

25th International QUENCH Workshop

22-24 October2019
Karlsruhe Institute of Technology
Karlsruhe, Germany

Editor: Martin Steinbrück

DOI: 10.5445/IR/1000100298

AGENDA

25th International QUENCH Workshop*

Karlsruhe Institute of Technology, Campus North, H.-von-Helmholtz-Platz 1, 76344 Egg.-Leopoldshafen, Germany
22-24 October 2019

Meeting Location: Fortbildungszentrum für Technik und Umwelt (FTU), Auditorium (Aula)

Tuesday, 22 Oct 2019

9:00	Welcome	W. Tromm/M. Steinbrück, KIT
	INTERNATIONAL PROGRAMS (Chair: M. Steinbrück, KIT)	
9:20	Main results of the IAEA Coordinated Research Project on Analysis of Options and Experimental Examination of Fuels for Water Cooled Reactors with Increased Accident Tolerance (ACTOF)	M.S. Veshchunov, IAEA
9:50	Progress in the OECD TCOFF project in support of Fukushima Decommissioning	D. Bottomley, JAEA
10:10	**Coffee break (Group Photo)**	
	QUENCH PROGRAM: RECENT RESULTS (Chair: M. Veshchunov)	
10:40	Update of the QUENCH program	M. Steinbrück, KIT
11:00	First results of the QUENCH-20 experiment with BWR test bundle	J. Stuckert, KIT
	25 YEARS QUENCH PROGRAM (Chair: T. Haste, Imperial College)	
11:20	25 years QUENCH-Program: Highlights of separate-effects tests	M. Steinbrück, KIT
12:05	Main results of the QUENCH bundle tests	J. Stuckert, KIT
12:50	**Lunch**	
13:50	Investigations of Hydrogen in Cladding Materials by means of Neutron Imaging	M. Grosse, KIT
14:30	Impact of QUENCH Experiments for ISP, Benchmarks and Code Validation	T. Hollands, GRS
15:10	**Coffee break**	
	MODELLING AND CODE APPLICATION I (Chair: C. Allison, ISS)	
15:40	Simulation of Quench-17 with ATHLET-CD	C. D'Alessandro, GRS
16:00	Comparative analysis of simulations of the air ingress experiments QUENCH-16 and QUENCH-18 using AC² - ATHLET-CD	F. Krist, RUB

**** In Cooperation with the International Atomic Energy Agency (IAEA)***

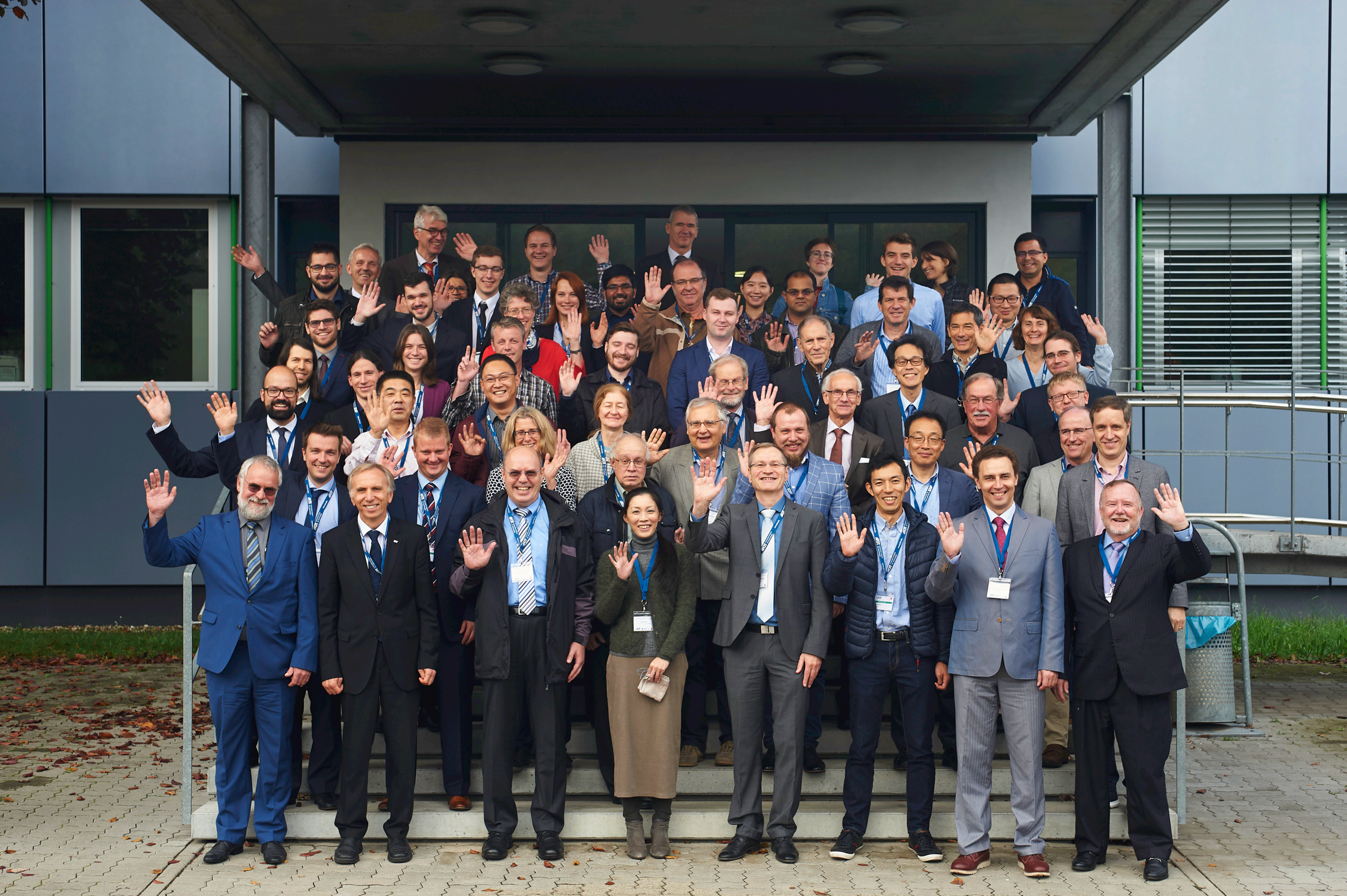
16:20	Post-test modelling of the experiment QUENCH-19 with ATF-cladding FeCrAl using SOCRAT code	A. Vasiliev, IBRAE
16:40	Simulation of recent QUENCH experiments with AC2	L. Tiborcz, GRS
17:15	***QUESA meeting (Chair: T. Hollands, GRS; for partners only)***	

Wednesday, 23 Oct 2019

	MODELLING AND CODE APPLICATION II (Chair: T. Hollands, GRS)	
8:40	Pre-test analysis of the QUENCH-20 BWR test with ASTEC	S. Wang, KIT
9:00	Preliminary Assessment of the new ASYST - ISA Integral Analysis Code Using Selected Integral Thermal Hydraulic - Fuel Assembly Experiments	C. Allison, ISS
9:20	MELCOR Analysis of Separate Effect Test's with PSI-KIT Nitriding Model	B. Jäckel, PSI
9:50	Evaluation of the process in the BWR and VVER spent fuel pools during severe accident conditions	T. Kaliatka, LEI
10:10	Numerical modelling of in-vessel melt-retention: The LIVE experiments	A. Joshi, Imp. College
10:30	**Coffee break**	
11:00	Preliminary results for simulations of the DEBRIS test facility conducted with the Severe Accident Analysis Code ASTEC V2.1	J.M. Peschel, RUB
11:20	Anticipated Benefit of CrAl_Coated_Zr Cladding under Beyond Design Basis Accidents	T.-H. Chun, KAERI
	ATF CLADDING (Chair: M. Grosse, KIT)	
11:50	Multi- elemental coatings on Zirconium alloy – INCT oxidation experiments	B. Sartowska, INCT
12:10	Testing of Cr Cold Spray-coated Cladding with Enhanced Accidental Tolerance	M. Sevecek, CTU
12:40	**Lunch**	
13:40	Coated cladding behaviour during high-temperature transients	A. Chalupová, CTU
14:00	Chromium coatings deposited by magnetron sputtering for accident tolerant nuclear fuel cladding	D. Sidelev, TPU
14:20	High-Temperature Oxidation of Chromium-Coated Optimized ZIRLO™ in air and steam	G. Bourdon, CVUT
14:45	**Bus to Annweiler, Trifels castle, and invited dinner**	

Thursday, 24 Oct 2019

	ATF CLADDING cont. (Chair: M. Sevecek, CTU)	
8:40	Behavior upon high temperature under steam environment of outer Cr (or inner DLIMO CVD CrCx) coated Zr based nuclear fuel claddings	J.-C. Brachet, CEA
9:10	Oxidation and quenching behavior of cold spray Cr-coated Zr alloy fuel cladding	C. Tang, KIT
9:30	Results of corrosion and thermomechanical tests of ATF-cladding samples	A. Mokrushin, LUCH
	EXPERIMENTS I (Chair: J. Stuckert, KIT)	
9:50	High temperature oxidation of cladding material in SFP-LOC conditions examined with 18O tracer techniques and Raman imaging	C. Duriez, IRSN
10:10	The oxidation behavior of Zr-1%Nb cladding alloy in air-steam mixtures	J. Krejci, UJP
10:30	**Coffee break**	
11:20	Towards and Improved Understanding of the Causes of Increased Hydrogen Uptake of Zr based Claddings at High Burnups	S. Abolhassani, PSI
11:50	Steam oxidation of hafnium at high temperature	S. Guilbert-Banti, IRSN
12:10	The CODEX-NITRO experiment	R. Farkas, MTA
12:30	**Lunch**	
	EXPERIMENTS II (Chair: C. Duriez, IRSN)	
13:30	Experimental investigation of the Ag-In-Cd system	M. Barrachin, IRSN
13:50	Physicochemical interaction between U-Zr-O melt and Fe-based structure during core degradation	A. Ito, Tokyo IT
14:10	Difference in oxidation behavior of heterogeneous BWR fuel assembly under steam-starved condition	Y. Nagae, JAEA
14:30	Post-test analysis of the CMMR-4 test bundle	H. Madokoro, JAEA
14:50	Status and results of the CLADS-MADE-02 BWR control blade degradation test under steam-rich conditions related to 1F Unit 3 accident	A. Pshenichnikov, JAEA-CLADS
15:30	**Closure of the Workshop**	M. Steinbrück, KIT




KIT
Karlsruhe Institute of Technology
IAEA
25th
International QUENCH Workshop
Karlsruhe Institute of Technology, Germany
22-24 October 2019
In cooperation with
the International
Atomic Energy Agency
Internet
SSID: KA-WLAN


TOSHIBA

Karlsruhe Institute of Technology

Welcome Address:
25th QUENCH workshop at KIT

Outlook Programme NUSAFE at KIT and HGF

Th. Walter Tromm, Programme Nuclear Waste Management, Safety and Radiation Research







Structure of the Program NUSAFE

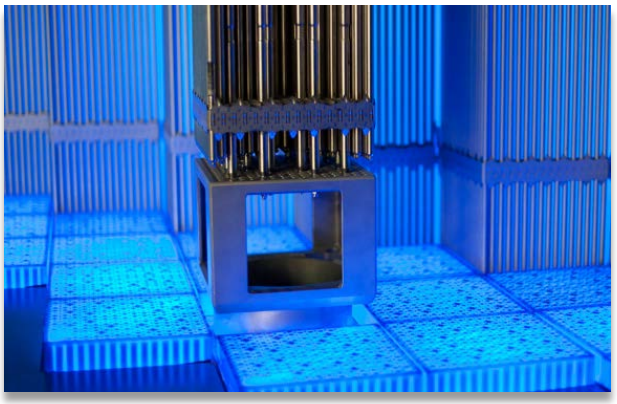
- **Topic 1 – Nuclear Waste Management (151 FTE, 63%)**
  - nuclear waste disposal
  - predisposal
  - fundamental scientific aspects
- **Topic 2 – Reactor Safety (89 FTE, 37%)**
  - design basis accidents & materials research
  - beyond design basis accidents & emergency management

Strategy

- **cutting-edge fundamental research** using a unique combination of **state-of-the-art infrastructures** and **theoretical tools**
- develop and integrate advanced experimental, instrumental (spectroscopy, microscopy etc.) as well as multiphysics and multiscale simulation tools
- synergistically **combine Helmholtz competencies** from Research Fields Energy and Earth & Environment
- development of dedicated **advanced data science methods and techniques** as well as digitalization initiatives
- **internationalization** via cooperating with key research organizations
- strong link to regional **universities** (e.g. joint appointments)
- **attracting young scientists** by providing a unique research infrastructure as a basis for excellent research







Strategic Goal of Reactor Safety Research

- Contribution to and assessment of the international developments in **reactor safety** technology
  - Lifetime extension for existing reactors
  - New builds and innovative concepts
- Leading edge research on **key aspects** of reactor safety
  - To remain a competent partner in international projects, bodies and committees
  - To ensure Germany's lasting influence on reactor safety in Europe and worldwide
- Providing an attractive education, training and research hub for **next generation experts**



Competences

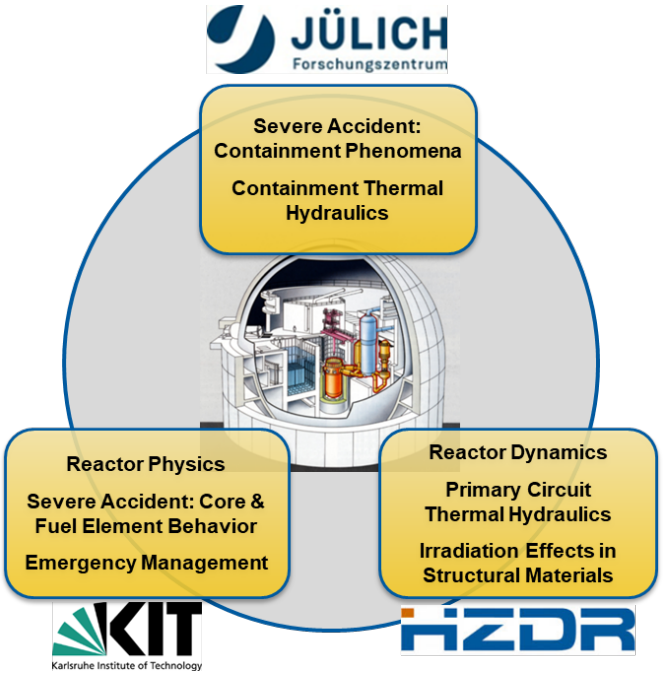
Experimental facilities

- Unique research infrastructures
  - High-pressure thermal hydraulic two-phase flow tests
  - Hot cells for investigation of irradiated materials
  - Facilities for core melt investigations and severe accident containment phenomena
- Groundbreaking results
  - CFD-grade data on condensation phenomena in the primary circuit and on containment walls
  - Accident-tolerant-fuel tests at the Helmholtz QUENCH facility
- Important Severe Accident Facilities in Europe (EU project SAFEST)



Conclusion

- NUSAFE provides leading edge research on key aspects of reactor safety as contribution to the international developments in reactor safety technology
- Unique combination of experimental infrastructures with high-level expertise in modeling of multiphysics and multiscale reactor safety issues
- Attractive education/training/research hub for next generation experts to ensure Germany's lasting influence on reactor safety in Europe and worldwide
- Implementation of results through cooperation with important international players in research, industry and authorities



Thank you for your attention



Th. Walter Tromm
Karlsruhe Institute of Technology
Programme Nuclear Safety Research

walter.tromm@kit.edu

Main results of the IAEA Coordination Research Project (CRP) on Analysis of Options and Experimental Examination of Fuels for Water-Cooled Reactors with Increased Accident Tolerance (ACTOF)

M.S. Veshchunov

Nuclear Fuel Cycle and Materials Section, Division of Nuclear Fuel Cycle and Waste Technology, Department of Nuclear Energy, International Atomic Energy Agency

Vienna International Centre, PO Box 100, 1400 Vienna, Austria

Abstract

The IAEA encourages and assists research on and development and practical use of atomic energy and its applications for peaceful purposes throughout the world. It brings together research institutions from its developing and developed Member States to collaborate on research projects of common interest, so-called Coordinated Research Projects (CRPs).

Fuel modelling is a recurrent priority in the IAEA sub-programme "Nuclear Power Reactor Fuel Engineering". Development and verification of computer codes are possible only on the basis of good experimental data that requires long and expensive in-reactor and post-irradiation studies. That is why international cooperation in this area is highly desirable, and the IAEA traditionally supports interested Member States in their efforts to enhance the capacities of their computer codes to predict fuel behaviour. Coordinated Research Projects (CRPs) are the main IAEA programme implementation tools in the area of fuel engineering.

The Fukushima accident also highlighted the vulnerability of zirconium fuel cladding to severe accident conditions. In this accident, cooling was lost for many days and the overheating cladding reacted with water to produce hydrogen. This induced hydrogen explosions and fuel melting as temperature rose. It was therefore considered important to investigate other fuel designs that would be more resistant to such severe accidents, whilst retaining the reliability and burnup potential of current fuel designs. Many Member States are considering new fuel types that range from using an oxidation resistant coating on zirconium-based cladding to alternate fuel and cladding materials. These new fuels/claddings under development must be licensed before being deployed industrially and therefore research is undertaken to assess their behaviours in reactor. This is time consuming and costly but can be modelled.

The respective CRP T12030 on “Analysis of Options and Experimental Examination of Fuels for Water-Cooled Reactors with Increased Accident Tolerance” (ACTOF) complements this effort by considering the modelling and development of advanced fuel concepts, supporting the collection of experimental data and model development that will be required to allow the introduction of such fuels into commercial reactors.



IAEA
International Atomic Energy Agency

Main results of the IAEA Coordinated Research Project (CRP) on Analysis of Options and Experimental Examination of Fuels for Water Cooled Reactors with Increased Accident Tolerance (ACTOF)

M. Veshchunov

Technical Lead (Fuel Engineering)

Nuclear Fuel Cycle and Materials Section

Division of Nuclear Fuel Cycle and Waste Technology

Department of Nuclear Energy

IAEA, Vienna, Austria

m.veshchunov@iaea.org



25th International QUENCH Workshop
Karlsruhe Institute of Technology, 22-24 October 2019

Outline

- **Who are we?**
  - IAEA organization
  - IAEA Fuel Engineering Programme
  - CRPs
- **CRP ACTOF**
  - Background and Objectives
  - Joint Actions
    - Round Robin Tests
    - Benchmark exercises
    - Severe Accident Experimental and Modelling Exercise
  - Conclusions
  - Perspectives and recommendations
  - New CRP on ATF

IAEA: Statute and objectives

Established in 1957

171 Member States

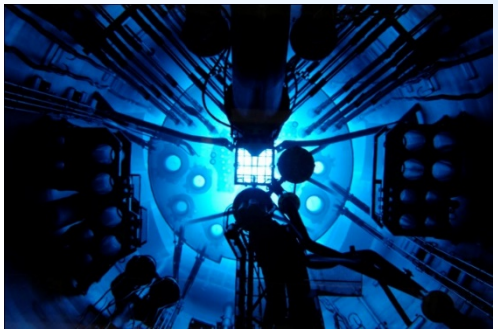
~ 2,560 multidisciplinary professional and support staff from more than 100 countries



ATOMS FOR PEACE AND DEVELOPMENT

The Agency shall seek to accelerate and enlarge the contribution of atomic energy to peace, health and prosperity throughout the world.

Research Reactors



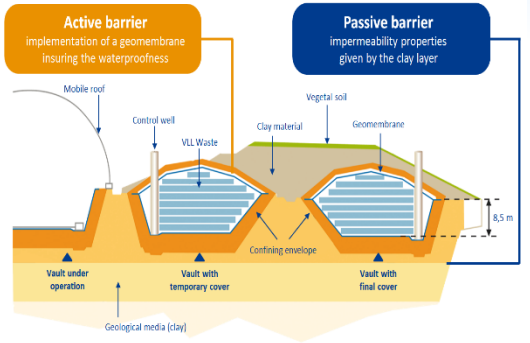
Division of Nuclear Fuel Cycle and Waste Technology

NEFW

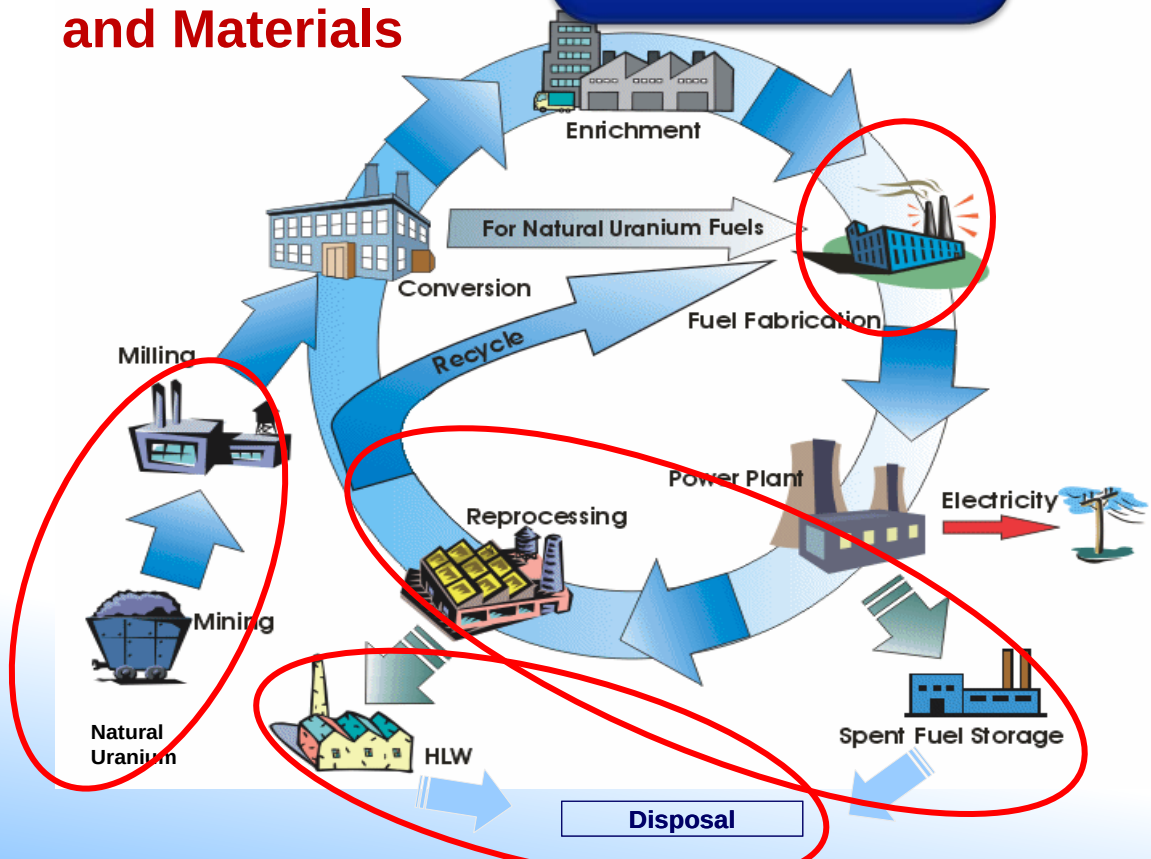
Waste Management







Nuclear Fuel Cycle and Materials



Decommissioning Environmental Remediation









Fuel Engineering Programme

- Major Programme (MP) 1: NUCLEAR POWER AND FUEL CYCLE
  - Programme (P) 1.2: Nuclear Fuel Cycle and Materials Technologies
    - Subprogramme (SP) 1.2.2: Nuclear Power Reactor Fuel
      - ✓ Project 1.2.2.1: Nuclear Power Reactor Fuel Engineering

- **Objective:** Support Member States (MSs) to understand and address factors affecting the design, fabrication and in-pile behaviour of currently operating and innovative nuclear fuels and materials for power reactors
- **Advised by the Technical Working Group on Fuel Performance and Technology (TWGFPT):** a group of recognized experts from MSs to provide advice and support programme implementation, reflecting a global network of excellence and expertise in the area of nuclear power reactor fuel engineering (25 Members)

Coordinated Research Projects (CRPs)

- CRPs are a mechanism for coordinating international research within the IAEA programme of work
- A CRP theme is scoped in consultation with experts and authorized by the IAEA for proposals of work from Member States
- Typically ~4 years, organized around 3 Research Coordination Meetings (RCMs)
- A very good opportunity to work with many groups around the world
- CRP direction is largely defined in the first RCM by the CRP participants
- Research results finalized as an IAEA TECDOC
- Results are available, free of charge, to scientists, engineers and other users from all Member States

Coordinated Research Projects
(Fuel Engineering Programme)

Coordinated Research Projects (CRPs)	14	15	16	17	18	19	20	21	22	23
Fuel modelling in accident conditions (FUMAC)										
Reliability of high power, extended burnup and advanced PHWR fuels										
Analysis of options and experimental examination of fuels for water-cooled reactors with increased accident tolerance (ACTOF)										
Accelerator simulation and theoretical modelling of radiation effects (SMoRE-2)										
Fuel Materials for Fast Reactors (embedded meeting in FR-17, June 2017; CM in 2018; RCM-1 on 2-4 October 2019)										
Testing, Modelling and Simulations for ATF (TS-ATF)										

CRP on Analysis of Options and Experimental Examination of Fuels with Increased Accident Tolerance (ACTOF)

❑ Background

- Fukushima accident: zirconium cladding worsened the problem
- New and improved fuel designs are being considered by many Member States
- TWG FPT recommendation arising from post-Fukushima review
- IAEA expertise in supporting fuel modelling – CRP FUMAC considers standard fuel modelling under accident conditions
- Technical Meeting on Accident Tolerant Fuel held in US, 2014

❑ Objective

- To support options for the development of nuclear fuel with an improved tolerance of severe accident conditions
- To support modelling of new fuel designs with advanced cladding or fuel
- To acquire data through experiments on new fuel types and cladding materials to support their use for fuel with improved accident tolerance

IAEA CRP T12030 (ACTOF)

- **Participants** (17 organizations from 13 MSs)

  Argentina (CNEA), Brazil (USP), China (CNPRI, CIAE, NPIC), Finland (VTT), Germany (KIT), India (BARC), Italy (NINE), Korea (KAERI), Poland (INCT), Russian Federation (VNIINM, IBRAE), United States (Westinghouse, Batelle), Czech Republic (CTU), JAEA (Japan) [*joined at RCM-2*]

- **Observers**

  OECD-NEA, EPRI (USA), US NRC, GRS (Germany) – *active*

- **Status**
  - In closure (2014-2019)
  - Research Coordination Meetings:
    - RCM-1: November 2-4, 2015 in Vienna
    - RCM-2: June 20-22, 2017 in Vienna
    - RCM-3: November 26-29, 2018 in Vienna
  - CM on preparation of TECDOC: February 28 - March 1, 2019

ACTOF Joint Actions

- Round Robin Tests
- Benchmark Exercise
- Severe Accident Experimental and Modelling Exercise

Round Robin Tests

- 7 participants
  - WEC (Westinghouse): coordination
  - CTU: Czech Technical University /UJP Praha (Czech Republic)/ MTA EK (Hungary)
  - Karlsruhe Institute of Technology (KIT), Germany
  - VTT Materials for Power Engineering, Finland
  - Institute of Nuclear Chemistry and Technology (INCT), Poland
  - University of Sao Paulo (USP), Brasil
- Activity was divided into three subtasks (the involvement is summarized in Table):
  - Sample production
  - Long-term corrosion test (VVER or PWR chemistry)
  - High-temperature steam oxidation

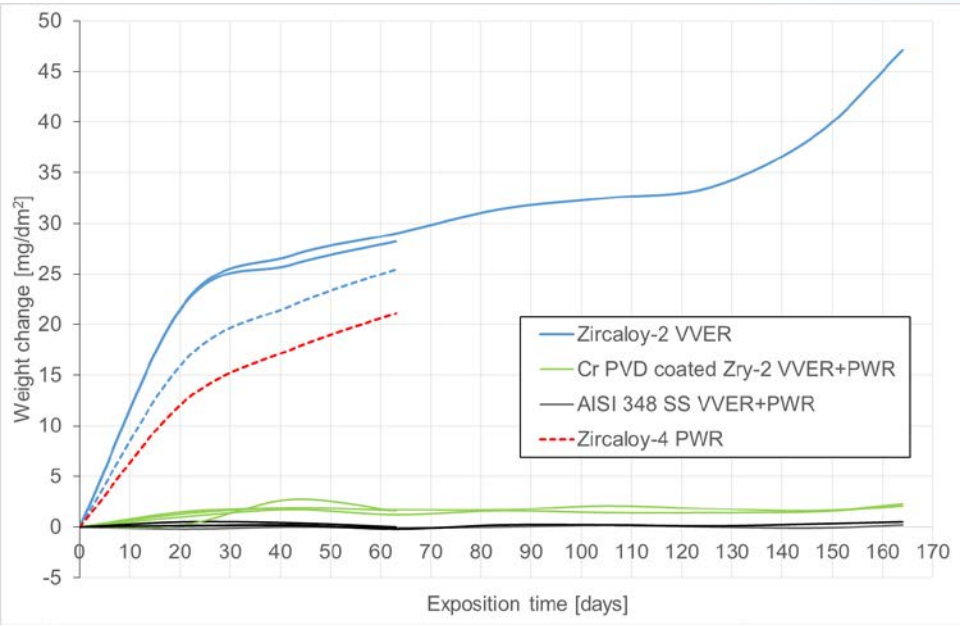
	CTU	KIT	INCT	VTT	USP	MTA EK
SAMPLE PRODUCTION	X	X	X		X	
LONG-TERM CORROSION	X		X	X		
HIGH-TEMPERATURE OXIDATION	X	X		X		X

ATF Sample Production

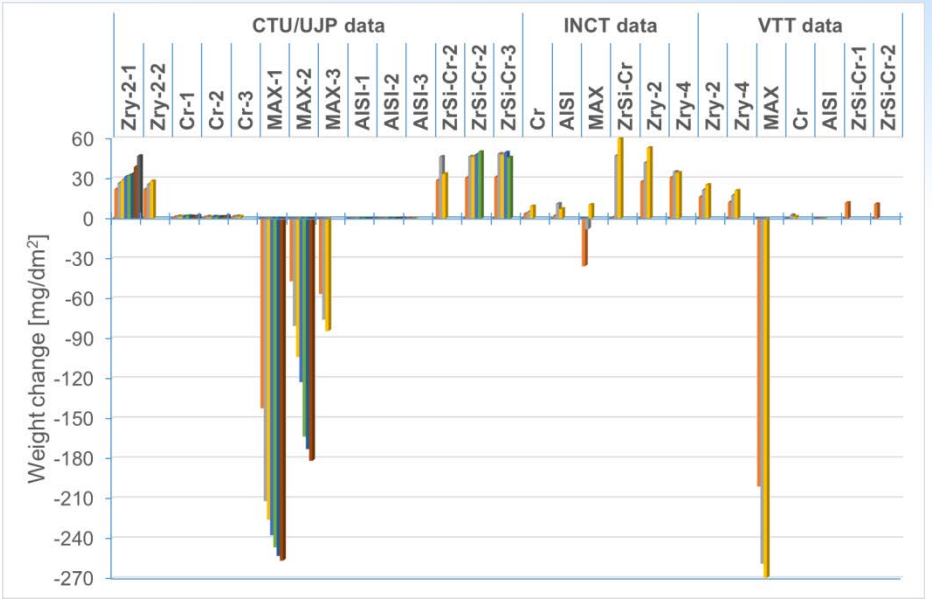
- Four types of ATF candidate cladding samples produced (3 coated cladding concepts + advanced steel)
  - Cr PVD coated Zry-2 and E110 (Zr1%Nb) cladding – produced by CTU
  - $Cr/Cr_2AlC/Cr$ PVD coated Zry-4 – produced by KIT
  - ZrSi-Cr PVD coated Zry-2 – produced by INCT
  - AISI 348 stainless steel – produced by USP
- Westinghouse Electric Company provided Zry-2 substrates for Cr and ZrSi-Cr coated samples
- UJP Praha provided Zry1%Nb substrates

Post Test Examinations

Selected results – Long term corrosion tests



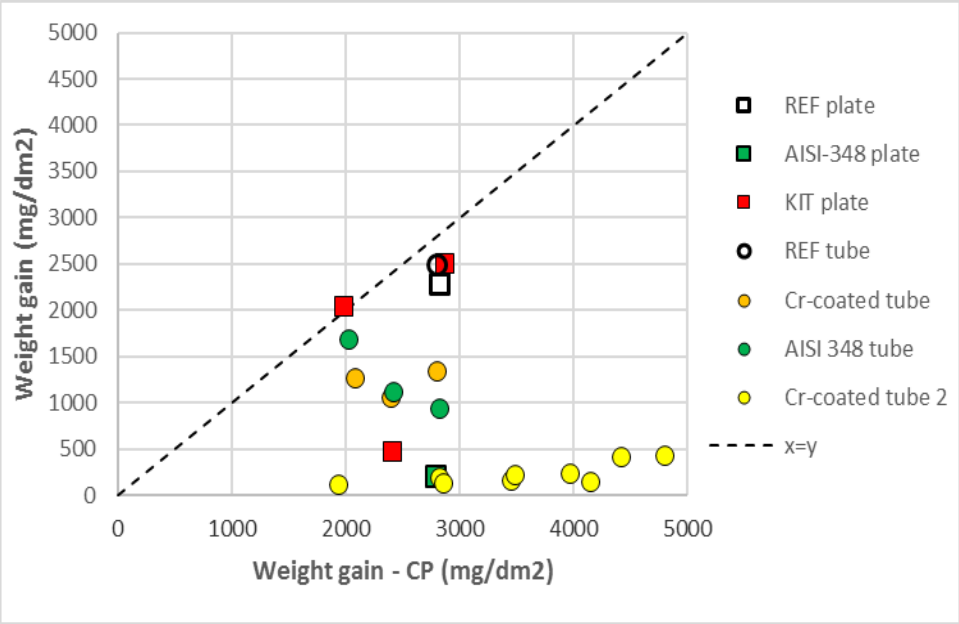
Weight gains from the corrosion test in VVER and PWR water chemistry



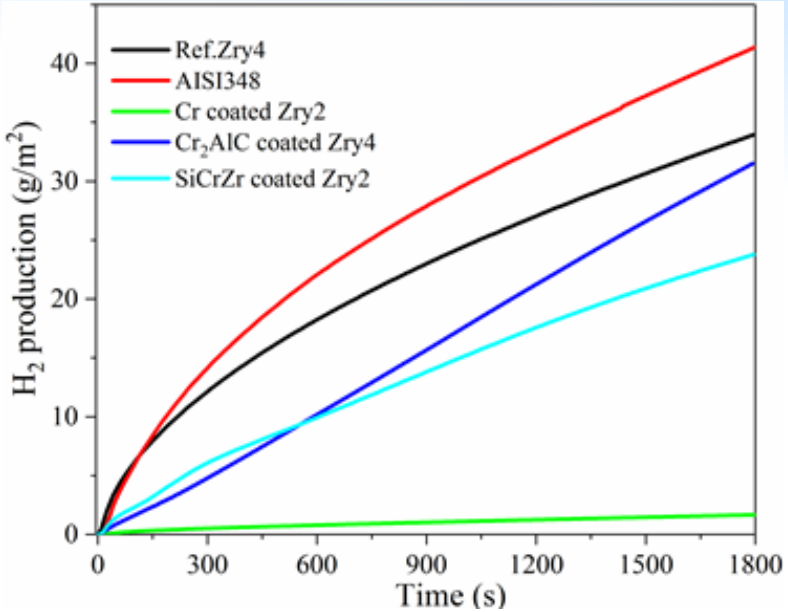
Dissolution and spallation of MAX phase coated samples in both VVER and PWR conditions

Post Test Examinations

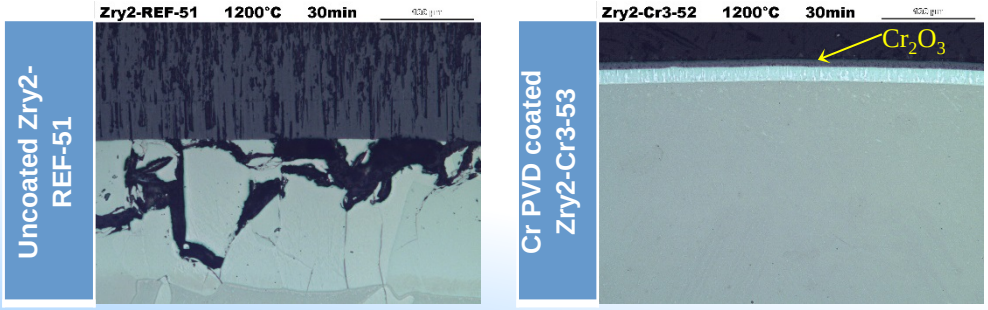
Selected results – HT Oxidation



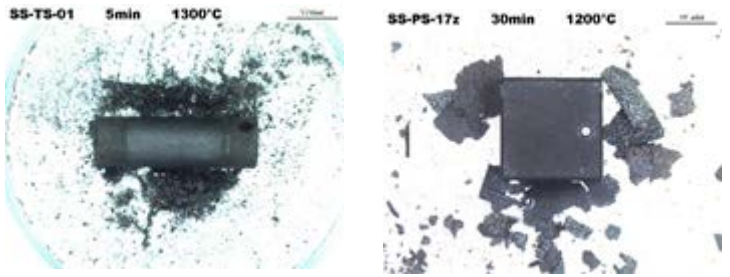
Measured against calculated/expected weight gains (using Cathcart-Pawel correlation) in HT oxidation tests



Hydrogen production in HT oxidation tests



Metallography of uncoated and Cr-coated Zry-2



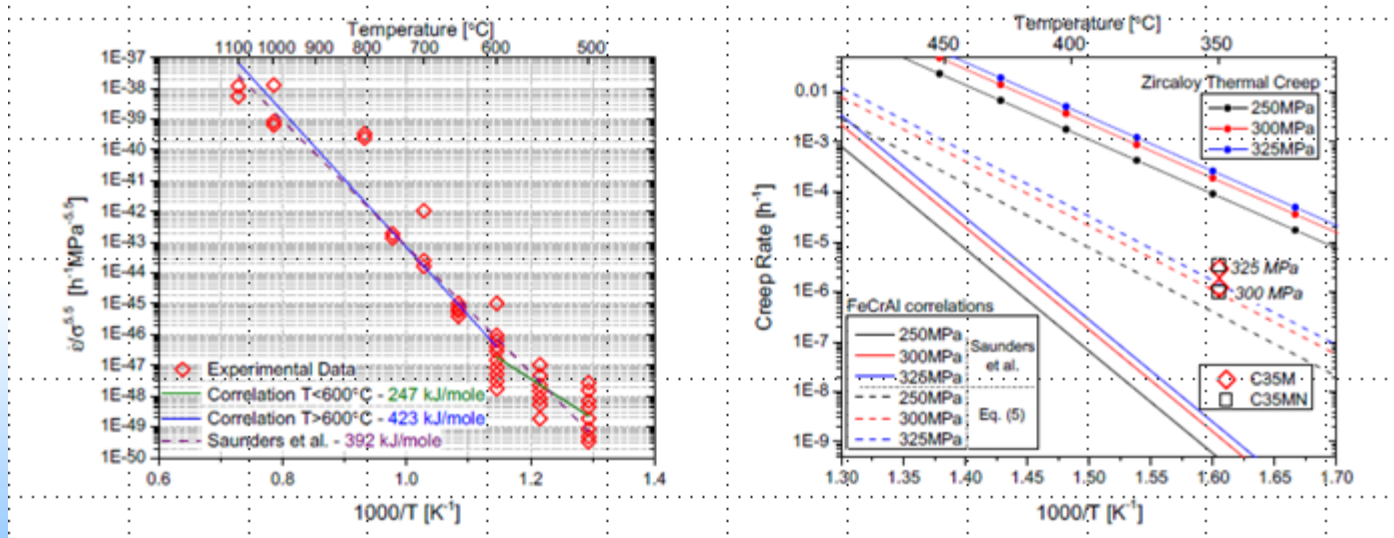
Spallation of oxide of AISI 348 alloy

ACTOF Joint Actions

Benchmark Exercise (FeCrAl against Zry-4)

❑ Scope

- ➢ Provide material property data for FeCrAl (INL)
- ➢ Benchmark calculation for FeCrAl
  - Provide modelling input, normal operation case specification (UO_2-FeCrAl) and LOCA case specification, output format for FeCrAl (INL)
  - Perform benchmark calculation using different codes
  - Prepare report for benchmark calculation



ORNL correlations for thermal and irradiation creep of C35M

Benchmark Exercise

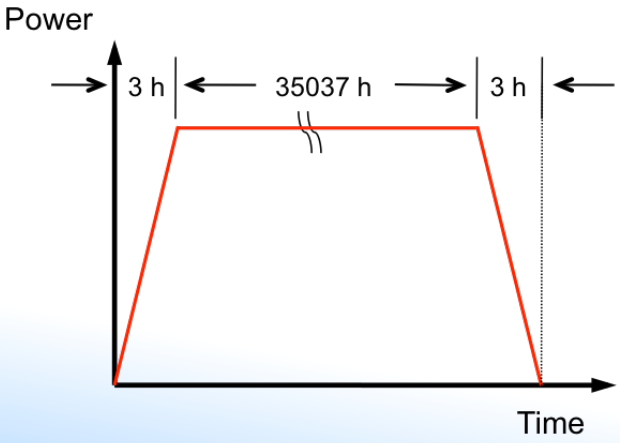
Participants

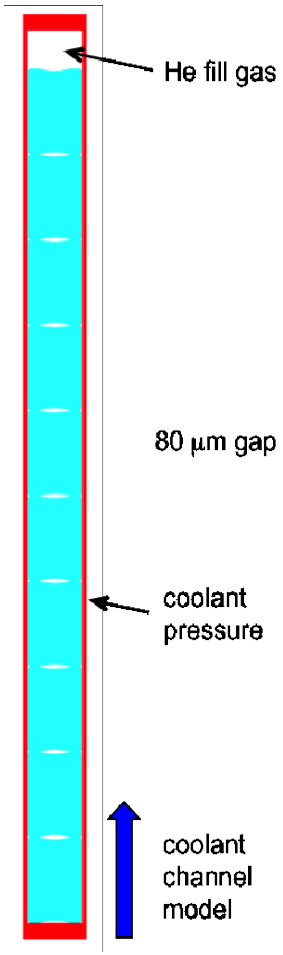
- Idaho National Laboratory (USA), BISON code
- N.IN.E – Nuclear and Industrial Engineering (Italy), TRANSURANUS code
- University of São Paulo (Brazil), modified FRAPCON-3.4 code
- CNEA – National Atomic Energy Commission (Argentina), BACO code
- JAEA – Japan Atomic Energy Agency (Japan), FEMAXI-7 code

Benchmark Exercise

Normal operation

- Simulation of a 10-pellet fuel rodlet with typical PWR specifications
- Constant LHR=25 kW/m for 4 years with start-up and final shut-down
- Both FeCrAl and Zry-4



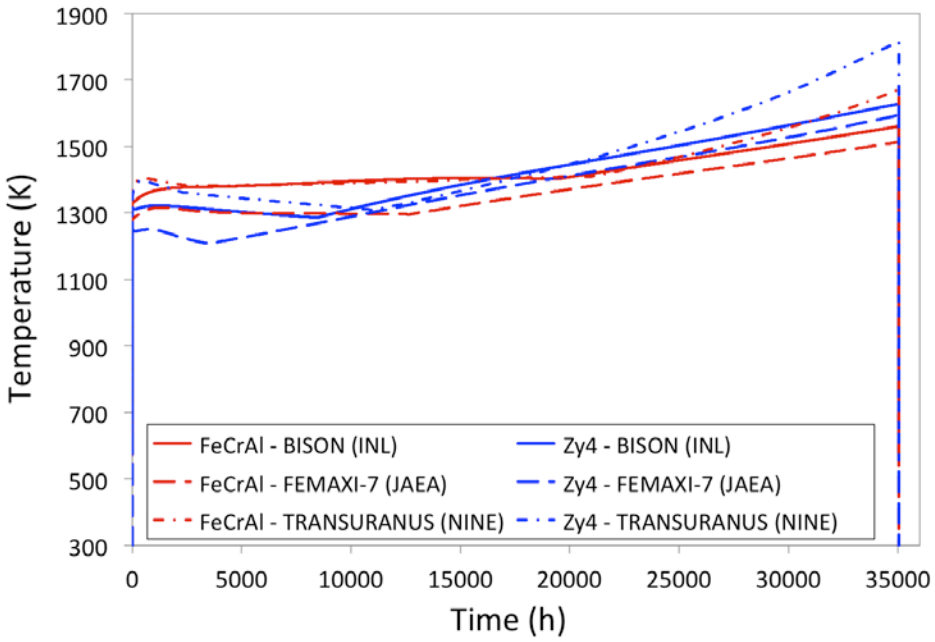


	UO_2/Zircaloy-4 Rodlet	UO_2/FeCrAl Rodlet
Number of pellets	10	10
Pellet length (mm)	11.86	11.86
Pellet inner diameter (mm)	0	0
Pellet outer diameter (mm)	8.19	8.57
Chamfers, dishes	no	no
Initial fuel density (%TD)	95	95
Initial fuel density (kg/m^3)	10431	10431
Initial fuel enrichment (%)	5	5
Initial fuel grain radius (3D) (μm)	5	5
Radial gap width (μm)	80	80
Initial fill gas	He	He
Initial fill pressure (MPa)	2	2
Cladding inner diameter (mm)	8.35	8.73
Cladding thickness (mm)	0.575	0.385
Cladding outer diameter (mm)	9.5	9.5
Upper plenum height (mm)	26	26
Lower plenum height (mm)	1	1
Total free volume (cc)	1.725	1.874
Total rodlet length (incl. plugs) (mm)	150	150
Coolant inlet mass flux (kg/m^2-s)	3800	3800
Coolant inlet temperature (K)	580	580
Coolant pressure (MPa)	15.5	15.5
Pin pitch (mm)	12.6	12.6

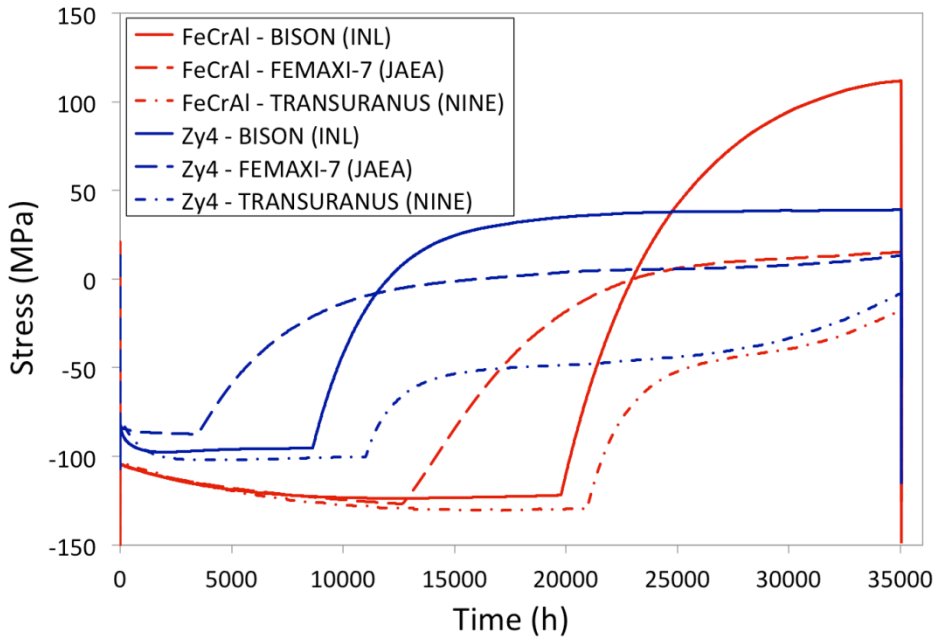
Benchmark Exercise

Selected results

Normal operation conditions



Centerline temperature

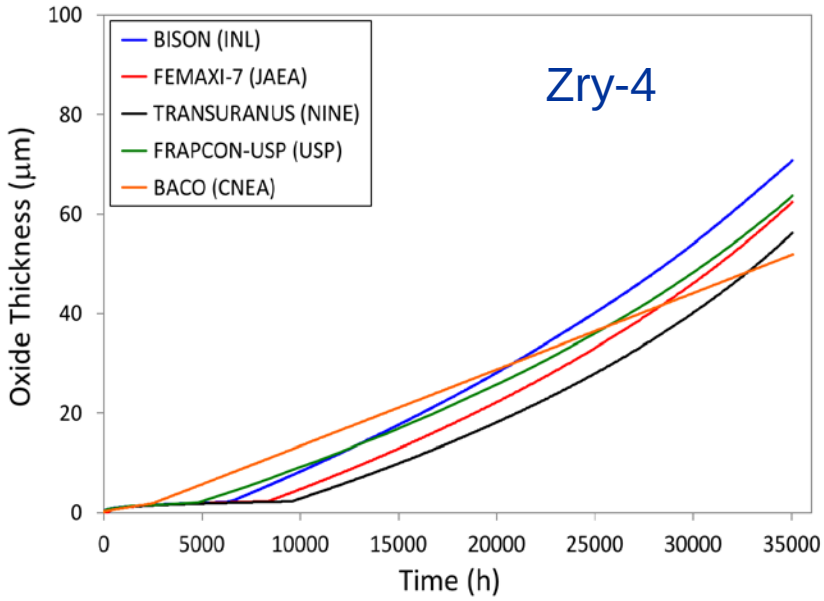


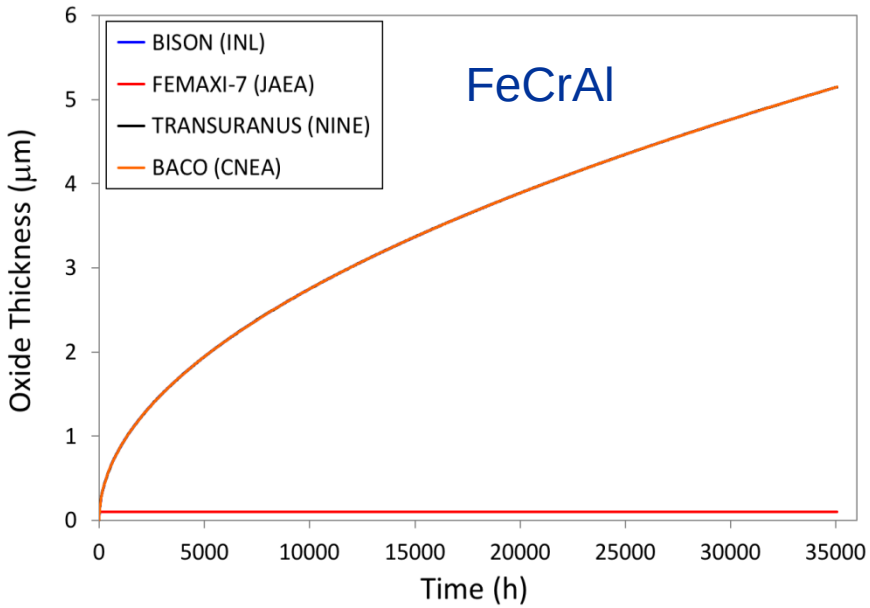
Cladding hoop stress

Benchmark Exercise

Selected results

Normal operation conditions



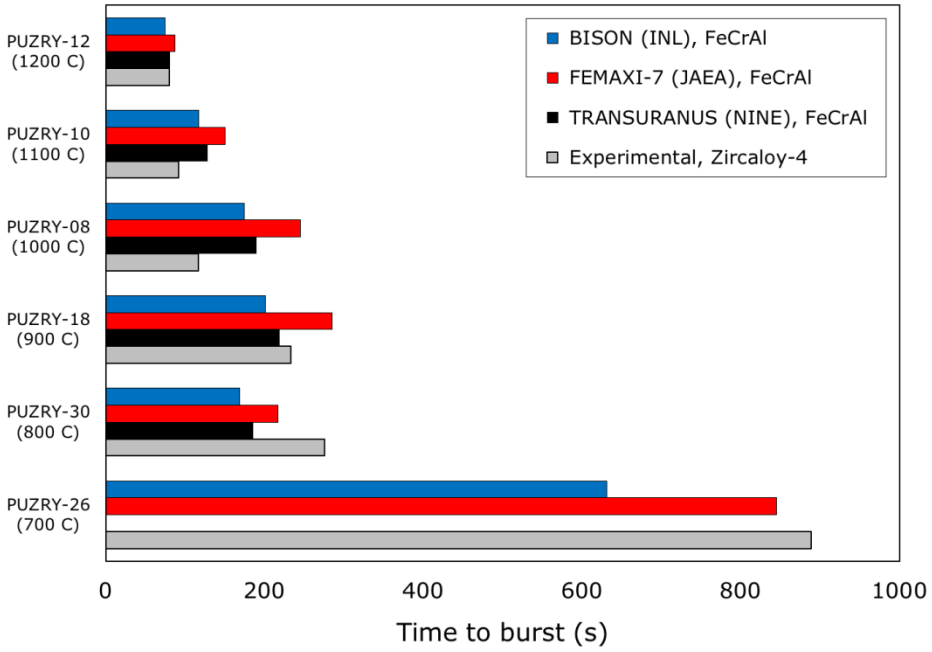


Oxide layer thickness

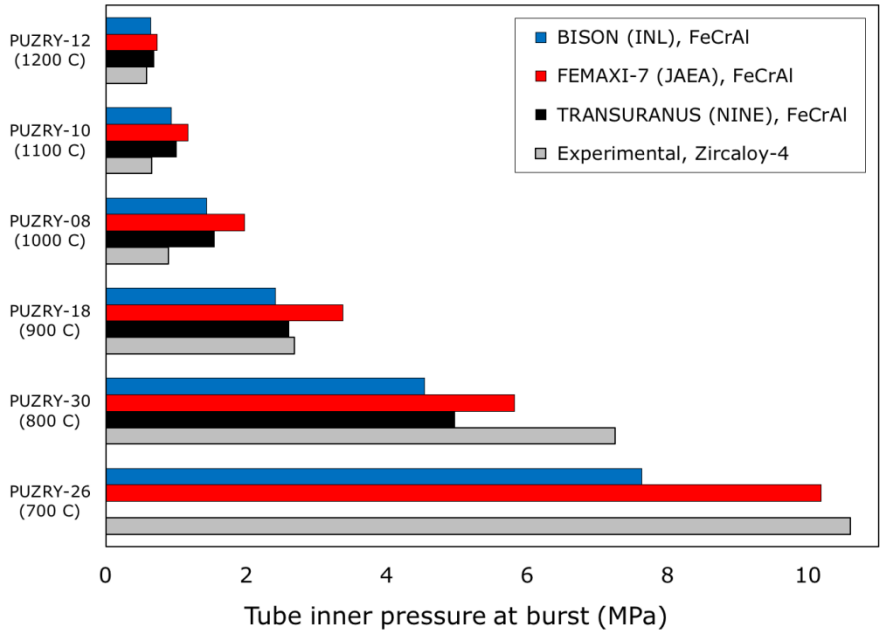
Benchmark Exercise

Selected results

LOCA



Time to burst



Burst pressure

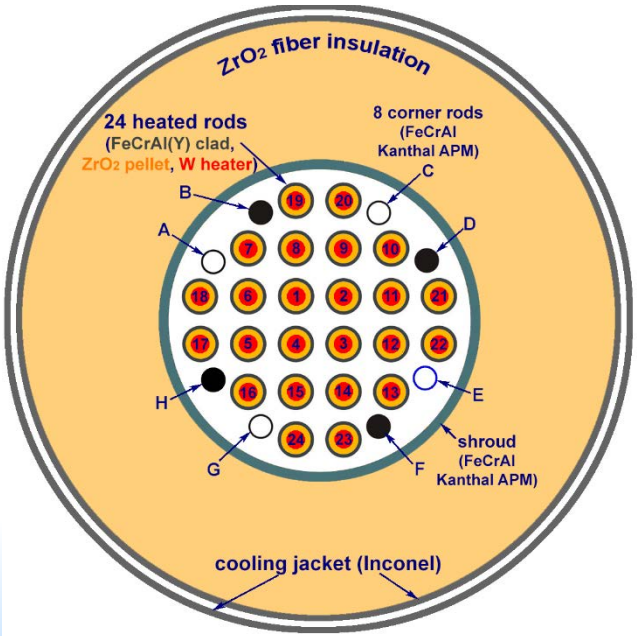
ACTOF Joint Actions

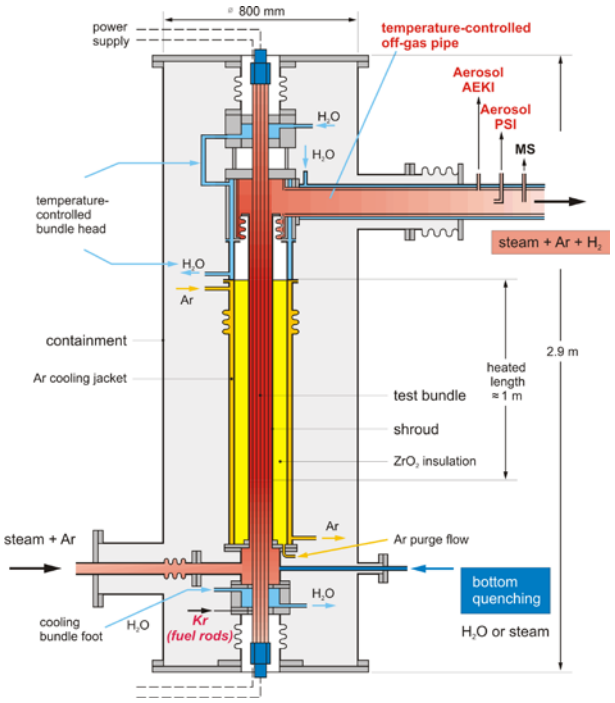
Severe Accident Experimental and Modelling Exercise

QUENCH-19 (FeCrAl) bundle test at KIT



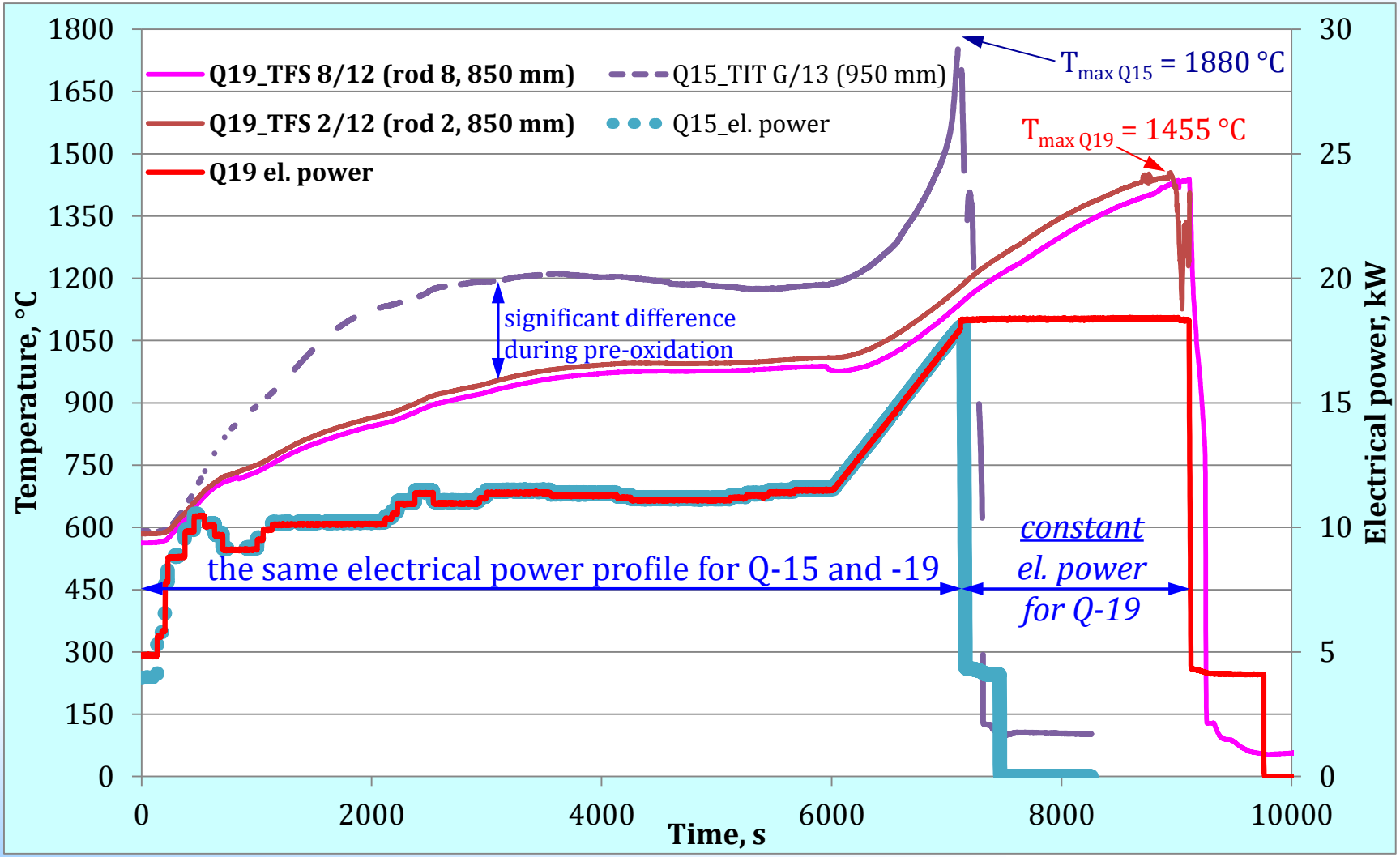
- Provide results of severe accident testing, including separate single rod test and Quench-19 FeCrAl test (KIT)
- Calculation for high temperature QUENCH-19 (FeCrAl) test using ATHLET-CD (GRS) and SOCRAT (IBRAE)





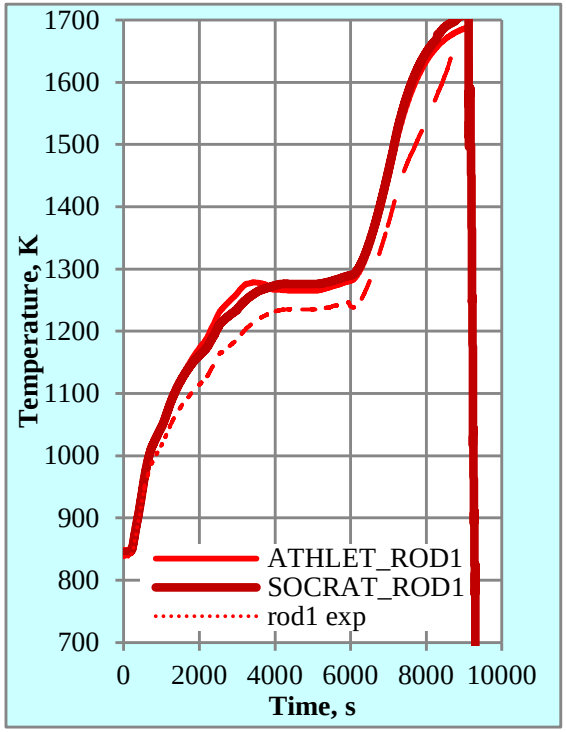
Severe Accident Experimental and Modelling

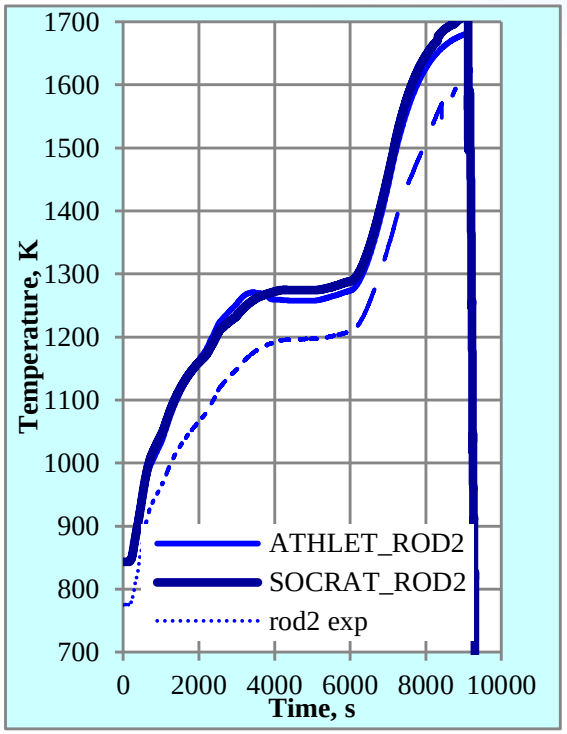
Test performance: comparison of QUENCH-15 (ZIRLO) and -19 (FeCrAl)

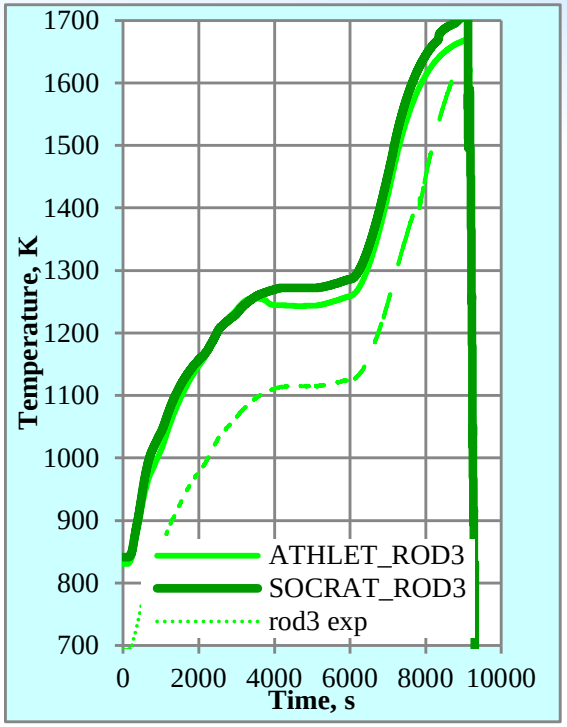


Severe Accident Experimental and Modelling

Selected results



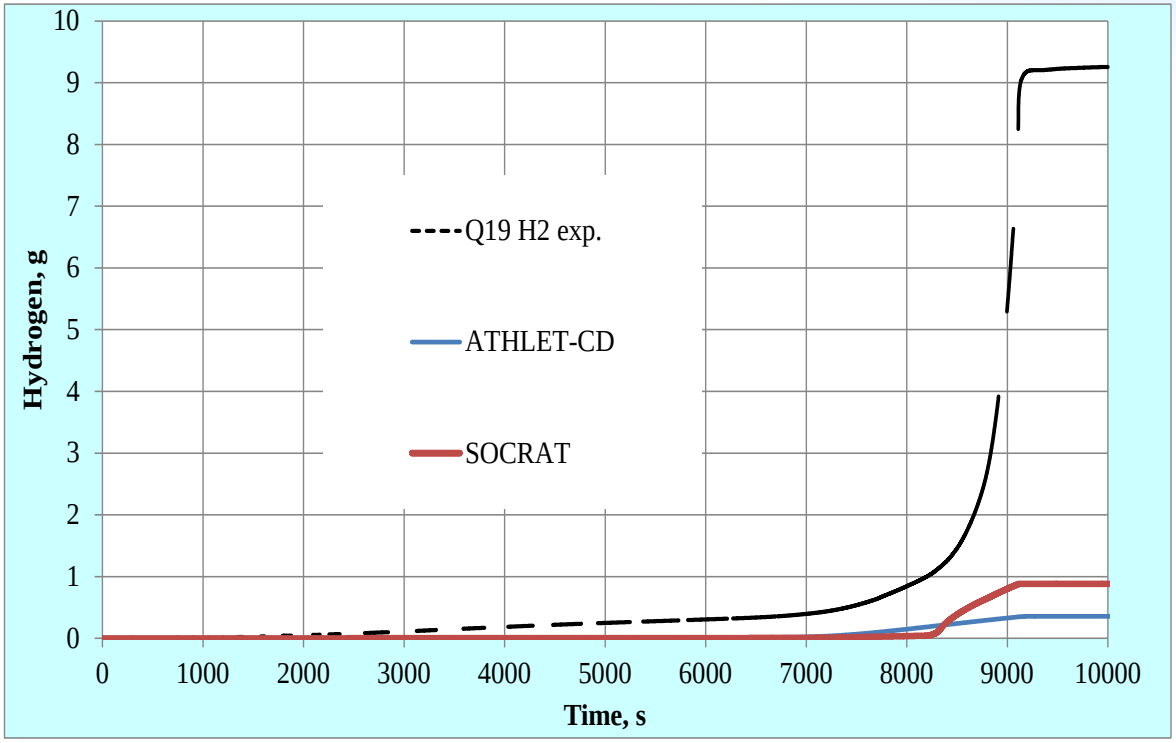




Temperature simulation for elevation 950 mm

Severe Accident Experimental and Modelling

Selected results



Simulation of hydrogen release: integral values

Conclusions:

- Currently available correlations for FeCrAl underestimate the oxidation kinetics
- New separate-effect tests on high temperature oxidation of FeCrAl alloys in a wider temperature range are needed

Conclusions

- Various ATF options were analyzed resulting in improved understanding of the ATF behaviours and advancing ATF technology developments in Member States
  - Several coated cladding materials were produced, tested, characterized, and analyzed
  - The feedbacks are important for MSs to improve their ATF concepts and development
- Fuel performance codes from participating organizations were significantly extended to the analysis of several ATF concepts (including FeCrAl and SiC claddings, coated Zircaloy claddings and U_3Si_2 fuel)
- Benchmark was organized and finalized where the extended codes were compared for the analyses of fuel rod with FeCrAl cladding under both normal operation and design-basis accident conditions
- Integral codes (ATHLET-CD and SOCRAT) have been applied and benchmarked against the severe-accident bundle test QUENCH-19 (KIT) with FeCrAl claddings
- CRP triggered new collaborations between some organizations beyond the ACTOF project timeframe (especially a great interest to international programs with ATF at QUENCH facility (KIT)

Perspectives and recommendations

- To extend and foster collaborations among MSs to advance ATF technologies
- To further enhance the database for ATF through coordinated round robin tests and tests from MSs for better understanding and evaluation of ATF behaviour and performance
- To extend the benchmarking of MSs fuel performance codes to cover other materials and conditions, and to enhance codes development
- To closely couple experimental work with modelling and simulation so that we can produce good quality sets of test data to validate and improve modelling and analysis for ATF
- To carry out deeper analysis of failure criteria for ATF for better understanding of safety and economic benefits of ATF and to enhance ATF acceptance for public by demonstrating the safety benefits of ATF
- To organize a new CRP on Testing and Simulation of Advanced Technology Fuels (ATF-TS) (2020-2023), to support sustainability of nuclear technology, diversification of fuel supply, and innovation in fuel technology developments

New CRP on Testing and Simulation of Advanced Technology Fuels (ATF-TS) (2020-2023)

- CM on preparation of new CRP Proposal: October 15-17, 2019
- Experimental Program:
  - **Round Robin tests**
    - Cr coated Zr claddings:
      - ballooning and burst isothermal (CTU,…)
      - ballooning and burst transient and/or LOCA (Quench Rig facility, KIT)
    - FeCrAl:
      - high temperature oxidation tests (Thermo Balance facility, KIT)
      - autoclave oxidation tests and mechanical tests, etc. (CRIEPI, CTU, …)
    - SiC
      - autoclave oxidation, high temperature oxidation, collection of material properties data base *(CNPRI, NPIC, JRC-Karlsruhe,…)*
  - **Bundle tests**
    - DEGREE facility with ATF rods (Coated Zry-4) under SA and/or LOCA
  - **Irradiation tests data**
    - Doped fuel pellets HALDEN tests – TBC

New CRP on Testing and Simulation of Advanced Technology Fuels (ATF-TS) (2020-2023)

- Modelling Program
  - **Fuel performance codes benchmarks, including modeling improvements and uncertainty analysis**
    - Material properties database for ATF *(ISS?)*
    - FeCrAl / coated Zr cladding / uncoated Zr cladding against new RRT burst tests
    - Doped fuel pellets HALDEN tests – TBD
  - **SA Modelling benchmark**
    - Database: Quench-19, DEGREE
    - SA Codes : ASTEC, ATHLET-CD, MELCOR, MAAP, SOCRAT…
  - **LOCA evaluation methodology development for NPP applications**
    - Qualification of Fuel rod codes for LOCA application based on IFA 650.10 with SOCRAT TH boundary conditions and uncertainty analysis, prediction for FeCrAl and/or coated Zr cladding
    - Application to PWR prototypic fuel rod with TH boundary conditions (2 scenarios: LB and SB LOCA) and uncertainty analysis, prediction for FeCrAl and/or coated Zr cladding

IAEA
International Atomic Energy Agency

THANK YOU,
and welcome to the new CRP!



25th International QUENCH Workshop, Karlsruhe Institute of Technology Campus North, (Karlsruhe, Germany), 22-24 October 2019

Progress in the OECD TCOFF project in support of Fukushima Decommissioning.

By David Bottomley[1], Davide Costa[2], Akira Nakayoshi[1], Tadahiro Washiya[1] and Masaki Kurata[1].

[1] Japan Atomic Energy Agency-CLADS LAboratory, Iwaki, Japan,

[2] Division of Nuclear Science, NEA-OECD, Billancourt-Paris, France

ABSTRACT

The 3-year TCOFF (Thermodynamic Characterisation of Fuel Debris and Fission Products) project had a preliminary meeting before starting in Jan. 2017 with 18 institutes from 11 member countries (including EC) and 2 associated member institutes. The project aims to improve the thermodynamic databases and so enhance severe accident simulation models. It identified compounds/conditions needing more characterisation by thermodynamic measurements, calculations or improved modelling. Tasks were grouped into fuel-based and fission product-based areas. The work was carried out by members or associated research centres. In addition to the in-kind contributions from members; there was also 2 annual calls for research proposals. Other activities included Workshops and collaboration with Pre-ADES and ARC-F projects, by means of joint meetings and information exchanges. This project will be entering its final reporting stages and the presentation will show selected results and also the links and interactions built up between TCOFF and other currently running projects.


TOSHIBA

Collaborative Laboratories for Advanced Decommissioning Science

OECD BETTER POLICIES FOR BETTER LIVES

Nuclear Energy Agency

NEA NUCLEAR ENERGY AGENCY

Progress in the OECD TCOFF project in support of Fukushima Decommissioning.

TCOFF = Thermodynamic Characterization Of Fuel Debris & Fission Products based on Scenario Analysis of Severe Accident Progression at FDNPS

David Bottomley[1], Davide Costa[2], Akira Nakayoshi[1], Tadahiro Washiya[1] and Masaki Kurata[1].

[1] Japan Atomic Energy Agency-CLADS Laboratory, Japan

[2] Division of Nuclear Science, NEA

Outline

- Outline of TCOFF
- Project work programme- progress as at July2019
  - TF1 (corium and debris)
  - TF2 (Fission Products)
- Results from additional TCOFF research programme (international calls for proposals)
- Dissemination - 2nd TCOFF Intl. Workshop 2019, Iwaki
- Links with other OECD-NEA-CSNI projects
- Concluding Remarks

Background of TCOFF

- **Motivation: Support for Fukushima Daiichi decommissioning. There is an internationally-recognised need for continual updating of thermodynamic knowledge and databases to understand fuel degradation: also for**
  - Improvement of fuel degradation and FP-behaviour models, applied to SA-codes;
  - Severe accident management and fuel debris characterization.

- MEXT/Japan proposed a 3-year joint project (**2017-2019**) to NEA/NSC (*Nuclear Science Committee*), to maximise synergies with the related joint projects, **TAF-ID** (@NSC), **BSAF-2**, **PreADES**, **ARC-F** (@NEA/CSNI), *Committee of Safety Nuclear Installations*)

- Fully funded by MEXT/Japan (720 kEuros for 3 years), for

1) project management,
2) NEA technical support
3) *International calls for R&D proposals* (2x1 year: **2018/19**).

Objectives of TCOFF

1. **Improve quality and/or inventory of thermodynamic databases** with a reference to SA-progression analysis for FDNPS accident. (TAF-ID, NUCLEA, HERACLES, SGTE)
   - ◆ **Benchmark calculations** under conditions experienced during FDNPS accident;
   - ◆ **Identification and prioritization of material science concerns** of current thermodynamic databases;
   - ◆ **Improvement and/or enlargement of thermodynamic databases** through experimental and analytical knowledge, provided as in-kind contribution;

2. **Conduct joint thermodynamic evaluations** of SA-progression at in-vessel and ex-vessel phases of FDNPS unit-1,2, and 3.
   - Fuel melting and molten core relocation;
   - FP-behaviour, including volatilization/deposition/re-vaporization and leaching;
   - Fuel debris chemical and phase composition, including long term degradation;
   - Thermodynamic evaluation of formation of materials *which may potentially be detected at the FDNPS*.

Members

TCOFF member organizations:

- CVR (Czech Rep.)
- JRC (EC)
- CEA, IRSN (France)
- KIT (Germany)
- CRIEPI, JAEA, TITECH (Japan)
- KAERI (Korea)
- Tech. Univ. Delft (the Netherlands)
- IBRAE, KRI, NITI (Russian Federation)
- KTH, SSM (Sweden)
- PSI (Switzerland)

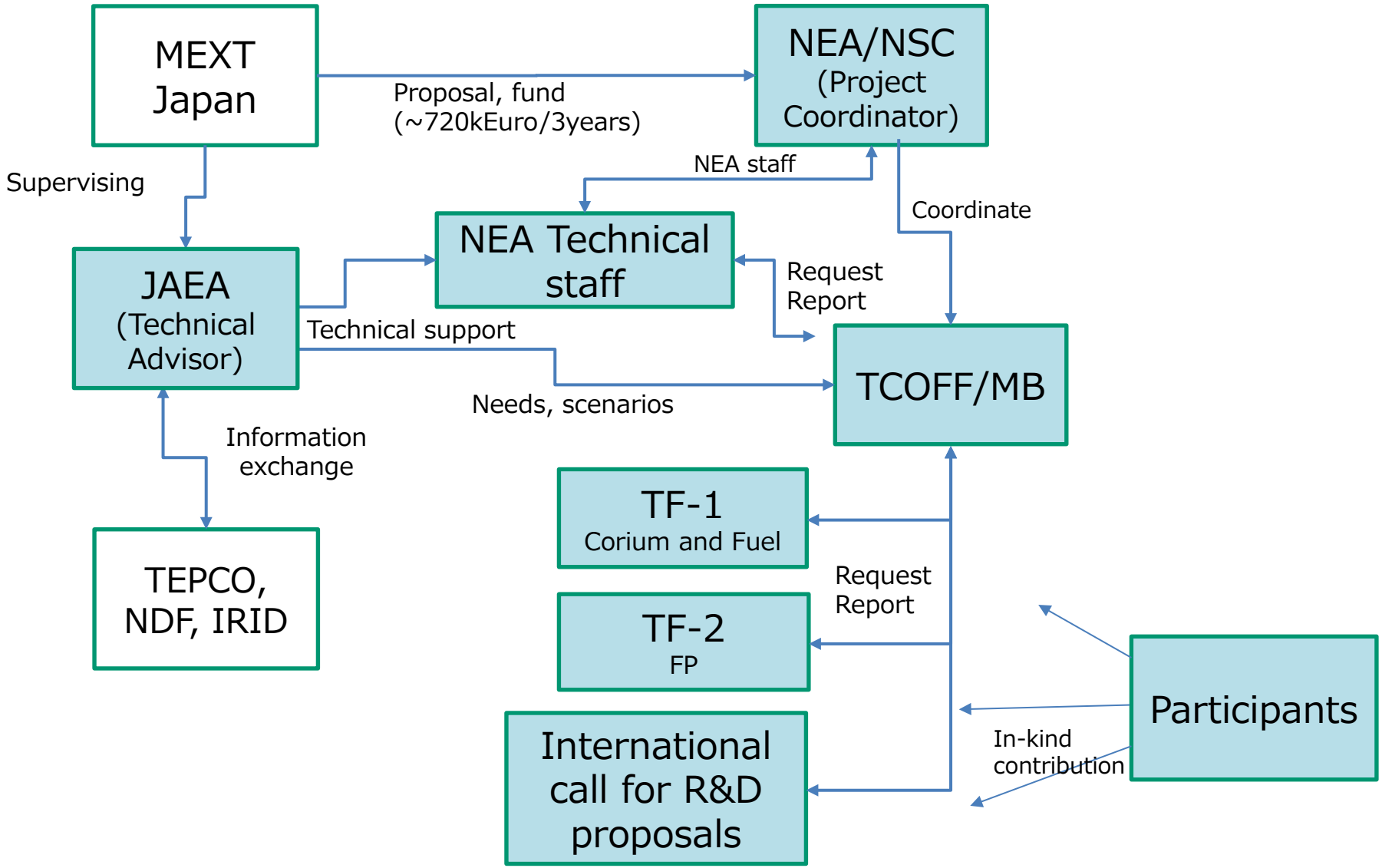
New members organizations (from 2018):

- NRC/SNL (US)
- St. Petersburg State Univ. (Russia)

Other organizations who showed their interests to TCOFF:

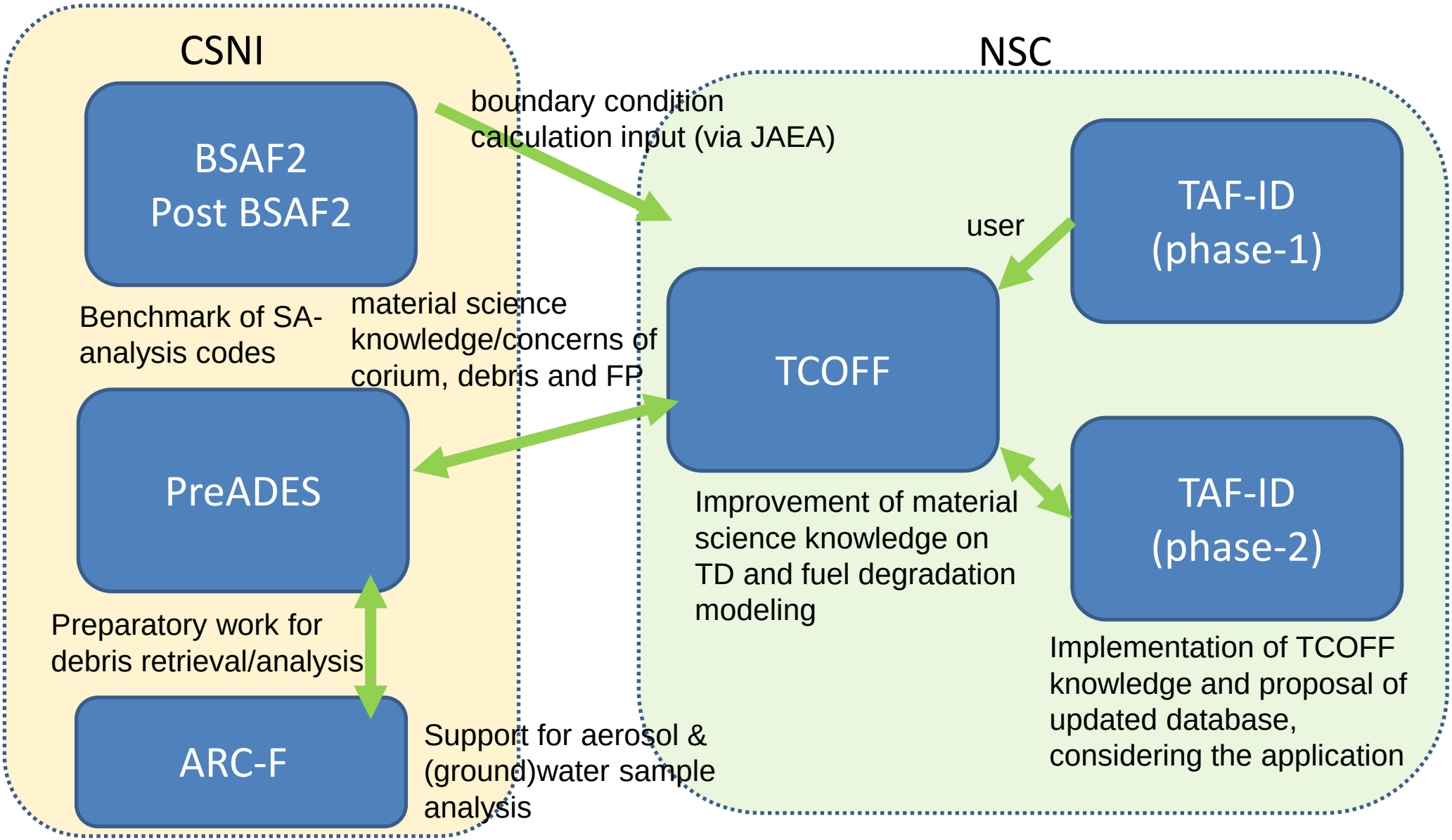
- Aix-Marseilles Univ. (IM2NP, France)
- Joint Institute for High Temperatures (Russia)

Structure and Workflow of TCOFF



Collaborative Laboratories for Advanced Decommissioning Science

Collaboration with related projects in NEA



Project work programme- progress as at July2019

Task Force Activities –Identified as major issues for improvement

TF-1: Corium and Debris

Activity-1	FP Thermodynamic database benchmark
Activity-2	U-Zr-O system (exptl. & liquefaction modelling)
Activity-3	Other extended (eg U-Zr-Fe-O (-B) (-N) or sub-systems),
Activity-4/5	Physical-chemistry of corium & MCCI (Vulcano)
Activity-6	FDNPS-issues

TF-2: Fission Products

Activity-1	Improvements of Cs (compound)-SS interactns. (in-kind)
Activity-2	Cs-complex interactions & volatility
Activity-3	FP-leaching
Activity-4	Long term impact incl. Sr, Cs, also Ba (Ru)

TF-1: Corium and Debris
U-Zr-O system (activity-2) and other sub-systems (activity-3)

In-kind contributions to TCOFF-related updates:

- Overviews of HERACLES & benchmark (PSI)
- Thermodynamic dataset from MELCOR modelling (KTH)
- Outline of improvement of Cd/In/Ag/Zr database for NIUCLEA/MEPHISTA (IRSN)
- TAF-ID extension (phase 2) (TAF-ID)
- Outline of Zircobase (CEA)
- Sim-test results on Zry oxidation and Hydrogen uptake (JAEA)
- Vapour pressure data of U-Zr-O system (SPSU)
- Experimental work on the Zr-N-O-H system (JRC-KA)
- Experimental work on the Zr-Fe-O-H system (Osaka Univ., as observer)

Discussion (IK) on improvement of fuel degradation model using TCOFF findings:

- Requirement from MELCOR standpoints (SNL)
- Review of the basic problems in thermodynamic approach (IRSN)
- Proposal of advanced simplified UO_2/Zry liquefaction model by thermodynamic approach (JAEA)

TF-1: Corium and Debris

Physical-chemistry of corium and MCCI (activity-4/5) and FDNPS-issues (activity-6)

In-kind TCOFF-related updates (Activity-4/5):

- Review of Chernobyl lava and update of leaching test (KRI)
- BWR bundle degradation test results under steam-starved conditions (JAEA)
- The influence of B on layered corium pool behaviour (NITI)
- MCCI interaction anticipated in FDNPS accident (CEA)
- Current status of thermodynamic analysis for TROI-50 and FK-1 tests (KAERI)

In-kind TCOFF-related updates (Activity-6):

- Proposal on measurement of aerosol particles generated from sim-MCCI sample cutting (CEA)
- Detailed evaluation on corium relocation in Unit-2 and Unit-3 (JAEA)

TF-2: FPs

<u>In-kind</u> contributions and TCOFF-related updates on Cs-steel interaction (activity-3) and Cs-complex (activity-4):

- FP release model from molten corium (IBRAE)
- Research activities related to FDNPS decommissioning (JAEA)
- Proposal of benchmark regarding FP-database (NEA)

Discussion on improvement of thermodynamic data of Cs-complex:

➔ TCOFF will focus on Cs-Mo-O, Cs-Fe-O, Cs-B-O, Cs-Si-O and Cs-Cr-O, including the influence to I-chemistry.

<u>In-kind</u> FP-leaching (activity-3) and long term impact (activity-4):

- R&D plan on secondary source term via aqueous phase from MCCI-debris (Tohoku Univ., as observer)
- Discussion on details of experimental method, tabulation manner of thermodynamic data and prototypic modelling

TCOFF R&D Call for Proposals

Following proposals were selected for funding and R&Ds are ongoing (2018):

- **NITI:** Phase equilibria in the U-Zr-O and U-Zr-Fe-O systems;
- **TUDelft:** Experimental studies of the Ba-Sr-Cs-Mo-O system;
- **SPSU:** Vaporization and thermodynamics of Cs-bearing compounds in the Cs-Si-O, Cs-B-O, Cs-Mo-O, Cs-Cr-O, Cs-Fe-O systems;
- **KRI:** Water leaching tests of radionuclides from matrices of aged Chernobyl “lava” and corium;
- **TITECH:** Thermodynamics of Cs and Si compounds.

Nomination process in 2019:

- Nomination of TCOFF technical committee (Jul. 2018)
- Proposal to TCOFF technical committee (Sep. 2018)
- Prioritization of proposals in technical committee (Nov. 2018)
- Selection (Jan. 2019, @4th meeting)

➔ **Currently, MG considering NITI, KRI, TITECH and JIHT for proposals in 2019.**

Status of TCOFF R & D Activities (in-kind & from 2 calls for proposals) (at July8-9th Meeting):

- Modelling
  - Current results of the fission products benchmark (TITECH)
- Experimental & Measurements
  - Testing for phase equilibria in the corium U-Zr-Fe-O-B-C system (NITI)

In-kind activity

  - Physical chemistry of long term fission product phases of Ba-Sr-Cs-Mo-O system (TUDelft)

IK + Call-Prop

  - Leaching of radionuclides from matrices of aged Chernobyl “lava” and corium: (KRI)

Calls for Proposals

  - KEMS, time-of-flight MS combined with laser heating measurements on ZrO2 and Fe-Zr-O systems (JIHT)
  - Solution calorimetry of Cs polymolybdates formation enthalpies (IM2NP)

TCOFF Activities
– selected results, in-kind & calls for proposals

Collaborative Laboratories for Advanced Decommission

Benchmark of Thermodynamic Databases (TF-1/A-1) –Main Reactor zones

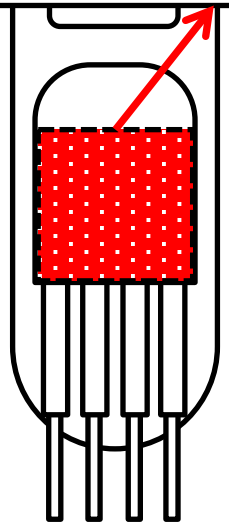
Objective

To identify high priority R&D issues for efficient improvement of thermodynamic databases and of material science knowledge (experiment, model, etc.).
TAF-ID (NEA/NSC/TAF-ID project), NUCLEA (IRSN), HERACLES (PSI)

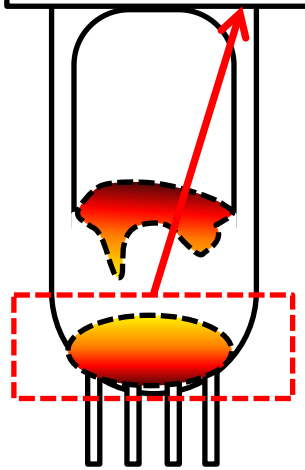
In-vessel

U-Zr-Fe-[Ni-Cr]-O-B-C

① Average composition of "Core"



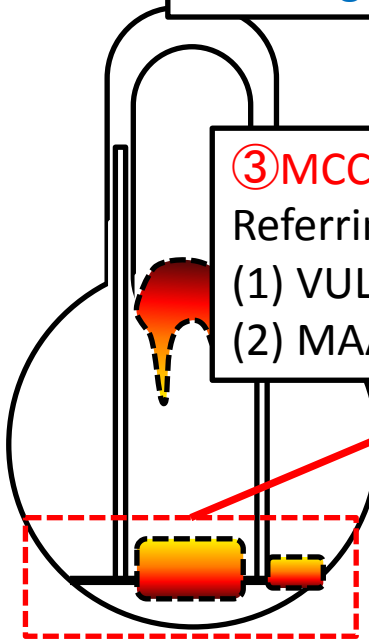
② Lower plenum referring to MAAP result for unit1 (BSAF)



Ex-vessel

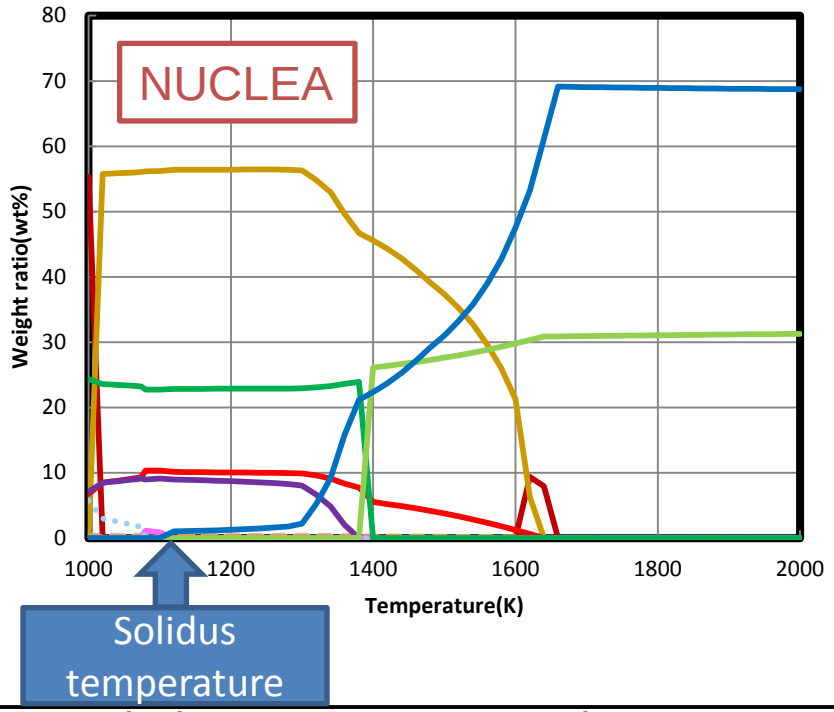
U-Zr-Fe-[Ni-Cr]-O-B-C (corium)
Si-Ca-Mg-Al-Fe-O (concrete)

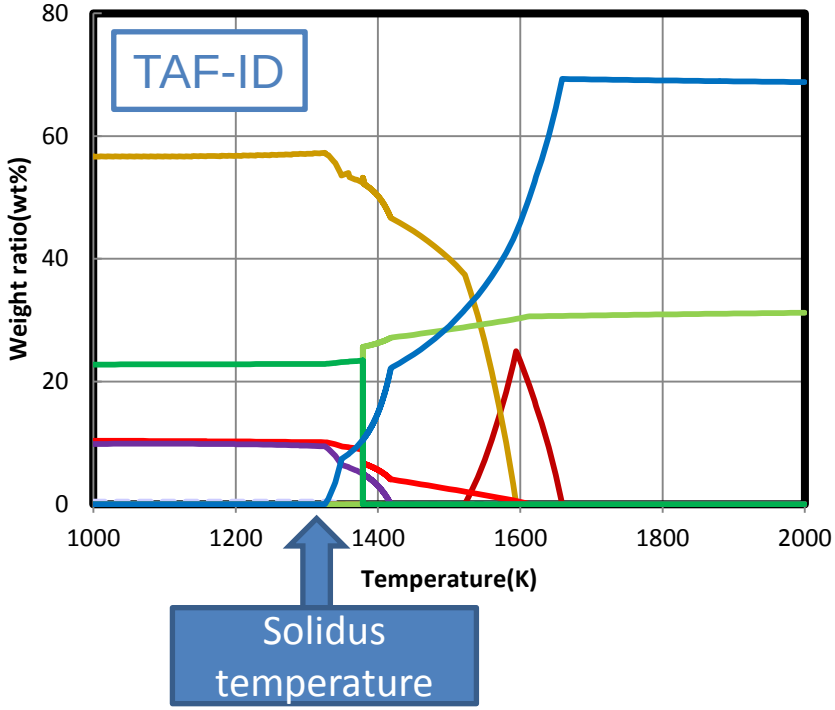
③MCCI
Referring to
(1) VULCANO test result
(2) MAAP result for unit1



TAF-ID kindly allows the free use of TAF-ID database on TCOFF objectives (by NEA technical staff).
IRSN kindly allows, as its in-kind contribution, to TCOFF-members the free use of NUCLEA Toolbox on TCOFF objectives (NRC/SNL, KTH, and KAERI are using it for their in-kind contributions).

TF-1:Thermodynamic database benchmark (Act-1) FDNPS (MAAP) MCCI





②Solidus Temperature：NUCLEA→1079K, TAF-ID→1326K→TAF-ID
(Ni-Zr compound was not formed in the TAF-ID case

Hiroshi Ogi

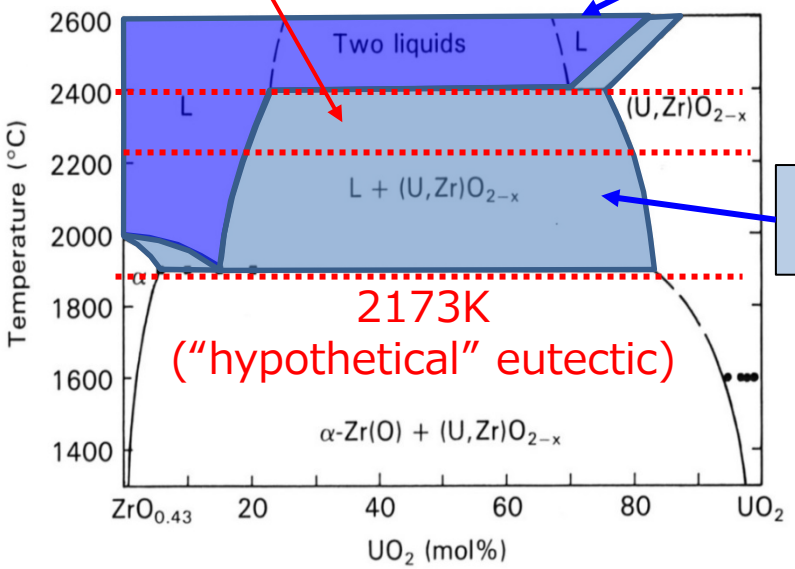
U-Zr-O base system (TF-1/A-2)

Proper simplification of UO_2/Zry liquefaction by TD approach

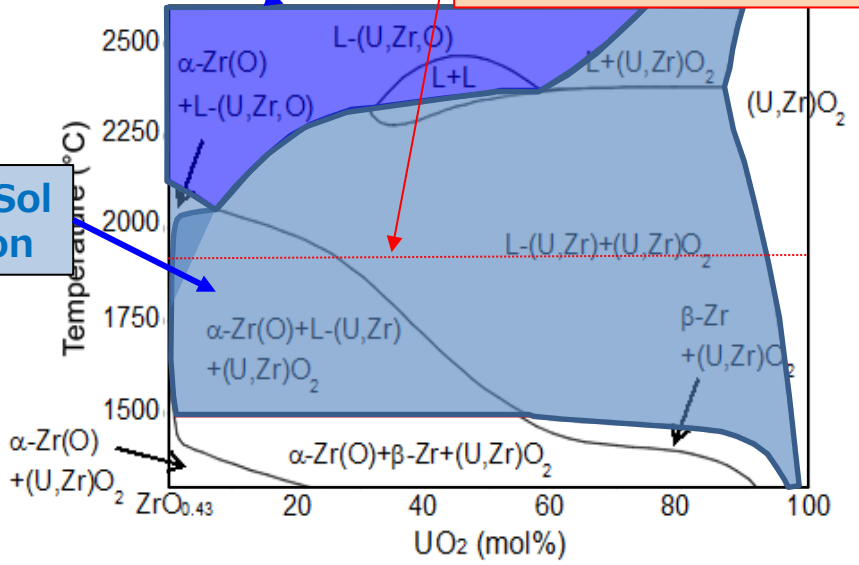
~2500K
("magic" eutectic)

Liquid region

Question: what happen in temperatures between "hypothetical" eutectic and "magic" eutectic?



Liq/Sol region



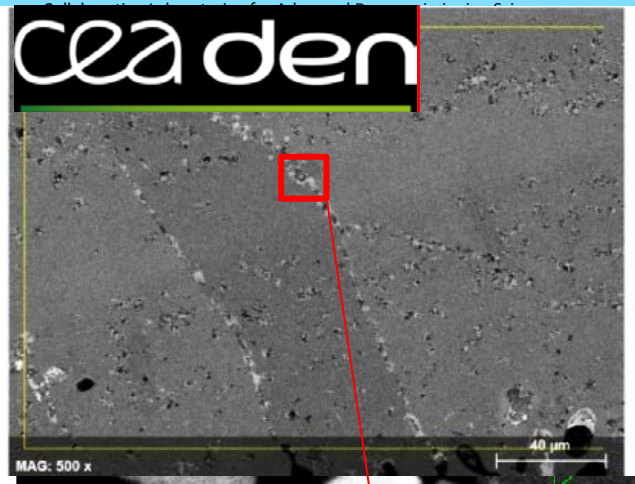
"Previously utilized" phase diagram

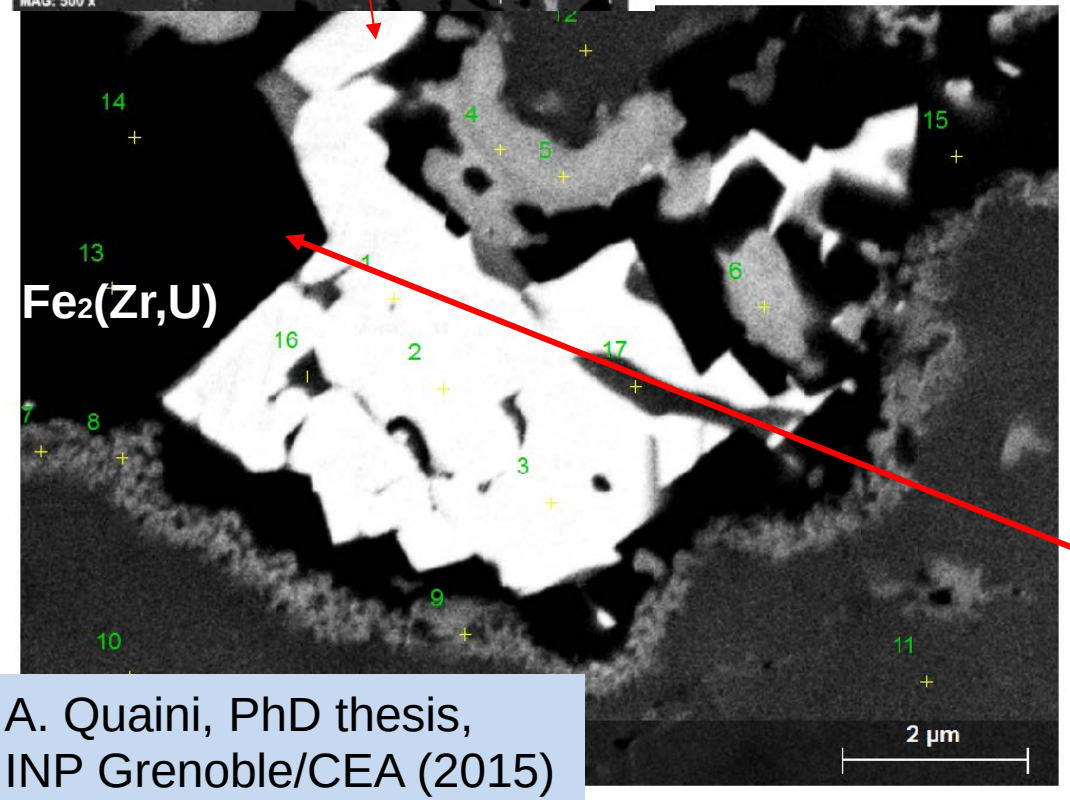
"Theoretically true" phase diagram

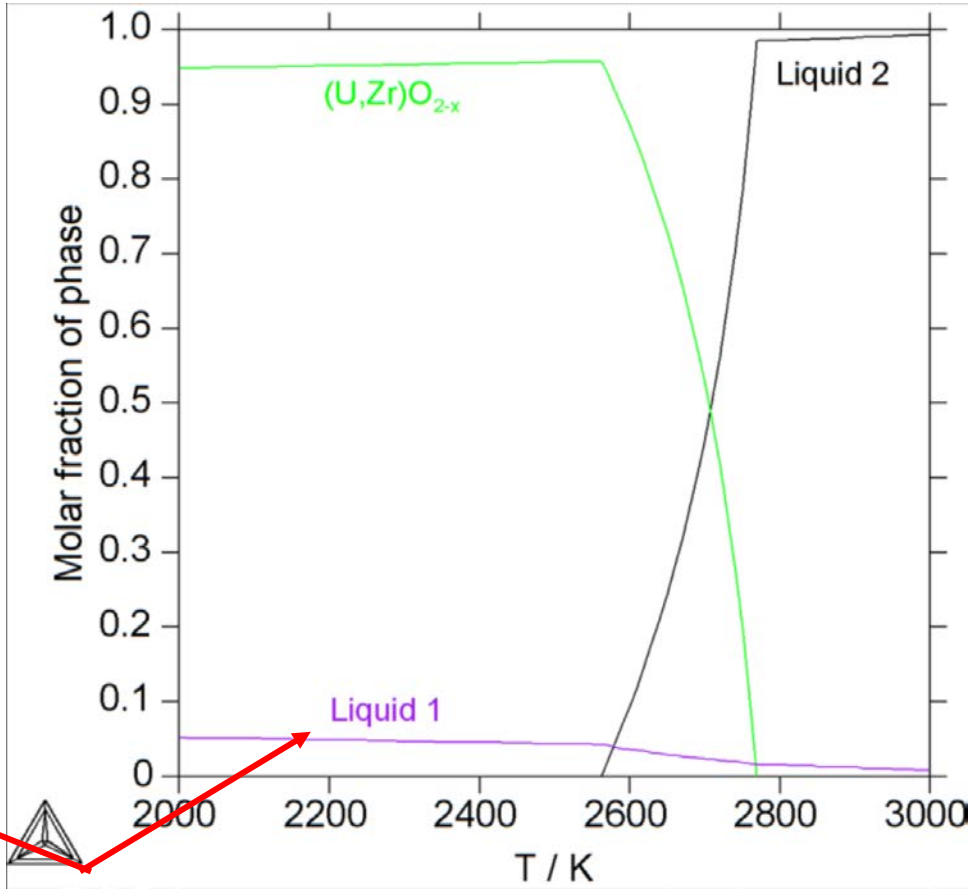
- Previous quasi-binary UO_2-$ZrO_{0.43}$ phase diagram was drawn by *binary phase rule* and then **"hypothetical" eutectic (2173K)** was identified and implemented in SA-analysis codes.
- Then, for better fitting to observation in Phebus and other sim-tests, a **"magic" eutectic (~2500K)** was currently implemented without sufficient theoretical background.
- But, phase boundaries of U-Zr-O should be drawn *by ternary phase rule*. In theoretically true phase diagram, wider liq/sol mixture region must play important roles.

TF-1: Corium and Debris (Activity 2)

U-Zr-O system- exptl. & liquefaction modelling







Liquid 1 ($Fe_{0.432}U_{0.247}Zr_{0.306}O_{0.015}$) relocates to the grain boundaries

A. Quaini, PhD thesis, INP Grenoble/CEA (2015)

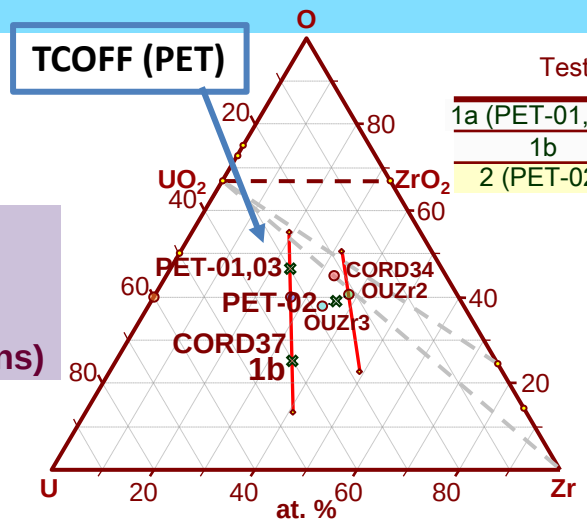
NITI - International Call Proposal 2018

Collaborative Laboratories for Advanced Decommissioning Science

Tests to understand the physical chemistry of key corium systems U-Zr-O and U-Zr-Fe-O

U-Zr-O system

CORPHAD and CEA tests vs TCOFF tests (impact of IMCC conditions)



Test matrix

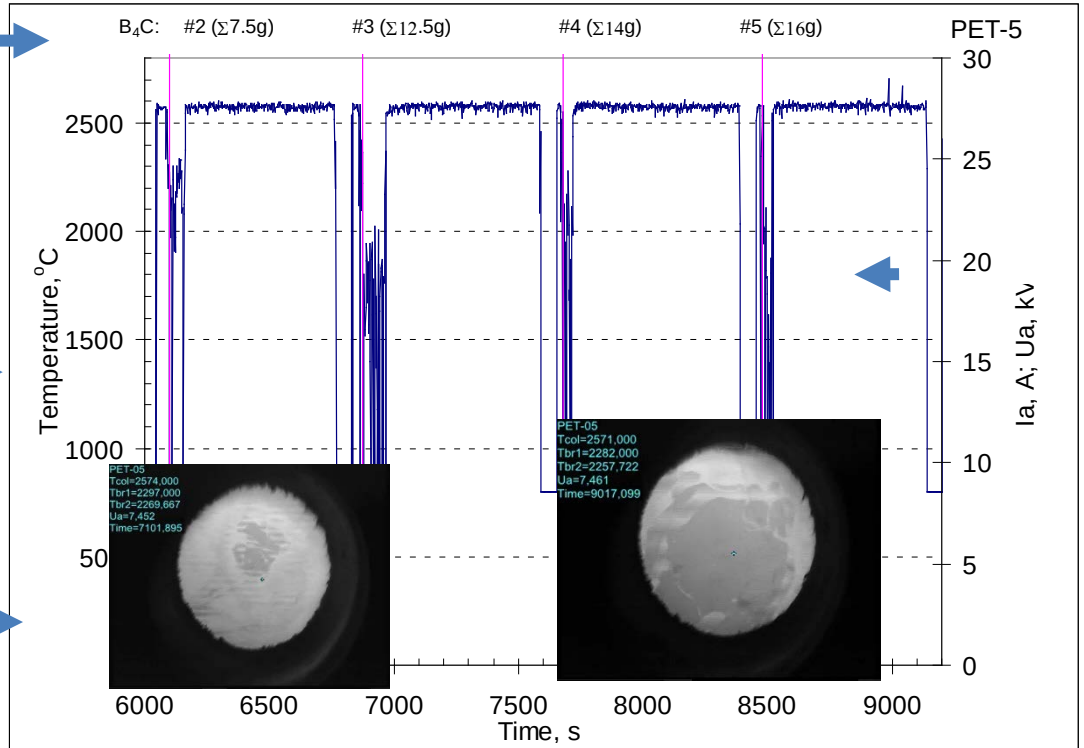
Test	Charge composition, at. %		
	U	Zr	O
1a (PET-01,03)	30.0	23.0	47.0
1b	40.0	34.0	26.0
2 (PET-02)	25.0	36.0	39.0

A. Quaini, C. Gueneau, S. Gosse, N. Dupin, B. Sundman, E. Brackx, R. Domenger, M. Kurata, F. Hodaj. **Contribution to the thermodynamic description of the corium – The U-Zr-O system** // JNM. 2018. V. 501. P. 104–131

Additions of B_4C to melt

Temperature (from pyrometer)

View of melt from Pyrometric camera



Additions of B4C resulted in metal layer meovement

Alexandrov RIT (NITI)

ROSATOM

TF1: Activity-3 Other extended (eg U-Zr-Fe-O (-B) (-N) or sub-systems)

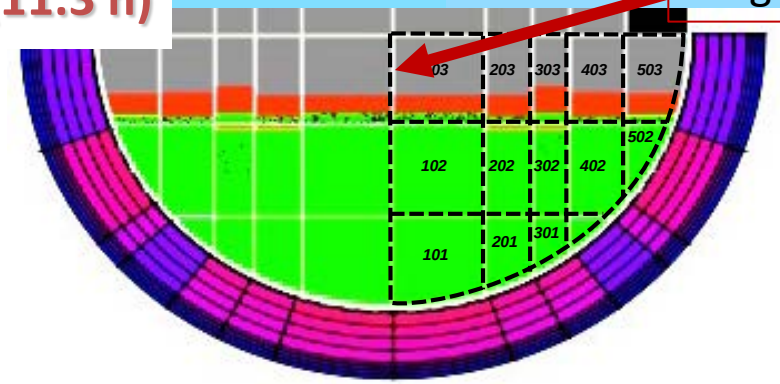
Thermodynamic assessment of corium composition (11.3 h)

MELCOR
output data (Ring 103):

Components	Mass, kg	
	PD	MM
UO_2	1192	-
Zr	6	-
ZrO_2	369	-
SS	-	2334
SS oxide	-	-
B_4C	0.0055	-
Inconel	-	45
Temperature, K	1967	1844

NUCLEA
input data (Ring 103):

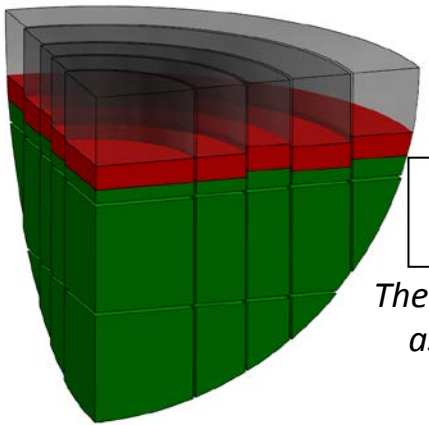
Element	Mass, kg	Temperature, K
U	1051	1873 *(Determined by mixing masses and enthalpies of relocates predicted by MELCOR)*
Zr	280	
O	242	
Fe	1741	
Cr	450	
Ni	308	
B	0.0043	
C	0.0012	



Metallic molten pool (MM)

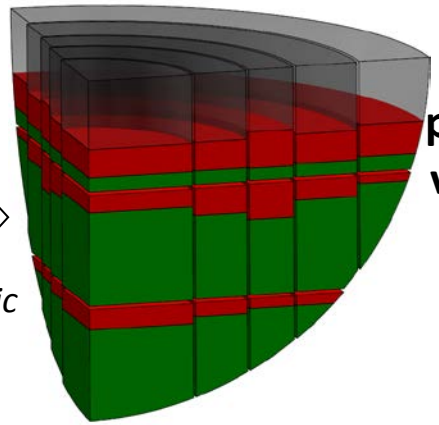
Particulate debris (PD)

MELCOR results



Thermodynamic assessment

NUCLEA results



Thermodynamic assessment of corium composition was performed for each ring

Results are presented as schematic of metallic molten pool and solid particulate debris volume fractions in ¼ of reactor lower head (RPV is not shown)

ROYAL INSTITUTE OF TECHNOLOGY

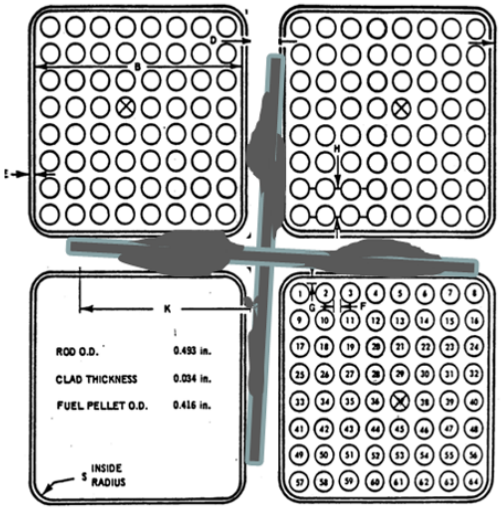
Strål säkerhets myndigheten
Swedish Radiation Safety Authority

NPS Kärnkraftsäkerhet

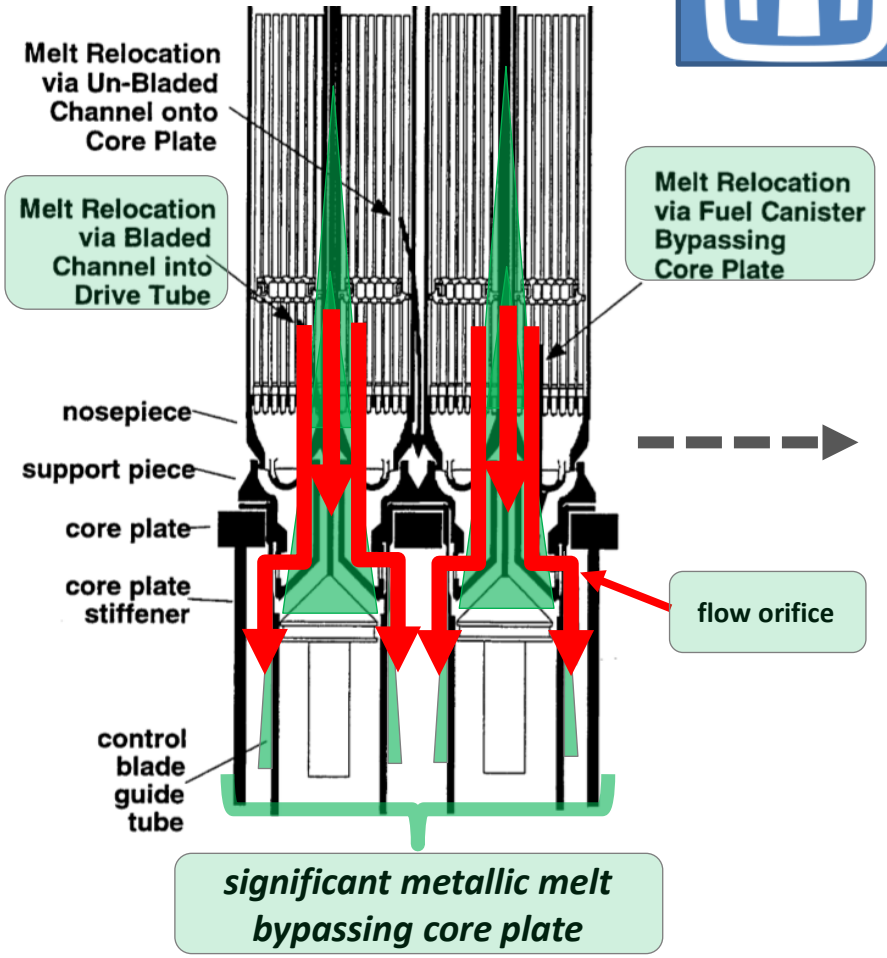
Attack of Channel Box (Zr) by Liquefied Blade Material (SS/B_4C)

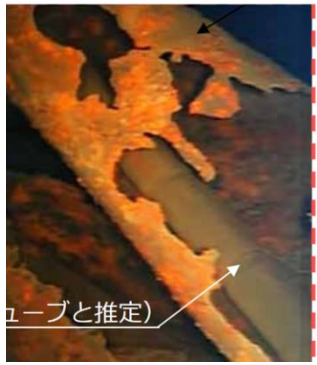
DF-4 BWR Experiment in ACRR (SNL)





- UO_2/Zr(O) liquefactions → ~2400K
- B_4C/SS liquefactions → ~1500K
- B_4C/SS/Zr liquefactions → ~1200K to 150C





MELCOR Modelling Improvement (SNL) - Examination of BWR Channel box structure, degradation & passages for debris to lower vessel head

1.Benchmark:Step-1 (Result : Mo-O-H steam rich, gas/liq/sol)

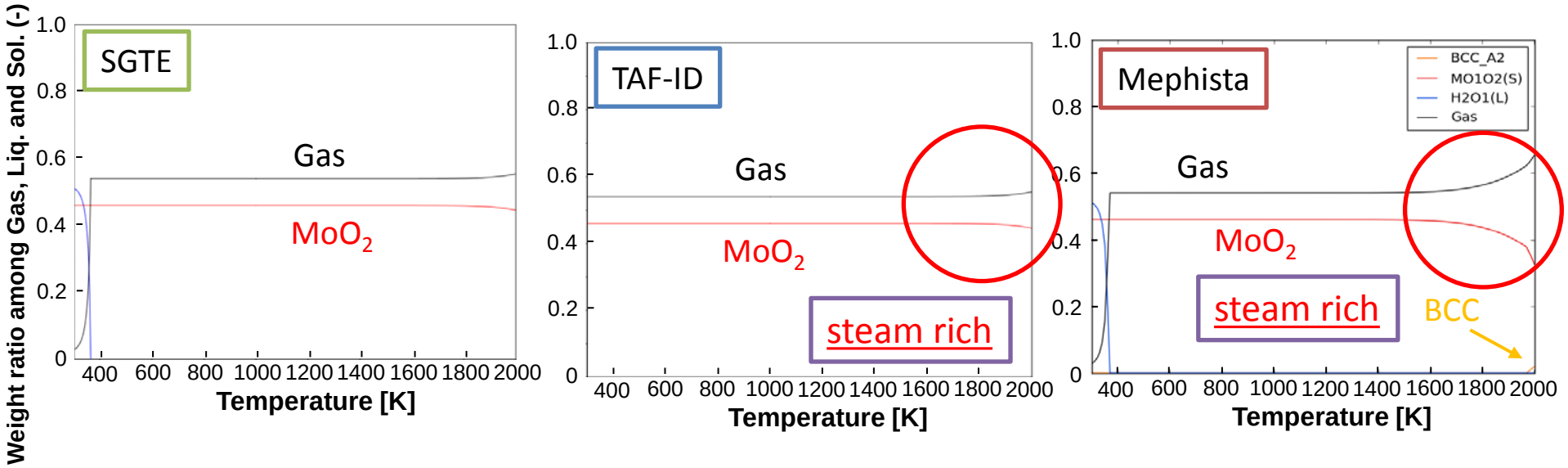
Pressure

1.0 atm.

Temperature

300-2000 K

	(Cs, Mo, I, B, Si)	H_2	H_2O
Case 1 (Mo-O-H)	0.1	0.1 (steam rich)	1



- Solid-MoO_2 appeared in each database. However, the vaporization tendency (temperature and weight ratio) of solid-MoO_2 were slightly different from each other.

TF2: Activity-2 –Fission product Thermo-dynamic Data SrO-MoO_3 from Knudsen Cell –Mass Spec.

Collaborative Laboratories for Advanced Decommissionin

- ***Content of vapor:***

  $SrMoO_4$,

  $SrMoO_3$ (?, T=2150 K)

- Temperature range:

  1570-1738 K

- Thermodynamic functions:

  p_i, $\Delta H_{s,0}$, $\Delta H_{f,0}$

$SrMoO_3(g) + 2Sr(g) \rightarrow 3SrO(g) + Mo(s)$,

$SrMoO_3(g) + 3MoO_2(g) \rightarrow 3MoO_3(g) + Sr(g) + Mo(s)$,

$SrMoO_4(g) + 3Sr(g) \rightarrow 4SrO(g) + Mo(s)$,

$SrMoO_4(g) + 4MoO_2(g) \rightarrow 4MoO_3(g) + Sr(g) + Mo(s)$.

Dissociation energy of strontium molybdates into gaseous oxides and atomization energy

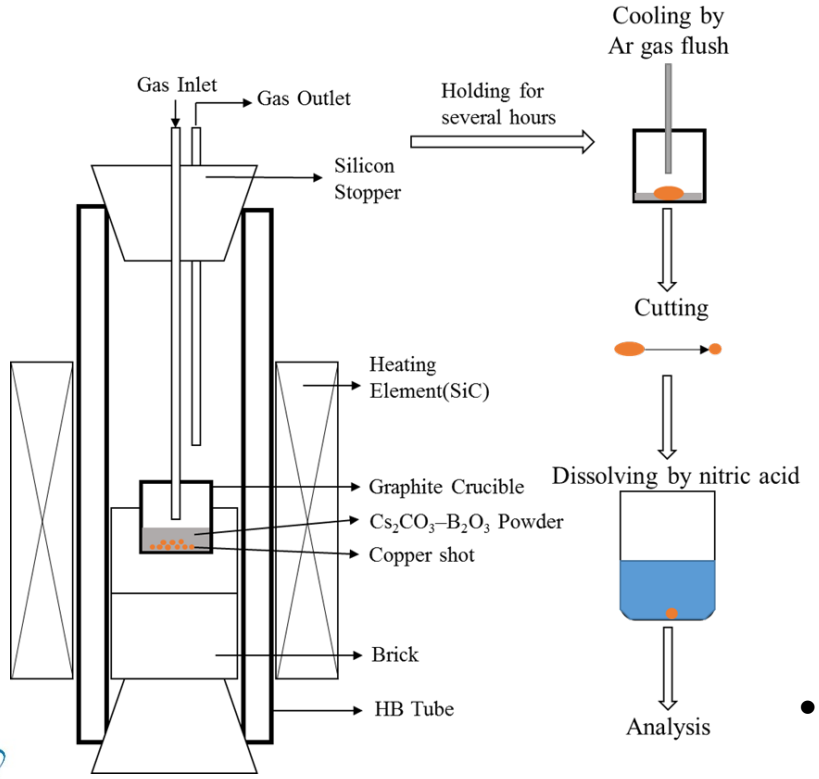
Molecule	$\Delta H°_0$, KJ/mol	$D°$(SrO-$MoO_{2,3}$), kJ/mol	Proposed value, kJ/mol	Atomization energy, eV
$SrMoO_3$	237 ± 8	655	657 ± 63	22.3 ± 1.0
	-359 ± 12	655		
$SrMoO_4$	510 ± 17	731	741 ± 63	30.0 ± 1.0
	-261 ± 13	753		

St. Petersburg University,
www.spbu.ru

TF2: Activity-2 –Chem.Equilib. Technique for TD data of Cs-Si-compounds

TITECH

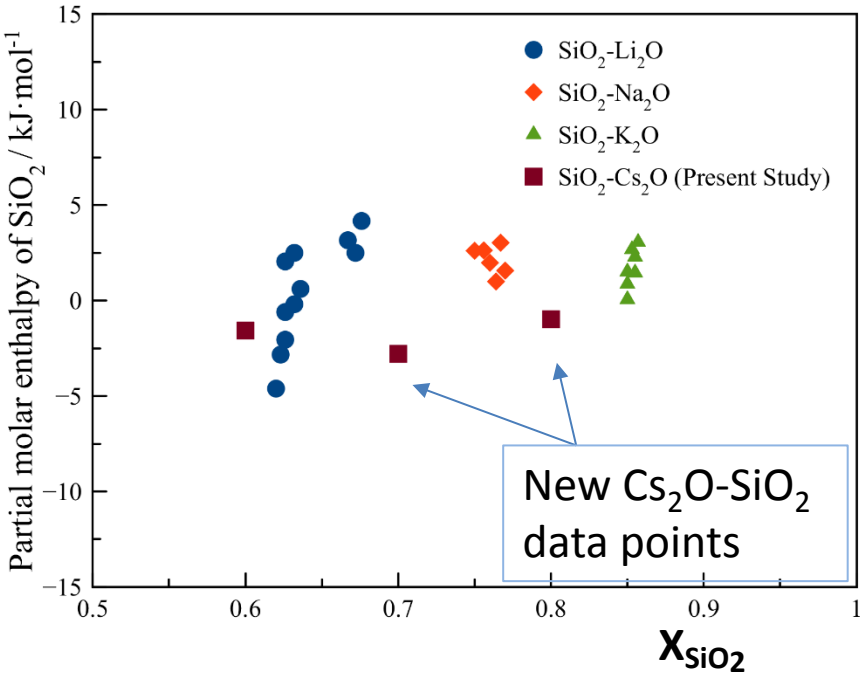
Furnace for preparation of compounds (Cs_2O-B_2O_3-Cu for B_2O_3 activity) or Cs_2O-SiO_2-Cu for Cs_2O activity in Cu)



Analysis by ICP-OES, AA & ICP-MS

Partial Molar Enthalpy of SiO_2 in Binary Alkali-Silica System

Cs-Si-O



- It can be shown that in SiO_2-Cs_2O system, $\Delta\bar{H}_{SiO_2}$ values are more negative than other alkali-metal silicate system from Morishita et al.[1] at 1663 K.

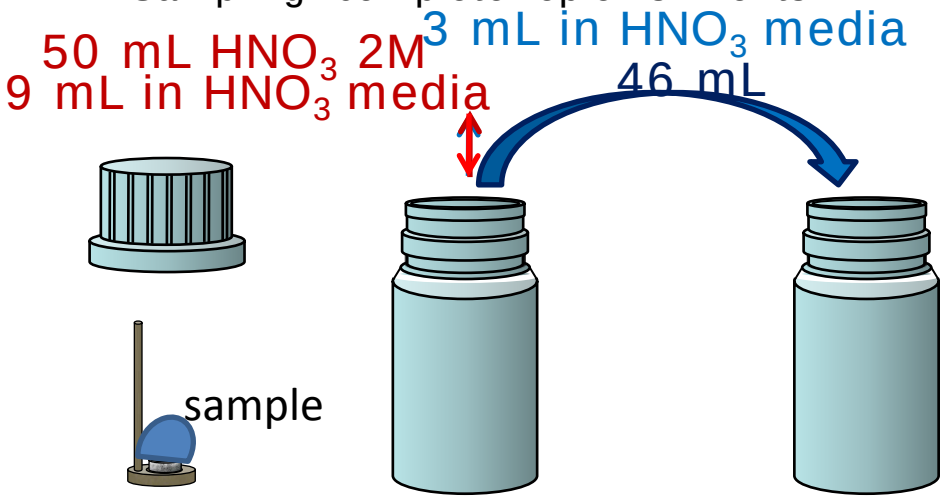
[1] M. Morishita, A. Navrotsky, M.C. Wilding, "Direct Measurement of Relative Partial Molar Enthalpy of SiO_2 in SiO_2-M_2O (M=Li, Na, K, Cs) Binary and SiO_2-CaO-Al_2O_3 Ternary Melts", J. Am. Ceram. Soc., 87 [8] 1550-1555 (2004)

Collaborative Laboratories for Advanced Decommissioning Science

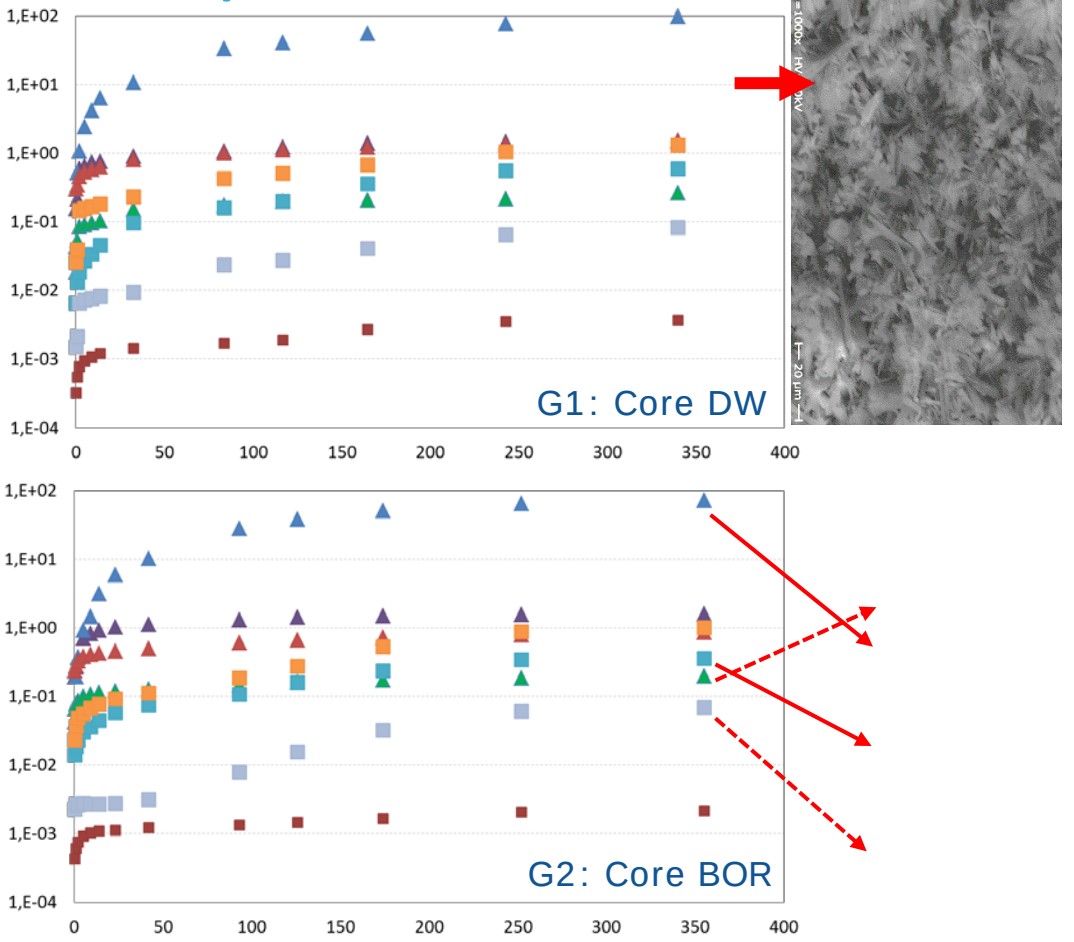
TF2: Activity-3 –Leach Testing

Leach Testing of TMI-2 core & agglomerate samples

- Gas phase: air, oxidising condition
- Volume: 50±1 mL
- Temp: 25±5 °C
- Duration: 350 days
- PE-bottles with Pt-wire sample holder
- Sampling: complete replenishments



Cumulative FIAP (%) vs time



$$CumFIAP_i = \frac{m_{i,aq}}{SS \times m_{SNF} \times H_i}$$

CRIEPI Central Research Institute of Electric Power Industry

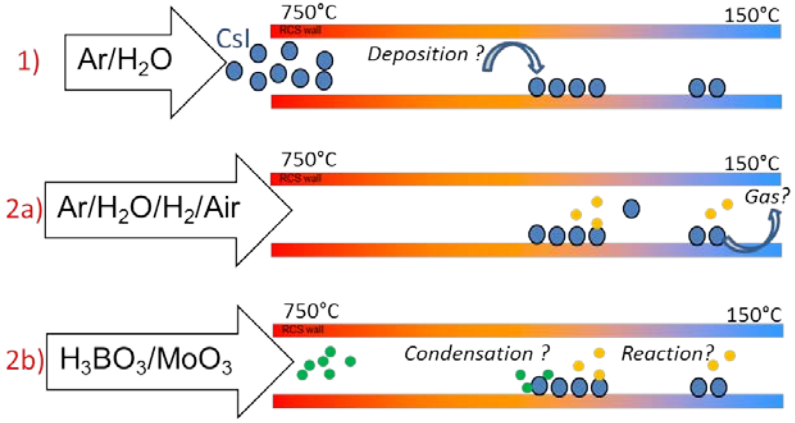
European Commission

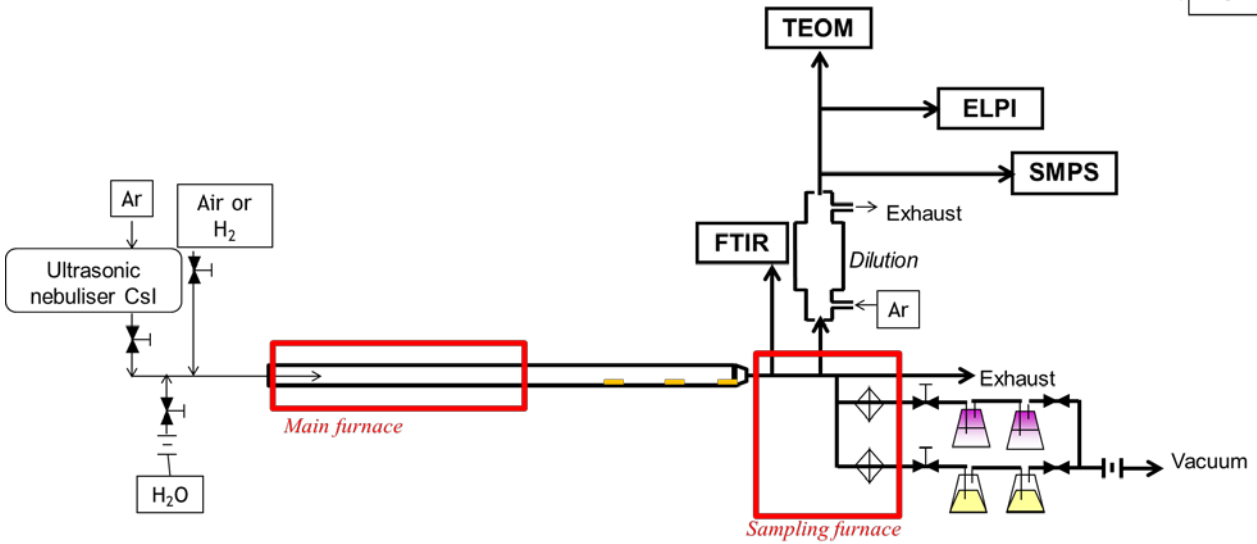
TF2: Activity-4 –FP's of LT Radiological impact

Key phenomena studied at VTT Oy.: Iodine behaviour in the primary circuit

- FP release from primary circuit surfaces (*Academy of Finland project - Collaboration with JAEA & IRSN*)

→ to **verify** the reactions on condensed phase from deposited aerosols and **revaporisation** effects by changing the carrier gas composition and flow rate;
→ Reproductive test of FP release and transport **(Cs-I-B-H-O system)** at JAEA and VTT;
→ Analysis with **SOPHAEROS,** module of the ASTEC code at IRSN.





2nd International TCOFF workshop (10-12, July, 2019)

- **CEA** and **NEA** assisted with the organisation of the 2nd TCOFF-related international workshop (10-12 July, 2019, Joban Hawaiian Center and J-village, Fukushima, Japan), which was co-hosted by **JAEA/CLADS** as **FRC** (Fukushima Research Conference)

• 'Materials Science for Severe Accident & Fukushima-Daiichi Decommissioning'.

- Over 130 representatives from 21 countries (research and academic institutes, fuel vendors, utilities, so on), 29 oral + 43 posters.

Sessions

- Session1: SA-code, accident analysis of FDNPS, individual models
- Session2: High temperature experiments (integral, separate effect, fundamentals)
- Session3: Thermodynamic database
- Session4: Accident Tolerant Fuel
- Panel: Role of this community/occasion, synergy to be developed between thermodynamics and severe accident codes, uncertainties propagation, synergy between SA and ATF R&Ds, expectation for TCOFF phase2

Collaboration between TCOFF and PreADES/ARC-F

- **TCOFF/PreADES**
  - Collaborative analysis/evaluation of FDNPS-samples (especially Ubearing particles) → to be carried out under the frame of PreADES
  - Remarks form TCOFF to PreADES by material science standpoints for 'property table of re-criticality' → CRIEPI leading this topic.
- **TCOFF/ARC-F**
  - Delivery of thermodynamic data regarding Cs-complex with remarks from TCOFF expertise, i.e. influence of updated data to volatile-FP behaviour.

❖ Treatment of IP (discussed in the last TCOFF-MB): TCOFF final report will be disclosed to PreADES and ARC-F. As for TCOFF R&D call reports, they will be disclosed after the publication by academic contributors (within one year, a guideline)

TCOFF: Timeline in Last Year

- 18 organisations from 10 NEA member countries, plus the EC.
- Two times TCOFF-MB meeting; July 8-9 and Feb. 5-7, 2020 (under discussion, last meeting)
- TCOFF co-organized workshop; July 10-12 @J-village, Fukushima, Japan
- TCOFF last workshop: in 2020 (where?)
- TCOFF report:
  - Outline was agreed and authors were nominated in July meeting
  - Section titles to be fixed by end July
  - Format to be distributed by mid Aug.
  - Skype meeting
  - First draft will be distributed by end Nov.
  - Draft will be reviewed in the last meeti

Already delayed!

Collaborative Laboratories for Advanced Decommissioning Science

Future Plan (addressed in preliminary meeting)

OECD Nuclear Energy Agency

Task 1: Contribution to decommissioning of FDNPS

Debris characterization using TCOFF phase-1 knowledge, review of previous knowledge by TD approach (*i.e.,* TMI-2, Chernobyl, integral sim-tests (in-pile, out of pile), separate effects tests etc., thermodynamic interpretation of mechanisms (including chemical condition) of debris formation and FP-behavior in FDNPS conditions using FDNPS sample data (reverse analysis approach), collaboration with ARC-F and PreADES

Task 2: Contribution to model behavior of conventional UO2/Zry and other materials interactions, including ATF-fuel/cladding

Improvement of individual models on accident progression, core degradation and source term (*e.g.,* fuel liquefaction progression, U-Zr-O melt/SS interaction, influence of FP-chemical forms and so on), suitable simplification of the individual models for the implementation into SA-analysis codes and the application to ATF

Task 3: Improvement of materials science knowledge regarding severe accident

Discussion on chemical equilibrium approach (as extended approach), including reaction kinetics, diffusion, local quasi-equilibrium, influence of boundary conditions etc. , efficient continuation of TD database improvement, Identification of collaborative experimental study for concrete requirements and training course on how to use thermodynamic knowledge and collaborative workshops.

Task 4: Leaching Discussion on secondary source term and irretrievability, performance assessment by TD approach and influence of volatile FP-behavior before and after leaching

Collaborative Laboratories for Advanced Decommissioning Science

Expected Timeline for TCOFF phase 2

OECD BETTER POLICIES FOR BETTER LIVES

Nuclear Energy Agency

NEA NUCLEAR ENERGY AGENCY

Preliminary discussion among potential participants by Feb. 2020 (before the last TCOFF meeting)

- Tasks, framework (under NSC or both of NSC/CSNI), funding + in-kind, relation with other NEA projects and so on

- Preparation of a few page draft (to be distributed to reach consensus)

✓ Introduction of TCOFF phase 2 in NSC meeting in June 2020

✓ A kick-off workshop among TCOFF phase 2 participants in July 2020

✓ Considerable duration of TCOFF phase 2: July 2020 – June 2023

CONCLUDING REMARKS

1) TCOFF project identified important issues in thermodynamic data or modelling for understanding severe accident progression.

1) It has successfully launched a series of investigations to tackle problem areas through a wide range of techniques carried out by its members.

2) It has also carried out further studies in these areas by means of a yearly call for proposals; this has enabled new samples, new techniques to be used for improved measurements or data that is difficult to access.

3) In the coming 6 months the final reports will be drafted to crystallise the advances made and the future research necessary.

4) On the basis of this report and the TCOFF-related workshops, a preliminary proposal on post-TCOFF is being discussed.

Thank you for your attention !!

25. International QUENCH Workshop, 22-24 Oct 2019, KIT, Karlsruhe, Germany

Update of the QUENCH program

Martin Steinbrück, Juri Stuckert, Mirco Große et al.

The main objective of the QUENCH program at KIT is the investigation of the hydrogen source term and materials interactions during LOCA and the early phase of severe accidents including reflood. Bundle experiments as well as separate-effects tests are conducted to provide data for the development of models and the validation of severe fuel damage code systems.

The QUENCH bundle facility is a unique out-of-pile bundle facility with electrically heated fuel rod simulators and extensive instrumentation. So far, 20 experiments with various severe accident (SA) scenarios as well as a series of seven DBA LOCA experiments were conducted. The QUENCH-LOCA series was completed in 2016. One of the main results is the definition of the conditions for secondary hydriding around the burst position and its influence on the mechanical properties of the cladding rods.

The last SA test QUENCH-20 planned in the framework of the EC SAFEST project and proposed by SSM was conducted in October 2019, just two weeks before the QWS. It was the first experiments in the QUENCH facility with BWR geometry including boron carbide absorber cross, channel box and water cross ring. First results of this test were presented by J. Stuckert.

Separate-effects tests during 2019 were focused on the high-temperature behavior of various ATF cladding candidates. Many of these experiments were done in the framework of the EC ILTROVATORE and IAEA ACTOF programs.

QUENCH bundle tests are part of the validation matrices of most SFD code systems which was also reflected during the session “Modelling and code validation”.

Finally, the status of reporting and publishing as well as the numerous national and international cooperations were briefly described and acknowledged.


operation with
the I national
Ato ergy Agency

Karlsruhe Institute of Technology

Institute for Applied Materials

Update of the QUENCH Program

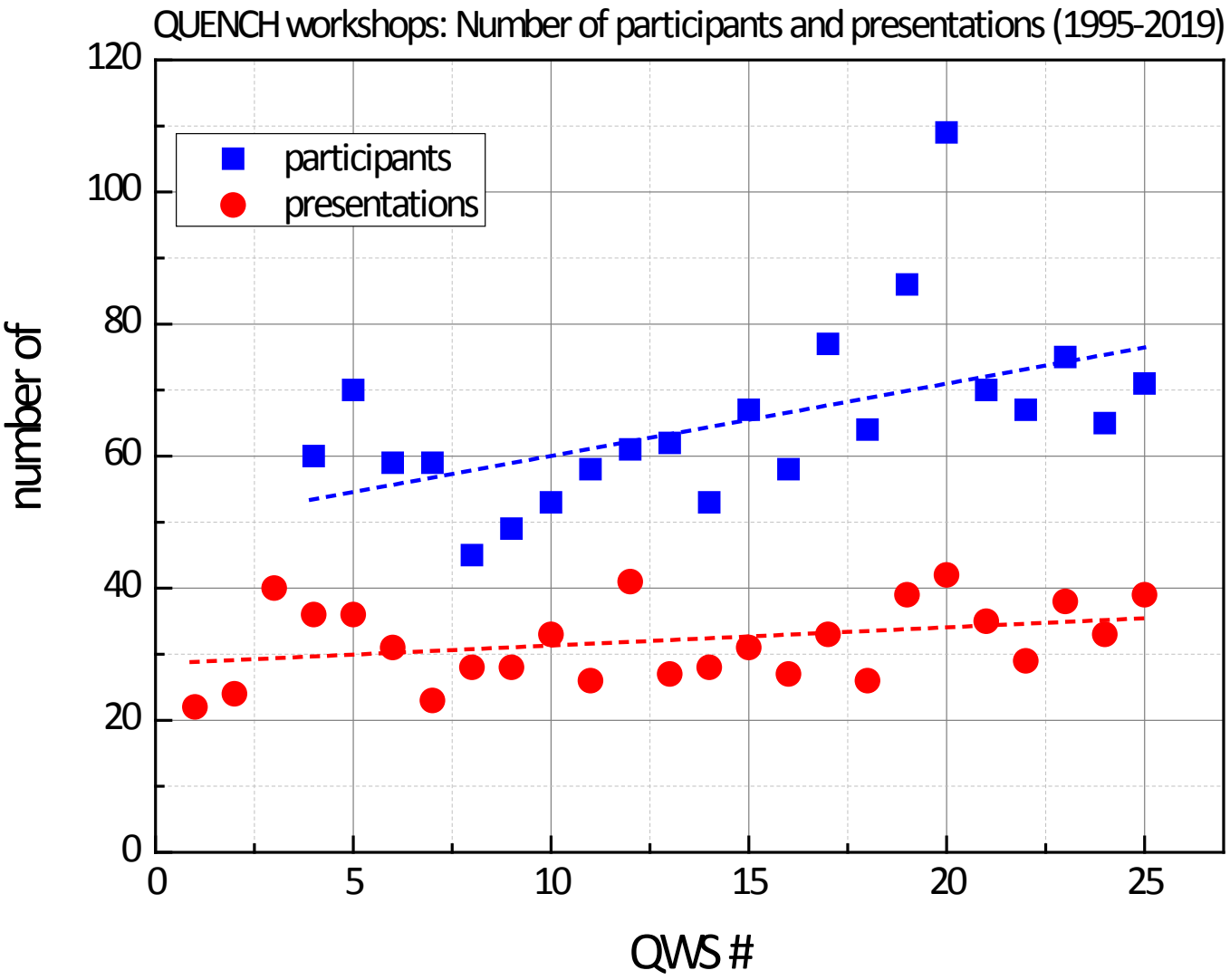
M. Steinbrück, J. Stuckert, M. Große et al.

25th International QUENCH Workshop, Karlsruhe, 22-24 October 2019

Institute for Applied Materials, Programme NUSAFE

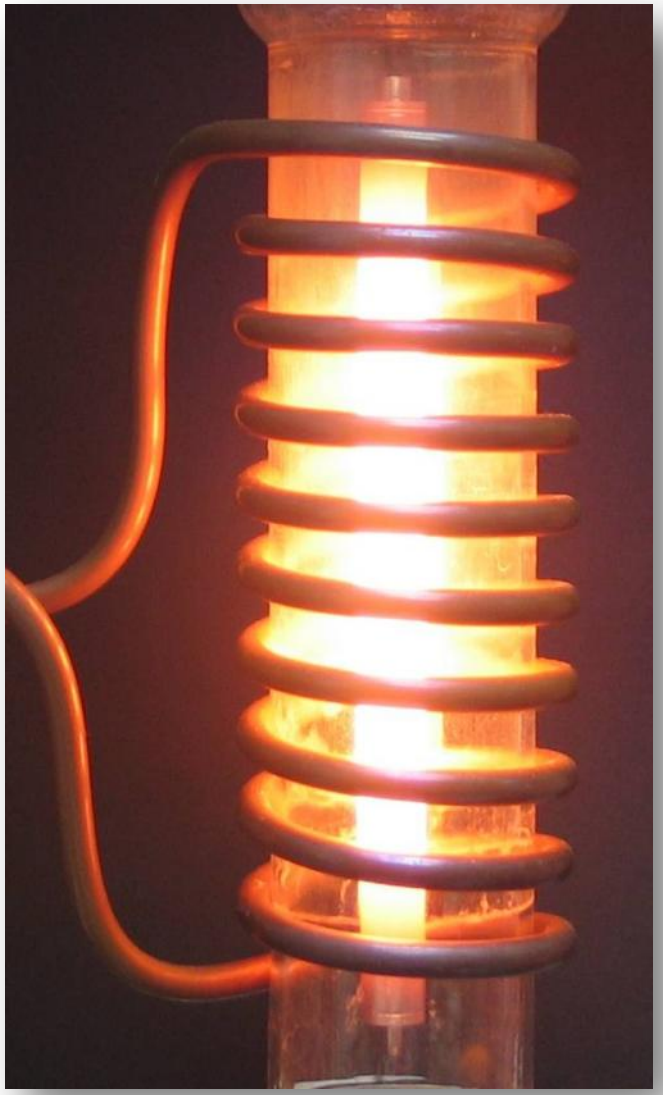


QWS statistics 1995-2019



Outlook

- Motivation
- Bundle experiments
- Separate-effects tests
- ATF activities
- Modelling / Code validation
- Future planning



Motivation

- Reflood is a prime accident management measure to terminate a nuclear accident
- Reflood may cause temperature excursion connected with increased hydrogen and FP release (severe accidents) and embrittlement of cladding and secondary hydriding (LOCA)
- Coolability of a degraded core is a matter of high priority (Fukushima)
- QUENCH experiments (bundle+SET) provide data for development of models and validation of SFD code systems

QUENCH Programme

Investigation of hydrogen source term and materials interactions during LOCA and early phase of severe accidents including reflood



Separate-effects tests

Modelling → CODES → Application

Validation



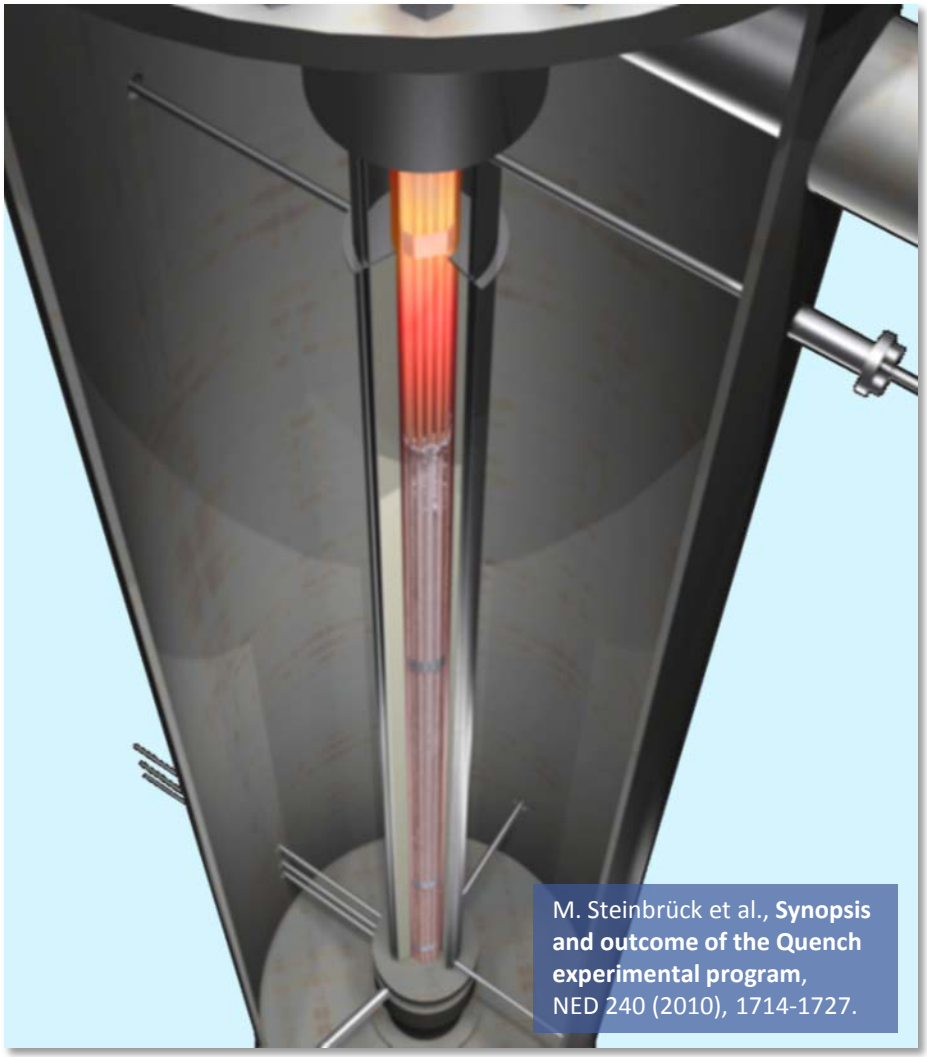
Bundle experiments



PWR fuel element

QUENCH facility

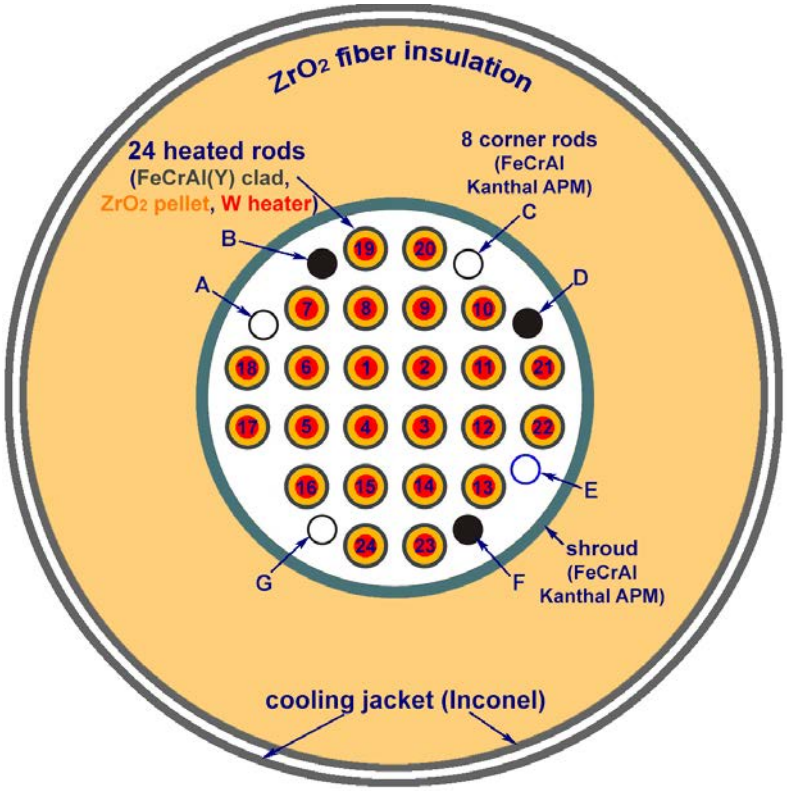
- Unique out-of-pile bundle facility to investigate reflood of an overheated reactor core
- 21-31 electrically heated fuel rod simulators; T up to >2000°C
- Extensive instrumentation for T, p, flow rates, level, etc. + MS
- So far, 20 experiments on SA performed (1996-today)
  - Influence of pre-oxidation, initial temperature, flooding rate
  - B_4C, Ag-In-Cd control rods
  - Air ingress; debris formation
  - Advanced cladding alloys
- 7 DBA LOCA experiments with separately pressurized fuel rods



M. Steinbrück et al., **Synopsis and outcome of the Quench experimental program**, NED 240 (2010), 1714-1727.

QUENCH-19

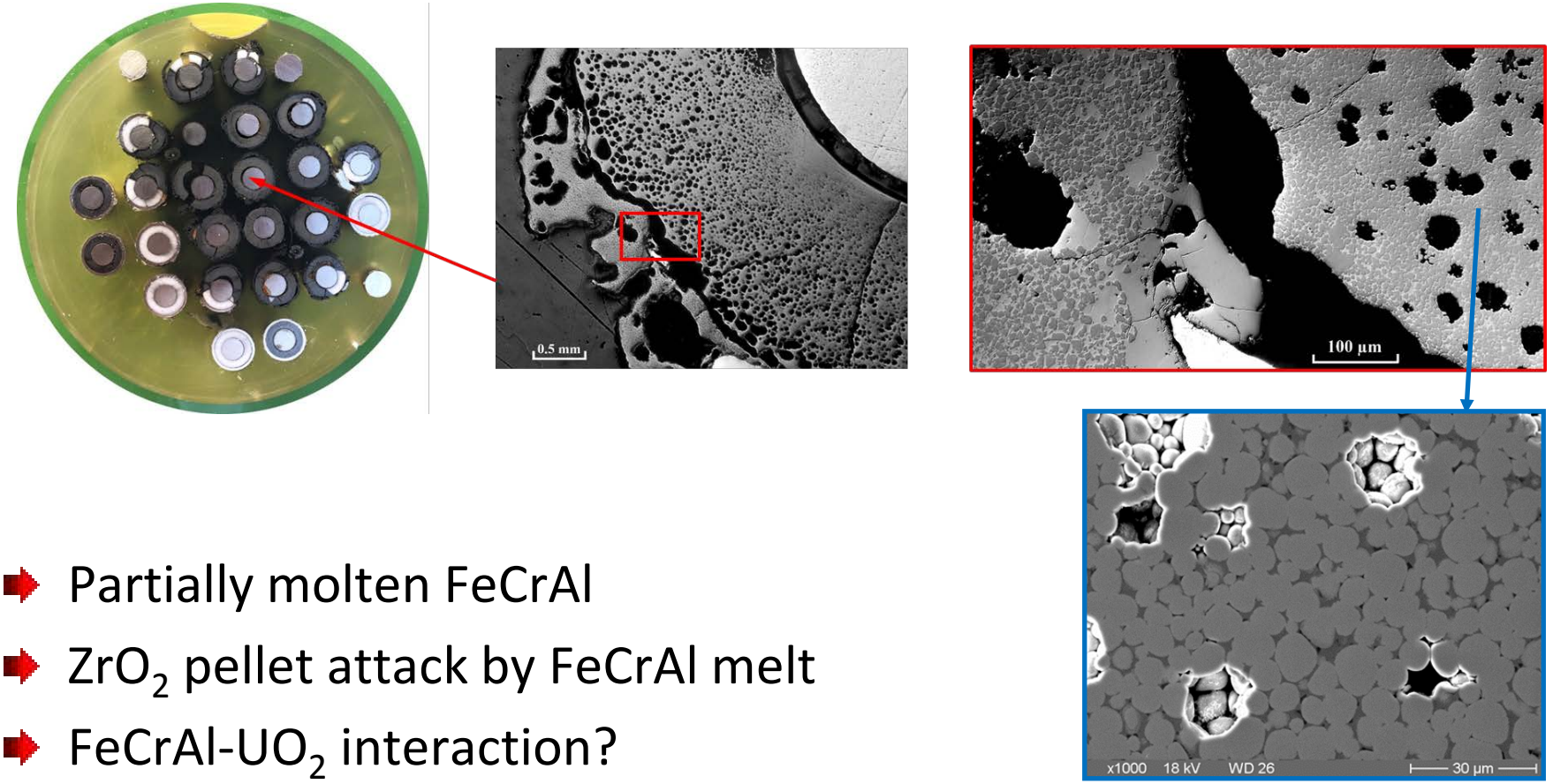
- Worldwide first bundle test with ATF cladding
- With FeCrAl cladding, shroud and spacer grids
- In cooperation with ORNL
- Scenario similar to QUENCH-15 (same bundle geometry, same electrical power input)
- Conducted on August 2018





QUENCH-19 post-test examination

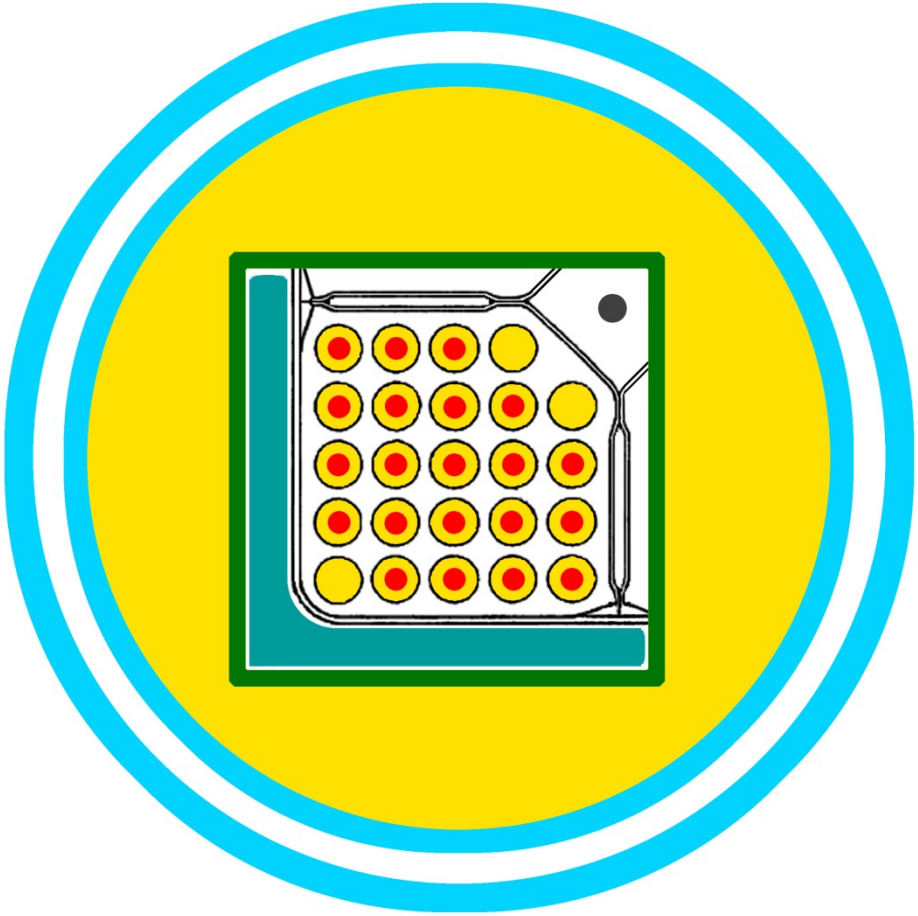
- Polished cuts from various bundle elevations under investigation at KIT and ORNL



- Partially molten FeCrAl
- ZrO_2 pellet attack by FeCrAl melt
- FeCrAl-UO_2 interaction?

BWR bundle test QUENCH-20

- Conducted 09 Oct 2019 in the framework of the EC SAFEST program
- Proposed by Swedish regulatory body and supported by Westinghouse and KTH
- Square bundle cross section
- Including boron carbide absorber blades and water channels



Test section with thermal insulation and cooling jacket

BWR bundle test QUENCH-20: First results

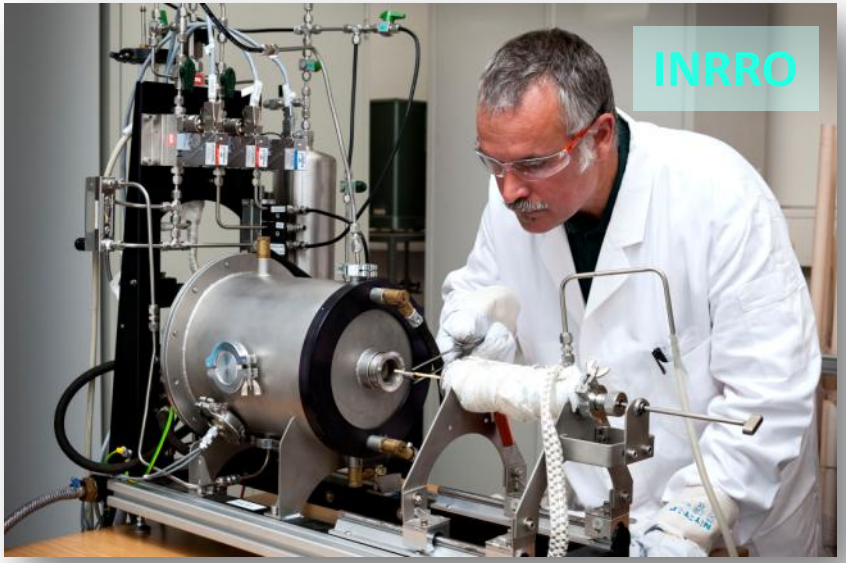




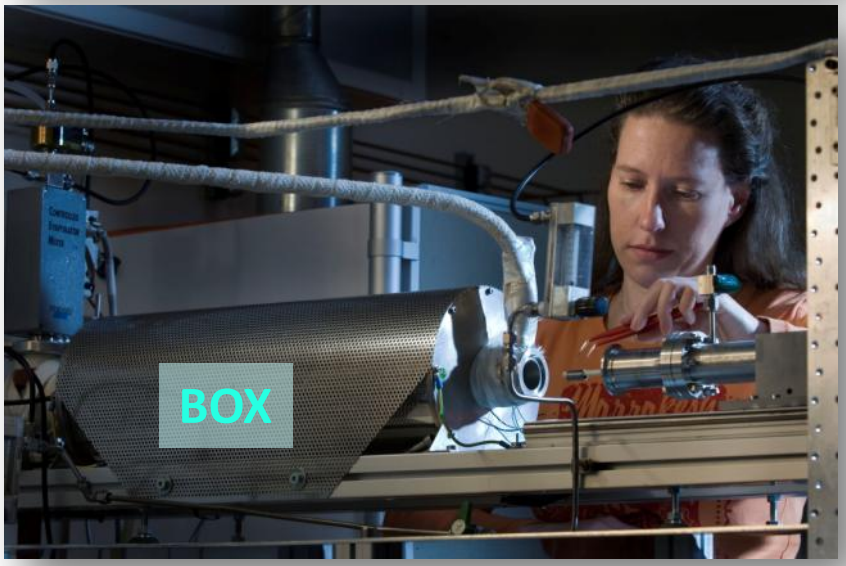


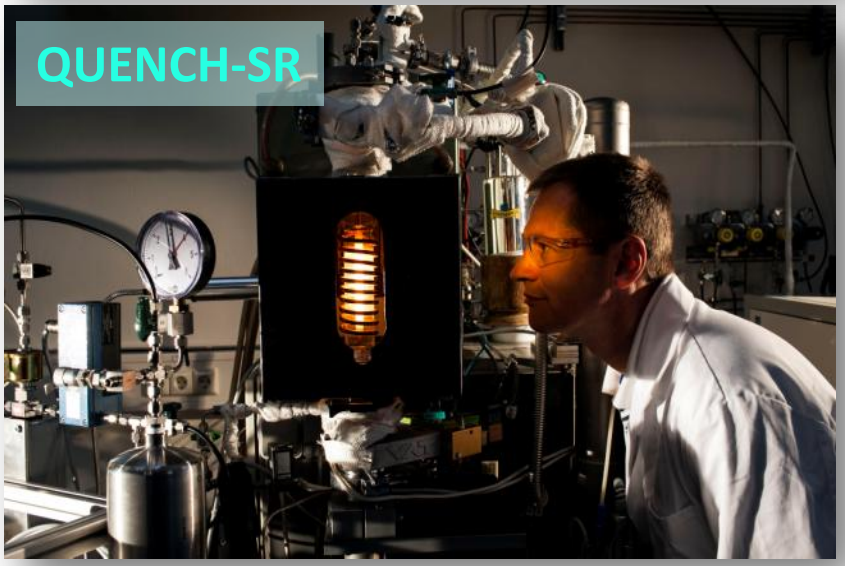
First views on test bundle after extraction from the cooling jacket

QUENCH Separate-effects tests: Main setups









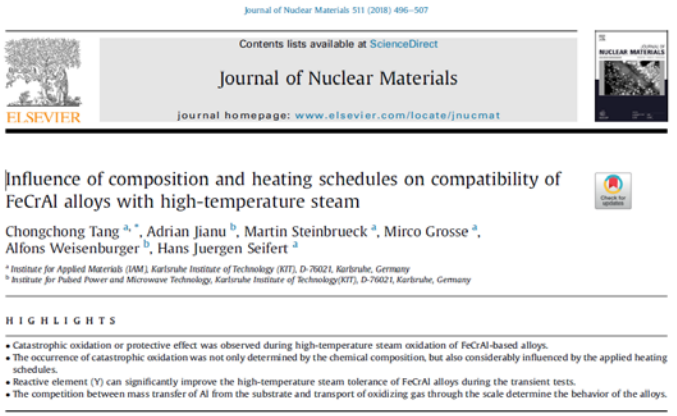
QUENCH activities for Accident Tolerant Fuel Claddings

- Single-rod oxidation and quench tests with Cr-coated Zr alloy
- Ultra-high temperature oxidation tests with SiC_f-SiC
- Oxidation kinetics of various FeCrAl alloys
- Development of MAX phase coatings for Zr alloys

- Participation in various international collaborations on ATF
  - EC IL TROVATORE (Lead WP “Coolant-cladding-fuel interaction”)
  - IAEA ACTOF
  - OECD NEA EGATFL, TOPATF, and QUENCH-ATF (under discussion)
  - Westinghouse CARAT
  - Various bilateral collaborations with General Atomics, CEA, CTU Prague, Tomsk Polytechnic University, …

SETs on high-temperature oxidation of FeCrAl alloys

- Influence of composition and heating rates on HT oxidation in steam
  - Published JNM 2018
  - Oxidation kinetics strongly dependent on the development of a protective alumina scale
  - Catastrophic oxidation possible at high heating rates
- Oxidation kinetics of APM, APMT, B136Y3, and C26M2 from 600 to 1500°C
  - Ongoing activity
  - Change of mechanism at around 1000°C
    - No extrapolation of data to lower temperatures



Journal of Nuclear Materials 511 (2018) 496–507

Contents lists available at ScienceDirect

Journal of Nuclear Materials

journal homepage: www.elsevier.com/locate/jnucmat

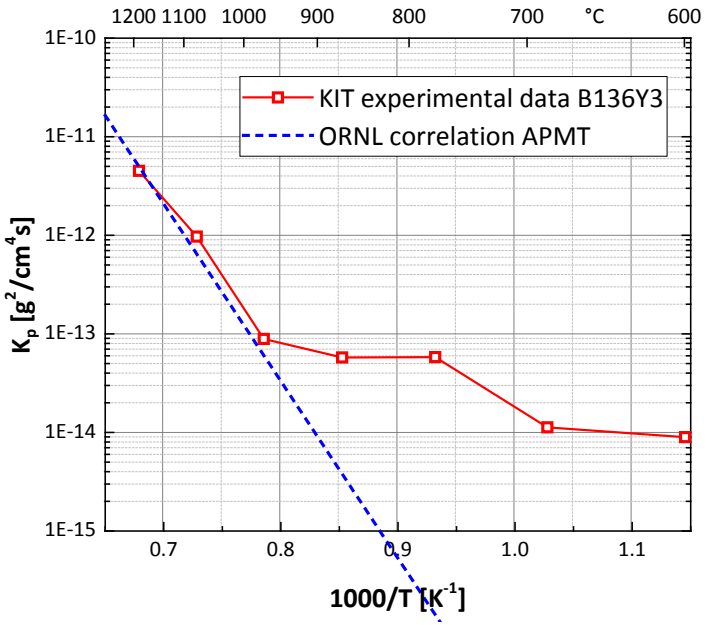
Influence of composition and heating schedules on compatibility of FeCrAl alloys with high-temperature steam

Chongchong Tang [a, *], Adrian Jianu [b], Martin Steinbrueck [a], Mirco Grosse [a], Alfons Weisenburger [b], Hans Juergen Seifert [a]

[a] Institute for Applied Materials (IAM), Karlsruhe Institute of Technology (KIT), D-76021, Karlsruhe, Germany
[b] Institute for Pulsed Power and Microwave Technology, Karlsruhe Institute of Technology(KIT), D-76021, Karlsruhe, Germany

HIGHLIGHTS

- Catastrophic oxidation or protective effect was observed during high-temperature steam oxidation of FeCrAl-based alloys.
- The occurrence of catastrophic oxidation was not only determined by the chemical composition, but also considerably influenced by the applied heating schedules.
- Reactive element (Y) can significantly improve the high-temperature steam tolerance of FeCrAl alloys during the transient tests.
- The competition between mass transfer of Al from the substrate and transport of oxidizing gas through the scale determine the behavior of the alloys.



Proposal for a NEA Joint Undertaking

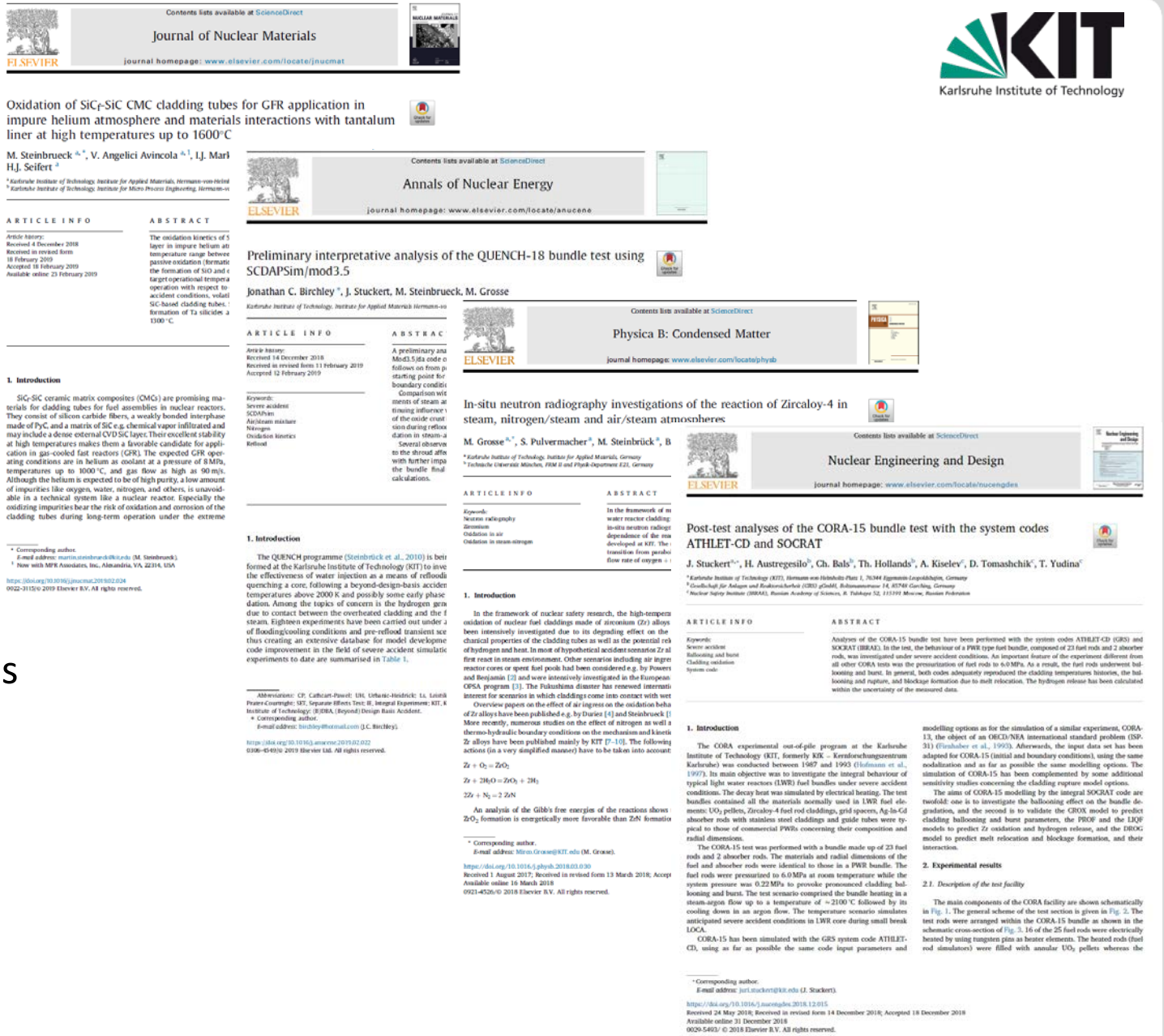
- Time frame: 2020-2024
- Experiments
  - Three bundle tests with DBA and/or BDBA scenarios:
    - Focus on-near term ATF cladding concepts (Cr coated Zr alloy)
  - To be discussed and decided between the project partners
- Costs: 1.5 M€ (approx. 500 000 €/test including materials, work and manpower)
- Requirements
  - Vendors for > 2 m long cladding tubes
  - Adaption of other bundle components to the cladding material, like shroud, spacer grids and TC sheaths
- Partners conducting pre- and post-test calculations welcome
- Supporting small-scale SETs

Modelling and code validation

- QUENCH bundle tests are part of validation matrices of most SFD code systems
- Pre-test calculations for QUENCH-20 by GRS
- Post-test calculations for QUENCH-18 in the framework of the NUGENIA QUESA project by GRS, PSI, IBRAE, LEI, EdF and of QUENCH-19 by GRS
- QUENCH data were used in the frame of IAEA FUMAC project
- RELAP5/SCDAPSIM analyses of various QUENCH tests by ISS
- Separate-effects test data on air oxidation of Zr alloys are used by PSI, RUB, EdF, ISS and others for model development

Reporting

- LOCA summary paper for ASTM Symp. Zr in Nucl. Ind. 2019
- Two book chapters for Comprehensive Nuclear Materials
- Papers and conference contributions (>10 Scopus references)



Contents lists available at ScienceDirect

Journal of Nuclear Materials

journal homepage: www.elsevier.com/locate/jnucmat

Oxidation of SiC_f-SiC CMC cladding tubes for GFR application in impure helium atmosphere and materials interactions with tantalum liner at high temperatures up to 1600°C

M. Steinbrueck [a,*], V. Angelici Avincola [a,1], I.J. Mari
H.J. Seifert [a]

[a] Karlsruhe Institute of Technology, Institute for Applied Materials, Hermann-von-Helmi
[b] Karlsruhe Institute of Technology, Institute for Micro Process Engineering, Hermann-v

ARTICLE INFO

Article history:
Received 4 December 2018
Received in revised form
18 February 2019
Accepted 18 February 2019
Available online 23 February 2019

ABSTRACT

The oxidation kinetics of 5
layer in impure helium at
temperature range betwee
passive oxidation (formatio
the formation of SiO and
target operational tempera
operation with respect to
accident conditions, volati
SiC-based cladding tubes.
formation of Ta silicides a
1300 °C.

1. Introduction

SiC_f-SiC ceramic matrix composites (CMCs) are promising materials for cladding tubes for fuel assemblies in nuclear reactors. They consist of silicon carbide fibers, a weakly bonded interphase made of PyC, and a matrix of SiC e.g. chemical vapor infiltrated and may include a dense external CVD SiC layer. Their excellent stability at high temperatures makes them a favorable candidate for application in gas-cooled fast reactors (GFR). The expected GFR operating conditions are in helium as coolant at a pressure of 8 MPa, temperatures up to 1000 °C, and gas flow as high as 90 m/s. Although the helium is expected to be of high purity, a low amount of impurities like oxygen, water, nitrogen, and others, is unavoidable in a technical system like a nuclear reactor. Especially the oxidizing impurities bear the risk of oxidation and corrosion of the cladding tubes during long-term operation under the extreme

* Corresponding author.
E-mail address: martin.steinbrueck@kit.edu (M. Steinbrueck).
[1] Now with MPR Associates, Inc., Alexandria, VA, 22314, USA

https://doi.org/10.1016/j.jnucmat.2019.02.024
0022-3115/© 2019 Elsevier B.V. All rights reserved.

Contents lists available at ScienceDirect

Annals of Nuclear Energy

journal homepage: www.elsevier.com/locate/anucene

Preliminary interpretative analysis of the QUENCH-18 bundle test using SCDAPSim/mod3.5

Jonathan C. Birchley *, J. Stuckert, M. Steinbrueck, M. Grosse

Karlsruhe Institute of Technology, Institute for Applied Materials Hermann-vo

ARTICLE INFO

Article history:
Received 14 December 2018
Received in revised form 11 February 2019
Accepted 12 February 2019

Keywords:
Severe accident
SCDAPsim
Air/steam mixture
Nitrogen
Oxidation kinetics
Reflood

ABSTRAC

A preliminary ana
Mod3.5jda code c
follows on from p
starting point for
boundary conditi
Comparison wit
ments of steam at
tioning influence
of the oxide crust
sion during reflo
dation in steam-a
Several observa
to the shroud affe
with further impa
the bundle final
calculations.

1. Introduction

The QUENCH programme (Steinbrück et al., 2010) is bei
formed at the Karlsruhe Institute of Technology (KIT) to inve
the effectiveness of water injection as a means of refloodi
quenching a core, following a beyond-design-basis acciden
temperatures above 2000 K and possibly some early phase
dation. Among the topics of concern is the hydrogen gen
due to contact between the overheated cladding and the f
steam. Eighteen experiments have been carried out under
of flooding/cooling conditions and pre-reflood transient sc
thus creating an extensive database for model developme
code improvement in the field of severe accident simulatio
experiments to date are summarised in Table 1.

Abbreviations: CP, Cathcart-Powell; UH, Urbanic-Heidrick; La, Leistik
Prater-Courtright; SET, Separate-Effects Test; IE, Integral Experiment; KIT, K
Institute of Technology; (B)DBA, (Beyond) Design Basis Accident.
* Corresponding author.
E-mail address: birchley@hotmail.com (J.C. Birchley).

https://doi.org/10.1016/j.anucene.2019.02.022
0306-4549/© 2019 Elsevier Ltd. All rights reserved.

Contents lists available at ScienceDirect

Physica B: Condensed Matter

journal homepage: www.elsevier.com/locate/physb

In-situ neutron radiography investigations of the reaction of Zircaloy-4 in steam, nitrogen/steam and air/steam atmospheres

M. Grosse [a,*], S. Pulvermacher [a], M. Steinbrück [a], B
[a] Karlsruhe Institute of Technology, Institute for Applied Materials, Germany
[b] Technische Universität München, FRM II and Physik-Department E21, Germany

ARTICLE INFO

Keywords:
Neutron radiography
Zirconium
Oxidation in air
Oxidation in steam-nitrogen

ABSTRACT

In the framework of m
water reactor claddin
in-situ neutron radiogr
dependence of the ma
developed at KIT. The
transition from parabo
flow rate of oxygen

1. Introduction

In the framework of nuclear safety research, the high-tempera
oxidation of nuclear fuel claddings made of zirconium (Zr) alloys
been intensively investigated due to its degrading effect on the
chanical properties of the cladding tubes as well as the potential rel
of hydrogen and heat. In most of hypothetical accident scenarios Zr al
first react in steam environment. Other scenarios including air ingre
reactor cores or spent fuel pools had been considered e.g. by Powers
and Benjamin [2] and were intensively investigated in the European
OPSA program [3]. The Fukushima disaster has renewed internati
interest for scenarios in which claddings come into contact with wet
Overview papers on the effect of air ingress on the oxidation beha
of Zr alloys have been published e.g. by Duriez [4] and Steinbrueck [5
More recently, numerous studies on the effect of nitrogen as well a
thermo-hydraulic boundary conditions on the mechanism and kineti
Zr alloys have been published mainly by KIT [7–10]. The following
actions (in a very simplified manner) have to be taken into account

$$Zr + O_2 = ZrO_2$$

$$Zr + 2H_2O = ZrO_2 + 2H_2$$

$$2Zr + N_2 = 2\,ZrN$$

An analysis of the Gibb's free energies of the reactions shows
ZrO_2 formation is energetically more favorable than ZrN formatio

* Corresponding author.
E-mail address: Miros.Grosse@KIT.edu (M. Grosse).

https://doi.org/10.1016/j.physb.2018.03.030
Received 1 August 2017; Received in revised form 13 March 2018; Accep
Available online 16 March 2018
0921-4526/© 2018 Elsevier B.V. All rights reserved.

Contents lists available at ScienceDirect

Nuclear Engineering and Design

journal homepage: www.elsevier.com/locate/nucengdes

Post-test analyses of the CORA-15 bundle test with the system codes ATHLET-CD and SOCRAT

J. Stuckert [a,*], H. Austregesilo [b], Ch. Bals [b], Th. Hollands [b], A. Kiselev [c], D. Tomashchik [c], T. Yudina [c]

[a] Karlsruhe Institute of Technology (KIT), Hermann-von-Helmholtz-Platz 1, 76344 Eggenstein-Leopoldshafen, Germany
[b] Gesellschaft für Anlagen und Reaktorsicherheit (GRS) gGmbH, Boltzmannstrasse 14, 85748 Garching, Germany
[c] Nuclear Safety Institute (IBRAE), Russian Academy of Sciences, B. Tulskaya 52, 115191 Moscow, Russian Federation

ARTICLE INFO

Keywords:
Severe accident
Ballooning and burst
Cladding oxidation
System code

ABSTRACT

Analyses of the CORA-15 bundle test have been performed with the system codes ATHLET-CD (GRS) and SOCRAT (IBRAE). In the test, the behaviour of a PWR type fuel bundle, composed of 23 fuel rods and 2 absorber rods, was investigated under severe accident conditions. An important feature of the experiment different from all other CORA tests was the pressurization of fuel rods to 6.0 MPa. As a result, the fuel rods underwent ballooning and burst. In general, both codes adequately reproduced the cladding temperatures histories, the ballooning and rupture, and blockage formation due to melt relocation. The hydrogen release has been calculated within the uncertainty of the measured data.

1. Introduction

The CORA experimental out-of-pile program at the Karlsruhe Institute of Technology (KIT, formerly KfK – Kernforschungszentrum Karlsruhe) was conducted between 1987 and 1993 (Hofmann et al., 1997). Its main objective was to investigate the integral behaviour of typical light water reactors (LWR) fuel bundles under severe accident conditions. The decay heat was simulated by electrical heating. The test bundles contained all the materials normally used in LWR fuel elements: UO_2 pellets, Zircaloy-4 fuel rod claddings, grid spacers, Ag-In-Cd absorber rods with stainless steel claddings and guide tubes were typical to those of commercial PWRs concerning their composition and radial dimensions.

The CORA-15 test was performed with a bundle made up of 23 fuel rods and 2 absorber rods. The materials and radial dimensions of the fuel and absorber rods were identical to those in a PWR bundle. The fuel rods were pressized to 6.0 MPa at room temperature while the system pressure was 0.22 MPa to provoke pronounced cladding ballooning and burst. The test scenario comprised the bundle heating in a steam-argon flow up to a temperature of ~2100 °C followed by its cooling down in an argon flow. The temperature scenario simulates anticipated severe accident conditions in LWR core during small break LOCA.

CORA-15 has been simulated with the GRS system code ATHLET-CD, using as far as possible the same code input parameters and modelling options as for the simulation of a similar experiment, CORA-13, the object of an OECD/NEA international standard problem (ISP-31) (Firnhaber et al., 1993). Afterwards, the input data set has been adapted for CORA-15 (initial and boundary conditions), using the same nodalization and as far as possible the same modelling options. The simulation of CORA-15 has been complemented by some additional sensitivity studies concerning the cladding rupture model options.

The aims of CORA-15 modelling by the integral SOCRAT code are twofold: one is to investigate the ballooning effect on the bundle degradation, and the second is to validate the CROX model to predict cladding ballooning and burst parameters, the PROF and the LIQF models to predict Zr oxidation and hydrogen release, and the DROG model to predict melt relocation and blockage formation, and their interaction.

2. Experimental results

2.1. Description of the test facility

The main components of the CORA facility are shown schematically in Fig. 1. The general scheme of the test section is given in Fig. 2. The test rods were arranged within the CORA-15 bundle as shown in the schematic cross-section of Fig. 3. 16 of the 25 fuel rods were electrically heated by using tungsten pins as heater elements. The heated rods (fuel rod simulators) were filled with annular UO_2 pellets whereas the

* Corresponding author.
E-mail address: jurl.stuckert@kit.edu (J. Stuckert).

https://doi.org/10.1016/j.nucengdes.2018.12.015
Received 24 May 2018; Received in revised form 14 December 2018; Accepted 18 December 2018
Available online 31 December 2018
0029-5493/ © 2018 Elsevier B.V. All rights reserved.

Outlook 2019-2020

- Post-test examinations of QUENCH-18/-19/-20
- Discussion with various international partners on further bundle tests with ATF claddings
- SETs on various further topics
  - Focus on ATF cladding high temperature oxidation, partially in the framework of the H2020 project IL TROVATORE and the IAEA CRP ACTOF as well as in bilateral cooperation
- Activities on safety of long-term dry intermediate storage
  - BMBF sponsored SPIZWURZ project (H in Zr alloys)
  - HOVER (Helmholtz Research Platform for Nuclear Waste Management and Decommissioning Research)

Co-operations

Programs

- NUGENIA
- HORIZON 2020
- IAEA
- OECD-NEA

Bilateral

- PSI
- MTA EK
- IRSN, CEA, EdF
- RUB-LEE
- GRS
- Westinghouse
- USNRC
- KONICOF
- NECSA, BAM, HMI
- NRA, JAEA
- ISS
- ORNL
- Tomsk PTU
- Various Chinese Organizations

Acknowledgement

- Helmholtz Association for funding program NUSAFE at KIT
- Program NUSAFE and IAM institute's management for broad support of our activities
- IAEA for financial support of a number of participants

- And last but not least the QUENCH team:
  J. Laier, J. Moch, H. Muscher, U. Peters, U. Stegmaier, C. Tang, M. Walter

Karlsruhe Institute of Technology

Institute for Applied Materials

Update of the QUENCH Program

M. Steinbrück, J. Stuckert, M. Große et al.

25th International QUENCH Workshop, Karlsruhe, 22-24 October 2019

Institute for Applied Materials, Programme NUSAFE



First results of the QUENCH-20 test with BWR bundle

J. Stuckert, M. Große, J. Laier, J. Moch, U. Peters, U. Stegmaier, M. Steinbrück

Abstract

Experiment QUENCH-20 with BWR geometry simulation bundle was successfully conducted at KIT on 9th October 2019. This test was performed in the framework of international access SAFEST infrastructure with the users from Swedish Radiation Safety Authority (SSM) in cooperation with Westinghouse Sweden, GRS and KTH.

The test objective was the investigation of a BWR fuel assembly degradation including a B_4C control blade. The test bundle mock-up represents one quarter of a BWR fuel assembly. The 24 electrically heated fuel rod simulators were filled separately with krypton (overpressure of 4 bar).

According to the pre-test calculations performed with ATHLET-CD, the bundle was heated to a temperature of 1230 K at the cladding of the central rod at the hottest elevation of 950 mm. This pre-oxidation phase in steam lasted 4 hours. Towards the end of this phase, the reference rod was extracted from the test bundle for determination of the oxide thickness axial distribution.

During the transient stage, the bundle was heated to a maximal temperature of 2000 K. The cladding failures were observed at temperature about 1700 K and lasted about 200 s. Massive absorber melt relocation was observed 50 s before the end of transition stage.

The test was terminated with the quench water injected with a flow rate of 50 g/s from the bundle bottom. Fast temperature escalation from 2000 to 2300 K during 20 s was observed. The mass spectrometer measured release of CO_x and few CH_4 during the reflood as products of absorber oxidation; corresponding production of B_2O_3 should be about 97 g. Hydrogen production during the reflood amounted to 32 g (57.4 g during the whole test) including 10 g from B_4C oxidation.



Karlsruhe Institute of Technology

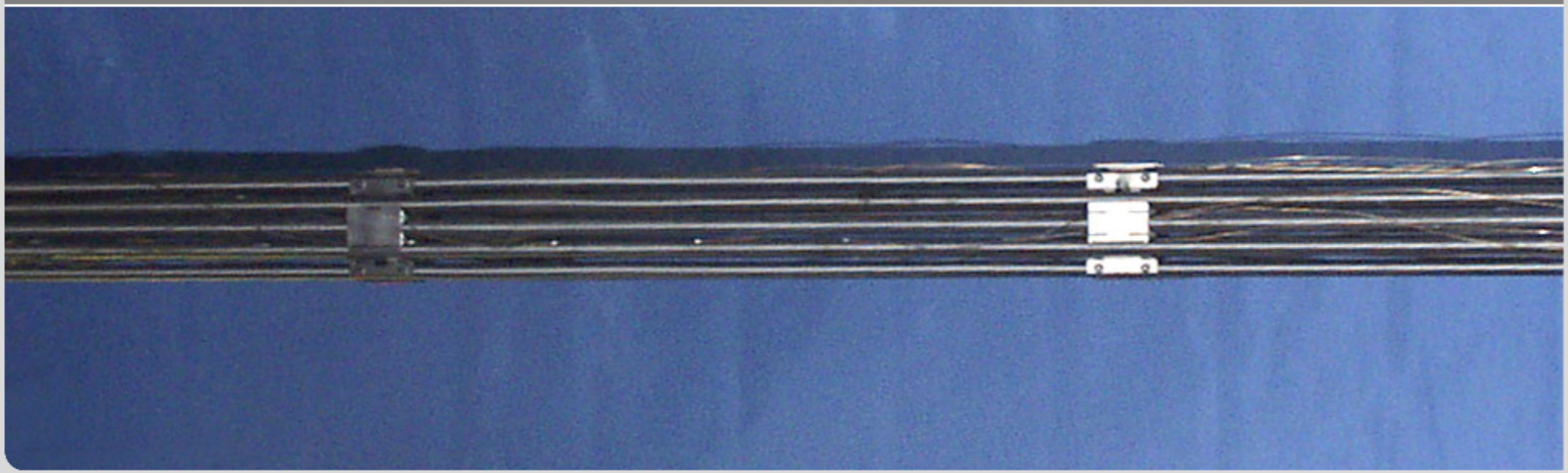
Institute for Applied Materials

First results of the QUENCH-20 test with BWR bundle

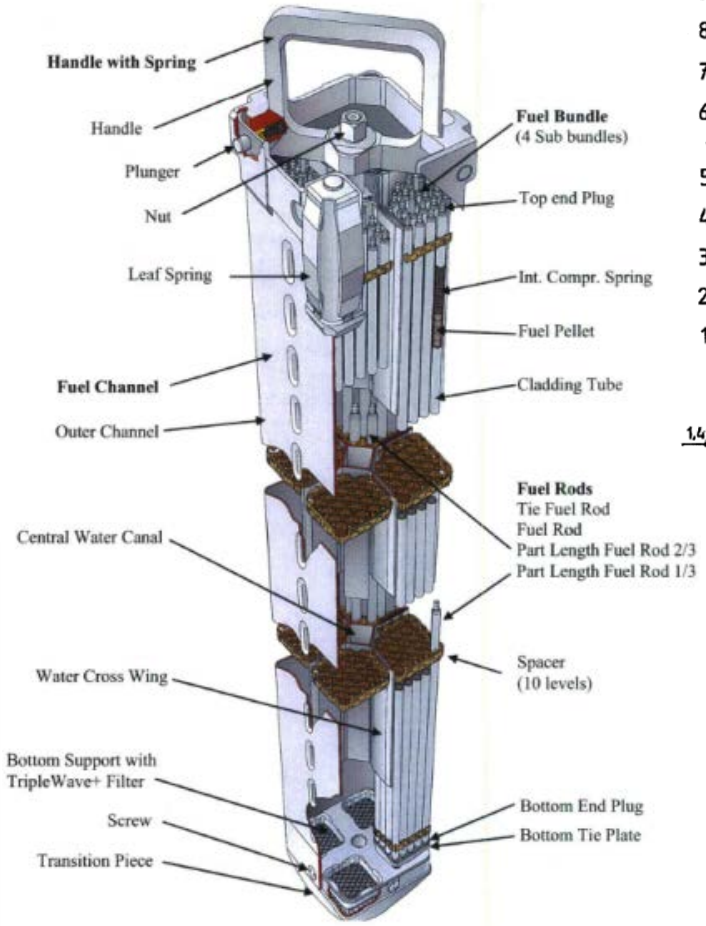
J. Stuckert, M. Große, J. Laier, J. Moch, U. Peters, U. Stegmaier, M. Steinbrück

QWS-25, Karlsruhe

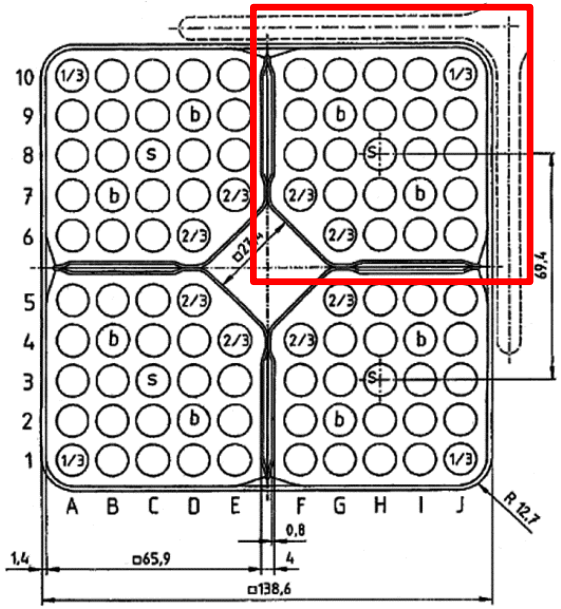
Institute for Applied Materials; Program NUSAFE



QUENCH-20 (SAFEST): Choice of BWR elements, which should be simulated during QUENCH-SAFEST

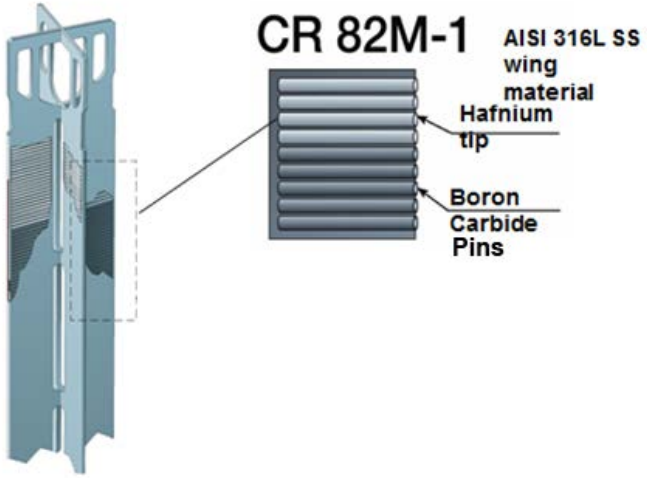


assembly SVEA-96 Optima



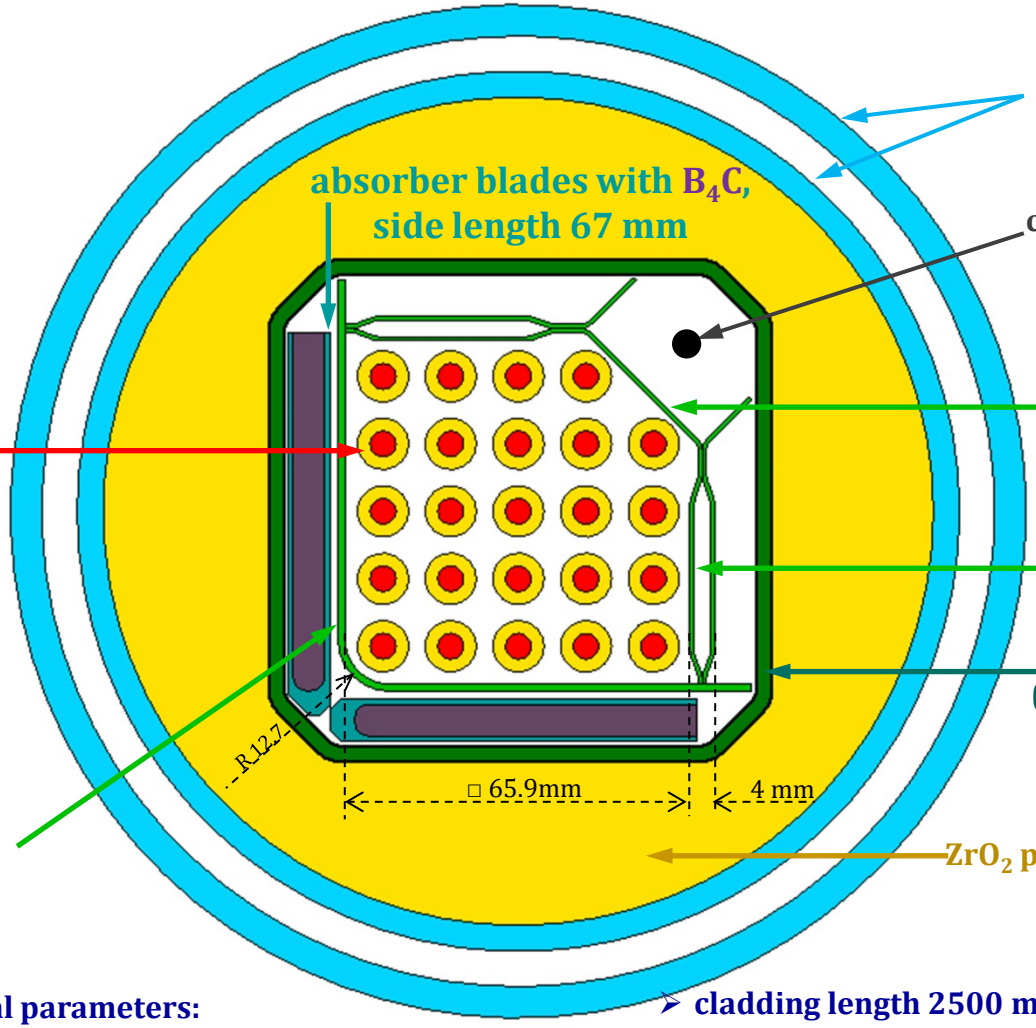
assembly cross section

***SSM proposal*: study of high temperature degradation of BWR assembly mock-up in QUENCH facility (melt formation due to <u>eutectic material interaction</u> inside absorber cross)**



absorber cross

QUENCH-20: suggested test bundle composition (¼ SVEA-96 OPTIMA2 assembly)



Inconel cooling jacket, inner tube ID=158.3 mm

corner rod (Zry-4, OD 6 mm)

heated rods (24): cladding Zy-2 with inner ZrSn-liner (10% of clad),

ZrO_2 pellet OD 8.48±0.05 ID 5.45±0.1 mm, length 11 mm,

W heater OD 5.25±0.025 mm

water channel box (ZIRLO), side length 27.4 mm

water cross wing (ZIRLO), wall thickness 0.8 mm

Zr shroud 90 mm x 114 mm (inner clearance dimensions), wall thickness 3 mm

advanced low tin ZIRLO fuel channel box, wall thickness 1.4 mm

ZrO_2 porous thermal insulation

Geometrical parameters:

- bundle pitch 12.898 mm;
- outer diameter of claddings 9.84 mm;
- thickness of claddings 0.605 mm;
- absorber blades: thickness 8.05 mm
- cladding length 2500 mm
- absorber and cannel box lengths 1600 mm
- water gap between channel box and absorber blade 2.5 mm (nominal inter-assembly gap in BWR-PROTEUS core is 13.8 mm -> water gap 2.875 mm)

QUENCH-20: delivered parts



Zr shroud



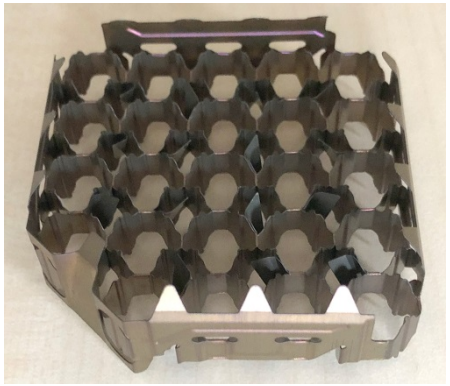
channel box (low tin ZIRLO)



absorber blade (stainless steel)

horizontal holes for B_4C pins

B_4C pin

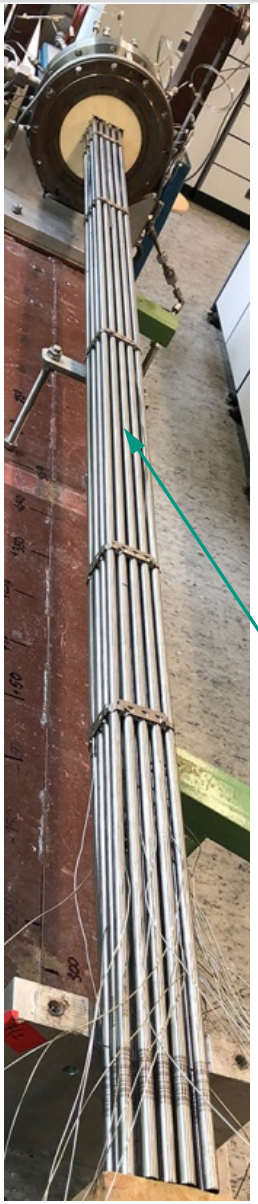


sleeve type spacer grid Inconel X750



claddings (Zry-2 with inner ZrSn liner)

QUENCH-20: instrumentation and preparation of parts



Q20 bundle instrumented with TCs



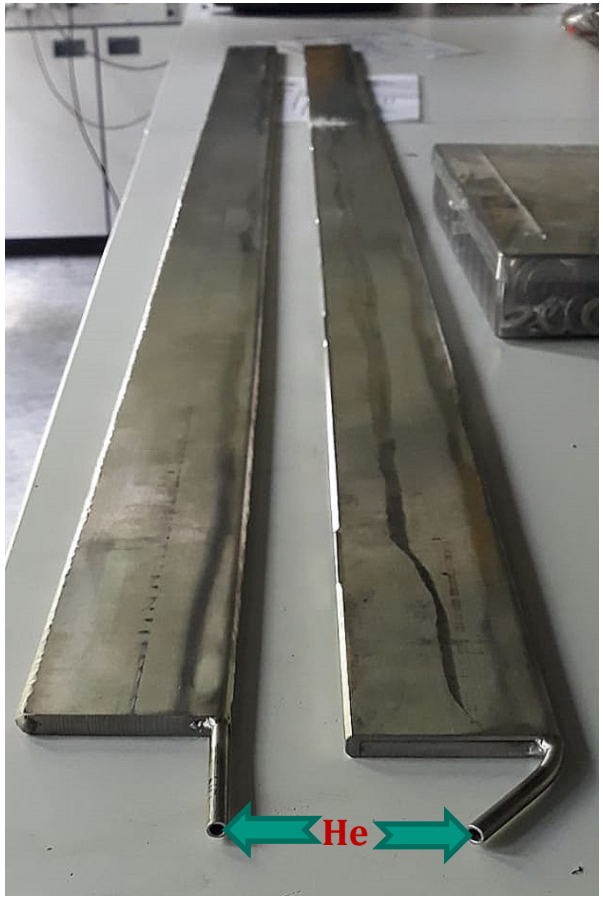
low temperature TC at shroud surface



high temperature TC at clad surface

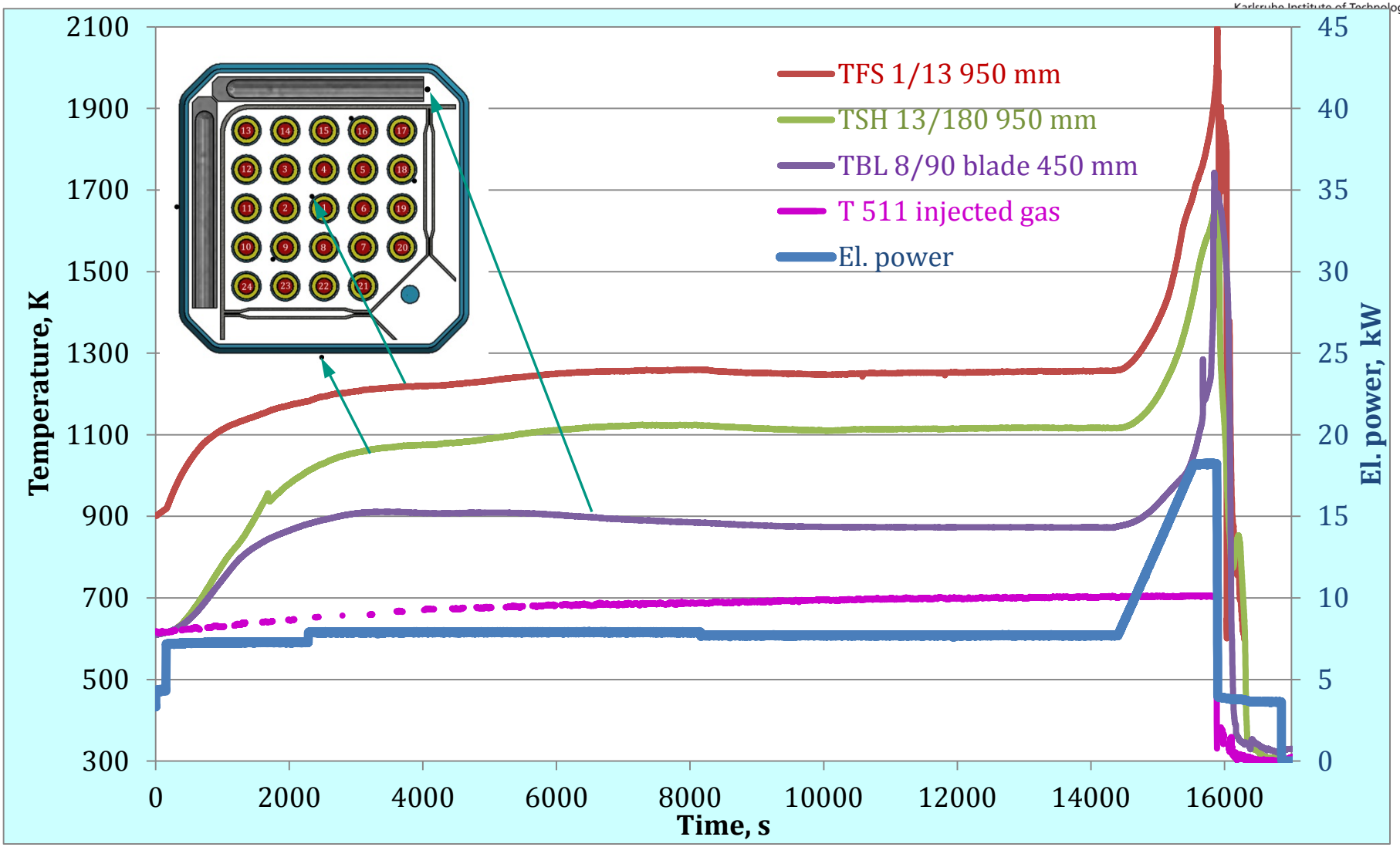


Zr shroud connected to bundle foot



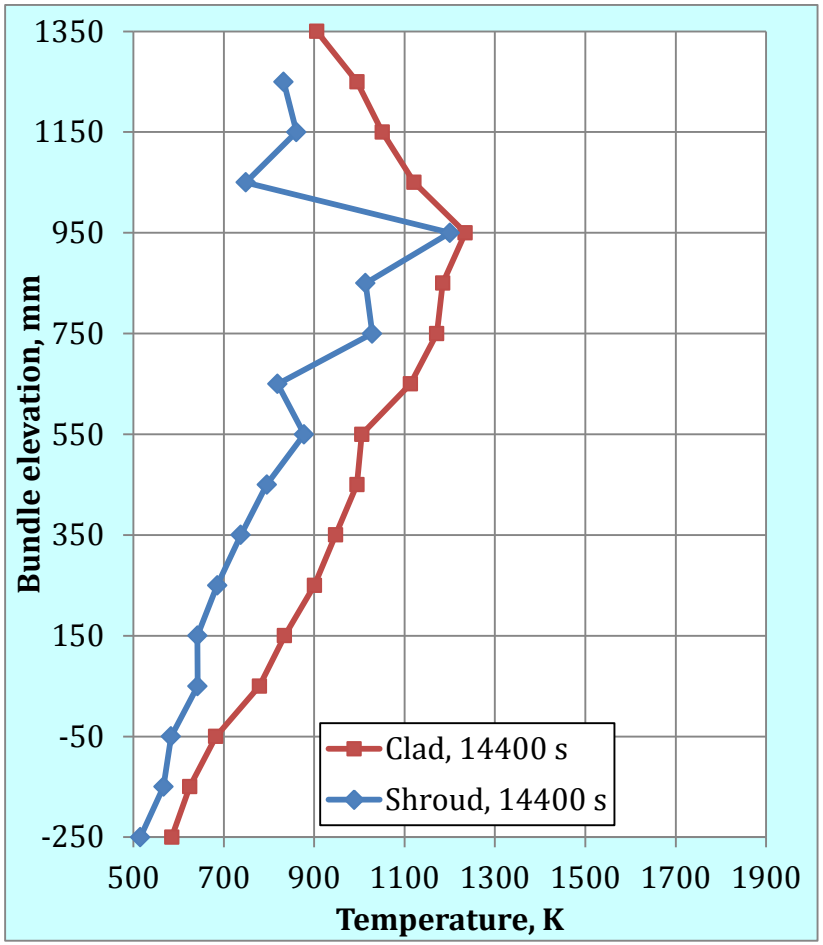
absorber blades filled with B4C pins and prepared for filling with He, then welded

QUENCH-20: test scenario

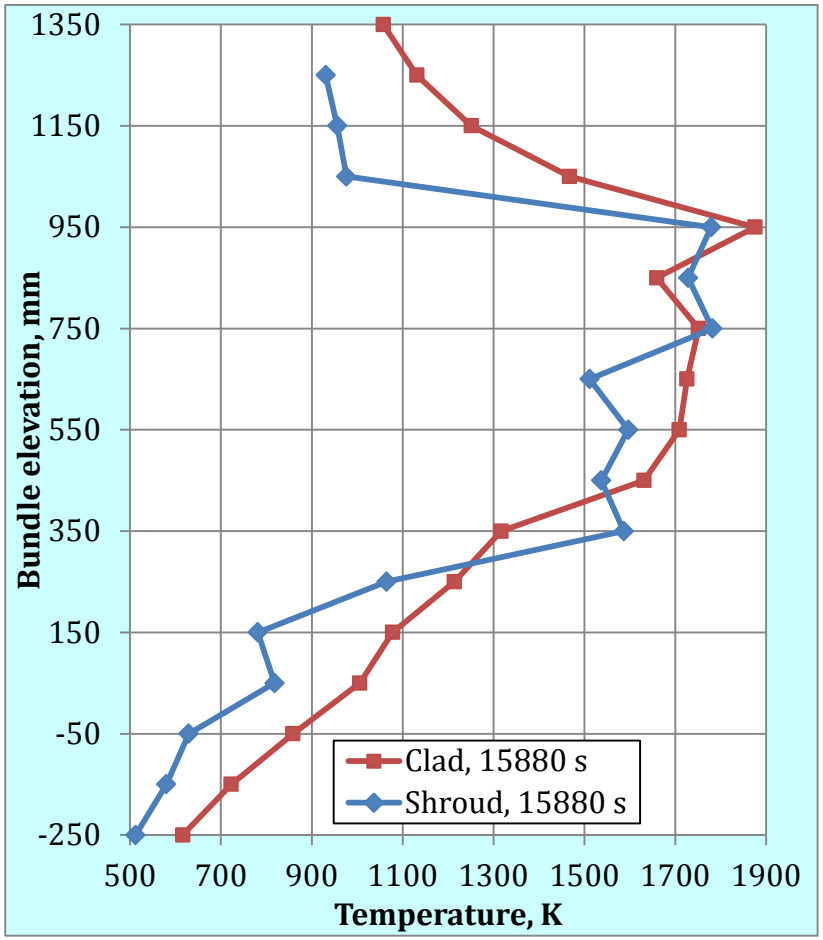


gas injection: Ar 3g/s during the whole test; superheated steam 3 g/s until the quench initiation

QUENCH-20: axial temperature profiles of outer cladding surfaces and outer shroud surface (temperatures averaged through the cross-section for each elevation)

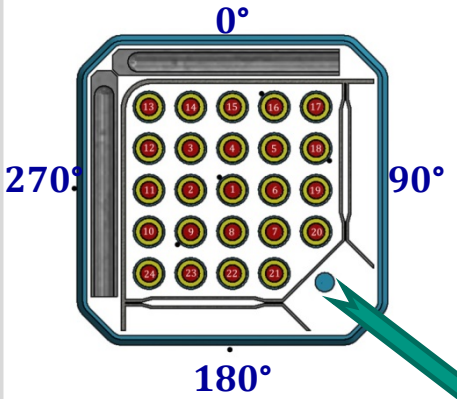


on the end of pre-oxidation (14400 s)

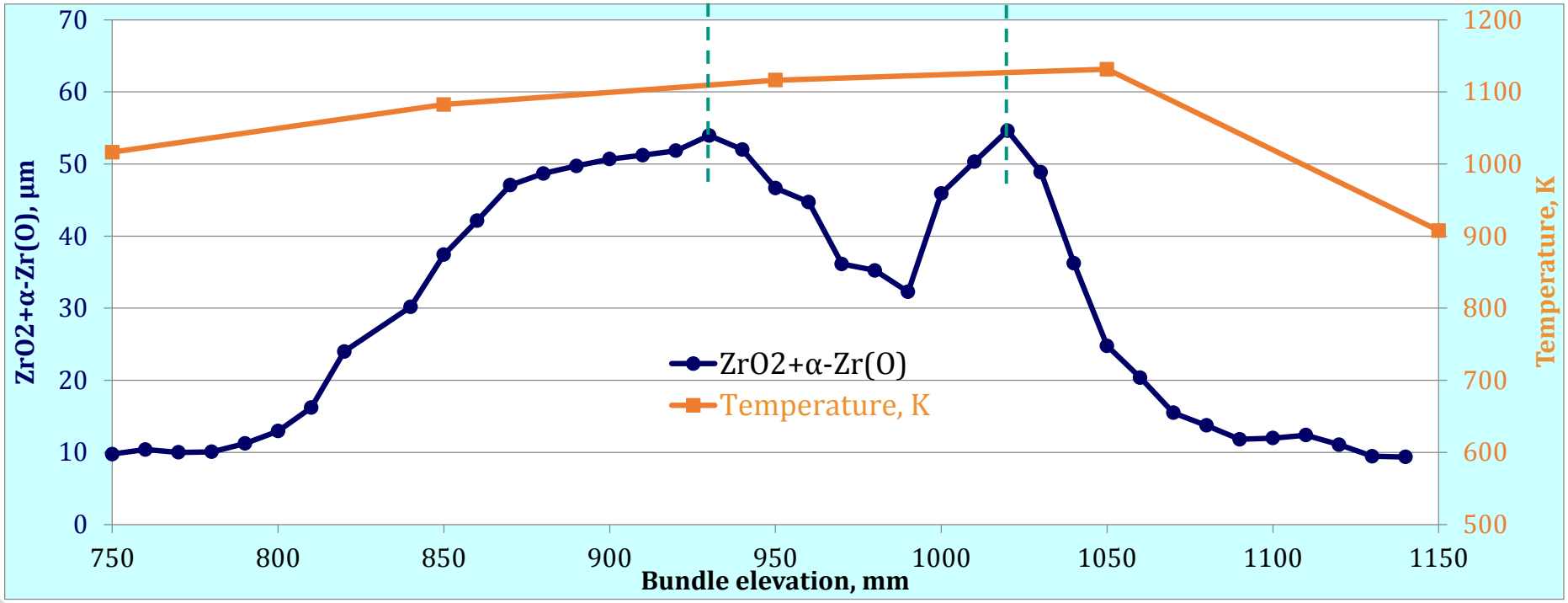


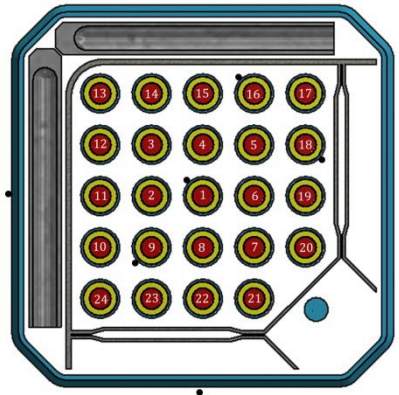
on the end of transient (15880 s)

QUENCH-20: oxidation of Zry-4 corner rod withdrawn on the end of pre-oxidation



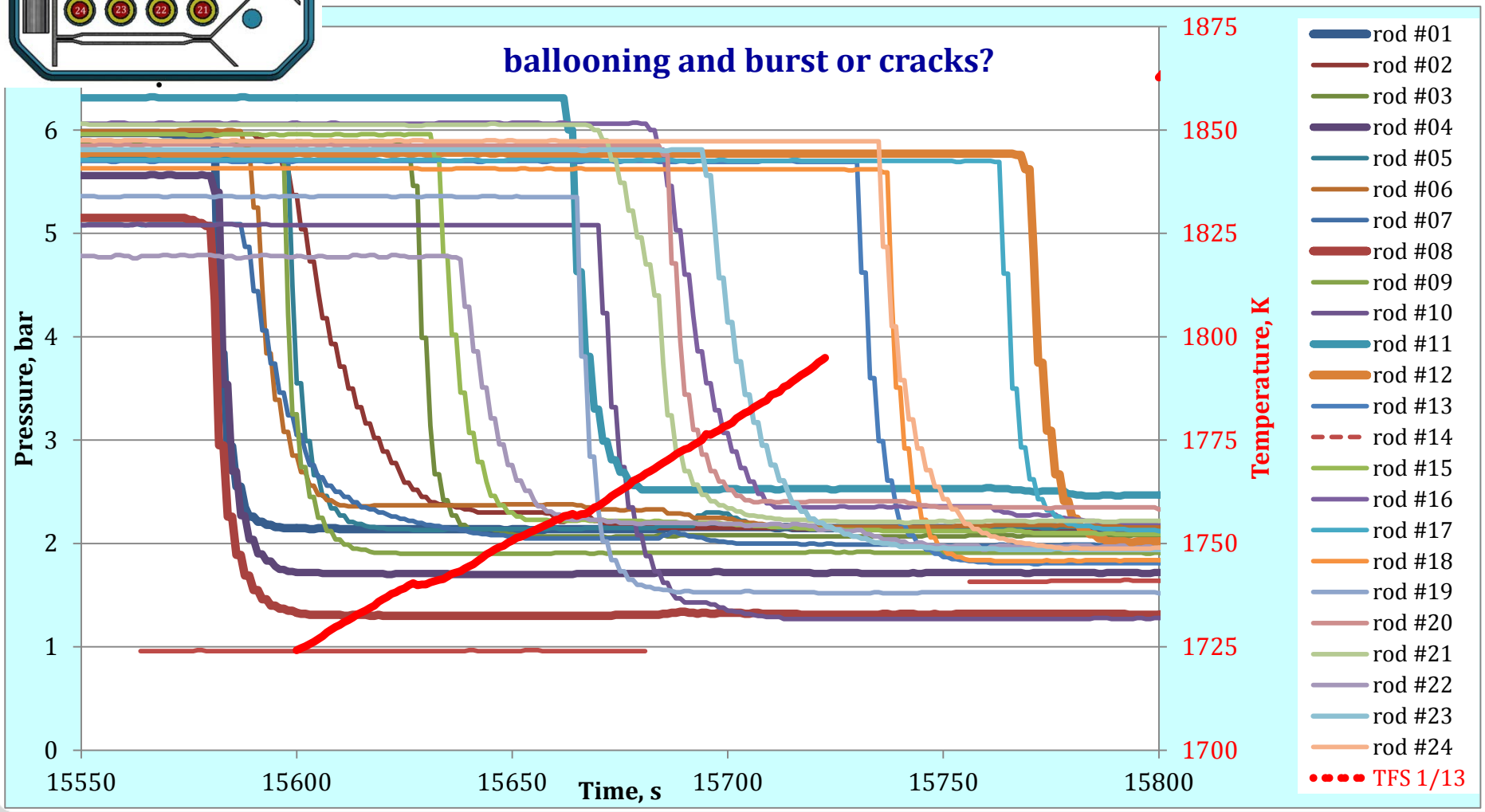




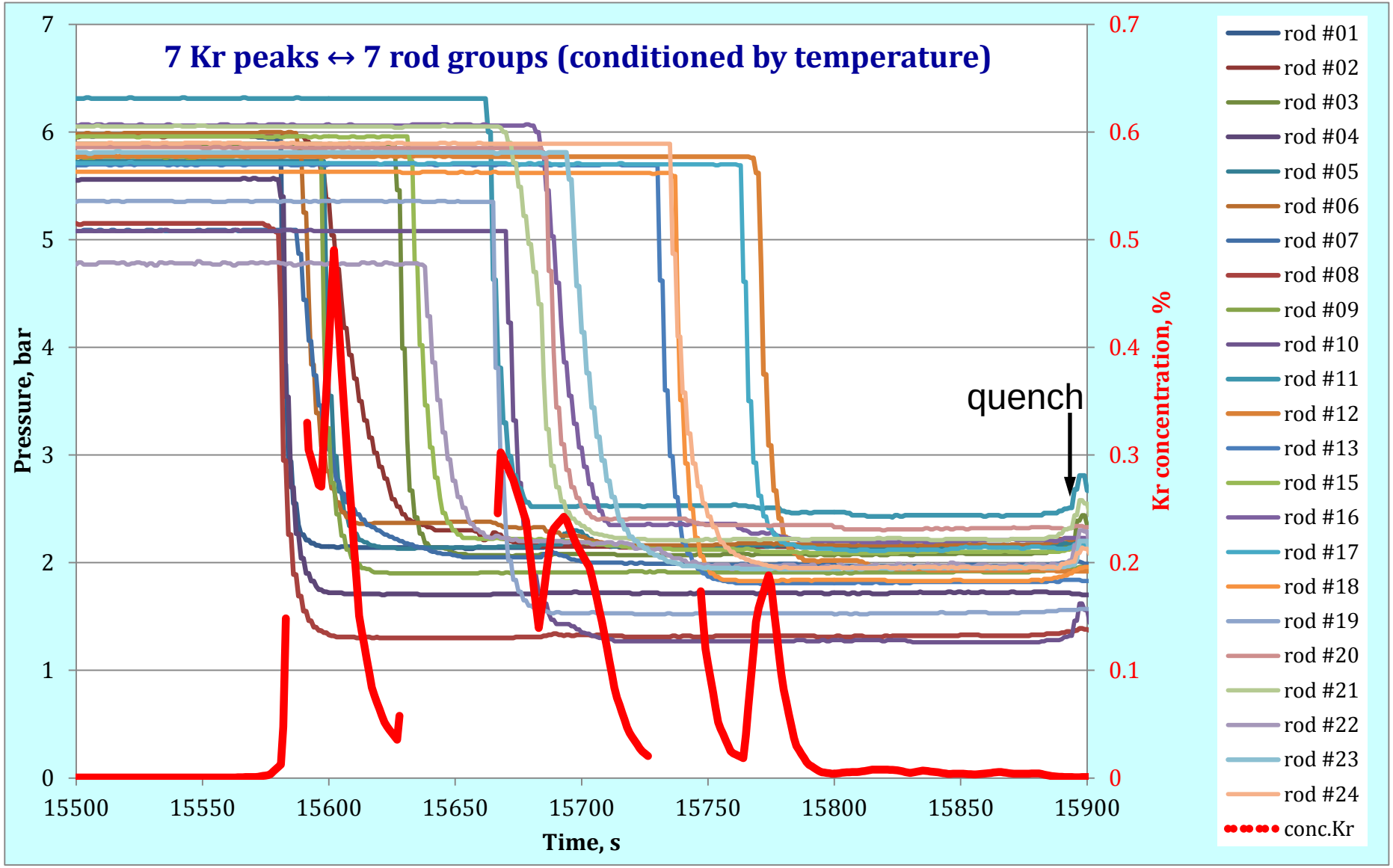


QUENCH-20: failure of rods; first failures: inner rods 1, 4, 8; last failure: outer rod 12

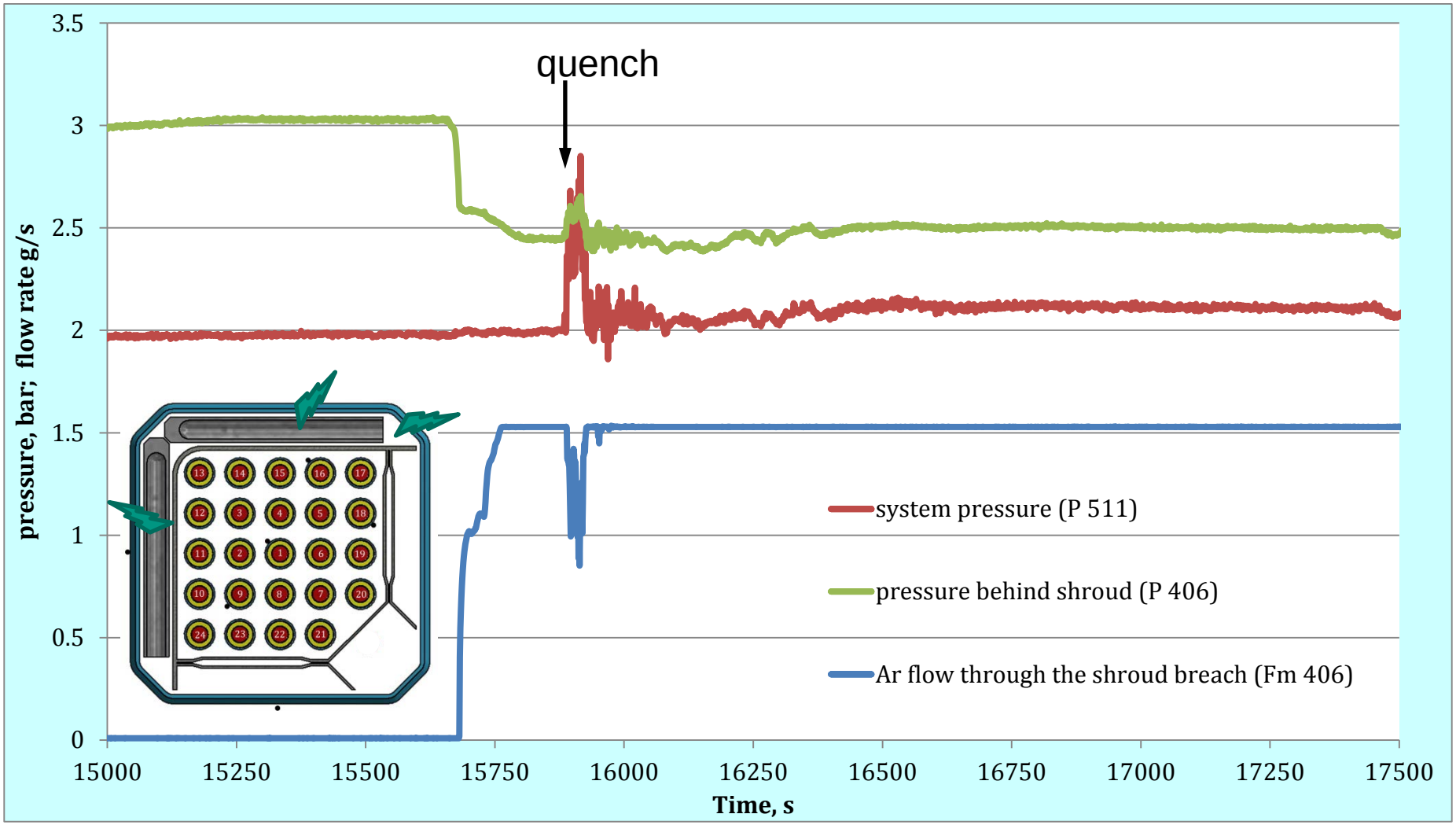
Karlsruhe Institute of Technology



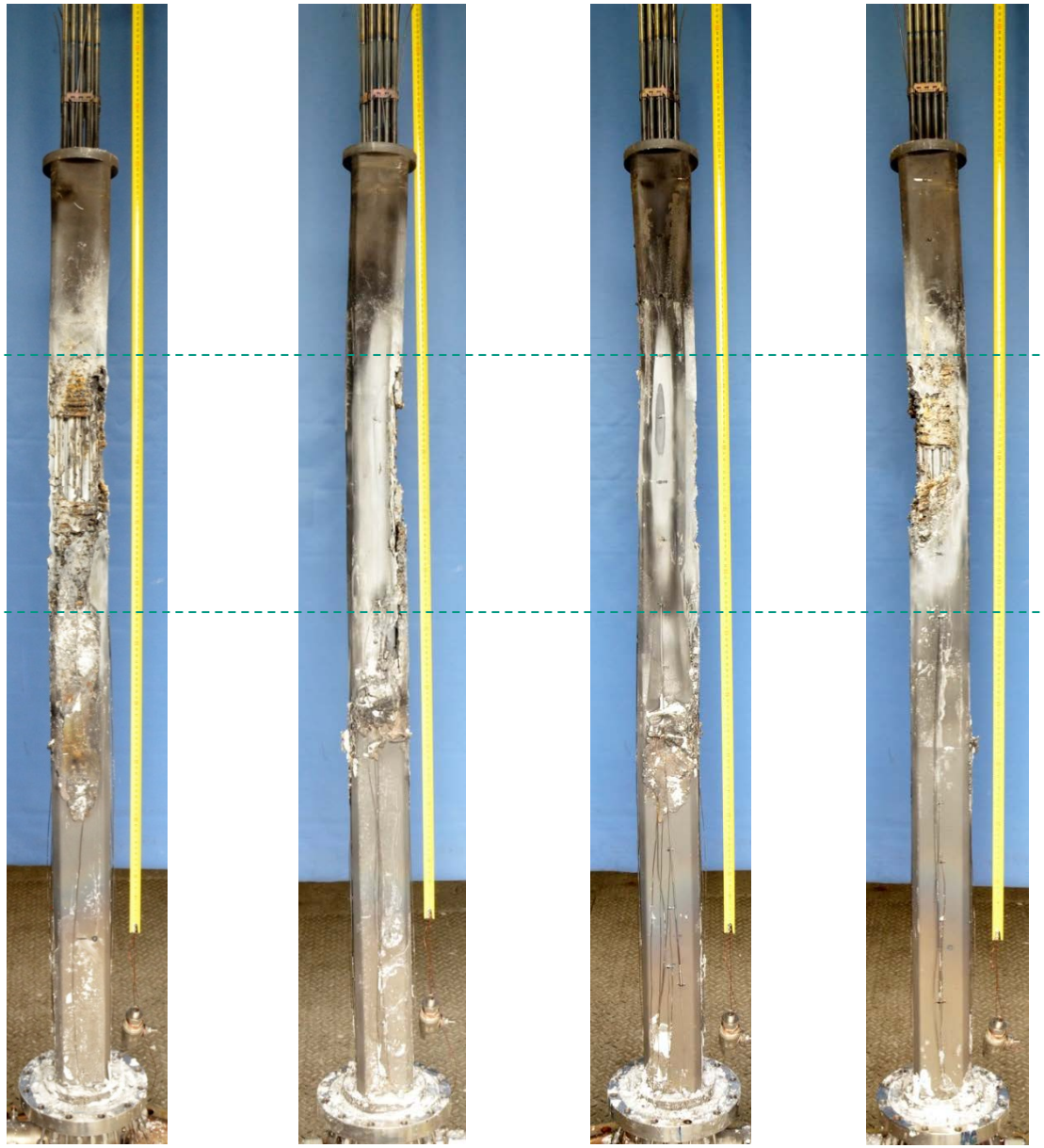
QUENCH-20: indication of rod failures by Kr release

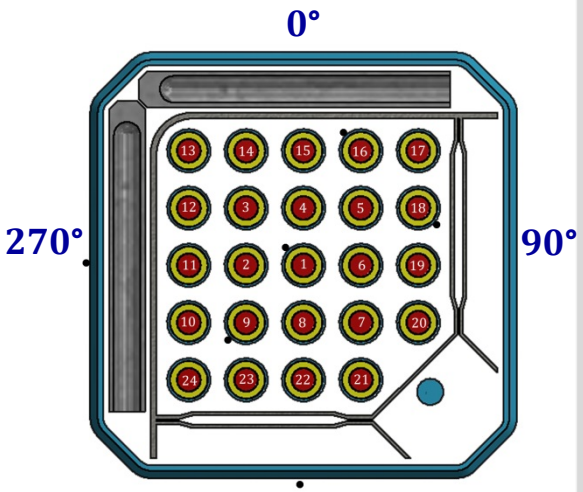


QUENCH-20: shroud failure



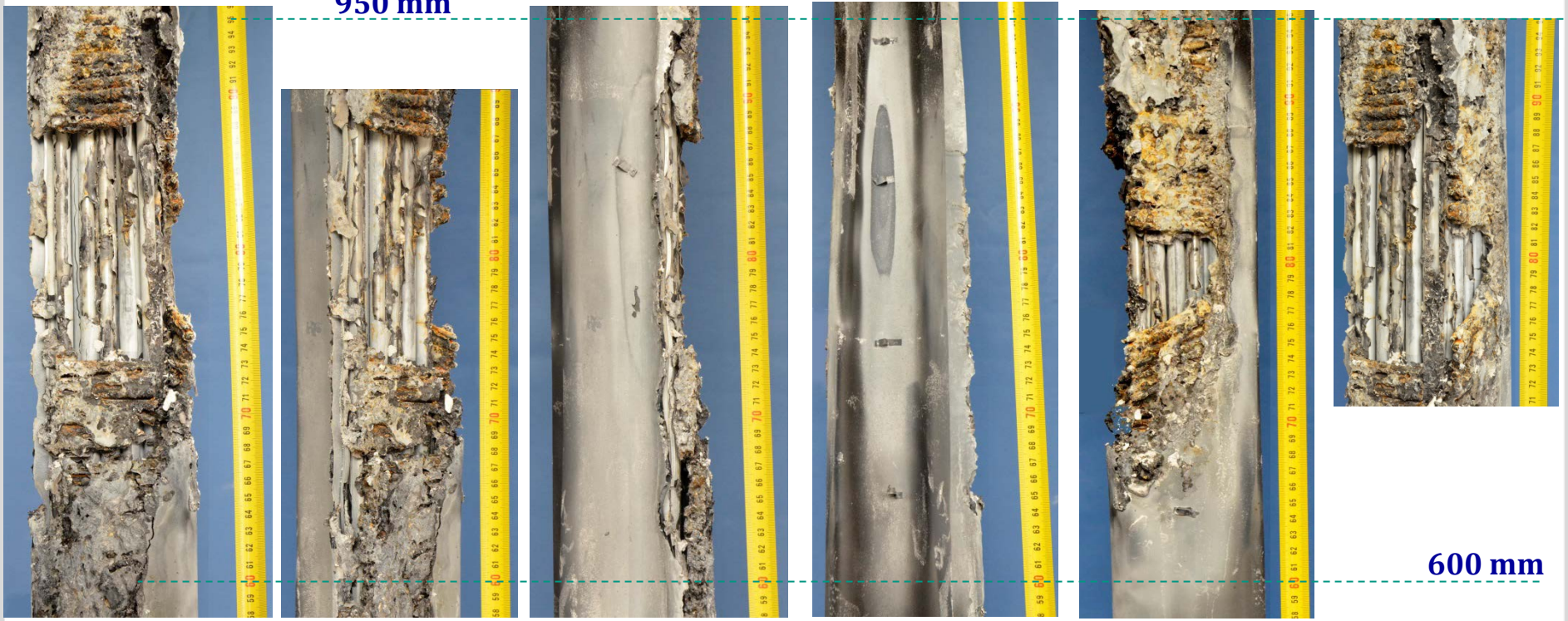
QUENCH-20 bundle surrounded by shroud: post-test view

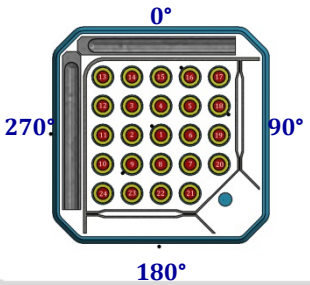




bundle cross-section, top view

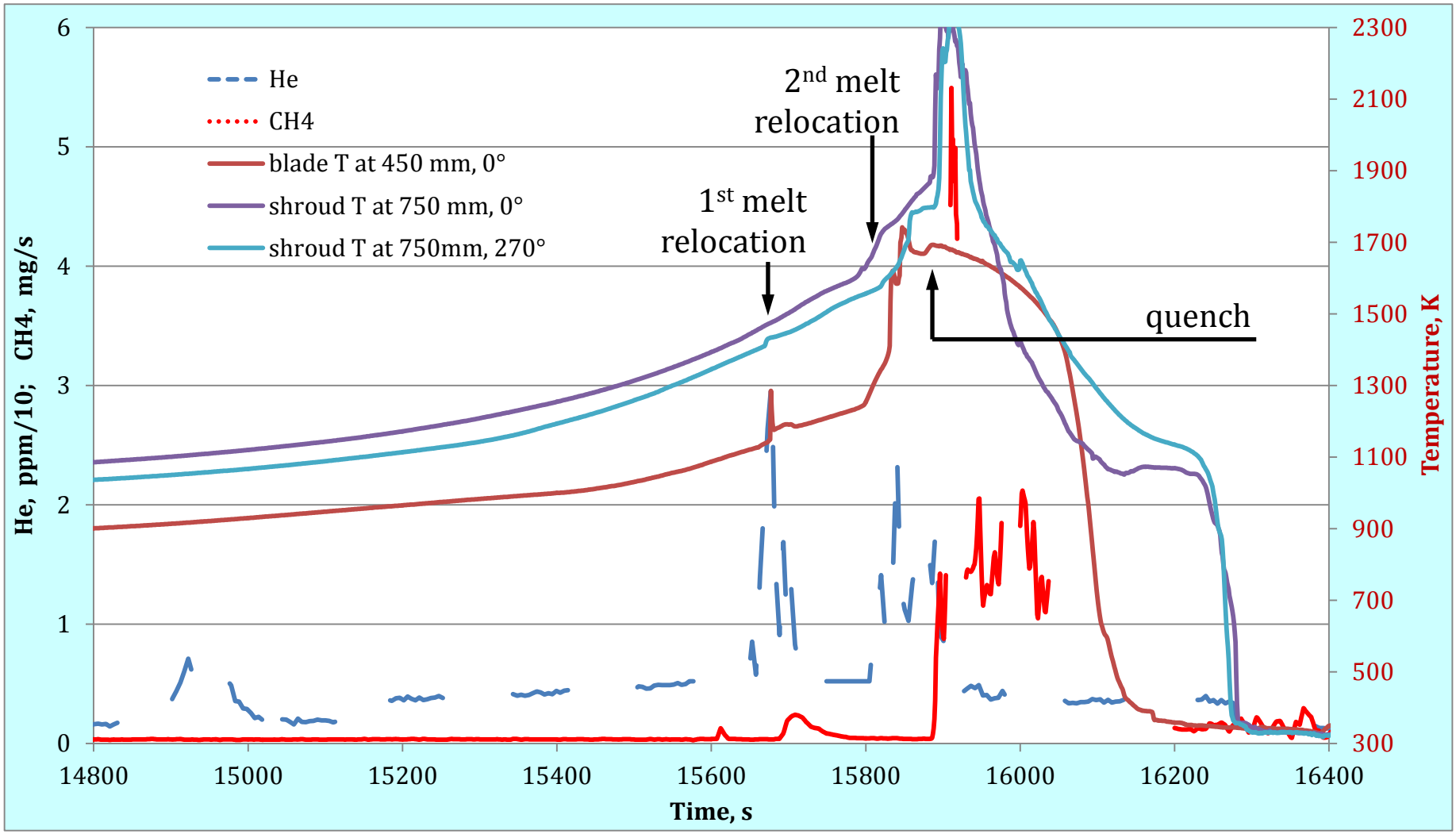
QUENCH-20 bundle surrounded by shroud: post-test view



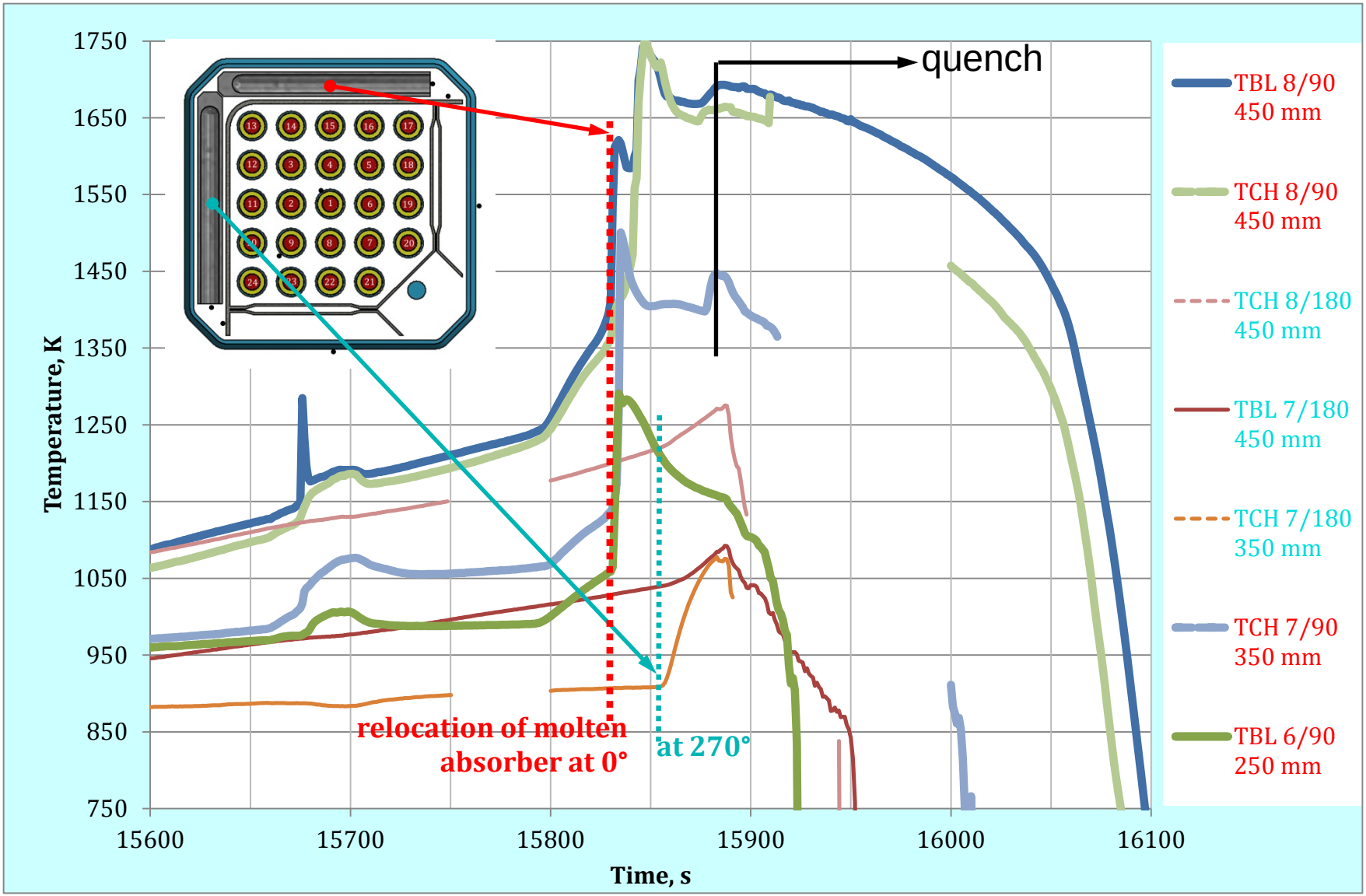


Strong degradation of absorber blades, channel box and shroud between elevations 650 and 950 mm at angle positions 0° and 270°

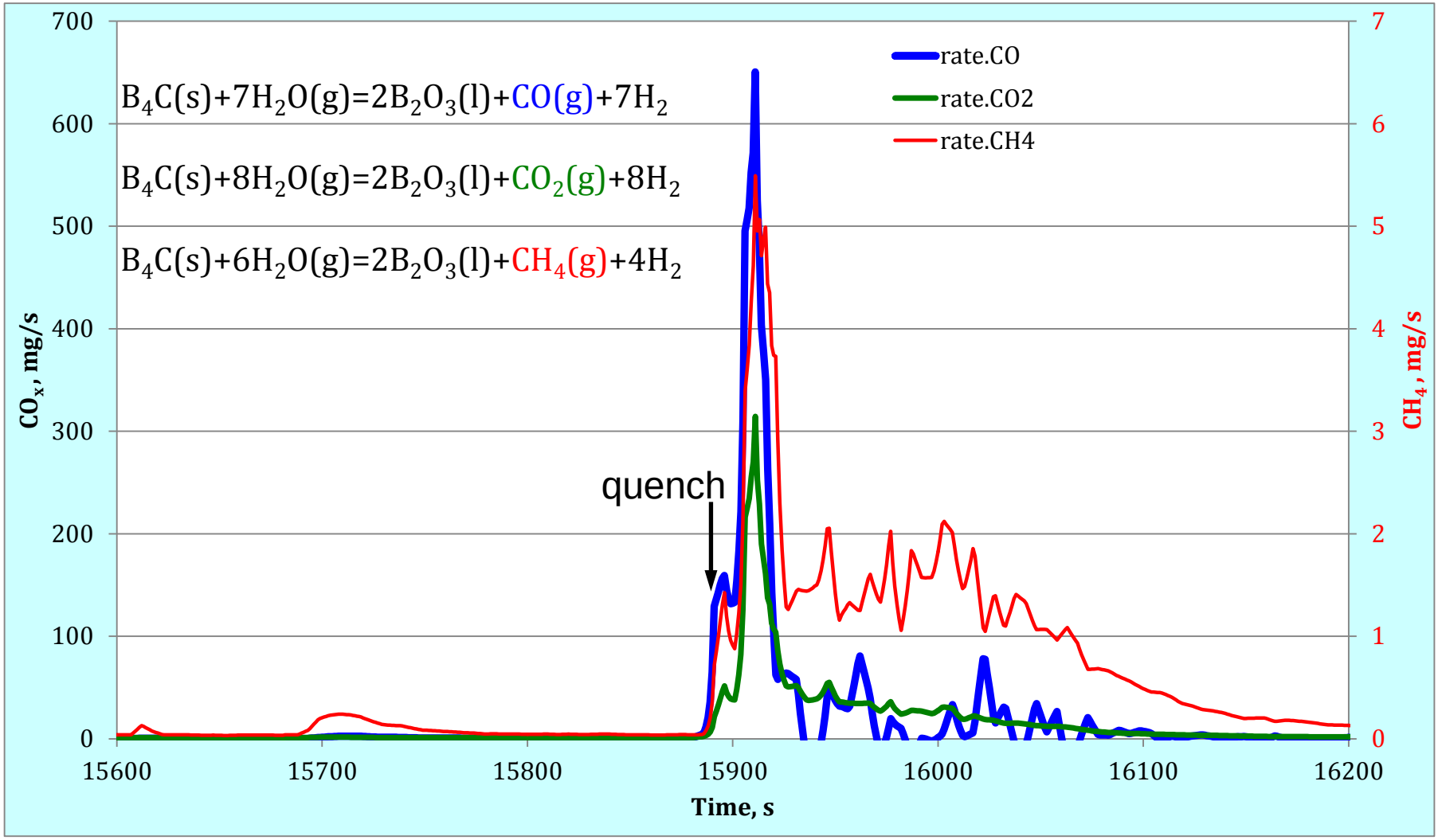
QUENCH-20: absorber melt formation at above 750 mm and relocation to lower elevations



QUENCH-20: absorber melt relocation from hottest bundle elevations to elevations 250-450 mm

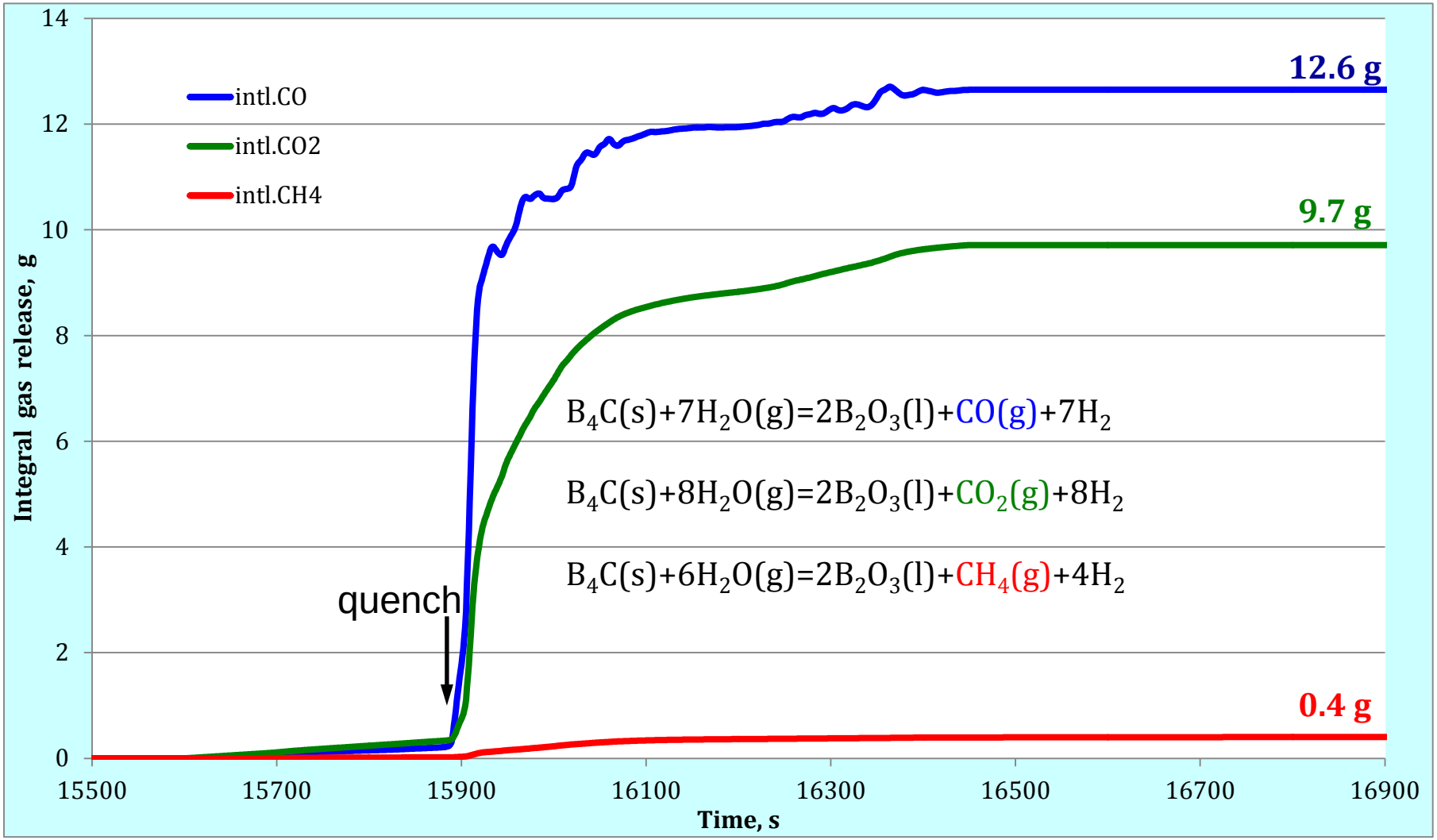


QUENCH-20: reaction of B_4C with steam



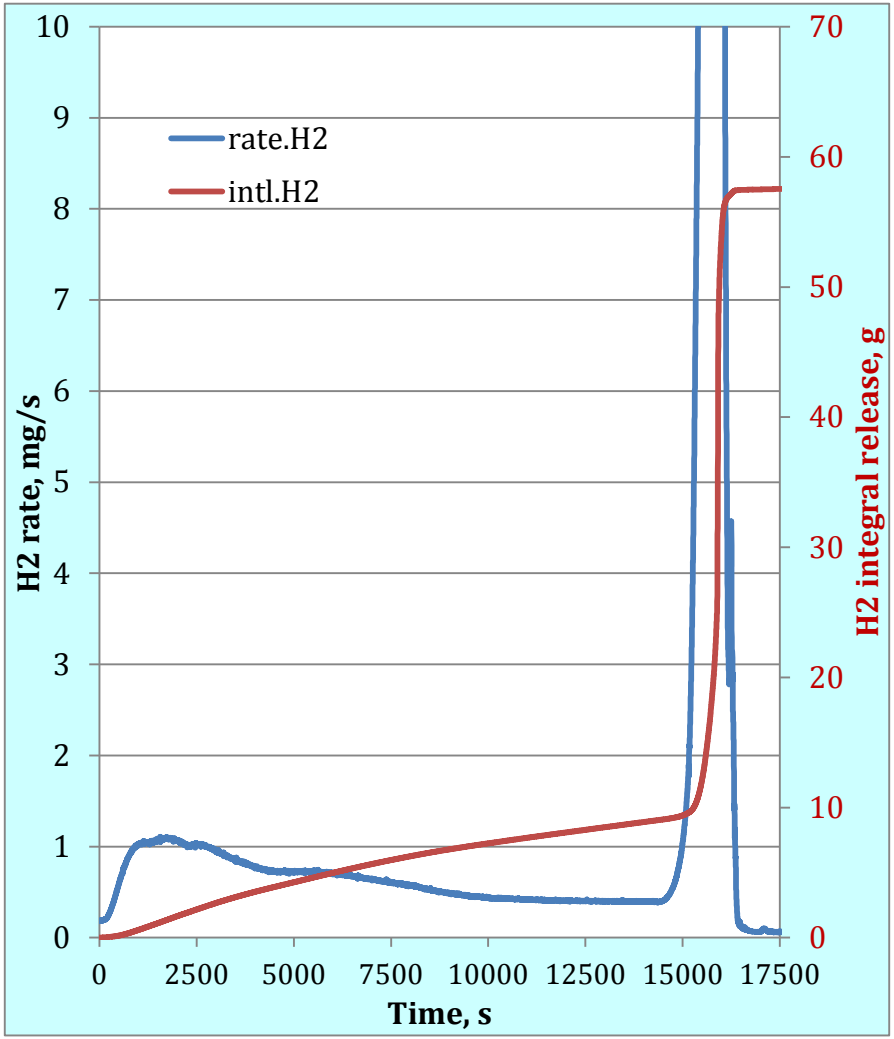
only small release of CH_4 before quench; CO and CO_2 formation firstly in the quench stage

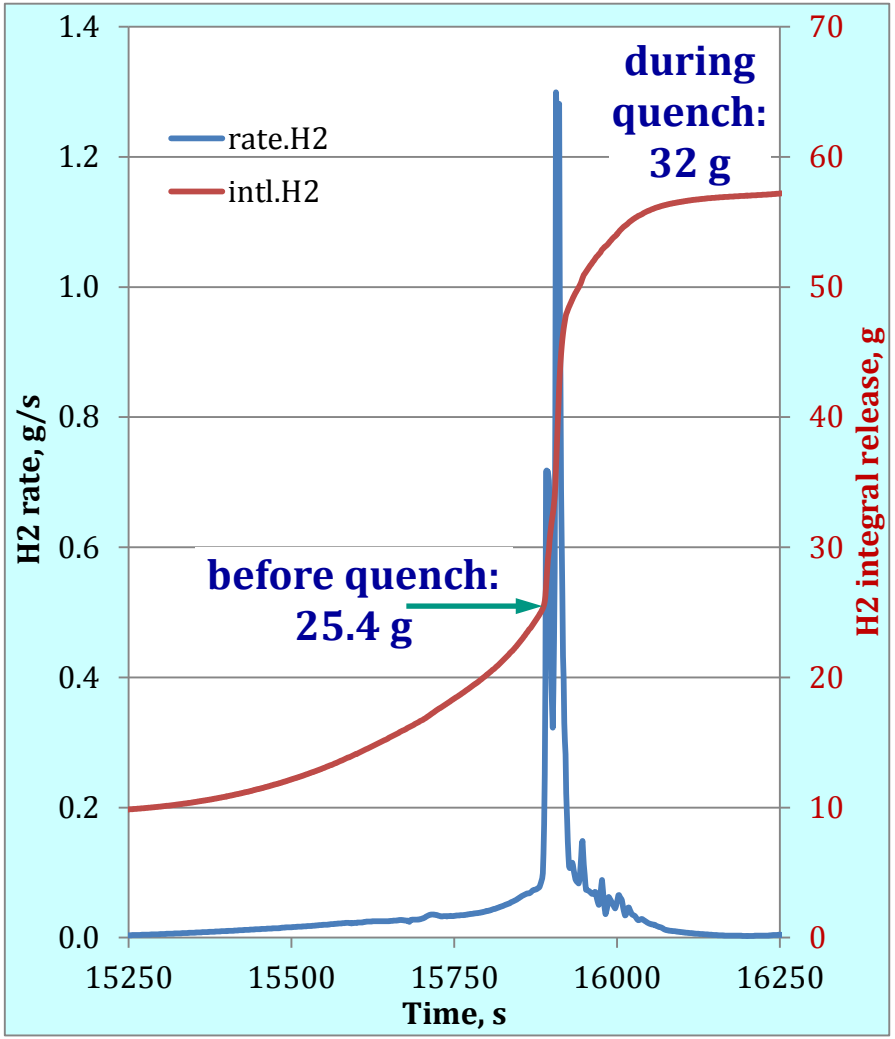
QUENCH-20: reaction of B_4C with steam, integral gas release



According to CO_x and CH_4 release: corresponding mass of B_2O_3 is 96.8 g; H_2 is 10.0 g

QUENCH-20: hydrogen release

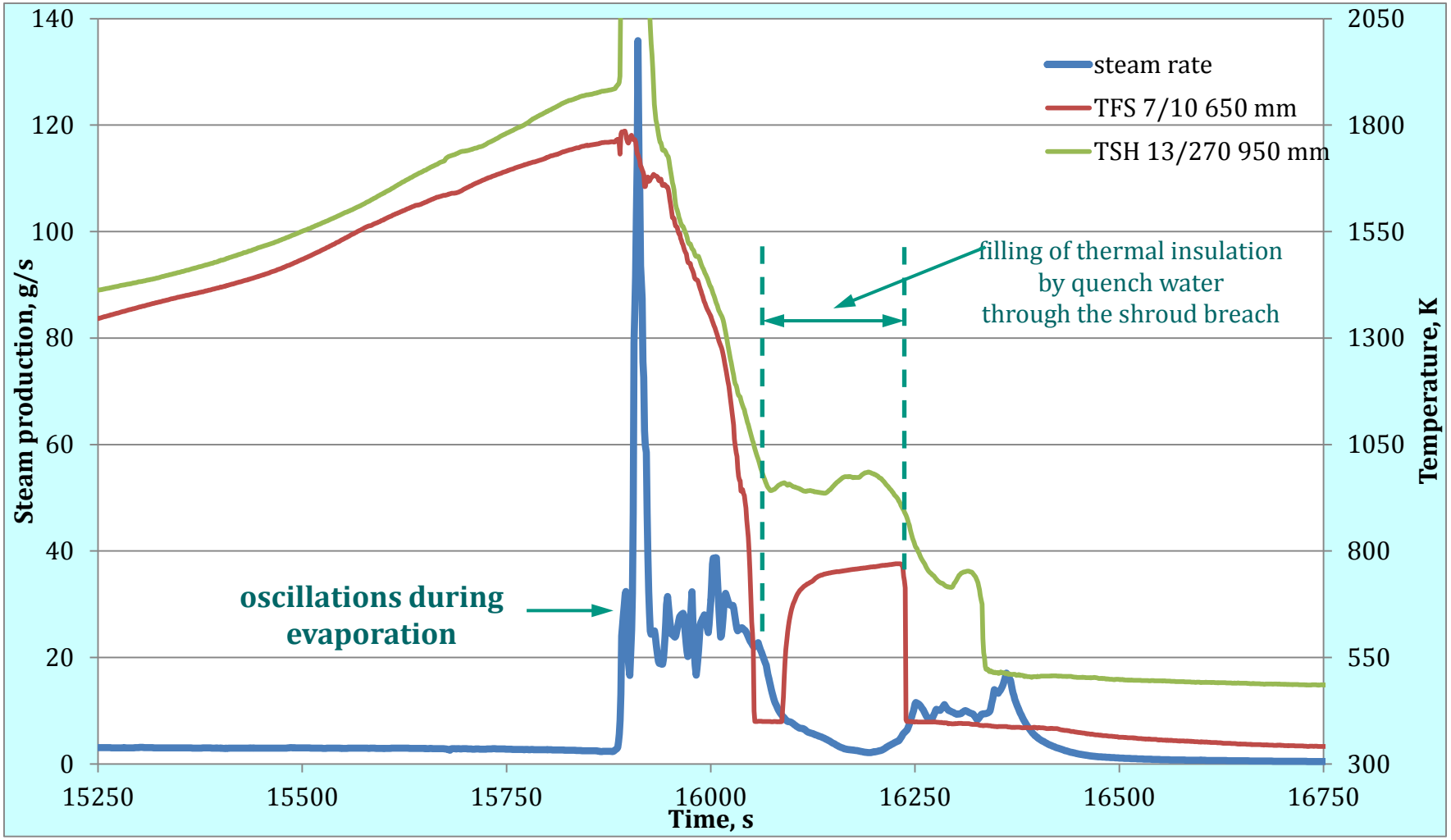




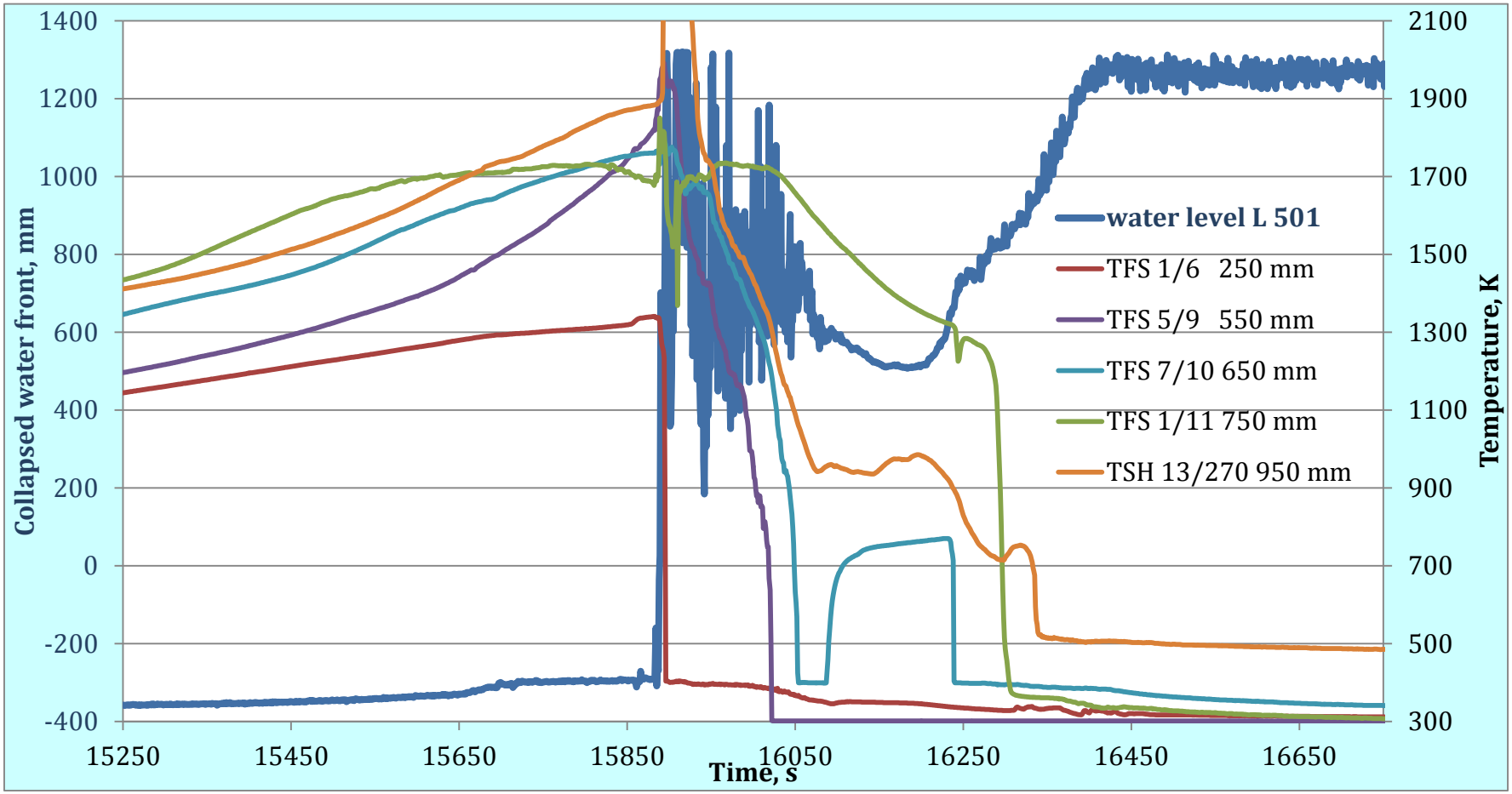
H_2 release during the whole test: 57.4 g;
before quench – interaction of steam with Zry,
during quench – steam interaction with Zry and absorber

H_2 release during quench:
22 g (from Zry and molten steel) +
+ 10 g (from B_4C)

QUENCH-20: steam production during the quench stage



QUENCH-20: filling of bundle with quench water and wetting of thermocouples



delayed cooling of the bundle (>450 s) due to filling of insulation annulus through the shroud breach at ≈550 mm

Summary and conclusions

- Experiment QUENCH-20 with BWR geometry simulation bundle was successfully conducted at KIT on 9th October 2019 in the framework of the international SAFEST project. The test bundle mock-up represented one quarter of a BWR fuel assembly with 24 electrically heated fuel rod simulators and B_4C control blade. The rod simulators were filled with Kr to inner pressure of 6 bar at peak cladding temperature of 900 K.
- The pre-oxidation stage in the flowing gas mixture of steam and argon (each 3 g/s) and system pressure of 2 bar lasted 4 hours at the peak cladding temperature of 1250 K. The Zry-4 corner rod, withdrawn at the end of this stage, showed the maximal oxidation at elevations between 930 and 1020 mm with signs of breakaway.
- During the transient stage, the bundle was heated to a maximal temperature of **2000 K**. *The cladding failures were observed at temperature about 1700 K and lasted about 200 s*. During the period of rod failures also the first absorber melt relocation accompanied by shroud failure were registered. *Massive absorber melt relocation was observed 50 s before the end of transition stage*.
- The test was terminated with the quench water injected with a flow rate of 50 g/s from the bundle bottom. Fast *temperature escalation* from 2000 to **2300 K** during 20 s was observed. The mass spectrometer measured *release of CO (12.6 g), CO_2 (9.7 g) and CH_4 (0.4 g) during the reflood as products of absorber oxidation; corresponding production of B_2O_3 should be 96.8 g .*
- Hydrogen production during the reflood amounted to **32 g** (57.4 g during the whole test) including 10 g from B_4C oxidation.

Acknowledgment

The QUENCH-20 experiment was performed in the framework of the SAFEST project in cooperation with Swedish Radiation Safety Authority (SSM), Westinghouse Sweden, GRS and KTH and supported by the KIT program NUSAFE. Personal thanks to Mr. Isaksson (SSM), Mr. Bechta (KTH), Mr. Hollands (GRS), Ms. Korske (Westinghouse) for their help and fruitful cooperation. The bundle materials and absorbers were provided by Westinghouse Sweden.

The authors would like to thank all colleagues involved in the pre-test calculations.

Thank you for your attention

http://www.iam.kit.edu/awp/666.php
http://quench.forschung.kit.edu/

25. International QUENCH Workshop, 22-24 Oct 2019, KIT, Karlsruhe, Germany

25 years QUENCH program. Highlights of separate-effects tests

Martin Steinbrück, Juri Stuckert, Mirco Große et al.

The main objective of the QUENCH program at KIT is the investigation of the hydrogen source term and materials interactions during LOCA and the early phase of severe accidents including reflood. Bundle experiments as well as separate-effects tests are conducted to provide data for the development of models and the validation of severe fuel damage code systems.

In the framework of the QUENCH jubilee session highlights of 25 years separate-effects tests were presented in this talk. The focus of the QUENCH SETs are clearly on high-temperature (> 600°C) oxidation and materials interactions of zirconium alloys (cladding), absorber materials, and structure materials in well-defined atmospheres. In this context, hydrogen release and uptake by the Zr alloy cladding materials was investigated as well. More recent experiments concentrated on the high-temperature behavior of new ATF cladding materials.

The main takeaways from this presentation were:

- Zirconium oxidation at high temperatures is a source of significant release of hydrogen and heat affecting nuclear accident progression.
- Oxidation is not always of parabolic kinetics and may be strongly dependent on experimental boundary conditions.
- Eutectic interactions may lead to melt formation far below the melting points of the individual materials. These melts may slowly relocate and severely oxidize.
- ATF claddings could strongly decrease the risk of temperature escalation and hydrogen detonation during BDB accidents as well as significantly increase the coping time for AMMs.
- Most experimental results were used to improve models, especially in cooperation with IBRAE, GRS, and IRSN as well as internally by H. Steiner and M. Große.



Karlsruhe Institute of Technology

Institute for Applied Materials

25 years QUENCH program. Highlights of separate-effects tests

M. Steinbrück, J. Stuckert, M. Große et al.

25th International QUENCH Workshop, Karlsruhe, 22-24 October 2019

Institute for Applied Materials IAM-AWP & Program NUSAFE





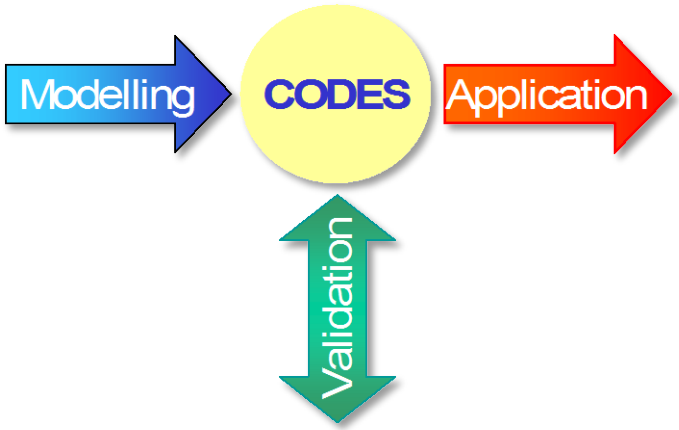


QUENCH program at KIT

Investigation of hydrogen source term and materials interactions during LOCA and early phase of severe accidents including reflood



Separate-effects tests



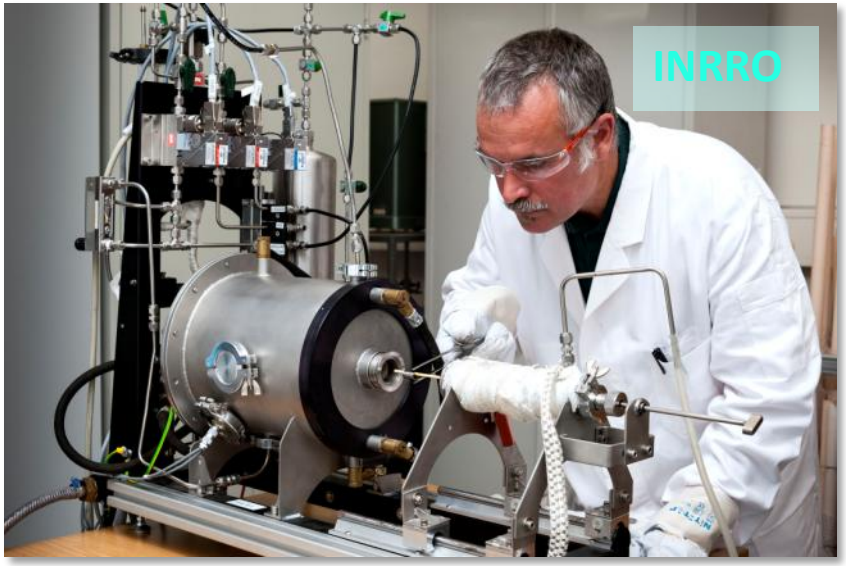


Bundle experiments

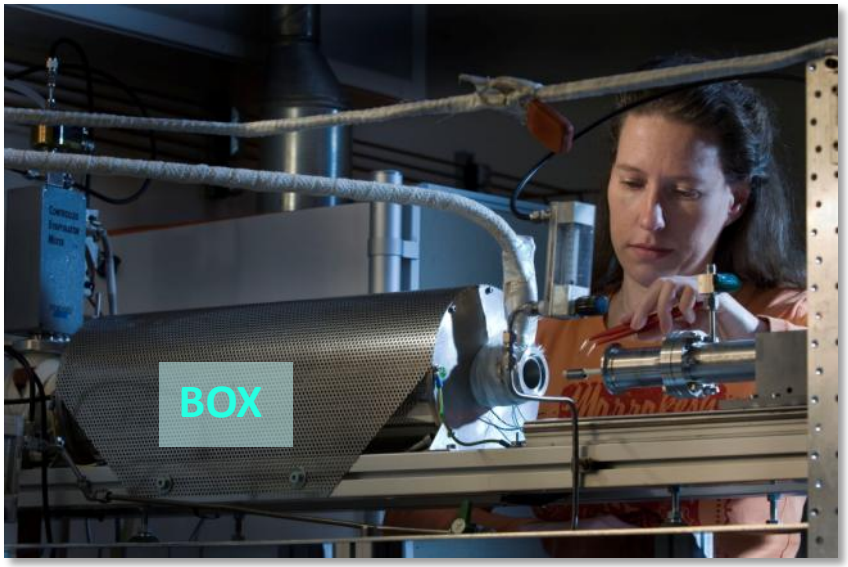


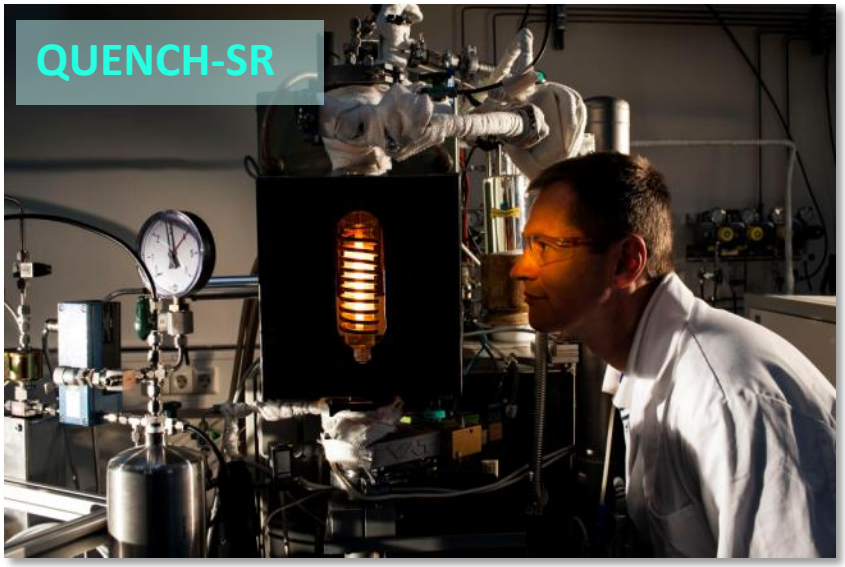
PWR fuel element

QUENCH separate-effects tests: Main setups









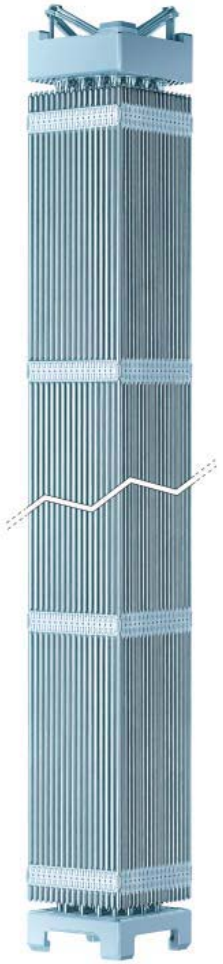
Core materials in Light Water Reactors

- UO_2(/PuO_2) fuel: 100-200 t
- Zry cladding + grid spacers: 20-40 t
- Zry canister (BWR): 40 t
- Various steels, Inconel: >500 t (incl. RPV)
- B_4C absorber (BWR, VVER, …): 0.3-2 t
- AgInCd absorber (PWR): 3-5 t

Environment

- **Water, steam**
- Air
- Nitrogen

} After failure of RPV/primary circuit and in spent fuel pool



PWR fuel assembly



BWR control blade

Topics

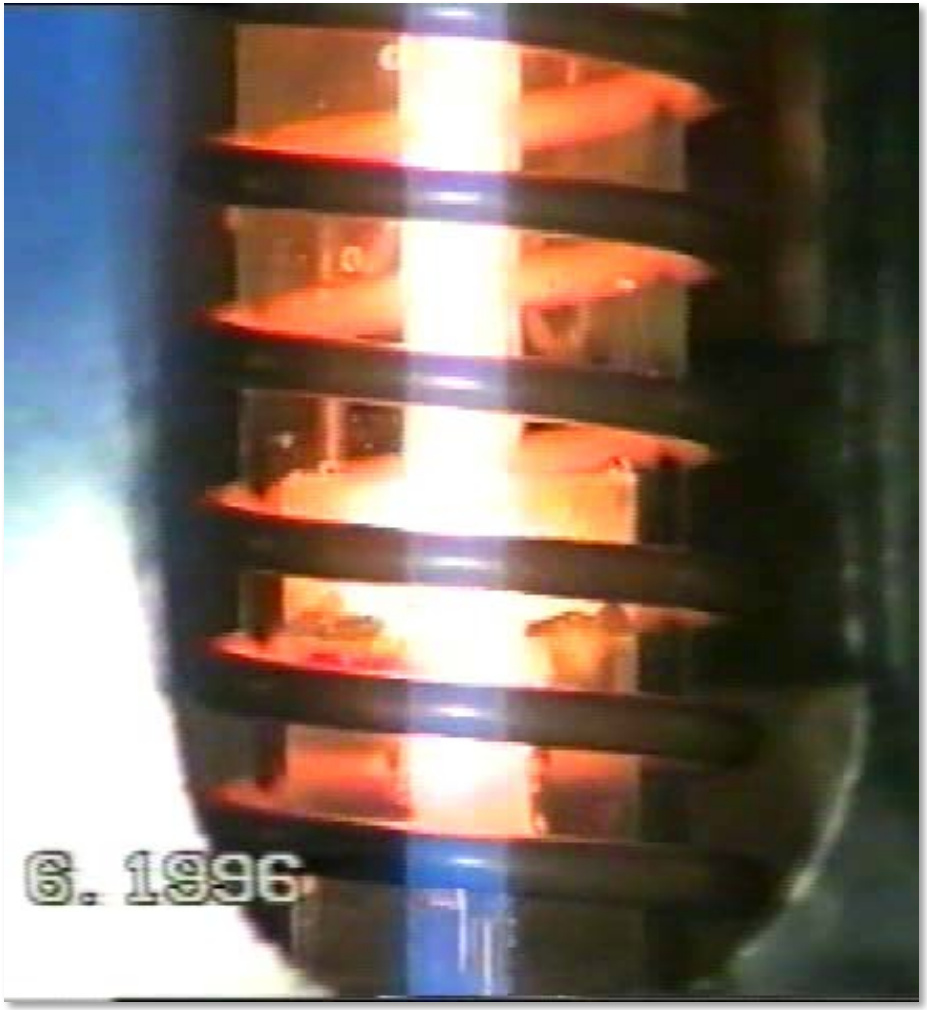
- Generally, high-temperature (> 600°C) oxidation and materials interactions of zirconium alloys (cladding), absorber materials, and structure materials in well-defined atmospheres
- Quenching of pre-oxidized cladding
- Oxide shell failure criterion
- Interaction between Zr melt and ZrO_2 (UO_2) ceramic
- Zr alloy oxidation in steam, oxygen, air, mixtures
- Hydrogen release and absorption
- B_4C absorber rod oxidation degradation
- AgInCd absorber rod failure
- ATF cladding materials
- …

➢ SETs were made mostly in connection with corresponding bundle tests

Early experiments

Single-rod QUENCH tests

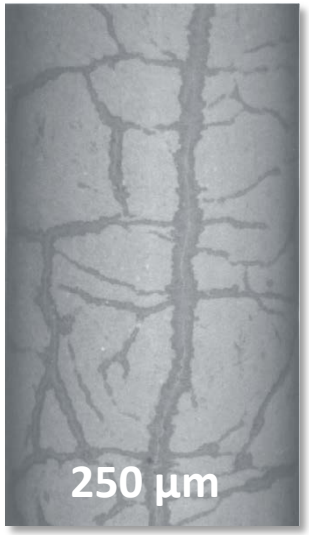
- 15-cm rods filled with ZrO_2 pellets
- Direct inductive heating
- Video recording
- Mass spectrometer for analysis of hydrogen release
- Parameters:
  - Pre-oxidation 0-350 µm
  - 1000-1600°C at onset of quenching
  - Quenching with hot/cold water or steam
  - Flooding rate 1.5 cm/s



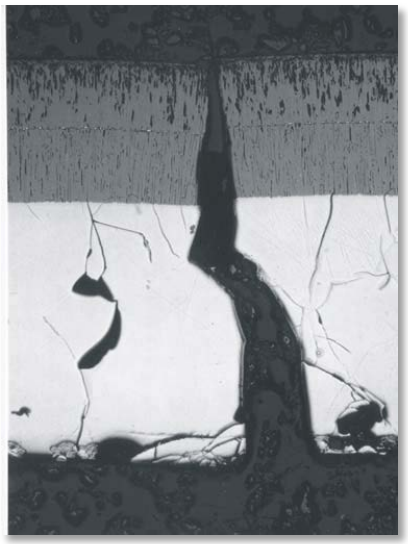
Reflood from 1400°C

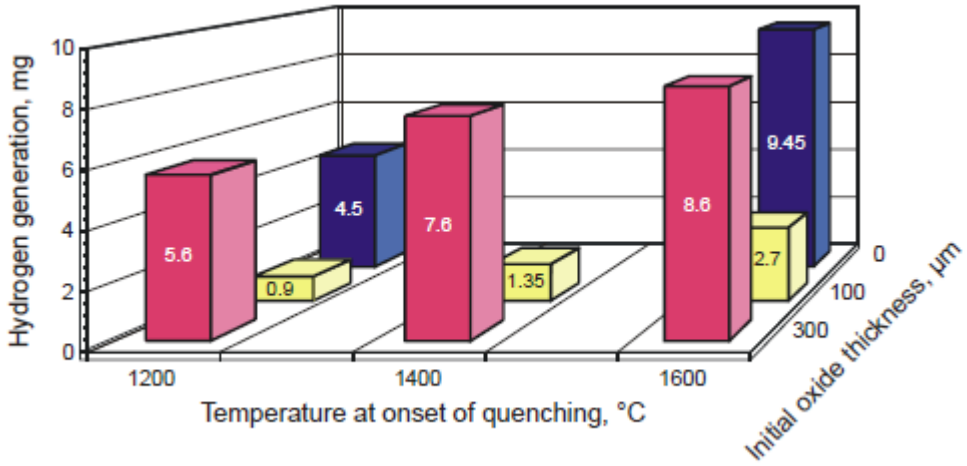
Single-rod QUENCH tests – Main results

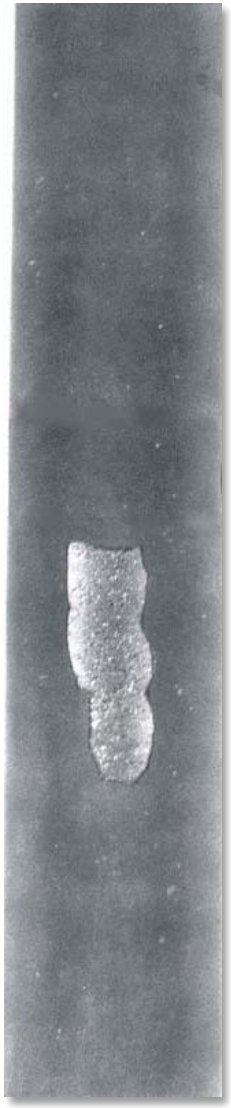




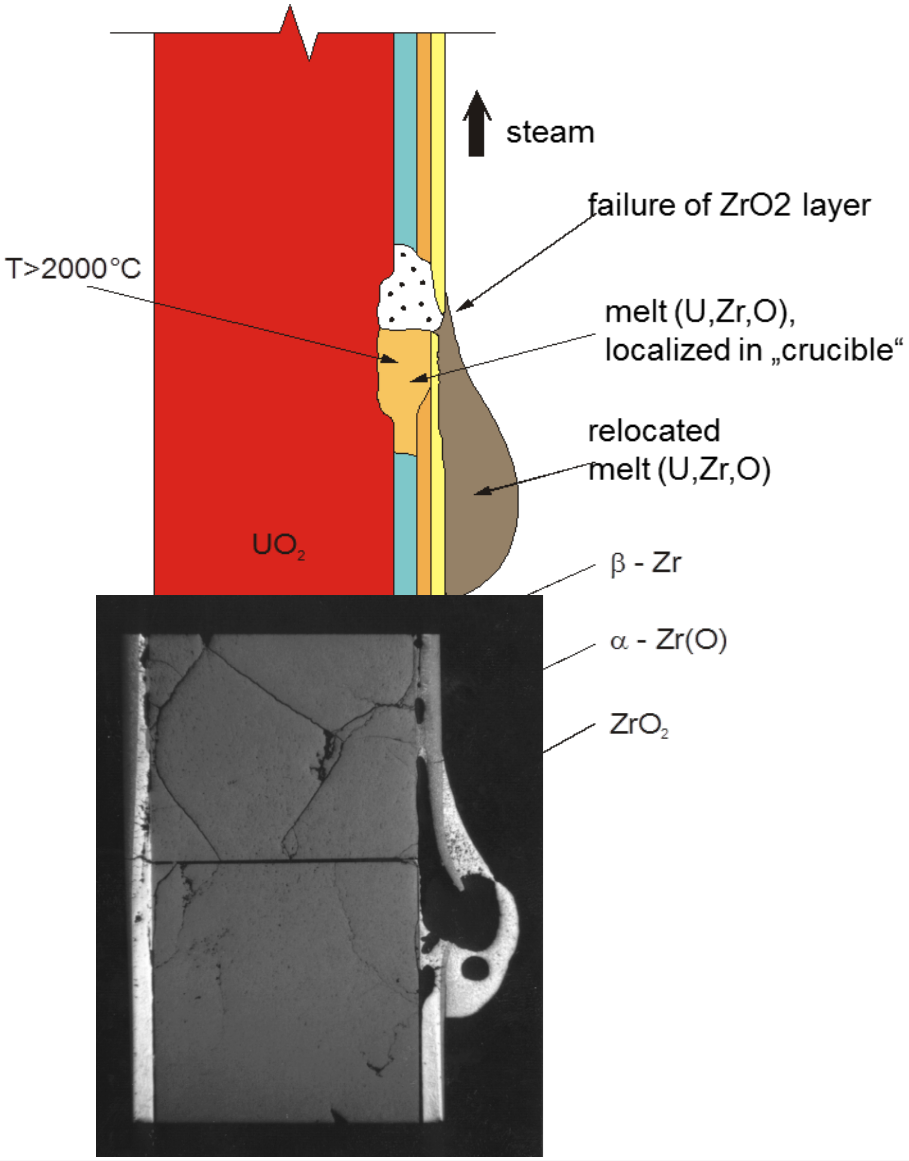
- Through-wall crack for pre-oxidation >200 µm with a density of 0.5 mm/mm²
- Oxidation of crack surfaces connected with hydrogen absorption by the metal
- Localized spalling of thick oxide scales

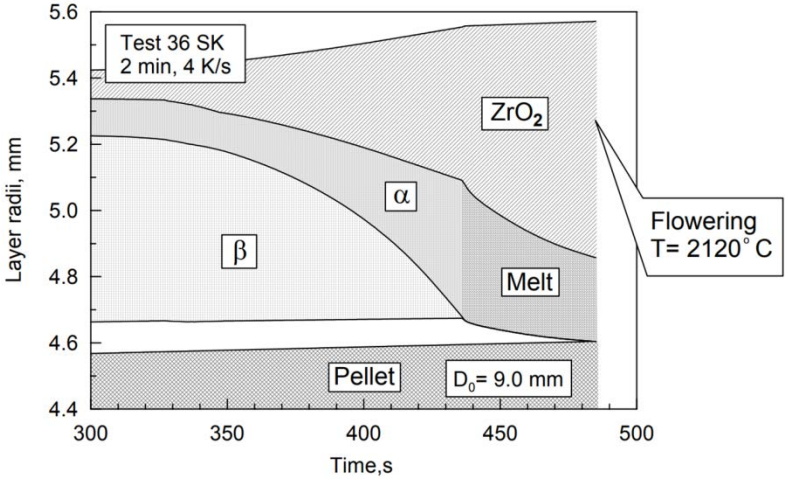




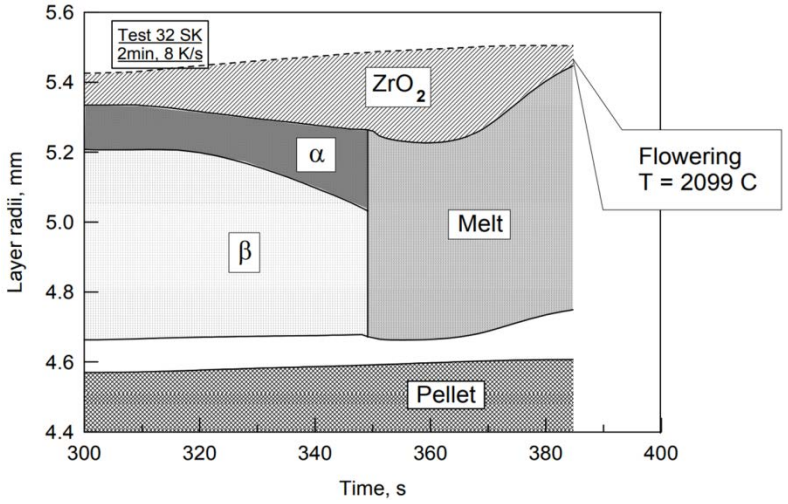


Oxide shell failure



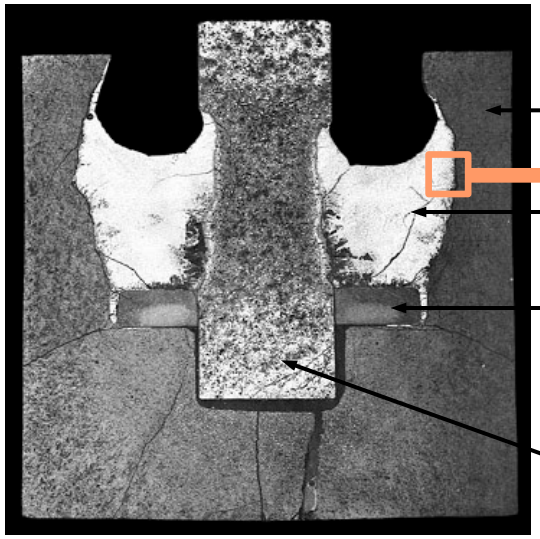


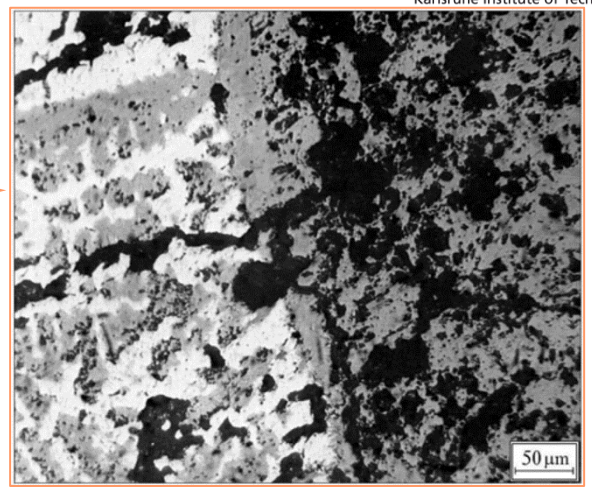
SVECHA simulation: slow heating



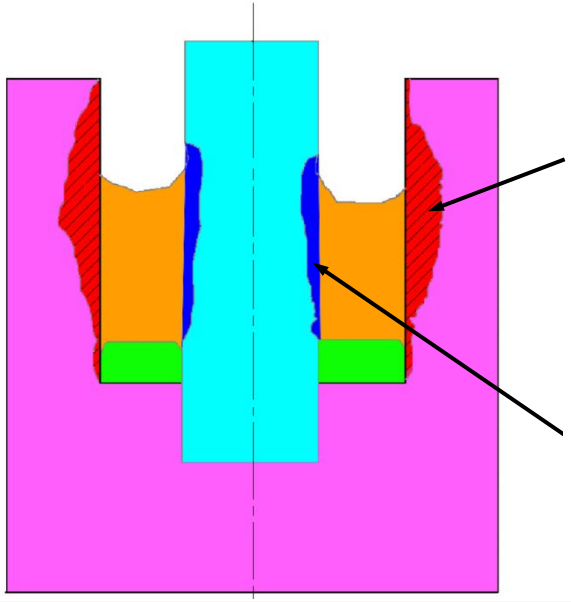
SVECHA simulation: rapid heating

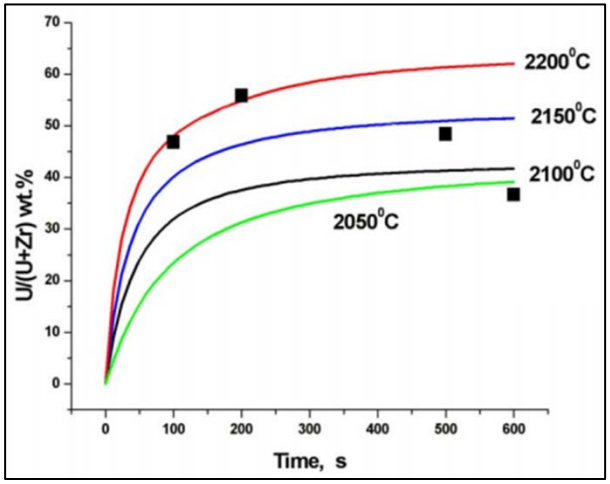
UO_2/ZrO_2 dissolution by Zr melt (COLOSS project)





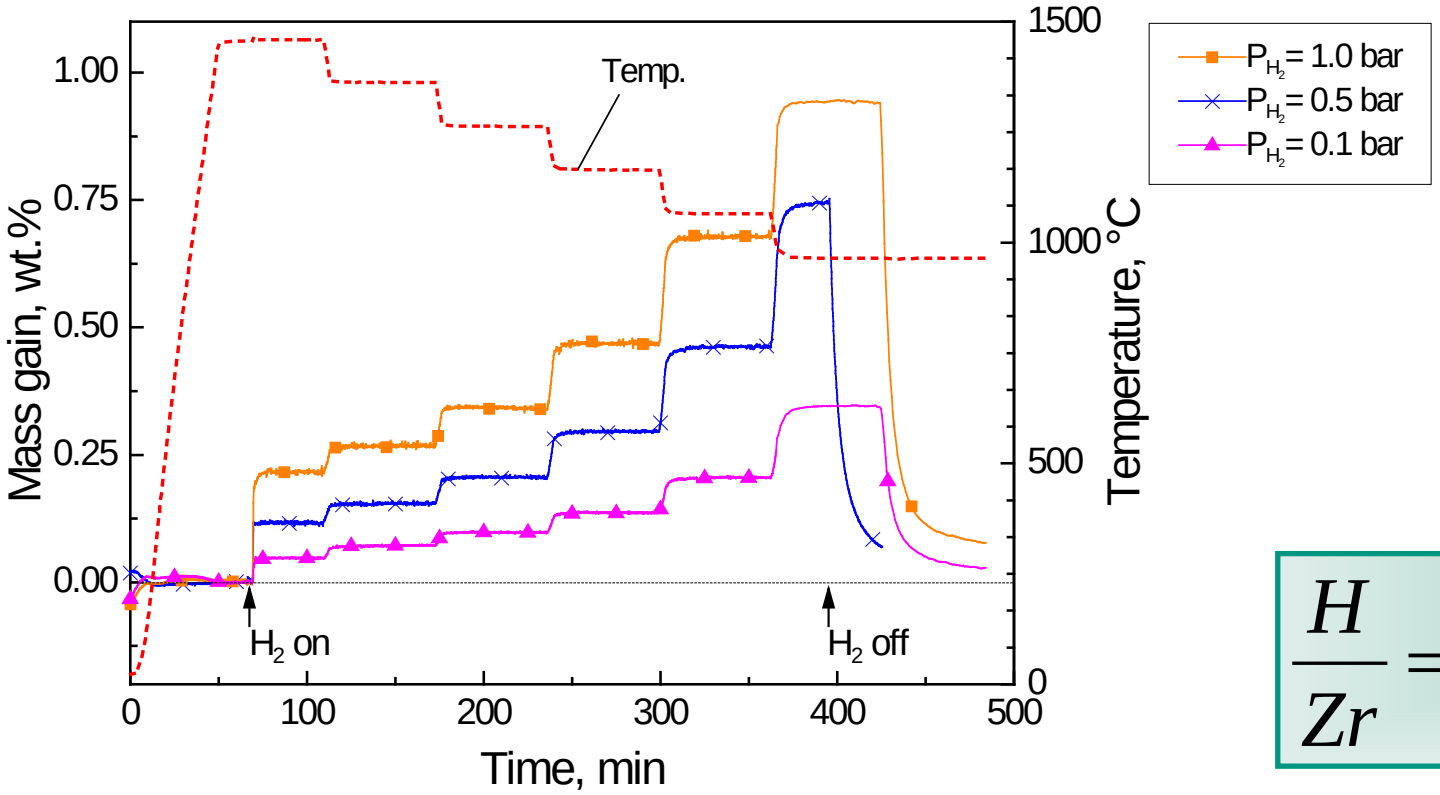
$(U, Zr)O_{2-x}$ precipitates in melt and transition zone between melt and crucible





SVECHA simulation: calculated and measured U content in the melt

Hydrogen uptake of Zircaloy-4

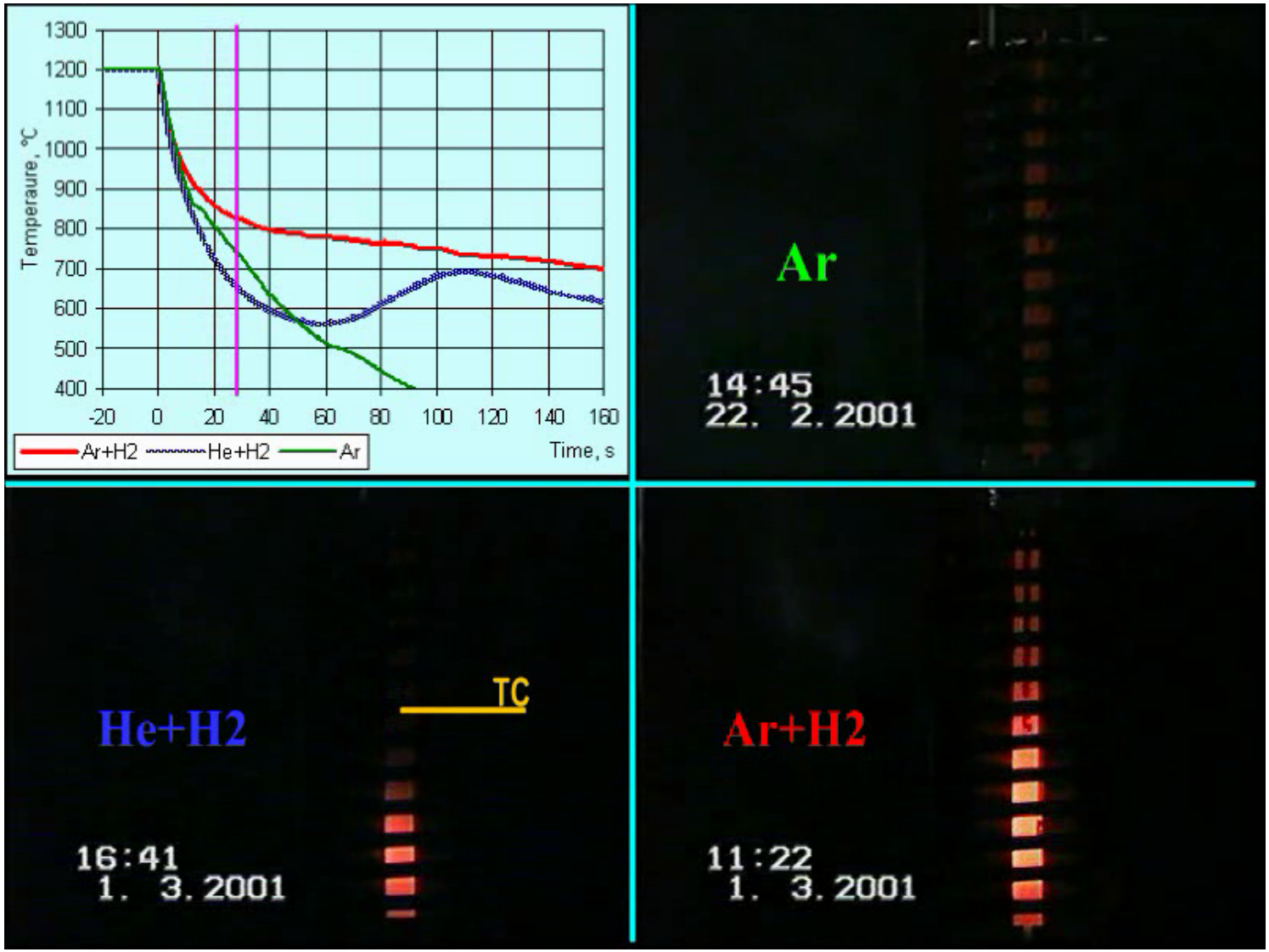


$$\frac{H}{Zr} = k_S \cdot \sqrt{P_{H_2}}$$

Sieverts' law

- Sieverts' law constant determined
- No difference between Zry-4 and M5®
- Reduced H solubility with increasing O content in the metal
- Fast establishment of equilibrium

Exothermal effect of hydrogen uptake



Oxidation of zirconium alloys and hydrogen behavior

High-temperature oxidation of zirconium alloys

- Most cladding alloys consist of 98-99 wt% zirconium plus some alloying elements (Sn, Nb, Fe, Cr, …)

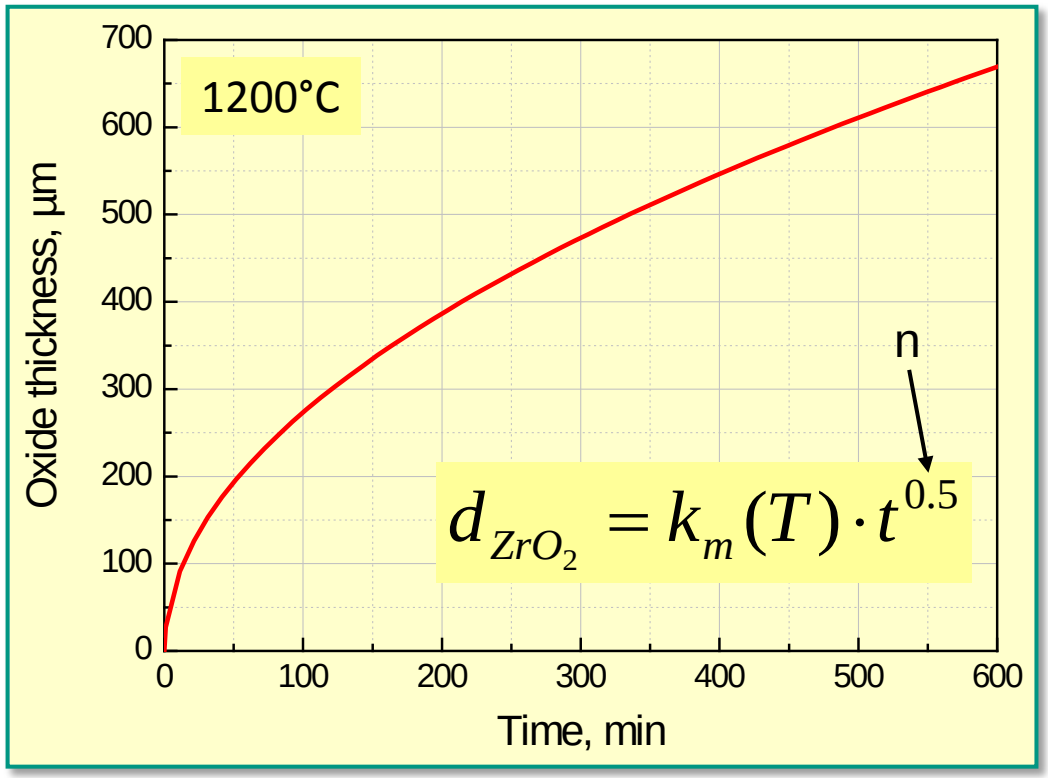
Element	Zircaloy-4	D4	M5	E110	ZIRLO
Nb	-	-	**1**	**1**	**1**
Sn	**1.5**	**0.5**	0.01	**-**	**1**
Fe	0.2	**0.5**	0.05	0.008	0.11
Cr	0.1	0.2	0.015	0.002	< 0.01

- In steam, oxygen, nitrogen, air, and various mixtures
- Temperature: 600-1600°C

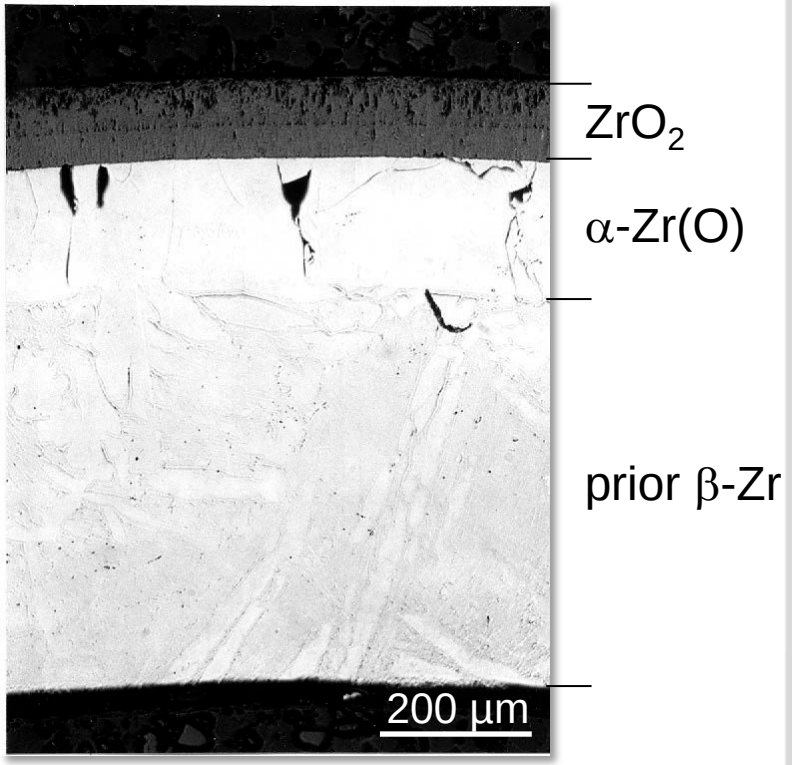


Oxidation in steam (oxygen): Text book knowledge

- Parabolic oxidation correlations determined by the diffusion of oxygen through growing oxide scale



Oxide thickness during oxidation of Zry at 1200°C in steam

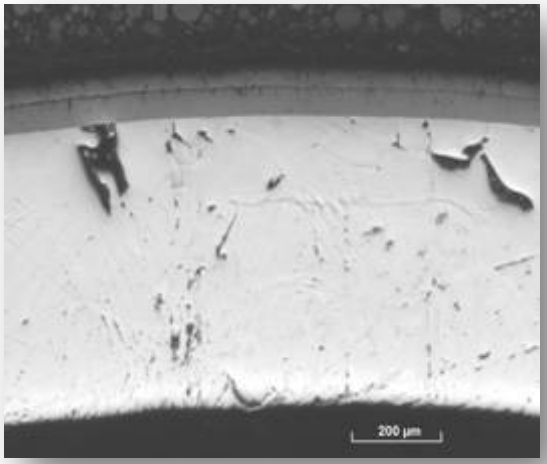


20 min at 1200°C in steam

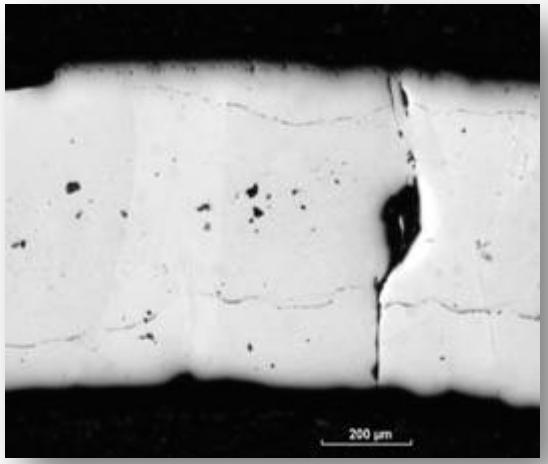
Deviation from parabolic kinetics

- Starvation conditions at low oxidant flow rates
- Cubic (sub-parabolic) kinetics for T < 1000°C (n < 0.5)
- Breakaway (n ≈ 1 after transition)
- Nitrogen (n ≈ 1 after transition)

Steam starvation

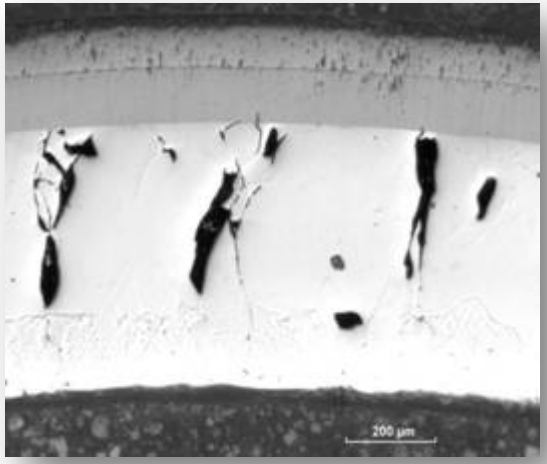


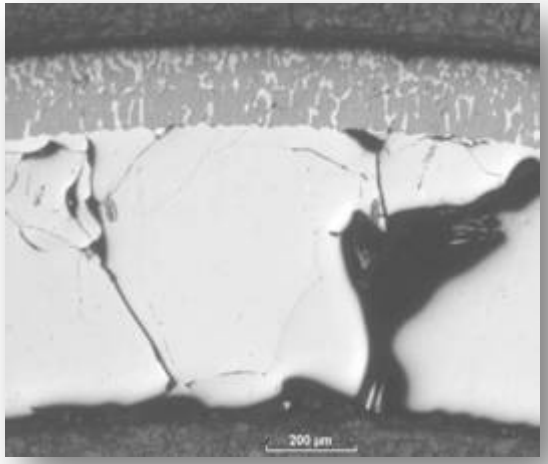
Oxidation



Steam starvation at 1700 K

Dissolution of oxide scale



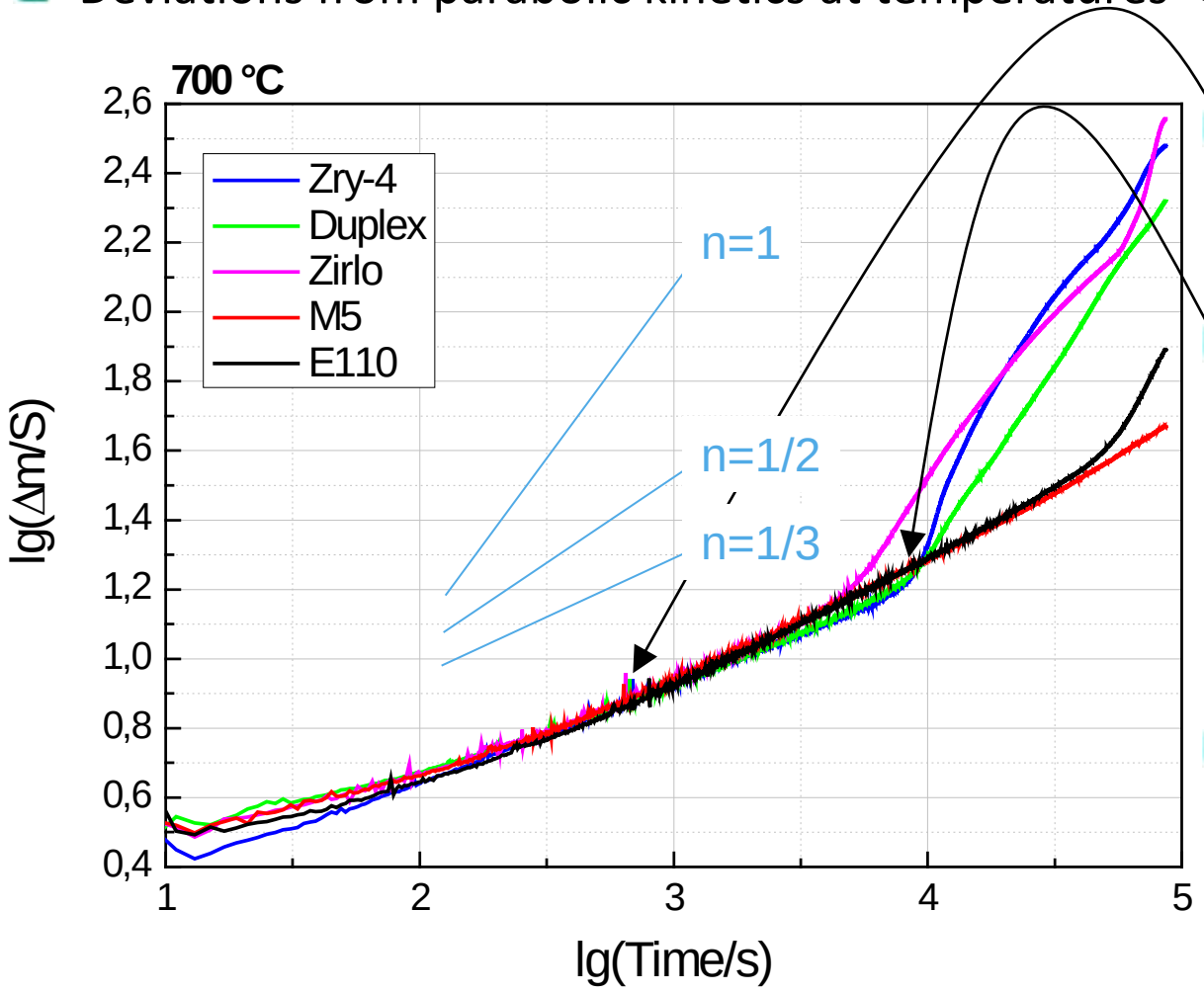


Thinning of oxide scale and precipitation of α-Zr(O) in oxide

- Weakening of protective effect of ZrO_2 oxide layer

Oxidation in steam (oxygen)

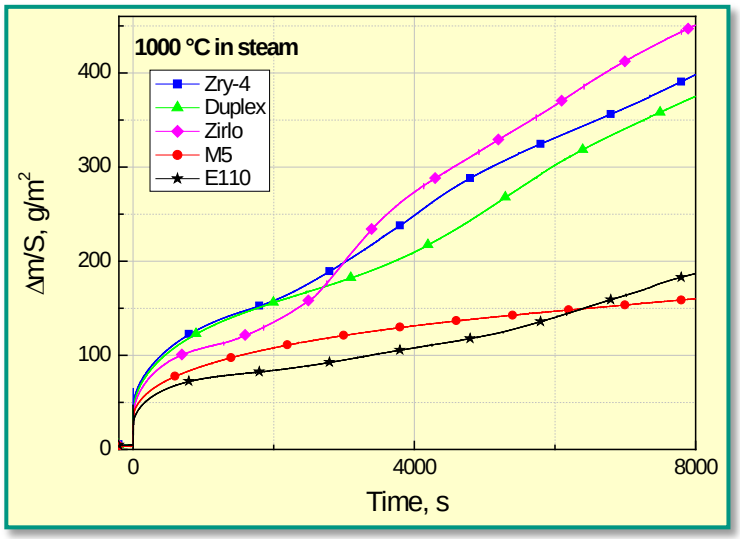
- Deviations from parabolic kinetics at temperatures <1050°C

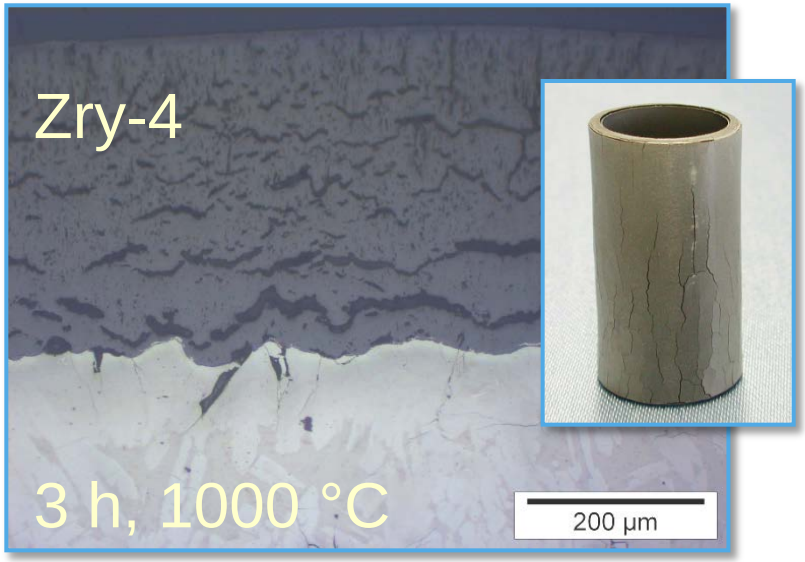


- Sub-parabolic (cubic) kinetics
- Transition from (sub-) parabolic to linear kinetics after critical time / oxide thickness due to breakaway
- Similar kinetics of all alloys before transition, but strongly varying behavior at and after transition

Breakaway oxidation

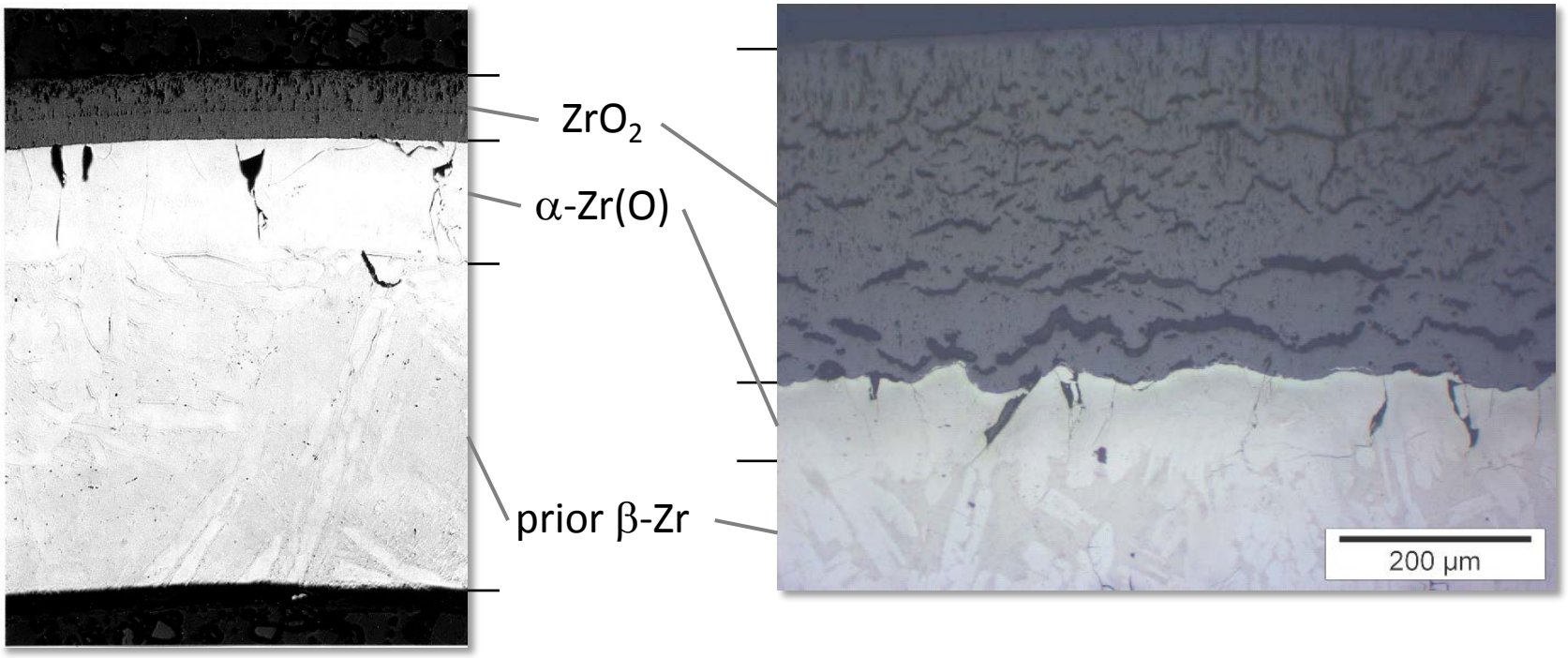
- Loss of protective properties of oxide scale due to its mechanical failure.
- Breakaway is caused by phase transformation from meta-stable tetragonal to monoclinic oxide and corresponding change in density up to ca. 1050°C.
- Critical times and oxide thicknesses for breakaway strongly depend on type of alloy and boundary conditions (30-60 min at 1000°C and 8 h at 600°C).
- During breakaway significant amounts of hydrogen can be absorbed (>40 at.%, 7000 wppm) due to local enrichment of H_2 in pores and cracks near the metal/oxide boundary ("hydrogen pump").





Hydrogen uptake during HT oxidation of Zry in steam

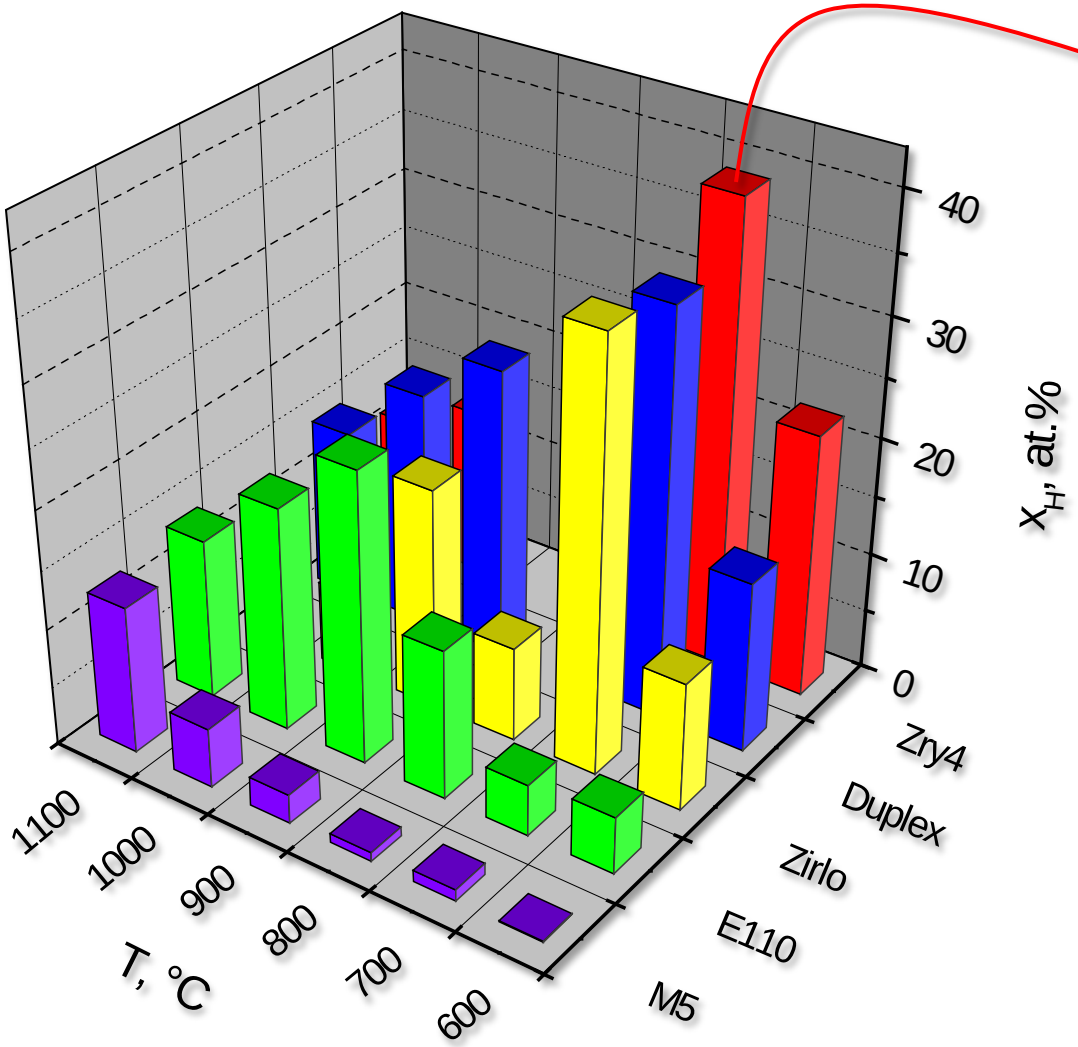
- $Zr + 2H_2O \rightarrow ZrO_2 + 2H_2$
- $H_2(gas) \leftrightarrow 2H(diss)$
- Oxide scale acts as a barrier for uptake and release of hydrogen

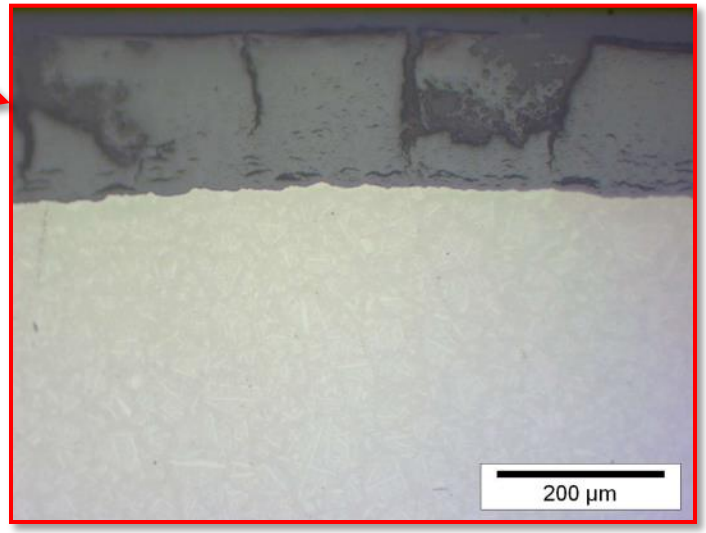


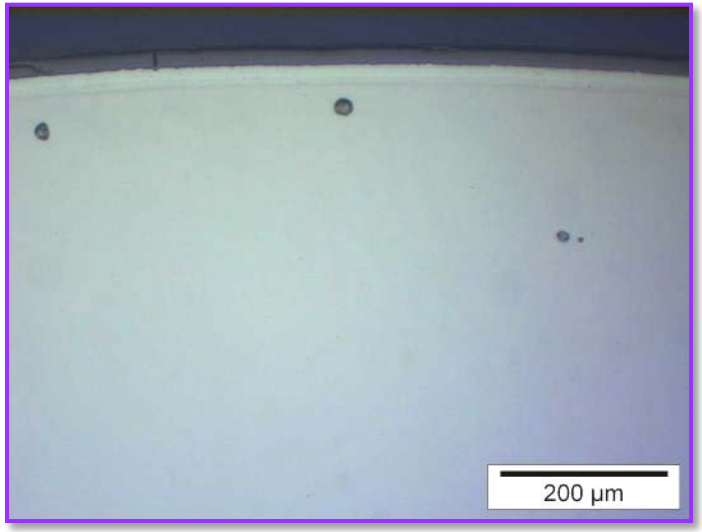
20 min at 1200°C in steam

3h at 1000°C in steam

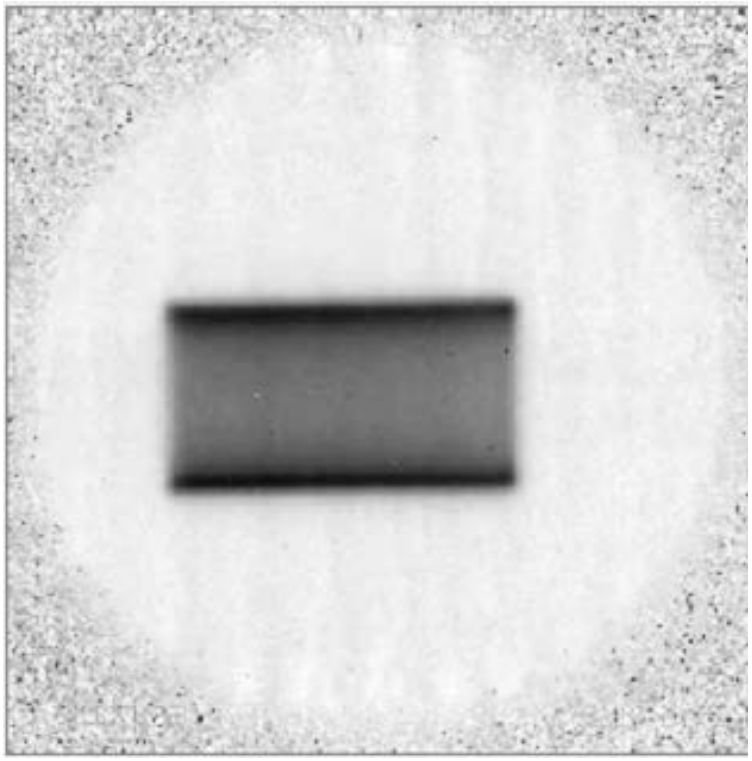
Correlation of H absorption and oxide morphology

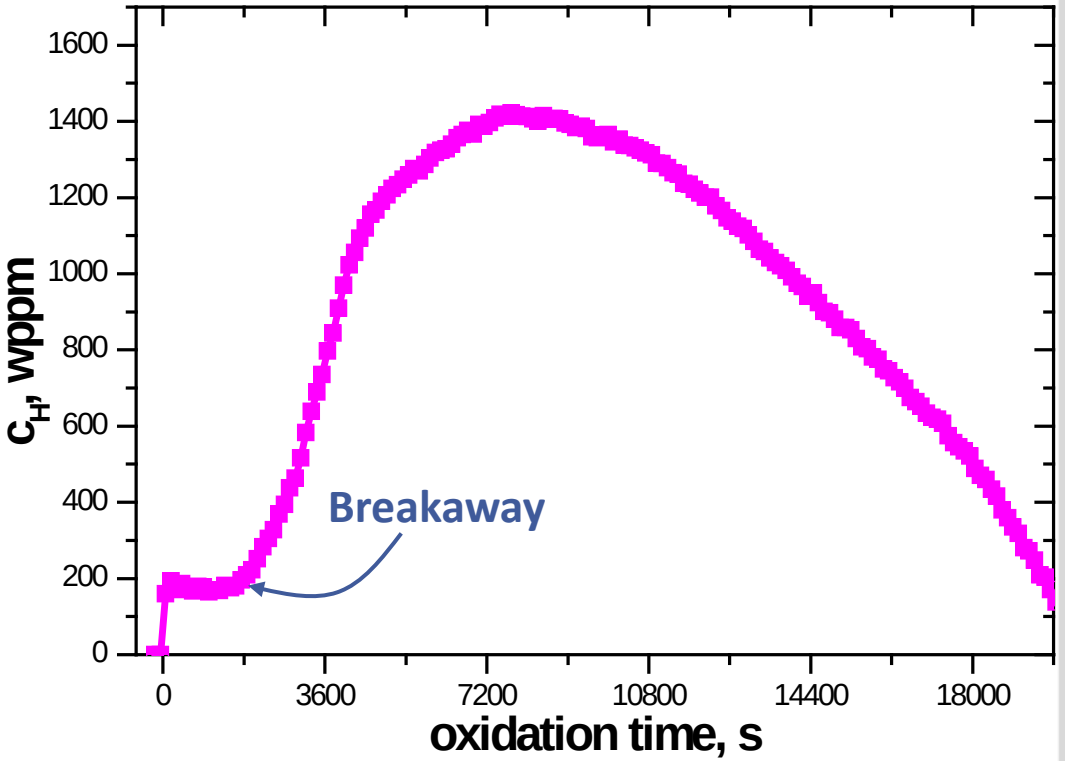






In-situ investigation of hydrogen uptake during oxidation of Zry in steam by neutron radiography





Zry-4, 1000°C
30 g/h steam, 30 l/h argon

- Rapid initial hydrogen uptake
- Further strong hydrogen absorption after transition to breakaway

Oxidation in atmospheres containing nitrogen

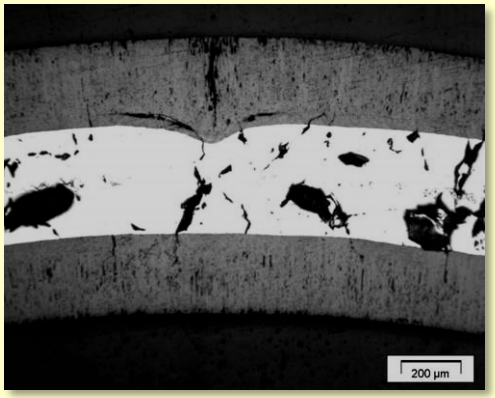
… under prototypical conditions, including

- Pre-oxidation in steam/O_2
- Tests in mixed air(N_2)-steam atmospheres

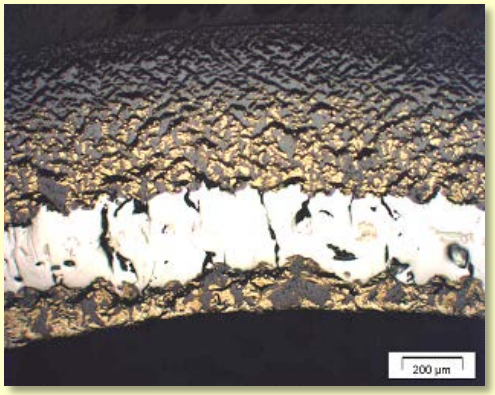
1 hour at 1200 °C in



steam | 50/50 steam/air | air



1.5 h steam

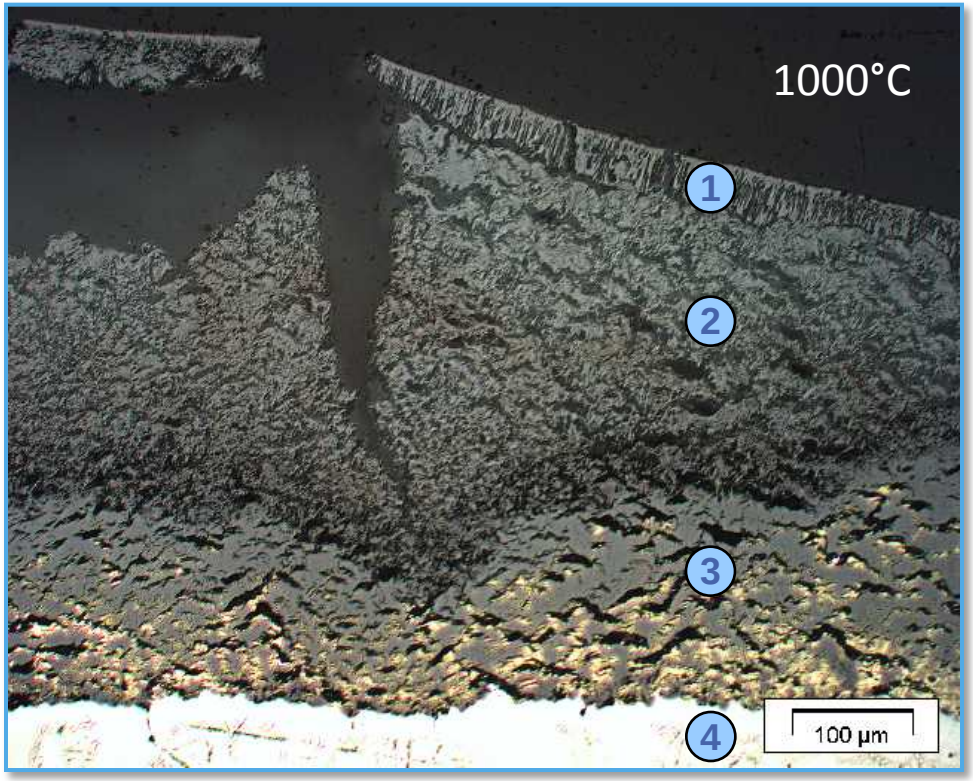


1 h steam/N_2 (50/50)

➧ Loss of barrier effect against FP product release

Mechanism of air oxidation

- Diffusion of air through imperfections in the oxide scale to the metal/oxide interface
- Consumption of oxygen
- Remaining nitrogen reacts with zirconium and forms ZrN
- ZrN is re-oxidized by fresh air with continuing reaction associated with a volume increase by 48%
- Formation of porous and non-protective oxide scales



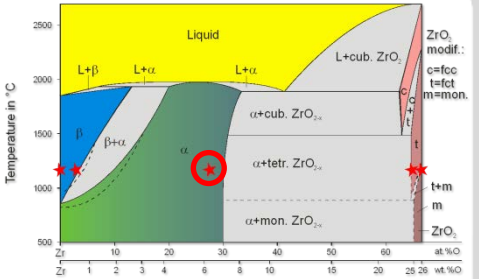
1 – initially formed dense oxide ZrO_2

2 – porous oxide after oxidation of ZrN

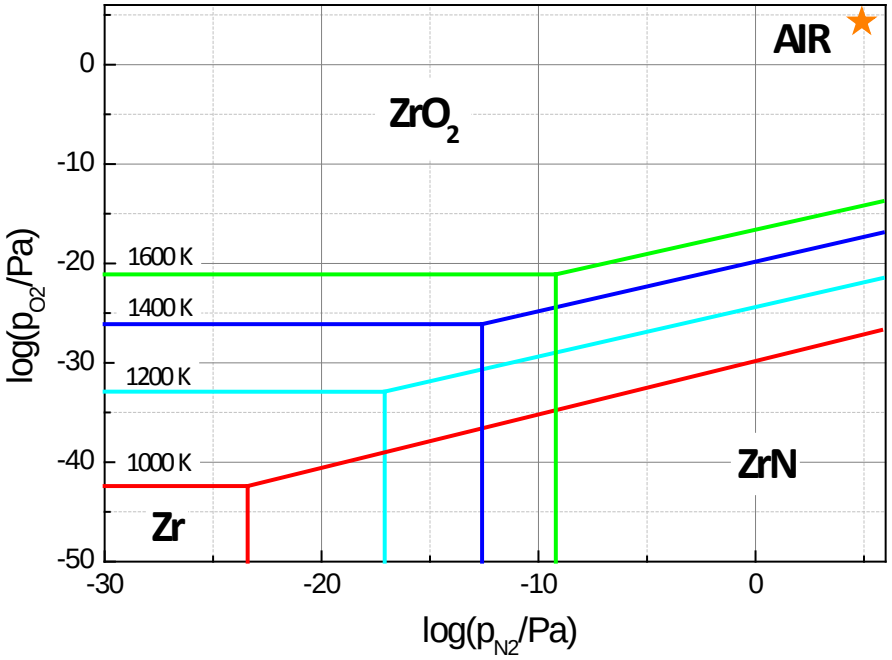
3 – ZrO_2 / ZrN mixture

4 – α-Zr(O)

Mechanism of air oxidation

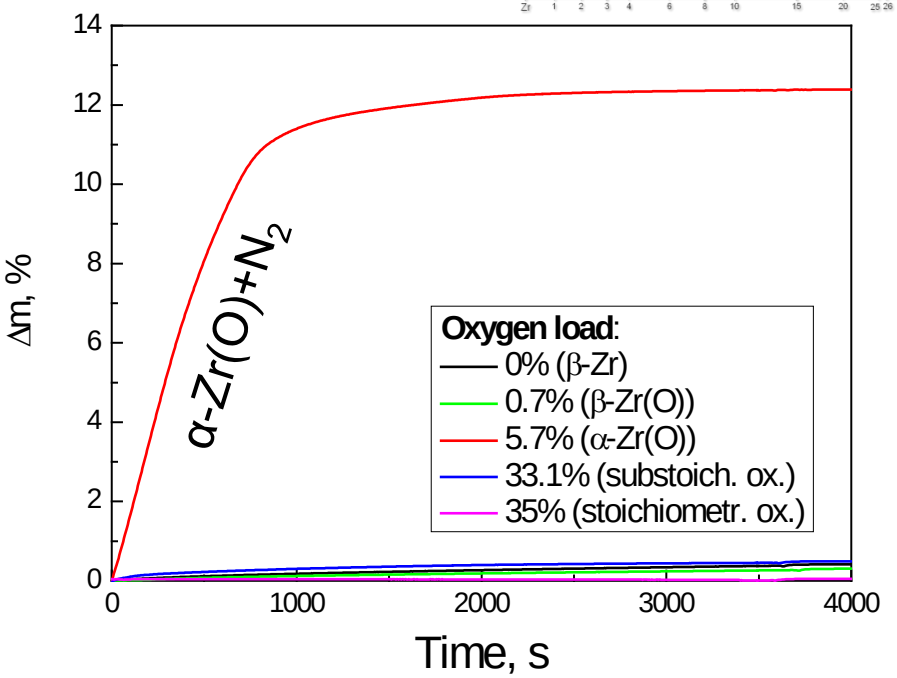


Thermodynamic view



Stability diagram Zr-O-N

Kinetic view



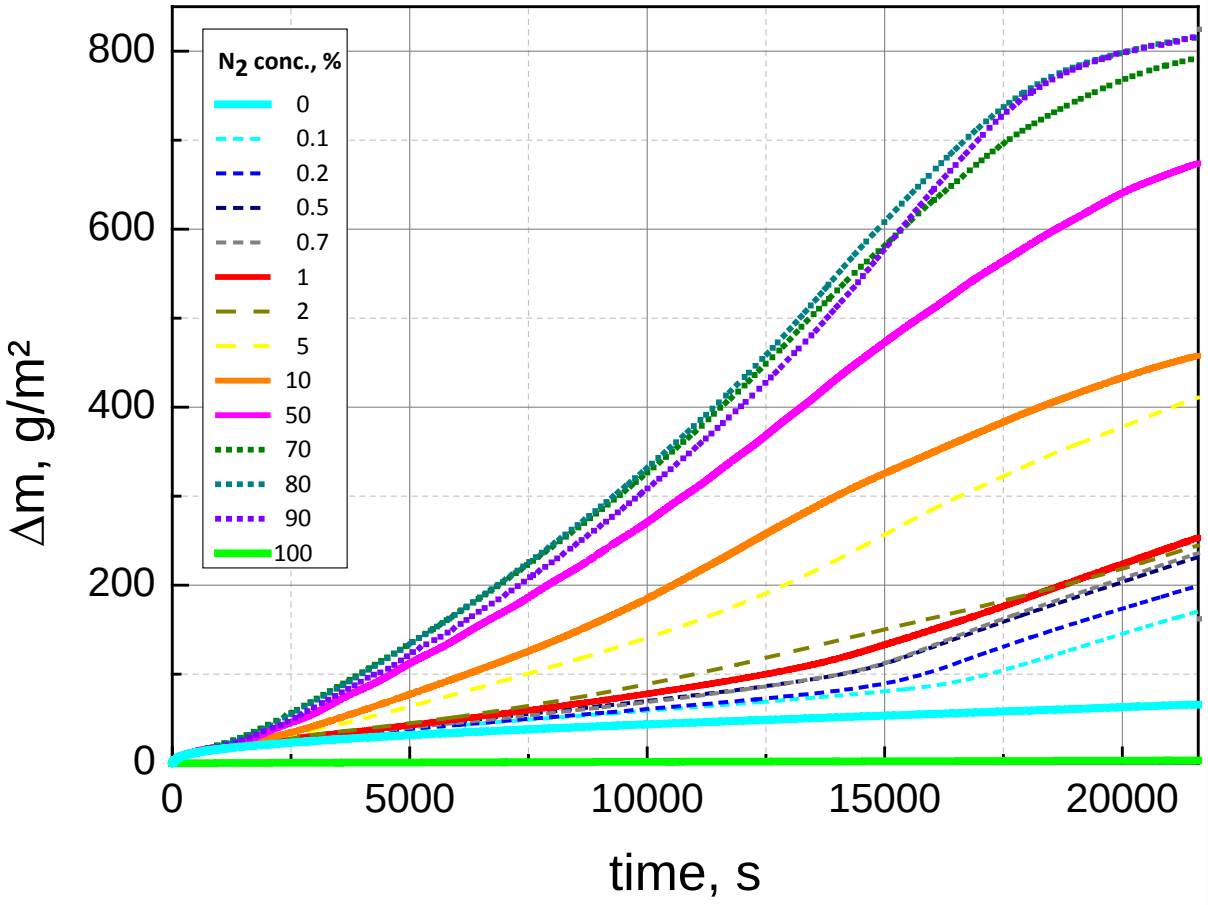
Reaction of ZrO_x with nitrogen (1200°C)

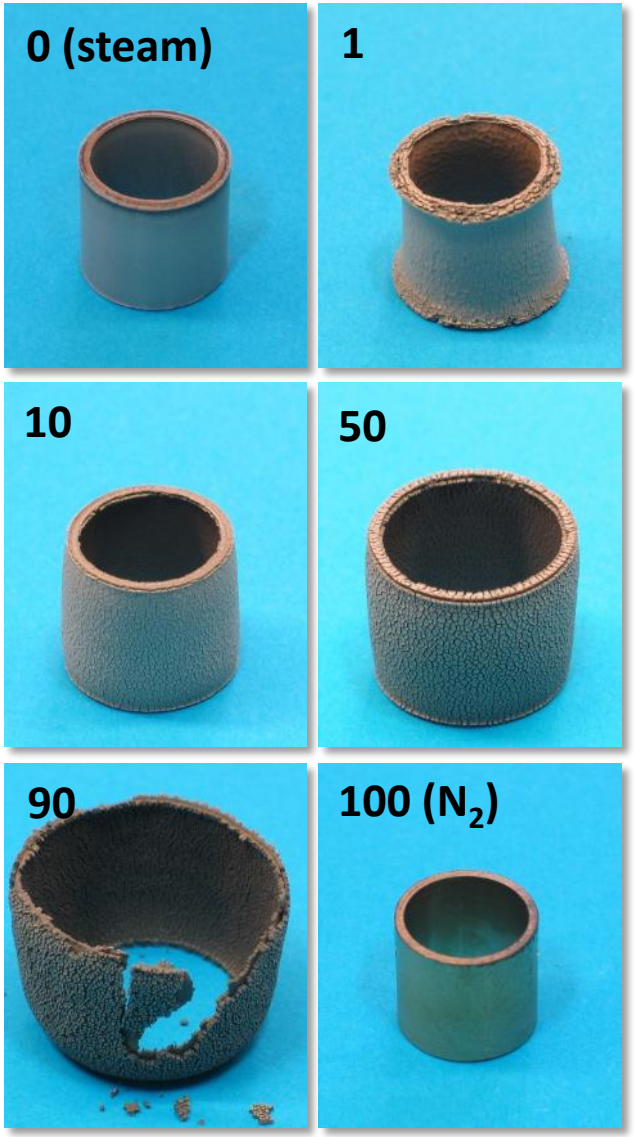
- ZrN only stable at very low oxygen partial pressure (activity)
- Fast reaction of oxygen-stabilized Zr with nitrogen
- Both conditions are present <u>locally</u> at the metal-oxide interface

IAM Institute for Applied Materials

Oxidation in mixed steam-nitrogen at 800°C

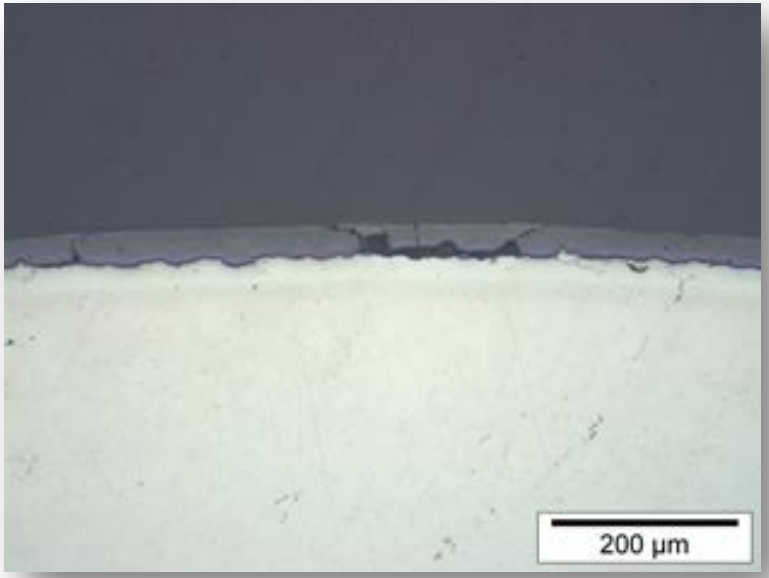
TG results at 800°C, 6 hours



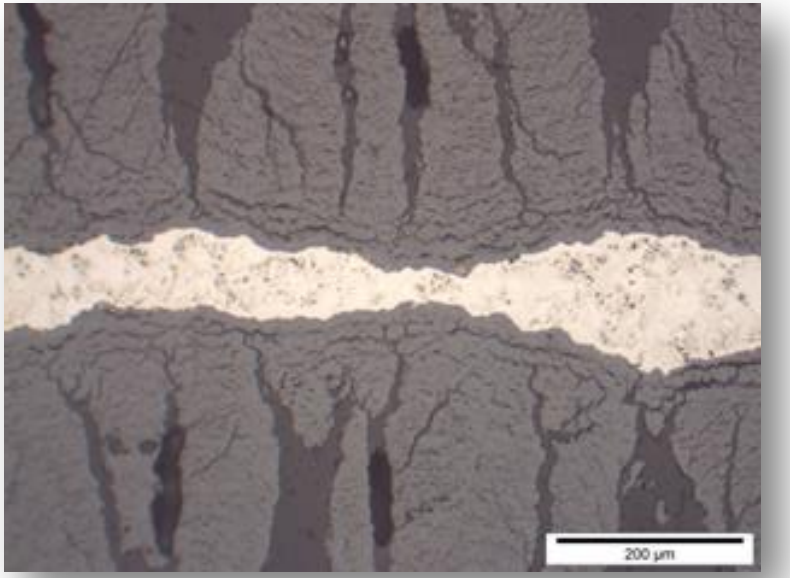


Oxidation in mixed steam-nitrogen at 800°C

6 hour at 800 °C in steam

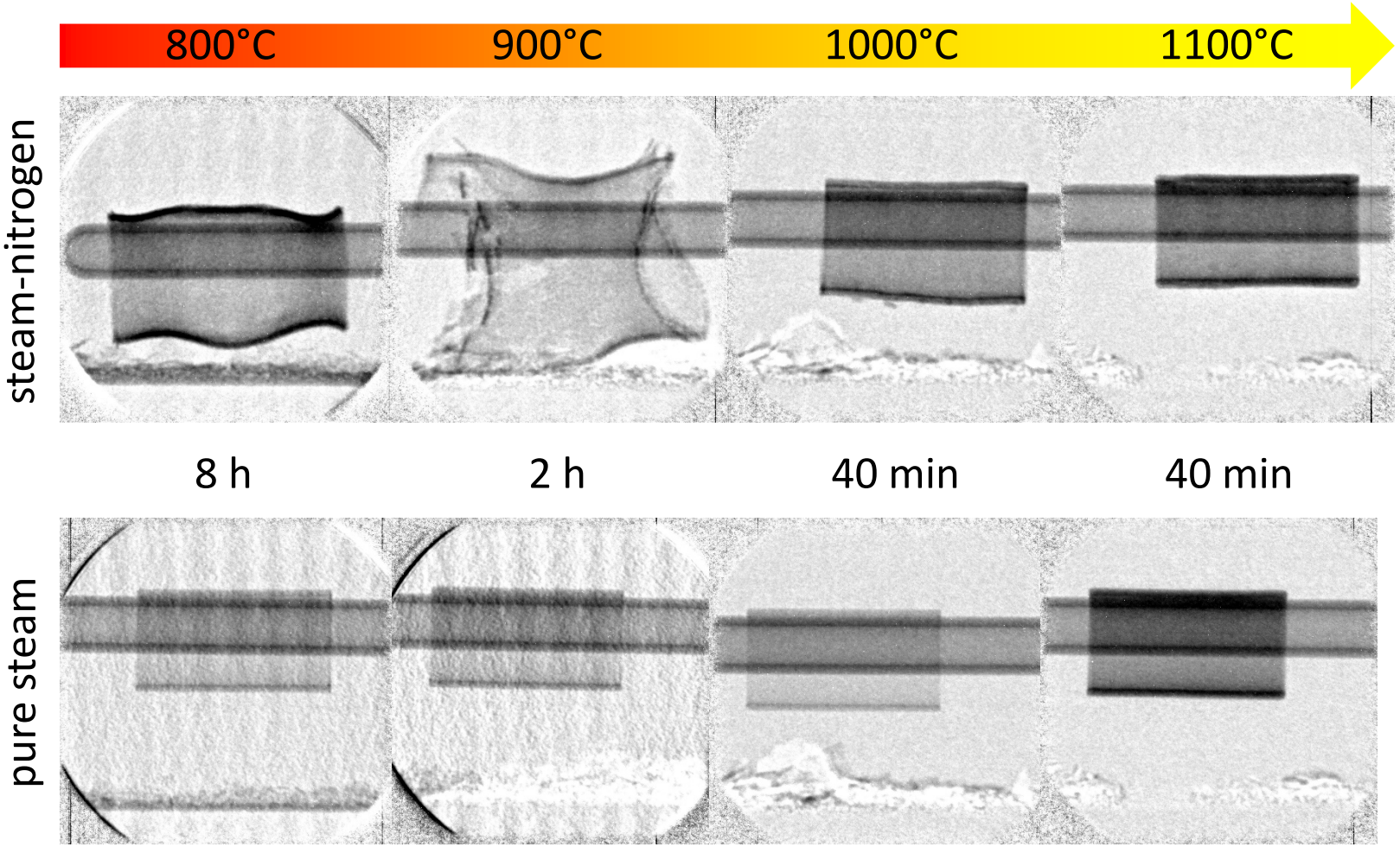


6 hour at 800 °C in 50/50 steam/N_2

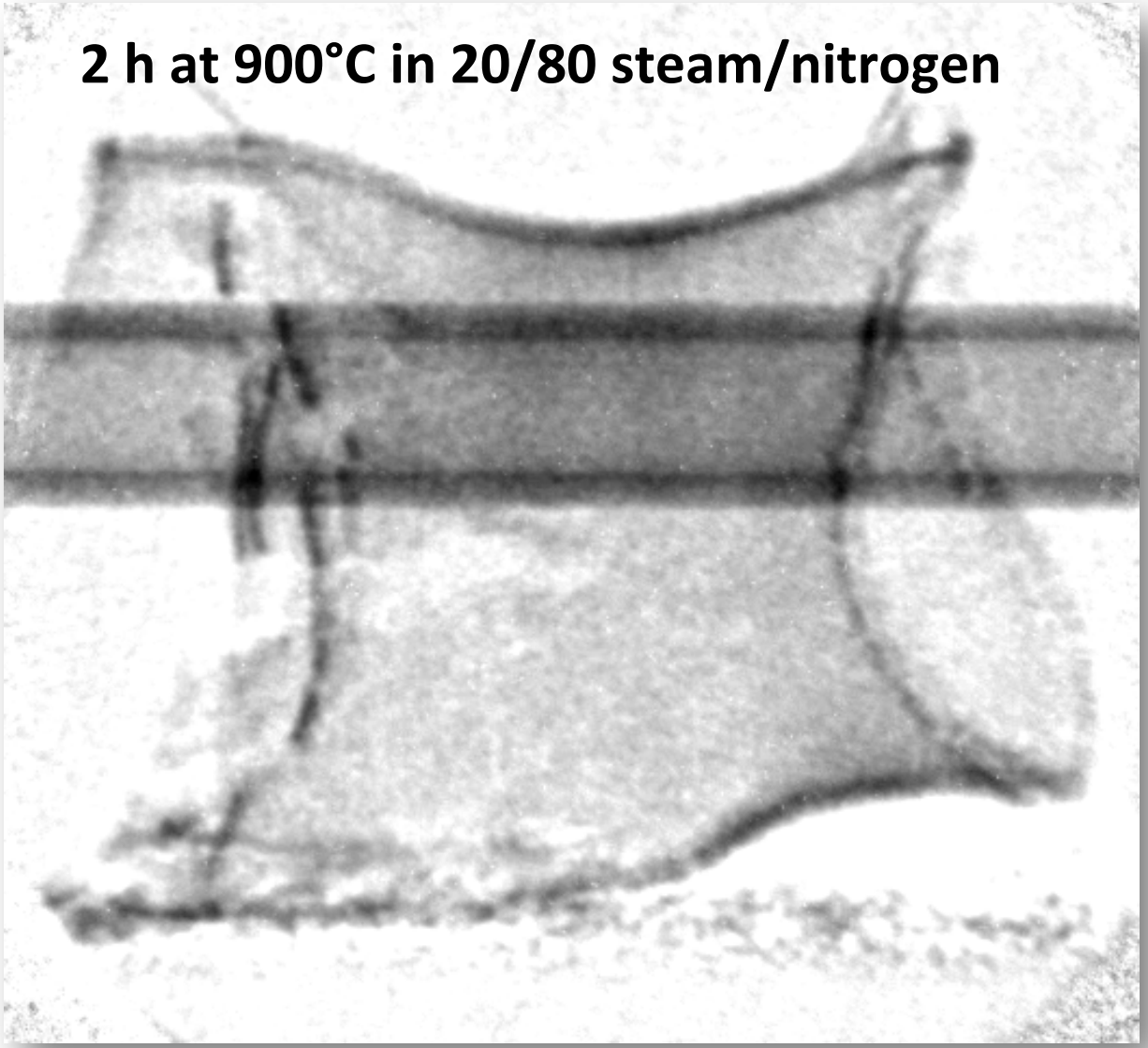


- Strong effect of nitrogen on oxidation and degradation
- Nitrogen acts like a catalyst (NOT like an inert gas)
- Enhanced hydrogen source term by oxidation in mixtures containing nitrogen

In-situ NR of Zircaloy-4 in steam and steam-nitrogen



In-situ NR of Zircaloy-4 in steam-nitrogen

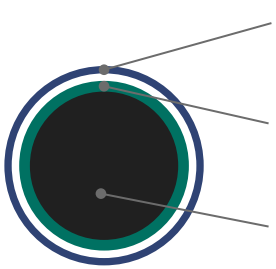


Control rod behavior

Absorber materials in LWRs

Boron carbide

- Used in boiling water reactors (BWR), VVERs, some pressurized water reactors (PWR)
- Control rods (PWR) or cross-shaped blades (BWR)
- Surrounded by stainless steel (cladding, blades) and Zry (guide tubes, canisters)

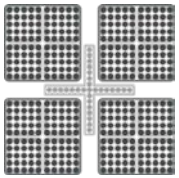


Zry guide tube
T_{melt}=1900°C

SS cladding
T_{melt}=1450°C

B_4C
T_{melt}=2450°C

BWR control rod





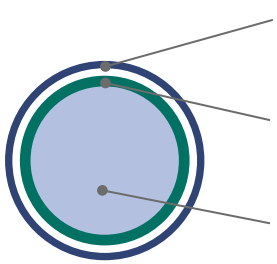
BWR control blade

AgInCd alloy

- Used in PWRs
- Surrounded by stainless steel cladding and Zry guide tubes
- Rods in Zry guide tubes combined in control rod assemblies



PWR control rod assembly



Zry guide tube
T_{melt}=1900°C

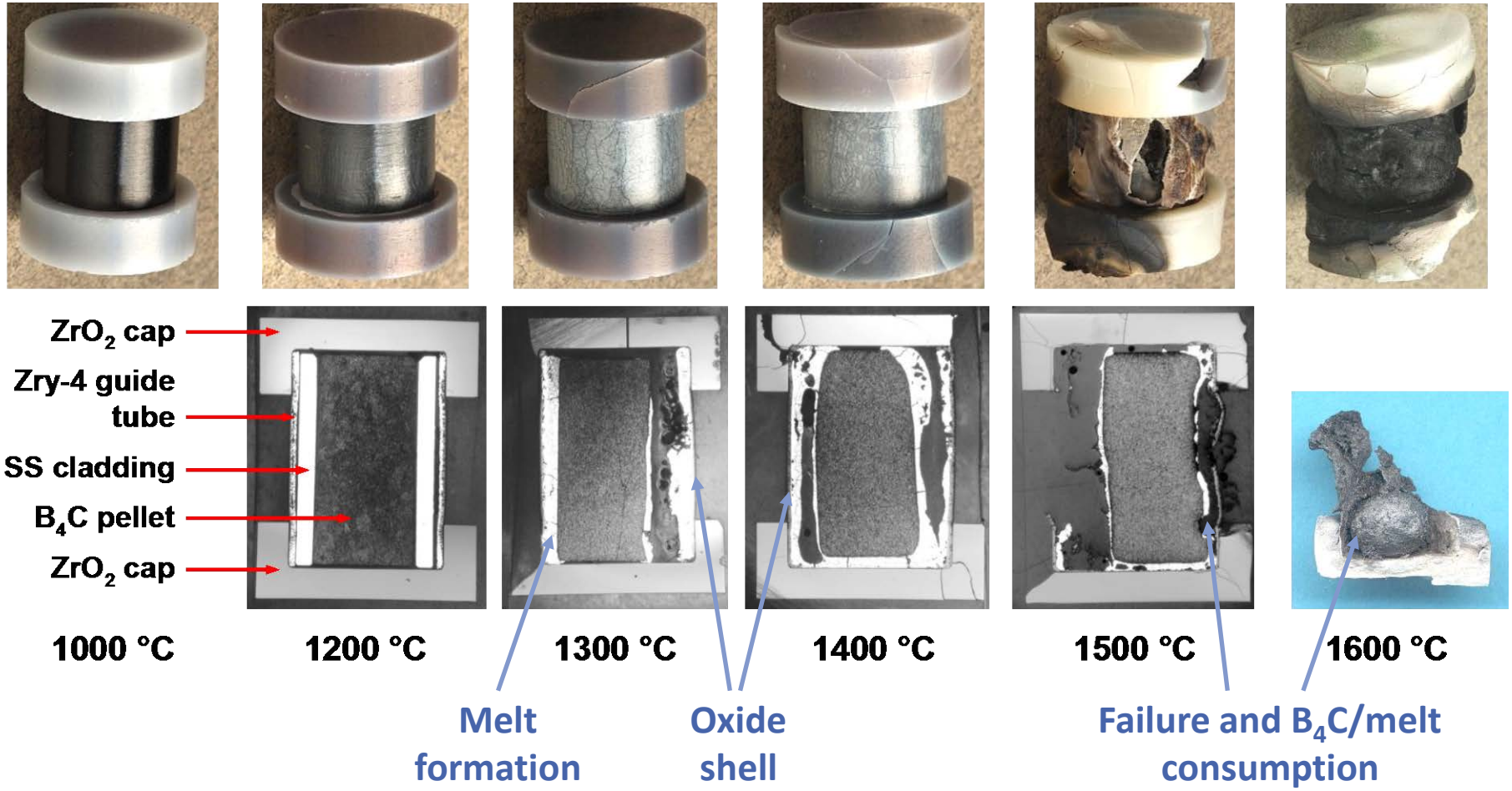
SS cladding
T_{melt}=1450°C

AgInCd
T_{melt}=800°C

PWR control rod

Degradation of B_4C control rods (1-pellet)

Post-test appearance and axial cross section of B_4C/SS/Zry specimens after 1 hour isothermal tests at temperatures between 1000 and 1600 °C

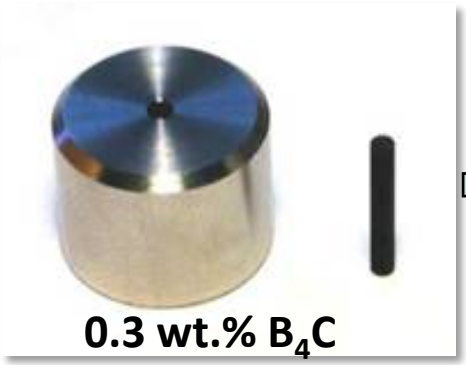


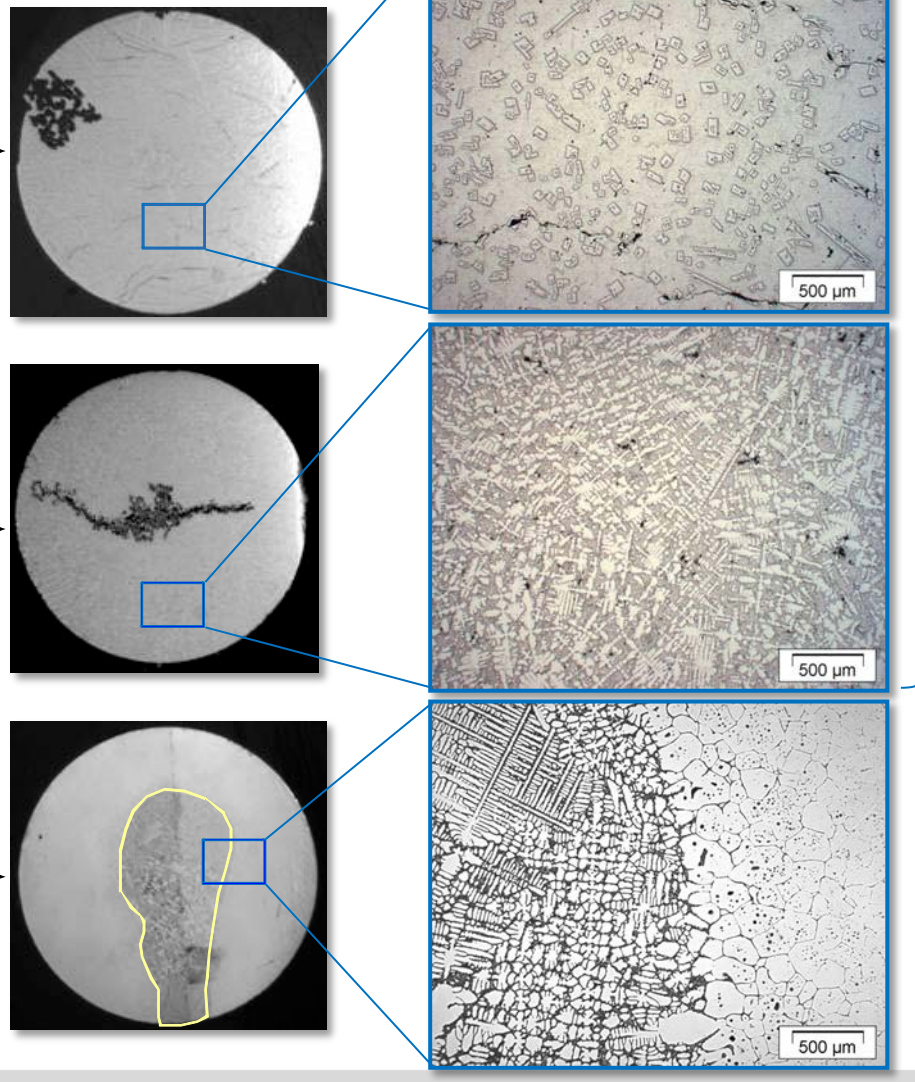
Eutectic interaction of stainless steel with B_4C

1 h at approx. 1250 °C





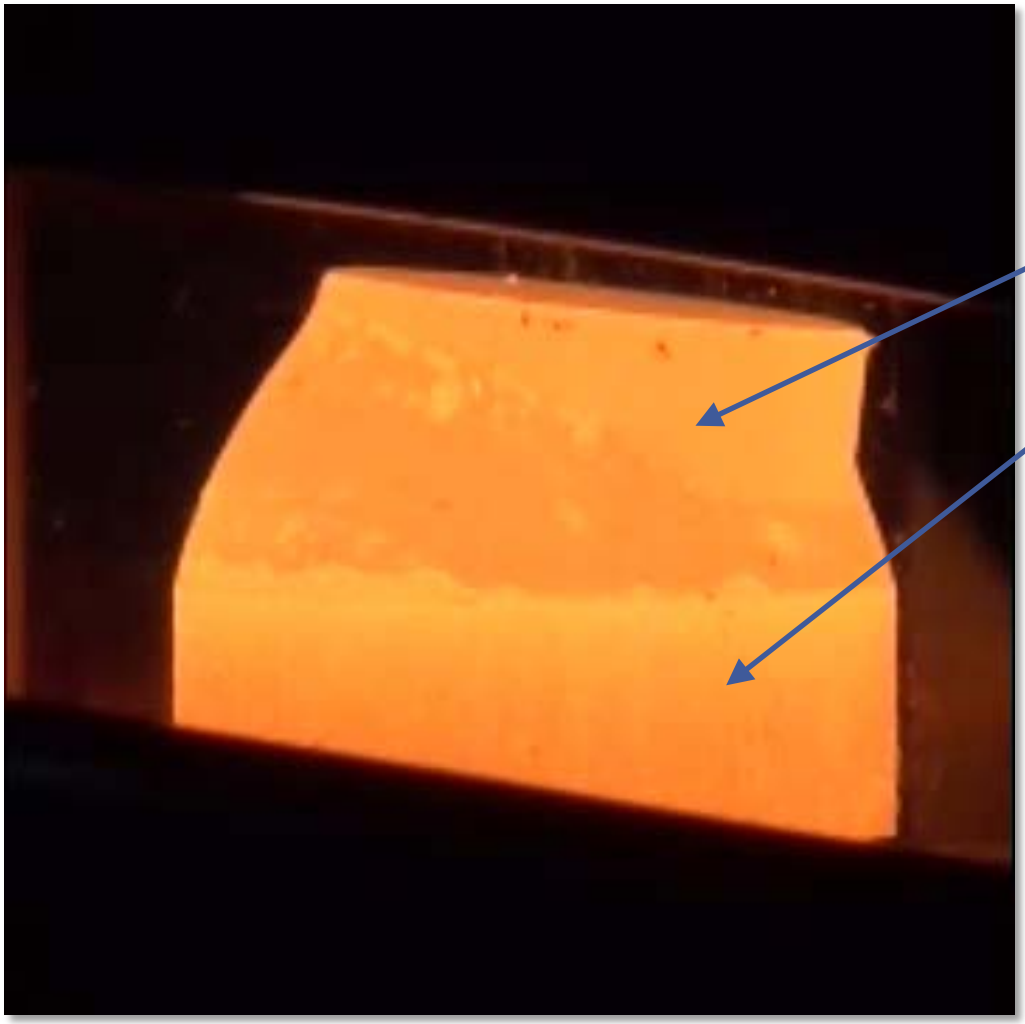


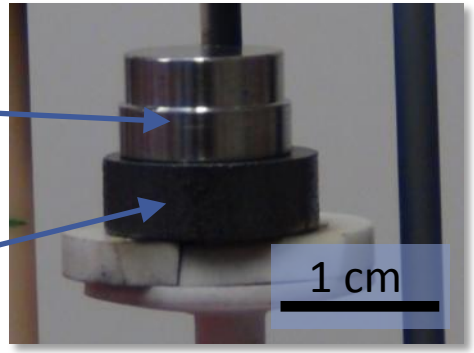


Complete liquefaction of stainless steel

1/3 of SS liquefied

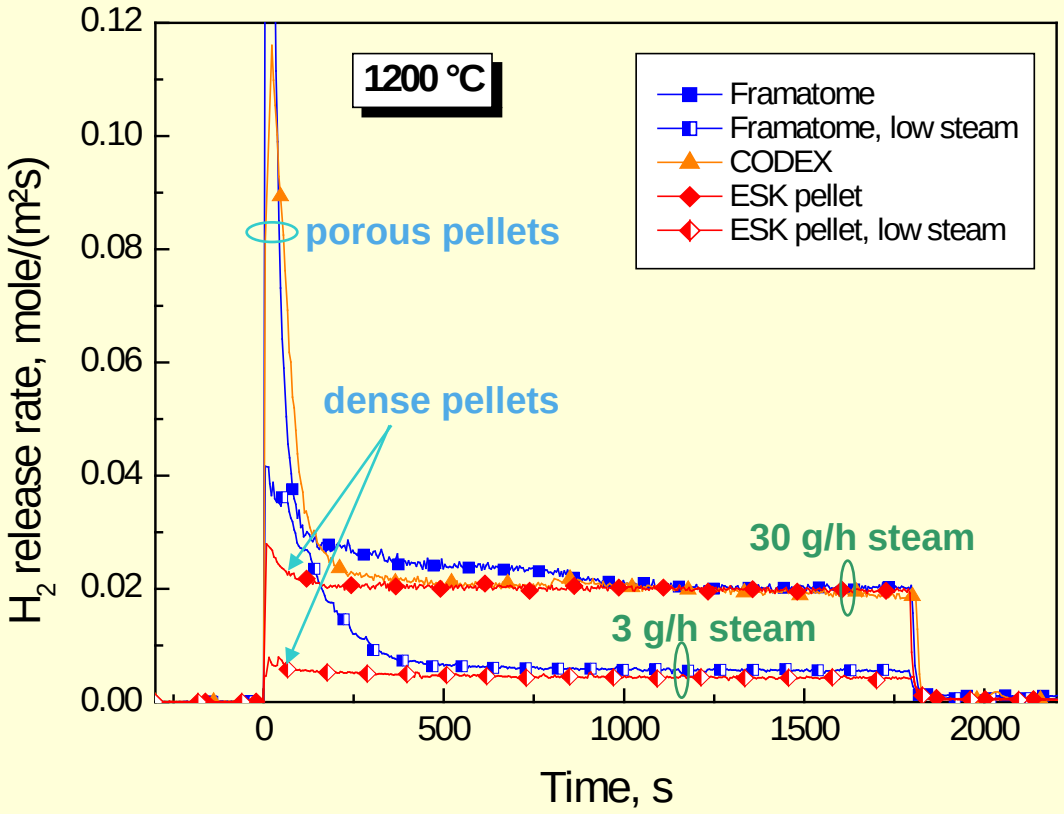
Eutectic interaction of stainless steel with B_4C





- Rapid and complete melting of SS at 1250°C starting at B_4C/SS interface

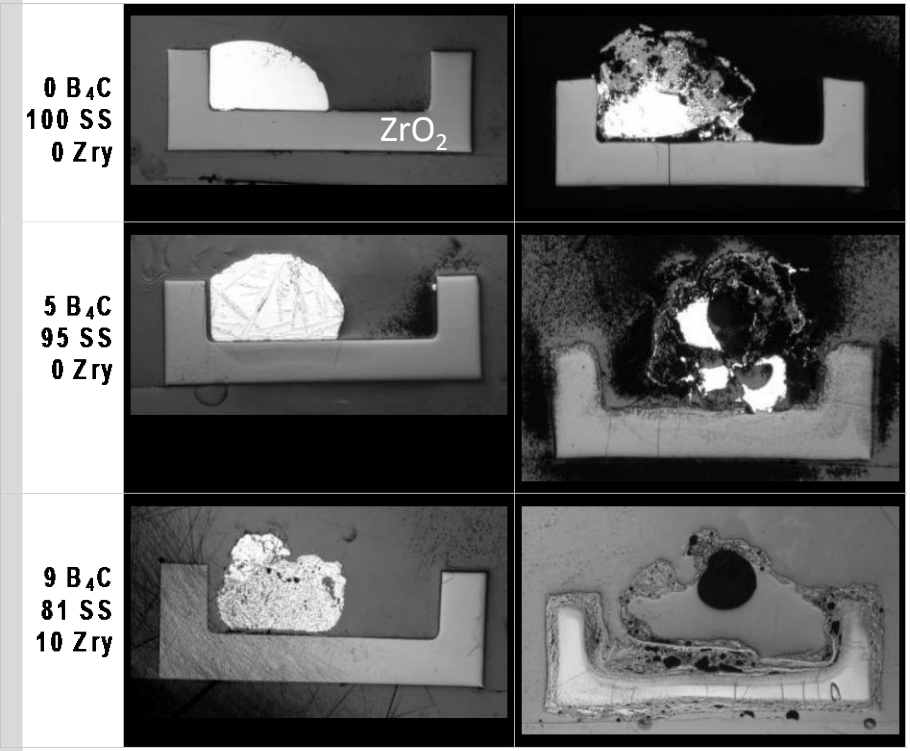
Oxidation kinetics of B_4C in steam



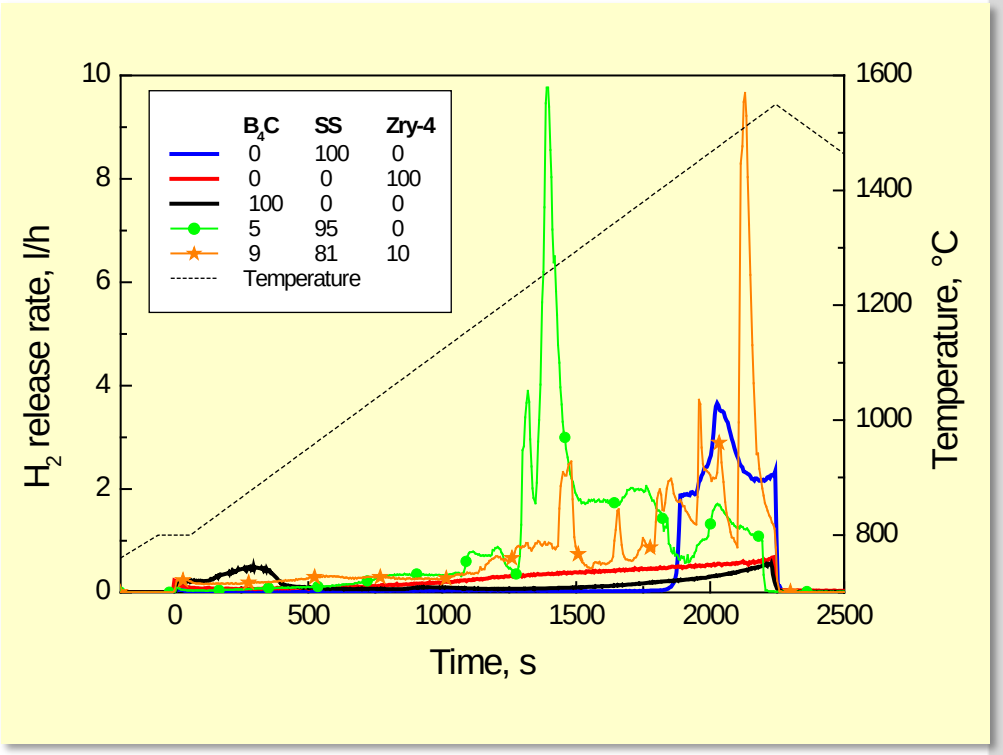
- Strongly dependant on B_4C structure and thermo-hydraulic boundary conditions like pressure and flow rate

Oxidation of B_4C absorber melts

Transient oxidation of B_4C/SS/Zry-4 absorber melts
in steam between 800 and 1550 °C



before oxidation after oxidation

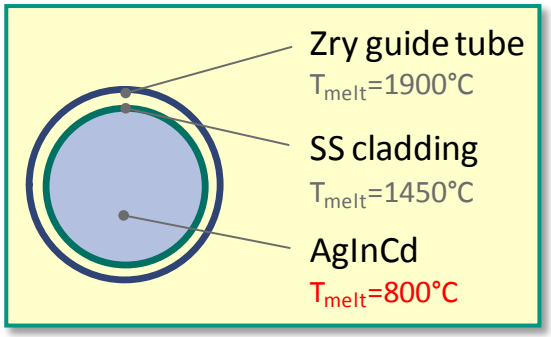


Oxidation rate during reaction of absorber melts and pure CR components in steam

Failure of AgInCd absorber rod

- Ag-In-Cd control rods fail at temperatures above 1200°C due to the eutectic interaction between SS and Zry-4
- Failure is very stochastic (from local to explosive) with the tendency to higher temperatures for symmetric samples and specimens with inner oxidation
- No ballooning of the SS cladding tube was observed before rupture
- Burst release of cadmium vapour is followed by continuous release of indium and silver aerosols and absorber melt





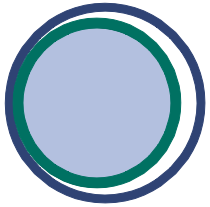
IAM Institute for Applied Materials

Different failure types of AgInCd absorber rod





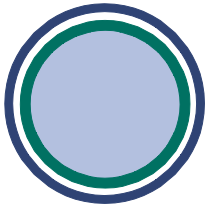
SIC-02 (asym. rod)
Local failure at 1230°C







SIC-05 (symmetric rod)
Global failure at 1350°C



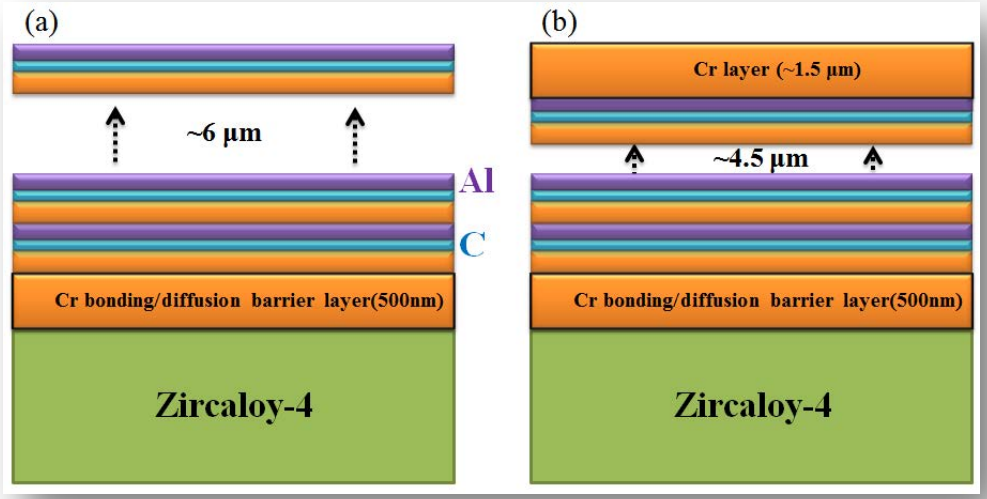
ATF cladding

KIT activities on ATF

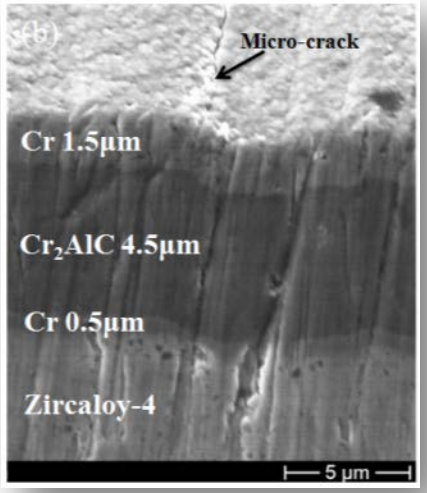
- QUENCH bundle tests with FeCrAl cladding in cooperation with ORNL
- Single-rod oxidation and quench tests with Cr-coated Zr alloy
- Ultra-high temperature oxidation tests with SiC_f-SiC
- Development of MAX phase coatings for Zr alloys

- Participation in various international collaborations on ATF
  - EC IL TROVATORE
  - IAEA ACTOF
  - OECD NEA EGATFL, TOPATF, and QUENCH-ATF (under discussion)
  - Westinghouse CARAT

MAX-phase coated cladding alloys (Cr_2AlC)

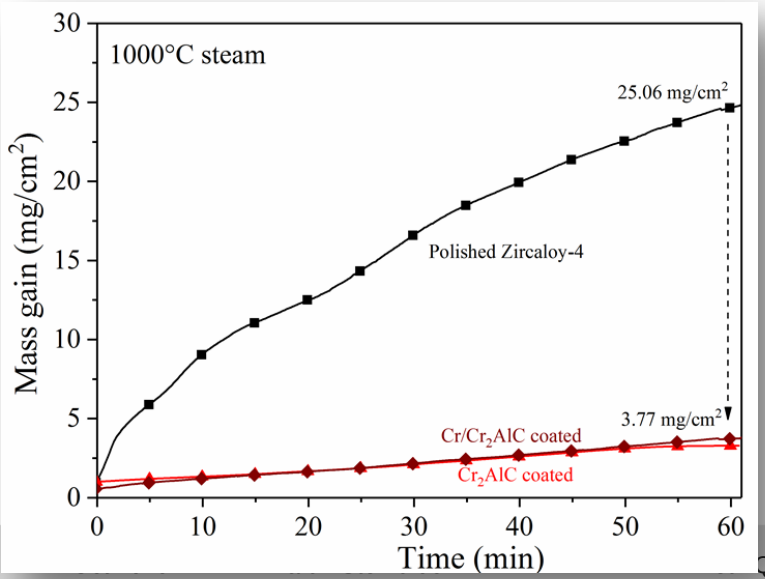


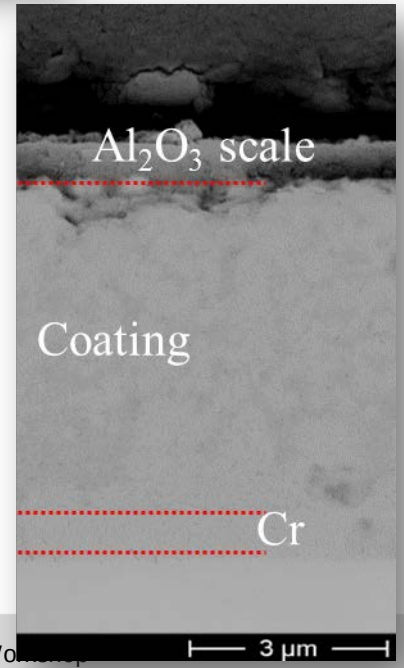
Annealing

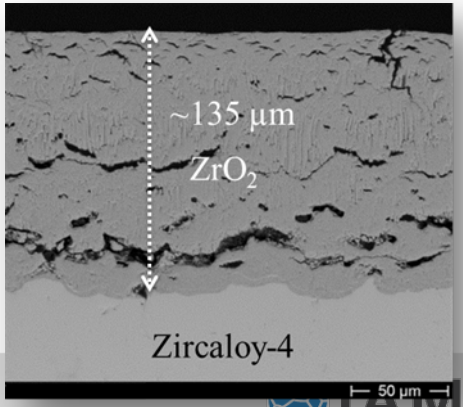


Magnetron sputtered Cr/C/Al nano layers

Pure MAX phase



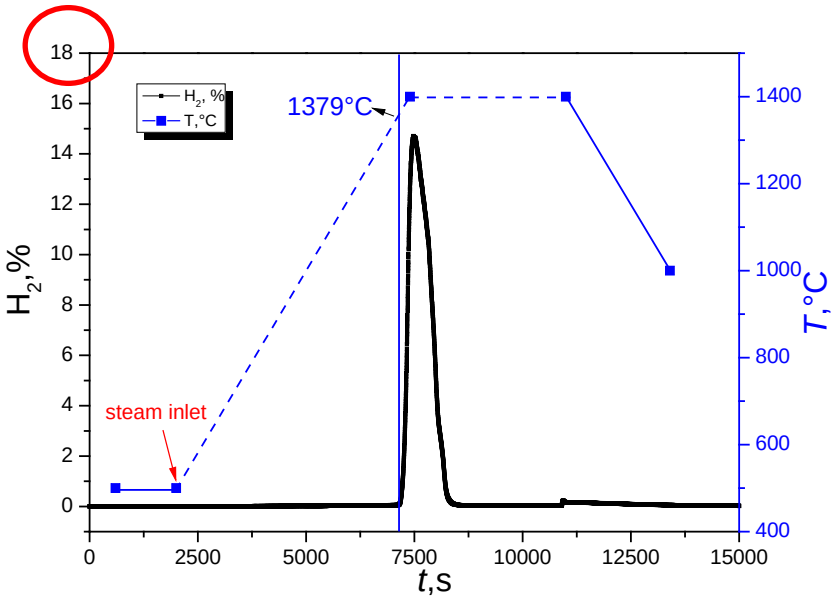




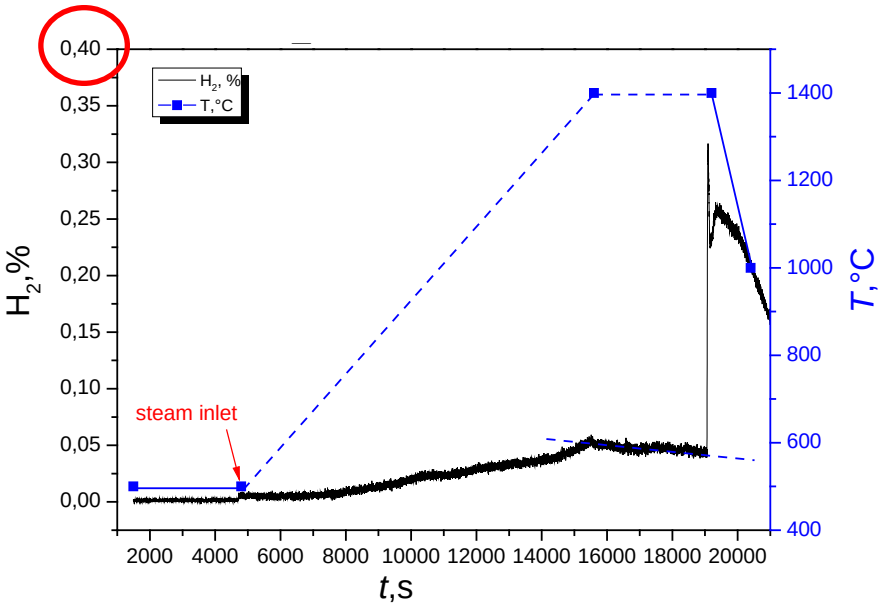
Tang, KIT, PhD 2019

Institute for Applied Materials

Oxidation of Kanthal-APM (FeCrAl) in steam



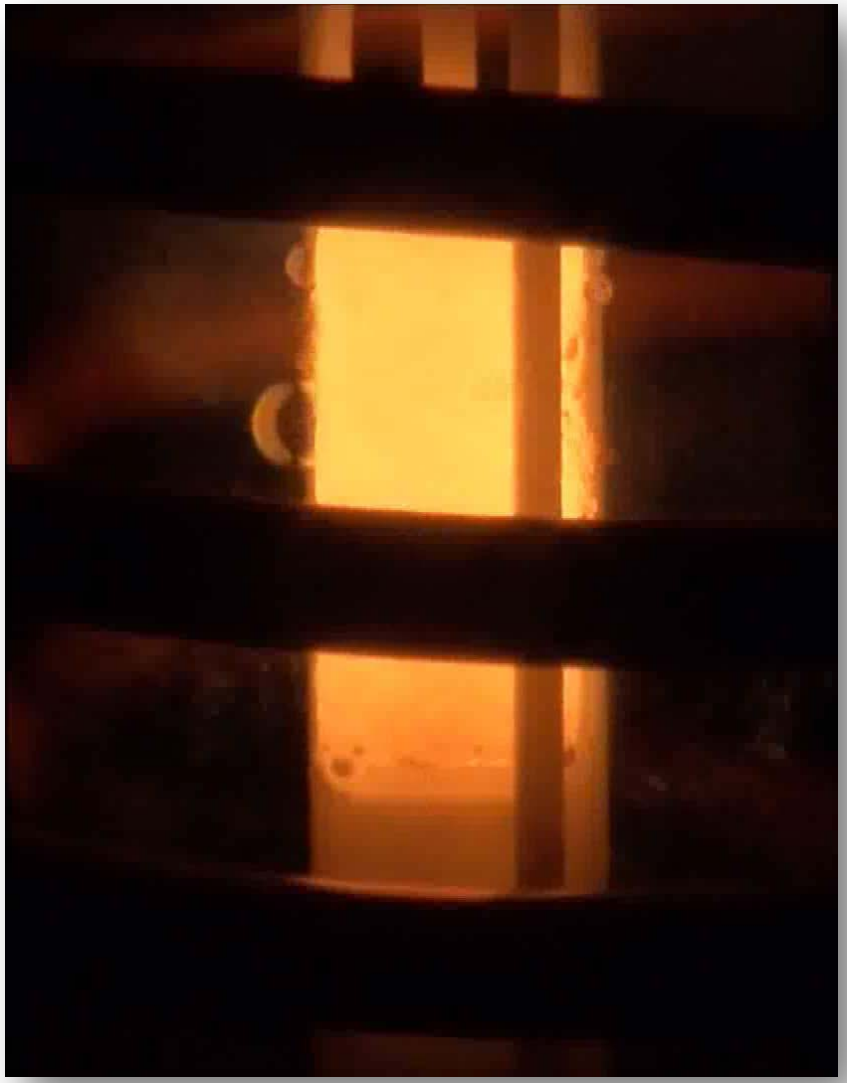
Heating with 10 K/min to 1400°C and subsequent isothermal annealing for 1 h in steam



Heating with 5 K/min to 1400°C and subsequent isothermal annealing for 1 h in steam

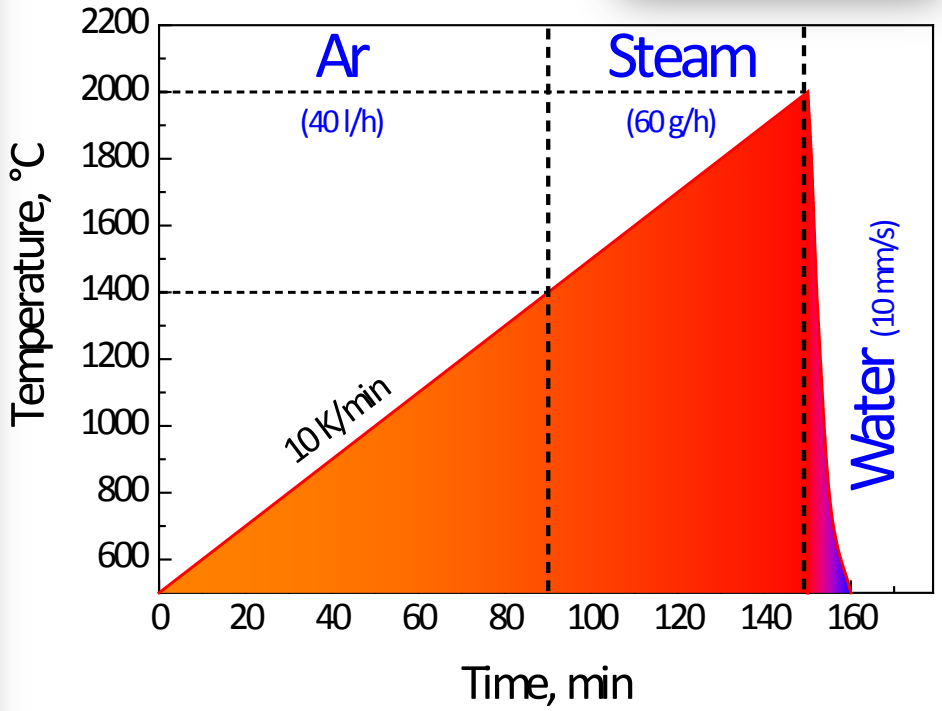
- Formation of a protective alumina scale during slow heatup or pre-oxidation at lower temperatures
- Otherwise, rapid and complete oxidation of the FeCrAl alloy

Steam oxidation of SiC and quench from 2000°C





Post-test appearance of SiC-SiC sample



Test conduct

Avincola, NED 2015
Avincola, KIT, PhD 2016

Takeaways

- Zirconium oxidation at high temperatures is a source of significant release of hydrogen and heat affecting nuclear accident progression.
- Oxidation is not always of parabolic kinetics and may be strongly dependent on experimental boundary conditions.
- Eutectic interactions may lead to melt formation far below the melting points of the individual materials. These melts may slowly relocate and severely oxidize.
- ATF claddings could strongly decrease the risk of temperature escalation and hydrogen detonation during BDB accidents as well as significantly increase the coping time for AMMs.
- Most experimental results were used to improve models, especially in cooperation with IBRAE, GRS, and IRSN as well as internally by H. Steiner and M. Große.

Acknowledgement

- The QUENCH group at KIT for their excellent work and support
- Program NUSAFE at KIT
- Various projects in the 3rd to 7th EU Framework Programs for Research and Innovation
- National and international partners

- You, for your kind attention

Karlsruhe Institute of Technology

Institute for Applied Materials

25 years QUENCH program
Highlights of separate-effects tests

M. Steinbrück, J. Stuckert, M. Große et al.

25th International QUENCH Workshop, Karlsruhe, 22-24 October 2019

Institute for Applied Materials IAM-AWP & Program NUSAFE







Key papers: Oxidation of Zr alloys and hydrogen behavior

Grosse, M., Pulvermacher, S., Steinbrück, M., Schillinger, B.
In-situ neutron radiography investigations of the reaction of Zircaloy-4 in steam, nitrogen/steam and air/steam atmospheres
(2018) Physica B: Condensed Matter, 551, pp. 244-248. Cited 2 times.
DOI: 10.1016/j.physb.2018.03.030

Grosse, M., Steinbrueck, M., Schillinger, B., Kaestner, A.
In situ investigations of the hydrogen uptake of zirconium alloys during steam oxidation
(2018) ASTM Special Technical Publication, STP 1597, pp. 1114-1135. Cited 3 times.
DOI: 10.1520/STP159720160041

Steinbrück, M., da Silva, F.O., Grosse, M.
Oxidation of Zircaloy-4 in steam-nitrogen mixtures at 600–1200 °C
(2017) Journal of Nuclear Materials, 490, pp. 226-237. Cited 11 times.
DOI: 10.1016/j.jnucmat.2017.04.034

Stuckert, J., Hózer, Z., Kiselev, A., Steinbrück, M.
Cladding oxidation during air ingress. Part I: Experiments on air ingress
(2016) Annals of Nuclear Energy, 93, pp. 4-17. Cited 9 times.
DOI: 10.1016/j.anucene.2015.12.034

Steinbrück, M., Schaffer, S.
High-Temperature Oxidation of Zircaloy-4 in Oxygen–Nitrogen Mixtures
(2016) Oxidation of Metals, 85 (3-4), pp. 245-262. Cited 23 times.
DOI: 10.1007/s11085-015-9572-1

Steinbrück, M., Grosse, M.
Deviations from parabolic kinetics during oxidation of zirconium alloys
(2015) ASTM Special Technical Publication, STP 1543, pp. 979-1001. Cited 5 times.
DOI: 10.1520/STP154320130022

Key papers: Oxidation of Zr alloys and hydrogen behavior

Pshenichnikov, A., Stuckert, J., Walter, M.
Microstructure and mechanical properties of Zircaloy-4 cladding hydrogenated at temperatures typical for LOCA conditions
(2015) Nuclear Engineering and Design, 283, pp. 33-39. Cited 12 times.
DOI: 10.1016/j.nucengdes.2014.06.022

Steinbrück, M.
High-temperature reaction of oxygen-stabilized α-Zr(O) with nitrogen
(2014) Journal of Nuclear Materials, 447 (1-3), pp. 46-55. Cited 24 times.
DOI: 10.1016/j.jnucmat.2013.12.024

Große, M., Steinbrück, M., Stuckert, J., Kastner, A., Schillinger, B.
Application of neutron radiography to study material processes during hypothetical severe accidents in nuclear reactors
(2012) Journal of Materials Science, 47 (18), pp. 6505-6512. Cited 12 times.
DOI: 10.1007/s10853-011-5553-1

Steinbrück, M., Vér, N., Grosse, M.
Oxidation of advanced zirconium cladding alloys in steam at temperatures in the range of 600-1200 °c
(2011) Oxidation of Metals, 76 (3-4), pp. 215-232. Cited 58 times.
DOI: 10.1007/s11085-011-9249-3

Steinbrück, M., Böttcher, M.
Air oxidation of Zircaloy-4, M5® and ZIRLO™ cladding alloys at high temperatures
(2011) Journal of Nuclear Materials, 414 (2), pp. 276-285. Cited 72 times.
DOI: 10.1016/j.jnucmat.2011.04.012

Steinbrück, M., Große, M., Sepold, L., Stuckert, J.
Synopsis and outcome of the QUENCH experimental program
(2010) Nuclear Engineering and Design, 240 (7), pp. 1714-1727. Cited 84 times.
DOI: 10.1016/j.nucengdes.2010.03.021

Key papers: Oxidation of Zr alloys and hydrogen behavior

Grosse, M.
Comparison of the high-temperature steam oxidation kinetics of advanced cladding materials
(2010) Nuclear Technology, 170 (1), pp. 272-279. Cited 20 times.
DOI: 10.13182/NT10-A9464

Steinbrück, M.
Prototypical experiments relating to air oxidation of Zircaloy-4 at high temperatures
(2009) Journal of Nuclear Materials, 392 (3), pp. 531-544. Cited 79 times.
DOI: 10.1016/j.jnucmat.2009.04.018

Große, M., Lehmann, E., Steinbrück, M., Kühne, G., Stuckert, J.
Influence of oxide layer morphology on hydrogen concentration in tin and niobium containing zirconium alloys after high temperature steam oxidation
(2009) Journal of Nuclear Materials, 385 (2), pp. 339-345. Cited 68 times.

Steinbrück, M.
Oxidation of zirconium alloys in oxygen at high temperatures up to 1600 °c
(2008) Oxidation of Metals, 70 (5-6), pp. 317-329. Cited 35 times.
DOI: 10.1007/s11085-008-9124-z

Grosse, M., Steinbrueck, M., Lehmann, E., Vontobel, P.
Kinetics of hydrogen absorption and release in zirconium alloys during steam oxidation
(2008) Oxidation of Metals, 70 (3-4), pp. 149-162. Cited 39 times.
DOI: 10.1007/s11085-008-9113-2

Steinbrück, M.
Hydrogen absorption by zirconium alloys at high temperatures
(2004) Journal of Nuclear Materials, 334 (1), pp. 58-64. Cited 62 times.
DOI: 10.1016/j.jnucmat.2004.05.007

Key papers: Control rod degradation

Kurata, M., Barrachin, M., Haste, T., Steinbrueck, M.
Phenomenology of BWR fuel assembly degradation
(2018) Journal of Nuclear Materials, 500, pp. 119-140. Cited 5 times.
DOI: 10.1016/j.jnucmat.2017.12.004

Steinbrück, M., Stegmaier, U., Grosse, M.
Experiments on silver-indium-cadmium control rod failure during severe nuclear accidents
(2017) Annals of Nuclear Energy, 101, pp. 347-358. Cited 7 times.
DOI: 10.1016/j.anucene.2016.11.039

Steinbrück, M.
Influence of boron carbide on core degradation during severe accidents in LWRs
(2014) Annals of Nuclear Energy, 64, pp. 43-49. Cited 19 times.
DOI: 10.1016/j.anucene.2013.09.027

Steinbrück, M.
Degradation and oxidation of B4C control rod segments at high temperatures
(2010) Journal of Nuclear Materials, 400 (2), pp. 138-150. Cited 32 times.
DOI: 10.1016/j.jnucmat.2010.02.022

Dubourg, R., Austregesilo, H., Bals, C., Barrachin, M., Birchley, J., Haste, T., Lamy, J.S., Lind, T., Maliverney, B., Marchetto, C., Pinter, A., Steinbrück, M., Stuckert, J., Trambauer, K., Vimi, A.
Understanding the behaviour of absorber elements in silver-indium-cadmium control rods during PWR severe accident sequences
(2010) Progress in Nuclear Energy, 52 (1), pp. 97-108. Cited 19 times.
DOI: 10.1016/j.pnucene.2009.09.012

Steinbrück, M.
Oxidation of boron carbide at high temperatures
(2005) Journal of Nuclear Materials, 336 (2-3), pp. 185-193. Cited 53 times.
DOI: 10.1016/j.jnucmat.2004.09.022

Key papers: ATF cladding materials

Steinbrueck, M., Angelici Avincola, V., Markel, I.J., Stegmaier, U., Gerhards, U., Seifert, H.J.
Oxidation of SiC f -SiC CMC cladding tubes for GFR application in impure helium atmosphere and materials interactions with tantalum liner at high temperatures up to 1600°C
(2019) Journal of Nuclear Materials, 517, pp. 337-348.
DOI: 10.1016/j.jnucmat.2019.02.024

Tang, C., Jianu, A., Steinbrueck, M., Grosse, M., Weisenburger, A., Seifert, H.J.
Influence of composition and heating schedules on compatibility of FeCrAl alloys with high-temperature steam
(2018) Journal of Nuclear Materials, 511, pp. 496-507.
DOI: 10.1016/j.jnucmat.2018.09.026

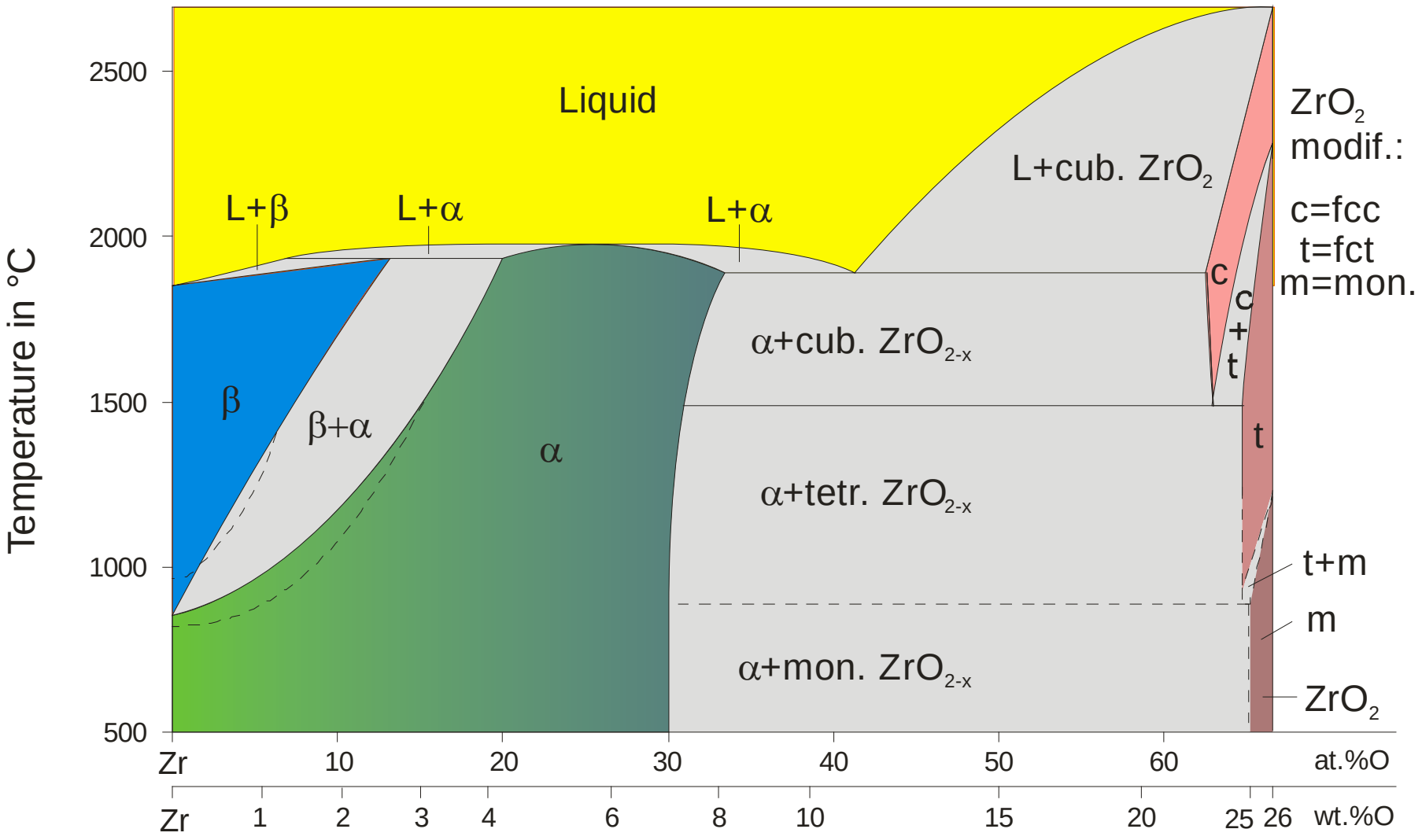
Tang, C., Steinbrueck, M., Stueber, M., Grosse, M., Yu, X., Ulrich, S., Seifert, H.J.
Deposition, characterization and high-temperature steam oxidation behavior of single-phase Ti2AlC-coated Zircaloy-4
(2018) Corrosion Science, 135, pp. 87-98. Cited 7 times.
DOI: 10.1016/j.corsci.2018.02.035

Tang, C., Stueber, M., Seifert, H.J., Steinbrueck, M.
Protective coatings on zirconium-based alloys as accident-Tolerant fuel (ATF) claddings
(2017) Corrosion Reviews, 35 (3), pp. 141-165. Cited 36 times.
DOI: 10.1515/corrrev-2017-0010

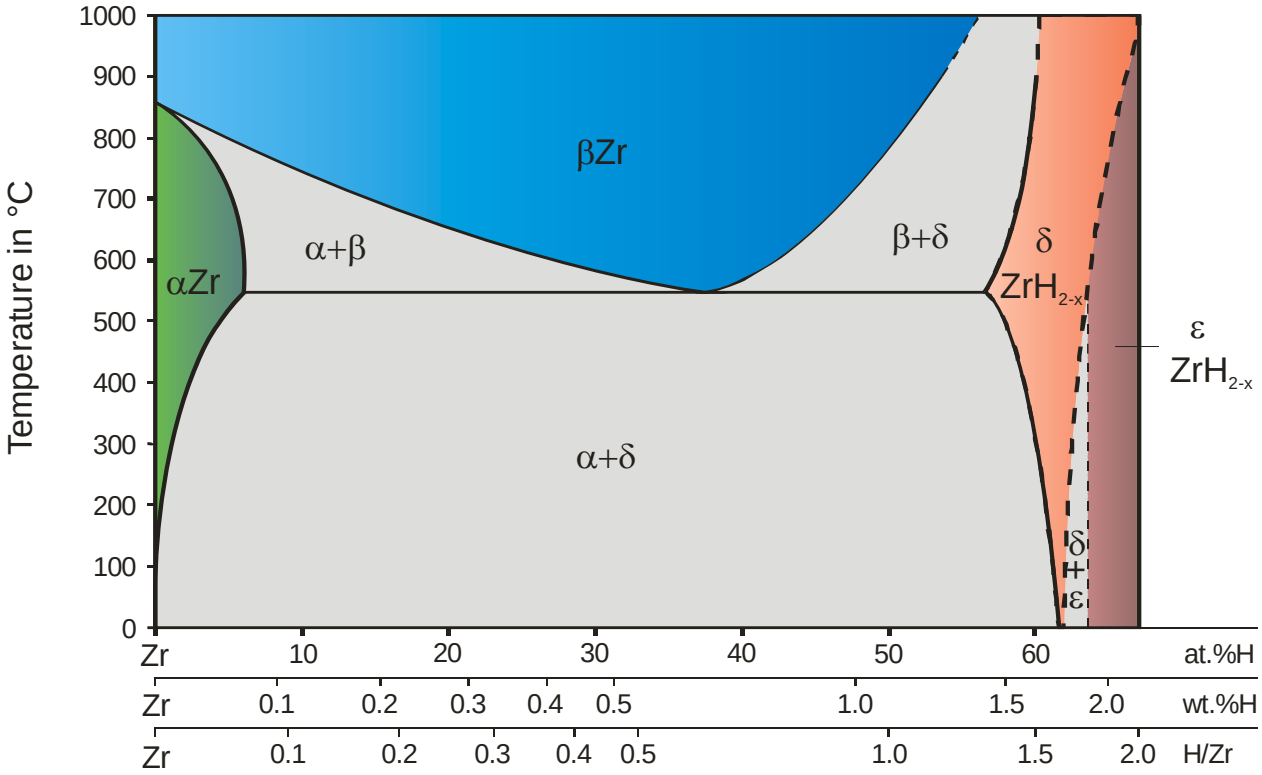
Tang, C., Steinbrück, M., Große, M., Bergfeldt, T., Seifert, H.J.
Oxidation behavior of Ti2AlC in the temperature range of 1400 °C–1600 °C in steam
(2017) Journal of Nuclear Materials, 490, pp. 130-142. Cited 8 times.
DOI: 10.1016/j.jnucmat.2017.03.016

Avincola, V.A., Grosse, M., Stegmaier, U., Steinbrueck, M., Seifert, H.J.
Oxidation at high temperatures in steam atmosphere and quench of silicon carbide composites for nuclear application
(2015) Nuclear Engineering and Design, 295, pp. 468-478. Cited 20 times.
DOI: 10.1016/j.nucengdes.2015.10.002

Phase diagram Zr - O



Phase diagram Zr - H



Sieverts' law:

$$\frac{H}{Zr} = k_S \cdot \sqrt{p_{H_2}}$$

with

$$k_S = A \cdot e^{\frac{-B}{RT}}$$

Main results of the QUENCH bundle tests

J. Stuckert, M. Große, M. Steinbrück

Abstract

In the framework of the QUENCH program at KIT, over the past 22 years, 21 bundle tests were performed under severe accident conditions with different cladding materials. Additionally, 7 QUENCH-LOCA bundle tests with fresh and pre-hydrogenated different cladding materials (Zry-4, M5®, opt. ZIRLO™) were performed according to a temperature/time-scenario typical for a LBLOCA in a German PWR.

Main purposes of severe accident tests were hydrogen source term, as well as investigation of phenomena on melt relocation, debris, and aerosol formation. Concerning the hydrogen source term, six parameters, enhancing hydrogen production during reflood, have been identified: 1) low reflood flow rates < 1 g/s/rod; 2) breakaway effect with weakness and spallation of protective oxide layer; 3) steam starvation; 4) nitride formation by air ingress with formation of very porous oxide layer during following reflood; 5) high temperatures with melt relocation outside claddings and intensive melt oxidation; 6) eutectic interactions between B_4C, stainless steel and Zircaloy-4 leading to low melting point.

Post-test tensile experiments, performed in the framework of the QUENCH-LOCA program, evidenced fracture at hydrogen bands (formed during secondary hydriding) for claddings with local hydrogen concentrations >1500 wppm.


ologie

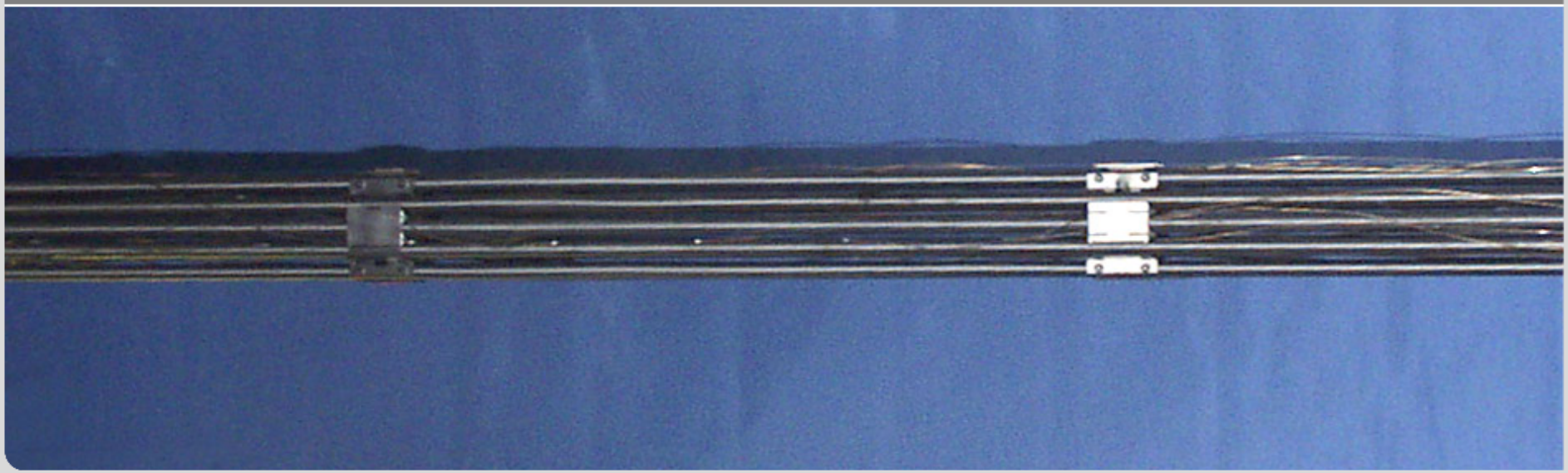
Karlsruhe Institute of Technology

IAM
Institute for Applied Materials

Main results of the QUENCH bundle tests

J. Stuckert, M. Große, M. Steinbrück

Institute for Applied Materials; Program NUSAFE



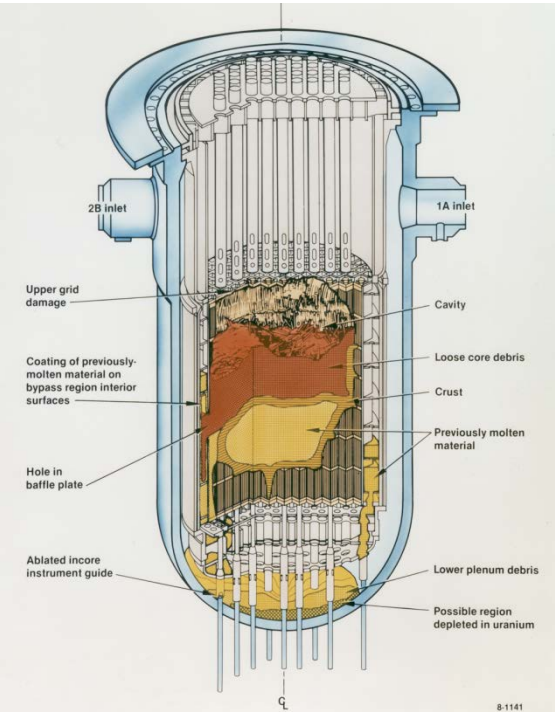
Investigations to core degradation:

TMI-2-Accident ➡ CORA ➡ QUENCH

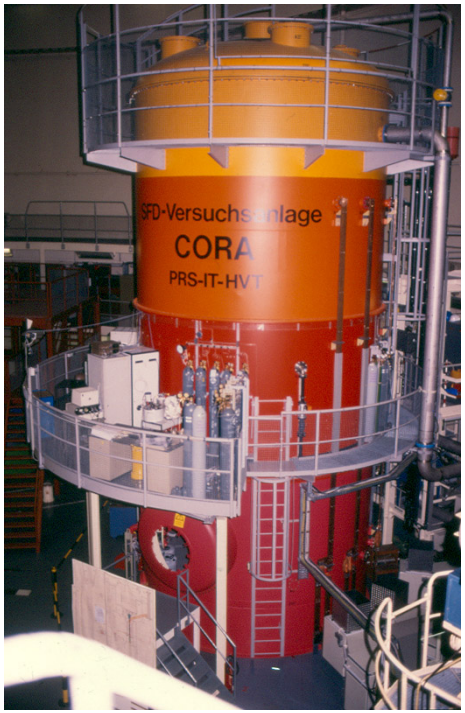
28 March 1979:
50% reactor core fragmented or melted, H_2 generation

1986 - 1993, 19 Tests:
Investigation of melt formation and -relocation

1997 ⟶ now, 21 Tests (+7 LOCA):
Material behavior,
Hydrogen source term



Backgrounder on the Three Mile Island Accident, NRC



G. Schanz et al., . **Information on the evolution of severe L WR fuel element damage obtained in the CORA program**, JNM 188 (1992) 131-145

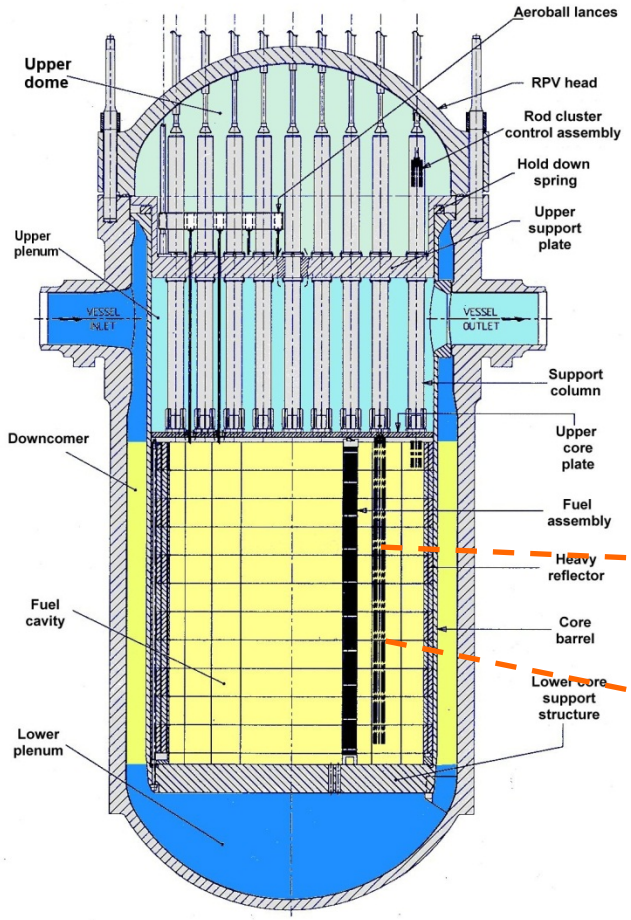


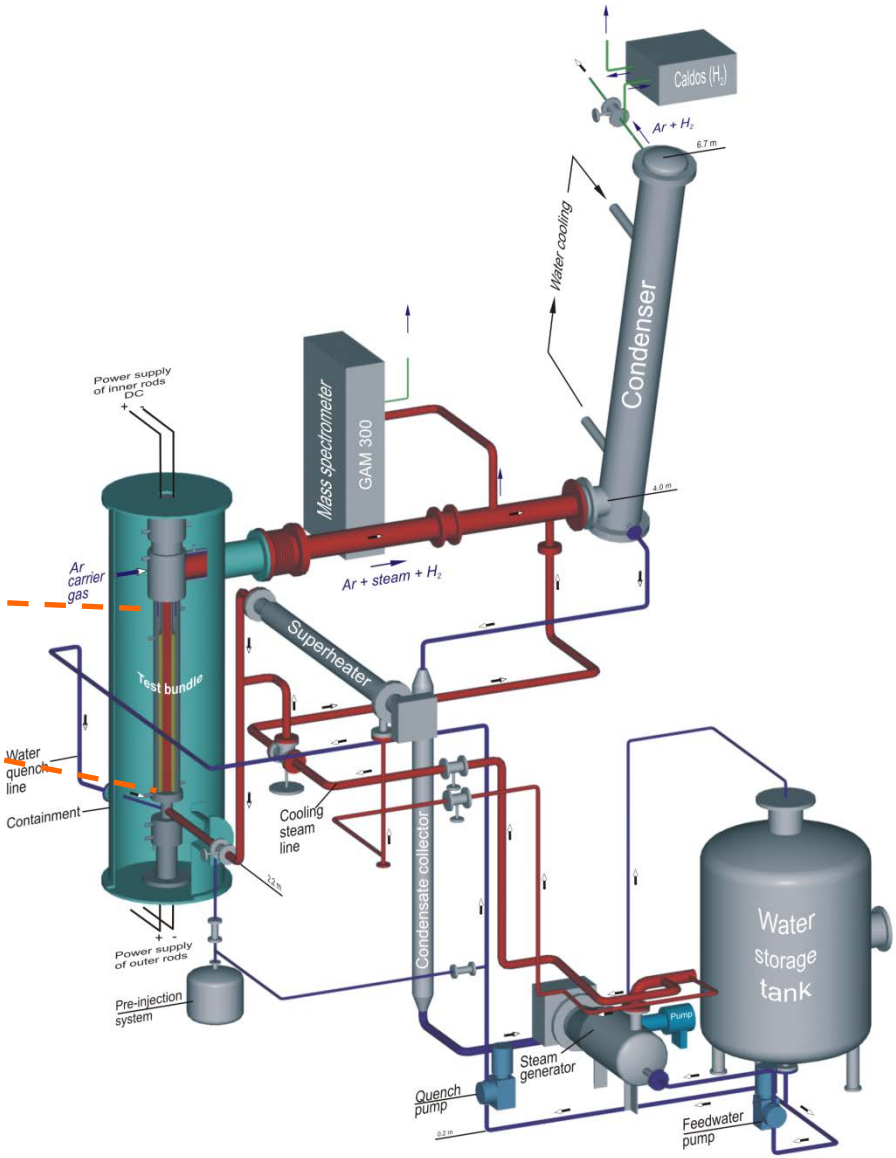
M. Steinbrück et al., Synopsis and outcome of the QUENCH experimental program, NED 240 (2010) 1714–1727

T. Haste et al., A comparison of core degradation phenomena in the CORA, QUENCH, Phébus SFD and Phébus FP experiments, NED 283(2015) 8–20

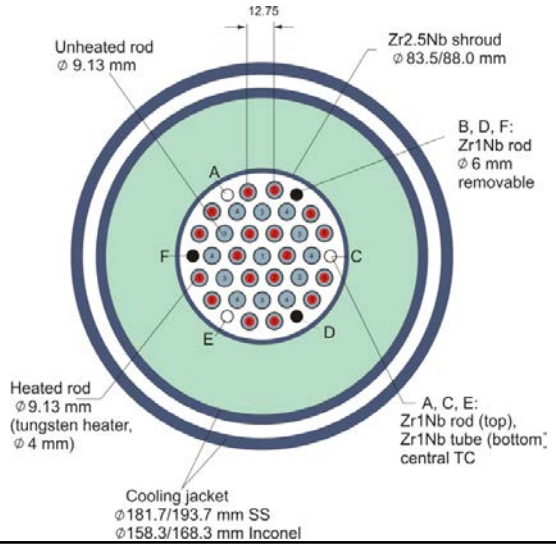
QUENCH-facility

PWR-Reactor





Composition of bundles

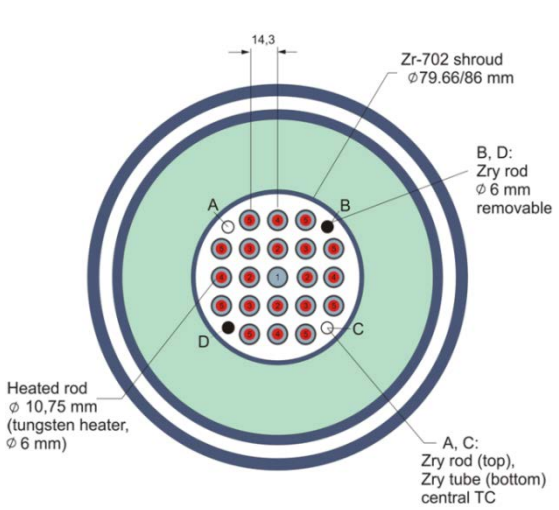


WWER, pitch 12.75 mm

claddings: **E110** - alloy

Fuel rod simulators:

18 heated,13 not heated, 6 corner rods

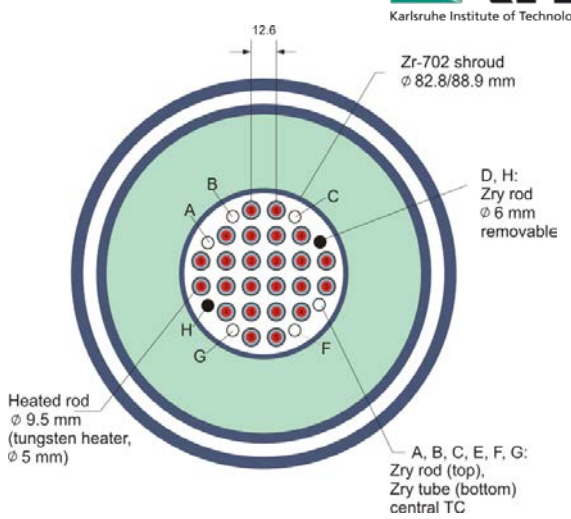


PWR, pitch 14.3 mm

claddings: **Zry-4** or **M5®** alloys

Fuel rod simulators :

20 heated, 1 not heated (or absorber), 4 corner rods

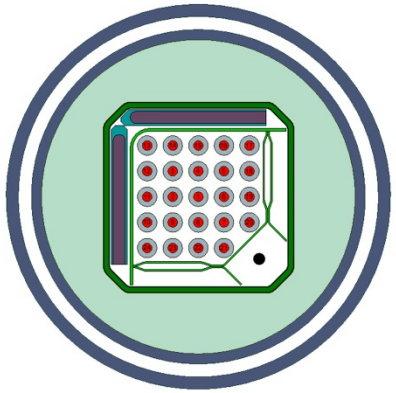


PWR, pitch 12.6 mm

claddings: **ZIRLO™** or **M5®** alloys

Fuel rod simulators :

24 (22) heated, 0 not heated (or 2 AgInCd absorber), 8 corner rods



BWR, pitch 12.898 mm

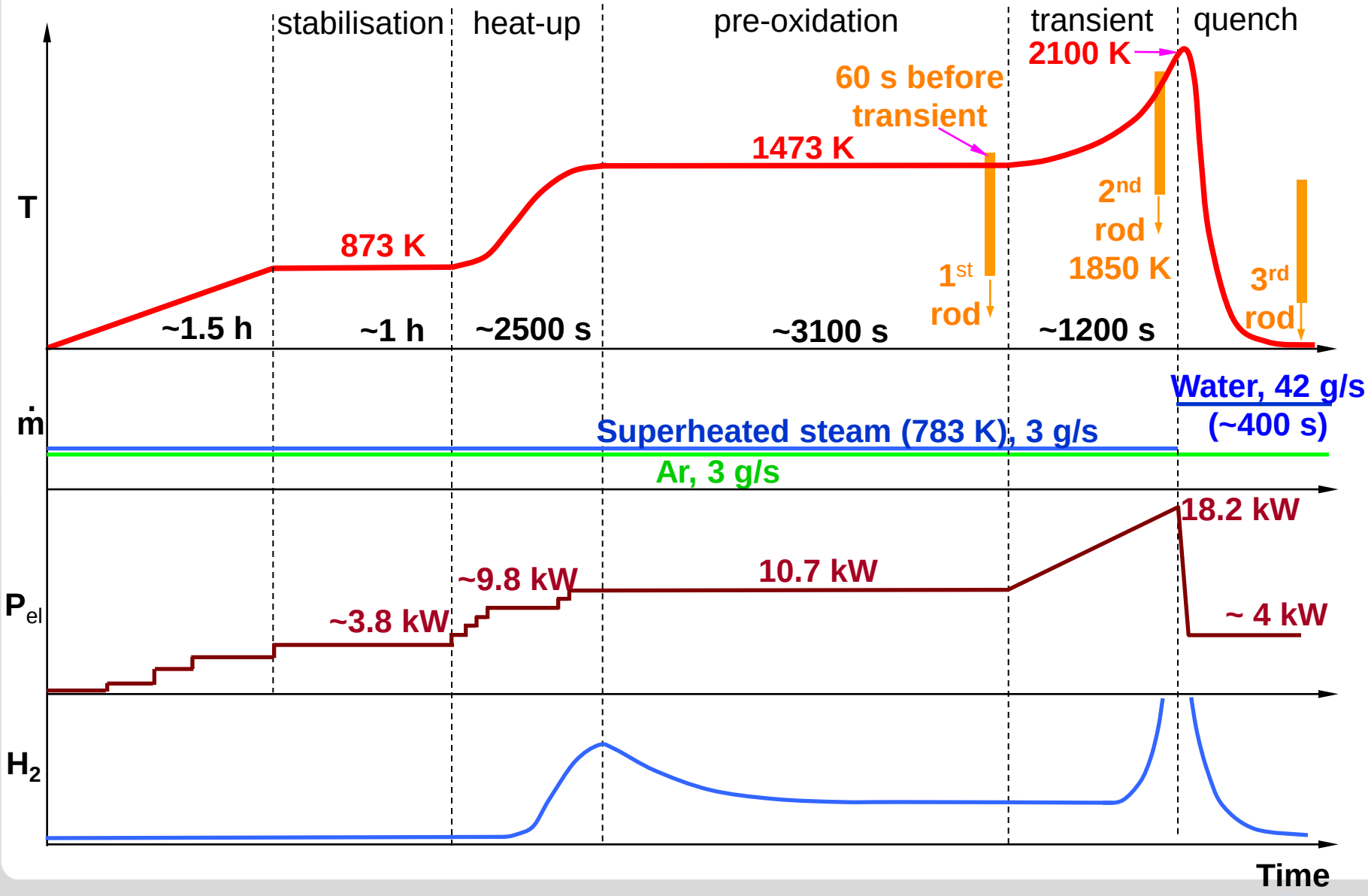
claddings: **Zry-2** alloy

Fuel rod simulators :

24 heated, 1 corner rod

Absorber blades with B_4C pins

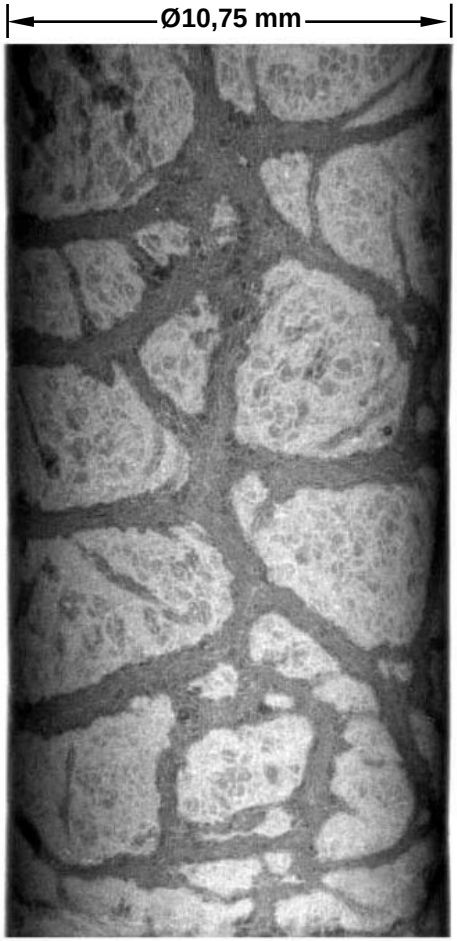
Typical QUENCH scenario: performance of QUENCH-14 (M5®) similar to Q-06 (Zry-4), Q-12 (E110) and Q-15 (ZIRLO™)



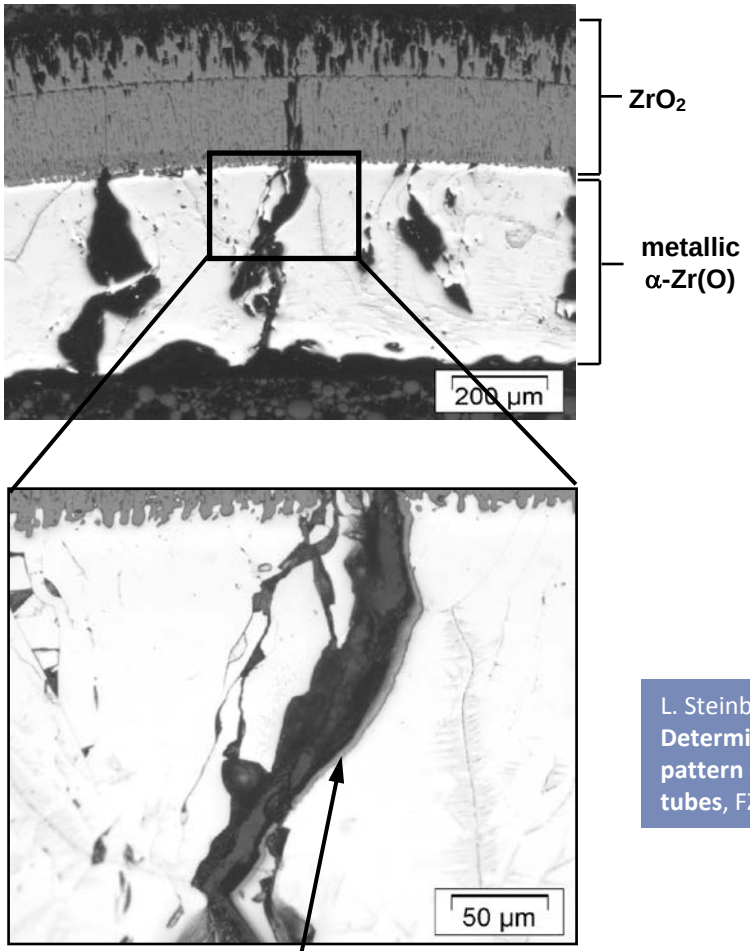
QUENCH test matrix

Test	Quench medium / Injection rate	Temp. at onset of flooding	Max. oxide before transient	Max. oxide before flooding	Max. oxide after test	H_2 production before / during cooldown	Remarks, objectives
QUENCH-00 Oct. 9 - 16, 97	Water 80 g/s	≈ 1800 K			completely oxidized		commissioning test
QUENCH-01 February 26, 98	Water 52 g/s	≈ 1830 K	312 µm		500 µm at 913 mm	**36 / 3**	pre-oxidized cladding
QUENCH-02 July 7, 98	Water 47 g/s	≈ 2400 K			completely oxidized	**20 / 140**	no additional pre-oxidation, **melt**
QUENCH-03 January 20, 99	Water 40 g/s	≈ 2350 K			completely oxidized	**18 / 120**	no additional pre-oxidation, **melt**
QUENCH-04 June 30, 99	Steam 50 g/s	≈ 2160 K	82 µm		280 µm	**10 / 2**	slightly pre-oxidized cladding
QUENCH-05 March 29, 2000	Steam 48 g/s	≈ 2020 K	160 µm		≈ 420 µm	**25 / 2**	pre-oxidized cladding
QUENCH-06 Dec. 13 2000	Water 42 g/s	≈ 2060 K	207 µm	300 µm	≈ 630 µm	**32 / 4**	*OECD-ISP 45*
QUENCH-07 July 25, 2001	Steam 15 g/s	≈ 2100 K	230 µm		completely oxidized	**66 / 120**	EU COLOSS B_4C**, eutectic melt**
QUENCH-09 July 3, 2002	Steam 49 g/s	≈ 2100 K			completely oxidized	**60 / 400**	EU COLOSS B_4C, **eutectic melt**
QUENCH-08 July 24, 2003	Steam 15 g/s	≈ 2090 K	274 µm		completely oxidized	**46 / 38**	EU COLOSS; reference for QUENCH-07, **melt**
QUENCH-10 July 21, 2004	Water 50 g/s	≈ 2200 K	514 µm	613 µm (at 850 mm)	completely oxidized	**48 / 5**	EU LACOMERA; air ingress
QUENCH-11 Dec 08, 2005	Water 18 g/s	≈ 2040 K		170 µm	completely oxidized	**9 / 132**	EU LACOMERA; boil-off, **melt;** *benchmark*
QUENCH-12 Sept 27, 2006	Water 48 g/s	≈ 2100 K	160 µm, breakaway	300 µm, breakaway	completely oxidized	**34 / 24**	ISTC; WWER, **melt**
QUENCH-13 Nov. 7, 2007	Water 52 g/s	≈ 1820 K		400 µm	750 µm	**42 / 1**	EU SARNET; Ag/In/Cd (aerosol)
QUENCH-14 Sept 27, 2006	Water 41 g/s	≈ 2100 K	170 µm	470 µm	900 µm	**34 / 6**	M5® cladding
QUENCH-15 Nov. 7, 2007	Water 41 g/s	≈ 2100 K	145 µm	320 µm	620 µm	**41 / 7**	ZIRLO™ cladding
QUENCH-16 July 27, 2012	Water 50 g/s	≈ 1870 K	135 µm	140 µm	850 µm: outer **porous,** inner dense	**16 / 128**	EU LACOMECO; air ingress, **melt;** *benchmark*
QUENCH-17 Jan. 31, 2013	Water 10 g/s	≈ 1800 K		completely oxidized	completely oxidized	**110 / 1**	*EU SARNET-2; DEBRIS formation*
QUENCH-18 Sept. 27, 2017	Water 53 g/s	≈ 2000 K	90 µm		partially dissolved by **melt**	**56 / 238**	EU ALISA; **AgInCd** absorber (**melt** and aerosols); *air ingress*
QUENCH-19 August 29, 2018	Water 41 g/s	≈ 1740 K				**8.8 / 0.5**	ATF (FeCrAl) clads; cooperation with ORNL
QUENCH-20 October 9, 2019	Water 50 g/s	≈ 2000 K	≈ 100 µm		t.b.d.	**25.4 / 32**	EU SAFEST; BWR bundle with B4C absorber

Oxidation of cracks developed during flooding: low contribution to hydrogen production



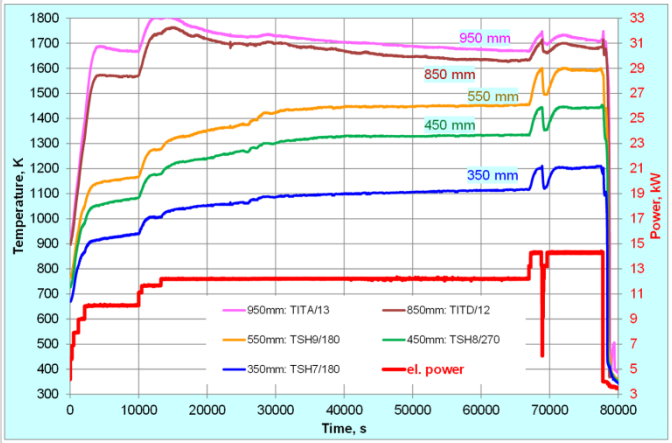
Development of cracks in the cladding with thick oxide layer (>150 µm) and cooled down with steam. Crack density ~ 4 cm/cm²



L. Steinbock and J. Stuckert. **Determination of the crack pattern of quenched zircaloy tubes**, FZKA-6013 (1997)

Negligible oxidation of crack edges gives only some percent of generated hydrogen

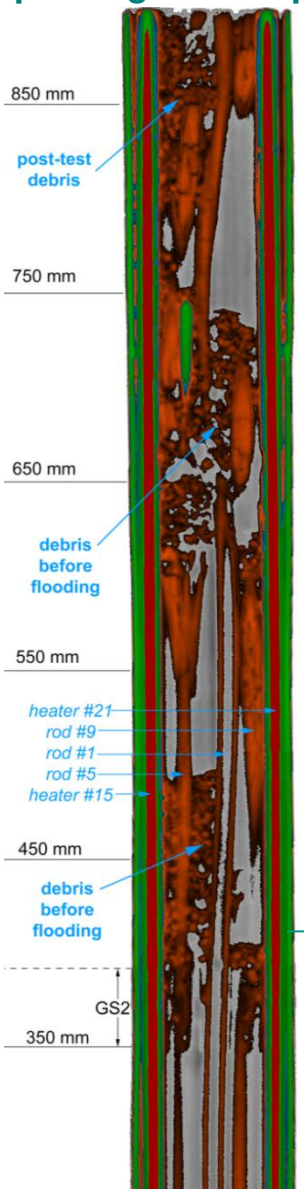
QUENCH-17: Debris formation after degradation of strongly oxidized cladding and release of pre-segmented pellet simulators



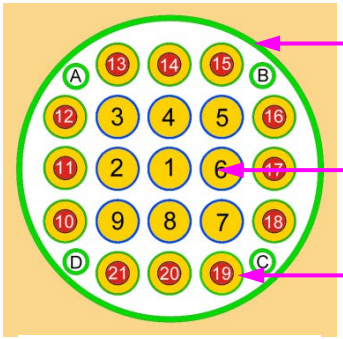
test scenario



debris: 1) separated parts of fuel pellets simulator; 2) large segments of failed Zry claddings.



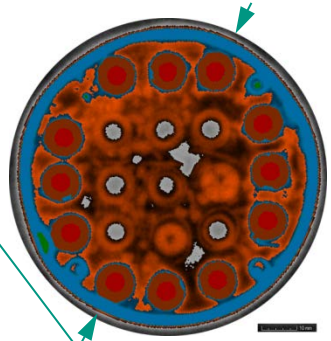
X-ray tomography



bundle composition



cross-section at 400 mm: metallography; debris bed porosity 50%



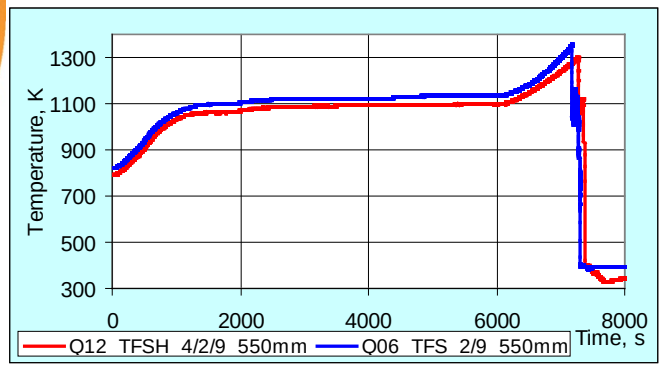
cross-section at 400 mm: tomography; blockage 85%

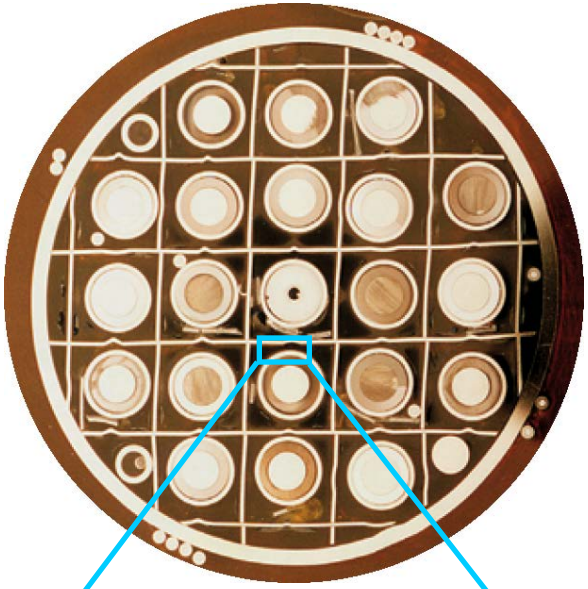
J. Stuckert et al., **Results of the QUENCH-DEBRIS test**, ICAPP 2014, Paper 14150

Weakening of protective oxide layer by breakaway oxidation: QUENCH-12 (WWER, electrolytic E110) vs. QUENCH-06 (Zry-4)

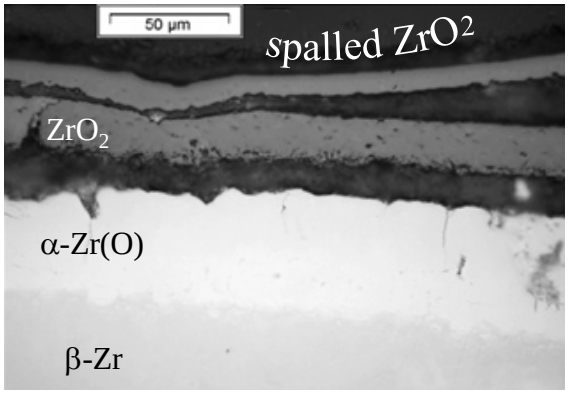


Q12: rubble on spacer grid consists of spalled cladding scales and fragments of partially oxidized cladding



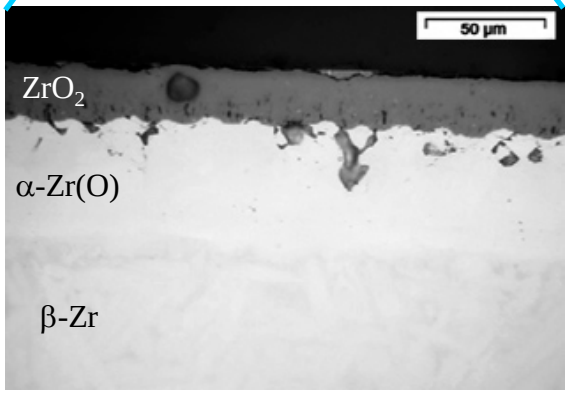


Q06 cross-section



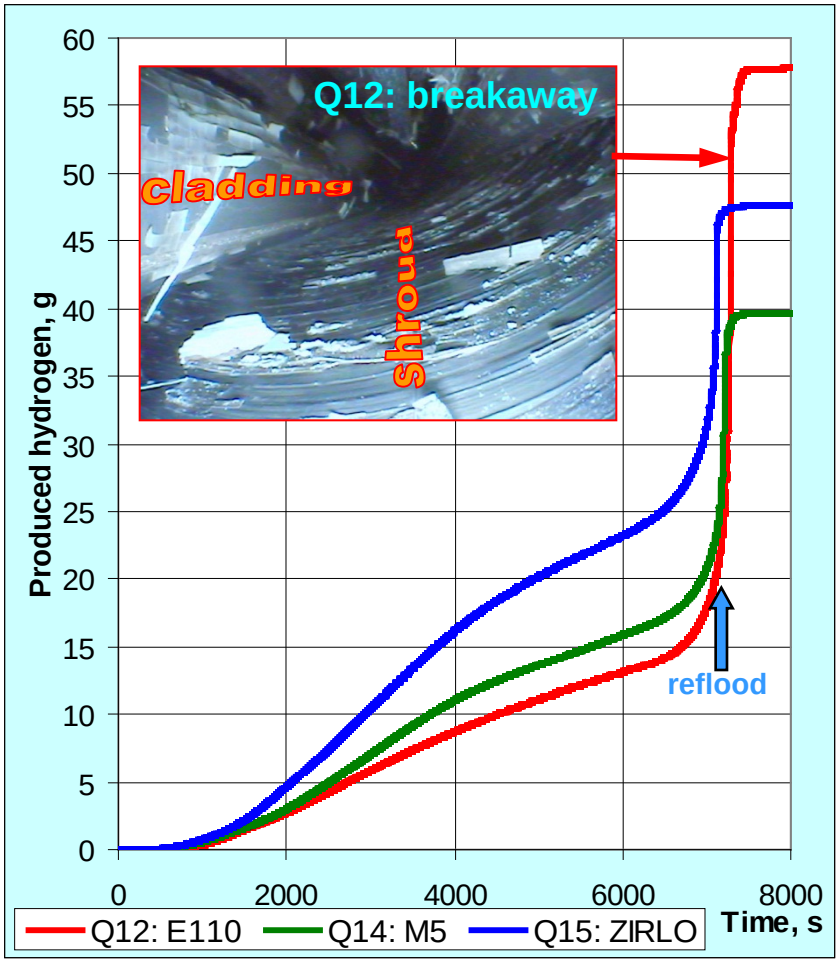
Q12 cladding: spalling of oxide scales due to breakaway effect

J. Stuckert et al. **Experimental and post-test calculation results of the integral reflood test QUENCH-12 with a VVER-type bundle**, ANE 36 (2009) 183–192

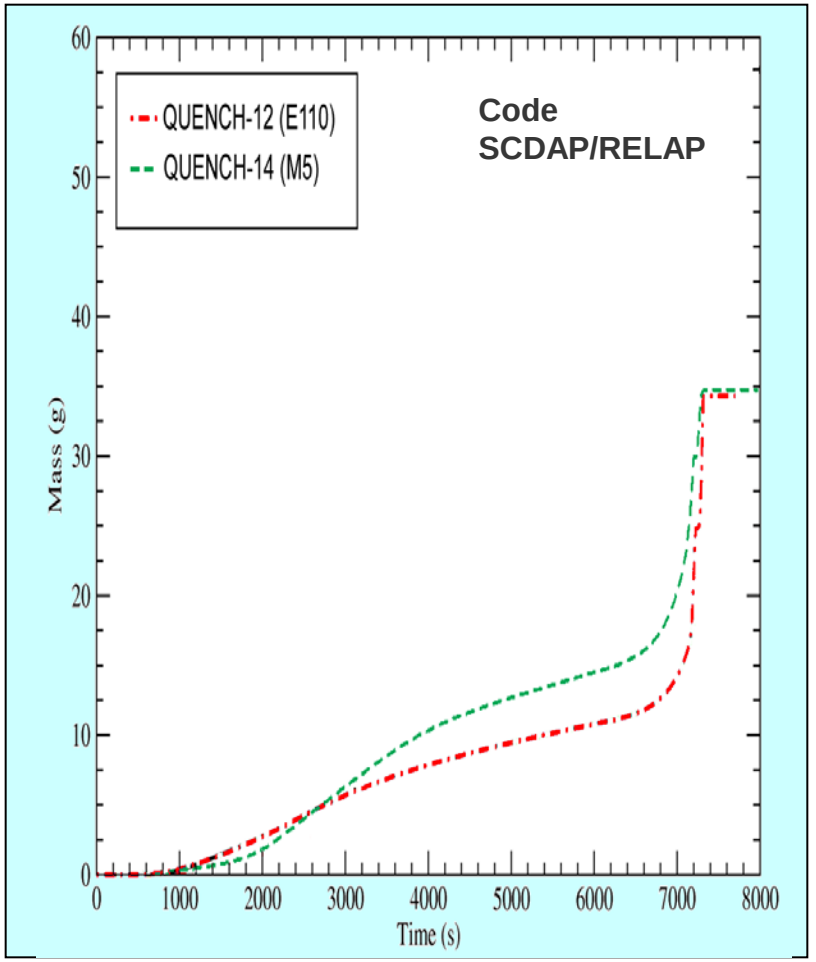


Q06 oxidized cladding

Increased hydrogen production during reflood after breakaway: QUENCH-12 (electrolytic E110) vs. QUENCH-14 (M5®)

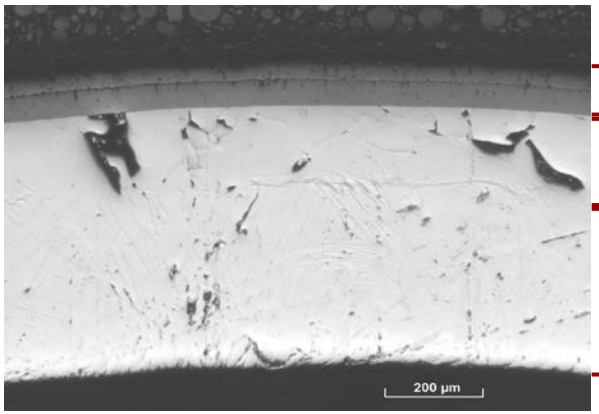


Consequences of breakaway enhanced hydrogen release: 1) new metallic surfaces, 2) melt release outside cladding, 3) release of hydrogen absorbed in metal.



Post-test calculations: need for improvement of model for quench phase

Influence of pre-reflood steam or oxygen starvation conditions (QUENCH-09, -11, -16, -18)

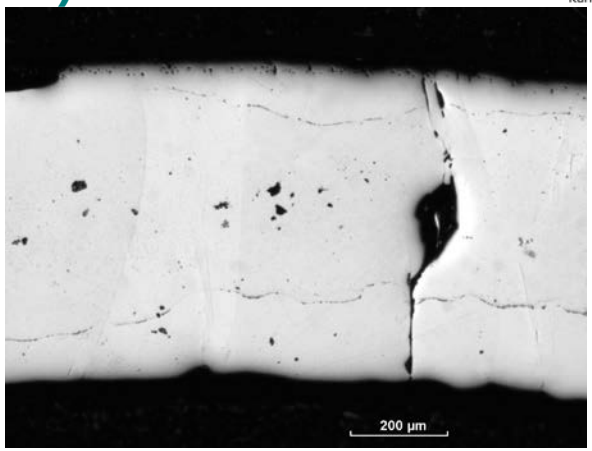


ZrO_2, 134 µm

α-Zr(O), 182 µm

β-Zr, 431 µm

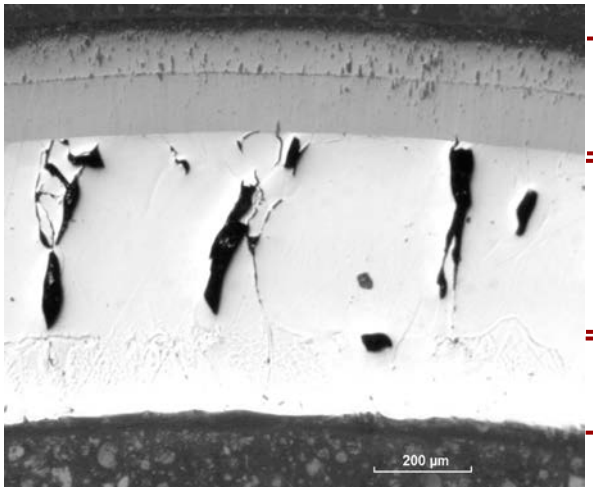
Steam starvation at 1700K



α-Zr(O), 733 µm

„Thin“ oxide layer

Complete decomposition of oxide layer

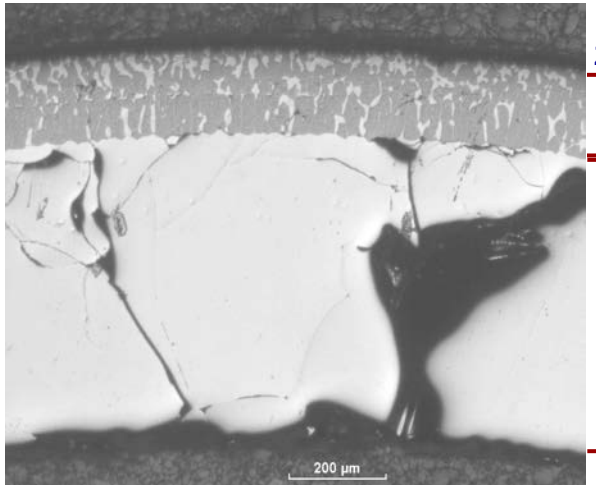


ZrO_2, 228 µm

α-Zr(O), 397µm

β-Zr, 177 µm

Steam starvation at 1700K



ZrO_2: 186µm, Metallic precipi-tations 24%

α-Zr(O), 646 µm

„Thick“ oxide layer

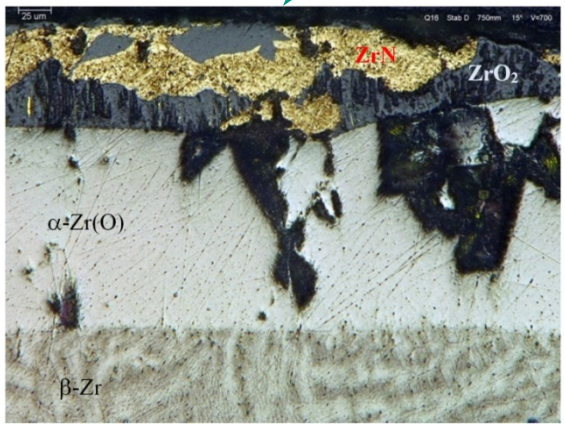
J. Stuckert and M. Veshchunov **Behaviour of Oxide Layer of Zirconium-Based Fuel Rod Cladding under Steam Starvation Conditions**, FZKA-7373 (2008)

Development of metallic precipitations inside oxide layer. Precipitates will expose to intensive oxidation during following flooding

Air ingress after moderate pre-oxidation (QUENCH-10, -16): massive nitride formation during *oxygen starvation* and their intensive re-oxidation during quench

Q16 pre-reflood



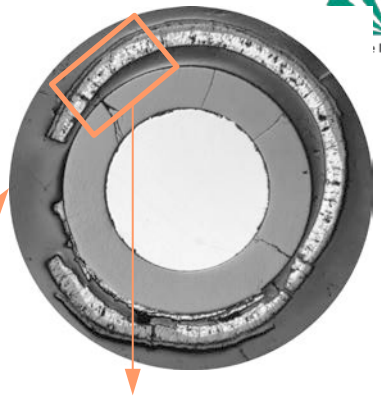


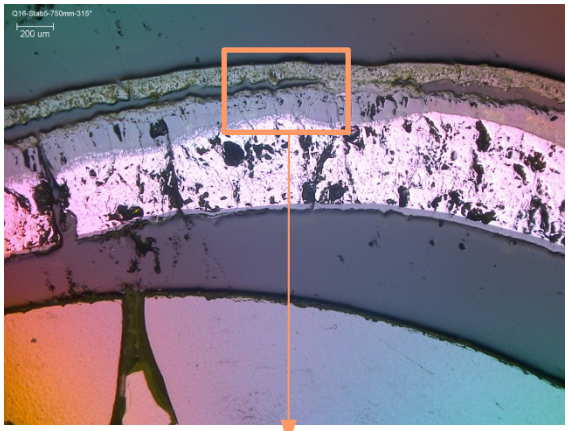
nitride formation inside oxide layer

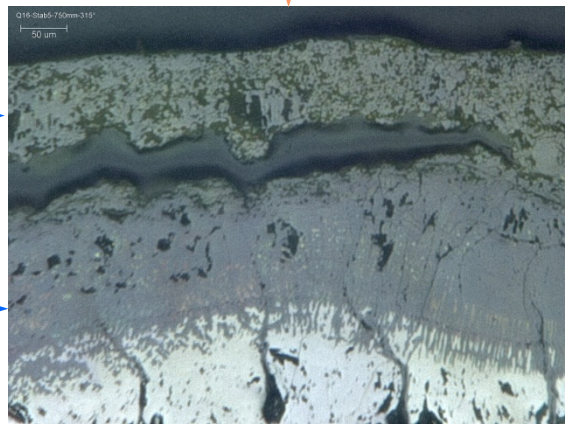
Q16 post-reflood



Endoscope observation at ~850 mm







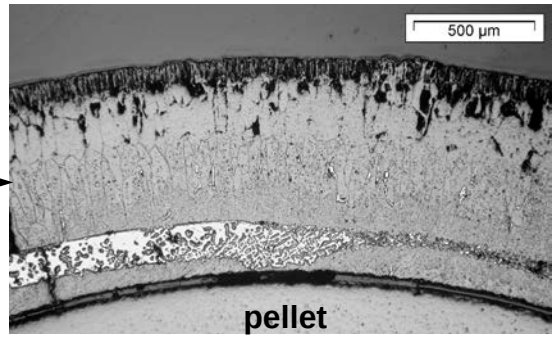
prior nitrided scale *re-oxidised* during quench and spalled

from internal ZrO_2 layer growing during quench

J. Stuckert and M. Steinbrück **Experimental results of the QUENCH-16 bundle test on air ingress**, PNE 71 (2014) 134-141

Typical layer structure of strong oxidised cladding at hottest bundle elevation of 1000 mm after reflood

outer ZrO_2
formed during pre-oxidation and reflood

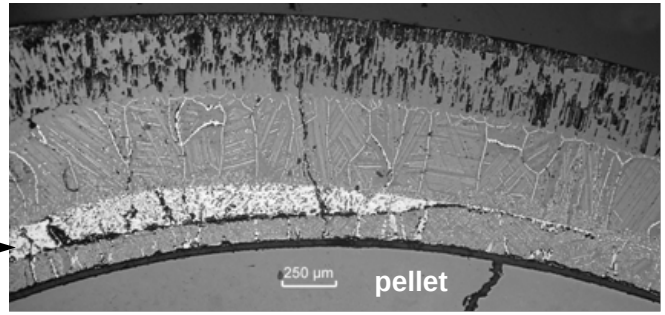


QUENCH-15 (ZIRLO™)

rod #17

J. Stuckert et al., **Experimental and calculation results of the integral reflood test QUENCH-15 with ZIRLO™ cladding tubes in comparison with results of previous QUENCH tests**, NED 241 (2011) 3224–3233

melt
formed at ~2030 K
and partially oxidised
due to dissolution of ZrO_2

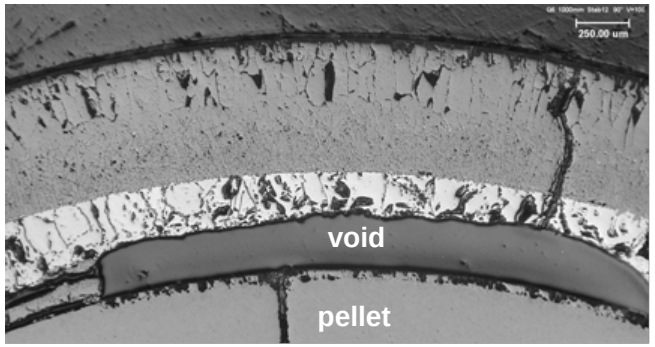


QUENCH-14 (M5®)

rod #11

J. Stuckert et al., **Experimental and calculation results of the integral reflood test QUENCH-14 with M5® cladding tubes**, ANE 37 (2010) 1036–1047

inner ZrO_2
formed during reflood
(due to interaction with steam penetrated under breached cladding; no interaction with pellet)

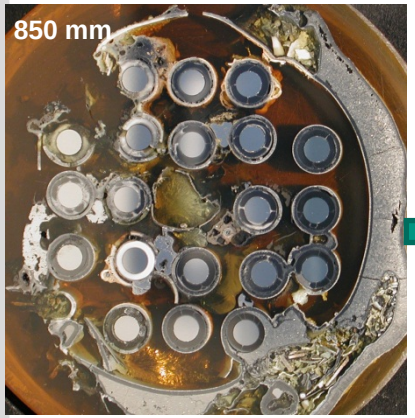


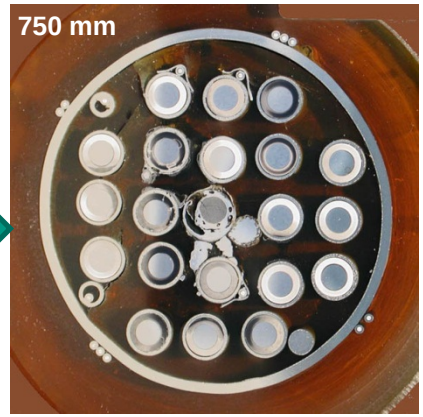
QUENCH-06 (Zry-4)

rod #12

L. Sepold et al., **Experimental and computational results of the QUENCH-06 test (OECD ISP-45)**, FZKA-6664 (2004)

Eutectic melt induced upper 1200°C by absorber rod: *complementary* tests Q-07 (B_4C rod) and Q-08 (without absorber)



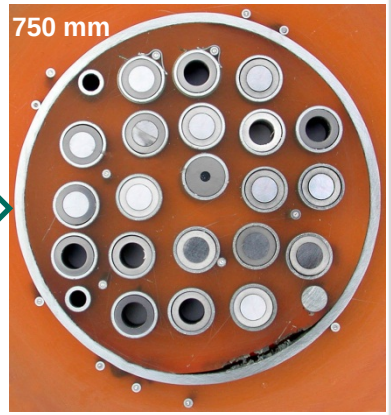


QUENCH-07: formation of significant melt amount and melt relocation

B_4C<->Fe eutectic at ~1150°C

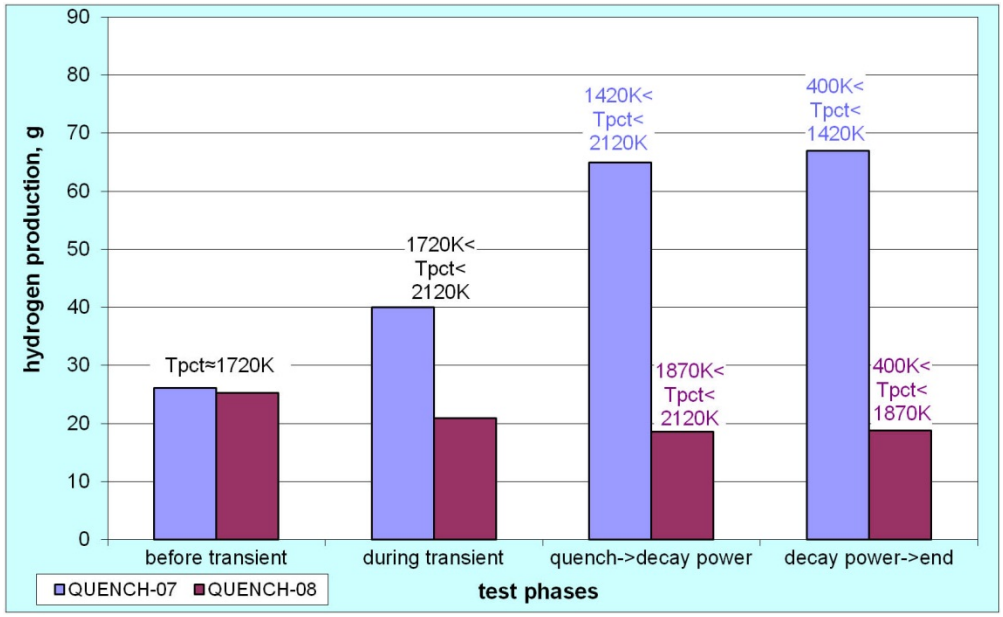
Zry <-> SS eutectic at ~1300°C





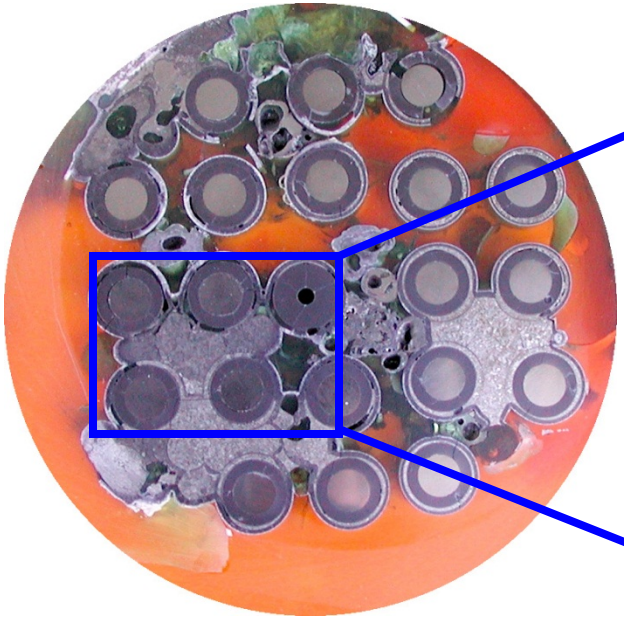
QUENCH-08: moderate melt formation; no noticeable melt relocation

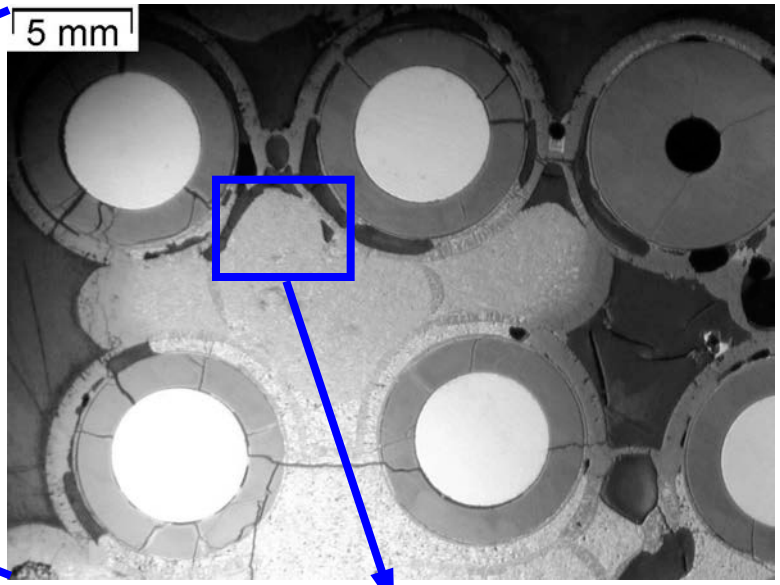
hydrogen productions for different test phases with indication of temperature evolution during the phase:

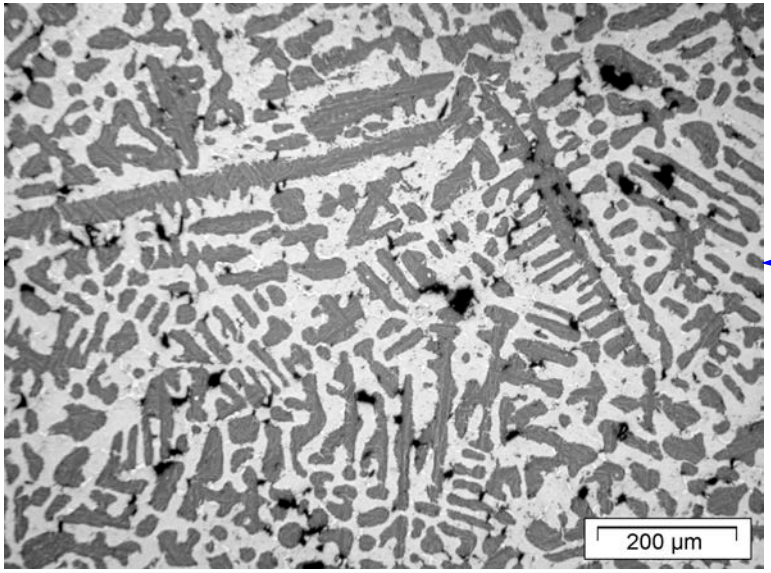


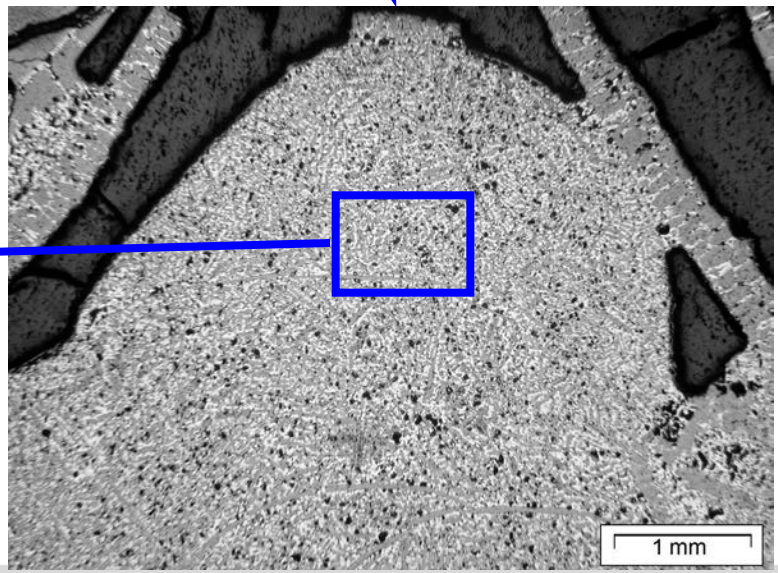
J. Stuckert et al., **Experimental and Computational Results of the QUENCH-08 Experiment (Reference to QUENCH-07)**, FZKA-6970 (2005)

QUENCH-11, elev. 837 mm: melt relocated outside fuel rods and oxidised in steam







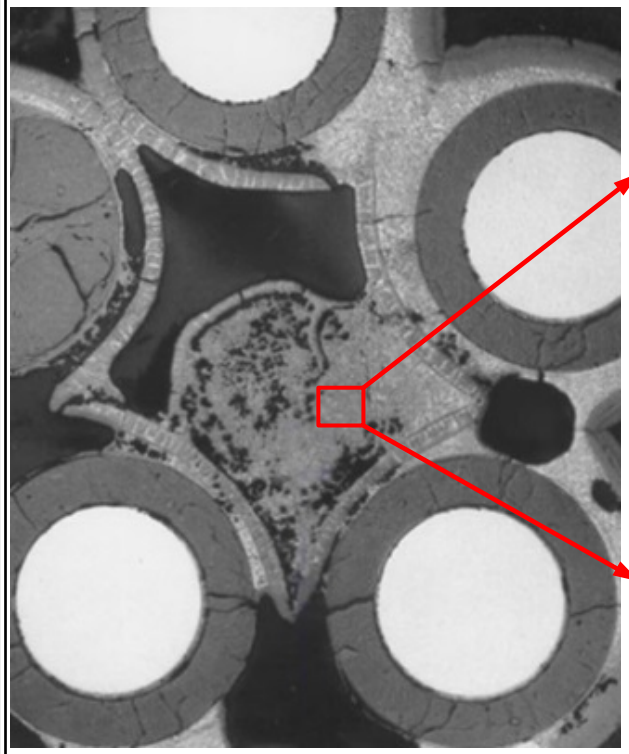


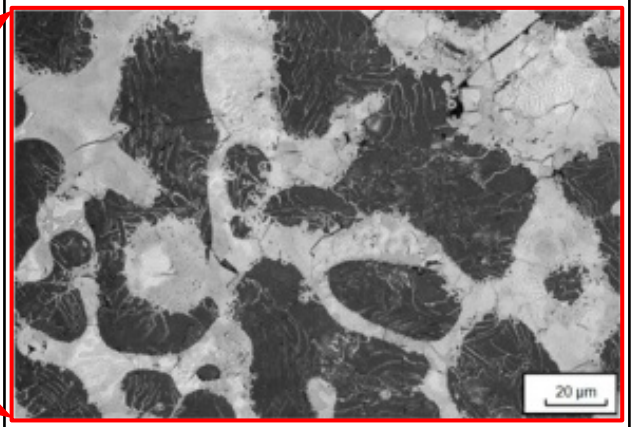
Molten pools frozen at middle and upper elevations of the PWR QUENCH-03 bundle flooded from the bundle bottom at $T_{pct} \approx 2350$ K by water with flow rate $F_q \approx 1$ g/s/rod

		
650 mm	**950 mm**	**1150 mm**

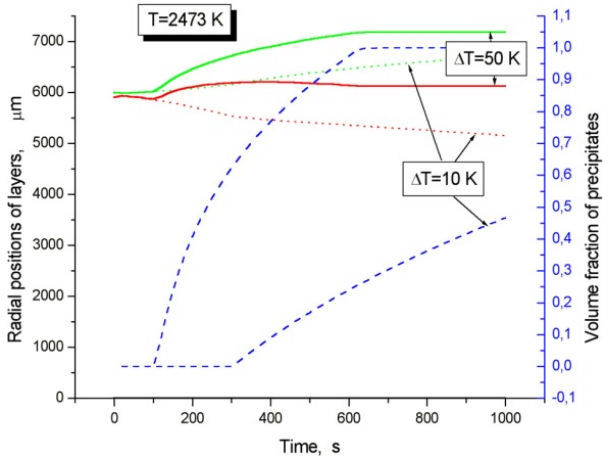
P. Hofmann et al., **Experimental and calculation results of the experiments QUENCH-02 and QUENCH-03**, FZKA-6295 (2000)

Analysis of the melt composition formed in the PWR QUENCH-02 bundle flooded from bottom at $T_{pct} \approx 2400$ K with flow rate $F_q \approx 1$ g/s/rod





M. Veshchunov et al., **Modelling of Zr-O and U-Zr-O melts oxidation and new crucible tests**, FZKA-6792 (2002)

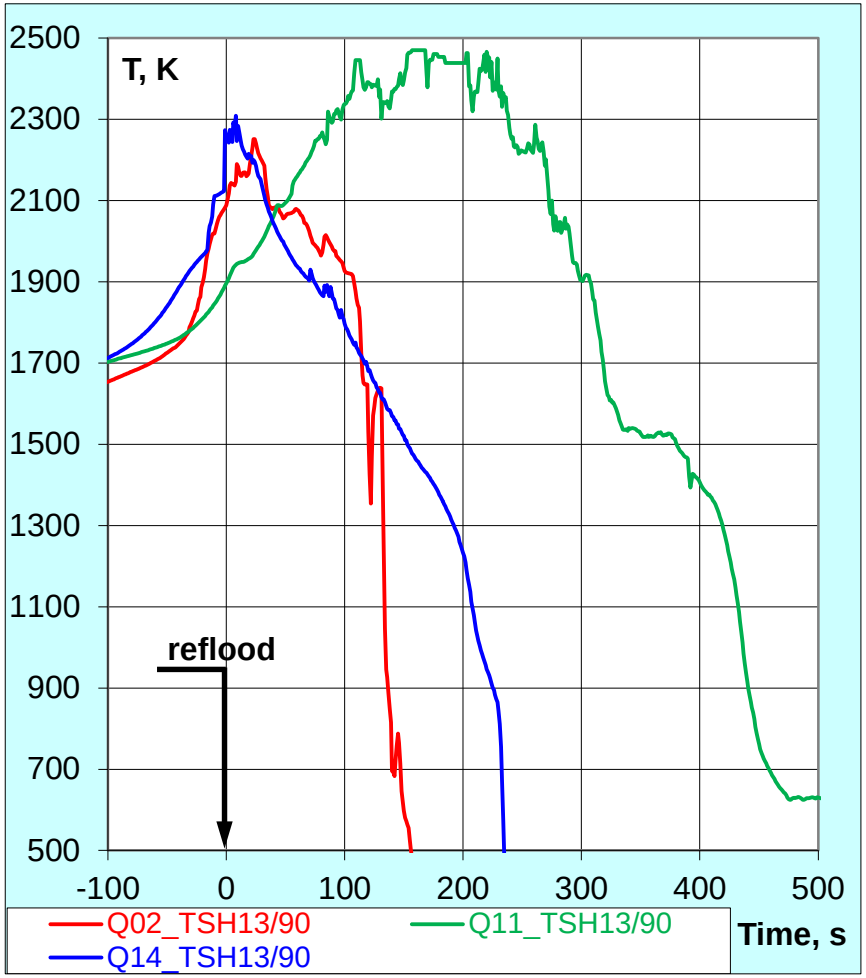


Post-test image of cross section of the QUENCH-02 bundle at elevation of 850 mm showing an oxidized molten pool surrounded by oxide

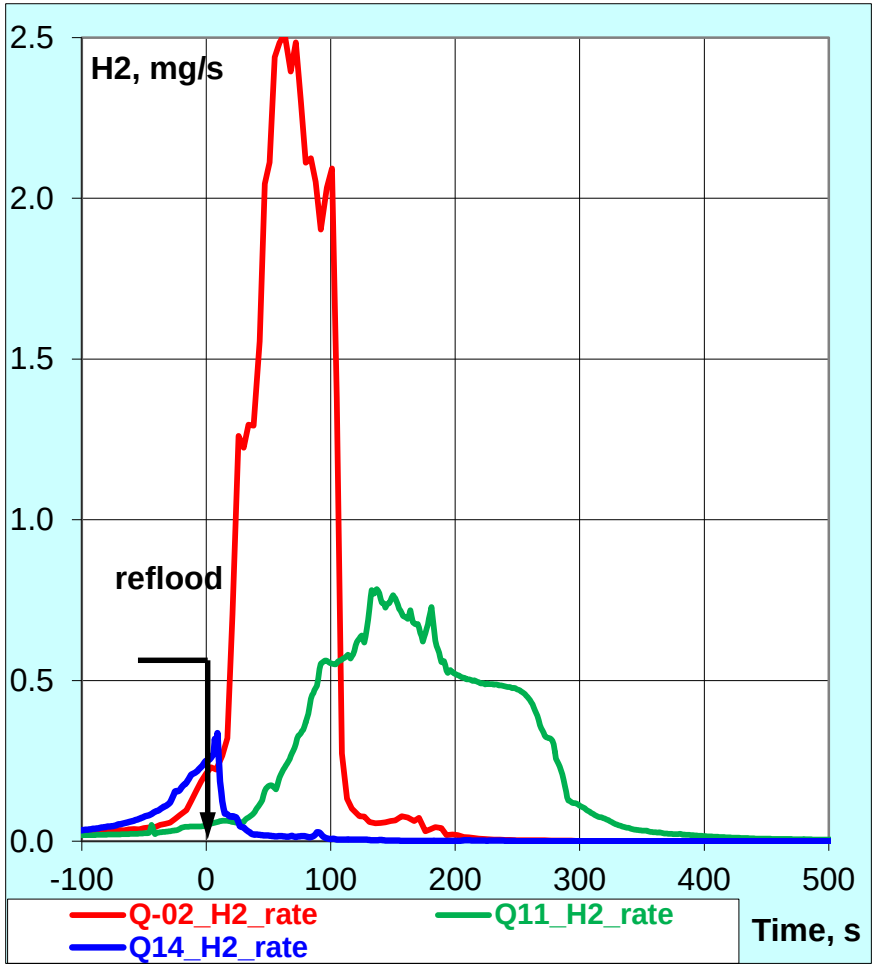
Ceramic precipitates inside QUENCH-02 molten pool, oxygen concentration 53 at% (image analysis): above saturation limit of 46%

SVECHA simulation of Zr melt oxidation at 2473 K for two temperature drops in the boundary oxide layer ΔT = 10 K and 50 K for cylindrical molten pool with radius of 6 mm;
solid and dotted curves: radial positions of internal (red) and external (green) oxide layer boundaries; dashed curves: volume fraction of precipitates

Hydrogen release
with (Q-02, Q-11) and without (Q-14) melt oxidation in steam



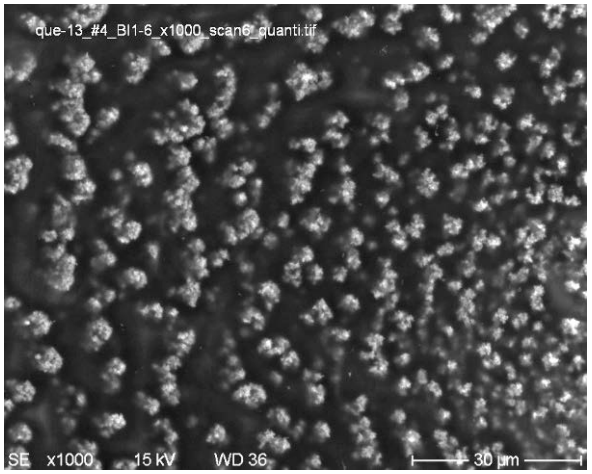
temperature histories

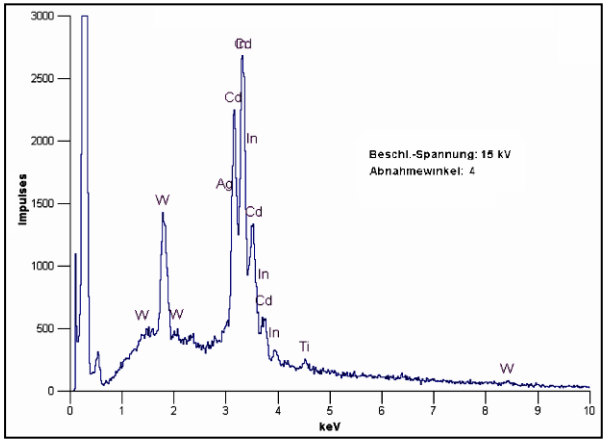


hydrogen releases

QUENCH-13: aerosol release after failure of AgInCd absorber rod

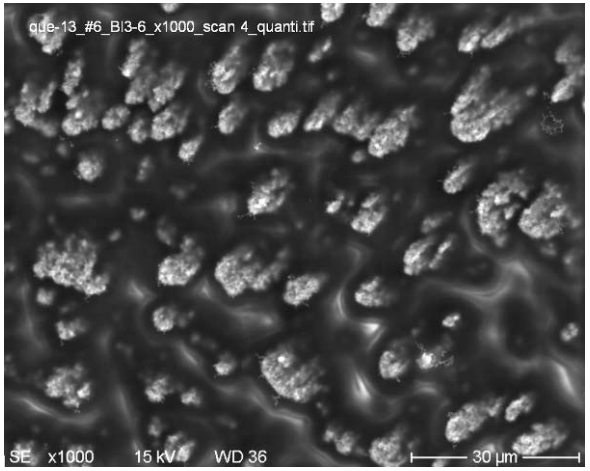
Sample PSI BI1/6 (D_{ae}=0.4-0.7 µm): collected after control rod failure

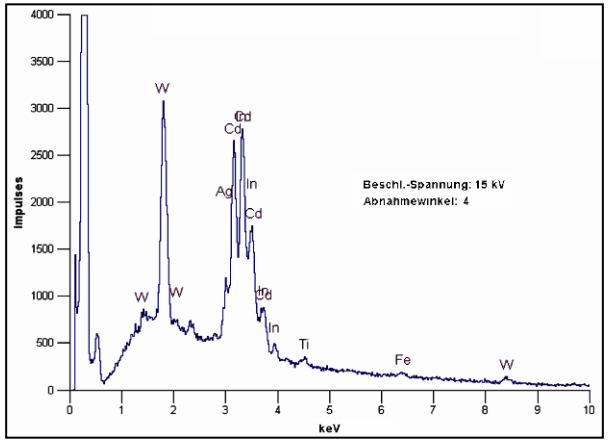




	Cd	In	Ag	W
wt%	42	41	2.5	14.5

Sample PSI BI3/6 (D_{ae}=0.4-0.7 µm): collected before reflood

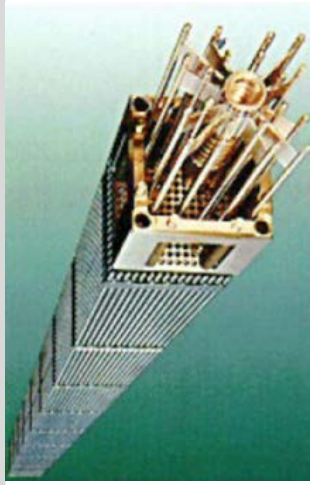




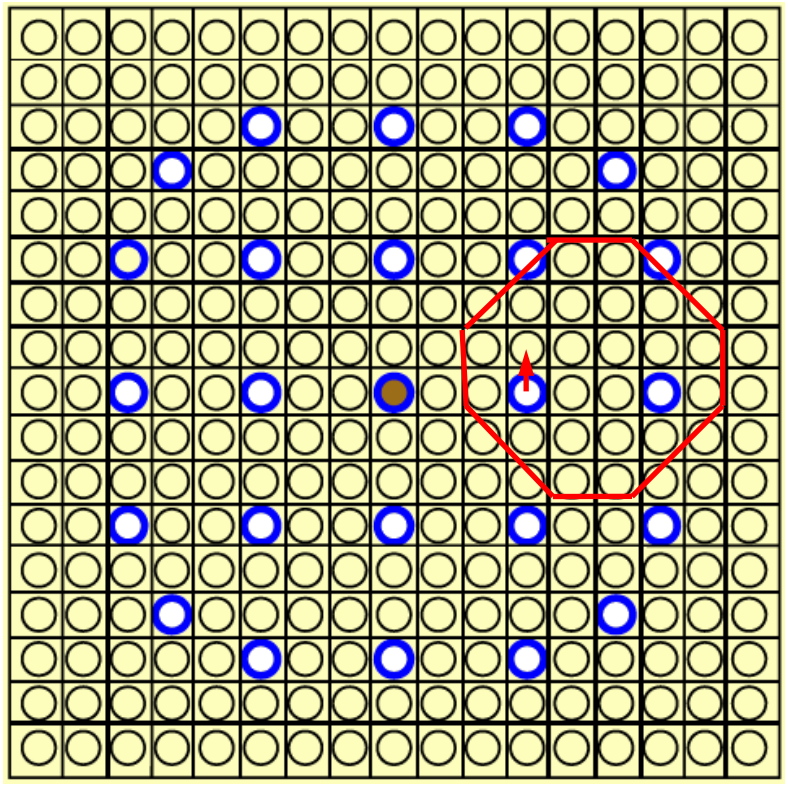
	Cd	In	Ag	W	Fe
wt%	33	31	8	27	1

T. Lind et al., **Aerosol behavior during SIC control rod failure in QUENCH-13 test**, JNM 397 (2010) 92–100

QUENCH-18 test on air ingress and aerosol release



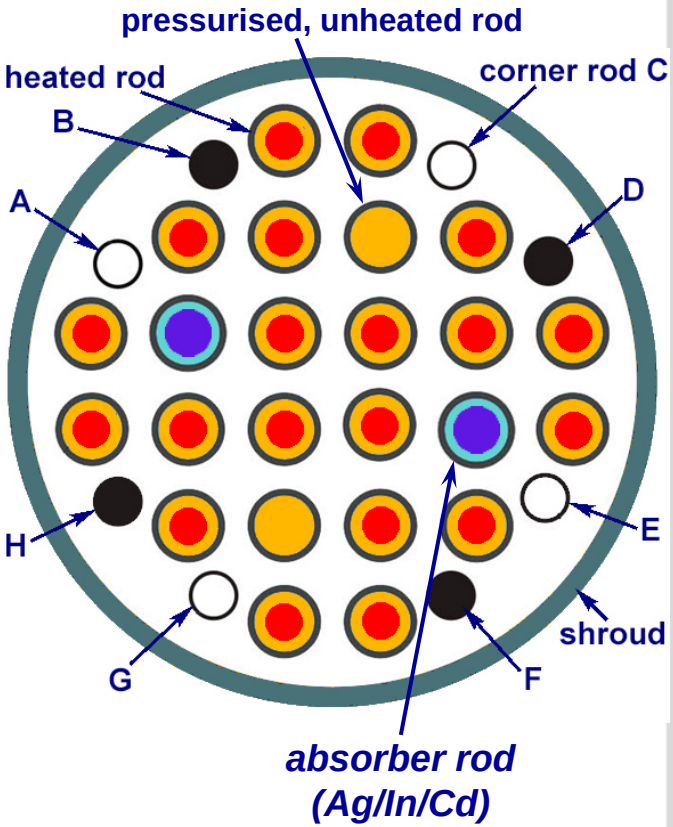
fuel assembly **17x17**



- fuel rod (264)
- guide tube for AgInCd control rod (24)
- instrument thimble

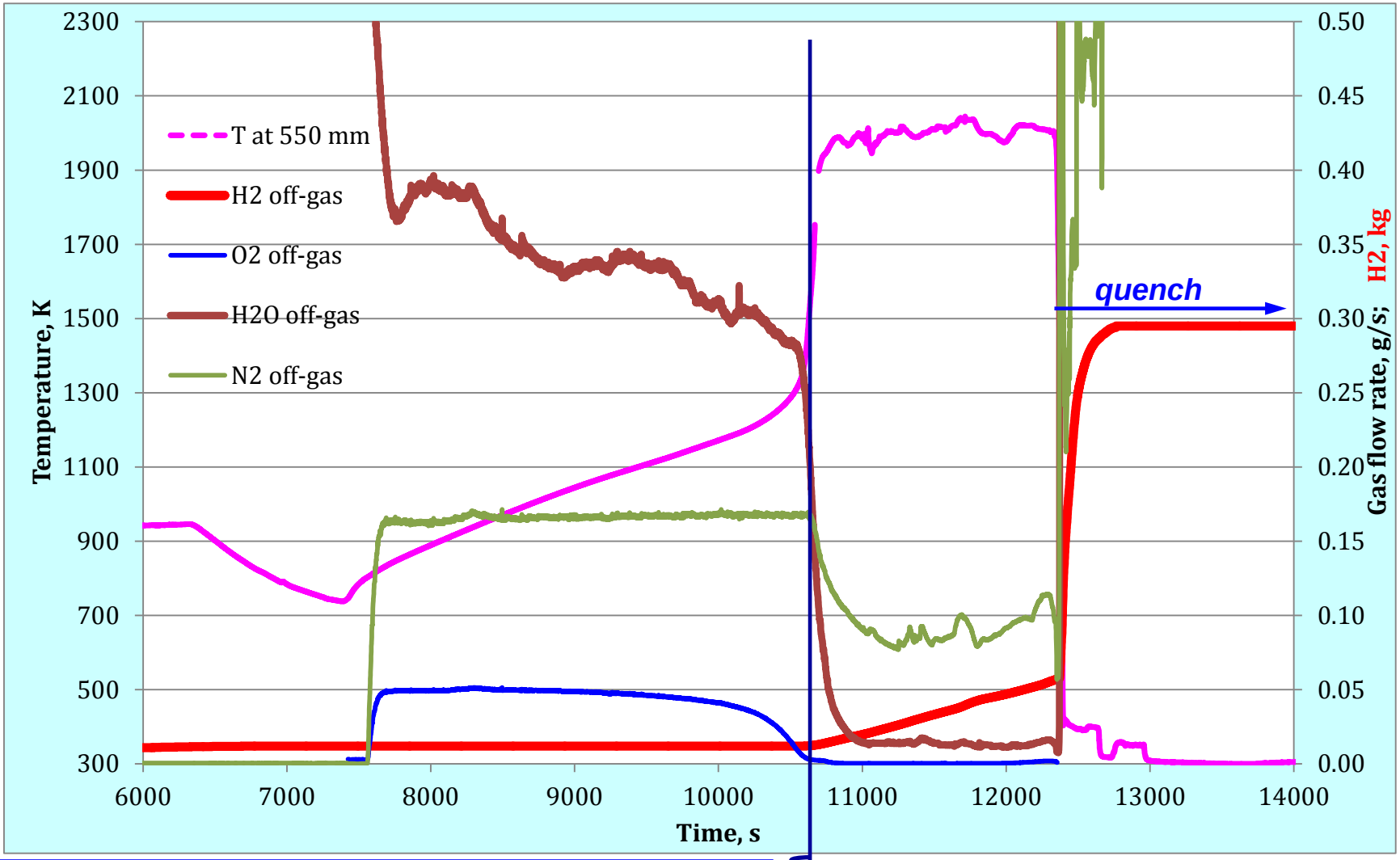
10:1

proposed QUENCH test bundle



J. Stuckert et al., **First results of the QUENCH-ALISA bundle test**. NUTHOS-2019 (2019)

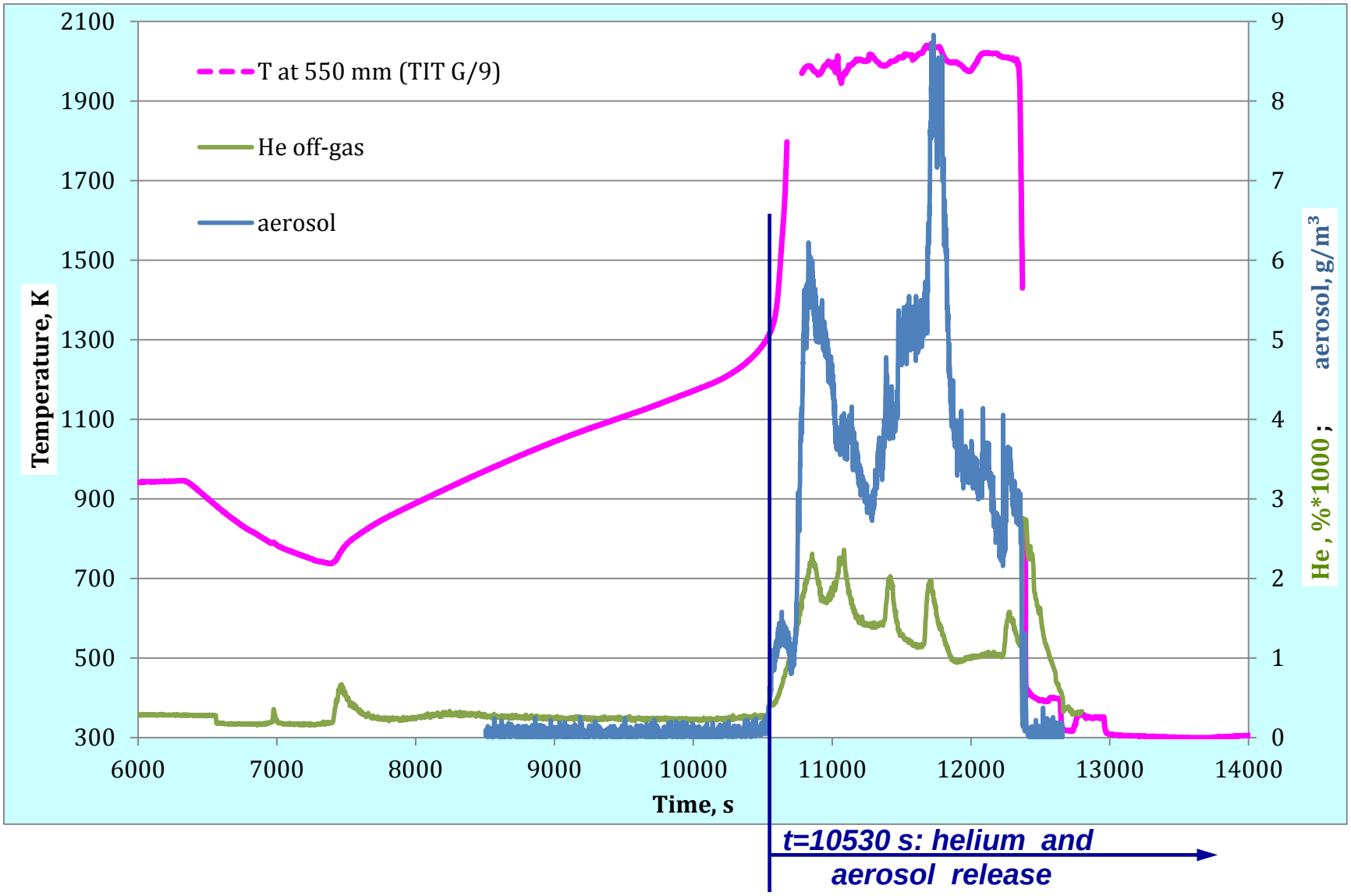
Outlet gas behaviour during air ingress in QUENCH-18: starvation phenomena



consumed oxygen: 100 g; consumed nitrogen: 120 g;
consumed steam: 450 g; released hydrogen: 45 g

t≈10600 s: oxygen starvation, H_2 increase steam and nitrogen consumption

Failure of absorber rods and aerosol release in QUENCH-18

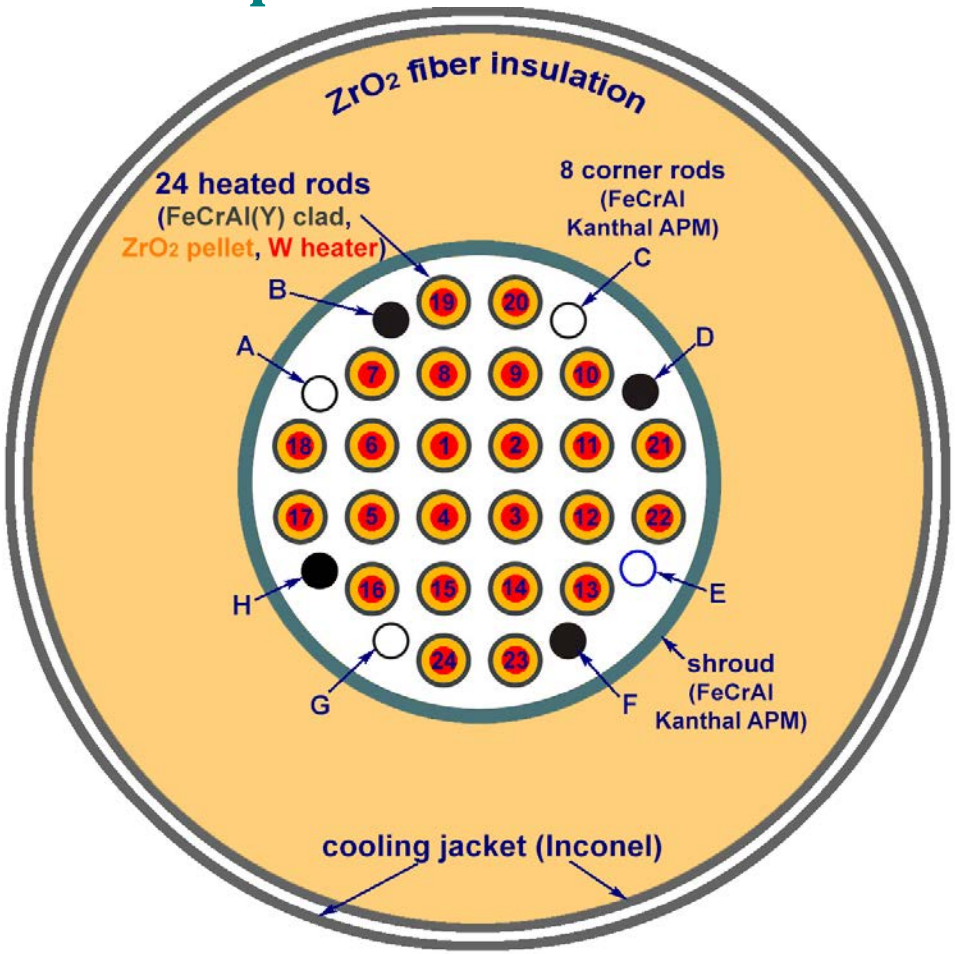


Aerosols in QUENCH-18: release of Cd, Ag, In

Element	Released, g	fraction of total mass in control rods, %
Cadmium	**9.0**	**14.3**
Silver	6.6	0.6
Indium	1.2	0.7
Total	*16.8*	*1.3*

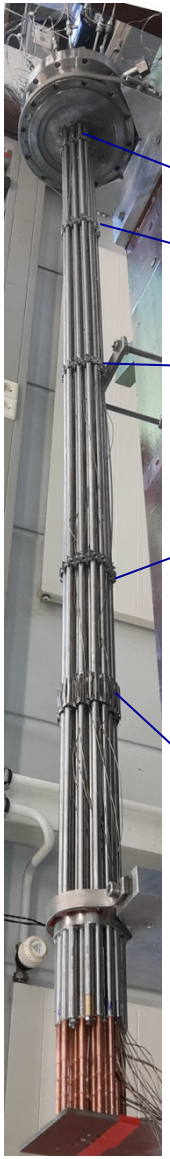
J. Kalilainen et al., **The measurement of Ag/In/Cd release under air-ingress conditions in the QUENCH-18 bundle test**. JNM 517 (2019), pp. 315-327

Composition of the test bundle QUENCH-19 (FeCrAl)

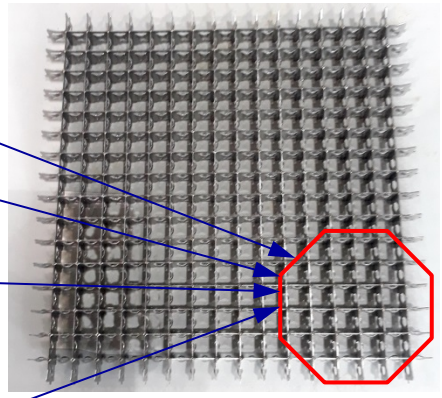


cross section
(arrangement the same as for QUENCH-15)

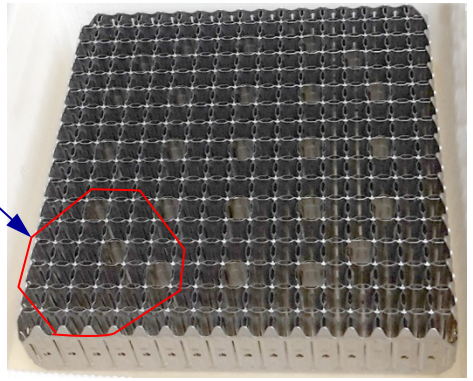
J. Stuckert et al., **First results of the bundle test QUENCH-19 with FeCrAl claddings**. QWS-24 (2018), Karlsruhe



test bundle (length 2m)

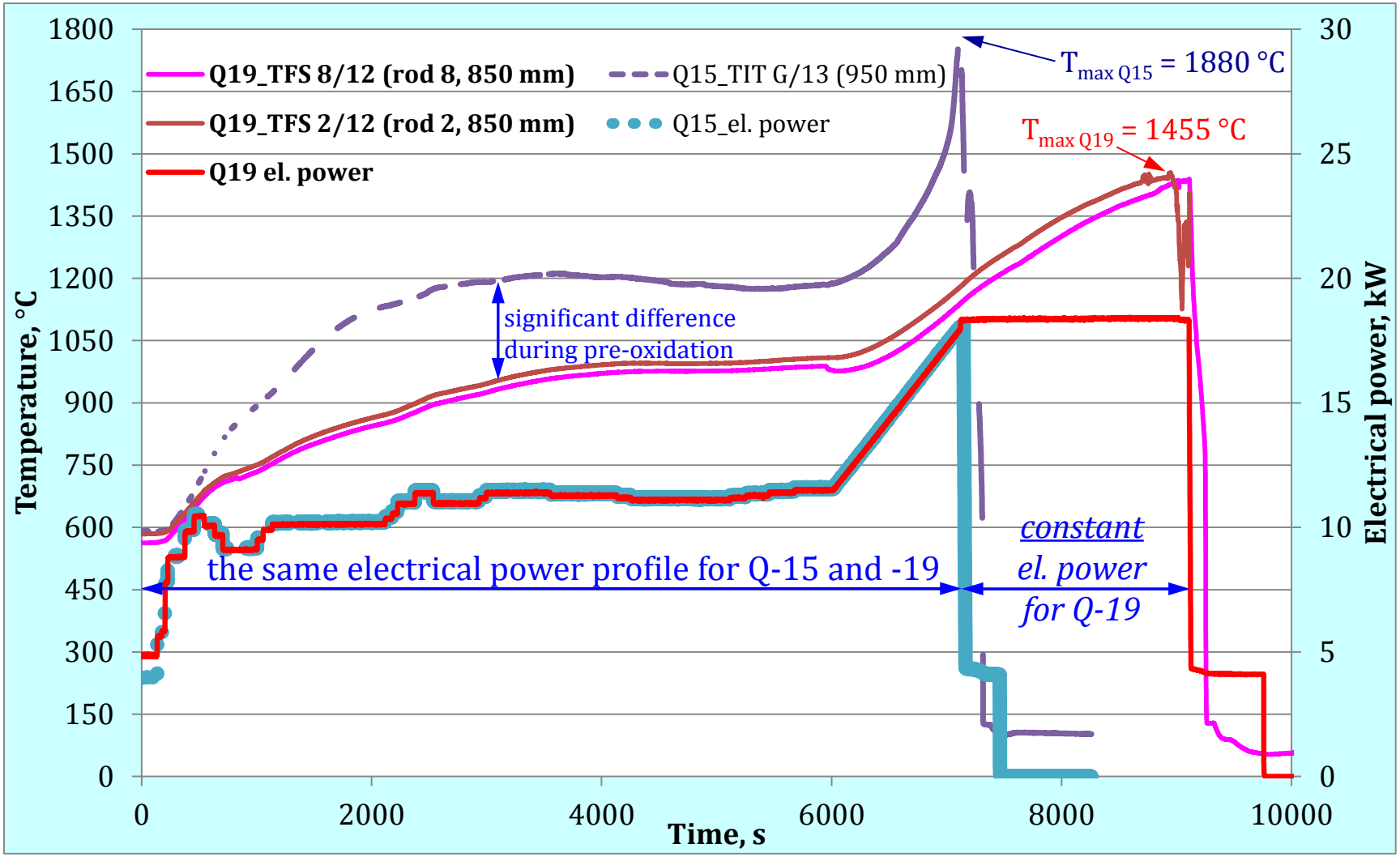


ORNL Kanthal AF **spacer grids**:
height 22 mm,
sheet thickness 0.5 mm



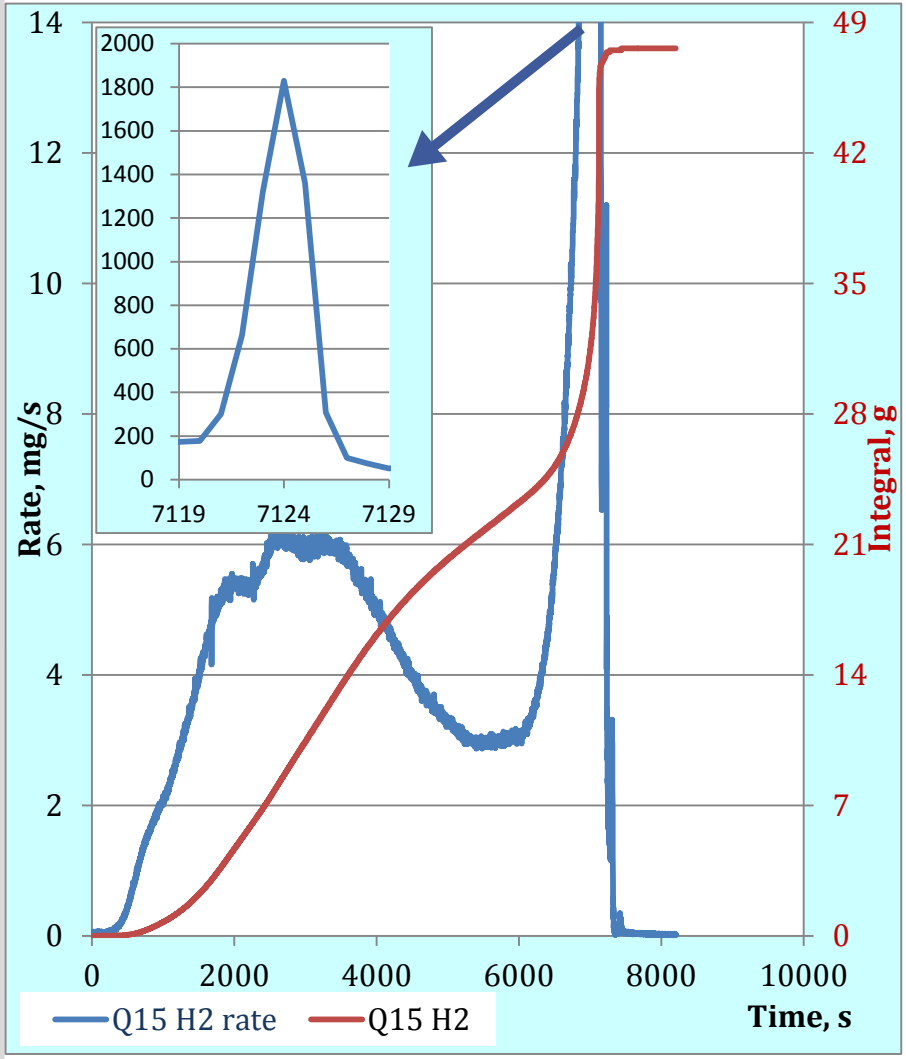
AREVA Inconel **spacer grid**:
height 45 mm,
sheet thickness 0.5 mm

Test performance: comparison of QUENCH-15 (ZIRLO) and -19 (FeCrAl)

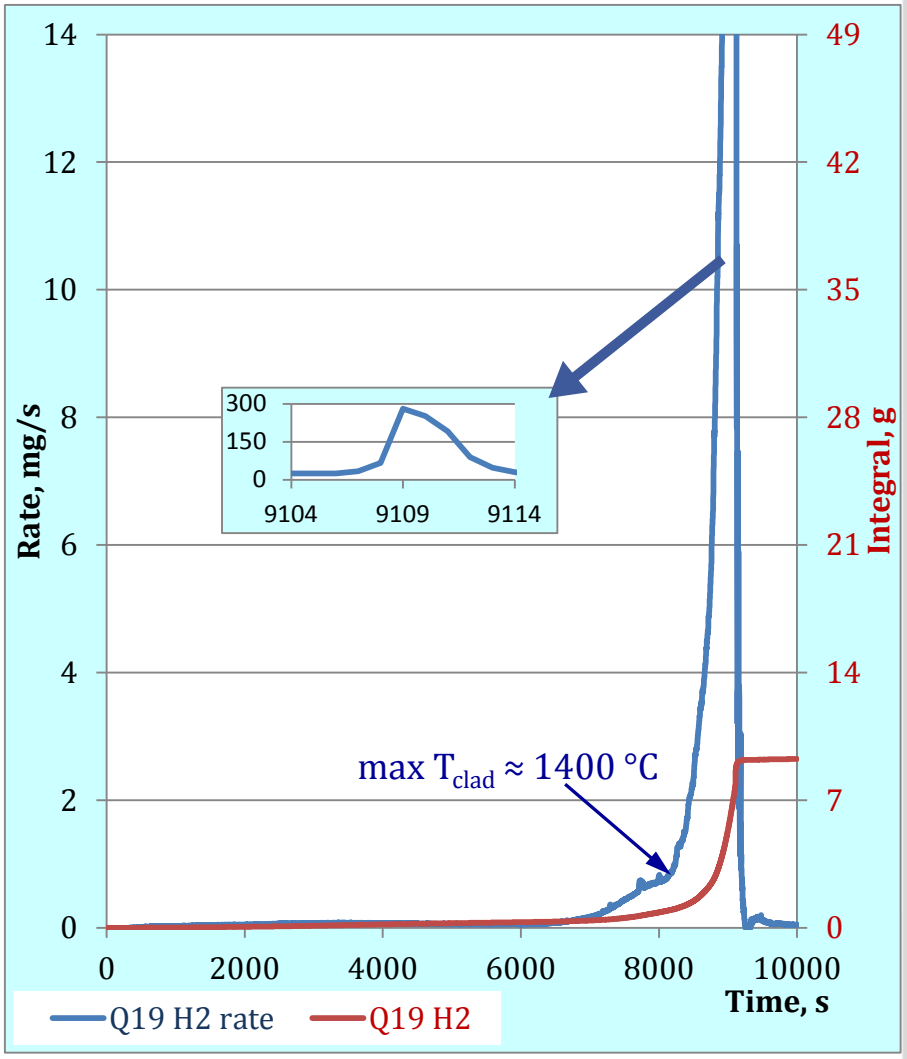


Energy release during Q15 pre-oxidation (i.e. until 6000 s): electrical $E_e = 63.7$ MJ, chemical $E_{ch} = 3.5$ MJ $\Rightarrow$ $E_{ch} \ll E_e$

Hydrogen release in QUENCH-15 (ZIRLO) and -19 (FeCrAl)

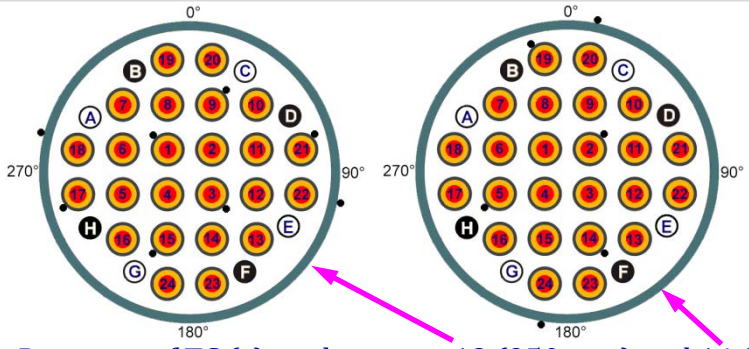


QUENCH-15: max rate 1830 mg/s; totally 47.6 g H_2



QUENCH-19: max rate 280 mg/s; totally 9.2 g H_2

QUENCH-19 bundle at elevations between 900 and 1100 mm: cladding damages by molten thermocouple steel (AISI 304) sheaths

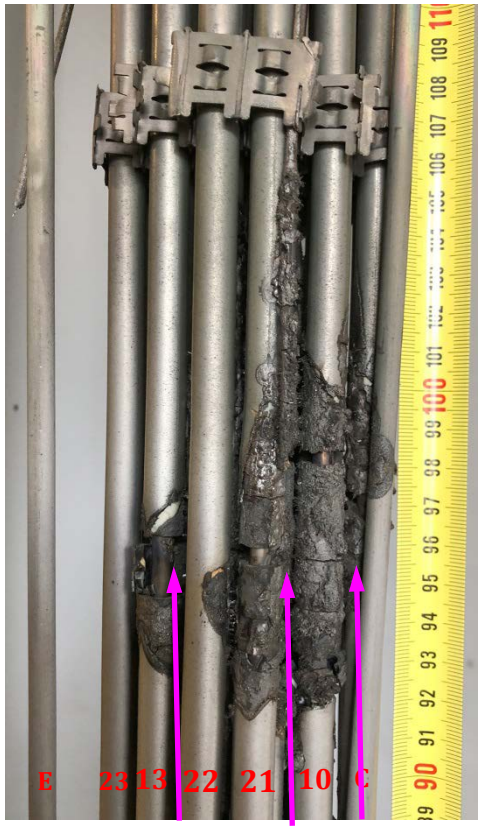


Positions of TC (•) at elevations 13 (950 mm) and 14 (1050 mm)

- the melting range of 304 steel is 1400…1450°C
- the melting range of FeCrAl alloys is 1500…1520°C



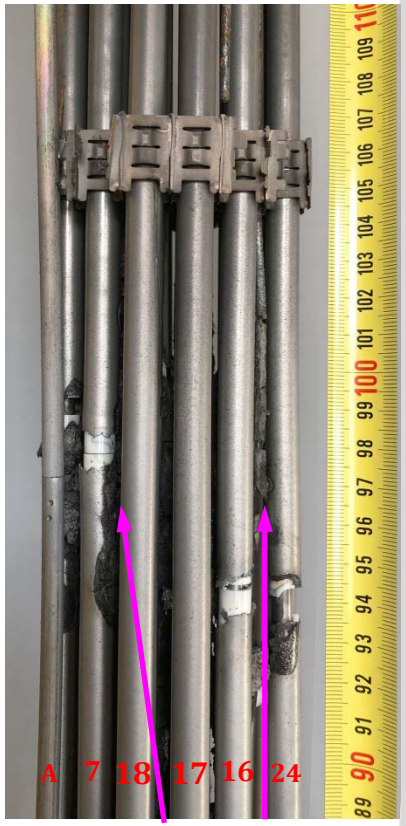
0°: TFS 9/13 and 19/14



90°: TFS 3/13, 21/13, 9/13

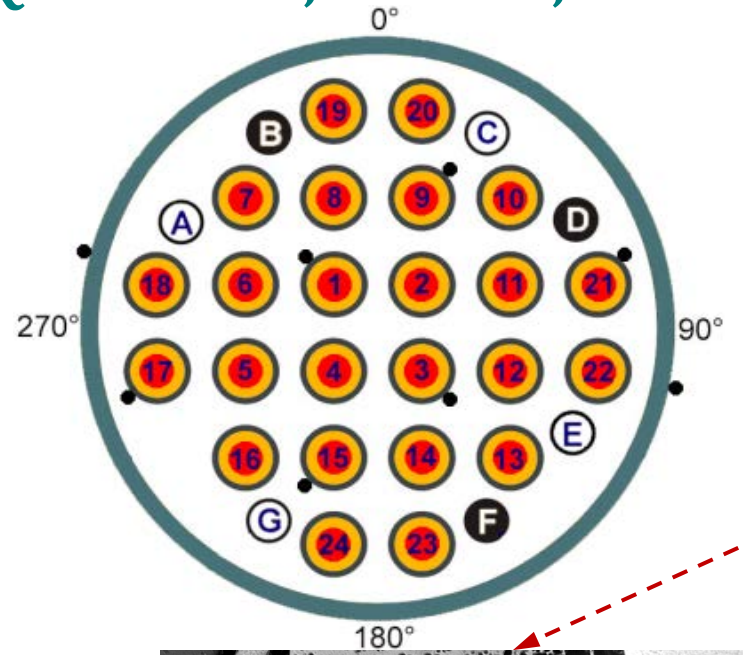


180°: TFS 15/13 and 14/14

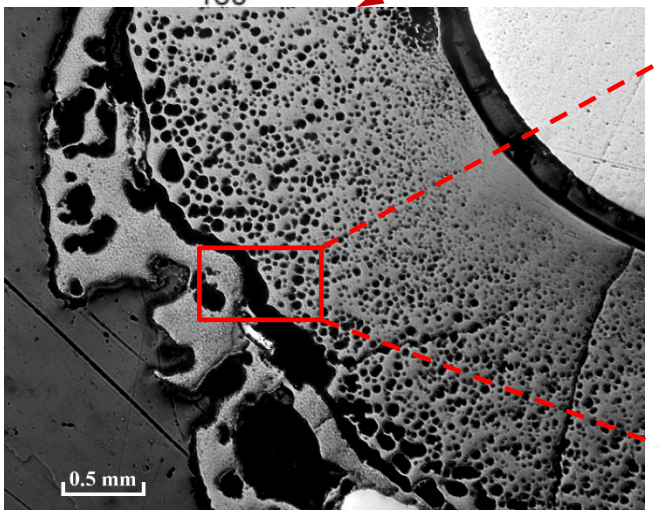


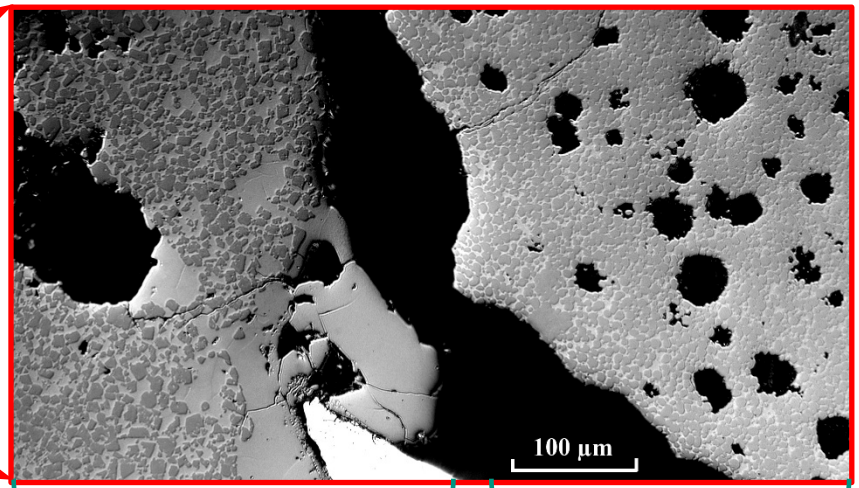
270°: TFS 1/13, 15/13

QUENCH-19, 950 mm, rod 2: molten claddings of central rods





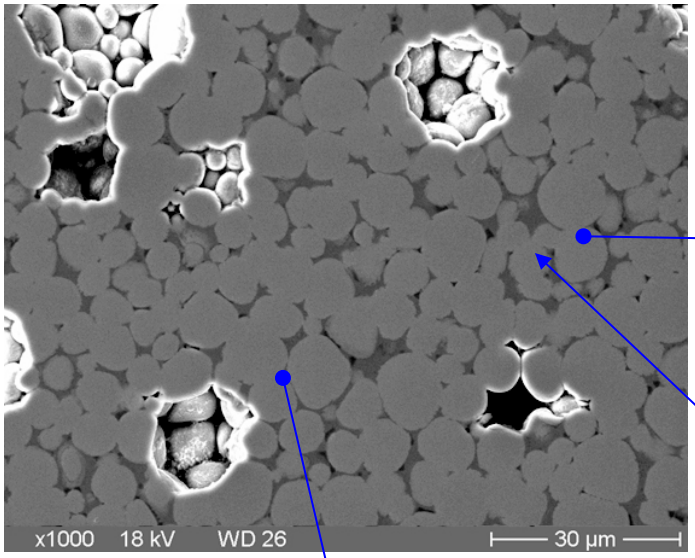


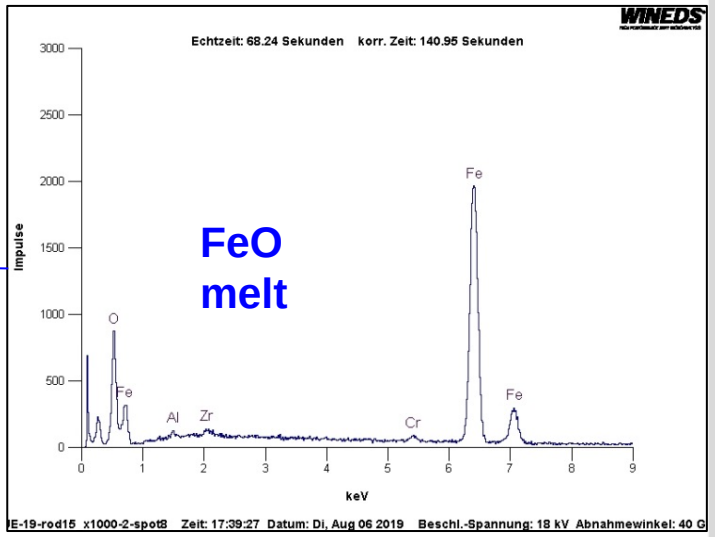


frozen cladding melt

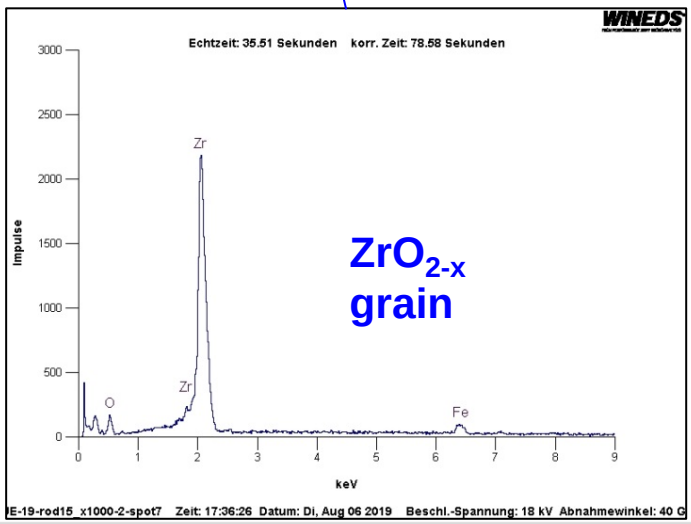
melt-interacting ZrO_2 pellet

QUENCH-19, 950 mm: penetration of FeO melt into pellet

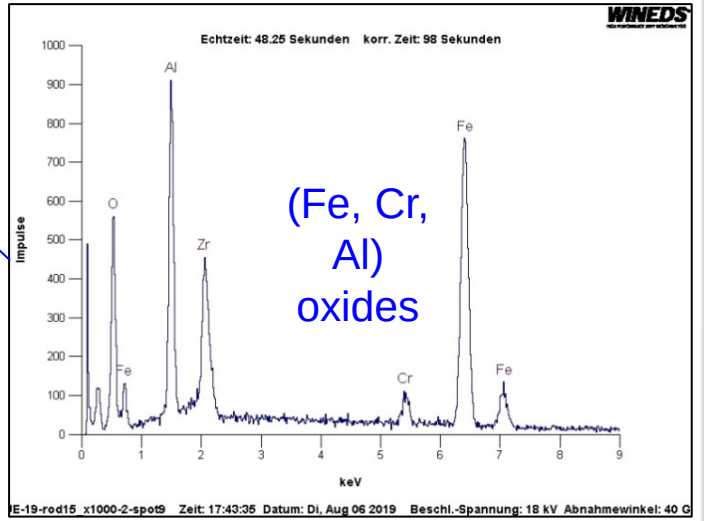




FeO melt

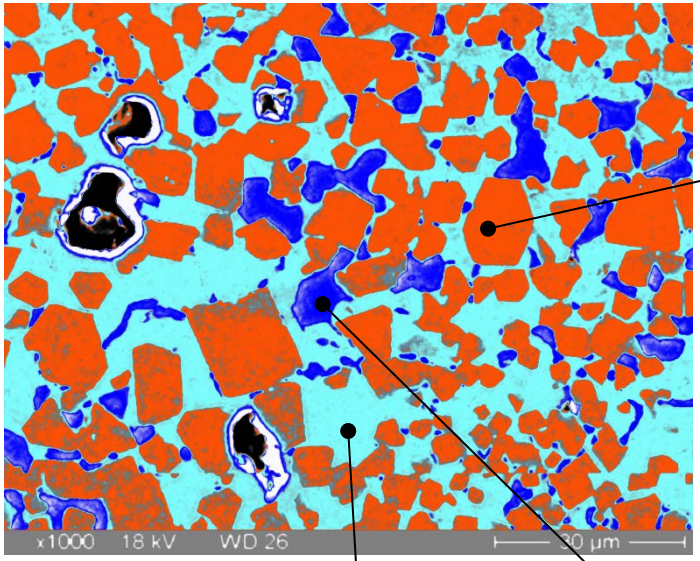


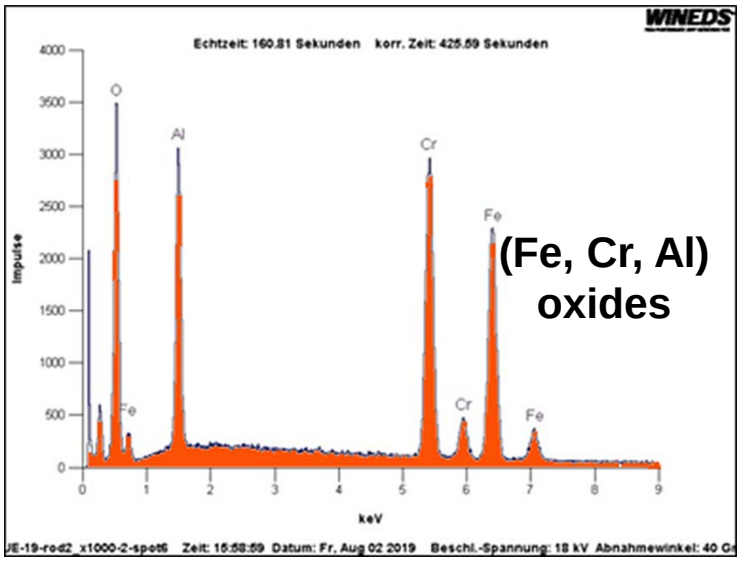
ZrO_{2-x} grain

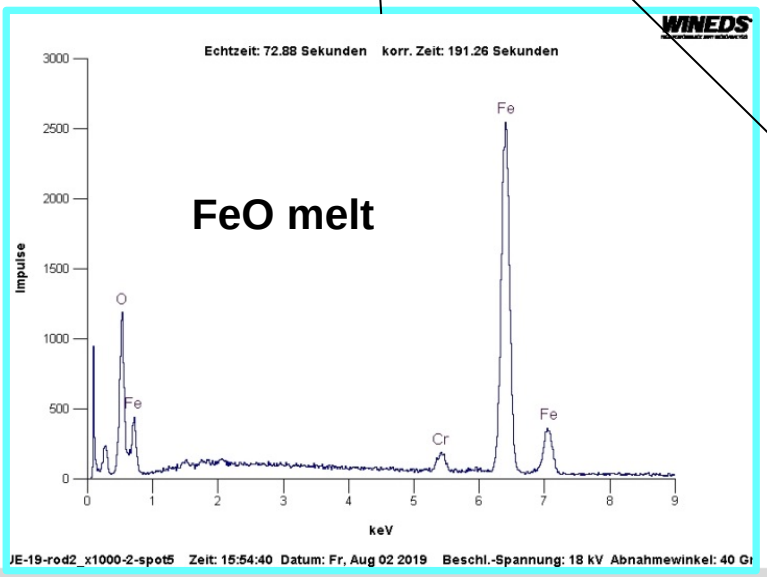


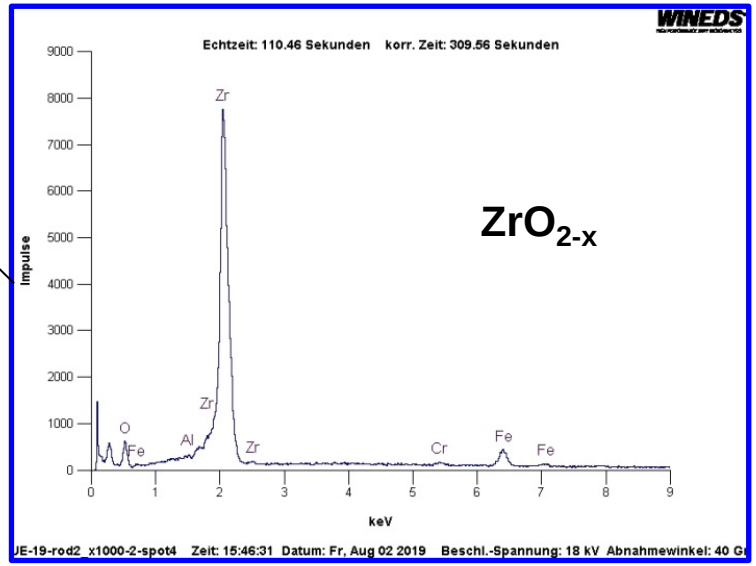
(Fe, Cr, Al) oxides

QUENCH-19, 950 mm: oxide precipitates inside molten FeO formed already at 1370 °C

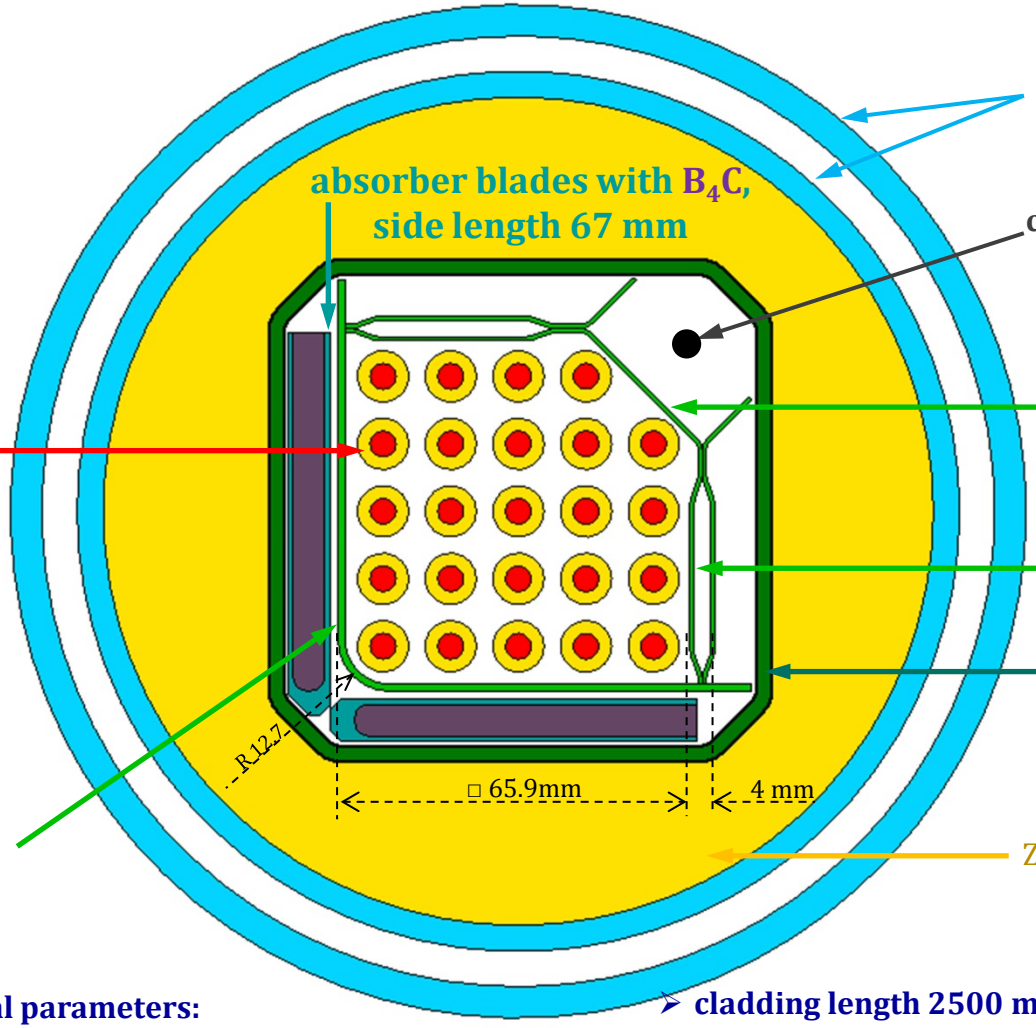








QUENCH-20: test bundle composition
¼ SVEA-96 OPTIMA2 assembly (BWR)



Inconel cooling jacket, inner tube ID=158.3 mm

corner rod (Zry-4, OD 6 mm)

heated rods (24): cladding Zy-2 with inner ZrSn-liner (10% of clad),

ZrO_2 pellet OD 8.48±0.05 ID 5.45±0.1 mm, length 11 mm,

W heater OD 5.25±0.025 mm

water channel box (ZIRLO), side length 27.4 mm

water cross wing (ZIRLO), wall thickness 0.8 mm

Zr shroud □ 86 mm, wall thickness 3 mm

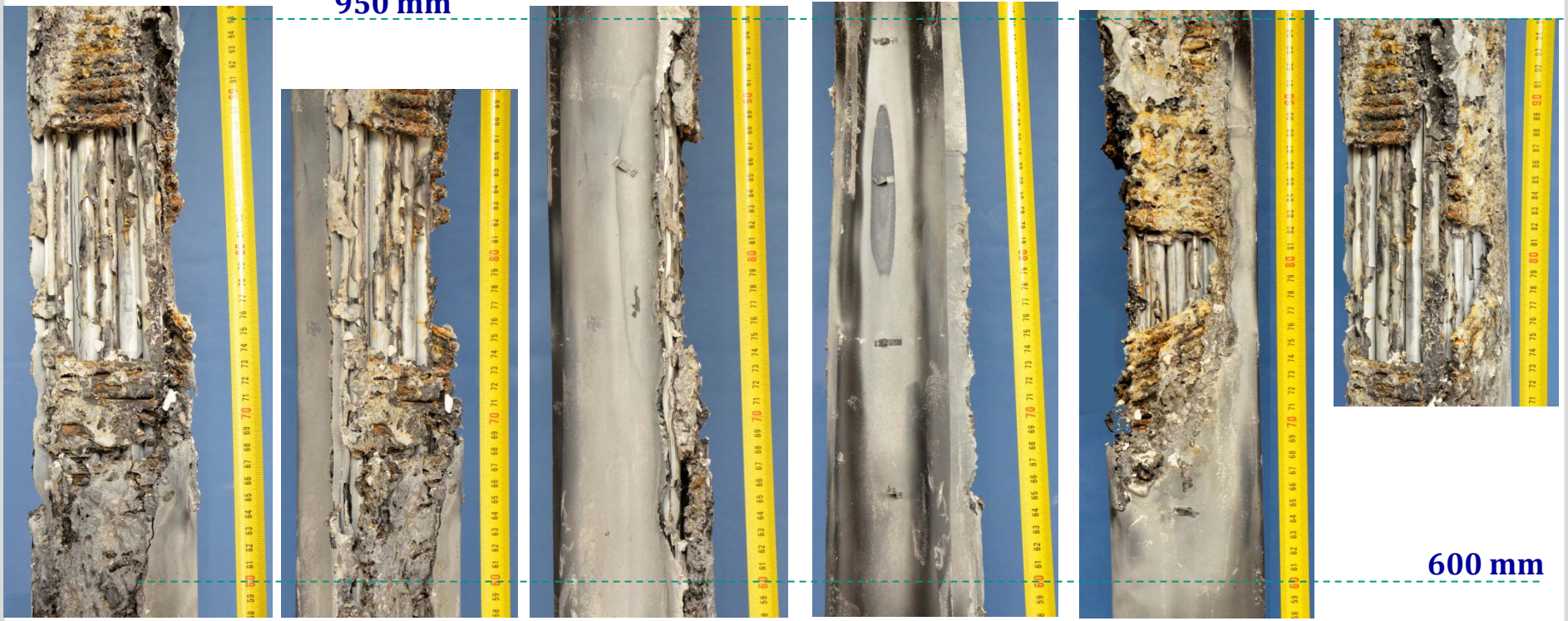
advanced low tin ZIRLO fuel channel box, wall thickness 1.4 mm

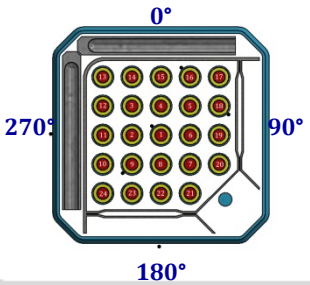
ZrO_2 porous thermal insulation

Geometrical parameters:

- bundle pitch 12.898 mm;
- outer diameter of claddings 9.84 mm;
- thickness of claddings 0.605 mm;
- absorber blades: thickness 8.05 mm
- cladding length 2500 mm
- absorber and cannel box lengths 1600 mm
- water gap between channel box and absorber blade 2.5 mm (nominal inter-assembly gap in BWR-PROTEUS core is 13.8 mm -> water gap 2.875 mm)

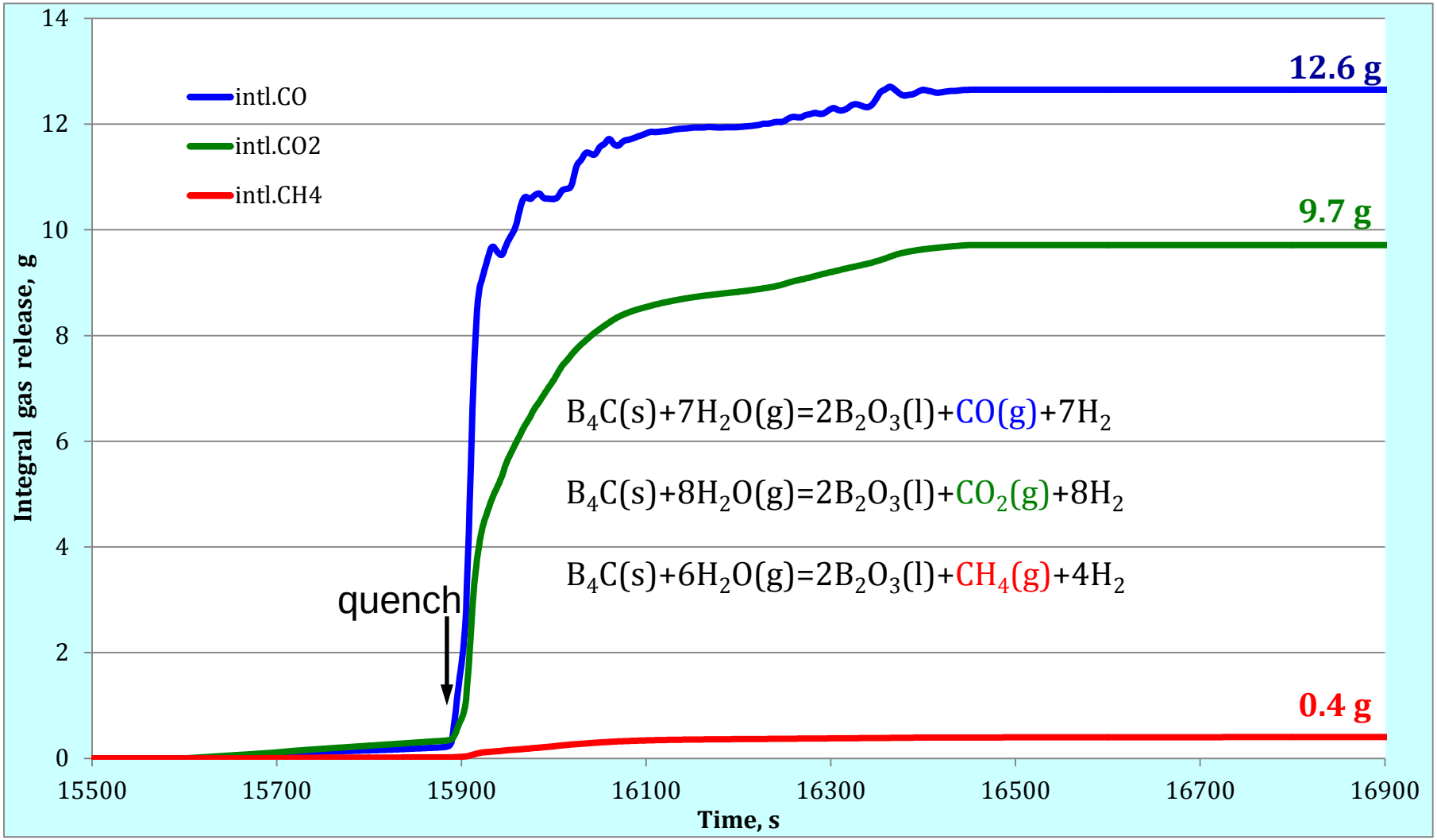
QUENCH-20 bundle surrounded by shroud: post-test view





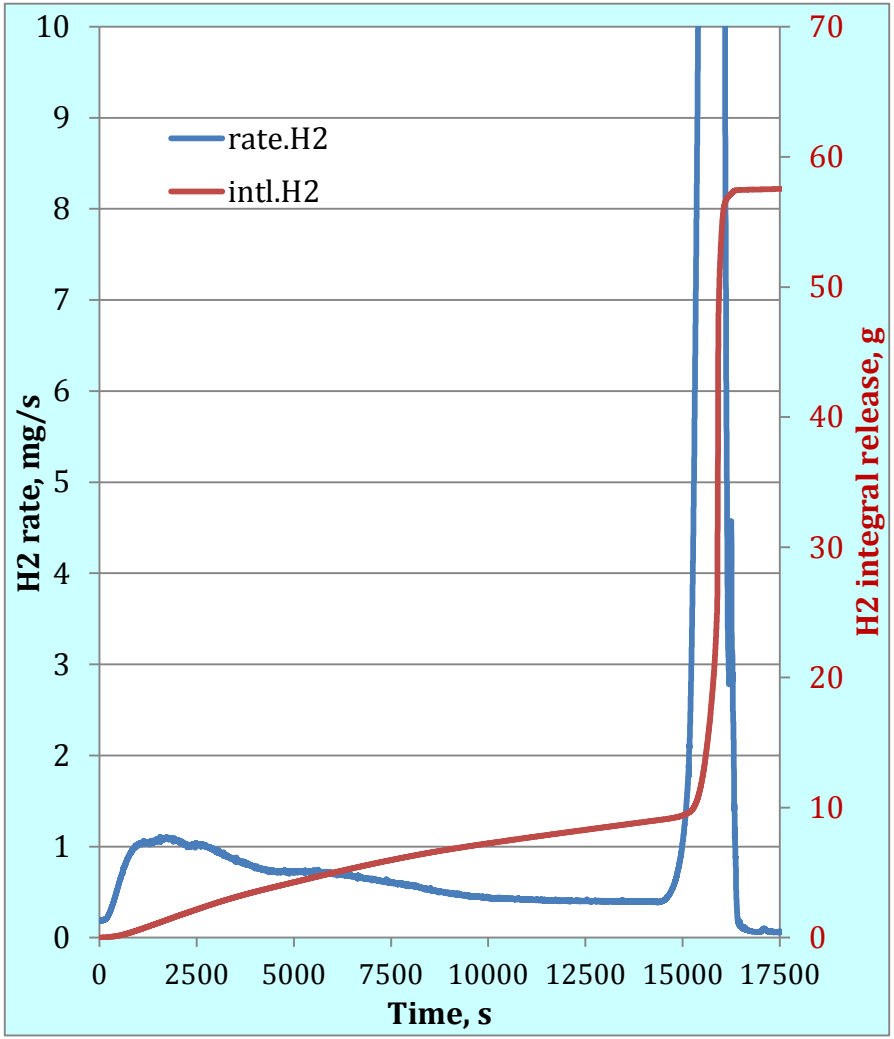
Strong degradation of absorber blades, channel box and shroud between elevations 650 and 950 mm at angle positions 0° and 270°

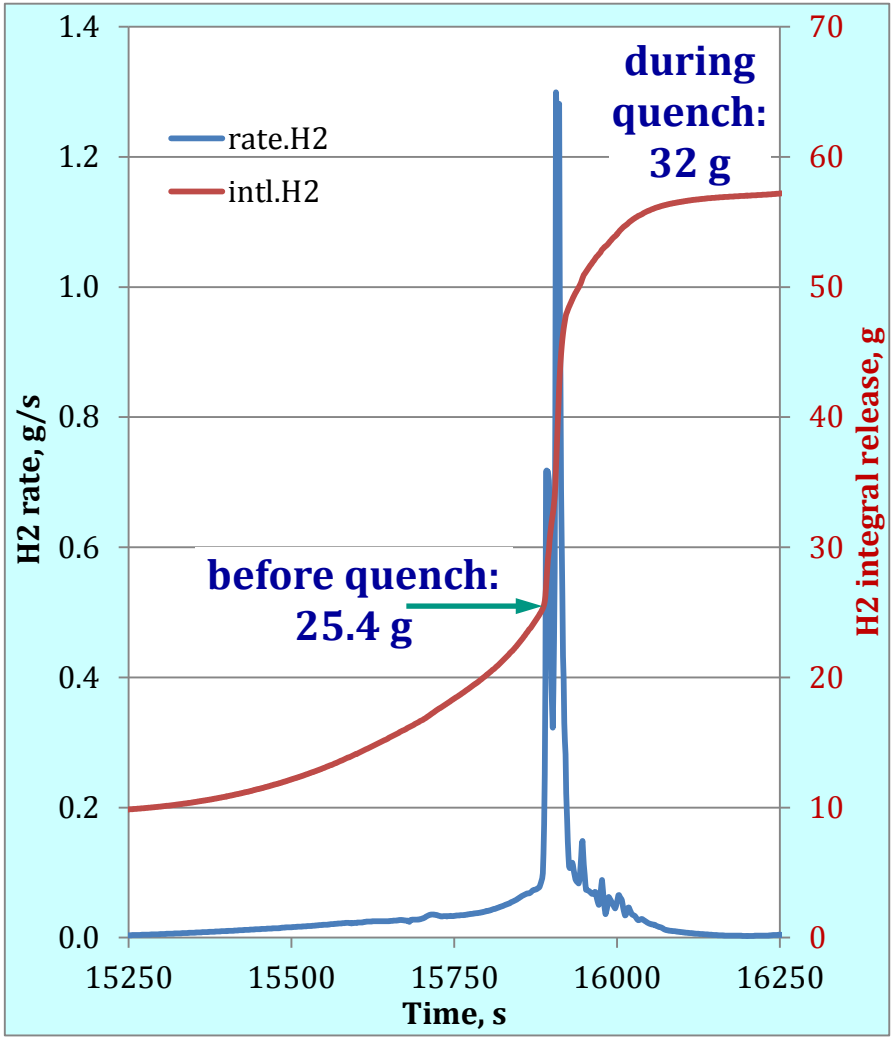
QUENCH-20: reaction of B_4C with steam, integral gas release



According to CO_x and CH_4 release: corresponding mass of B_2O_3 is 96.8 g; H_2 is 10.0 g

QUENCH-20: hydrogen release





H_2 release during the whole test: 57.4 g;
before quench – interaction of steam with Zry,
during quench – steam interaction with Zry and absorber

H_2 release during quench:
22 g (from Zry and molten steel) +
+ 10 g (from B_4C)

Database: contents

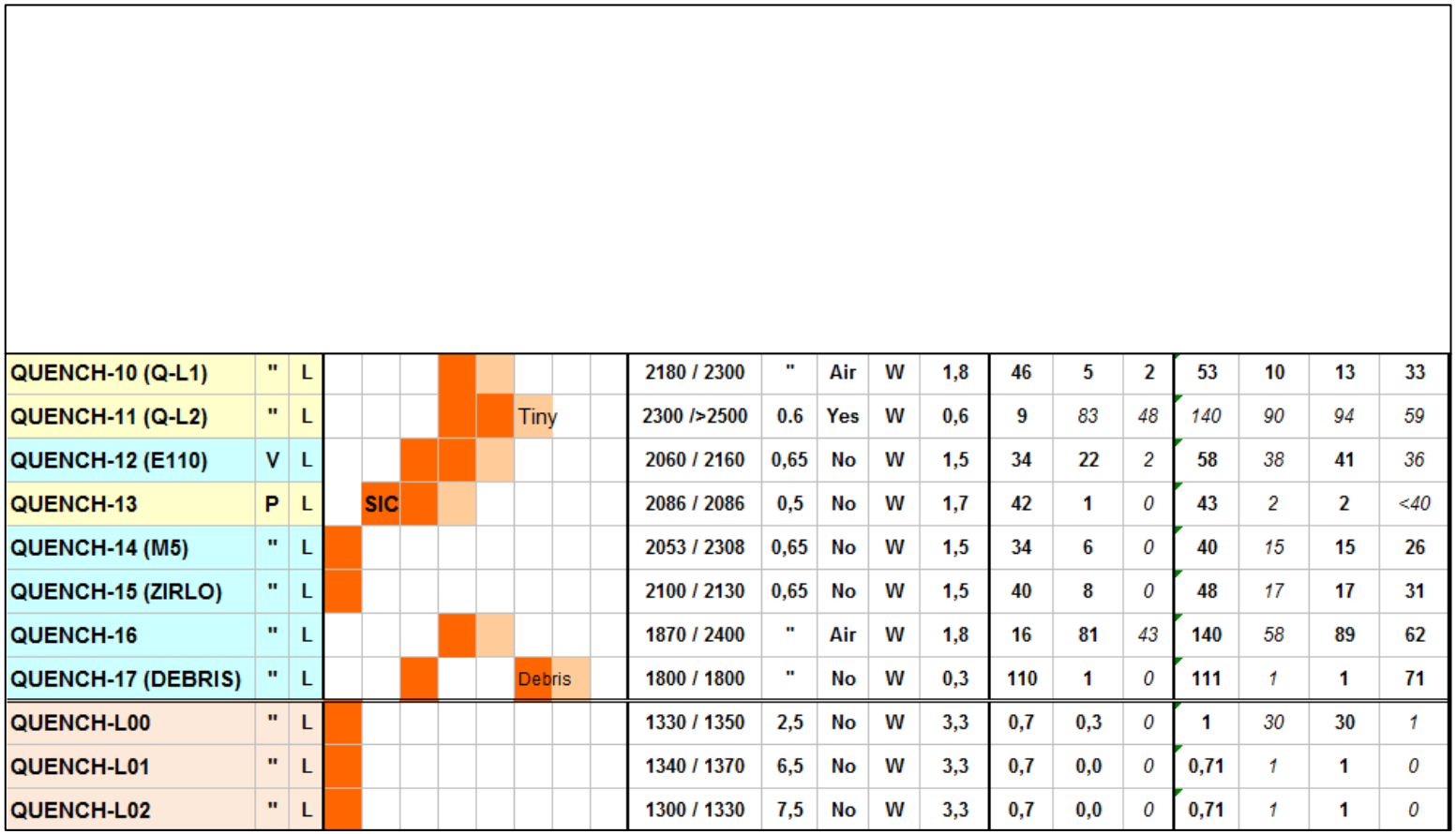
- Core damage state and evolution
- Temperatures, Heat-up rates Steam starvation prior to reflood(?)
- Reflood medium and mass flow rate
- Hydrogen data
- Fraction of Zry consumed for H_2 production
- PARAMETER: top, top + bottom flooding

W. Hering et al., **Integration of New Experiments into the Reflood Map**, ICAPP 2015 Paper 15465

Core damage evolution in reflood experiments	Reactor type	Pressure at reflood	Intact / loc. ballooning	Absorber damaged	Fuel rod damaged	Metallic melt relocated	Local debris	Local debris / pool	Global debris / pool	Material relocation ->LH	PCT prior to reflood / during test	Heat-up rate	Steam starvation prior to reflood	Reflood medium	Reflood mass flow rate (RMFR)	Hydrogen before quench	Corrected H2 mass during quench	H2 due to facility effects	Total measured Hydrogen mass	Corrected fraction of total H_2 mass released during quench	Original fraction of total H_2 mass released during quench	Fraction of available Zry mass consumed for H2 production
Data source			0	1	2	3	4	5	6	7	K	K/s			$\frac{g}{s*rod}$	g	g	g	g	%	%	%
CODEX 3/1	V	L									1420 / 1430	0,3		W	0,9	?	?	?	?	?		?
CODEX 3/2	V	L									1773 / 1923	0,6		W	0,9	1	0	?	1	<5		<5
PARAMETER 2	V	L	B								1700 /~1700	?	No	W	5	---	---	?	---	---		---
PARAMETER SF1 (top)	V	L						Tiny			2123 /~2300	2	No	W	1,4	20	54	17	91	73	78	60
PARAMETER SF2 (t+b)	V	L									1770 / 1850	0,2	No	W	5	23,5	1,5	0	25	6	6	
PARAMETER SF3 (top)	V	L									1870 / 1900	0,3	No	W	1,4	31	4,5	0	35,5	13	13	
PARAMETER SF4 (air)	V	L									1900 / 2300	"	Air	W	3,2	21	66	20	107	76	80	
QUENCH IBS05	P	L									1700 / 1750	?	---	W	2,6	20	33	5	58	62	66	34
QUENCH-01	"	L									1830 / 1900	0,7	No	W	1,8	36	1	2	39	3	8	24
QUENCH-02	"	L									2470 / 2500	"	No	W	1,7	20	109	31	160	84	88	83

Database: (cont.)

- ZIRLO™ and M5® claddings
- QUENCH-12: WWER
- QUENCH-17: DEBRIS

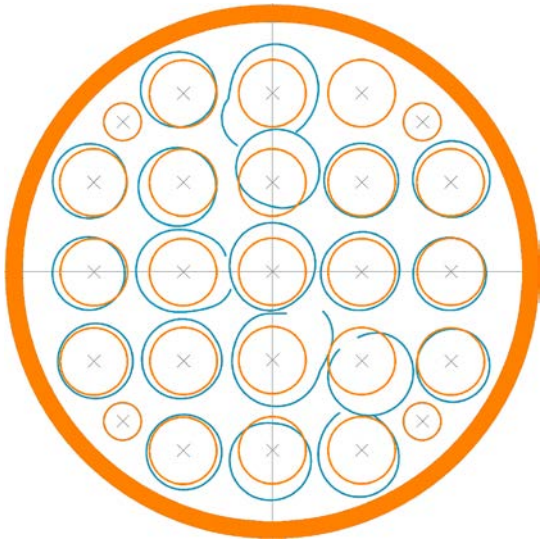


QUENCH-10 (Q-L1)	"	L	2180 / 2300	"	Air	W	1,8	46	5	2	53	10	13	33
QUENCH-11 (Q-L2)	"	L	2300 />2500	0.6	Yes	W	0,6	9	*83*	*48*	*140*	*90*	*94*	*59*
QUENCH-12 (E110)	V	L	2060 / 2160	0,65	No	W	1,5	34	22	*2*	58	*38*	41	*36*
QUENCH-13	P	L	2086 / 2086	0,5	No	W	1,7	42	1	*0*	43	*2*	2	*<40*
QUENCH-14 (M5)	"	L	2053 / 2308	0,65	No	W	1,5	34	6	*0*	40	*15*	15	26
QUENCH-15 (ZIRLO)	"	L	2100 / 2130	0,65	No	W	1,5	40	8	*0*	48	*17*	17	31
QUENCH-16	"	L	1870 / 2400	"	Air	W	1,8	16	81	*43*	140	*58*	89	62
QUENCH-17 (DEBRIS)	"	L	1800 / 1800	"	No	W	0,3	110	1	*0*	111	*1*	1	71
QUENCH-L00	"	L	1330 / 1350	2,5	No	W	3,3	0,7	0,3	*0*	1	*30*	30	*1*
QUENCH-L01	"	L	1340 / 1370	6,5	No	W	3,3	0,7	0,0	*0*	0,71	*1*	1	*0*
QUENCH-L02	"	L	1300 / 1330	7,5	No	W	3,3	0,7	0,0	*0*	0,71	*1*	1	*0*

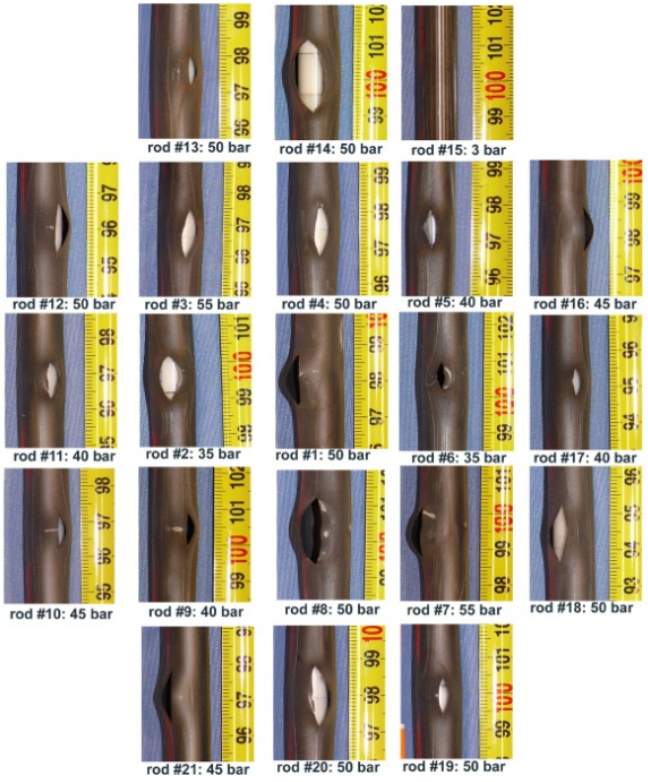
QUENCH-LOCA test matrix

Test	Type of cladding tubes	Max heat-up rate, K/s	Max T on the end of heat-up, K	Duration of inner cladding oxidation at T > 1123 K, s	Secondary cladding hydriding	Post-test fracture due to secondary hydriding
QUENCH-L0 July 22, 2010 Commissioning test	Zry-4	2.5	1350	110	**yes**	**yes**
QUENCH-L1 Feb. 02, 2012 Reference test	Zry-4	7	1373	105	**yes**	**no**
QUENCH-L2 July 30, 2013	M5®	8	1373	88	**yes**	**no**
QUENCH-L3HT March 21, 2014	Opt. ZIRLO™	8	1623	252	**yes**	**yes**
QUENCH-L4 July 30, 2014	Pre-hydriding M5® (100 wppm H)	8	1385	100	**yes**	**yes**
QUENCH-L3 March 17, 2015	Opt. ZIRLO™	8	1346	84	**yes**	**no**
QUENCH-L5 Feb. 17, 2016	Pre-hydr. opt. ZIRLO (300 wppm H)	8	1257	45	**no**	**-**

QUENCH-LOCA program at KIT (2010-2016): Influence of hydrogen uptake after LOCA-burst on mechanical properties of claddings



ballooning and burst of claddings in comparison to pre-test fuel rod positions in the QUENCH-LOCA bundle: 25% blockage of cooling channel



axial burst positions after bundle QUENCH-LOCA test with Zry-4 claddings

secondary hydriding



hydrogen bands inside cladding detected with n^0-radiography: >2000 wppm hydrogen content



double rupture of cladding along hydrogen bands during tensile tests for C_H>1500 wppm

J. Stuckert et al., **QUENCH-LOCA program at KIT on secondary hydriding**, NED 255 (2013), 185-201.

J. Stuckert et al., **Lessons learned from the QUENCH-LOCA experiments**, QWS-23 (2017).

M. Grosse et al., **Secondary hydriding during LOCA – Results from the QUENCH-L0 test**, JNM 420 (2012), 575-582.

SUMMARY

• 21 bundle tests were performed under severe accident conditions with different cladding materials.

• Six parameters, enhancing hydrogen production during reflood, have been identified:

1) Low reflood flow rates < 1 g/s/rod (QUENCH-07, -08, -11);

2) Breakaway effect with weakness and spallation of protective oxide layer (QUENCH-12);

3) Steam starvation (QUENCH-09, -11, -16);

4) Nitride formation by air ingress with formation of very porous oxide layer during following reflood (QUENCH-10, -16);

5) High temperatures with melt relocation outside claddings and intensive melt oxidation (QUENCH-02, -03, -09, -11, -16, -18);

6) Eutectic interactions between B_4C, stainless steel and Zircaloy-4 leading to low melting point (QUENCH-07, -09, -20).

• Additionally to hydrogen source term, other phenomena on melt relocation, debris, and aerosol formation were investigated.

• 7 QUENCH-LOCA bundle tests with fresh and pre-hydrogenated different cladding materials (Zry-4, M5®, opt. ZIRLO™) were performed according to a temperature/time-scenario typical for a LBLOCA in a German PWR. Post-test tensile experiments evidenced fracture at hydrogen bands (formed during secondary hydriding) for claddings with local hydrogen concentrations >1500 wppm.

Thank you for the fruitful cooperation and attention

http://quench.forschung.kit.edu/

http://www.iam.kit.edu/awp/666.php

Investigations of Hydrogen in Cladding Materials by means of Neutron Imaging

Mirco Grosse
Karlsruhe Institute of Technology

Hydrogen in nuclear fuel claddings made of zirconium alloys is still an important topic even it is investigated since decades. Neutron Imaging is a powerful tool for the quantitative investigation of hydrogen in zirconium alloys. This contribution to the 25. International QUENCH workshop gives an overview about the quantitative calibration of the method. Highlights of the application of neutron imaging during the last 14 years are presented.

Basis of the contrast in neutron images are differences in the total macroscopic neutron cross section and/or in the path length of the neutron through the sample. The total macroscopic neutron cross section depends more or less linearly on the number density ratio between hydrogen and zirconium. This dependence can be derived theoretically and is confirmed experimentally.

The following investigations are presented as highlights:

- In-situ investigations of the hydrogen diffusion in Zircaloy-4 at temperatures between 900 and 1300°C
- In-situ investigations of the hydrogen uptake during annealing of Zircaloy-4 in Ar/H_2 atmosphere at 550°C including phase transformation in the zirconium alloy
- In-situ investigations of the hydrogen uptake during steam oxidation between 1000 and 1300°C
- Post-test determination of the hydrogen uptake and distribution during design basis large break loss of coolant accidents (LB-LOCA)
- In-situ investigations of the reaction of Zircaloy-4 in nitrogen-steam and air-steam atmospheres
- Ex-situ investigations of the hydrogen diffusion in Zircaloy-2 and Zr-2.5%Nb at temperatures between 250 and 350°C depending on the orientation and
- Dependence of the hydrogen uptake and distribution in stressed pre-notched Zircaloy-4 specimens at temperatures of 350°C

An outlook on further investigations planned in the framework of the SPIZWURZ project is given too.

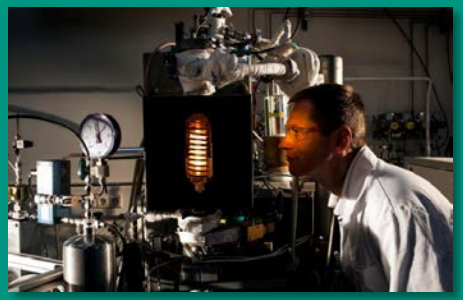


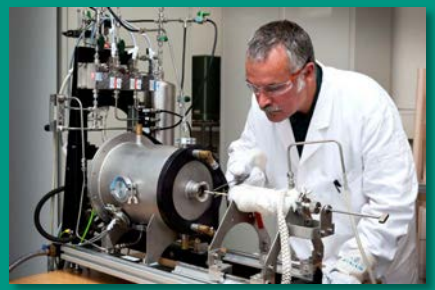
Karlsruhe Institute of Technology

Investigations of Hydrogen in Cladding Materials by means of Neutron Imaging

KIT / Institute for Applied Materials – Applied Material Physics / Program NUSAFE

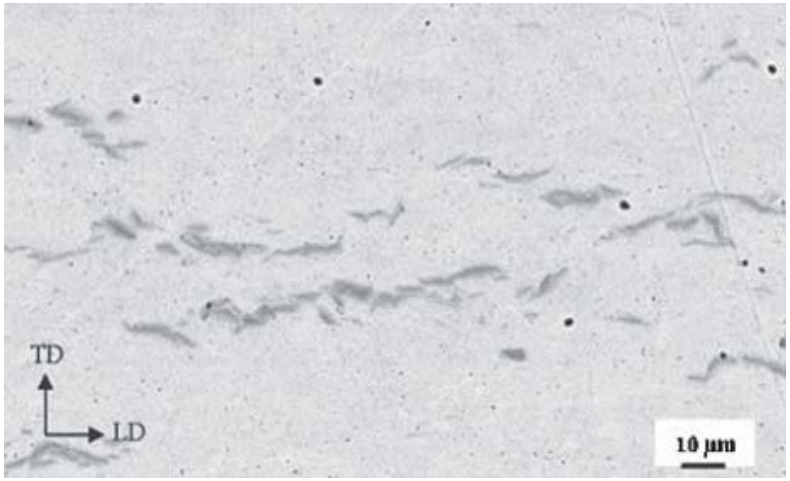
Mirco Große

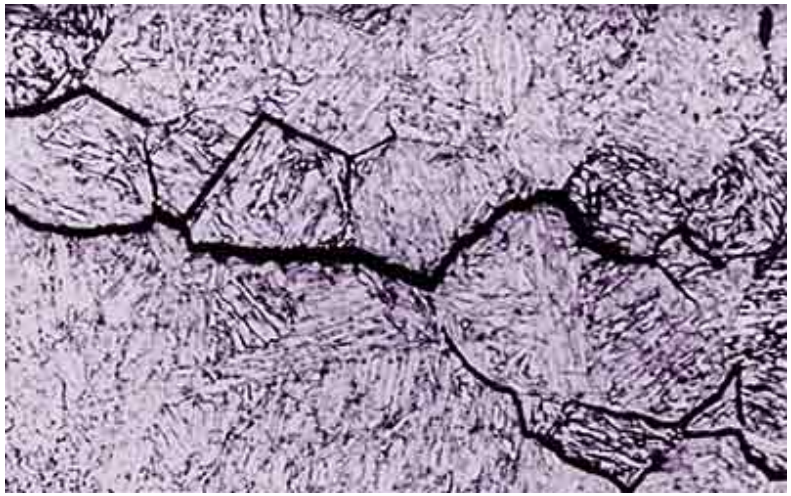





Hydrogen in Zirconium Alloys

- Hydrogen uptake during operation: 70 .. 150 wt.ppm
- At hot spots (spacer grid, spalled oxide scale, fretting) : some 10^3 wt.ppm
- Degradation of the mechanical properties of the cladding tube: e.g. brittle thermo-shock behaviour during emergency cooling to terminate an accident.
- Effect of hydrogen strongly depends on the orientation of the hydrides.
- Delayed hydride cracking (DHC)





Hydrogen in Zirconium Alloys

- Hydrogen in zirconium is investigated since decades.
- Actually, large efforts to understand and describe hydrogen related processes in zirconium alloys were made by a lot of groups:

  15 of 40 oral presentations and 10 of 15 posters at the ASTM Symposium “Zirconium in Nuclear Industries” (May 20-23, 2019) were belong hydrogen in zirconium alloys
- Secondary hydrogenation during LOCA
- Hydride re-orientation in the cladding wall from circumferential to radial orientation if $p_i > p_o$
- Dependence of hydrogen diffusivity and solubility on elastic lattice strain of the zirconium matrix

Investigations of Hydrogen in Zirconium alloys at KIT

Available online at www.sciencedirect.com
SCIENCE DIRECT®
Journal of Nuclear Materials 334 (2004) 58–64
journal of nuclear materials
www.elsevier.com/locate/jnucmat

Hydrogen absorption by zirconium alloys at high temperatures

Martin Steinbrück *

Forschungszentrum Karlsruhe GmbH, Institut für Materialforschung I, Postfach 3640, D-76021 Karlsruhe, Germany

Received 18 March 2004; accepted 30 April 2004

Abstract

At high temperatures, e.g. during a hypothetical severe accident, zirconium and its alloys are not stable to other materials and to oxidising atmospheres. Exothermic reactions with steam cause the production of hydrogen which will be released to the atmosphere and, thus, endanger the containment or may be absorbed by the remaining metal. The hydrogen solubility in Zircaloy-4 and Zr–1Nb was measured in the temperature range of 1230–1730 K and at hydrogen partial pressures between 10 and 100 kPa. The parameters of the Sieverts constant were determined. No significant differences between the two alloys were observed. The hydrogen solubility of oxygen containing Zircaloy-4 decreases with increasing oxygen content.
© 2004 Elsevier B.V. All rights reserved.

1. Introduction

Zirconium and its alloys are widely used in nuclear and chemical industries because of their low neutron absorption and their excellent mechanical and corrosion properties. In today's nuclear reactors, optimised Zircaloy and zirconium–niobium alloys are used for structural components like fuel claddings, guide tubes, and grid spacers.

At Forschungszentrum Karlsruhe (FZK), the hydrogen source term during a hypothetical severe nuclear accident, especially during the reflood phase, is being investigated within the QUENCH program [1–3]. Hydrogen is produced by the strongly exothermic zirconium-steam reaction (Eq. (1)). It is either released as a gas into the atmosphere or may be absorbed by the remaining zirconium metal (Eq. (2)):

$$2H_2O + Zr \Longleftrightarrow ZrO_2 + 2H_2 + \Delta_r H \quad (1)$$

$$H_{2(gas)} \Longleftrightarrow 2H_{(abs)} + \Delta_s H \quad (2)$$

where $\Delta_r H$ and $\Delta_s H$ are the enthalpies of reaction and solution, respectively. The latter reaction which is subject of this paper may considerably affect the course of events during and after quenching of an overheated, partially degraded core. The zirconium alloy may act as a sink or source of hydrogen, depending on the conditions prevailing (temperature, pressure). In this way, the hydrogen solubility of the cladding material may alter the time of hydrogen release from the core. Furthermore, the heat of solution of hydrogen in zirconium relative to 1 mol H_2 is about half the enthalpy of the strongly exothermic oxidation reaction by steam and may therefore influence the energy balance during severe accident transients at least temporarily.

The hydrogen absorption by zirconium alloys was studied extensively in the past, in particular with regard to the embrittlement of cladding material during long-term operation, which is beyond the scope of this work. Some publications also deal with higher temperatures [4–8], but actually only Moalem and Olander [9] published data for the temperature region above 1270 K which is considered in this paper.

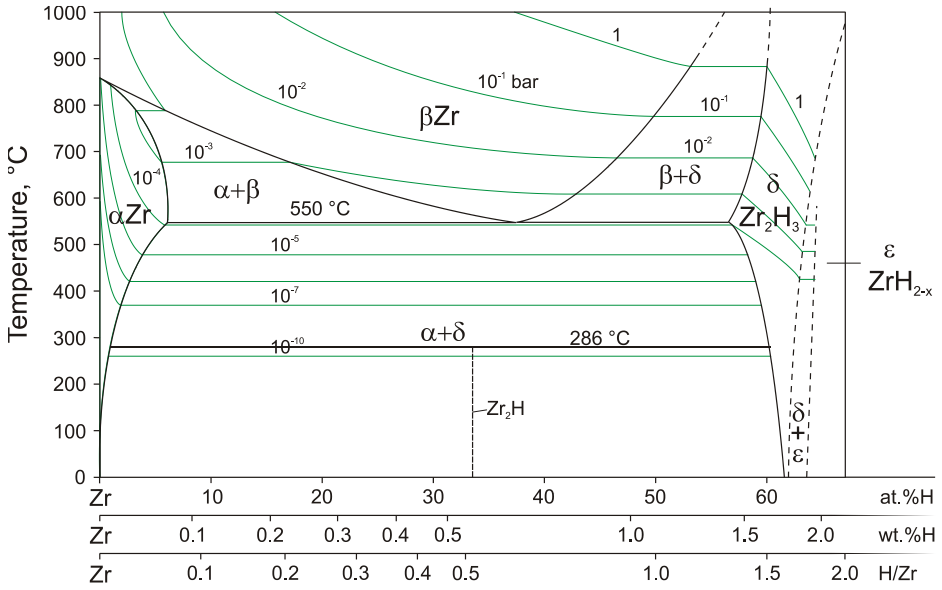
It is well known that the hydrogen solubility in zirconium follows the Sieverts law (Eq. (3)), according to which the amount of hydrogen absorbed in a diluted solution is a function of the hydrogen partial pressure:

* Tel.: +49-7247 822517; fax: +49-7247 824567.
E-mail address: martin.steinbrueck@imf.fzk.de (M. Steinbrück).

0022-3115/$ - see front matter © 2004 Elsevier B.V. All rights reserved.
doi:10.1016/j.jnucmat.2004.05.007

At KIT hydrogen in zirconium is investigated since decades.

Determination of the dependence of Sieverts coefficients on temperature and oxygen concentration.



Determination of hydrogen concentrations by means of neutron imaging

X-ray radiography

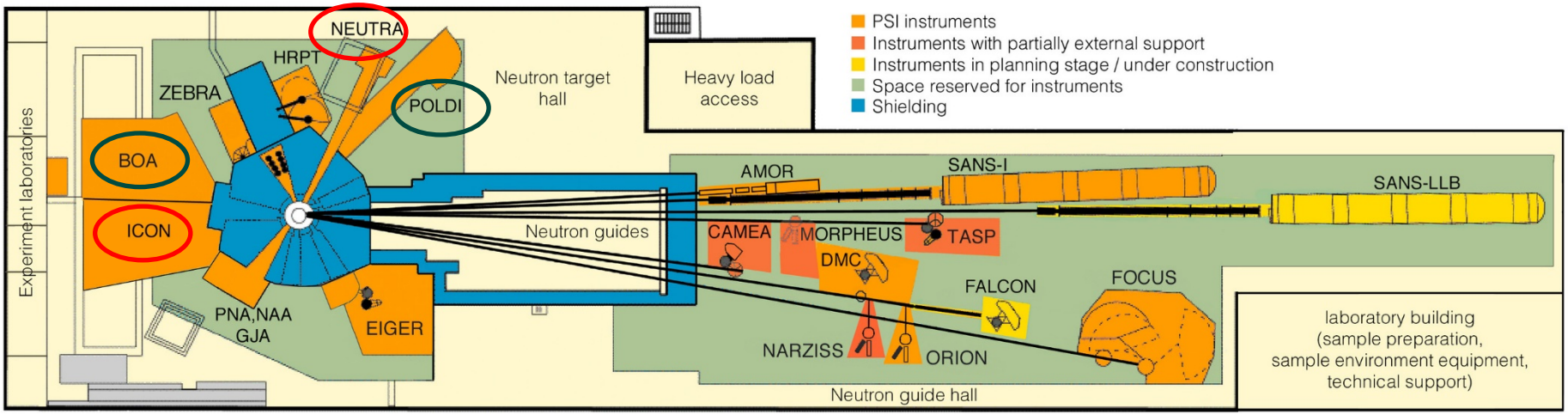


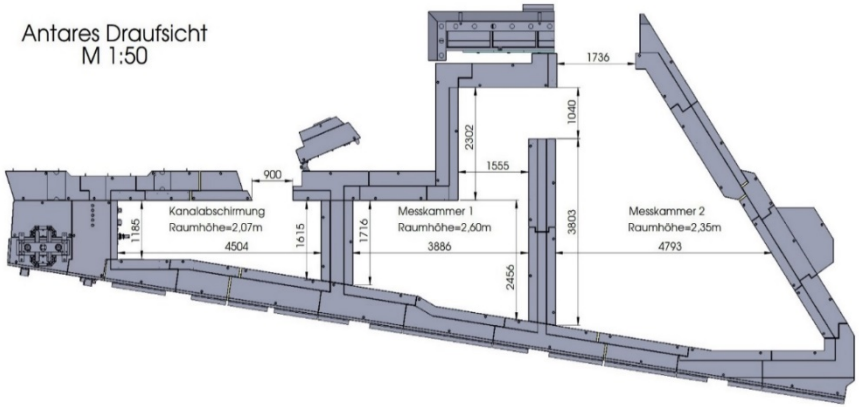
neutron radiography

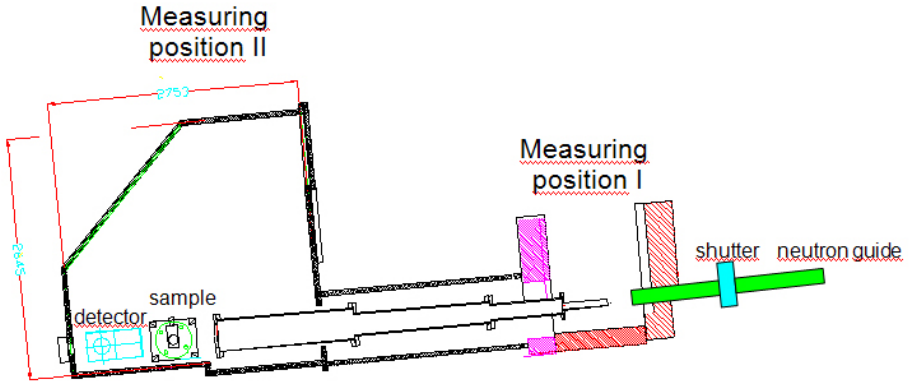


GKSS Geesthacht 1991

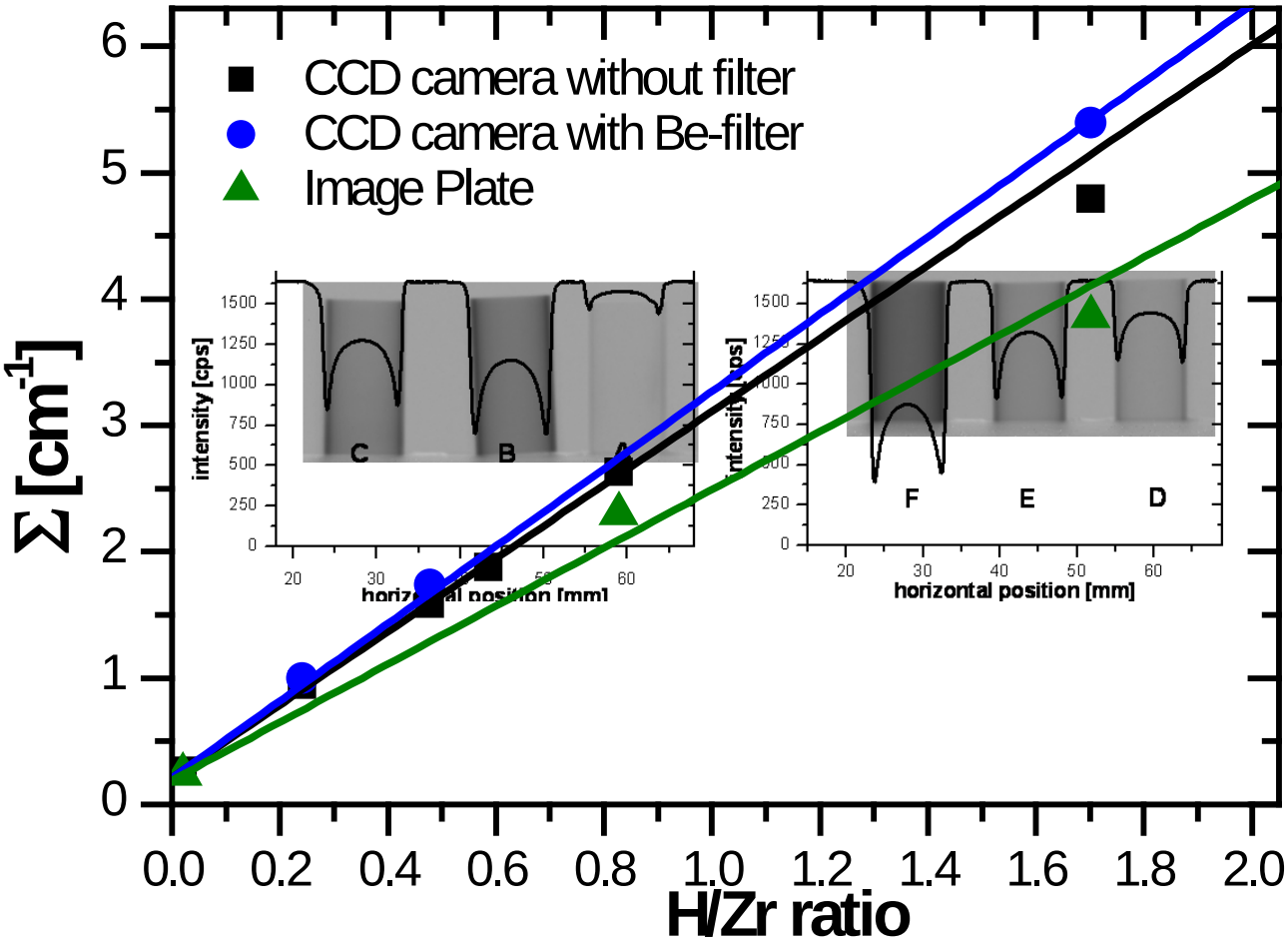
Neutron Imaging facilities used







Determination of hydrogen concentrations by means of neutron imaging



M. Grosse, E. Lehmann, P. Vontobel, M. Steinbrueck,

Quantitative determination of absorbed hydrogen in oxidised zircaloy by means of neutron radiography,

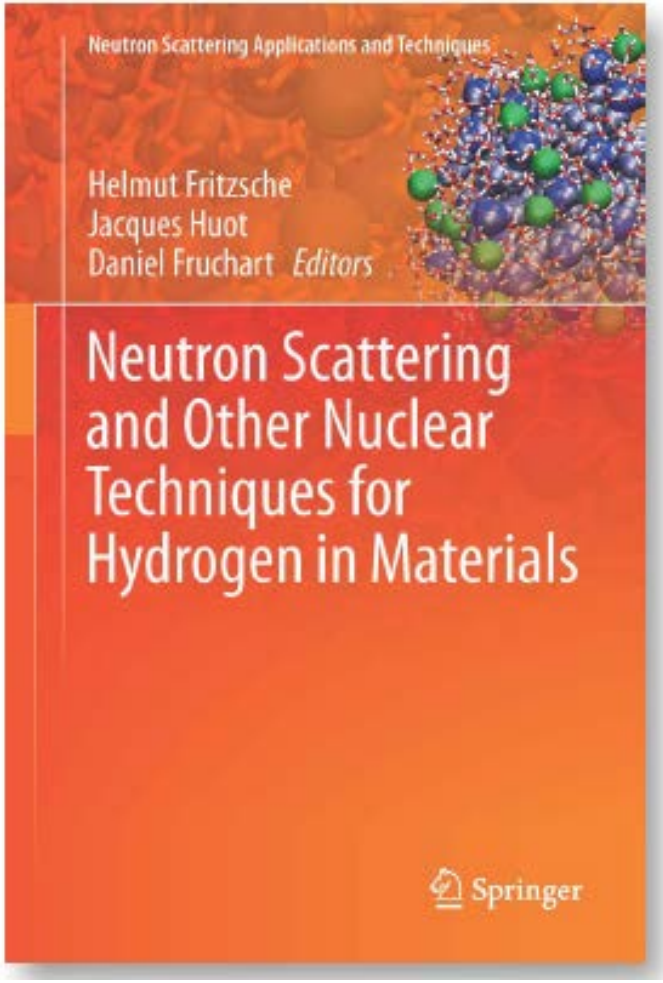
Nucl. Instr. Methods A566 (2006), 739-745

Neutron Imaging

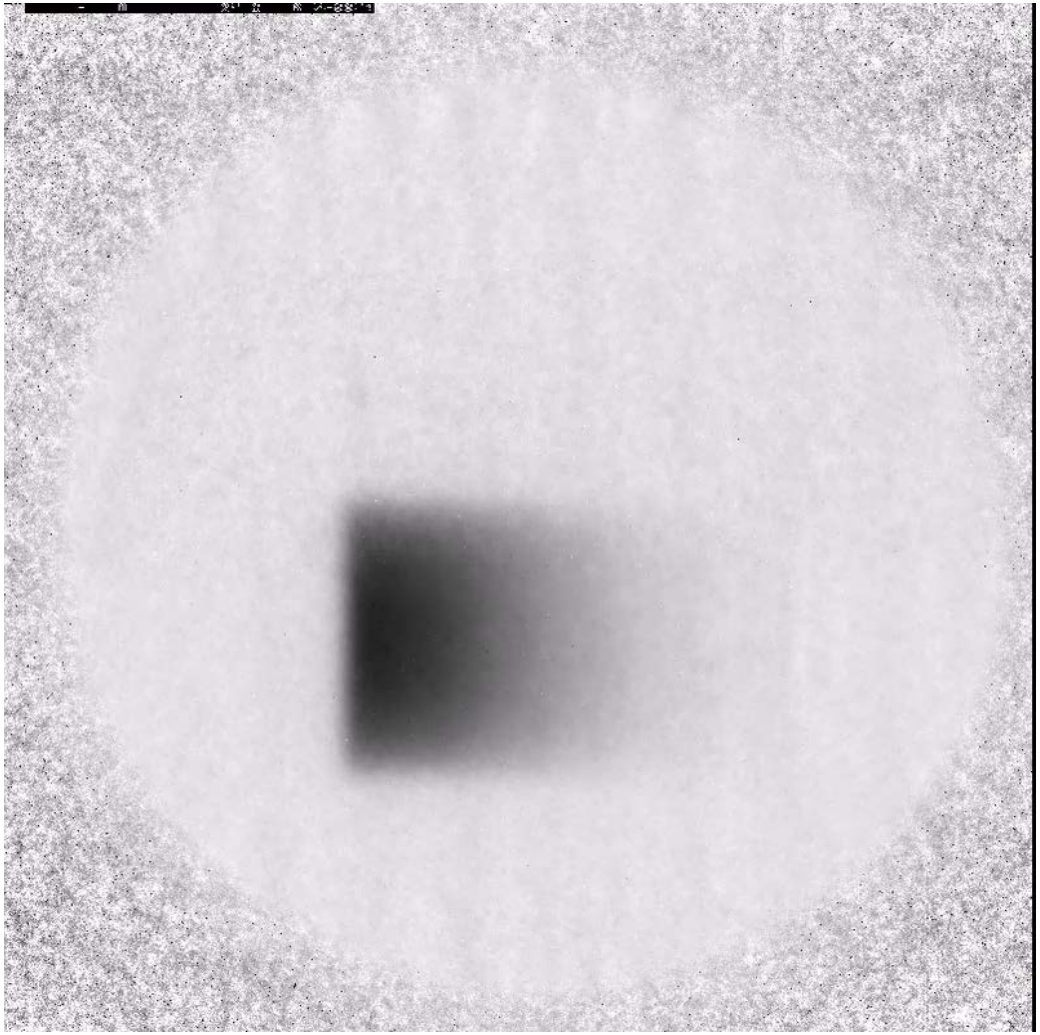
$$\Sigma_{total} = \frac{-\ln\left(\frac{I - I_B}{I_0 - I_B}\right)}{s}$$

$$= \sum_i N_i \sigma_i$$

$$= \underbrace{N_{Zr}\sigma_{Zr} + \ldots}_{\Sigma_{Zry}} + N_H \sigma_H + N_O \sigma_O$$



Separate Effect Tests



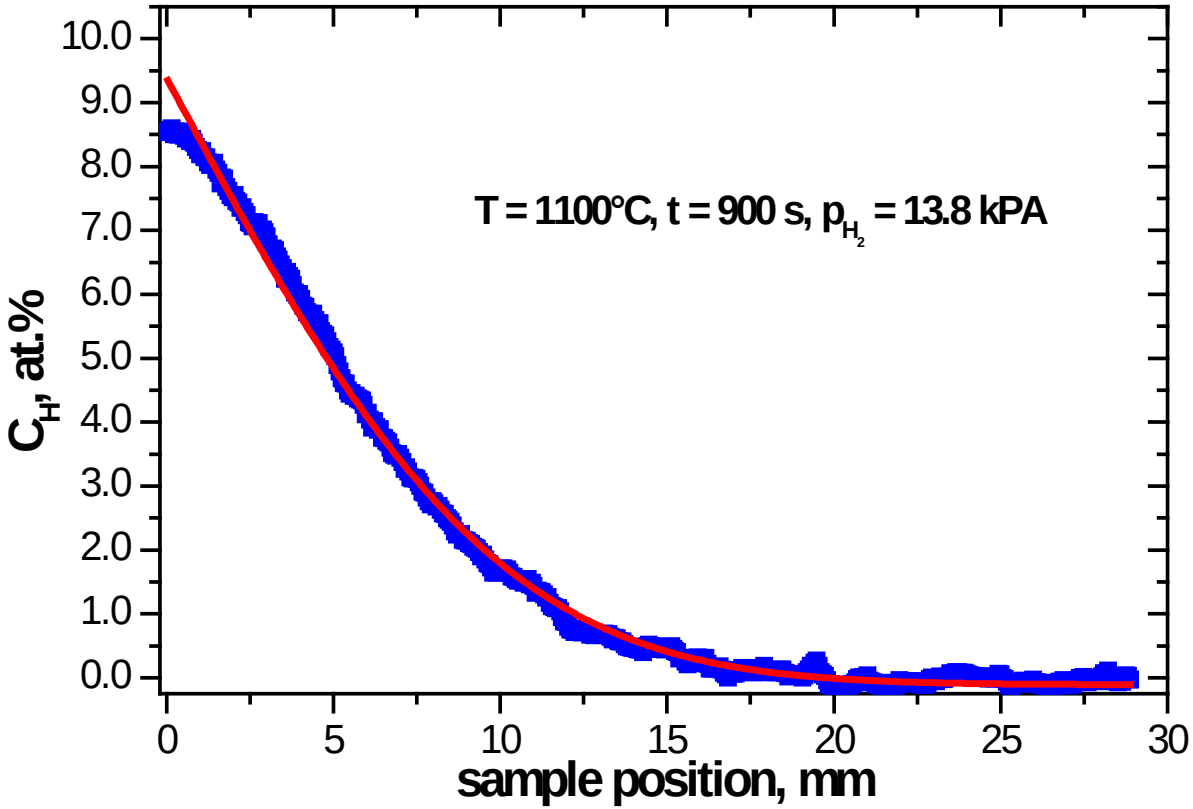
Zry-4 solid cylinder,
12 mm diameter, 20 mm height
Pre-oxidized in O_2 at 1100°C

At one base plane the oxide layer was removed by grinding and polishing.

Annealing in flowing Argon – 5% H_2 gas mixture at tempertures between 900 and 1300°C

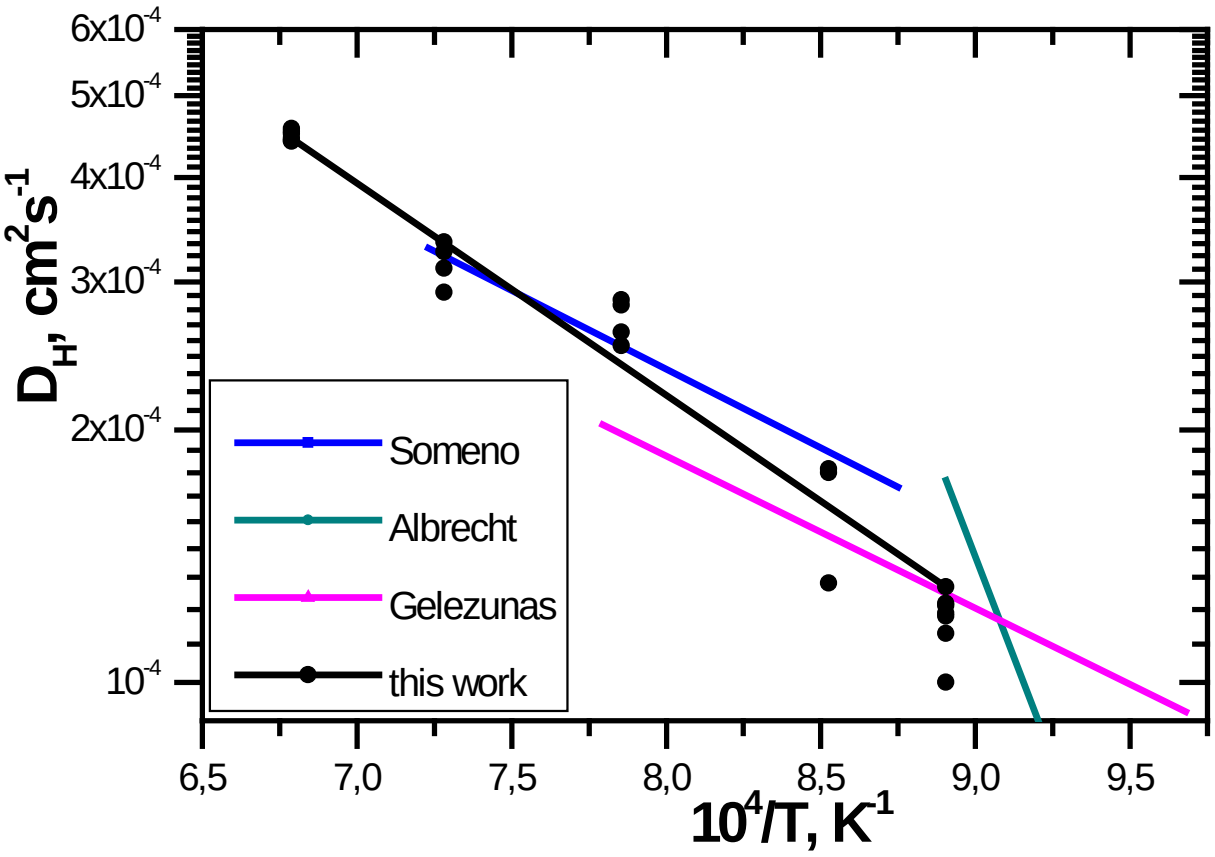
1100°C

Separate Effect Tests



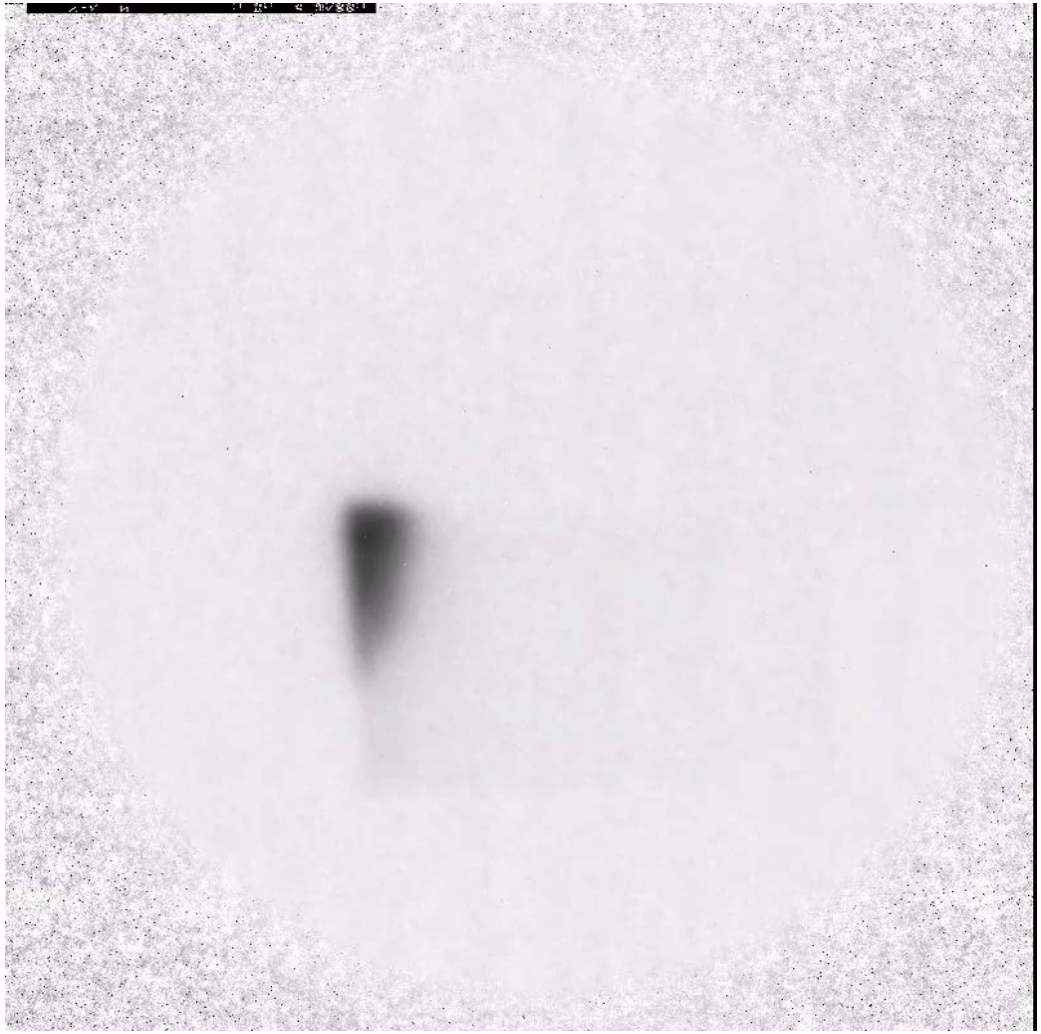
The hydrogen distribution can be determined from each image corresponding with a certain time

Separate Effect Tests



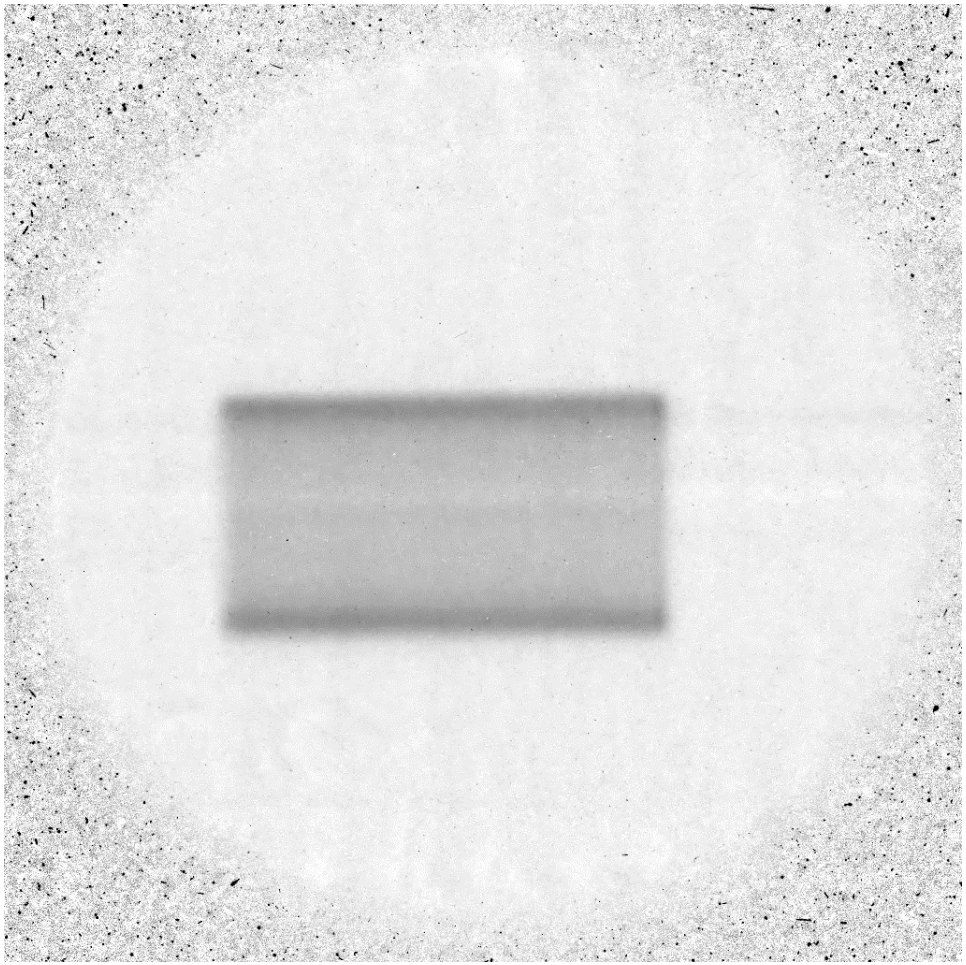
Comparison of the results with temperature correlations from literature

Separate Effect Tests



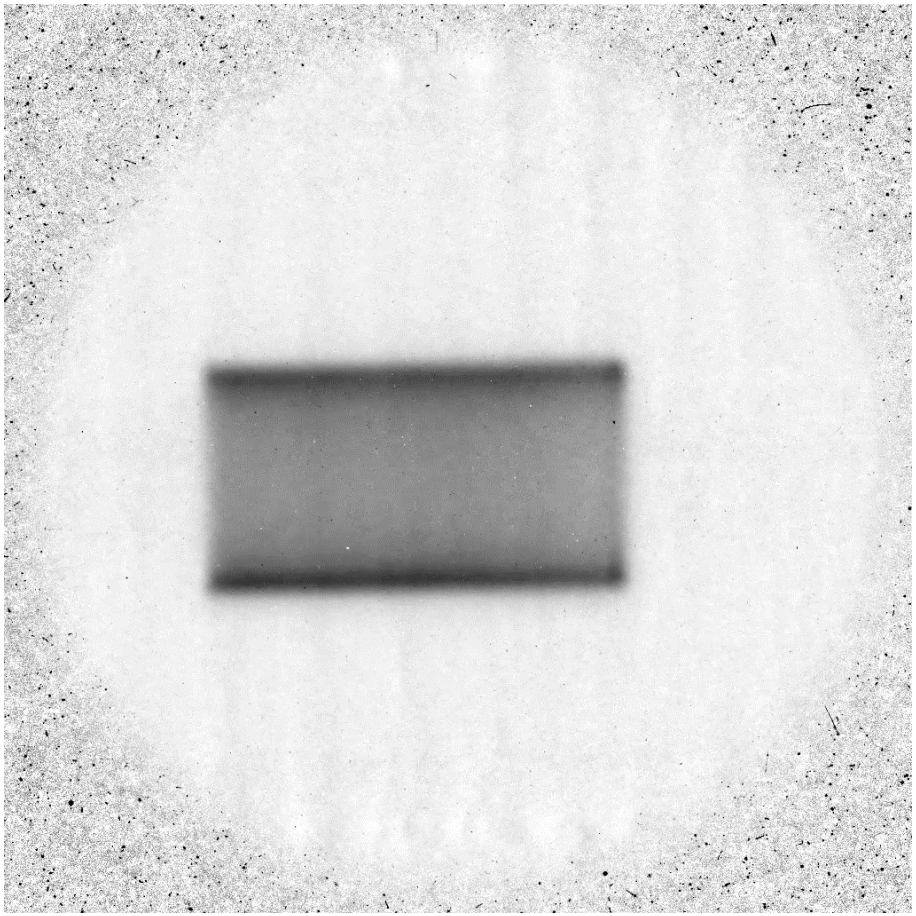
Test at 550°C in the α-β phase region

Separate Effect Tests



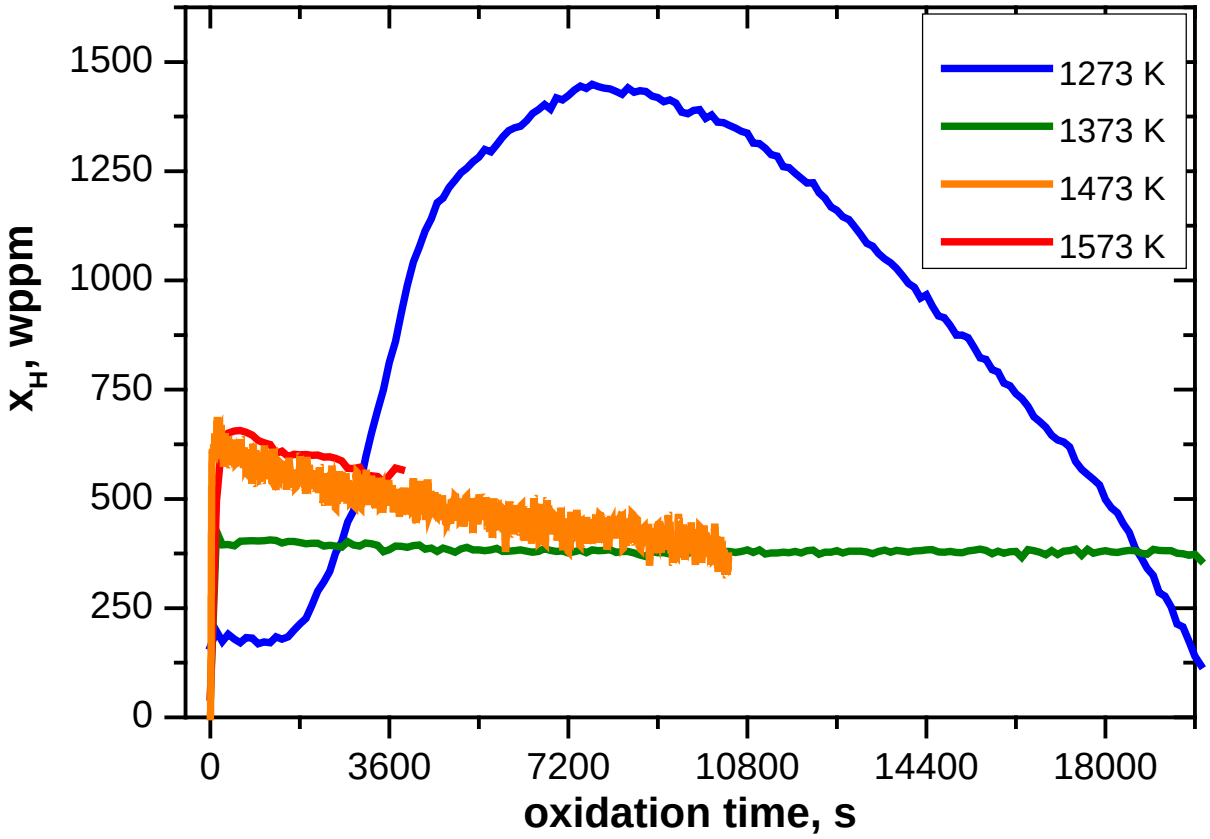
Reguläre Oxidation bei 1100°C

Separate Effect Tests



Breakaway Oxidation bei 1000°C

Results



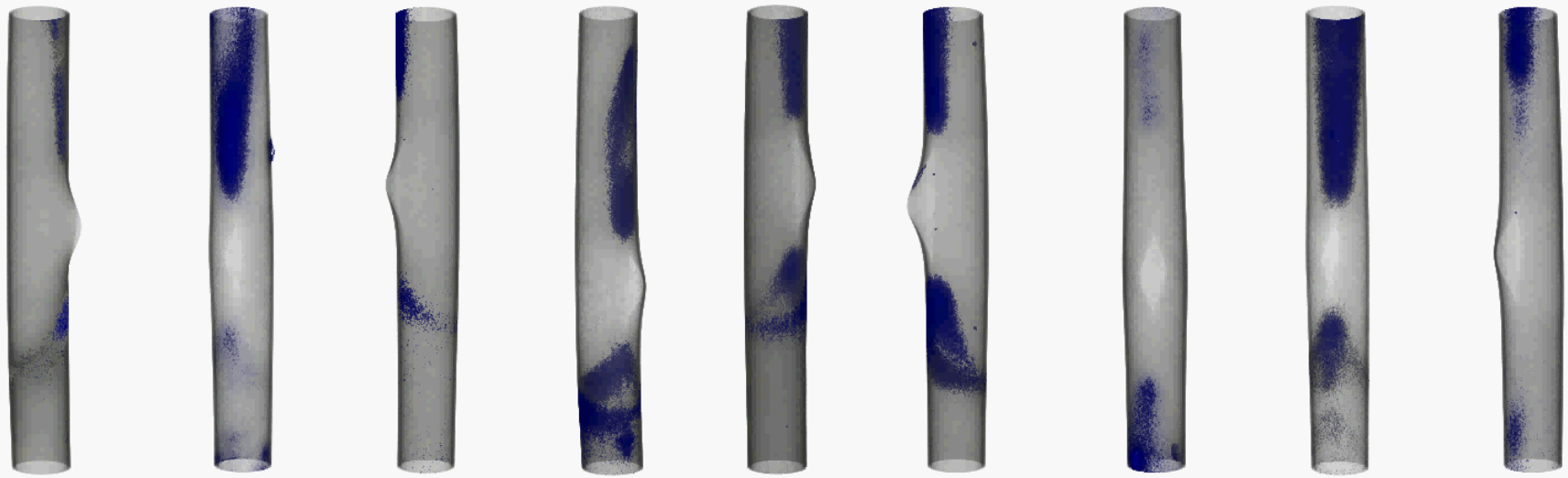
Very fast hydrogen uptake at the beginning

Later the hydrogen concentration decreases with time

Enhanced hydrogen uptake due to breakaway

Results QUENCH-L3 rods

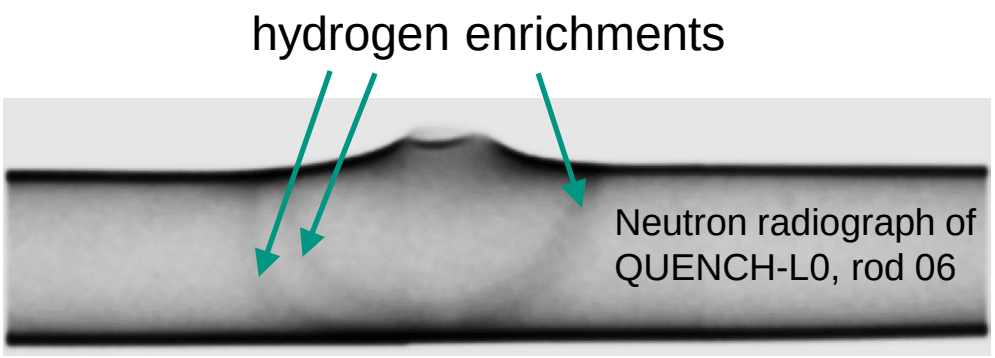
inner rods

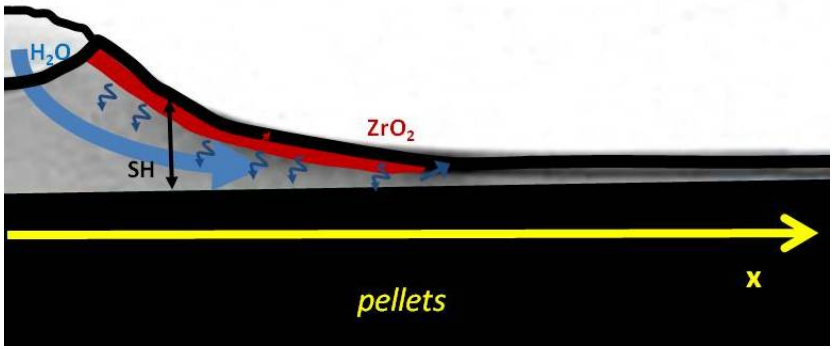


01 02 03 04 05 06 07 08 09

Maximal hydrogen concentration 1240 wppm at rod 06

Investigations of Hydrogen in Zirconium alloys at KIT





Steam:

Diffusion into the cladding

$$\frac{dc_{H_2O}(x)}{dt} = D_{H_2O}(T)\frac{\partial^2 c_{H_2O}}{\partial x^2}$$

with $c_{H2O}(x=0) = c_{H2O}(\text{bundle})$

Consumption:

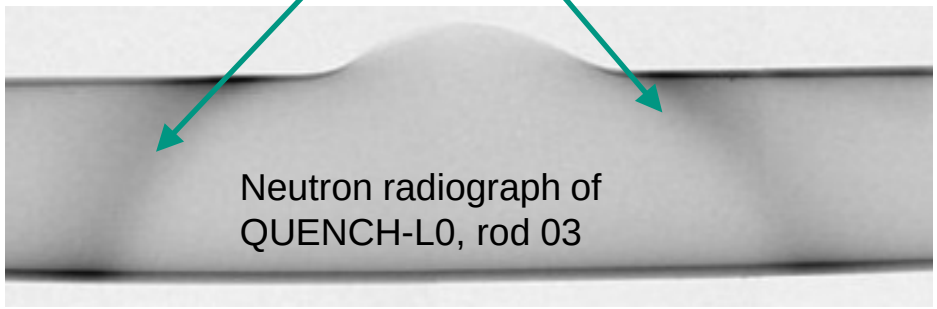
$$\frac{dc_{H_2O}(x)}{dt} = \frac{K_{ox}(T)}{2\sqrt{t}}$$

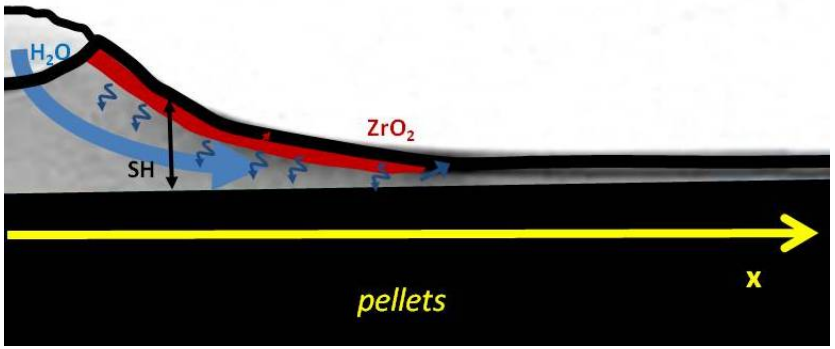
$$dc_{H_2O}(x) = \left(D_{H_2O}(T)\frac{\partial^2 c_{H_2O}}{\partial x^2} - \frac{K_{ox}(T)}{2\sqrt{t}} \right) dt$$

$$c_{H_2O}(x) \geq 0$$

Investigations of Hydrogen in Zirconium alloys at KIT

hydrogen enrichments





Gaseous hydrogen:

Source term

$$\frac{dc_{H_2}(x)}{dt} = \frac{K_{ox}(T)}{2\sqrt{t}}$$

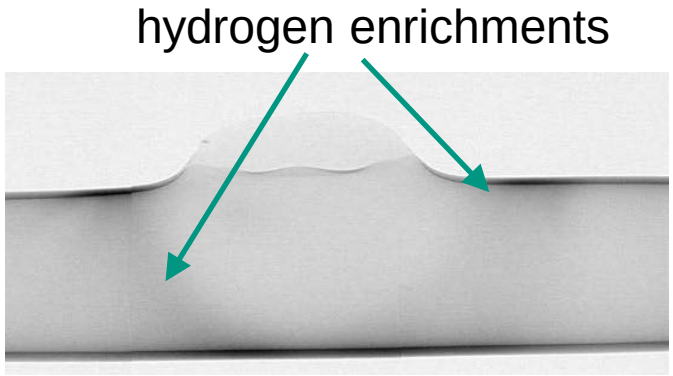
Diffusion

$$\frac{dc_{H_2}(x)}{dt} = D_{H_2}(T)\frac{\partial^2 c_{H_2}}{\partial x^2}$$

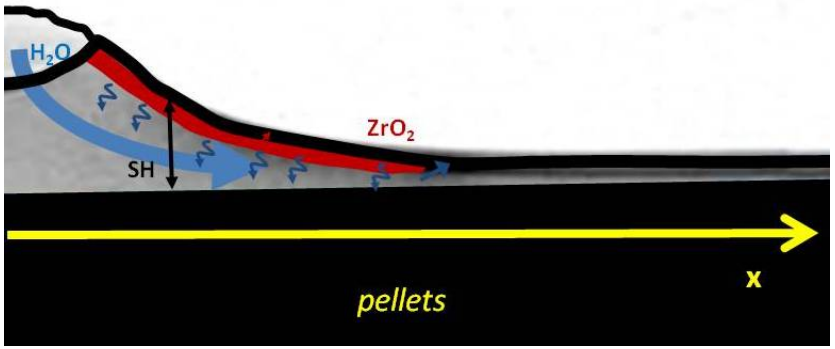
with $c_{H2}(x=0) = 0$

$$dc_{H_2}(x) = \left(D_{H_2}(T)\frac{\partial^2 c_{H_2}}{\partial x^2} + \frac{K_{ox}(T)}{2\sqrt{t}} \right) dt$$

Investigations of Hydrogen in Zirconium alloys at KIT



Neutron radiograph of QUENCH-L0, rod 08



Hydrogen uptake:

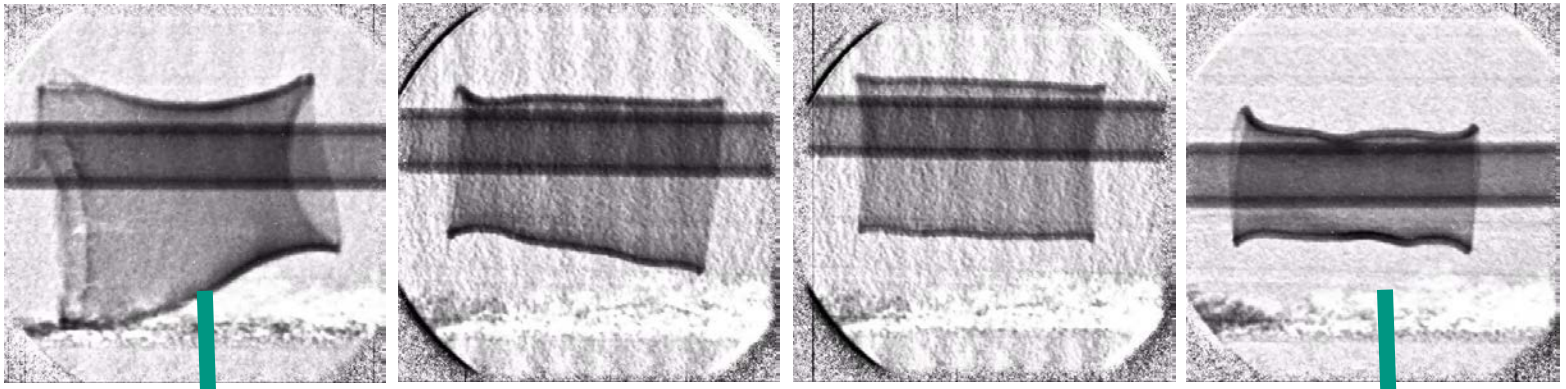
At first metal layer the hydrogen concentration is in equilibrium to the partial pressure of hydrogen gas in the gap between pellets and inner cladding surface.

$$x_H^m(x, r=0) = \frac{K_S(T)\sqrt{c_{H_2}(x)\,R\,T}\,M_H}{\left(1+K_S(T)\sqrt{c_{H_2}(x)\,R\,T}\right)M_{Zr}}$$

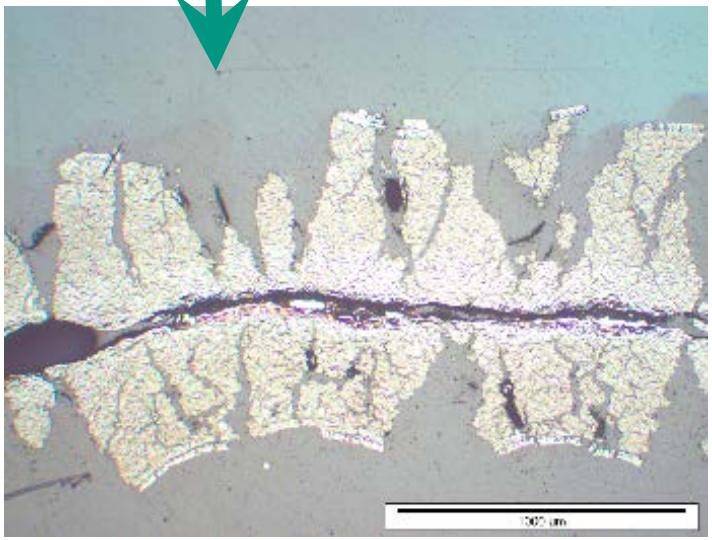
$$\Delta n_H^{gas} = -\Delta n_H^{metal}$$

In-situ Neutron imaging – influence of flow rate

steam-nitrogen
900°C



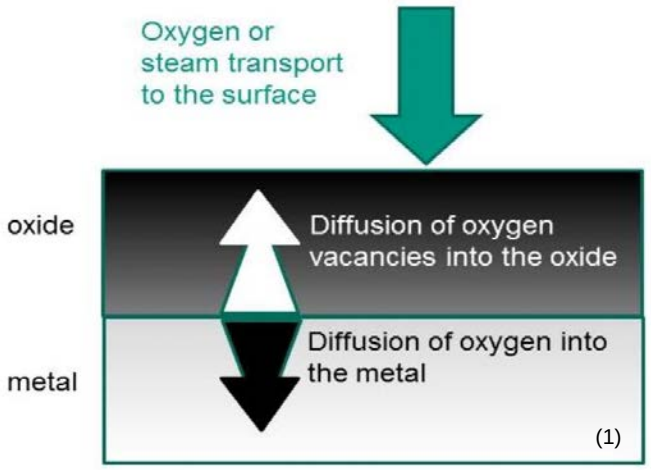
24 l/h | 36 l/h | 48 l/h | 72 l/h





Flow rate model

[M. Grosse et al. ICAPP 2016]



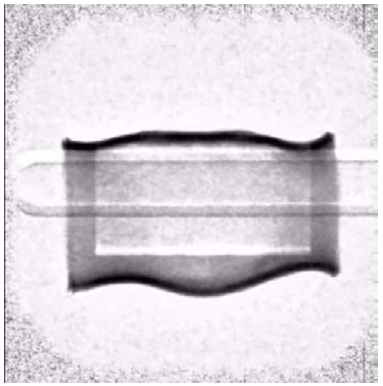
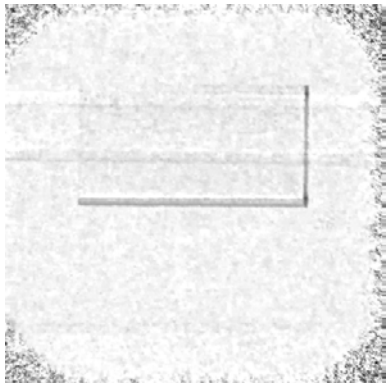
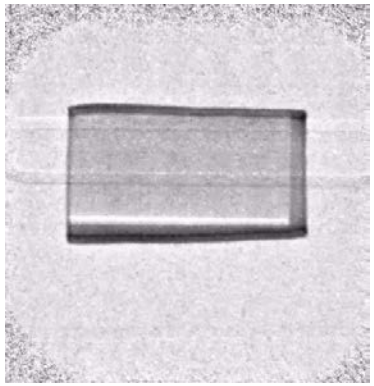
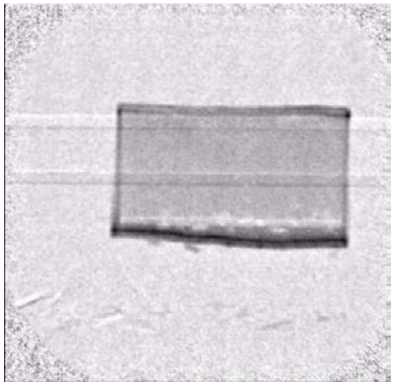
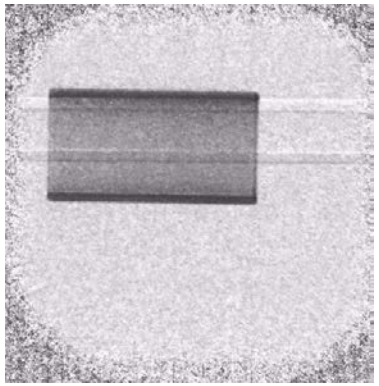
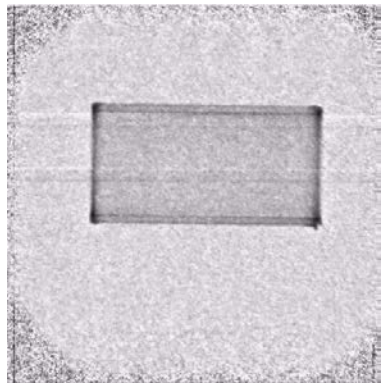
- Basic reaction with steam if an oxide layer is already formed
  - $ZrO + V_o^{2+} + 2e^- + H_2O \rightarrow 2\,ZrO_2 + 2H$
- $\dot{n}_{V_O^{2+}} = \dot{n}_{oxygen,react} = \frac{K_{n_{ox}}}{2\sqrt{t}}$ for saturation
- In the case of steam + oxygen starvation

$$\rightarrow \frac{K_{n_{ox}}}{2\sqrt{t}} - \frac{\dot{n}_{O_2}}{2} - \dot{n}_{H_2O} = \frac{\dot{n}_{N_2}}{4}$$

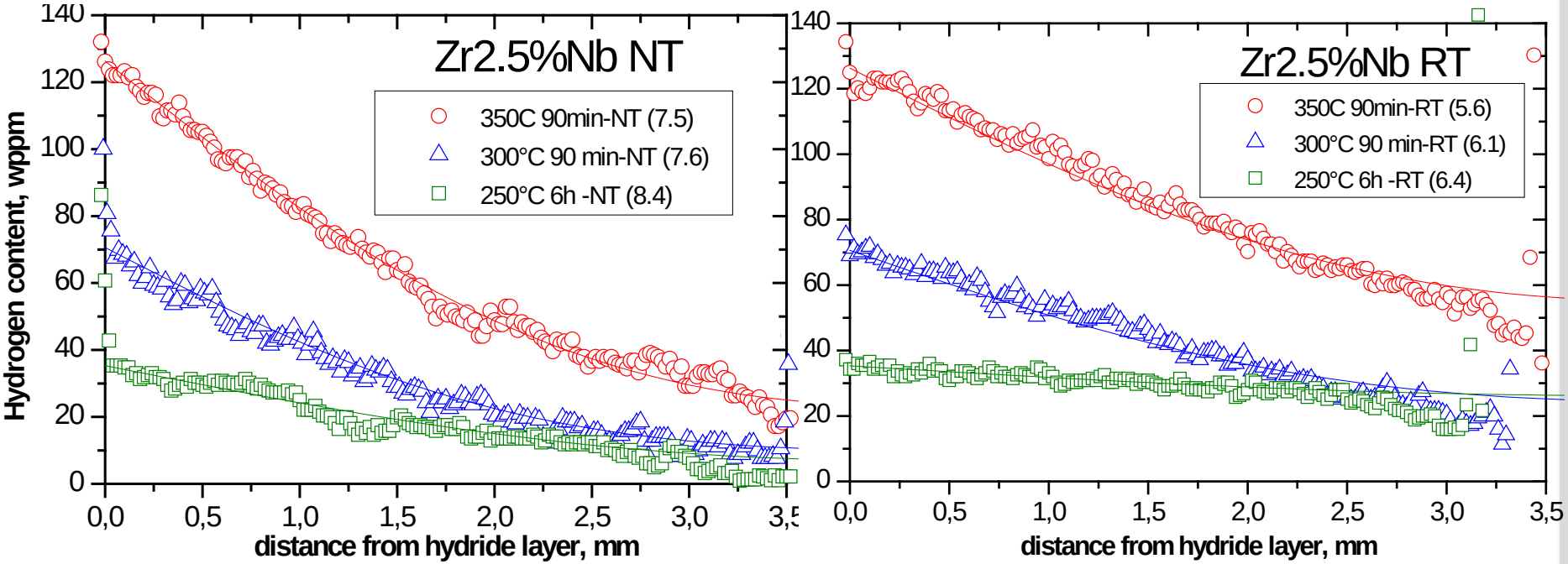
- If $c_N > c_{N,critical}$ -> ZrN precipitation and formation of cracks
- $\dot{x}_{res} = IF_{cracks} * \dot{x}_{linear} + (1 - IF_{cracks}) * \dot{x}_{parabolic}$

(1) ICAPP 2016,INFLUENCE OF THE STEAM AND OXYGEN FLOW RATE ON THE REACTION OF ZIRCONIUM IN

In-situ Neutron imaging – different atmospheres

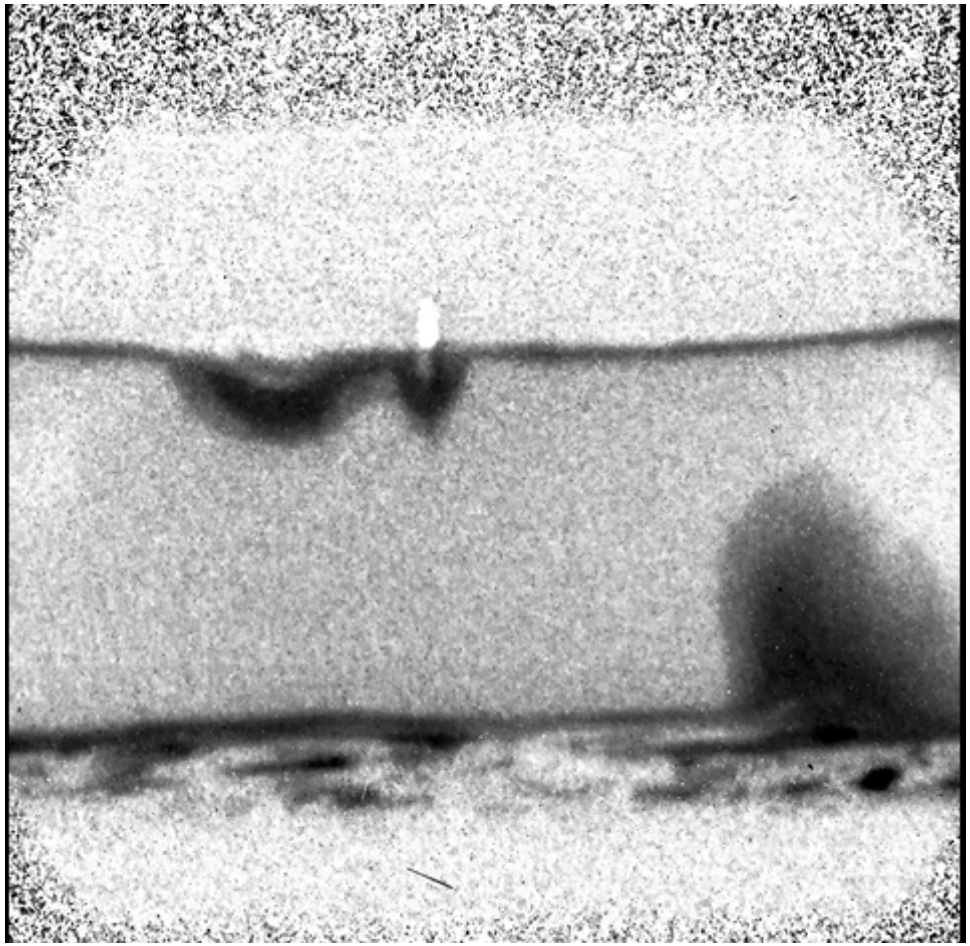
	steam-nitrogen	steam	steam-air
800°C			
1000°C			

Hydrogen behaviour at T < 400°C

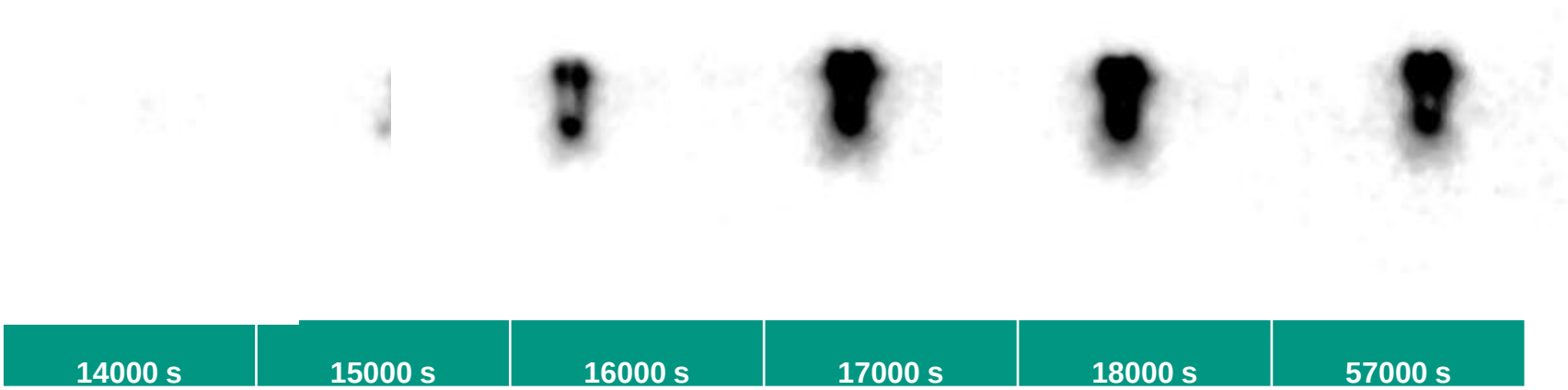


- Temperature dependence of hydrogen solubility
- Faster diffusion in normal direction than in rolling direction (may be caused in a better continuity of the β phase network normal to RT direction

Hydrogen behaviour at T < 400°C

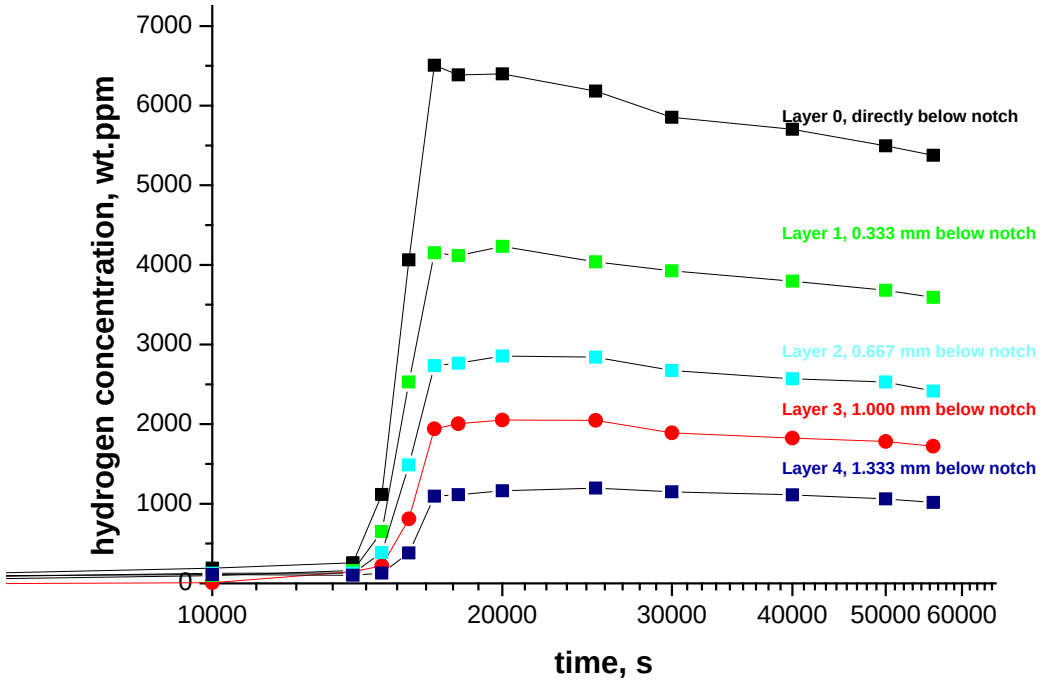


Hydrogen behaviour at T < 400°C



Hydrogen uptake at a notch and crack tip in a stresses pre-cracked Zry.4 specimen

Hydrogen behaviour at T < 400°C



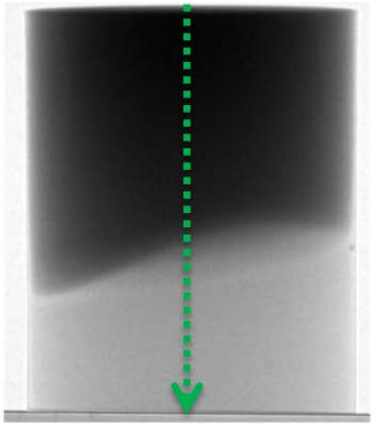
Delayed hydrogen uptake, only very low changes after switch off of the hydrogen supply at 18 ks.

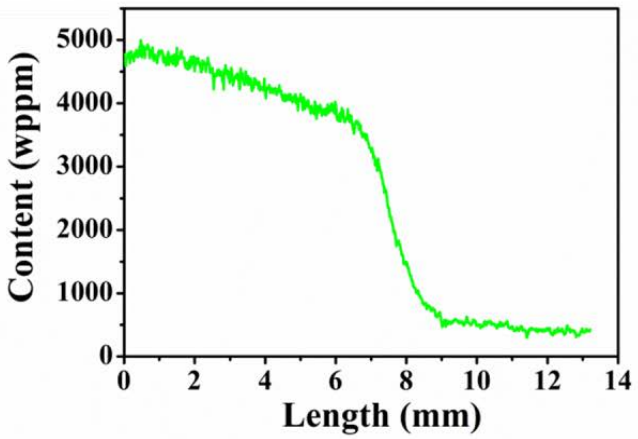
Protection against hydrogen uptake - coated Zry

as received

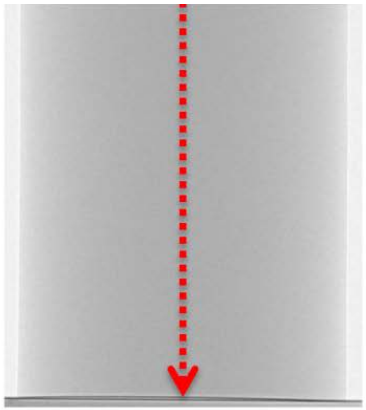


uncoated

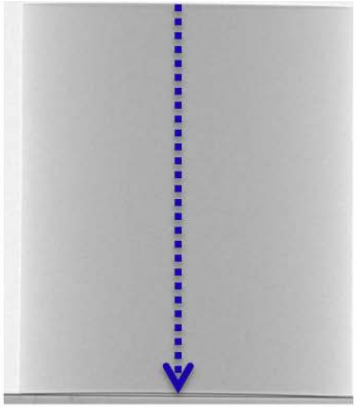


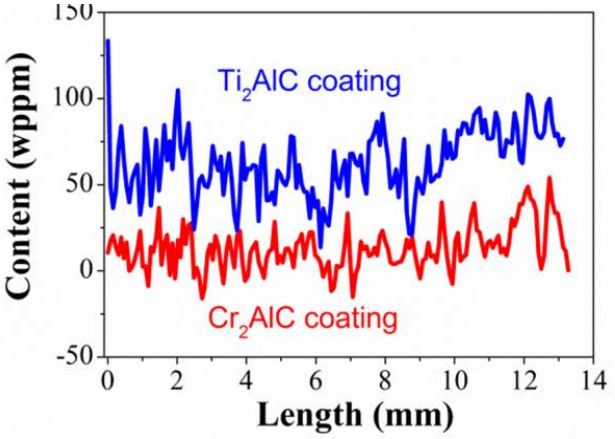


Cr_2AlC coated



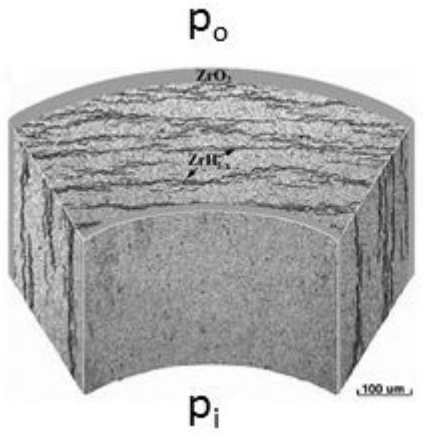
Ti_2AlC coated



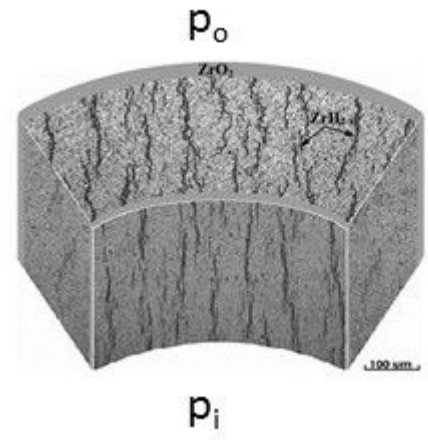


Hydrogen behaviour during long term dry storage of spent fuel rods

- Hydrogen uptake of the cladding tube made of Zircaloy during operation:
  - 70 .. 150 wt.ppm
  - oriented in hoop direction
  - at some positions (friction between grid spacers and cladding tubes, blisters at positions were the oxide layer spalled) hydrogen enrichments can reach several thousands wt.ppm



- Hydrogen keeps an issue even after usage of the fuel rods:
  - re-distribution of hydrogen and
  - re-orientation of hydrides



The SPIZWURZ project

SPIZWURZ (**Sp**annungs**i**nduzierte **W**asserstoff**u**mlagerung in Brennstabhüllrohren während längerfristige**r** **Z**wischenlagerung

Joined project GRS, KIT-INE, KIT-IAM

KIT-IAM contributions to SPIZWURZ:

Quantifying of the hydrogen diffusion in zirconium alloys depending on orientation,

- Hydrogen diffusion in Zr single crystals
- Hydrogen diffusion depending on texture
- Hydrogen diffusion and solubility depending on elastic stress



Credit: Audrius Meskauskas

Purpurner Enzian (Spitzwurz)

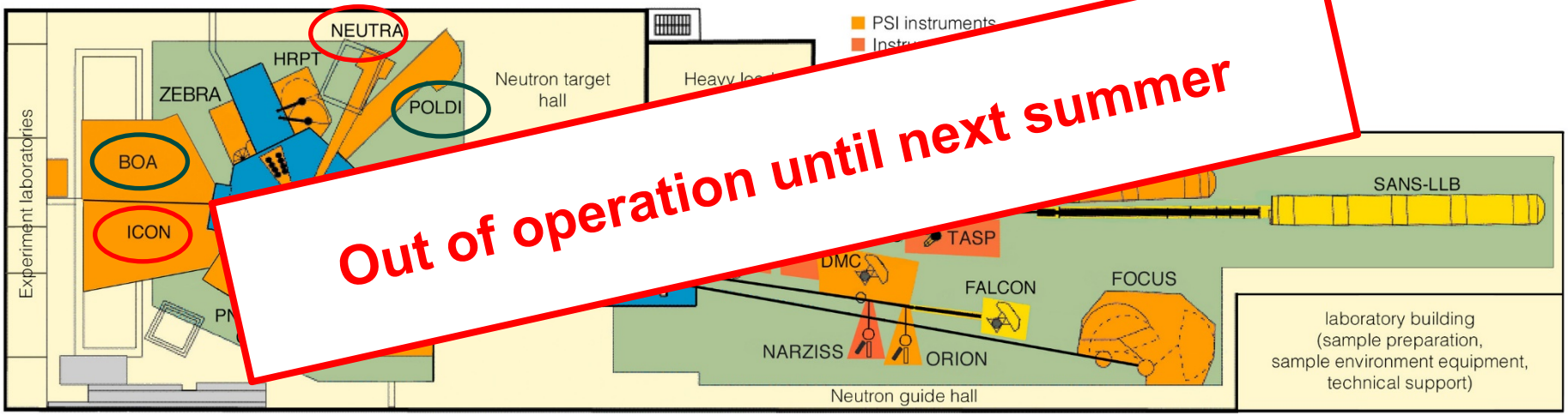
Summary

- Hydrogen in zirconium alloys is investigated worldwide including at KIT since decades. However, there are still a lot of open questions.
- Neutron imaging is a powerful tool to investigate hydrogen in zirconium.
- Hydrogen uptake at high temperatures strongly depends on the oxide morphology
- Coatings suppress hydrogen uptake of zirconium alloys.
- Hydrogen solubility and diffusion depends in zirconium alloys on elastic lattice strain. Quantification is needed for modelling.

Plans for the future

- Project Spizwurz:
  - Systematic separate effect tests to investigate hydrogen diffusion and solubility dependence on lattice direction, texture, elastic stress/strain
  - Cooperation with GRS, KIT-INE, CNL, ?
  - Fuel rod bundle test (21 fuel rod simulators with original claddings, 2.5 m long, three-angular temperature gradient):
    - duration: 250 days
    - start temperature: 500°C at the hottest axial and radial position,
    - Cooling rate: 1 K/day
  - Intensive post-test examinations

Neutron Imaging facilities



Out of operation until next summer

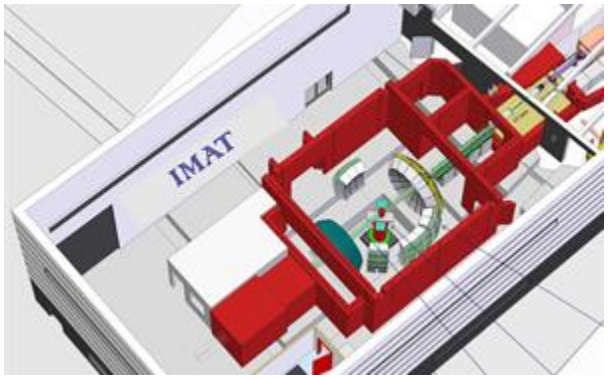


Out of operation at least until next summer



End of operation at this December

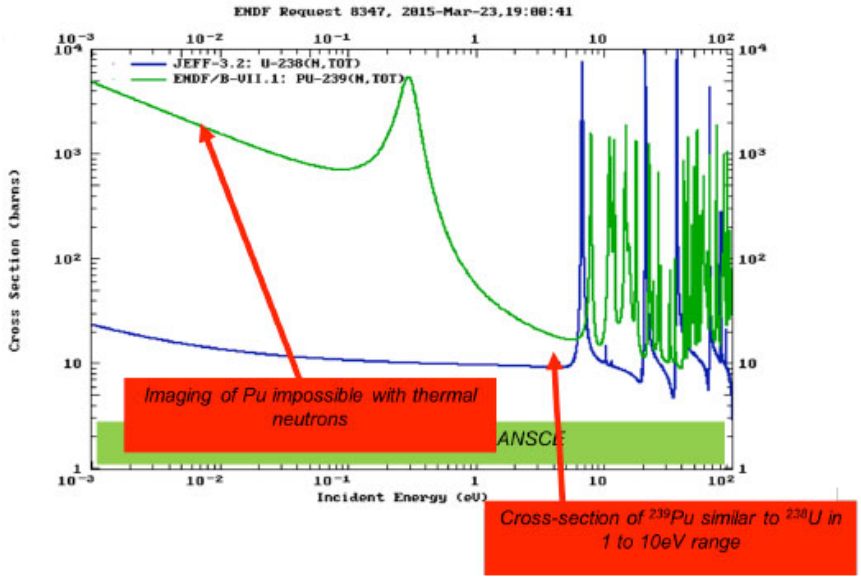
Alternatives



IMAT @ ISIS



Imagine @ Orphée



ERNI @ LANSCE

Acknowledgements

Thanks to

- The whole QUENCH team at KIT for preparing the samples and conducting the test.
- The KIT program NUSAFE, VGB, EU for sponsoring these activities.
- Neutron Sources (FRM2, SINQ, BER for providing beam-time for the Neutron Imaging investigations and for the support during the experiments.

Thank you for your attention!

Impact of QUENCH Experiments for ISPs, Benchmarks and Code Validation

Thorsten Hollands
Gesellschaft für Anlagen- und Reaktorsicherheit (GRS) gGmbH, Germany

Abstract

For the development of software tools applied in the field of nuclear safety requirements and procedures are defined for quality assurance purposes. For example, the IAEA published a general document concerning requirements, that need to be fulfilled during code development, including verification and validation (IAEA SAFETY STANDARDS SERIES No. SSG-2). In general development, verification and validation should be separated, while the validation process should cover a phenomena orientated validation matrix, single effect tests (SET), and integral tests. The available experiments for severe accident scenarios and phenomena were reviewed and documented in OECD reports in which validation matrices were defined and the test series were classified according to their applicability for validation (NEA/CSNI/R(2000)21). All investigated experiments are classified in category 1 (experiments are amongst the best qualified for code validation in their field, ISPs normally fall into this category) or 2 (experiments are well qualified for code validation and could be used to increase the degree of confidence in a code's suitability for a given application). The evaluated QUENCH tests at that time were classified as category 2. QUENCH-06, which was subject of ISP-45, can be classified as category 1.

The QUENCH test matrix shows that several topics are covered in the history of the test series to investigate the material behavior of fuel rod simulators during flooding of superheated cores. First, classical PWR tests were performed, followed by three tests focusing on B_4C oxidation. Additionally, the scope was on the investigation of different cladding materials like E110, Zirlo™ or M5®. Furthermore, three air-ingress tests were conducted as well as one debris test. The latest two tests dealt with ATF cladding material and a BWR configuration. These wide field of subjects as well as the well instrumented test section and the documentation are the basis for many validation cases of several severe accident codes. The fact that QUENCH-06 was chosen for ISP-45, three tests were used for SARNET benchmarks, one test for a NUGENIA benchmark and one for an IAEA ACTOF benchmark show the high importance of QUENCH tests for the international code validation. In addition to the severe accident tests six LOCA tests were performed, one of them was the topic of an IAEA FUMAC benchmark.

Additionally, QUENCH tests and comparable test series are widely used by beginners in the field of simulation of nuclear systems/plants with respect to severe accident studies or by users of new codes to assure knowhow transfer, because the number of phenomena is limited, and the tests are well documented.



Impact of QUENCH Experiments for ISP, Benchmarks and Code Validation

Thorsten Hollands

Gesellschaft für Anlagen- und Reaktorsicherheit (GRS) gGmbH

25th International QUENCH Workshop

Karlsruhe Institute of Technology (KIT)

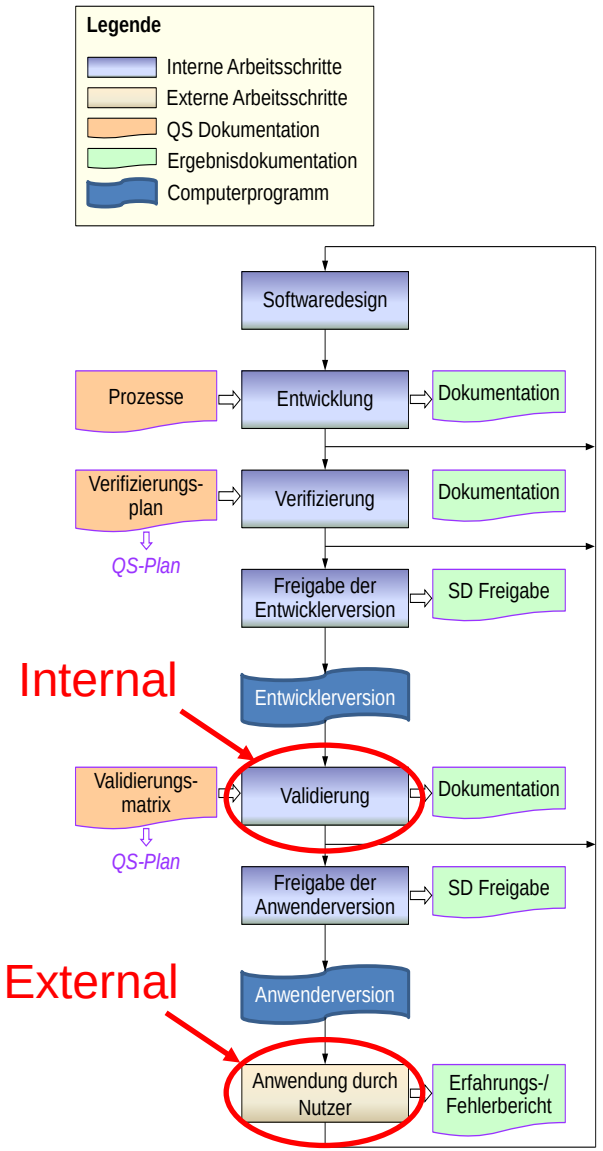
22 – 24 October 2019

Outline

- Validation of computer codes
- QUENCH Matrix and Application
- ISP-45: QUENCH-06
- SARNET/NUGENIA-Benchmarks
- QUENCH Tests for Education and Knowhow Transfer
- Conclusions and Outlook

Validation of computer codes
General process

- IAEA SAFETY STANDARDS SERIES No. SSG-2
- QM Guidelines for computer programs
- Separation of *Development and Verification* and *Validation*
  - Verification: check, whether models are implemented correctly
  - Validation: check, whether physical phenomena are described by the correct models
    - Phenomena orientated validation matrix
    - Single effect tests (SET): selected effects, clearly defined initial and boundary conditions, high instrumentation density and quality
    - Integral tests: interaction of different effects, normally scaled test facilities, common special instrumentation



Validation of computer codes
Requirements for code validation

- IAEA SAFETY STANDARDS SERIES No. SSG-2
- OECD/CSNI In-Vessel Core Degradation Code Validation Matrix (NEA/CSNI/R(2000)21)
  - **Category 1** experiments are amongst the best qualified for code validation in their field. ISPs normally fall into this category. Data are well documented and boundary conditions are well defined (these conditions may be relaxed if there are specific unique features). Category 1 tests are strongly recommended for the validation of system codes (depending on their specific objectives)
  - **Category 2** experiments are well qualified for code validation, and could be used to increase the degree of confidence in a code's suitability for a given application. The experiment may not be unique, but valuable in the sense of parameter range.
  - **Category 3** and **4** were not considered due to the database and quality of the evaluated experiments.
  - Cross References Matrices were generated to evaluate the investigated experiments

QUENCH Matrix and Application (I)

Experiment	Topic	Used for
QUENCH-01	partial fragmentation of pre-oxidized cladding	Validation
QUENCH-02	no additional pre-oxidation; quenching from high temperatures	Validation
QUENCH-03	delayed flooding; 240 s after temperature escalation has started	Validation
QUENCH-04	cool-down behavior of slightly pre-oxidized cladding by injected cold steam	Validation
QUENCH-05	cool-down behavior of pre-oxidized cladding by injected cold steam	Validation
QUENCH-06	prediction of H_2 source term by different code systems	**ISP-45**
QUENCH-07	impact of B_4C absorber rod failure on H_2, CO, CO_2 and CH_4 generation	Validation
QUENCH-08	Reference test to QU-07 without absorber rod	Validation
QUENCH-09	impact of B_4C absorber rod failure on H_2, CO, CO_2 and CH_4 generation in steam-starved conditions	Validation
QUENCH-10	air ingress during spent fuel storage container accident	**SARNET Benchmark**

QUENCH Matrix and Application (II)

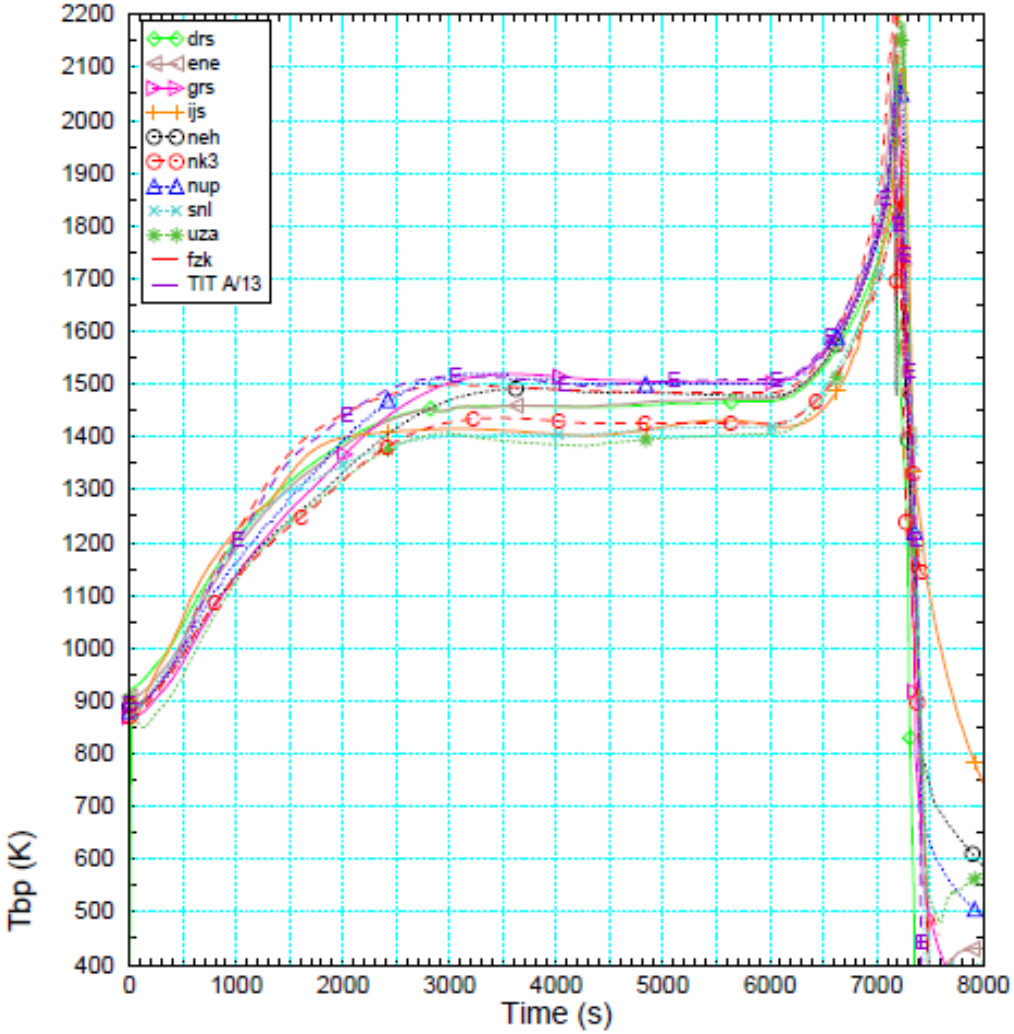
Experiment	Topic	Used for
QUENCH-11	boil-off test with subsequent flooding	**SARNET Benchmark**
QUENCH-12	physico-chemical behavior of VVER type cladding (Zr1%Nb) during flooding	Validation
QUENCH-13	AgInCd absorber rod, aerosol	Validation
QUENCH-14	ACM series, M5® cladding	Validation
QUENCH-15	ACM series, ZIRLO™ cladding	Validation
QUENCH-16	air ingress	**SARNET Benchmark**
QUENCH-17	Debris formation and coolability	Validation
QUENCH-18	air ingress, AgInCd absorber rods	**NUGENIA QUESA Benchmark**
QUENCH-19	ATF, FeCrAl cladding	**IAEA ACTOF Benchmark**
QUENCH-20	BWR configuration	Under Investigation

QUENCH Matrix and Application (III)

Experiment	Topic	Used for
QUENCH-L0	VGB Project; Commissioning test with Zry-4.	Validation
QUENCH-L1	VGB Project; Reference test.	**IAEA FUMAC Benchmark**
QUENCH-L2	VGB Project; M5® claddings.	Validation
QUENCH-L3HT	VGB Project; Opt. ZIRLO™ claddings.	Validation
QUENCH-L3	VGB Project; Optimised ZIRLO™ claddings.	Validation
QUENCH-L4	VGB Project; Pre-hydrogenated (100 wppm) M5® claddings	Validation
QUENCH-L5	VGB Project; Pre-hydrogenated (300 wppm) optimised ZIRLO™ claddings.	Validation

ISP-45: QUENCH-06
– Open phase –

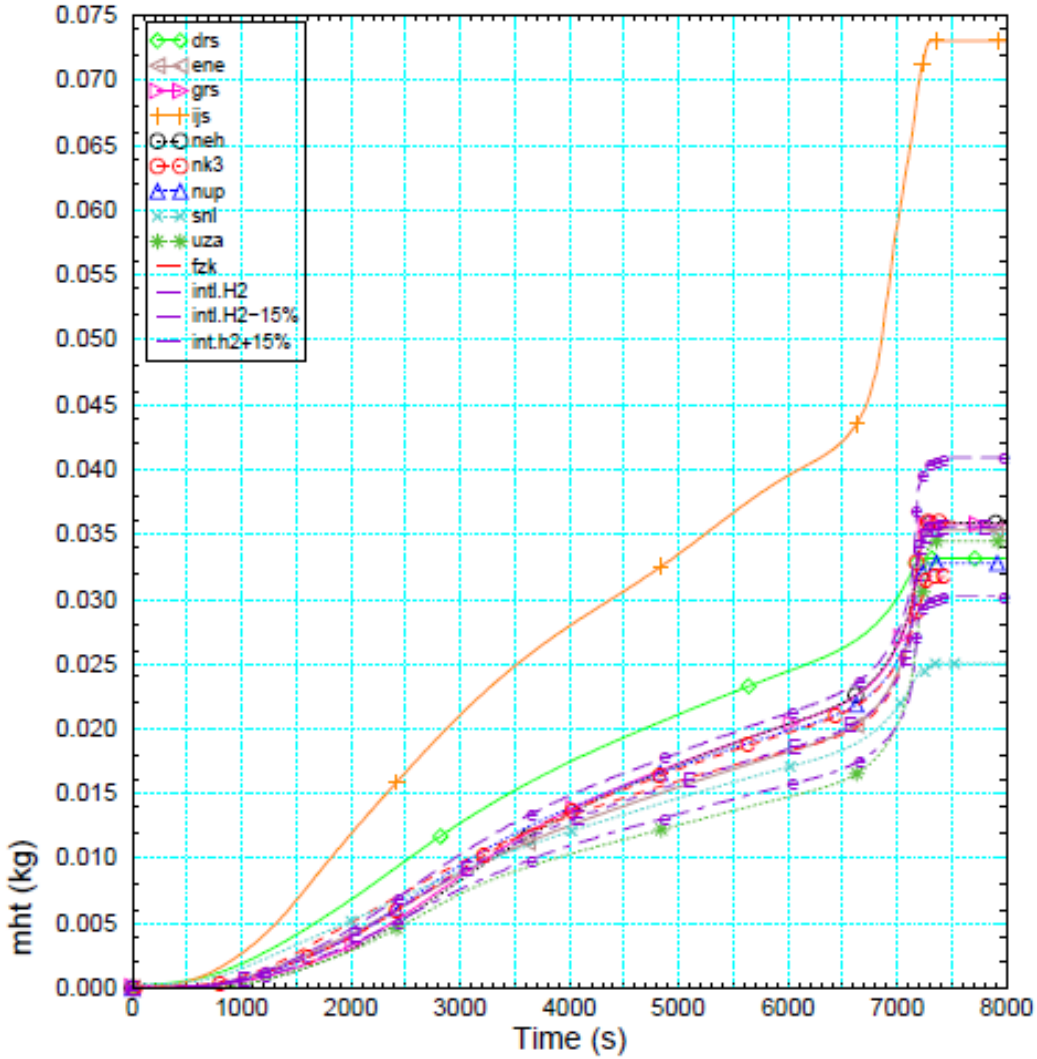
- Maximum cladding temperatures



FZKA 6722

ISP-45: QUENCH-06

- Hydrogen generation



FZKA 6722

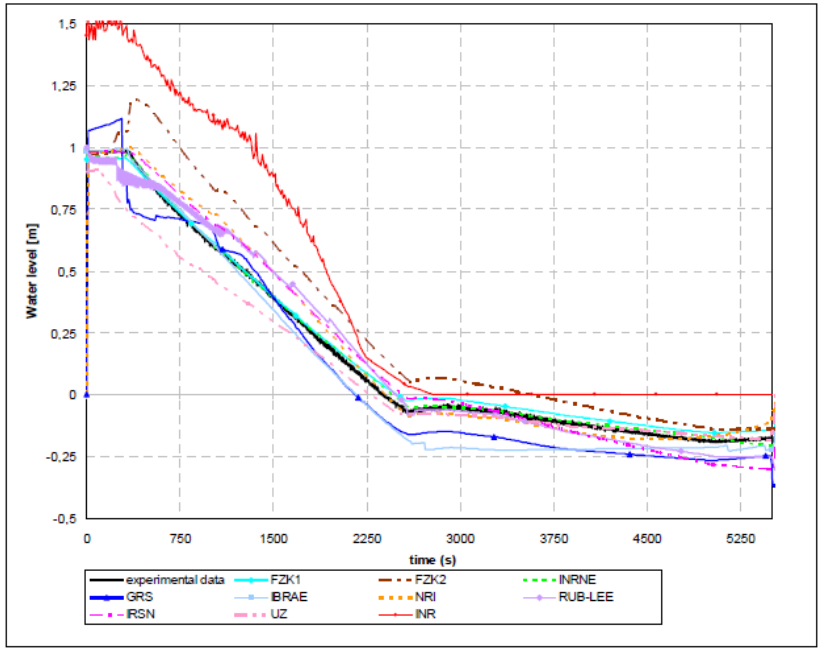
ISP-45: QUENCH-06
– Main findings (FZKA 6722) –

- Despite some large discrepancies between some measured and calculated results, especially during the quench phase, a blind exercise like ISP-45 has turned out to be valuable, because the participants are forced to assess the code capabilities in a more profound way than simply to modify input parameters to fit the code predictions to known experimental results.
- Comparing results of the blind phase indicates not only differences in the mechanistic treatment of phenomena but also some inadequate balancing between them. It is most important for the simulation of severe situations not only to consider all pertinent phenomena, but also their interdependencies.
- A reasonably revised ranking of the relevant phenomena will help to limit the necessary analytical effort also for more severely damaged bundles. It is emphasized that this ranking must be done carefully to avoid inappropriate model development.
- ISP-45 may be considered to be a first step for further code validation concerning the aims of the QUENCH program. Future tests are intended to enlarge, to verify or to precise the findings drawn from the past tests, including the influence of absorber components. This will contribute to an improvement of the mechanistic basis for future code development and verification efforts.

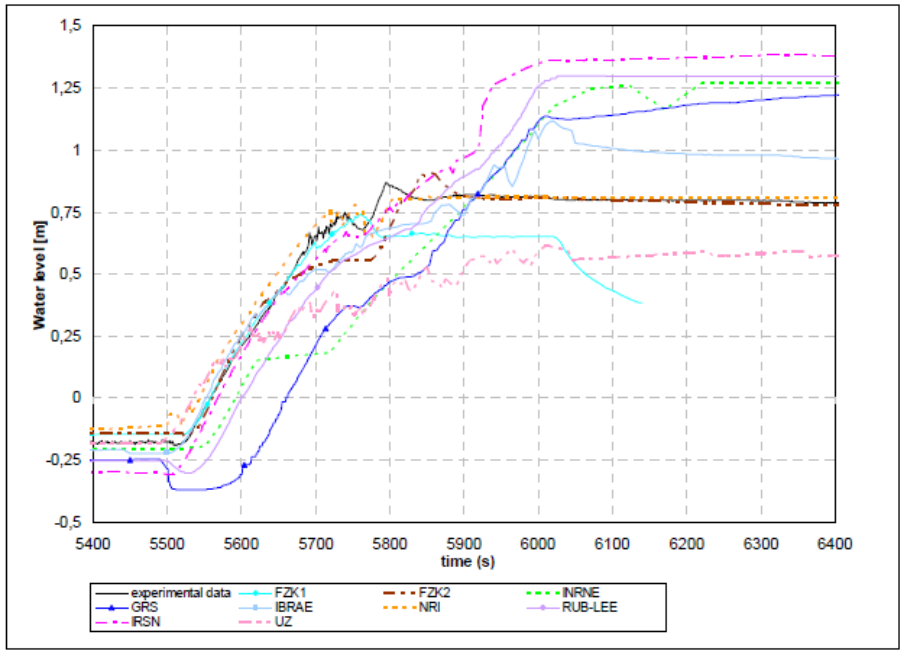
SARNET Benchmark: QUENCH-11

- Water level

During boil-off



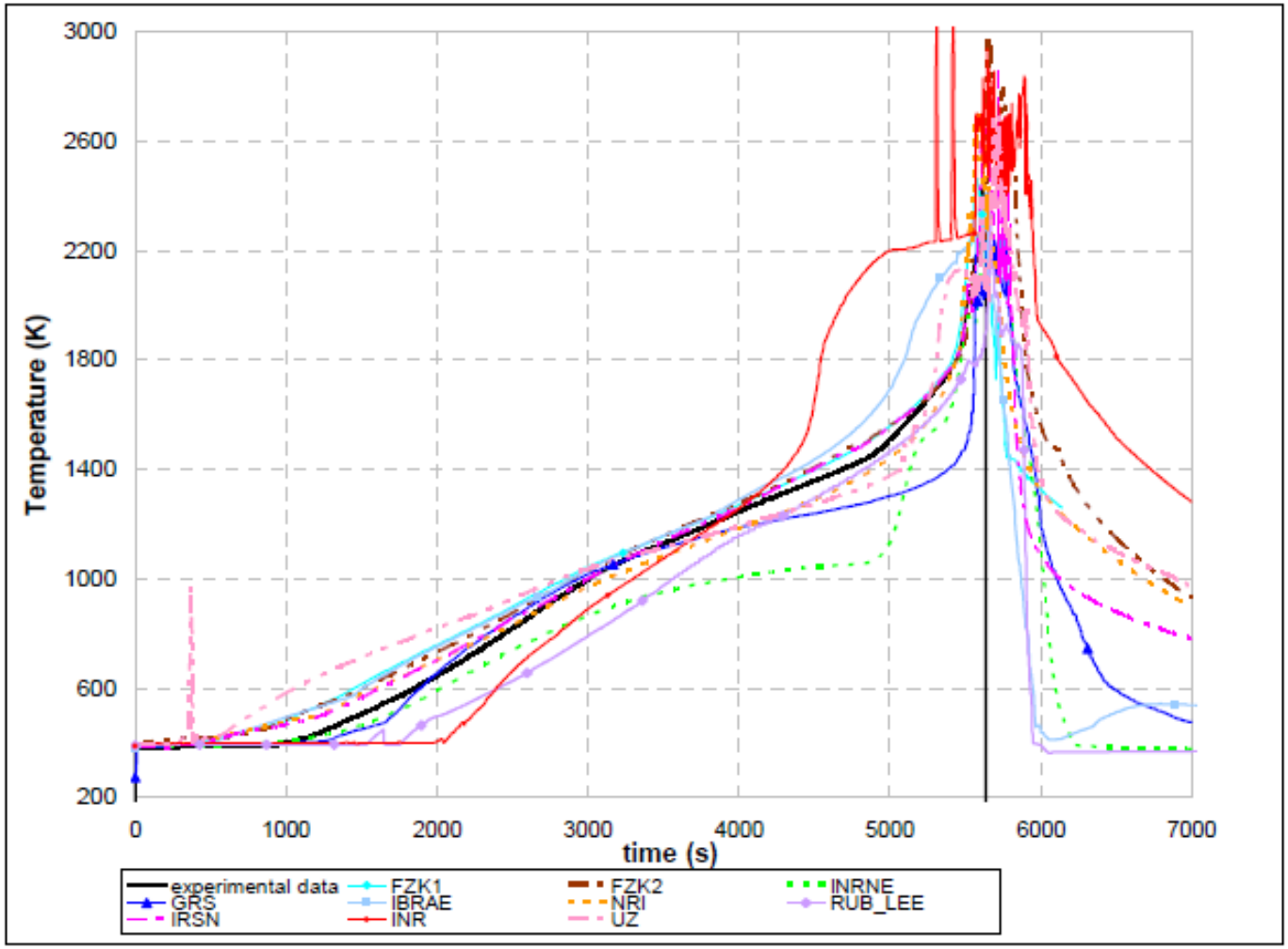
and reflood



FZKA 7368

SARNET Benchmark: QUENCH-11

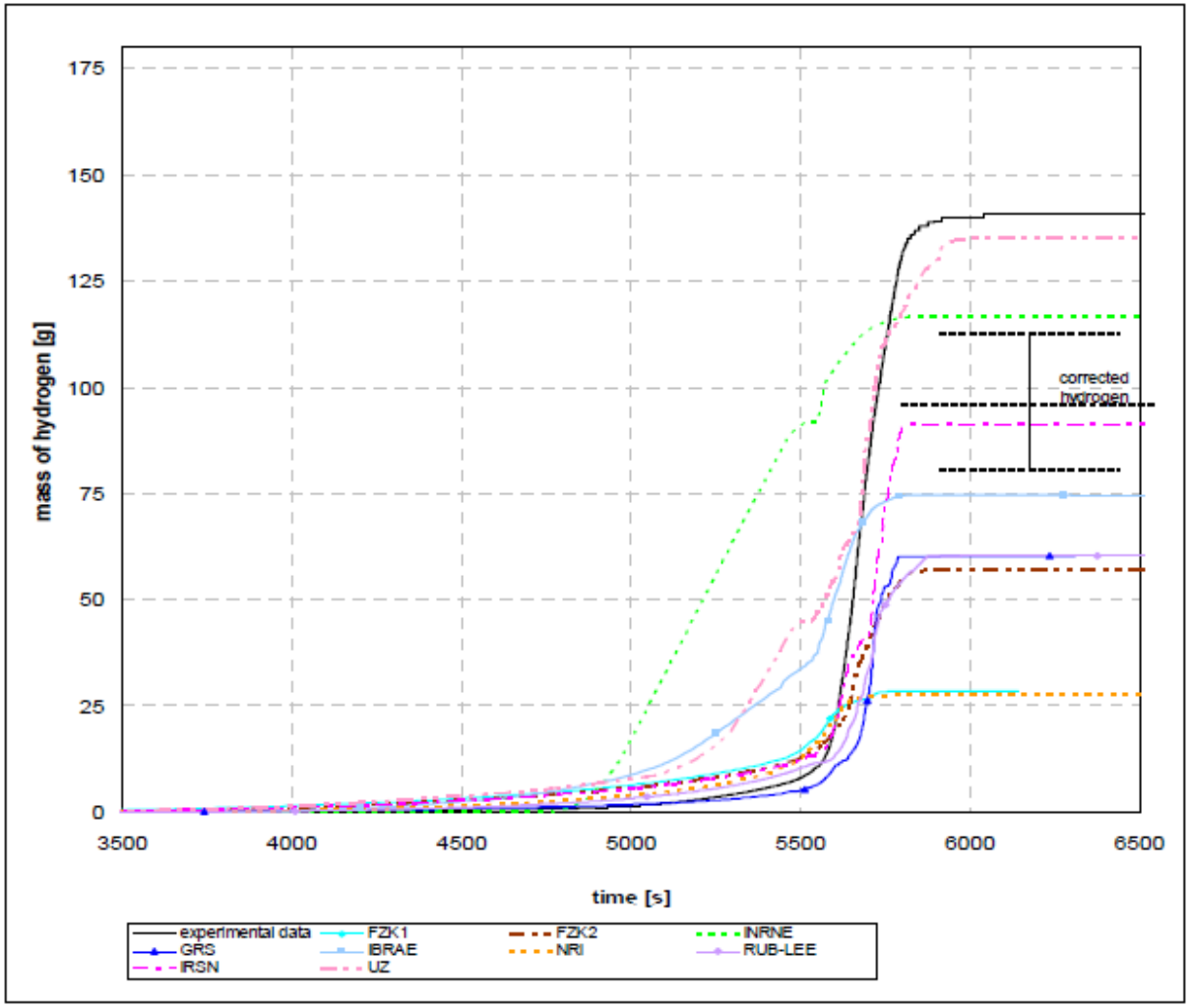
- Maximum cladding temperatures



FZKA 7368

SARNET Benchmark: QUENCH-11

- Hydrogen generation



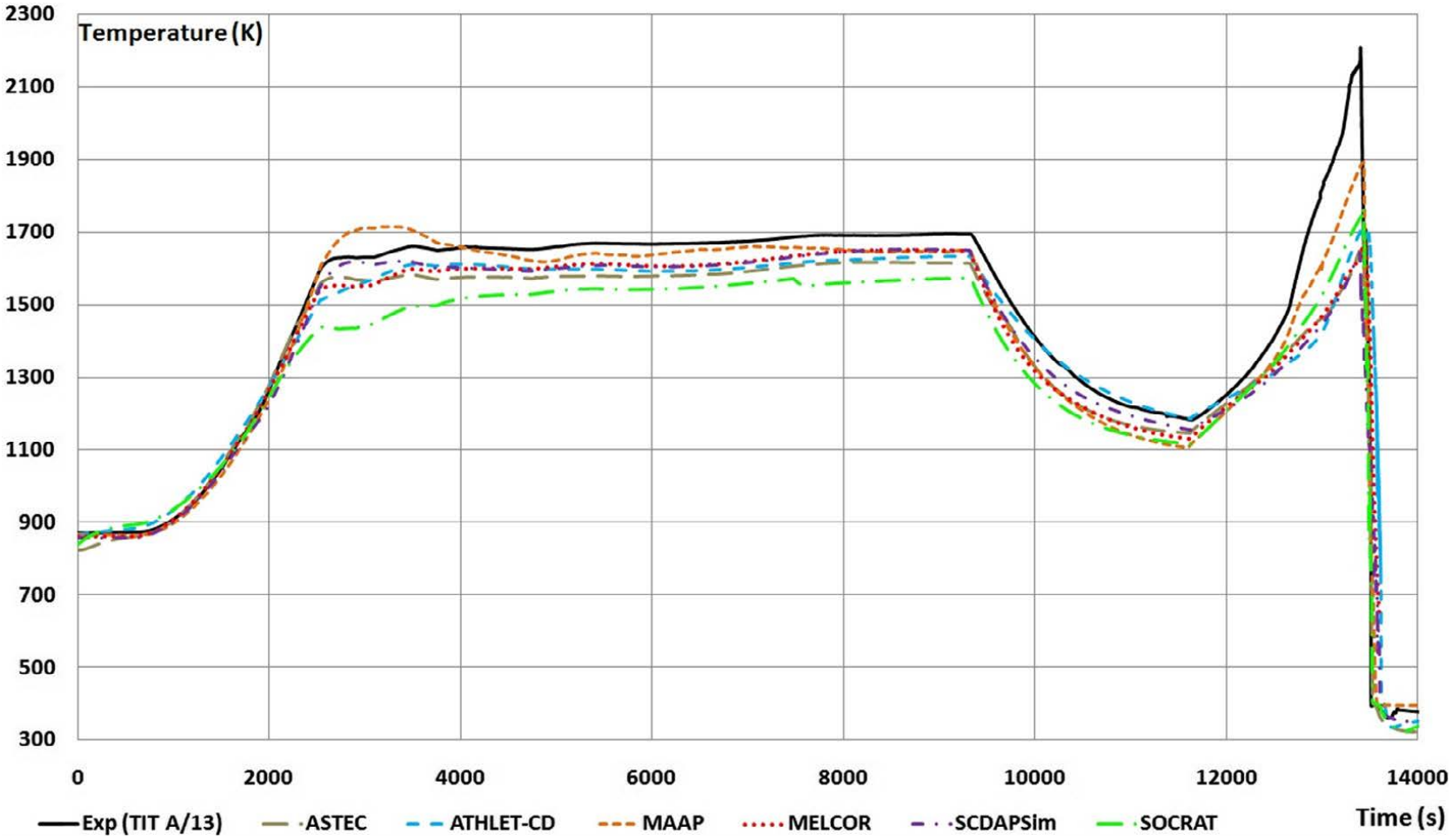
FZKA 7368

SARNET Benchmark: QUENCH-11 – Main findings (FZKA 7368) –

- The development of the water level and the axial temperature and oxide profiles gave %an important insight of the performance of the calculation. The increased importance of thermal-hydraulic aspects with respect to other QUENCH tests also implied larger efforts than for previous tests even for those participants who are acquainted with this experimental program.
- Larger discrepancies are seen in the hydrogen production and the related oxide scale thickness. They can partly be attributed to less experienced users as it is well-known from other benchmarks that the skill of the code user to model a test and his understanding of the code plays an important role for the quality of the results. Experimental uncertainties and inherent limitations of the codes add to the differences in the results.
- A comparison with other experiments not outlined in this report generally shows a further demand for an improvement concerning oxidation of severe damaged structures during a reflood scenario.
- Having in mind the inherent limitations of severe accident codes to simulate complex tests like QUENCH-11, as well as the experimental uncertainties, the limited bandwidth of calculated mainstream results, including hydrogen is a good outcome of the code benchmark.

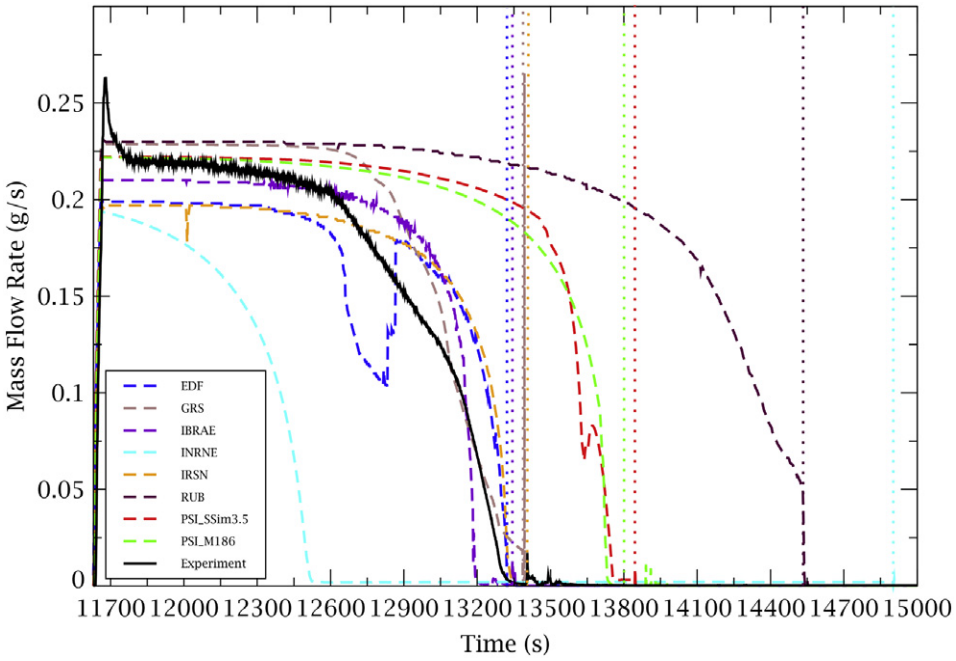
SARNET Benchmark: QUENCH-10/-16
– Results of QUENCH-10 –

- Cladding temperatures at 950 mm

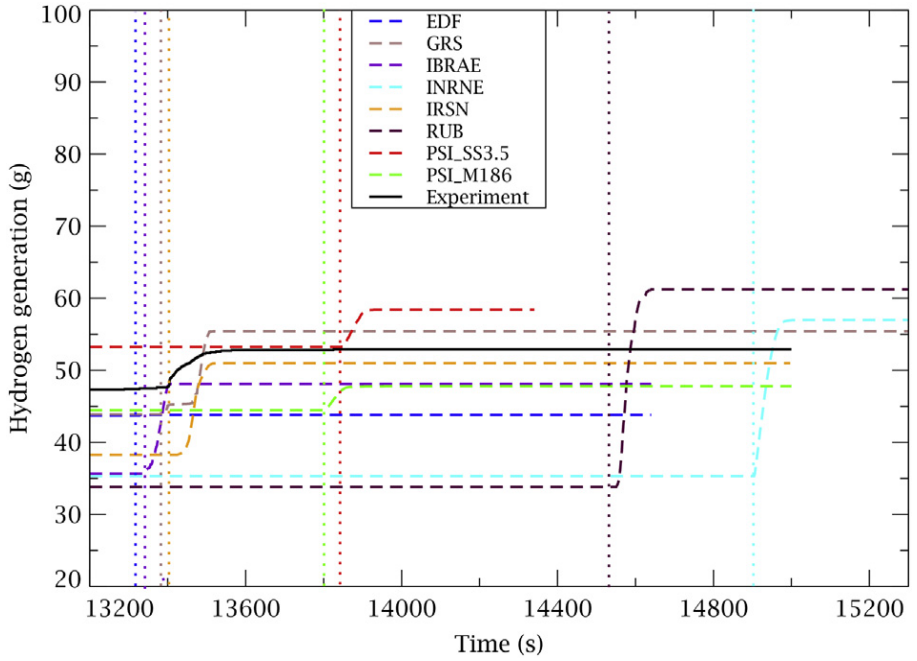


SARNET Benchmark: QUENCH-10/-16
– Results of QUENCH-10 –

- Oxygen consumption

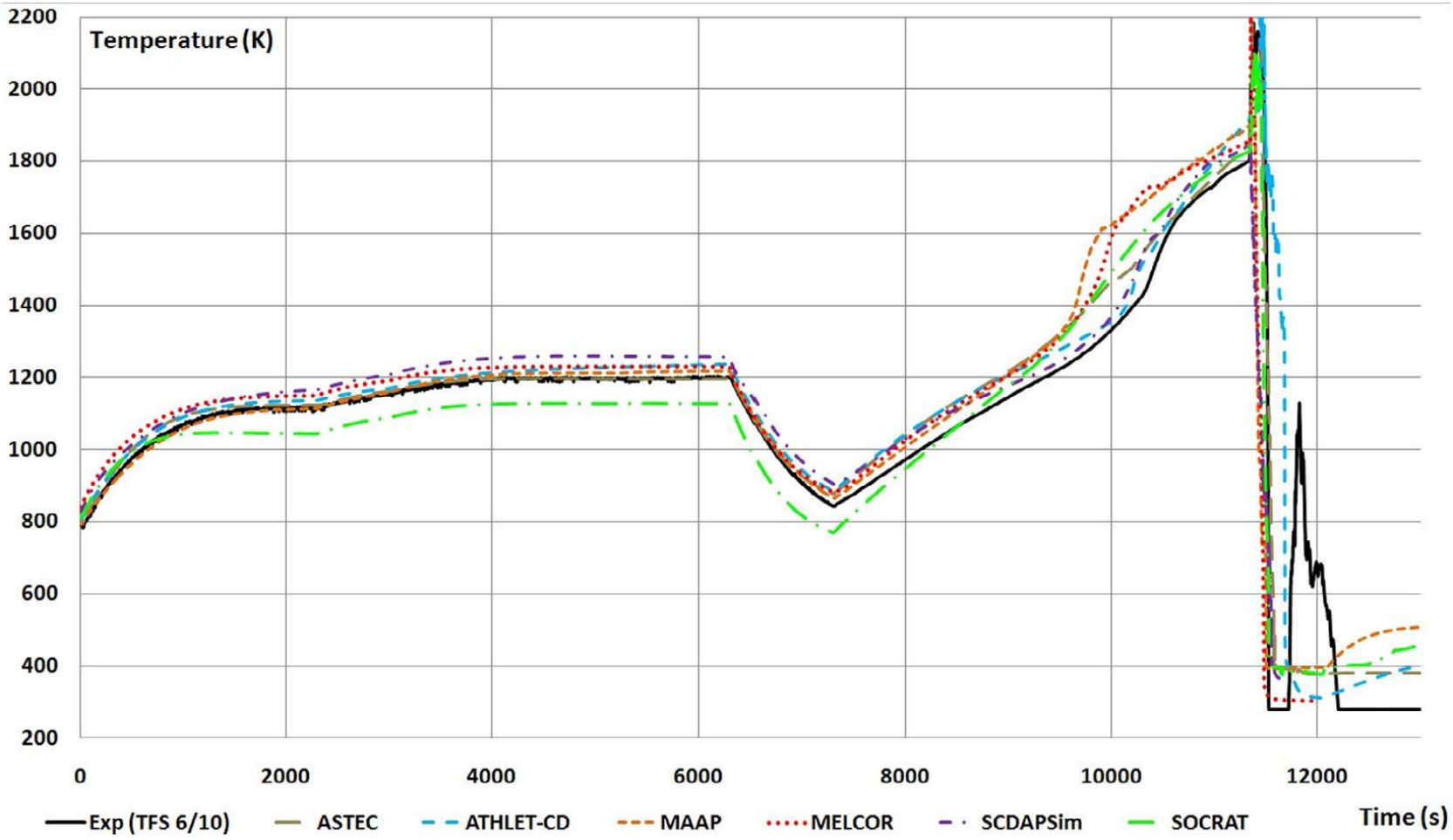


Hydrogen generation during reflood



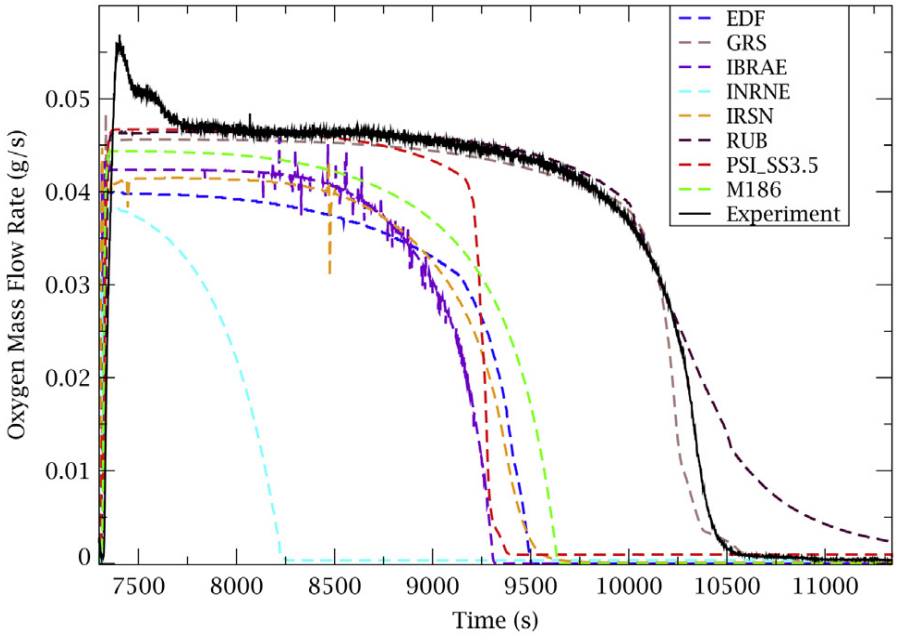
SARNET Benchmark: QUENCH-10/-16
– Results of QUENCH-16 –

- Cladding temperatures at 650 mm

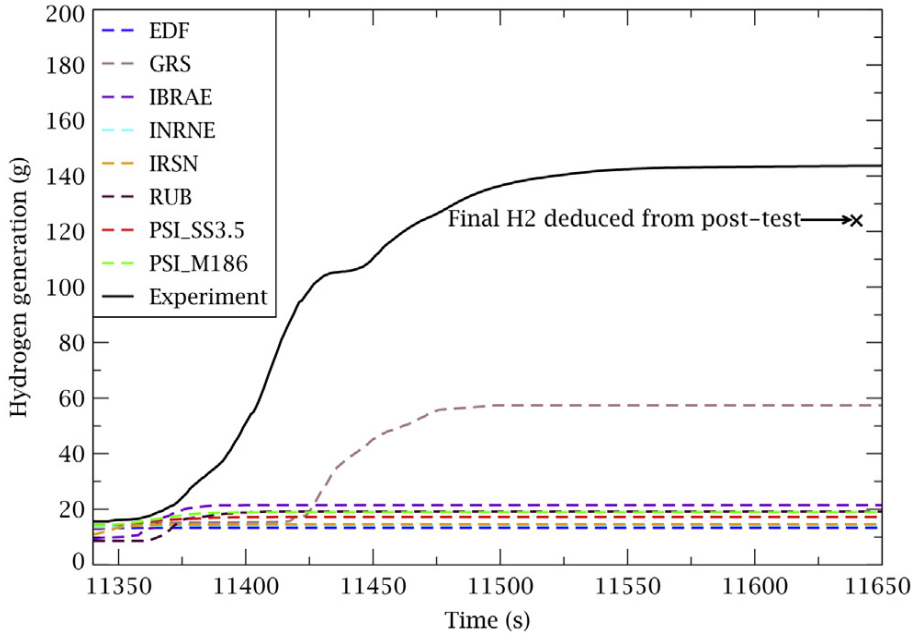


SARNET Benchmark: QUENCH-10/-16
– Results of QUENCH-16 –

- Oxygen consumption



Hydrogen generation during reflood



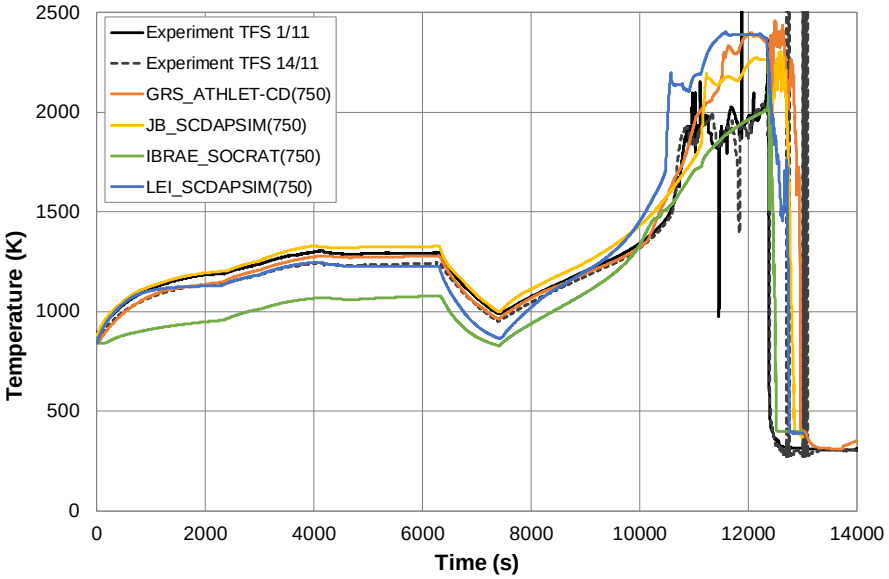
SARNET Benchmark: QUENCH-10/-16
Main findings

- The adoption of identical input models for the two experiments whose conduct were qualitatively similar but quantitatively very different presented a stiff test to the codes and constituent models.
- Taking these points into account, the simulations reproduced the experimentally observed phenomenology except:
  - The oxygen starvation in Q-10, whose occurrence was somewhat marginal and may have been affected by the idealized boundary conditions, especially the constant power during the air ingress phase, was reproduced by 5 of the 8 simulations;
  - The strong reflood excursion in QUENCH-16 which was reproduced by only one simulation (ATHLET-CD)
  - The nitriding which was reproducible only with codes that included a model for the zirconium-nitrogen reaction (ICARE/CATHARE and ATHLET-CD).
- The air ingress benchmark exercise has provided valuable lessons on the modelling of an air ingress scenario.

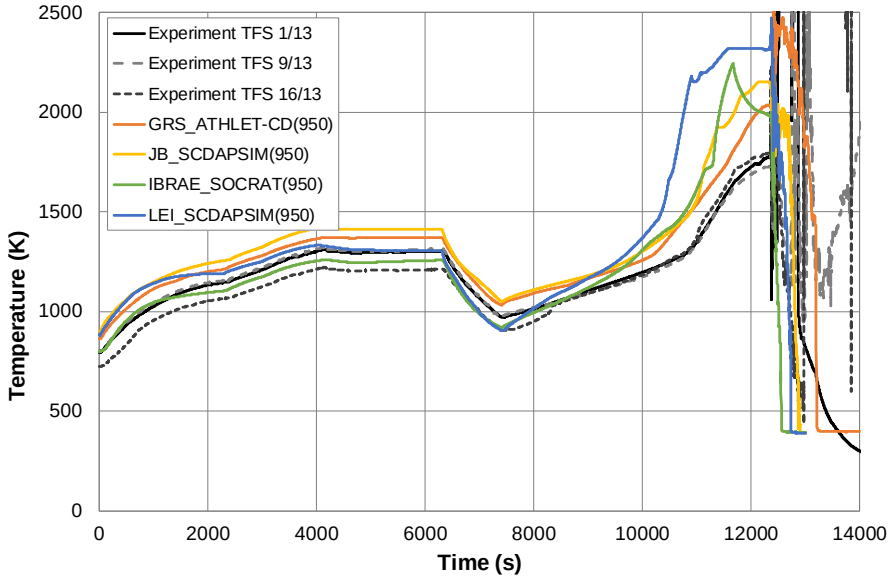
NUGENIA QUESA Benchmark: QUENCH-18 – Results of the Post-Test Benchmark –

- Cladding temperatures

750 mm



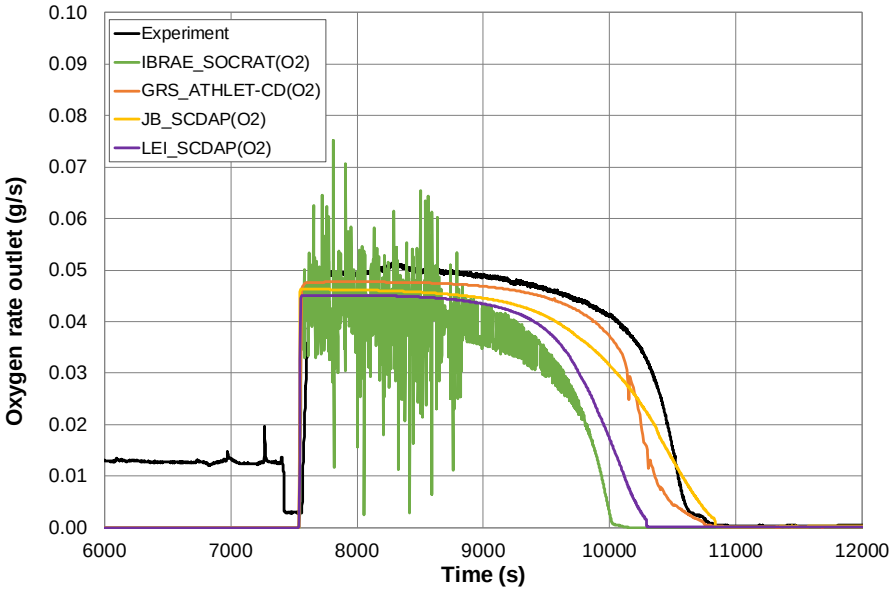
950 mm



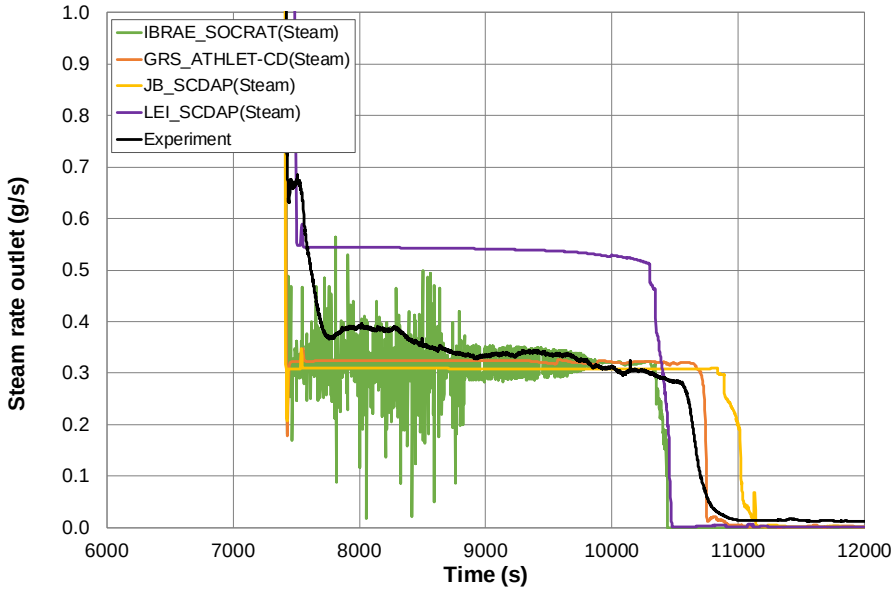
NUGENIA QUESA Benchmark: QUENCH-18 – Results of the Post-Test Benchmark –

- Outlet flow rates

Oxygen



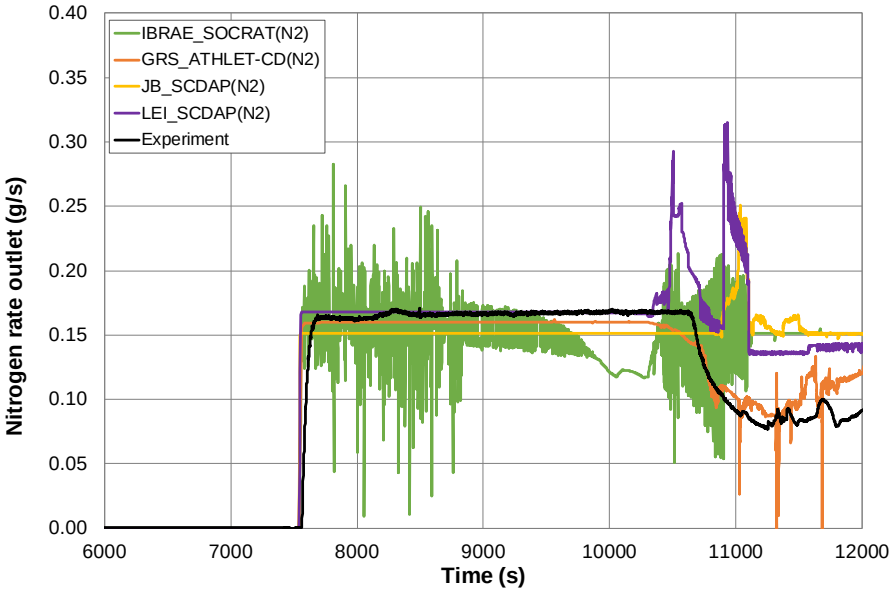
Steam



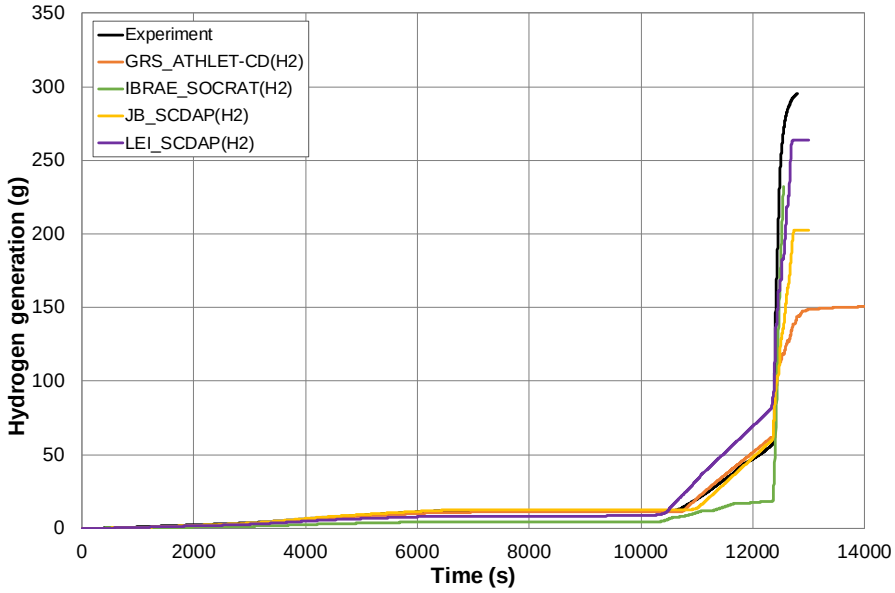
- Complete oxygen starvation in the experiment at 10700 s is also simulated by the codes mostly a bit earlier
- Almost complete steam starvation in the experiment at 11000 s is also predicted by the codes in the range -500 s to +150 s

NUGENIA QUESA Benchmark: QUENCH-18
– Results of the Post-Test Benchmark –

- Nitrogen flow rate outlet



Cumulated Hydrogen Generation



- Nitrogen consumption is only calculated by ATHLET-CD and SOCRAT, but underestimated compared to the experiment
- Hydrogen generation is predicted by all codes during the mixed air/steam phase, but underestimated by all codes during reflooding

NUGENIA QUESA Benchmark: QUENCH-18 – Main findings –

- In general, all codes predict the experimental behaviour for post-test simulations, but already the pre-test calculations are mostly close to each other
- Oxygen and steam starvation is calculated in all simulations
- Lowest elevation of O_2 starvation is much lower for ATHLET-CD (150 mm) compared to SCDAPSim (550/650 mm) and SOCRAT (550 mm)
- Steam and nitrogen consumption in parallel calculated by ATHLET-CD and SOCRAT
- No dedicated nitrogen consumption model for SCDAPSim
- The hydrogen generation or release during quenching is underestimated by all codes
  - Final experimental quantification for each component is necessary to evaluate the simulation results
- The post-test benchmark is still ongoing

QUENCH Tests for Validation and Code Release

- QUENCH tests are used for the validation of severe accident codes, like
  - AC^2 (ATHLET-CD)
  - ASTEC
  - ICARE/CATHARE
  - MAAP
  - MELCOR
  - RELAP/SCDAM(SIM)
  - SOCRAT
  - RATEG/SVECHA
- Each QUENCH severe accident test is at least used for validation by one code
- From QUENCH-03 onwards all test are used for code validation, because a wide field of issues and phenomena is covered by the tests
- The distribution of application is quite uniform, with slightly higher application of ISP-45 and the SARNET Benchmarks
- The codes are applied for QUENCH test by developing institutes and external institutes, which allows also an independent validation

QUENCH Tests for Education and Knowhow Transfer

- QUENCH tests and comparable test series are widely used for beginners in the field of simulation of nuclear systems/plants with respect to severe accident studies or users of new codes:
  - The experiments are well documented
  - The number of phenomena is limited, but complexity exists
  - Experienced users can assist the newcomers based on already existing input decks

- With this experience by application of QUENCH tests beginners and already advanced users are able to perform simulations of more complex systems up to plant simulations

  ➢Learning on a car to be able to drive also a lorry, **not starting with the lorry**!

- The topics of QUENCH tests and corresponding SETs were used for a number of Doctoral Theses, e. g. B_4C oxidation, Air ingress Phenomena….

Conclusion and Outlook

- QUENCH tests are widely used for code validation
- One ISP and four SARNET/NUGENIA Benchmarks on QUENCH tests were conducted
- Several topics are covered which led also to code improvements to be able to perform calculations
- This wide field of topics provides many data for code validation
- Beside the QUENCH tests for severe accident conditions also a series of LOCA tests was performed which was also used for code validation
- The new topics of QUENCH tests considering ATF rods are challenging for the codes, but this will again force model development and validation efforts

- **Hopefully, the data base for code validation will be further enlarged by performing several new QUENCH tests**

Thank you for your attention!

Simulation of QUENCH-17 with ATHLET-CD

Christophe D'Alessandro,

Gesellschaft für Anlagen- und Reaktorsicherheit (GRS) gGmbH, Boltzmannstraße 14, 85748 Garching bei München, Germany, ✉christophe.dalessandro@grs.de, ☎+498932004459

Prediction capabilities of ATHLET-CD, as code within GRS' AC² system code package, concerning the reflooding of a hot debris bed in the core region was previously assessed back in 2013 by simulating QUENCH-17 performed by KIT. In ATHLET-CD, the specific issue of two-phase flow in porous media is addressed by the module MEWA, developed by IKE at the University of Stuttgart. Since ATHLET-CD has been further improved between versions v2.2c (in 2013) and v3.2 (current version), but MEWA was not changed, the coupling of MEWA with ATHLET-CD must be verified anew.

The QUENCH-17 test investigated a bundle of 21 rods: 9 central unheated rods, with a Zry cladding, and 12 outer rods electrically heated, with a Hafnium cladding. Pellets with preformed debris were embedded in the unheated rods. The rods were placed within a shroud of Hafnium. The test started with a pre-heating phase, followed by a pre-oxidation phase by injecting steam from the bottom. Once the oxidation was completed, rod power was increased to start a transient phase, where debris was released from the failed rods and formed a debris bed on the middle space grid. At the end of the transient phase, cold water was injected from the bottom in order to reflood and cool down the oxidized rods and the debris bed.

The current simulation with ATHLET-CD v3.2 is based on the same input as the one used for the previous simulation with ATHLET-CD v2.2c. The QUENCH-17 bundle was discretized into three representative rings: the two inner rings containing the unheated rods and the outer ring containing the heated rods. Spacer grids were also simulated. Oxidation is calculated based on Cathcart's correlation. MEWA is only activated at the end of the simulation, as the debris bed is first formed at the end of the transient phase (MEWA initiation time has been defined according to the experimental outcomes).

The pre-oxidation phase is quite well reproduced and in good agreement with the experiment and the previous simulation. Hydrogen production and oxide layer thickness are comparable to those computed with ATHLET-CD v2.2c. However, the new results show a significant overestimation of cladding temperature prior to reflooding. This can be explained as cladding rupture of the heated and unheated rods is predicted at that time, leading to oxidation of the inner surface of the cladding. Previously, no rupture of the Hafnium cladding was calculated. Simulation of the quenching of the debris bed couldn't be carried out since the current coupling between MEWA and ATHLET-CD v3.2 leads to strong instabilities so that the calculation crashes approximately 150 s after MEWA initiation. It is worth mentioning that the flow through the bed is still one phase at that time. This problem must be solved jointly with MEWA developers, in order to evaluate properly the capabilities of MEWA as part of ATHLET-CD, regarding simulations of reflooding of porous media.



SIMULATION OF QUENCH-17 WITH ATHLET-CD

Christophe D‘Alessandro

Gesellschaft für Anlagen- und Reaktorsicherheit (GRS) gGmbH, Germany

25th International QUENCH Workshop

KIT, Karlsruhe
22-24.10.2019

Content

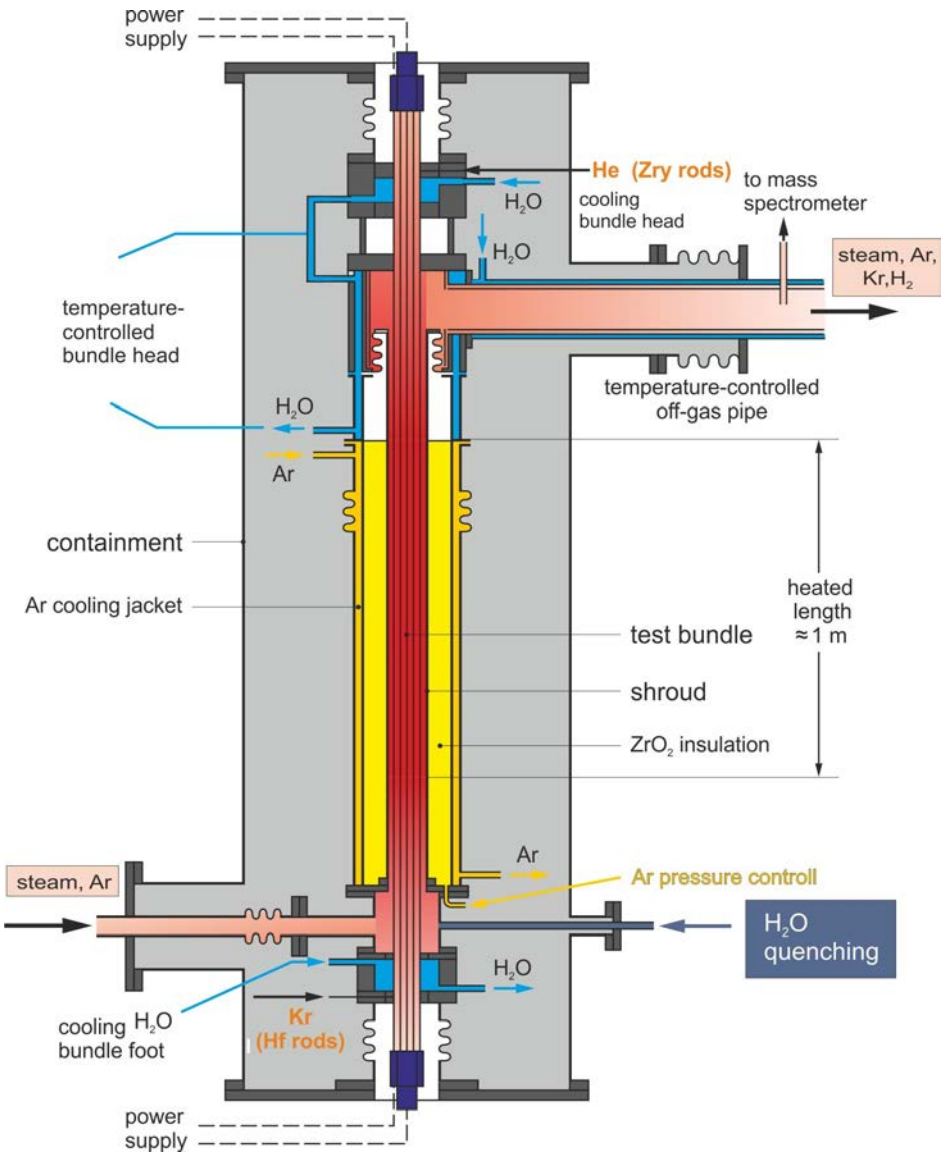
- QUENCH-17 test
  - Facility
  - Test conduct
- QUENCH-17 simulation with ATHLET-CD
  - Nodalization
  - Debris bed modelling
- Post-test simulation (without MEWA)
- Post-test simulation (with MEWA)
- Conclusion, comments and outlook

Motivation

- Validation of current version ATHLET-CD 3.2 as part of AC^2
- Regarding the coupling with MEWA module
  - Module developed by IKE, University of Stuttgart
  - Coolability of particle bed
- Last validation of MEWA, with ATHLET-CD 2.2c (in 2013)

QUENCH-17 test : Facility

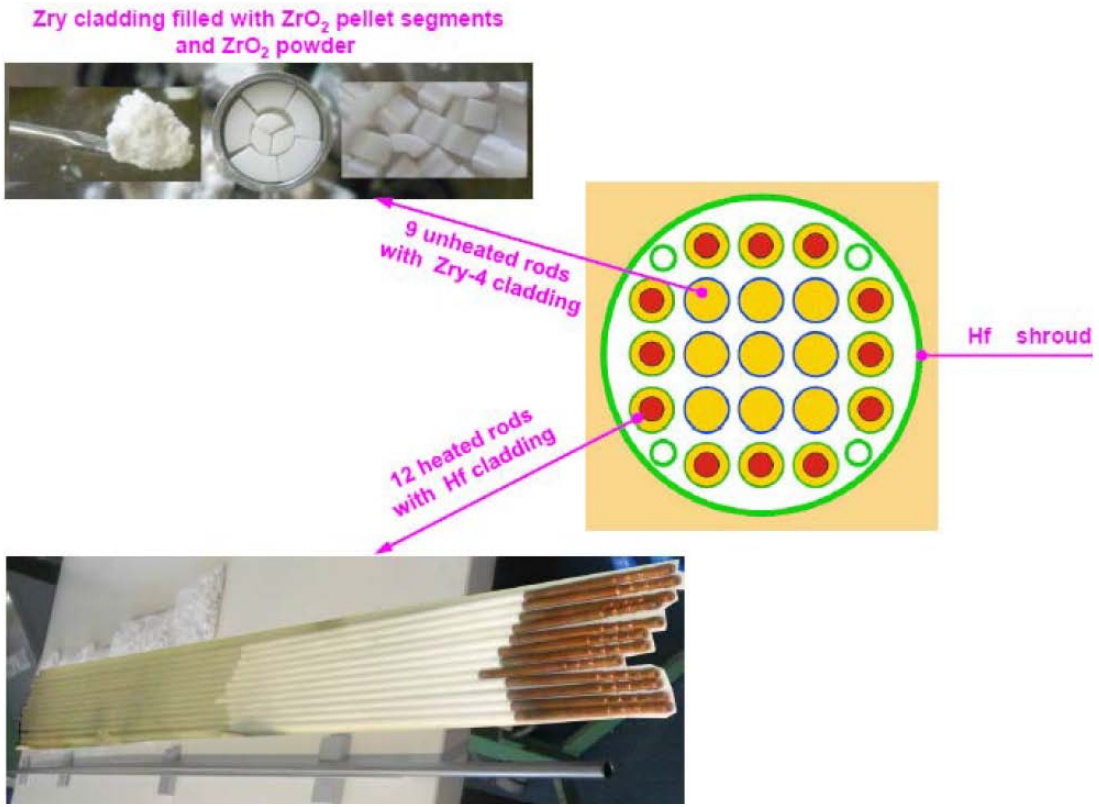
- Performed by KIT in January 2013
- Test purpose:
  - Debris bed formation inside a completely oxidized bundle region
  - Coolability during reflooding
- Test bundle:
  - 9 unheated inner rods (Zry-4 cladding)
  - 12 heated outer rods (Hf cladding)
  - 4 corner rods with thermocouples (Hf cladding)
- Debris bed formation:
  - Inner rods filled with pre-fragmented Zirconia pellets
  - Pre-oxidation to produce complete oxidation of Zry-4 cladding within 0.5m
  - Collapse of oxidized region before/at the start of the reflooding



J. Stuckert et al.: Results of the QUENCH-DEBRIS (QUENCH-17) test with strongly oxidized Zircaloy-4 and hafnium claddings filled with segmented pellet simulators, NUSAFE 3572 , 2018, KIT

QUENCH-17 test : Facility

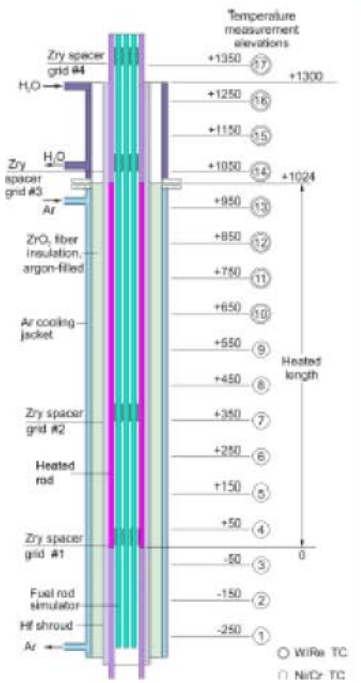
- Performed by KIT in January 2013
- Test purpose:
  - Debris bed formation inside a completely oxidized bundle region
  - Coolability during reflooding
- Test bundle:
  - 9 unheated inner rods (Zry-4 cladding)
  - 12 heated outer rods (Hf cladding)
  - 4 corner rods with thermocouples (Hf cladding)
- Debris bed formation:
  - Inner rods filled with pre-fragmented Zirconia pellets
  - Pre-oxidation to produce complete oxidation of Zry-4 cladding within 0.5m
  - Collapse of oxidized region before/at the start of the reflooding

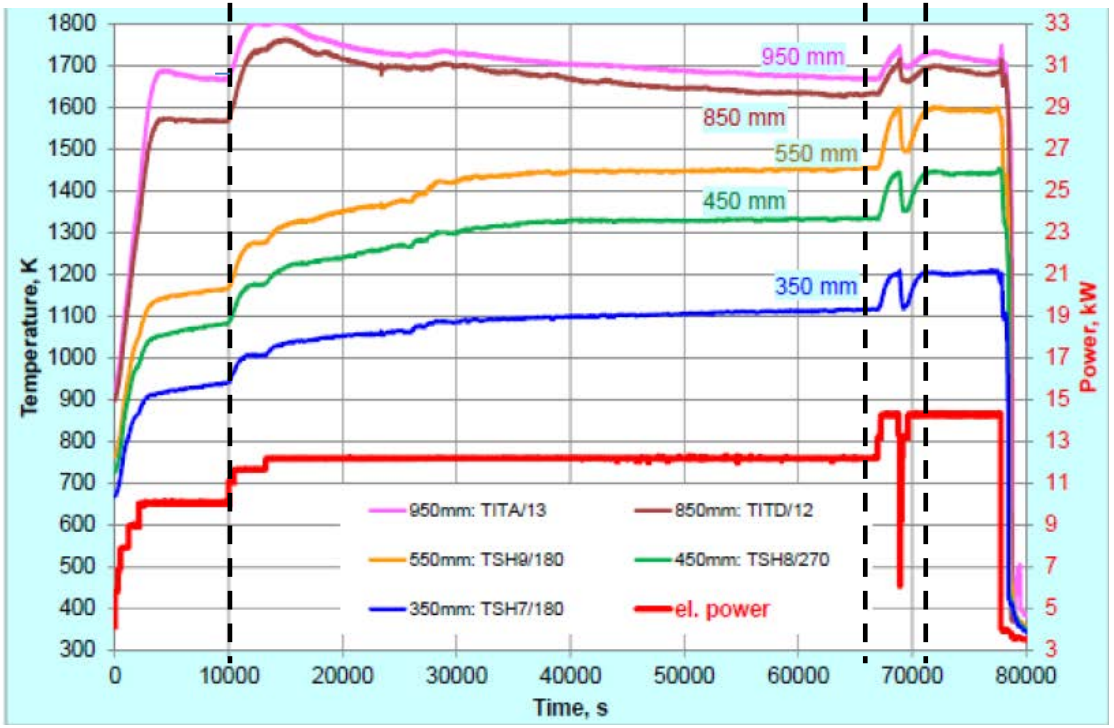


J. Stuckert: Status of the preparation of the Quench-Debris experiment, 18th IQWS, Nov.2012, KIT

QUENCH-17 test : Test conduct

J. Stuckert: Conduct and first results of the QUENCH-17 experiment, Feb.2013, KIT



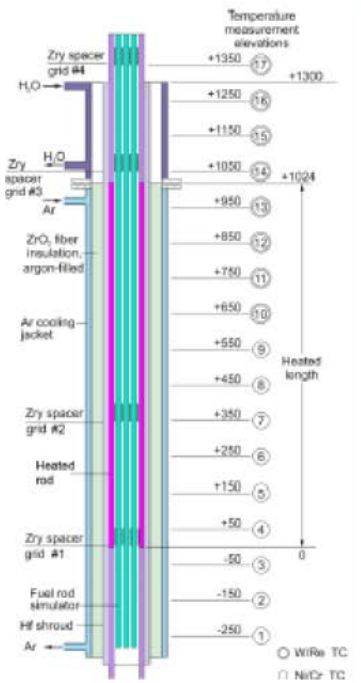


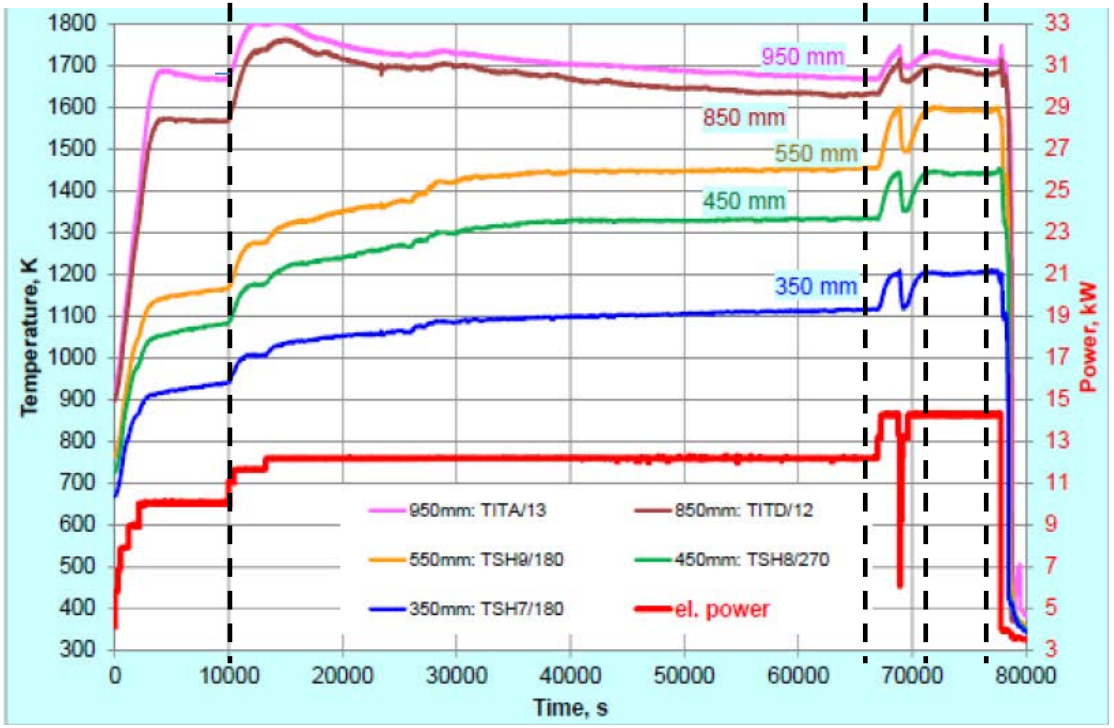
Oxidation:

- Stepwise increase of electrical power to 10 kW heats the bundle to a max. temperature of ~1700 K
- After 10000 s: stepwise increase to 12 kW to reach a max. temperature of 1800 K
- After 64000 s: increase to 14 kW
- End of oxidation at 72000s: devices show complete oxidation at 650 mm elevation

QUENCH-17 test : Test conduct

J. Stuckert: Conduct and first results of the QUENCH-17 experiment, Feb.2013, KIT





Debris bed formation:

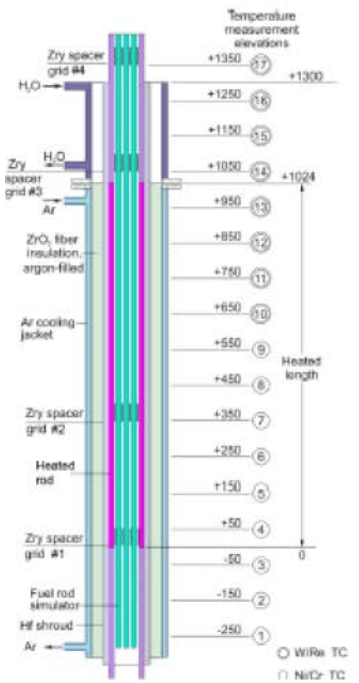
- Collapse of surviving Zry-4 claddings by application of an axial mechanical force
- Material relocation → formation of a heterogeneous debris bed at middle grid spacers (confirmed by response of fluid thermocouples)

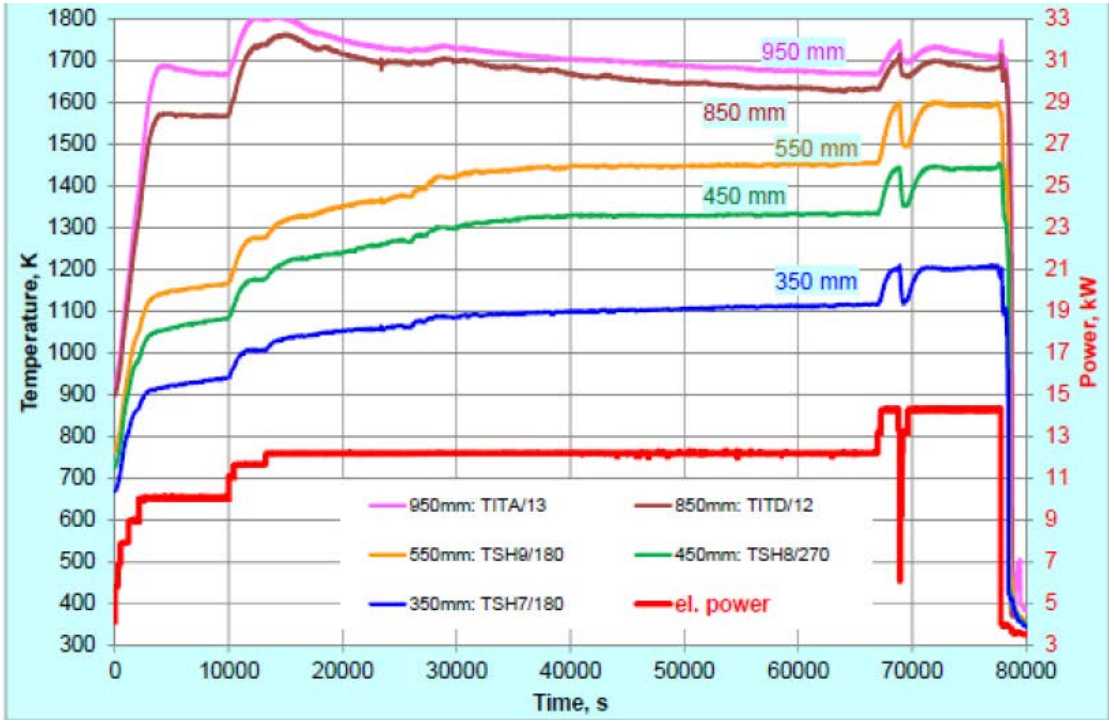
Reflooding:

- 77773 s: start of water injection with 10g/s, power reduction to 4 kW
- Steam and Argon flow at the bottom stopped
- Argon injection from the top

QUENCH-17 test : Test conduct

J. Stuckert: Conduct and first results of the QUENCH-17 experiment, Feb.2013, KIT





Debris bed cooling:

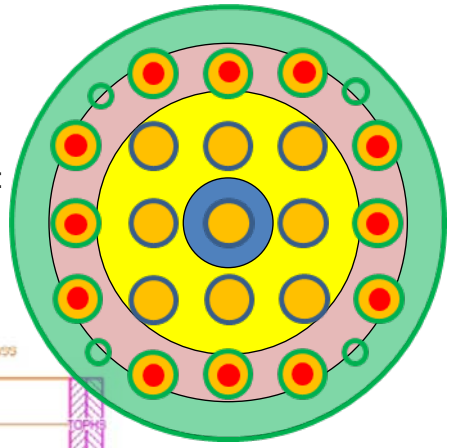
- After 78200 s: temperature reduction of debris + quenching of rods at bottom of bundle
- Steady progression of Quench Front up to debris region, then constant evaporation rate due to water ingression in the debris bed → slower Quench Front progression
- 78720 s: water level stagnation at 850 mm elevation due to shroud failure

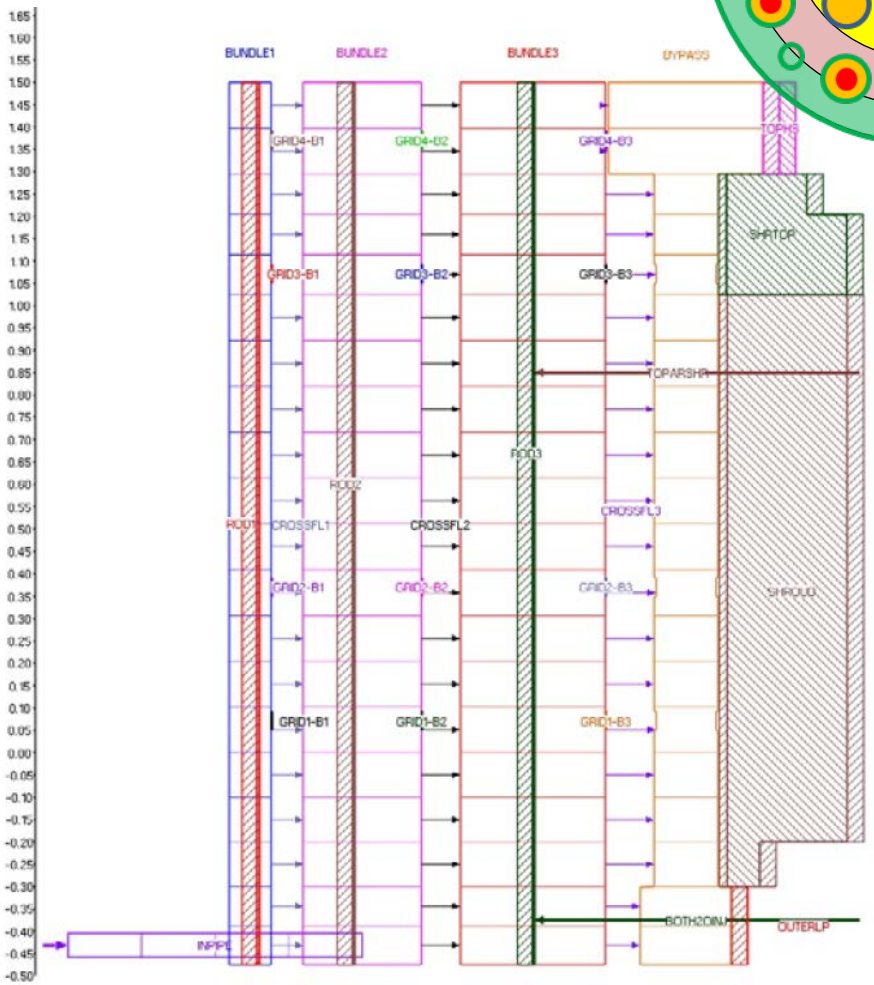
QUENCH-17 simulation with ATHLET-CD

Nodalization:

- BUNDLE1 with ROD1
  - → Inner unheated rod (Zry)
- BUNDLE2 with ROD2
  - → Inner unheated ring (Zry)
  - → 8 rods
- BUNDLE3 with ROD3
  - → Outer heated ring (Hf)
  - → 12 rods
- BYPASS
  - → Outer bundle region
- CROSSFL1,2,3
  - → Cross connections
- 4 GRIDS in each bundle region
- Active fill BOTH2INJ
  - → Water cooling
- INPIPE/OFFPIPE
  - → inlet/oulet pipes

Top view of **BUNDLE1, 2, 3 and BYPASS**:





QUENCH-17 simulation with ATHLET-CD

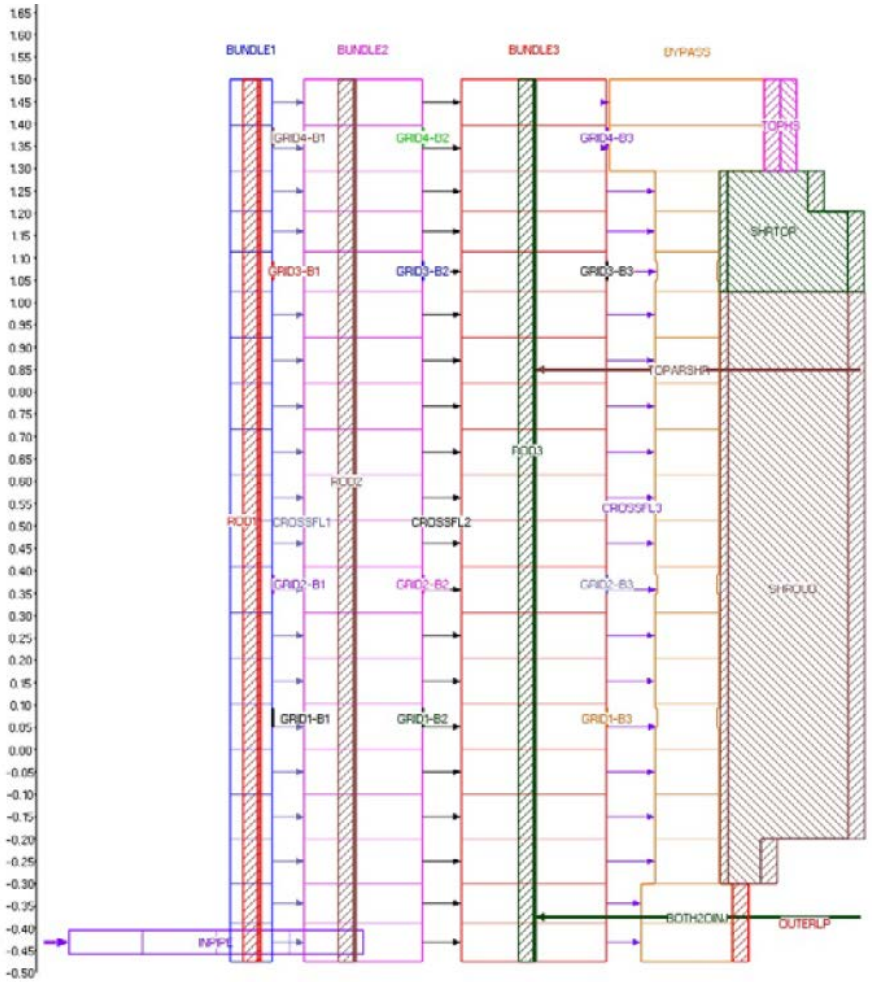
Oxidation models:

- 1273 - 1800 K: Cathcart
- 1800 - 2600 K: transition range
- 2600 - 2673 K: Prater/Courtright

- Hafnium oxidation:
  - ATHLET-CD 3.2 with material properties for Hf/HfO2 and Hf oxidation kinetics (as given by KIT)
  - These features were also applied into ATHLET-CD 2.2c for the previous post-test calculations

Initial / boundary conditions:

- Pressure = 2.1 bar
- Initial gas temperature = 600 K
- Water temperature= 23°C (296 K)

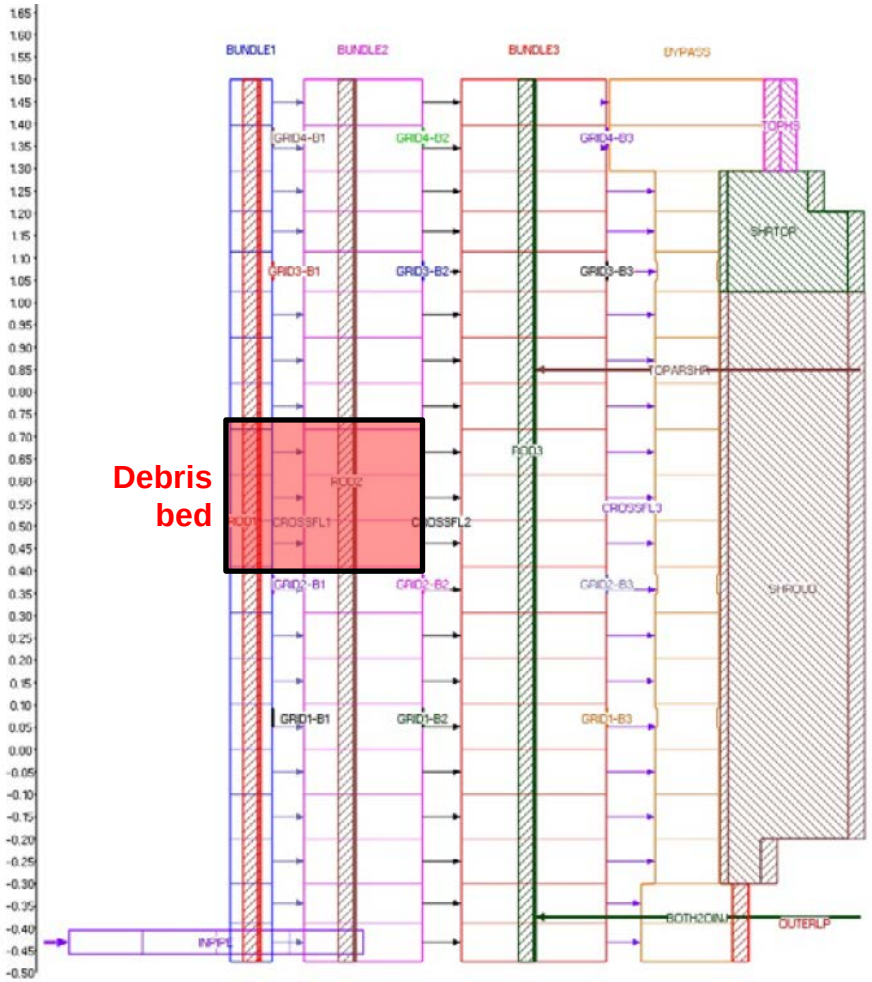


QUENCH-17 simulation with ATHLET-CD

Debris bed modelling:

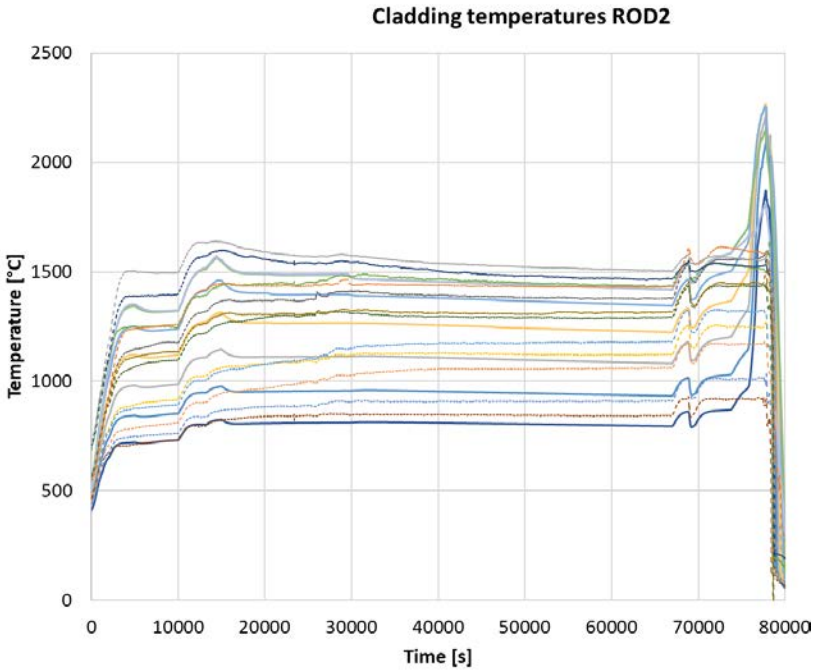
- MEWA module:
  - 2-phase flow in porous media
  - ATHLET-CD differential eq. model switched off
  - And replaced MEWA 6-eq. model
  - Coupling MEWA/ATHLET-CD as boundary conditions

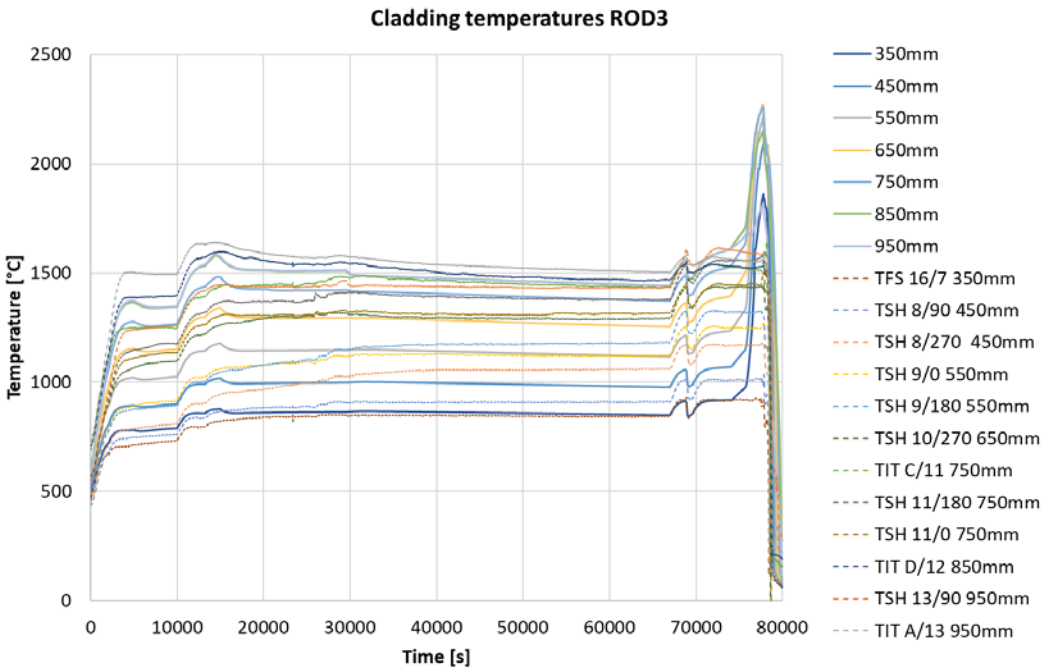
- Start: 77500 / 77800 s (~reflooding start)
- Position:
  - Radial: BUNDLE1 and 2
  - Axial: from 0.392 to 0.77 m
- Particle diameter: 3.5 / 5 mm



Post-test simulation without application of MEWA - Results

Rod cladding temperatures

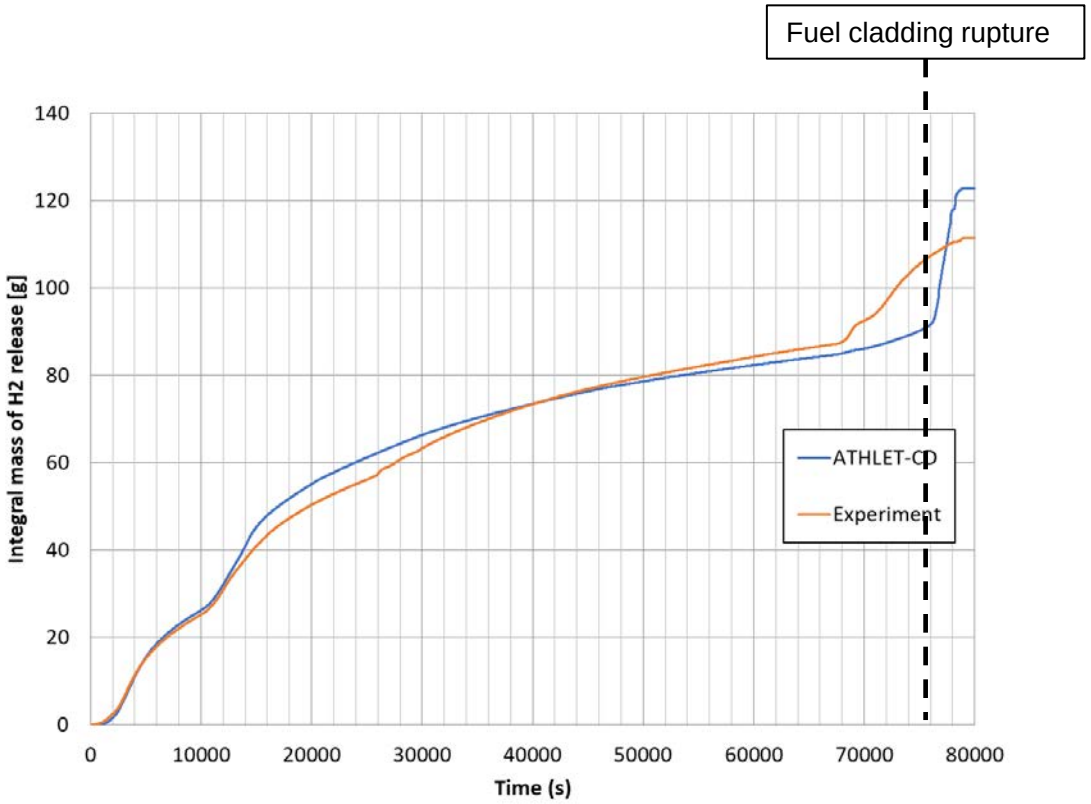




- Until ~76000 s: same trend than in experiment.
- Pre-oxidation phase:
  - 350 – 850 mm: ~850°C – ~1450°C, agrees with exp.
  - 950 mm: ~1450°C, underestimation (in exp.: ~1550°C)
- Significant temperature increase before start of reflooding

Post-test simulation without application of MEWA - Results

Hydrogen generation



- Good agreement during heat up and pre-oxidation (until ~67000 s)
- The increase of hydrogen generation rate after the power increase and before start of reflooding (until 77800 s) is underestimated

→ Similar to the previous calculation with ATHLET-CD 2.2c

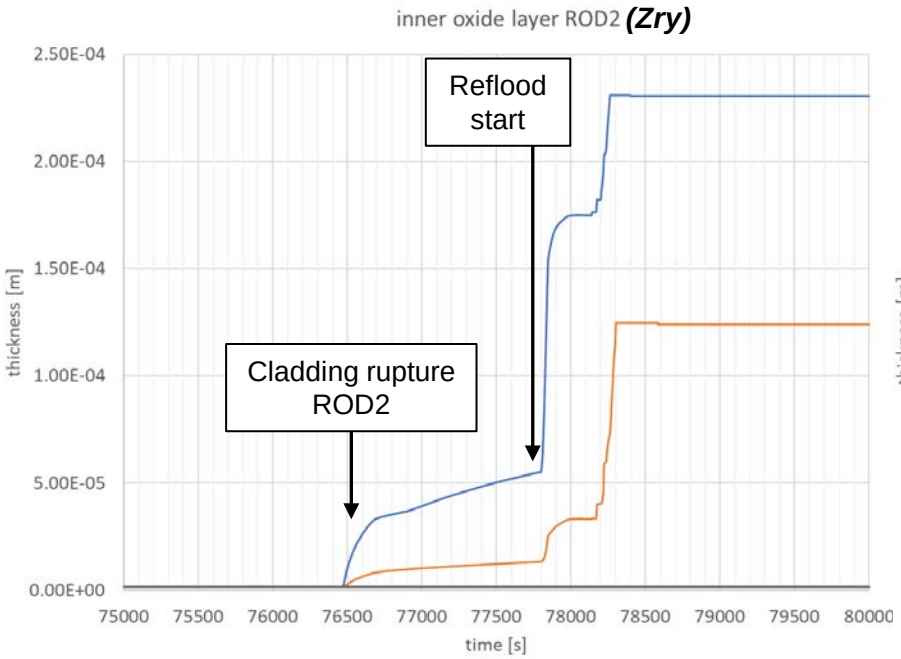
- After starting water injection, hydrogen generation is strongly overestimated

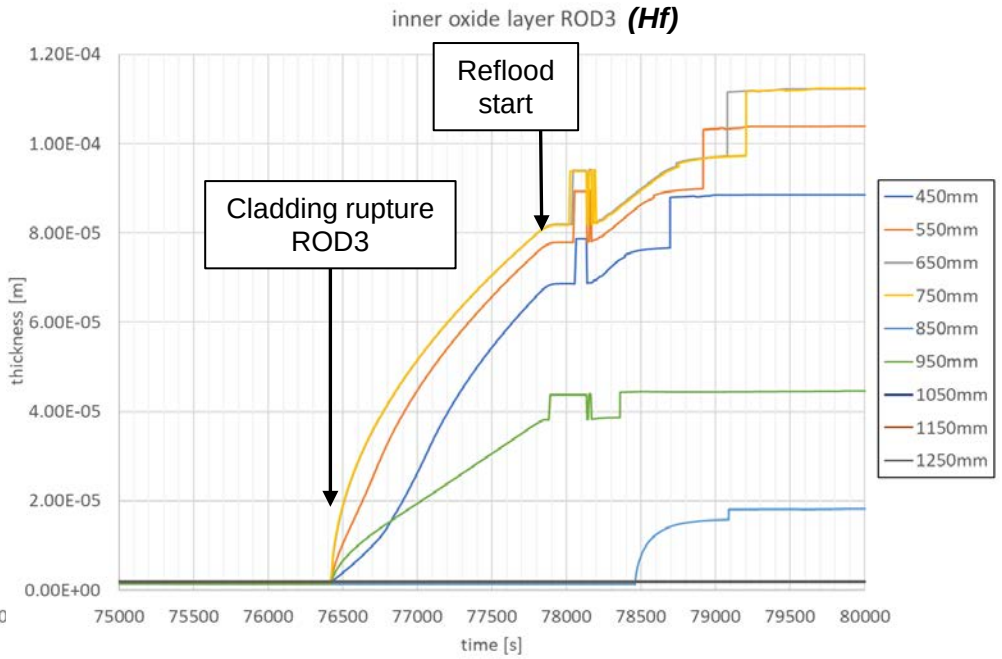
→ due to cladding ruptures at 76420 s (ROD3), 76473 s (ROD2) and 76478 s (ROD1)

→ Inner cladding oxidation

Post-test simulation without application of MEWA - Results

Inner oxide layer of cladding

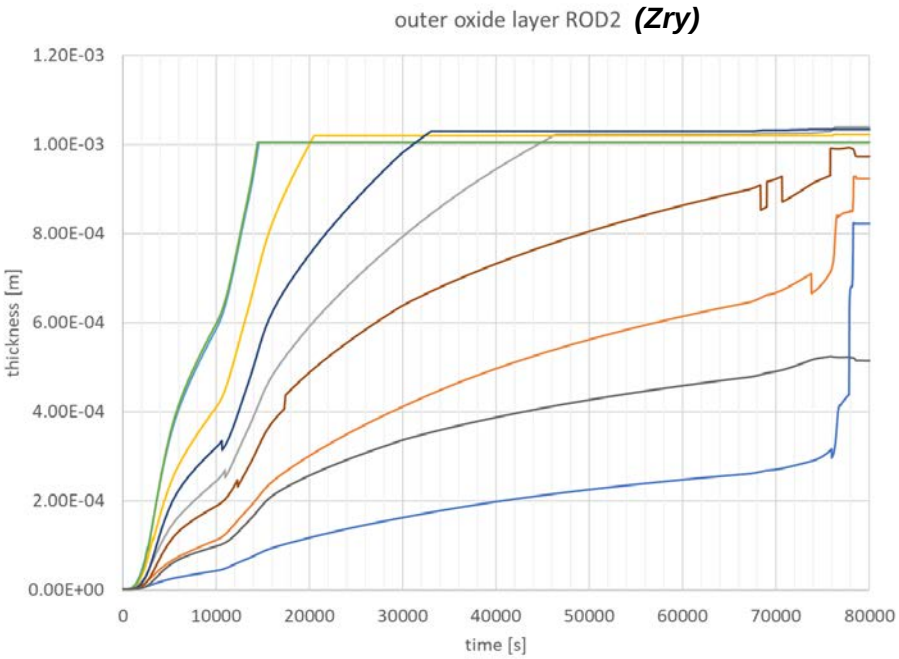


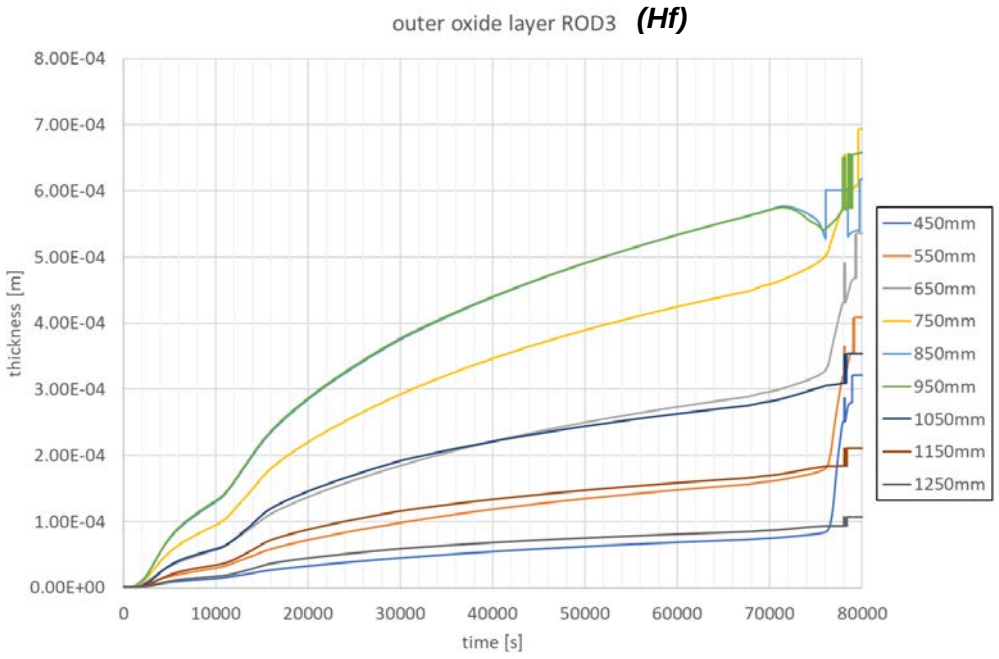


- Exponential then linear growth after cladding rupture
- ROD2:
  - Second growth at water injection start
  - Highest values ~230 µm at z = 450 mm (previous calc.: ~100 µm at z = 850/950mm)
- ROD3:
  - Highest values ~110 µm at z = 650/750 mm (previous calc.: no oxidation)

Post-test simulation without application of MEWA - Results

Outer oxide layer of cladding

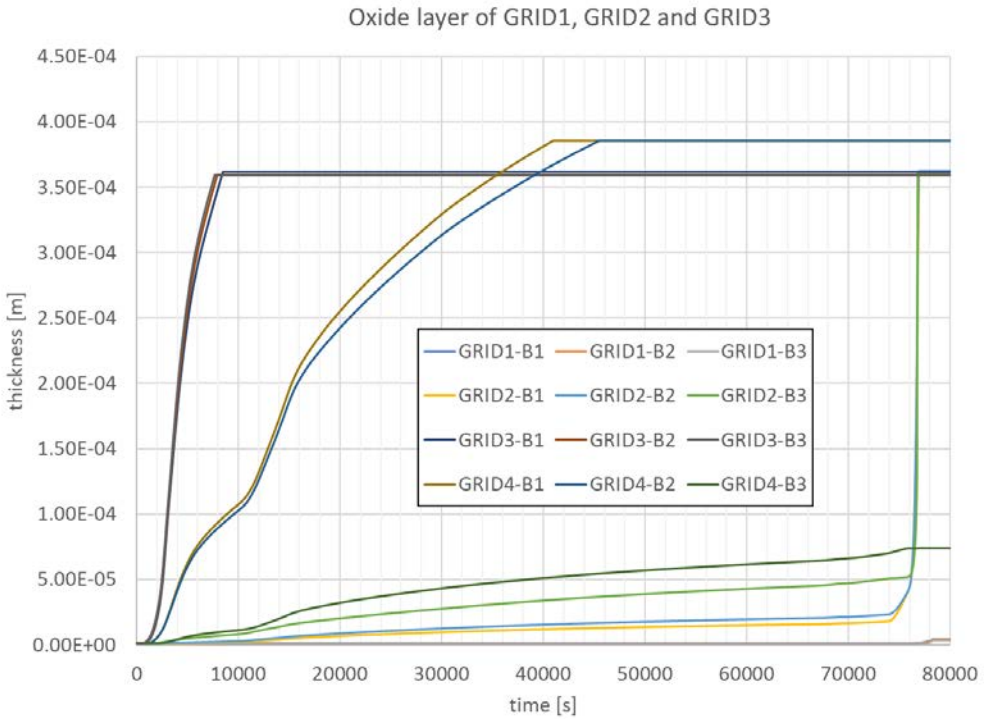




- ROD2:
  - Complete oxidation of Zry cladding was reached at z= 650 mm after 46000s (in exp.: after 72000s; previous calc: 56000s)
  - Unlike in exp. and previous calc., not completely oxidized at z = 1150mm after 78000s. But at 1050mm completely oxidized after 33000 s like in previous calc.
- ROD3:
  - Max. oxide layer thickness for Hf cladding low compared to that of Zry
  - No complete oxidation

Post-test simulation without application of MEWA - Results

Oxide layer of grids



- GRID3 and GRID4 are totally oxidized after 50000 s
- Same results as the previous calculation with ATHLET-CD 2.2c
- Agrees with first results from experiments where grid spacer 4 was completely oxidized after the test

Post-test simulation with MEWA - Results

Start of MEWA

- Start = 77800 s
- Coupling of MEWA with ATHLET-CD at debris bed boundaries

→ Strong instabilities

→ Time step reduced to $\sim 10^{-10}$

Simulation finally fails at 77965 s (165 s after MEWA start)

Conclusion, comments and outlook

- Pre-oxidation phase well reproduced
- Inner oxidation of Hafnium cladding seems to lead to an overestimation of Hydrogen generation
- Instabilities by coupling MEWA with the current ATHLET-CD 3.2

→ Need for further development with support from IKE, University of Stuttgart

Thank you for your attention!

Supported by:



Federal Ministry
for Economic Affairs
and Energy

on the basis of a decision
by the German Bundestag

Comparative Analysis of simulations of the air ingress experiments QUENCH-16 and QUENCH-18 using AC² - ATHLET-CD

25th International QUENCH Workshop, October 2019, Karlsruhe

Florian Krist and Marco K. Koch

Plant Simulation and Safety Group (PSS),
Ruhr-Universität Bochum (RUB)
florian.krist@pss.rub.de, marco.koch@pss.rub.de
ORCID-ID: 0000-0002-4089-5801, 0000-0001-7260-5250

As part of the research project “External Validation and Analysis of Selected Models of the Accident Analysis Codes ASTEC, ATHLET and ATHLET-CD” post-test calculations of the air ingress experiments QUENCH-16 and QUENCH-18 are conducted in order to further validate and analyse the air ingress as well as the oxidation model basis. The simulations are performed with the severe accident analysis code AC² - ATHLET-CD (Analysis of Thermal-Hydraulic of Leaks and Transients – Core Degradation), developed by GRS. ATHLET-CD is able to perform simulations of thermal-hydraulic processes during an incident with core degradation.

The investigated experiments were performed at the QUENCH test facility by KIT. In both bundle tests conditions of loss of cooling accidents in light water reactors with re-flooding are reproduced in order to analyse the bundle behaviour during the air ingress and the re-flooding with water. Distinctive features can be found in the bundle set-up and in the conduct of the tests. In contrast to QUENCH-16, where the steam flow through the bundle is switched off during the air ingress stage, in QUENCH-18 the test section is in a mixed air/steam atmosphere from the beginning of the air ingress.

The analysis of the simulation results examines in particular the code’s capability to represent the thermal behaviour of the fuel and absorber rods as well as the oxidation behaviour in the air or air/steam atmosphere respectively. To assess the code’s development progress comparative calculations using ATHLET-CD 3.1A in patch version 4 and 5 are conducted. The simulated temperature evolutions are overall in good accordance with the experimental data. Especially the thermal behaviour during the experimental period before the air ingress stage are reproduced well. The nitrogen behaviour is significantly better reproduced in the runs with patch 5. Further, the reproduction of the hydrogen release during reflooding shows clear improvements in the updated version. However, the simulated oxygen mass flow rates show potential in refining the reaction kinetics. In both patch version 4 and 5 the oxygen consumption is calculated too early and thus an overestimation of the zirconium oxidation.

Supported by:



on the basis of a decision
by the German Bundestag

This work was funded by the German Federal Ministry of Economic Affairs and Energy under grant number 1501522 on the basis of a decision by the German Bundestag.

The simulations were performed with the code version ATHLET-CD 3.1A Patch 4 and 5 developed by GRS.


Technologie



RUB

RUHR-UNIVERSITÄT BOCHUM

Comparative Analysis of simulations of the air ingress experiments QUENCH-16 and QUENCH-18 using AC² - ATHLET-CD

Florian Krist and Marco K. Koch

25th International QUENCH Workshop, Karlsruhe

Tuesday, 22th October 2019

PSS Plant Simulation and Safety
Prof. Dr.-Ing. Marco K. Koch

Content

- Introduction
- Experimental Setup
- Modelling approach
- Simulation Results
- Conclusion

Introduction

The QUENCH testing programme

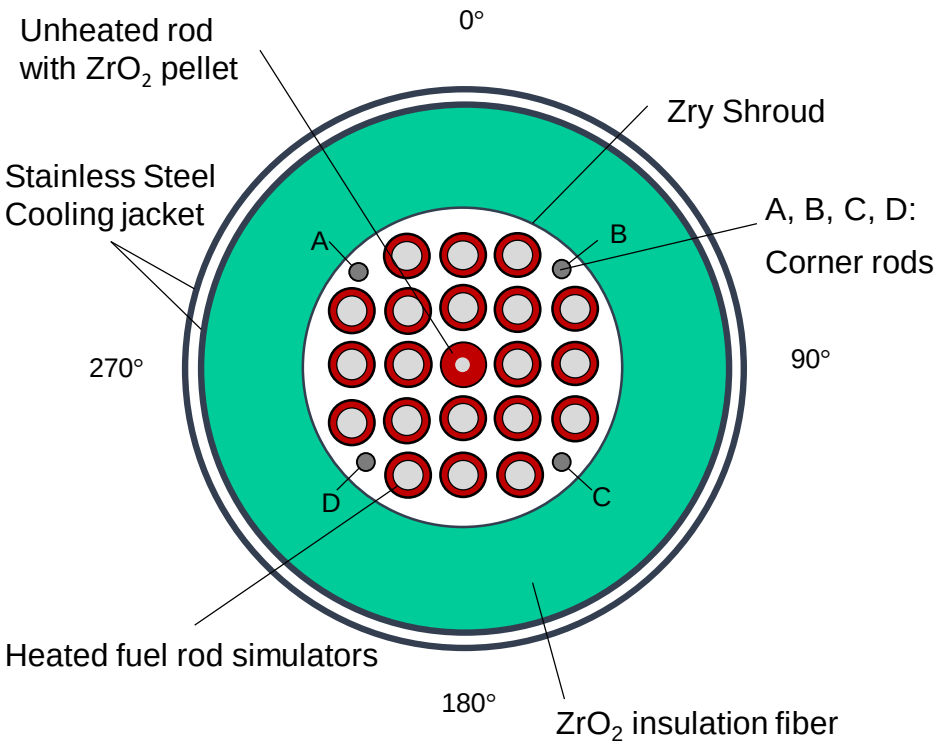
Test	Quench medium & flooding rate	Temp. at onset of flooding*	Max. ZrO_2 layer thickness	Remarks, objectives	Date of test conduct
16	Water 53 g/s	≈ 1.870 K	135 µm	LACOMECO Project air ingress	27.07.11
18	Water 53 g/s	≈ 1.950 K	completely oxidized	ALISA Project air ingress; AgInCd absorber rods	27.09.17

* at 950 mm

https://quench.forschung.kit.edu/24.php

Description of experiments

QUENCH-16 Test bundle



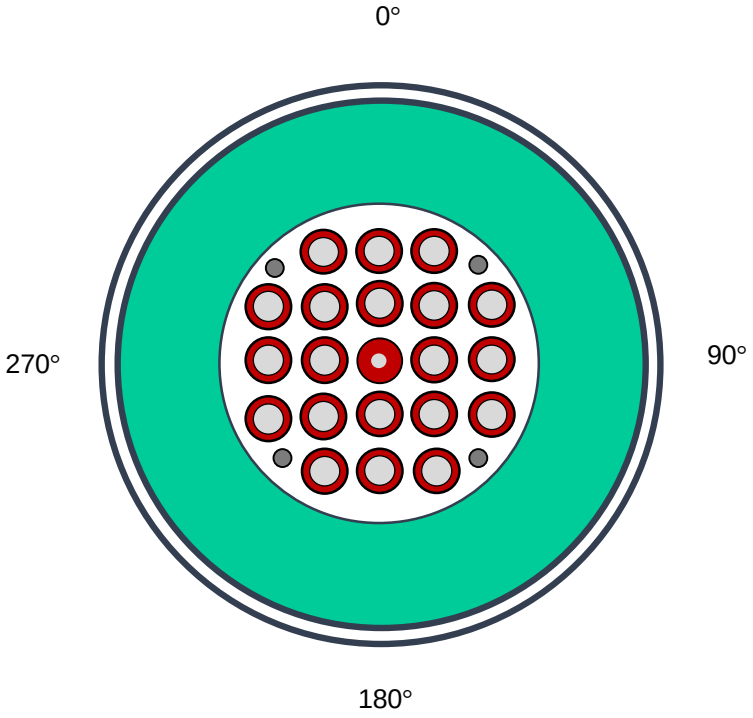
- Cooling jacket
- Insulation fiber
- Shroud
- 20 heated fuel rod simulators
  - In a 5x5 matrix arranged
- Four corner rods
- One unheated central rod simulator
  - ZrO_2 pellet

Q-16: Exp. data from: Stuckert et. al.: KIT-SR-7634

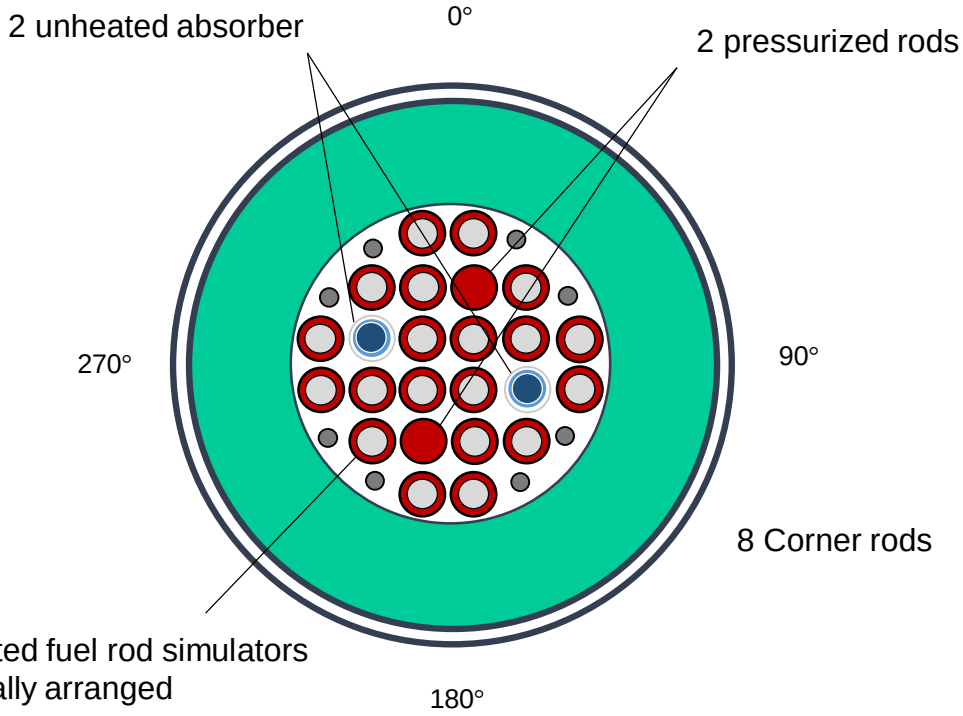
Description of experiments

Test bundle

QUENCH-16



QUENCH-18

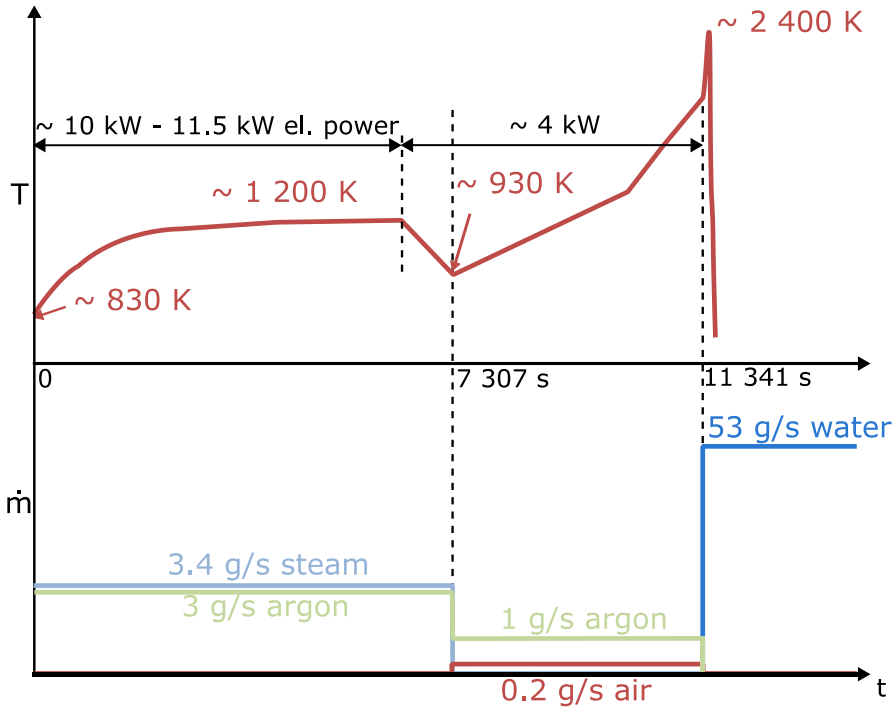


Q-18: exp. data from: Stuckert et. al. 2018

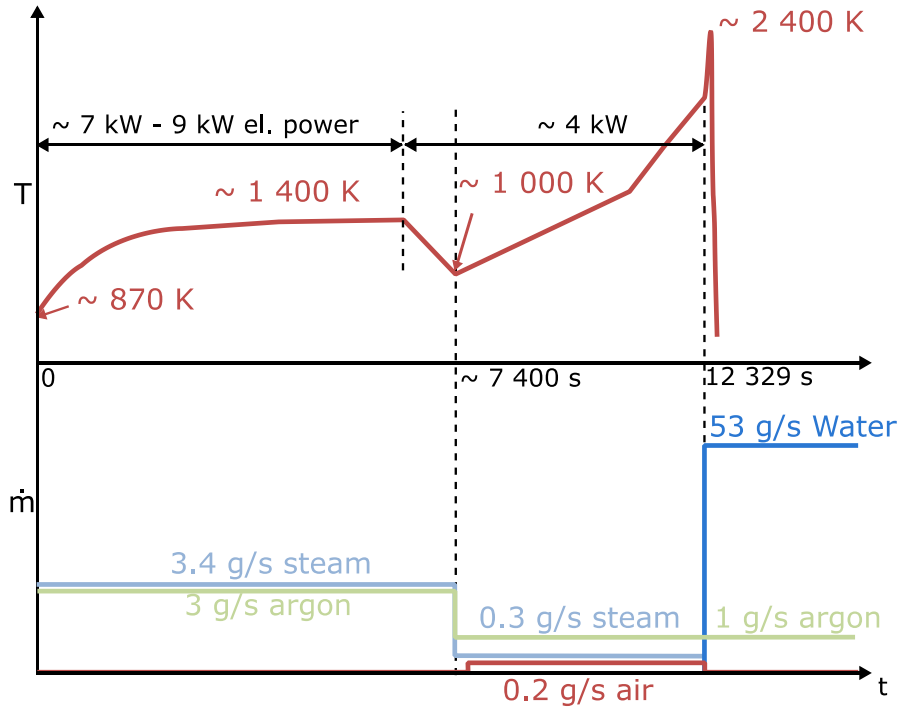
Description of experiments

Comparison of Test Conducts

QUENCH-16



QUENCH-18



Modelling approach
QUENCH-16

- ATHLET-CD input deck based on an existing PSS setup for previous QUENCH simulations
- Three core sections
- Flow channel: 10 equidistant nodes
- Comparative simulations with different patches of ATHLET-CD 3.1A

Run	Steam oxidation model (IOXMOD)	Air oxidation model (IOXAIR)	Set of rod oxidation parameters
1	Leistikow - Prater/Courtright	AEKI for Air	Based on previous QUENCH simulations
2	Cathcart - Prater/Courtright		Upper limits
(3)			Lower limits

Modelling approach
QUENCH-18

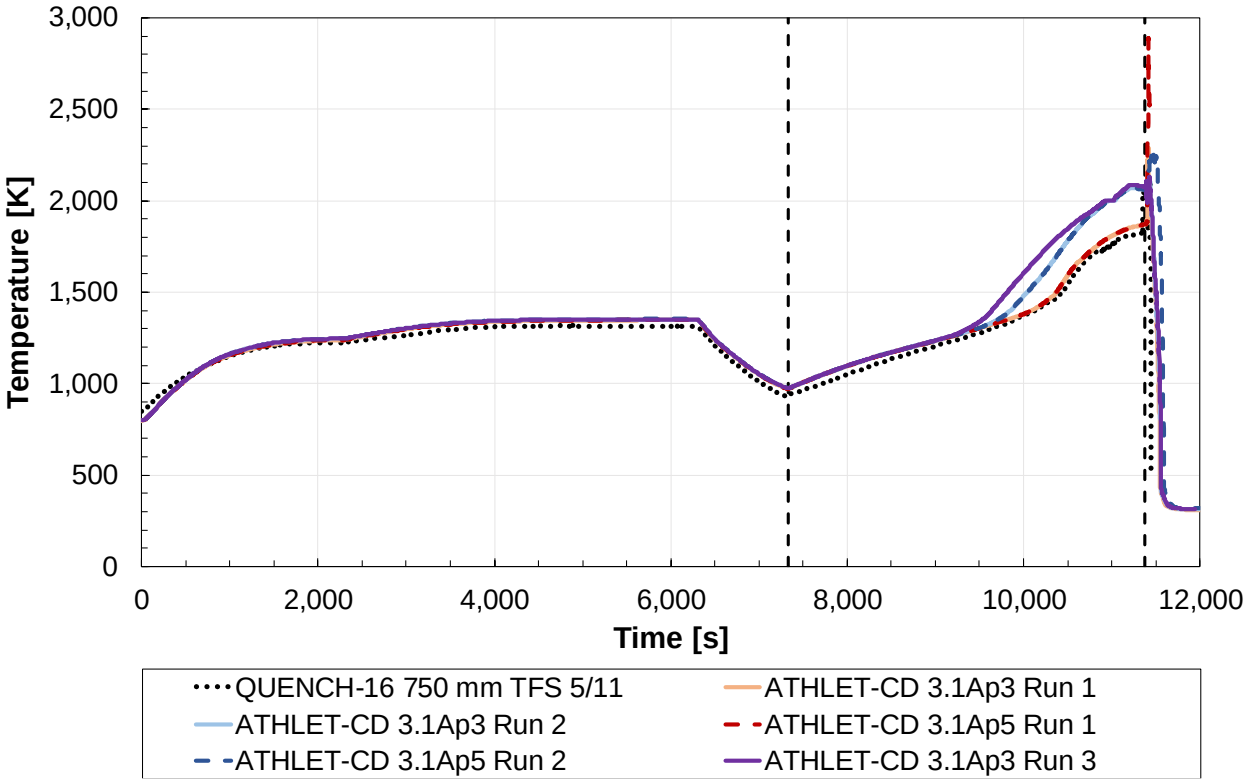
- Rod oxidation:
  Upper Limits
- Change of air oxidation model
  - NUREG1, NUREG2
- Consideration of fast injection in Run B
- Modified bundle geometry
  - Fourth core section added
  - Absorber rods in core section 2

Run	Steam oxidation model (IOXMOD)	Air oxidation model (IOXAIR)	Set of rod oxidation parameters	Fast injection considered
A	Cathcart - Prater/Courtright	NUREG2 (T<1180K); NUREG1 (T>1450K)	Upper Limits	–
B				✓

Simulation Results

QUENCH-16 – Cladding Temperature (950 mm)

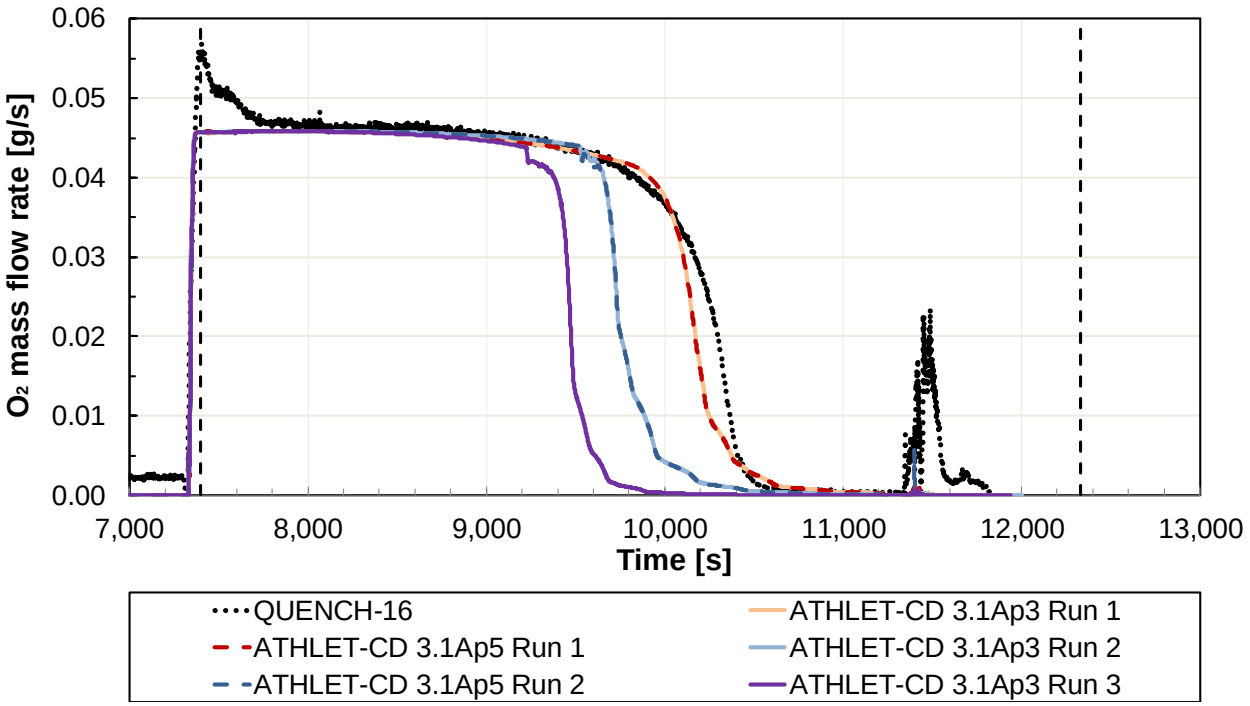
- All simulation runs in good accordance until oxidation stage
- Runs 2 and 3: Overestimation of the temperature during air starvation
- Run 1:
  - Precise reproduction during air starvation
  - Patch 5: Overestimation of the temperature excursion



Simulation Results

QUENCH-16 – Oxygen flow rate at outlet

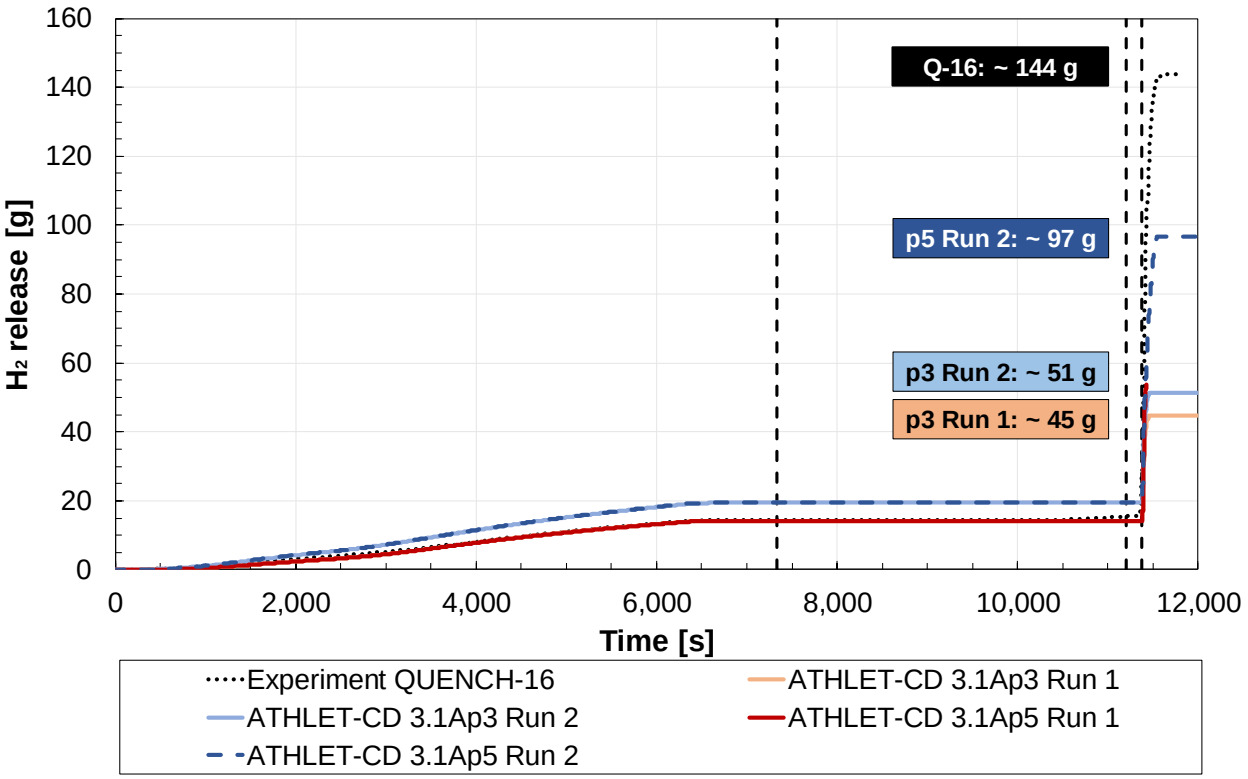
- Run 1 in good accordance with the experiment
- Runs 2 and 3:
  Air starvation calculated too early
- No changes when using the newer patch version



Simulation Results

QUENCH-16 – Total hydrogen generation

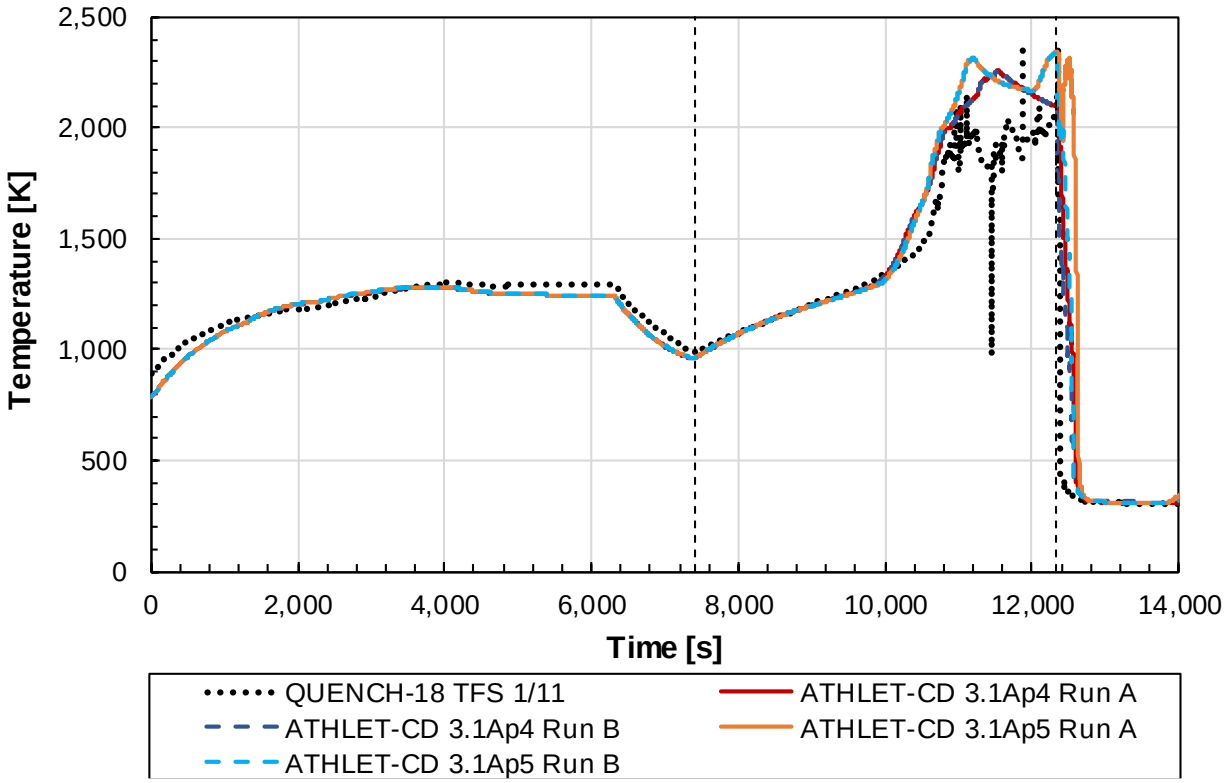
- Hydrogen generation related to quenching significantly underestimated when using patch 3
- Run 2, patch 5: clear improvement regarding the H_2 release during quenching



Simulation Results

QUENCH-18 – Cladding Temperature (750 mm)

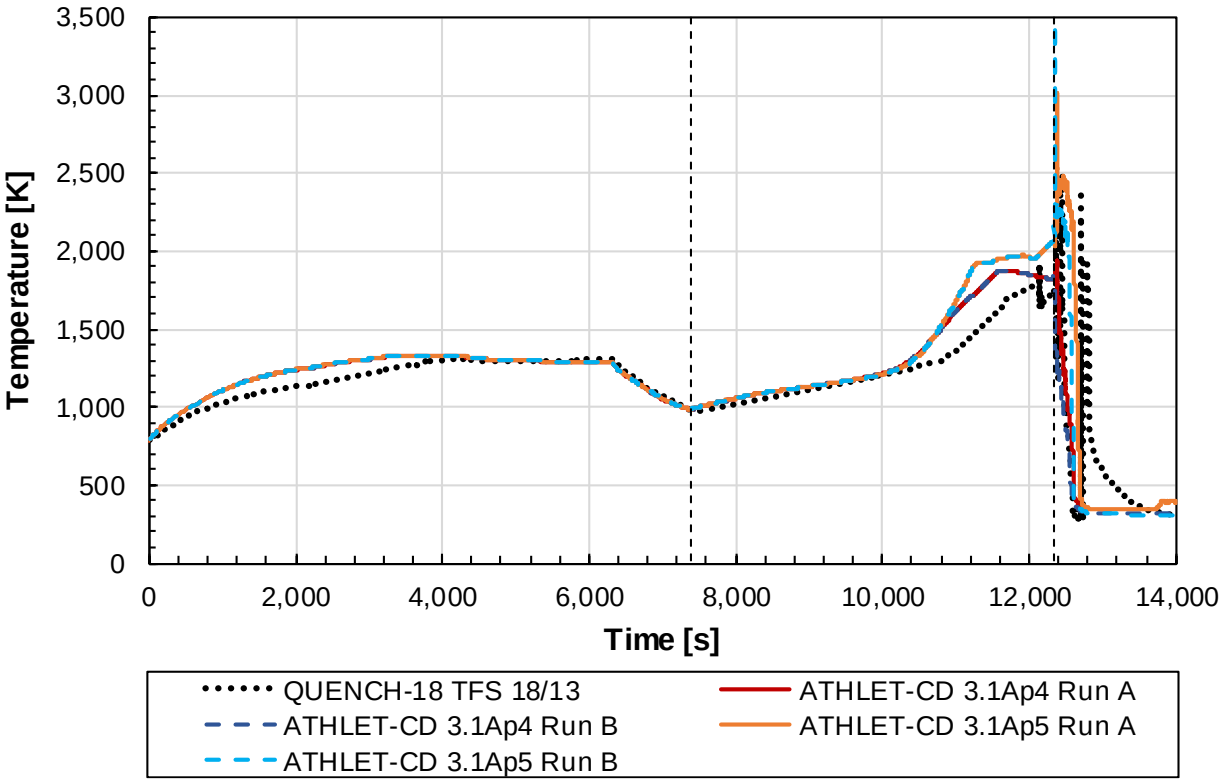
- All runs:
  Good qualitative accordance during air ingress
- Run A, p5:
  Delayed cool down after quenching



Simulation Results

QUENCH-18 – Cladding Temperature (950 mm)

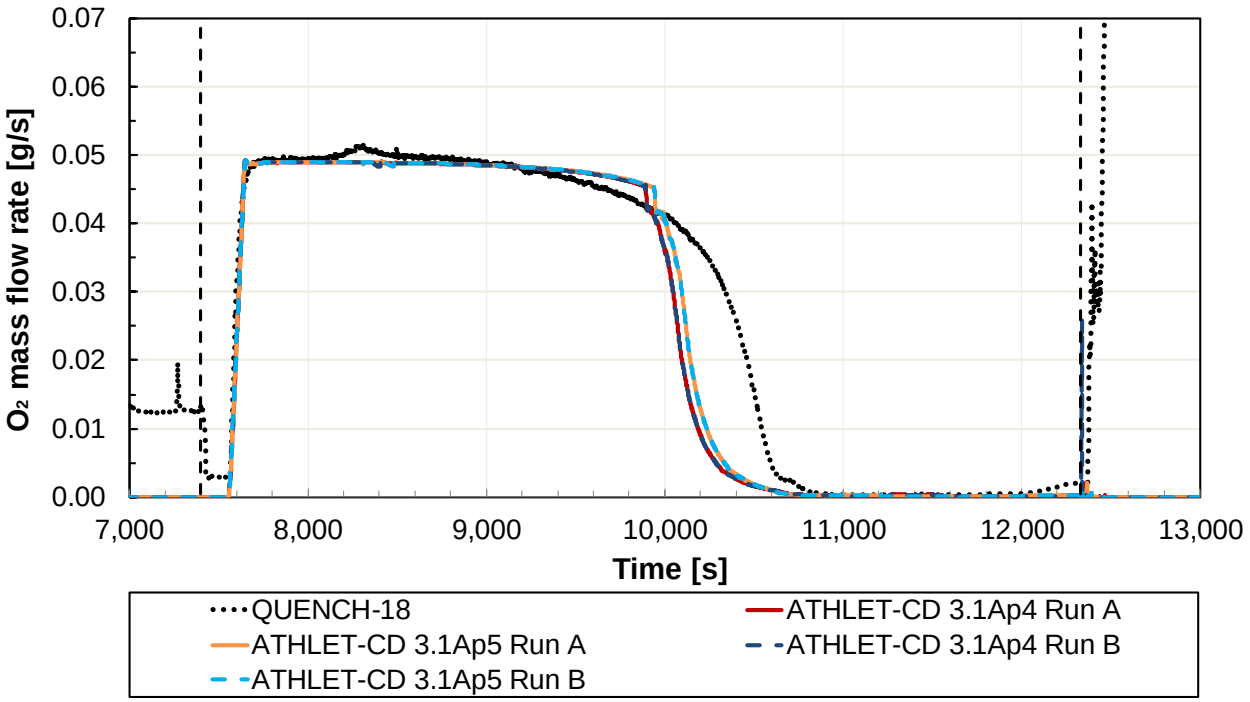
- All runs: Overestimation of temperature during steam/air starvation
- Substantial overestimation during quenching



Simulation Results

QUENCH-18 – Oxygen flow rate at outlet

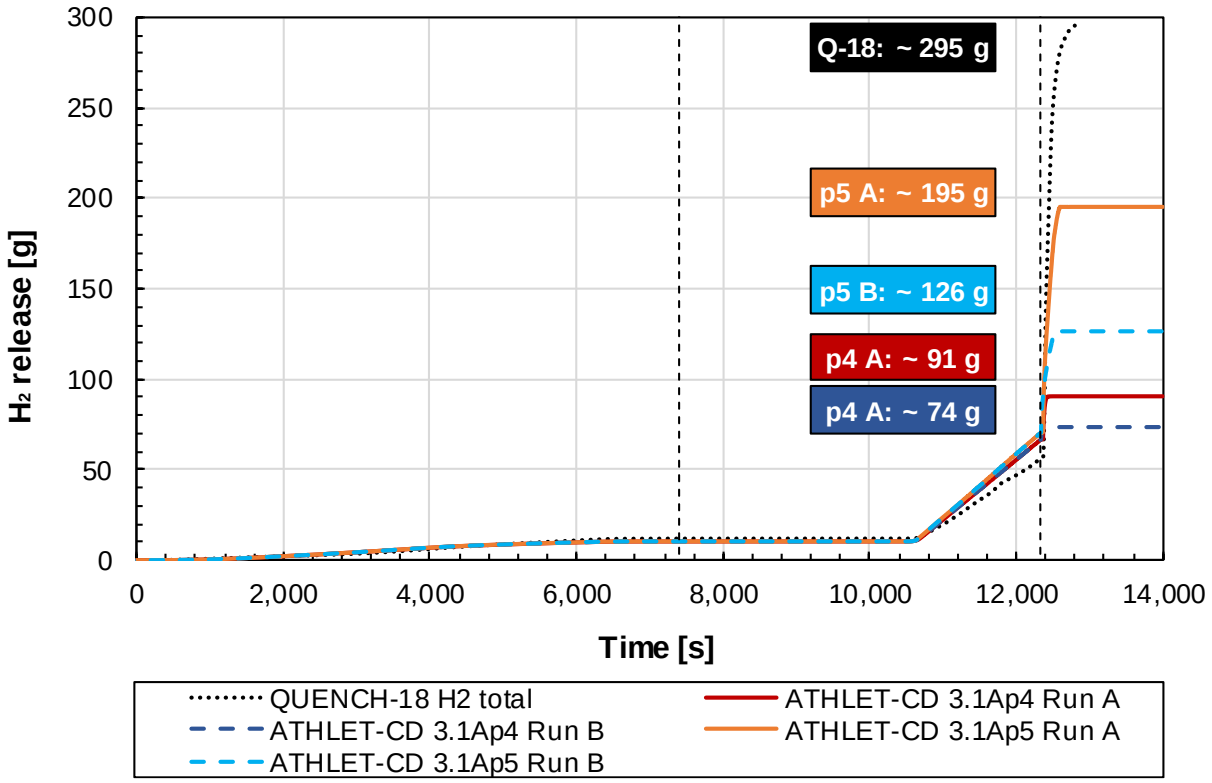
- All runs:
  Air starvation reached too early
- Only minor deviations between different patch versions



Simulation Results

QUENCH-18 – Total hydrogen generation

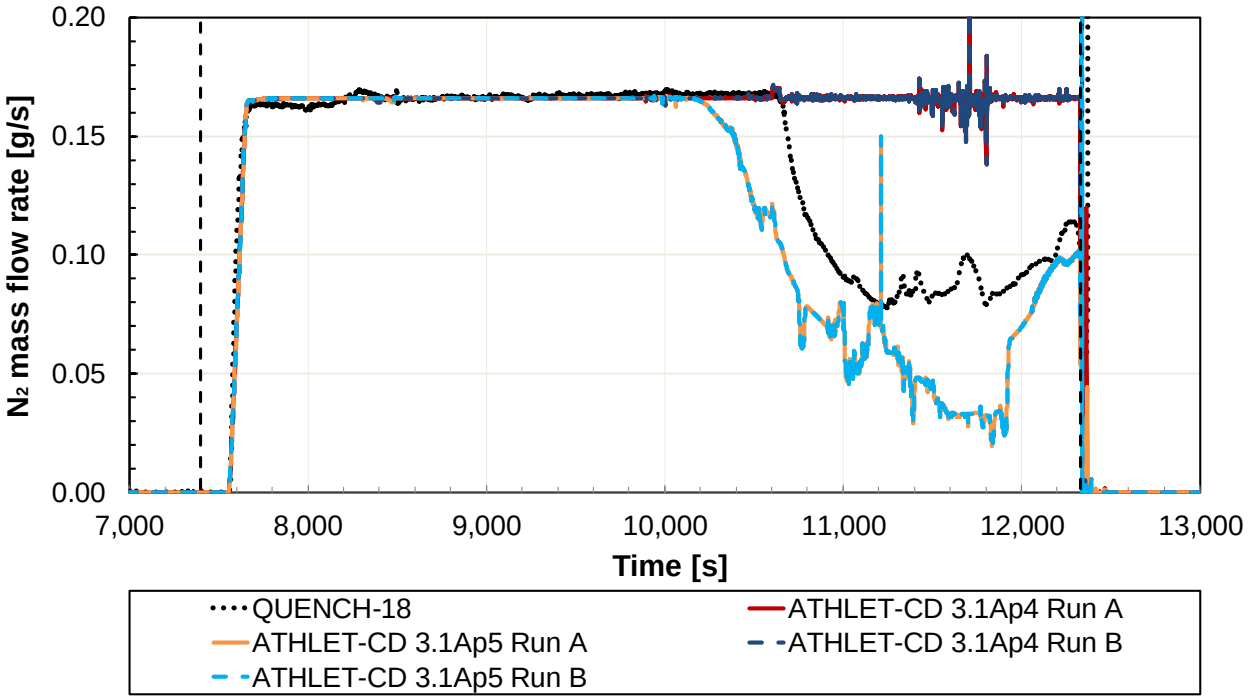
- Runs with patch 4: Extreme underestimation of H_2 release during quenching
- Run A, p5: H_2 release clearly improved
- Run B, p5: Consideration of fast injection reduces H_2 release during quenching



Simulation Results

QUENCH-18 – Nitrogen flow rate at outlet

- Improved simulation of the N_2 consumption with patch 5



Conclusion

- AC² - ATHLET-CD provides adequate modelling options to represent the oxidation behaviour of QUENCH-16 and QUENCH-18
- Generally good reproduction of the cladding temperature evolution
- Potential for an improved representation of the air starvation in refining the modelling of the rod oxidation
- Improvements in the simulation of the hydrogen generation during reflooding
- An adequate modelling of the fast injection could possibly improve the cooling behaviour

Acknowledgements

The used code system **AC² - ATHLET-CD** is developed by GRS.

This work is funded by the German Federal Ministry of Economic Affairs and Energy under grant number **1501522** on the basis of a decision by the German Bundestag. Responsibility for the content lies with the authors.



Thank you for your attention

Thank you for your attention

The Authors



Florian Krist

florian.krist@pss.rub.de

+49 (0) 234 32 26909



Marco K. Koch

marco.koch@pss.rub.de

+49 (0) 234 32 26368

Post-Test Modelling of the Experiment QUENCH-19 with ATF-Cladding FeCrAl Using SOCRAT Code

Alexander Vasiliev
Nuclear Safety institute (IBRAE)
B.Tulskaya 52
115191, Moscow, Russia
vasil@ibrae.ac.ru

ABSTRACT

The thermal hydraulic and SFD (Severe Fuel Damage) best estimate computer modelling code SOCRAT/V3 has been used for the calculation of QUENCH-19 experiment with new advanced tolerant fuel cladding made of FeCrAl alloy.

The QUENCH-19 test conditions simulated a representative scenario of LOCA (Loss of Coolant Accident) nuclear power plant accident sequence in which the overheated up to 1700K core would be reflooded from the bottom by ECCS (Emergency Core Cooling System). The QUENCH-19 experiment included the following phases: first heat-up phase, pre-oxidation phase, final heat-up phase and bottom water flooding phase. The important feature of QUENCH-19 test was the use of new FeCrAl material as claddings material.

The QUENCH-18 with ATF FeCrAl claddings test was successfully conducted at the KIT, Karlsruhe, Germany, on August 29, 2018. The primary objective of this test was to investigate the high-temperature oxidation of FeCrAl cladding in the steam following a pre-oxidation in the steam. Expectedly low cladding oxidation rate was detected during the test which resulted in very moderate integral hydrogen production in QUENCH-19. It was due to low parabolic oxidation coefficient for FeCrAl.

In this paper, the special attention was paid to the ability of the SOCRAT to predict the test behaviour using two correlations for FeCrAl parabolic oxidation: 1) the correlation given by manufacturer and recommended by Oak Ridge Nat. Lab.; 2) the correlation of Zhong. Those correlations are occurred to differ approximately by order of magnitude.

The calculated temperature dynamics results obtained for all phases are in a reasonable agreement with experimental data which justifies the adequacy of thermal hydraulic modelling capabilities of SOCRAT code. However, the SOCRAT underestimated the hydrogen generation and integral production during final heat-up phase for both parabolic correlations used. Besides that, the SOCRAT drastically underestimates hydrogen generation during pre-oxidation phase for calculation with Oak Ridge Nat. Lab oxidation correlation.

The main reason for disagreement between calculated and experimental data may be the higher real parabolic oxidation constant compared to this parameter in the recommended correlation which underestimates very much oxidation and hydrogen generation rate. The second reason for underestimation in calculations may be due to not adequate taking into account of FeCrAl melt oxidation rate in the code.


KIT
Institut für Technologie

Post-Test Modelling of the Experiment QUENCH-19 with ATF-Cladding FeCrAl Using SOCRAT Code

Alexander Vasiliev

IBRAE

B.Tulskaya 52, 115191 Moscow, Russia

QUENCH 2019, Karlsruhe, Germany, October 22-24, 2019

Content of presentation

1. Introduction
2. FeCrAl as one of perspective ATF cladding
3. QUENCH-19: initial and boundary conditions
4. Reason for expressed bundle temperature profile
5. Results of SOCRAT QUENCH-19 calculations
6. Conclusions


October 4-6, 1995
FORTBILDUNGSZENTRUM FTU

October 4-6, 1995



FeCrAl Cladding Parabolic Oxidation. Two Kinetics Used

Recommended Kanthal oxidation kinetics – variant 1

$$K(T) = 2.80 \cdot 10^{1} \exp\left(-\frac{172000}{RT}\right) \approx 2.80 \cdot 10^{1} \exp\left(-\frac{20700}{T}\right)$$

kg/(m^{2}s$^{1/2}$)

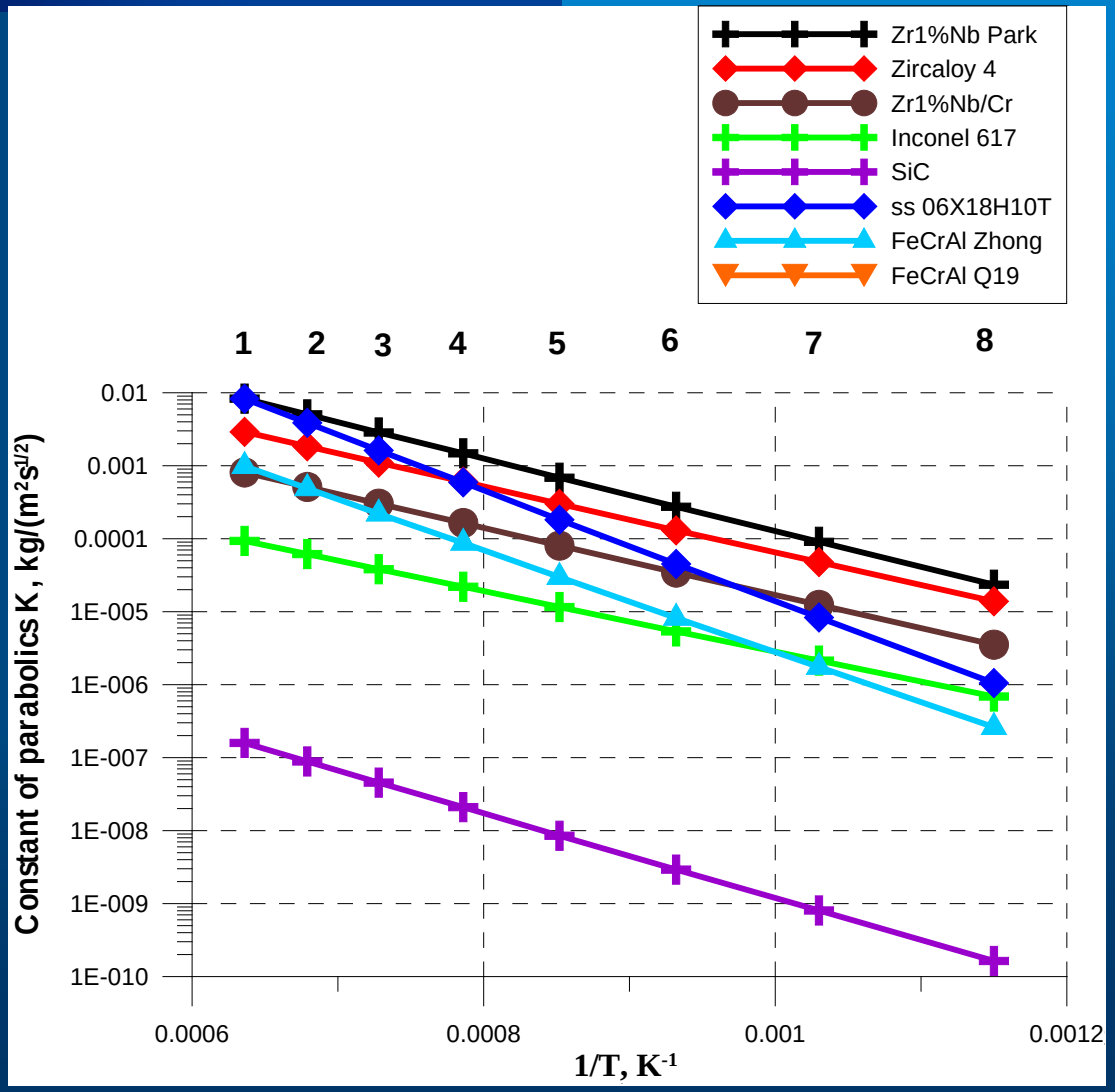
FeCrAl oxidation kinetics - variant 2

$$K(T) = 2.83 \cdot 10^{1} \exp\left(-\frac{16150}{T}\right)$$

kg/(m^{2}s$^{1/2}$)

Zhong W., Mouche P.A., Han X. et al. Performance of Iron-Chromium-Aluminium Alloy Surface Coatings on Zircaloy 2 under High-Temperature Steam and Normal BWR Operationg Conditions. J. of Nuclear Materials, 2016, V. 470, P. 327-338.

Perspective ATF-Claddings Candidates/ Parabolic Kinetics



1 – 1300°C

2 – 1200°C

3 – 1100°C

4 – 1000°C

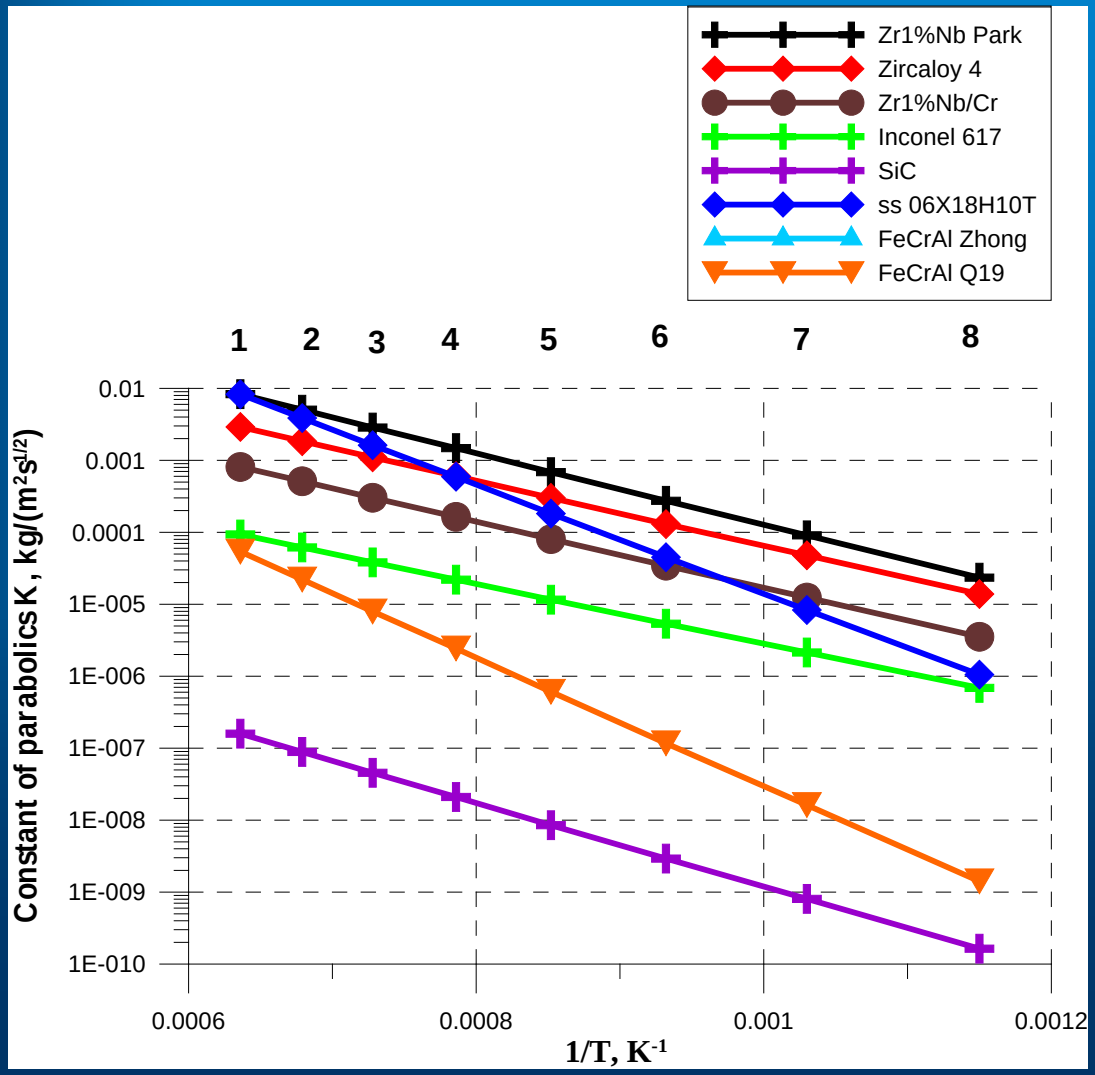
5 – 900°C

6 – 800°C

7 – 700°C

8 – 600°C

Perspective ATF-Claddings Candidates/ Parabolic Kinetics



1 – 1300°C

2 – 1200°C

3 – 1100°C

4 – 1000°C

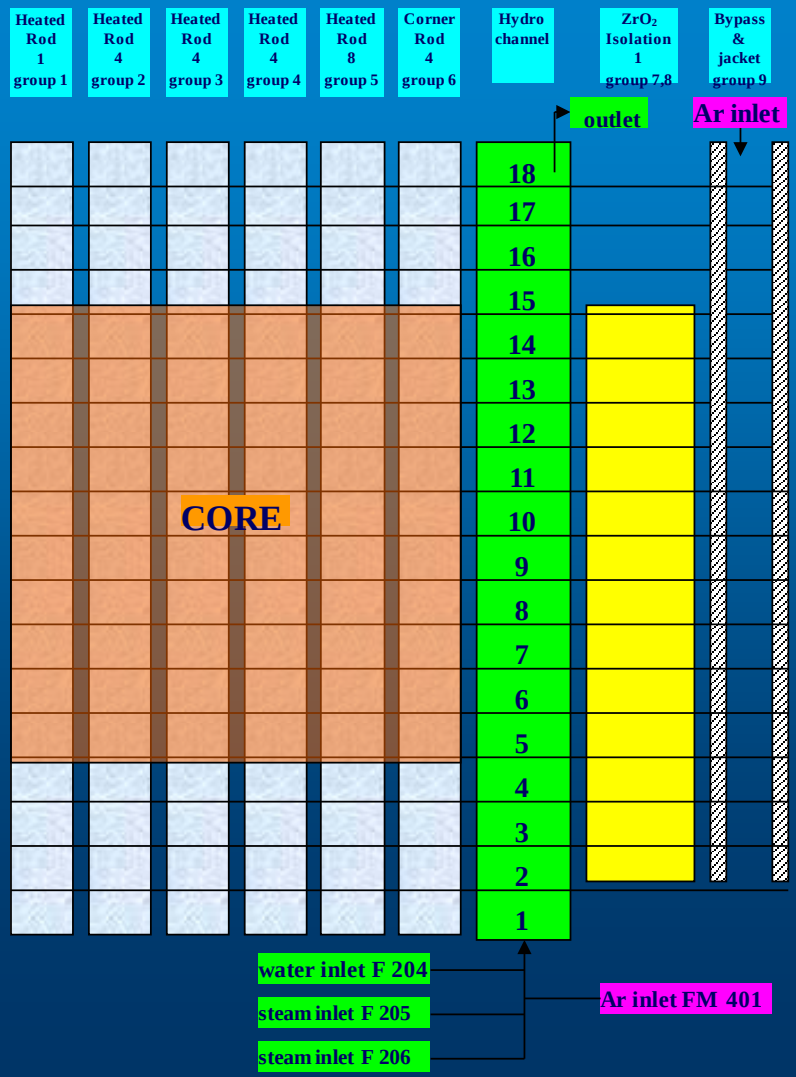
5 – 900°C

6 – 800°C

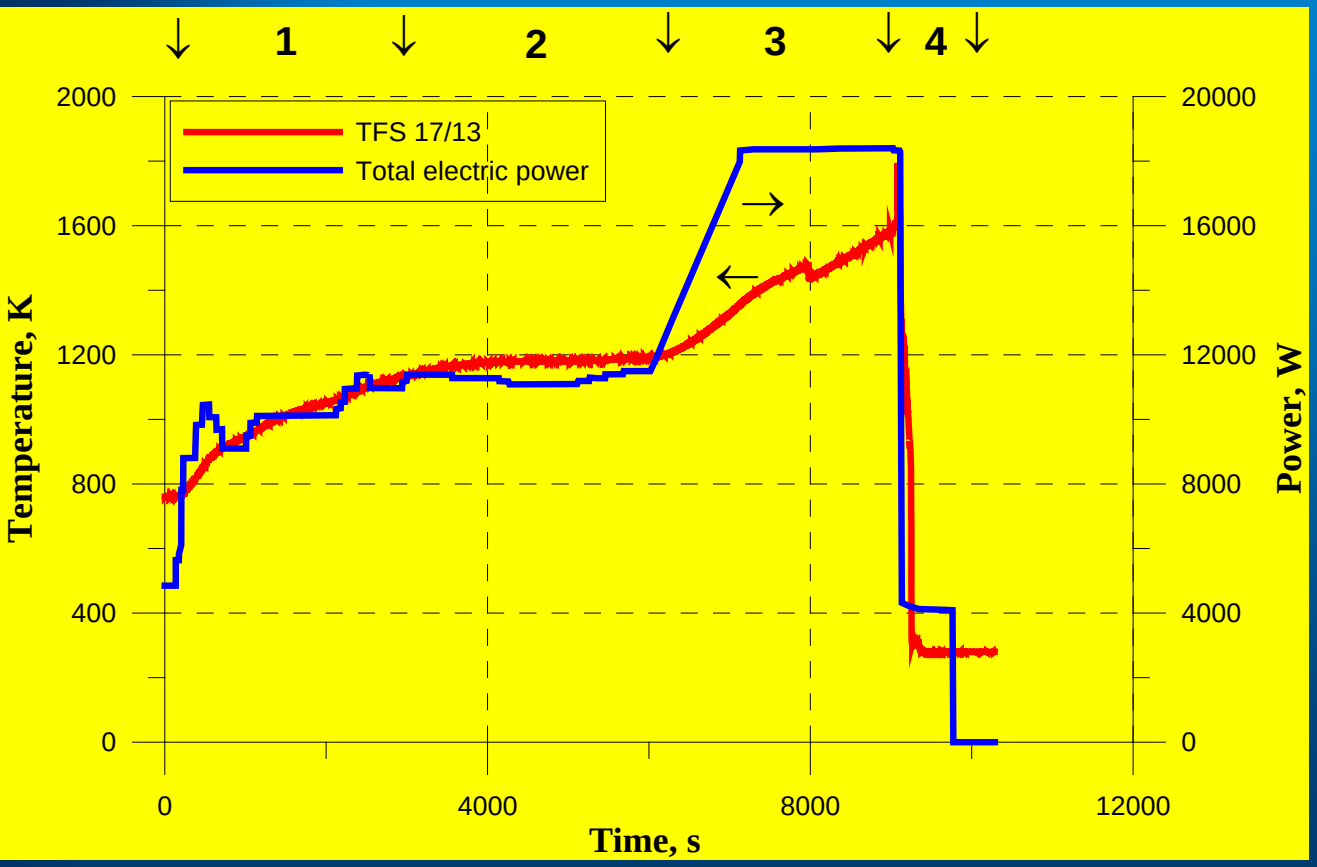
7 – 700°C

8 – 600°C

SOCRAT/V3 nodalization for QUENCH-19



QUENCH-19 Phases



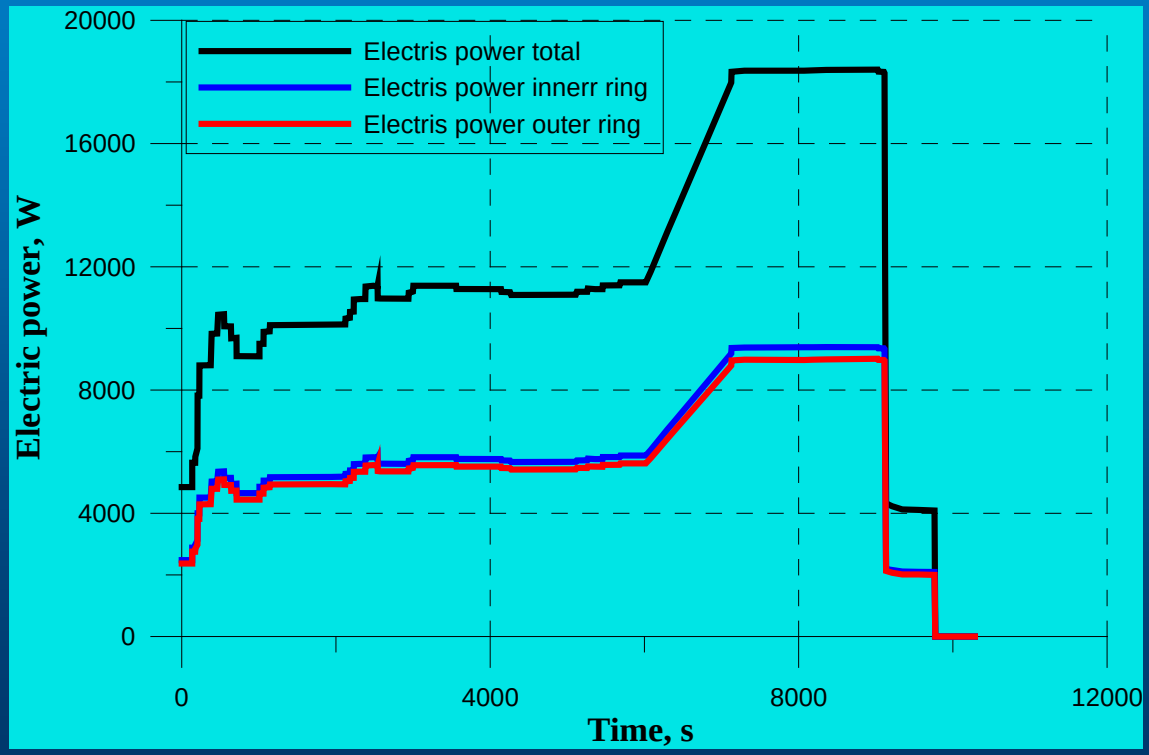
1 – first heat-up

2 – preoxidation

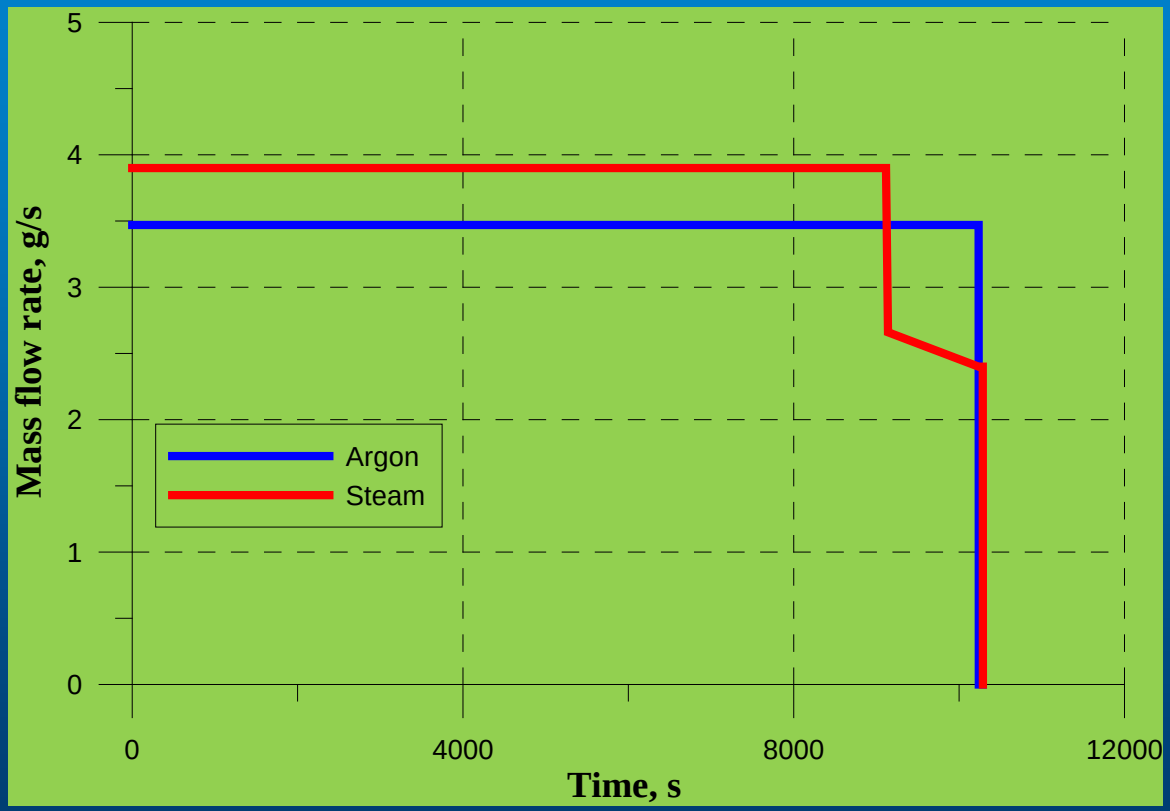
3 – final heat-up

4 – reflood

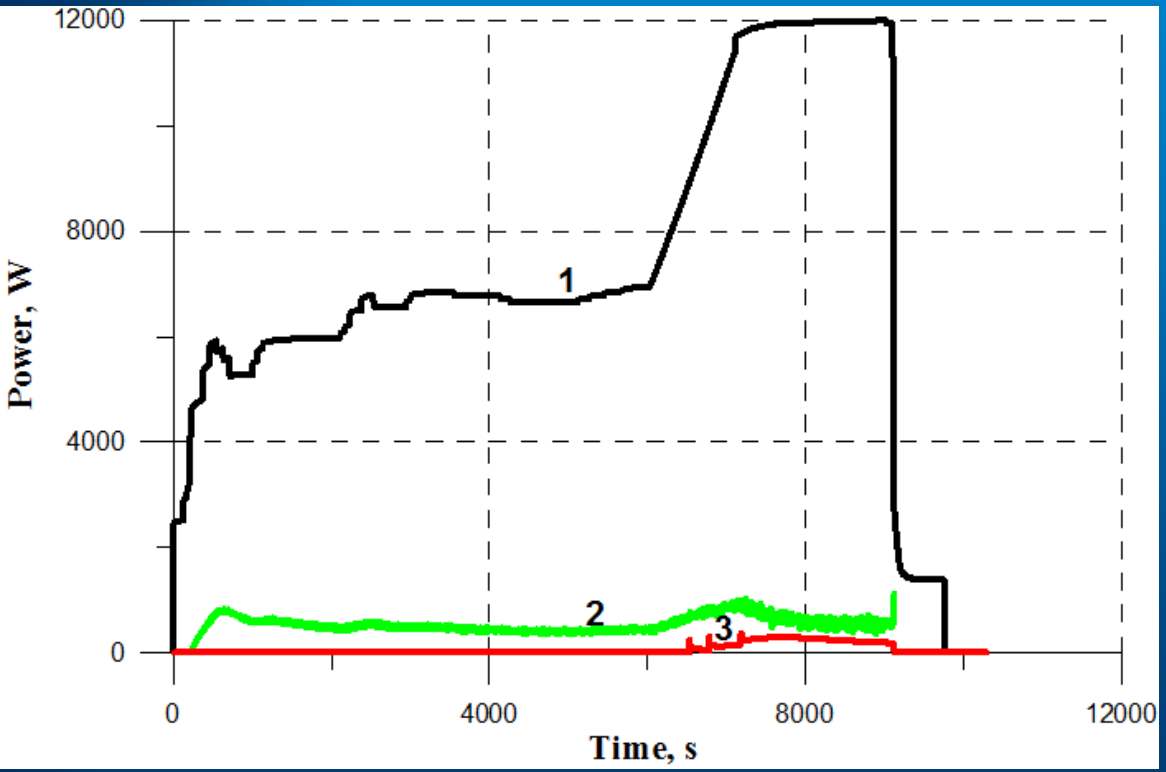
Electric Power



Gas Mass Flow Rates



QUENCH-19 Bundle Heat Fluxes

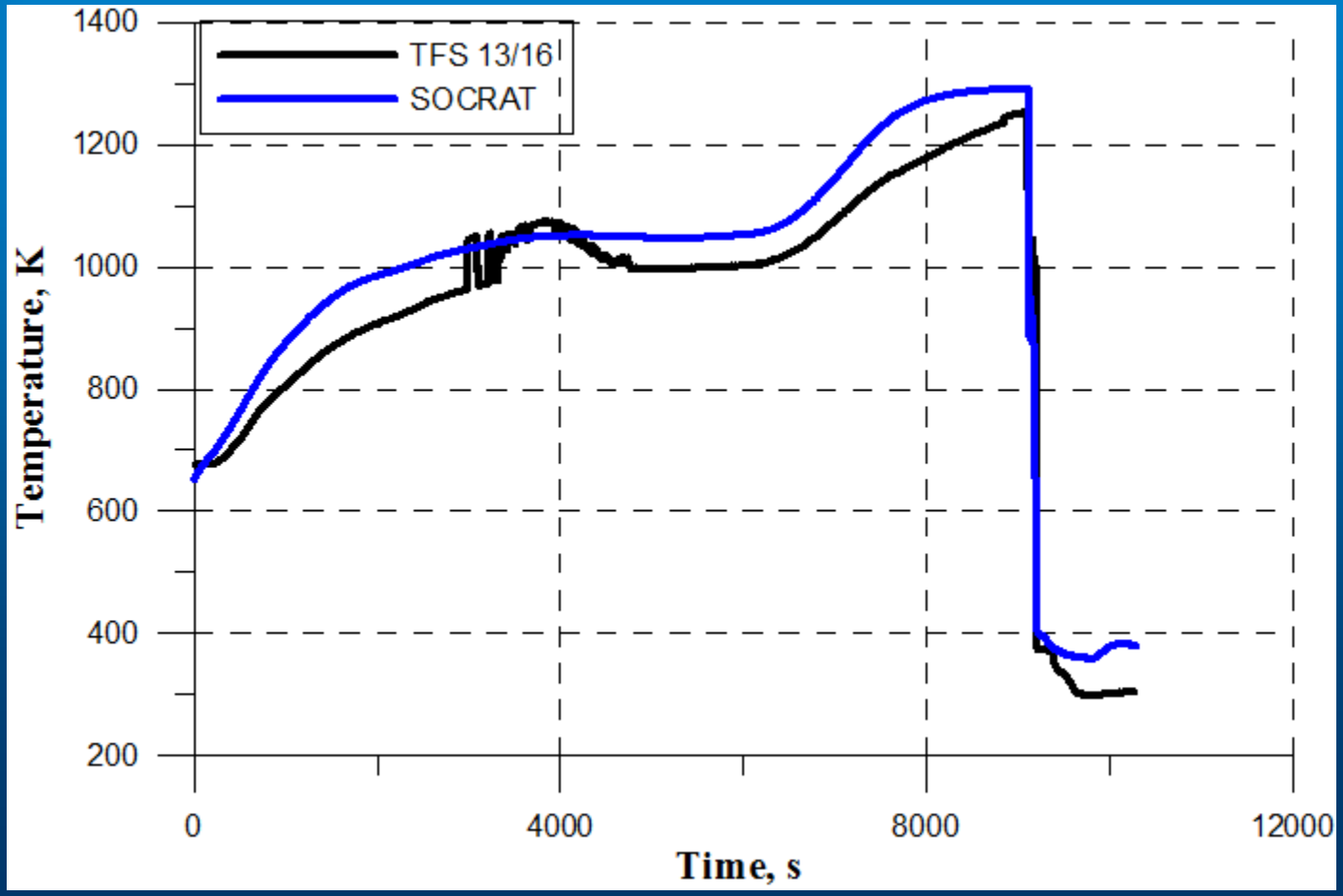


1 – **total electric power**

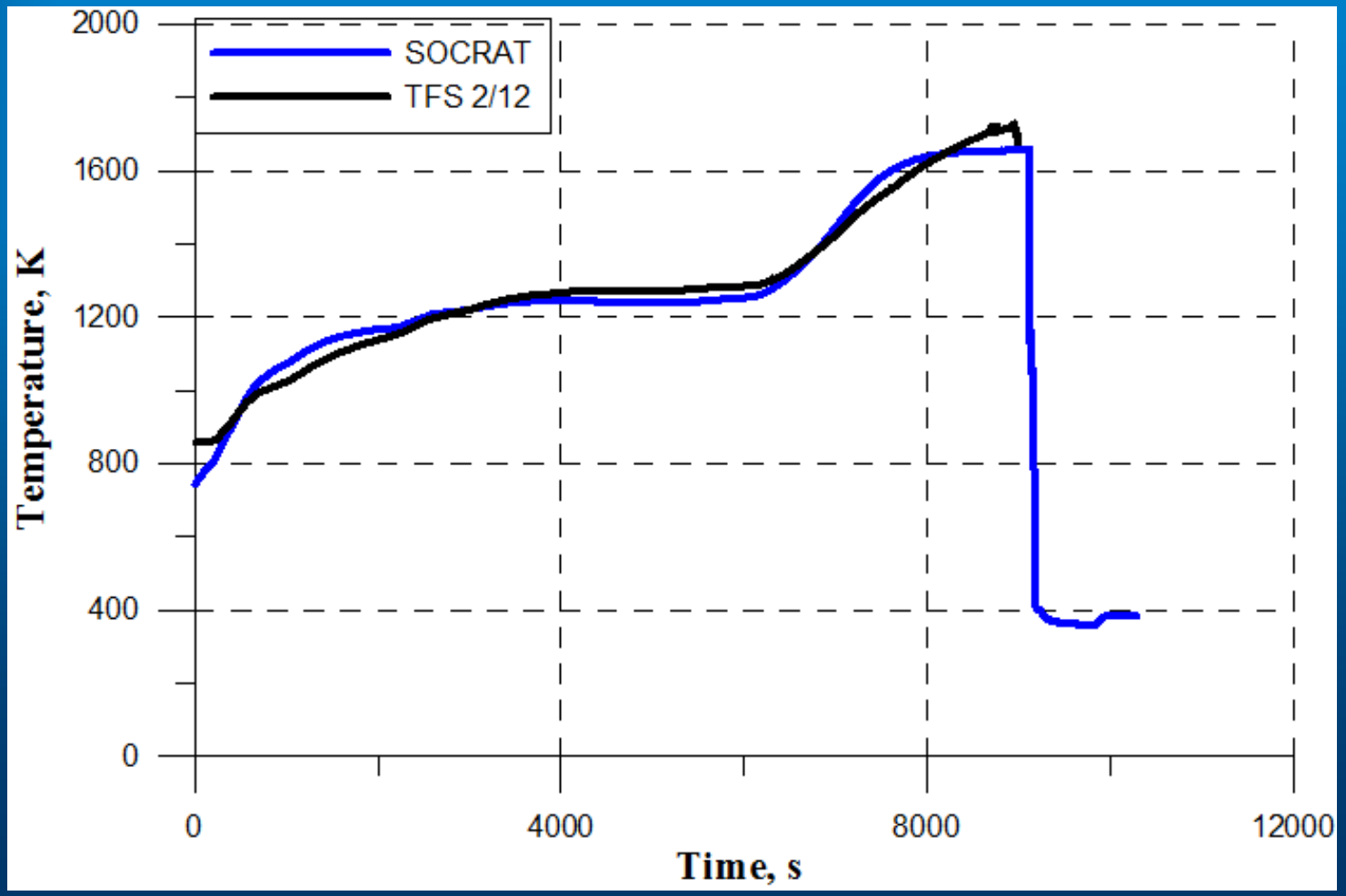
2 – **heat to shroud**

3 – **chemical heat**

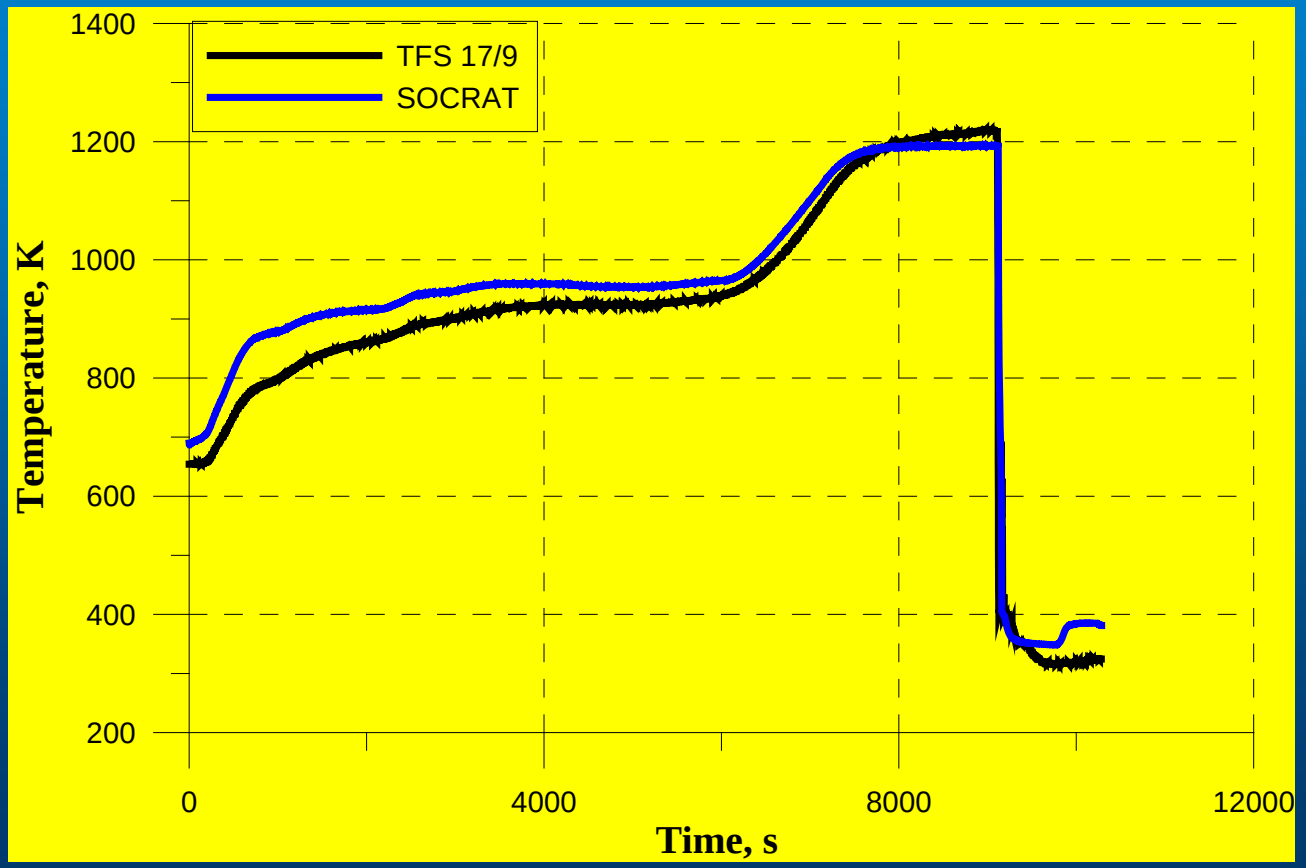
Temperature at Level 1250 mm



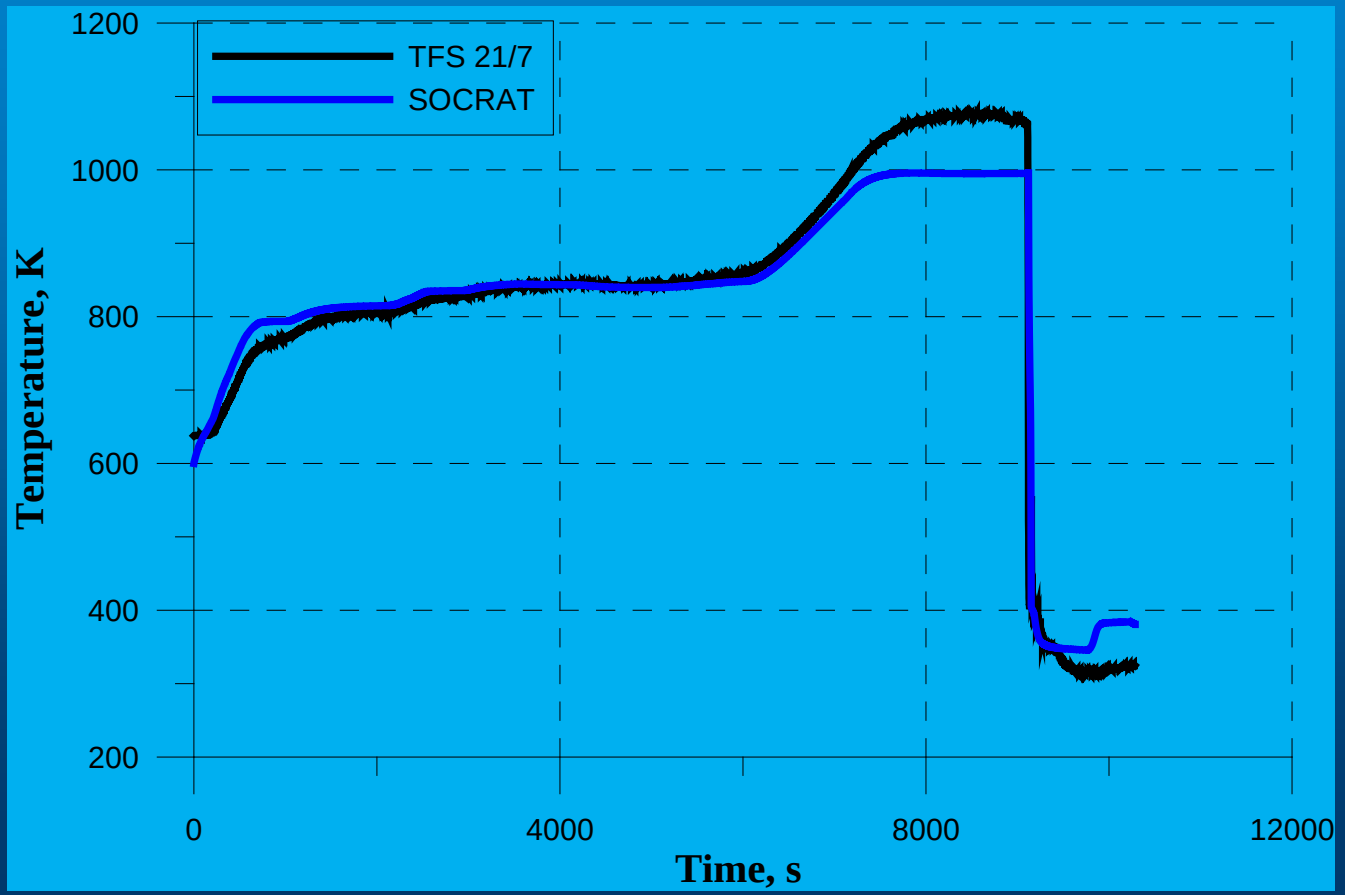
Temperature at Level 850 mm



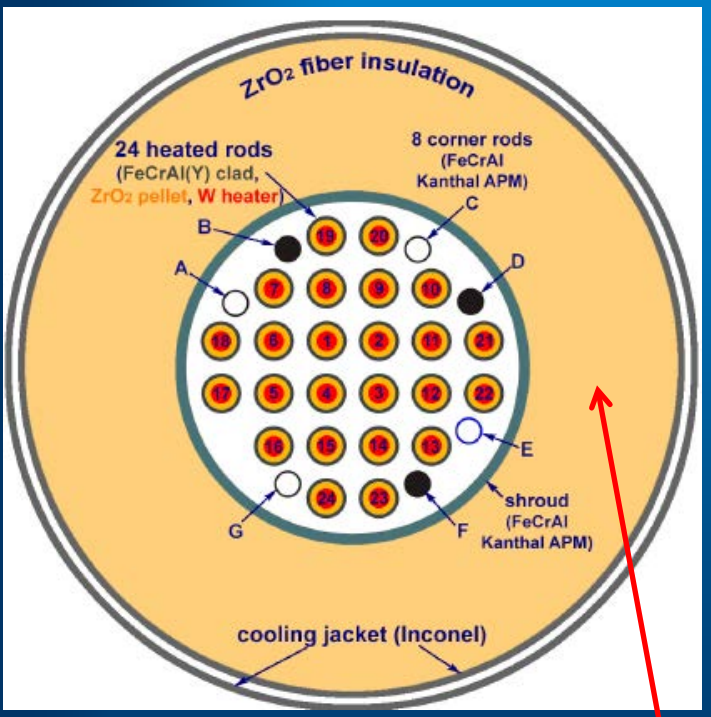
Temperature at Level 550 mm

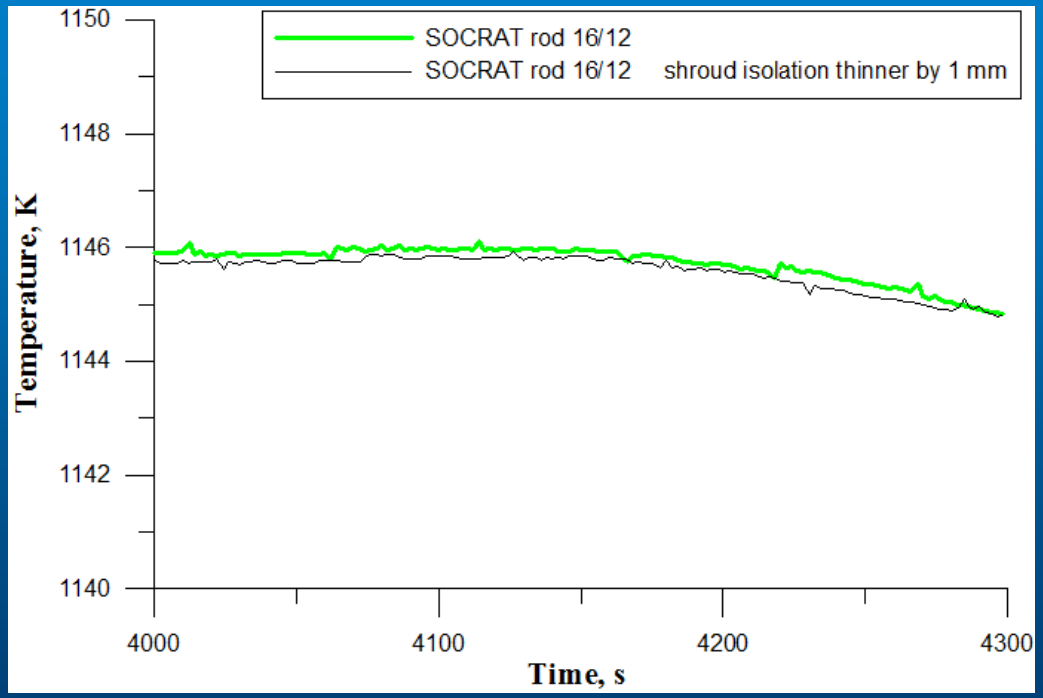


Temperature at Level 350 mm



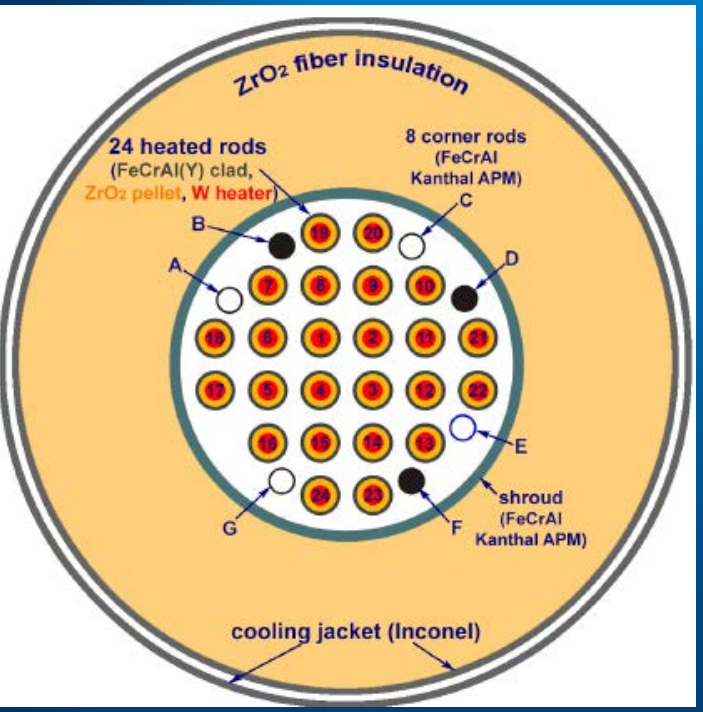
Clear Expressed Non-Uniform Radial Temperature Profile in QUENCH-19

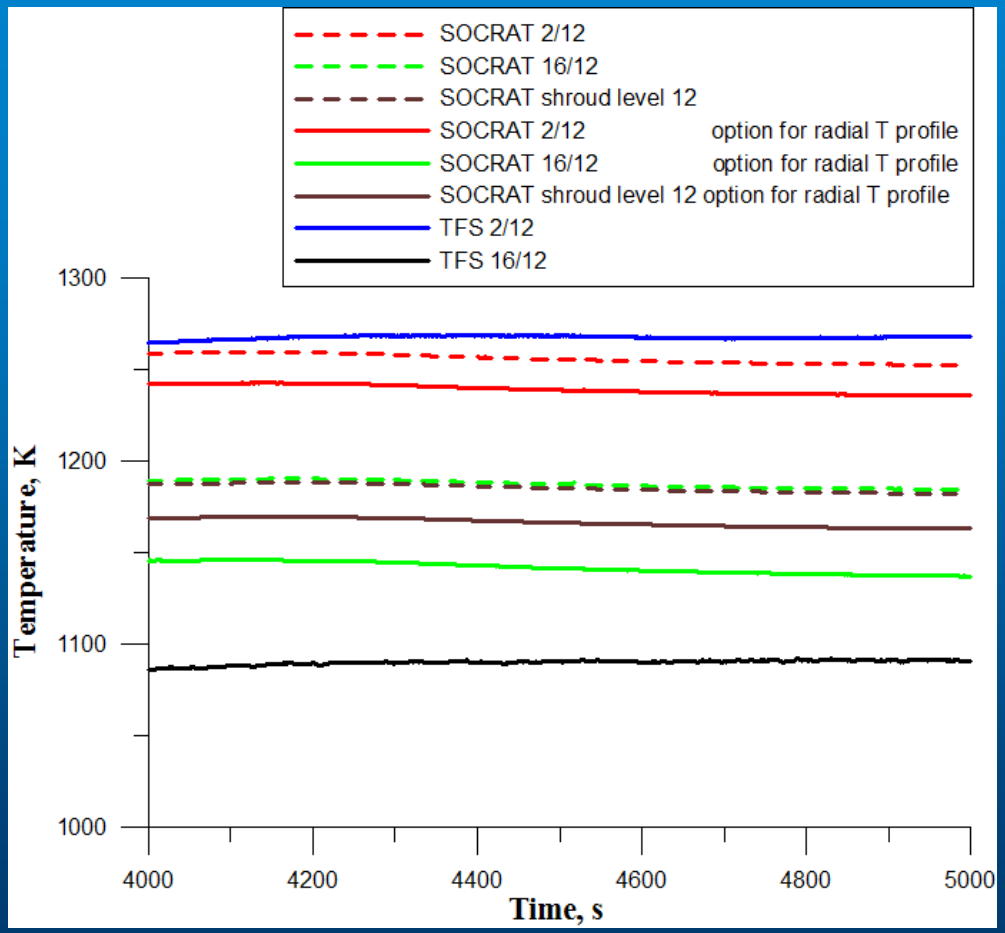




The non-uniform radial temperature profile is not a result of thinner shroud isolation in QUENCH-19 compared to standard thichkness!

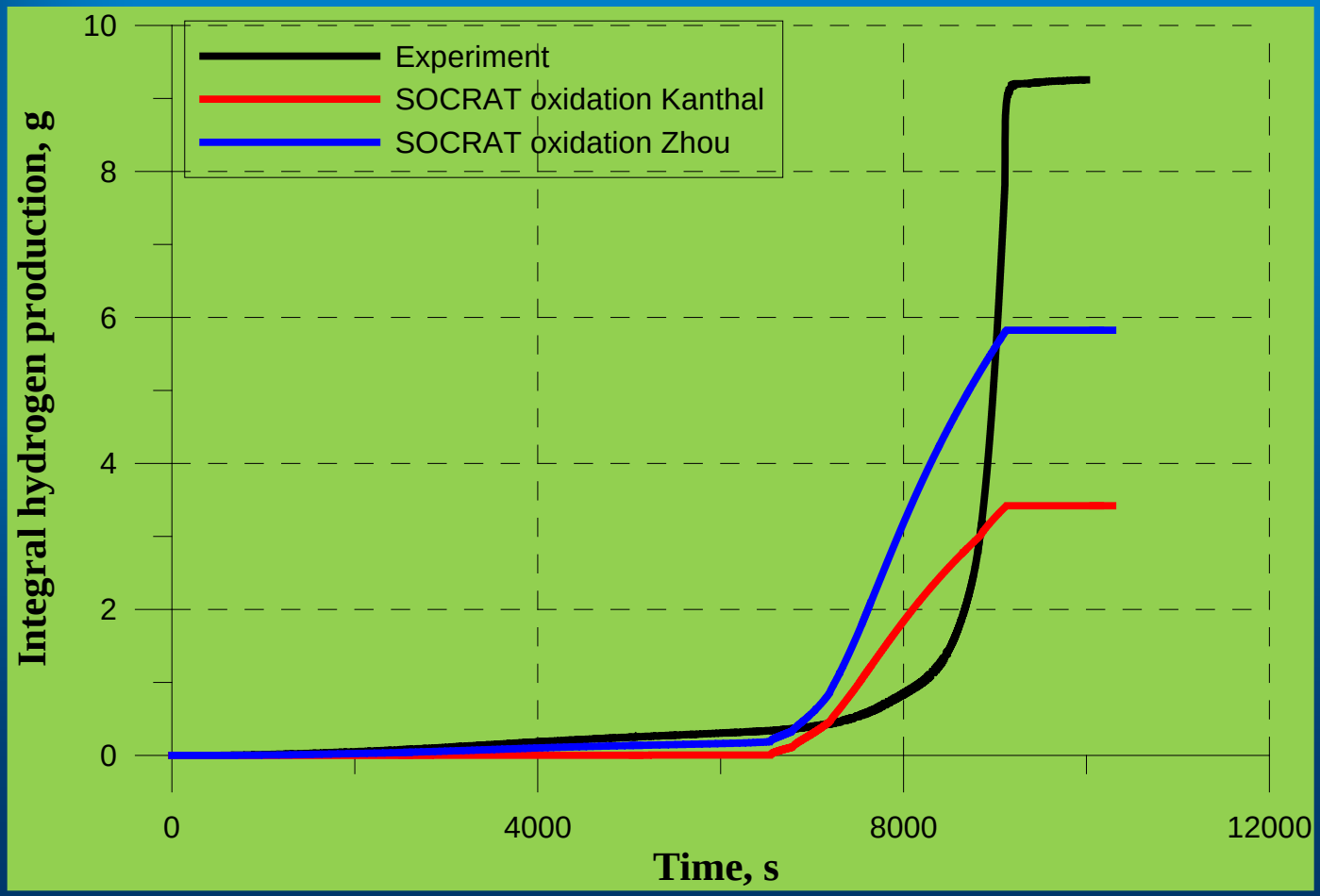
Clear Expressed Non-Uniform Radial Temperature Profile in QUENCH-19



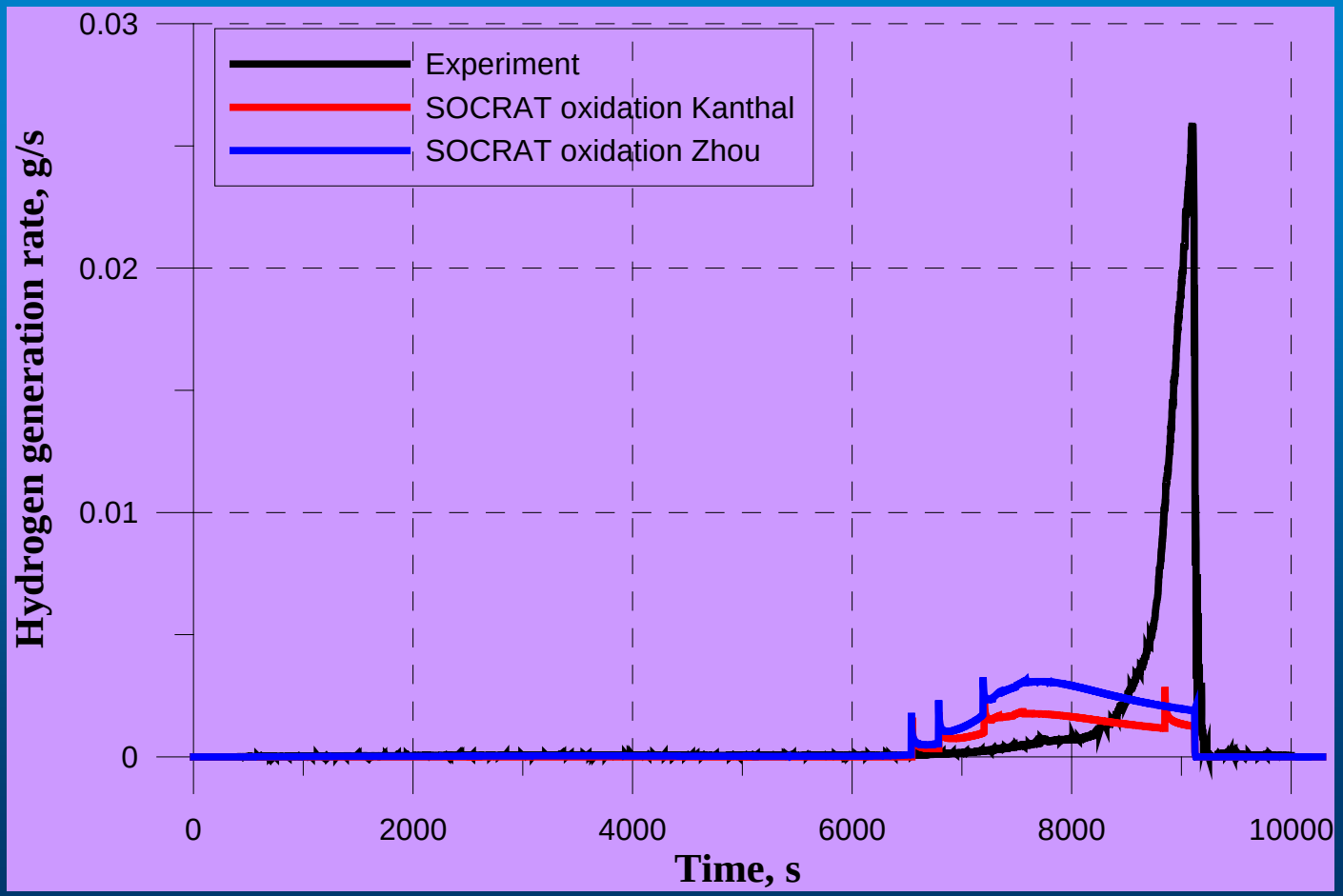


The non-uniform radial temperature profile is a result of lower heat conduction of FeCrAl compared to Zr alloys!

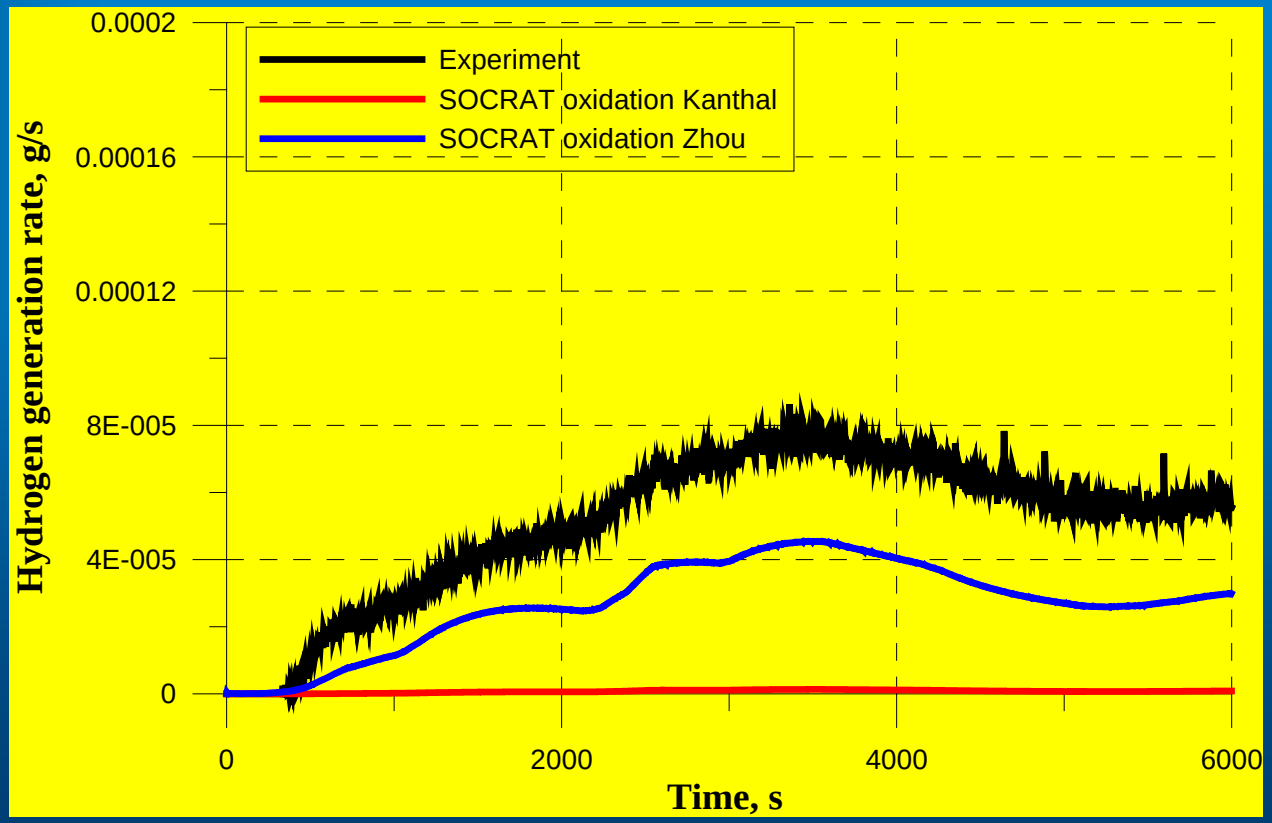
Integral H_2 Production



H_2 Generation Rate

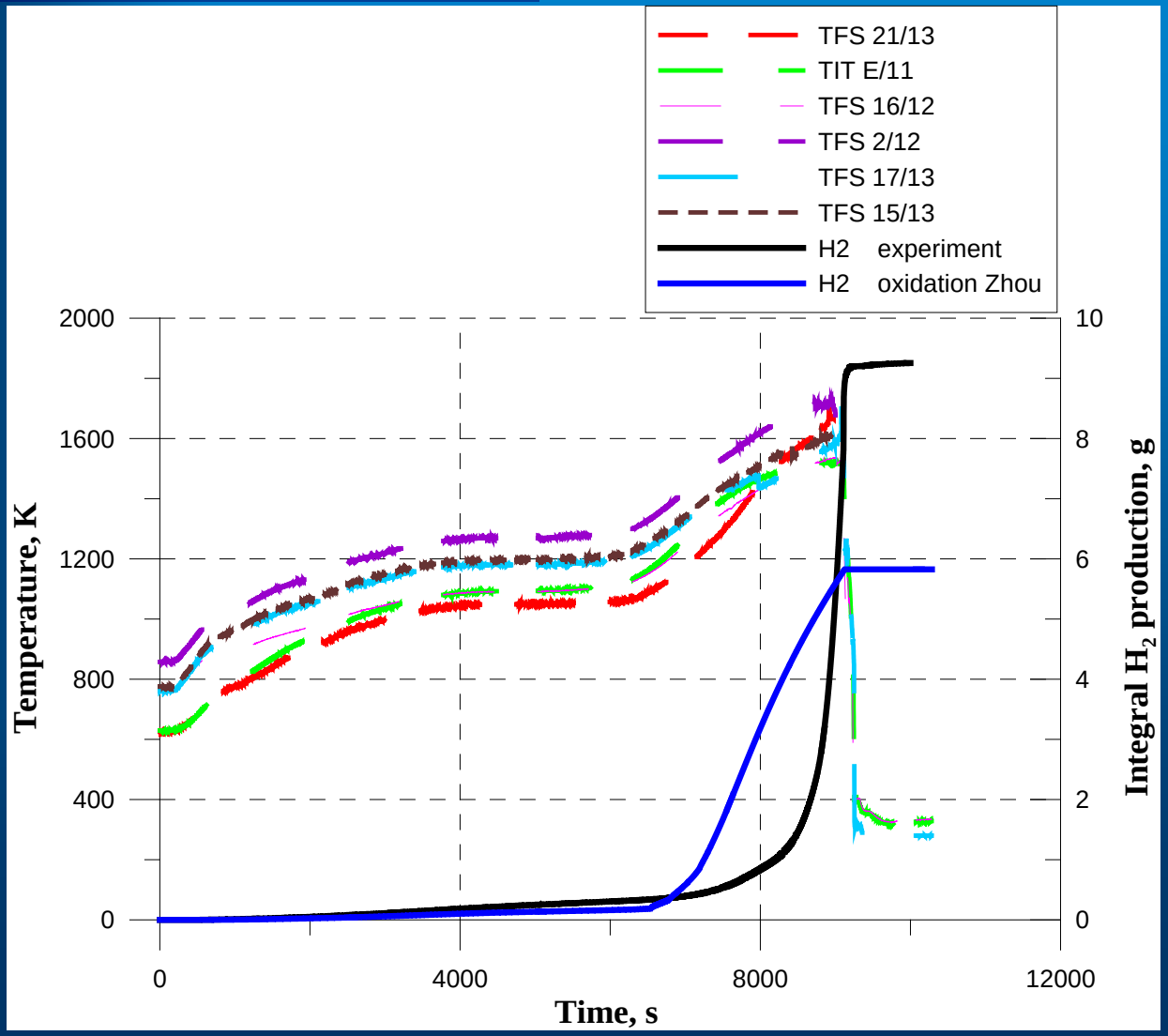


H_2 Generation Rate
First Heat-Up and Preoxidation



Kanthal oxidation kinetics drastically underestimates the experimental behaviour !

H_2 Generation Behaviour in Experiment QUENCH-19



Let 25 years have rushed
Years are flying, running
Sometimes 5 minutes can change the world
Don’t say about 25 years

Summary



The use of FeCrAl instead of general Zr-based claddings drastically influenced the test behaviour if compared to QUENCH-15 test with the same electric power history through the test.

The calculated and experimental thermal-hydraulic are in a reasonable agreement, which shows the adequacy of modelling the complicated thermo-hydraulic behaviour in the QUENCH-19 test. Hydrogen release rate underestimation by SOCRAT code with the use of two chosen FeCrAl oxidation correlations. Maybe, the real FeCrAl oxidation correlation exceeds the recommende one . The second reason for disagreement may be not adequate account of FeCrAl melt oxidation in the SOCRAT current version.

The hydrogen generation in QUENCH-19 was much lower in comparison to QUENCH-15 experiment. There was no temperature escalation in QUENCH-19 in contrast to QUENCH-15. The test was finished by about 2000 s earlier compared to QUENCH-15.

Simulation of recent QUENCH experiments with AC2

Livia Tiborcz, Thorsten Hollands
Gesellschaft für Anlagen- und Reaktorsicherheit (GRS) gGmbH

The QUENCH-19 experiment aimed to study an ATF cladding material, FeCrAl(Y), and its behavior under severe accident conditions. Post test analyses of the experiment has been carried out with the severe accident code ATHLET-CD as part of the code system AC^2. Compared to the pre-test analyses a dedicated oxidation model for the FeCrAl material has been implemented, with the assumption that only Aluminum will be oxidized. A modified correlation with a multiplication factor based on an IAEA Report has been also analyzed. Furthermore, temperature independent material properties of the FeCrAl material has been implemented. The simulation predicts well the overall thermal behavior of the rod alongside the heated length, while above that a slight overestimation of the temperatures can be seen. The radial spread of the temperatures within the bundle observed in the experiment however could not be captured with the calculations. The predicted hydrogen generation is significantly lower than measured, which could be due to the assumptions, that only Al is being oxidized. Another reason for this could be that the observed beginning of the melting, which was not modelled, could lead to an accelerated oxidation. Further improvements of the FeCrAl oxidation model taking into account the post-test analyses can improve the simulation results.

The QUENCH-20 experiment, carried out at KIT 2019.October.9, investigated for the first time a BWR configuration. The quadratic geometry of the bundle represented ¼ of a BWR bundle including two absorber blades. The ATHLET-CD model of the facility represented the core region with two thermo-fluid objects and one ROD object, which summed up all rods within the bundle due to its BWR configuration. The presented results are the first outcomes of a post-test analyses utilizing the BCs applied during the experiment. The thermal behavior, where first measurements are available, is well captured, though some overestimation of the cladding temperatures at 850mm, while a slight underestimation at 950mm can be seen. At the same time these deviations stay in the order of measurement uncertainties. The oxide layer of the corner rod at the end of the pre-oxidizing period was ~55µm, while the simulated value is ~65µm. In the middle of the bundle the simulation predicts an oxide layer thickness of 113µm, which is close to the target value of 100µm. The hydrogen production is very well captured till the quenching, after which it is underestimated. The simulation yields a total of ~41g, while ~58g has been measured. One of the reasons for this could be the observed failure of the shroud, which enabled the oxidation of the outer surface not modelled in our calculations.



Simulation of recent QUENCH experiments with AC2

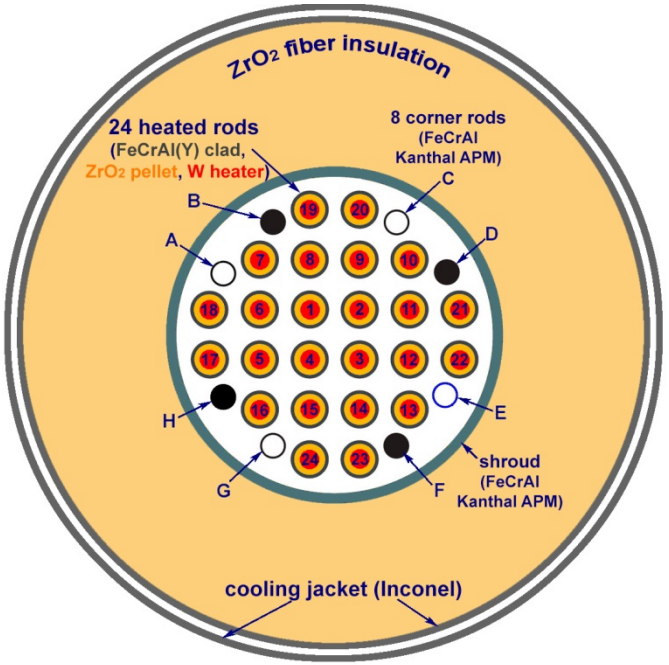
L. Tiborcz, T. Hollands
Gesellschaft für Anlagen- und Reaktorsicherheit (GRS) gGmbH

25th International QUENCH Workshop
Karlsruhe Institute of Technology
22-24 October 2019

QUENCH-19

QUENCH-19: Experiment

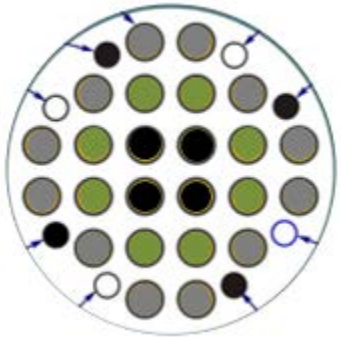
- Performed at KIT 2018
- FeCrAl claddings to investigate the cladding material behavior under SA conditions
- Scenario: similar to QUENCH-15 with Zirlo cladding
  - same bundle geometry
  - same electrical power input
- Bundle configuration made of different FeCrAl compositions:
  - 24 heated rods with tungsten heater and ZrO_2 pellet
  - 8 corner rods
  - 5 spacer grid
  - Shroud



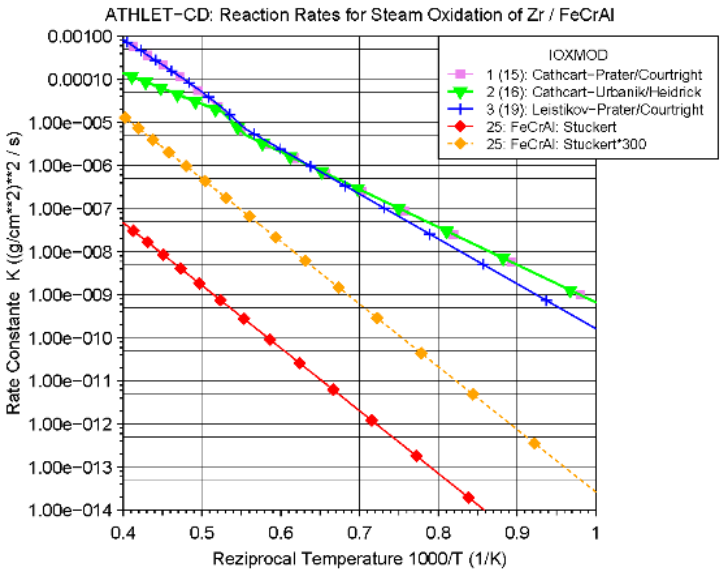
Source: KIT

QUENCH-19: Modelling with ATHLET-CD

- Standard ATHLET-CD input deck
- Bundle design implemented as given by KIT
- 2 Fluid Channels
  - Bundle → ROD1: 4 central rods — Rods 1, 2, 3, 4
  - Bypass
    - ROD2: 8 rods (intermediate ring) — Rods 5, 6, 8, 9, 11, 12, 14, 15
    - ROD3: 12 rods (outermost ring) — Rods 7, 10, 13, 16, 17, 18, 19, 20, 21, 22, 23, 24

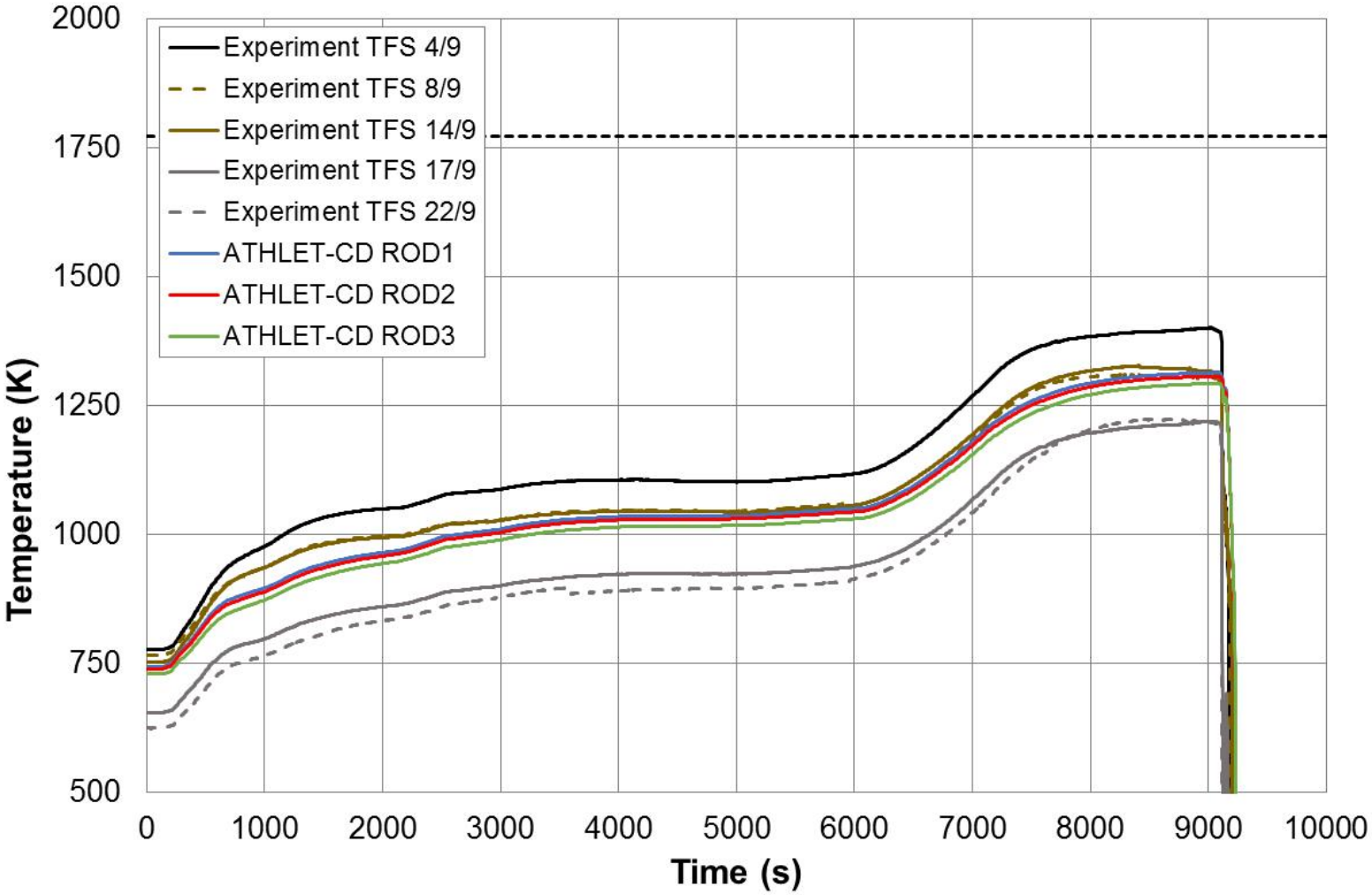


- Boundary conditions from data file
- Oxidation model for FeCrAl implemented as given by KIT
- Constant FeCrAl / Al_2O_3 properties instead of Zry / ZrO_2 properties



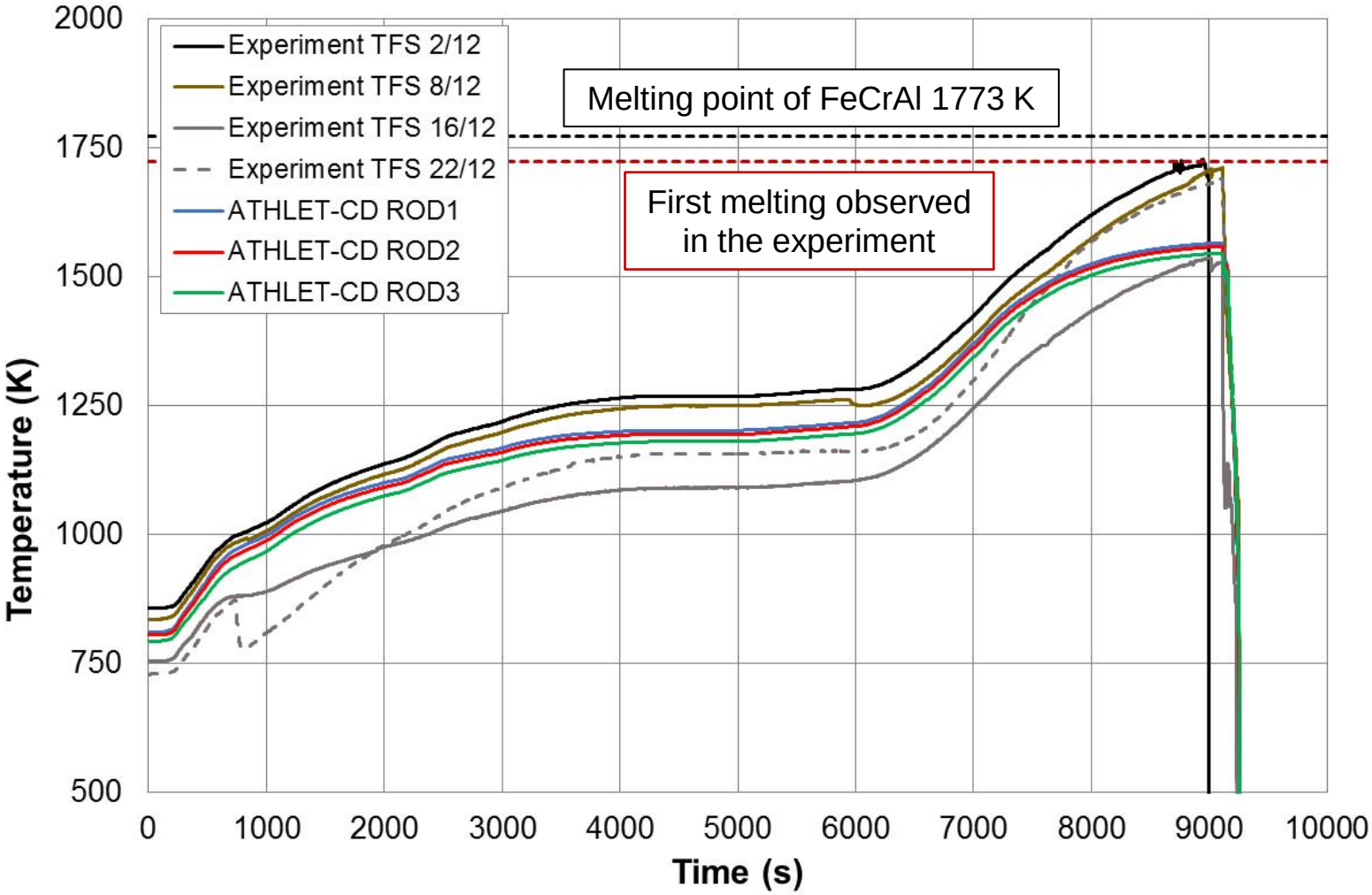
QUENCH-19: Results

- Temperatures at 550 mm



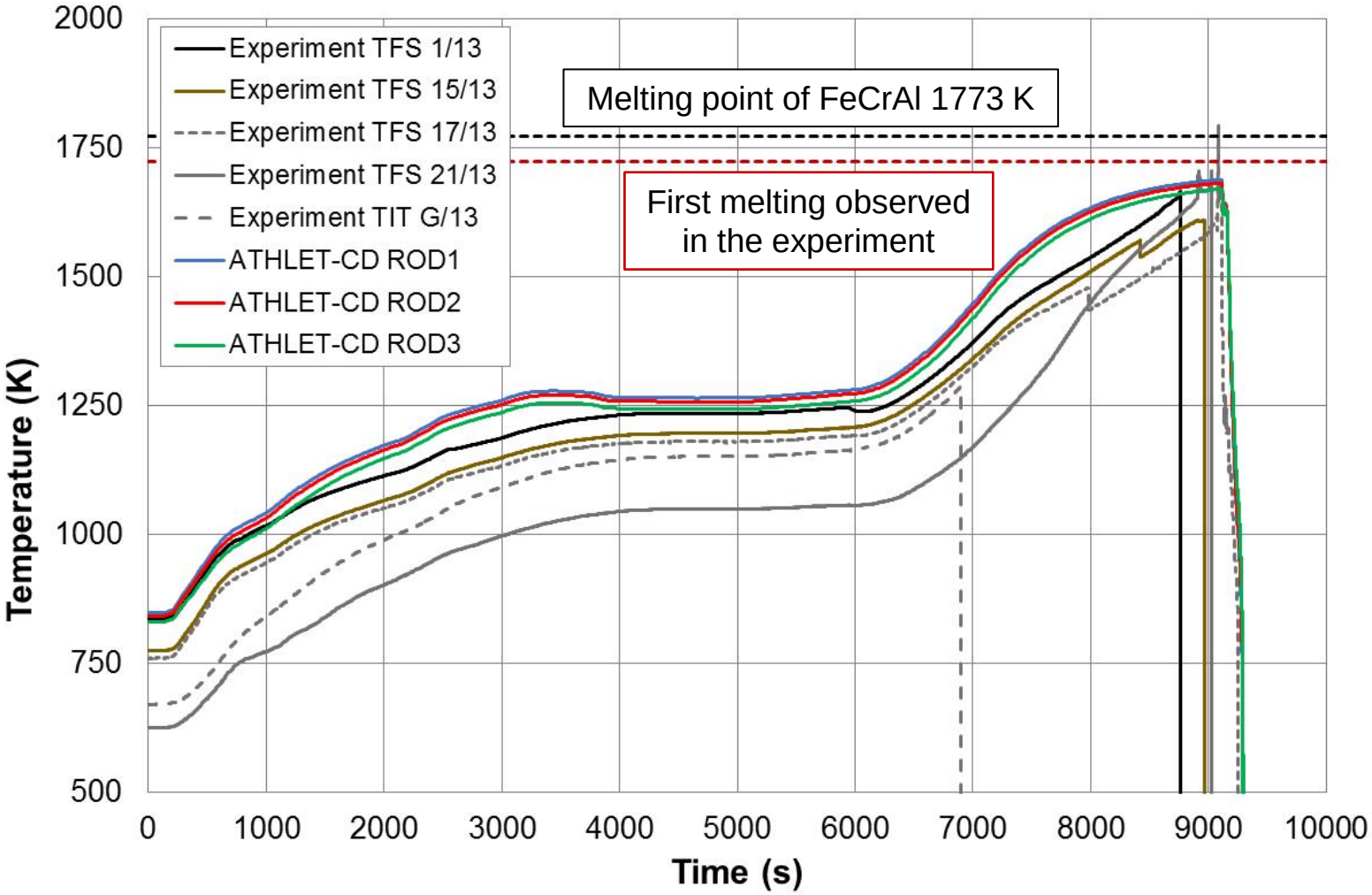
QUENCH-19: Results

- Temperatures at 850 mm



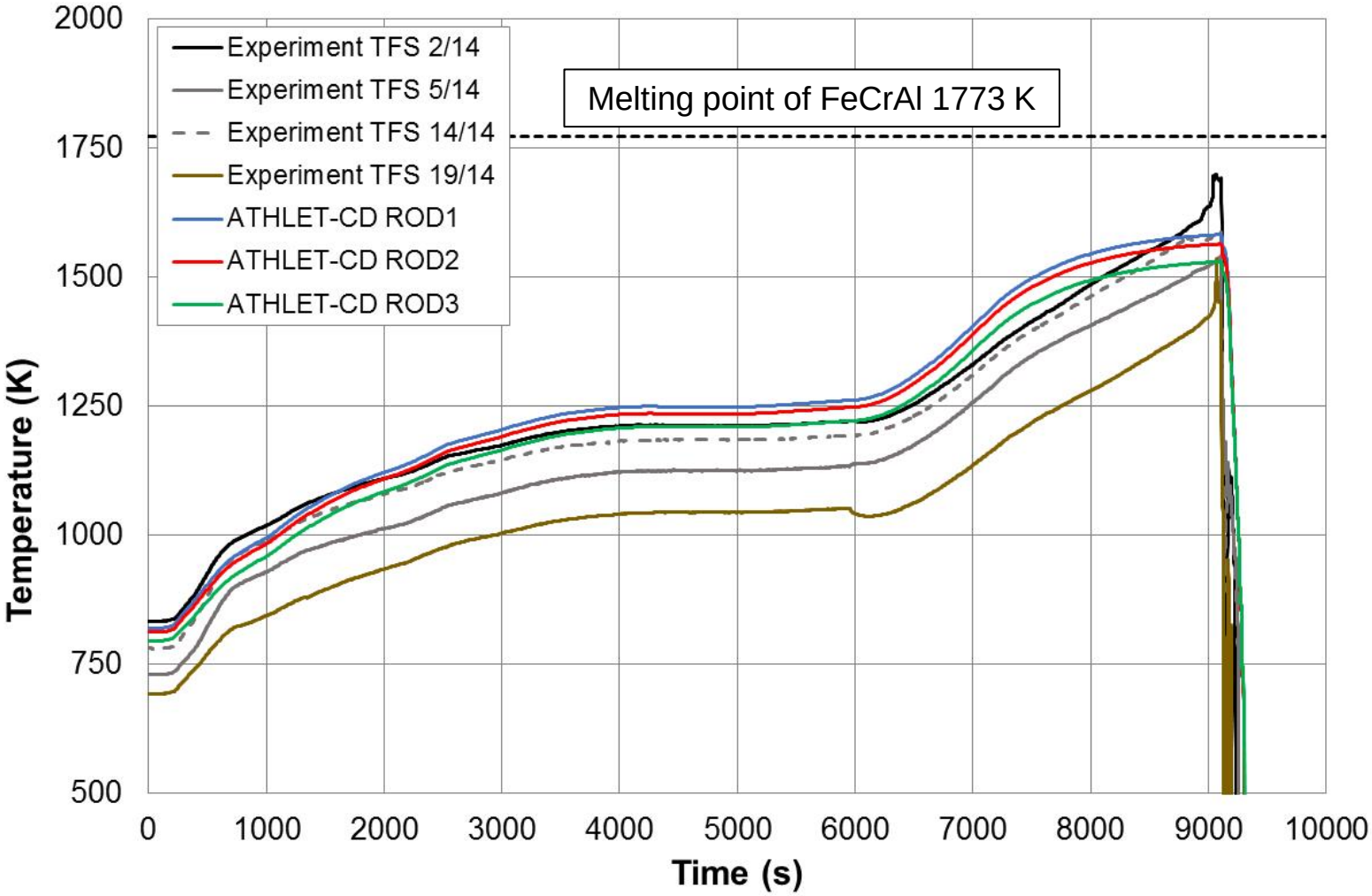
QUENCH-19: Results

- Temperatures at 950 mm



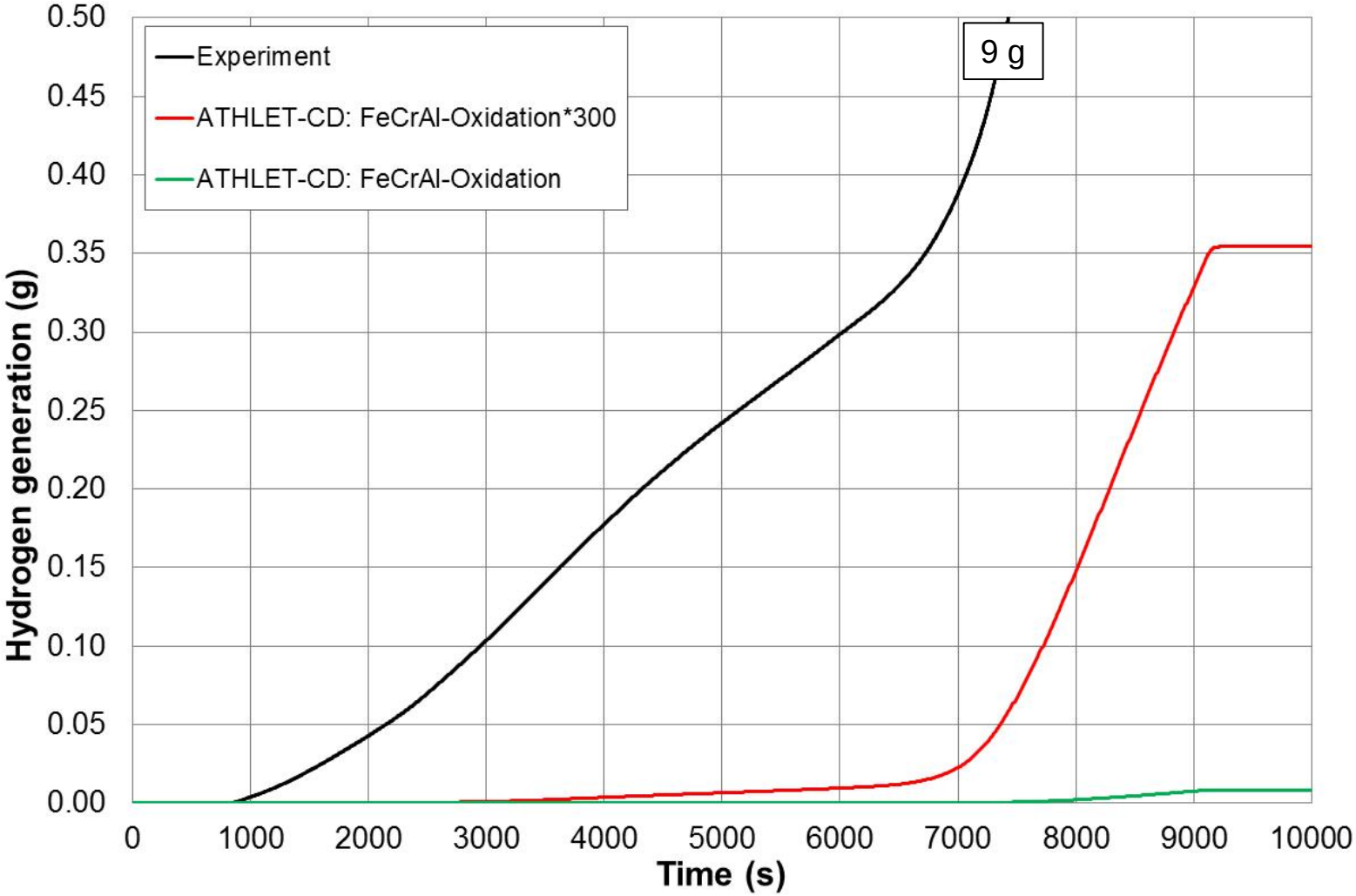
QUENCH-19: Results

- Temperatures at 1050 mm



QUENCH-19: Results

- Hydrogen production



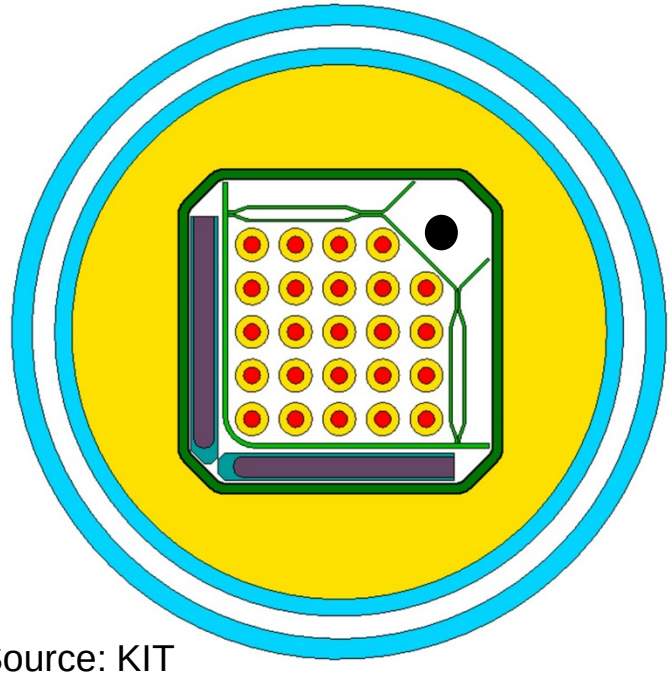
QUENCH-19: Conclusions

- No temperature escalation is simulated
  - Max T_{exp} 1730K @ 850mm
  - Max T_{sim} 1685K @ 950mm
- No further temperature increase in agreement with the test
- Good agreement of temperature along the heated length
- Overestimation of temperature above the heated length
- H2 generation is significantly lower than measured
  - Further development of FeCrAl oxidation is needed
- Furthermore, the observed beginning of melting which may lead to accelerated oxidation is not modelled and could be one additional point for model improvement

QUENCH-20

QUENCH-20: Experiment

- Performed at KIT 2019. October 9.
- BWR configuration
- Westinghouse bundle parts (clad, channel box, spacer grids, absorber blades, part of B_4C pins)
- Quadratic Zr shroud
- Bundle configuration:
  - 24 heated rods with tungsten (W) heater
  - ZrO_2 pellets
  - Zy-2 clad with ZrSn inner liner
  - 1 corner rod (withdrawn after pre-oxidation)
  - 5 spacer grids



Source: KIT

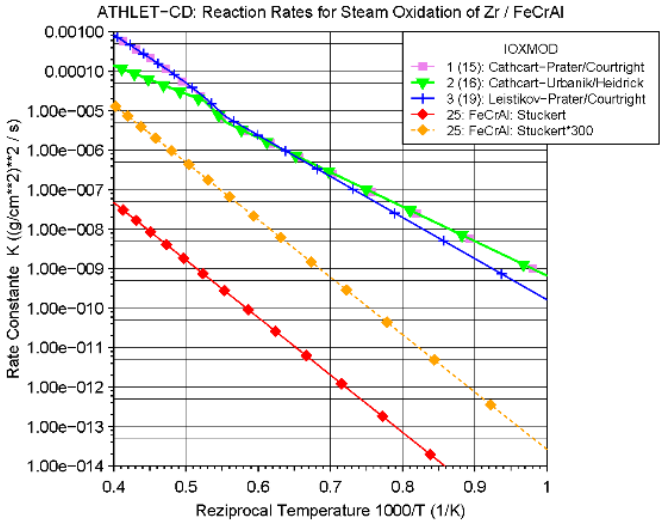
QUENCH-20: Modelling with ATHLET-CD

- Basis: standard ATHLET-CD input deck for Quench 15
- Bundle configuration implemented as given by KIT (1)
- Fluid Channels
  - Bundle: 53% of core within the canister → ROD1: all rods are summed up due to BWR configuration
  - Bypass: 47% of the core area surrounding the canister
- Boundary conditions as given by KIT
- Target values
  - T_{max} at beginning of quenching approx. 2000K @950mm
  - $T_{pre\text{-}oxid}$ 1223K
  - Oxide layer thickness ~100 µm after 4 hrs of pre-oxidation

(1) J. Stuckert, Status of the preparation of the QUENCH-SAFEST bundle test; Cadarache, 11.12.2018

QUENCH-20: Modelling with ATHLET-CD

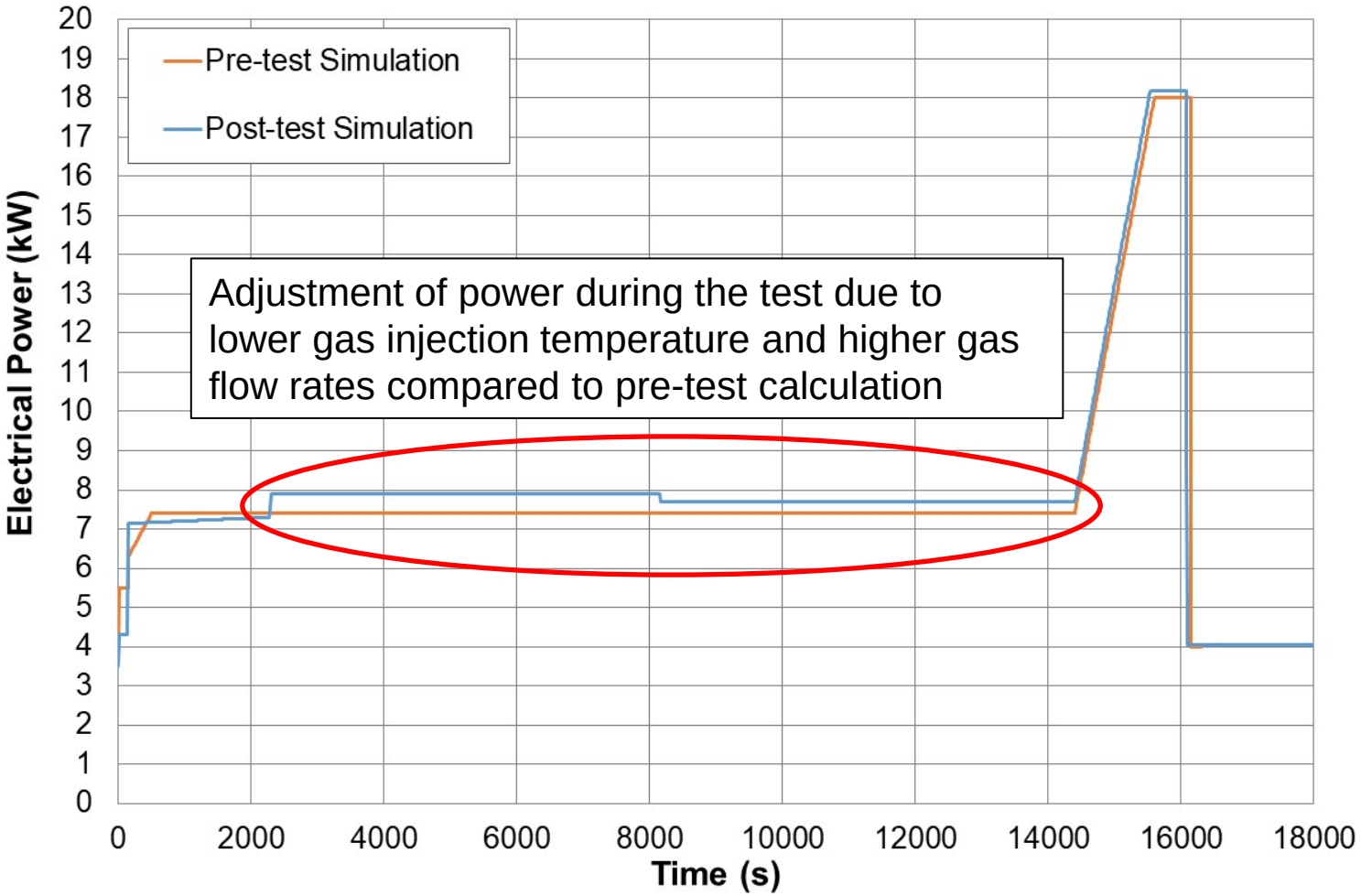
- New model for B_4C oxidation for BWR-absorber (2)
  - Based on PWR B_4C oxidation
  - Arrhenius approach
- BWR model for reactor applications is used
  - T_{melt} of eutectic SS/B_4C absorber blade 1550K
  - T_{melt} of Zry canister 2300K
- Oxidation model for fuel rods and BWR canister (Zr*)
  - Pre-test: Cathcart / Prater-Courtright
  - Post-test: Cathcart / Urbanic-Heidrick
- No transition to accelerated oxidation is considered



(2) C. Bals, H. Austregesilo, Modellierung der Borkarbid-Oxidation für Absorber-Elemente von Siedewasserreaktoren in ATHLET-CD 3.1B, TN-MIS-18/1, Juni 2018

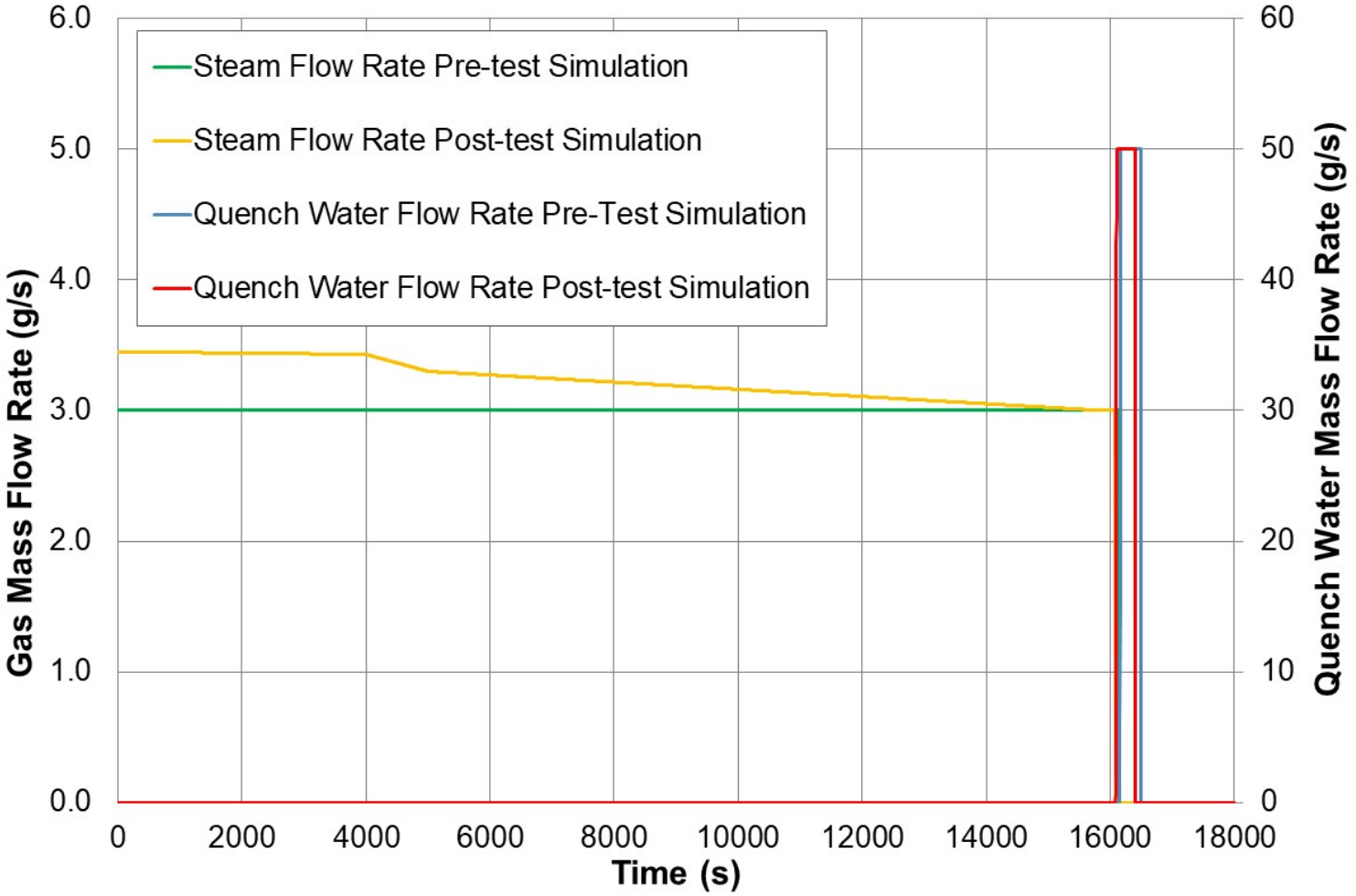
QUENCH-20: Results

- Boundary conditions



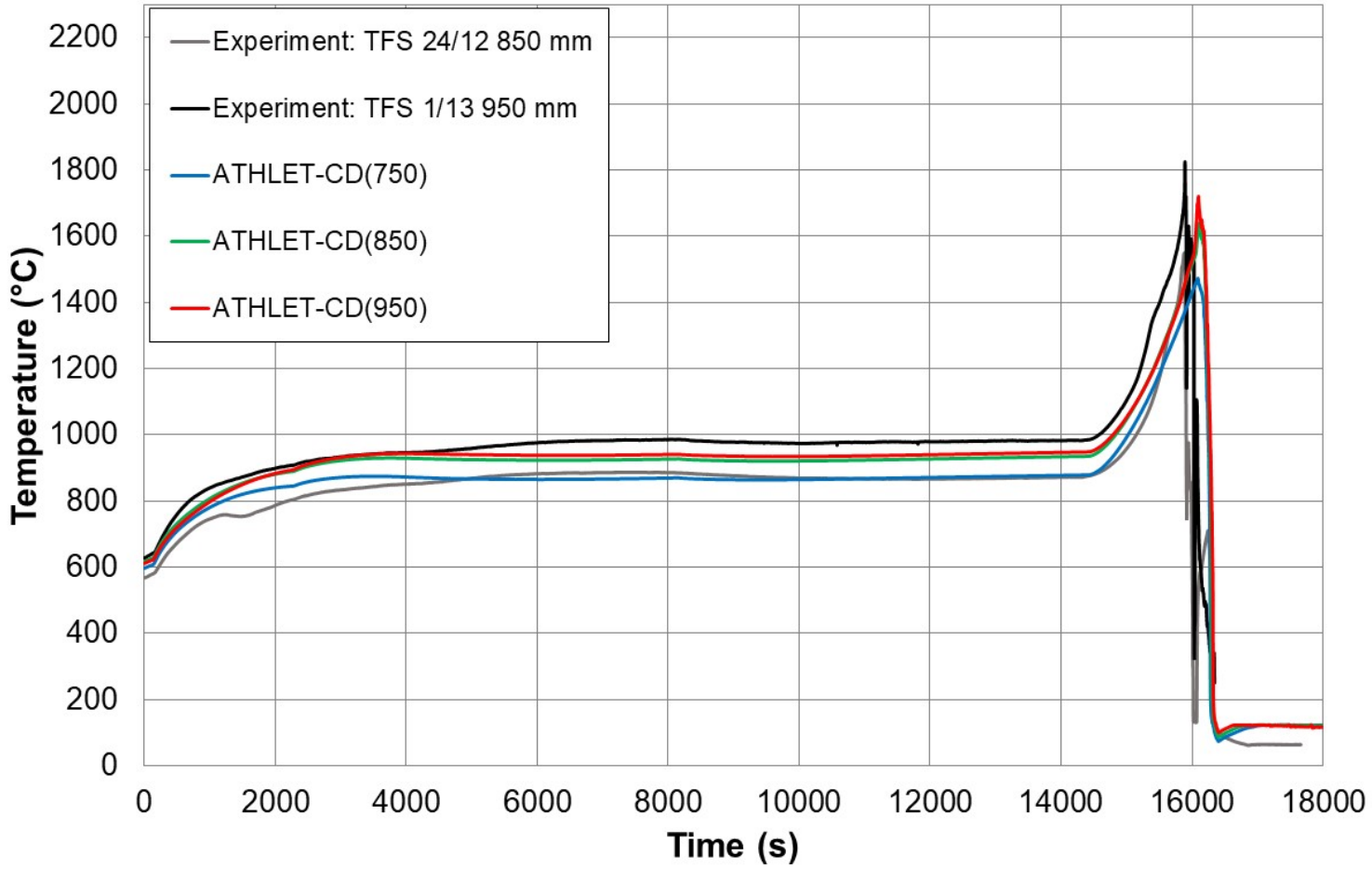
QUENCH-20: Results

- Boundary conditions



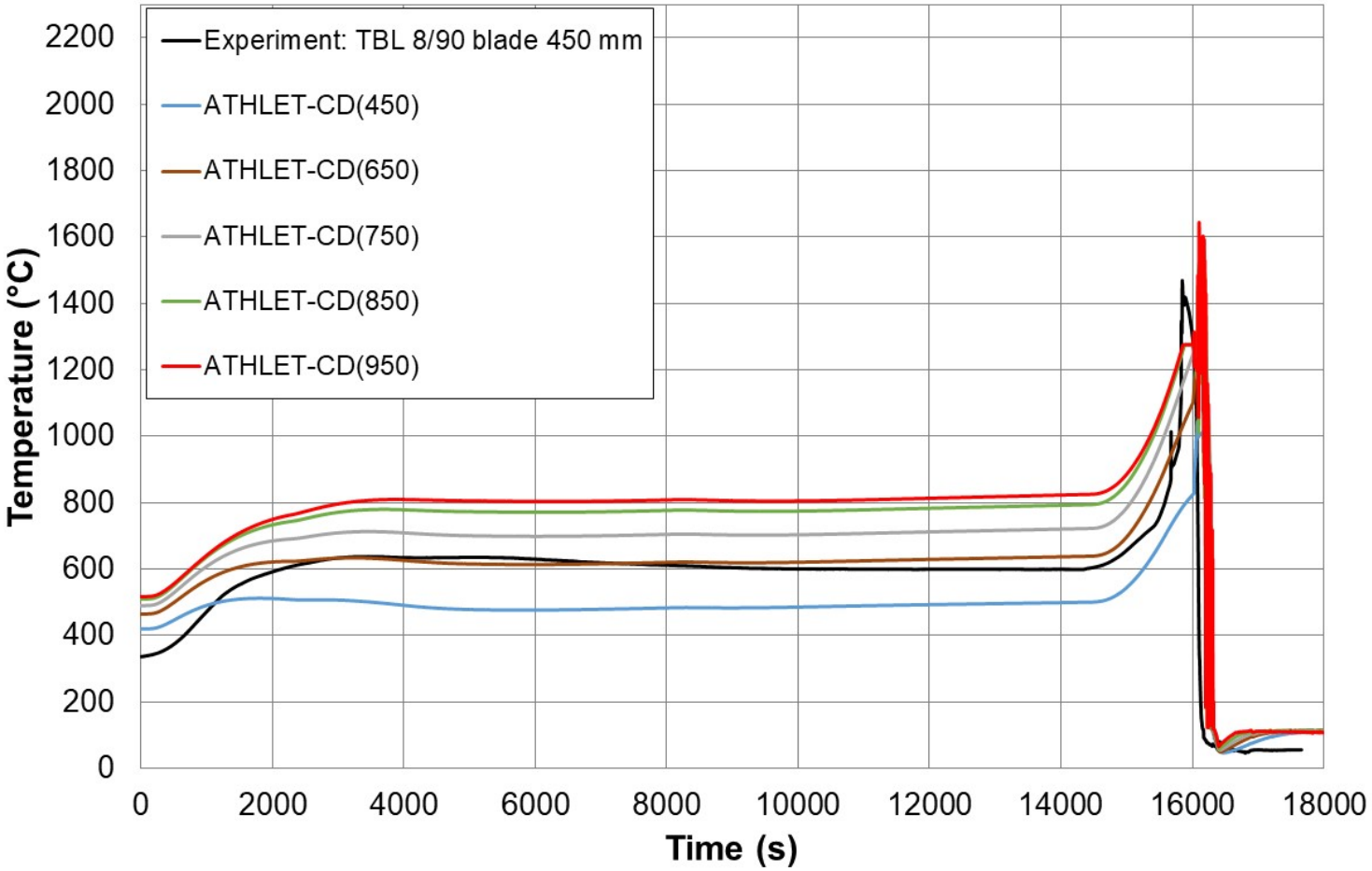
QUENCH-20: Results

- Cladding temperatures



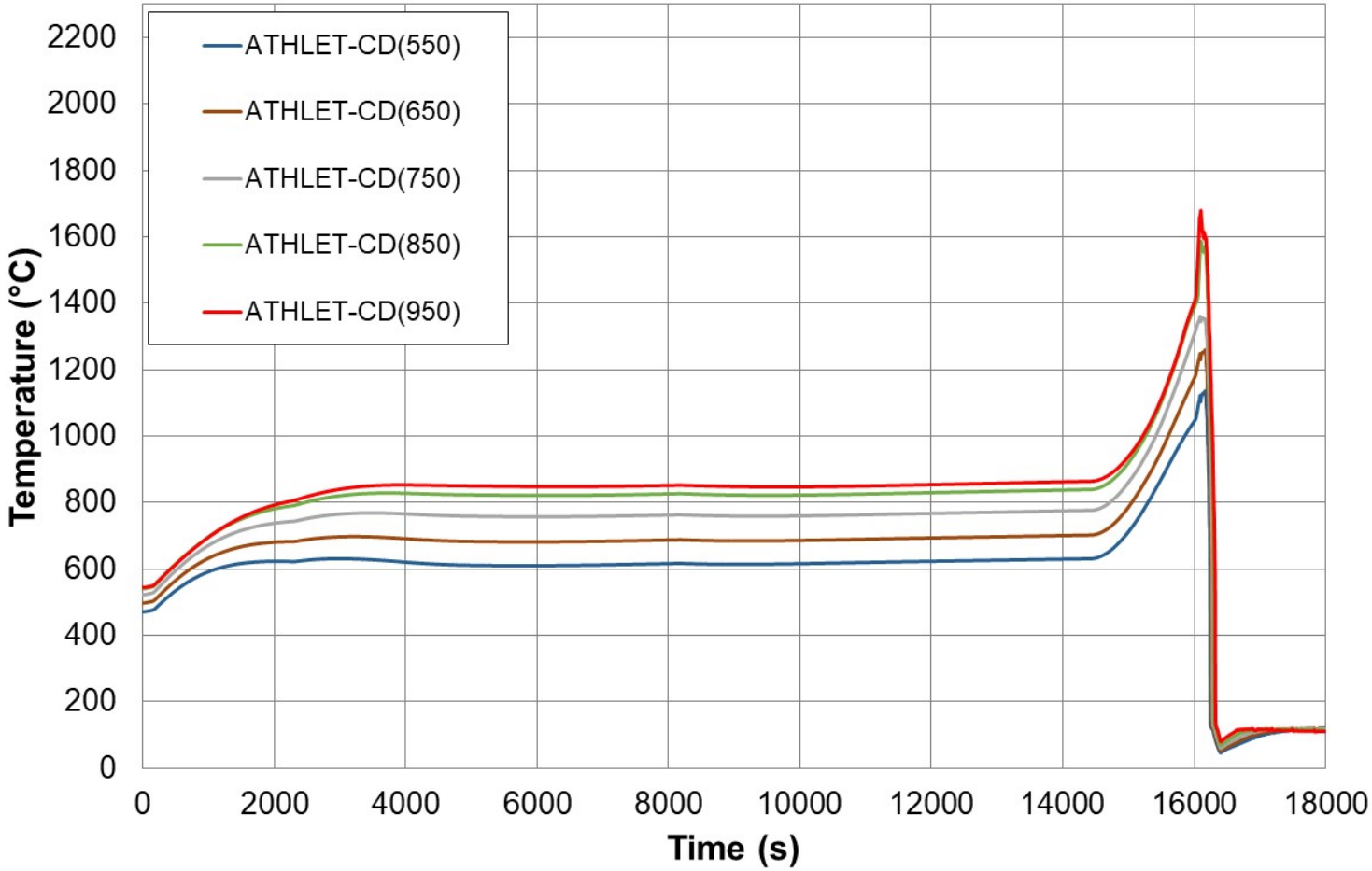
QUENCH-20: Results

- Absorber surface temperatures



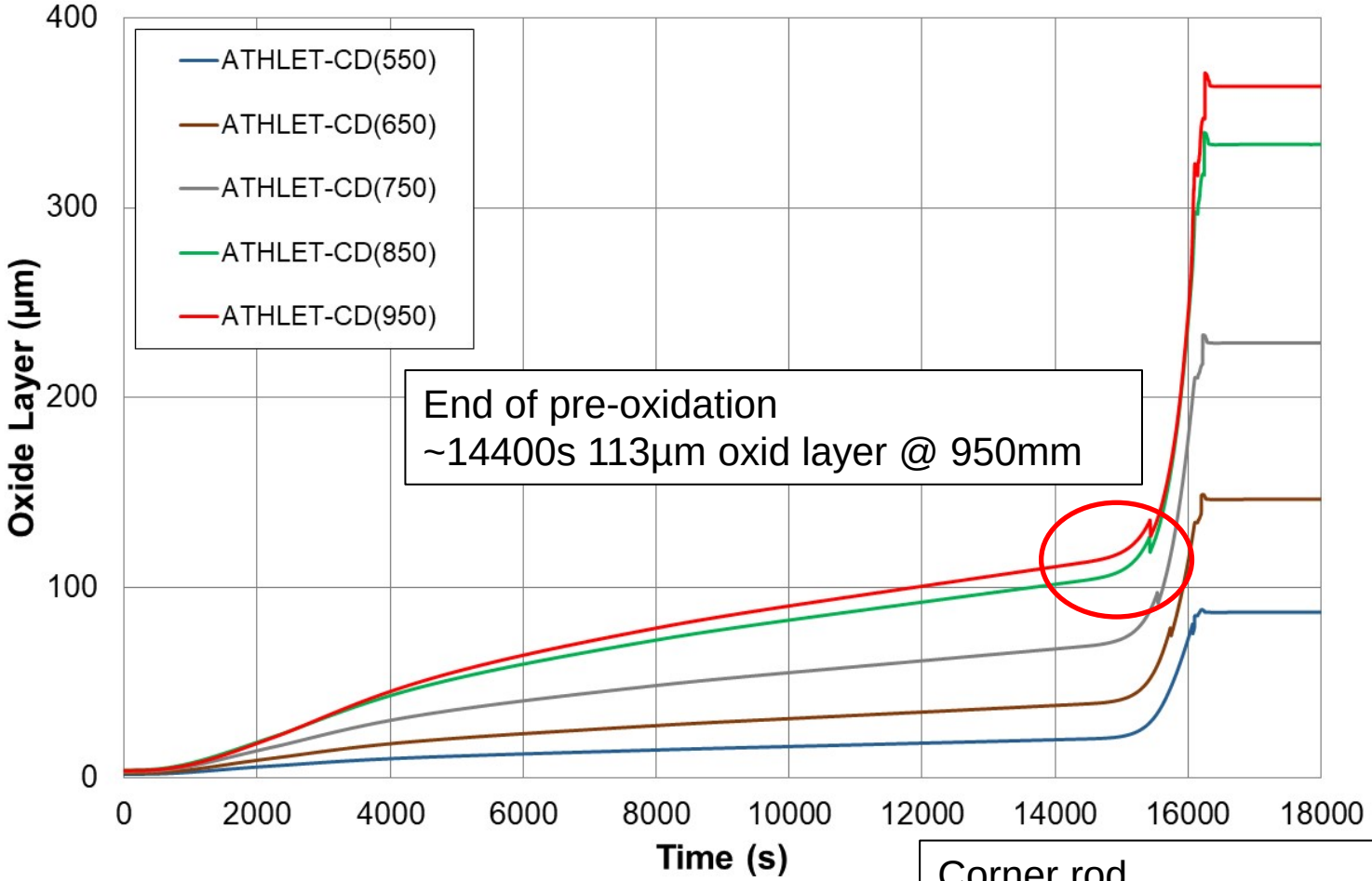
QUENCH-20: Results

- BWR canister temperatures



QUENCH-20: Results

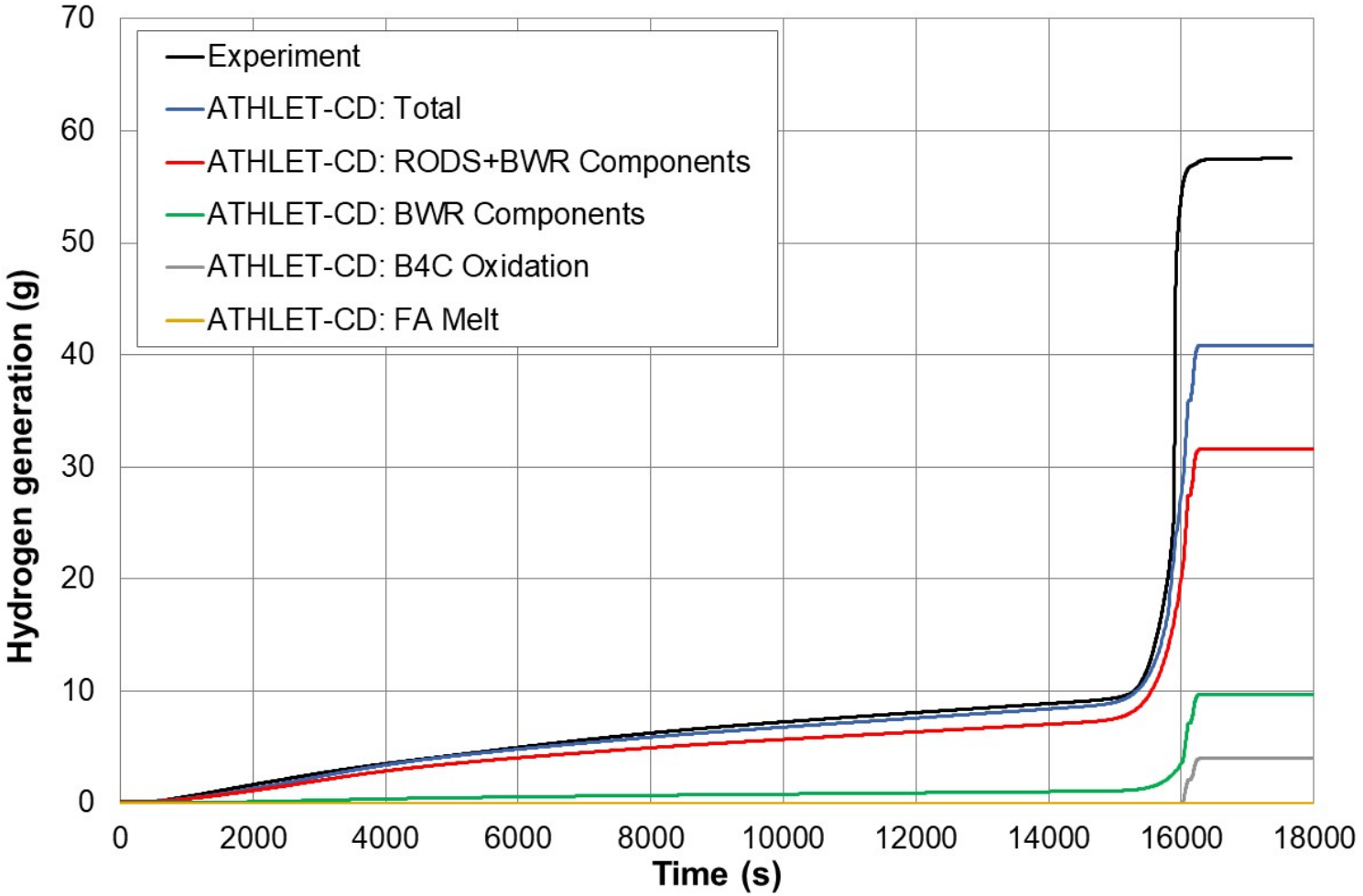
- Oxide layer thickness in the middle of the bundle



Corner rod
~14400s ~65µm oxid layer @ 950mm
Exp. : ~55µm

QUENCH-20: Results

- Hydrogen production



QUENCH-20: Conclusions

- First calculations applying the BCs of the experiment
- Pre-oxidation
  - Power adjustment due to lower steam T and higher mass flow rate
  - Corner rod: ∂_{ox} ~65µm @950mm <-> exp. ∂_{ox} ~55µm
- B4C oxidation
  - CO2 release app. at the same time in the experiment (beginning of reflood) and the calculation (end of transient)
  - CO, CO2 and CH4 composition of the experiment needed for the simulation
- Quench phase
  - Pre-test calc.: quenching at about 1730 °C would lead to a stronger T escalation
  - Experiment, post-test calc.: quenching at about 1700 °C only small T increase

Acknowledgement

The development and validation of AC^2 are sponsored by the German Federal Ministry for Economic Affairs and Energy (BMWi).

Thank you very much for your attention!

Pre-Test Analysis of QUENCH-20 BWR-Bundle with ASTEC

Shisheng Wang (INR), Heinrich Muscher (IAM), Victor Sanchez-Espinoza (INR)

KIT

A pre-test simulation and analysis for QUENCH-20, the first BWR Quench-bundle test ever, has been performed with the latest version of ASTEC code – ASTEC-V2.1.1.4 – being subject of this paper.

The objective of the Quench-20 test was the investigation of a BWR fuel assembly early degradation phase in case of a severe accident. The test bundle mock-up represented one quarter of a BWR fuel assembly, including a cruciform B_4C control blade in order to simulate the eutectic material interaction between stainless steel and B_4C inside absorber blade.

In the ASTEC geometrical modelling, in order to simulate the radiative heat transfer between fuel rods and the assembly canister, the canister itself has been modelled as an equivalent cylinder. The cruciform B_4C control blade has been modelled as equivalent cylinders inside the stainless steel cladding. The thermal boundary conditions on the inner tube of the Inconel cooling jacket were extrapolated from the former QUENCH-8 test results.

The pre-test calculations have shown, that the bundle is expected to be heated up to a temperature of 1030 K at the central rods cladding at the “hottest” elevation of 950 mm during the stabilization phase. During the pre-oxidation phase in steam, which has lasted 1 hour (11500 – 15100s), the corresponding temperature at the Zr cladding of the central heated rod at the “hottest” elevation of 950 mm reached 1710 K (this at 15100s),. In the following transient phase, the power was further increased to initiate the transient heat-up to a maximal temperature of 1910 K, (at 16300 s). At the end of transient phase, approximately one-fourth length of the steel cladding of the B_4C control rod was melted, its position measured from top of the control rod. Roughly, in the region of about half of the length of control rods the eutectic material interaction between stainless steel and B_4C happened.



Pre-Test Analysis of QUENCH-20 BWR-Bundle with ASTEC

ASTEC-Team at KIT
Presenter: S. Wang

Institute for Neutron Physics and Reactor Technology (INR)
Reactor Physics and Dynamic Group (RPD)



Content

- Motivation
- Quench-20 experiment
- ASTEC Modeling & Input
- Calculation Result & Analysis
- Summary

Motivation

- **The new Version of ASTEC, It's capabilities to simulate BWR-bundle tests;**
- **Pre-test Simulation Results to support experiment staffs;**
- **To review the ASTEC capabilities to simulate BWR Plants.**

Quench-20 Experiment

Quench Experimental Facility

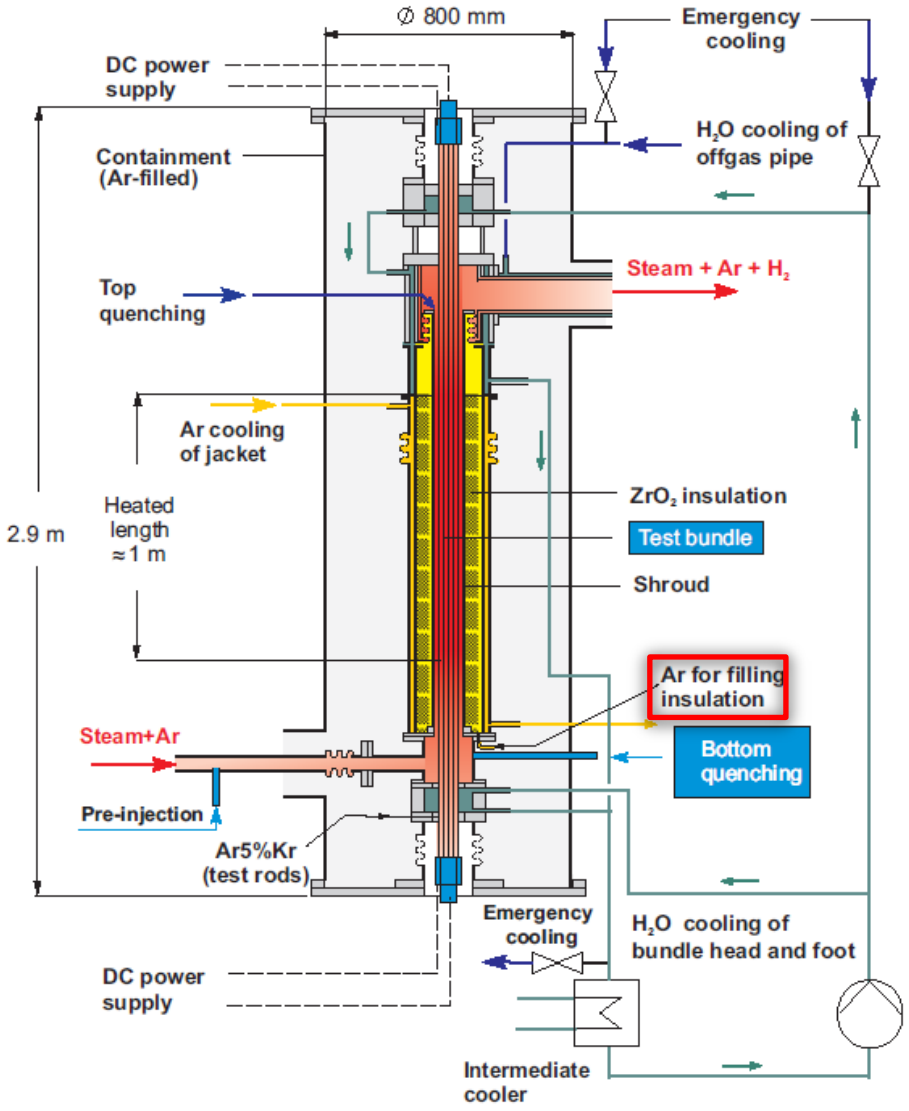
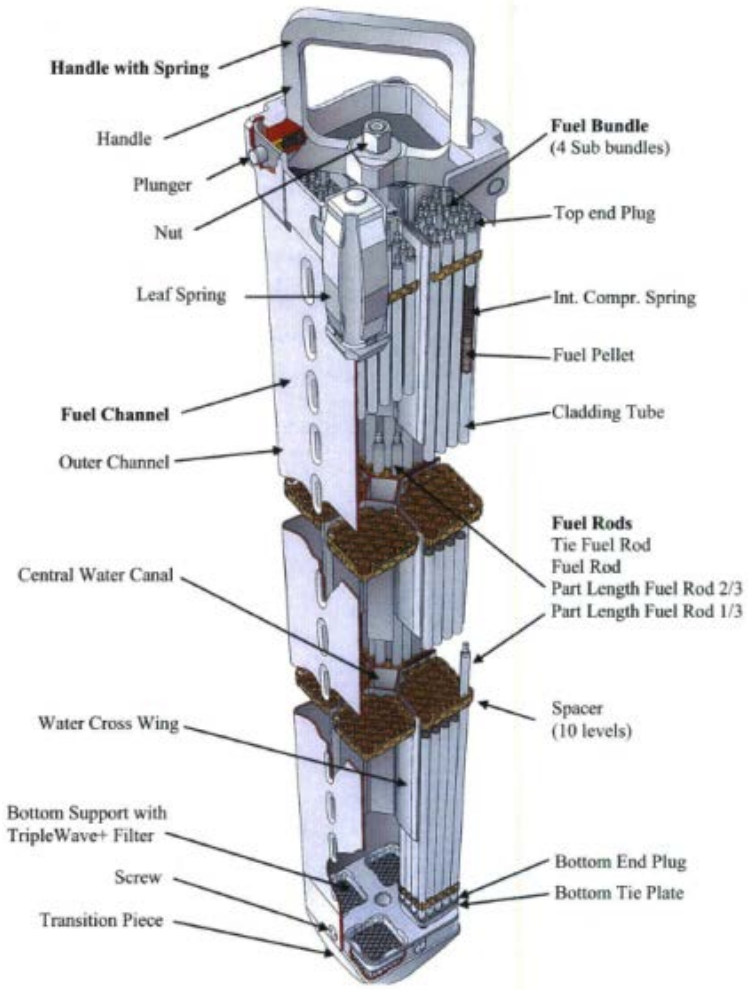


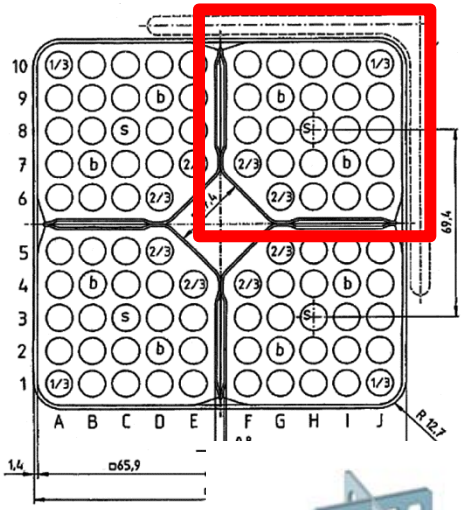
Fig. 4: QUENCH test section; flow lines

- The main component of the QUENCH facility is the test bundle
- Superheated steam + argon as a carrier gas enters the bundle at the bottom
- The argon, the not consumed steam, the generated hydrogen exit the bundle at the top.
- The reflooding water enters the test section through a separate line at the bottom of the bundle

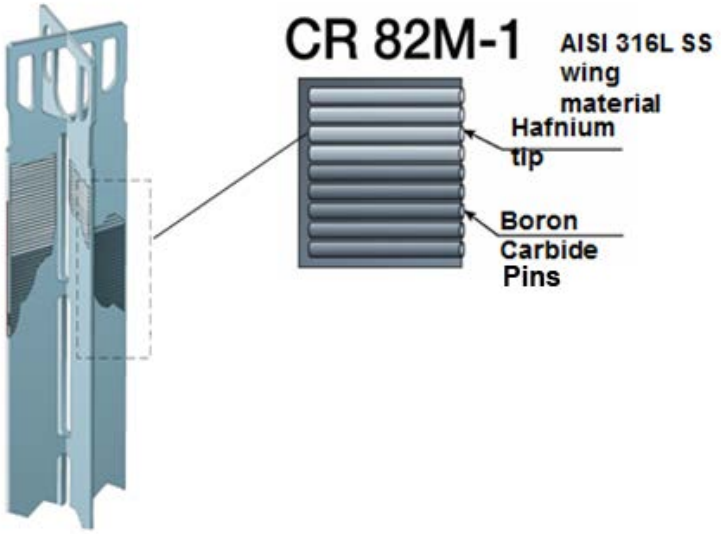
Pre-test simulation of QUENCH-20 (SAFEST)



Assembly SVEA-96 Optima

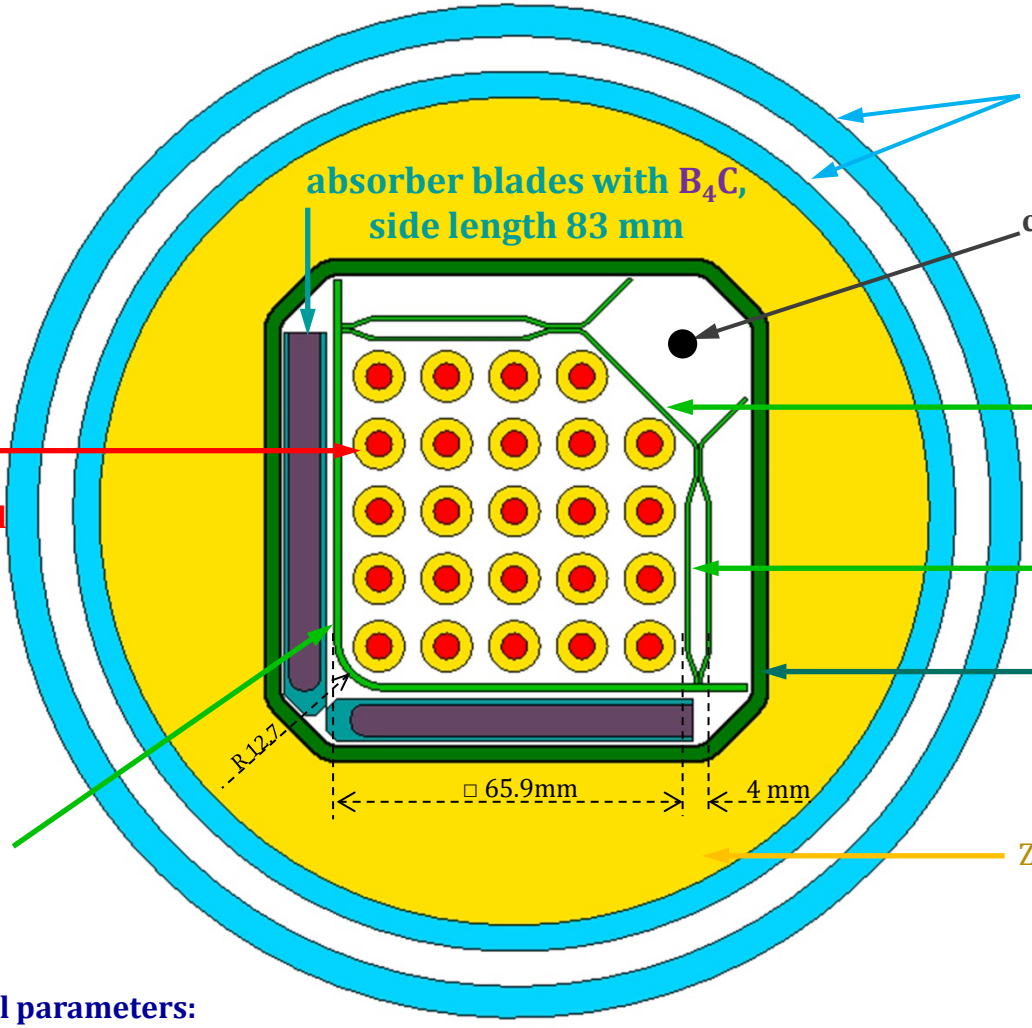


SSM proposal: study of high temperature degradation of BWR assembly mock-up in QUENCH facility (melt formation due to eutectical material interaction inside absorber cross)



Absorber cross blade

QUENCH-20: suggested test bundle composition (¼ SVEA-96 OPTIMA2 assembly)



Inconel cooling jacket, inner tube ID=158.3 mm

corner rod (Zry-4, OD 6 mm)

water channel box (ZIRLO), side length 27.4 mm

water cross wing (ZIRLO), wall thickness 0.8 mm

Zr shroud 86 mm, wall thickness 3 mm

ZrO_2 porous thermal insulation

heated rods (24): cladding Zy-2 with inner ZrSn-liner (10% of clad), ZrO_2 pellet OD 8.48mm and ID 5.2 mm, length 10 mm, W heater OD 5 mm

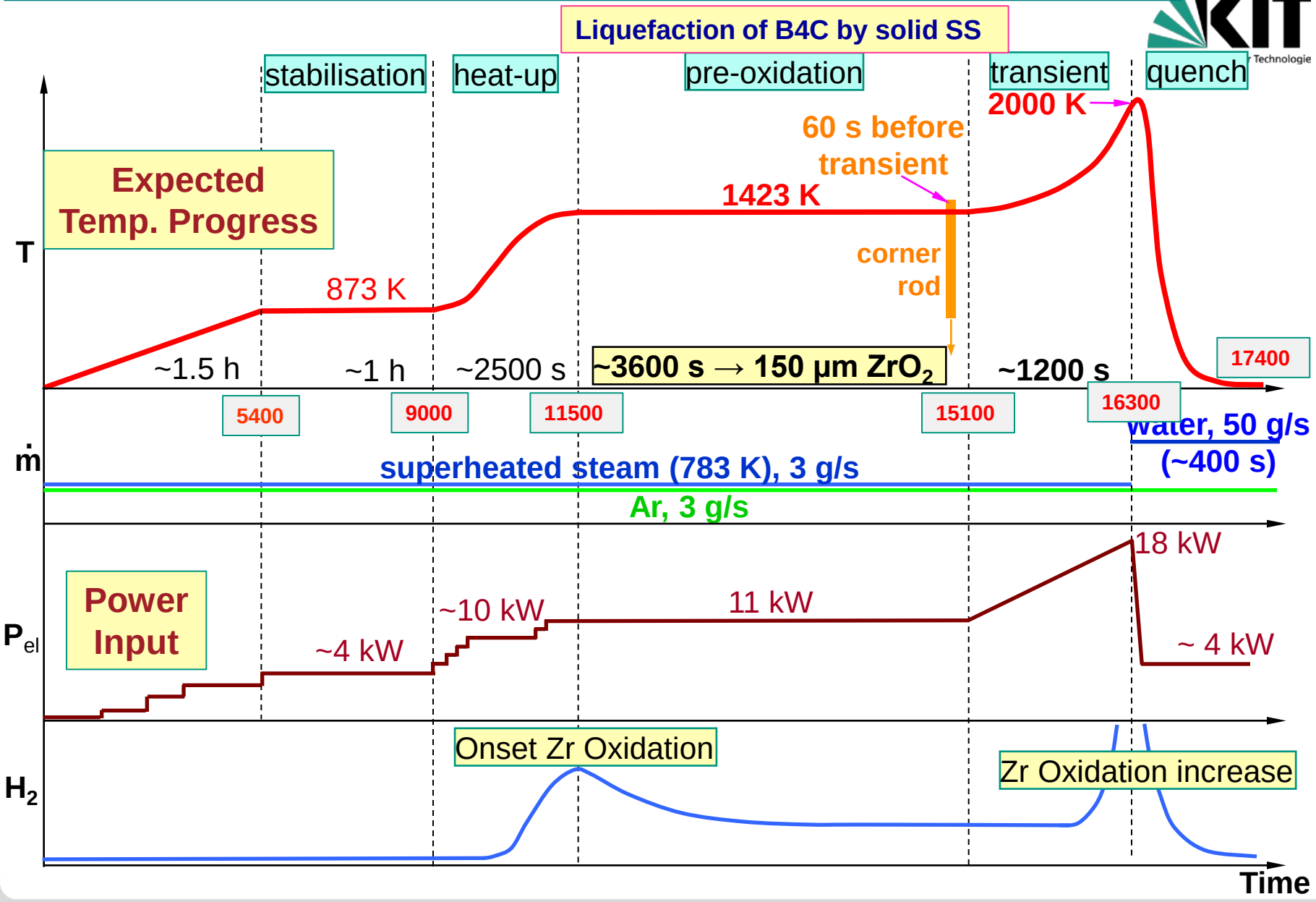
advanced low tin ZIRLO fuel channel box, wall thickness 1.4 mm

Geometrical parameters:

- bundle pitch 12.898 mm;
- outer diameter of claddings 9.84 mm;
- thickness of claddings 0.605 mm;
- absorber blades: thickness 8.05 mm

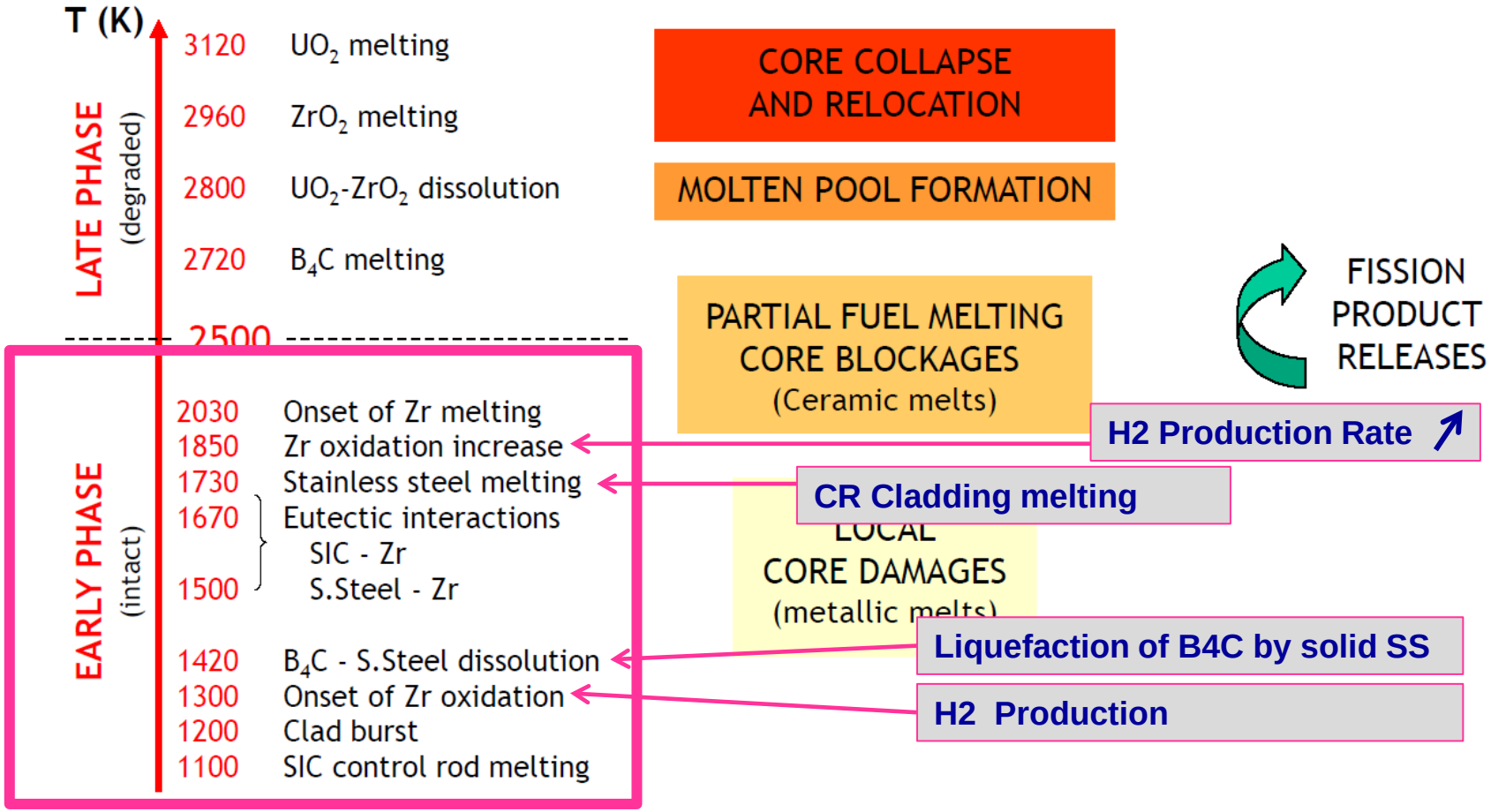
- cladding length 2500 mm
- absorber and channel box lengths 1600 mm

Suggested scenario for QUENCH20-SAFEST



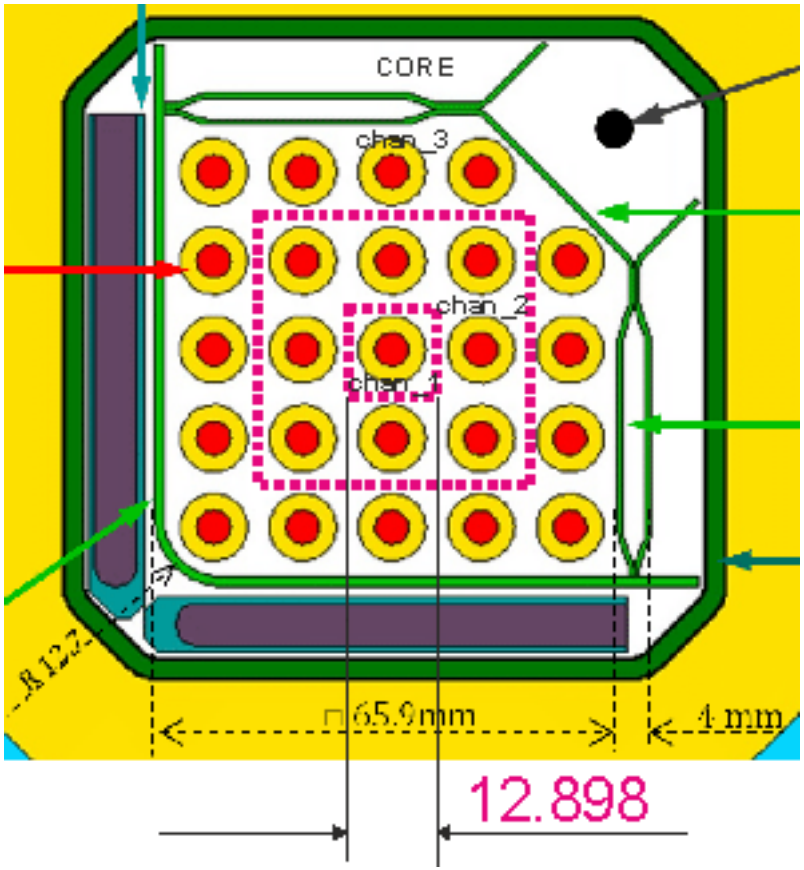
Core degradation modelling

Main phenomena to take into account

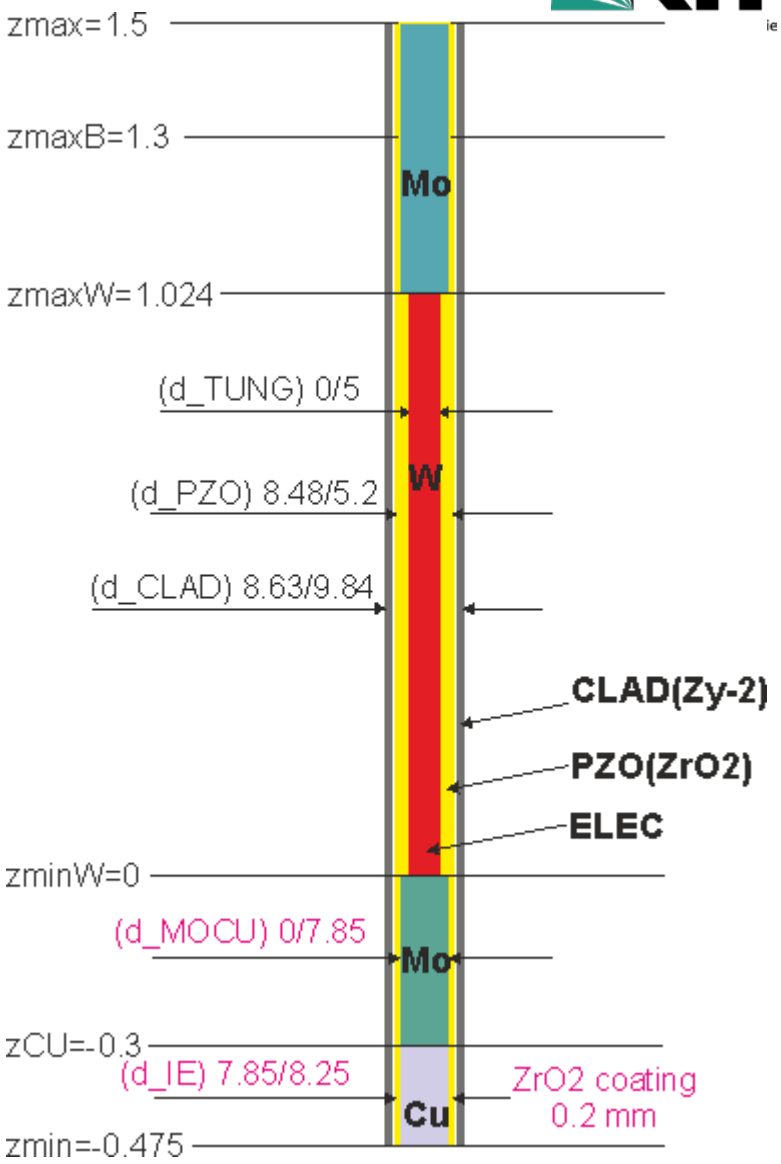


ASTEC Modeling & Input

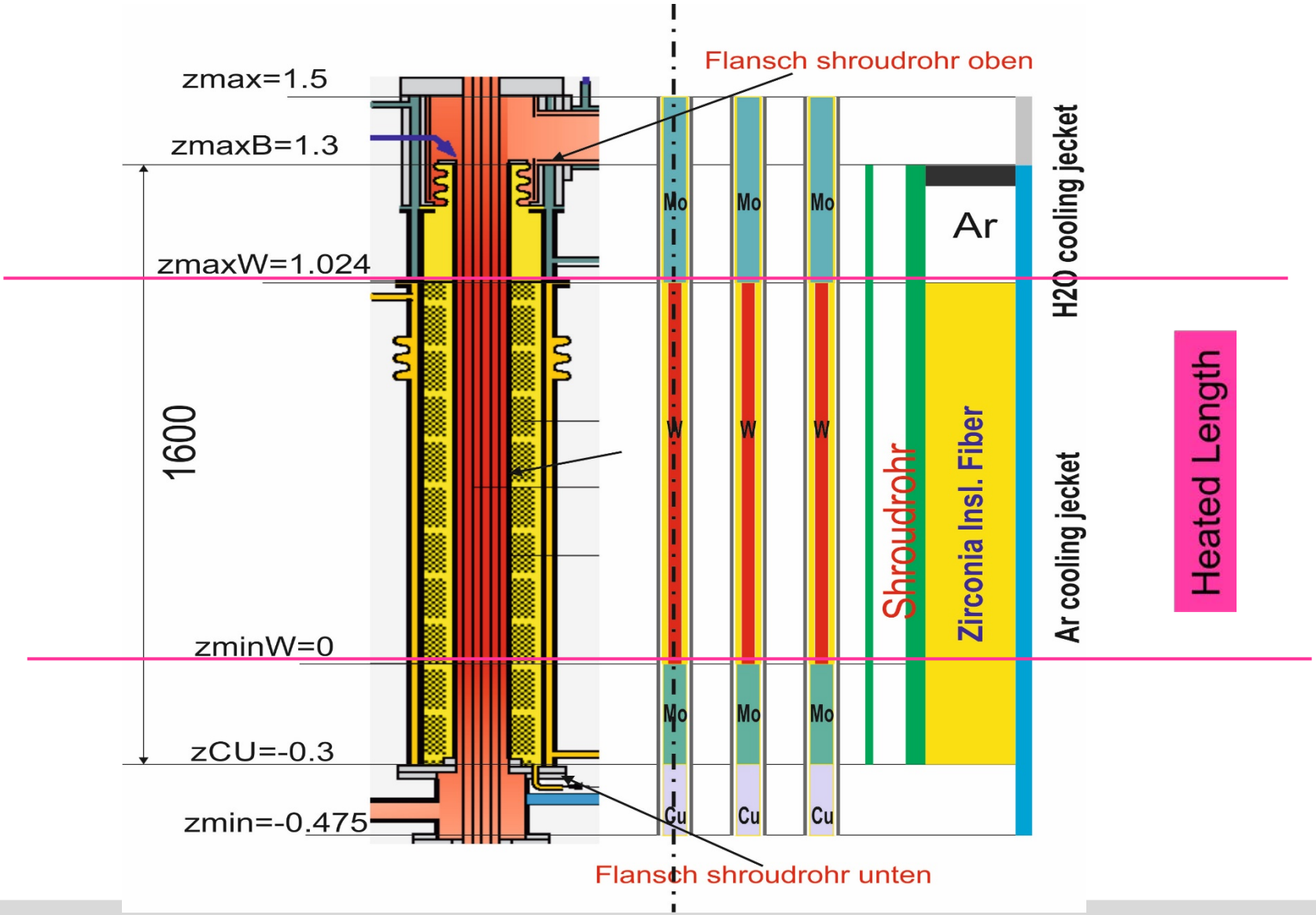
Quench-20 Cross Section and Heated Rod



3 Channels



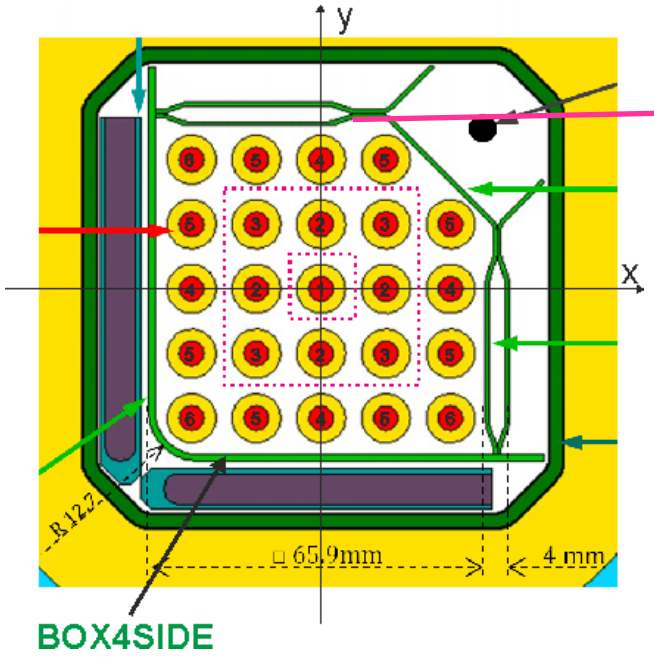
Quench- 20 Bundle Axial Arrangement

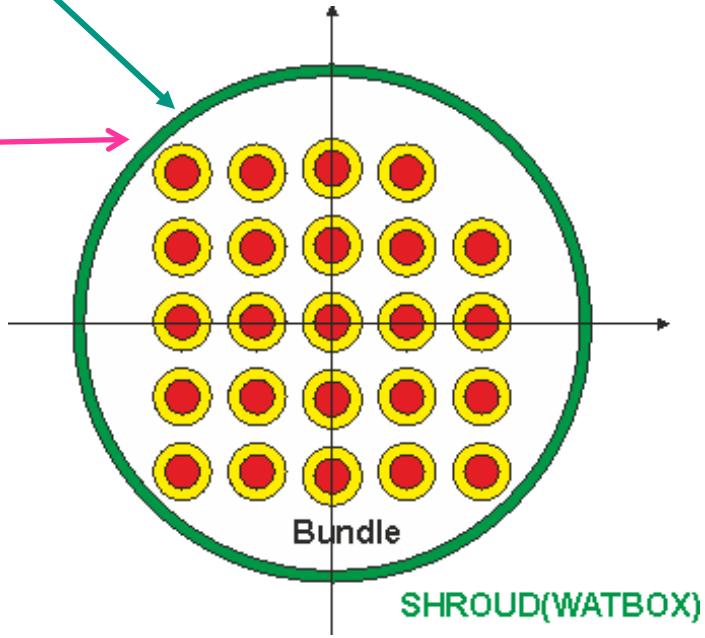


HT: Radiative heat exchanges in a bundle

STRU RADB

[bundle]: geometic parameters
[bundle]: location parameters
[**shroud**]: diameter; **Obligatory:** **cylinder**
[radiative model]: parameters

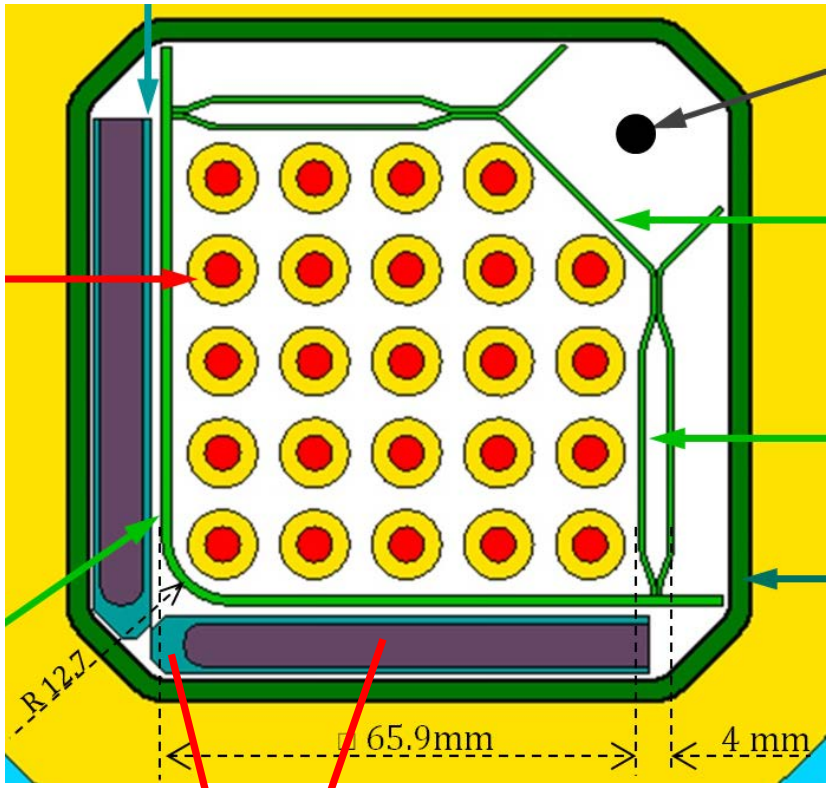




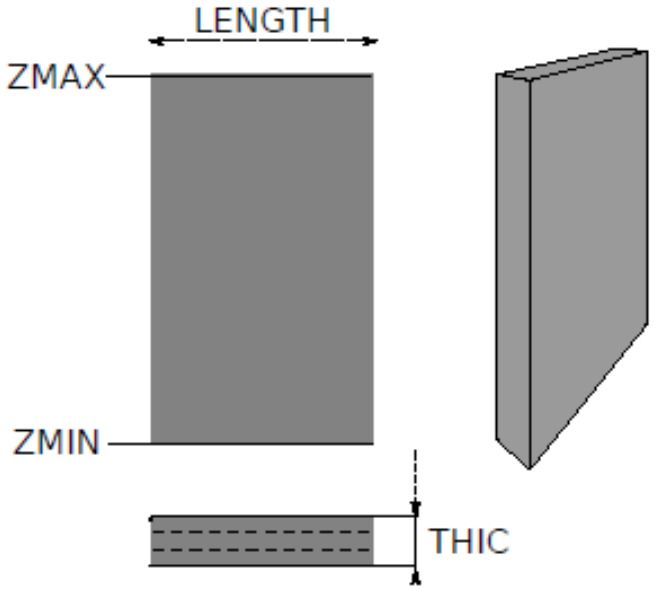
Shroud type: cylinder

Oxidation B4C & liquefaction of B4C by solid SS (1/4)

- **Oxidation of B_4C** module: **Vessel: BCOX**
- **B_4C – S. Steel** dissolution module: **Vessel: BCSS**



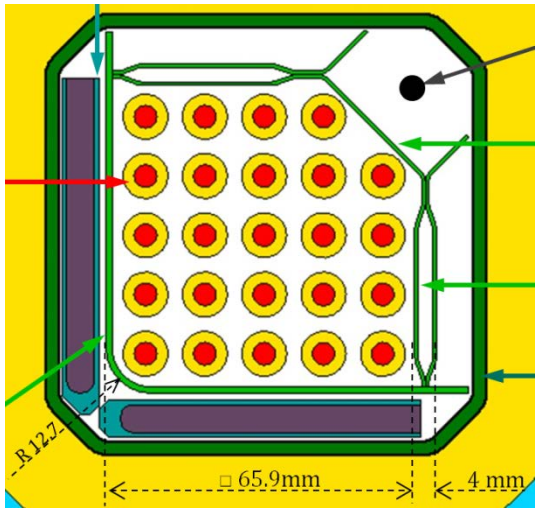
- **B_4C**
- **Stainless Steel**

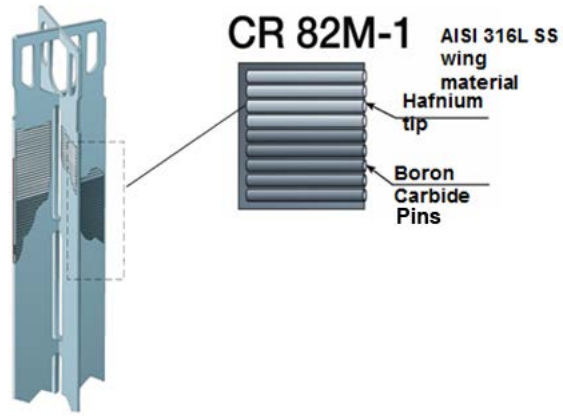


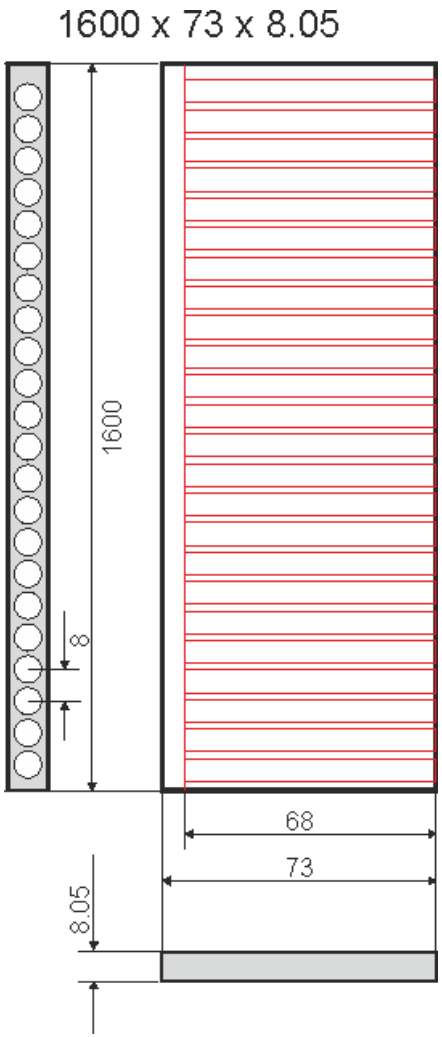
MACRO WALL

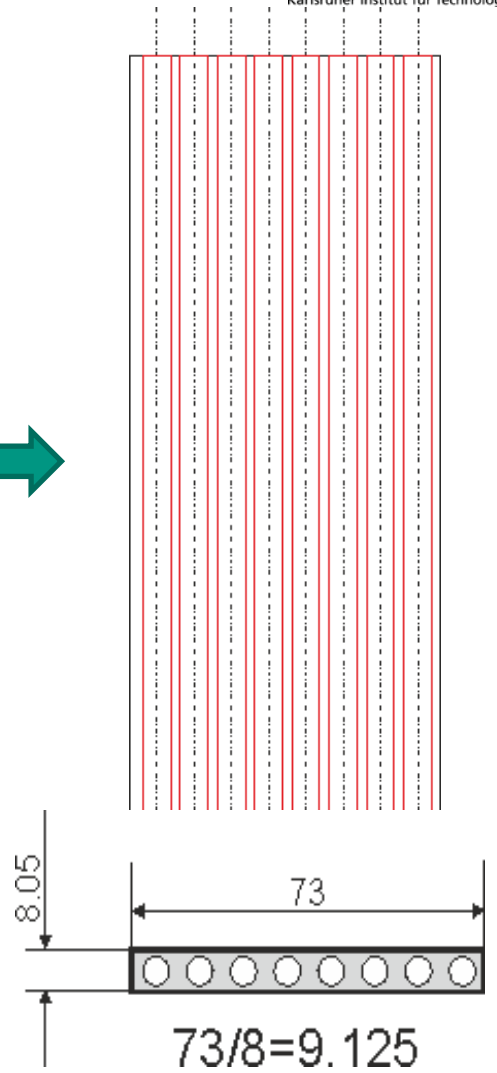
It is not possible: cylinder in wall .

Oxidation B4C & liquefaction of B4C by solid SS (2/4)





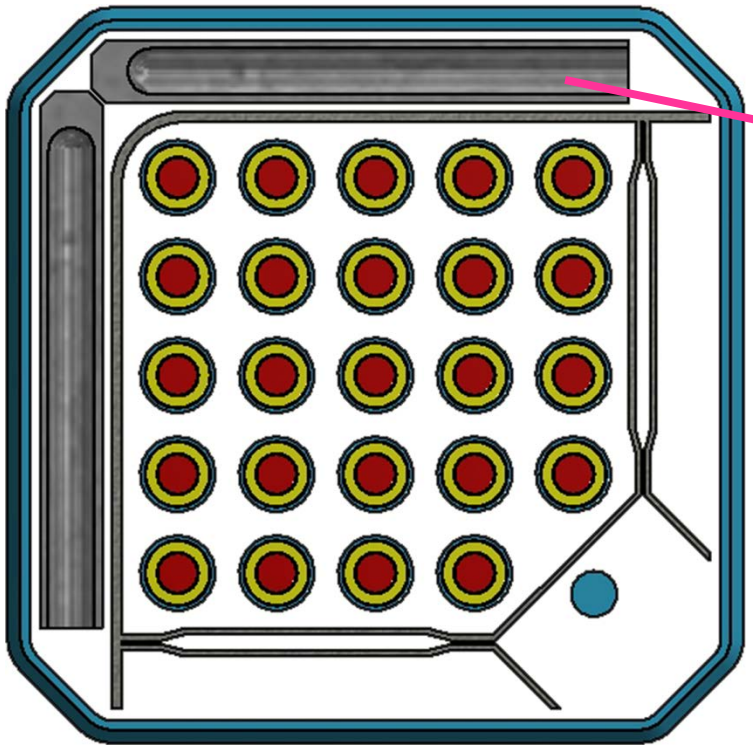


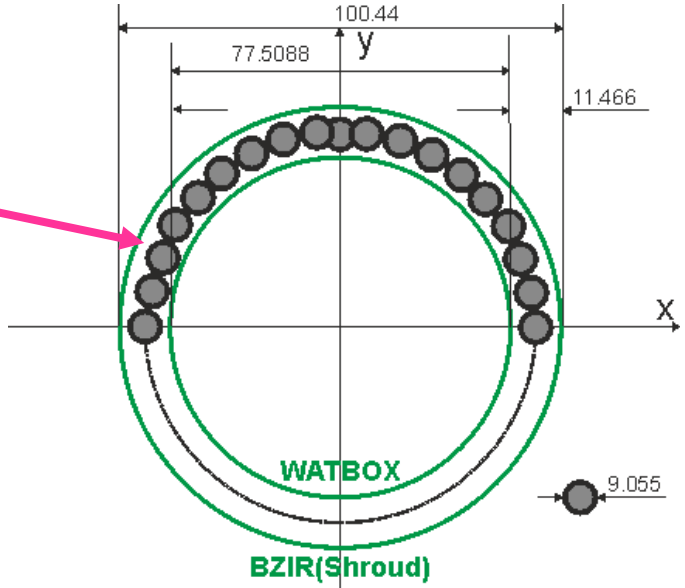


B_4C blade (Exp.)

B_4C blade (Model)

Oxidation B4C & liquefaction of B4C by solid SS (3/4)





WATBOX:d=77.5088 **BZIR(Shroud)=100.44**

CR_ring:d=(77.5088+100.44)/2=88.9744
r_CR_ring=44.4872

d=sqrt(8.05*8*4/Pi)=9.055

pitch=09.055

number=Pi*44.4872/pitch=15.43

Oxidation B4C & liquefaction of B4C by solid SS (4/4)

WATBOX-Bundle-Shroud radiation Heat exchange

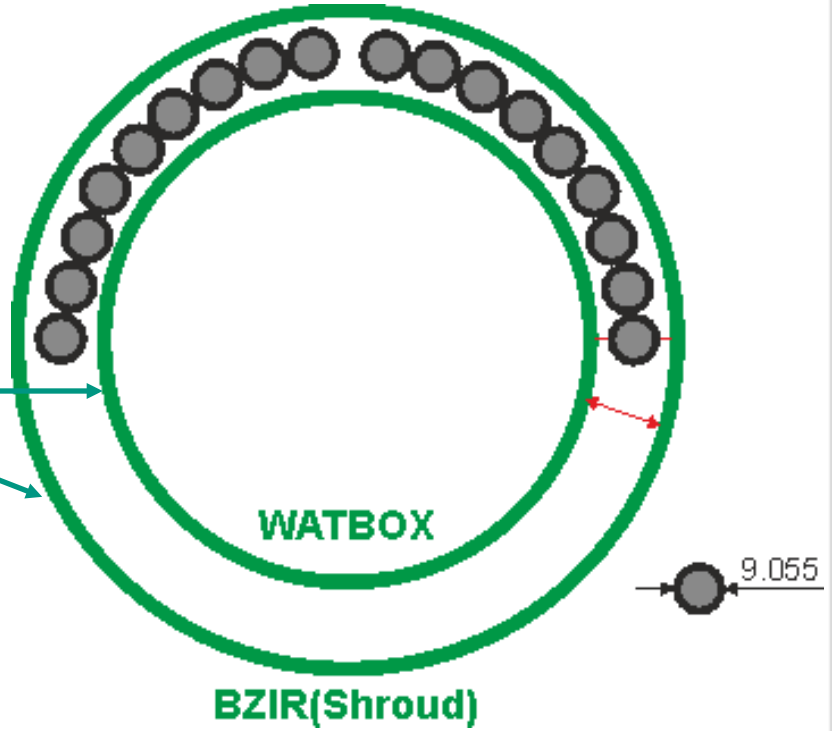
STRU RADB

[bundle]: **WATBOX: positon & geometry**

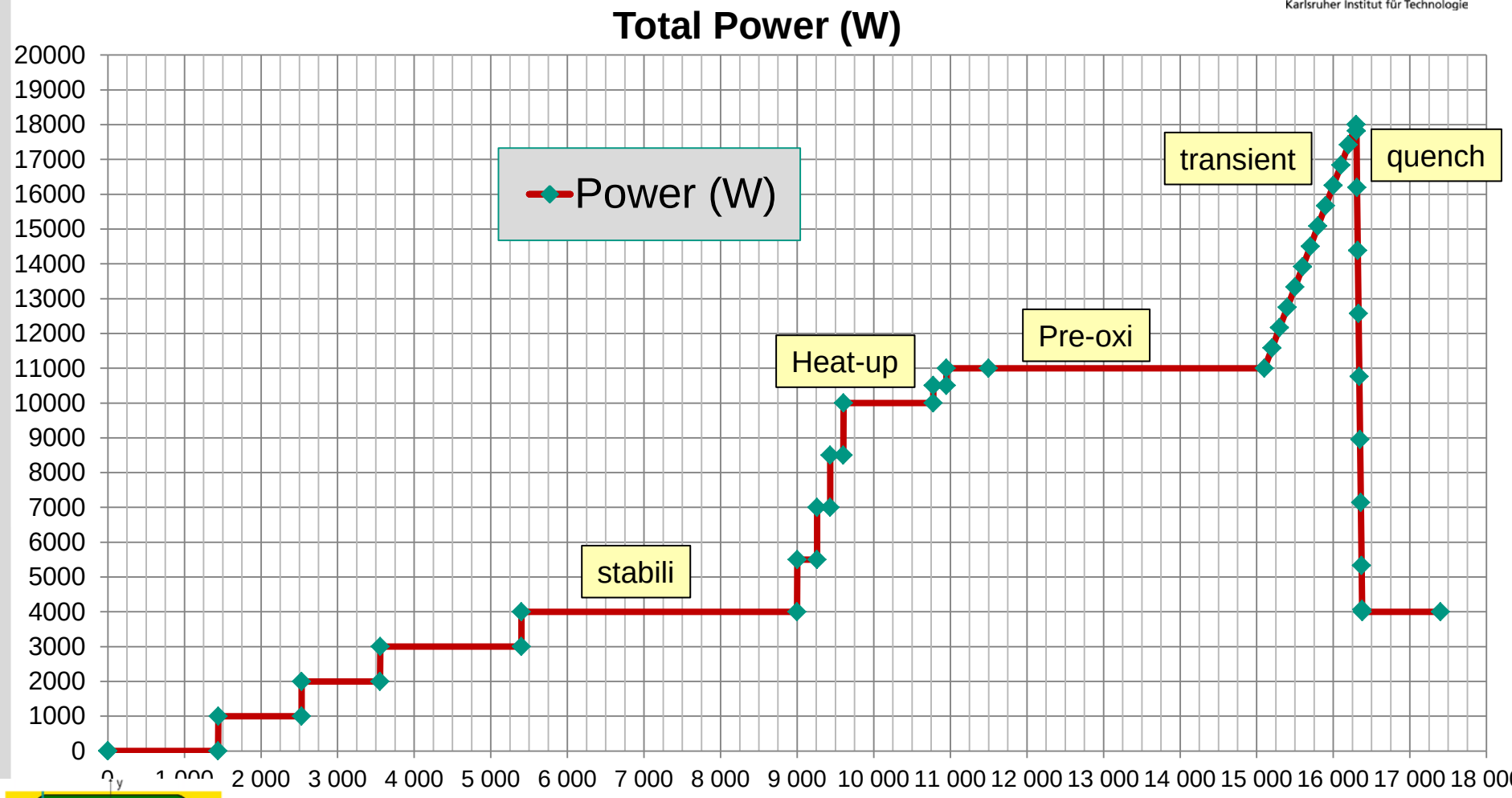
[bundle]: **CR cylinders: postions & geom.**

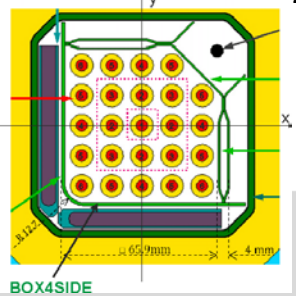
[**shroud**]:shroud ; Obligatory: **cylinder**

[radiative model]: parameters



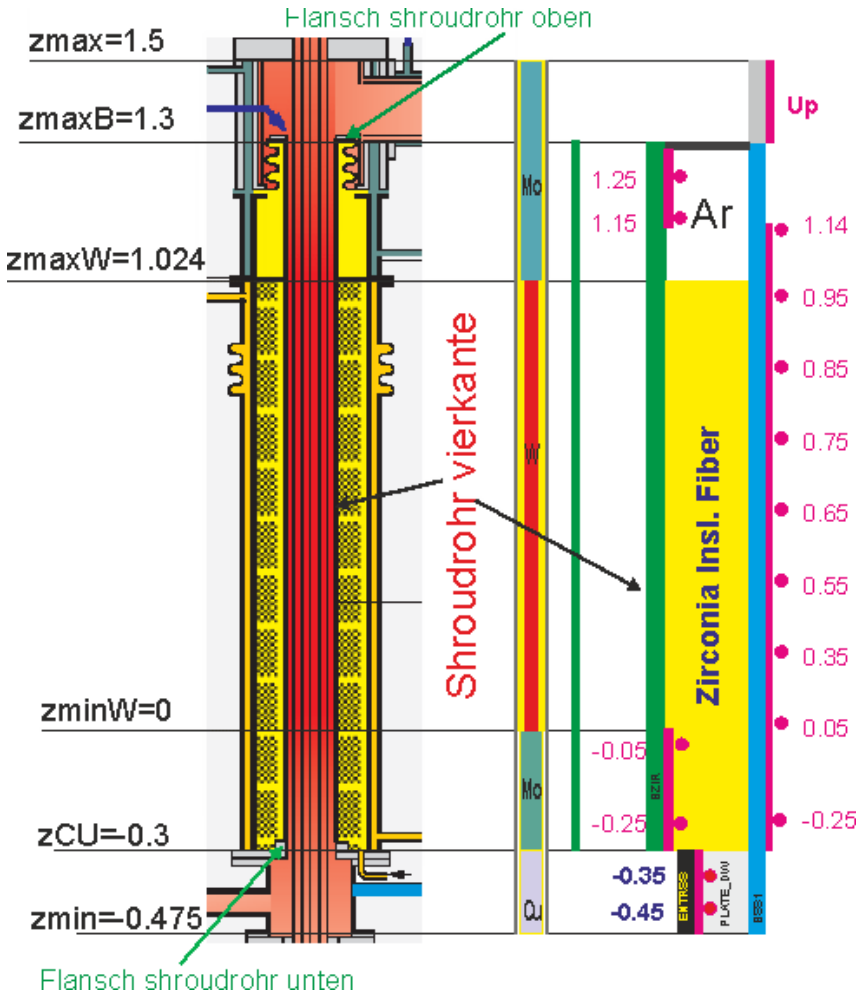
Total Power Input & Power distribution in bundles





Power in Channel (i)= Power * [(bundle_number_in_channel (i)] / [total_number]

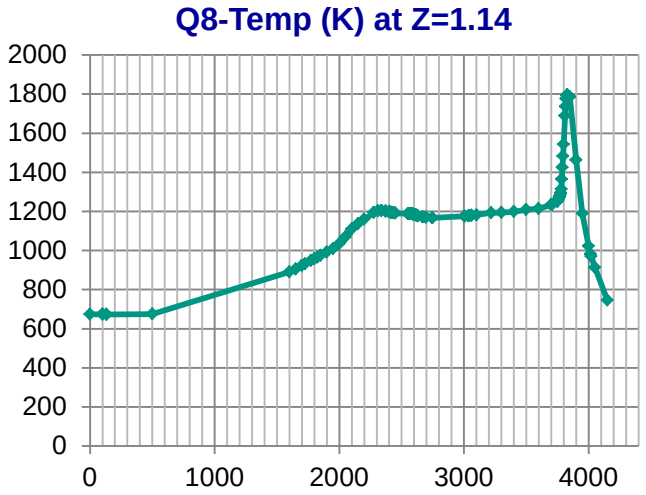
Thermal B.C.; BCTZ: Impose thermal conditions on a face of MACR at given elevations (1/2)

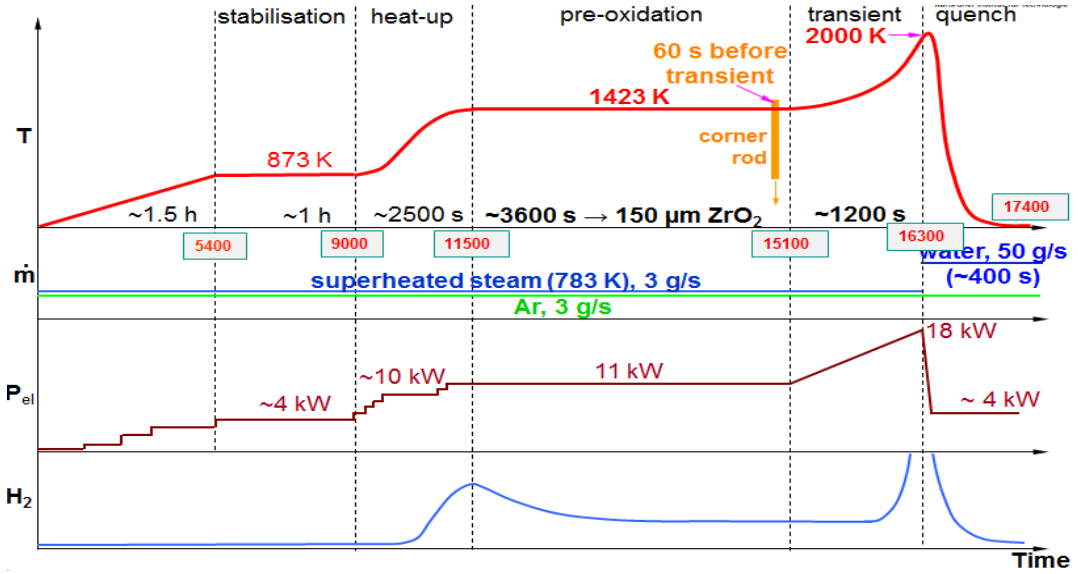


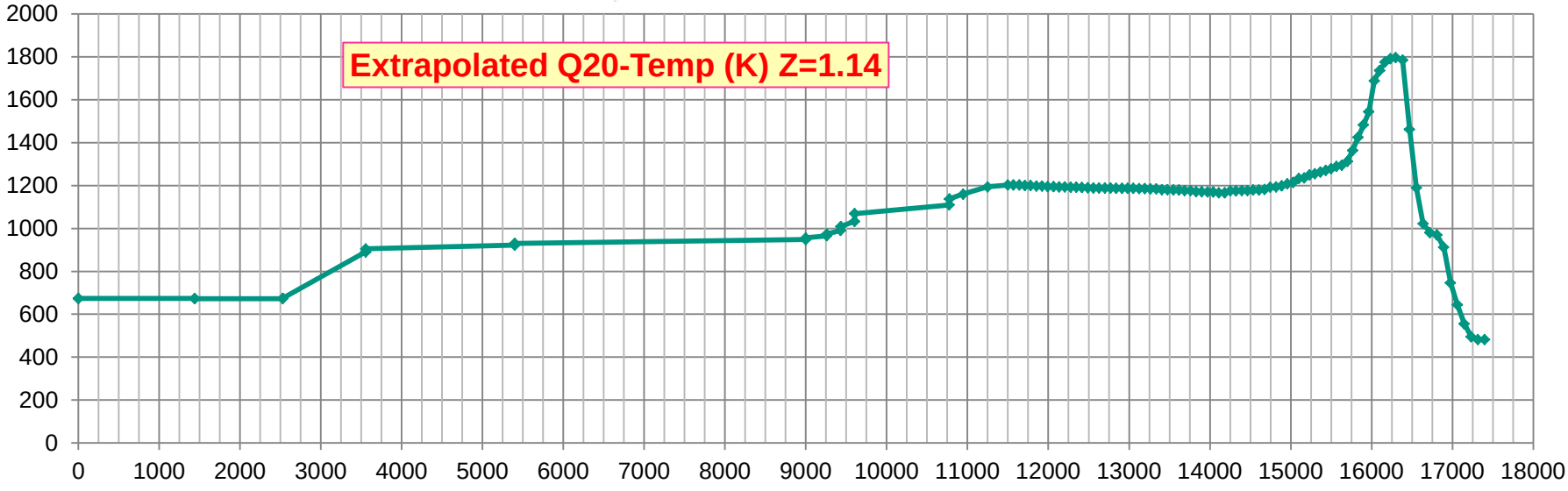
At given Macro Surface & Z-elevations:
e.g : cooling jacket z=1.14
{H(i), time(i), external_Temperature(i)}

```
MACR ‚BSS1‘   FACE  ‚EXTERNAL‘
TYPE  ‚BCTZ‘
ZMIN  ZMAX   ! restrict domain
Z  1.14
SR1  H(i)          !  [W/(m2.K)]
SR1 INST           ! Instant (s)
SR1 TIMP           ! External meidum
                   ! temperature (K)
```

Thermal B.C.; BCTZ: Impose thermal conditions on a face of MACR at given elevations (2/2)

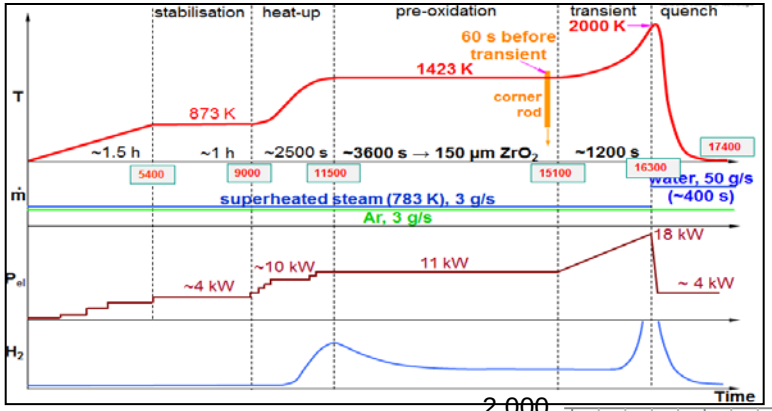






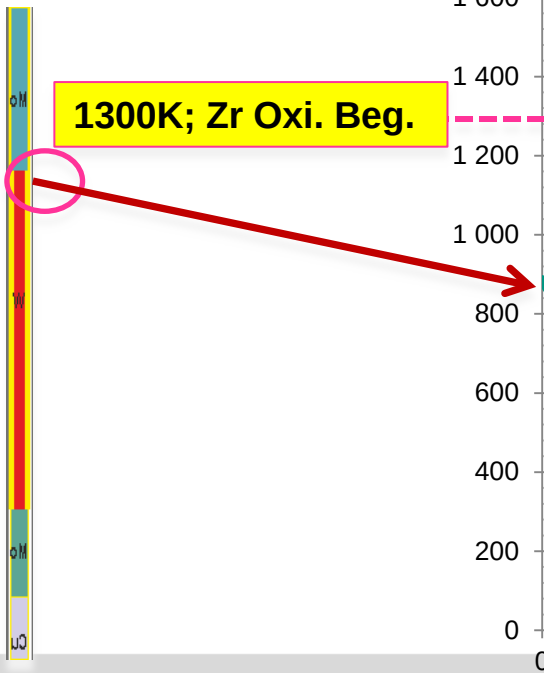
Calculation Results

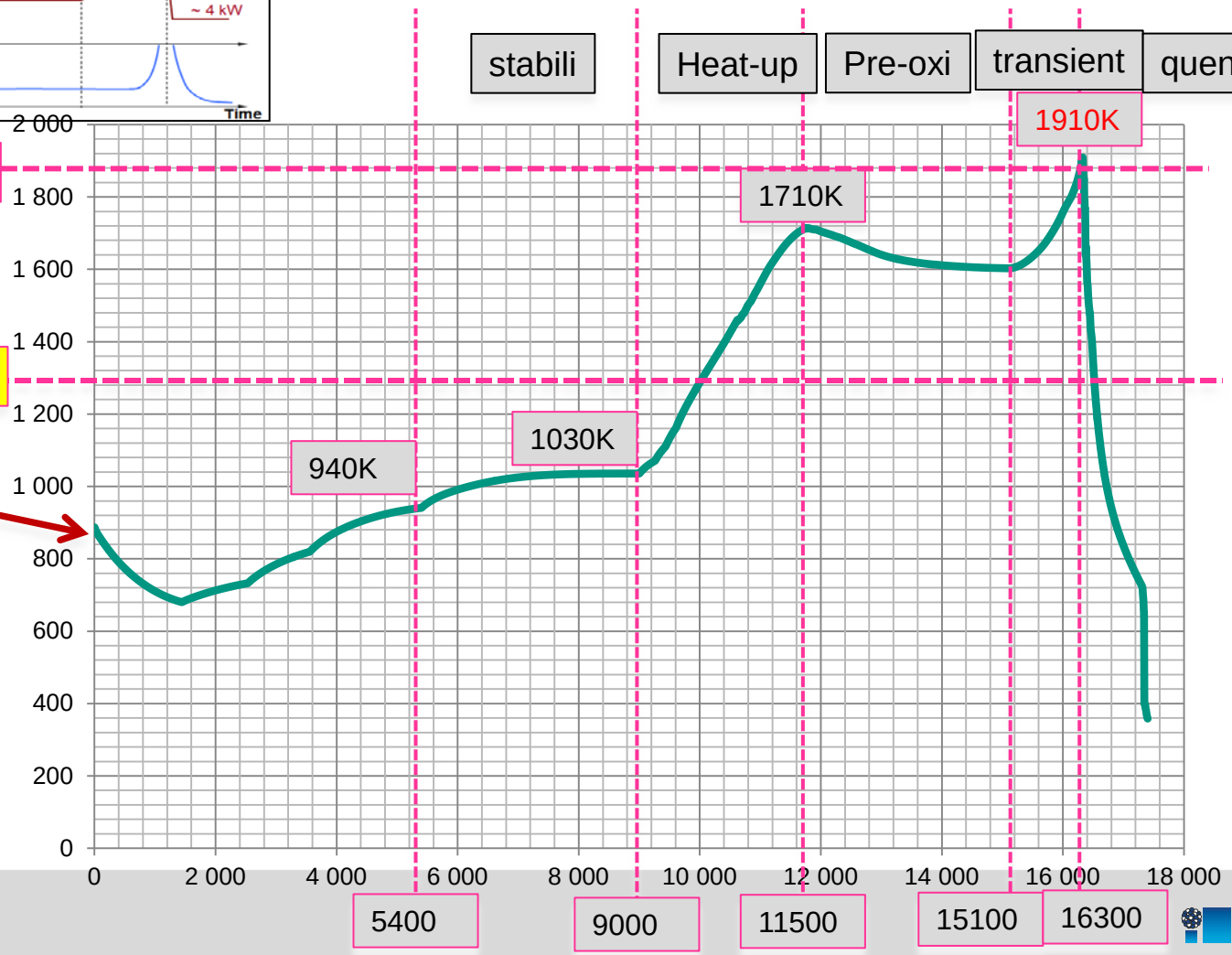
Central Rod max.Temp. Development



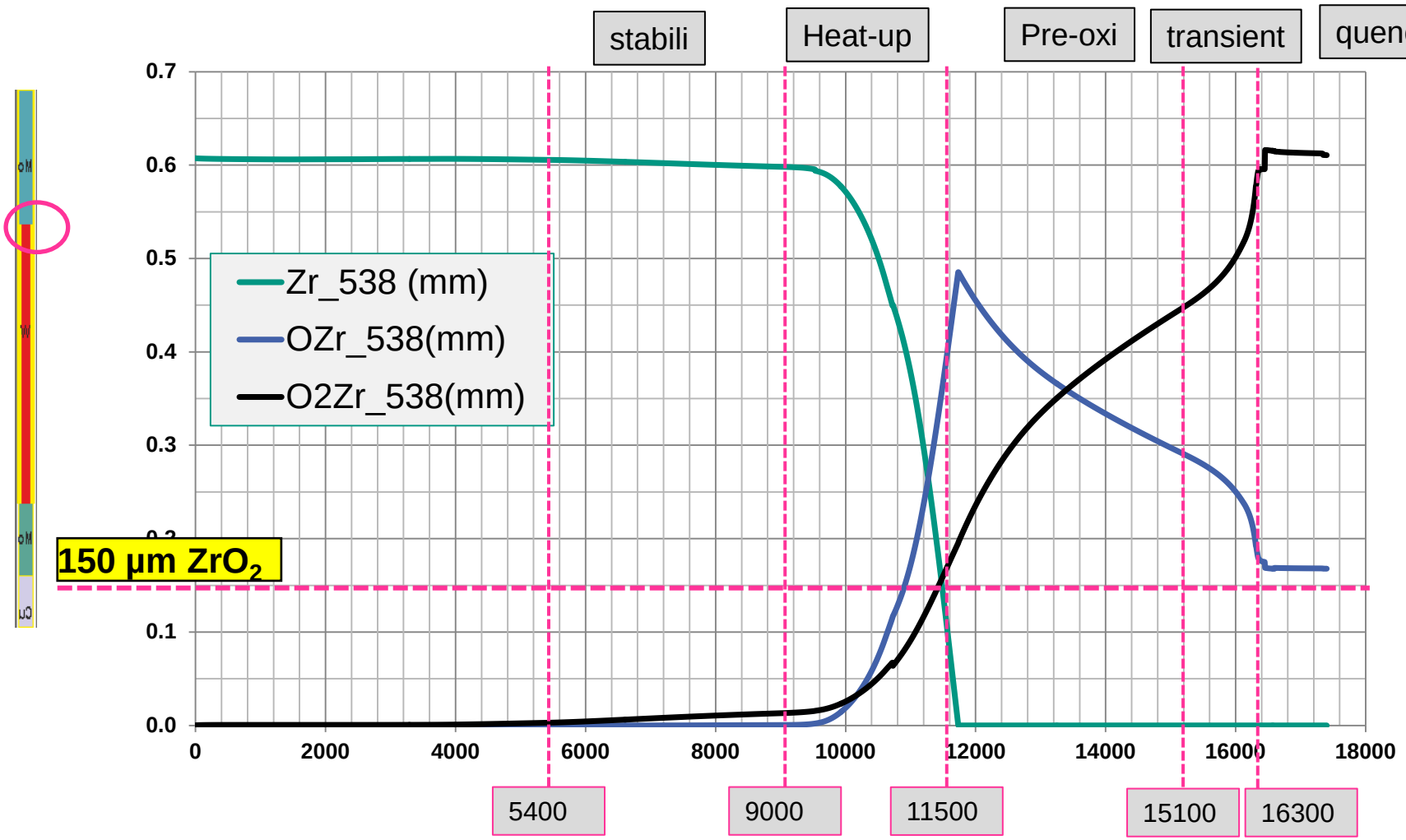
1850K; Zr Oxi. increase

1300K; Zr Oxi. Beg.

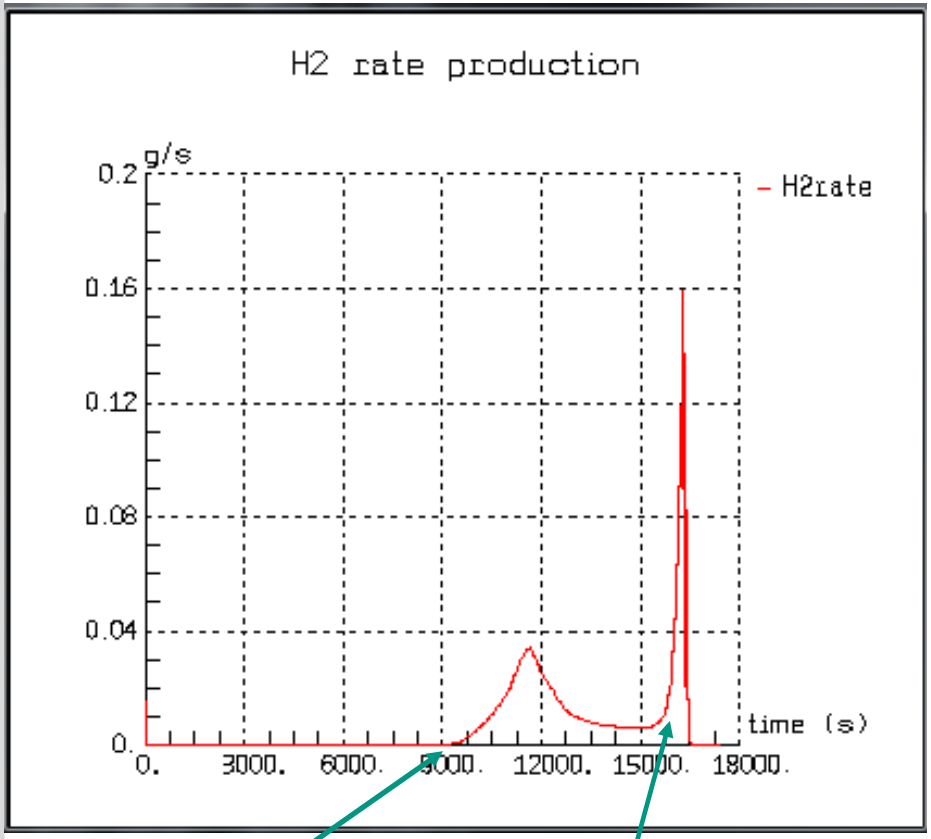


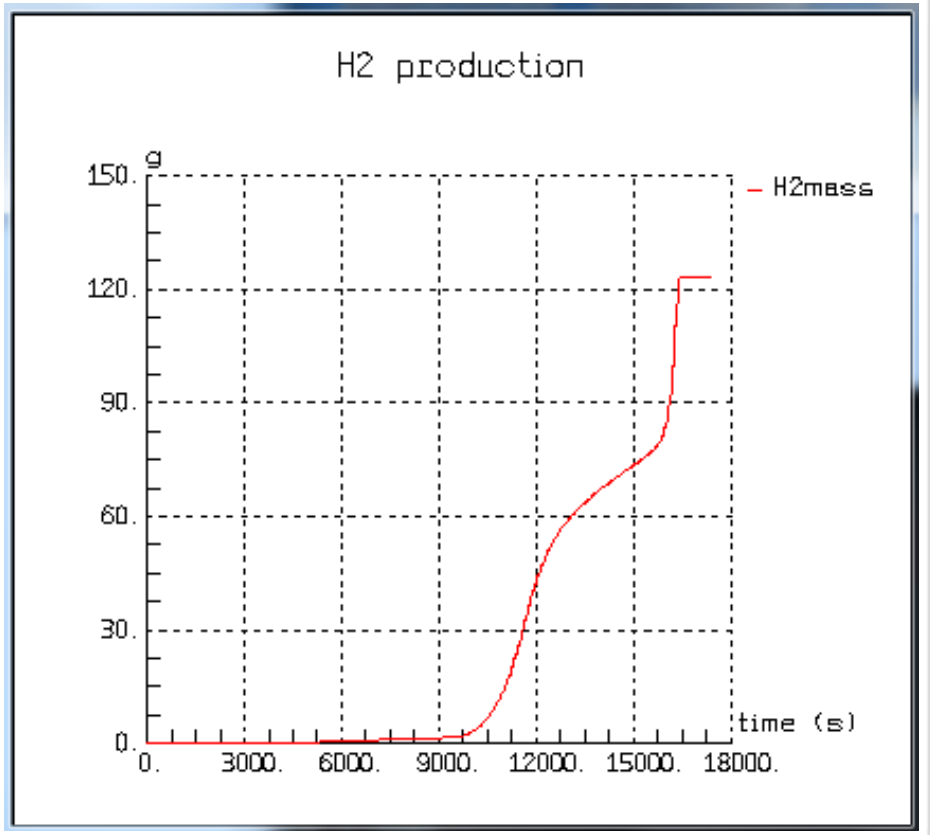


Heated Centr- Rod Zr, ZrO & ZrO2 Thicknesses



H2 production rate & Accumulated H2 mass

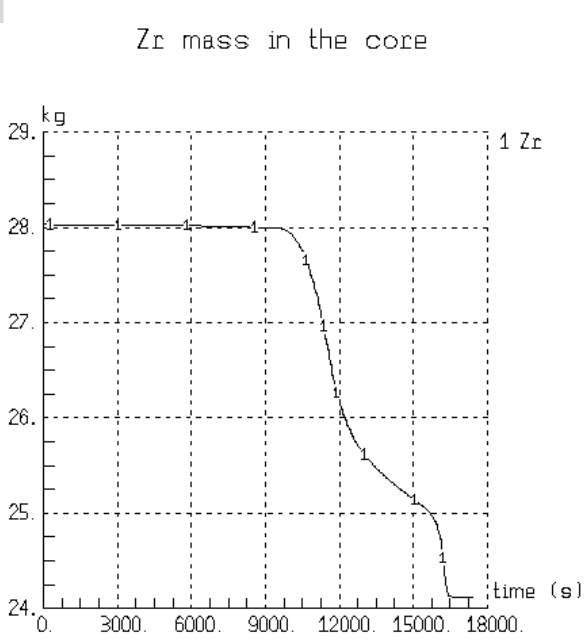


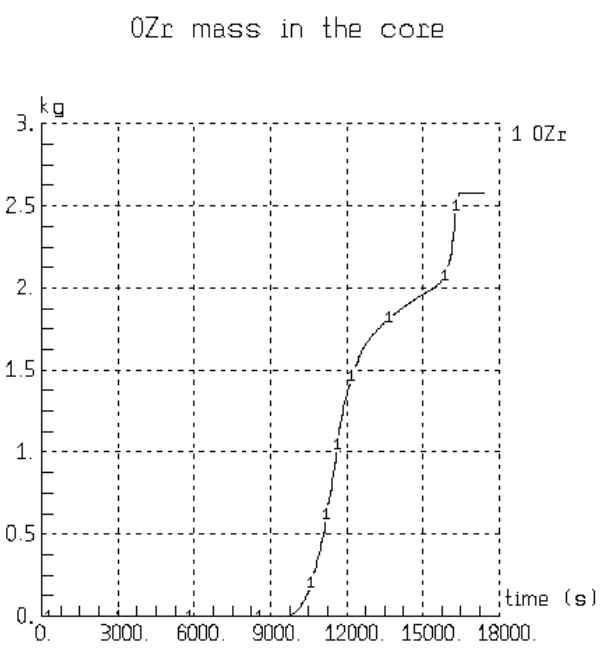


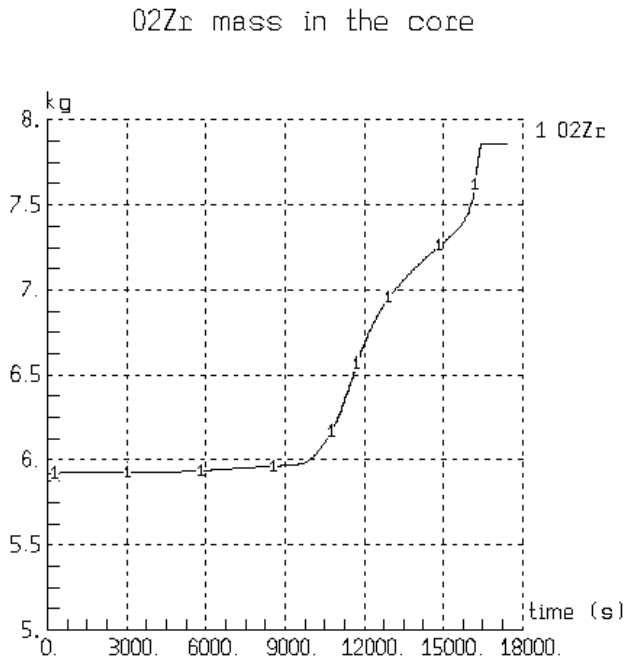
1850K, H2 Production Rate ↗

1300K: Onset of Zr Oxidation

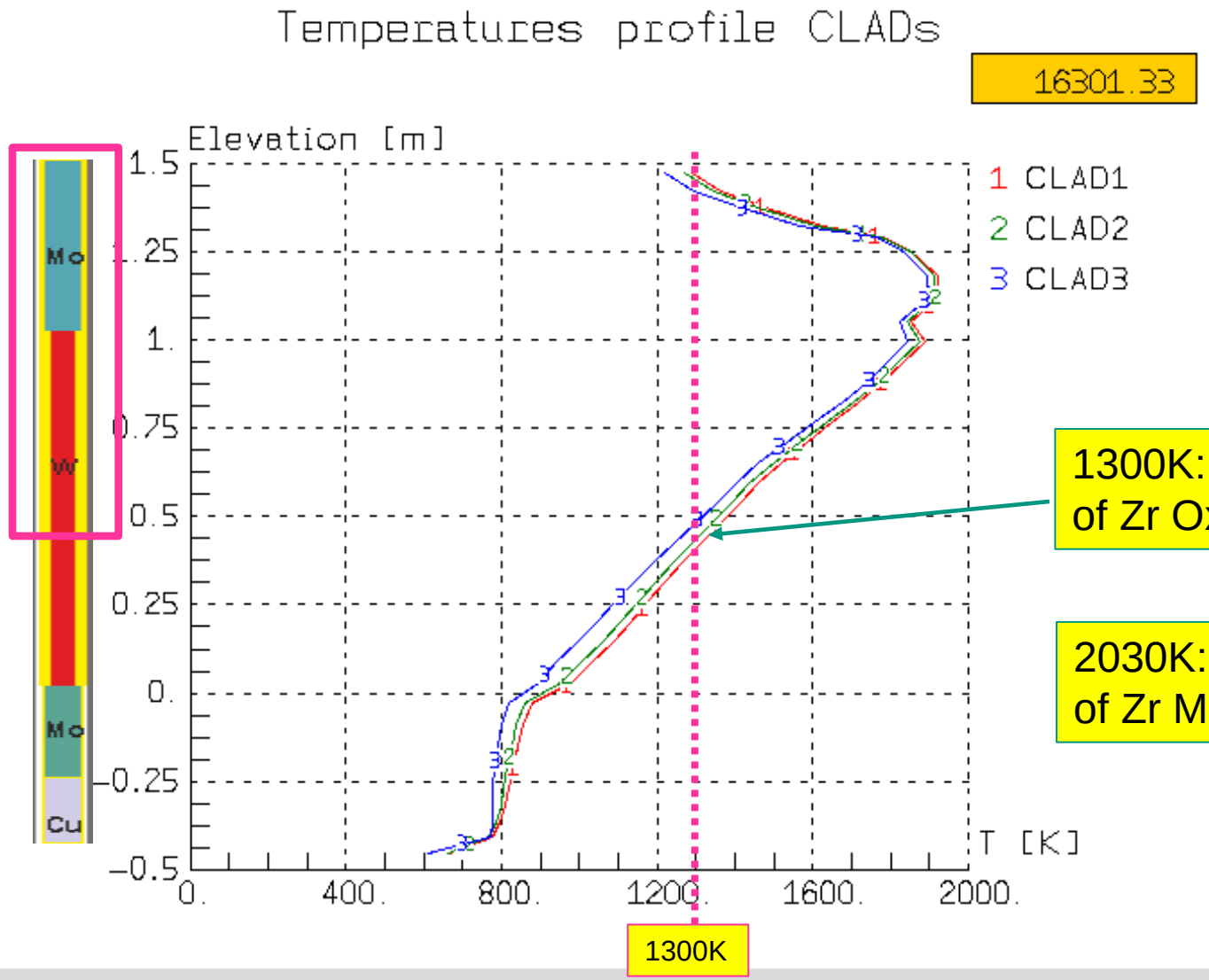
Total Zr, ZrO & ZrO2 Mass Development







Cladding Temperature Profile at max Power Instant

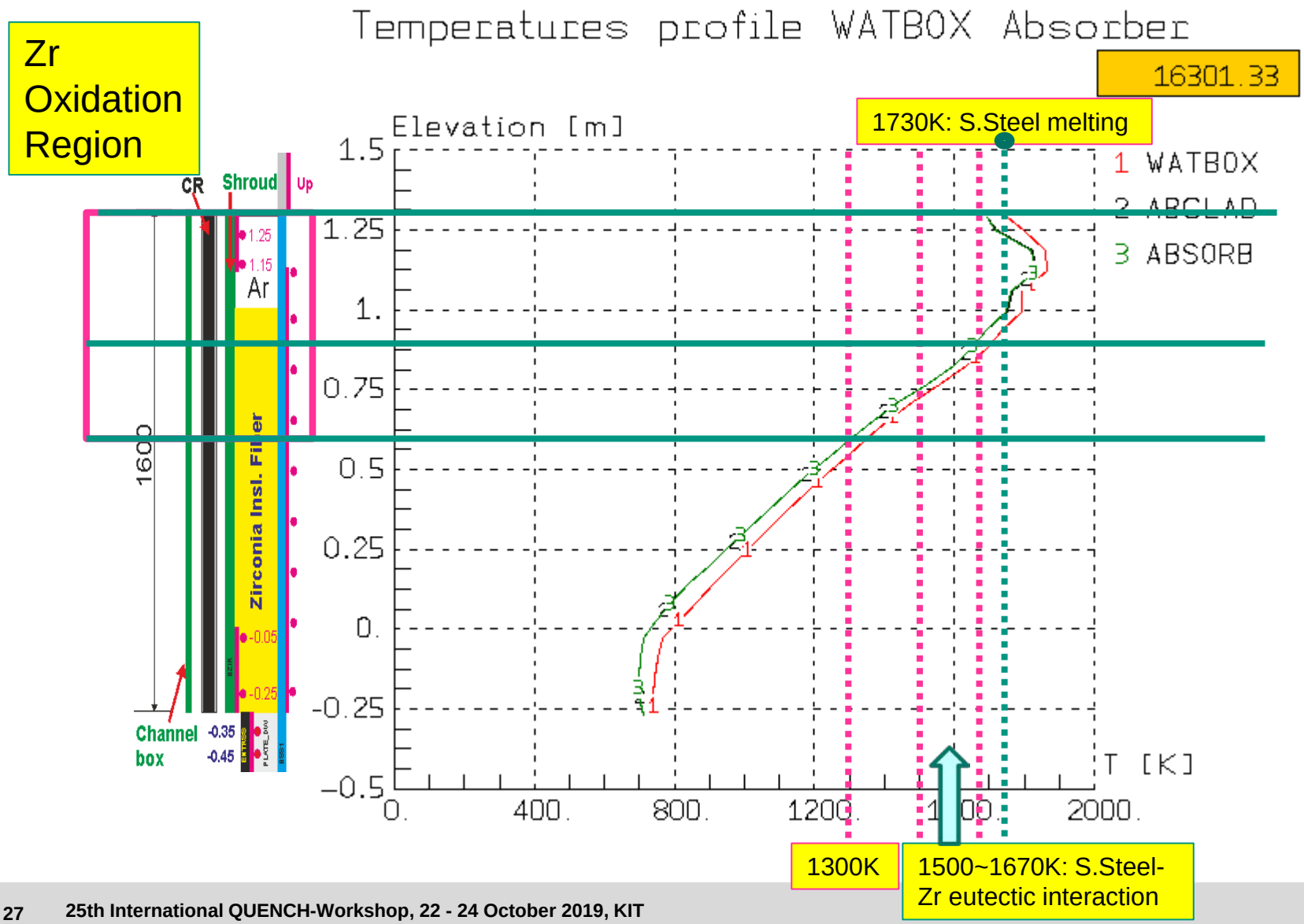


Zr Oxidation Region

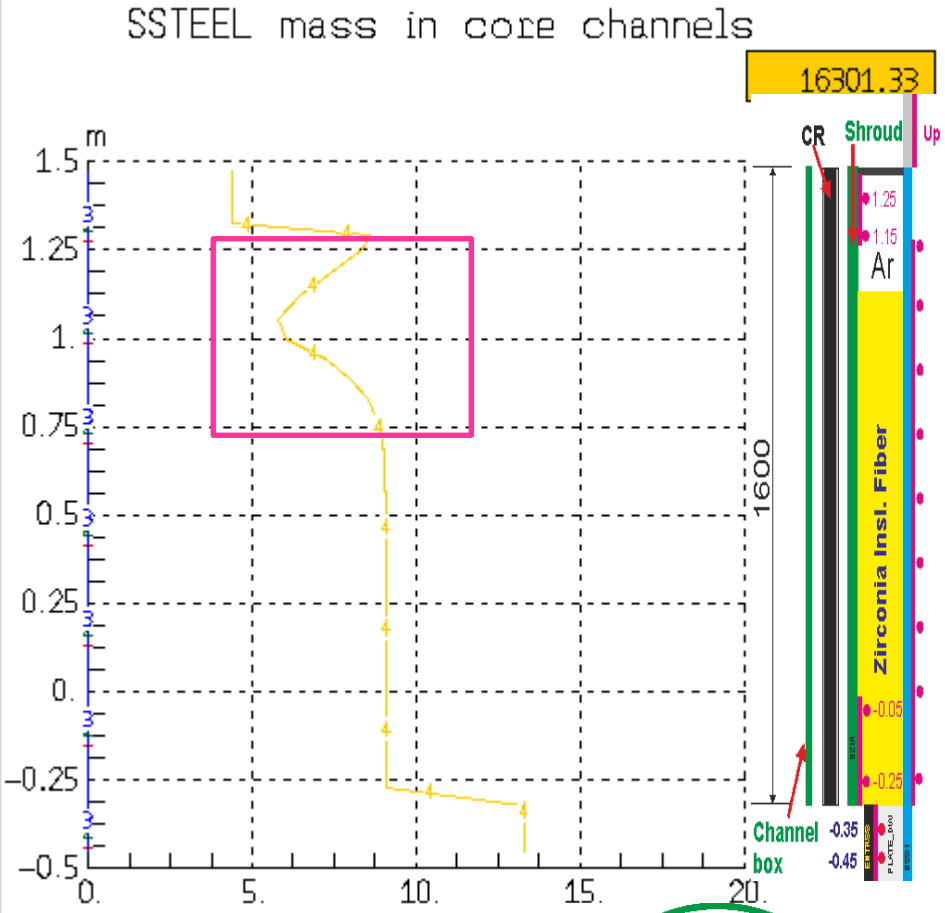
1300K: Onset of Zr Oxidation

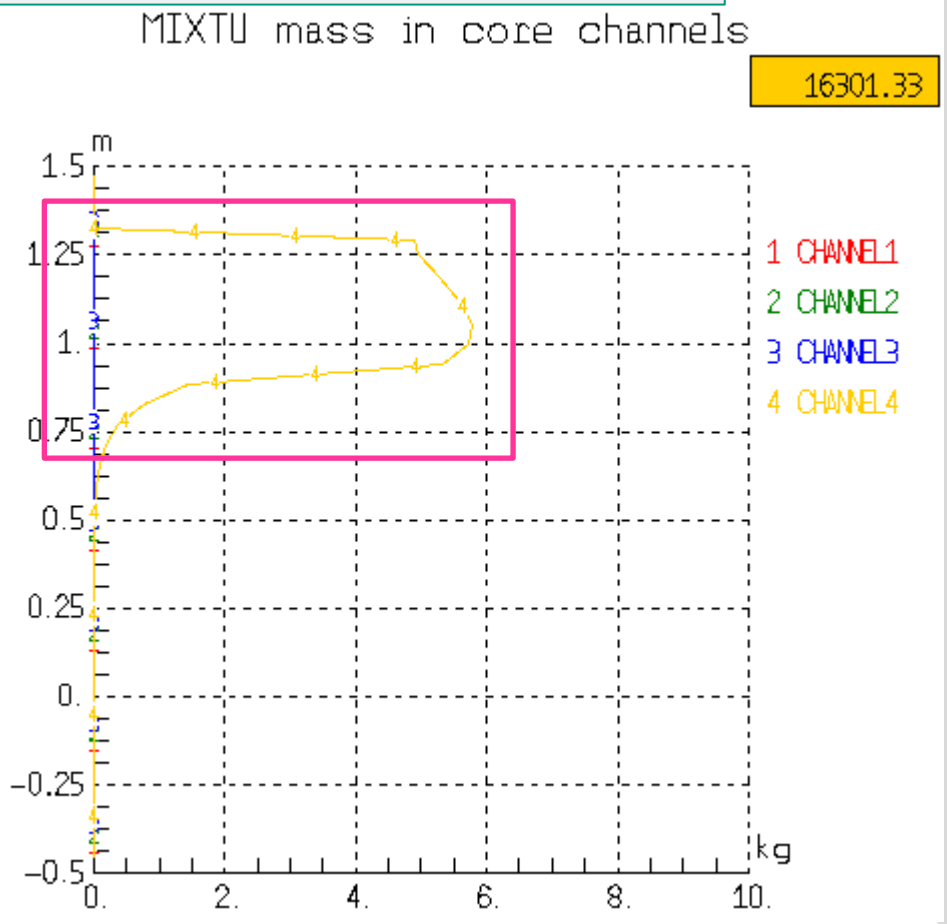
2030K: Onset of Zr Melting

Channel Box, CR-cladding & CR Temperature Profile

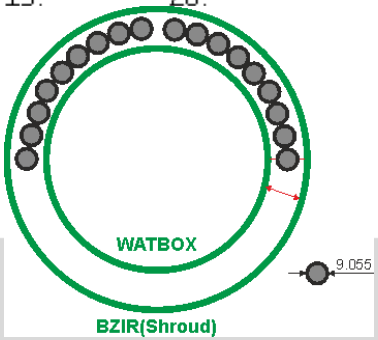


S.Steel & Mixture mass Axial Profile



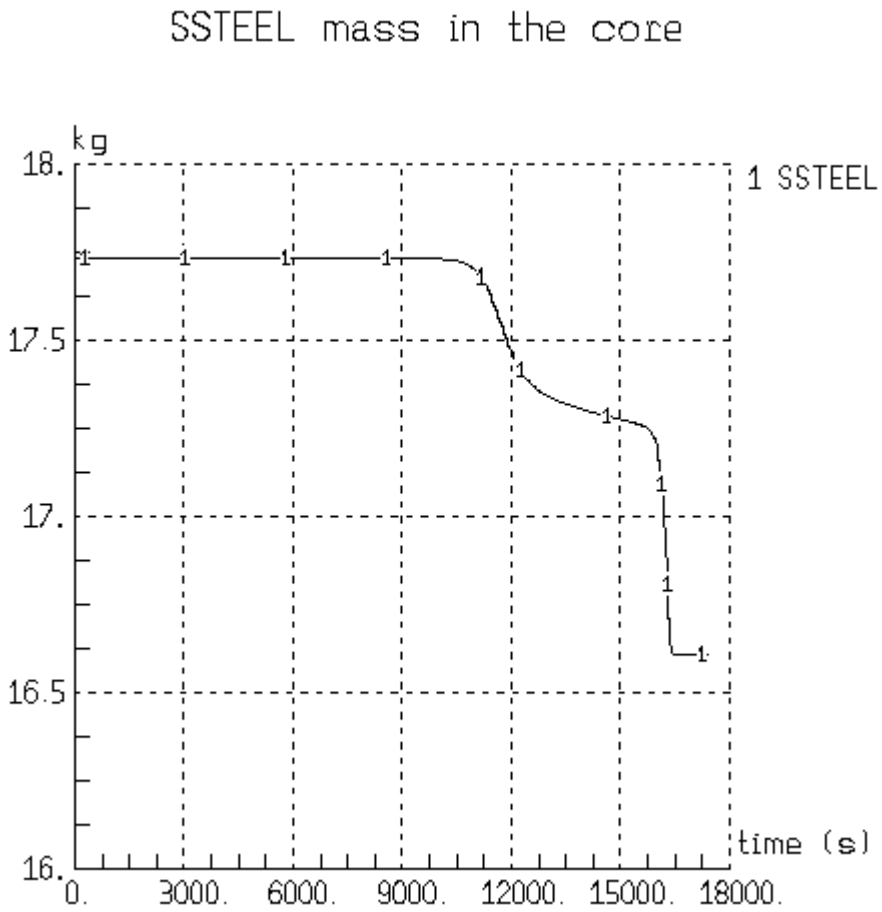


1730K S. Steel melting



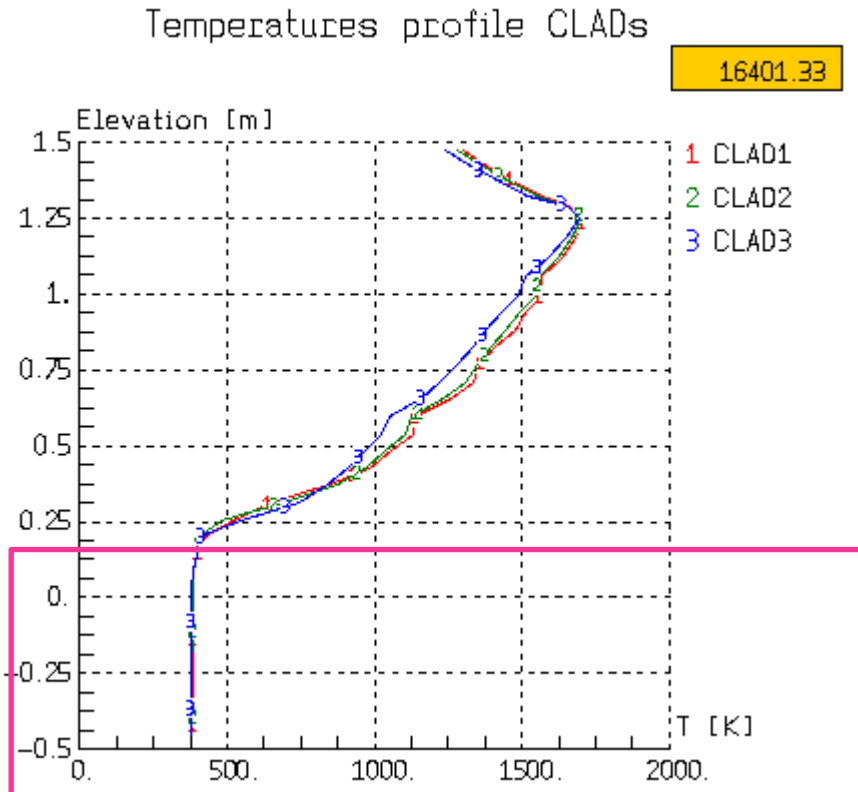
degradated materials:
(COMPACT or CRACKED) → (DISLOCAT).

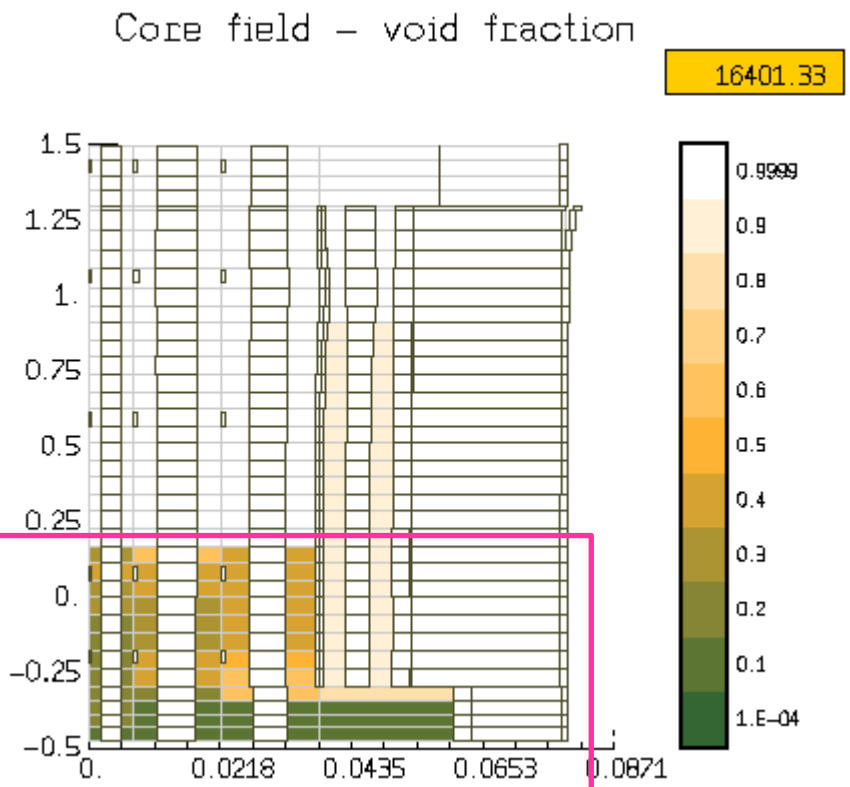
Total S.Steel mass Development



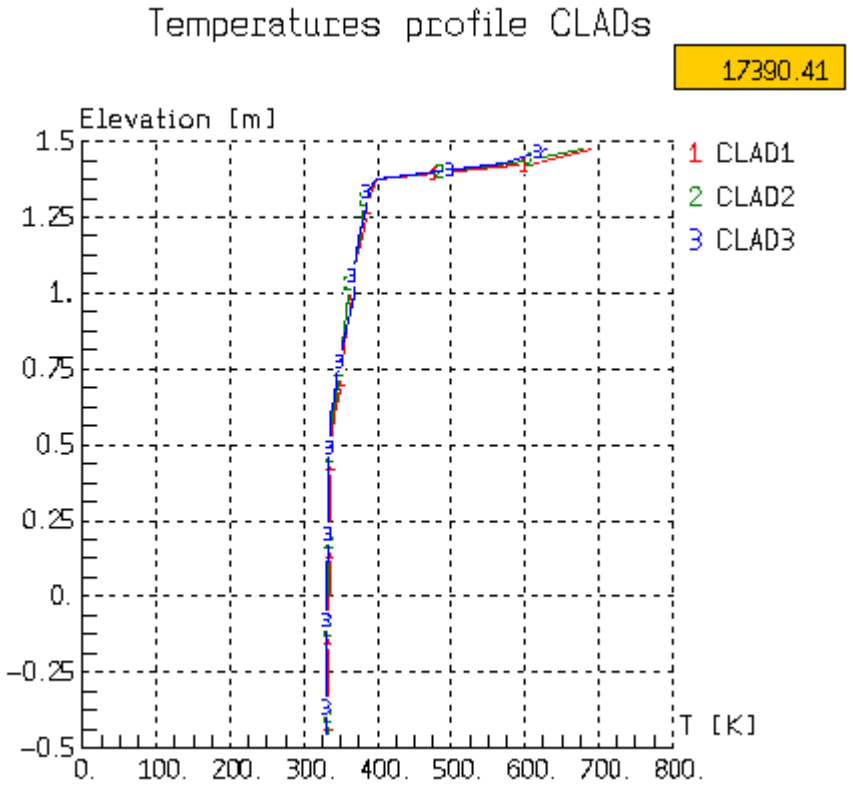
~ 1.5 Kg S. Steel melting

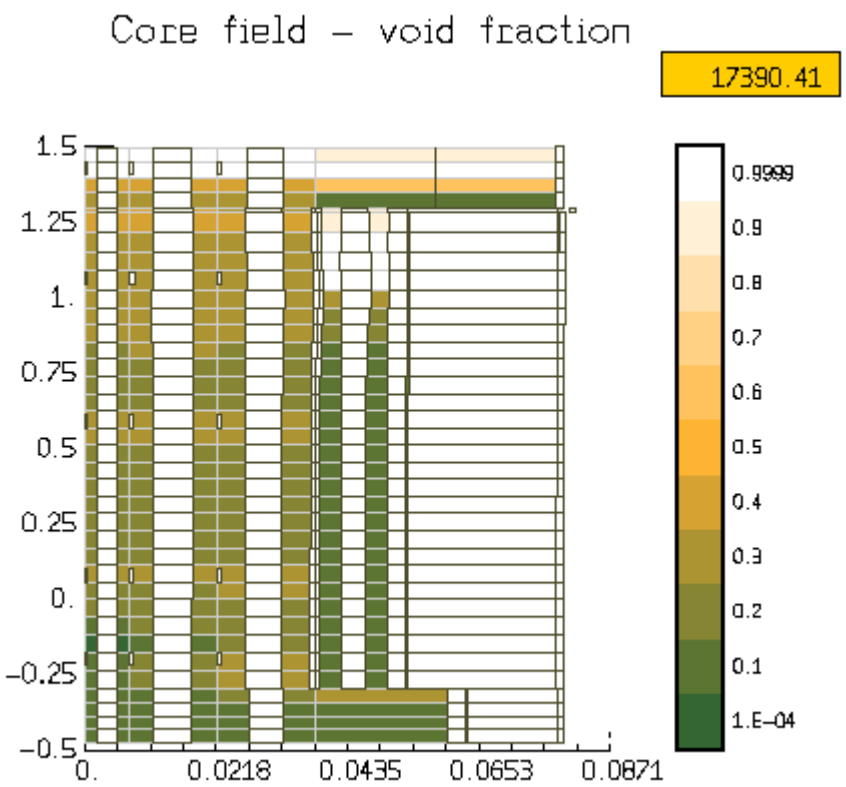
Quench Phase





Calculation End

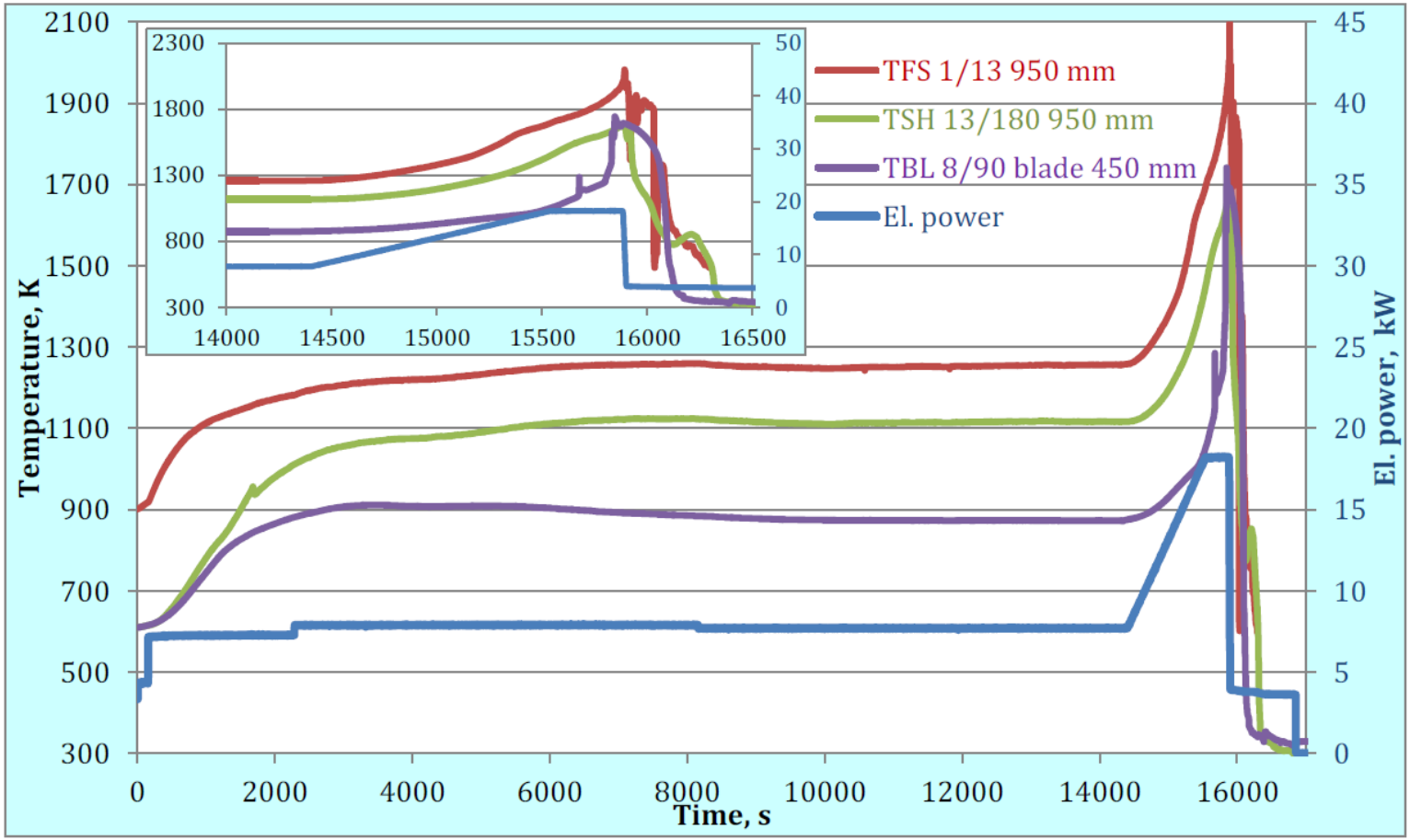




SUMMARY

- The present ASTEC version can be used to **simulate BWR bundle test**.
- In order to simulate the radiative heat exchanges between bundle rod and square channel box wall (e.g. Canister wall of BWR assembly), the square box should be modelled as **cylindrical geometry**.
- "**Cruciform control blade**": Present version can be applied for BWR case by modelling the **rectangular blade** as **equivalent cylinders**.
- The simulation results show ASTEC can give **reasonable results**. The results was used to support experimental staffs to design experiment progress.
- **OUTLOOK**: post-test calculations.

First information on QUENCH-20- bundle test



Electrical power profile during QUENCH-20 and readings of three selected thermocouples installed at cladding surface (TFS), shroud (TSH) (both at the hottest elevation of 950 mm) and at the absorber blade surface at the elevation of 450 mm.

Preliminary Assessment of the new ASYST - ISA Integral Analysis Code Using Selected Integral Thermal Hydraulic - Fuel Assembly Experiments

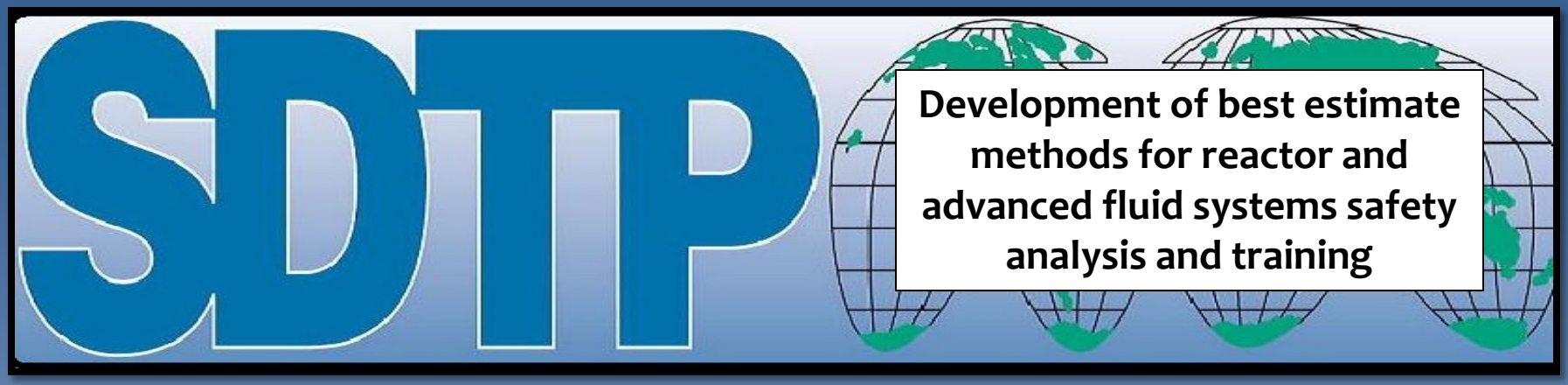
C.M. Allison[1], J.K. Hohorst[1], A. Ezzidi[2], and M. Naitoh[2]
[1]Innovative Systems Software (ISS)
[2]The Institute of Applied Energy (IAE)

ABSTRACT

ASYST (**A**daptive **SYS**tem **T**hermal-hydraulics) - ISA (Integral Simulation and Analysis) is a new code being developed jointly under the direction of the organizations noted above that combines the capabilities of SCDAPSIM and SAMPSON. The thermal hydraulic module, ASYST-THA, replaces the original US NRC-developed RELAP5 code used in RELAP/SCDAPSIM/MOD3.x and THA used in SAMPSON with a new system level hydrodynamic options that include multi-dimensional, multi fluid models originally developed by ISS and IAE. The ASYST reactor-specific modeling options include modules describing the behavior of (a) the core/fuel assembly structures, (b) late phase debris/melt relocation, (c) the containment including melt spreading and molten core-concrete interactions, and (d) fission product release and transport. The core/fuel assembly behavior module uses derivatives of SCDAPSIM/MOD3.x models and correlations while the late phase debris/melt relocation module uses a combination of SCDAPSIM/MOD3.x (2D based) models and SAMPSON MCRA, DCA, DSA (3D-based) models. The fission product release and transport module uses combinations of models from SCDAPSIM/MOD3.x and SAMPSON. The core-concrete interaction module uses a SCDAPSIM-based porous media model in combination with SAMPSON Debris-Concrete Interaction (DCRA) models and correlations. The reactor vessel, reactor coolant system and containment thermal hydraulic behavior is described by ASYST-THA in combination with the SAMPSON hydrogen combustion, hydrogen detonation and steam explosion modules, HYNA, DDOC and VESUVIUS, respectively. Funding and additional technical contributions for the development of ASYST comes from the contributors to the international SCDAP Development and Training Program (SDTP).

The presentation provides a brief overview and status of the development of the ASYST code along with preliminary comparisons of the initial version of the code with selected integral experiments conducted at KIT and the INL.





Preliminary Assessment of the new ASYST - ISA Integral Analysis Code Using PBF-SFD - ST

Presented Dr. Chris Allison
General Manager
Innovative Systems Software (ISS)
3585 Briar Creek Lane
Idaho Falls, Idaho 83406

ASYST-ISA is a new collaborative development initiated by ISS and IAE-NUPEC with international collaboration through SDTP

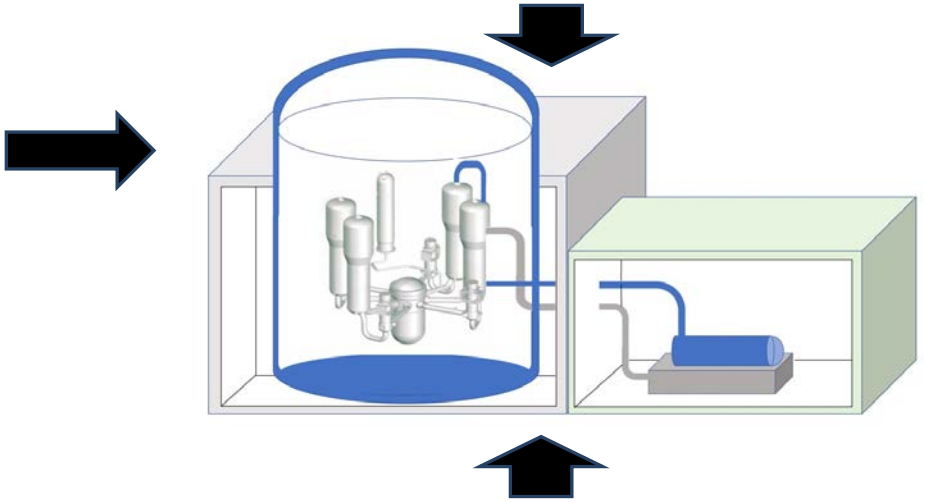
- Introduction to **ASYST - ISA** - (Adaptive SYStem Thermal-hydraulics - Integral Severe Accident)
- Motivation for development
  - Impact of user effects in simplified integral codes in Fukushima assessment
  - …
- Comparison with PBF-SFD-ST (Beta test version)

ASYST-ISA is a detailed integral BEPU accident analysis code being developed collaboratively through SDTP

ASYST adaptive system thermal hydraulic and control system module

* Describe behavior in RCS, containment, and aux. buildings
* Incorporates advanced multi-D, multi- fluid hydro models developed for SCDAPSIM/MOD4.x and SAMPSON
  * Advanced water properties developed for SCWRs and HPWRs
  * Molten salt/metals
  * Non-condensable gases

SAMPSON and SCDAPSIM **fission product release and transport module** can be used in combination with system thermal hydraulic module



SAMPSON **hydrogen combustion and steam explosion modules** can be used in conjunction with system thermal hydraulic module for containment and aux. buildings

ASYST - Adaptive multi-D, fluid system thermal hydraulic module will replace RELAP5 and SAMPSON THA(RCS)/CVA(containment) TH options

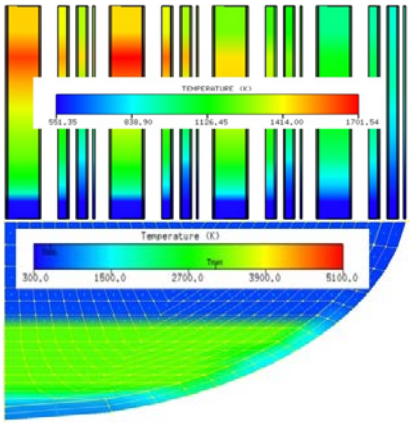
* Adaptive numerical techniques for single phase, two phase, and multi-fluid conservation equations
* "Open source" peer reviewed constitutive TH and material property correlation libraries
* Multi-D reactor kinetics with options for user supplied modules
* Standard control systems and trip logic options with options for MATLAB or user supplied functions
* User options - backwards compatibility for RELAP5/SCDAPSIM and SAMPSON based input/output, integral uncertainty analysis, GUI-based input editing and interactive desktop simulation with options for 3rd party options (ie GRAPE)

Combination of SCDAPSIM and SAMPSON models will describe in-vessel and ex-vessel behavior

"Open source" peer reviewed material property correlation libraries

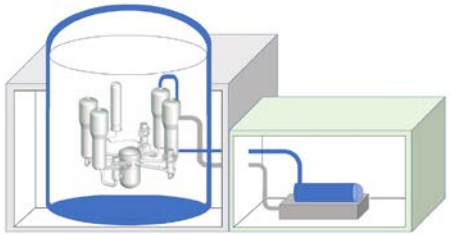
In-vessel modules

- Core/fuel assembly structures - SCDAPSIM(2D/3D)
- Late phase debris/melt relocation - SCDAPSIM(2D) with options for SAMPSON(3D)



Containment and Aux. Building modules (SAMPSON)

- Melt spreading (3D)
- Core-concrete interactions (2D)
- H2 combustion (3D)
- Melt-water interactions (2D/3D)

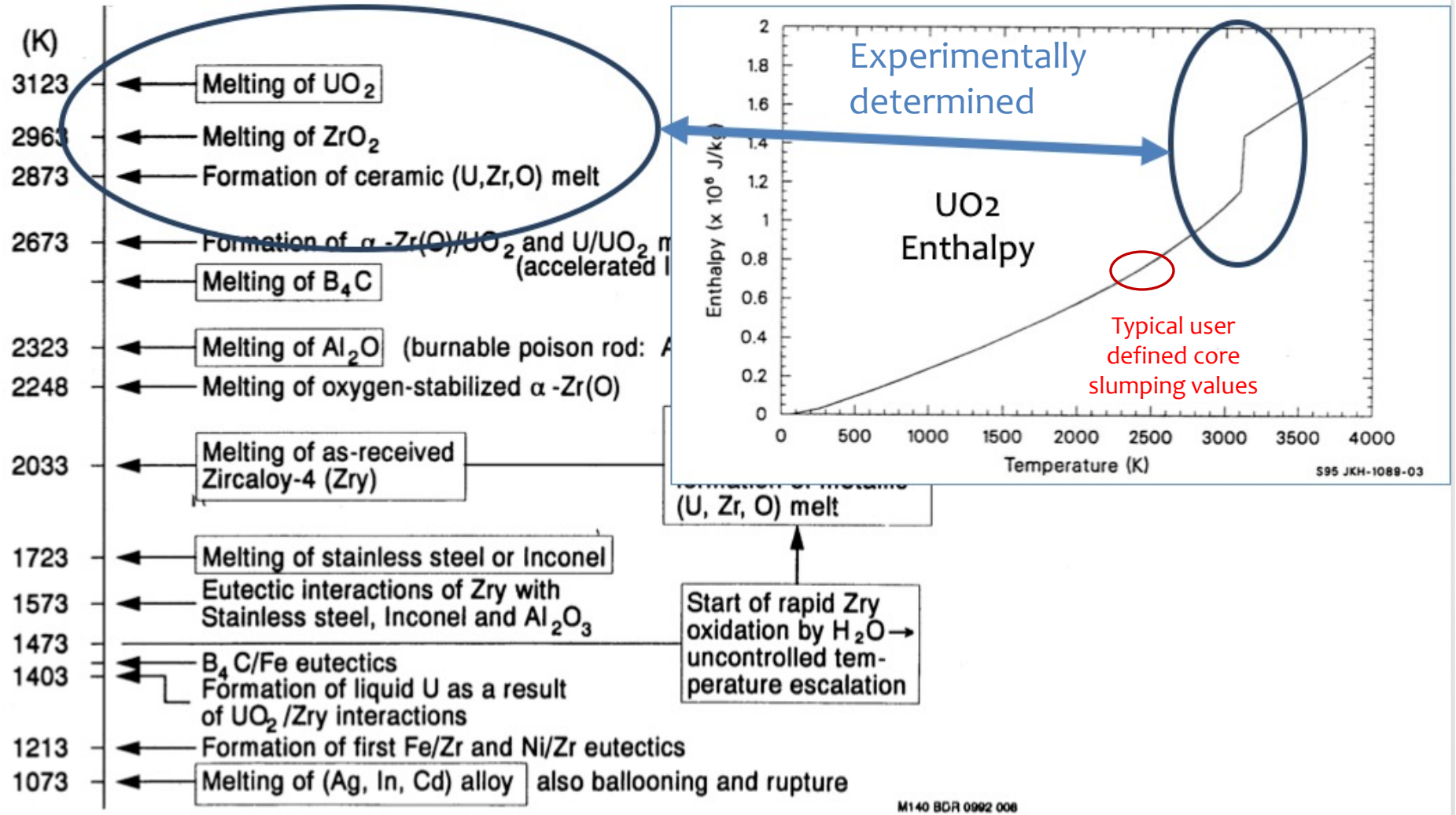


Sampson and SCDAPSIM fission product and transport models and correlations

ASYST-ISA is new collaborative development initiated by ISS and IAE-NUPEC with international collaboration through SDTP

- Introduction to **ASYST - ISA** - (Adaptive SYStem Thermal-hydraulics - Integral Severe Accident)
- Motivation for development
  - Impact of user effects in simplified integral codes in Fukushima assessment
- Comparison with PBF-SFD-ST

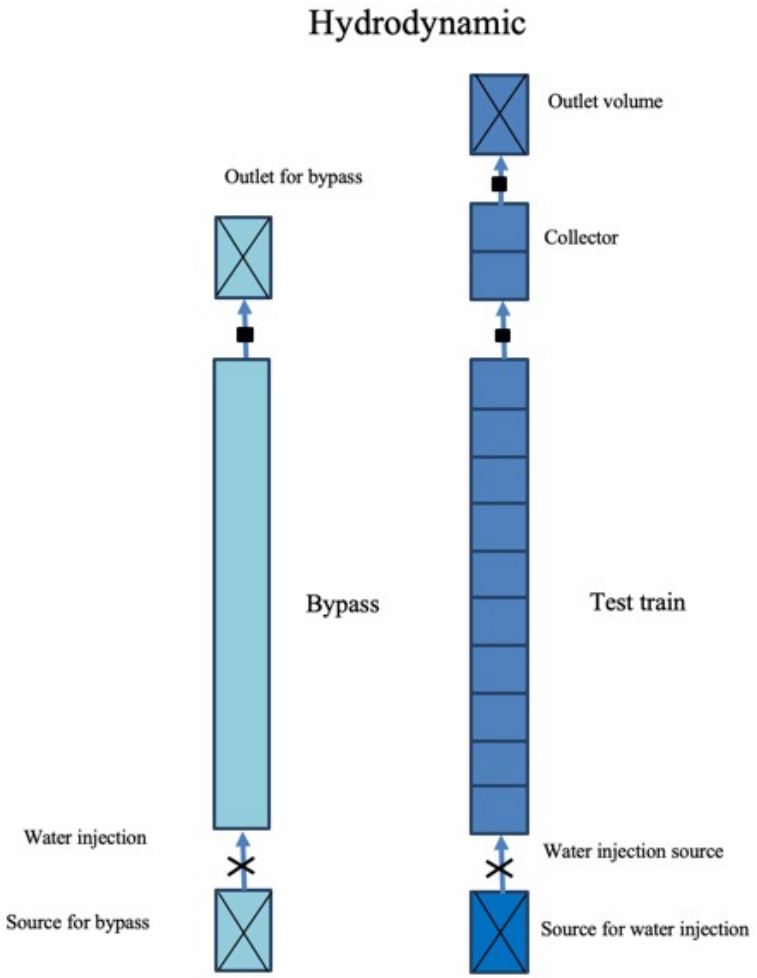
User-defined core slumping temperatures in simplified codes have significant impact on energy of molten [U-Zr] – O2 and source term

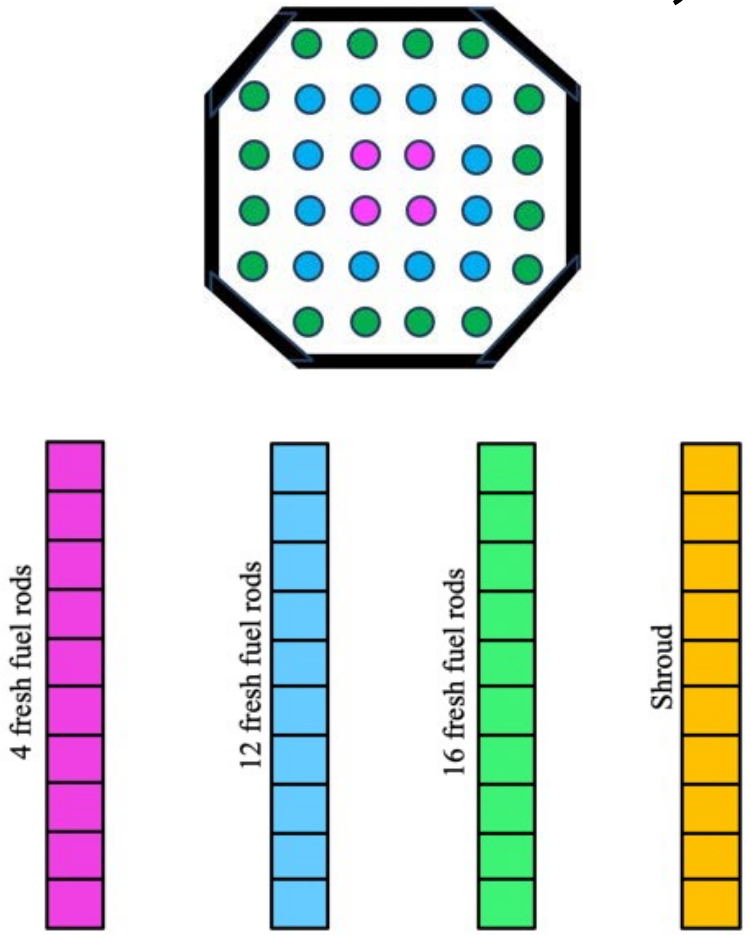


ASYST-ISA is new collaborative development initiated by ISS and IAE-NUPEC with international collaboration through SDTP

- Introduction to **ASYST - ISA** - (Adaptive SYStem Thermal-hydraulics - Integral Severe Accident)
- Motivation for development
  - Impact of user effects in simplified integral codes in Fukushima assessment
- Comparison with PBF-SFD-ST (Beta test version) – See additional slides for more detailed description of experiment and associated references
  - ASYST-ISA (beta) is based on RELAP/SCDAPSIM/MOD4.X

PBF – SFD ST (Bundle Nodalization)

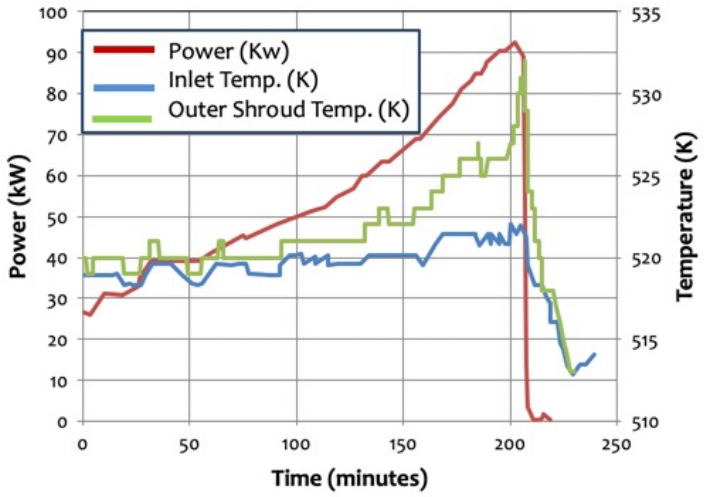


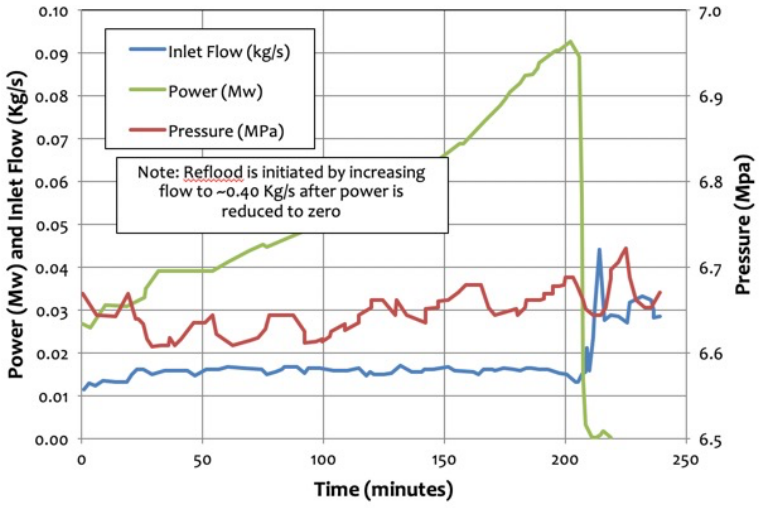


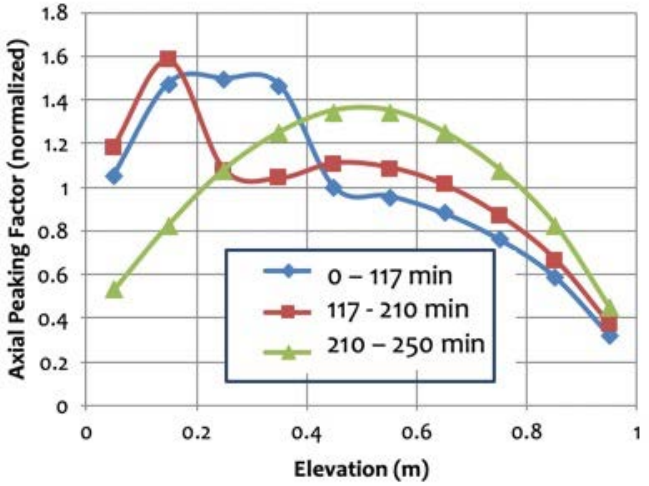
SCDAP Bundle Components

PBF – SFD ST (Boundary conditions used)

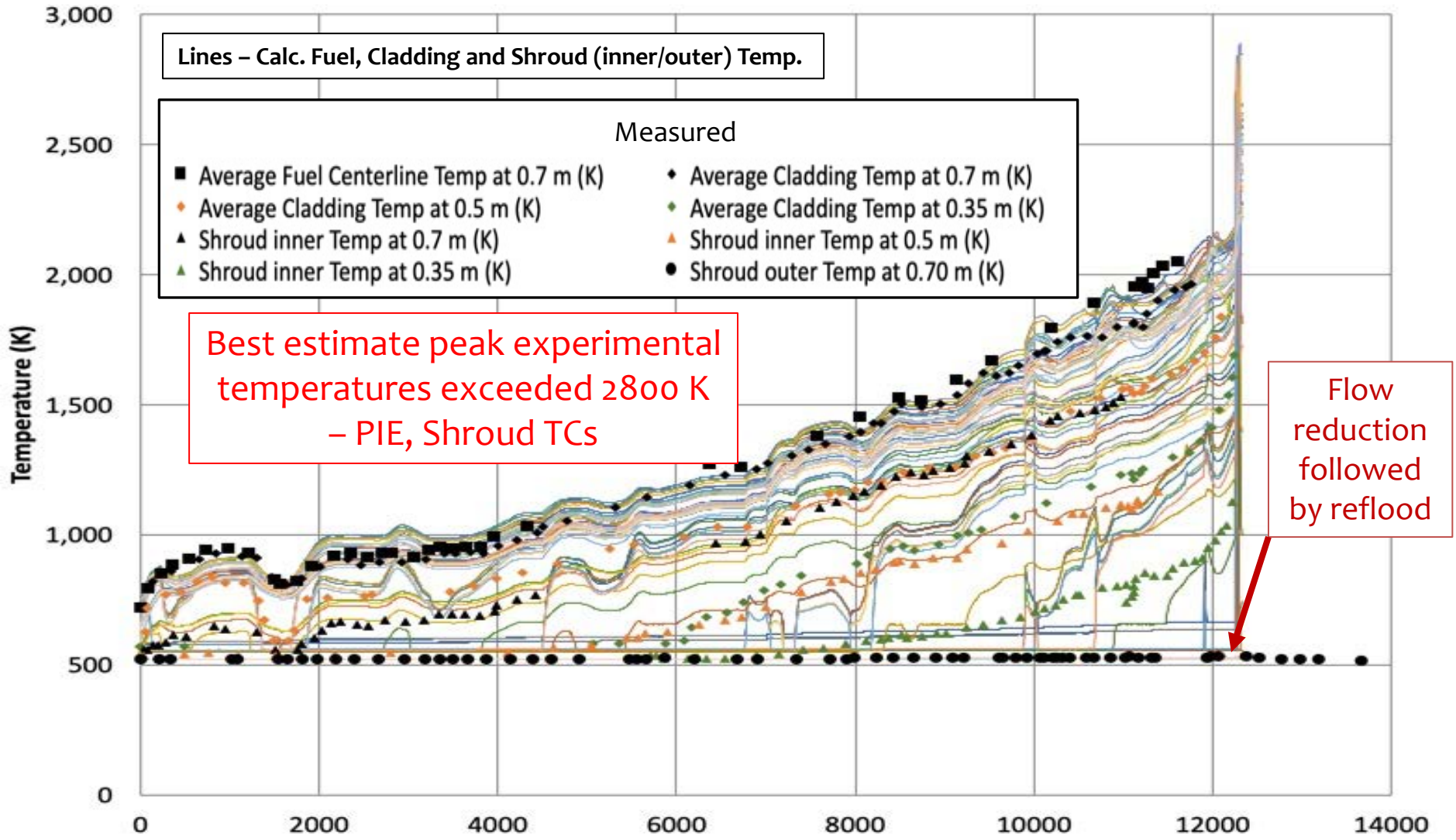
* Thermal hydraulic conditions
  * Pressure, inlet temperature, inlet flow, outside shroud temperatures
* Power
  * Time history
  * Axial power profiles







Comparison with PBF SFD-ST



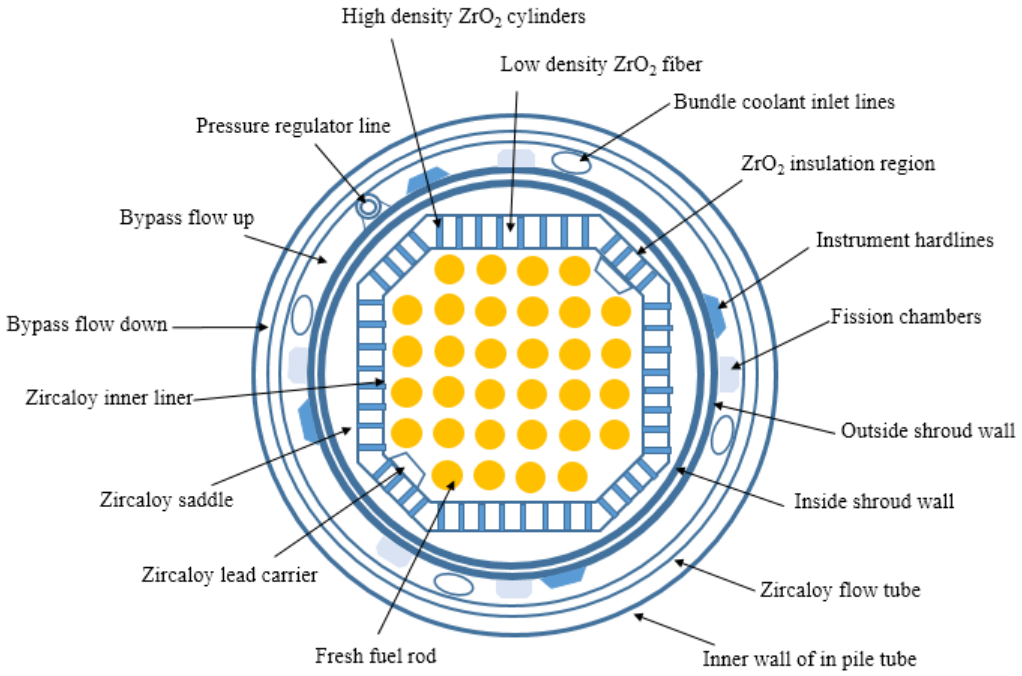
PBF SFD-ST Additional Slides

References

- PBE Severe Fuel Damage Scoping Test - Test result report, NUREG/CR-4883 EGG-2413, U.S. Nuclear Regulatory Commission, 1986

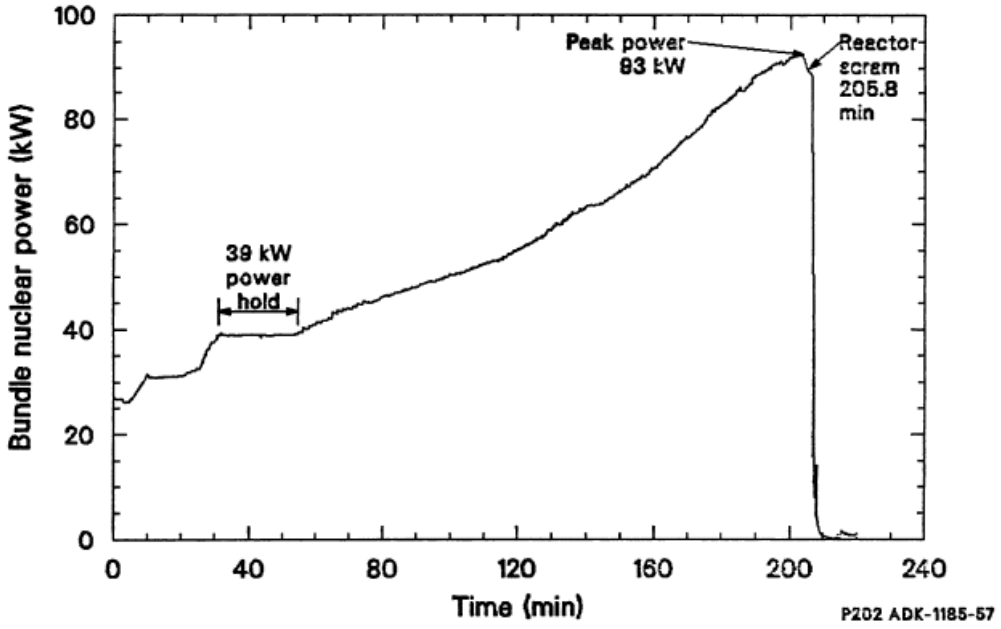
Test bundle

Description	Dimension	Note
Fuel rods		Pressurized water reactor (PWR)
	32 rods	Arranged in 6x6
	0.9144 m	Length
Inconel grid spacers	3 spacers	17 x 17 PWR fuel rod pitch of 12.75 ± 0.25 mm
Insulating shroud		Zirconia insulators

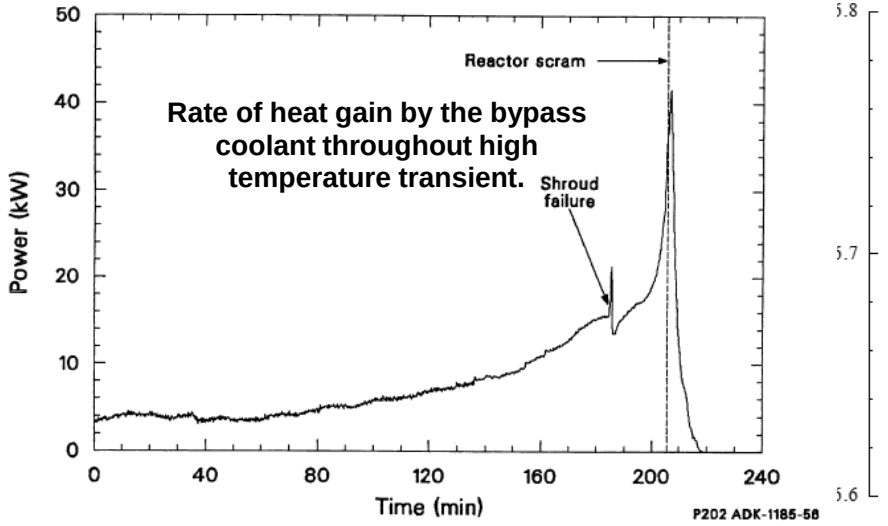


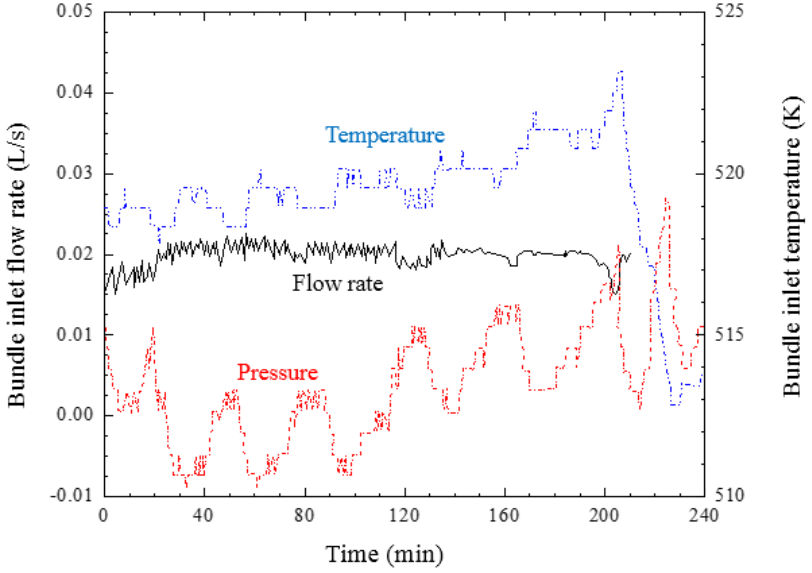
Ref. PBE Severe Fuel Damage Scoping Test - Test result report, NUREG/CR-4883 EGG-2413, U.S. Nuclear Regulatory Commission, 1986

Bundle Boundary Conditions

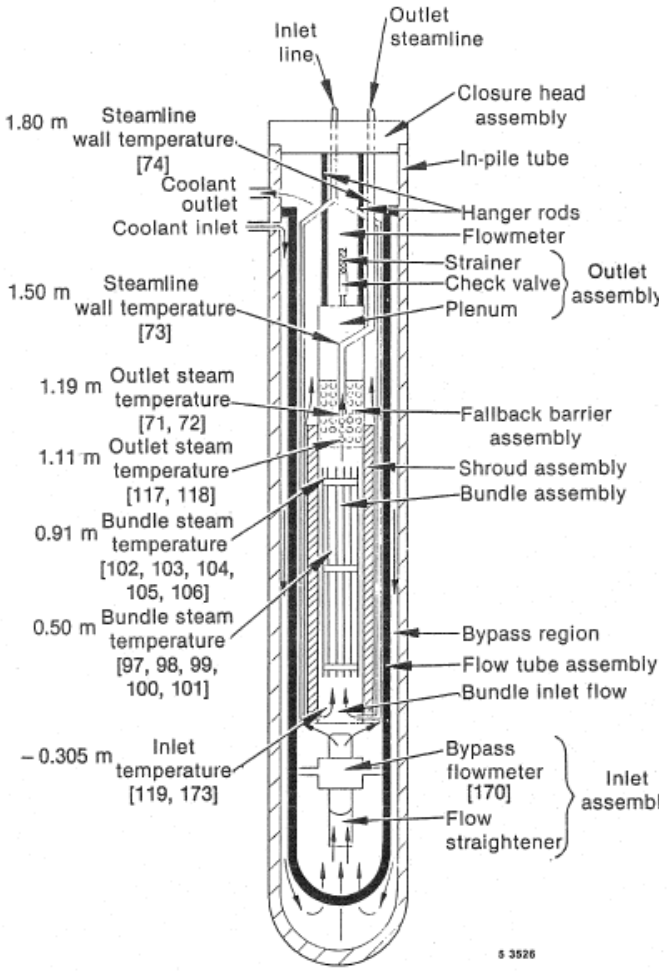


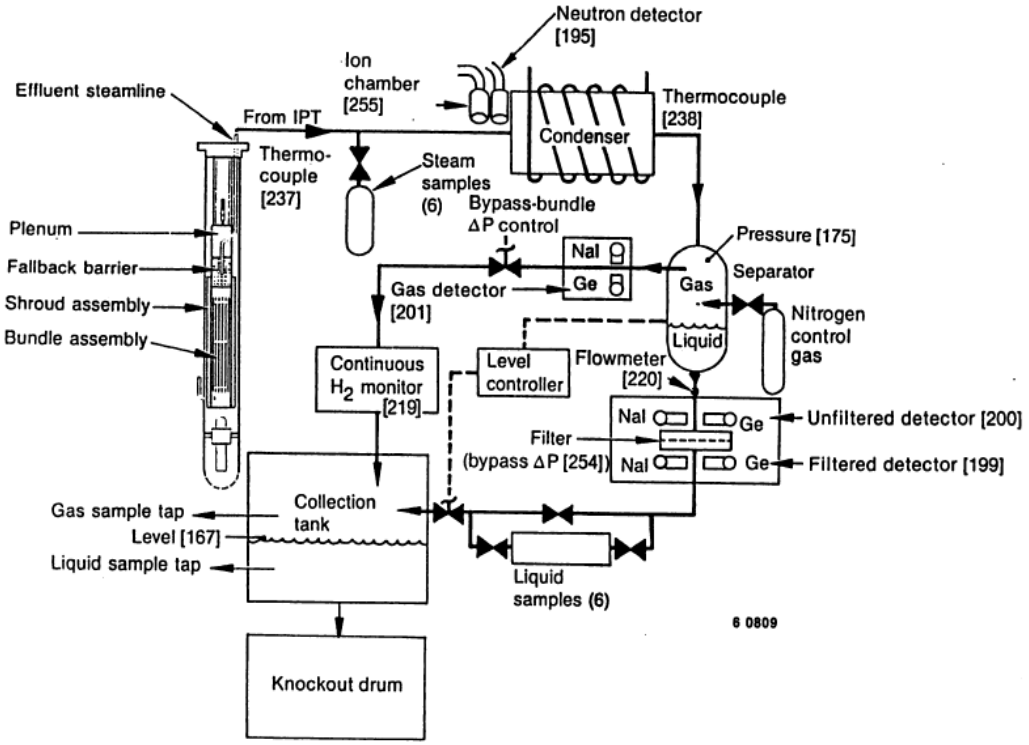
Ref. PBE Severe Fuel Damage Scoping Test - Test result report, NUREG/CR-4883 EGG-2413, U.S. Nuclear Regulatory Commission, 1986





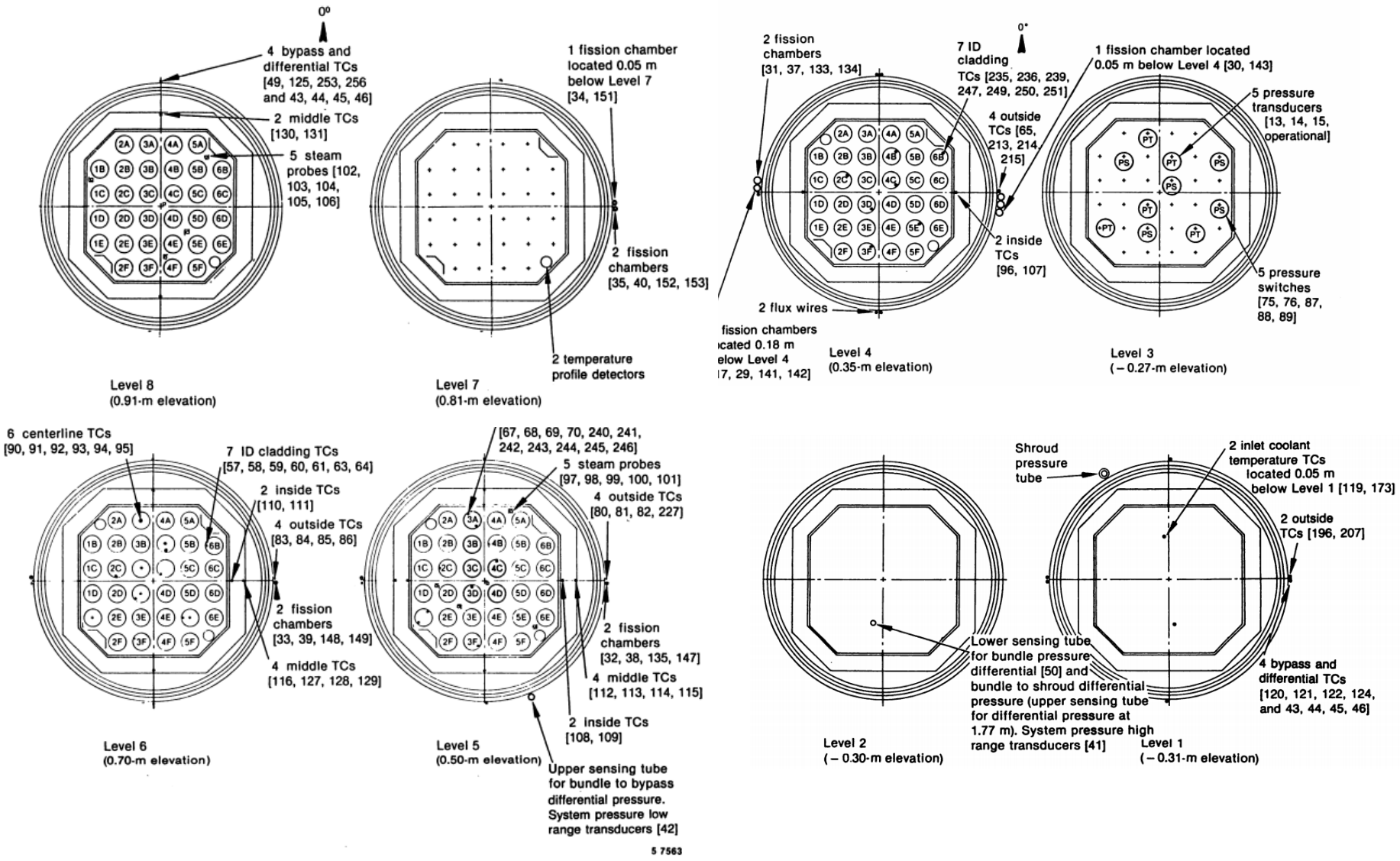
Instrumentation (1/2)





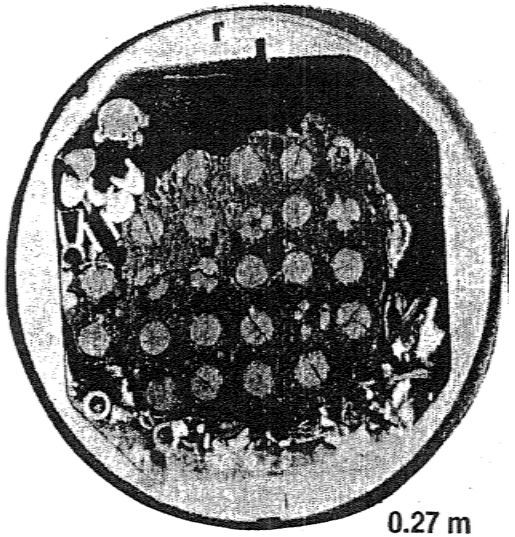
Elevation view of SFD-ST test train

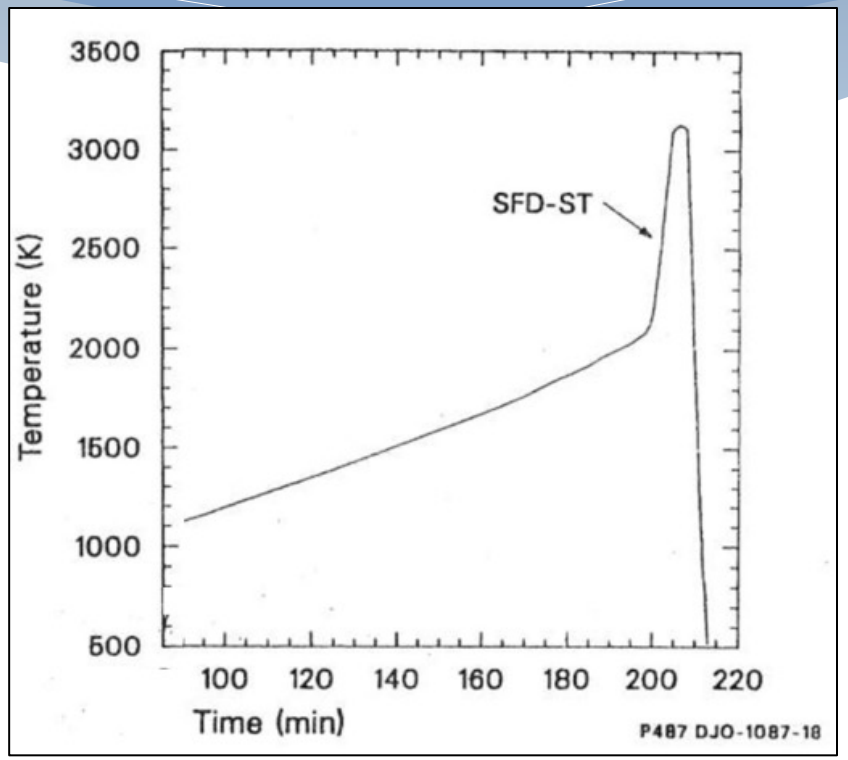
Instrumentation (2/2)



Best estimate peak experimental temperatures exceeded 2800 K

* Based on
  * Thermocouples in bundle shroud
  * Metallographic examinations
  * SCDAP/RELAP5 analysis





MELCOR Analysis of Separate Effect Test's with PSI-KIT Nitriding Model

B. Jäckel, J. Birchley, T. Lind, S. Park, M. Steinbrück

ABSTRACT

After Fukushima Dai-Ichi nuclear accident in 2011 the safety of spent fuel pools came into focus of the community. Integral experiments and separate effect tests, including during oxidant starvation but in the presence of nitrogen, showed the potential of a fast loss of the only barrier against fission product release due to formation of zirconium nitride (ZrN). A typical sequence might comprise pre-oxidation in steam, oxidation/nitriding in air/nitrogen, re-oxidation in steam.

PSI and KIT are carrying out a project to obtain data and hence develop a standalone computer model to calculate the behavior of the cladding material under different concentrations of oxygen and nitrogen. More than 70 separate effect tests are used to determine the temperature dependent reaction rates during four phases: pre-oxidation, annealing in inert gas, nitriding, and re-oxidation. The final phase investigates the separate oxidation of ZrN and oxidation of the remaining metal. The model distinguishes also between two regimes, the breakaway regime at temperatures below 1050°C and the non-breakaway regime above 1050°C. Accelerated oxidation results from the density and morphology differences between ZrN and ZrO_2, as these differences lead to breakaway-like effects and the produced ZrO_2 becomes very porous.

As a subroutine of the former PSI air oxidation and break-away model, which is implemented in the official release of the MELCOR 2.1 code version, the nitriding model is able to calculate the production of several components like oxygen stabilized alpha zirconium (α-Zr(O)), zirconium nitride (ZrN) and zirconium dioxide (ZrO_2). In addition, the consumption of oxygen, steam and nitrogen as well as the release of nitrogen during ZrN oxidation is calculated. The results of the MELCOR calculations with a local PSI version of MELCOR 1.8.6 in the different phases of the separate effect tests are compared with the experimental data.



PAUL SCHERRER INSTITUT

PSI



B. Jäckel, J. Birchley, T. Lind, S. Park, M. Steinbrück

MELCOR Analysis of Separate Effect Test's with PSI-KIT Nitriding Model

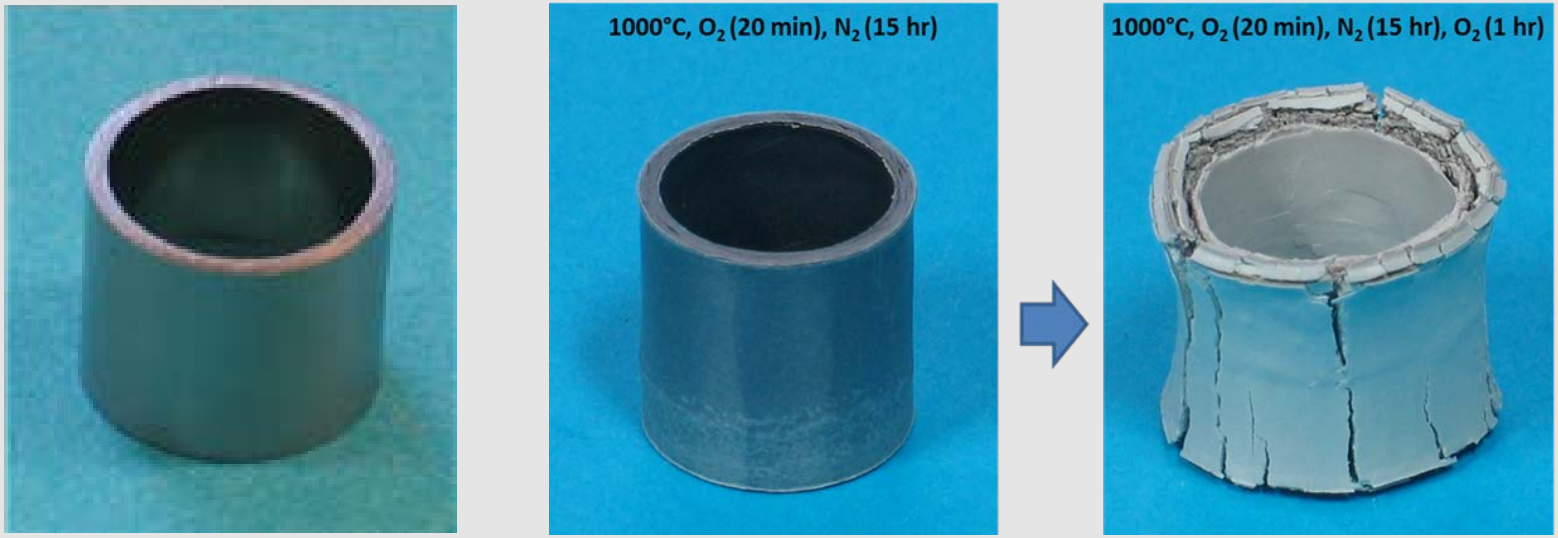
25th QUENCH Workshop, October 22-24, 2019

PAUL SCHERRER INSTITUT

Content

1. **Motivation**
2. **Separate-effect tests**
3. **Model**
4. **First Application**
5. **Outlook**

Separate-effect tests at KIT, Germany



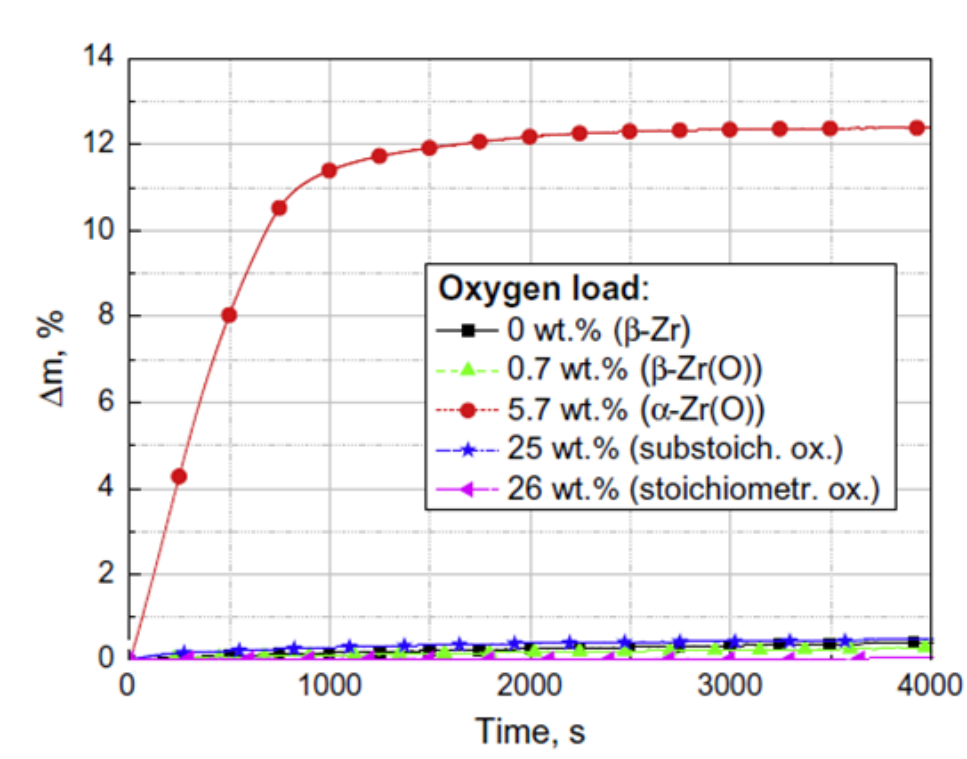
A fresh sample compared with a pre-oxidized and nitrided sample and finally a sample after re-oxidation with oxygen.

PAUL SCHERRER INSTITUT

Content

1. Motivation
2. Separate-effect tests
3. Model
4. First Application
5. Outlook

Nitriding Partners



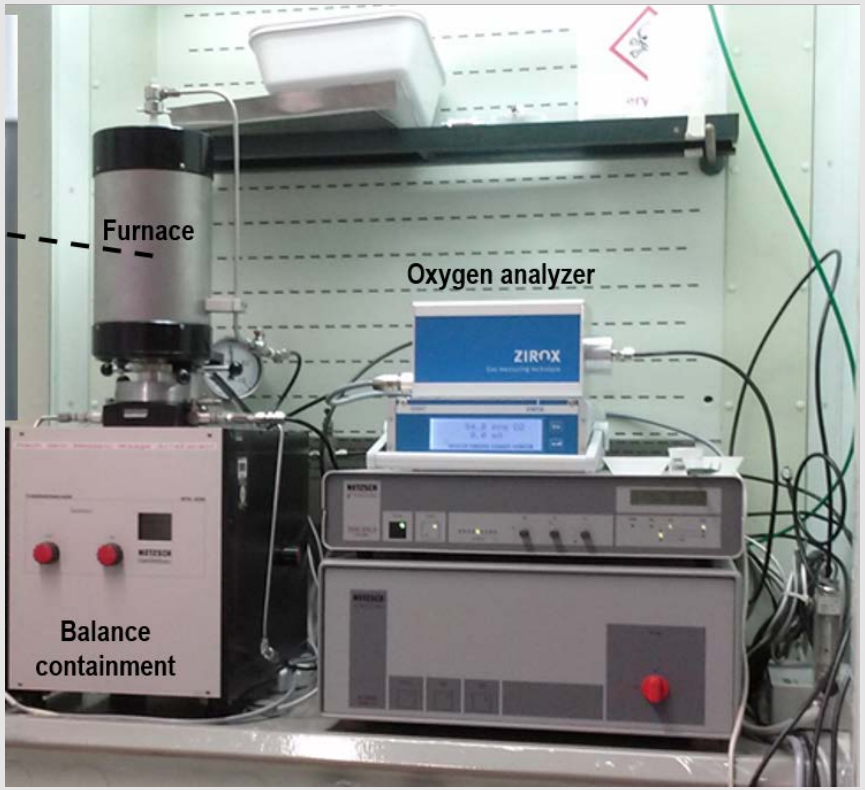
The preferred material for the nitriding reaction is α-Zr(O) as can be seen from investigations at KIT.

M. Steinbrück, 'High –temperature reaction of oxygen-stabilized α-Zr(O) with nitrogen', Journal of Nuclear Materials 447, pp. 46-55 (2014)

The Model includes oxidation of Zr metal to ZrO_2 and new to α-Zr(O), nitriding of α-Zr(O) to ZrN without release of oxygen and oxidation of ZrN with release of nitrogen. After complete consumption of ZrN, the remaining Zr metal and α-Zr(O) will be oxidised to ZrO_2.

Experimental Conditions

Two different thermal balance systems were used to perform the experiments at KIT, Germany: Netzsch STA-409 and Setaram TAG.



10 l/h Oxygen



0.9 l/h Oxygen for two tubes

Experimental Setup and Measurements

Heatup of the sample (1 cm of cladding tube) under argon atmosphere

Short time pre-oxidation by oxygen flow with argon as carrier gas (Phase I)

Long time nitriding by nitrogen flow with argon as carrier gas (Phase II)

Short time re-oxidation by oxygen flow with argon as carrier gas (Phase III)

Cool down of the sample under argon atmosphere

Measurements during test: weight gain measurement, off-gas measurement

Post test examination (micro graphs, Raman spectroscopy, X-ray spectroscopy, electron microscope imaging)

Some tests are stopped during phase II to investigate the nitriding history

Nitriding 0.5 h at 1000°C, no break away

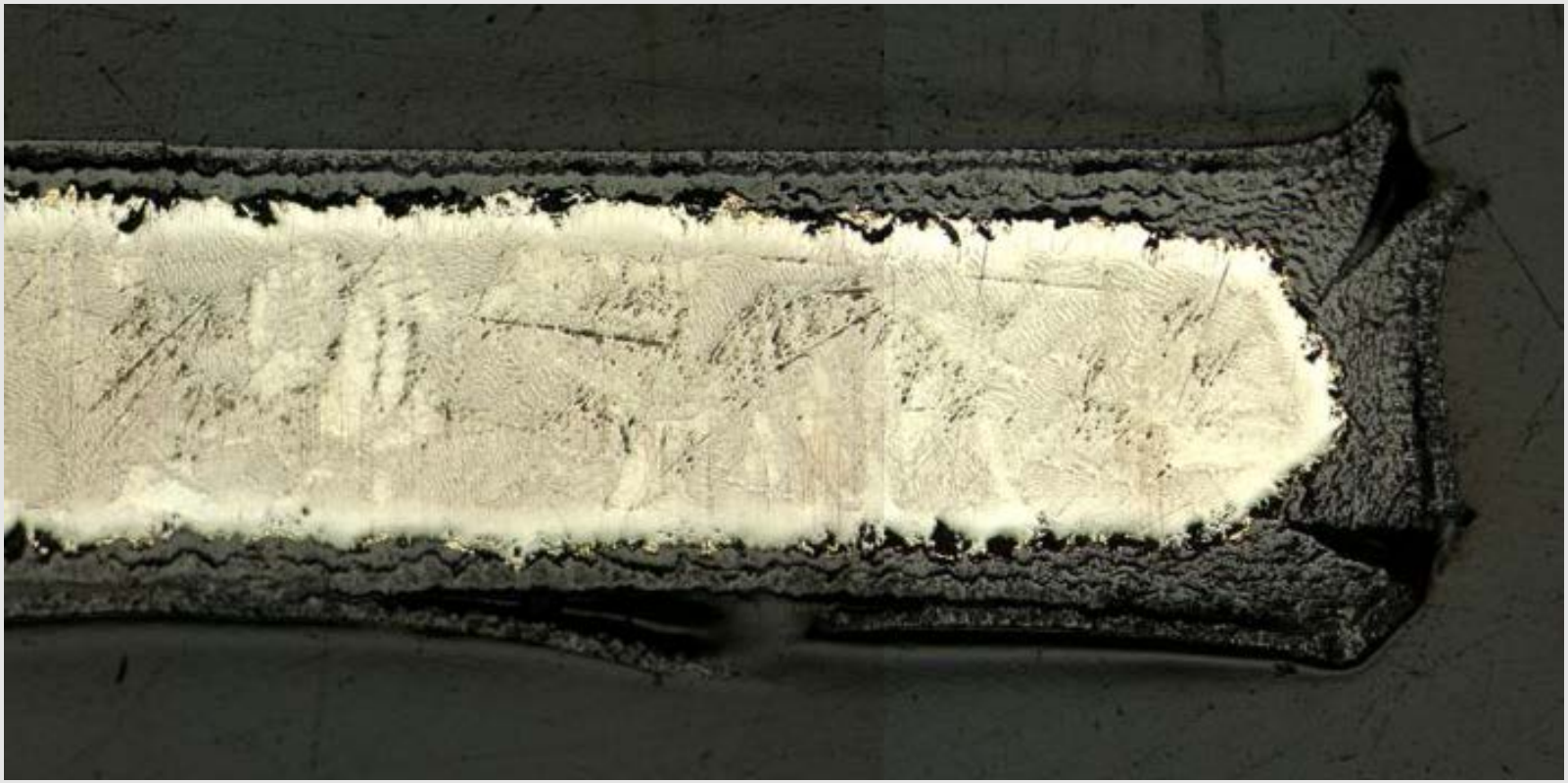
TAG facility, 20 minutes O_2 followed by 60 minutes N_2 gasflow



Attack of nitrogen only at broken edge

Nitriding 0.5 h at 1000°C, Break away

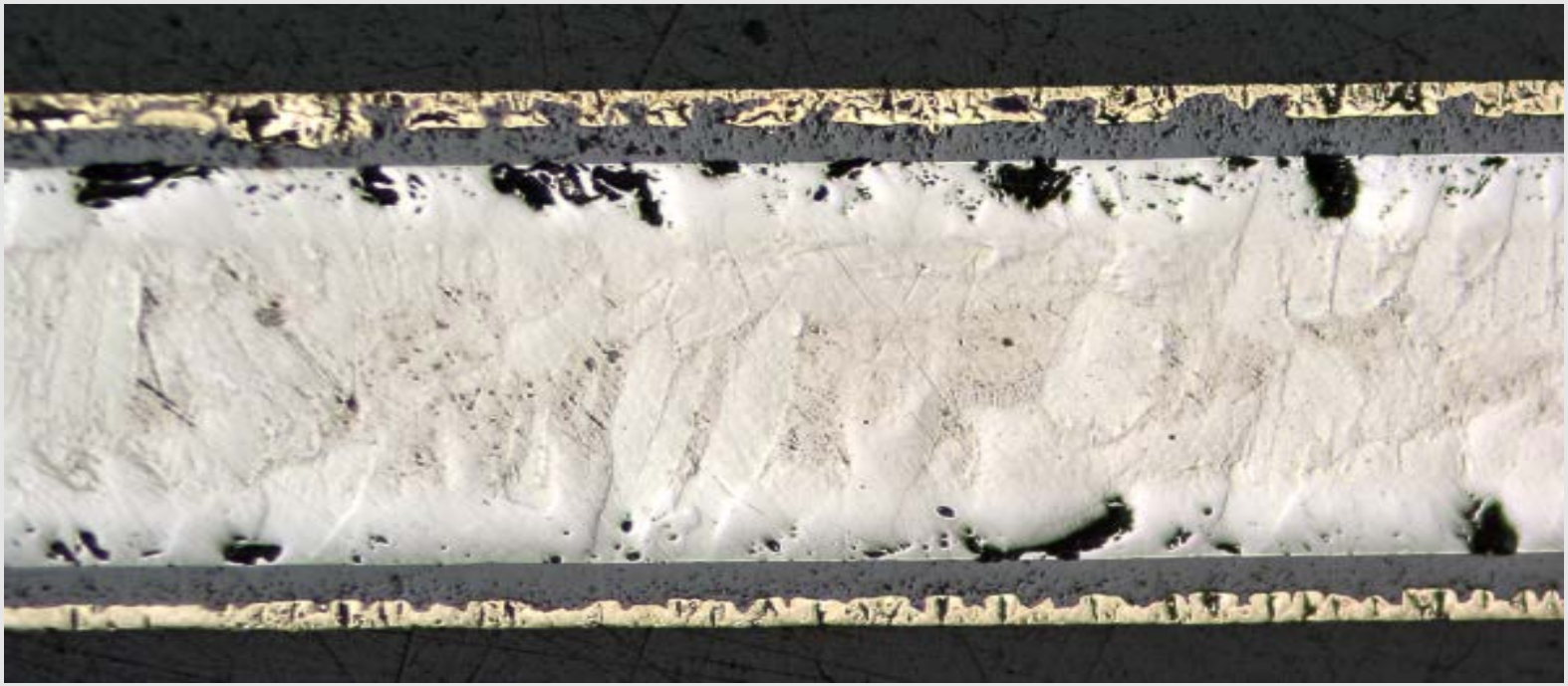
TAG facility, 60 minutes O_2 followed by 30 minutes N_2 gasflow



Attack of nitrogen after onset of break away effect

Nitriding 0.5 h at 1100°C

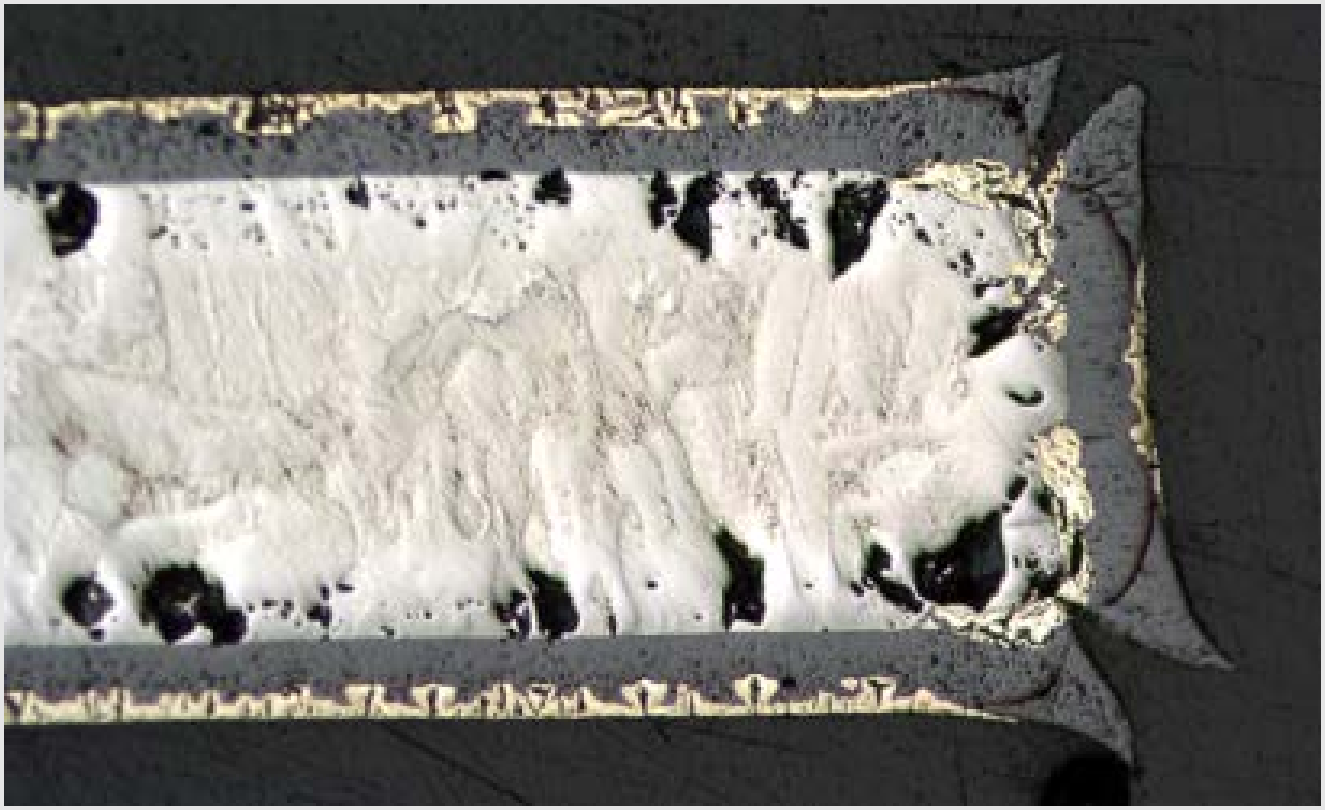
TAG facility, 20 minutes O_2 followed by 30 minutes N_2 gasflow



Attack of nitrogen only from the outer surface

Nitriding 0.5 h at 1100°C

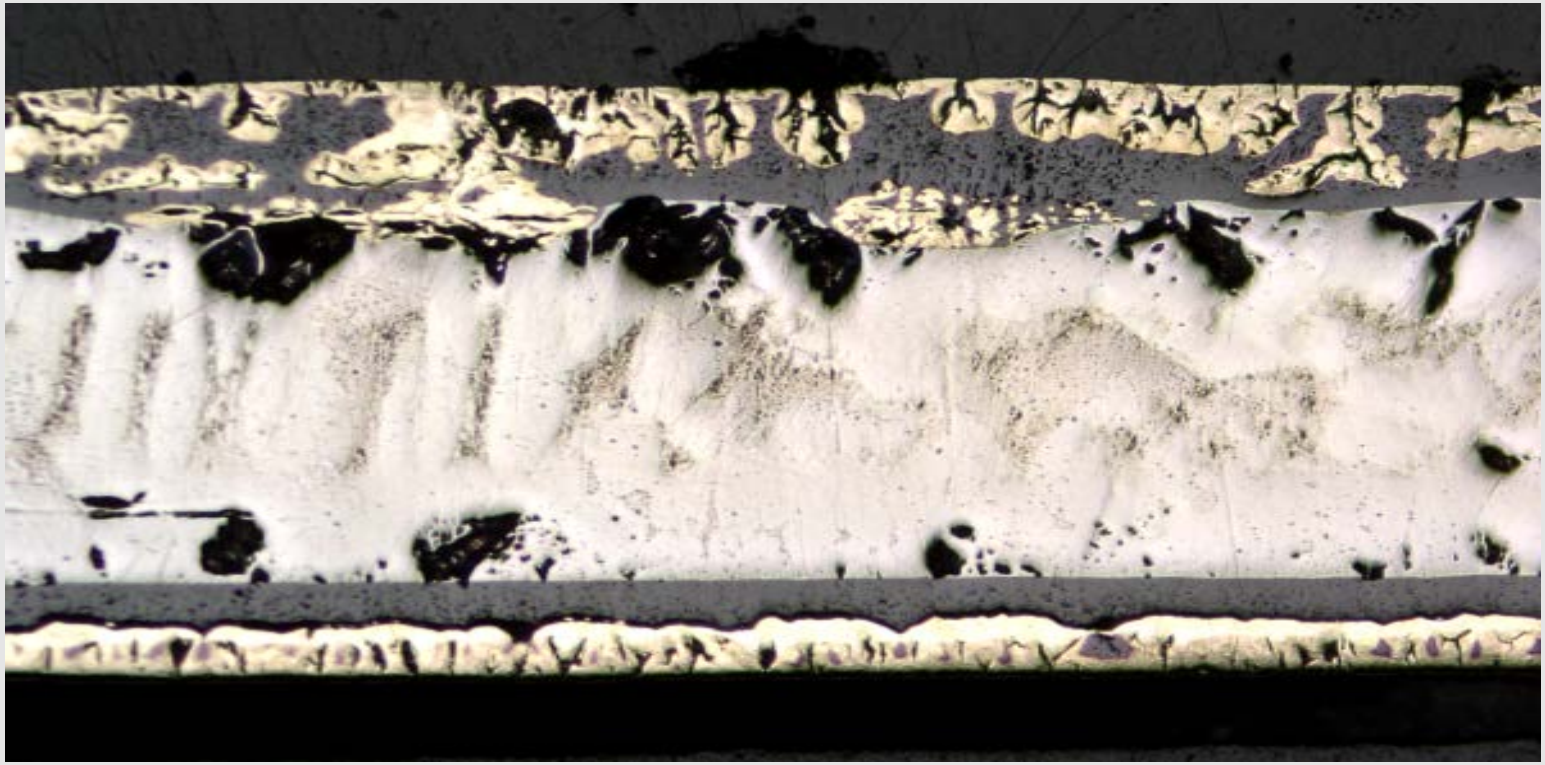
TAG facility, 20 minutes O_2 followed by 30 minutes N_2 gasflow



Attack of nitrogen only from the outer surface

Nitriding 1.0 h at 1100°C

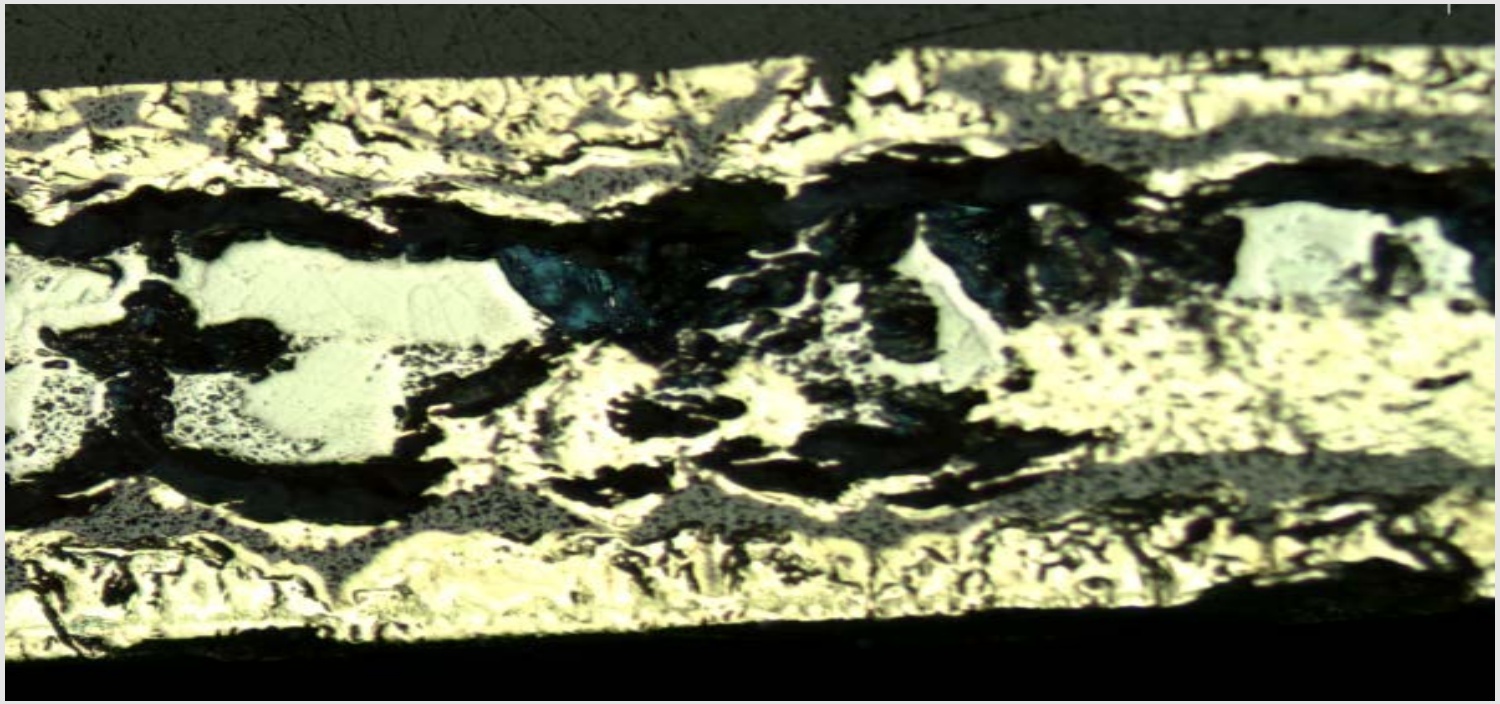
TAG facility, 20 minutes O_2 followed by 60 minutes N_2 gasflow



After breaking the oxide layer (upper part) nitrogen is reacting with the α-Zr(O) and producing ZrN between oxide crust and metal.

Nitriding 3.0 h at 1100°C

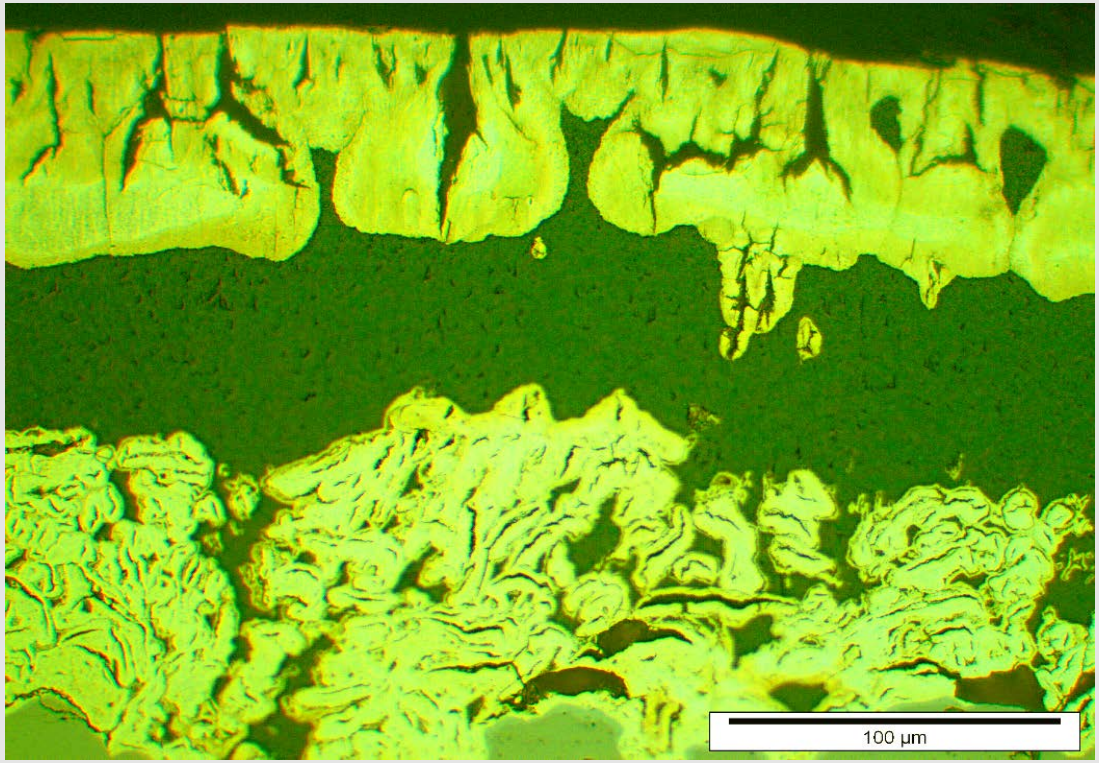
TAG facility, 20 minutes O_2 followed by 180 minutes N_2 gasflow



All α-Zr(O) has been consumed and now the slow nitriding process starts to consume slowly the remaining zirconium.

Nitriding

TAG facility, 1100°C, 10 minutes O_2 followed by 360 minutes N_2 gasflow



The nitriding process is following cracks in the oxide layer, which indicates that there is no diffusion of nitrogen through the oxide layer.

PAUL SCHERRER INSTITUT

Content

1. Motivation
2. Separate-effect tests
3. Model
4. First Application
5. Outlook

Pre-oxidation

Standard oxidation correlations are used to calculate oxidation by steam, air and oxygen under non starvation conditions.

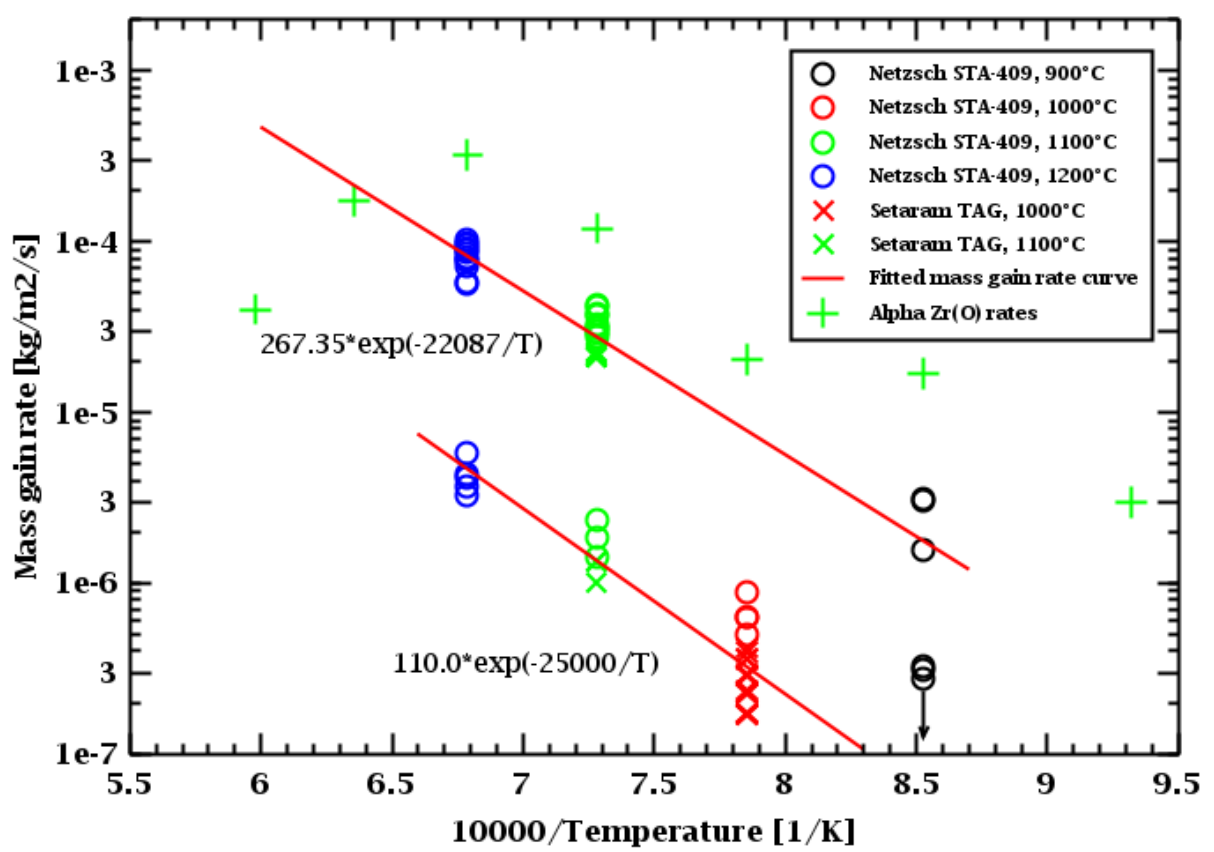
Below 1050°C PSI-breakaway model is used.

Above 1050°C PSI-breakaway model is used only for air.

Additional to earlier model α-Zr(O) is calculated using the Cathcard-Powell correlation.

(during partial oxygen and steam starvation production of α-Zr(O) is enhanced)

Nitriding



The nitriding correlations in Arrhenius plots are used as constant values for the temperatures. The nitriding reaction is not parabolic as the oxidation reaction which was observed during the SET's .

Re-oxidation

The re-oxidation starts fast with the oxidation of the ZrN and slows down when ZrN is oxidized.

In both temperature regimes the re-oxidation of zirconium metal reaches reaction rates which are deduced from breakaway experiments (at high temperatures only under presence of nitrogen).

The post breakaway reaction rates at high temperatures are attributed to the change in the morphology only.

ZrO_2 after re-oxidation of ZrN shows a porouse structure.

Model Overview

Presence of steam, oxygen or air:

using standard correlations and breakaway model plus α-Zr(O) production

Starvation of steam, oxygen without presence of N_2:

enhanced production of α-Zr(O) due to oxygen diffusion (standard correlations)

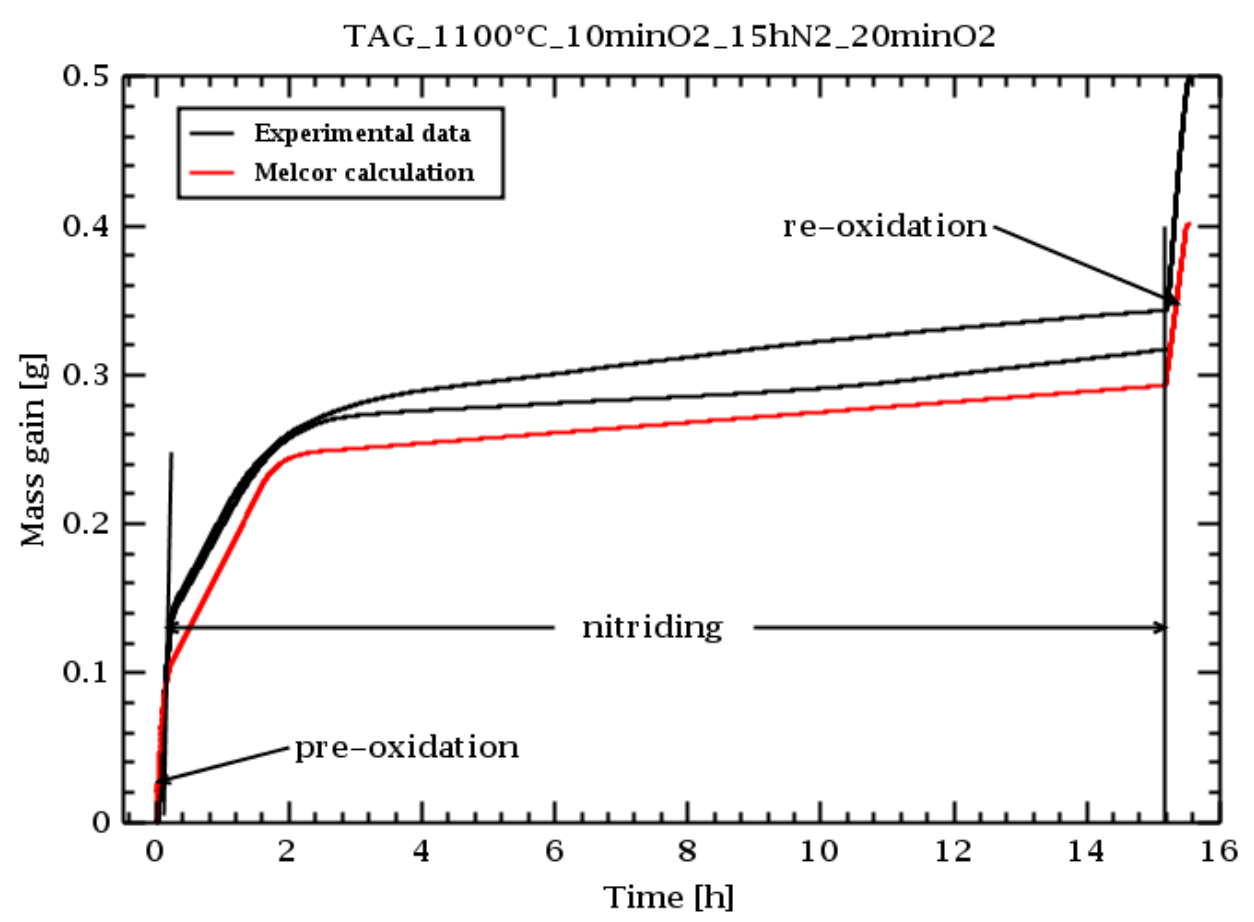
Starvation of steam, oxygen with presence of N_2:

Fast nitriding of α-Zr(O), slow nitriding w/o α-Zr(O)

Recovery of steam and oxygen:

Fast oxidation of ZrN, post breakaway oxidation of remaining α-Zr(O) and Zr metal

Mass Gain Measurement, TAG facility



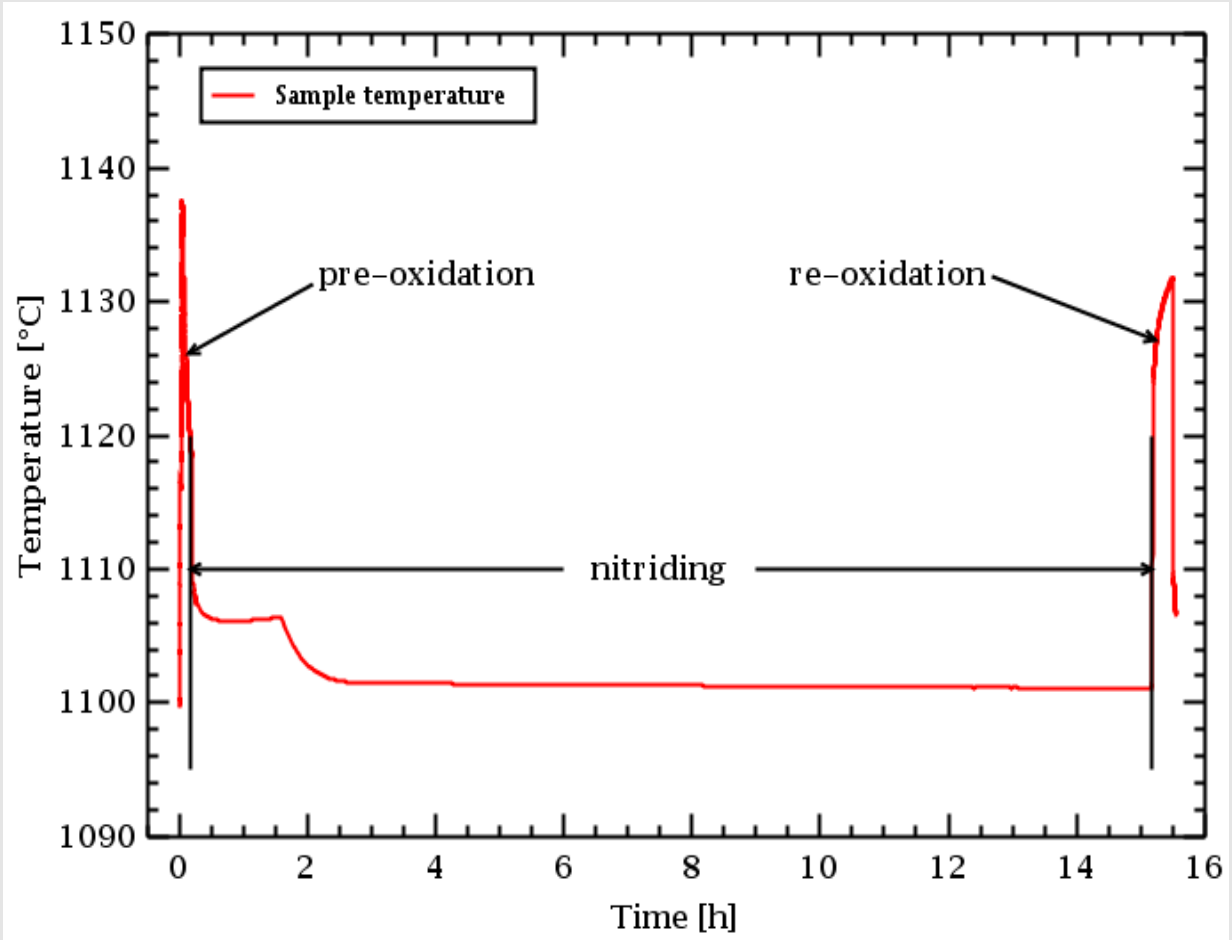
Pre-oxidation

Fast nitriding

Slow nitriding

Re-oxidation

Temperature overshooting, TAG facility



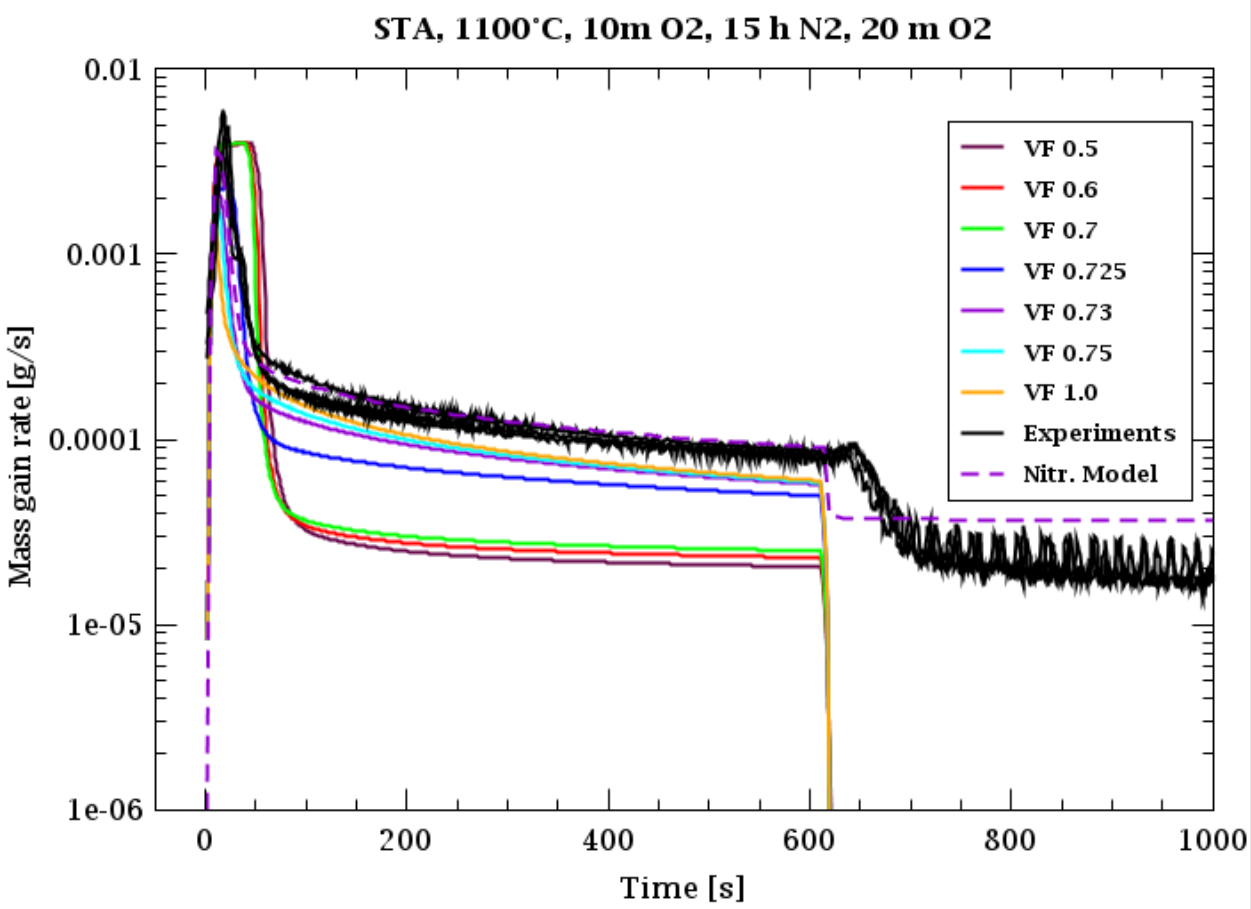
Pre-oxidation

Fast nitriding

Slow nitriding

Re-oxidation

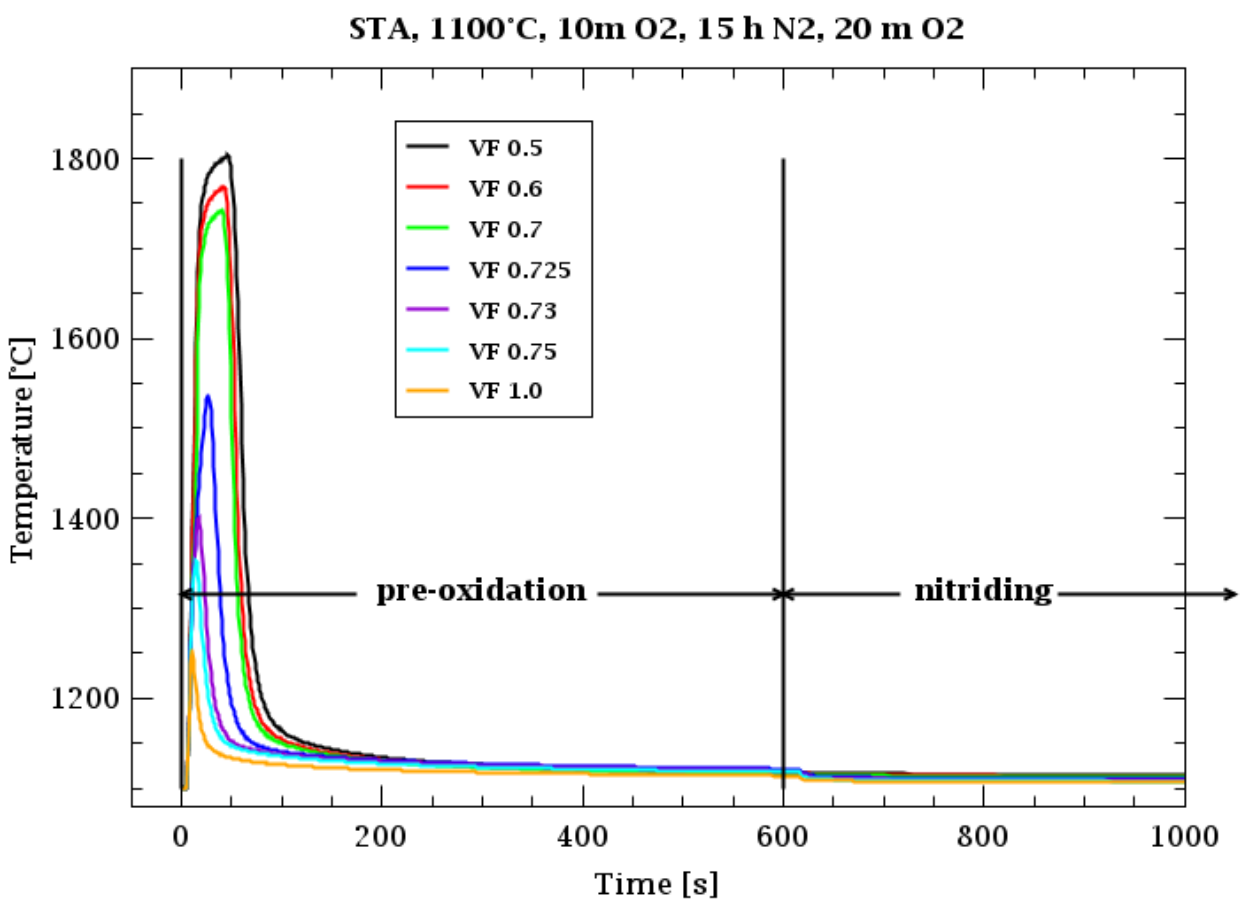
Mass Gain Rate Measurement, STA facility



Pre-oxidation

Fast nitriding

Temperature overshooting, STA facility

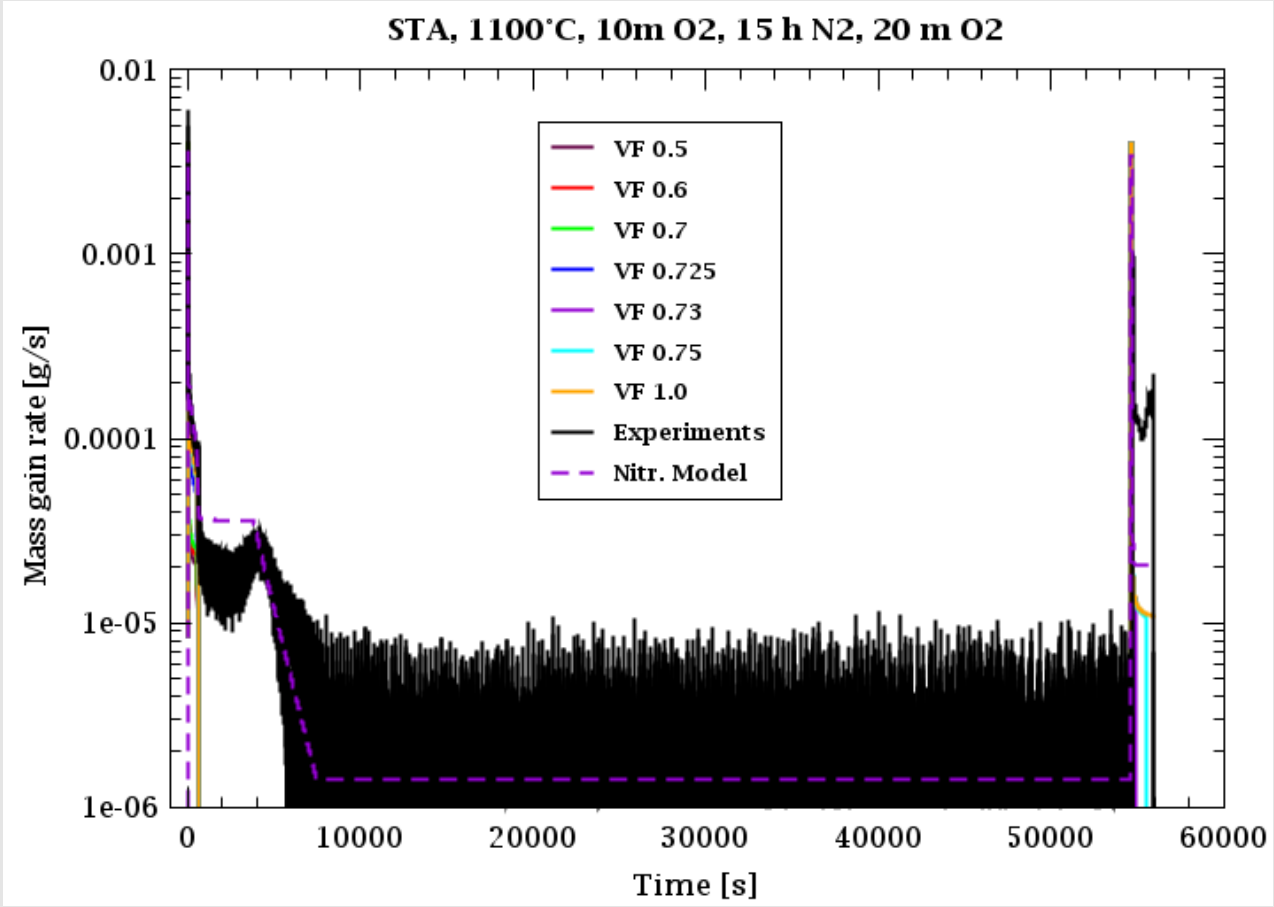


Pre-oxidation

Fast nitriding

The temperature overshooting at view factor 0.73 s in the order of 300K.

Mass Gain Rate Measurement, STA facility



Pre-oxidation

Fast nitriding

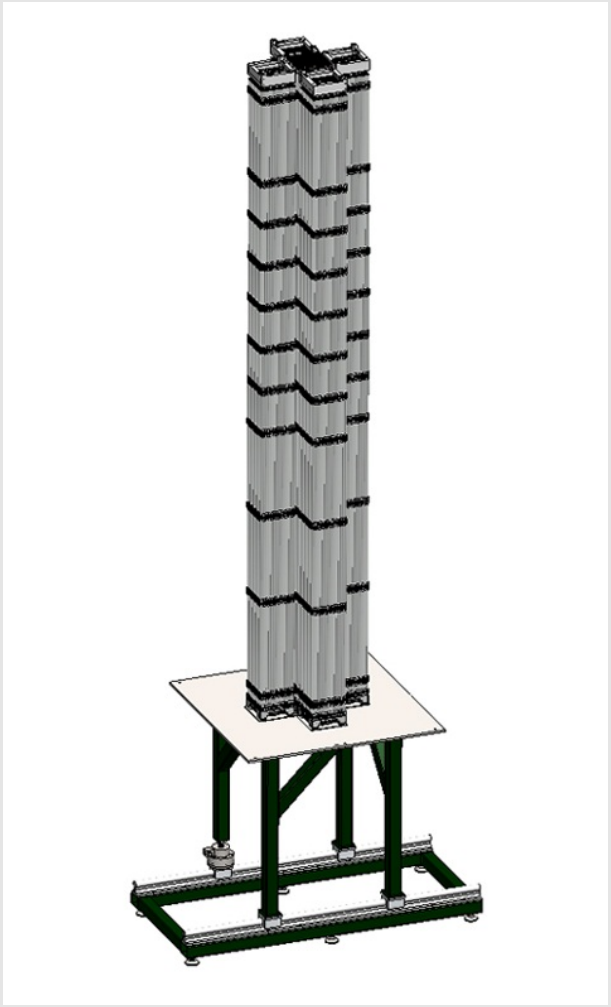
Slow nitriding

Re-oxidation

Content

1. Motivation
2. Separate-effect tests
3. Model
4. First Application
5. Outlook

Sandia Fuel Project Phase II



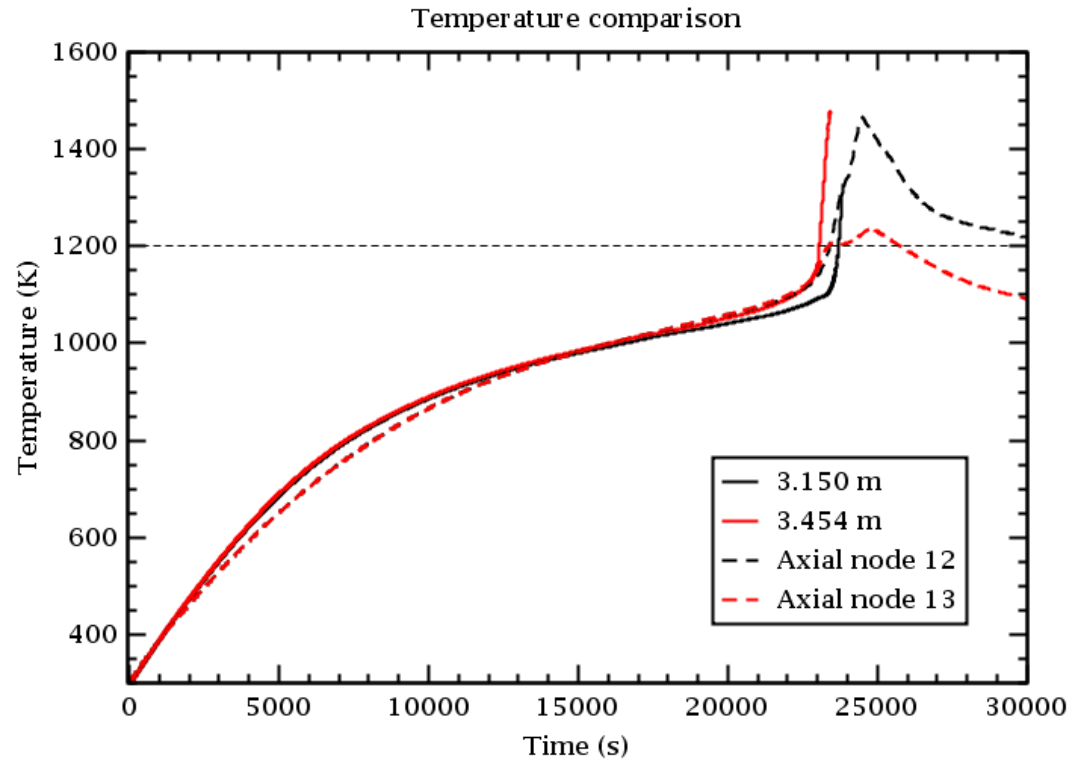
Five full lenght fuel assemblies, one heated in the center and four unheated in the periphery, cooled by buoancy driven air.

Heating power of 15 kW simulates FA three month after shutdown.





Sandia Fuel Project Phase II

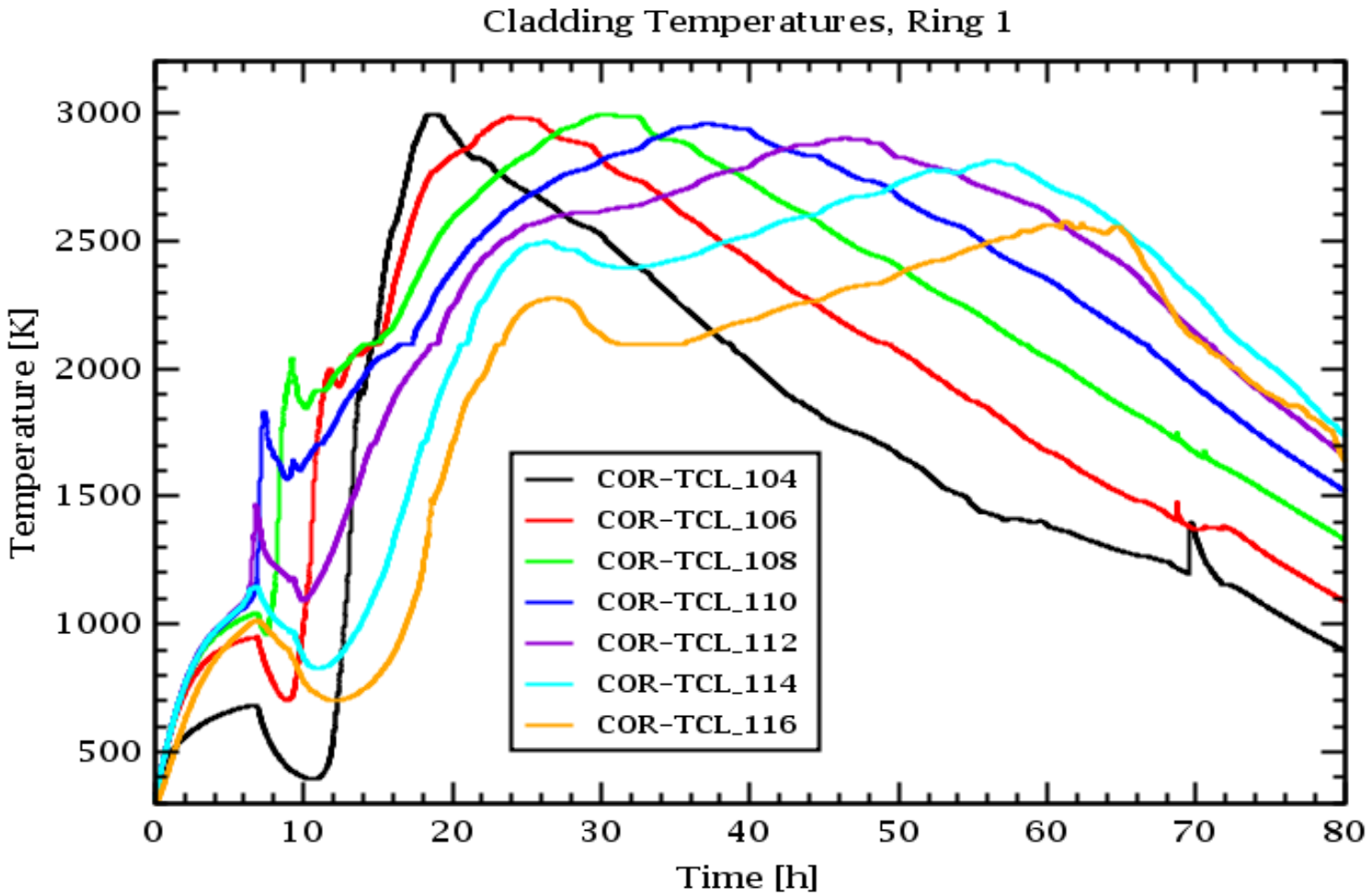


Calculated nitriding reaction in nodes 12 and 13 not self sustaining because of low temperatures.

The experimental data are reasonably met until failure of the thermo-couples.

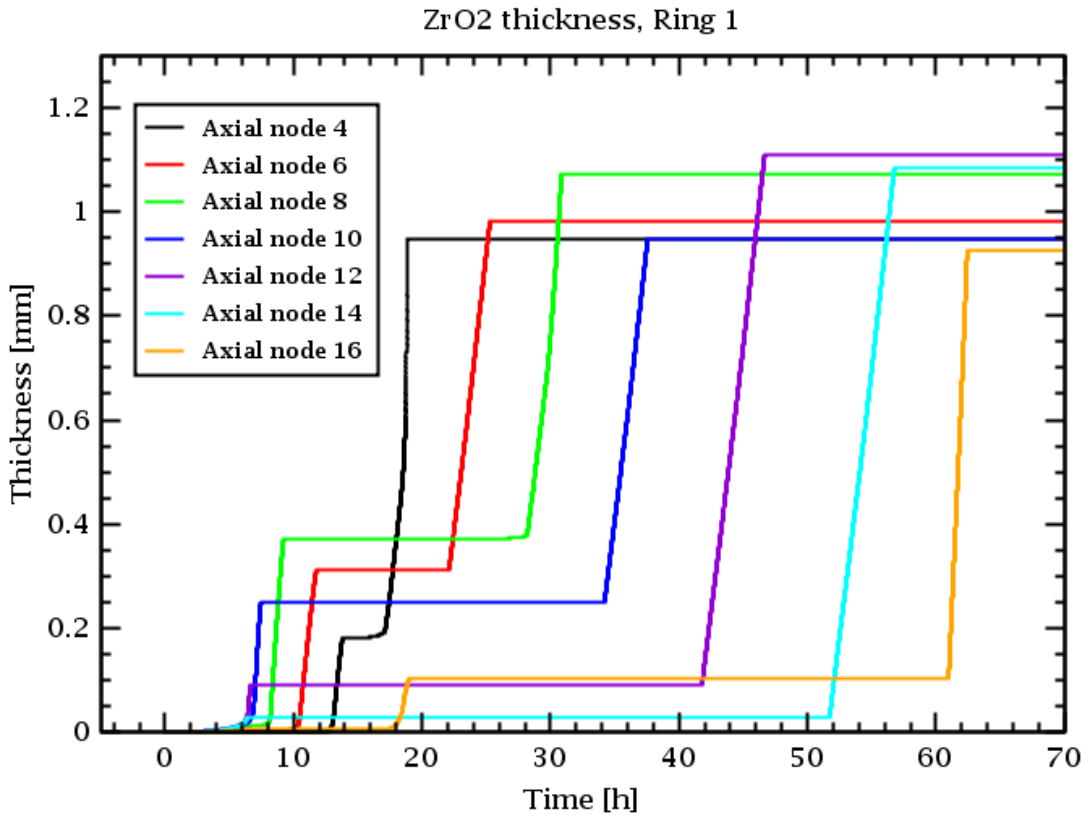
calculated by MELCOR code with nitriding model (MELCOR 1.8.6 PSI)

Sandia Fuel Project Phase II



T_{melt}: **Zr ~ 2125K** **ZrO_2 ~ 2988K** **ZrN ~ 3253K**

Sandia Fuel Project Phase II

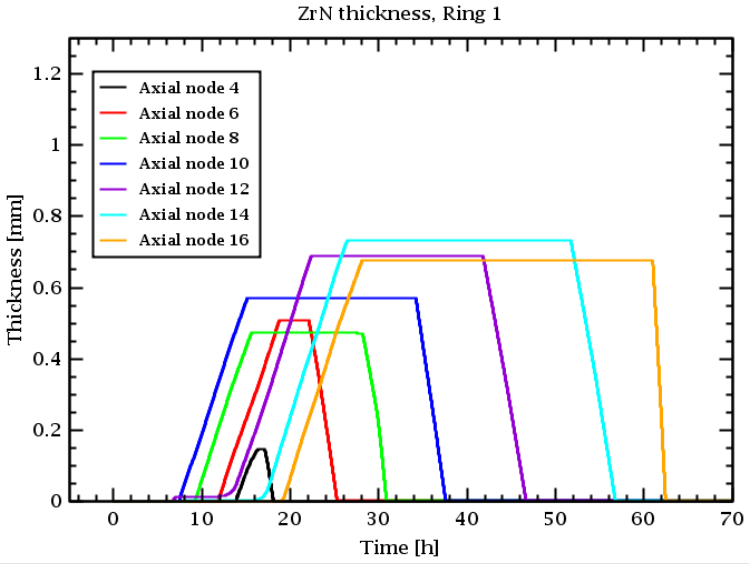


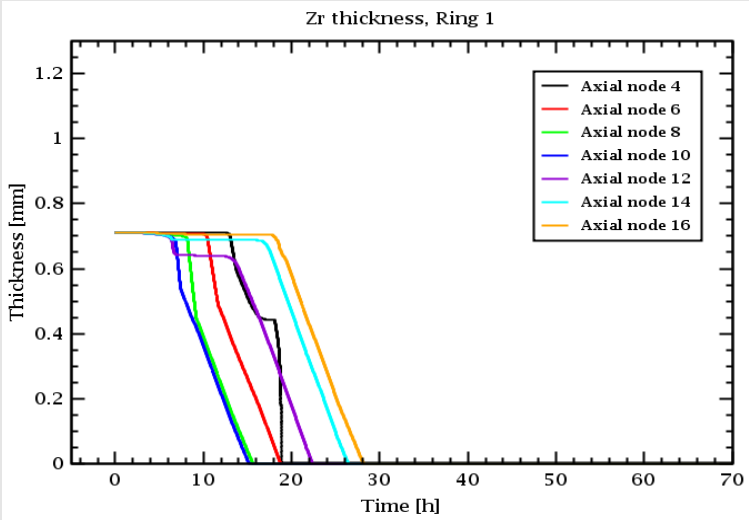
Mass loss by relocation may explain the different thickness of the oxide layer after full oxidation.

The zirconium fire firstly propagates downwards and then, after complete oxidation of the zirconium in the lowermost node, upwards again.

After about three days all the zircaloy was oxidized.

Sandia Fuel Project Phase II

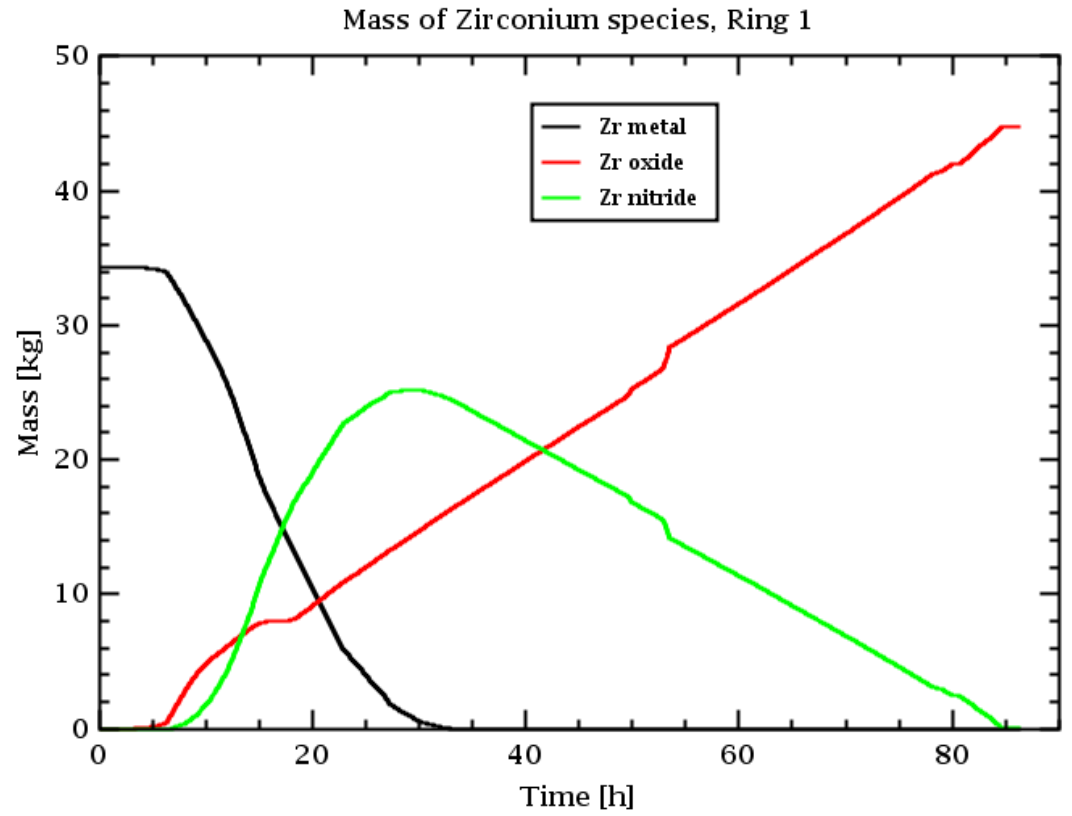




In contrary to the MELCOR calculation without nitriding model, the metal is completely consumed after about 30 hours.

All the remaining metal in the center region of the heated fuel element is nitrided.

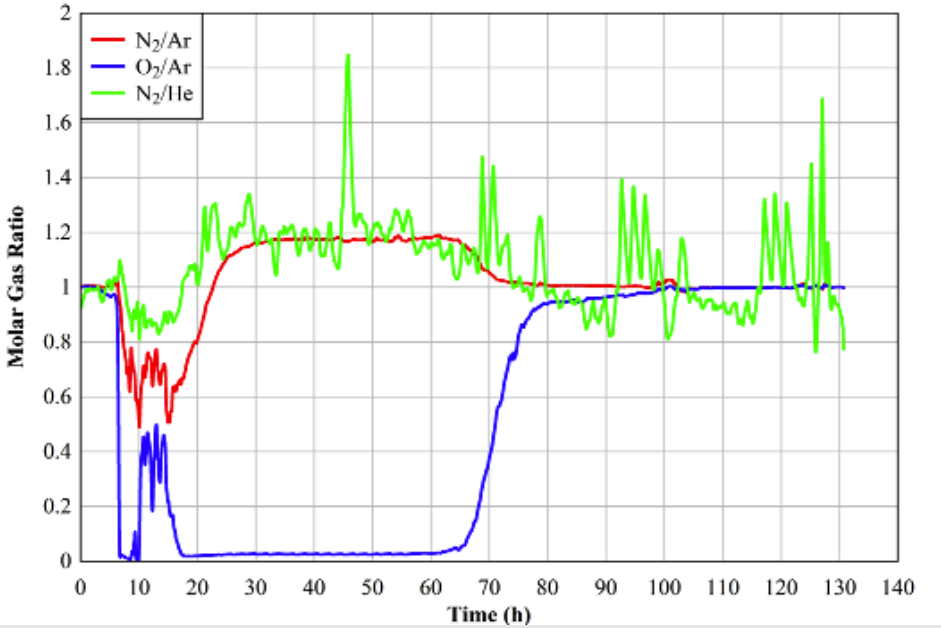
Sandia Fuel Project Phase II

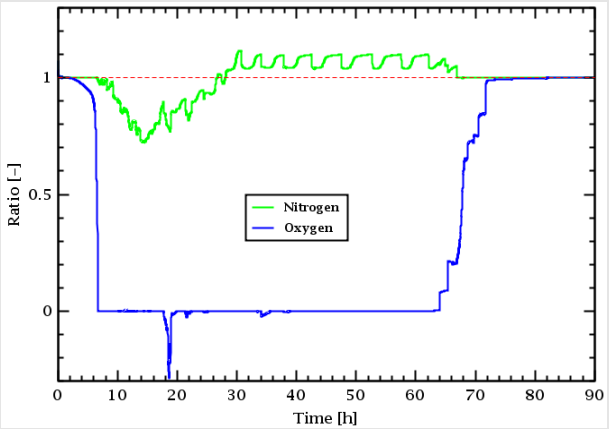


The metal is consumed after 30 hours and then the nitride is re-oxidized.

Limiting factor of the re-oxidation is the buoyancy driven air flow through the bundle.

Sandia Fuel Project Phase II





The relative gas composition at the outlet of the centered bundle is shown as normalized ratio between the reacting gases and argon from the experimental data.

This is compared with the ratio of outlet and inlet mass flow calculated from the MELCOR code.

The qualitativly good estimation shows the capability of the nitriding model to describe the chemical behaviour of the zirconium during the SFP experiment.

PAUL SCHERRER INSTITUT

Content

1. **Motivation**
2. **Separate-effect tests**
3. **Model**
4. **First Application**
5. **Outlook**

Outlook

- **The cuttoff of the nitriding reaction at high temperatures has to be investigated.**
- **Fine tuning of the temperature dependent reaction rate functions has to be done for the temperature range below 1050°C. The mechanical breakaway effect complicates the picture of the nitriding process.**
- **The model has to be validated with independent experiments and prepared for the full implementation into the severe accident codes MELCOR and SCDAP/Sim.**


Questions?

Evaluation of the process in the BWR and VVER spent fuel pools during severe accident conditions

T. Kaliatka, A. Kaliatka, V. Vileiniskis
Lithuanian Energy Institute, Breslaujos str. 3, LT-44403 Kaunas, Lithuania

ABSTRACT

The Tsunami that followed the earthquake at the Fukushima Daiichi nuclear plants in Japan showed that a loss of heat removal in the spent fuel pools (SFP) may lead to very serious consequences. The consequences of such an accident can be very serious creating a possibility of significant amount of radioactive material release to the environment. Thus, the loss of water, which leads to the loss of heat removal in SFP may lead to very serious consequences.

In order to investigate the processes and phenomena inside a spent fuel pool during severe accident conditions the codes which are developed for the analysis of accidents with fuel rods degradation (for example: RELAP/SCDAPSIM, ASTEC, MELCOR, etc.) could be used.

In this work RELAP/SCDAPSIM code were used for the modelling of the BWR and VVER type SFP. However, before the modelling of the SFP it is needed to make sure what code suitable correctly model the process in SFP during severe accidents. Scientists for Lithuanian Energy Institute have been validated RELAP/SCDAPSIM code against the QUENCH-3, QUENCH-6 and QUENCH-10 experiments. Validation results showed that the RELAP/SCDAPSIM code sufficiently reflect the main phenomena that occurred during QUENCH experiments and this code is suitable to model the processes in the SFP.

RELAP/SCDAPSIM code was used for the modelling the SFP of BWR (BWR4, MARK-1) and VVER (ZNPP Unit1) type reactors. Calculation results of RELAP/SCDAPSIM code were compared with calculation results of ASTEC. Comparison shows that RELAP/SCDAPSIM, ASTEC have the comparable and adequate results of calculation results. However highest differences in the calculation results are due to different calculation of produced hydrogen. In this work the reasons for the differences in calculation results are discussed.



LITHUANIAN ENERGY INSTITUTE
http://www.lei.lt

NATIONAL OPEN ACCESS SCIENTIFIC CENTRE FOR FUTURE ENERGY TECHNOLOGIES

OPEN R & D LITHUANIA

Evaluation of the processes in the BWR and VVER spent fuel pools during severe accident conditions

T. Kaliatka, A. Kaliatka, V. Vileiniskis

Outline

- Modeling of QUENCH-3, QUENCH-6 experiments using RELAP/SCDAPSIM and ASTEC codes
- Modeling of QUENCH-10 experiment using RELAP/SCDAPSIM for the preparation of modeling of spent fuel pools.
- Modelling of LOCA accident in the BWR spent fuel pool using RELAP/SCDAPSIM code

- Modelling of LOCA accident in the VVER spent fuel pool using RELAP/SCDAPSIM and ASTEC codes

Modeling of QUENCH-3, QUENCH-6 experiments using RELAP/SCDAPSIM and ASTEC codes

Modelling of QUENCH-03 and QUENCH-06 Experiments Using RELAP/SCDAPSIM and ASTEC Codes

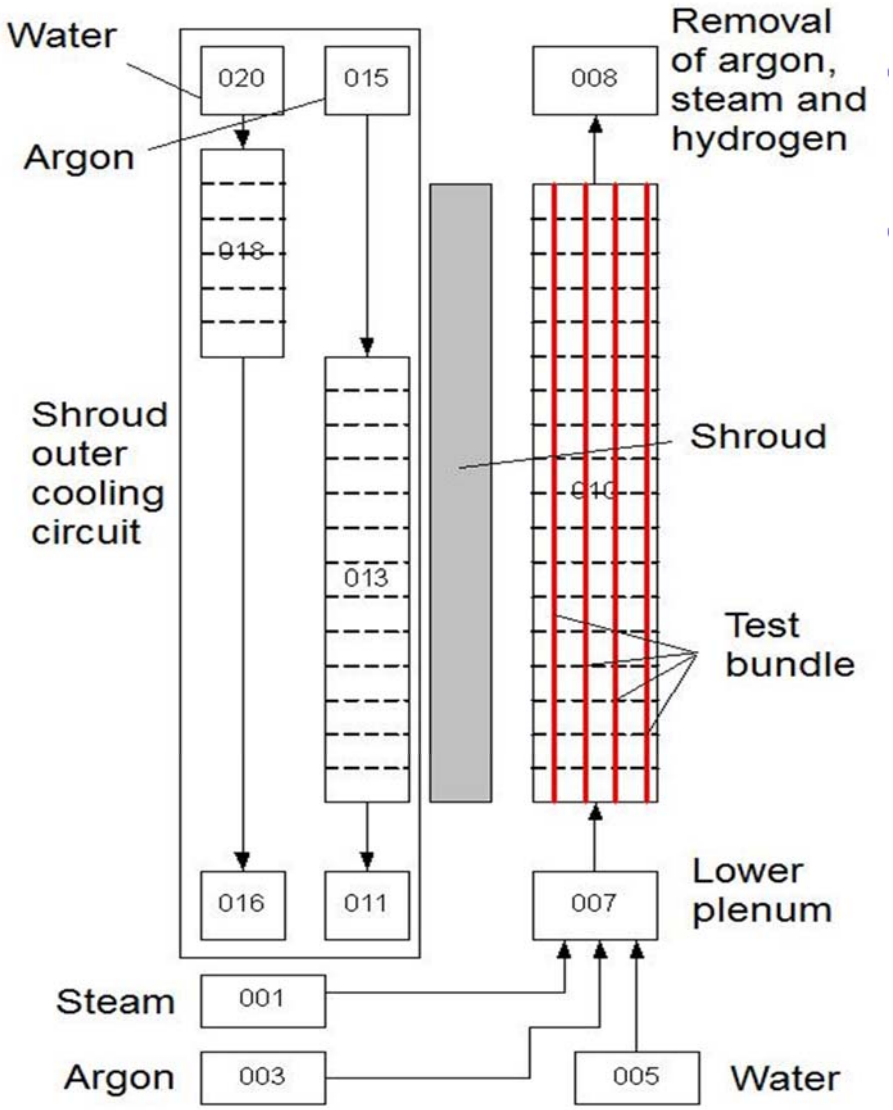
Science and Technology of Nuclear Installations
Volume 2014, Article ID 849480, 13 pages
http://dx.doi.org/10.1155/2014/849480

Application of Best Estimate Approach for Modelling of QUENCH-03 and QUENCH-06 Experiments

Nuclear Engineering and Technology
Volume 48, Issue 2, April 2016, Pages 419-433
https://doi.org/10.1016/j.net.2015.12.011

RELAP/SCDAPSIM model of the QUENCH test

RELAP/SCDAPSIM is designed to describe the overall reactor coolant system thermal hydraulic response and core behaviour under normal operating conditions or under design basis or severe accident conditions.



RELAP module (thermal hydraulics):

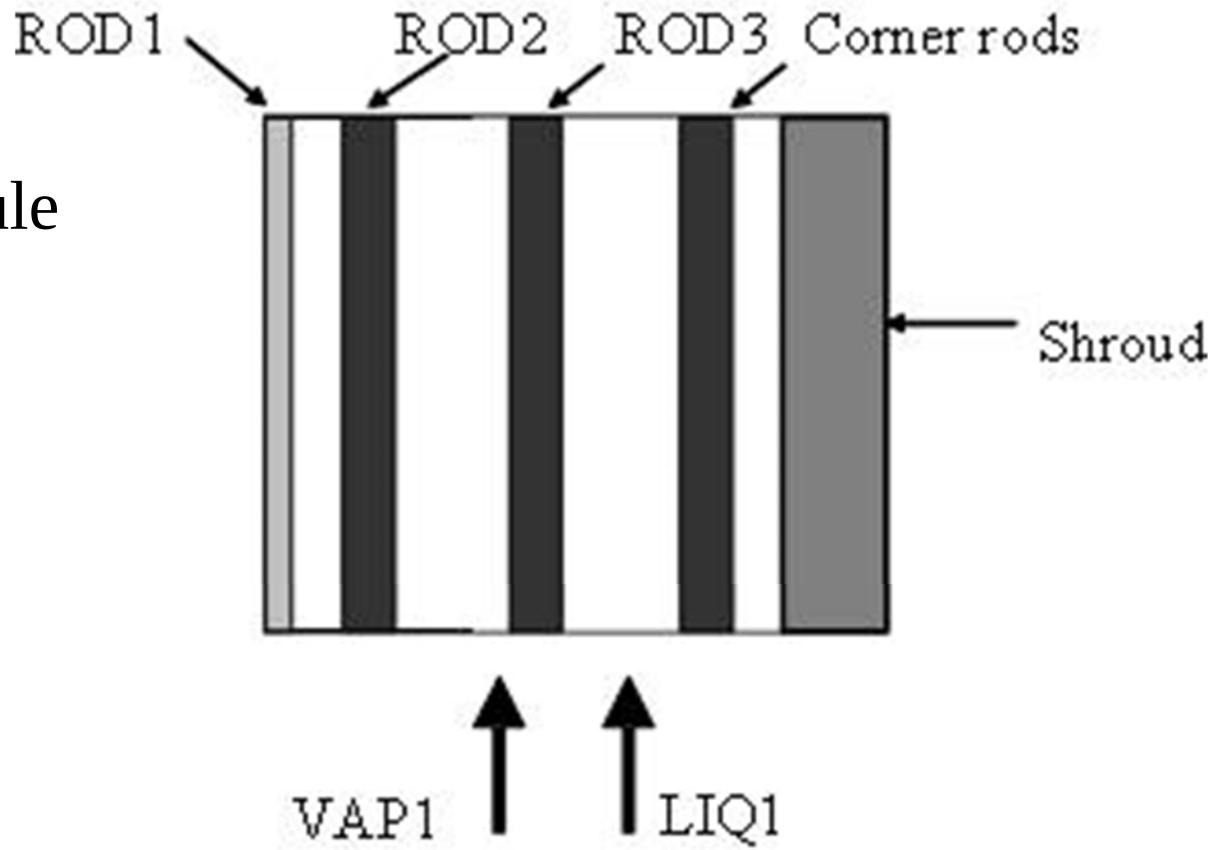
- All Elements

SCDAP module (behaviour of the core and vessel structures):

- component 1 - one central rod (not heated), modelled as a "fuel" element is composed of ZrO_2 pellets in the centre, a gas-filled gap and cladding of Zircaloy;
- component 2 - 8 heated rods (around the central rod) which simulates heated fuel rods, modelled using "Cora" component which is composed of tungsten heating elements in the centre, ZrO_2 pellets, gas-filled gap and cladding of Zircaloy;
- component 3 - 12 heated rods, modelled using "Cora" component;
- component 4 - the four rods in the corners, modelled as "fuel" component;
- component 5 – shroud of the bundle, modelled as "shroud" component, which consists of the inner Zircaloy layer, an insulating layer of ZrO_2 and Inconel layer (using properties of stainless steel).

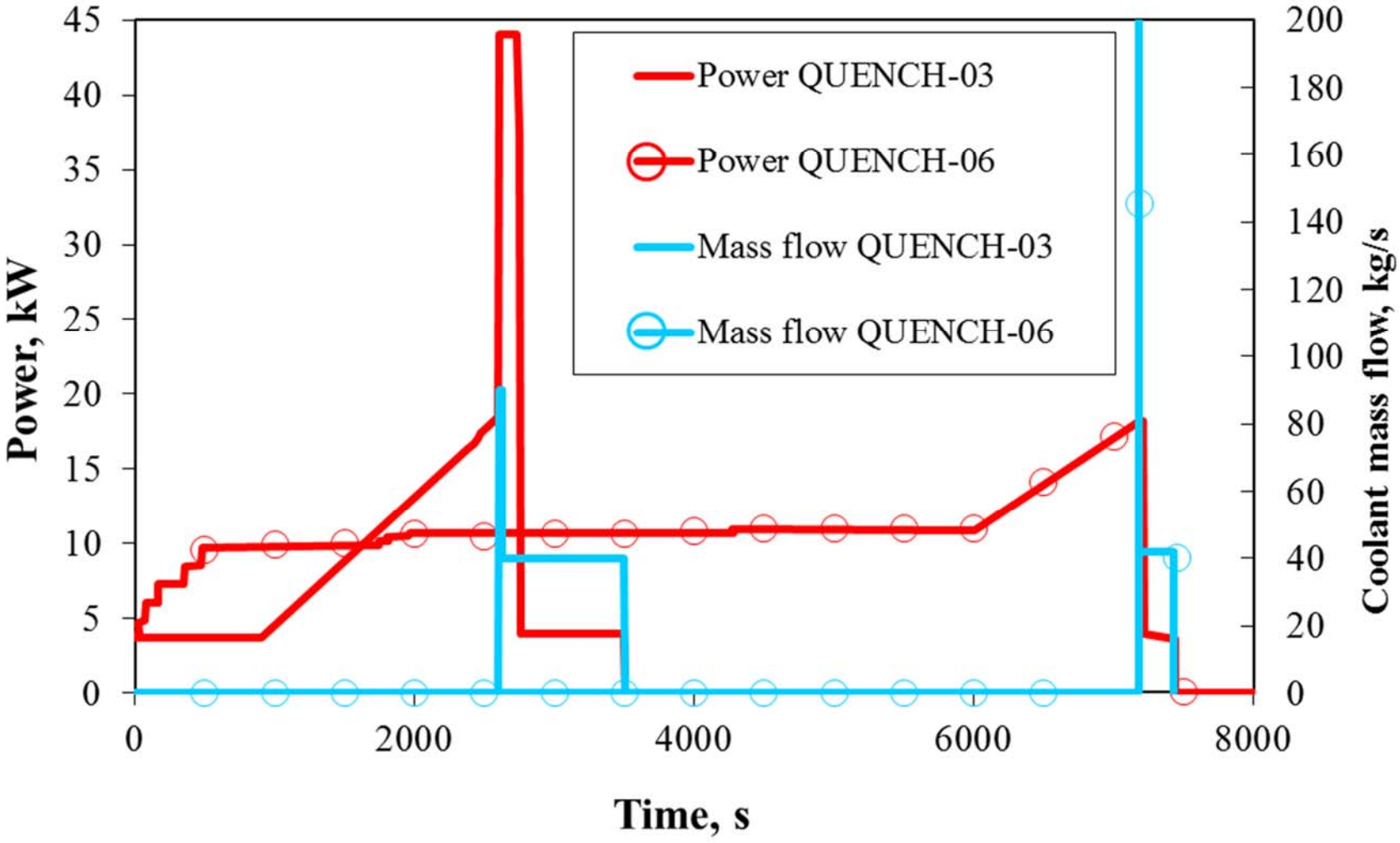
ASTEC model of the QUENCH test

ICARE module



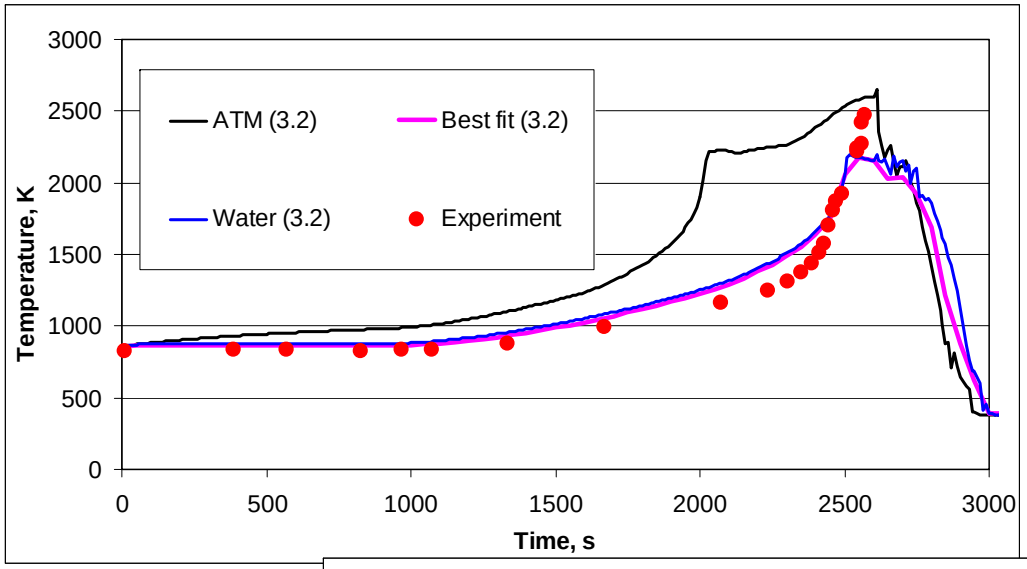
Nodalization scheme of QUENCH test, developed using ASTEC code ICARE module

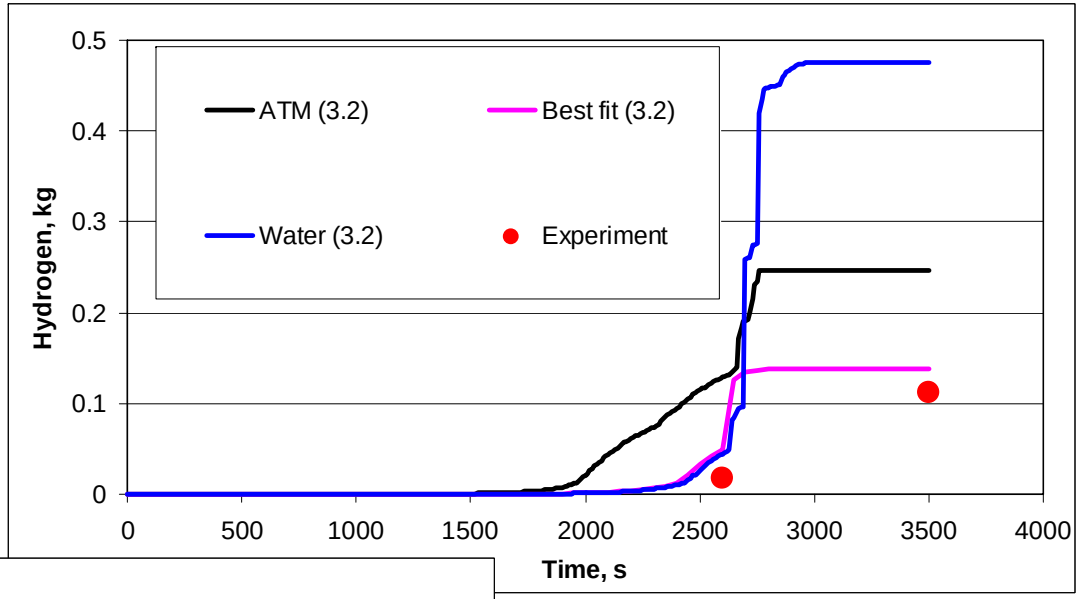
QUENCH-3 and QUENCH-6

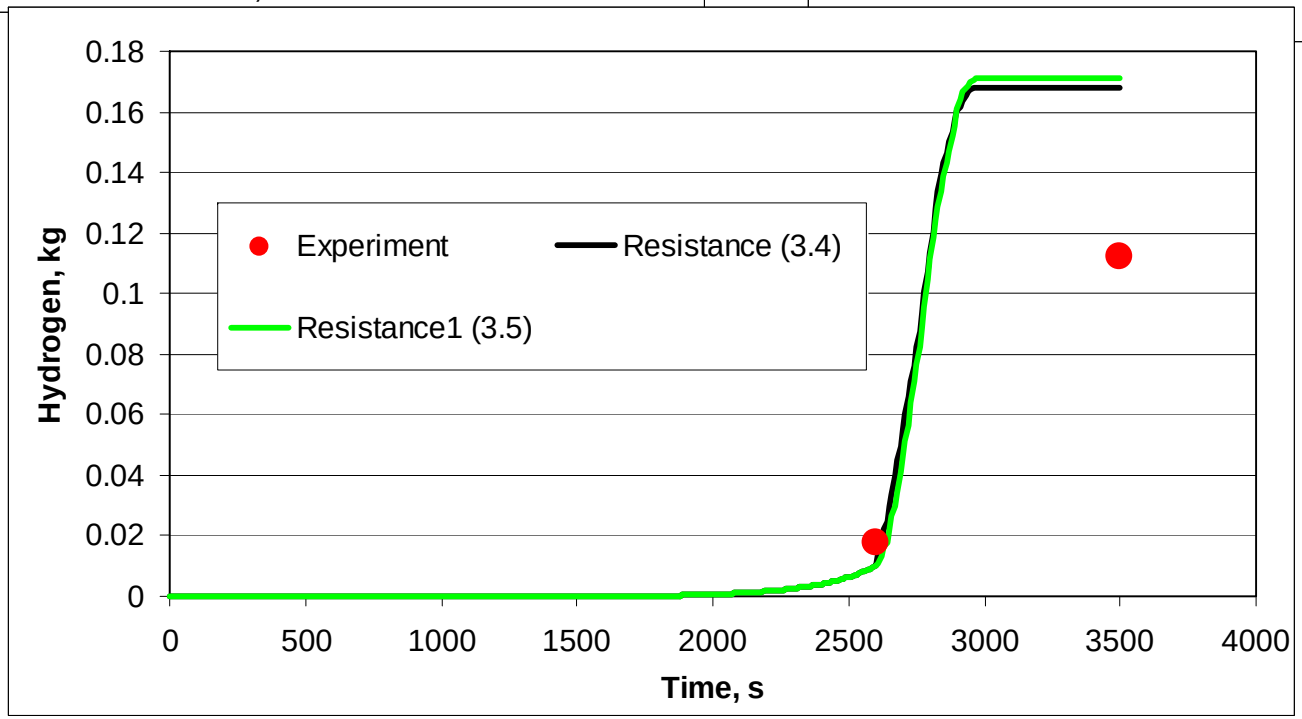


Progression of the QUENCH-03 and QUENCH-06

RELAP/SCDAPSIM / QUENCH-03

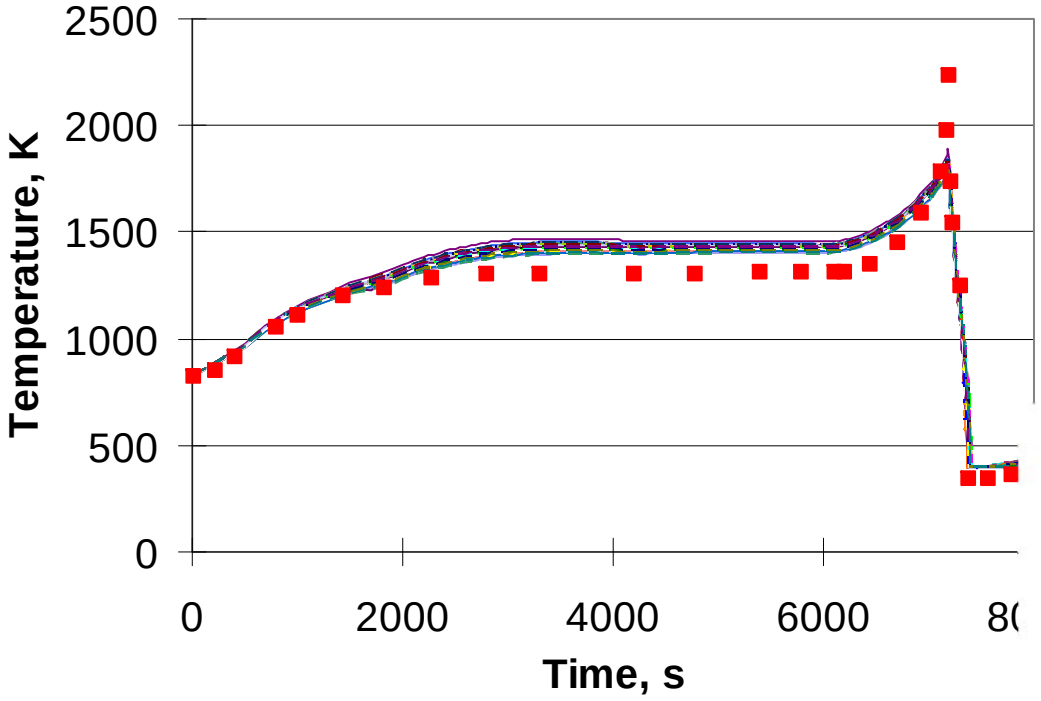






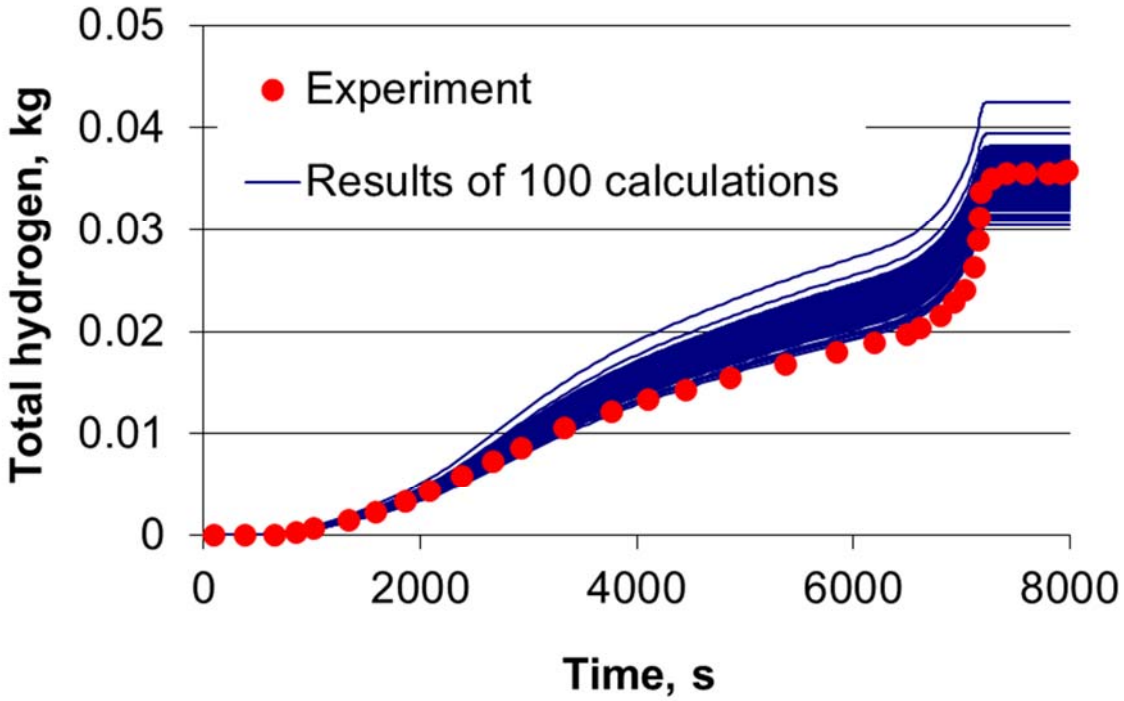
RELAP/SCDAPSIM / QUENCH-06

RELAP/SCDAPSIM mod 3.4



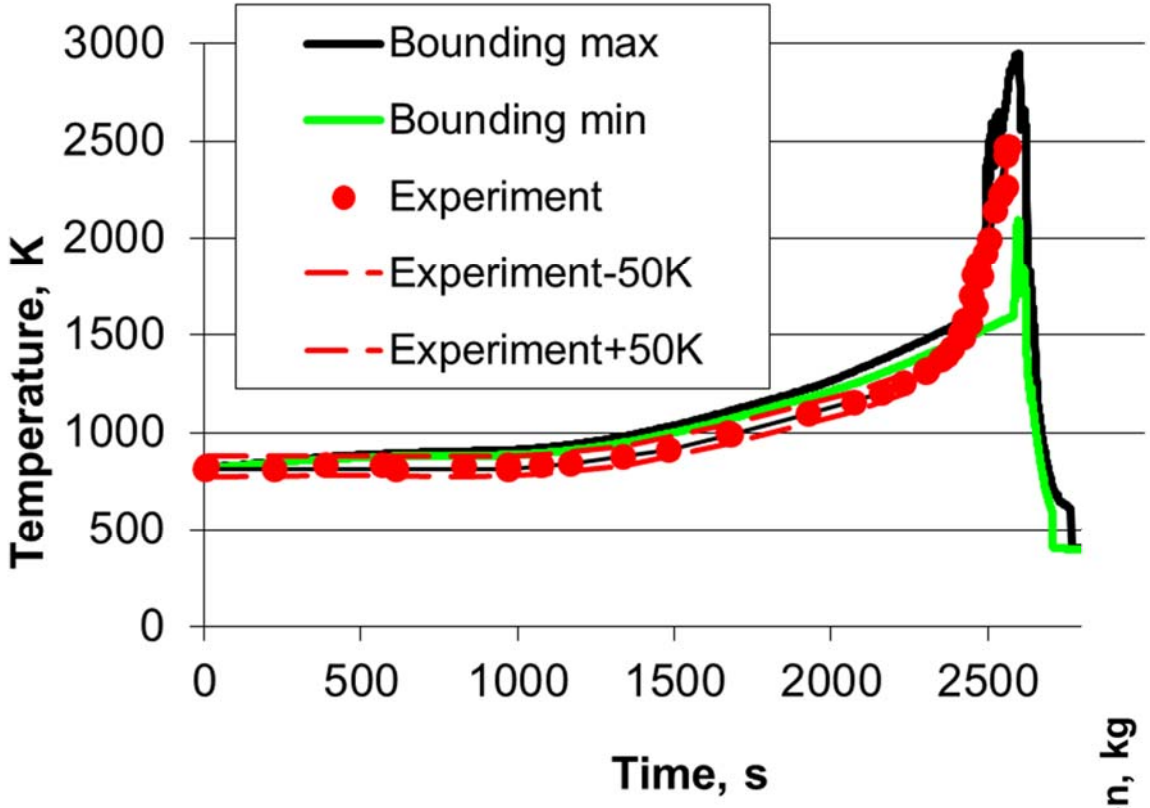
Results of RELAP/SCDAPSIM calculation of QUENCH-06 test. Behaviour of cladding temperatures of fuel rod imitator from inner rod ring at 750 mm height.

Result of RELAP/SCDAPSIM calculation of QUENCH-06 test, amount of generated hydrogen.



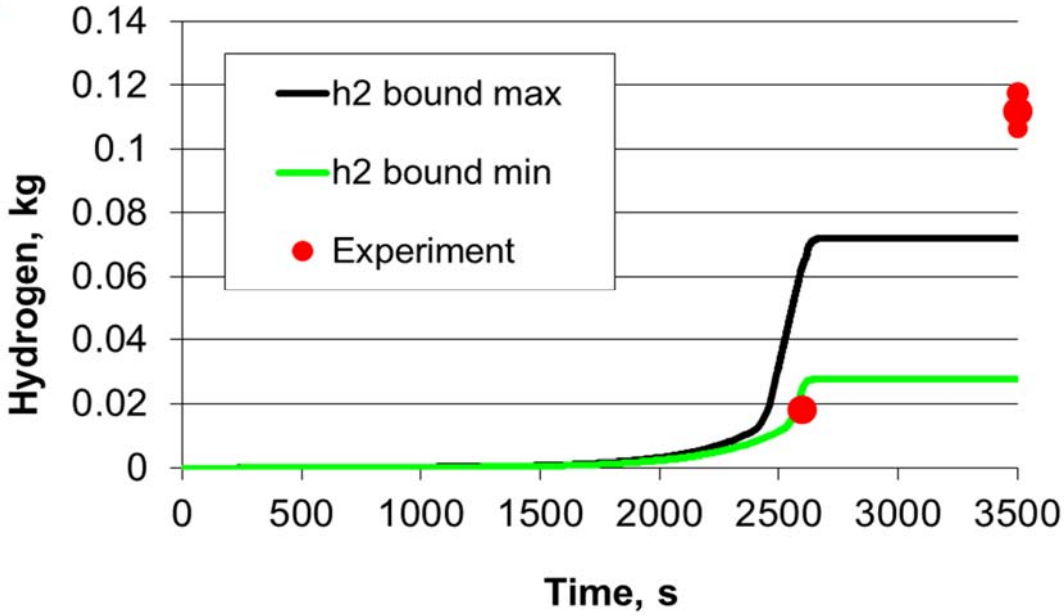
ASTEC / QUENCH-03

ASTEC –V2.0r3 code version

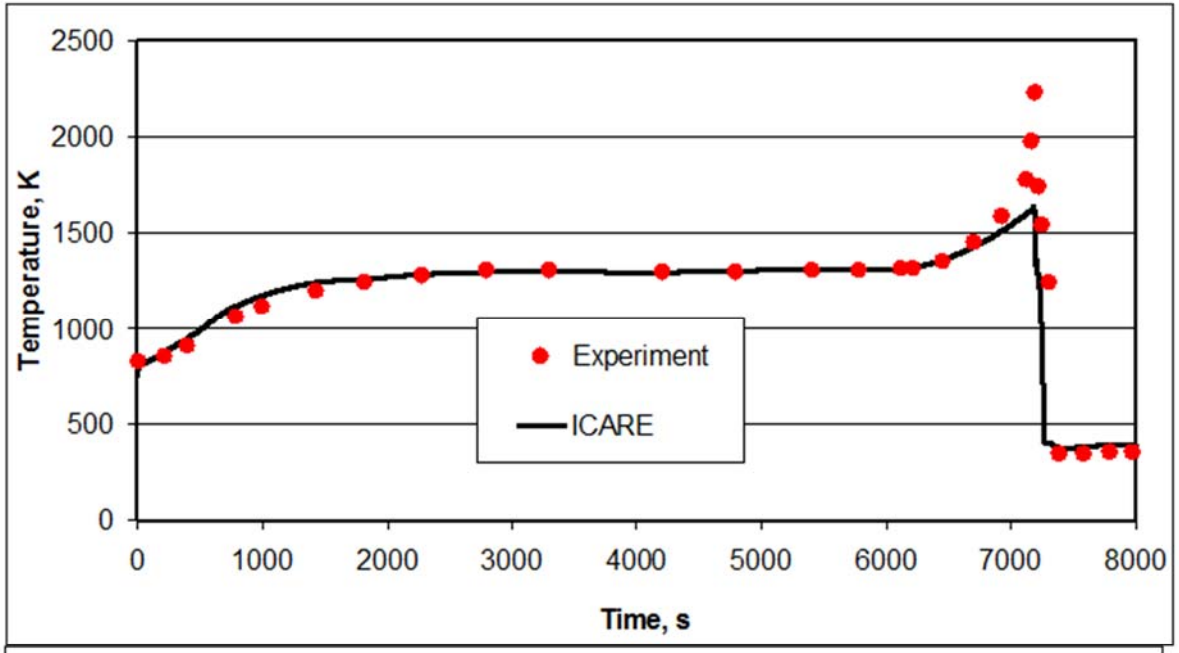


Results of ASTEC calculation of QUENCH-03 test, behaviour of cladding temperatures of fuel rod imitator from outer rod ring at 750 mm height.

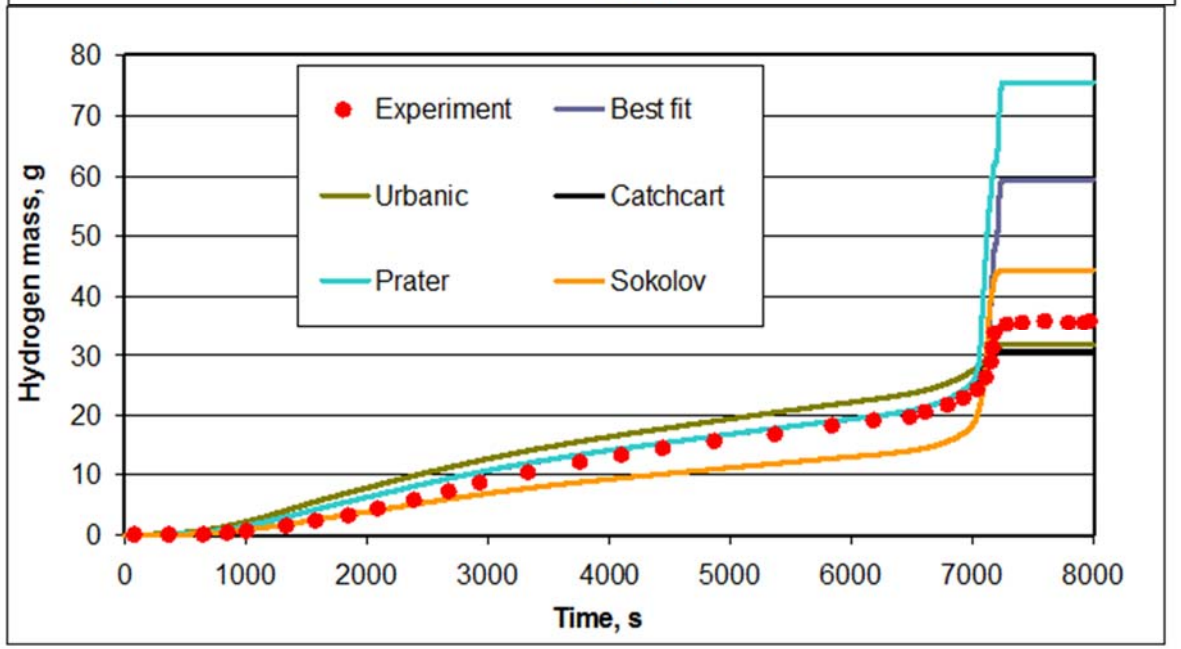
Result of ASTEC calculation of QUENCH-03 test, amount of generated hydrogen



ASTEC / QUENCH-06



QUENCH-06 test calculation using ASTEC code. Fuel rod imitator cladding temperature in outer ring of bundle at 750 mm height



QUENCH-06 test calculation using ASTEC code. Total hydrogen generation

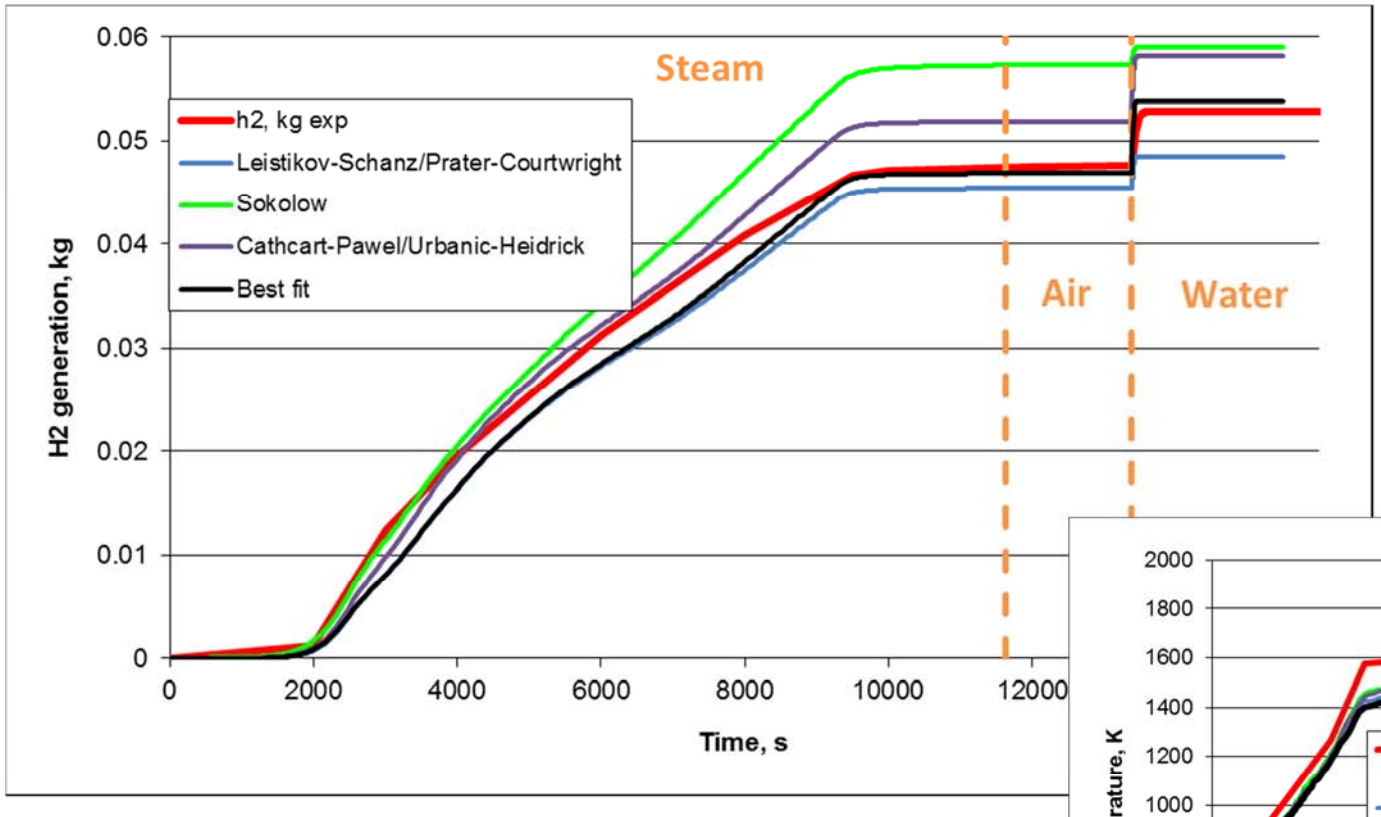
Modeling of QUENCH-10 experiment using RELAP/SCDAPSIM for the preparation of modeling of spent fuel pools.

Modelling of severe accidents in spent fuel pools, analysis of the heat-up of the fuel assemblies in the steam and air environment

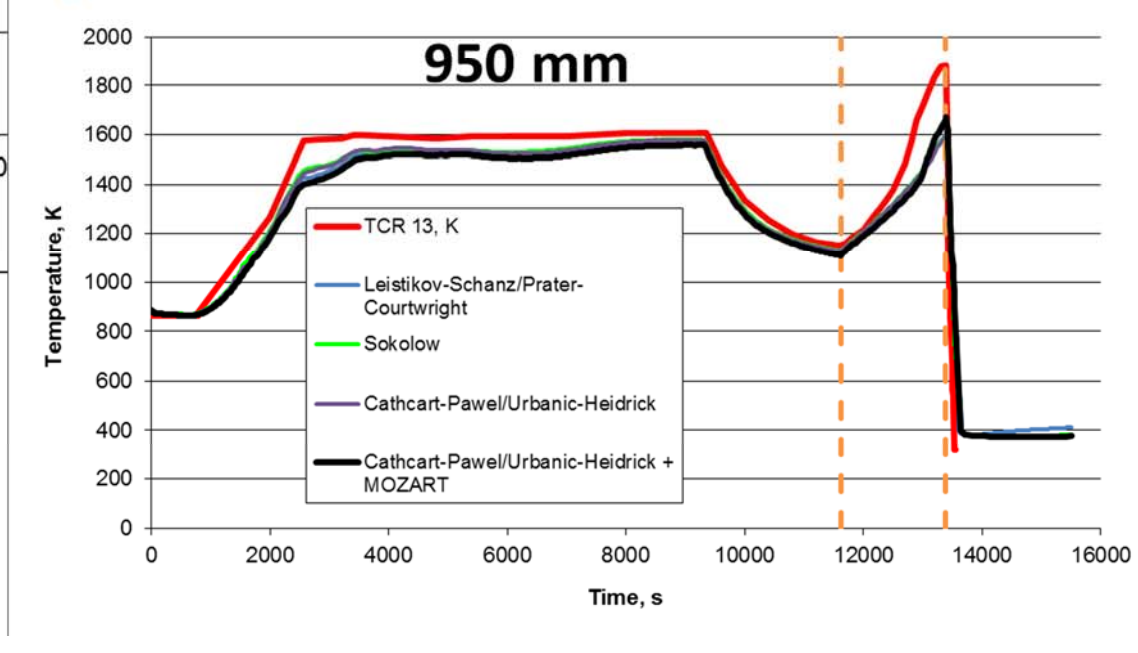
Nuclear Engineering and Design
Volume 337, October 2018, Pages 341-350
https://doi.org/10.1016/j.nucengdes.2018.07.016

RELAP/SCDAPSIM / QUENCH-10

Best fit calculation

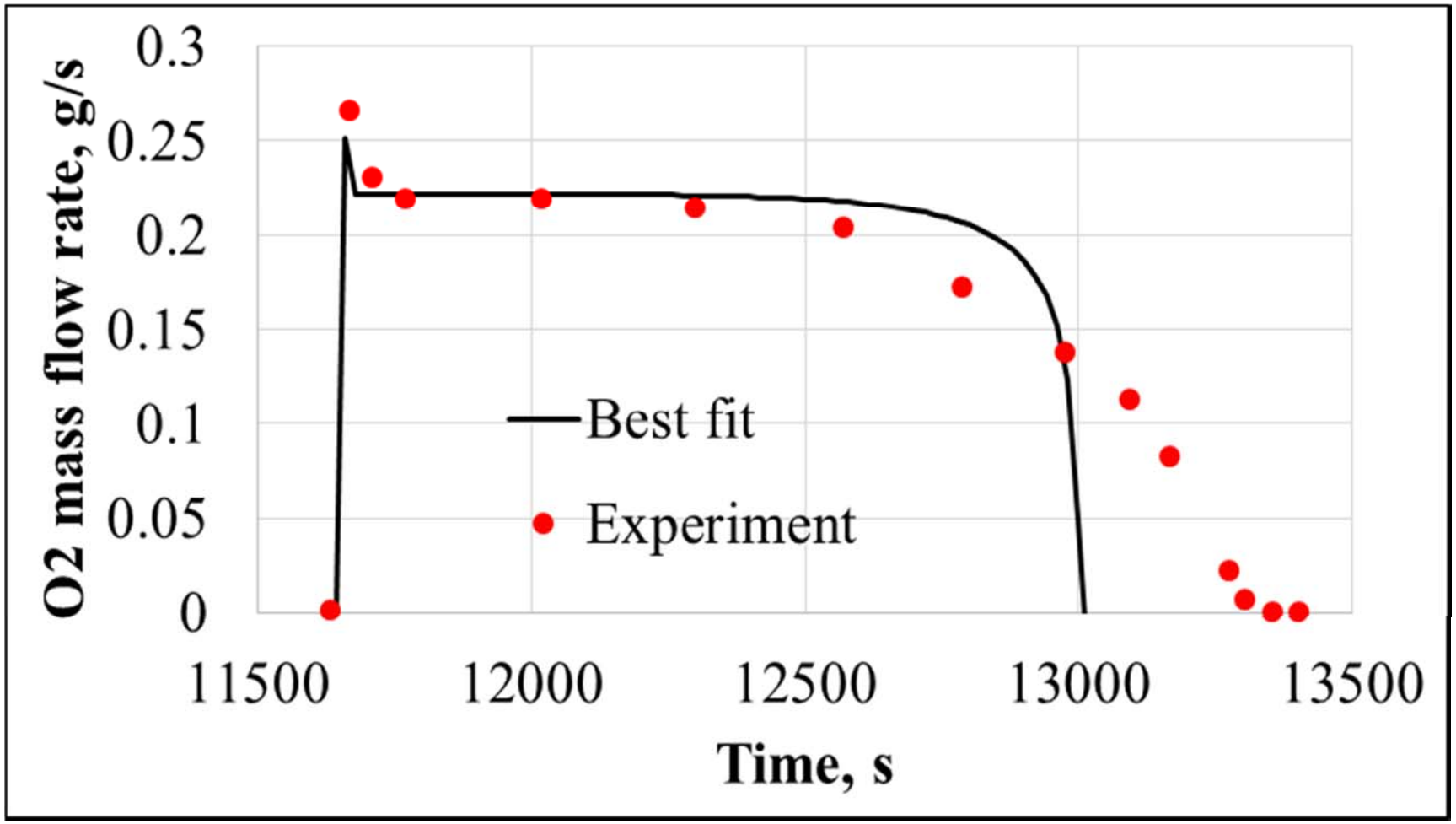


Calculation results using Cathcart-Pawel/Urbanic-Heidrick and MOZART oxidation models and **3.7 mOhm** resistance of sliding contacts are presented



RELAP/SCDAPSIM mod 3.5

QUENCH-10 test



Comparison of the O_2 mass flow rate measured during experiment and calculation results show good agreement in the first part of the air ingress phase. However, calculated O_2 mass flow rate start to decrease latter and decreases sharper than in the experiment (global oxygen starvation in the calculation achieved ~400 s earlier). In general it could be concluded that oxygen starvation process in the QUENCH-10 experiment is predicted reasonably well.

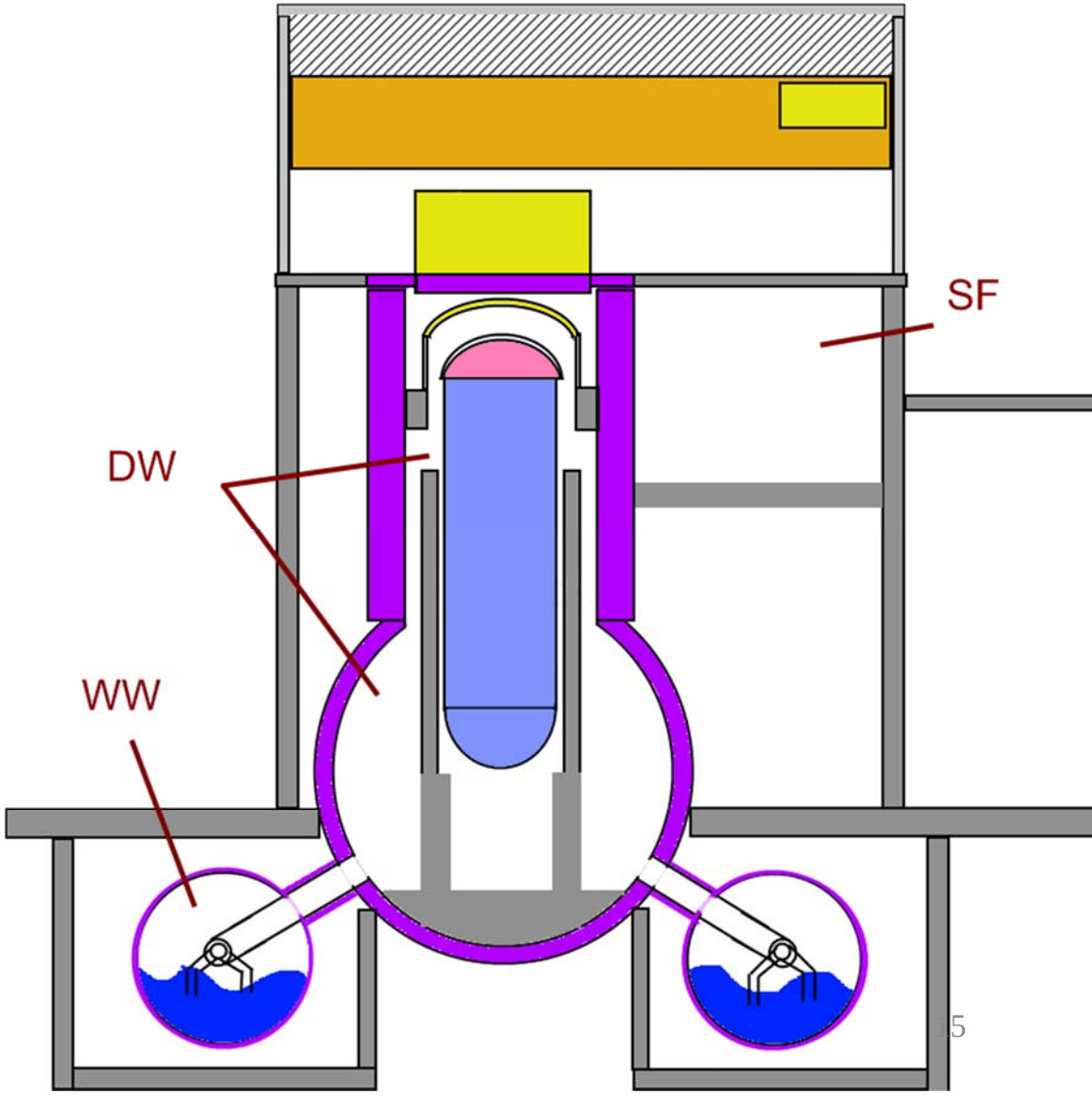
Modelling of LOCA accident in the BWR spent fuel pool using RELAP/SCDAPSIM code

Modelling of severe accidents in spent fuel pools, analysis of the heat-up of the fuel assemblies in the steam and air environment

Nuclear Engineering and Design
Volume 337, October 2018, Pages 341-350
https://doi.org/10.1016/j.nucengdes.2018.07.016

LOCA accident in the SFP of BWR type reactor

- The basic data of a BWR-4 type reactor with Mark-I type containment were used preparing this generic input deck.
- **Generic input deck was developed in the framework of the CESAM project (Euratom 7th FP under grant agreement No 604965).**
- For modelling of the processes in the SFP during a severe accident, the RELAP5 and RELAP/SCDAPSIM codes are used.

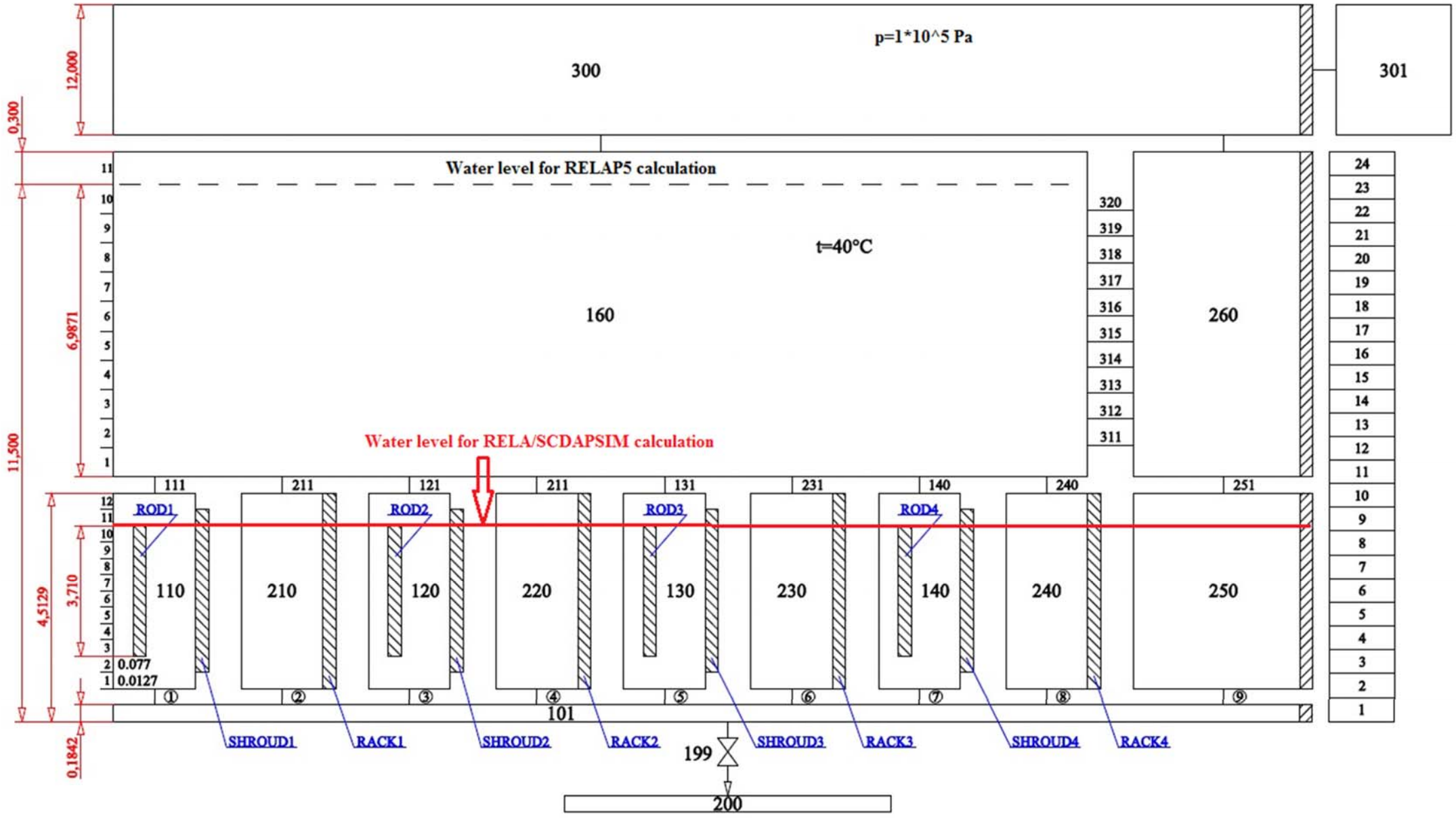


LOCA accident in the SFP of BWR type reactor

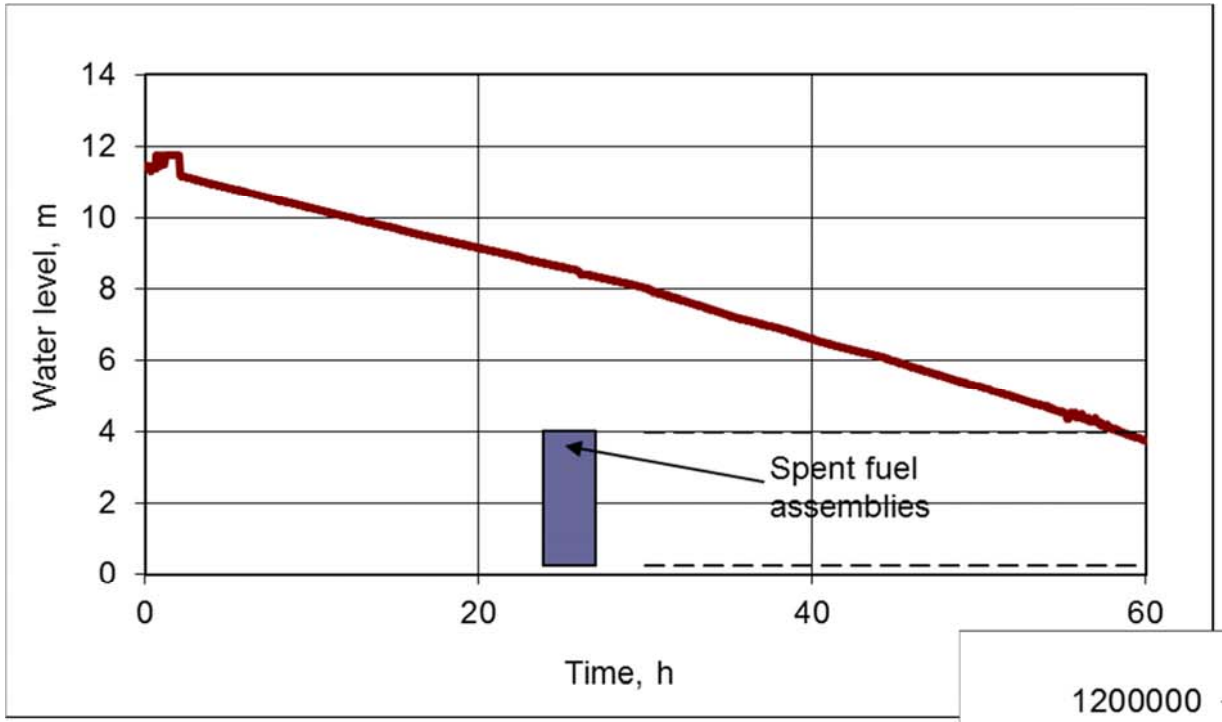
- SFP of the generic NPP is capable to store 3055 spent fuel assemblies, with total decay heat power 3.565 MW.
- Assumed air temp. in the pool is 303 K and water 313 K.
- The initiating event is a leak through broken 0.025 m diameter pipe (maximum leakage is equal to ~3 kg/s), connected to the bottom part of pool, together with total loss of electrical power.

Parameter	
Pool length, m	12.2
Pool width, m	9.9
Water height, m	11.5
Pool height, m	11.8
Steel liner thickness, m	0.0635
Concrete wall thickness, m	2.0
Pool bottom thickness, m	2.0

RELAP5 and RELAP/SCDAPSIM model of BWR SFP

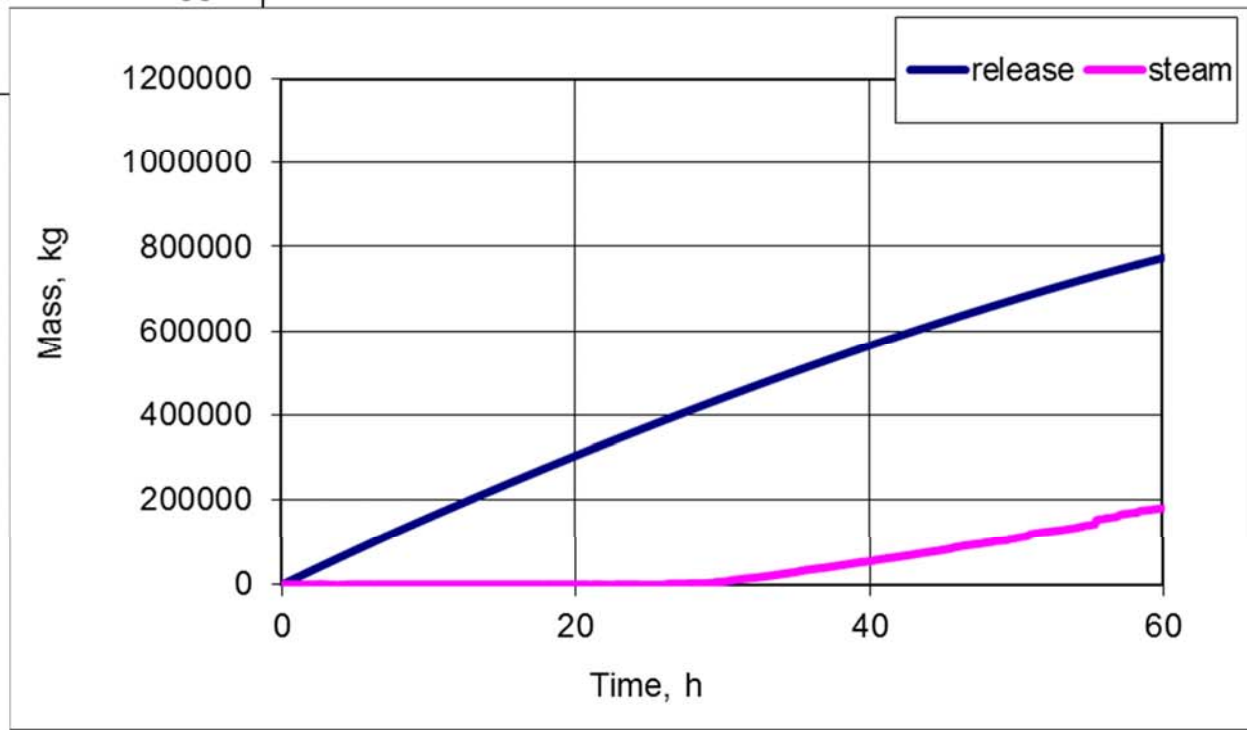


RELAP5 calculation results



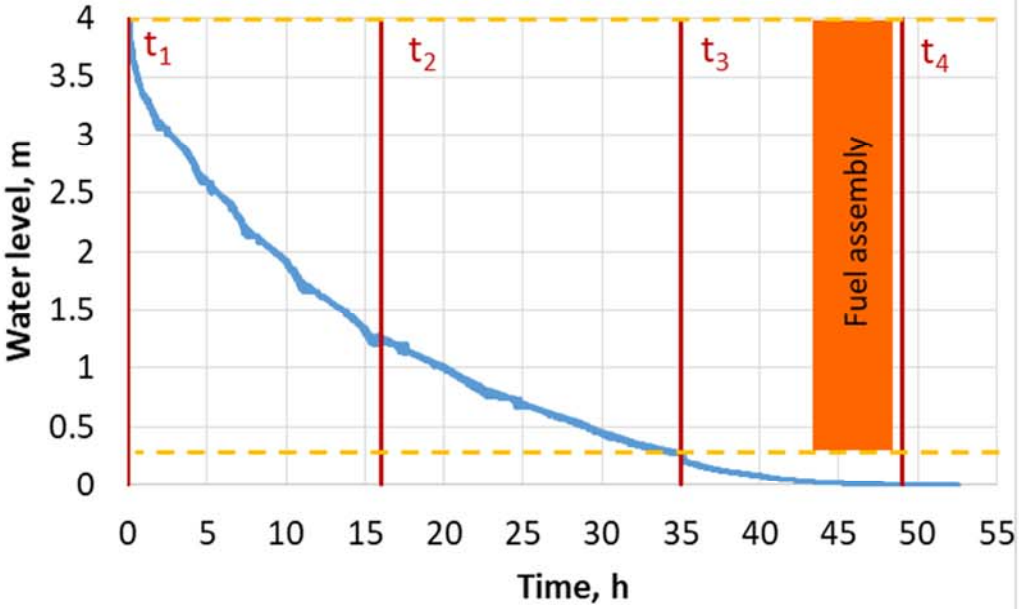
Behavior of pool water collapsed level

Comparison of integral water release and integral steam loss

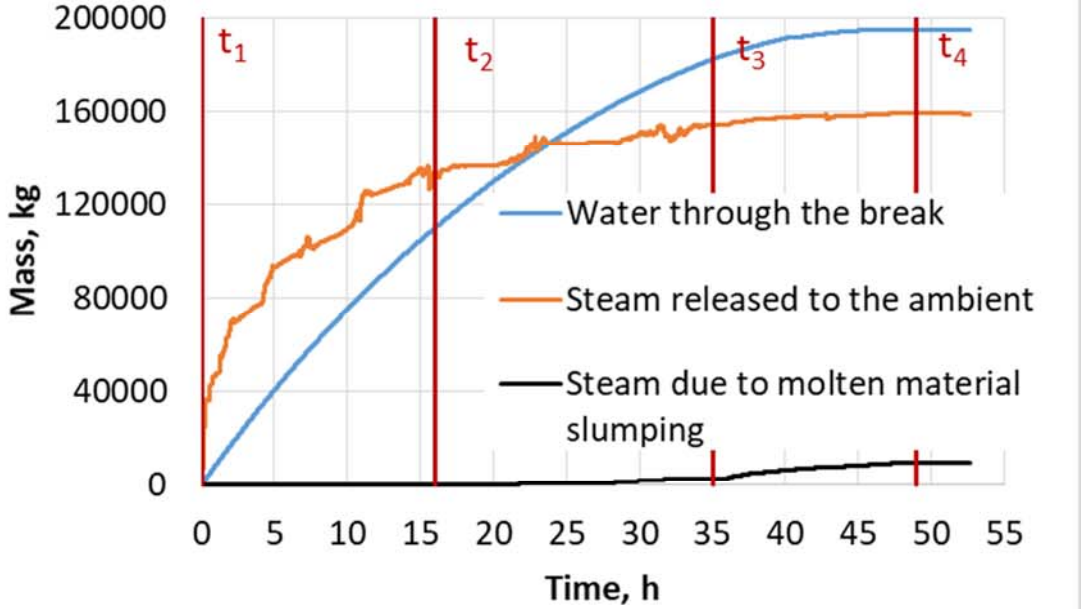


RELAP/SCDAPSIM calculation results

The calculation using RELAP/SCDAPSIM started when the water level in the pool is at ~4m (top of the active fuel) – this condition is assumed as the starting point (t = 0 s).



Water level in the *pool*



Water and steam released from the pool

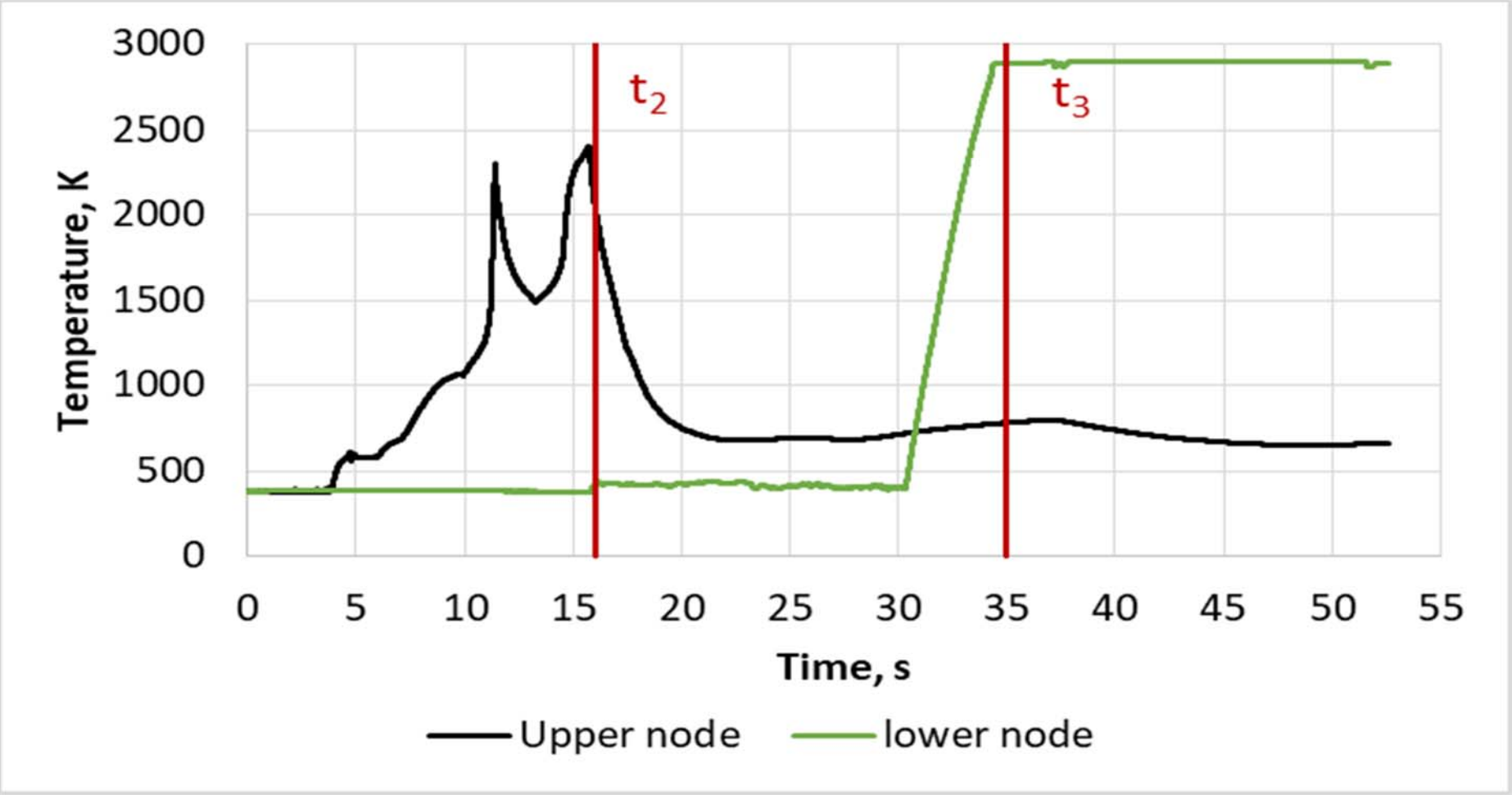
$0 - t_1$ – time up to the time when the water level decreases to the top part of the active fuel;

$t_1 - t_2$ – temperature increase in fuel rods (the duration of $t_1 - t_2$ interval is ~16 h); at the end of this interval first material relocation (1189 kg mass of liquefied material) to lower part of the SFP occurs;

$t_2 - t_3$ – water level decreases down to the bottom of the fuel assemblies; the duration of $t_1 - t_3$ interval is ~35 h;

$t_3 - t_4$ – water level decreases down to the bottom of pool – SFP is empty; the duration of $t_1 - t_4$ interval is ~49 h;

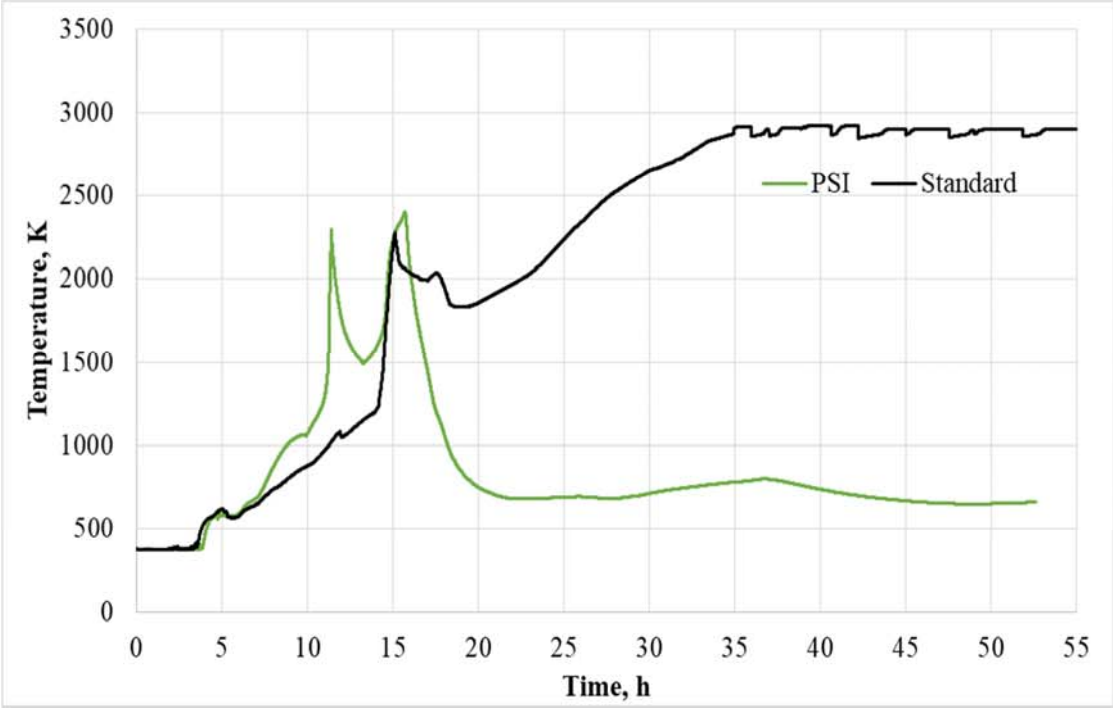
RELAP/SCDAPSIM calculation results

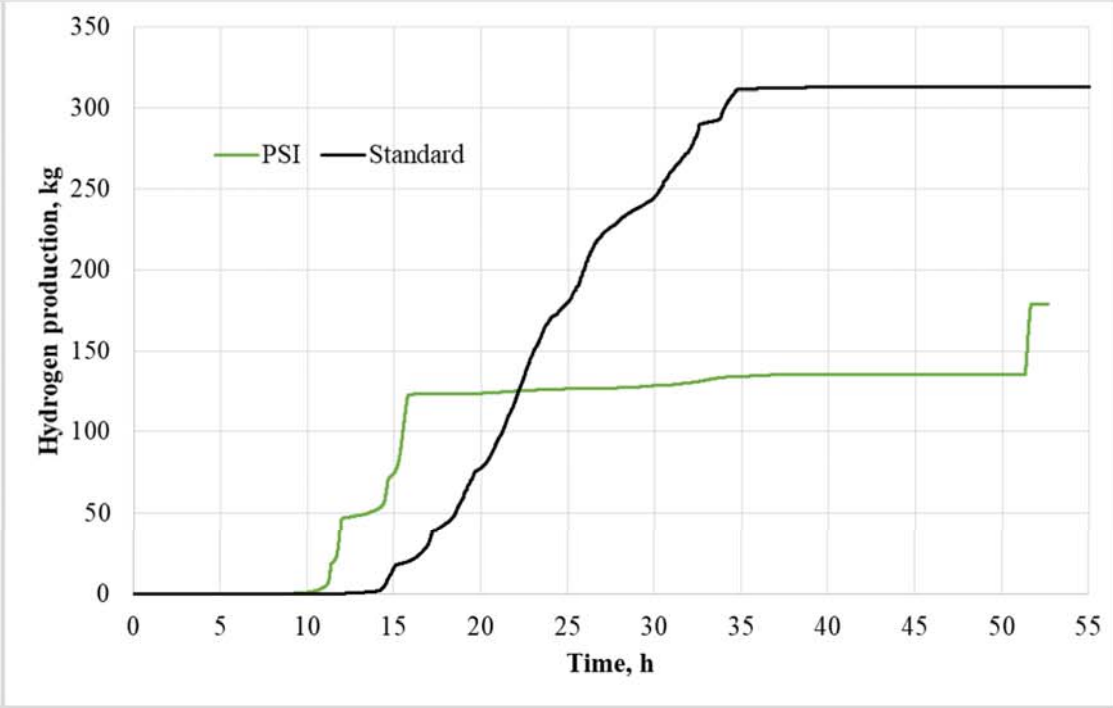


Cladding temperatures in the first group upper and lower parts of the fuel assemblies

Comparison of the calculated results using different Zr cladding oxidation models

Influence of the different Zr oxidation correlations



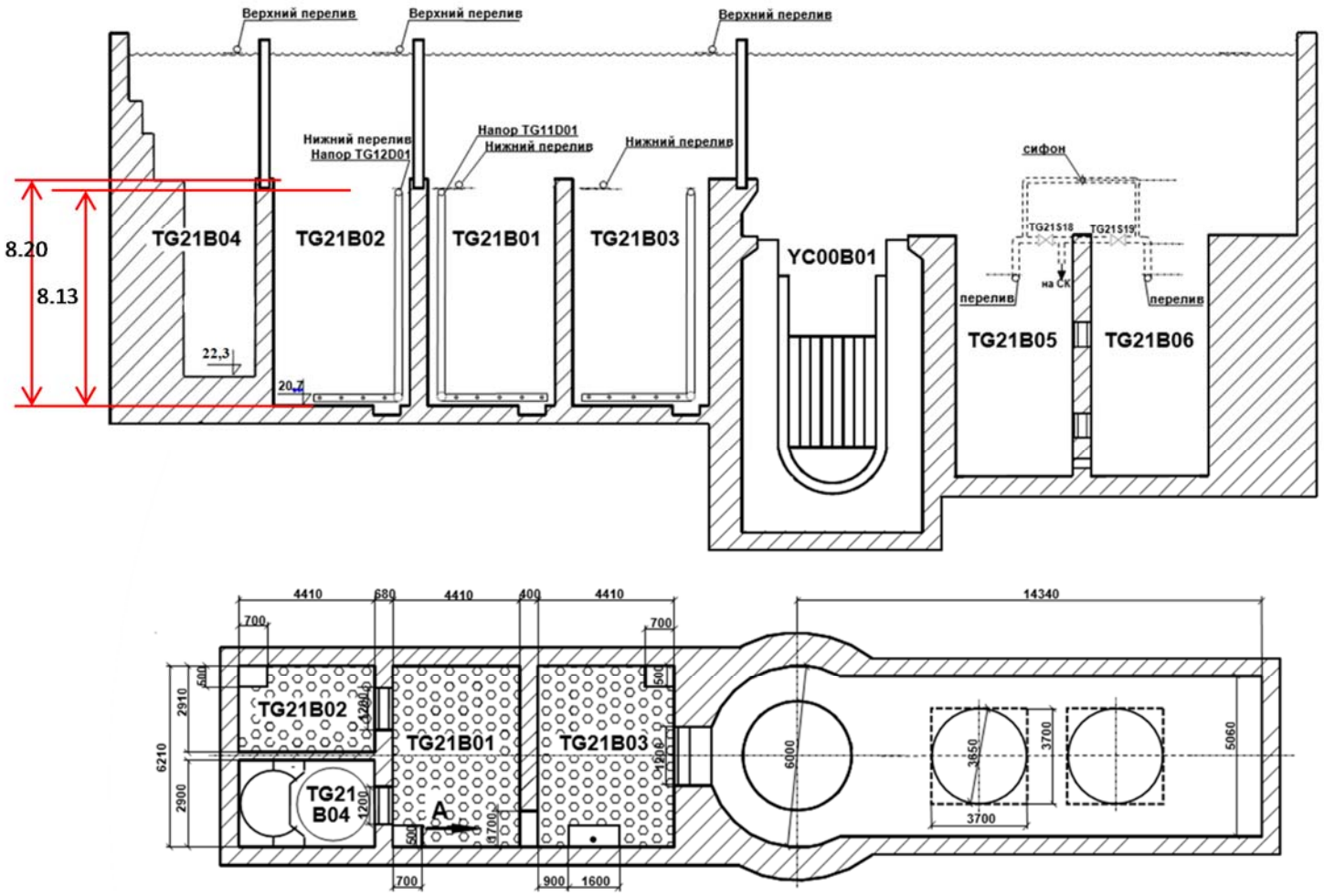


Using the standard oxidation model, the temperature in the upper part of the fuel assembly due to oxidation is increasing up to ~3000 K. The PSI model takes into account that steam and oxygen starvation is achieved. According to PSI model no energy due to the oxidation process is considered, thus the temperature in the upper part of the fuel assembly starts to decrease. However, temperature in the lower part of the fuel assembly increases due to oxidation, because there is enough steam available for cladding oxidation.

Modelling of LOCA accident in the VVER spent fuel pool using RELAP/SCDAPSIM and ASTEC codes

This work has been supported by the European Union's INSC programme For UKRAINE (Contract No. INSC/2017/385-967)

SBO in ZNPP-1 modelling

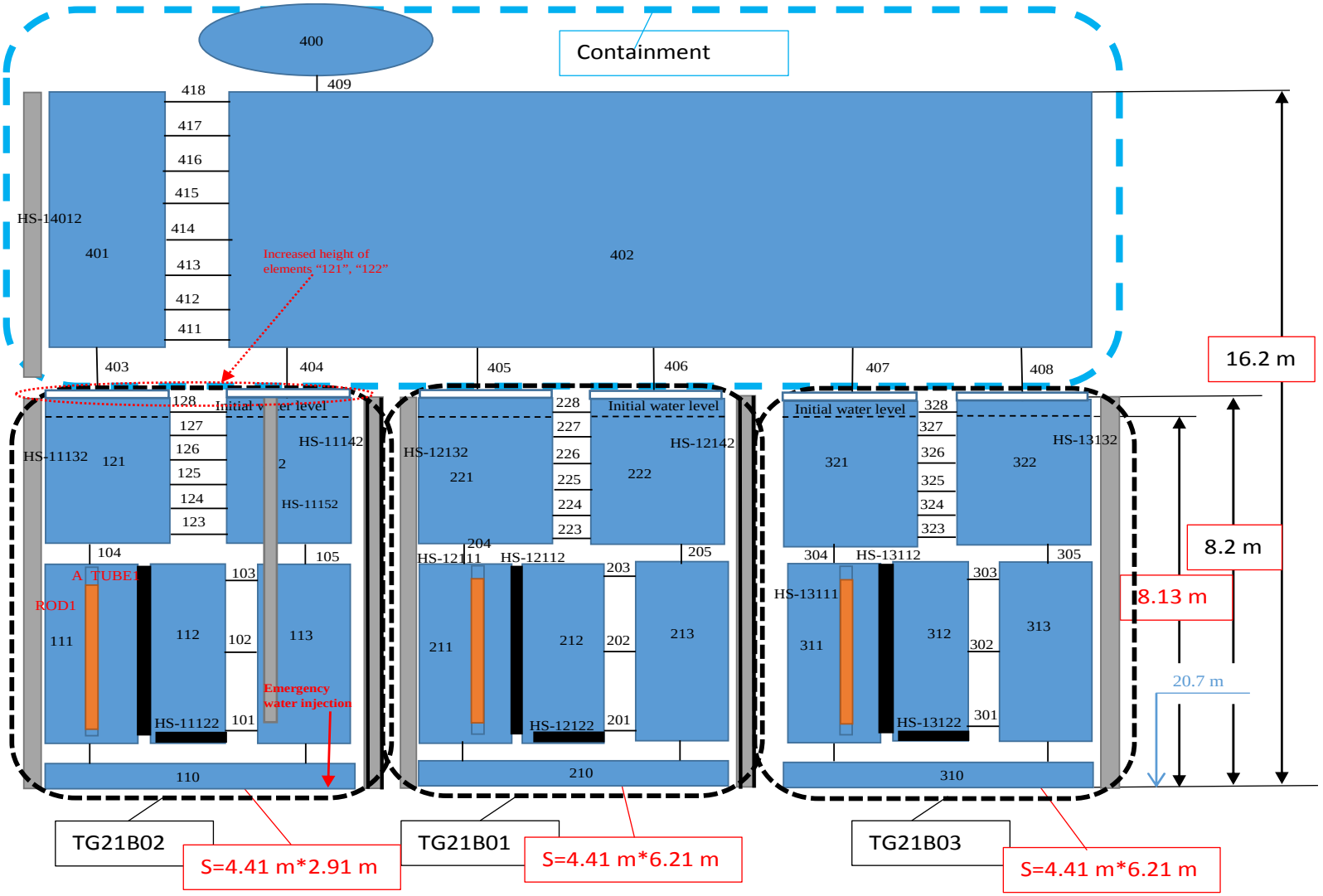


Spent fuel pool in ZNPP-1 (schematic)

Presented scenarios:

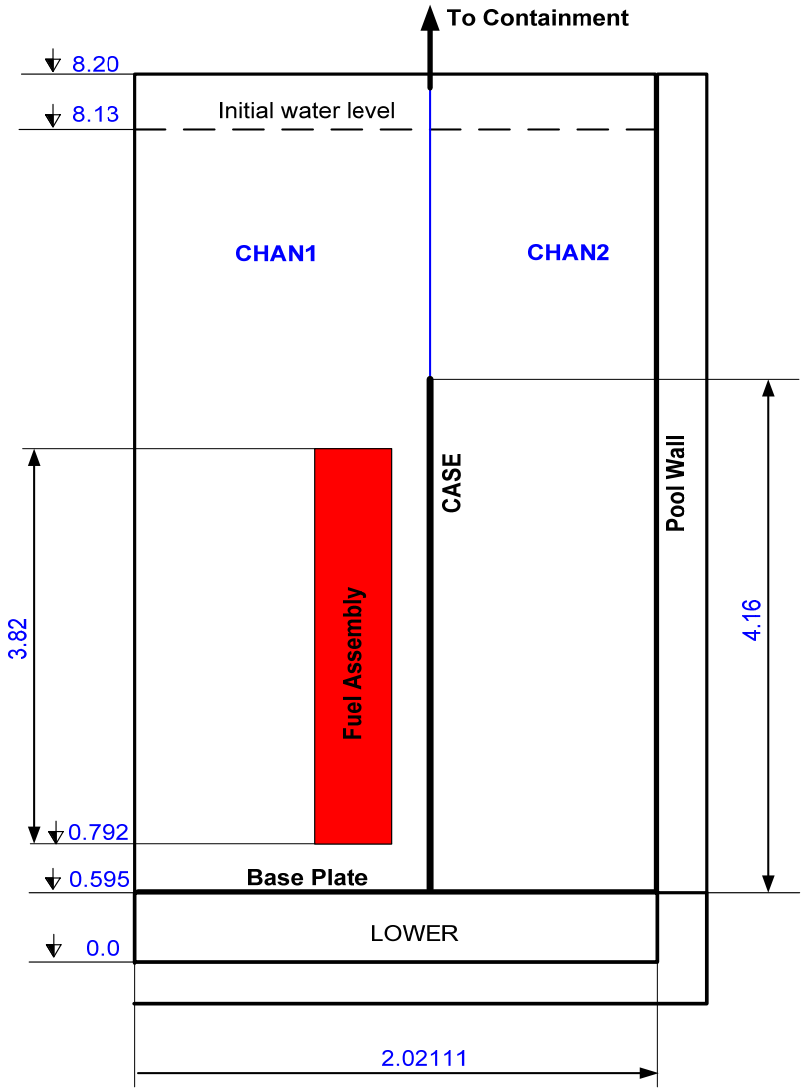
- without water injection
- with water injection in the later phase of the accident (1 h after reaching 1200 C)

RELAP/SCDAPSIM model



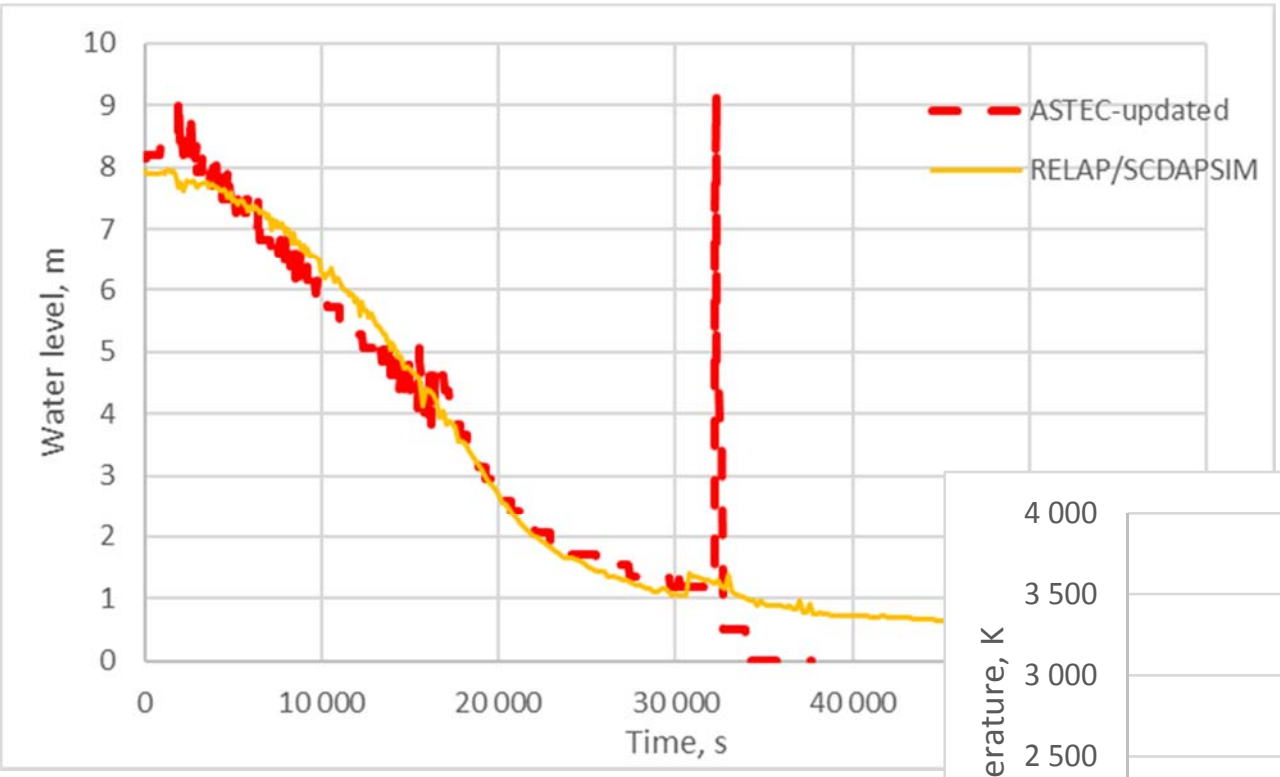
Nodalization scheme of SFP model of ZNPP Unit-1 for RELAP/SCDAPSIM mod3.4 code version

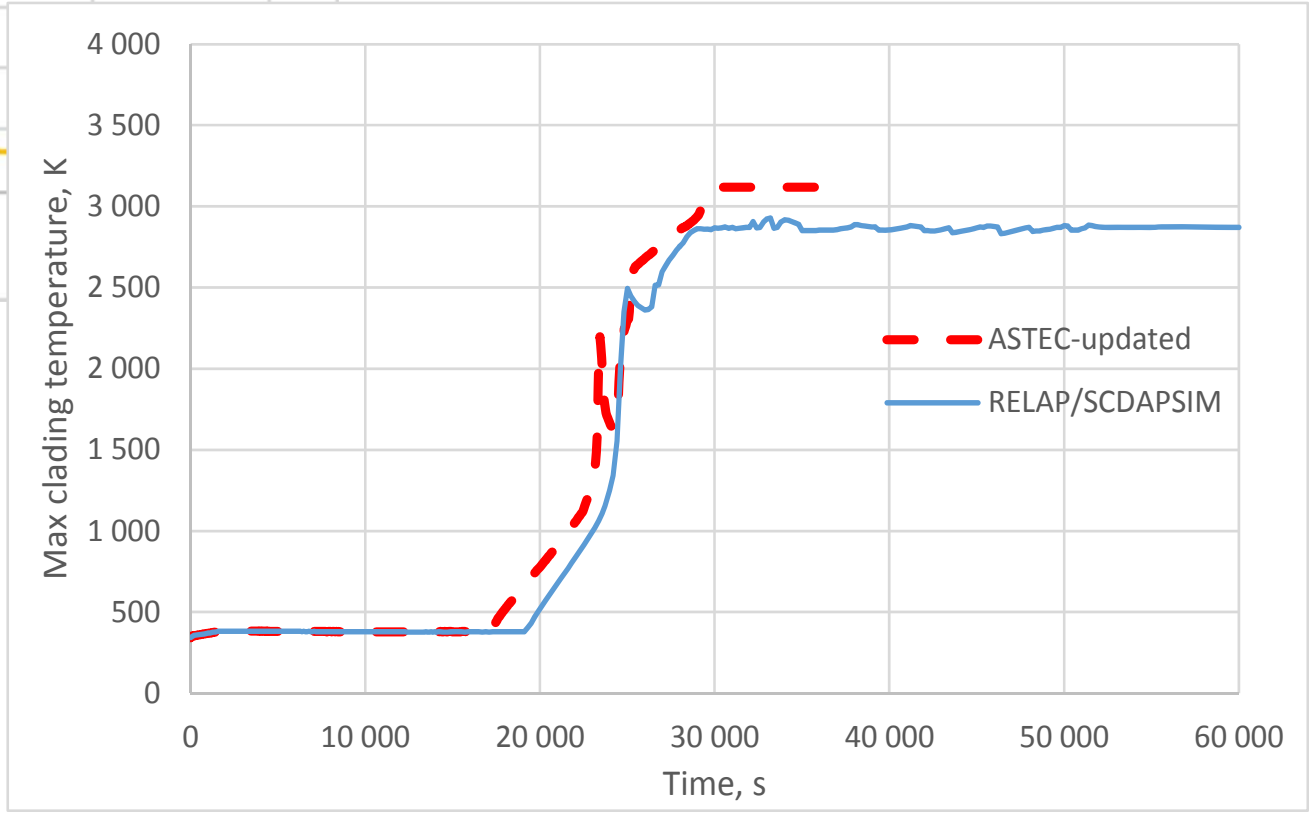
ASTEC model



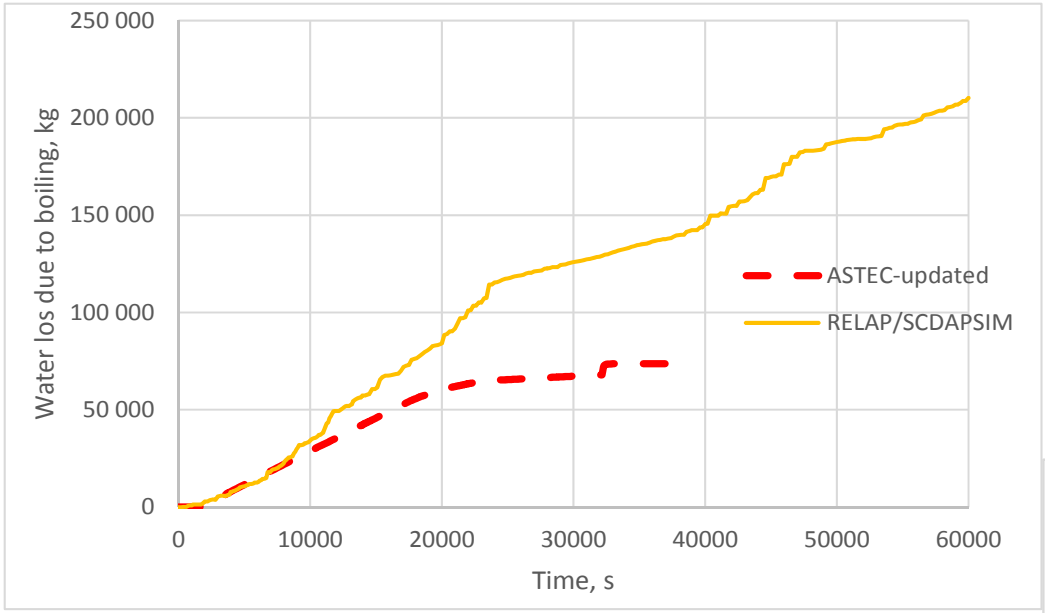
Nodalization scheme of SFP model of ZNPP Unit-1 using code ASTEC V2.1.1.4

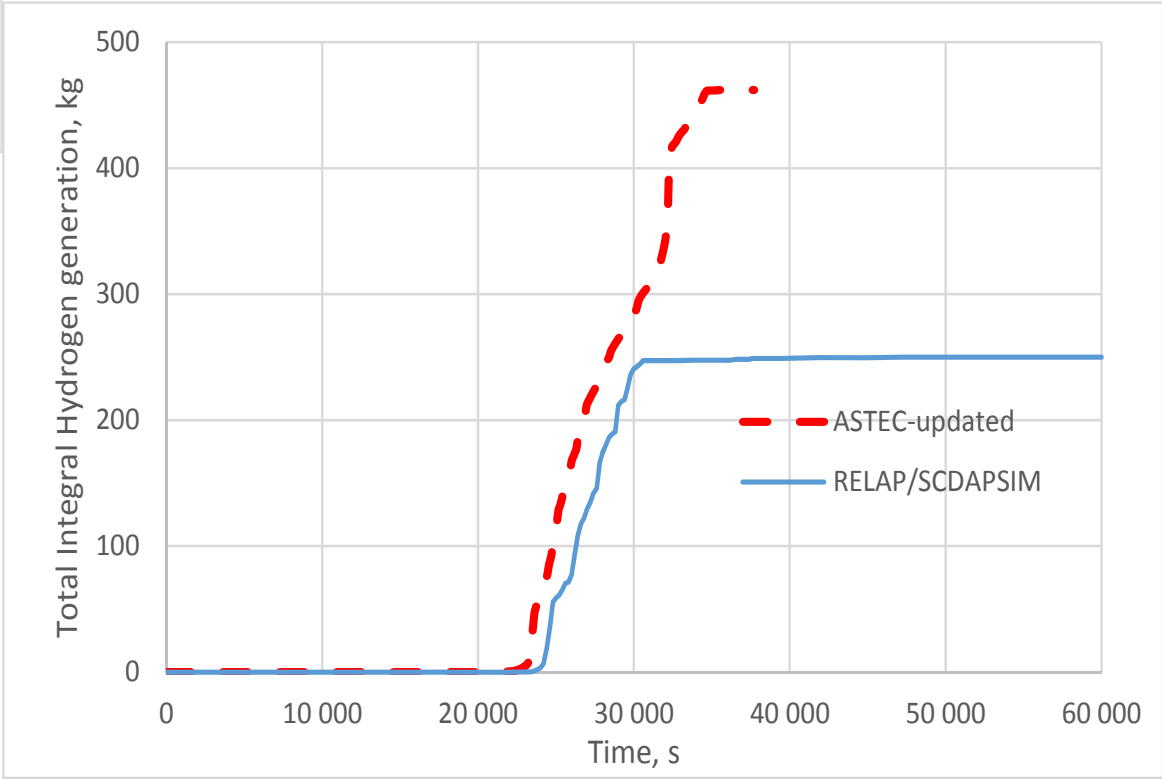
Scenario: without water injection



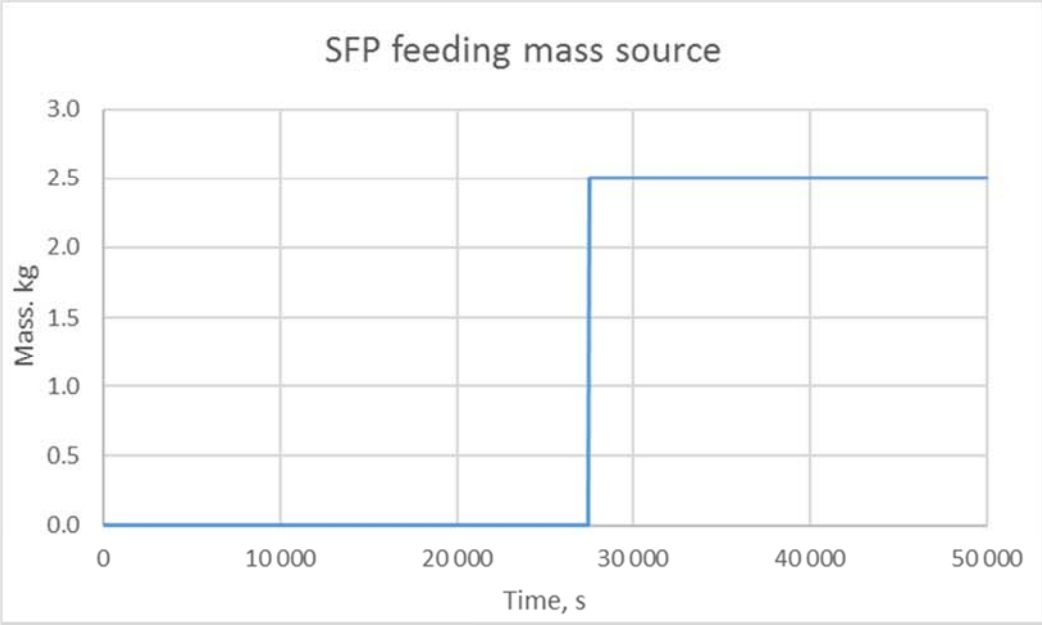


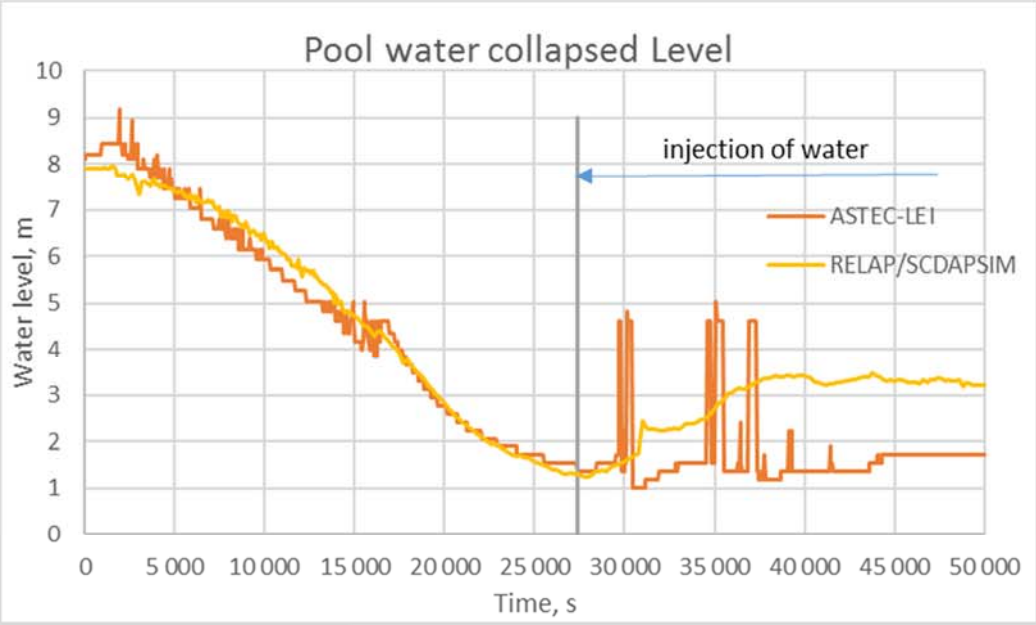
Scenario: without water injection

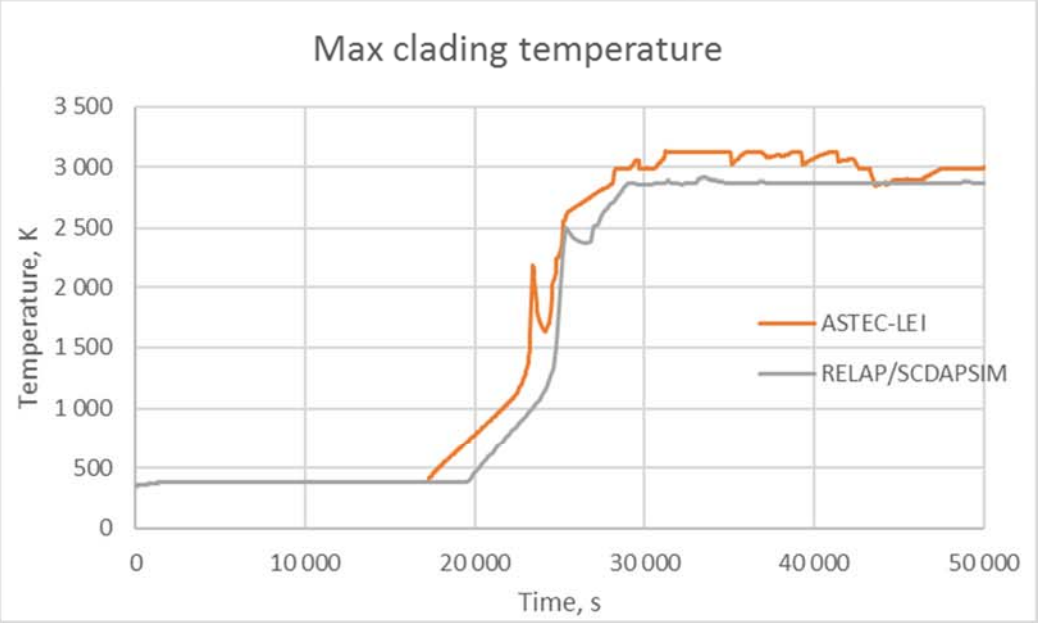




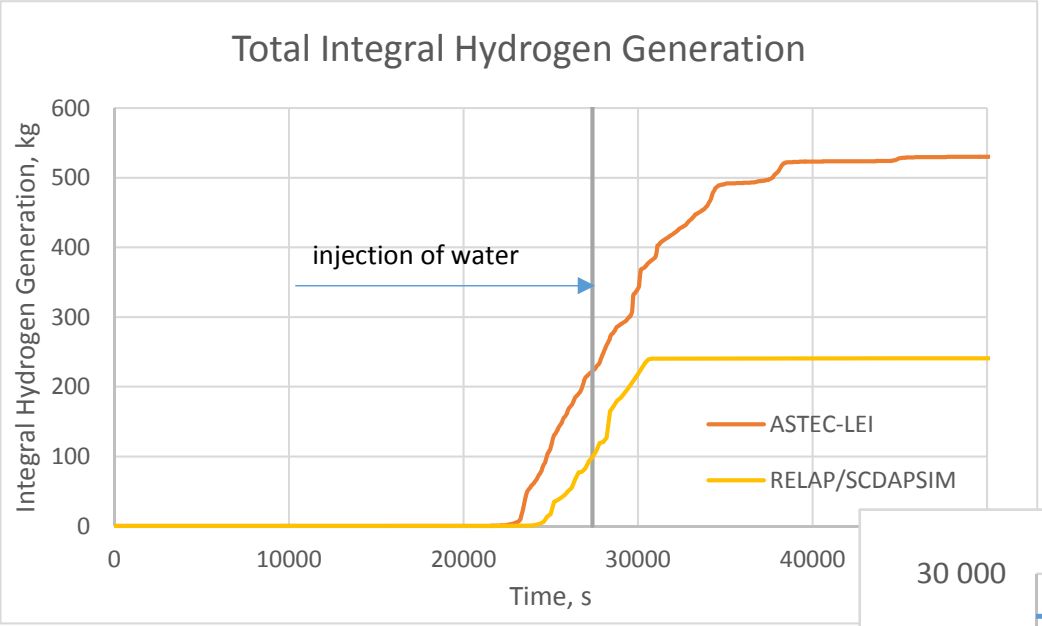
Scenario: with water injection

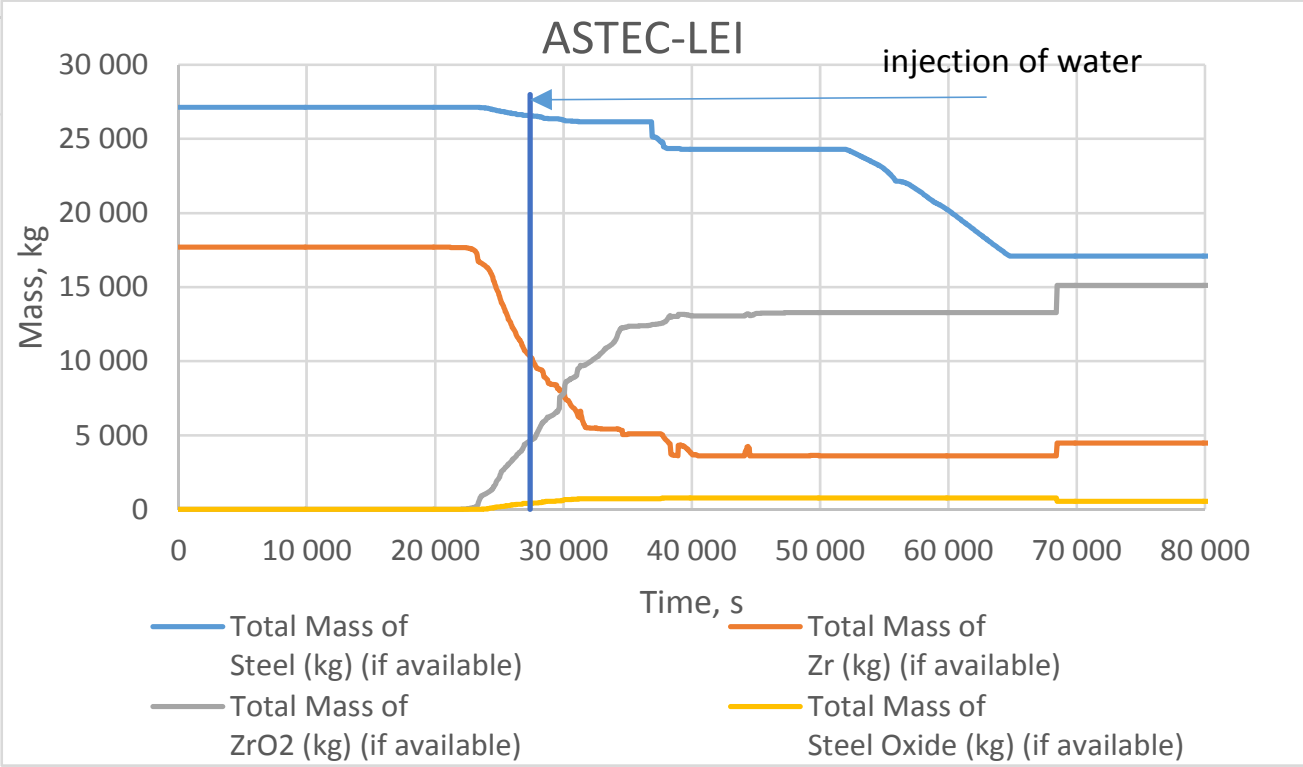




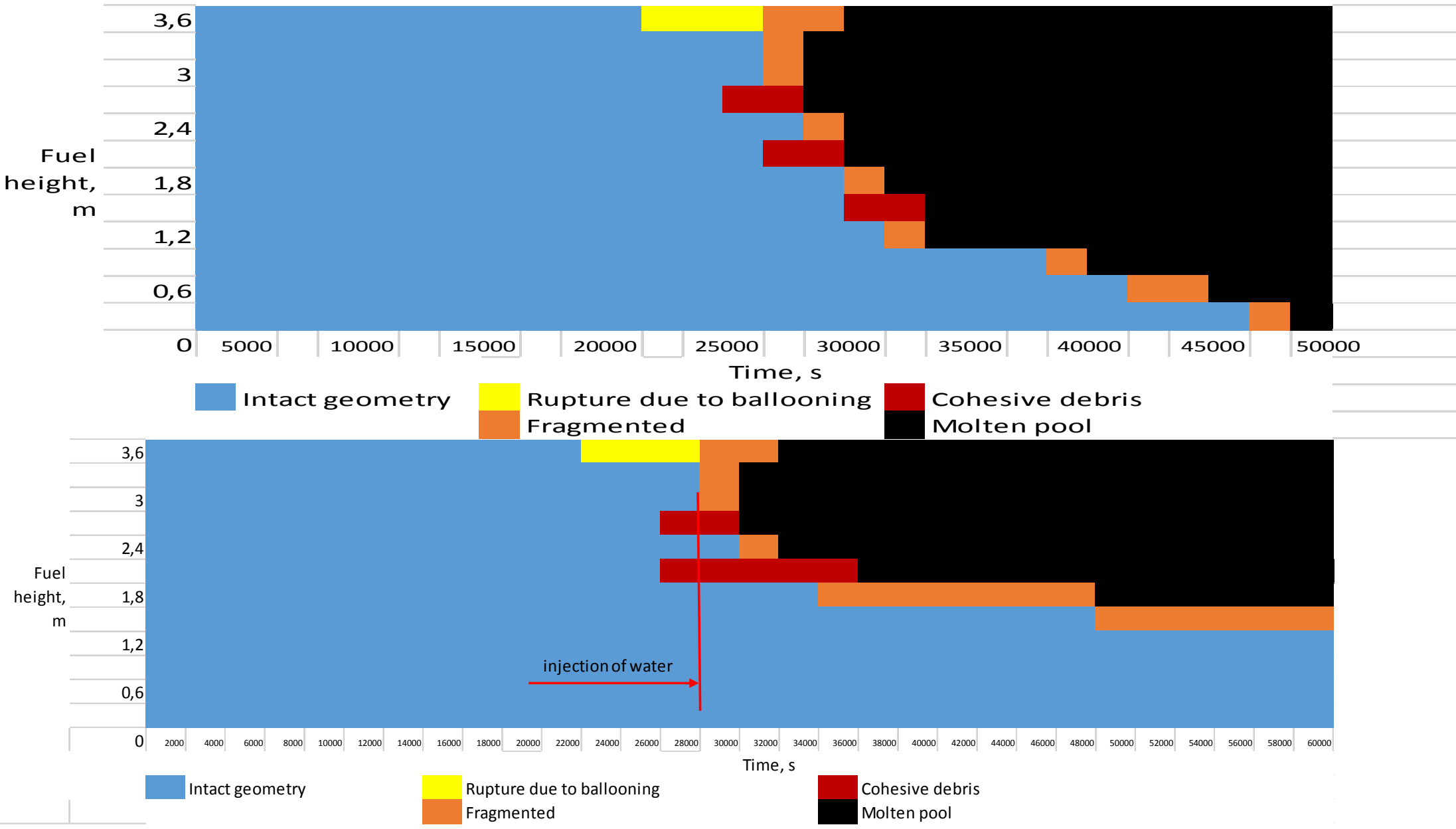


Scenario: with water injection





RELAP/SCDAPSIM calculation results



Conclusions

- Modeling of QUENCH-3, QUENCH-6 experiments using RELAP/SCDAPSIM and ASTEC codes
  - Modeling of QUENCH experiments were done in order to establish the knowledge as well as validation of program codes for this experimental setup.
  - Differnet RELAP/SCDAPSIM code versions have been tested. Also diferent Zr oxidation models for RELAP/SCDAPSIM and ASTEC codes.

Conclusions

- Modeling of QUENCH-10 experiment using RELAP/SCDAPSIM code.
  - Modelling of QUENCH-10 it was preparation for the modelling of BWR spent fuel pool. Modelling was done in order to understand the main phenomena which accruing during the experiment and to select the oxidation models.
- Modelling of LOCA accident in the BWR spent fuel pool using RELAP/SCDAPSIM code
  - Modelling of LOCA accident in the BWR spent fuel pool have been provided using RELAP5 and RELAP/SCDAPSIM program codes.
  - Influence of the different Zr oxidation correlations have been provided.

Conclusions

- Modelling of LOCA accident in the VVER spent fuel pool using RELAP/SCDAPSIM and ASTEC codes
  - Comparison shows that RELAP/SCDAPSIM, ASTEC have the comparable and adequate results of calculation results. However highest differences in the calculation results are due to different calculation of produced hydrogen. In this work the reasons for the differences in calculation results are discussed.

LITHUANIAN ENERGY INSTITUTE
http://www.lei.lt

NATIONAL OPEN ACCESS SCIENTIFIC CENTRE FOR FUTURE ENERGY TECHNOLOGIES

OPEN R & D LITHUANIA

Thank you for the attention

Tadas Kaliatka

Tadas.Kaliatka@lei.lt

QUENCH Workshop Presentation: Abstract

Numerical modelling of in-vessel melt retention: The LIVE Experiments

Aniket Joshi[a], Claire Heaney[b], Alan Jones[b], Liang Yang[b], Paul Smith[c], Ali Tehrani[d], Christopher C. Pain[b]

[a]Department of Materials, Imperial College London, London SW7 2AZ, United Kingdom
[b]Earth Science and Engineering Department, Imperial College London, London SW7 2AZ, United Kingdom
[c]John Wood Group PLC, Dorchester DT1 3BW, United Kingdom
[d]Office for Nuclear Regulation, Bootle L20 7HS, United Kingdom

The LIVE experiments were performed at Karlsruhe Institute of Technology to complement the existing experimental data on severe accidents. A series of experiments were performed varying parameters such as heating rate and cooling boundary conditions. These tests provide an insight into the core melt behaviour in the lower plenum of a reactor pressure vessel in both steady and transient states.

Originally developed for reservoir applications, Fluidity is a novel software package capable of performing dynamic mesh optimisation on unstructured meshes. About 10 years ago, this code was extended to be able to model multiphase flows.

In this work, Fluidity based packages are used to simulate the first two stages of the LIVE L3 test– air cooling and water cooling at 10 kW. The unmodified Rayleigh number is used instead of the traditionally used internal Rayleigh number, which is a function of the Rayleigh number and the Dammkohler number. The resulting effects on the heat transfer coefficient are analysed. The analysis is also compared against analytical solutions and the benefits of mesh adaptivity are illustrated.


KIT

Imperial College London

October 23, 2019

Numerical modelling of in-vessel melt retention: The LIVE Experiments

[1*]Aniket Joshi, [2]Claire Heaney, [2]Liang Yang, [2]Alan Jones, [3]Paul Smith, [4]Ali Tehrani, [2]Christopher Pain

[1]Department of Materials, Imperial College London, London SW7 2AZ, United Kingdom
[2]Department of Earth Science and Engineering, Imperial College London, London SW7 2AZ, United Kingdom
[3]John Wood Group PLC, Aberdeen AB11 6EQ, United Kingdom
[4]Office for Nuclear Regulation, Bootle L20 7HS, United Kingdom

Currently with The Open University, Milton Keynes MK7 6AA, United Kingdom. Email: aniket.joshi@open.ac.uk

Imperial College London

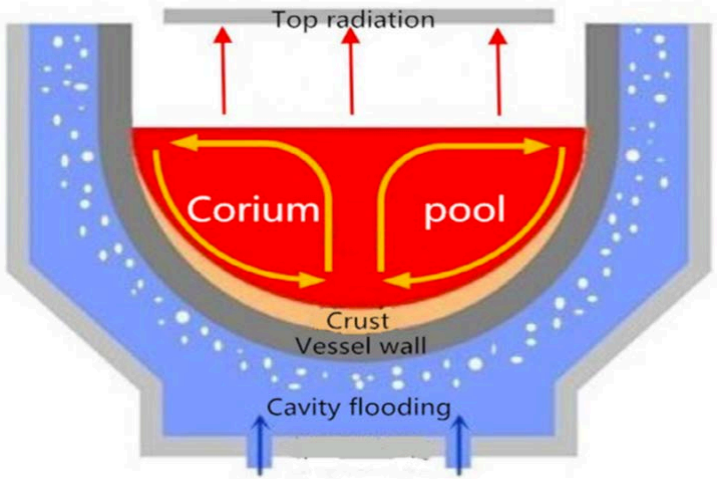
Severe accident phenomena

- Melt pool can be formed at the lower plenum of a Reactor Pressure Vessel (RPV)
- Molten materials need to be retained and need to prevent its leakage in the whole accident duration
- The melt pool (corium) is a self-heating substance and the RPV needs to withstand this
- Numerous experiments performed worldwide to understand this phenomena:
  - COPRA (CGN, China)
  - **LIVE (KIT, Germany)**
  - BALI (CEA, France)

Klein-Heßling W, Sonnenkalb M, Jacquemain D, Clément B, Raimond E, Dimmelmeier H, et al. Conclusions on severe accident research priorities. Annals of Nuclear Energy. 2014 Dec 1;74:4–11.

Imperial College London

Visualization



Visualization of severe accident experiments

Klein-Heßling W, Sonnenkalb M, Jacquemain D, Clément B, Raimond E, Dimmelmeier H, et al. Conclusions on severe accident research priorities. Annals of Nuclear Energy. 2014 Dec 1;74:4–11.

Imperial College London

The LIVE Experiments (Late In-Vessel Phase Experiments)

- Aimed at analyzing the retention and relocation of the melt pool
- Series of experiments performed in 2D and 3D
- Volumetrically heated pool to simulate corium heating in a 1/5th RPV scale model
- L3 test chosen for comparison due to data being publicly available
- L3 test parameters:
  - Melt simulant used: $NaNO_3$-KNO_3 (20% $NaNO_3$ and 80% KNO_3)
  - Melt heated up to 613 K (343℃) before pouring

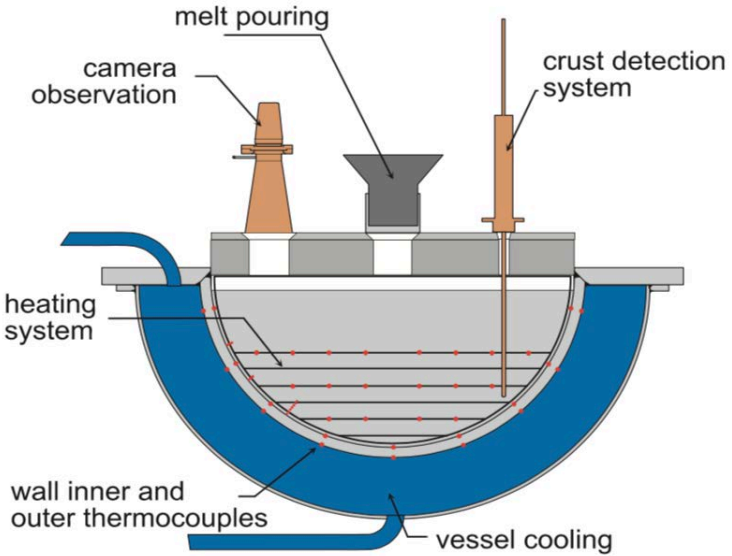
Gaus-Liu X, Mjasoedov A, Cron T, Foit JJ, Fluhrer B, Schmidt-Stiefel S, Wenz T. Test and simulation results of LIVE-L4+ LIVE-L5L. KIT Scientific publishing; 2011.

Imperial College London

The LIVE Experiments



The LIVE experimental vessel



Schematic of LIVE experiment

Fluhrer B, Miassoedov A, Cron T, Foit J, Gaus-Liu X, Schmidt-Stiefel S, Wenz T, Ivanov I, Popov D. The LIVE-L1 and LIVE-L3 experiments on melt behaviour in RPV lower head. Forschungszentrum Karlsruhe GmbH Technik und Umwelt (Germany).; 2008.

Imperial College London

Stages of the L3 test

1. Melt poured – Air cooling **(Phase 1)**
2. Heating at 18 kW (131 s)
3. Heating reduced to 14 kW (371 s)
4. Heating reduced to 12 kW (2,591 s)
5. Heating reduced to 10 kW (3,671 s)
6. Water supply switched on (7,200 s) **(Phase 2)**
7. Heating reduced to 7 kW (83,100 s) **(Phase 3)**
8. Experiment stopped (102,900 s)

Fluhrer B, Miassoedov A, Cron T, Foit J, Gaus-Liu X, Schmidt-Stiefel S, Wenz T, Ivanov I, Popov D. The LIVE-L1 and LIVE-L3 experiments on melt behaviour in RPV lower head. Forschungszentrum Karlsruhe GmbH Technik und Umwelt (Germany).; 2008.

Numerical modelling: Fluidity and dependent packages

- Open source general purpose code developed primarily at Imperial.
  - Fluidity based package (IC-FERST) has been used for numerical modelling.
- Uses unstructured meshing.
- Originally aimed to simulate porous media flows and aimed at reservoir modelling.
  - Extended to be able to model multi-phase flows such as droplet formation, flows in reactors.
- Simulates multi-phase flow with dynamic mesh optimization (DMO).
- Continuous and discontinuous galerkin discretisation methods used for spatial discretisation of the advection-diffusion equation.

Imperial College London

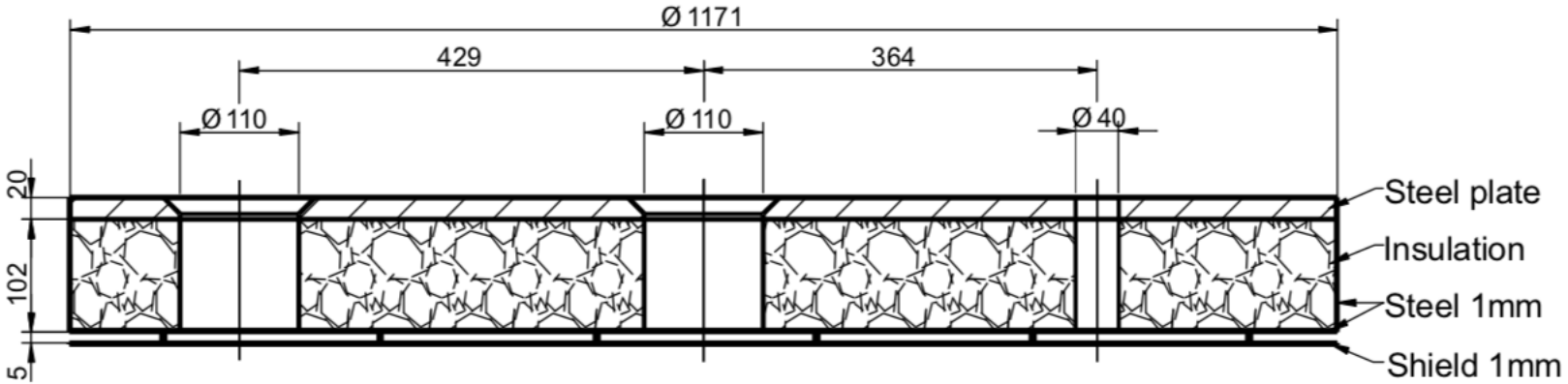
Simulating the L3 test– boundary conditions

- Boundary conditions are extremely important. Slight variations in the boundary condition parameters can give improper output since this is a natural convection phenomena
- Top and bottom boundary condition need to be defined
- Numerous heat transfer processes need to be taken into account

Fluhrer B, Miassoedov A, Cron T, Foit J, Gaus-Liu X, Schmidt-Stiefel S, Wenz T, Ivanov I, Popov D. The LIVE-L1 and LIVE-L3 experiments on melt behaviour in RPV lower head. Forschungszentrum Karlsruhe GmbH Technik und Umwelt (Germany).; 2008.

L3 test– Top boundary layer

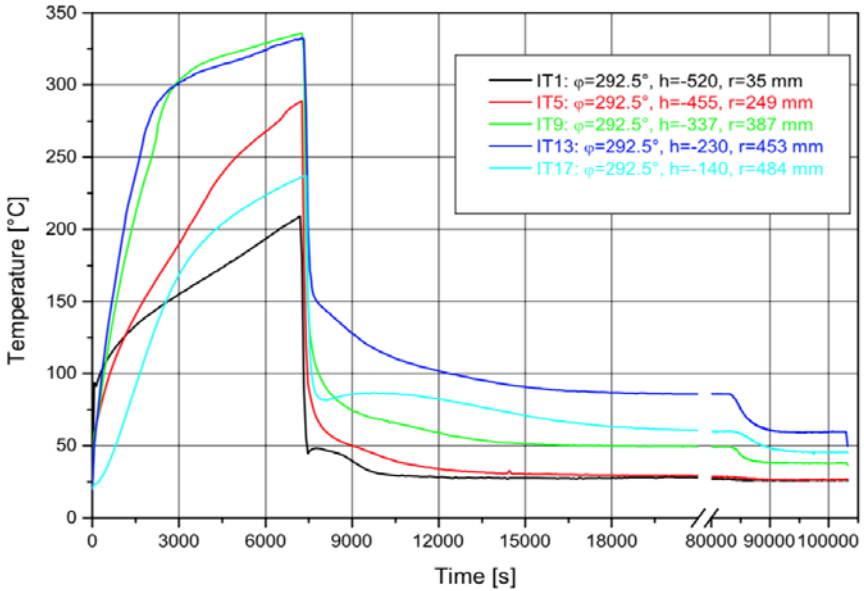
The observed temperature for L4 is 67.5 ℃. Top BC taken as 100 ℃ which is a very conservative estimate considering L3 heating power is lower



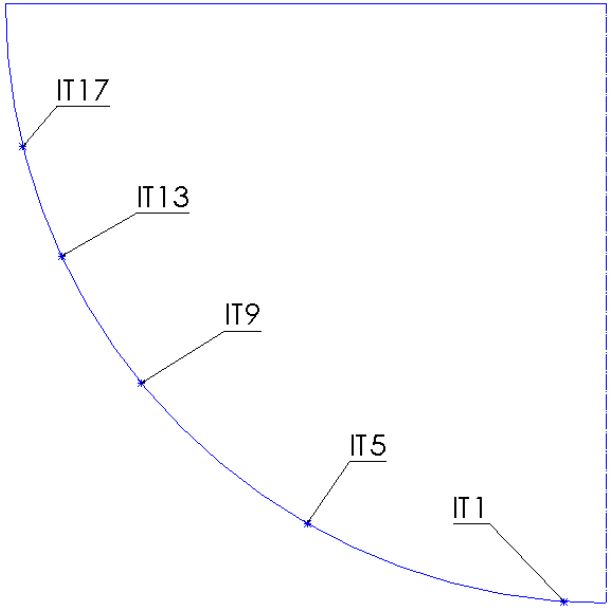
Schematic of top lid in LIVE experiments

Gaus-Liu X, Mjasoedov A, Cron T, Foit JJ, Fluhrer B, Schmidt-Stiefel S, Wenz T. Test and simulation results of LIVE-L4+ LIVE-L5L. KIT Scientific publishing; 2011.

L3 test– bottom boundary layer



Inner wall temperatures- L3 test

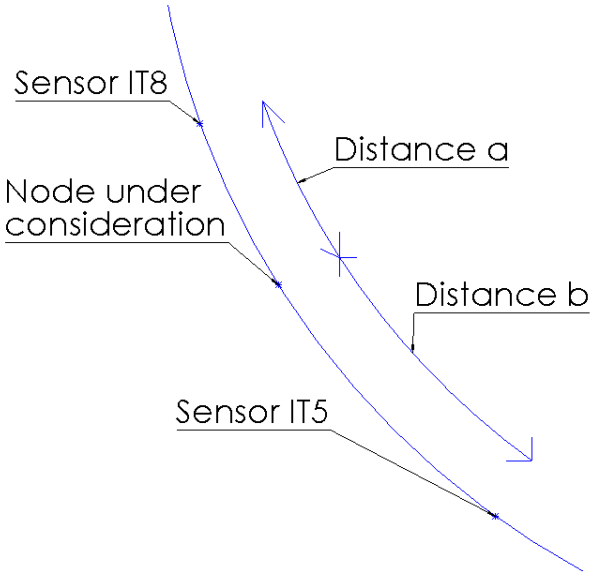


Position of inner wall temperature sensors

Fluhrer B, Miassoedov A, Cron T, Foit J, Gaus-Liu X, Schmidt-Stiefel S, Wenz T, Ivanov I, Popov D. The LIVE-L1 and LIVE-L3 experiments on melt behaviour in RPV lower head. Forschungszentrum Karlsruhe GmbH Technik und Umwelt (Germany).; 2008.

L3 test– bottom boundary layer

- Temperature function generated from the inner wall temperature graph
- Custom python script written
- Script checks nodal position and extrapolates the temperature based on the measured sensor temperatures



Illustrating nodal temperature calculation

Imperial College London

Simulating the L3 test– solidification

- Solidification is highly dependent on the input material parameters, which in this case is the $NaNO_3$-KNO_3 mixture.
- IC-FERST has a field called "Velocity Absorption" which arrests the fluid
  - Script also written to account for latent heat due to phase change
  - Path: ../vector field::Velocity/prognostic/vector field::Absorption
- $\partial c/\partial t = F(c, u, t) - \sigma c + F$
  - F(c, u, t) represent the advection and diffusion terms
  - Second term (σ) represents the absorption and last term (F) represents the source.
- One other way to change phase (liquid to solid) would be to change the viscosity (currently being modelled).

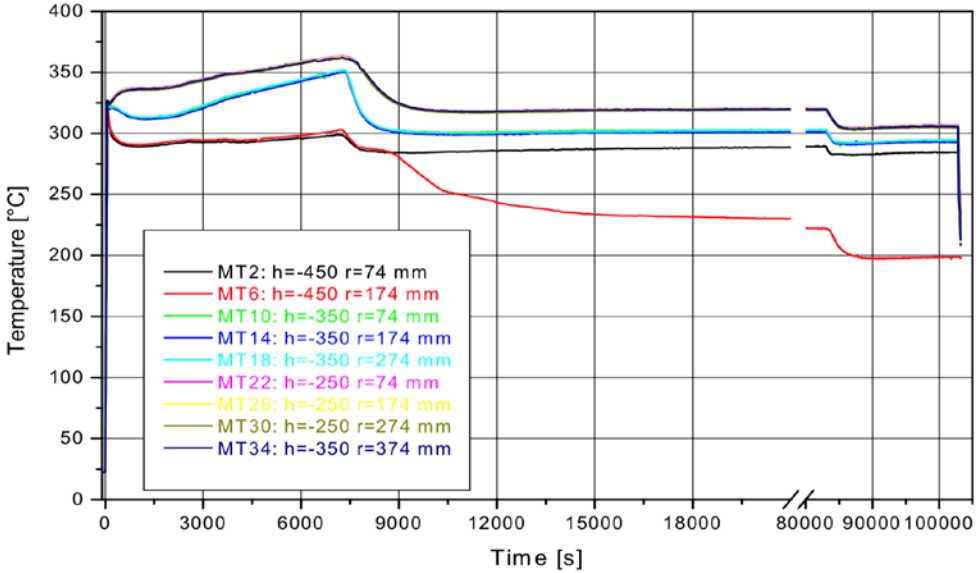
Imperial College London

Results

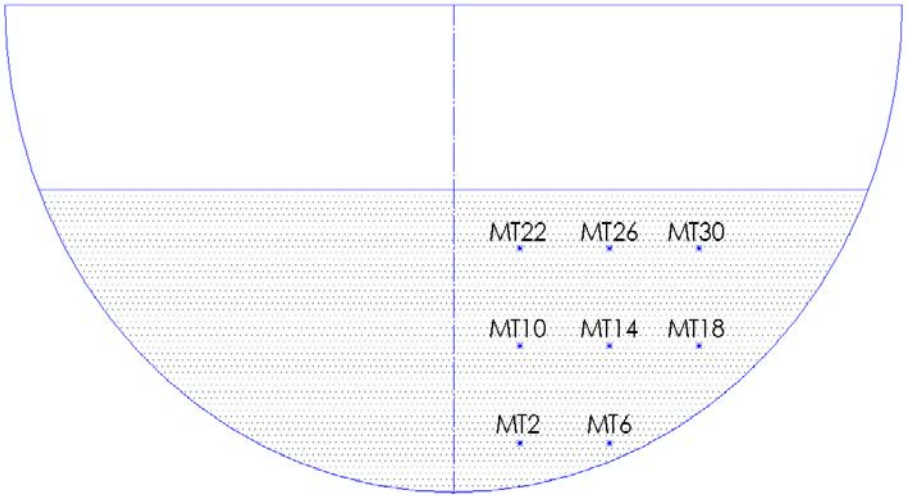
1) **Compared with first 2 phases of the L3 experiment**
2) **Compared with analytical solution**
3) **Illustrated the benefits of mesh adaptivity**
4) Analysed the temperature variation across the pool depth and compared the non-dimensional data generated with the BALI experiment

Imperial College London

Melt pool temperature (experimental)



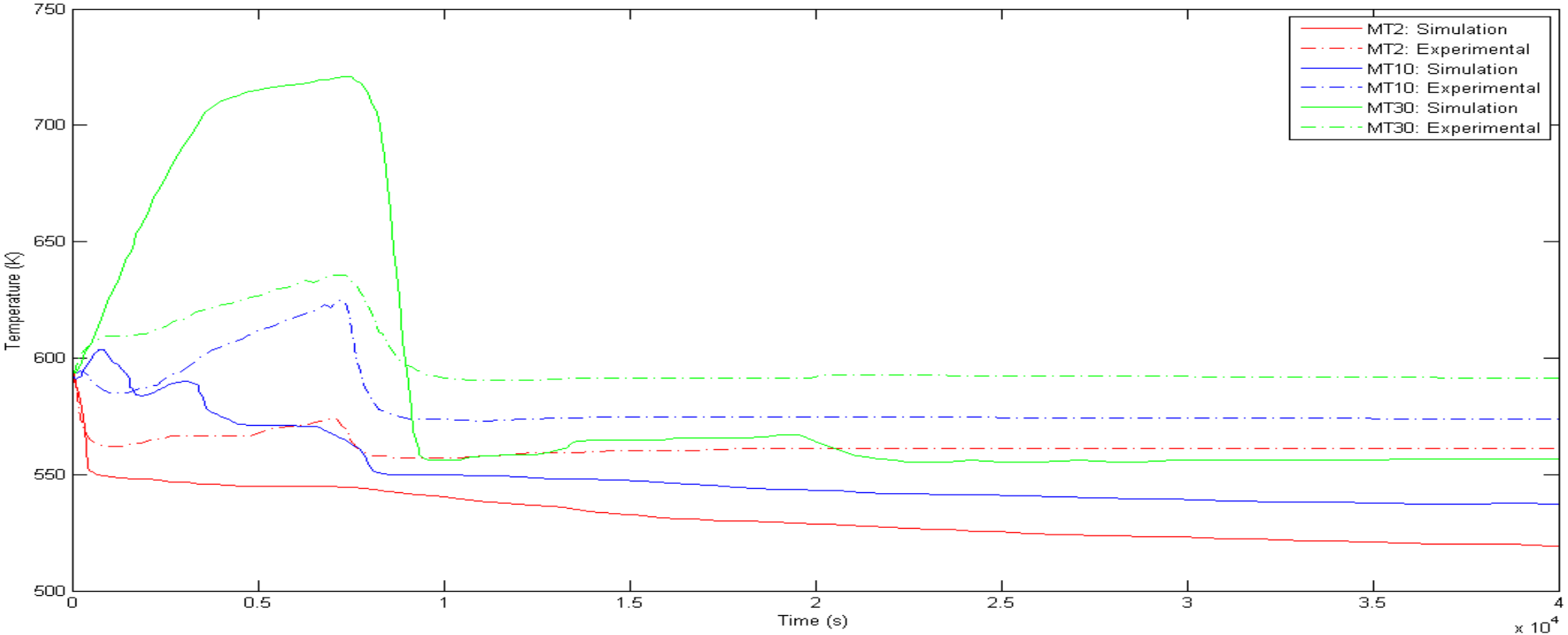
Melt pool temperatures- L3 test



Melt pool sensor positions

Fluhrer B, Miassoedov A, Cron T, Foit J, Gaus-Liu X, Schmidt-Stiefel S, Wenz T, Ivanov I, Popov D. The LIVE-L1 and LIVE-L3 experiments on melt behaviour in RPV lower head. Forschungszentrum Karlsruhe GmbH Technik und Umwelt (Germany).; 2008.

Comparing with L3 experiment



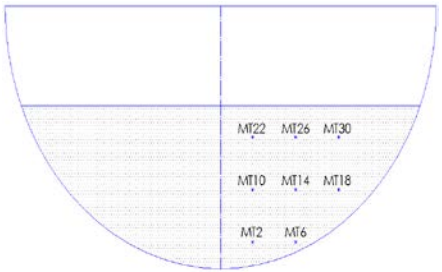
Imperial College London

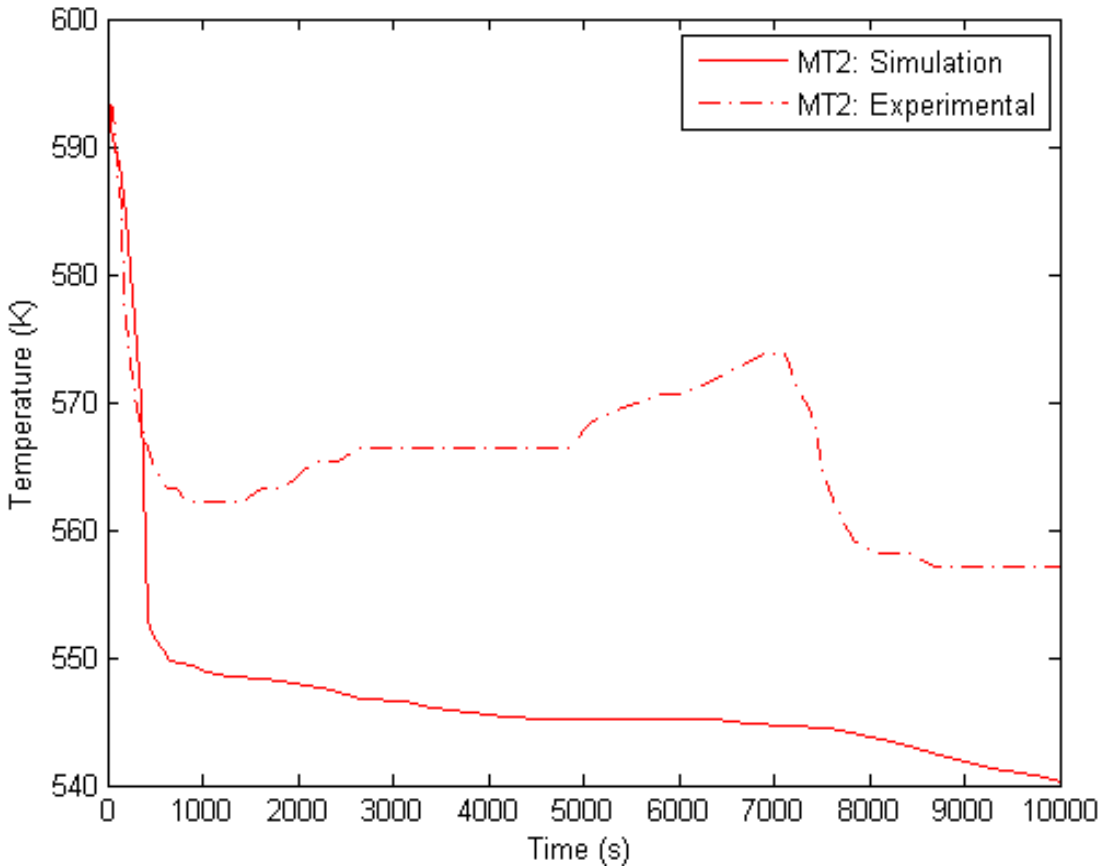
Comparing melt pool temperature

- Analysis done in 2D while experiment was done in 3D
- Maximum error of 14.5% at MT30 (end of phase 1)
- Steady state error always less than 8%
- Next few slides compare the sensors individually (air cooling phase)

Comparing with L3 experiment

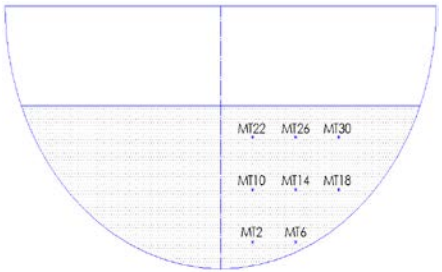
MT2 sensor

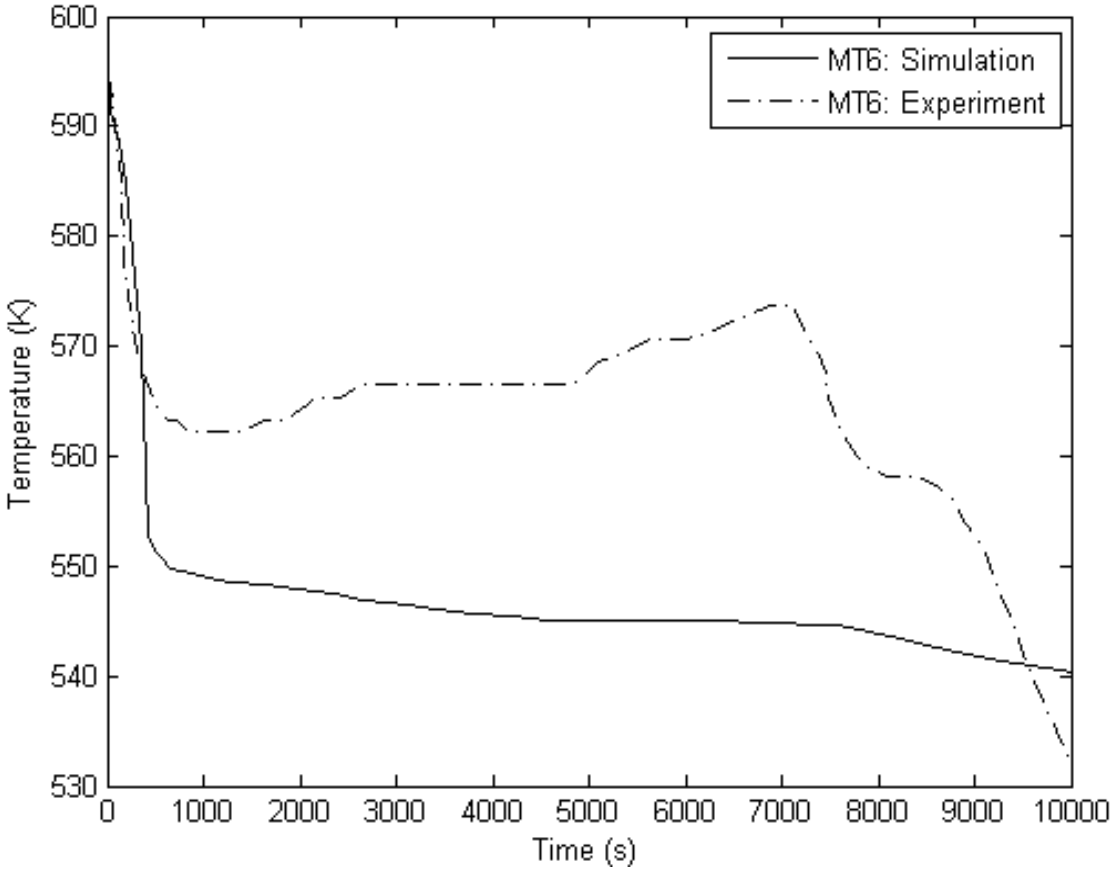




Comparing with L3 experiment

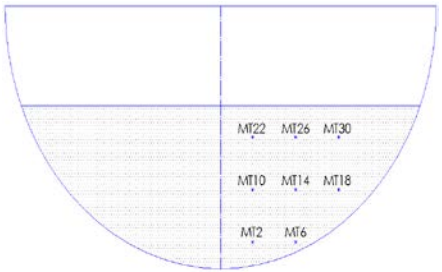
MT6 sensor

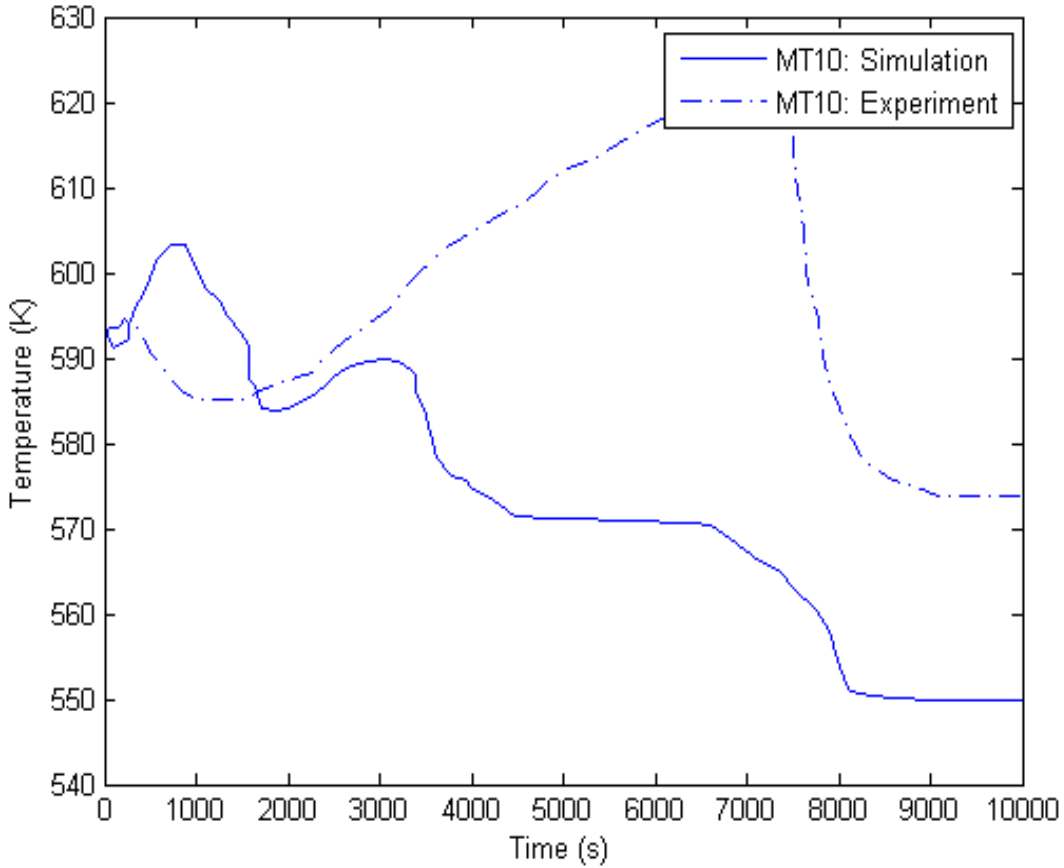




Comparing with L3 experiment

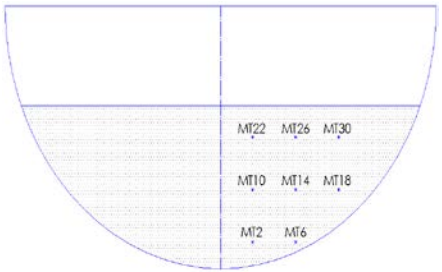
MT10 sensor

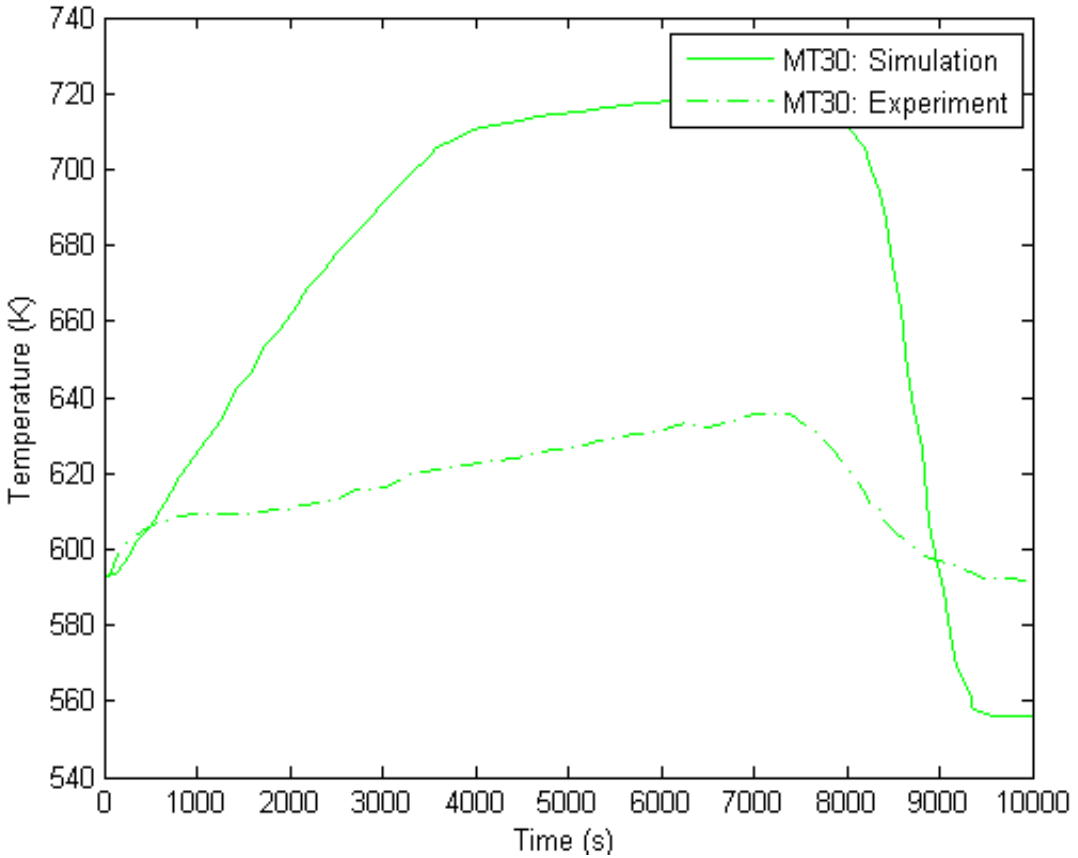




Comparing with L3 experiment

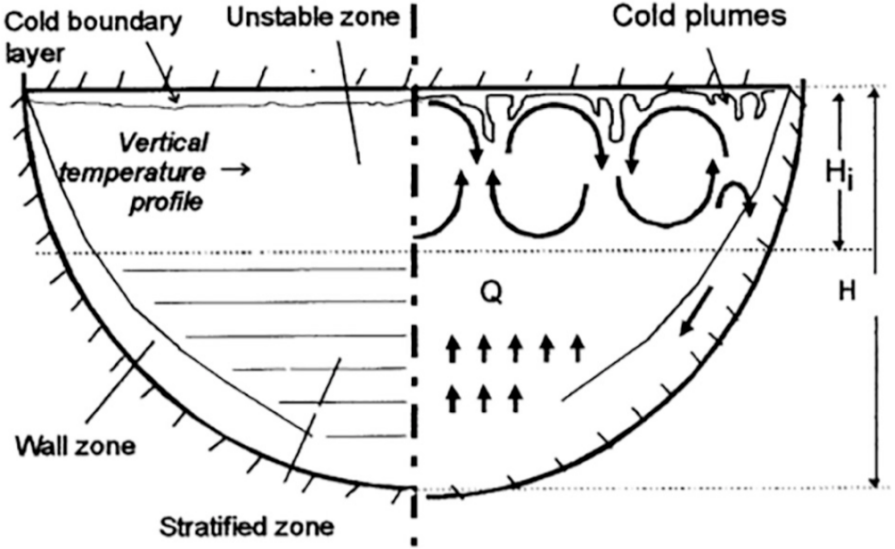
MT30 sensor



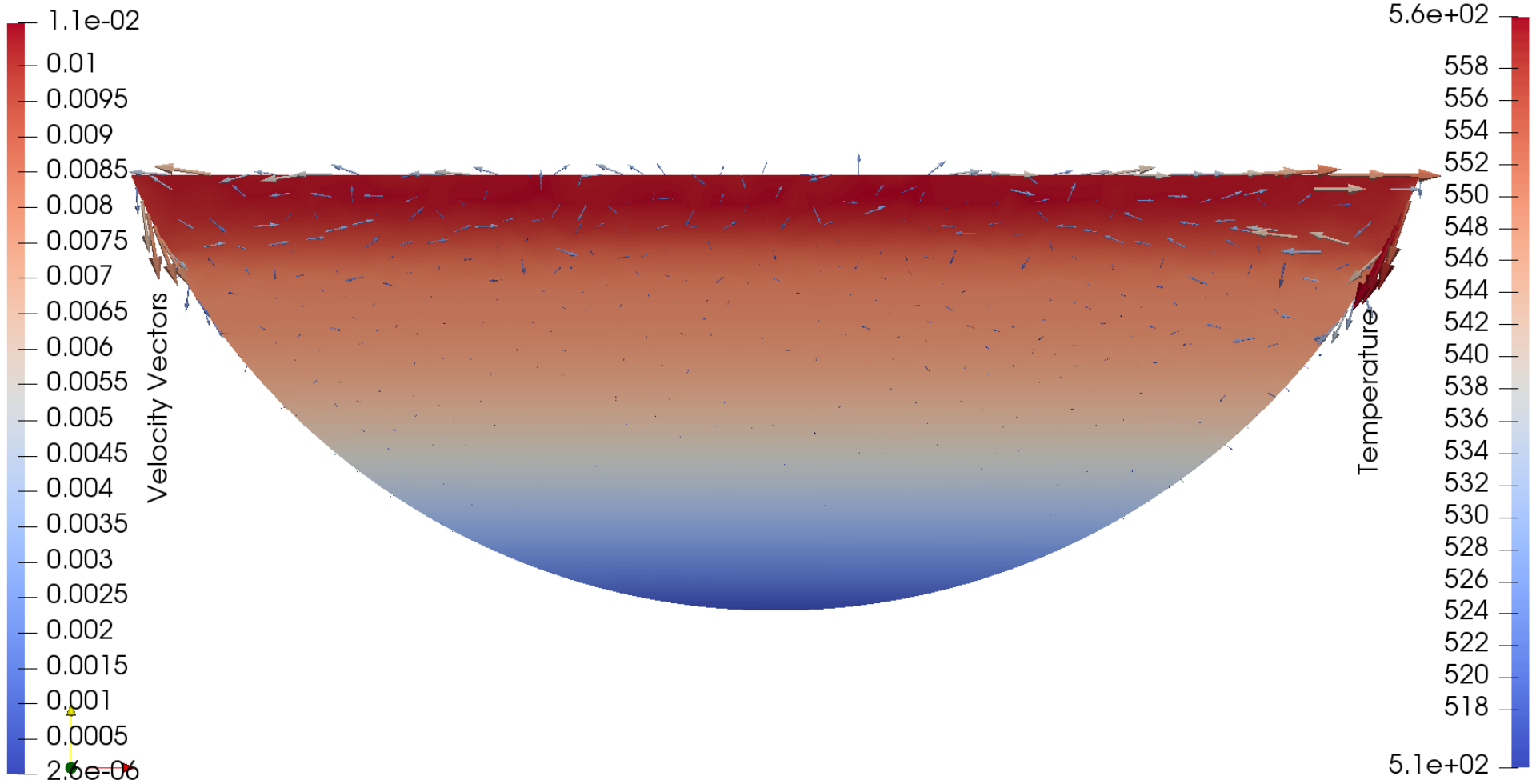


Imperial College London

Flow patterns (experimental and simulation)



Experimentally observed flow patterns



Flow patterns at steady state



Imperial College London

Analytical solution

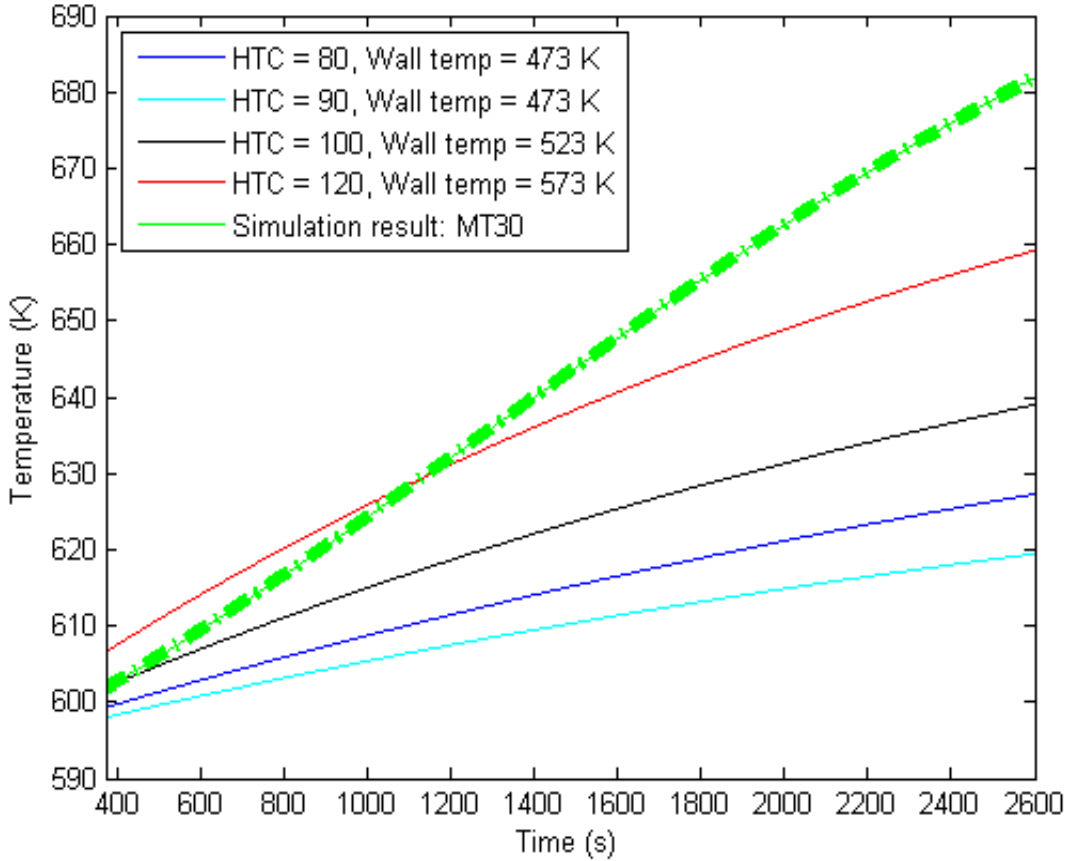
- To be used only as a guideline
- Shows whether the simulation is behaving in an expected manner

$$\underbrace{\rho V C_p \frac{DT}{Dt}}_{Internal\ energy} = Heat\ source - \underbrace{hA(T - T_{wall})}_{Bottom\ convection}$$

$$\underbrace{1862 \times 0.119 \times 1369 \frac{DT}{Dt}}_{Internal\ energy} = 18000 - \underbrace{70 \times 0.9(T - 373)}_{Bottom\ convection}.$$

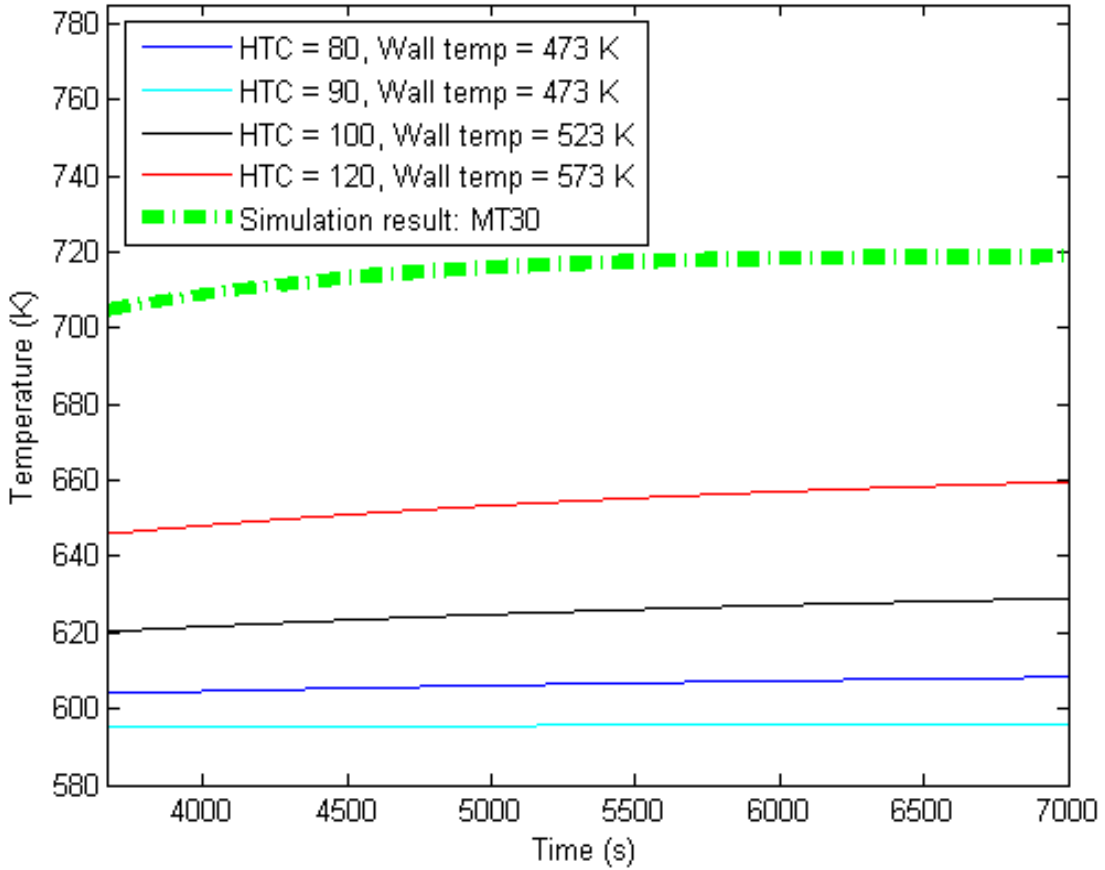
Comparing with analytical solution

14 kW phase



Comparing with analytical solution

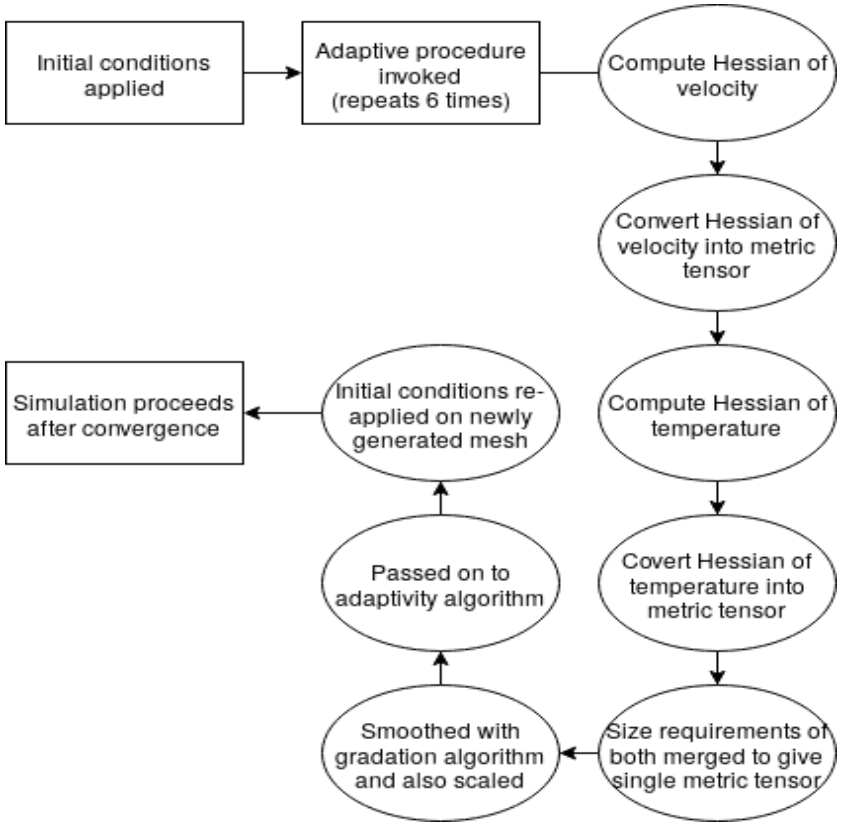
10 kW phase

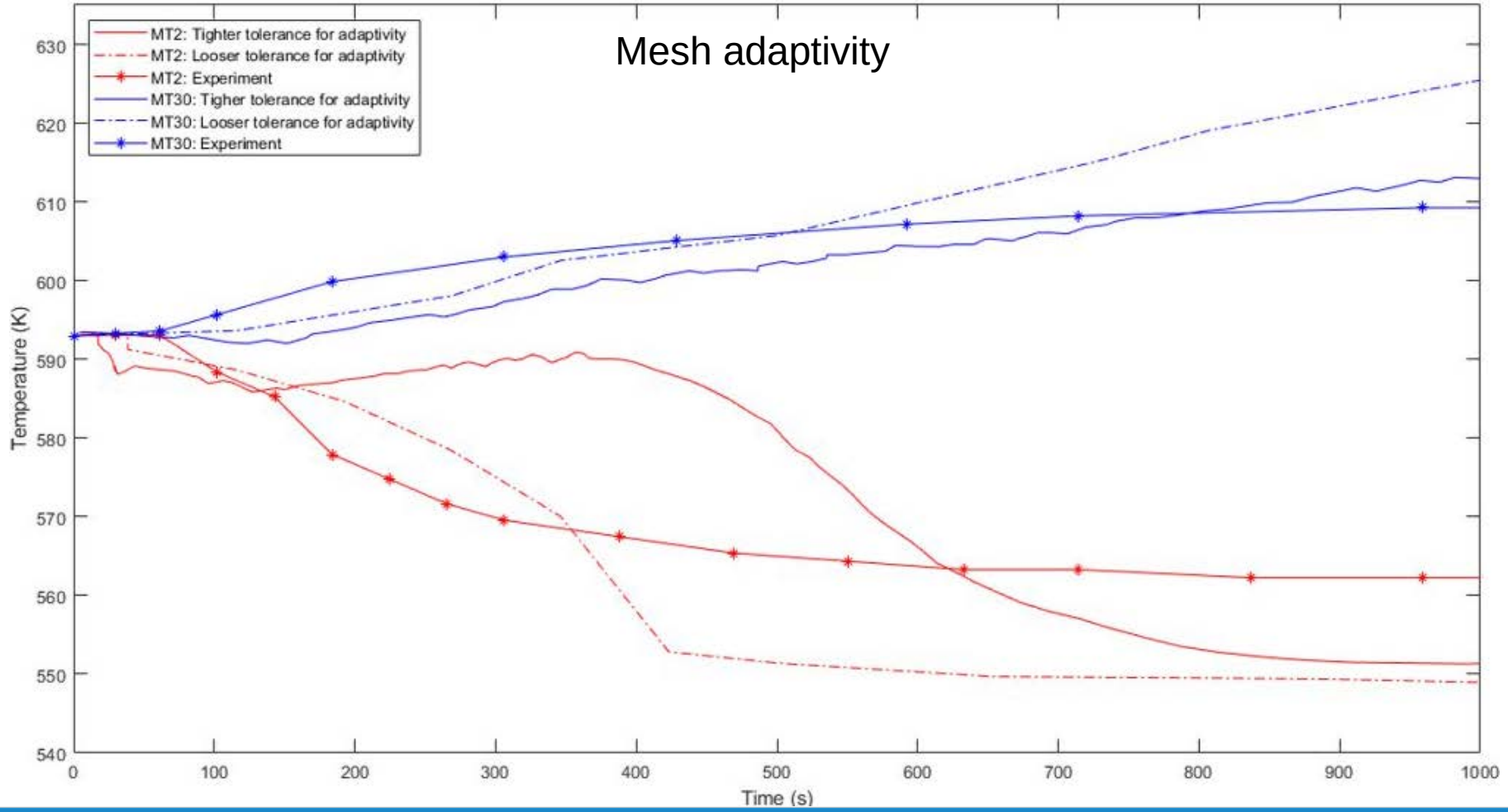


About mesh adaptivity

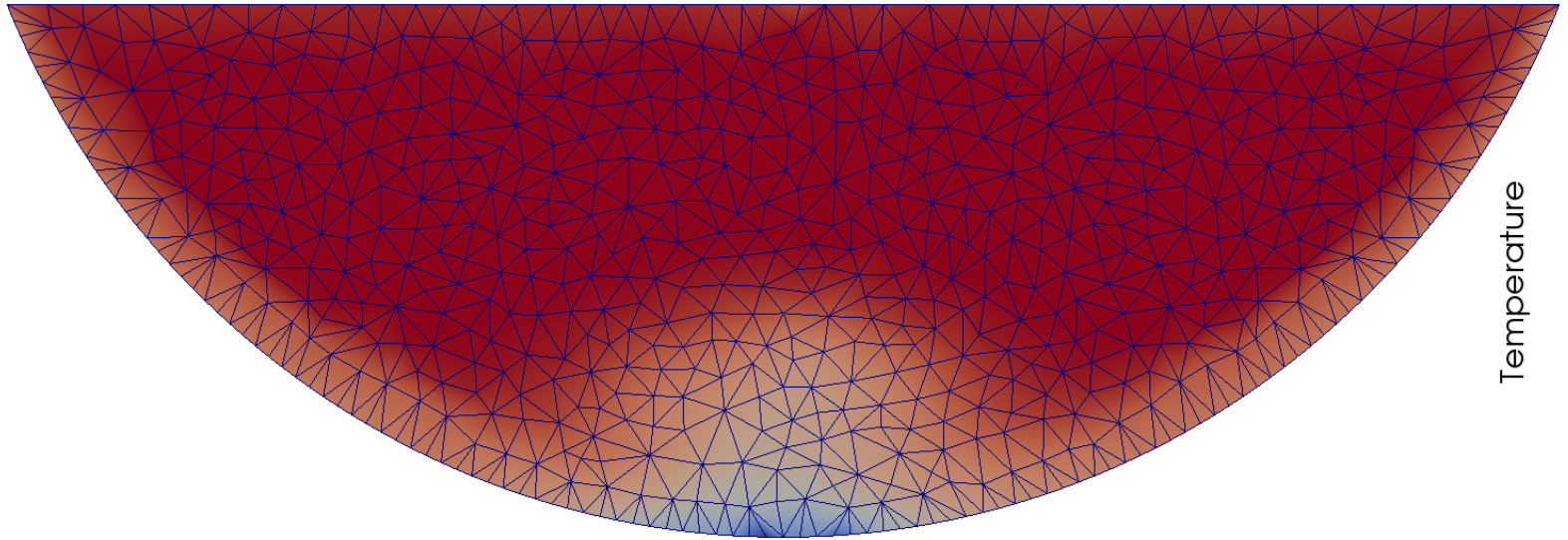
- One of the key highlights of IC-FERST
- The main analysis (against which experimental data is compared) is adapted to the velocity field. Relatively coarse mesh refinement parameters– minimum edge length of 15 mm and maximum edge length of 25 mm. Unit error 0.003
- Adaptivity test case is run. Adapted to temperature field. Relatively fine mesh refinement parameters– minimum edge length of 10 mm and maximum edge length of 30 mm. Unit error 0.0005.

Mesh adaptivity

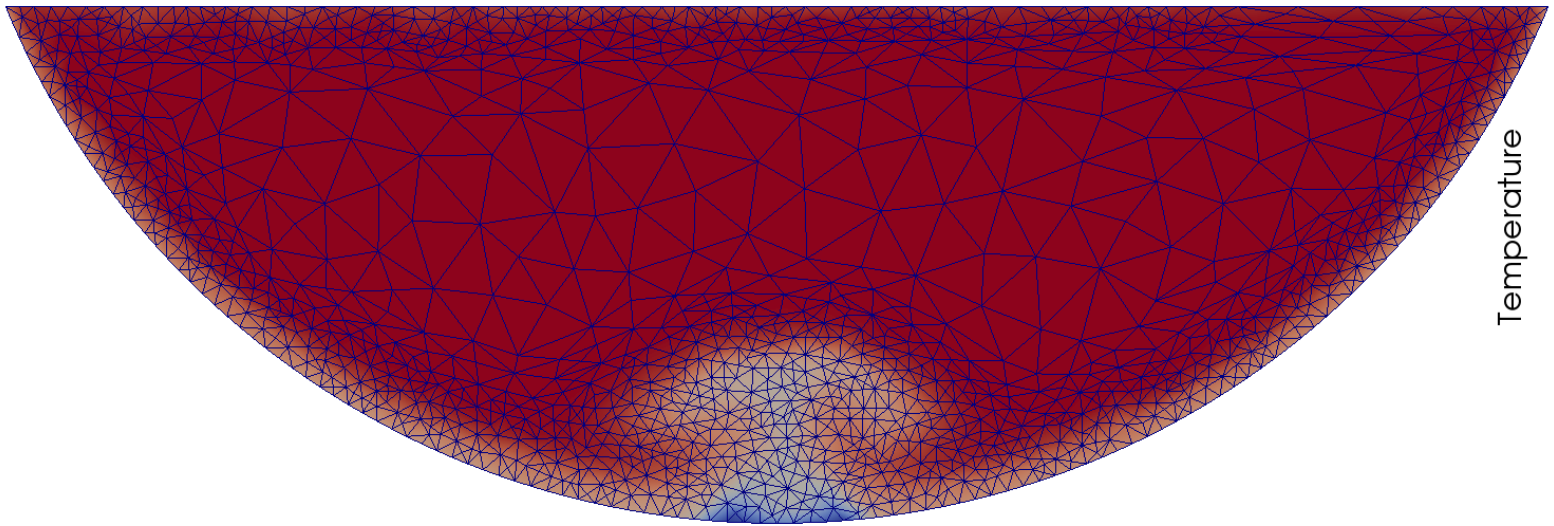




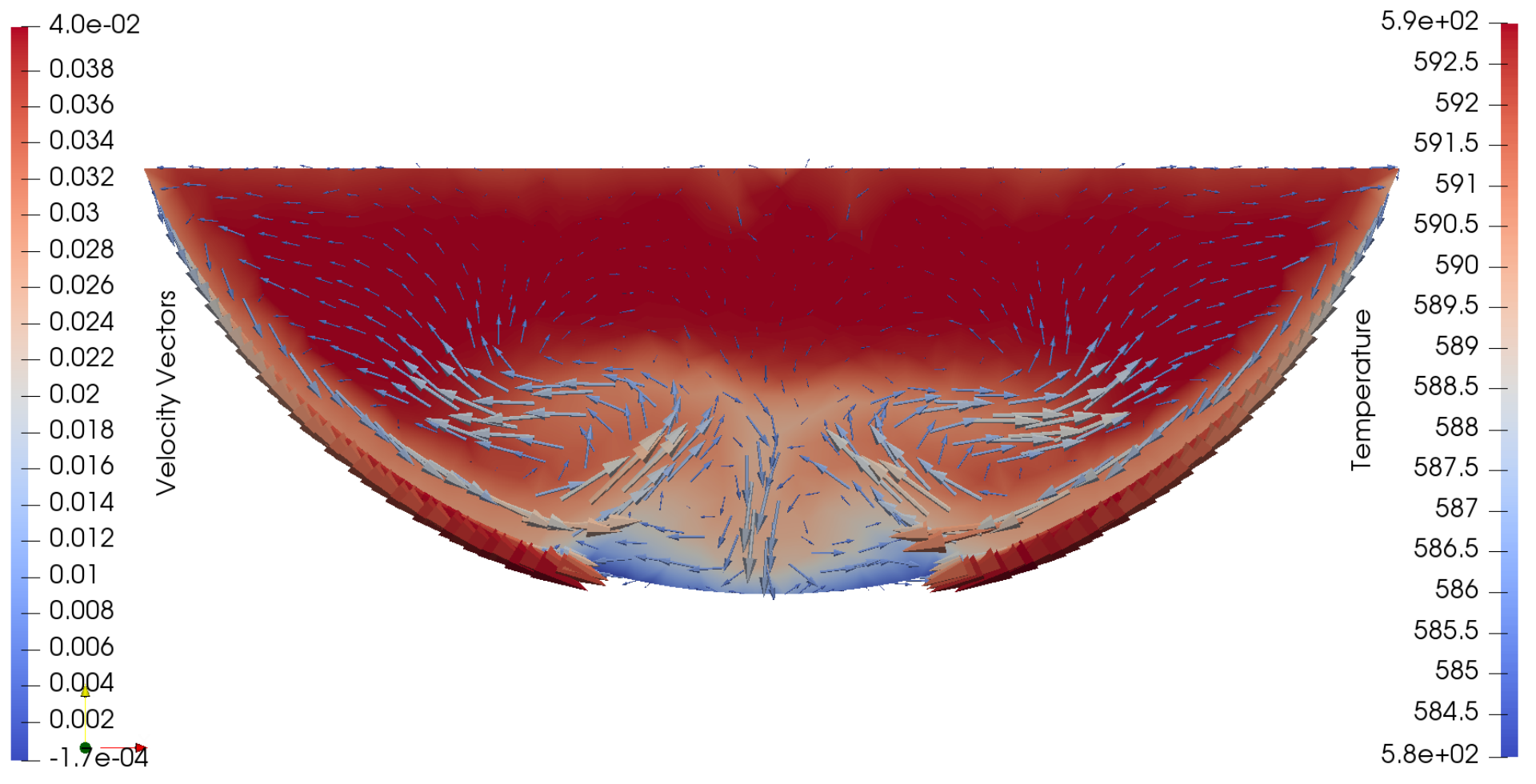
Comparison of different adaptivity scenarios with experiment



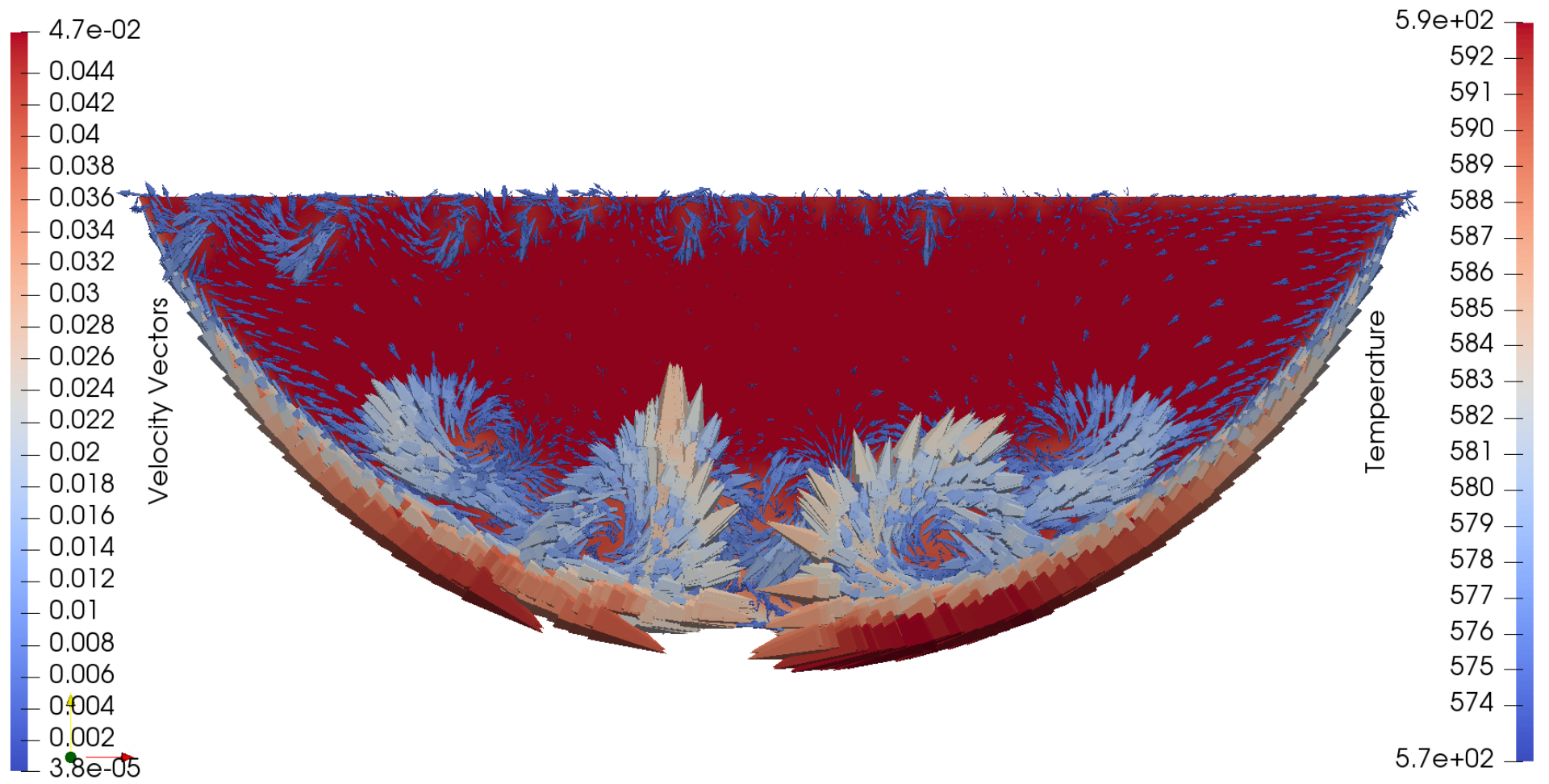
At t= 17s, relaxed criteria for mesh adaptivity. Temperature field.



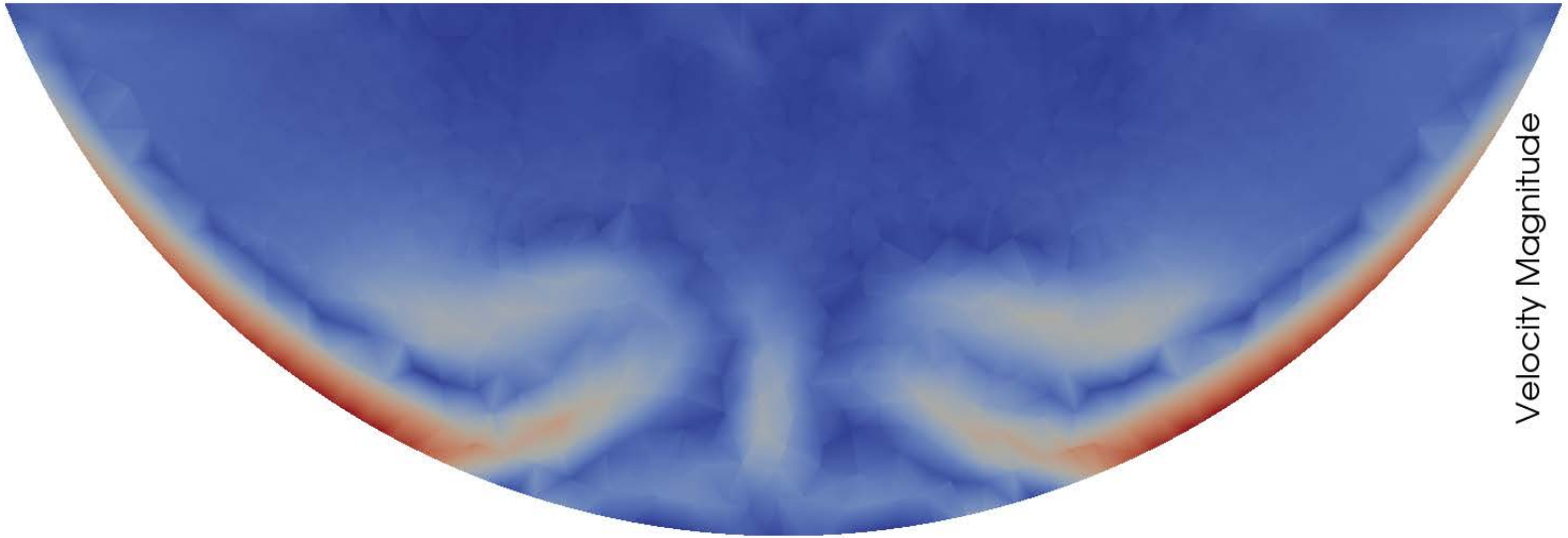
At t= 17s, strict criteria for mesh adaptivity. Temperature field.



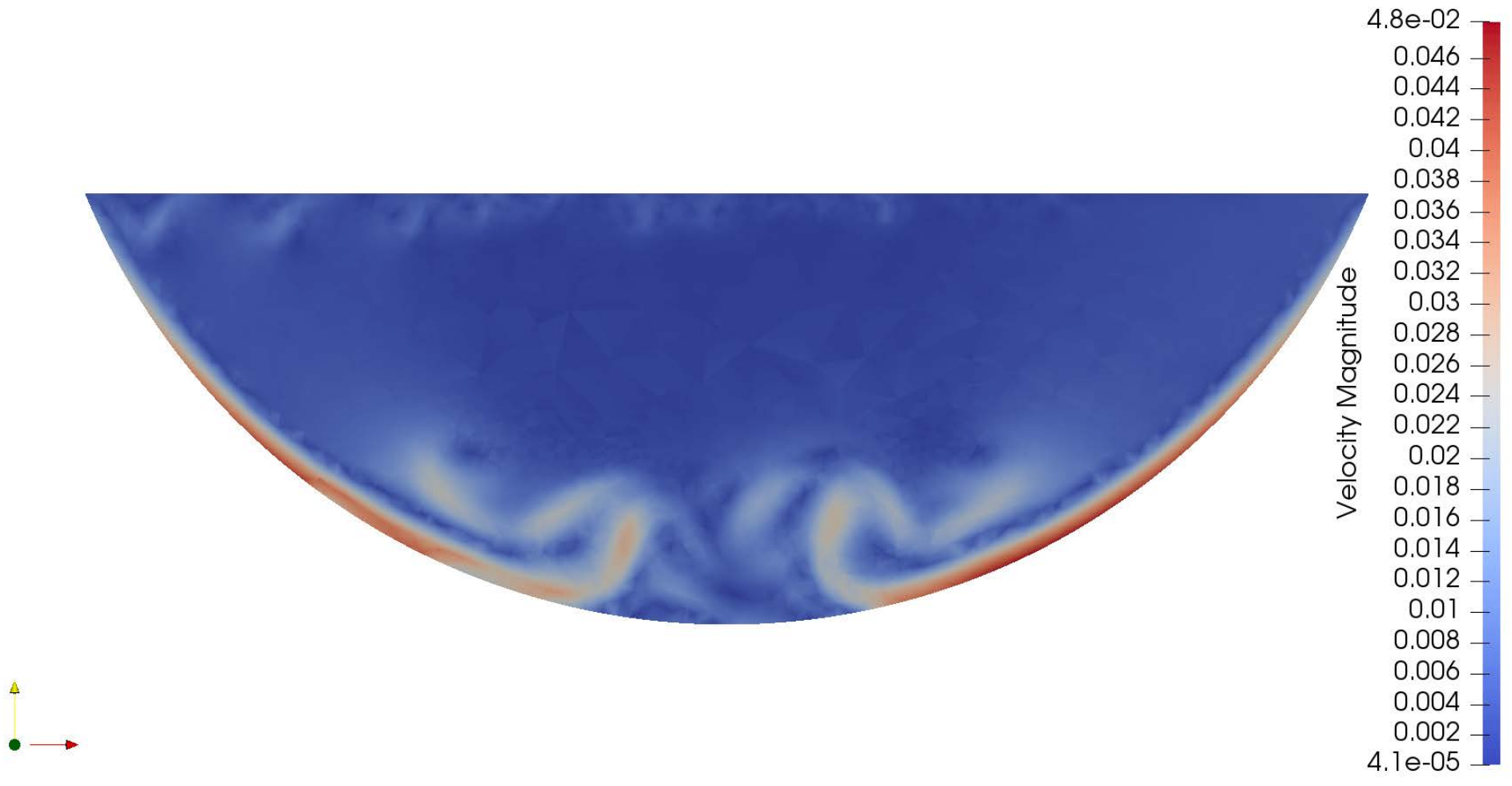
At t= 32s, relaxed criteria for mesh adaptivity. Temperature field with velocity vectors.



At t= 32s, strict criteria for mesh adaptivity. Temperature field with velocity vectors.



At t= 32s, relaxed criteria for mesh adaptivity. Velocity field.



At t= 32s, strict criteria for mesh adaptivity. Velocity field.

Cost of mesh adaptivity

- Strict criteria for mesh adaptivity- 48 hours (6 parallel nodes, 24 GB RAM). Ran for 1000s
- Relaxed criteria for mesh adaptivity- 72 hours (5 parallel nodes, 16 GB RAM). Ran for 40,000s
- Match with experimental data is better for fine mesh adaptivity simulation
  - 3x better in best case scenario (top layer of the melt)

CONCLUSIONS

Conclusions

- Compared with LIVE experiment – L3 test
  - Quasi steady-state reached (maximum error 14.5% at MT30 in phase 1)
  - Crust formation not as accurate as required
- Analysis compared with analytical solution
- Demonstrated the efficacy of mesh adaptivity
  - Adapting to the temperature field with stricter mesh refinement parameters resulting in better match with experimental values

Future work

- Improve crust formation modelling
  - Additional data required regarding viscosity of binary mixture for accurate modelling
- Analyse in 3D and perform sensitivity analysis
  - Gives a better insight into parameters controlling the phenomena
- Model LIVE L4 test and demonstrate robustness of Fluidity and its dependent packages

- Once the comparison between both is satisfactory, model the full vessel and water flow to make the analysis more realistic.

Thank you!

Preliminary results for simulations of the DEBRIS test facility conducted with the Severe Accident Analysis Code ASTEC V2.1

25th International QUENCH Workshop, October 2019, Karlsruhe

Jan Mathis Peschel and Marco K. Koch

Plant Simulation and Safety Group (PSS),
Ruhr-Universität Bochum (RUB)

jan.peschel@pss.rub.de, marco.koch@pss.rub.de
ORCID-ID: 0000-0002-6529-2492 / 0000-0001-7260-5250

As part of the research project “External validation and model analysis of the code systems AC² and ASTEC supported by detailed CFD analysis (VAMOCAAD)” simulations of degraded core sections, like debris beds and melt pools, are conducted. These are performed with the integral code ASTEC V2.1, that is developed by IRSN. The investigated experiments of the DEBRIS test facility were performed by the Institute of Nuclear Technology and Energy Systems (IKE) in Stuttgart.

Besides the investigated quenching experiments boling and dryout tests were also conducted by the IKE. Compared to previous experiments performed within the DEBRIS test facility, a couple of modifications like the addition of a pressure vessel allowed the extended variation of starting and boundary conditions. Besides to alternating temperature (up to 1,273 K) and pressure conditions (0.1, 0.3 and 0.5 MPa) two different particle types and varying flow conditions were tested. The PREMIX particle bed consists of a mixture of irregular shaped Al_2O_3 particles mixed with spherical stainless steel particles whereas the other bed consists of 3.0x5.75 mm cylindrical stainless steel particles. The testing area can be quenched from both the top and the bottom.

In this work the simulation of DEBRIS experiments performed with Bottom-Flooding will be presented. The investigated experiments will be simulated with both a fixed input signal and a gravity-driven quench water flow. Objective for the analysis of the simulation results is to validate the code capabilities to simulate the most relevant phenomena that occur while quenching the investigated debris bed formations. On the one hand the resulting temperature evolutions are overall in good accordance with the test results, showing the least deviations in the centre (axially and radially) of the debris bed. This also applies to the evolution of the quench front. On the other hand, the pressure evolution shows some larger deviations from the experimental results. The observed pressure oscillations that are calculated by ASTEC are closely connected to the resulting steam generation.

Supported by:

Federal Ministry for Economic Affairs and Energy

on the basis of a decision by the German Bundestag

This work was funded by the German Federal Ministry of Economic Affairs and Energy under grant number 1501568 on the basis of a decision by the German Bundestag.

The simulations were performed with the code version ASTEC V2.1, developed by IRSN.





RUB

RUHR-UNIVERSITÄT BOCHUM

Preliminary results for simulations of the DEBRIS test facility conducted with the Severe Accident Analysis Code ASTEC V2.1

Jan M. Peschel and Marco K. Koch

25th International QUENCH Workshop, Karlsruhe

Wednesday, 23rd October 2019

PSS Plant Simulation and Safety
Prof. Dr.-Ing. Marco K. Koch

Content

- Introduction
- Experimental Setup
- Modelling approach
- Simulation results
- Conclusion and Outlook

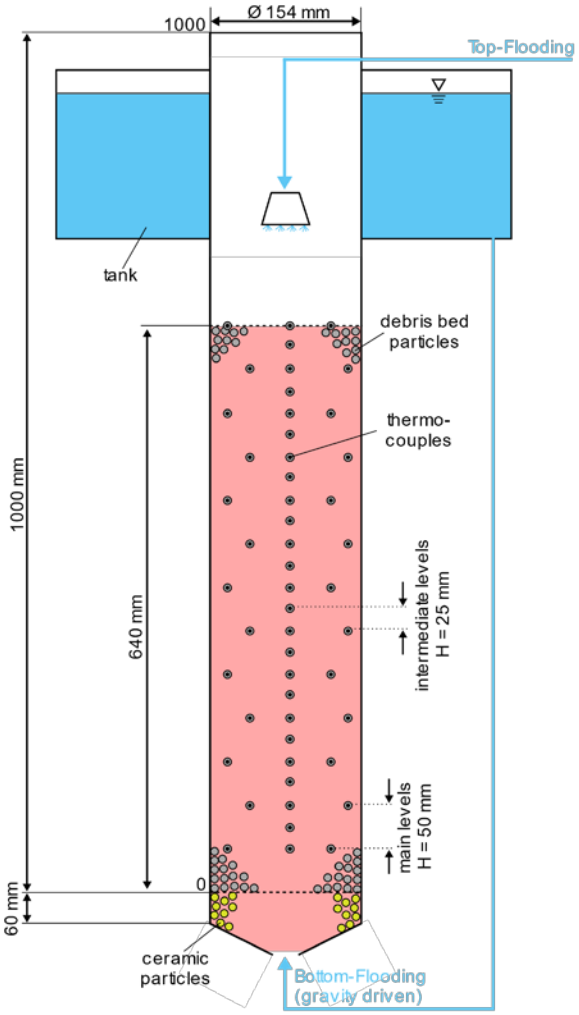
Introduction

- Motivation and aim
  - Simulation of most relevant phenomena during severe accidents with core degradation processes → DEBRIS cooling
  - Code validation and model analysis of the Severe Accident Analysis Code ASTEC V2.1
- Investigated DEBRIS experiments
  - DEBRIS test facility located at the Institute of Nuclear Technology and Energy Systems (IKE) in Stuttgart
  - Additional modifications (e.g. pressure vessel) compared to previous test series allow the extended variation of starting and boundary conditions

Experimental Setup

Structure of Test Section

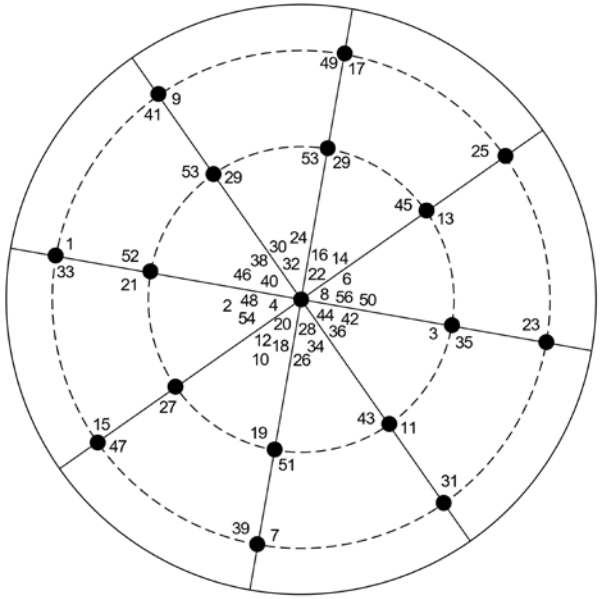
- Stainless steel test section
  - Integrated in pressure vessel (up to 4 MPa)
  - 60 mm ceramic particles (unheated)
  - 640 mm debris bed height
  - Bed can be quenched from top or bottom
  - Variation of initial temperature and pressure profile
- Instrumentation
  - 82 thermocouples (51 in debris bed)
  - Pressure transducers
  - Three magnetic-inductive flow meter (bottom-inlet, standpipe, condenser)



Experimental Setup

Structure of Test Section

- Stainless steel test section
  - Integrated in pressure vessel (up to 4 MPa)
  - 60 mm ceramic particles (unheated)
  - 640 mm debris bed height
  - Bed can be quenched from top or bottom
  - Variation of initial temperature and pressure profile
- Instrumentation
  - 82 thermocouples (51 in debris bed)
  - Pressure transducers
  - Three magnetic-inductive flow meter (bottom-inlet, standpipe, condenser)



Experimental Setup

Debris Particle Types

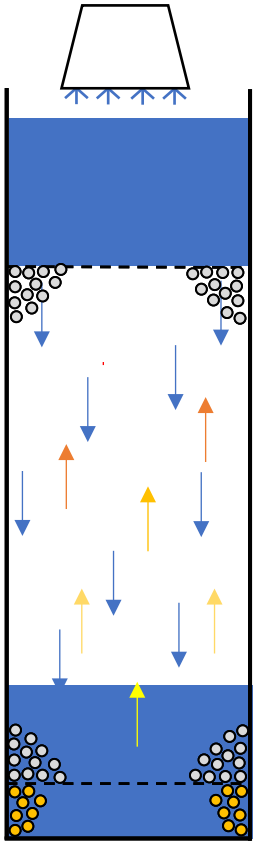
- Cylindrical particles
  - Stainless steel
  - 3.0x5.75 mm
- PREMIX particles
  - Irregular shaped AL_2O_3 particles
    - 10.7 % 2-5 mm → 3.5 mm
    - 20.8 % 5-10 mm → 7.5 mm
  - Mixed with stainless steel particles
    - Improvement of heat up
    - 24.8 % 3 mm
    - 43.7 % 6 mm



Experimental Setup

Flow Conditions

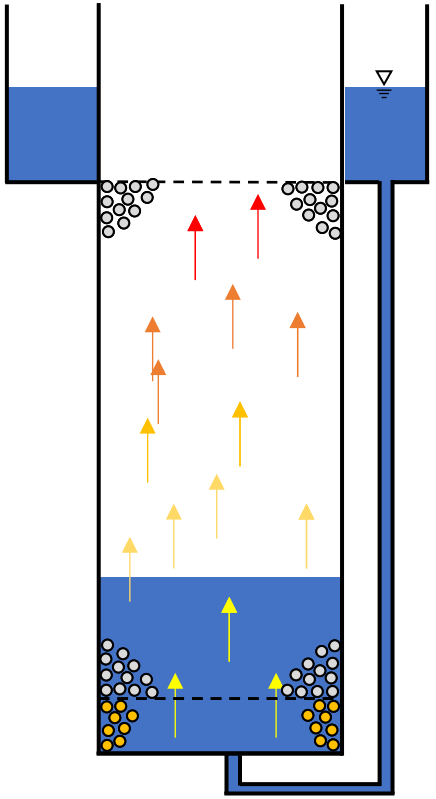
- **Top-Flooding**
  - Input via spray head
  - Establish (5 l/min) and maintain (1 l/min) constant water pool of 310 mm above debris bed
- Bottom-Flooding
  - Gravity driven input over a constant water head of 950 mm
  - Input flow rate is self-regulating depending on pressure inside the bed



Experimental Setup

Flow Conditions

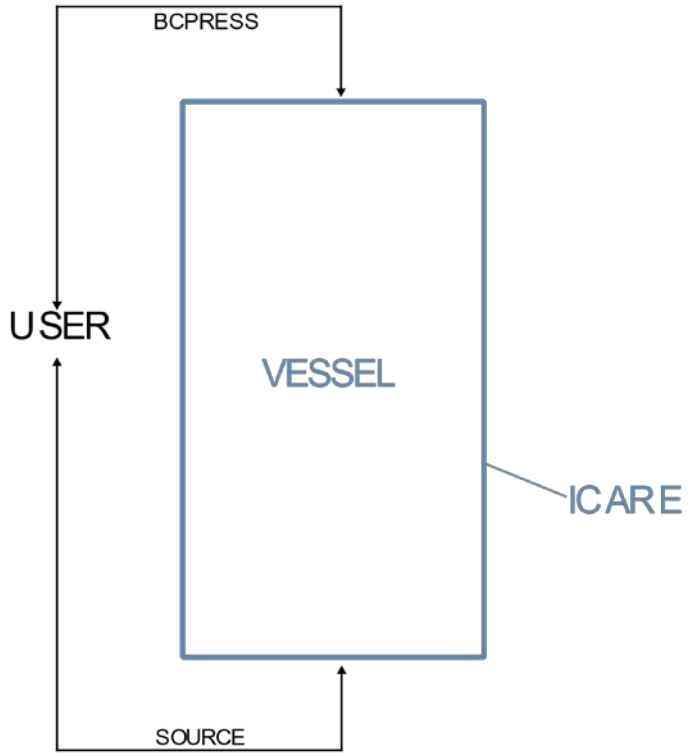
- Top-Flooding
  - Input via spray head
  - Establish (5 l/min) and maintain (1 l/min) constant water pool of 310 mm above debris bed
- **Bottom-Flooding**
  - Gravity driven input over a constant water head of 950 mm
  - Input flow rate is self-regulating depending on pressure inside the bed



Modelling approach

Schematic approach

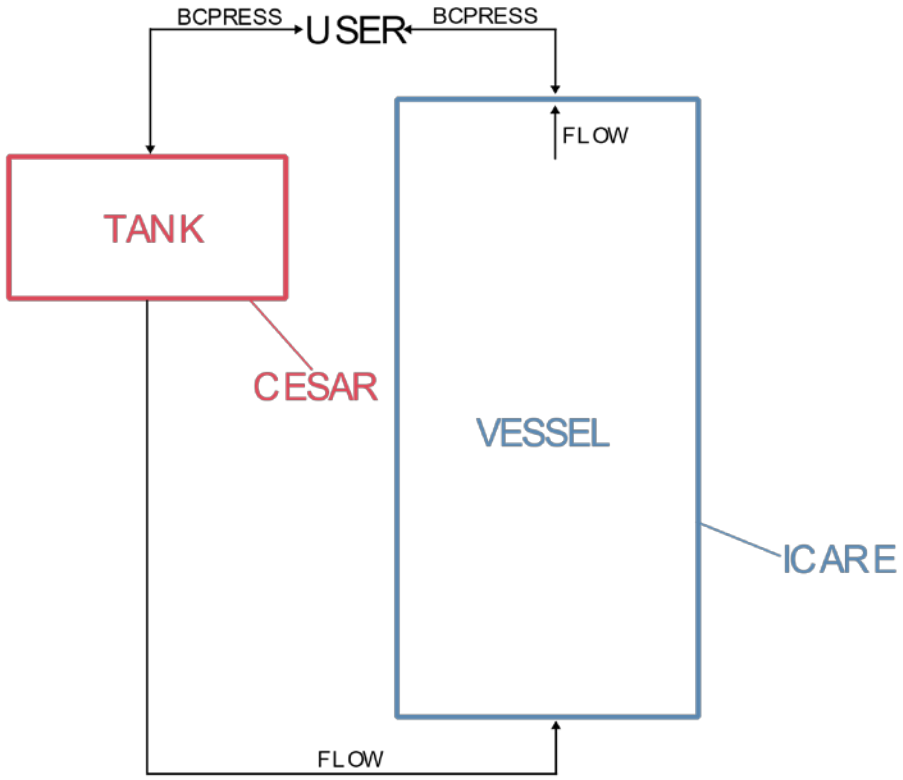
- Simulations conducted with ASTEC V2.1.1.6
- Only reflooding test phase will be simulated
  - No precise information about heat up of the test section
- **Fixed input flow**
  - Bottom- and Top-Flooding
  - Quench flow initiated via SOURCE
  - BCPRESS on outlet
- Gravity-driven input flow
  - Bottom-Flooding
  - BCPRESS on TANK and VESSEL
  - FLOW connection between TANK and VESSEL



Modelling approach

Schematic approach

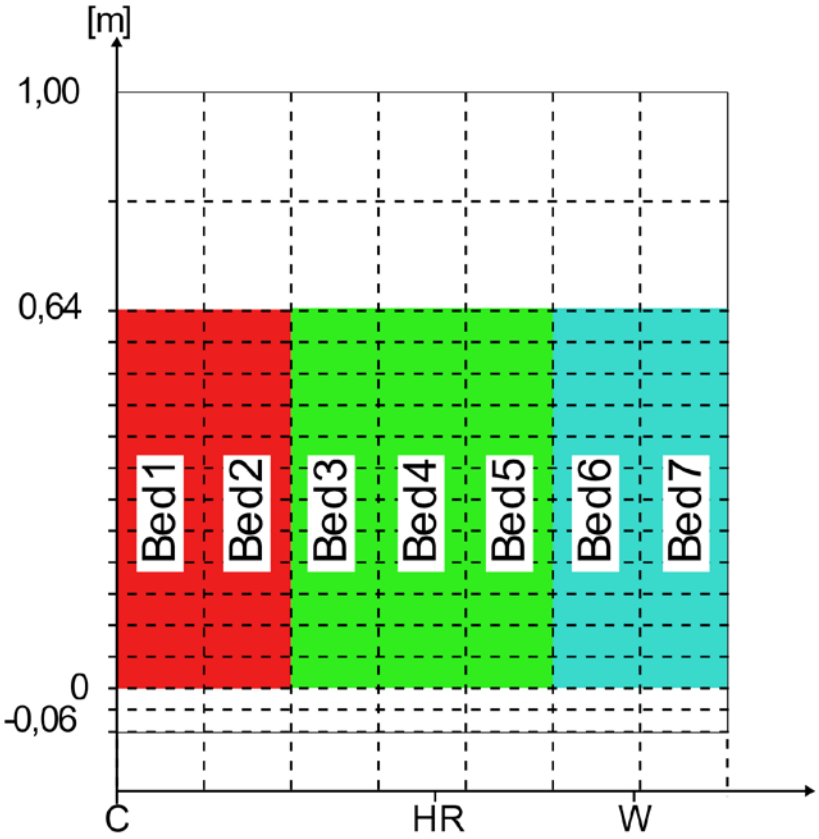
- Simulations conducted with ASTEC V2.1.1.6
- Only reflooding test phase will be simulated
  - No precise information about heat up of the test section
- Fixed input flow
  - Bottom- and Top-Flooding
  - Quench flow initiated via SOURCE
  - BCPRESS on outlet
- **Gravity-driven input flow**
  - Bottom-Flooding
  - BCPRESS on TANK and VESSEL
  - FLOW connection between TANK and VESSEL



Modelling approach

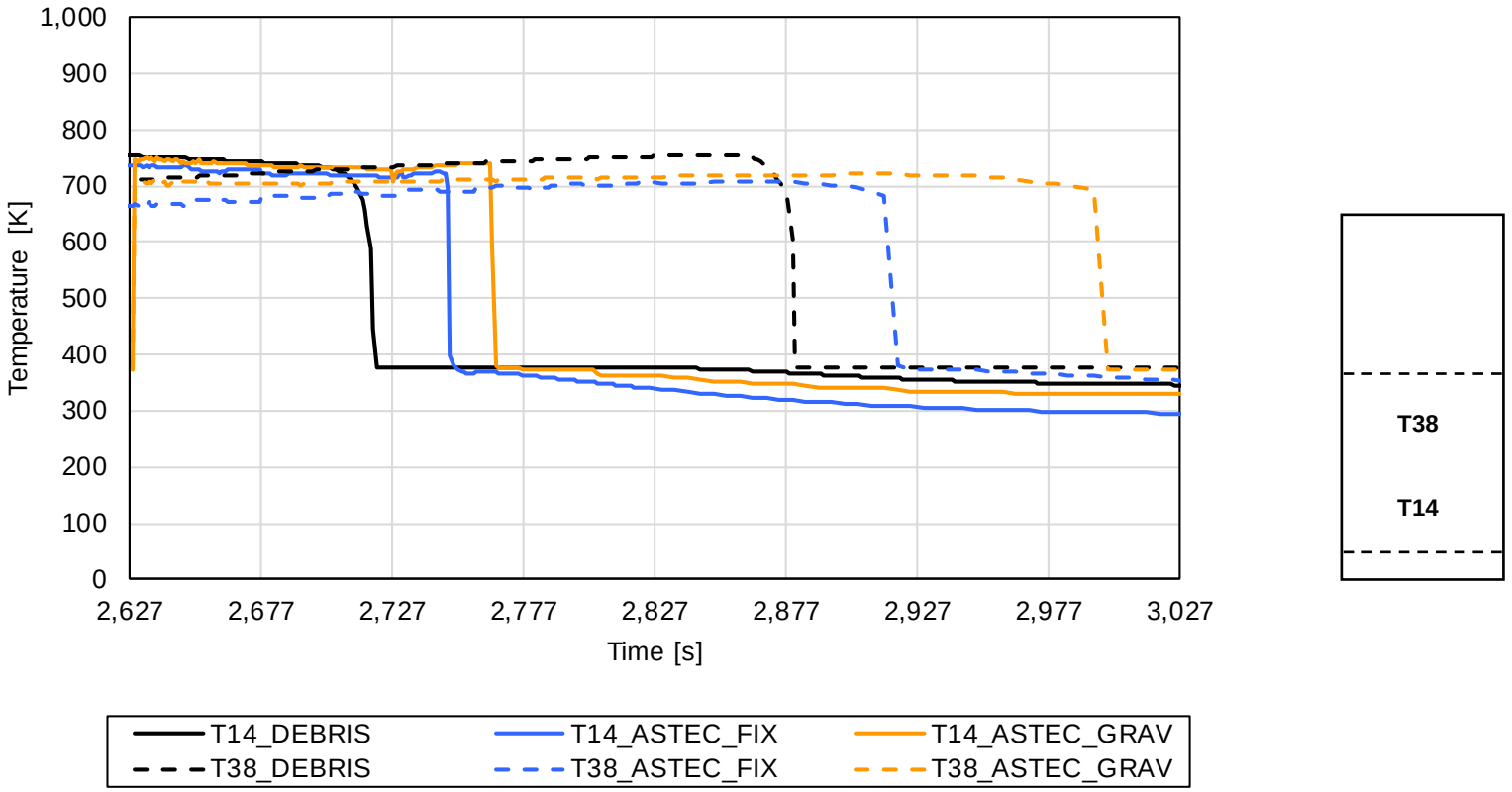
Debris Bed and Discretization

- Debris Bed
  - Two beds for premix and one for cylindric particle configuration
  - For cylindrical Particles: $V_{cyl} = V_{sph}$
- Discretization
  - Test area simulated with seven radial flow channels
  - Axially separated in 16 areas (more detailed in bed area)
- Wall of test section is not modelled
  - Information on temperature evolution currently not available



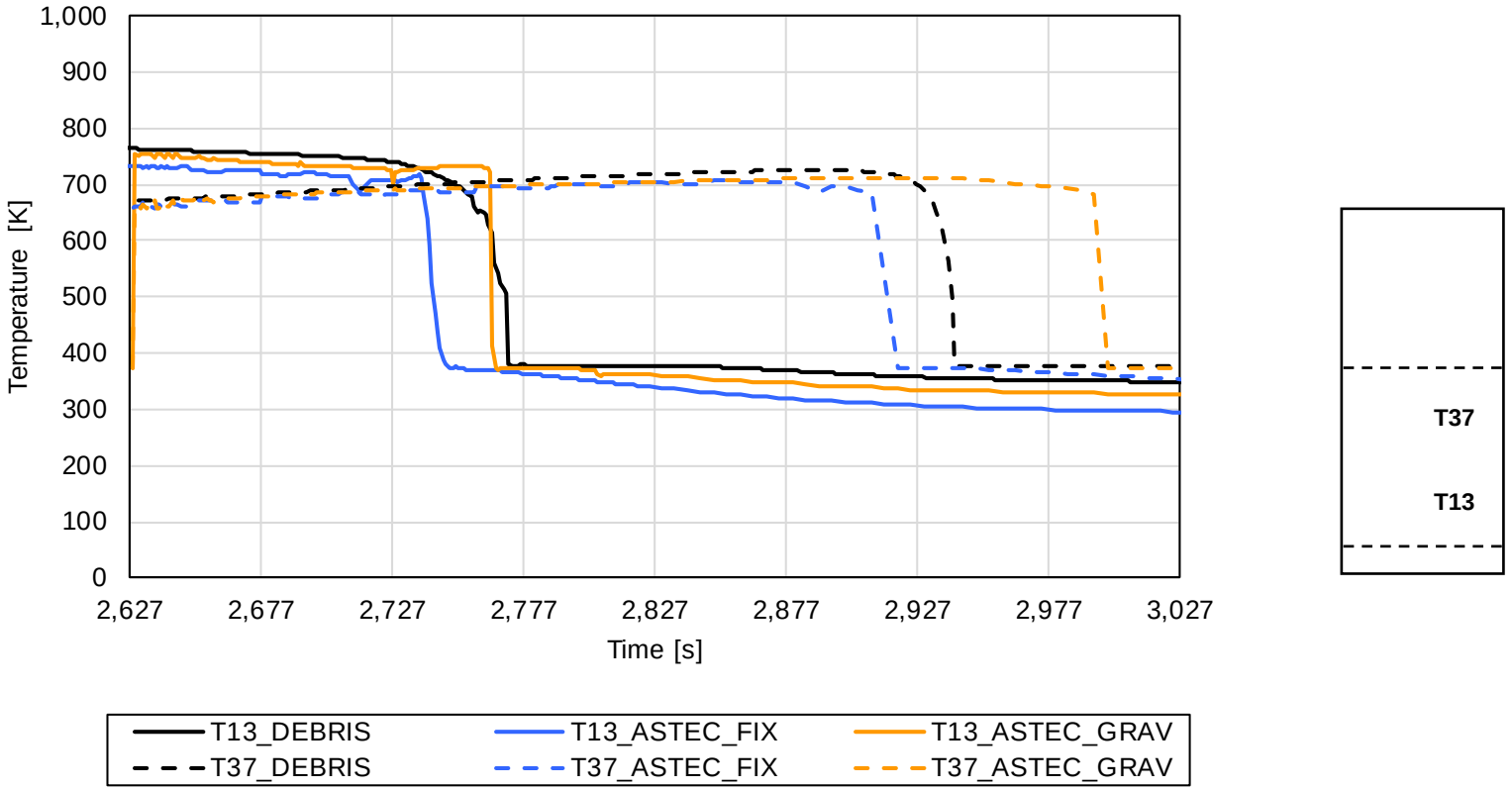
Simulation results

Temperature evolution – Cylindrical Particles, 1 bar – Center TCs



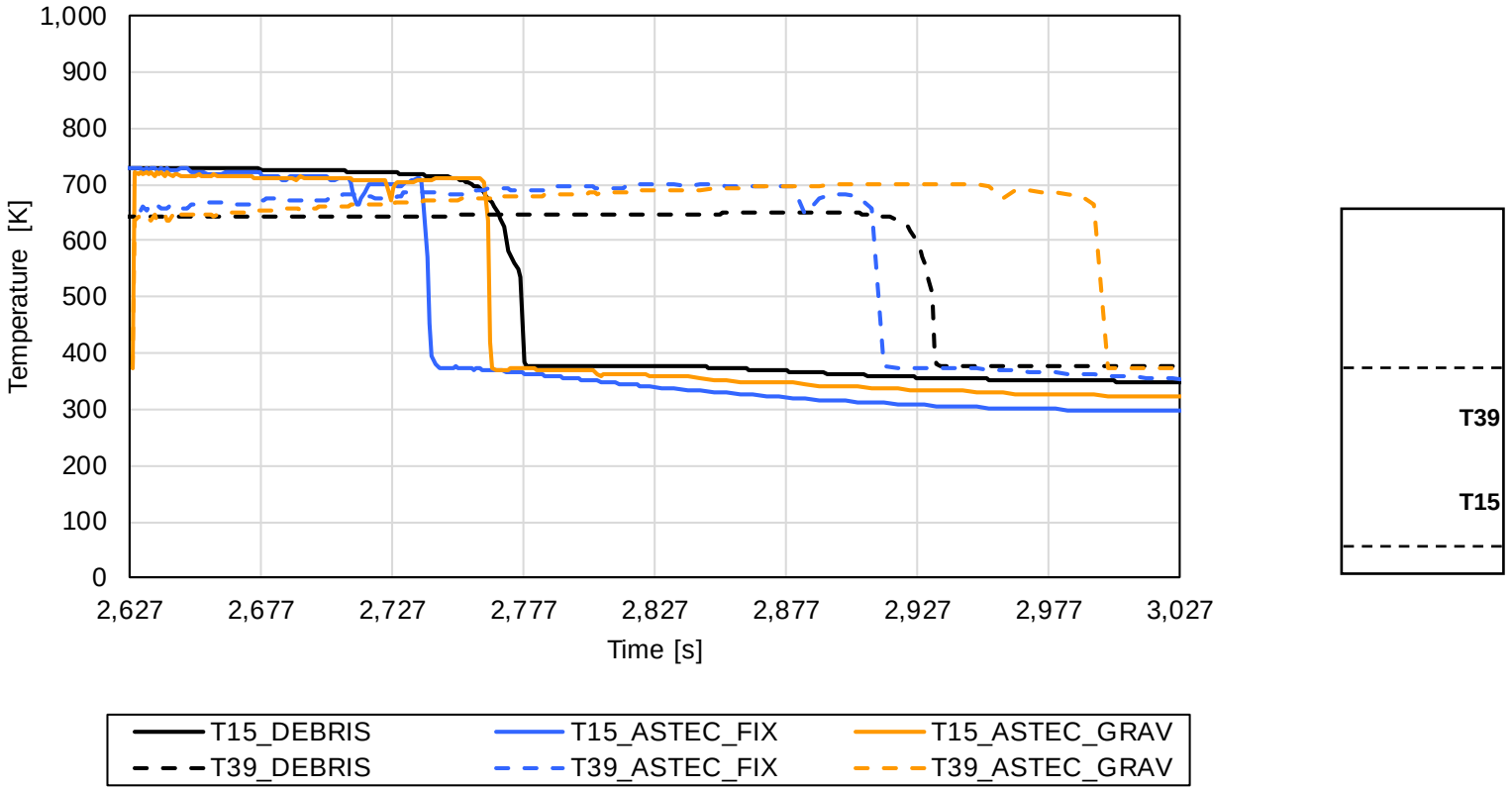
Simulation results

Temperature evolution – Cylindrical Particles, 1 bar – Half Radius TCs



Simulation results

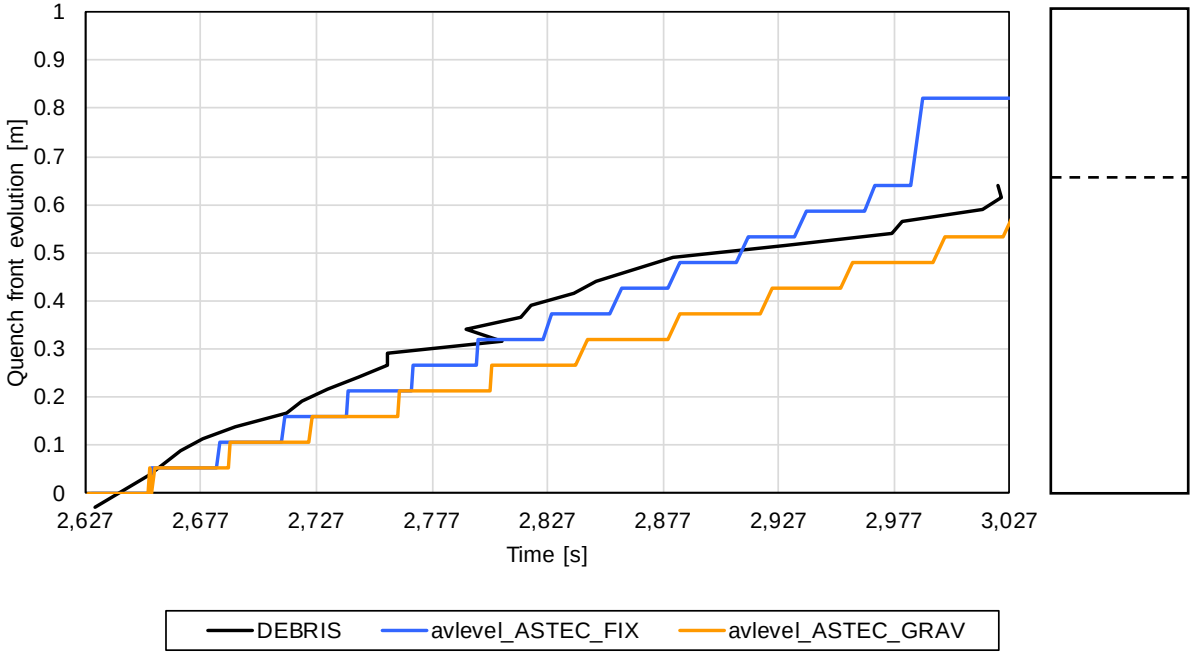
Temperature evolution – Cylindrical Particles, 1 bar – Wall TCs



Simulation results

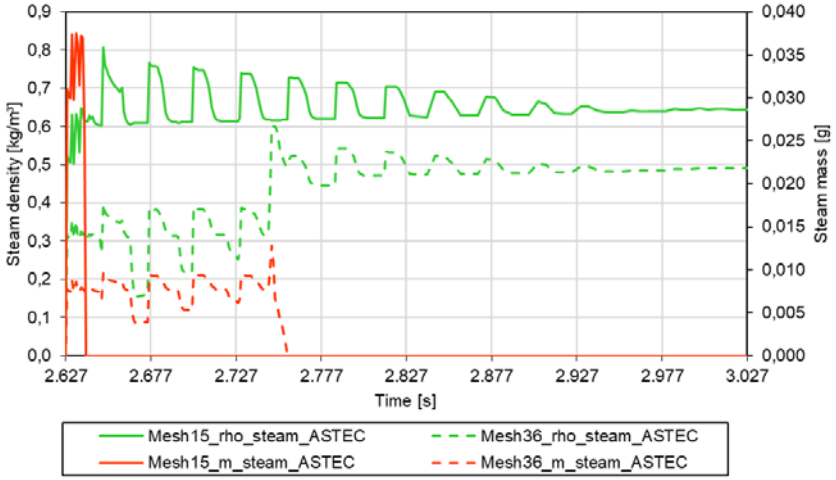
Evolution of Quench-Front – Cylindrical Particles, 1 bar

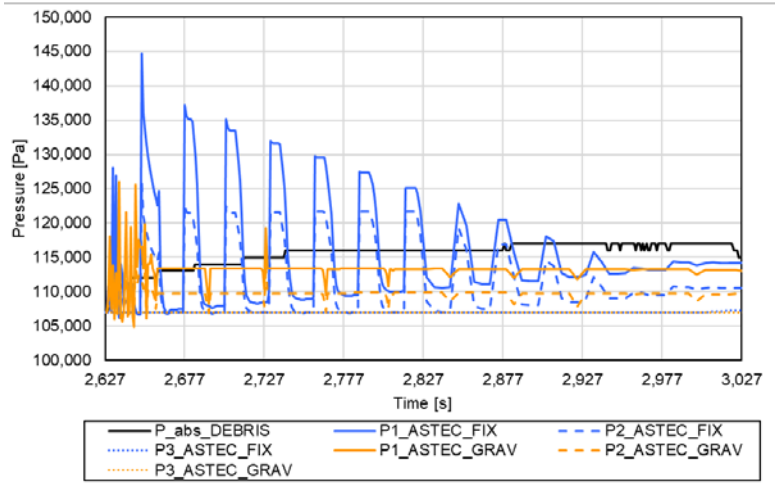
- No experimental results for the water level evolution
- For the experimental Quench front a zone is considered as quenched once T < Tsat

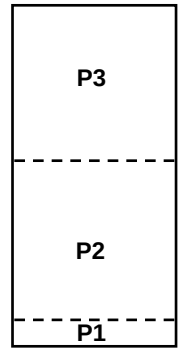


Simulation results

Pressure evolution – Cylindrical Particles, 1 bar







Conclusions and Outlook

- Conclusions
  - Good modelling options to represent the DEBRIS test facility
  - Temperature profiles overall in good accordance with experimental results (depending on radial position simulation results show different behavior)
  - Quench front evolution also in good accordance, bundle is quenched a bit too fast with fixed input flow and too slow with gravity driven input flow
  - Pressure evolution shows larger deviations compared to test results (fixed input)
- Outlook
  - Finish current work on gravity driven setup
  - Comparison of Test Results to COCOMO
  - Simulation of Top-Flooding experiments (DEBRIS and PEARL)

Acknowledgements

The used code system **ASTEC V2.1** is developed by IRSN.

These works were funded by the German Federal Ministry of Economic Affairs and Energy under grant number **1501568** on the basis of a decision by the German Bundestag. Responsibility for the content lies with the authors.



Thank you for your attention

The Authors



M. Sc. Jan M. Peschel

Jan.peschel@pss.rub.de

+49 (0) 234 32 26376



Prof. Dr.-Ing. Marco K. Koch

Marco.koch@pss.rub.de

+49 (0) 234 32 26368

Anticipated Benefits of CrAl_Coated_Zr Cladding under Beyond Design Basis Accidents

T.H. CHUN(*), C.H. SHIN, H.G. KIM
(*)thchun@kaeri.re.kr
Nuclear Fuel Safety Research Division, Korea Atomic Energy Research Institute
989 Beongil 111, Daedeok-daero, Yuseong-gu, Daejeon – KOREA

KAERI has been developing CrAl_Coated_Zr4 Cladding for PWR as a cladding candidate of the Accident Tolerant Fuel (ATF). The coating material of CrAl alloy showed a strong resistance to high temperature oxidation which would help some delay of reaching of fuel melting during the core uncovered environment. Here, the anticipated benefits of the cladding were assessed against the conventional Zr-4 cladding for the typical BDBA scenarios such as TMI-2, SBO, and SBLOCA+α using SCDAP-RELAP5 mod3.2. Those are estimated in terms of a delayed time to reaching core damage and amount of hydrogen generation. In the safety analyses, the suppressed oxidation kinetics of CrAl_Coated_Zr Cladding vs. temperature was assumed simply and conservatively, based on the CrAl alloy oxidation experiments, by factor of 1/100 of C-P model

Along with the TMI-2 accident scenario, it revealed that a rising trend of fuel temperature of the CrAl_coated cladding was turned down after operator actions such as PORV close, one RCP restart and HPSI activations actually taken in the middle of the accident and the core subsequently was reflooded again. However, the Zr4 cladding temperature kept increasing with no help of the advantageous actions. For the SBO accidents, short term and long-term scenarios are examined with OPR-1000. The short term SBO represents a total loss of power which result in no aux-feed water supply to the SGs. The long term SBO assumes that DC battery power is available for 4 hours and lead turbine-driven pumps work for a supply of aux-feed water. According to the results, following the core uncovered, the behaviors of fuel temperature rising are alike. So the delay times to fuel melting in short-term and long-term SBOs are also almost similar, 13 and 18 minutes, respectively. The accumulated H_2 generations of CrAl_coated cladding for both short and long term SBOs are approximately 10 % of that of Zr4 cladding at 10kg. In the SBLOCA+α, unlike a standard SBLOCA scenario with single failure of HPSI, all HPSIs are assumed unavailable in a 1.5 inch cold leg break accident. The analysis results showed the escalating temperature of uncovered CrAl_coated cladding was dropped a couple of times when the water of SITs were supplied as the core pressure decreased. But it was not the case of Zr4 cladding even with the SIT activation. This causes a delay of the core melting about 1 hour. The amount of accumulated H_2 generation is also about 10% of that of Zr4.

In summary, the anticipated benefits of the CrAl_coated cladding relative to the Zr4 cladding are following; core damage in TMI-2 be feasibly prevented, delay of core damage in SBO and SBLOCA+α marginal and rather beneficial, and accumulated H_2 generations in SBO and SBLOCA+α would be less than one order of magnitude.


nologie
KIT

Anticipated Safety Benefit of CrAl Coated Zr Cladding Under Beyond Design Basis Accidents

2019. 10. 23

Tae-Hyun Chun, Chang-Hwan Shin, Hyun-Gil Kim

KAERI 한국원자력연구원 Korea Atomic Energy Research Institute

Contents

- ATF Cladding in KAERI
- Objective
- BDBA Scenarios and Analysis Results
  - TMI-2
  - SBO
  - SBLOCA + α
- Summary

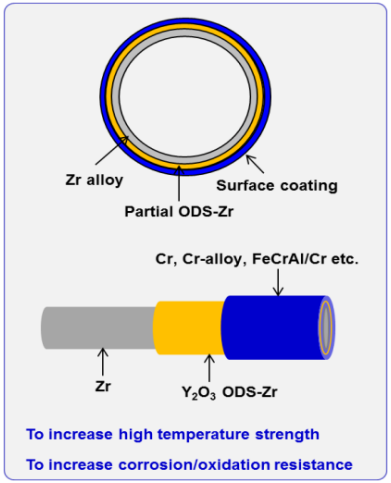
ATF Cladding in KAERI

❖ Alloy & structure design

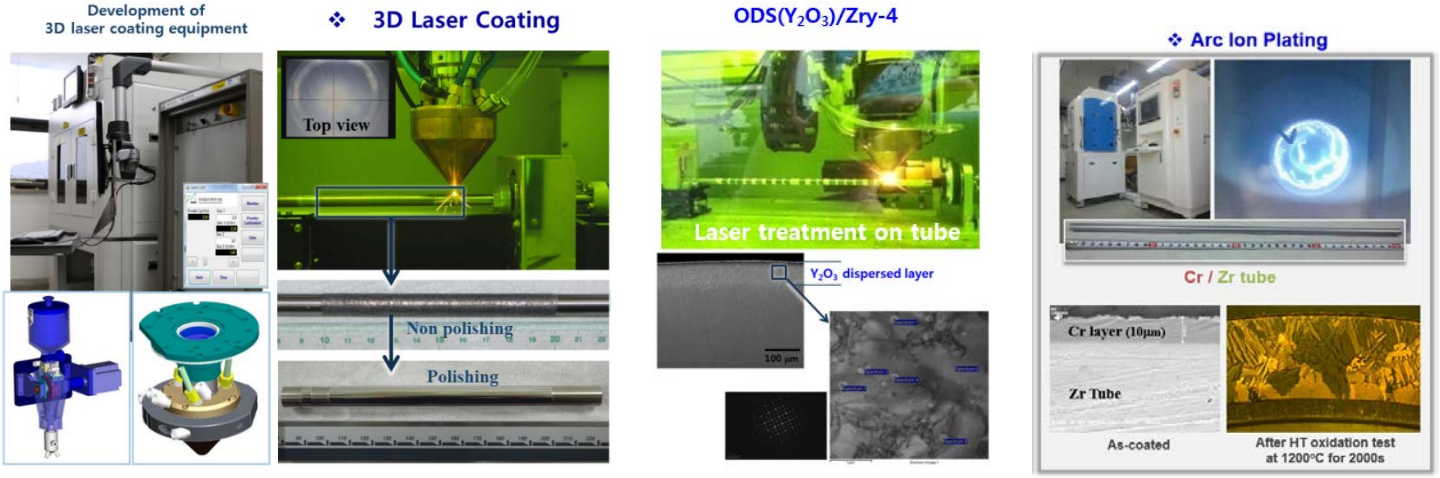
- CrAl alloy : Superior oxidation resistance & no pitting corrosion
- Partial ODS (Y_2O_3, Gd_2O_3, Er_2O_3): Increase deformation resistance, flexible reactivity control

❖ Fabrication processes

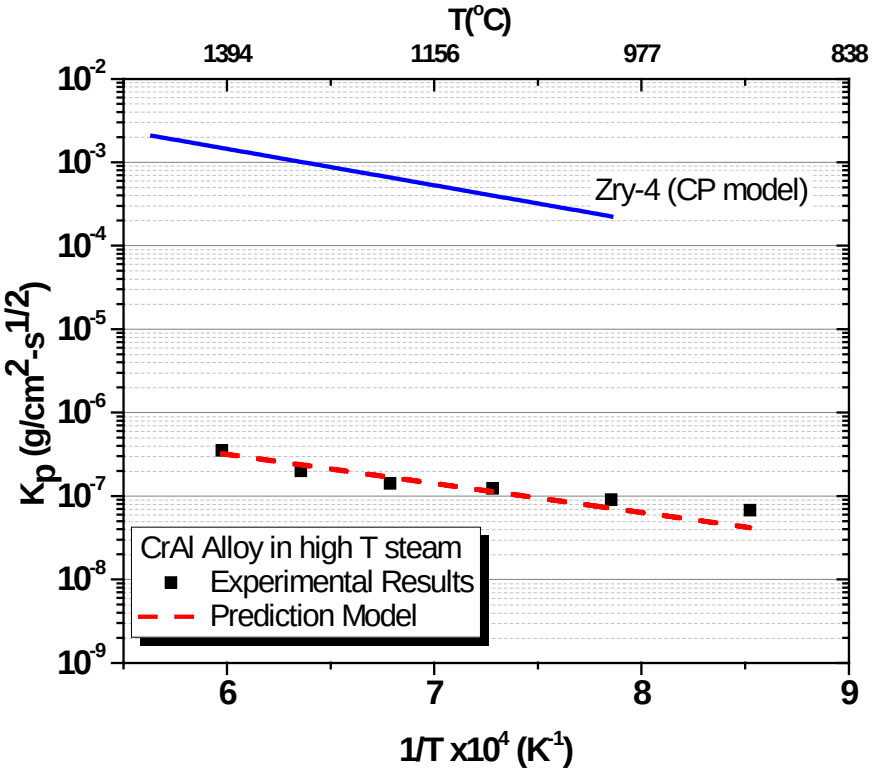
- 3D laser coating : coating & ODS treating
- Arc ion plating : thin layer and alloy coating



[ODS: Oxide Dispersion Strengthened]



CrAl_Coated Zr-4



The parabolic rate constant(K_p)

$$K_p = A * \exp(-\frac{Q}{RT})$$

A : Constant(mg/dm^4-s)
Q : Activation energy for the oxidation
R: Universal gas constant(8.314J/mole-K)
T : Oxidation Temperature (K)

For ATF

$$K_p = 4.149 \times 10^{-10} exp\left(-\frac{16040}{T(K)}\right) cm^2/s$$

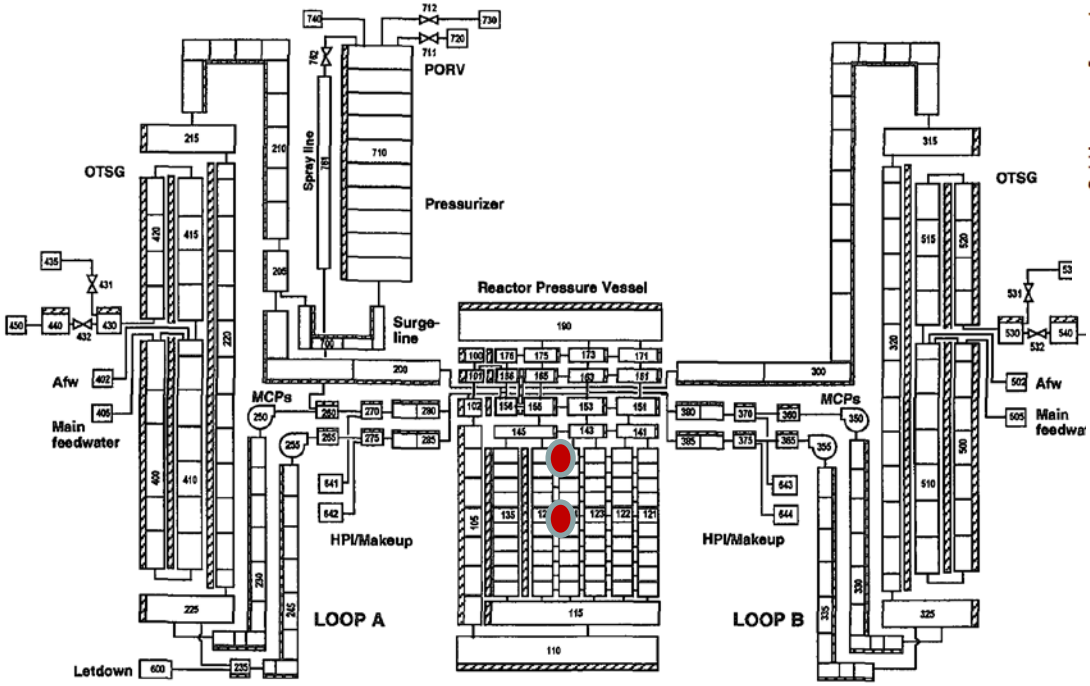
: Assume oxide density = 5 g/cm^2

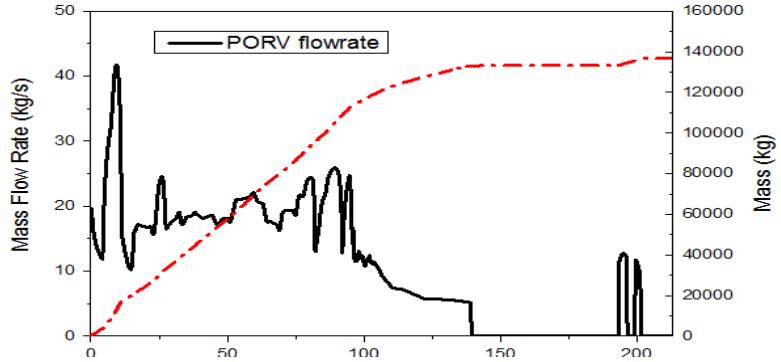
Objectives

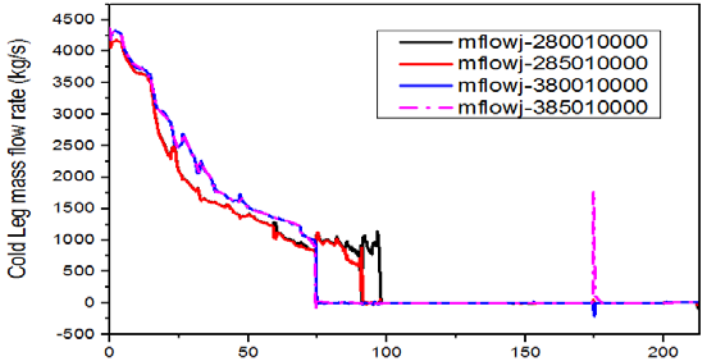
- To assess the potential safety benefit of ***CrAl_coated Zr cladding*** in terms of core damage and H_2 generation.
  - Beyond Design Basis Accident Scenarios
    - TMI-2
    - SBO : high P transient, No water supply
    - SBLOCA+ **α** : P decrease transient, SIT injection
  - Analysis code : **SCDAP/RELAP** mod.3.2
  - Oxidation kinetic model of CrAl_coated: **1/100** of C-P model

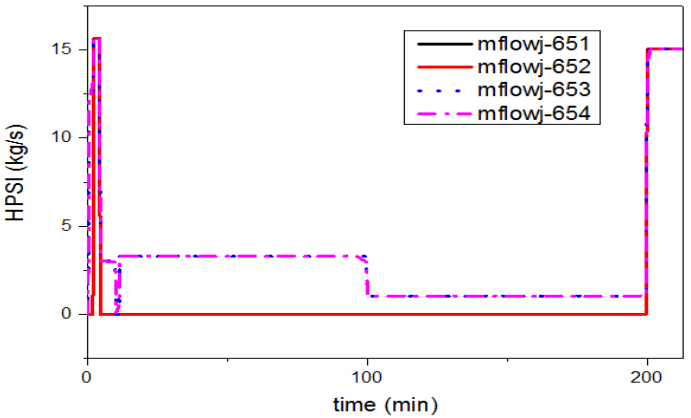
TMI-2

- **Scenario & Input :** G. Bandini (1999)
  - 0-139 min: PORV open
  - 139 min: **PORV close**
  - 100-174 min: Core heat-up & melting by core uncovery/ fuel rod oxidation
  - 174 min: **Restart of one RCP**
  - 200 min: **Activation of HPSI**

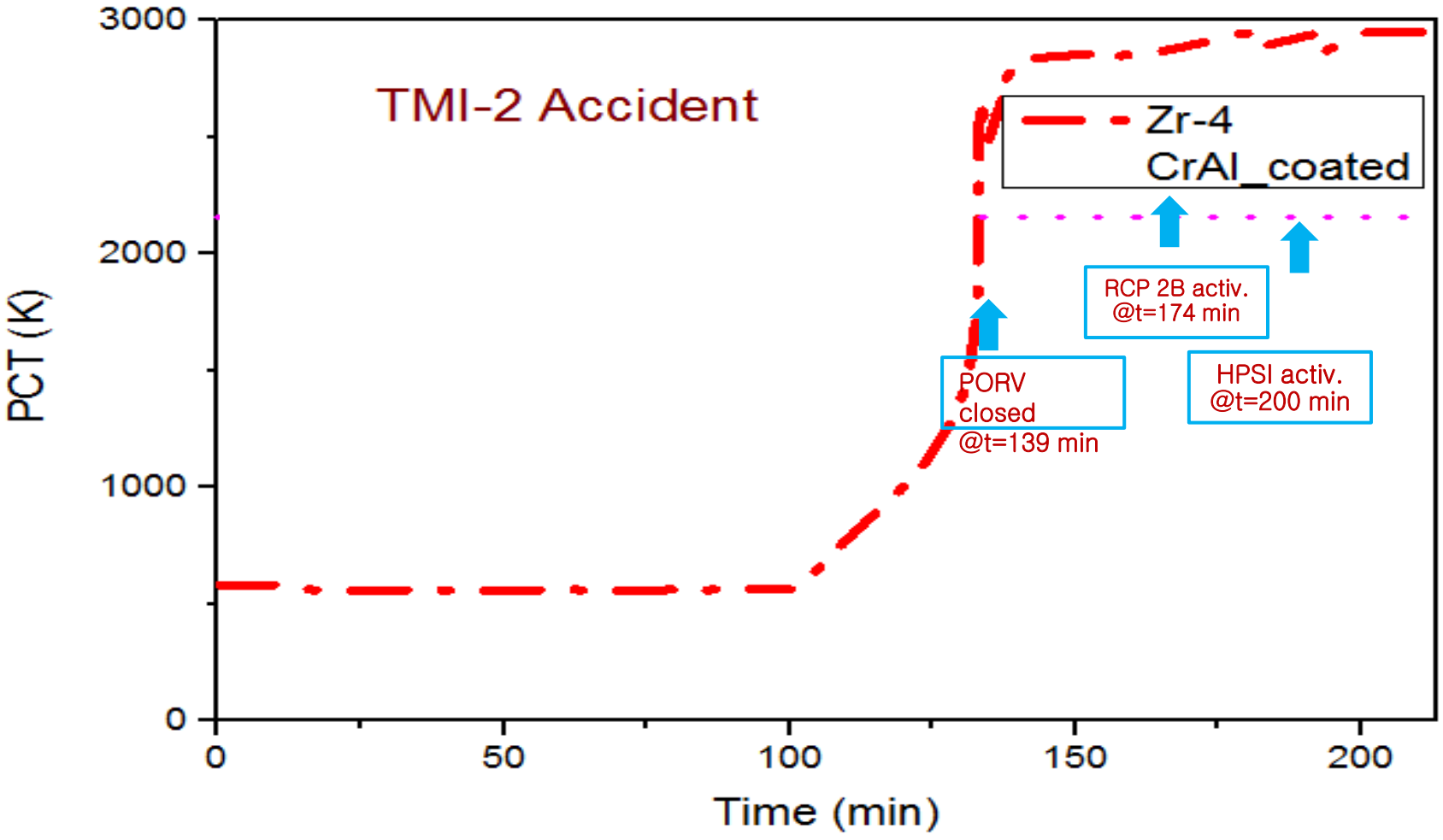






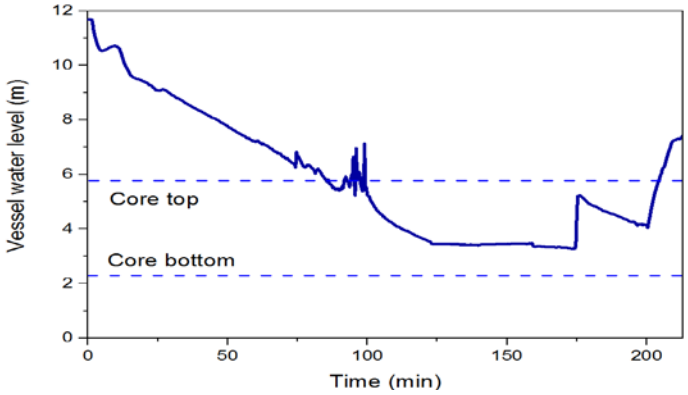


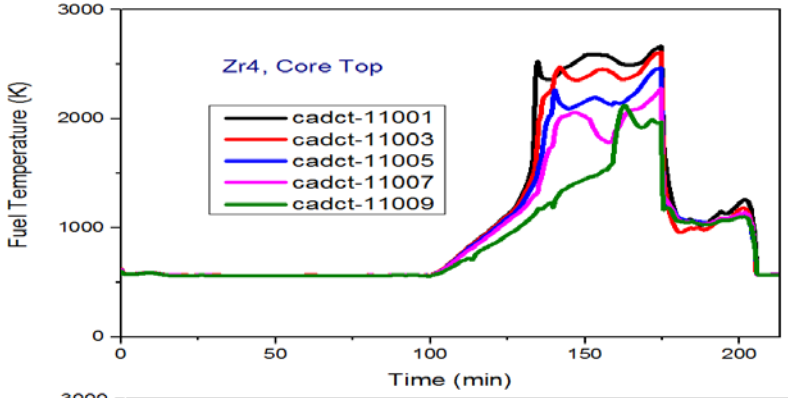
TMI-2 (continued)

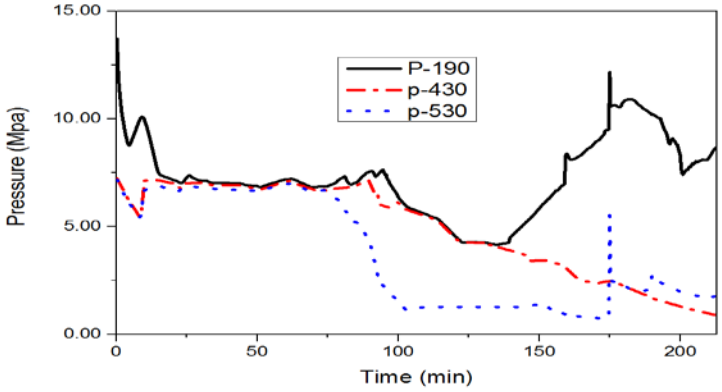


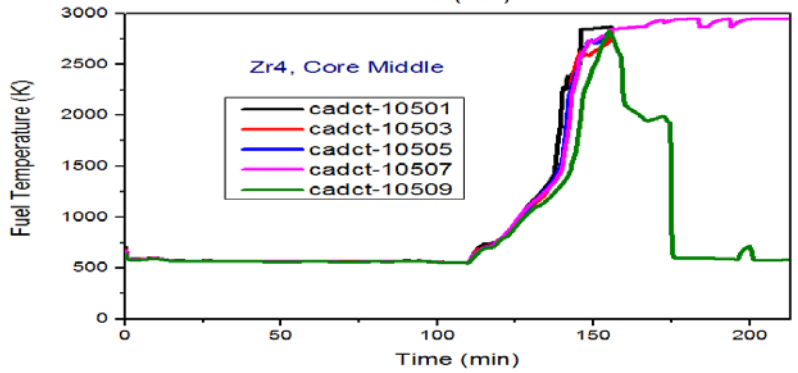
- Reaching core melting condition with no help of PORV close, RCP and HPSI operations

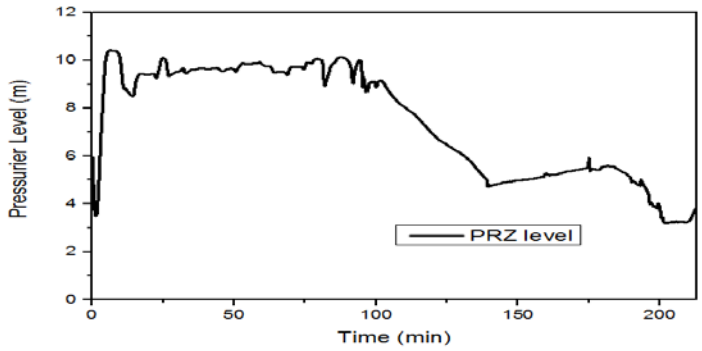
TMI-2 (continued)

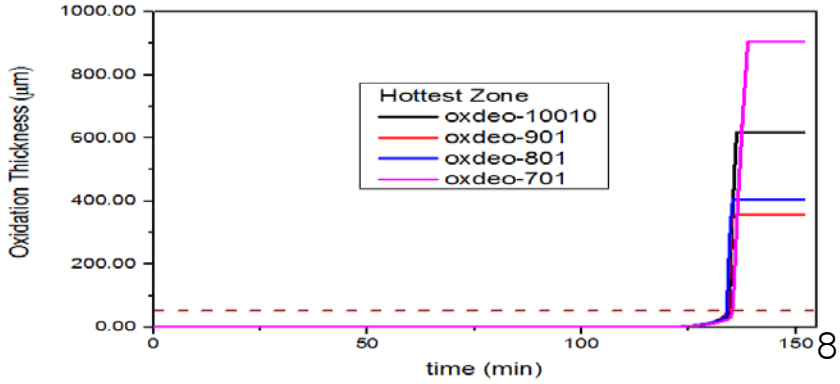




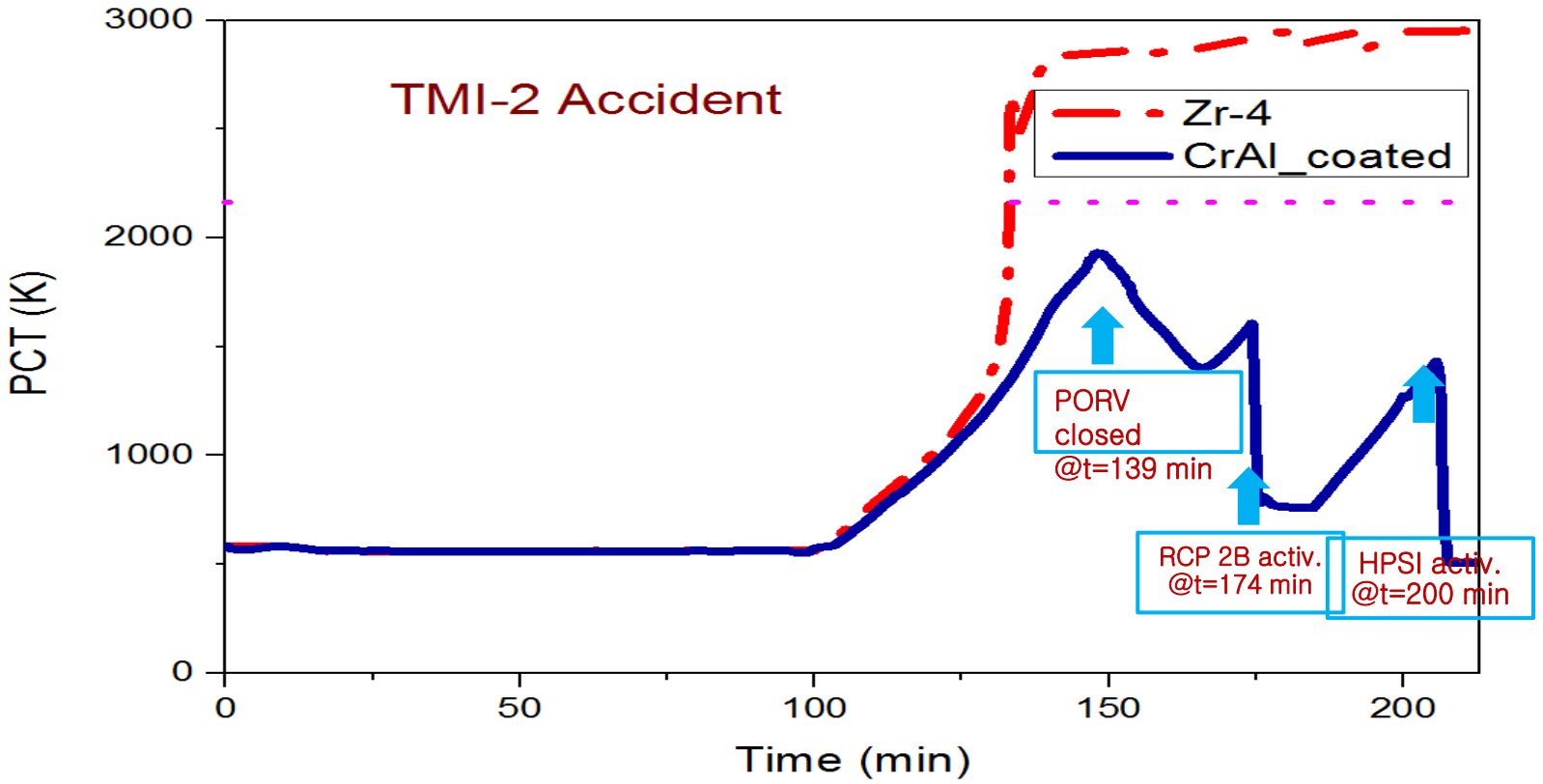






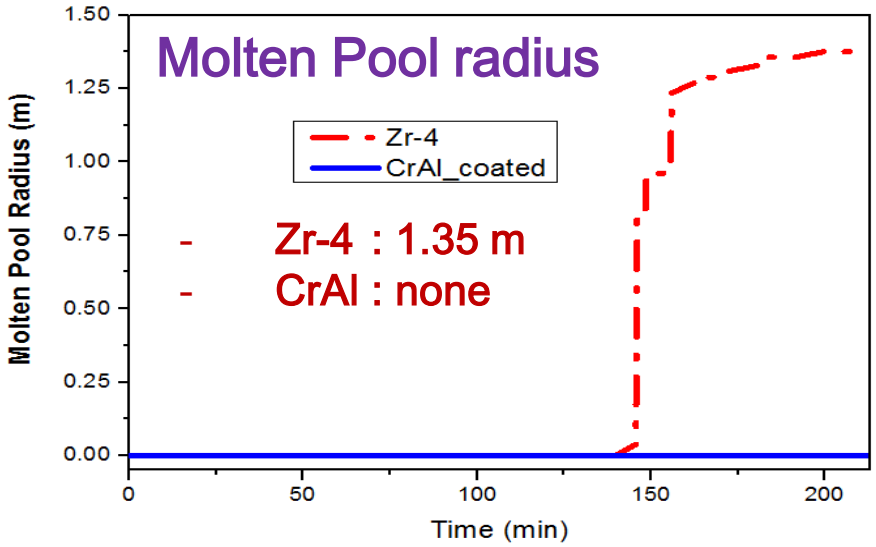


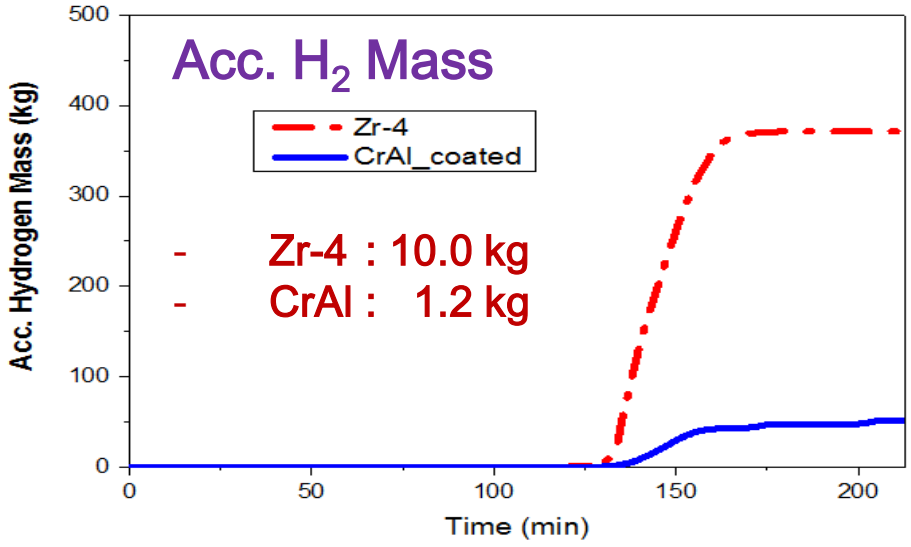
TMI-2 (continued)

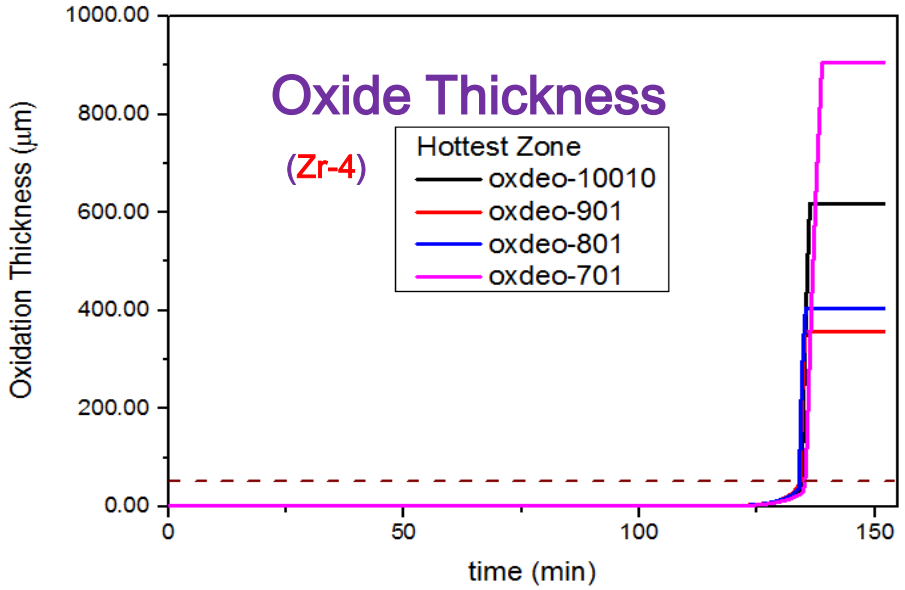


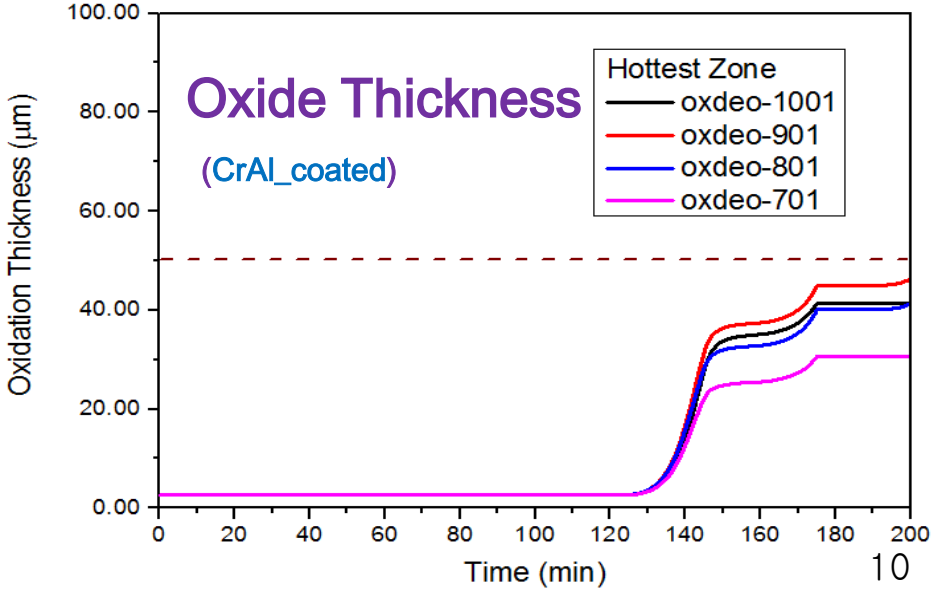
- No rapid temperature rise before PORV close and temperature drop through the RCP and HP activations
- Possibly preventing core melting in TMI-2 scenario

TMI-2 (continued)









SBO

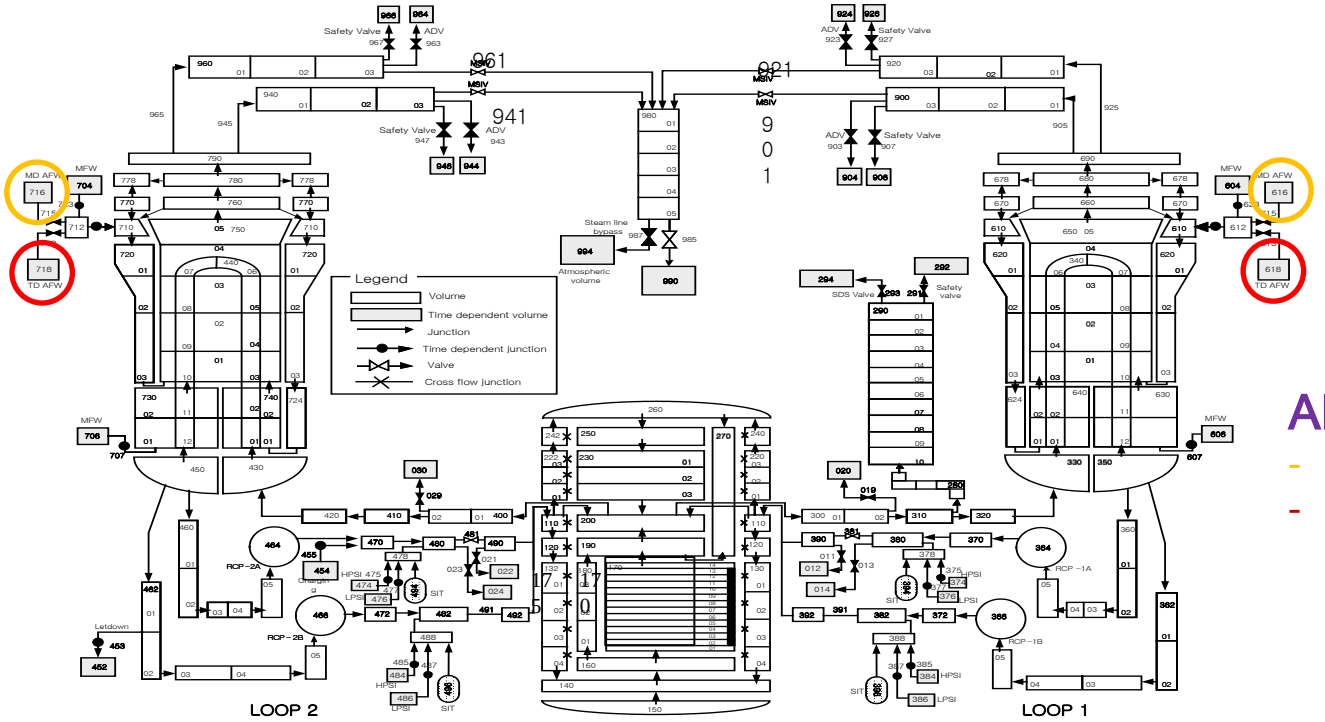
- Reference reactor: OPR-1000
- Scenario & Input :

– Short term SBO : On & Off-site AC power & DC power fail (No AFW)

– Long term SBO : AC power fail, DC power available (Turbine-Driven AFW)

① Battery life: 4 hr

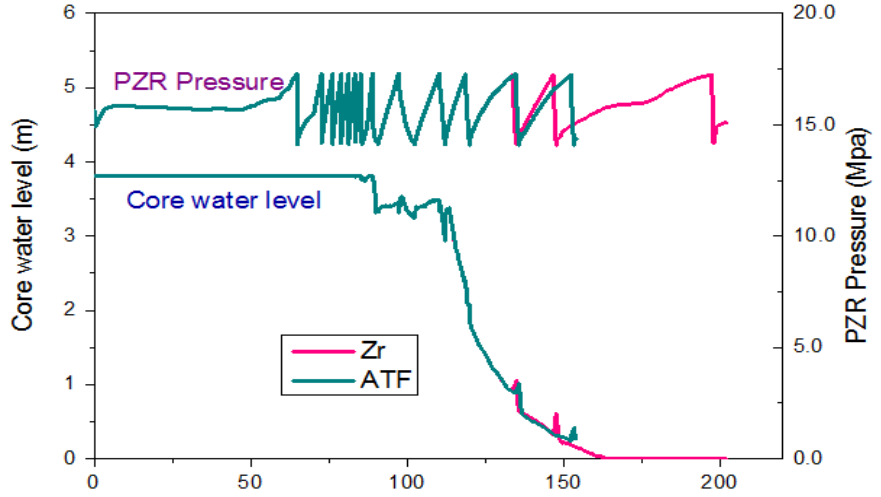
② TD_Pump performance: 100%, 75%

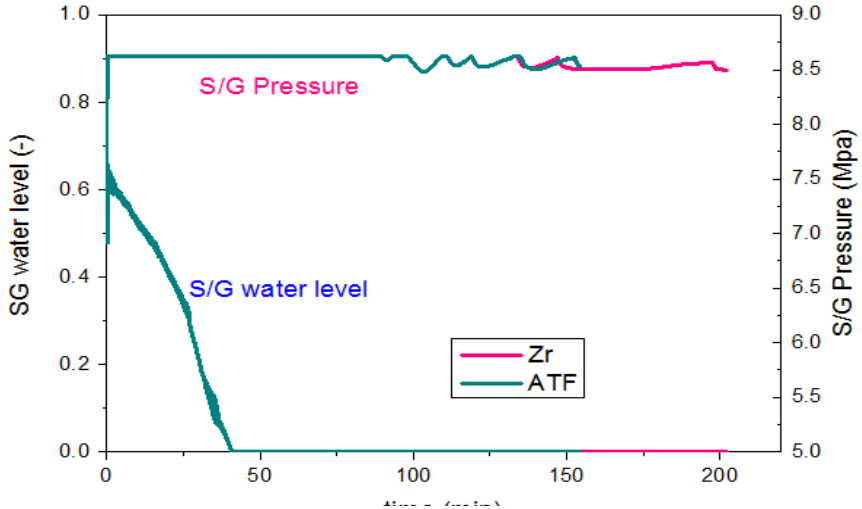


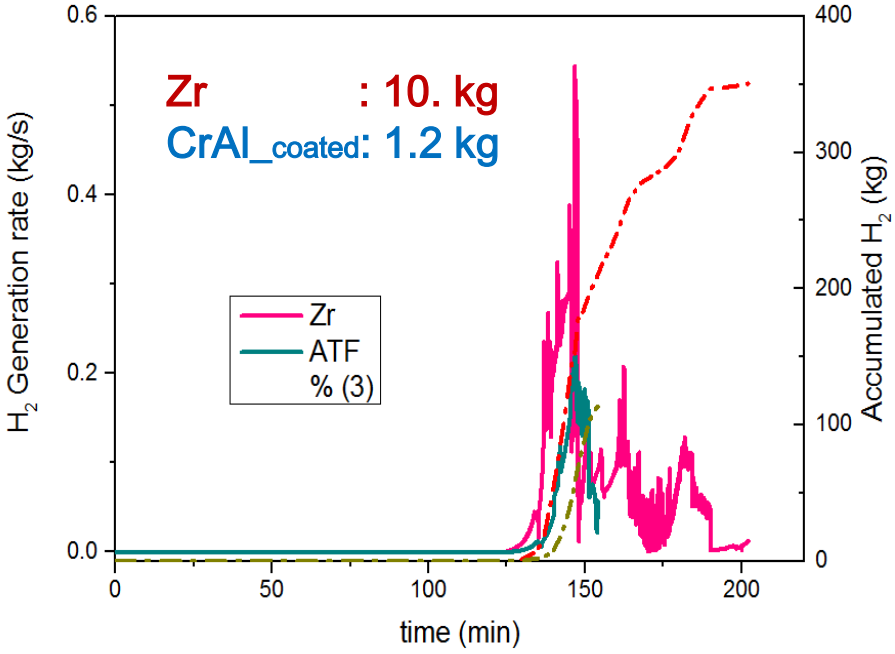
AFW Supply

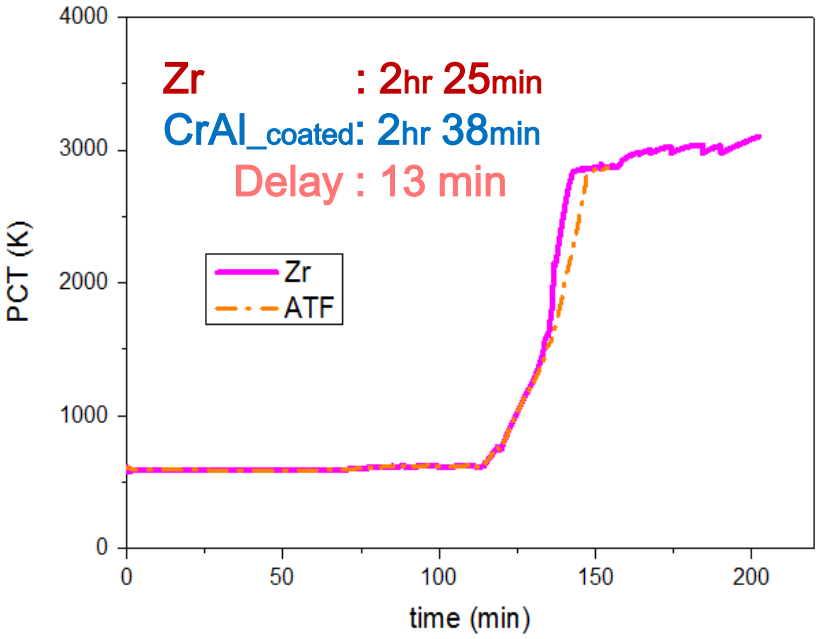
- Motor-driven pump (2)
- Turbine driven pump (2)

ST_SBO

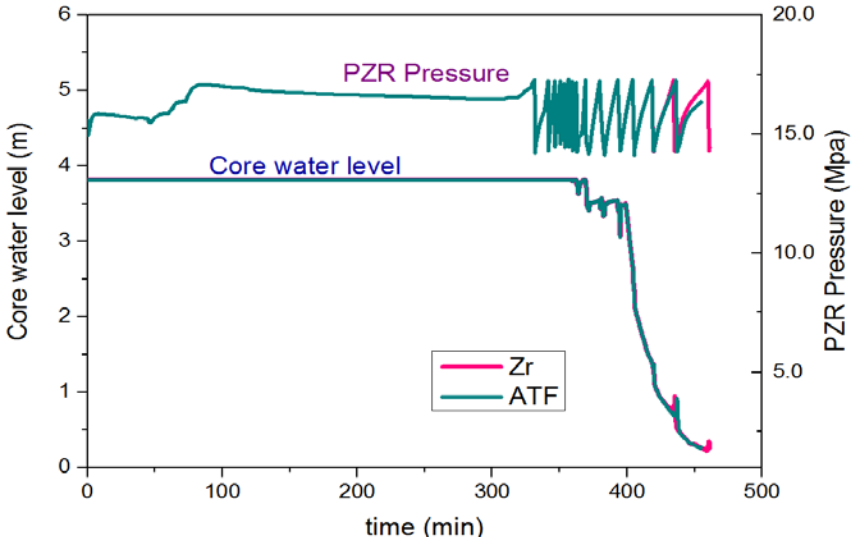

PZR Pressure
Core water level
Zr
ATF
Core water level (m)
PZR Pressure (Mpa)

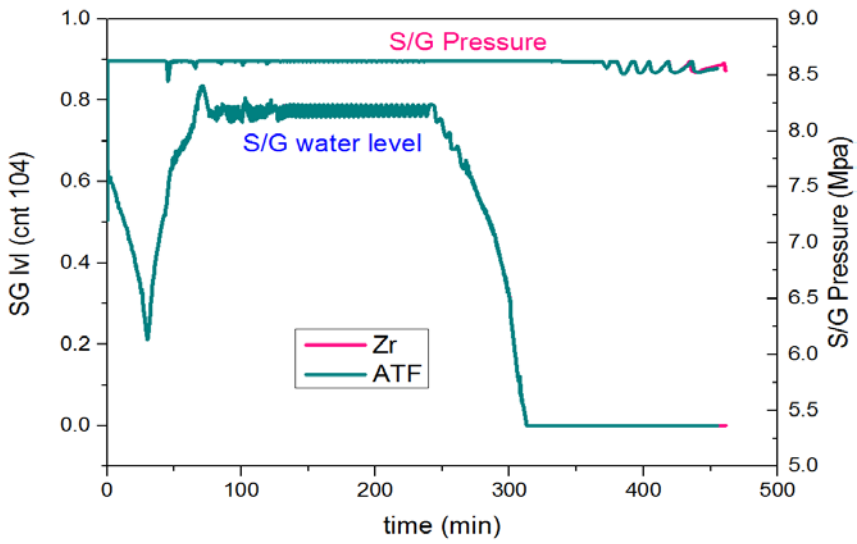

S/G Pressure
S/G water level
Zr
ATF
SG water level (-)
S/G Pressure (Mpa)

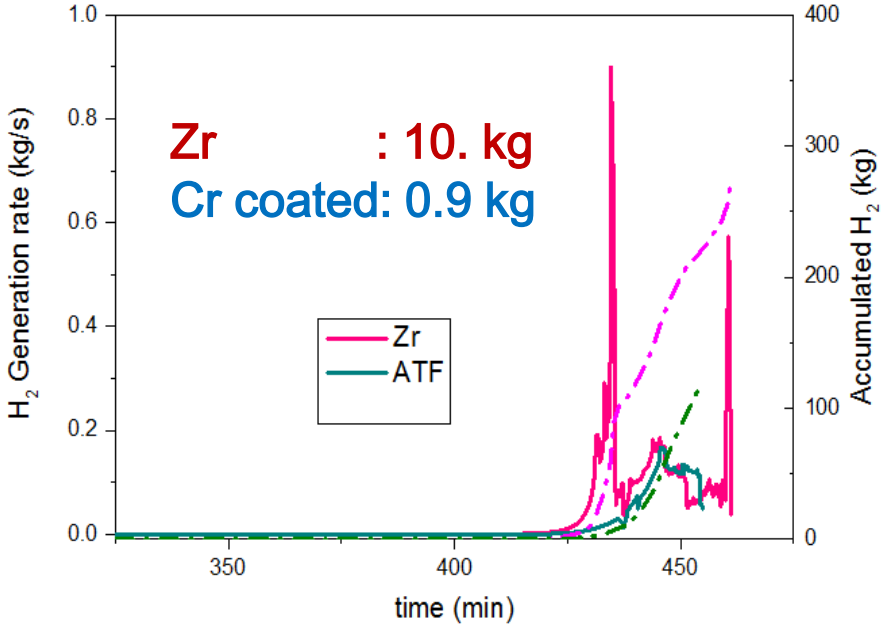

Zr : 10. kg
CrAl_coated: 1.2 kg
Zr
ATF
% (3)
H2 Generation rate (kg/s)
Accumulated H2 (kg)
time (min)

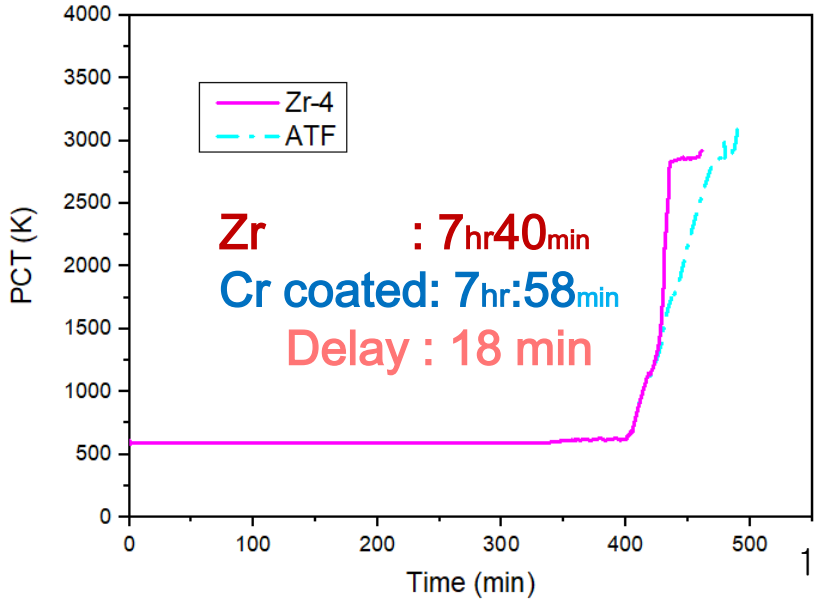

Zr : 2hr 25min
CrAl_coated: 2hr 38min
Delay : 13 min
Zr
ATF
PCT (K)
time (min)

LT_SBO


PZR Pressure
Core water level
Zr
ATF
Core water level (m)
PZR Pressure (Mpa)
time (min)

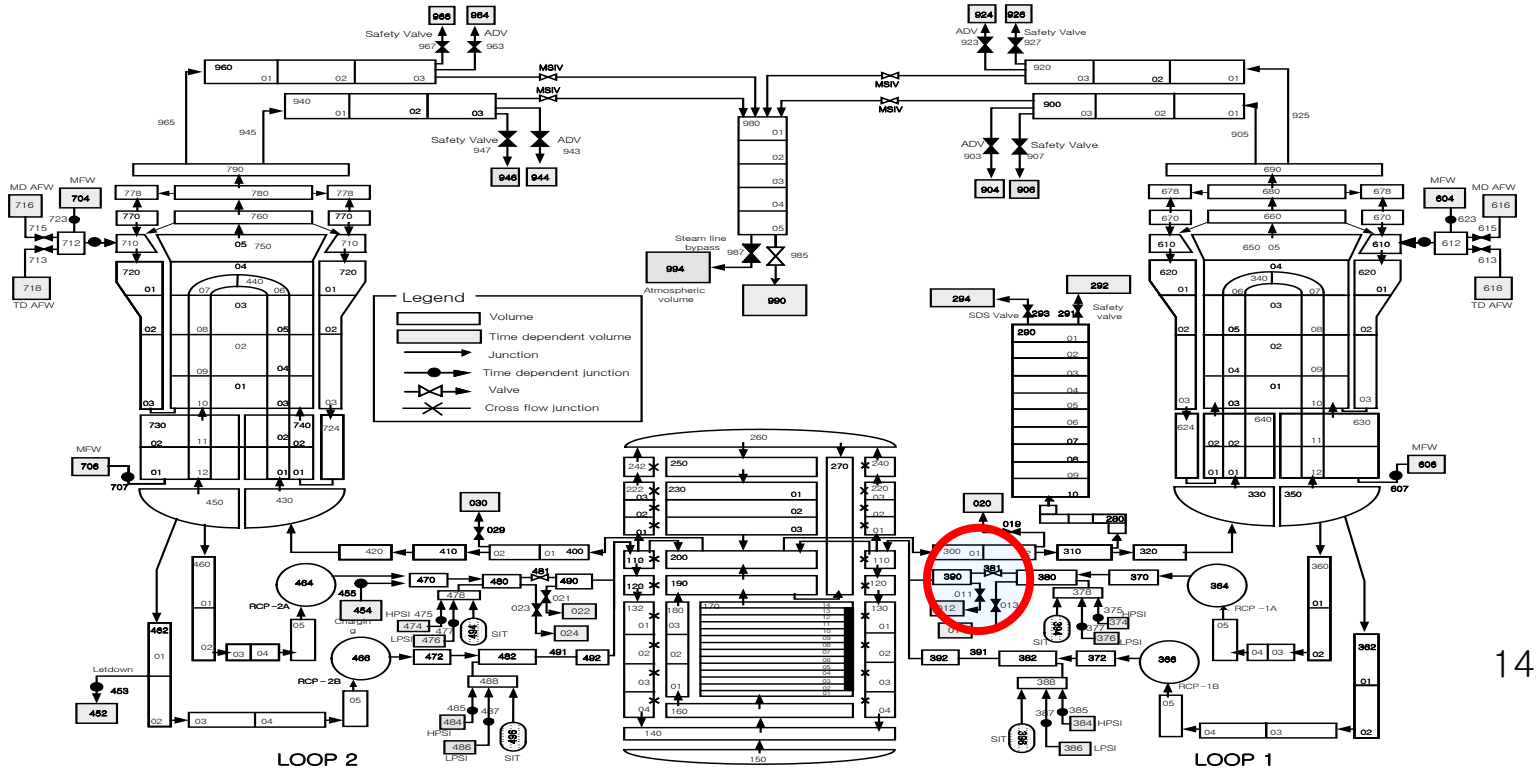

S/G Pressure
S/G water level
Zr
ATF
SG lvl (cnt 104)
S/G Pressure (Mpa)
time (min)


Zr : 10. kg
Cr coated: 0.9 kg
Zr
ATF
H2 Generation rate (kg/s)
Accumulated H2 (kg)
time (min)


Zr-4
ATF
Zr : 7hr40min
Cr coated: 7hr:58min
Delay : 18 min
PCT (K)
Time (min)

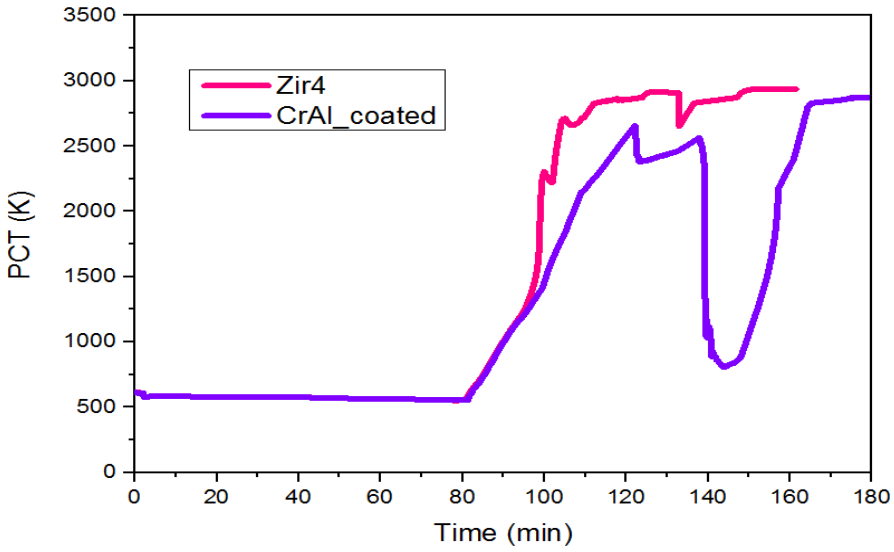
SBLOCA+α

- Reference reactor: OPR-1000
- Accident Scenario
  - 1.5 inch cold leg Break
  - RCP, Reactor Shut-down
  - All HPSIs failure
  - 2 SIT activation

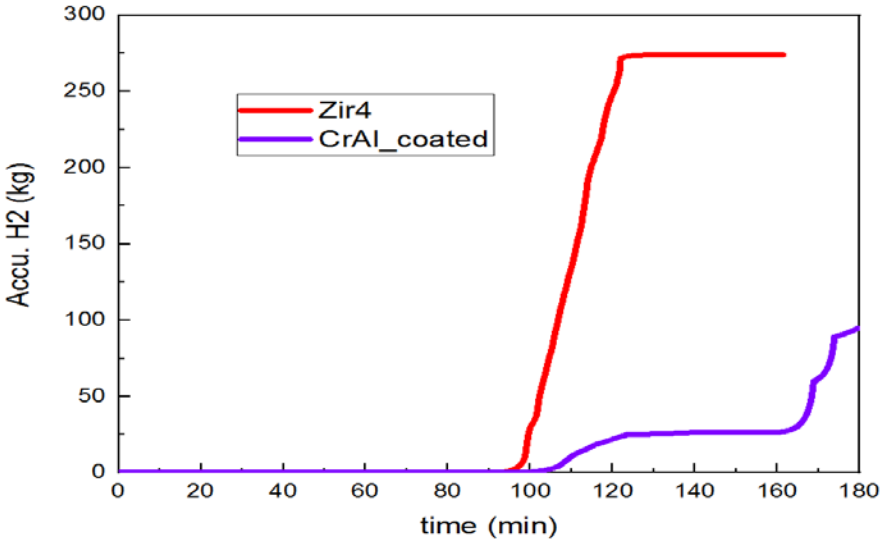


SBLOCA+α

PCT



Acc. H_2 Mass



- PCT of **ATF** decreases significantly with SIT, but increase again as water supply depletion
- Delayed reaching to core damage about 1hr

- H2 generation of **ATF is** about 10% of that of Zir4 at delayed time

Summary

Anticipated benefit of ATF candidate CrAl_coated Zr cladding for PWR in following scenarios;

- **Delay of Core Damage**
  - **TMI-2 : feasibly prevented**
  - **SBO : marginal benefit (10 or more min)**
  - **SBLOCA+ α: rather beneficial (about 1 hr)**
- **Delay of H2 explosion**
  - **One order of magnitude less in H2 generation**
  - **greatly helpful to reduce the probability of H2 explosion.**

Thank you
for your attention !

ACKNOWLEDGEMENTS

This work was supported by the National Research Foundation of KOREA (NRF) grant funded by the government (MSIT, Ministry of Science and ICT) (NRF-2017M2A8A5015064)

Multielemental coatings on Zirconium alloy – INCT oxidation experiments

Sartowska Bożena [1] *, Starosta Wojciech [1], Lech Waliś [1], Jerzy Smolik [2]

[1] Institute of Nuclear Chemistry and Technology, Warsaw, Poland
[2] Institute for Sustainable Technologies, Radom, Poland

ABSTRACT

Zirconium alloys are commonly used as cladding material for fuel elements in nuclear reactors. Zircalloys have very good water corrosion and radiation resistance at normal working conditions. But in the case of LOCA conditions, the fast oxidation of zirconium at steam atmosphere or/and air-steam mixture results in intense hydrogen generation.

Advanced materials that are intended to be more tolerant of severe accident conditions with the safe operation under normal conditions are looking for. The concept of Accident Tolerant Fuels (ATF) and Accident Tolerant Materials (ATM) has been developed for this purpose. There are two main ideas for the increasing of claddings' corrosion resistance:

(i) new materials for claddings production (SiC, FeCrAl)
(ii) surface layer of applied now claddings modification (protective layer of: MAX phases, FeCrAl, Cr).

Works carried out in INCT were aimed to develop multielemental coatings on zirconium alloys claddings and evaluation of their properties including behavior during oxidation processes. The examined materials were Zry-2 coated with $ZrSi_2$-Cr using PVD method. Oxidation tests were performed in 700^{o}C/1-5h/air. The results of experiments concerning coatings characterization and oxidation tests results are presented in this work.

Acknowledgements
This work has been partially supported under IAEA Research Contract No. 19026/R0 and by Polish Ministry of Science and Higher Education under decisions 3689/IAEA/2017/0



MULTIELEMENTAL COATINGS ON ZIRCONIUM ALLOY – INCT OXIDATION EXPERIMENTS

Sartowska Bożena *, Starosta Wojciech, Lech Waliś
Institute of Nuclear Chemistry and Technology, Warsaw, Poland

Jerzy Smolik,
Institute for Sustainable Technologies, Radom, Poland

WHAT WE KNOW



- Severe nuclear accidents have shown that under extreme conditions, nuclear fuel will fail and the high temperature reaction between zirconium alloys and water will lead to generation of hydrogen with the potential for explosion
  - The basic concept of uranium oxide fuel pellets clad with zirconium alloy tubing has reminded the choice for the majority of commercial nuclear power plants
  - There have been many improvements to the original design and materials used
- Development of the solution to minimize the risk related to the design and unforseable situations is needed
- The concept of Accident Tolerant Fuels **(ATF)** and Accident Tolerant Materials **(ATM)** - it means materials with increased accident tolerance - has been developed recently for this purpose

MULTIELEMENTAL COATINGS

- **Silicon based coatings** may provide a more protective barrier than the native ZrO2 films formed on alloy cladding during routine nuclear plant operations and may provide an protective barrier during high-temperature accident scenarios

14 Si 28.09

- Phase diagram for Zr-Si: intermetallic compounds - different Zr/Si ratios and stability regions, as for example:

40 Zr 91.22

ZrSi2 is stable up to 1620°C
ZrSi is stable up to 2210°C

- Zr and Si form their respective oxides at high temperatures and surface layers of ZrO_2 or SiO_2 or even **$ZrSiO_4$** may be formed depending on the stoichiometry

- **Chromium** metal left standing in air is passivated by oxidation, forming a thin, protective, surface layer
- The layer is a spinel structure only a few molecules thick. It is very dense, and prevents the diffusion of oxygen into the underlying metal

24 Cr 52.00

- Chromium, unlike such metals as iron and nickel, does not suffer from hydrogen embrittlement
- Chromium does suffer from nitrogen embrittlement, reacting with nitrogen from air and forming brittle nitrides at the high temperatures

THE AIM

- to develop the multielemental coatings on zirconium alloys claddings and evaluation of their properties at accident scenario as well as in the reactor normal working conditions
- to improve protective character of formed layer

INVESTIGATIONS



Material:

Zircalloy-2 (Zry-2)
Westinghouse

ELEMENT	CONCENTRATION
	wt.%
Sn	1.3 - 1.6
Fe	0.07 - 0.20
Cr	0.05 - 0.16
Ni	0.03 -0.08
Average (Fe+Cr+Ni)	0.23 - 0.32

Characterisation

1. Surface and cross-section observations: OM, SEMs including HR SEMs

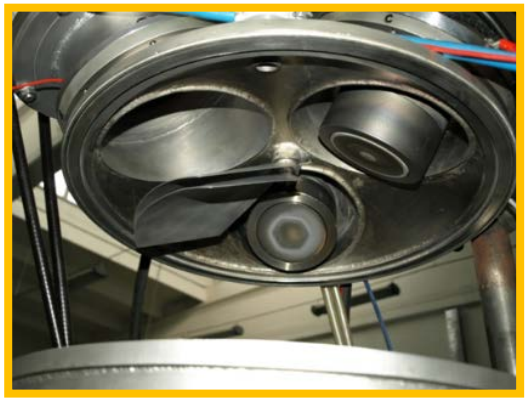
2. Elemental analysis: EDS with Quantax 400 (Bruker, Germany) in LSP mode

3. Phase analysis: X-ray diffractometer D8 Advanced (Bruker, Germany) with geometries Θ-2Θ, ω=5o, ω=10o

4. Oxidation tests :
   - 4.1. 700oC /1 - 5h/air
   - 4.2. 850oC and 1100oC/4h/argon
   - 4.3. autoclave: 360°C/196/bar/water/21, 42, 63 days

PHYSICAL VAPOUR DEPOSITION - PVD





Balzers system facility: general view, chamber view, position of flat circular magnetrons,

The multisource plasma magnetron sputtering system with 3 magnetron plasma sources allows to:

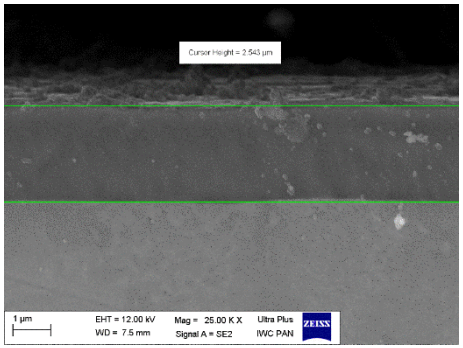
- deposit materials from separate targets
- obtain multielemental coatings

Used separate targets: (i) composite ZrSi2, (ii) chromium

Both sides covered

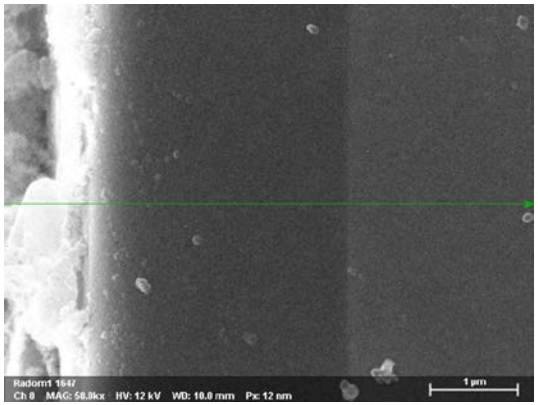
OBTAINED COATINGS

Thickness

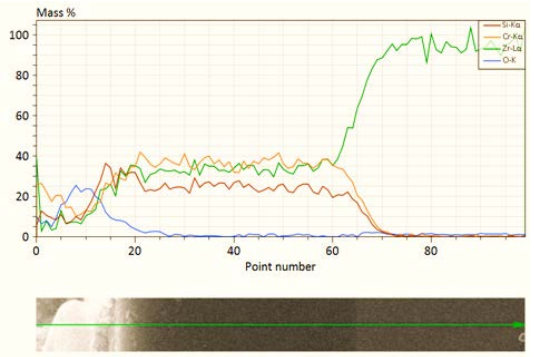


2.543 um

Elemental composition



	Si	Cr	Zr
at.%	43,30	34,80	21,90
wt.%	24,20	36,00	39,80

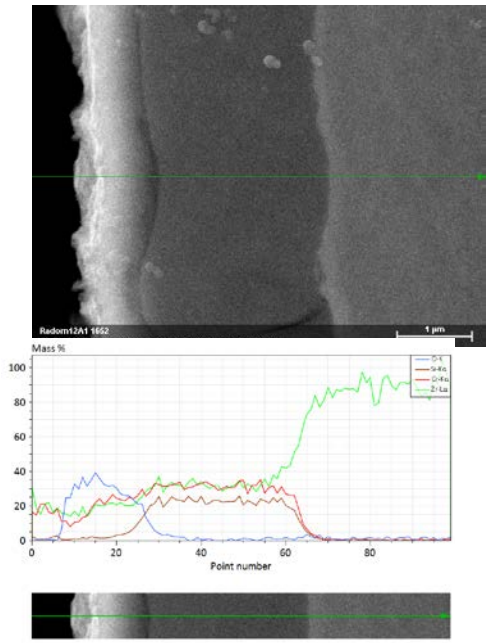


Zr
Cr
Si

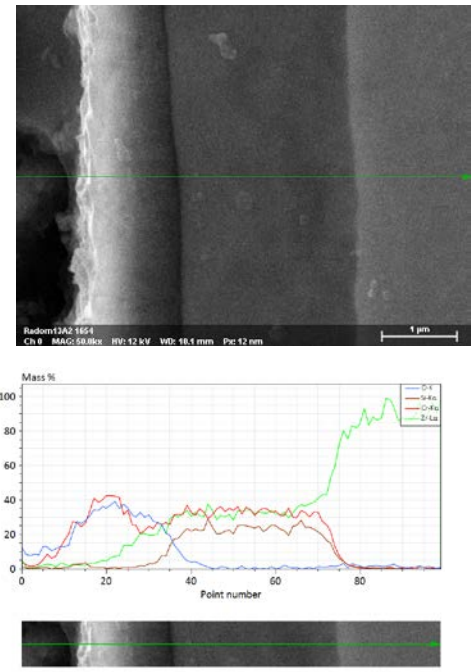
Zr40Si24Cr36

OXIDATION Zry-2 COATED - AUTOCLAVE

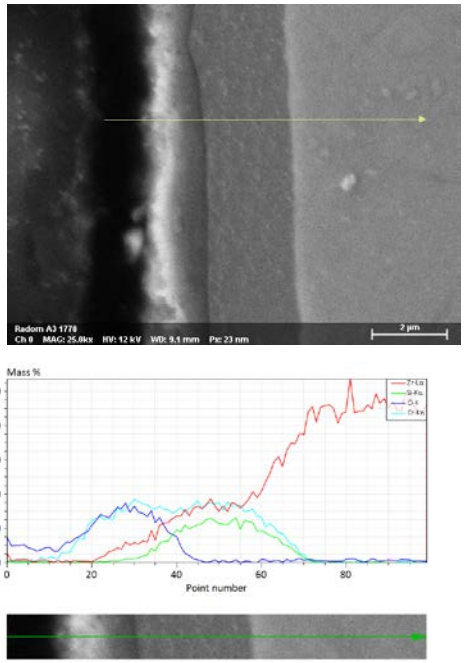
21 days (A1)



42 days (A2)



63 days (A3)



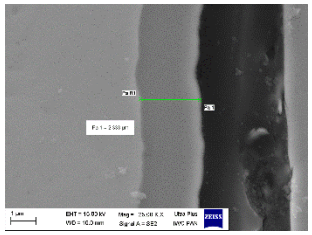
Thickness oxide layer [um]:
Coated A1: 0.5166 // A2: 1.090 // A3: 0.914
Zry-2: A1: 1.488 // A2: 2.074 // A3: 2.016

The oxidation process of $Zr_{40}Si_{24}Cr_{36}$ coatings took place and the base material remained not oxidized. Presence of $Zr_{40}Si_{24}Cr_{36}$ coatings slowed down Zry-2 oxidation and the protective character of $Zr_{40}Si_{24}Cr_{36}$ was observed.

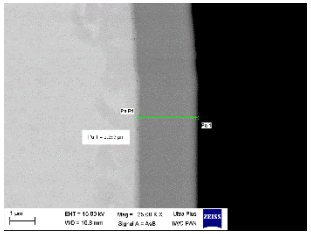
OXIDATION 700oC/air – surface layer quality

1h 2h 3h 4h 5h

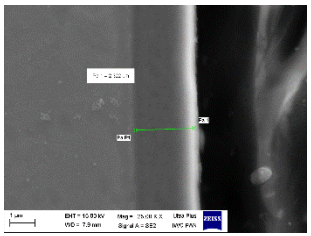
thickness



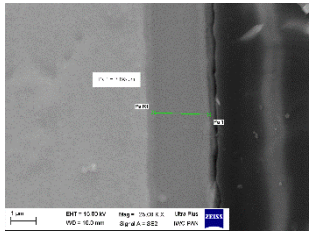
2.33 um



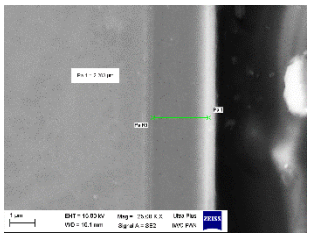
2.285 um



2.322 um

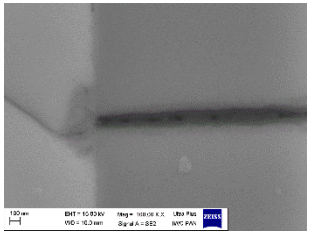


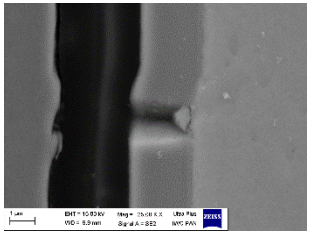
2.193 um

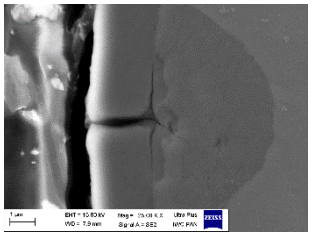


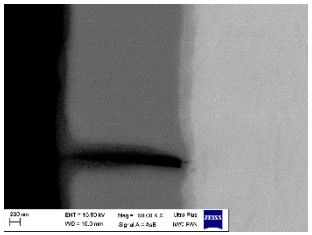
2.203 um

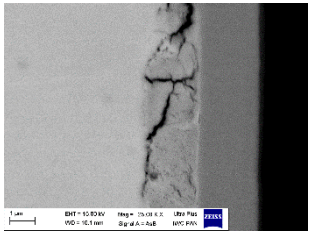
presence of cracks and oxidation - examples







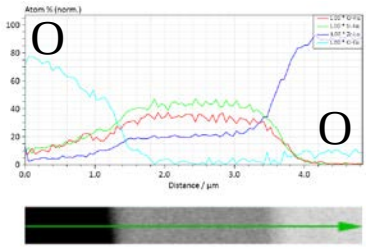




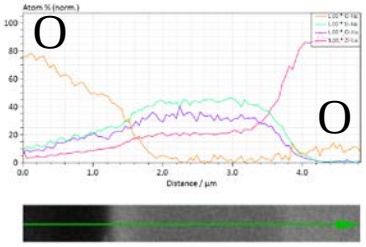
OXIDATION 700oC/air – cross-section investigations

Zry-2 coated with **Zr40Si24Cr36**

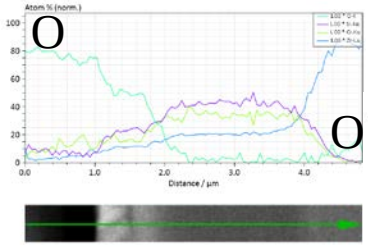
1h



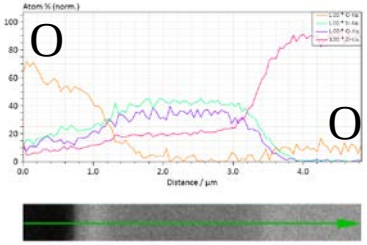
2h



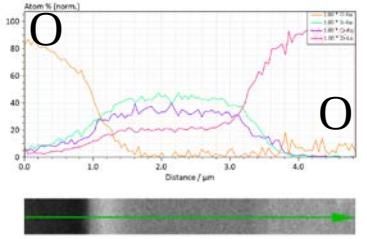
3h

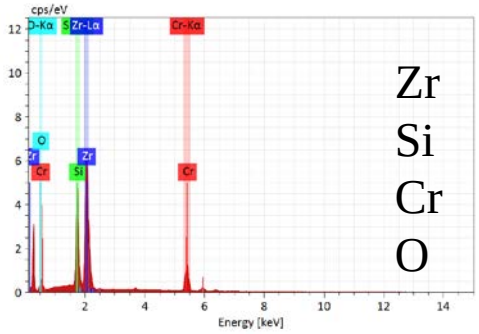


4h



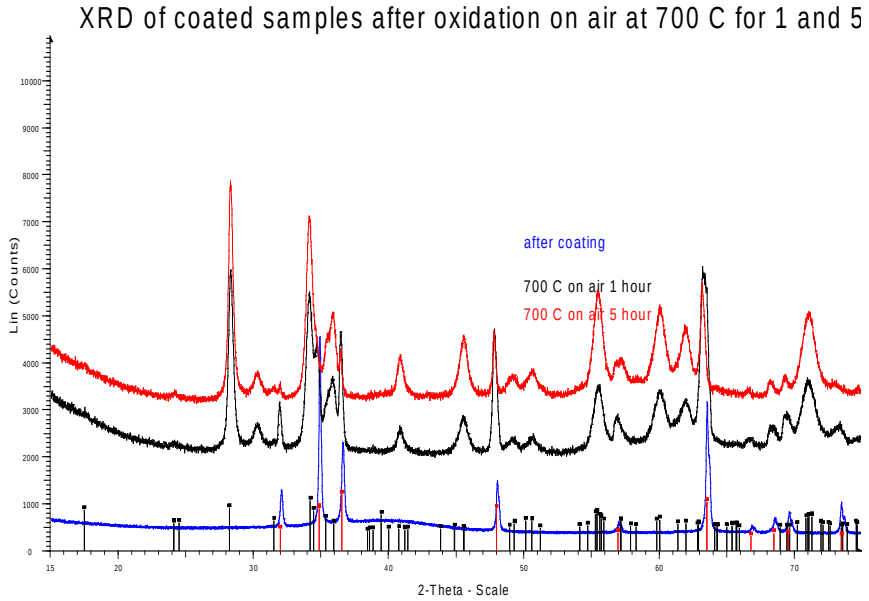
5h





Zr
Si
Cr
O

OXIDATION 700oC/air – phase analysis



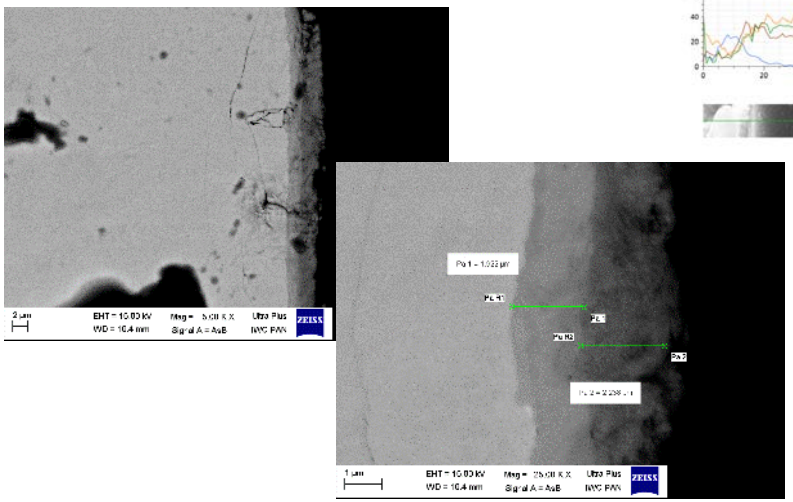
700oC/1h - **black line**
700oC/5h - **red line**
coated – blue line

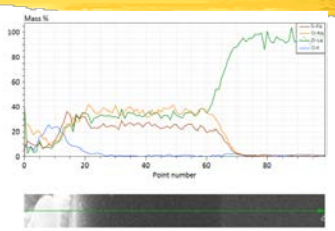
black markers – positions of ZrO_2 monoclinic phase
red markers – position of Zr hexagonal phase

- Growth of ZrO_2 with the time at the cost of Zr is clearly seen.
- The bulge at the position about $2\theta = 40$ deg at coated materials spectrum belongs to amorphous phase present in the coated Zry-2

OXIDATION 850oC and 1100oC/4h/argon – cross-section

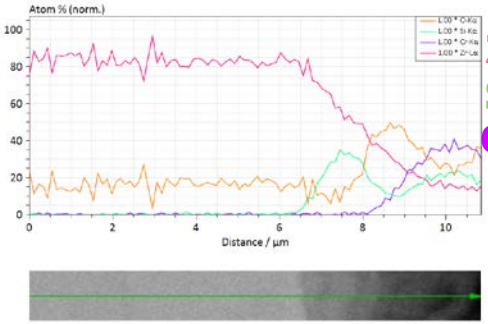
850oC



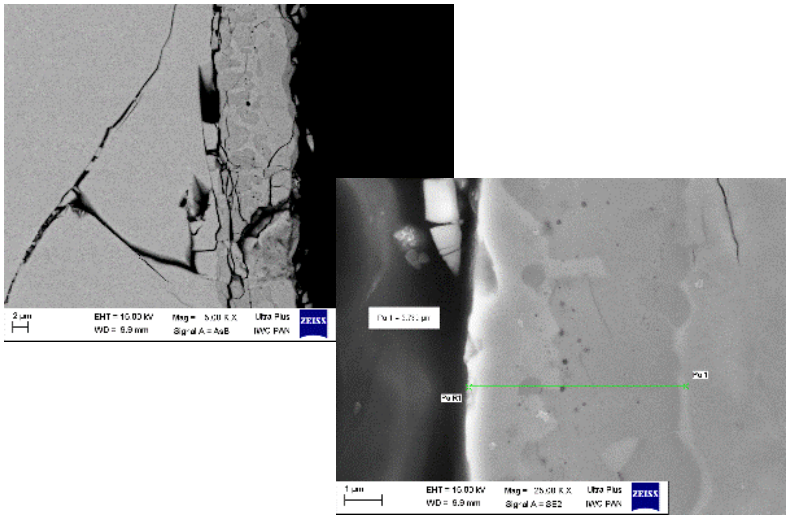


external: 2.238 um
internal: 1.922 um

Zr



1100oC

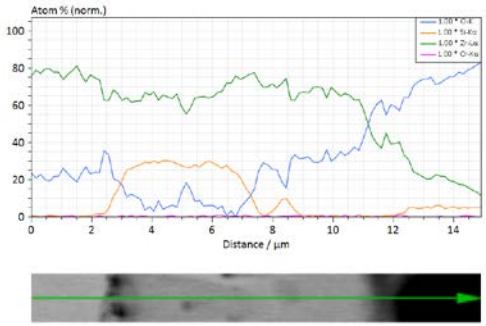


5.789 um

Zr

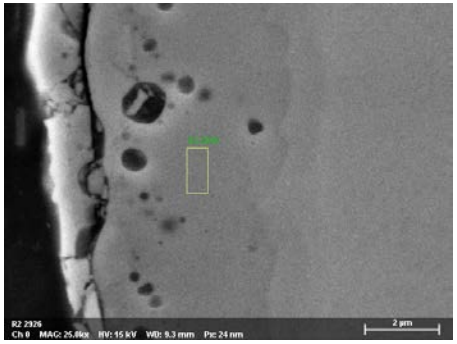
O

Si



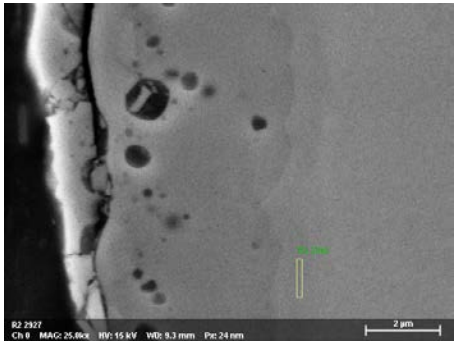
OXIDATION 1100oC/4h/argon

Elemental composition of the external and internal surface layer layer



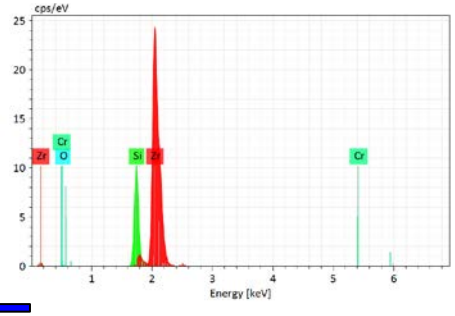
R2 3339

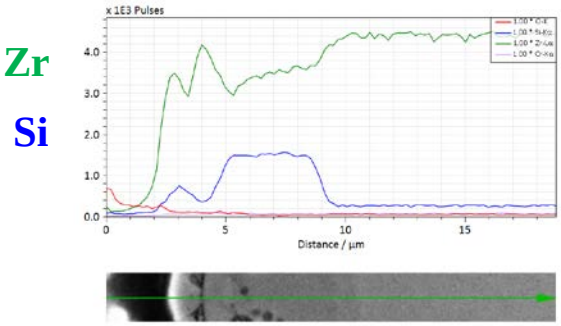
Element	At. No.	Netto	Mass [%]	Mass Norm. [%]	Atom [%]	abs. error [%] (1 sigma)	rel. error [%] (1 sigma)
Oxygen	8	459	0.77	0.81	3.52	0.25	31.89
Zirconium	40	199973	82.72	86.85	66.04	3.11	3.76
Chromium	24	42	0.03	0.03	0.04	0.00	16.36
Silicon	14	54891	11.72	12.31	30.39	0.52	4.40
		Sum	**95.24**	**100.00**	**100.00**		



R2 3340

Element	At. No.	Netto	Mass [%]	Mass Norm. [%]	Atom [%]	abs. error [%] (1 sigma)	rel. error [%] (1 sigma)
Oxygen	8	863	1.71	1.78	9.05	0.43	25.08
Silicon	14	6786	1.69	1.76	5.11	0.10	5.96
Zirconium	40	203398	91.51	95.59	85.16	3.44	3.76
Tin	50	889	0.72	0.76	0.52	0.06	8.34
Chromium	24	112	0.10	0.10	0.16	0.04	35.67
		Sum	**95.73**	**100.00**	**100.00**		



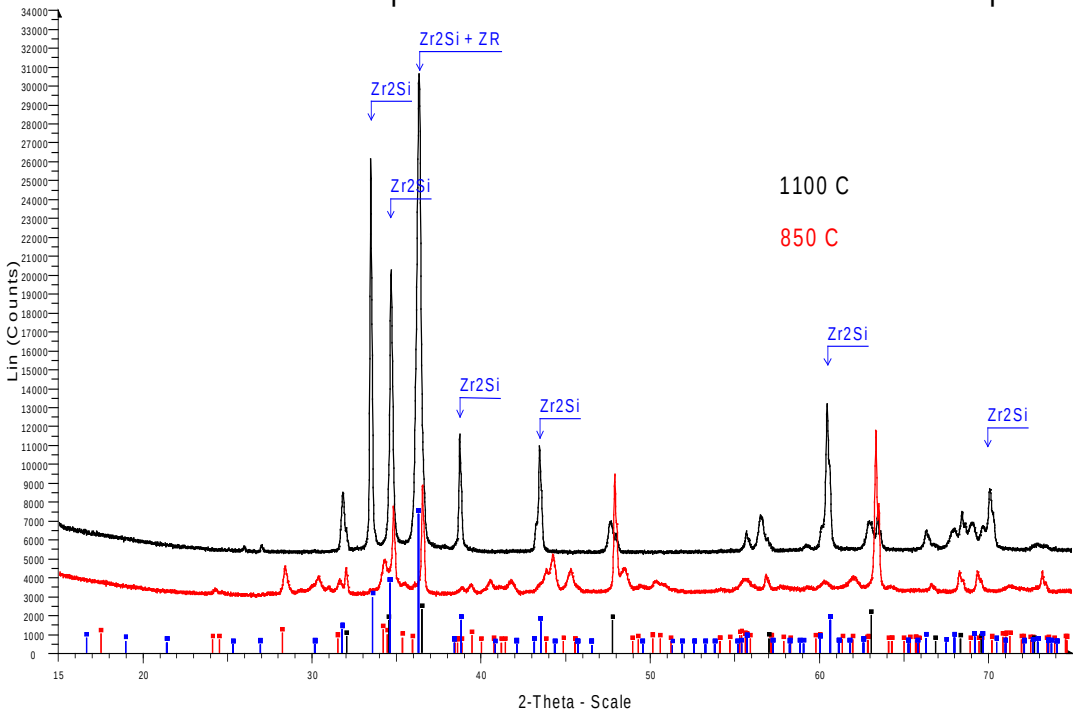


Distribution of elements across the surface layer

OXIDATION 850oC and 1100oC/argon

XRD of the samples coated with Zr, Si and Cr after thermal treatment

XRD of the samples after thermal treatment at Ar atmosphere



1100oC/4h/argon – black line

850oC/4h/argon – red line

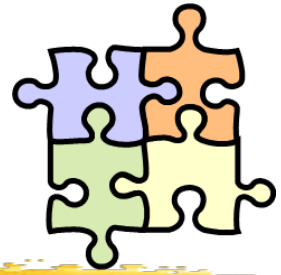
Zr2Si blue markers

Zr black markers

ZrO monoclinic phase - red markers

Identified Zr2Si phase is stable up to 1745oC

SUMMARY/CONCLUSIONS



1. Proposed material : Zr40Si24Cr36 for Zry2 coating can be considered as protective layer for Zry-2 during normal work in PWR conditions

2. Protective mechanism is assumed to two facts:
- chromium diffusion to the surafce
- presence of high temperature stable Si compounds

3. Obtained modified surface layers have to be improved using post formation proces for their better protective character

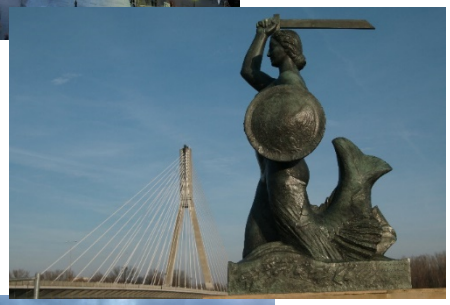
4. Plans for future:
- high temperature oxidation tests with different parametrs
- long time autoclave experiments 360oC/195 bar/21 days periods

NUTECH – 2020

Warsaw, 4 - 7 October 2020
International Conference on

Development and Applications of Nuclear Technologies







TOPICS OF THE CONFERENCE

- radiation processing of materials,
- radiation sterilization and health care products development,
- industrial application of the nuclear techniques,
- nuclear medicine & radiopharmaceuticals,
- nucleonic control systems,
- radioanalytical and radiotracer techniques,
- radiation technologies in environmental and earth studies and applications ,
- nuclear technologies in protection and identification of cultural heritage,
- radiation measurements, data processing and acquisition,
- radiation sources (eb, X-ray and gamma) development and applications,
- quality control and quality assurance in nuclear technologies,
- management of nuclear wastes,
- radioprotection and radiobiology,
- present status and future of nuclear energy,
- other topics related to nuclear and radiation related sciences.

nutech20@ichtj.waw.pl

GRADUATE SCHOOL OF PHYSICS AND CHEMISTRY

NATIONAL CENTRE FOR NUCLEAR RESEARCH ŚWIERK

The Graduate School of Physics and Chemistry was established in 2019 by the National Centre for Nuclear Research (NCBJ) and the Institute of Nuclear Chemistry and Technology (IChTJ).

Its goal is to leverage the expert knowledge of both institutions and take advantage of the resulting synergies to provide a coherent offer for individuals wishing to pursue a doctoral degree.

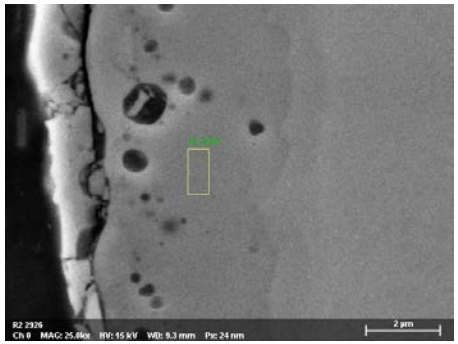
We build on the many years of experience in running graduate-level education and research programs at both institutions separately. **The School is uniquely focused on Nuclear Physics and Chemistry.**

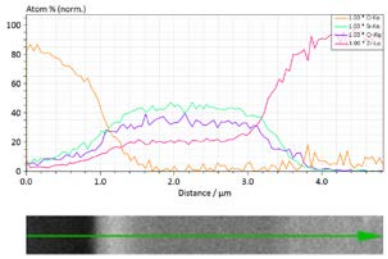
Applications for February 2020 are now accepting.
Application deadline for: Physics - 4th of November and Chemistry - 30th of November.

http://gradschool.ncbj.gov.pl/

MULTIELEMENTAL COATINGS ON ZIRCONIUM ALLOY – INCT OXIDATION EXPERIMENTS

Thank you for your attention





Acknowledgements

This work has been partially supported under IAEA Research Contract No. 19026/R0 and by Polish Ministry of Science and Higher Education under decision 3525/IAEA/2016/0 and 3689/IAEA/2017/0.

The finanical support under the framework of joint JINR Dubna- Polish research groups programme 04-5-1131-2017/2021 is greatfully acknowledged.

Testing of Cr Cold Spray-coated Cladding with Enhanced Accidental Tolerance

Martin Ševeček [a,c], Jakub Krejčí [b], Koroush Shirvan [c], Adéla Chalupová [a,b],

[a] Faculty of Nuclear Sciences and Physical Engineering, CTU in Prague
[b] UJP Praha a.s.
[c] Massachusetts Institute of Technology

Abstract:

This talk presents an overview of the experimental performance of non-commercial cold-spray (CS) chromium coated Zircaloy-4. Previously, high-temperature steam (500 to 1400 ^{o}C) and quench, room-temperature burst, autoclave creep, fatigue and corrosion testing along with thermo-mechanical modelling showed Cr-coating via cold spray process is a promising accident tolerant fuel (ATF) concept. Though, some concerns regarding crack initiation and propagation were also discussed. In this study, we expand the test matrix by investigating the accelerated creep and CRUD disposition after >800 hours of testing. The results indicate that the cold-spray chromium coating is expected to have similar performance during normal operation in terms of mechanical and thermal creep and CRUD deposition when compared to Zr-4. In addition, high-temperature ballooning/burst are reported. Noticeably superior performance in terms of burst time and burst size were also observed with the coated cladding samples at high temperature when compared to Zr-4. Single-sided steam oxidation at 1200 ^{o}C were also performed. While weight gain was found to be considerably smaller, hydrogen concentration was found to be higher inside Cr-coated samples compared to Zr-4 as well as post-quench ductility measured by ring compression tests. These data serve as a basis to motivate future testing and development of coated cladding models to predict the performance of this ATF concept for future commercial deployment with fully optimized deposition technique and parameters.


Technologie

Testing of Cr Cold Spray-coated Cladding with Enhanced Accidental Tolerance

Martin Ševeček [a,c], Jakub Krejčí [b], Koroush Shirvan [c], Adéla Chalupová [a,b],

[a] Faculty of Nuclear Sciences and Physical Engineering, CTU in Prague
[b] UJP Praha a.s.
[c] Massachusetts Institute of Technology

25th International QUENCH Workshop
Karlsruhe Institute of Technology, Germany

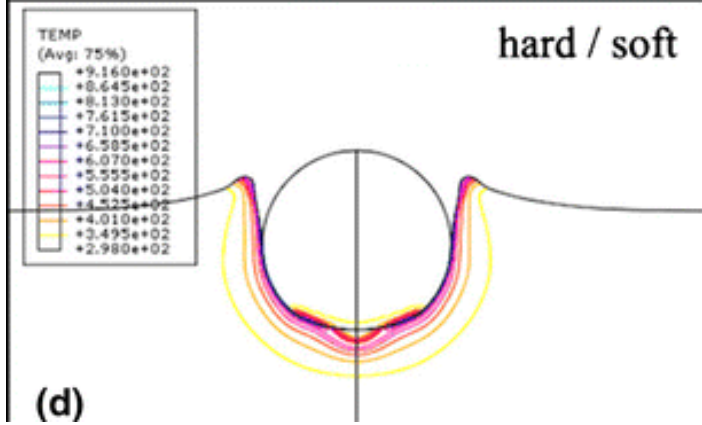
1. Coated cladding

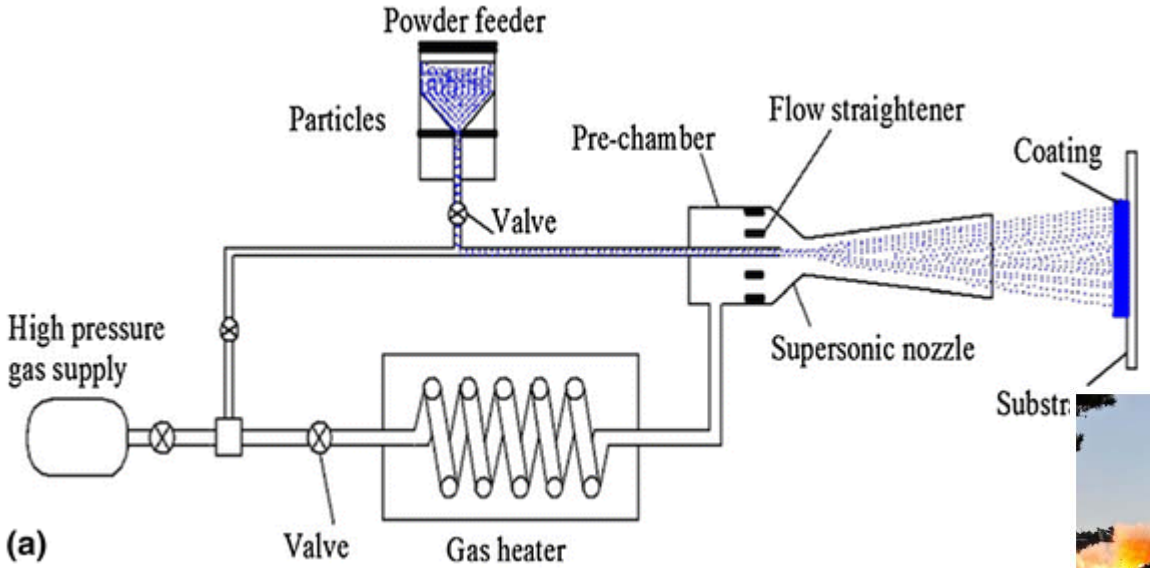
Coated Cladding with Enhanced Accidental Tolerance

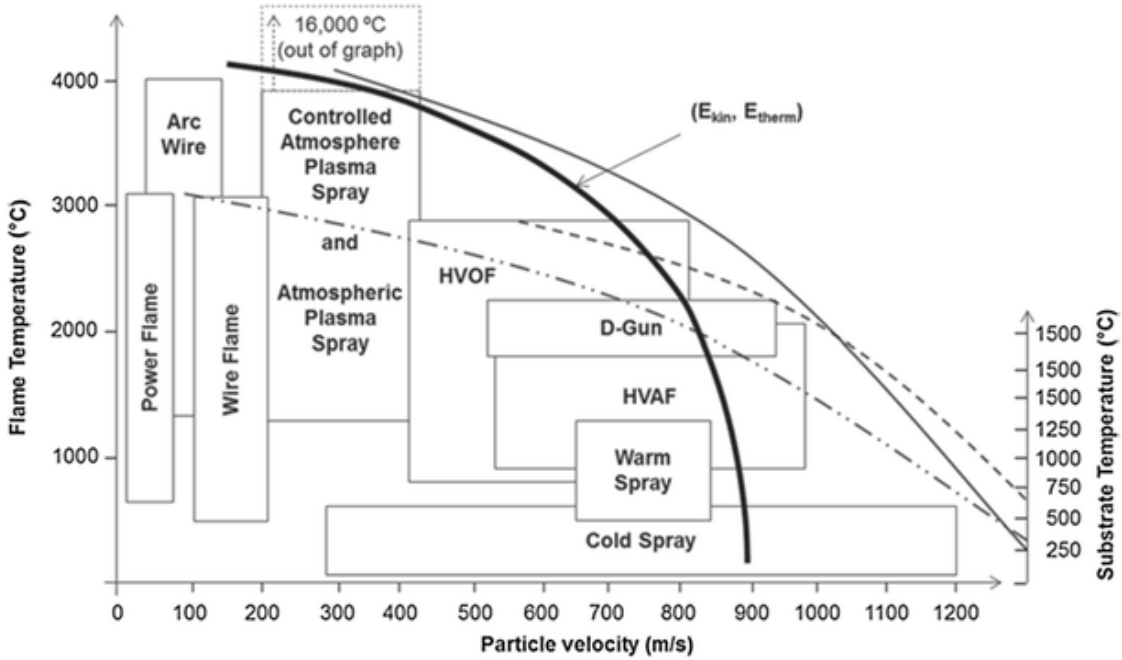
- Straightforward solution how to improve traditional Zr-based alloys = surface treatments (e.g. coating)
- Many coating materials tested and proposed to improve performance
- Cr-based coatings are considered as most mature and promising with LTRs and LTAs in commercial reactors
  - Framatome – Cr deposited by Physical Vapor Deposition (PVD)
  - Westinghouse Electric Company – Cr deposited by Cold Spray technique (CS)
  - TVEL – Cr deposited by PVD and CS
  - KNF – Cr-based Cr90Al10 coating deposited by arc ion plating
  - GNF – metallic fretting/oxidation resistant "ARMOR" coating for BWRs
  - CGN – Cr deposited by PVD, CS, laser deposition and plasma spraying

Cold-spray Process

- CS – one of the thermal spray techniques
- Many industrial applications (including nuclear)
- Hard coatings = challenging
- Mechanical properties – strongly process-dependent









Patriot Missile Launcher



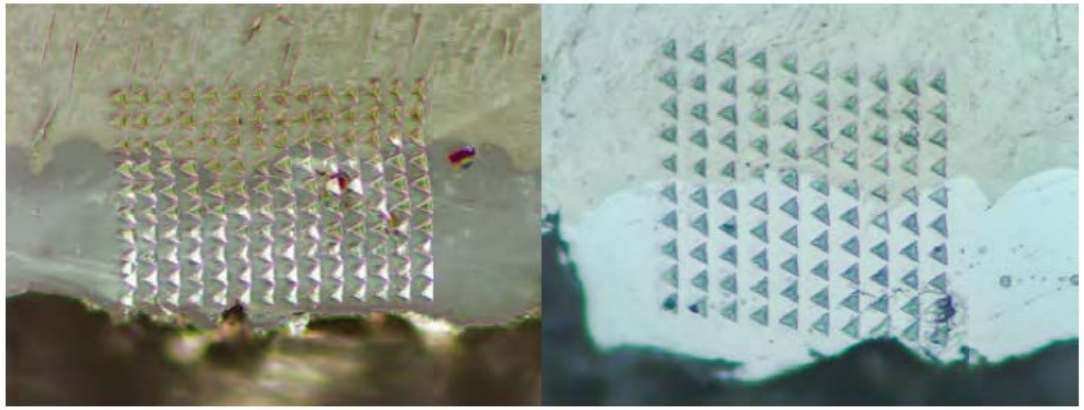
B1 Bombers Forward Equipment Bay Panels

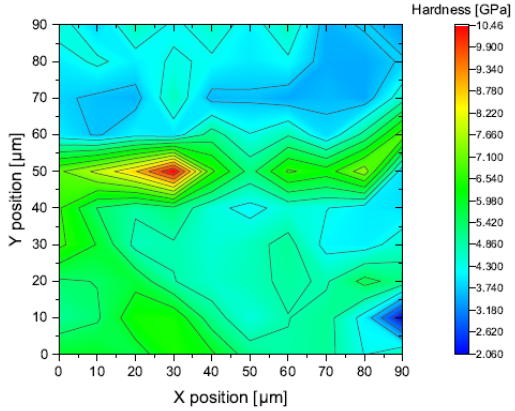


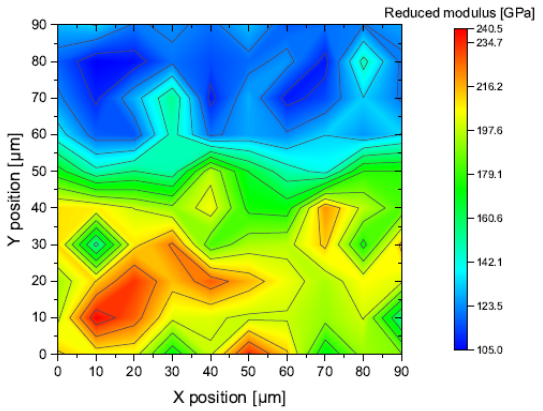
General Electric T700 Engine Front Housing

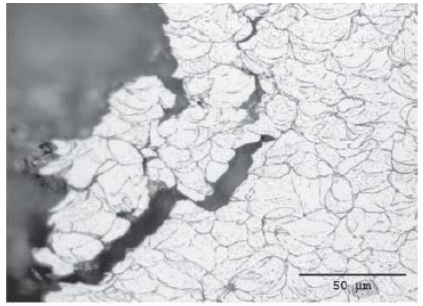
Mechanics of CS

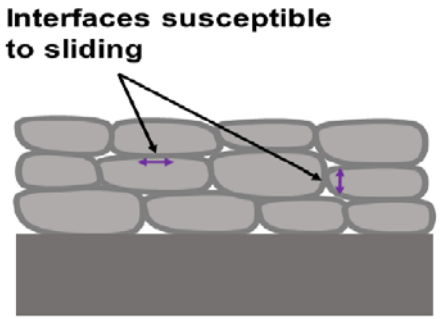
- Sprayed powder particles affect the substrate:
  - Hardening
  - Stress concentration
- CS coating
  - Very low ductility
  - Brittle failure due to incomplete bonding
  - Crack propagation along weak interfaces





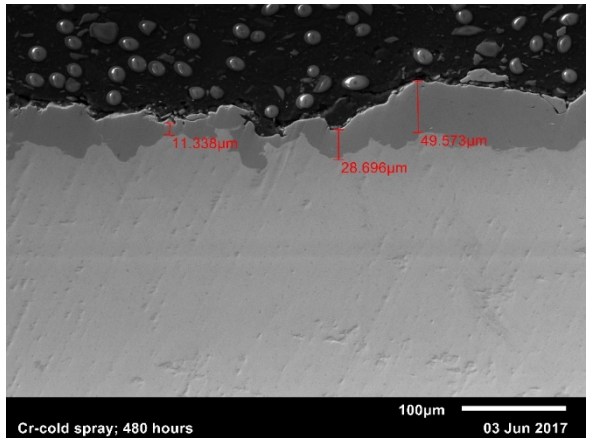


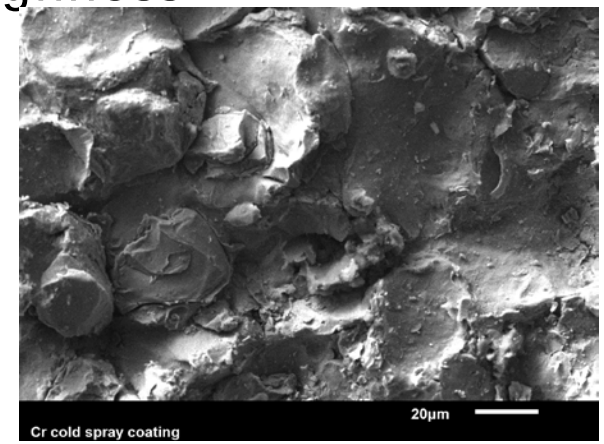


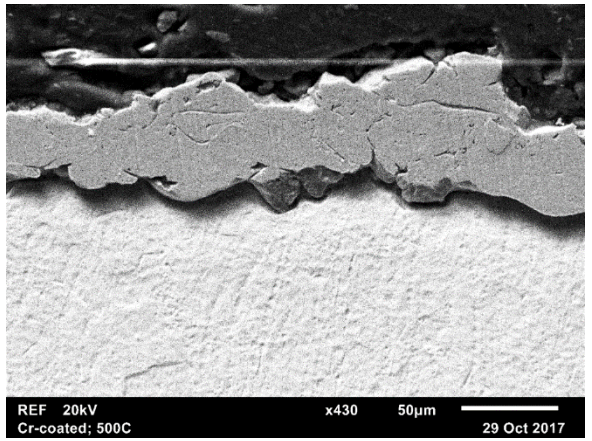


As-produced material

- Pure Cr (HP with He gas) – different powder suppliers (avg. powder size around 20 microns); three different coating suppliers; goal 20-30 microns
- Zircaloy-4 used as a substrate; no additional treatment (thermal or mechanical) = higher outer surface roughness



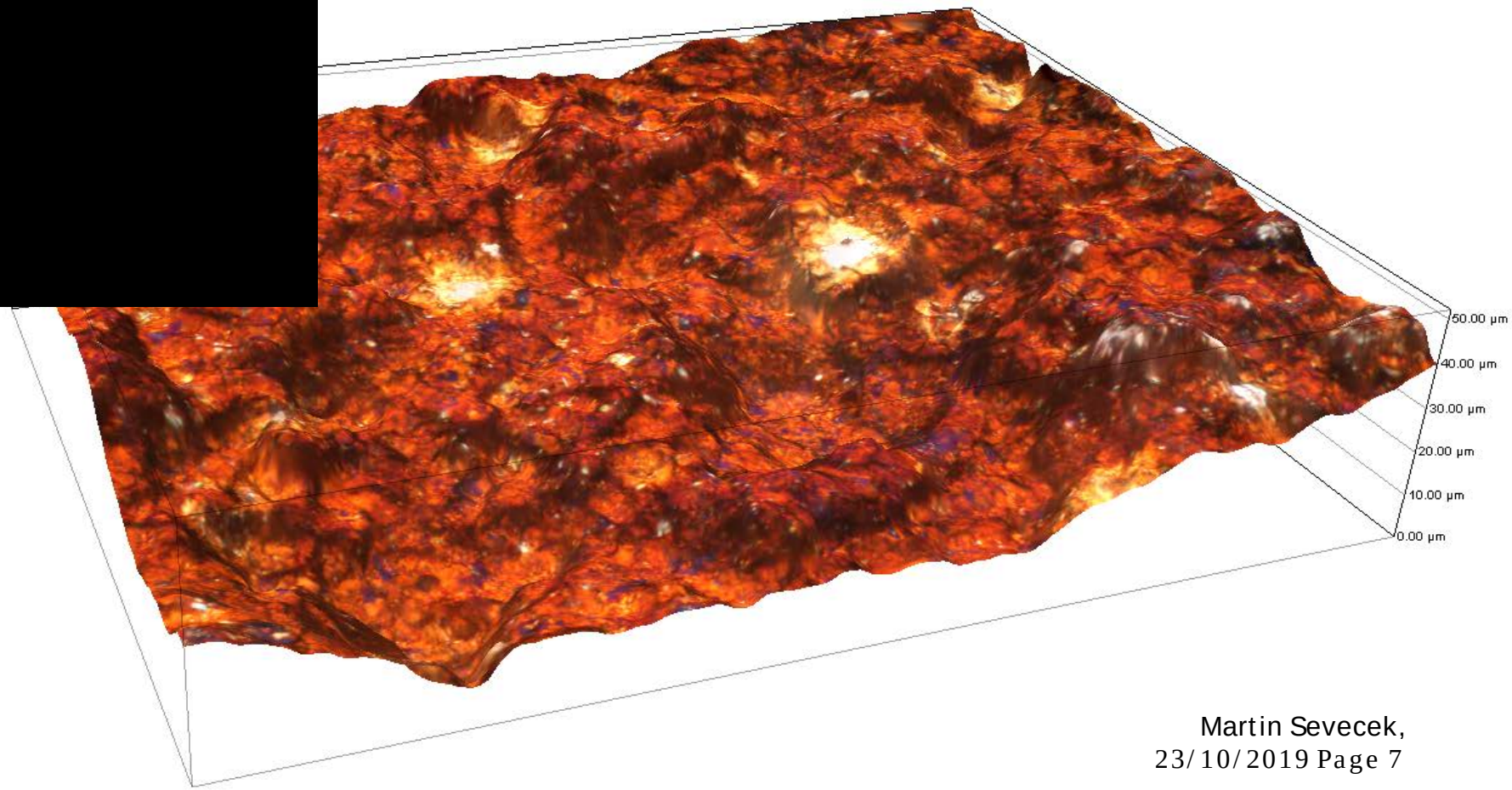






- Current commercial parameters – nominal thickness 25 microns, industrial polishing from outer side (same roughness as standard Zr); control of grit of polishing, process speed, pressure, number of passes + NDE



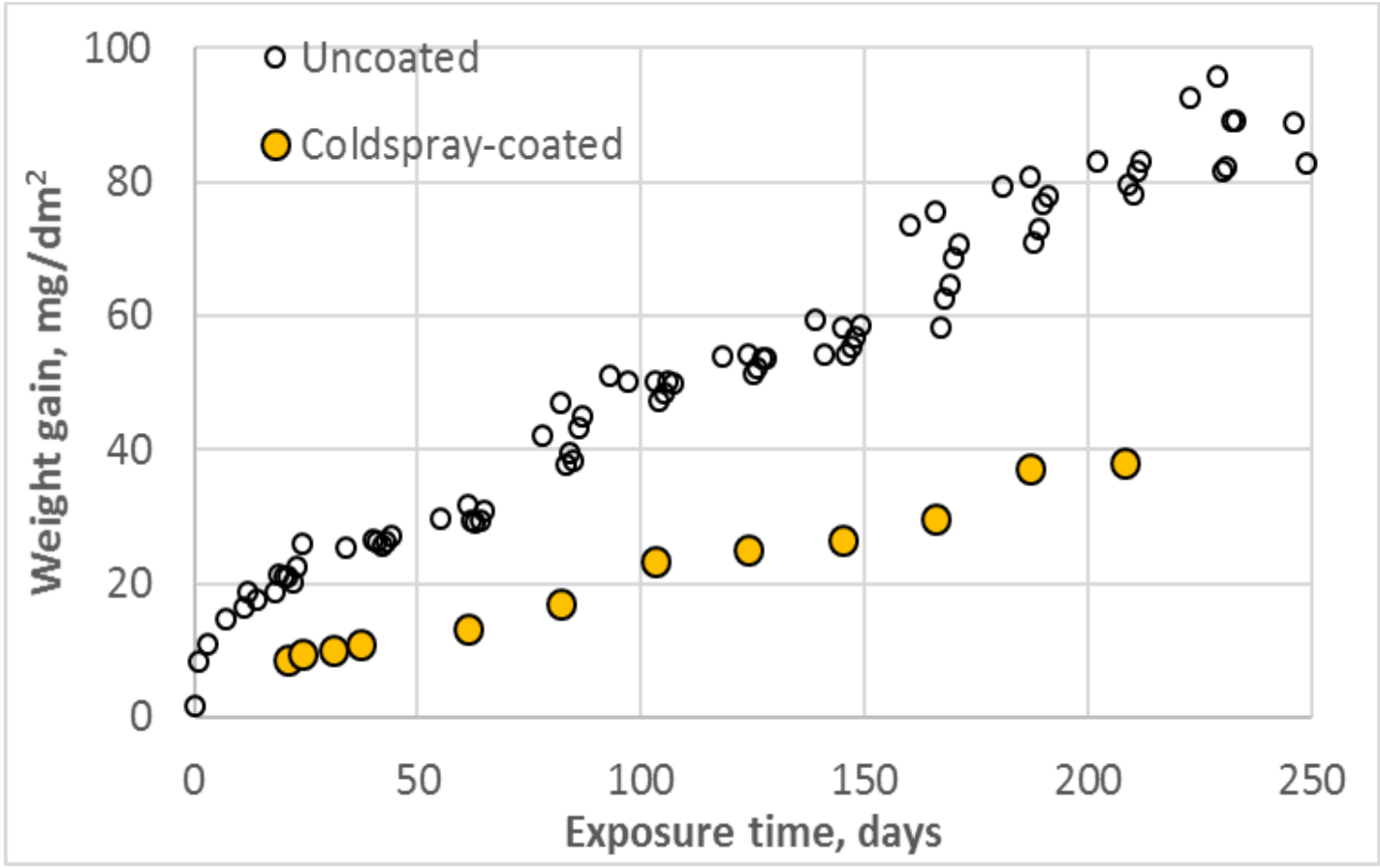

50.00 µm
40.00 µm
30.00 µm
20.00 µm
10.00 µm
0.00 µm

CTU
CZECH TECHNICAL UNIVERSITY IN PRAGUE

2. Normal operation

Long-term corrosion

- At 360°C, 18.4MPa, VVER chemistry
- Double-sided = strong effect of uncoated inner side
- Very low weight gains – even with high outer surface roughness
- Comparable to PVD coating – no acceleration, stable growth
- H-pickup not yet evaluated – not fully resolved question also for PVD



CRUD deposition

- MIT CRUD loop – aggressive chemistry for CRUD acceleration – might not be fully representative for real LWR conditions; allows for direct comparison
- No significant difference between Cr and Zr even with gamma irradiated coatings – in agreement with WEC results

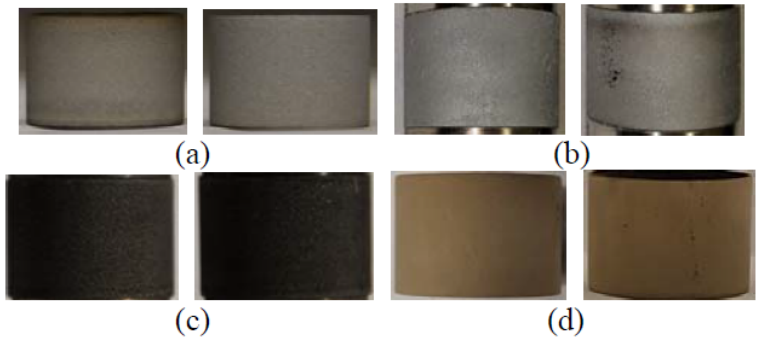
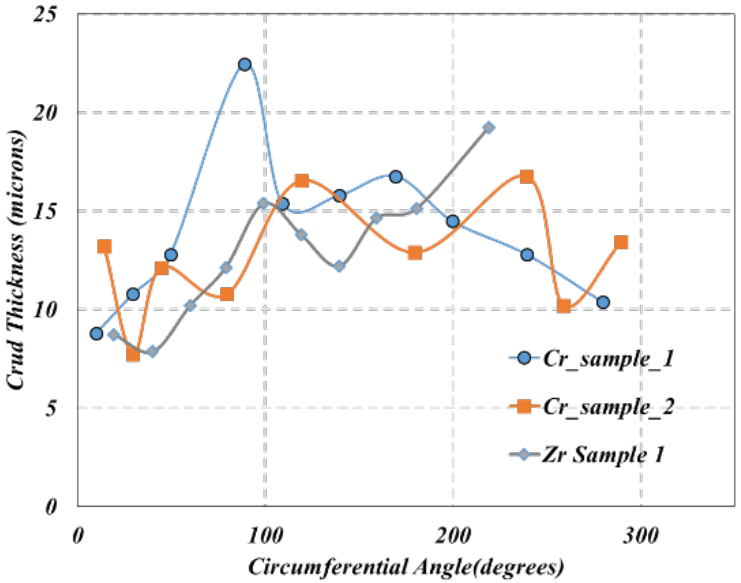


Fig. 3. Cr coated CRUD samples before the first set of tests (a) and after first set of tests (c) and samples before the second tests (b) and after second tests (d).



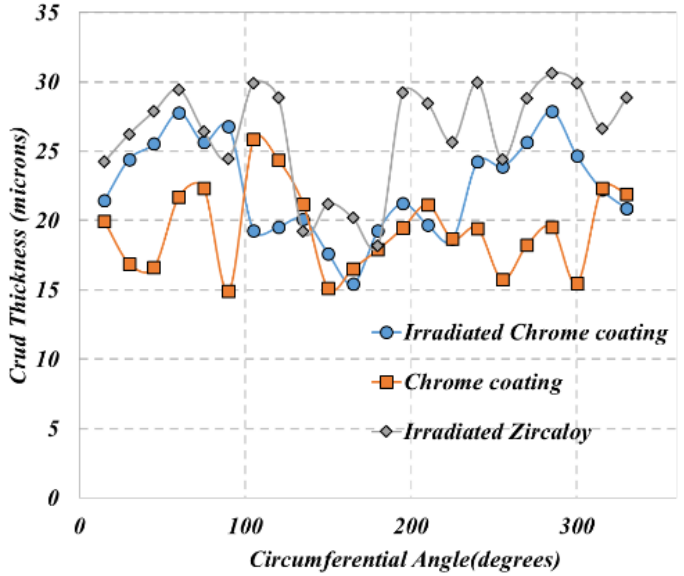
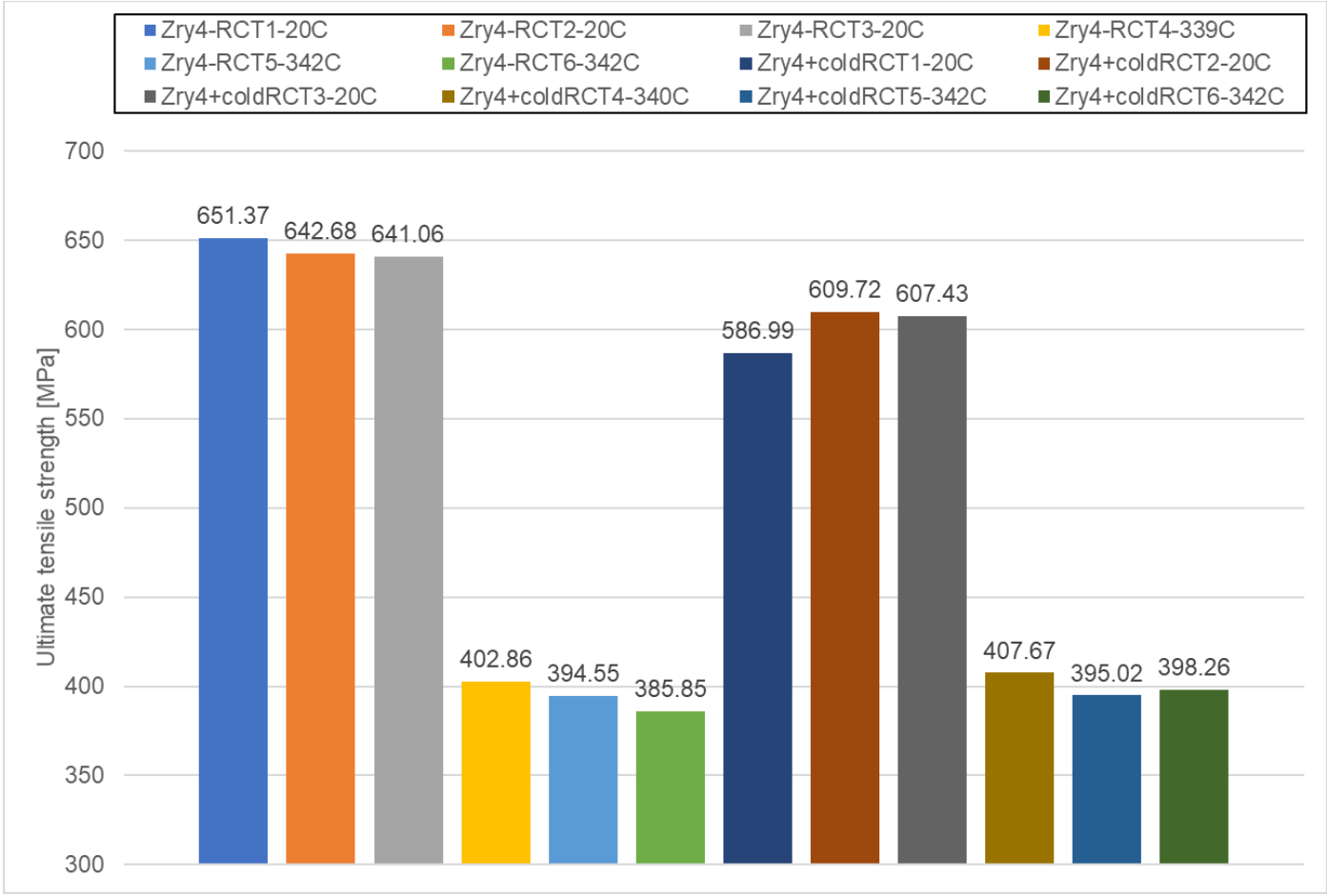


TABLE I. CRUD loop test conditions

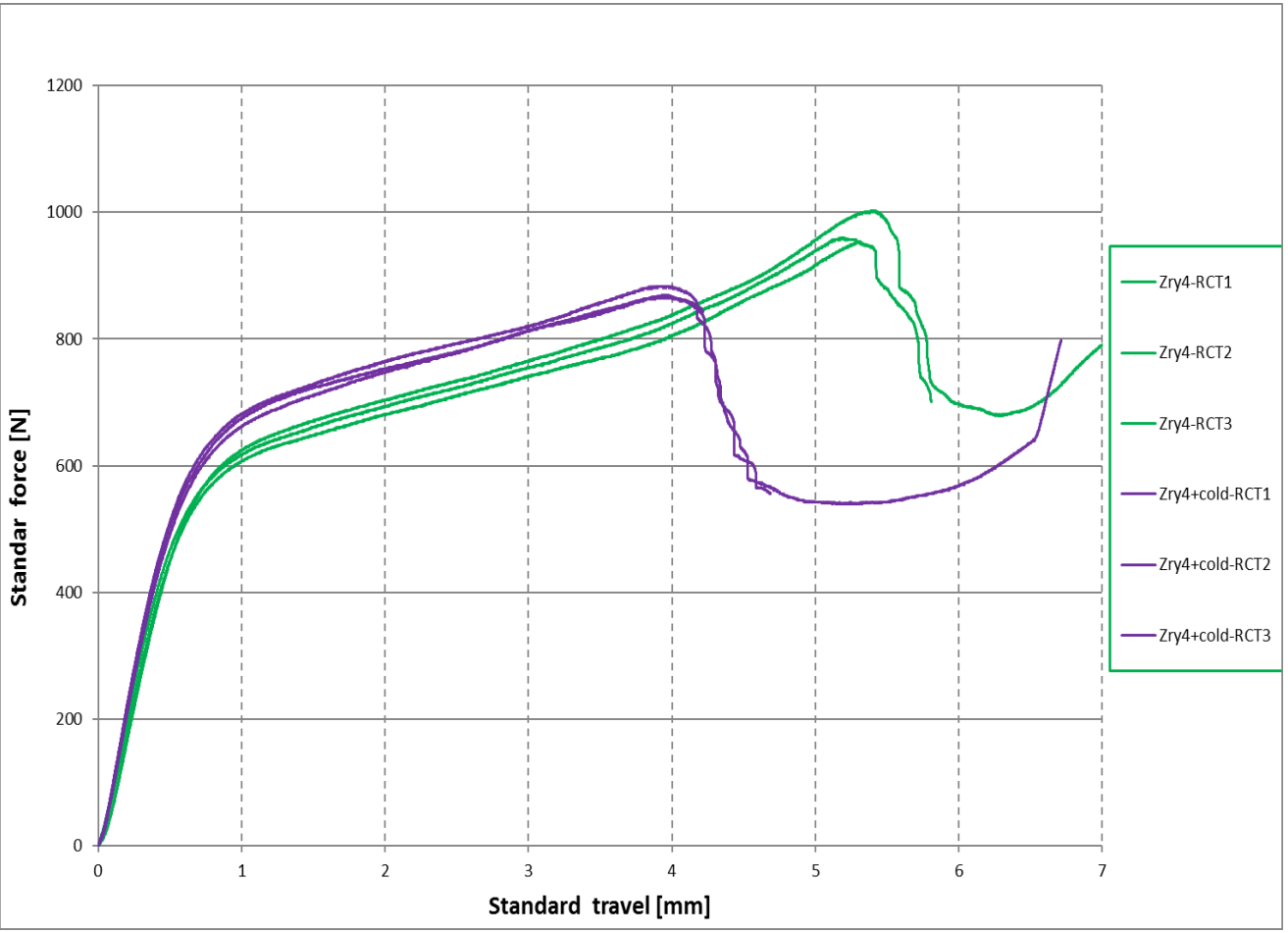
Parameter	Test #1	Test #2
Temperature	320 °C	320 °C
Pressure	15.5 MPa	11.5 MPa
Mass Flux	1920 kg/m²s	1920 kg/m²s
Test Duration	15 days	30 days
Boron	500 ppm	500 ppm
Lithium	2 ppm	2 ppm
Iron	12 ppm	12 ppm
Nickel	12 ppm	12 ppm
Zinc	-	12 ppm
H2	25-35 cc/kg	25-35 cc/kg
O2	<10 ppb	<10 ppb
pH	6.9-7.4	6.9-7.4
Conductivity	10-50 µS/cm	10-50 µS/cm

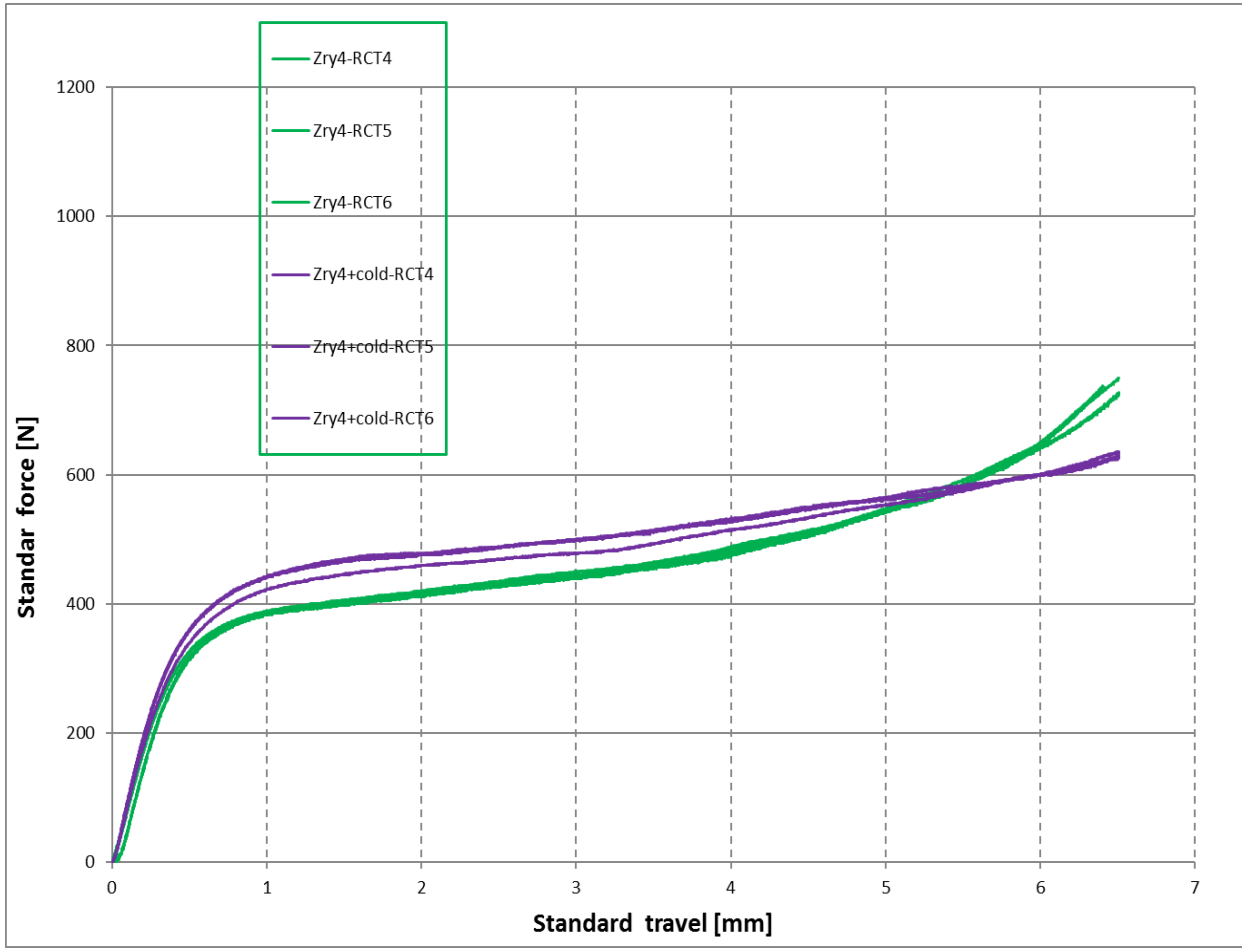
Mechanical tests – as-received RCT

- RCT with as-received material at 20 and 340°C
- UTS and ductility evaluated
- Residual ductility at 20°C is about 33% for coldspray Cr coated and about 46% for uncoated specimens.



RCT at 20 and 340°C





Fatigue tests and creep tests published previously

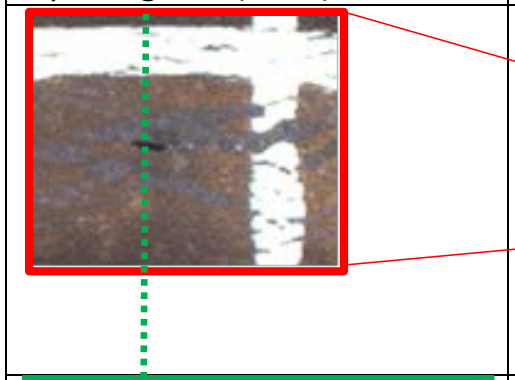
CTU
CZECH TECHNICAL UNIVERSITY IN PRAGUE

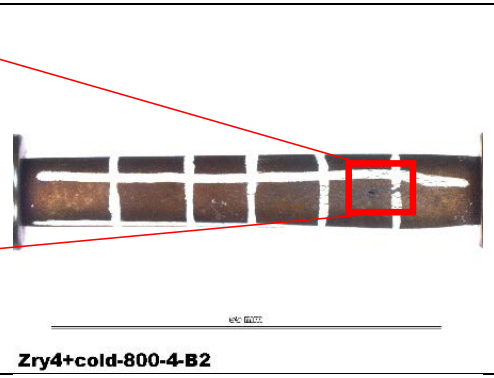
3. DBA Conditions

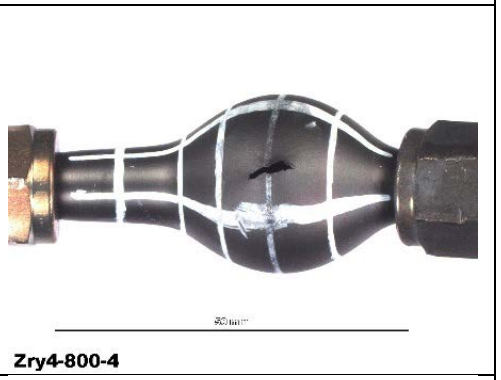
Burst test

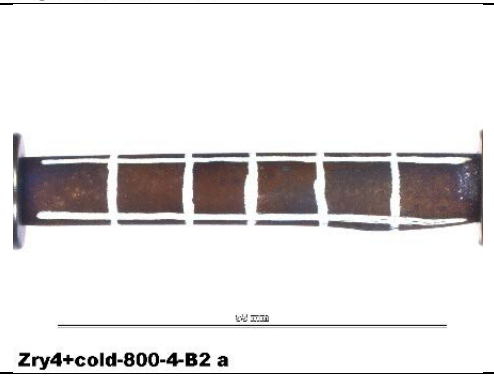
- Two CS coated specimens and uncoated were compared at 800 °C, with inner over-pressure 4 MPa, in Ar
- All parameters significantly improved
- FEM model at MIT used to calculate the fundamental parameters
- More tests needed => IAEA TS-ATF project – ballooning+burst RRT + benchmark exercise

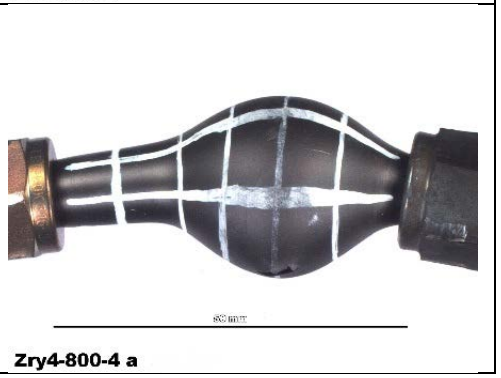
Specimen	Coldspray-coated	Uncoated
Stress (MPa)	27.5	30.9
Time to burst (sec)	1803	350
Maximal deformation (%)	14.5	178
Deformation 2 cm (%)	10.3	21.4
Opening size (mm^2)	0.1	5.6











CTU
CZECH TECHNICAL UNIVERSITY IN PRAGUE

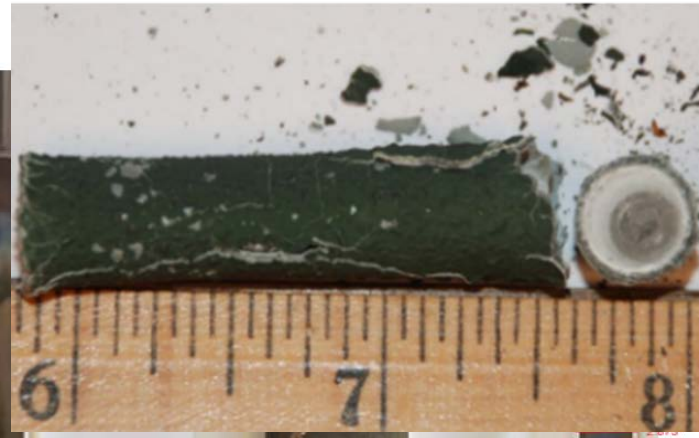
High-temperature steam oxidation

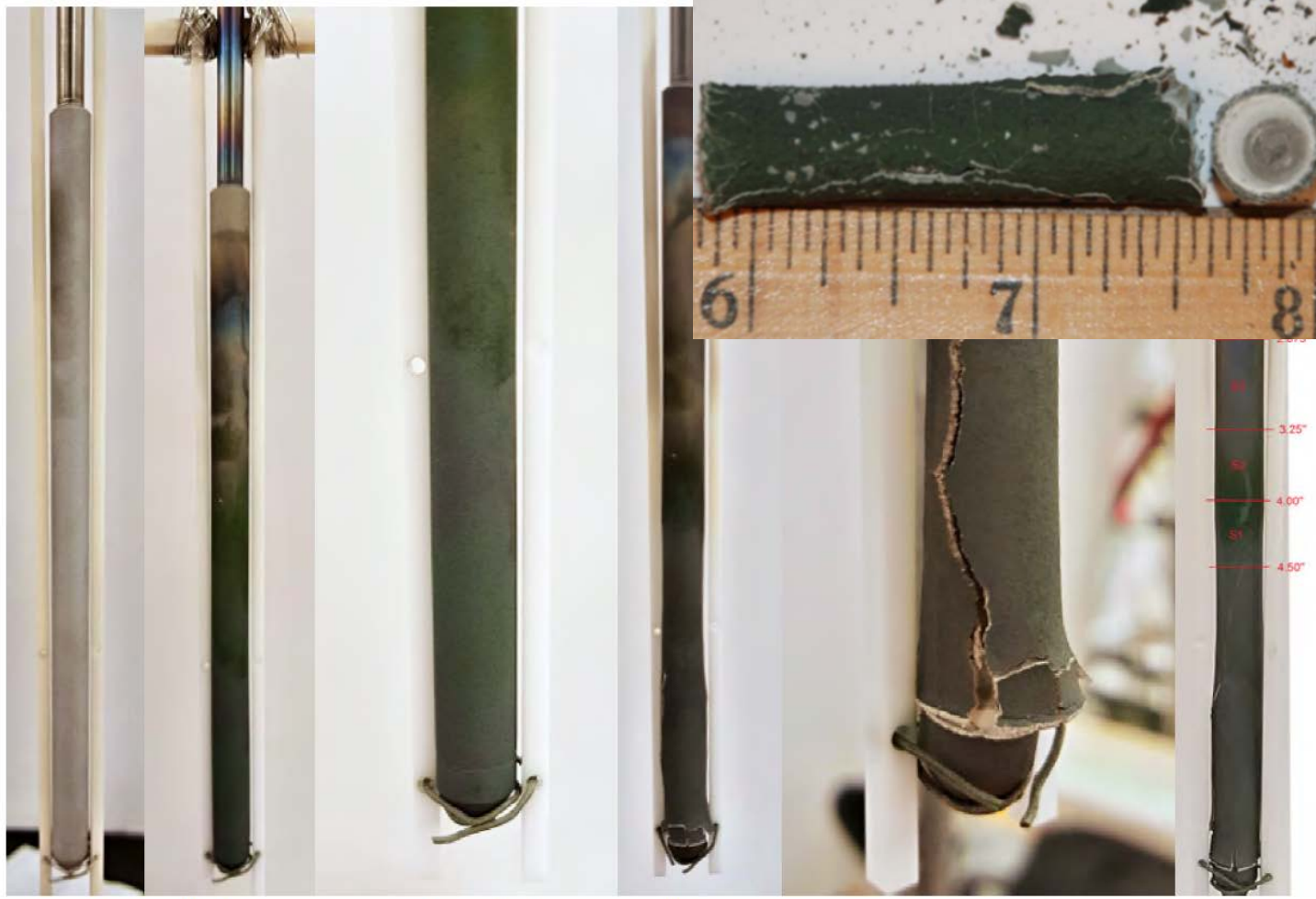
- Single-sided oxidation of 45mm long specimens with endplugs from Zr-alloy (uncoated)
- Comparison of two uncoated and two CS-coated specimens at 1200 °C (5 and 15 min).
- Based on temperature measurement and CP formula were calculated weight gain-CP, ECR-CP, and equivalent time-CP for isothermal exposition at 1200 °C

5 min @ 1400 °C Steam



20 min @ 1400 °C Steam



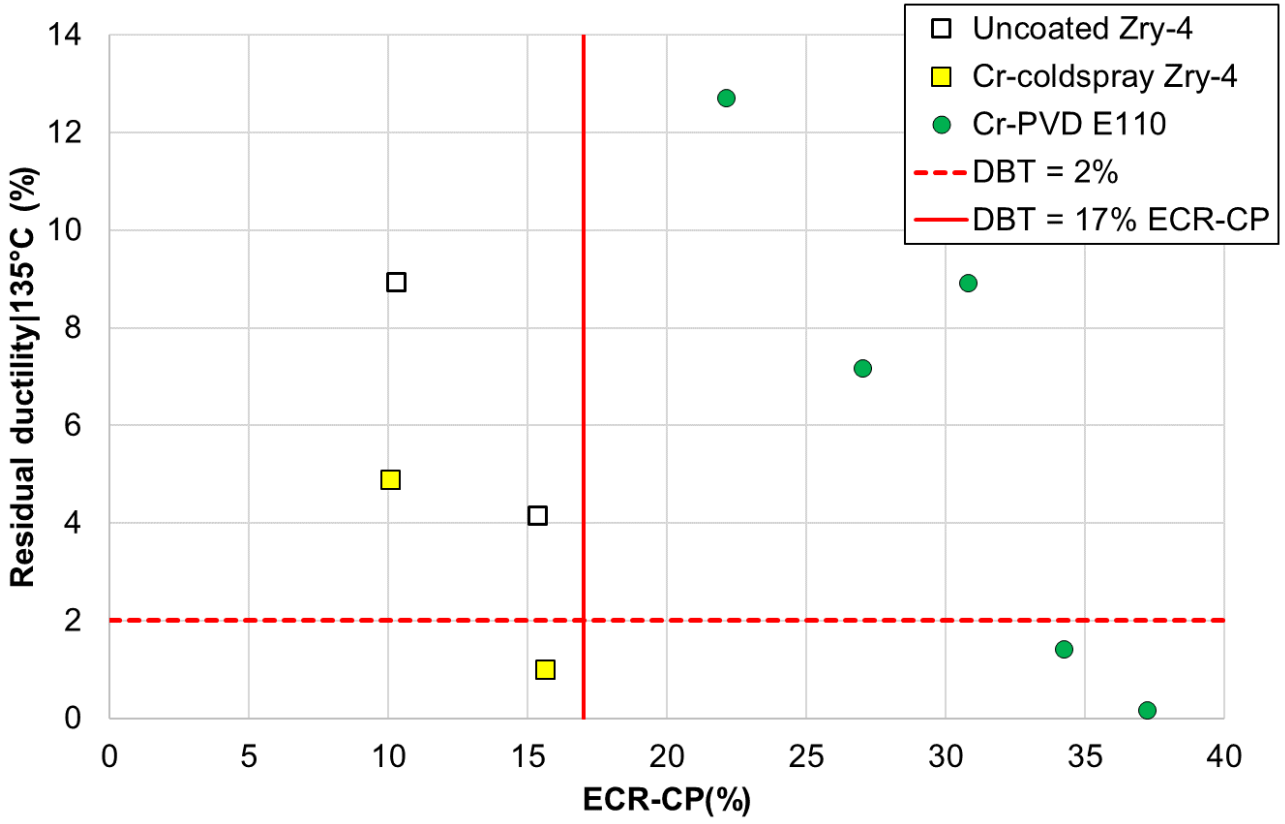


(a) Cr PT1 (b) 15min (c) 15min detail (d) 90min (e) 90min - detail (f) Cutting

Post quench DBT

- DBT transition according to time at temperature ECR (not experimental!!)
- Zry-4 – 17% (hydrogen/ burnup dependent)
- Cr PVD coated E110 – around 34%
- Cr CS – 15.6% ECR => 0.56, 0.55, 1.92 % RCT

ID	RCT1 (%)	RCT2 (%)	RCT3 (%)	ECR_{CP} (%)
Cr 5 min	5.0	4.8	4.9	10.1
Cr 10 min	0.6	0.6	1.9	15.6
Zr 5 min	8.5	-	9.3	10.3
Zr 10 min	2.5	5.7	4.3	15.4



Vickers Microhardness

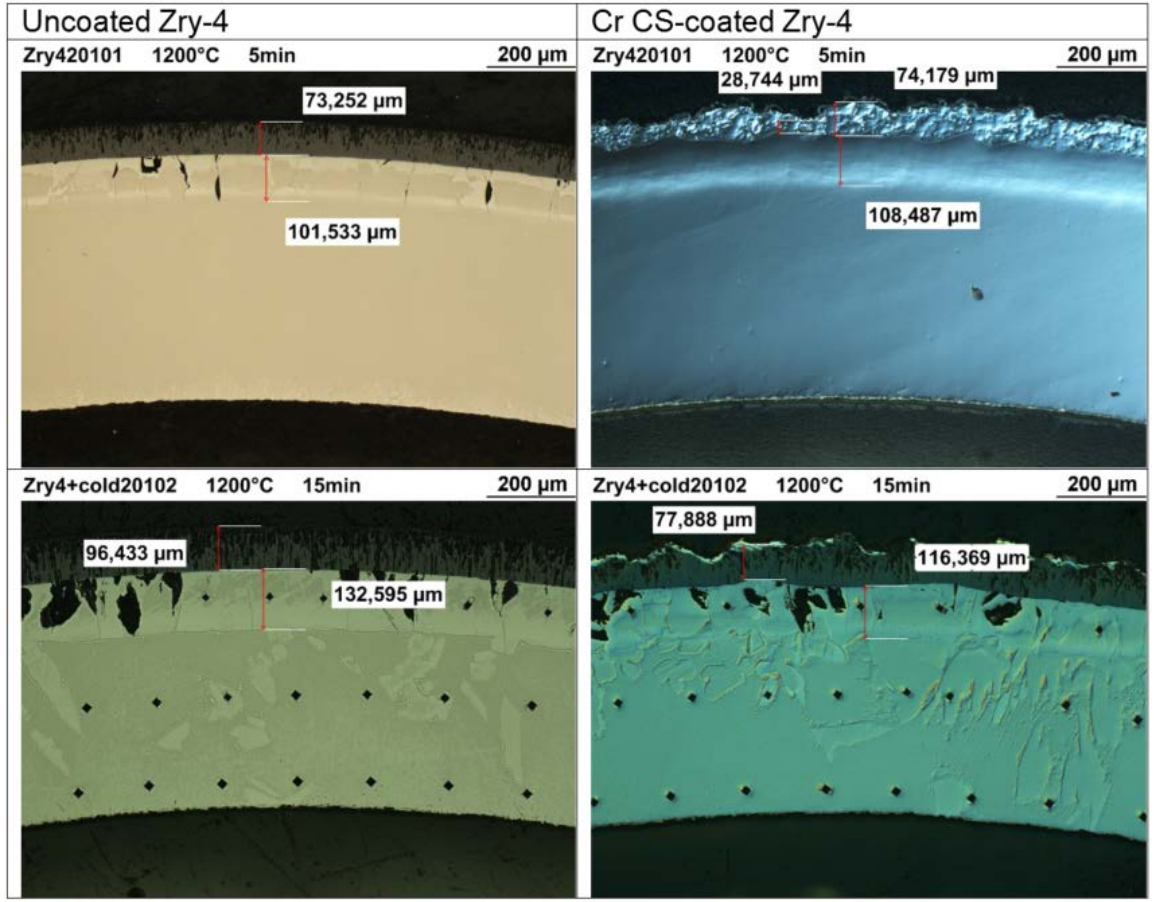
Three rows – under coating; middle; inner

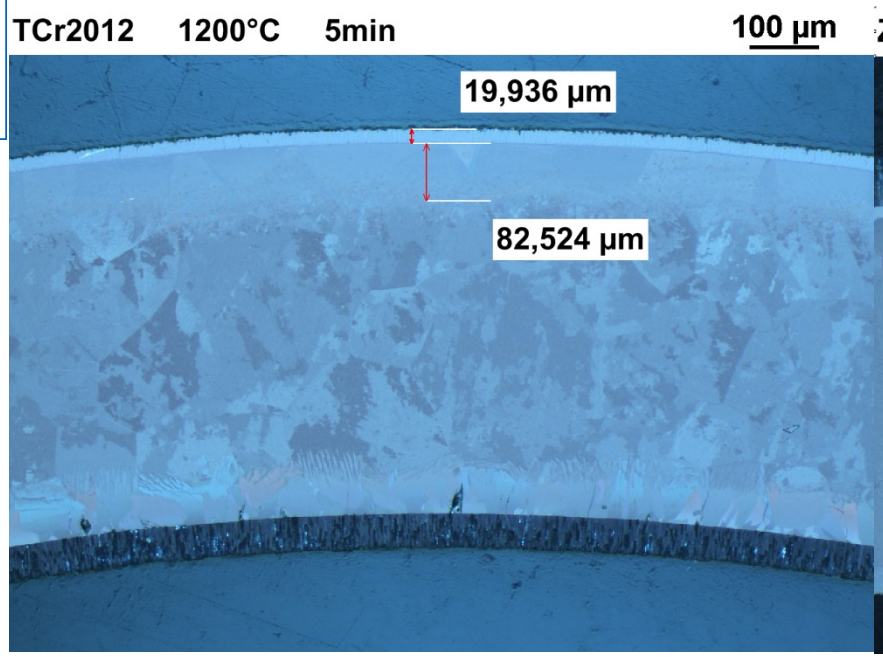
5 min – soft Zr =protective coating

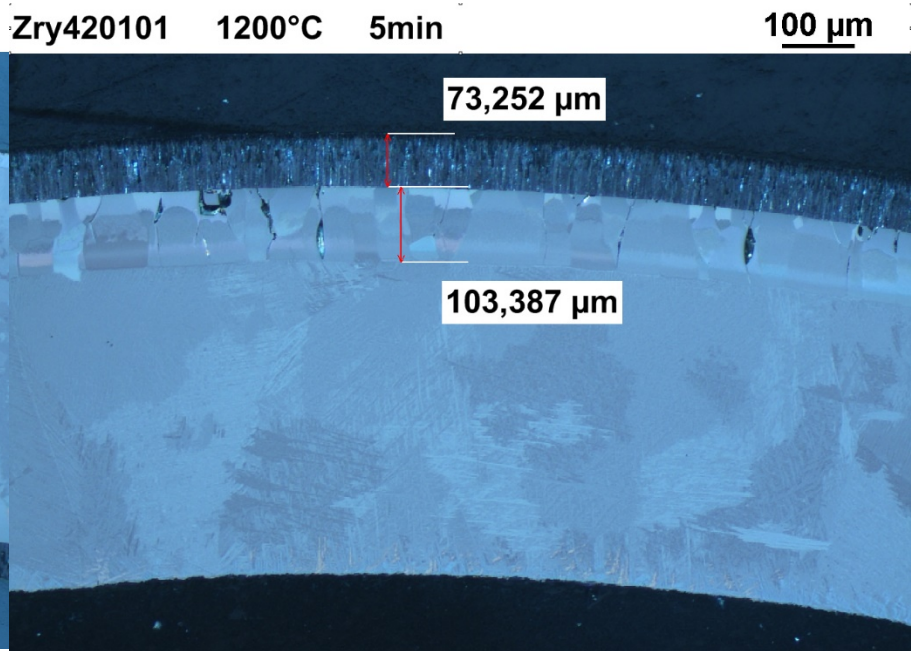
15 min – hard Zr – Cr enhanced O diffusion

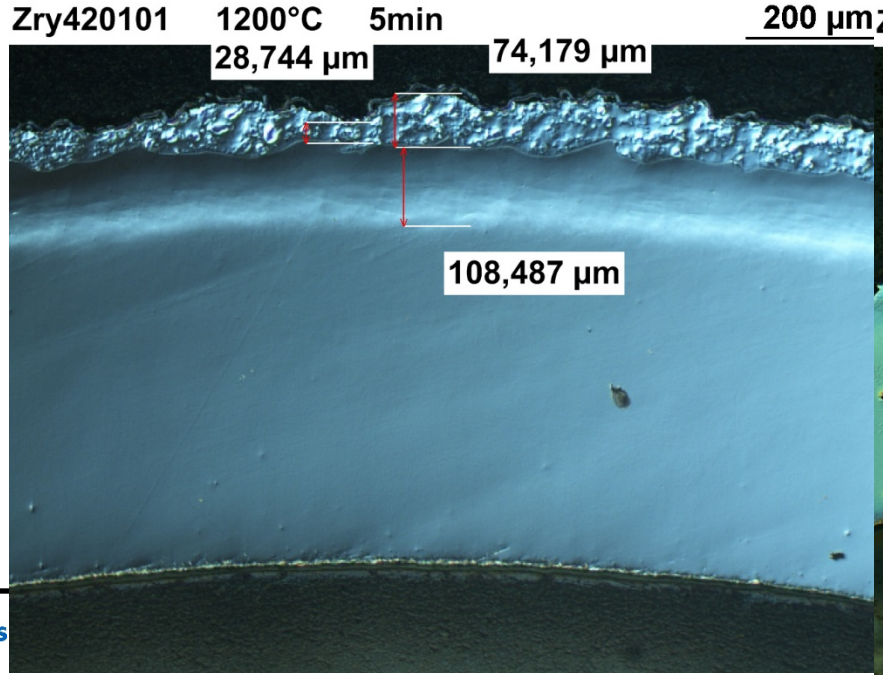
ID	VH out	VH mid	VH in
Cr 5 min	399	235	245
Cr 15 min	563	415	350
Zr 5 min	526	354	330
Zr 15 min	519	364	324

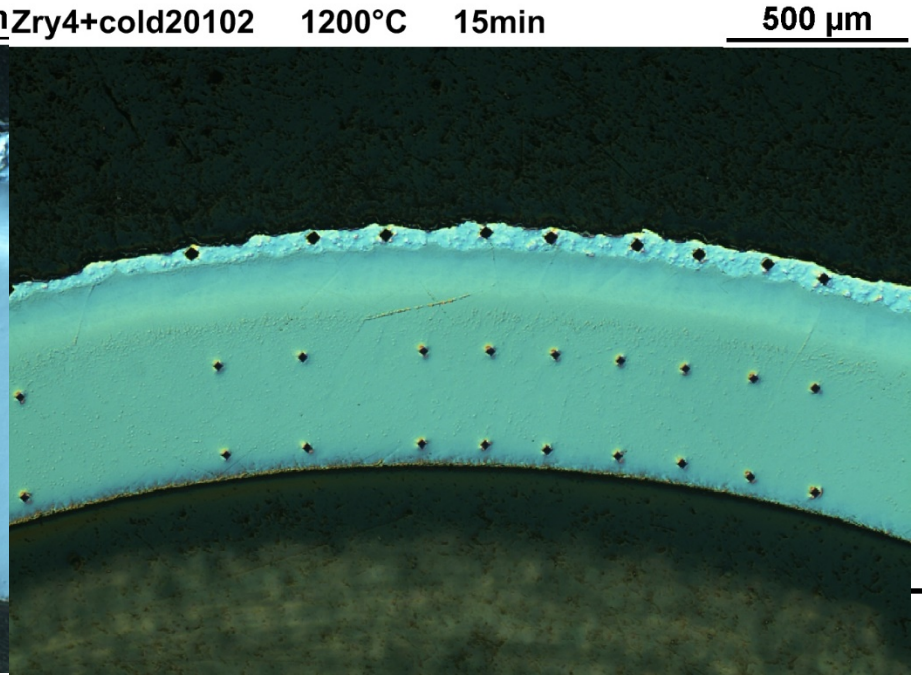
Cr stabilizes beta-Zr even with high O concentration = there is no clear alpha-Zr but hardness considerably increases




TCr2012 1200°C 5min
100 µm
19,936 µm
82,524 µm


Zry420101 1200°C 5min
100 µm
73,252 µm
103,387 µm


Zry420101 1200°C 5min
200 µm
28,744 µm
74,179 µm
108,487 µm

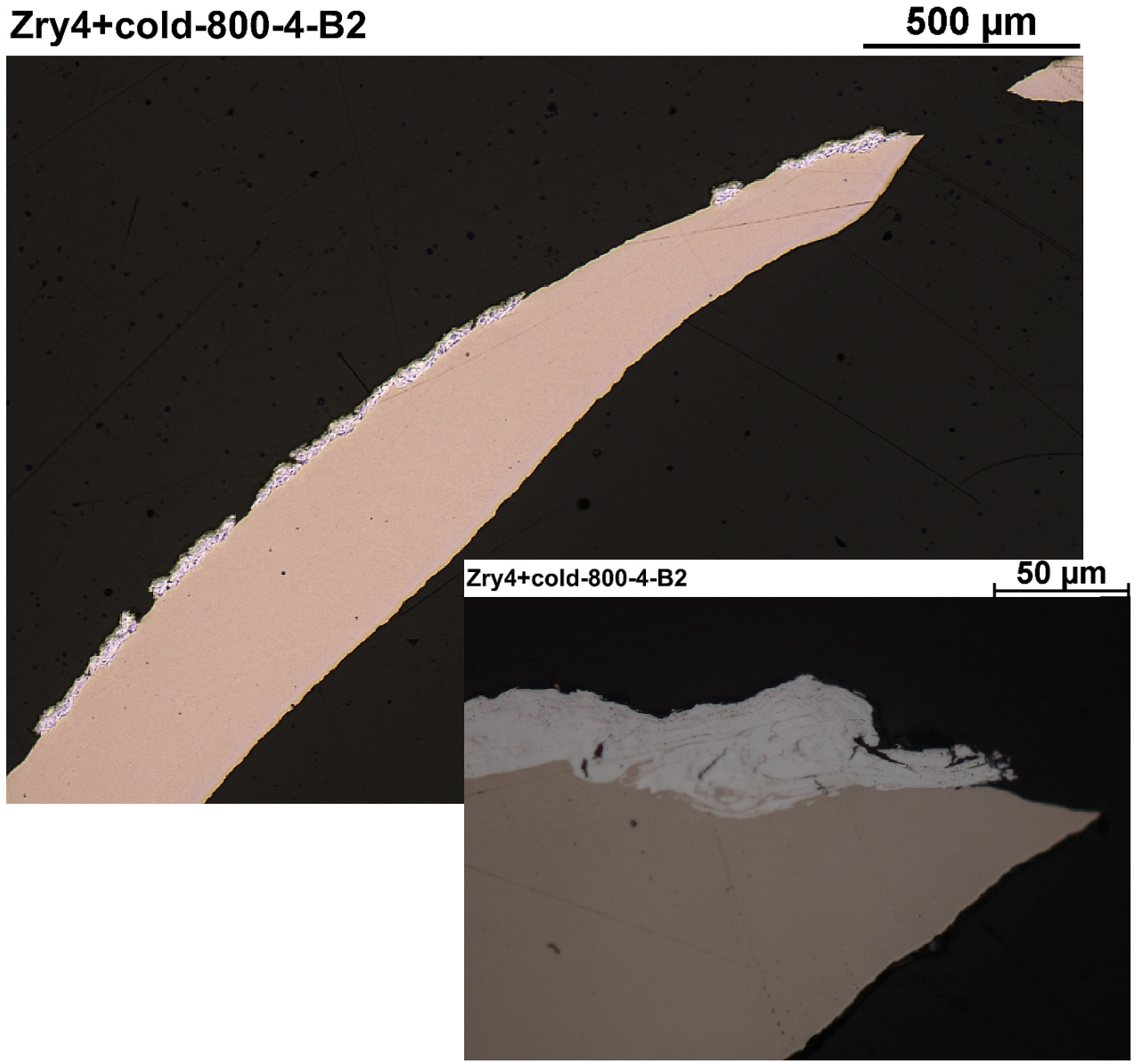

Zry4+cold20102 1200°C 15min
500 µm

Hydrogen

- Segments tested using IGF method (G8 Galileo analyzator: Bruker)
- Coating locally lost its protective behavior – local H increase

ID	WG-exp (mg/dm²)	H (wppm)
Cr 5 min	521	12; 12
Cr 15 min	880	100;107;116
Zr 5 min	1502	7.5; 7.5
Zr 15 min	1931	6.5; 6.1; 8.9

- H-increase after coating cracks (burst tests) – see our 2019 TopFuel paper = "hydrogen pump"



Summary

- Coated cladding materials are currently the main near-term ATF candidate of fuel vendors (Cr-based)
- Cold spray method used to produce samples with Zry-4 (3 CS types) – commercial CS optimized with surface treatments
  - Unlike PVD, interferes with substrate but does not provide substantial structural function
- Normal operation
  - Long-term corrosion – low weight gains; stable oxide several microns thick
  - CRUD deposition – comparable to uncoated Zr but depends on the chemistry and exact surface conditions
  - RCT – methodology questionable but at RT CS coated worse
- Ballooning + burst – considerable improvement
  - Thick coating without polishing
  - Expected lower benefits for commercial CS coating
- High-temperature steam oxidation
  - WG is significantly lower then for uncoated, but the results are influenced because of uncoated endplugs
  - CS-coated at 1200°C/ 15min: the coating locally lost its protective behavior, oxidation was connected with higher hydrogen absorption
  - Lower PQD than uncoated after the same exposition
- Hydrogen – still unresolved for normal operation (H-pickup) and issues at high temperature (hydrogen pump with failed coating)

CTU
CZECH TECHNICAL UNIVERSITY IN PRAGUE

Acknowledgement



COATED CLADDING BEHAVIOUR DURING HIGH-TEMPERATURE TRANSIENTS

Adéla Chalupová
CTU in Prague, V Holešovičkách 2, Praha 8, 18000, Czech Republic, chaluade@fjfi.cvut.cz

Jakub Krejčí
UJP PRAHA a.s., Nad Kamínkou 1345, Praha-Zbraslav, 15610, Czech Republic, krejci@ujp.cz

Ladislav Cvrček
CTU in Prague, Karlovo náměstí 13, Praha 2, 121 35, Czech Republic, ladislav.cvrcek@fs.cvut.cz

Martin Ševeček
CTU in Prague, V Holešovičkách 2, Praha 8, 18000, Czech Republic martin.sevecek@fjfi.cvut.cz

Vojtěch Rozkošný
UJP PRAHA a.s., Nad Kamínkou 1345, Praha-Zbraslav, 15610, Czech Republic, rozkosny@ujp.cz

Antonín Přibyl
UJP PRAHA a.s., Nad Kamínkou 1345, Praha-Zbraslav, 15610, Czech Republic

Patricie Halodová
Research Centre Rez, Hlavní 130, Husinec-Řež, 25068, Czech Republic, patricie.halodova@cvrez.cz

Petra Gávelová
Research Centre Rez, Hlavní 130, Husinec-Řež, 25068, Czech Republic, petra.gavelova@cvrez.cz

Severe nuclear accidents in past decades highlighted the potential threat from radiation release due to the physical and chemical degradation of nuclear reactor core once the local environment changes from normal operating conditions to design-basis accident scenario or design extension conditions. In response to the recent events at Fukushima Dai-ichi in 2011, investigation of core degradation processes and mainly nuclear fuel behaviour during accident transitions came to the fore. The concept of accident-tolerant fuels (ATF) has been proposed and widely investigated. ATF should tolerate the loss of active cooling in the core for a considerably longer period and up to higher temperatures than current Zirconium-based cladding system. There are many ATF concepts under development. The contribution is focused on one of the near-term approaches - the modification of the surface of existing Zirconium alloy claddings by a protective coating. A set of experiments of chromium and chromium nitride-based PVD and Cold Spray coated cladding concept was conducted at UJP PRAHA a.s.. Thermomechanical tests were designed to understand the cladding deformation and the burst condition during the LOCA phenomena.

Experiments were performed with the reference material (Zr1%Nb and Zircaloy-4) as well as coated specimens. The coatings were deposited on outer surfaces of samples either by magnetron sputtering or by Cold Spray deposition method. Pure chromium, multicomponent chromium nitride and chromium (CrN+Cr) and multi-layer chromium nitride/chromium coating (CrN/Cr) were chosen to be tested. In order to characterize the thermomechanical behaviour of fuel cladding during the LOCA transients, several burst tests were carried out. The experiments were made with several temperature levels between 600 and 1100°C and constant inner pressure from 1 to 10 MPa, in an argon environment.

Presented results show the influence of studied coatings on high-temperature cladding creep and related phenomena such as ballooning size, time to burst and cracking of the coating. There are many benefits related to coating usage such as reduction of the ballooning and prolongation of time to burst. Furthermore, oxidation from the outer side of the coating is reduced and hydrogen release is limited. Nevertheless, some negative effects were identified as well. The coating may be connected with larger opening size, the hydrogen content in the substrate is higher due to oxidation through cracks and the local mechanical properties can be deteriorated due to Cr diffusion into the substrate in the cracked areas.


TOSHIBA

Coated Cladding Behaviour During High–Temperature Transients

A. Chalupová [1,2], J. Krejčí [1], V. Rozkošný [1], A. Přibyl [1], J. Šustr [1], F. Manoch [1], J. Sýkora [1], M. Ševeček [2], L. Cvrček [2], P. Halodová [3], P. Gávelová [3]

[1] UJP PRAHA a.s., [2] CTU in Prague, [3] Research centre Rez

25th International QUENCH workshop, Karlsruhe

October 22-23, 2019

Presentation outlines

Centrum výzkumu Řež s.r.o.
Research Centre Řež

UJP PRAHA

Czech Technical University in Prague

IAEA



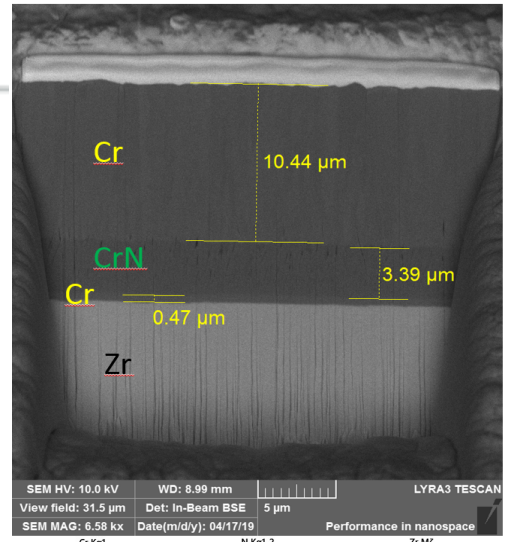
Material and coatings

- Substrates + deposited coatings:
  - Zr-1%Nb (⌀9.1 mm) + PVD: Cr (15.3µm)
  - Zr-1%Nb (⌀9.1 mm) + PVD: CrN/Cr (17.6µm)
    CrN+Cr (16.7µm)
  - Zry-4 (⌀9.5 mm) + Coldspray: Cr (20-100µm)
- Coating deposition: CTU in Prague
  - (Reactive) Magnetron Sputtering (RMS/MS)
  - Hauser Flexicoat 850

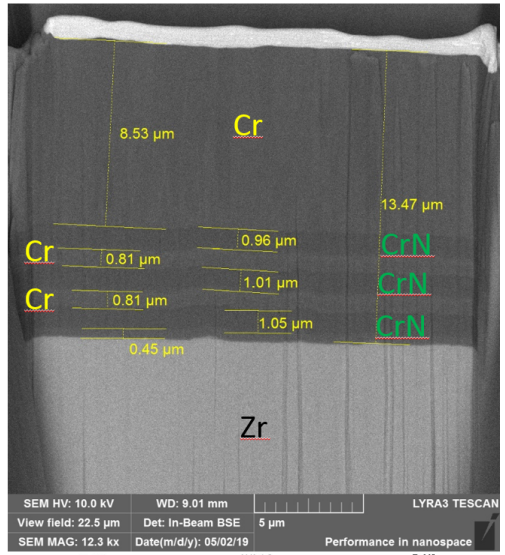


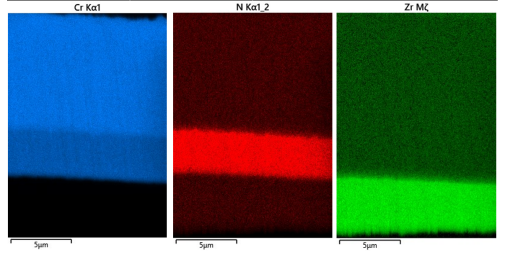
Coating	Cr	CrN+Cr	CrN /Cr
Layer 1: Cr [µm]	**15.3**	**11.4**	**10.8**
Layer 2: CrN [µm]	-	**5.3**	**1.6**
Layer 3: Cr [µm]	-	-	**1.2**
Layer 4: CrN [µm]	-	-	**1.2**
Layer 5: Cr [µm]	-	-	**1.0**
Layer 6: CrN [µm]	-	-	**1.3**
Layer 7: Cr [µm]	-	-	**0.6**
Total	**15.3**	**16.7**	**17.6**

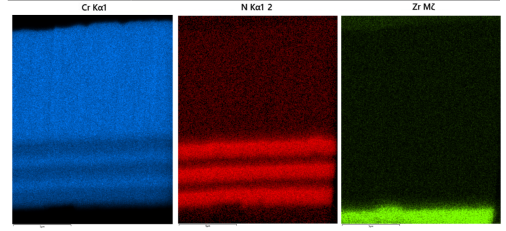
CrN+Cr (double-layer)

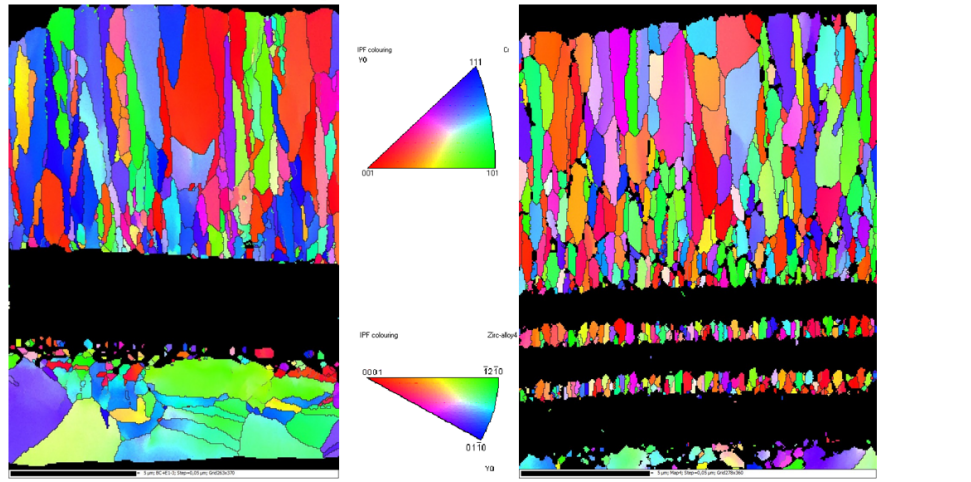


CrN/Cr (multi-layer)



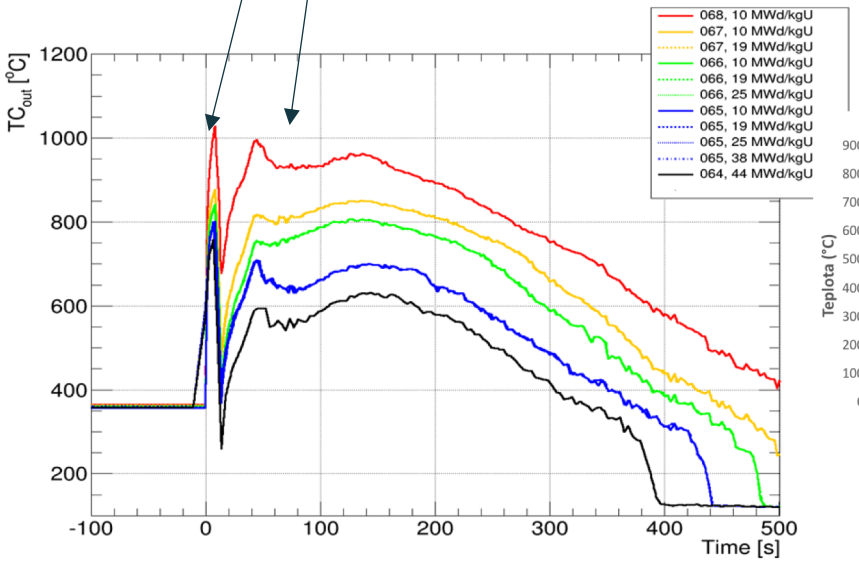


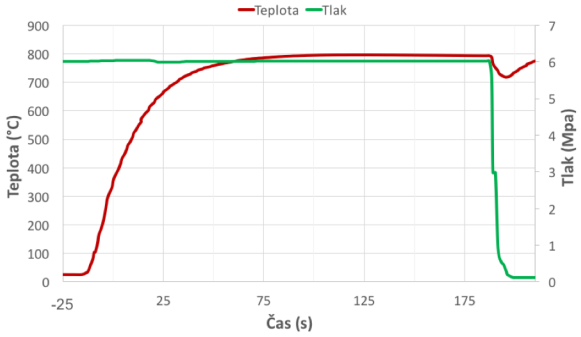




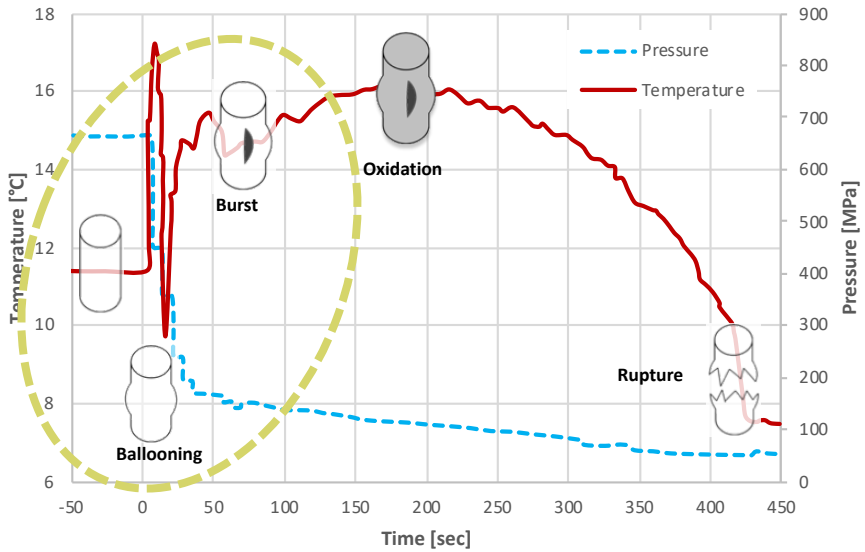
Burst test

- Resistance furnace, Ar atmosphere, RAMP test
- Exposition of reference as well as coated specimen
- Exposition:
  - pressure = 1-10 MPa
  - 1. peak LOCA (1100 °C, low inner pressure)
  - 2. peak LOCA (800 °C, high inner pressure)



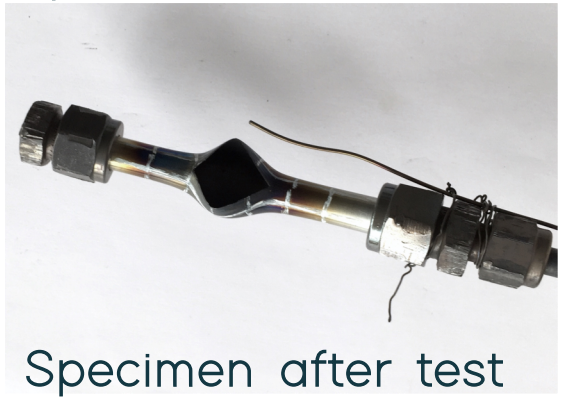


The course of the experiment





Specimen before test



Specimen after test



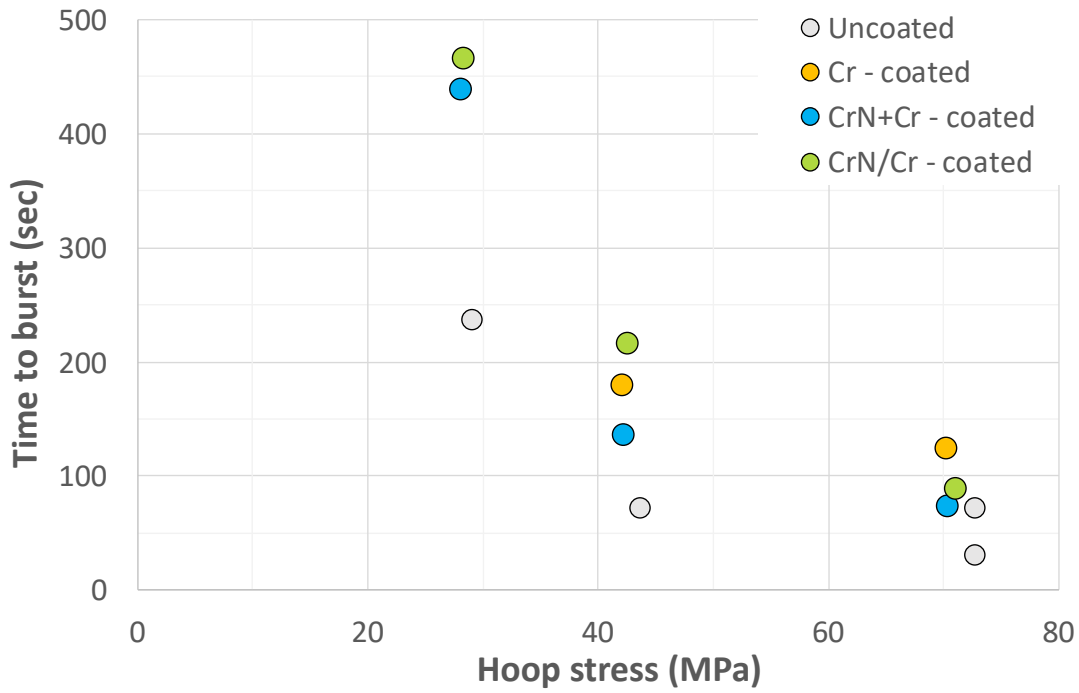
Resistance furnace

Time to burst

- Time to burst longer for coated specimens

Time to burst (Exposition 1100 °C)				
	Reference	Cr	CrN + Cr	CrN/Cr
2 MPa	**14 s**	**34 s**	**23 s**	**22 s**
4 MPa	**13 s**	**13s**	**18 s**	**20 s**

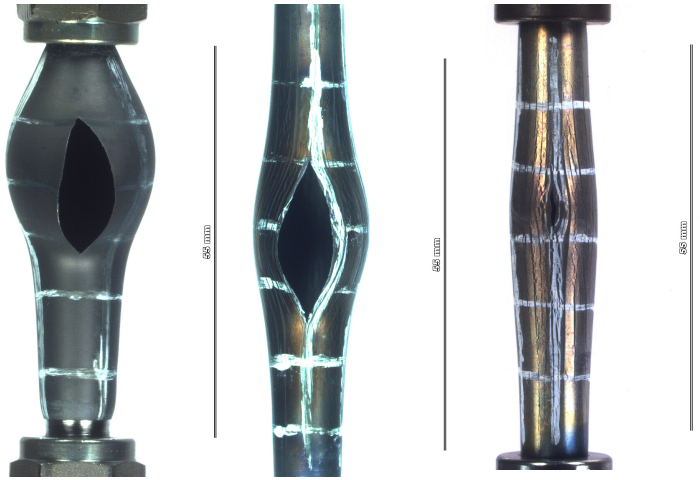
Time to burst (Exposition 800 °C)				
	Reference	Cr	CrN + Cr	CrN/Cr
4 MPa	**236 s**	**-**	**437 s**	**463 s**
6 MPa	**71 s**	**178 s**	**135 s**	**214 s**
10 MPa	**30 s**	**122 s**	**73 s**	**88 s**



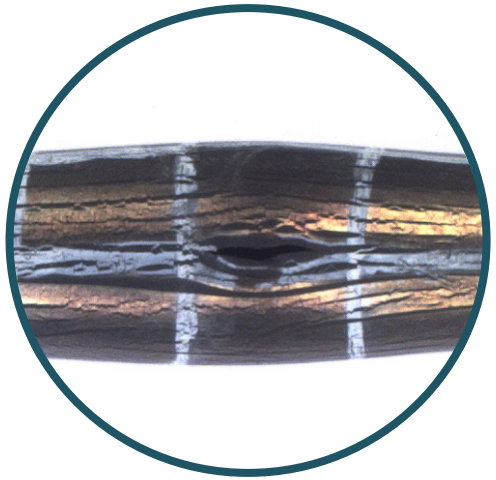
800 °C

Deformation, 800 °C

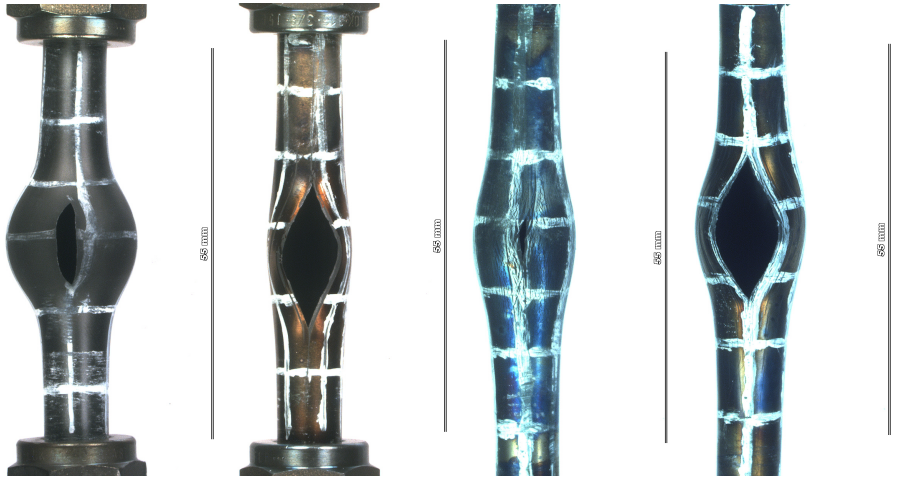
4 MPa



Zr-1%Nb CrN+Cr CrN/Cr+Cr

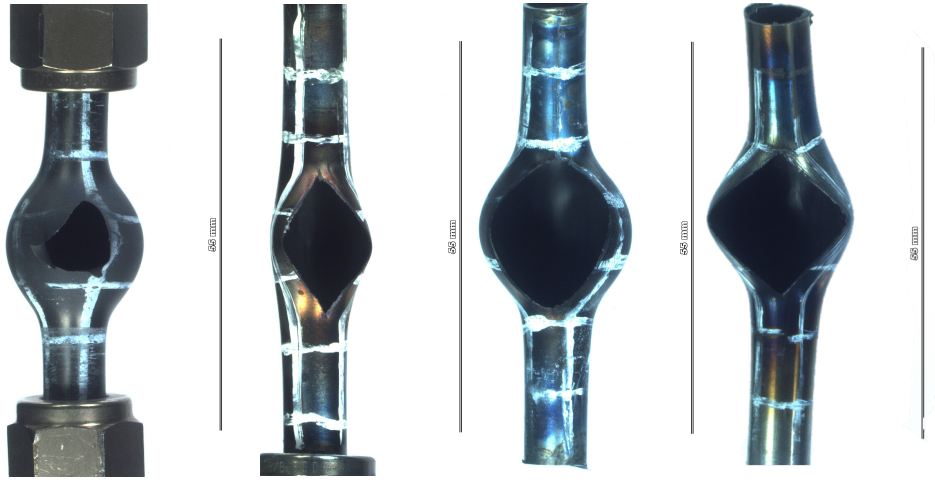


6 MPa



Zr-1%Nb Cr CrN+Cr CrN/Cr+Cr

10 MPa

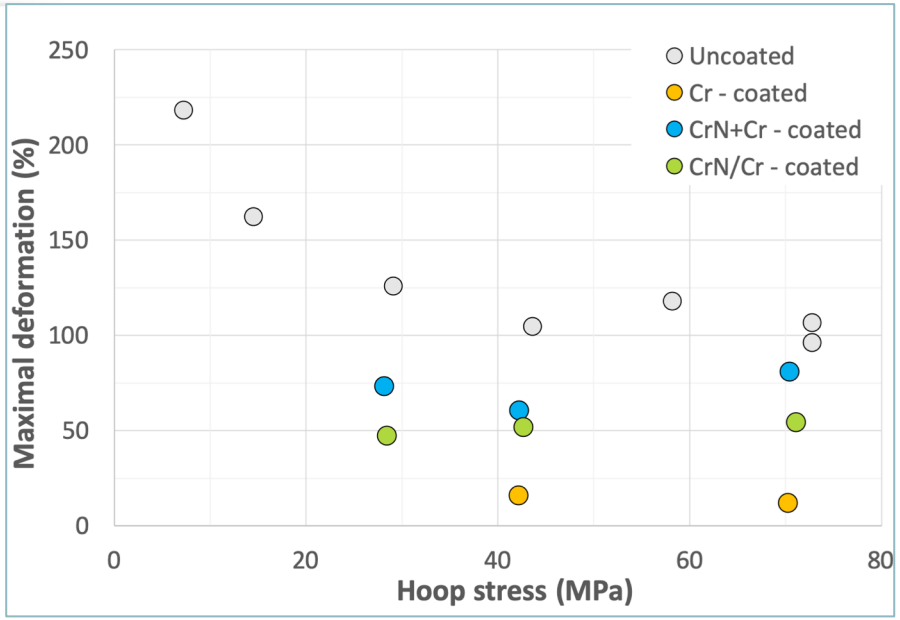


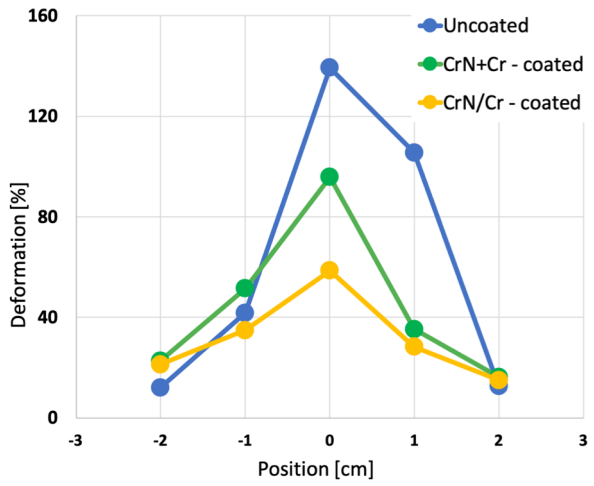
Zr-1%Nb Cr CrN+Cr CrN/Cr+Cr

Deformation, 800 °C

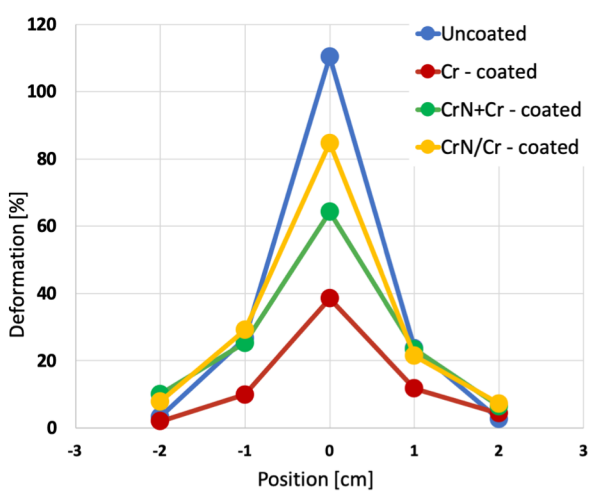
- Ballooning notably smaller for coated specimens
- Smallest deformation for metal Cr-coated

Maximal deformation (Exposition 800 °C)						
	Reference	Cr	CrN + Cr	CrN/Cr + Cr	Zry-4	Coldspray
4 MPa	**126%**	**-**	**73%**	**47%**	**178%**	**15%**
6 MPa	**105%**	**16%**	**61%**	**52%**	**-**	**-**
10 MPa	**107%**	**12%**	**81%**	**54%**	**-**	**-**

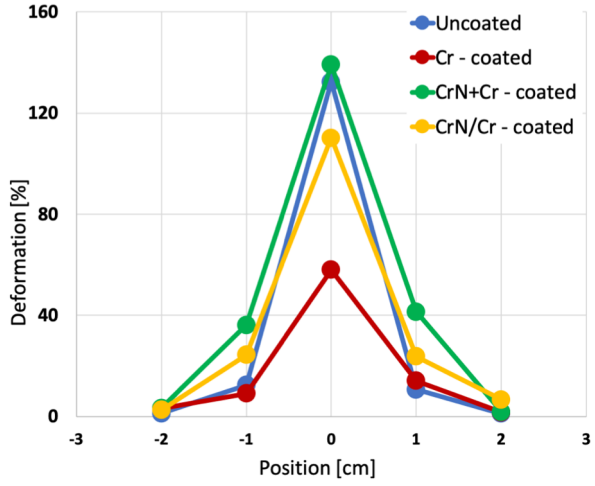




4 MPa



6 MPa

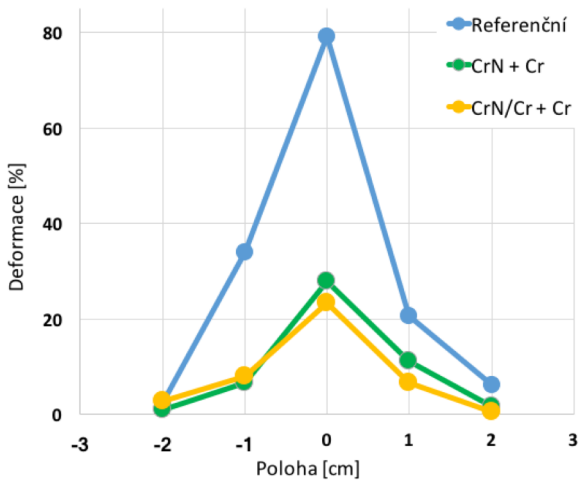


10 MPa

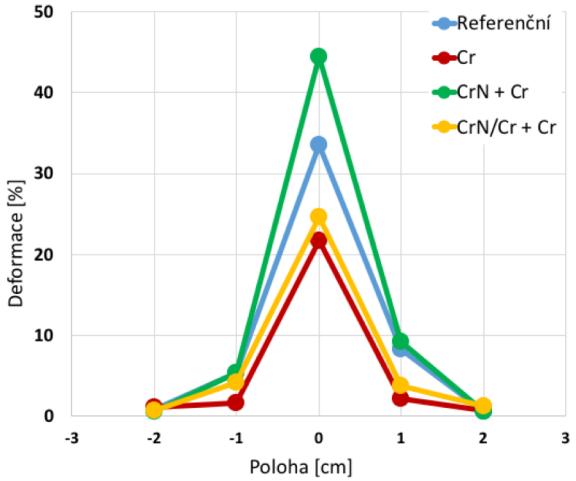
Deformation, 1100 °C

- Smaller for coated specimens

Maximal deformation (Exposition 1100 °C)				
	Reference	Cr	CrN + Cr	CrN/Cr + Cr
2 MPa	**78%**	**6%**	**28%**	**23%**
4 MPa	**34%**	**11%**	**44%**	**14%**

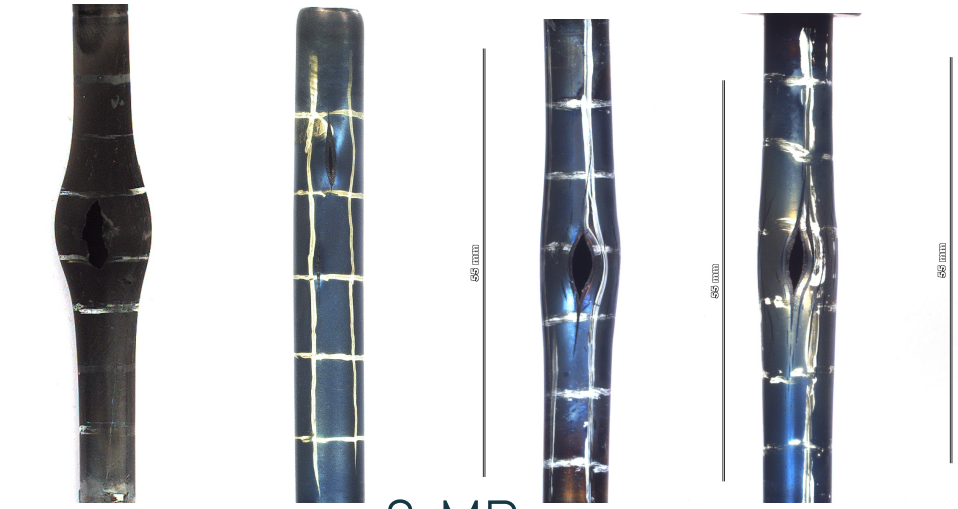


2 MPa



4 MPa

Zr-1%Nb | Cr | CrN+Cr | CrN/Cr+Cr



2 MPa

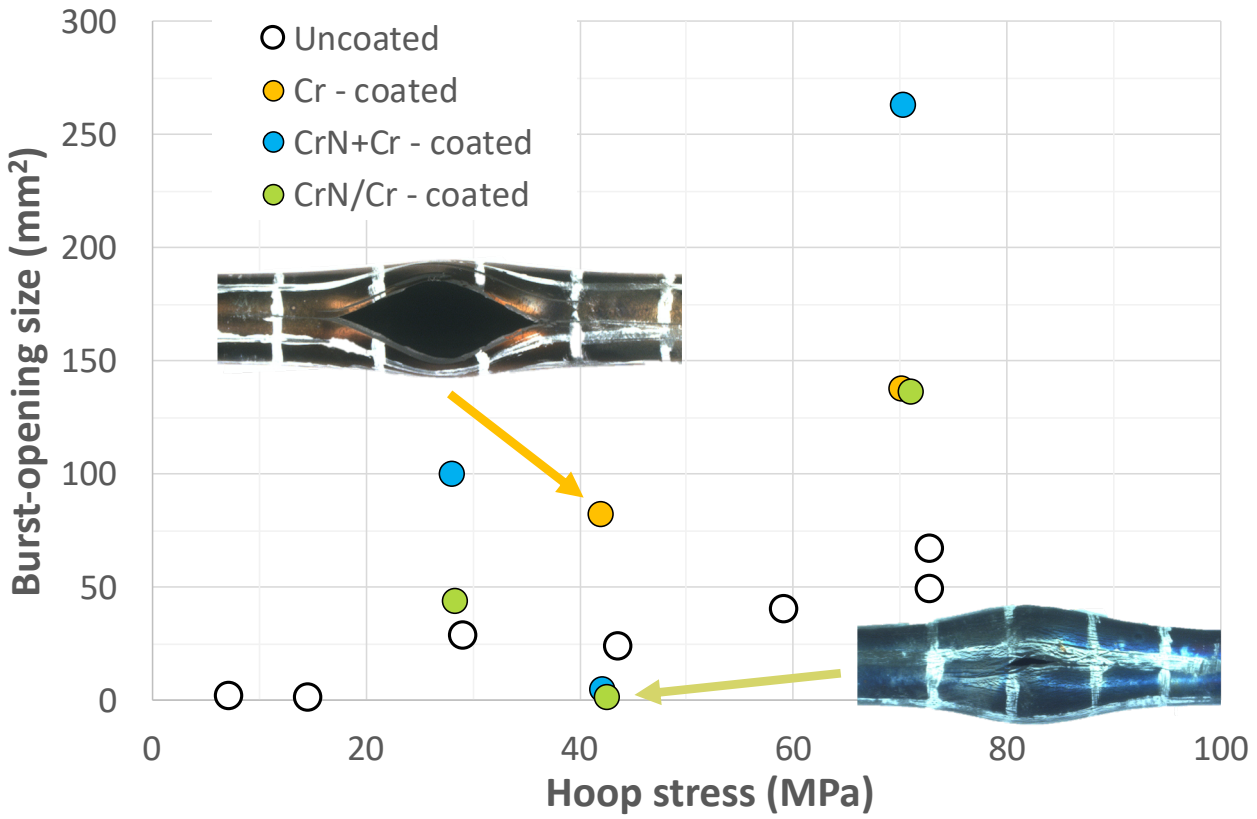


4 MPa

Burst opening size

Burst opening size (Exposition 800°C)				
	Reference	Cr	CrN + Cr	CrN/Cr + Cr
4 MPa	**28 mm²**	**-**	**99 mm²**	**36 mm²**
6 MPa	**24 mm²**	**81 mm²**	**4 mm²**	**103 mm²**
10 MPa	**49 mm²**	**137 mm²**	**262 mm²**	**212 mm²**

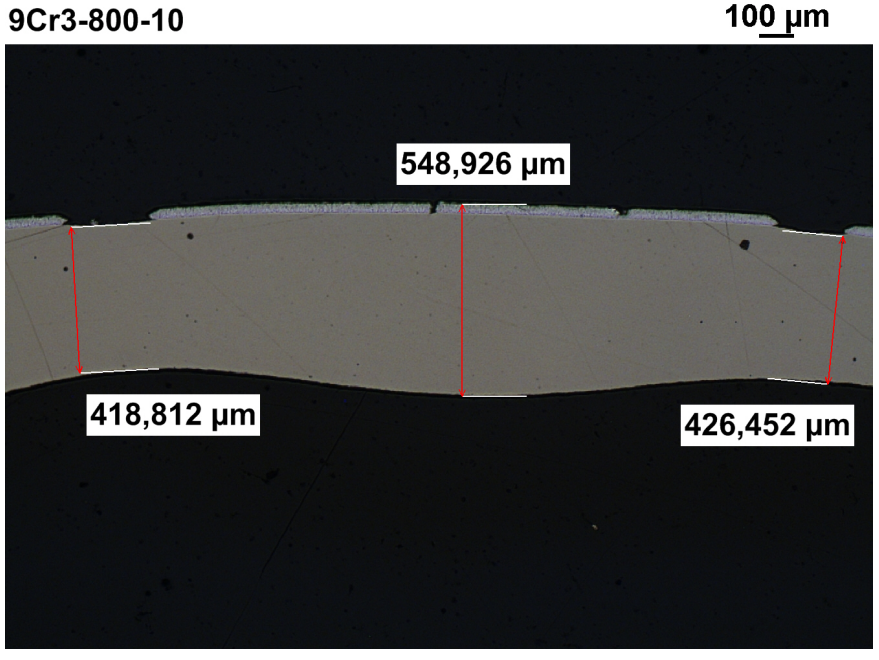
Burst opening size (Exposition 1100°C)				
	Reference	Cr	CrN + Cr	CrN/Cr + Cr
2 MPa	**15 mm²**	**2 mm²**	**16 mm²**	**9 mm²**
4 MPa	**28 mm²**	**23 mm²**	**28 mm²**	**24 mm²**

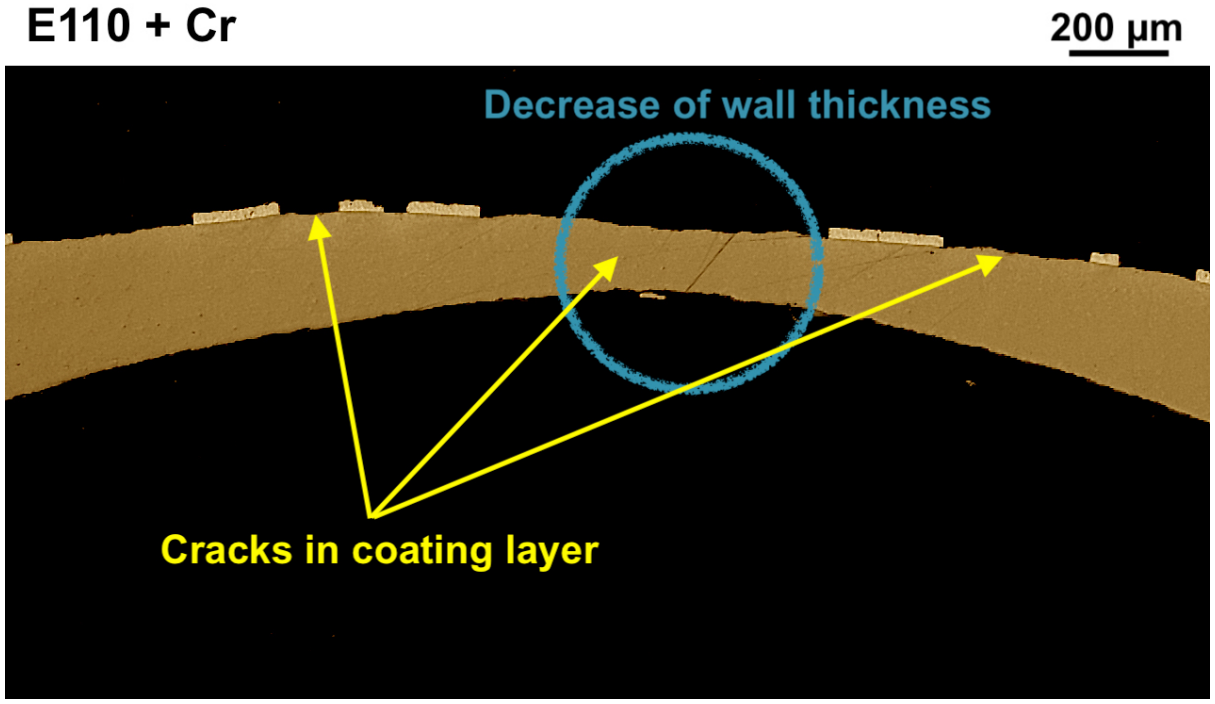


800 °C

Microstructure analysis

- Condition of coating
  - Cracking in coating layer (Extent of cracking corresponds to deformation of the cladding)
- Different Young's modules of Cr and Zr – creep acceleration in areas with damaged coating layer
- Ceramic layers – extensive cracking

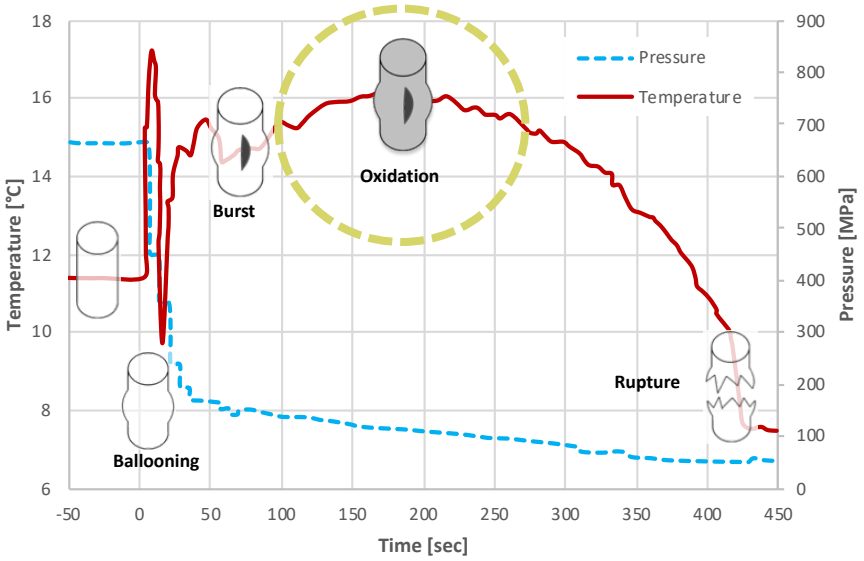




Local decrease in wall thickness in areas with damaged coating layer

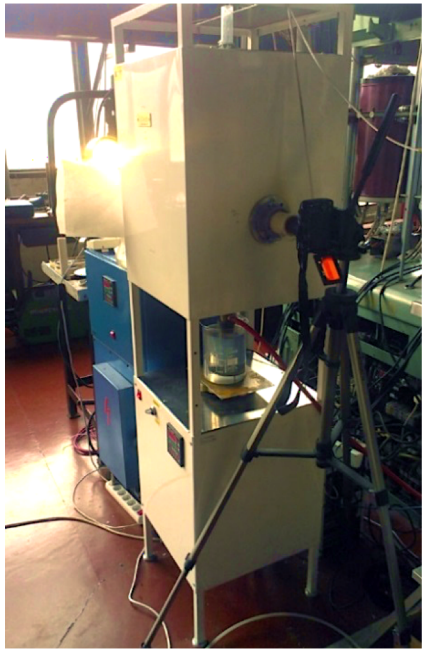
High temperature oxidation

- High temperature oxidation through coating & inner side of the cladding
- Resistance furnace, temperatures above Cr-Zr eutectic point (up to 1700°C)
- Double-side steam
- Temperature measured with welded thermocouple





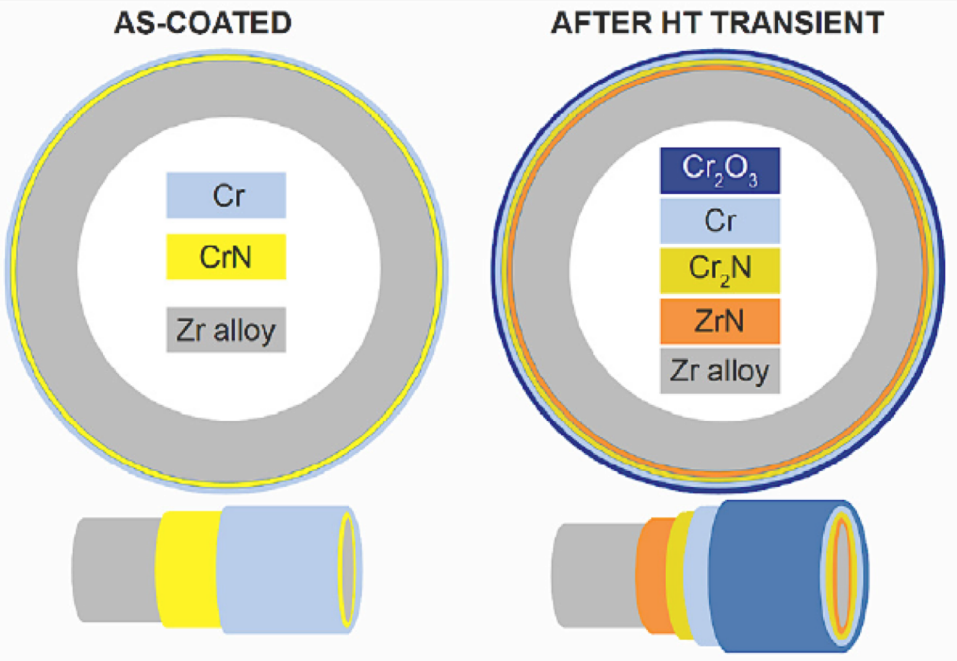
Specimen after test

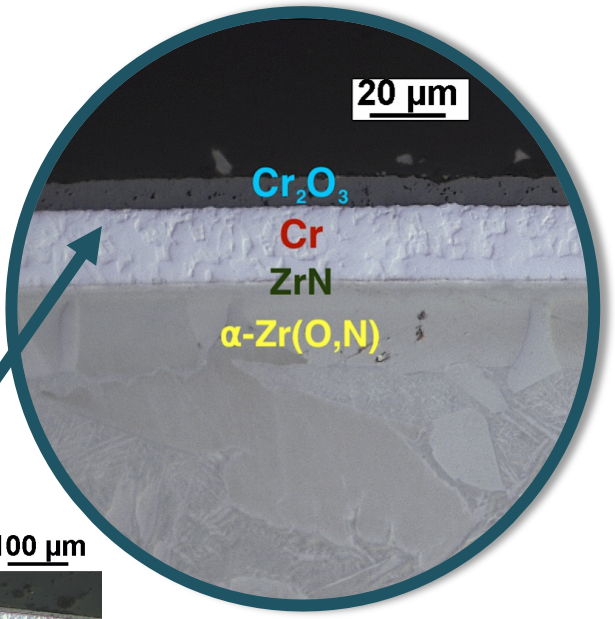


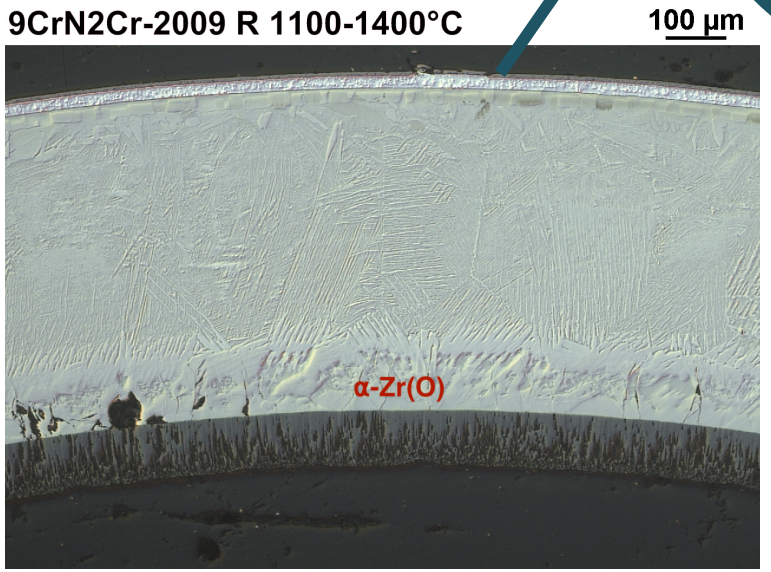
Resistance furnace

Multi-layer concept

- Bottom CrN layer
  - Decomposed during high temperature transient:
  - Stable ZrN formation
  - Prevent Cr diffusion
  - No Cr-Zr melting
- Top Cr – layer
  - Decrease of oxidation rate

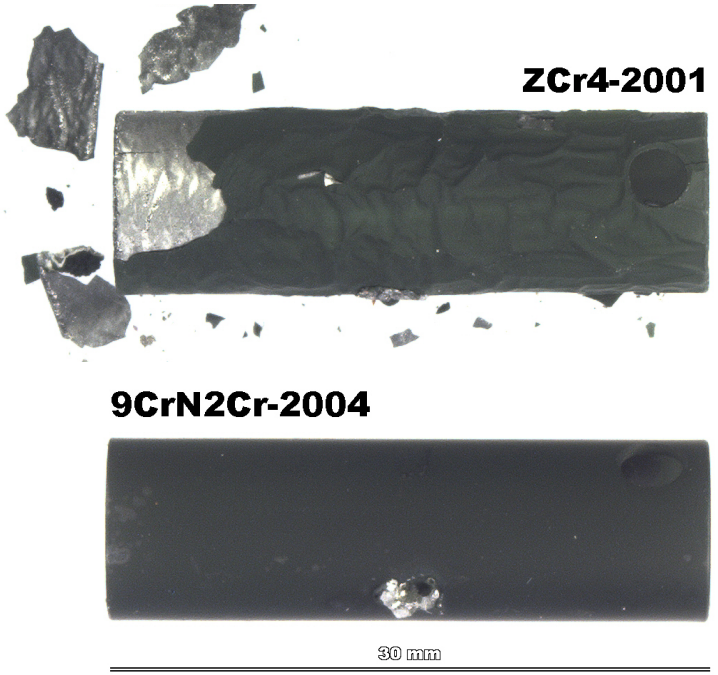






Multi-layer at high temperatures

- Cr coating
  - Wavy green-black oxide layer (Cr-Zr melting)
  - Similar WG to uncoated → no protective behaviour
- CrN+Cr
  - Compact black-green oxide layer
  - Prevents melting → protective behaviour



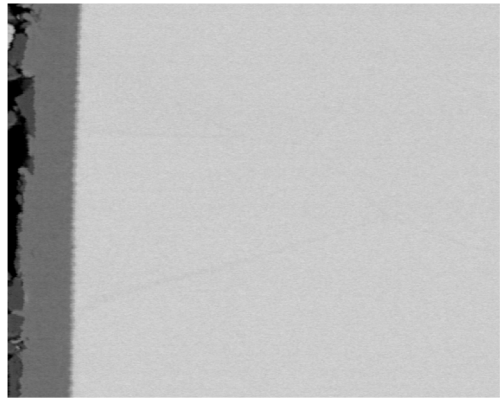
Multilayer at high temperatures					
Sample	Experiment	Temperature [°C]	WG-CP [mg/dm^2]	WG-exp [mg/dm^2]	QUENCH
ZCr4-2001	**IZOT + overshoot**	**1350-1508**	**1486**	**1761**	**cracks**
ZCr4-2002	**IZOT + overshoot**	**1350-1637**	**1217**	**1270**	**cracks**
9CrN2Cr-2002	**IZOT + overshoot**	**1400-1415**	**1316**	**700**	**no failure**
9CrN2Cr-2004	**IZOT + overshoot**	**1500-1579**	**1362**	**815**	**no failure**
9CrN2Cr-2007	**RAMP**	**1100-1300**	**1871**	**965**	**no failure**
9CrN2Cr-2008	**RAMP**	**1100-1350**	**1645**	**830**	**no failure**
9CrN2Cr-2009	**RAMP**	**1100-1400**	**1973**	**1031**	**no failure**

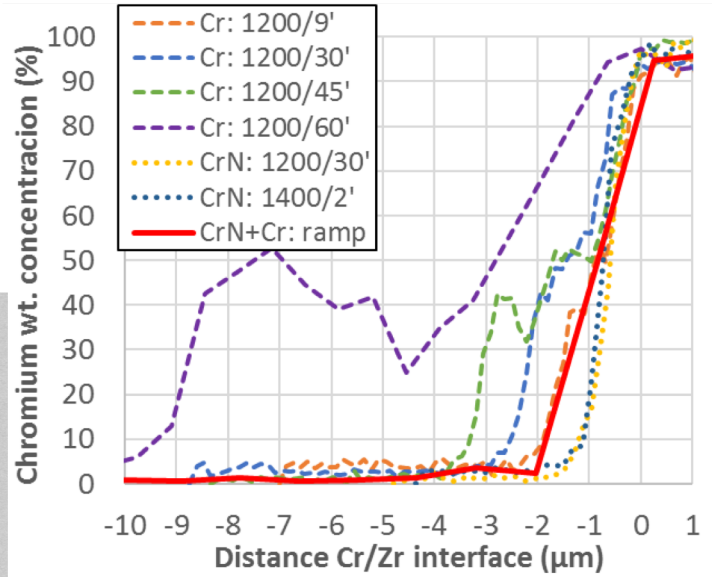
Chromium diffusion

- Measured using SEM/EDS

Chromium coating

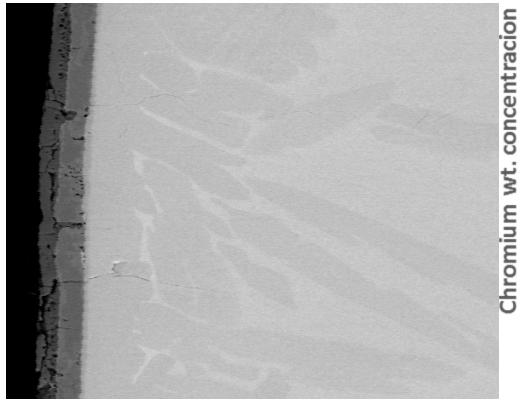
- Chromium diffusion into substrate was observed
- Cr-Zr eutectic can potentially occur
- Chromium stabilizes β-Zr → all diffused oxygen is in β-Zr dissolved → embrittlement for very low WG

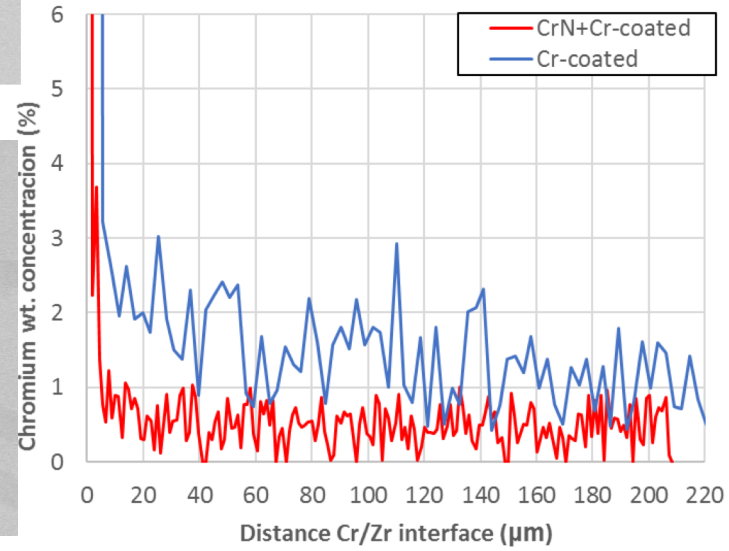




CrN+Cr coating

- Chromium diffusion is reduced
- α-Zr(O,N) is formed → oxygen stays localized in α-Zr(O) → less oxygen in β-Zr is dissolved





Conclusion

Comparison of reference Zr-1%Nb and coated cladding material			
	Cr	CrN + Cr	CrN/Cr + Cr
Time to burst	**Most prolongated (up to 300%)**	**Prolongated**	**Prolongated**
Ballooning size	**Reduction**	**Reduction under low inner pressure, comparable under high inner pressure**	**Reduction under low inner pressure, comparable under high inner pressure**
Burst opening size	**Larger under low inner pressure, comparable under high inner pressure**	**Larger under low inner pressure, comparable under high inner pressure**	**Larger under low inner pressure, comparable under high inner pressure**
Protective behaviour during HT oxidation	**Up to Cr-Zr eutectic point**	**Above Cr-Zr eutectic point**	**-**
Chromium diffusion	**Observed**	**Reduced**	**-**

Acknowledgements

UJP PRAHA, a.s.

J. Krejčí, V. Rozkošný, A. Přibyl, J. Šustr, F. Manoch, J. Sýkora

CZECH TECHNICAL UNIVERSITY IN PRAGUE

M. Ševeček , L. Cvrček

RESEARCH CENTRE REZ

P. Halodová, P. Gávelová

Financial support of this research through ČEZ a.s. company is gratefully acknowledged. Also, this work was supported by the Ministry of Education, Youth and Sport of the Czech Republic, programme NPU1, project No LO1207, National Programme of Sustainability II Project LQ1603 (Research for SUSEN), and IAEA CRP 21065, Technology Agency of the Czech Republic grants No. TH02020477, TH02020691, CZ.2.16/3.1.00/21563.

Acknowledgements

Financial support through IAEA



Date: 20-09-2019

Authors: Dmitrii V. Sidelev*, Egor B. Kashkarov, Maxim S. Syrtanov, Victor N. Kudiyarov, Valery P. Krivobokov

Affiliation: Tomsk Polytechnic University, Tomsk, Russia

Title of the presentation: Chromium coatings deposited by magnetron sputtering for accident tolerant nuclear fuel cladding

Abstract. Chromium coatings can be used as the protection of zirconium alloys from rapid oxidation in the case of loss of coolant accidents (LOCA) in light-water reactors. Magnetron sputtering is a one approach to deposit such coatings. This method has high reproducibility of operation parameters, no droplets in the particle flux, wide range of deposition parameters and coatings can be formed with good adhesion to a substrate. However, the productivity of the magnetron is relatively low, thus new construction of the magnetron diode should be considered to enable the high-rate deposition of Cr coatings onto fuel cladding.

This report is devoted to study the role of the type of magnetron diodes (classical construction and with "hot" target in Fig. 1) in structural properties of Cr films and the influence of thickness and microstructure of Cr films on resistance to oxidation of Cr-coated Zr-1Nb substrates at 1373 K in atmosphere during 20 min. The possibilities to use the magnetron sputtering systems for deposition a thick Cr coatings onto nuclear Zr fuel claddings are discussed.

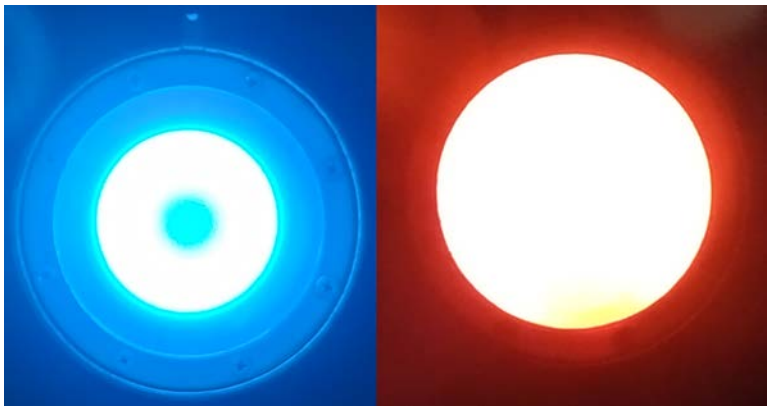


Fig. 1. Photographs of the "hot" Cr target magnetron during the sputtering (left) and after sputtering (right).

The analysis of Cr-coated Zr alloy after oxidation at 1373 K in atmosphere during 20 min reveals following results.

1. Higher Cr concentration, dense and uniform microstructure of coatings are desirable to protect of Zr-1Nb alloy.
2. Oxidation resistance of Zr-1Nb increases with thickness of protective Cr coating.
3. For coating deposition, magnetrons with a large ion fraction in the deposited flow should be used to improve coating microstructure.
4. New designs of magnetron diode can be considered to provide ultra-high deposition rates.

* Corresponding author.


KIT
für Technologie

25th International QUENCH Workshop

TOMSK POLYTECHNIC UNIVERSITY
ТОМСКИЙ ПОЛИТЕХНИЧЕСКИЙ УНИВЕРСИТЕТ

Chromium coatings deposited by magnetron sputtering for accident tolerant nuclear fuel cladding

Dmitrii V. Sidelev*, Egor B. Kashkarov, Maxim S. Syrtanov, Victor N. Kudiyarov, Maya R. Rombaeva

Tomsk Polytechnic University, Tomsk, Russia

22-24 October 2019

Tomsk Polytechnic University



1896 Technological institute for practical engineers **Present**

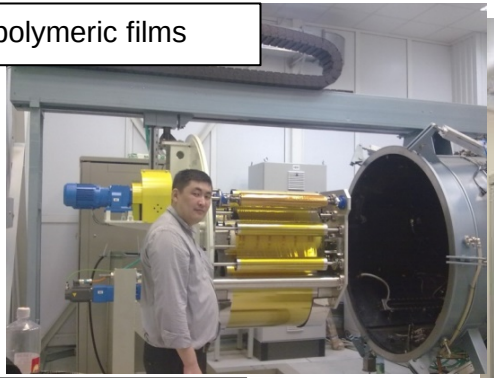
Main directions:

- New industrial technologies
- Energy and energetic systems
- Chemistry
- Material science
- IT technologies
- Nuclear energy and technologies → Weinberg Research Center

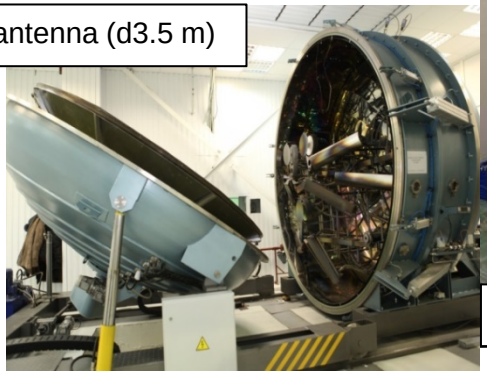
Weinberg Research Center

Focus area - development of new plasma equipment and technologies for material science.

polymeric films



antenna (d3.5 m)





Zr fuel cladding (length 0.5 m)

plasma sources



Zirconium nuclear fuel claddings

Zirconium alloys with Sn, Cr, Fe, Nb dopants are based material of fuel cladding in commercial light-water and pressurized nuclear reactors.

Under extreme condition (LOCA) Zr alloys are intensively oxidized in water steam or hydrogen explosion can be:

$$Zr + 2H_2O \rightarrow ZrO_2 + 2H_2\uparrow + Q. \quad (1)$$

Change of cladding material:
- ceramic (SiC);
- new type of steels;
- double-wall claddings.

Surface modification:
- welding deposition;
- implantation of Me ions.

Deposition of protection coatings:
- metals, nitrides, carbides, multilayer coatings, etc.;
- PVD or CVD methods.

Coating material and method

Requierements for coating:

- oxidation resistance at temperatures ~ 1073 ... 1673 K;
- hydrogen sorption rate is lower than for Zr alloys;
- resistance to cracking;
- adhesive strength;
- low diffusion coefficients in zirconium alloys.

→ **Cr-based coatings**

Requirements for deposition method:

- low heat flux - less than 0.5 ... 1.5 W /cm^2;
- no droplet fraction in deposited flow;
- uniformity of coating thickness - ± 5%;
- the ability for automate the process and its control;
- high productivity ~ 5-20 microns/h.

→ **Magnetron sputtering**

Magnetron sputtering

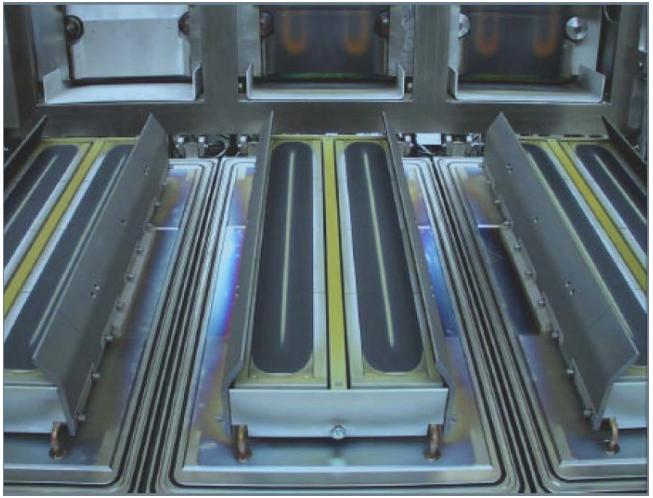


Fig. 1. Magnetron diode.

Parameters:

- atmosphere – inert (Ar) or reactive (Ar + N_2/O_2/C_2H_2);
- operation pressure – 0.1..0.5 Pa;
- deposition rate – 2…5 μm/h;
- magnetron length – substrate length x 125%;
- cathode materials – metals, alloys, etc.

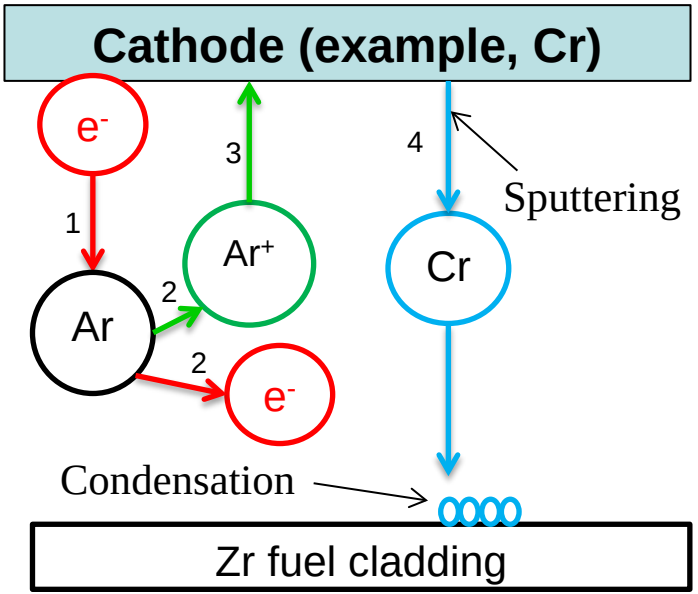


Fig. 2. The scheme of magnetron sputtering.

Equipment for experiments

Substrate – Zr-1%Nb.
Size – 25x25x2 mm^3.
Pretreatment: grinding and polishing (P4000) → degreasing → drying.





Fig. 3. The laboratory installation for coating deposition.

Coating deposition

Loading the samples into the chamber and pumping ($2x10^{-3}$ Pa) – 1 hour

↓

Etching of Zr surface - 10 min

↓

Coating deposition by single magnetron (or by multi-cathode system) – 1…6 hours

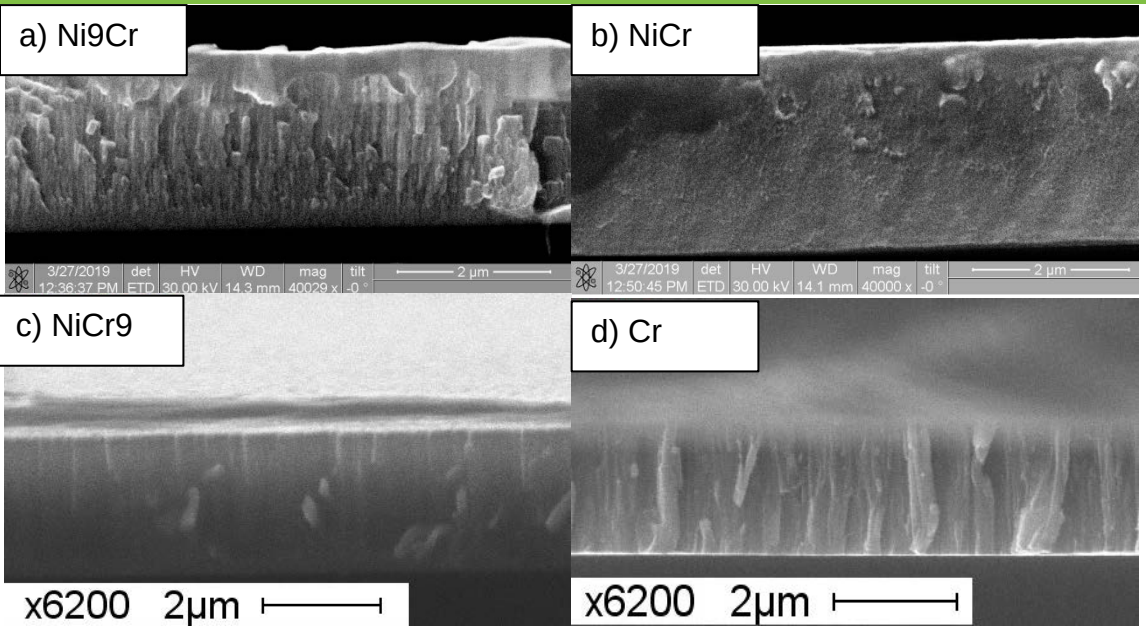
↓

Exposure of the samples in vacuum – 30 min

↓

Opening the chamber and pull of the samples – 10 min

Ni-Cr coatings



Thickness – **2,1±0,1 μm**.

Coating parametrs

Sample	*t*, min	Ni / Cr
Ni9Cr	111	83/17
NiCr	119	55/45
NiCr9	143	17/83
Cr	145	0/100

t – deposition time, Ni/Cr – ratio of Ni to Cr in the coatings (in at.%)

Fig. 4. Cross-section of the as-deposited coatings: a – Ni9Cr; b – NiCr; c – NiCr9; d – Cr.

Resistance to hydrogen uptake

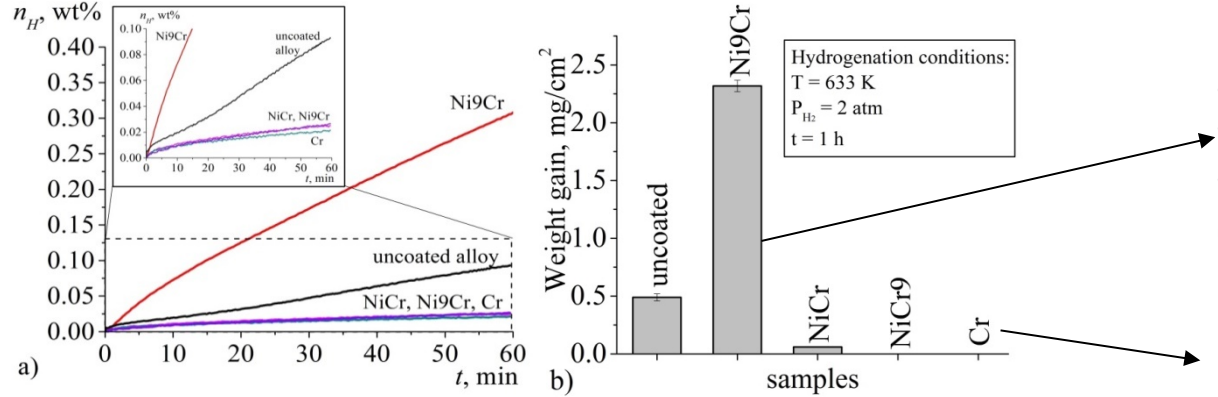


Fig. 5. The hydrogen sorption kinetics (a) and weight gain (b) at 633 K.

- The Ni-Cr coatings with high Ni concentration do not protect from hydrogen uptake. As the result - hydrogen embrittlement and destruction.



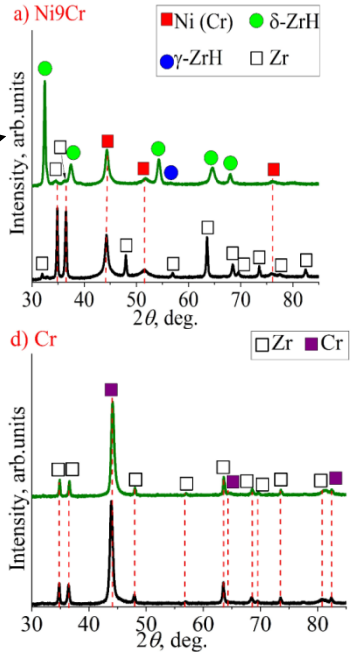
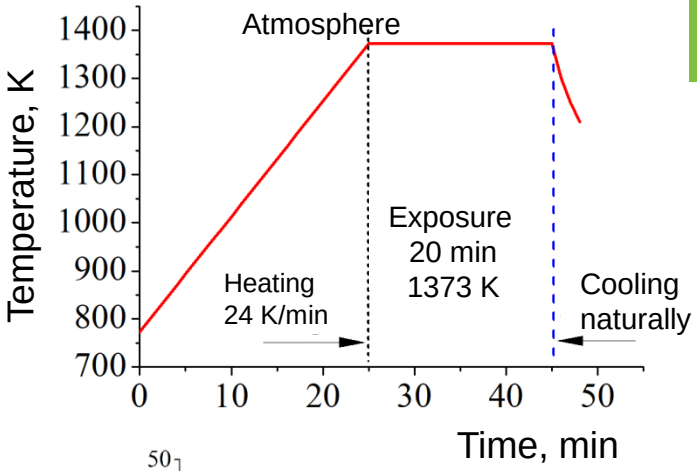


Fig. 6. X-ray spectra of as-deposited coatings (black) and after hydrogenation (green).

High-temperature oxidation (1)



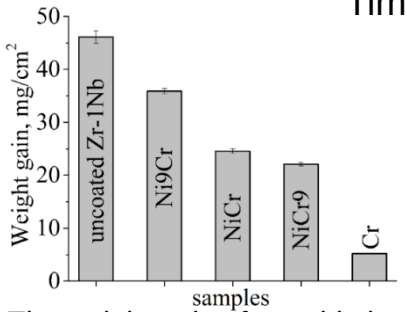
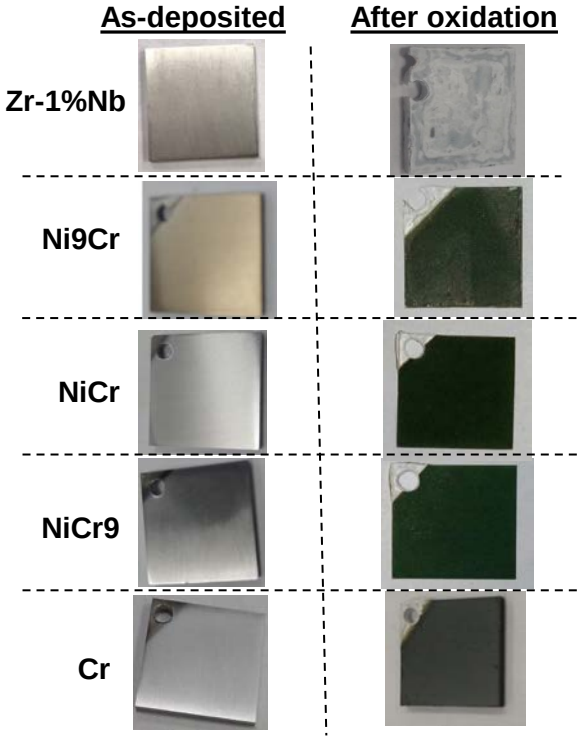
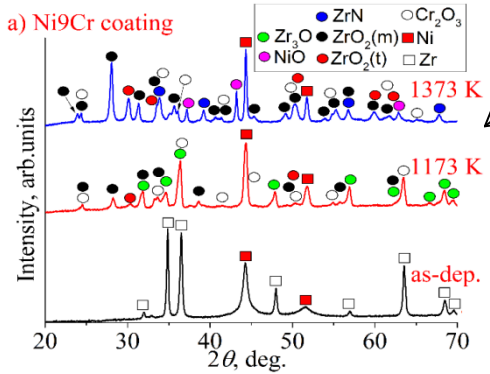


Fig. 7. The weight gain after oxidation at 1373 K.



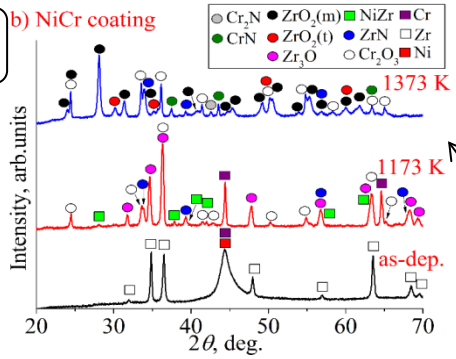
- The increase of Cr concentration in the coatings results in the decrease of weight gain (35.9 → 5.2 mg/cm^2).

Resistance to high-temperature oxidation (2)



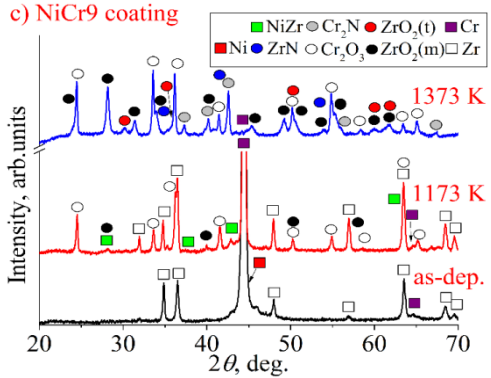
NiO protection layer
Zr oxidation

Ni/Cr in at.%
83/17



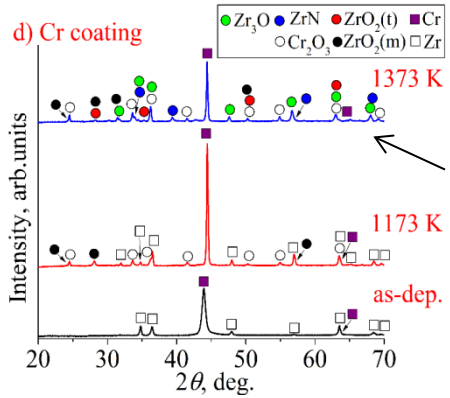
Ni/Cr in at.%
55/45

Diffusion of Ni to Zr
Formation of NiZr
Solution of Ni into Zr
Cr_2O_3 protection layer
Zr oxidation



Similar behaviour

Ni/Cr in at.%
17/83



Cr_2O_3 protection layer
Zr oxidation

Cr in at.%
100

Resistance to high-temperature oxidation (3)

Phase [vol.%]	Coating			
	Ni9Cr	NiCr	NiCr9	Cr
Cr_2O_3	17.0	42.3	64.5	30.9
NiO	7.5	-	-	-
ZrO_2 (m)	45.8	46.5	27.8	4.8
ZrO_2 (t)	8.9	3.2	1.9	1.1
Ni	15.4	-	-	-
ZrN	5.4	2.8	2.0	9.0
CrN		4.0	-	-
Cr_2N	-	1.2	3.8	-
Cr	-	-	-	42.8
Zr_3O	-	-	-	11.4
$\sum ZrO_x$	54.7	49.7	29.7	17.3

- Ni diffusion from the coating to alloy can **negatively influence** on oxidation resistance due to formation of structural defects.
- Cr_2O_3 layer has better protection properties.
- Cr coating does not full oxidized (α-Cr – **42.8 vol.%**), but no protect Zr from oxidation in total. This is due to the columnar microstructure of the deposited Cr coating, which leads to oxygen diffusion along the grain boundaries.

Resistance to high-temperature oxidation (4)

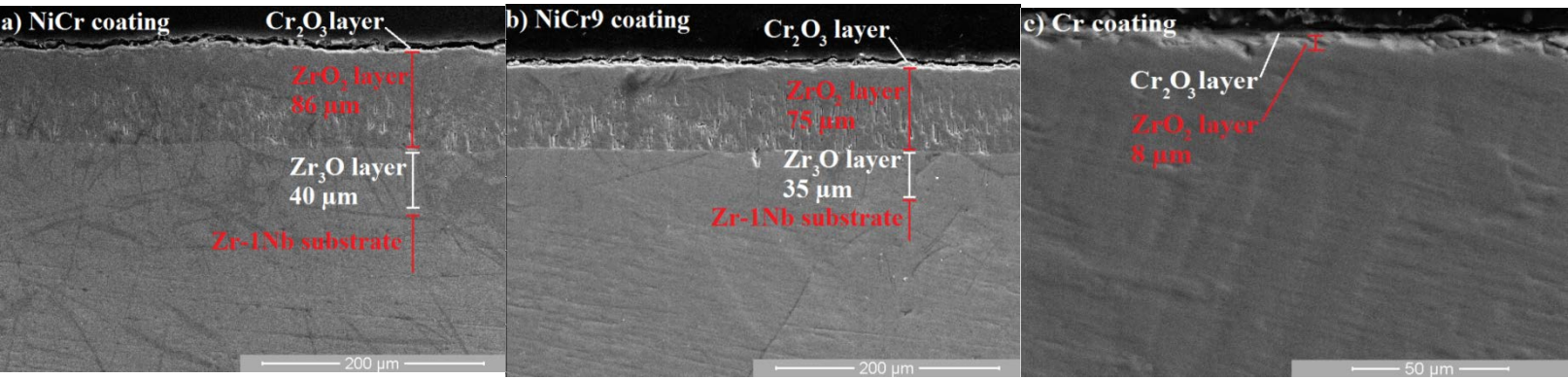


Fig. 10. Cross-section of the samples after oxidation at 1373 K: a – NiCr; b – NiCr9; c – Cr.

- Oxidation – uniform.
- Thickness of oxide layer decreases from **86 μm** (NiCr coating) to **8 μm** (Cr coating).

Mechanical properties of Ni-Cr coatings

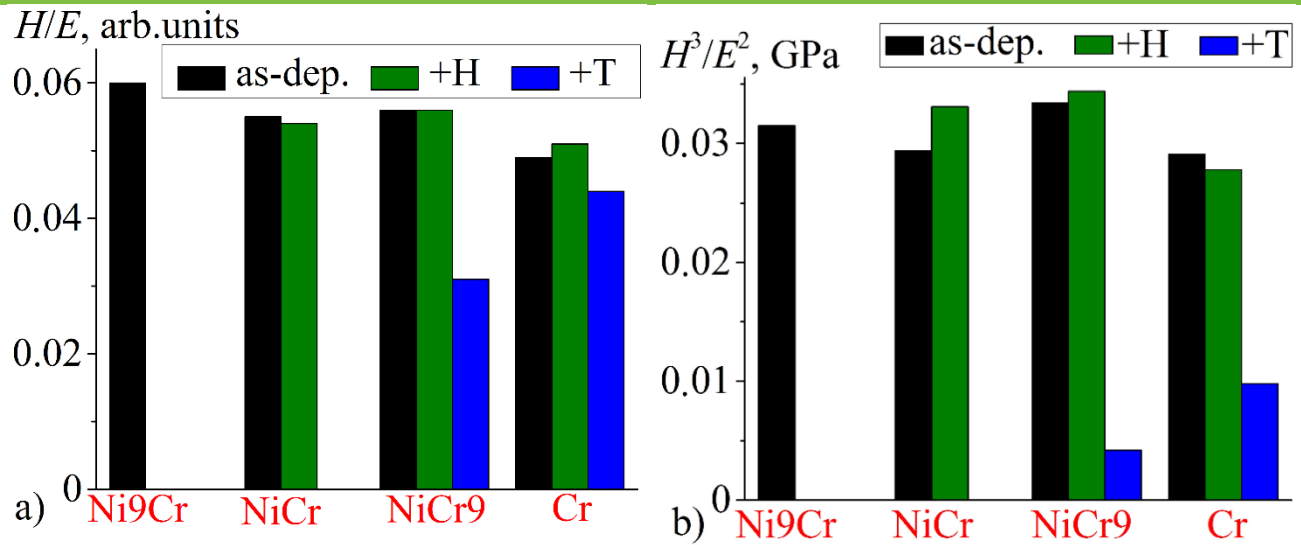


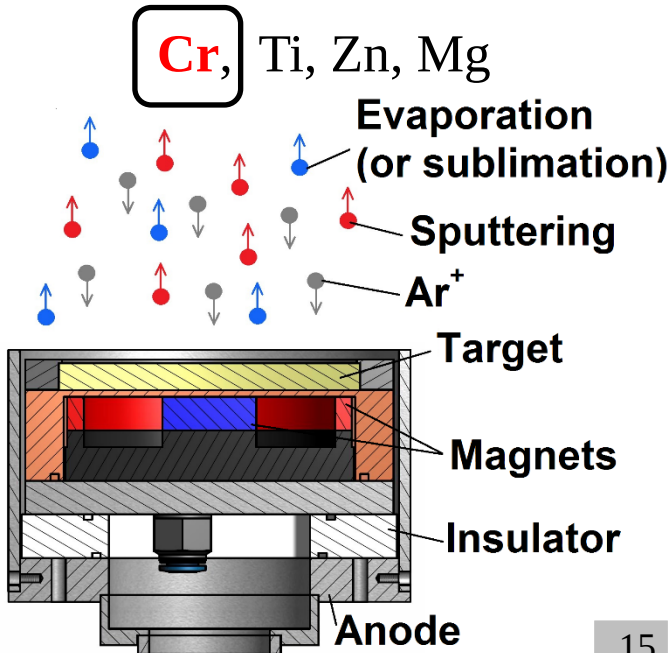
Fig. 11. H/E (a) and H^3/E^2 (b) ratios of nickel-chromium coatings deposited on Zr-1Nb substrates: (+H) – after hydrogenation; (+T) – after oxidation at 1373 K.

- Hydrogenation does no effect on mechanical properties of the coatings.
- The decrease of mechanical parameters is stronger for the coatings with higher Ni content. It indicates on denser microstructure of the oxidized layer of the coatings with Cr.

New requirements should be considered:

- to deposit the coatings with high concentration of Cr and with dense and uniform microstructure;
- increase deposition rate of the coatings.

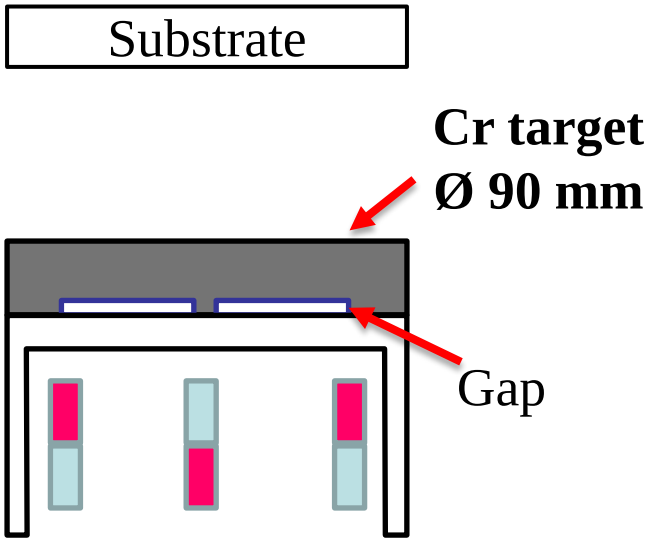
! Improve the energy per one deposited atom → Increase quantity of ions in deposited flow

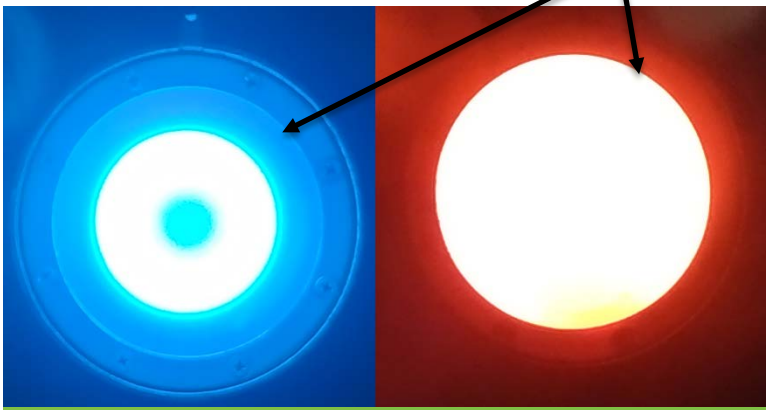


Magnetron with hot target

The photographs of magnetron with hot target

target temperature ~ up to **1700 K**





Sputtering **After sputtering**

- **decrease of heat contact between cooled magnetron body and sputtering target.**

Deposition rate can be higher 50 nm/s for single magnetron!

Cr coatings

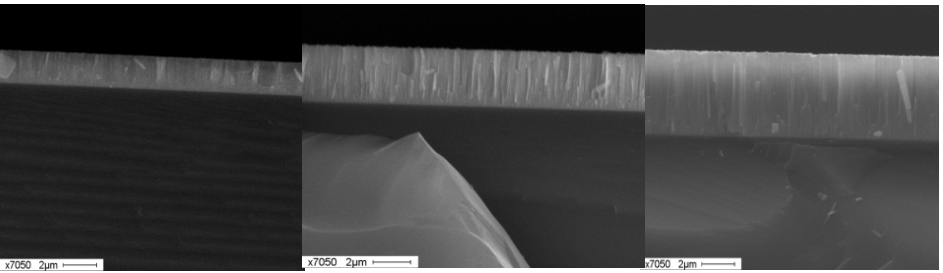
Magnetron with hot target

Deposition time – **25 min**

Cr-1 thickness – 1.8 μm

Cr-2 3.1 μm

Cr-3 4.5 μm

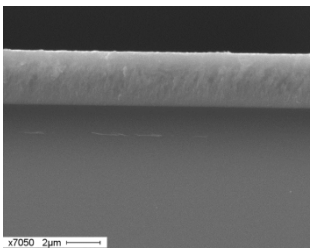


Dual magnetron system

Deposition time – **128 min**

Cr-4

thickness – 3.1 μm



Coating deposition

Loading the samples into the chamber and pumping ($2x10^{-3}$ Pa) – 1 hour

↓

Etching of Zr surface - 10 min

↓

Coating deposition by dual magnetron – 1…6 hours / or by using hot target magnetron **15-30 min**

↓

Exposure of the samples in vacuum – 30/**60** min

↓

Opening the chamber and pull of the samples – 10 min

Resistance to high-temperature oxidation

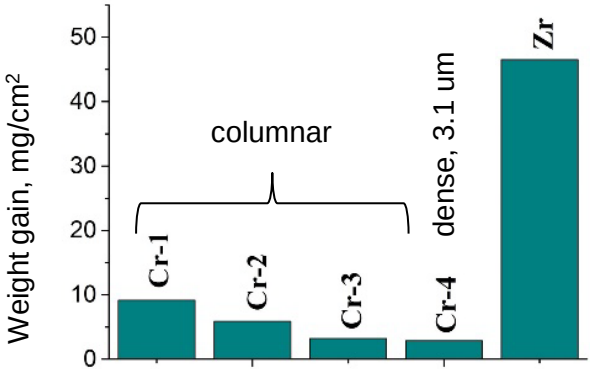
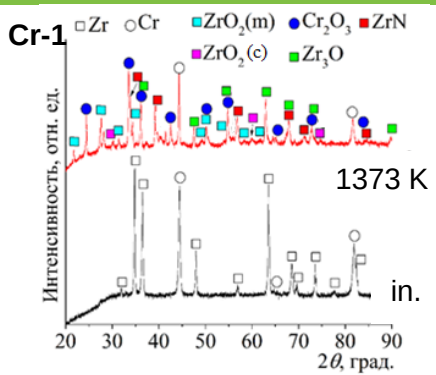
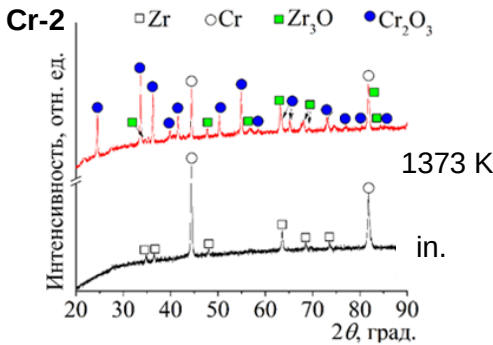
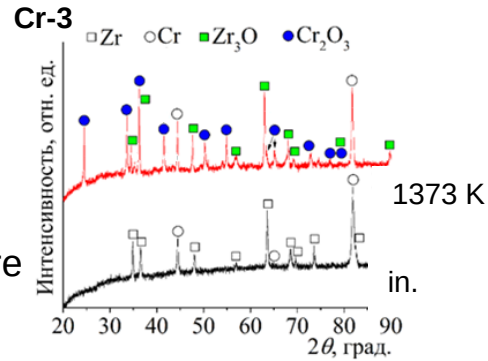
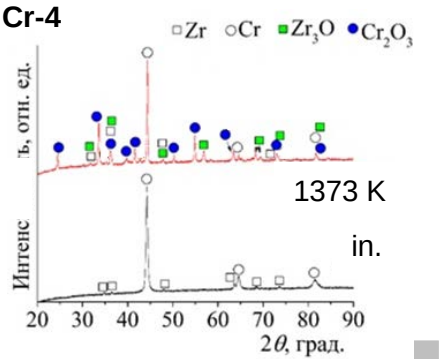


Fig. 12. Weight gain of the samples after oxidation at 1373 K.









- Higher thickness and denser microstructure of the Cr coatings are desirable.

Phase composition of the samples after oxidation

Phase [vol.%]	Cr-1	Cr-2	Cr-3	Cr-4
Cr_2O_3	52.7	78.6	84.8	66.9
Cr	16.6	11.6	13.1	31.9
Zr_3O	3.8	9.8	2.1	0.4
ZrN	15.8			
ZrO_2 (mono)	9.9			
ZrO_2 (cub)	1.2			
Zr				0.8
Total ZrO_x	**14.9**	**9.8**	**2.1**	**0.4**

Zirconium with dense Cr coating has higher resistance to high-temperature oxidation.

Conclusion

- Coatings deposited by magnetron sputtering can be used as a protection of Zr alloys in the case of high-temperature oxidation.
- High Cr concentration, dense and uniform microstructure of coatings are desirable.
- Oxidation resistance of Zr-1Nb increases with thickness of protective coating.
- For coating deposition, magnetrons with a large ion fraction in the deposited flow should be used.
- New designs of magnetron diode can be used to provide ultra-high deposition rates.

Future prospects

! To investigate the oxidation kinetics of Cr coatings by classical and hot target magnetron sputtering.

! To find new possibilities to tailoring of Cr coating microstructure for high-rate modes.

! To develop lengthy magnetron with hot target (the target length – 420 mm) and continue the examinations of Cr-coated Zr claddings.

25th International QUENCH Workshop

TOMSK POLYTECHNIC UNIVERSITY
ТОМСКИЙ ПОЛИТЕХНИЧЕСКИЙ УНИВЕРСИТЕТ

Thanks for attention!

Dmitrii V. Sidelev*, Egor B. Kashkarov, Maxim S. Syrtanov,
Victor N. Kudiyarov, Maya R. Rombaeva

Tomsk Polytechnic University, Tomsk, Russia

**** PhD, As. Professor***
E-mail: sidelevdv@tpu.ru

22-24 October 2019

High-Temperature Oxidation of Chromium-Coated Optimized ZIRLO™ in air and steam

Gauthier Bourdon (CTU-FJFI), Martin Ševecek (CTU-FJFI), Jakub Krejcí (UJP) , Ladislav Cvrcek (CTU-FME)

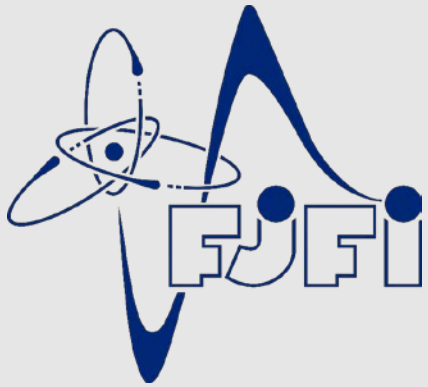
ABSTRACT

In design basis accidents such as LOCA or design extension conditions such as spent pool accident with air ingress, high-temperature oxidation of fuel cladding materials is one of the key phenomena for the accident progression. To enhance the claddings' behaviour, new materials are under investigation. They are called Accident Tolerant Fuels or Advanced Technology Fuels (ATFs). Among them, one of the most promising is the Chromium-coated cladding. Chromium-coated Optimized ZIRLO™ and uncoated Optimized ZIRLO™ high-temperature performance in steam and air have been investigated in detail. The coating was deposited using unbalanced magnetron sputtering which is considered as Physical Vapour Deposition technique. The experimental methods, test matrix, and parameters are first described followed by the results that mainly focus on the weight gain interpretation and the kinetics of reactions. Additionally, microstructure, microhardness, and hydrogen content have been studied to understand the oxidation mechanisms of these advanced materials. The experiments were carried out between 1000 and 1300°C. New kinetic correlations have been found in both air and steam. The results show that the steam oxidation rate is higher than the air oxidation rate, but in any case, the oxidation kinetics is much lower for coated than for uncoated materials. Oxidation hardening of a substrate is lower and slower in oxygen in comparison with steam. Metallographic analysis has been used to explain the oxidation mechanism. It has also been used to measure the thicknesses of coating and oxide layers. These measurements revealed that the decrease of the chromium coating thickness layer is related not only to oxidation but also diffusion of chromium inside zirconium that has been quantified. Moreover, it seems that after a while, the outer oxide thickness stops growing but the weight gain is still increasing. It is due to oxygen migration inside the cladding but without a formation of oxides. Measurements of hydrogen content were done for two temperature 1100 and 1200 °C allowing to compare hydrogen pickup for coated and uncoated material. It can be concluded that PVD Cr-coatings significantly increase the oxidation resistance of claddings both in air and steam. However, new issues have been raised such as strong diffusion of chromium inside the cladding which then leads to stabilization of beta-Zr allowing faster embrittlement due to oxygen ingress.

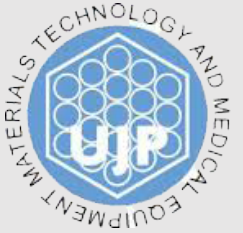


High-temperature oxidation of chromium coated Optimized Zirlo™ in air and steam

G. Bourdon, M. Ševeček, J. Krejčí



25th International QUENCH Workshop
Hosted by KIT
22-24 October 2019 in Karlsruhe



UJP PRAHA

Scenario of a severe accident with air ingress

Air ingress

- Reactor core (mismanaged LOCA, failed ECCS), spent fuel pool (Fukushima-Daiichi), transportation cask accident, fuel handling accident (Paks NPP)

Oxidation

- Air following with steam and mixture of them

Consequences

- Chemical heat release
- Cladding material degradation
- Hydrogen production

Experimental setup



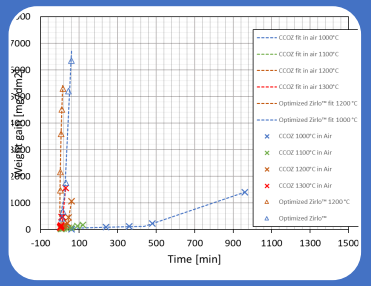
Samples

- **Optimized Zirlo™**, OD = 9.18 mm, ID = 8 mm, L = 30 mm , HD = 2-3 mm
- **Cr-coated Optimized Zirlo™ ,** OD = 9.18 mm, ID = 8 mm, L = 30 mm , HD = 2-3 mm, coating thickness = 18.6 ± 0.1 µm (PVD coating)



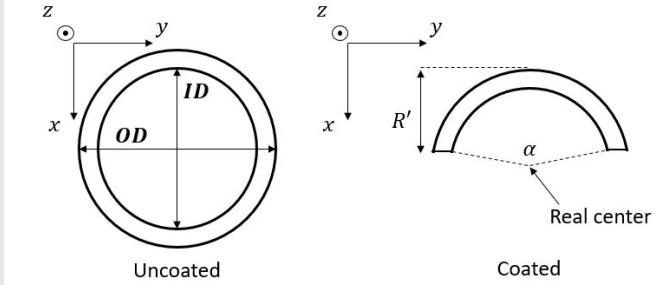
Flow rates

- **Air oxidation:** synthetic air flow = 100 $L.h^{-1}$, argon flow = 50 $L.h^{-1}$
- **Steam oxidation:** steam flow = 85 $g.h^{-1}$, argon flow = 50 $L.h^{-1}$



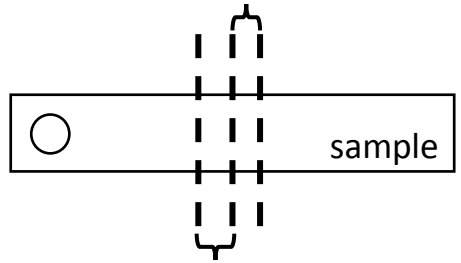
Characterization

- Weight gain, visual evaluation, microstructure, microhardness, hydrogen content



Top view scheme of samples

Hydrogen content



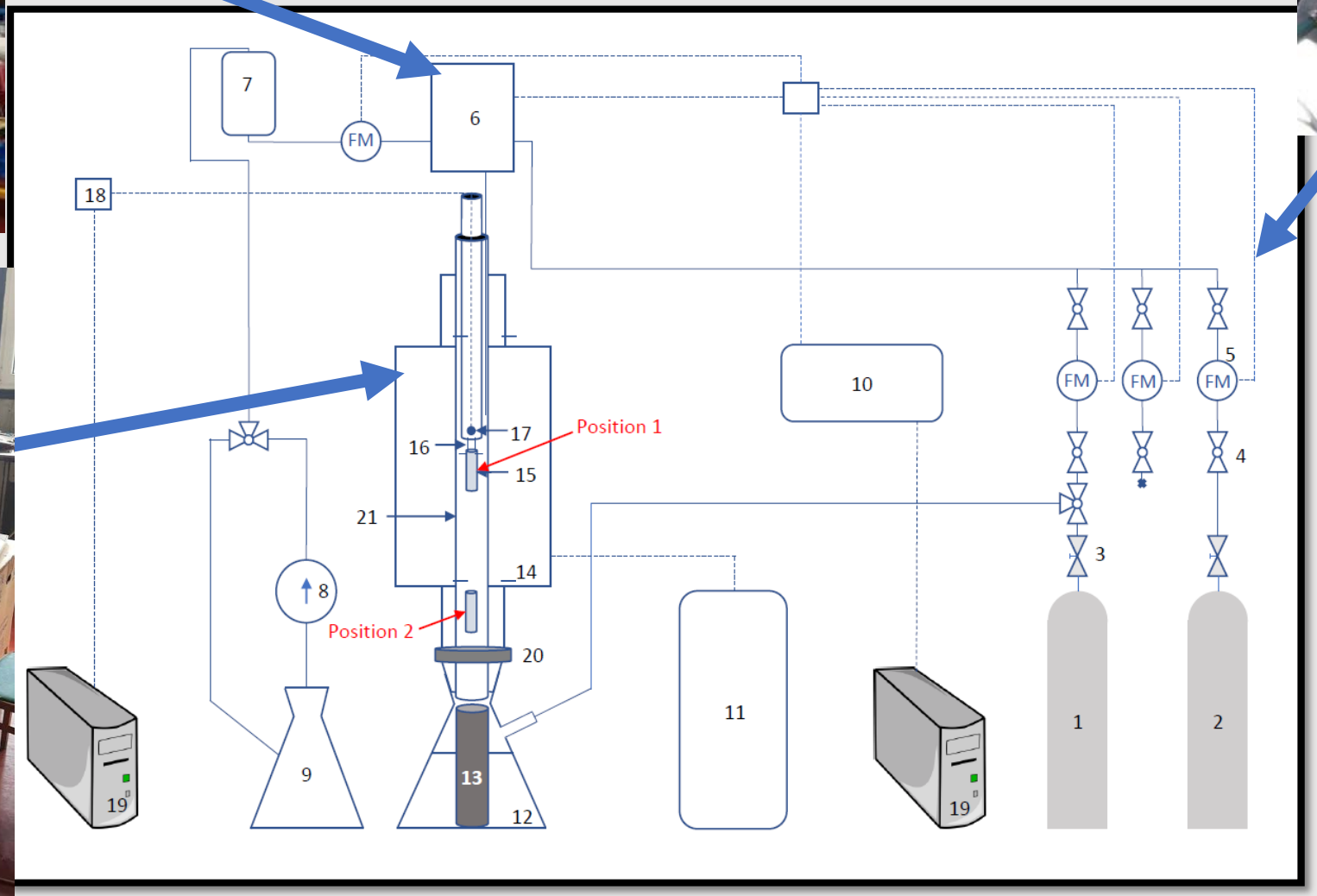
Microstructure

OD: Outer Diameter, ID: Inner Diameter, L: Length, HD: Hole Diameter, PVD: Physical Vapor Deposit

Experimental procedure







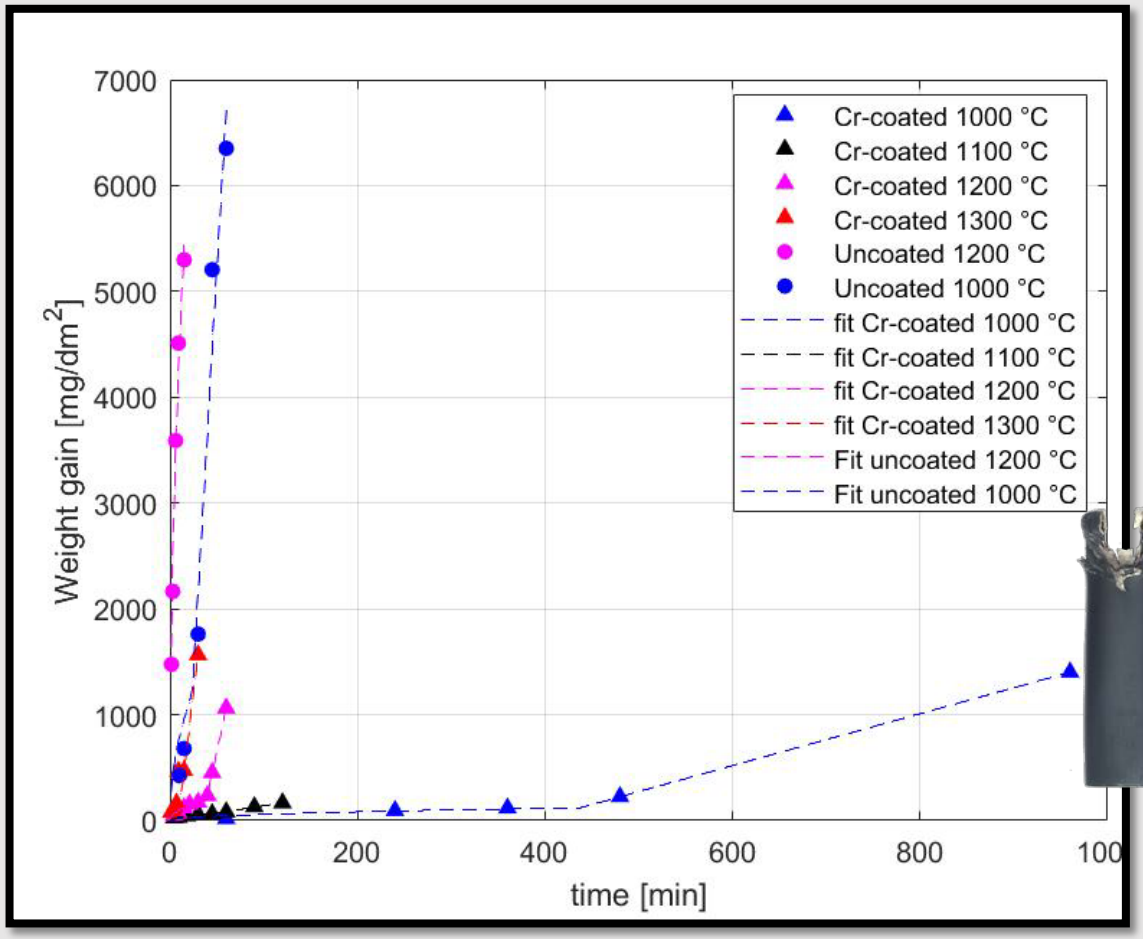


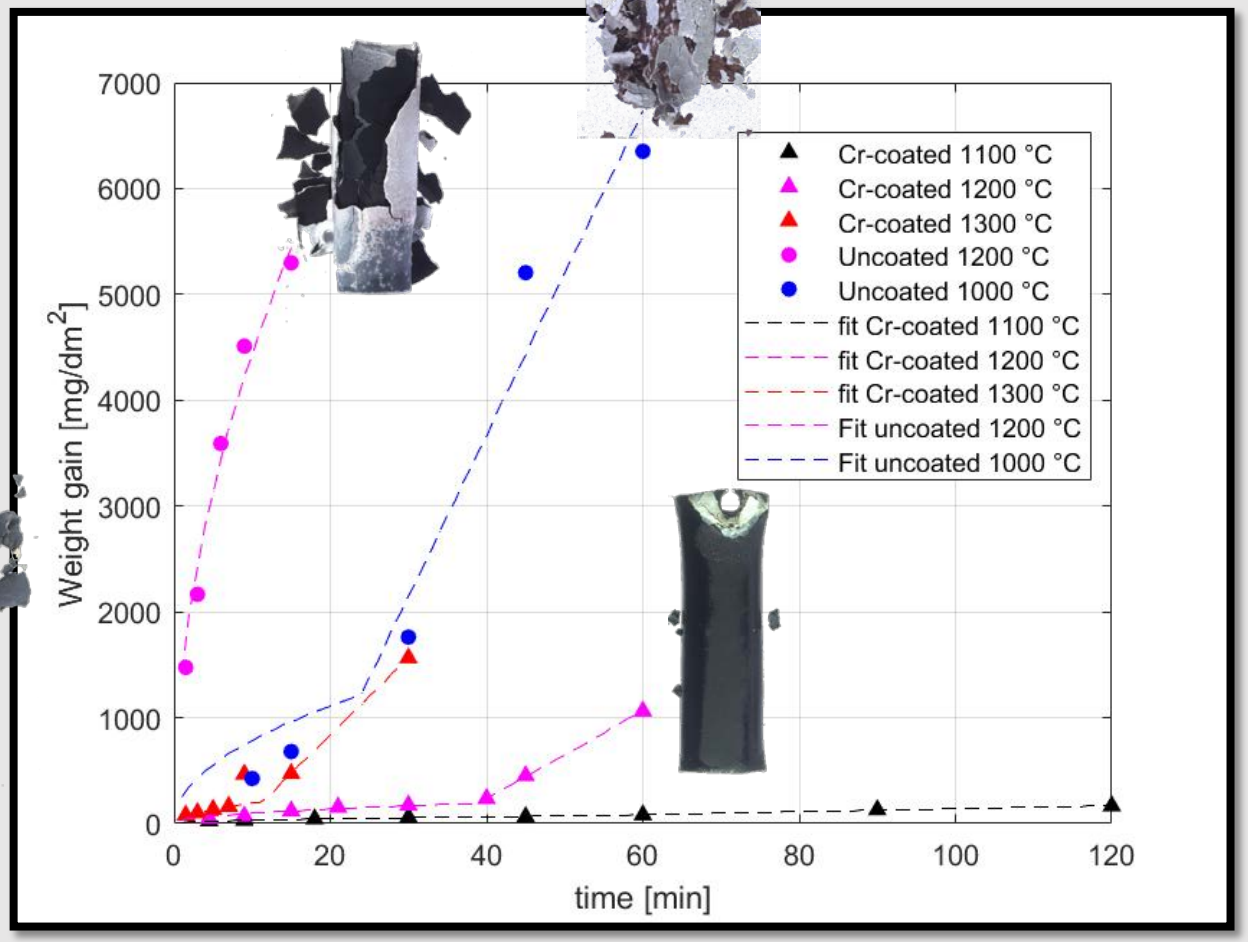
1. Argon bottle
2. Air bottle
3. Valve
4. Valve
5. Flowrate meter
6. CEM
7. Water for steam
8. Pump
9. Water tank for steam
10. Flowrate controller
11. Thermostatic control
12. Water at 0°C (cooling with ice cubes)
13. Tube to collect the sample
14. Furnace
15. Sample
16. Hook
17. Thermocouple
18. Analog-to-digital converter
19. Computer
20. Seal
21. Quartz tube (Ø = 24 mm)

Information wire

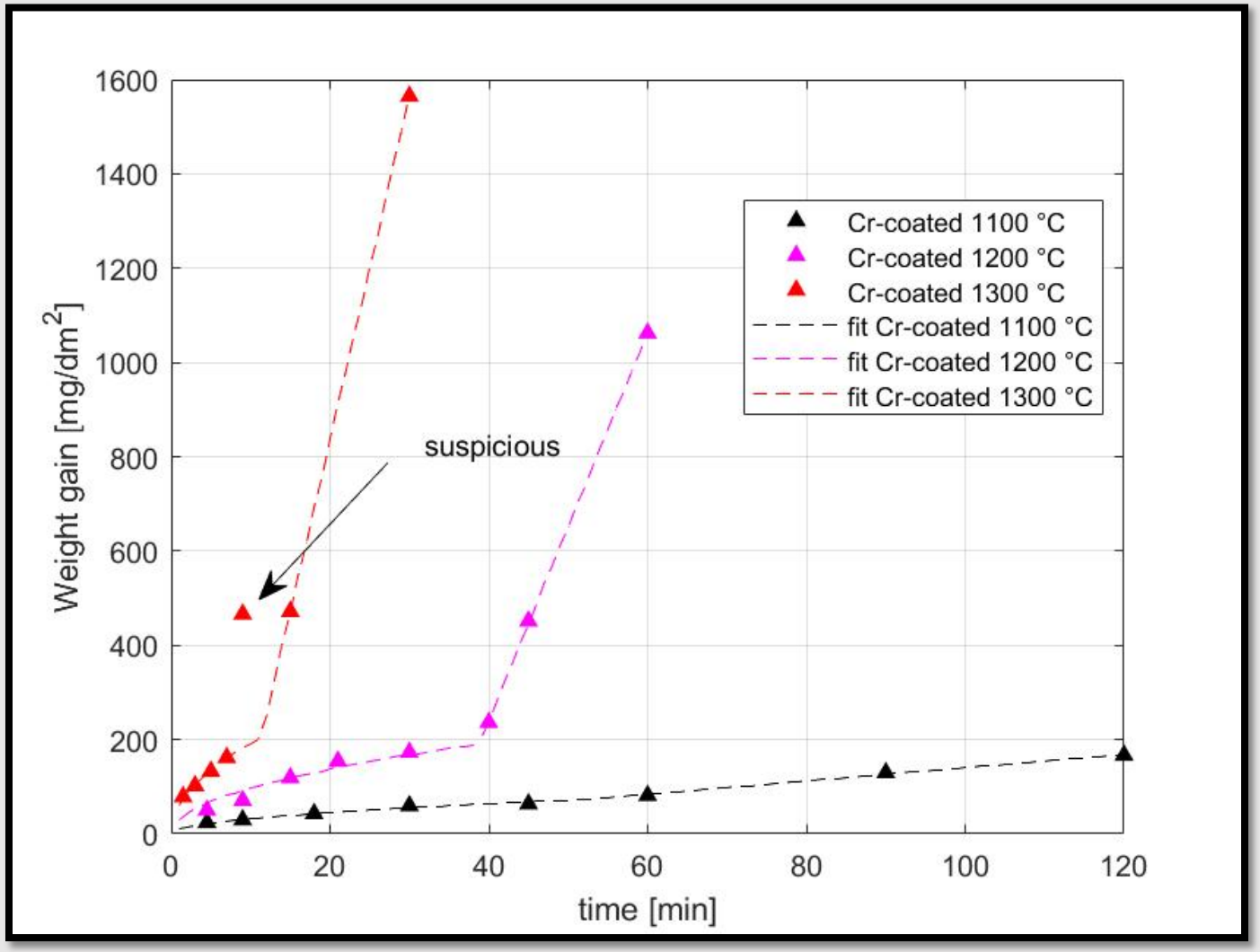
Tube with fluid

Results in air – Weight gain in air



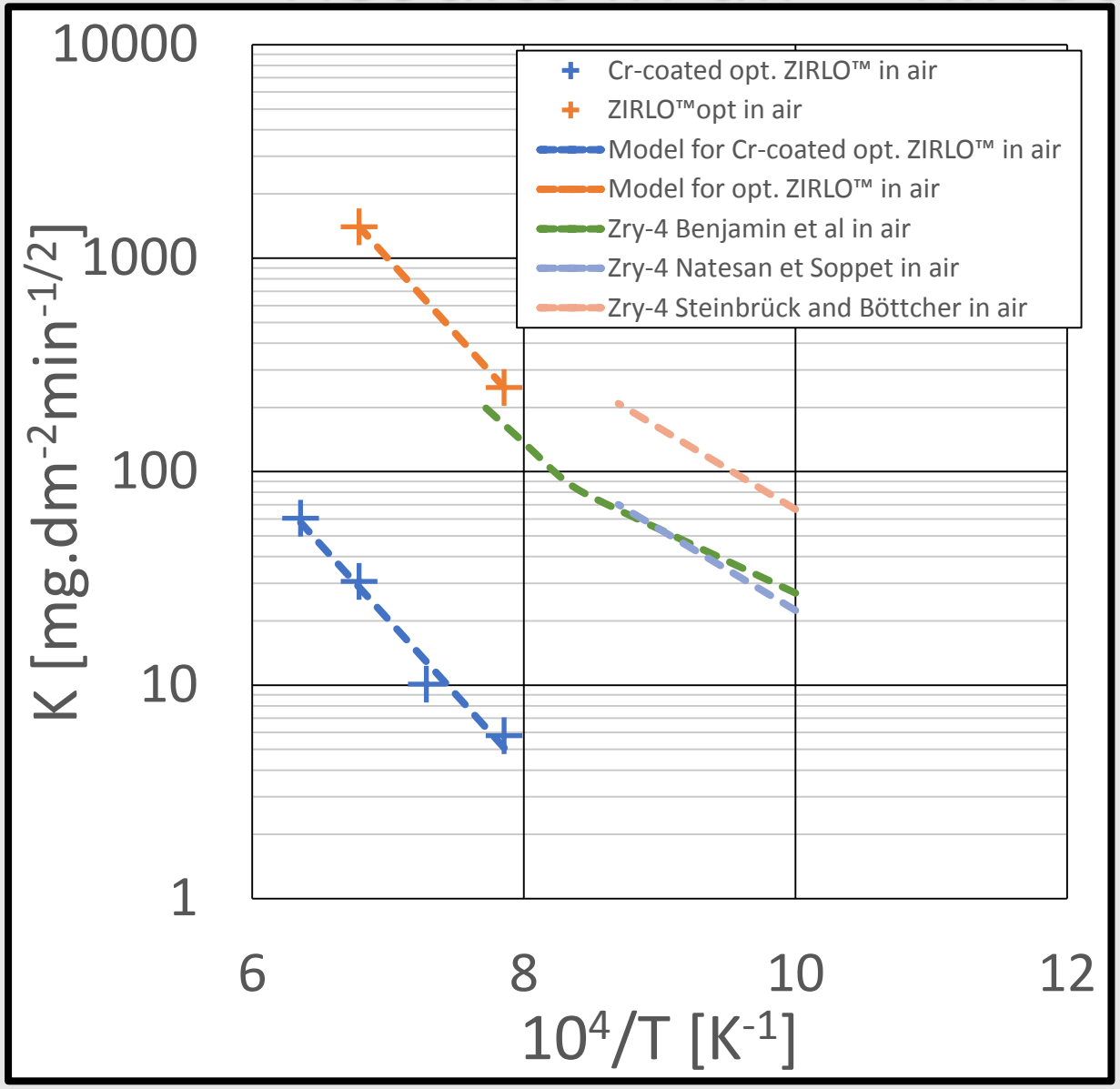


Results in air – Weight gain in air



For all temperature, there is a kinetic change → loss of protective nature of coating

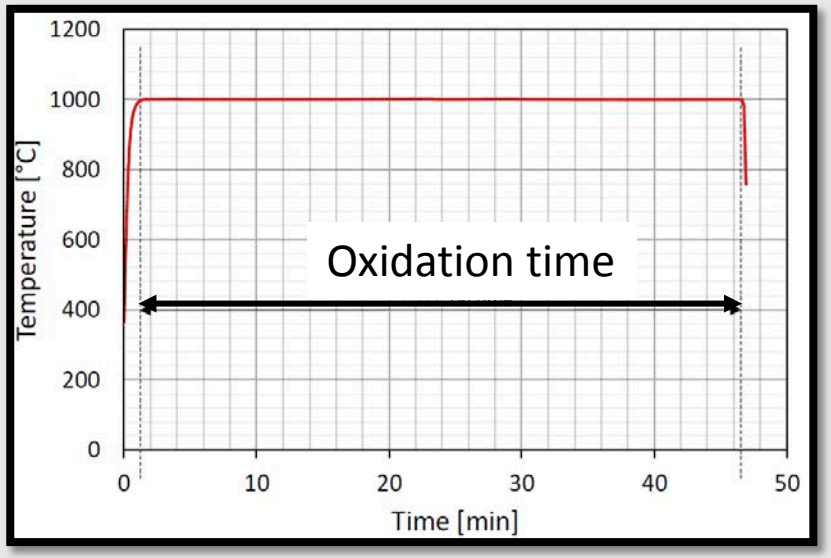
Results in air – kinetic correlation



Oxidation kinetic law before breakaway:

$$\frac{\Delta m}{S} = \sqrt{m_0 + k(T)(t - t_0)^2} \approx K t^{0.5}$$

- m_0: Oxide mass formed during the heating of the sample
- t_0: Heating time
- t: Oxidation time at set temperature
- k: oxidation rate

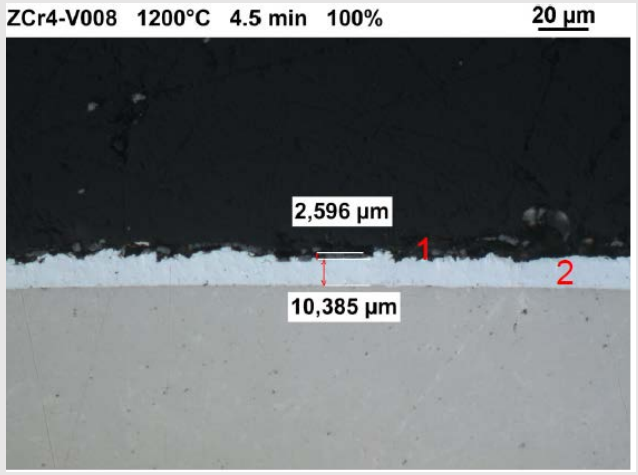


Temperature profile for Optimized Zirlo™ oxidation in air at 1000°C

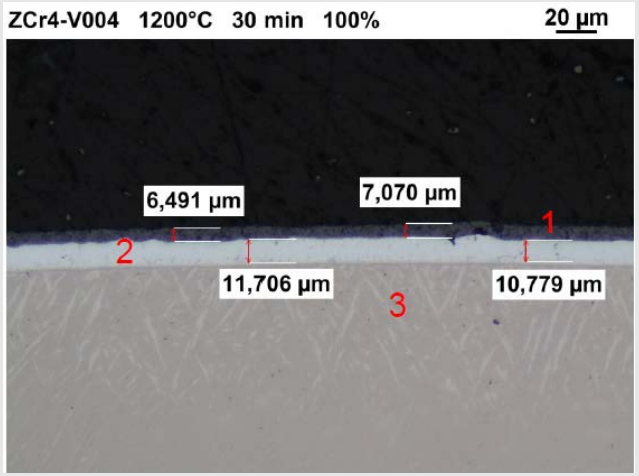
Results in air – Microstructures

Cr-coated Optimized Zirlo™

1200 °C – 4.5 min

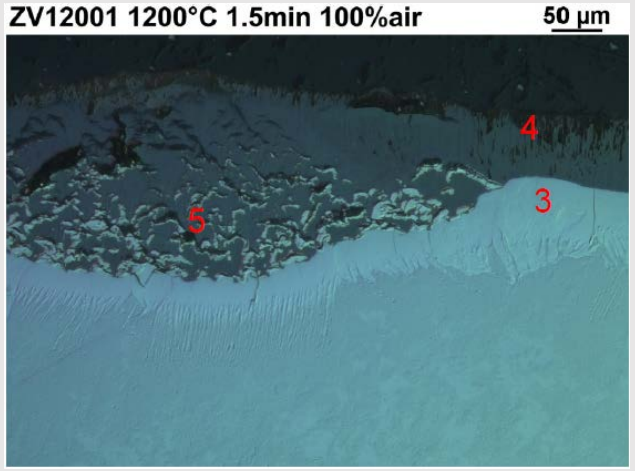


1200 °C – 30 min

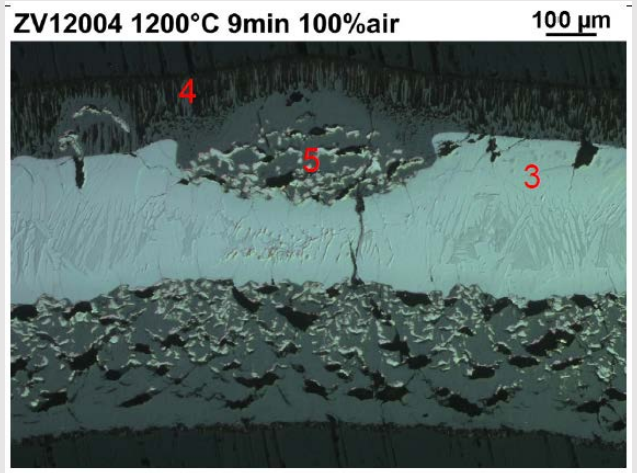


Optimized Zirlo™

1200 °C – 1.5 min



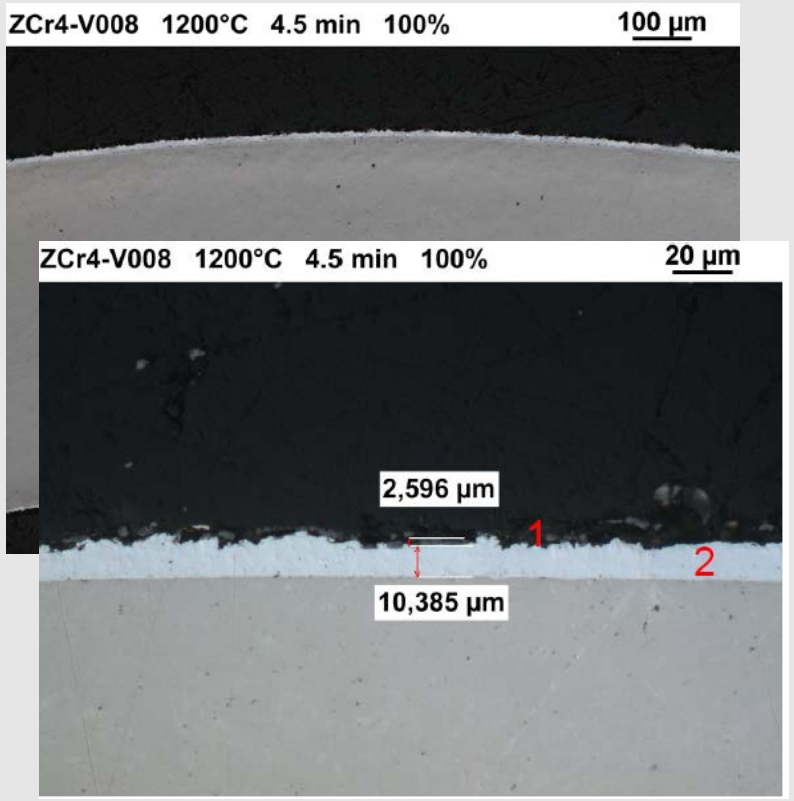
1200 °C – 9 min



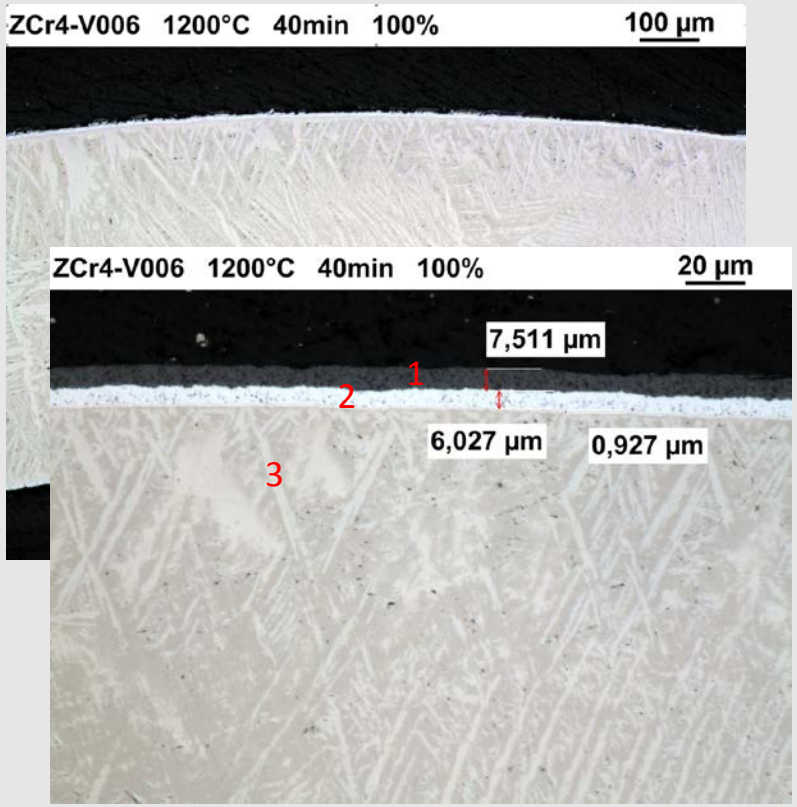
1. Cr_2O_3
2. Cr
3. $\alpha - Zr\ (O);\ \alpha - Zr\ (N)$
4. ZrO_2
5. $Porous\ ZrN$

Results in air – Microstructures

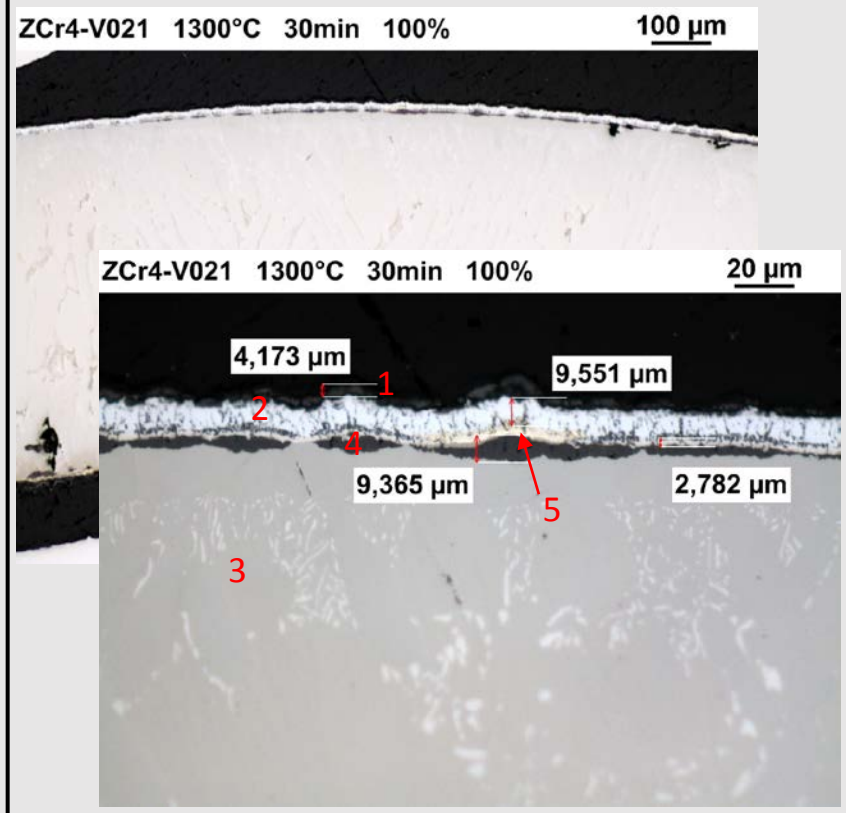
Cr-coated Optimized Zirlo™
1200°C - 4.5 min (pre-breakaway)



Cr-coated Optimized Zirlo™
1200°C - 40 min (breakaway point)

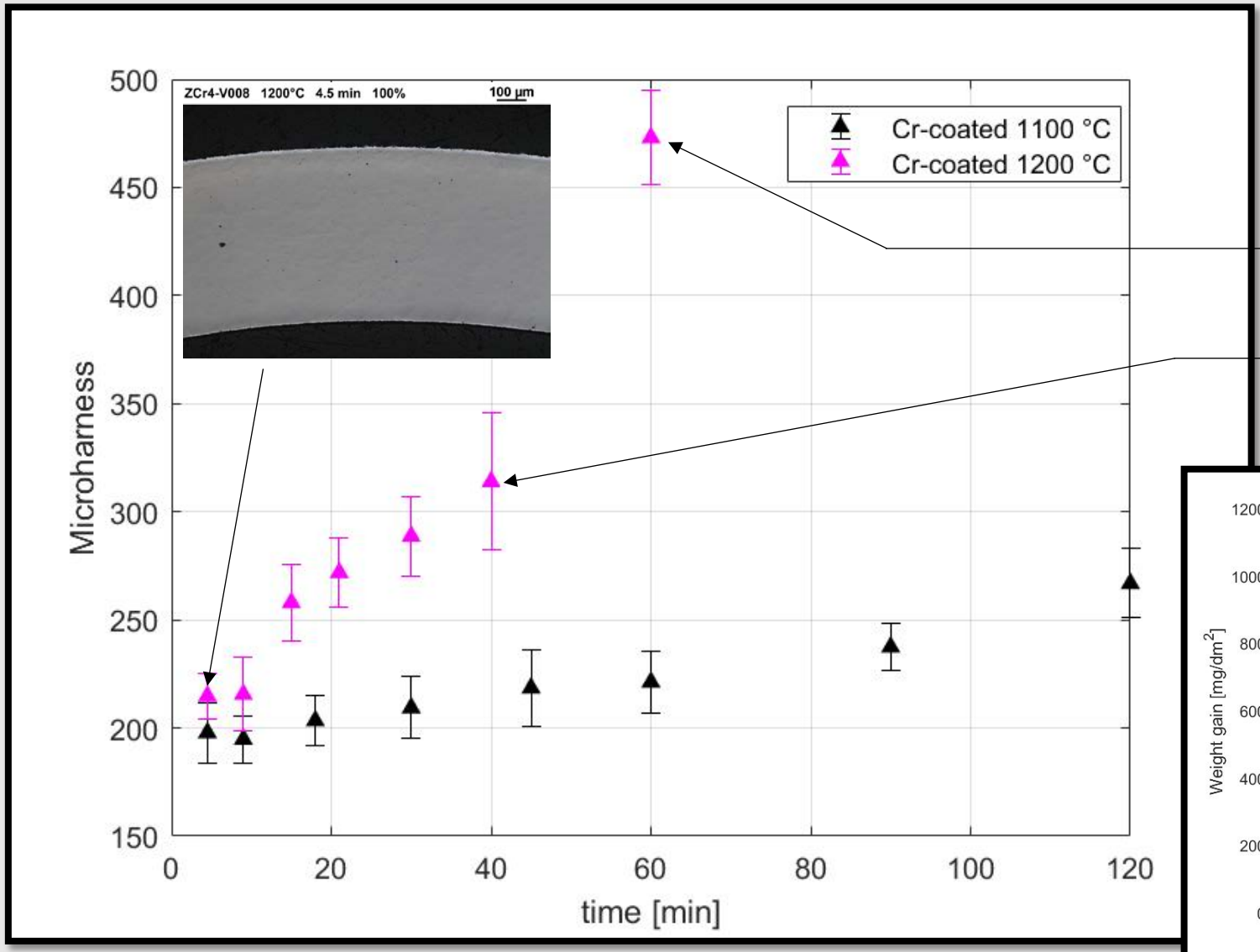


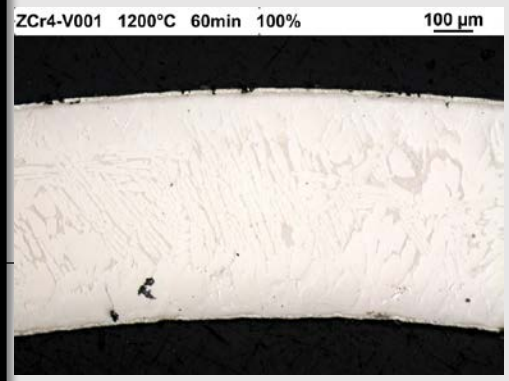
Cr-coated Optimized Zirlo™
1300°C - 30 min (post-breakaway)

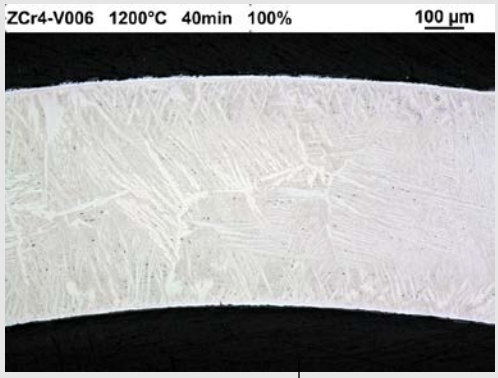


$3.\ \alpha - Zr\ (O); \alpha - Zr\ (N)\ \ 4.\ ZrO_2\ \ 5.\ ZrN + CrN$

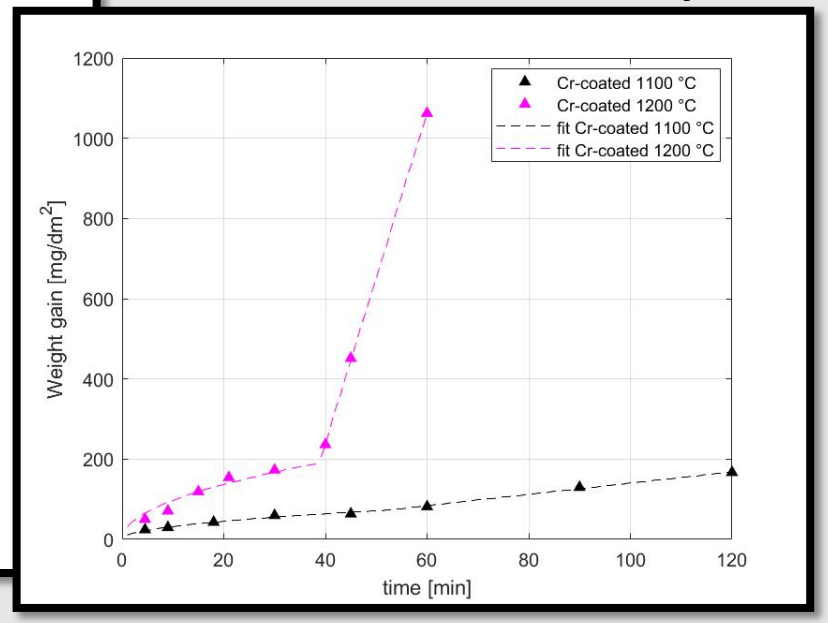
Results in air – Microhardness



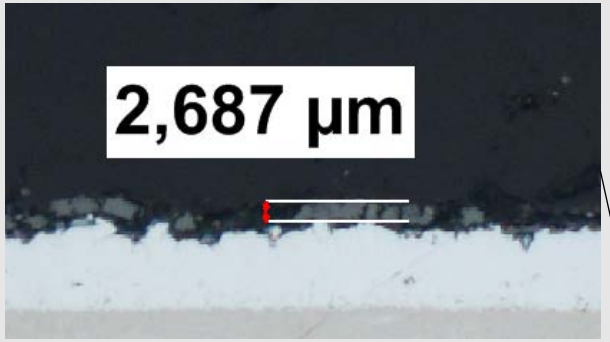


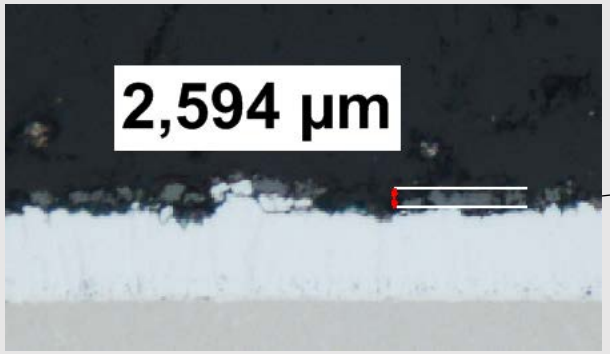


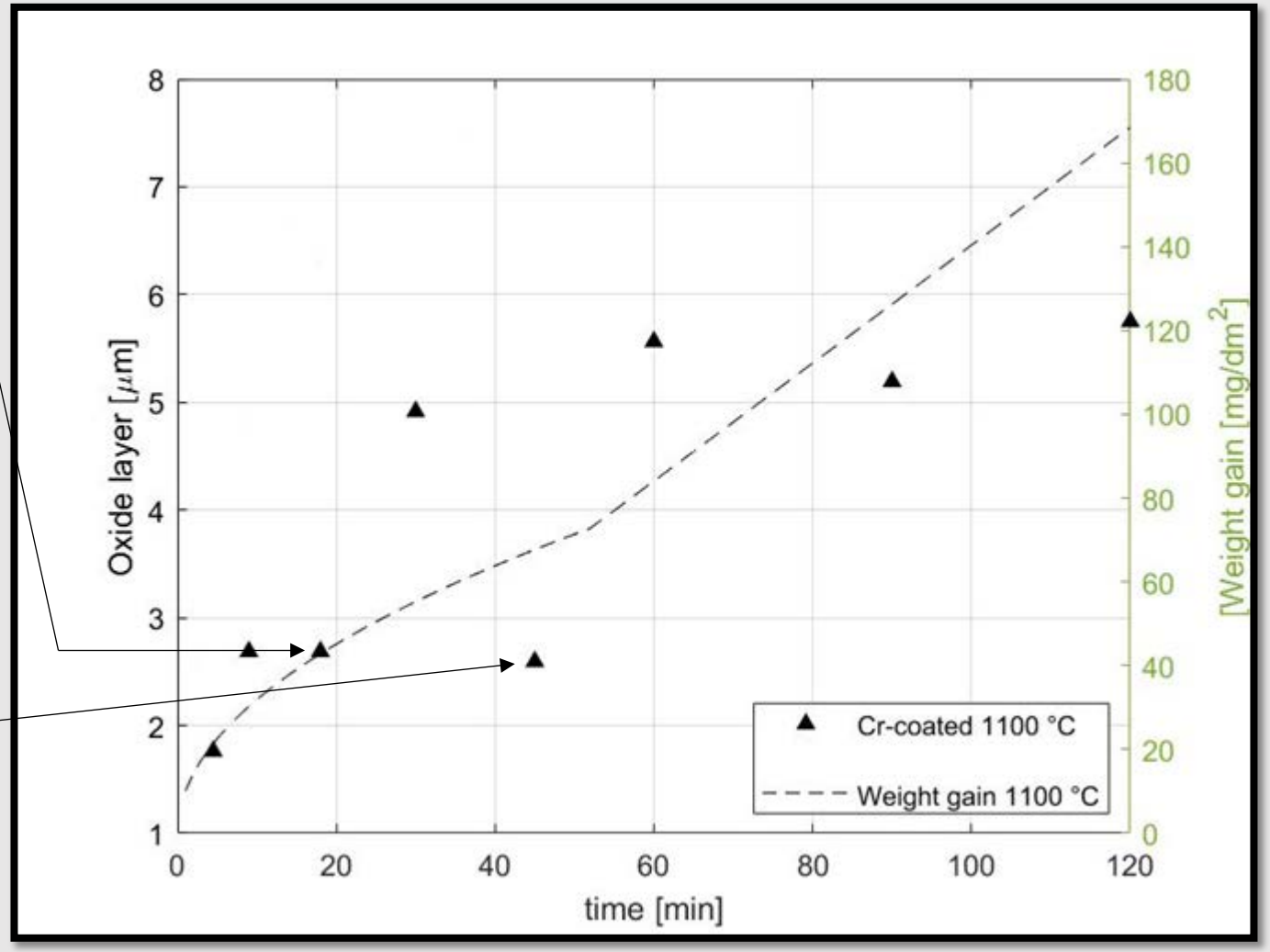
Considerable increase of microhardness after breakaway



Results in air – Cr-oxide layer

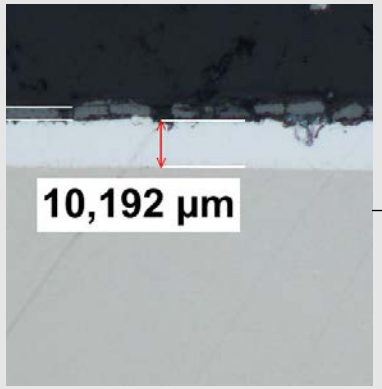


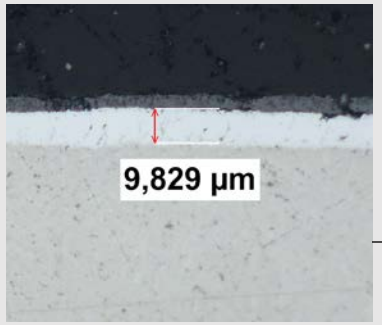


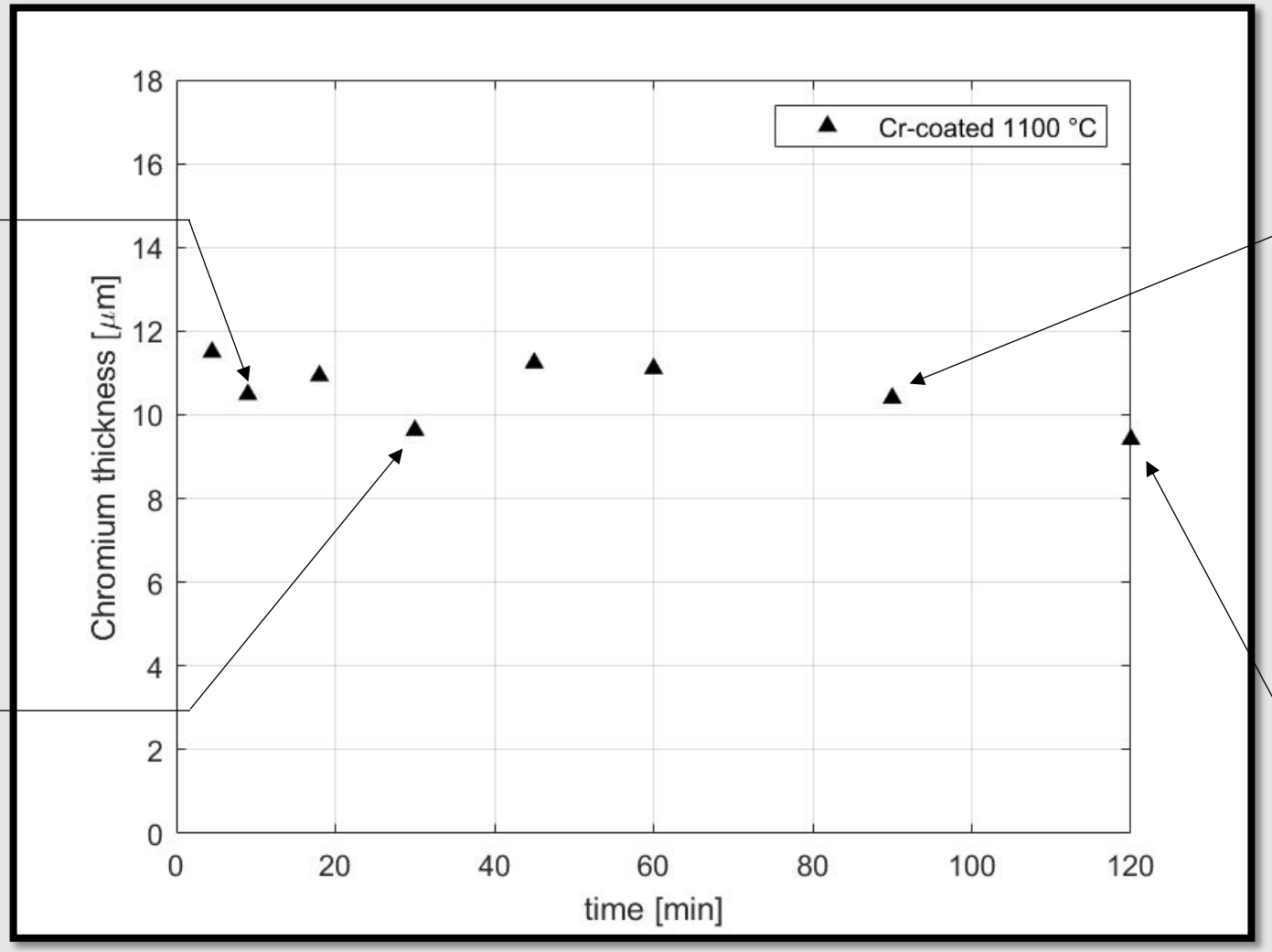


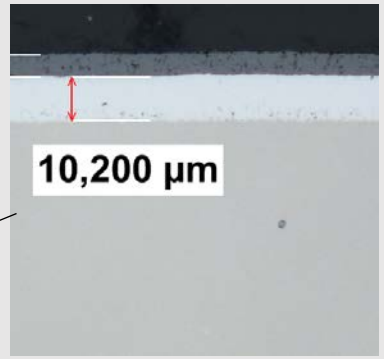
Oxide thickness does not increase after breakaway

Results in air – Microstructures

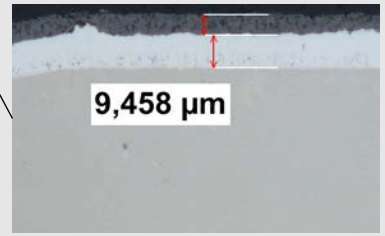




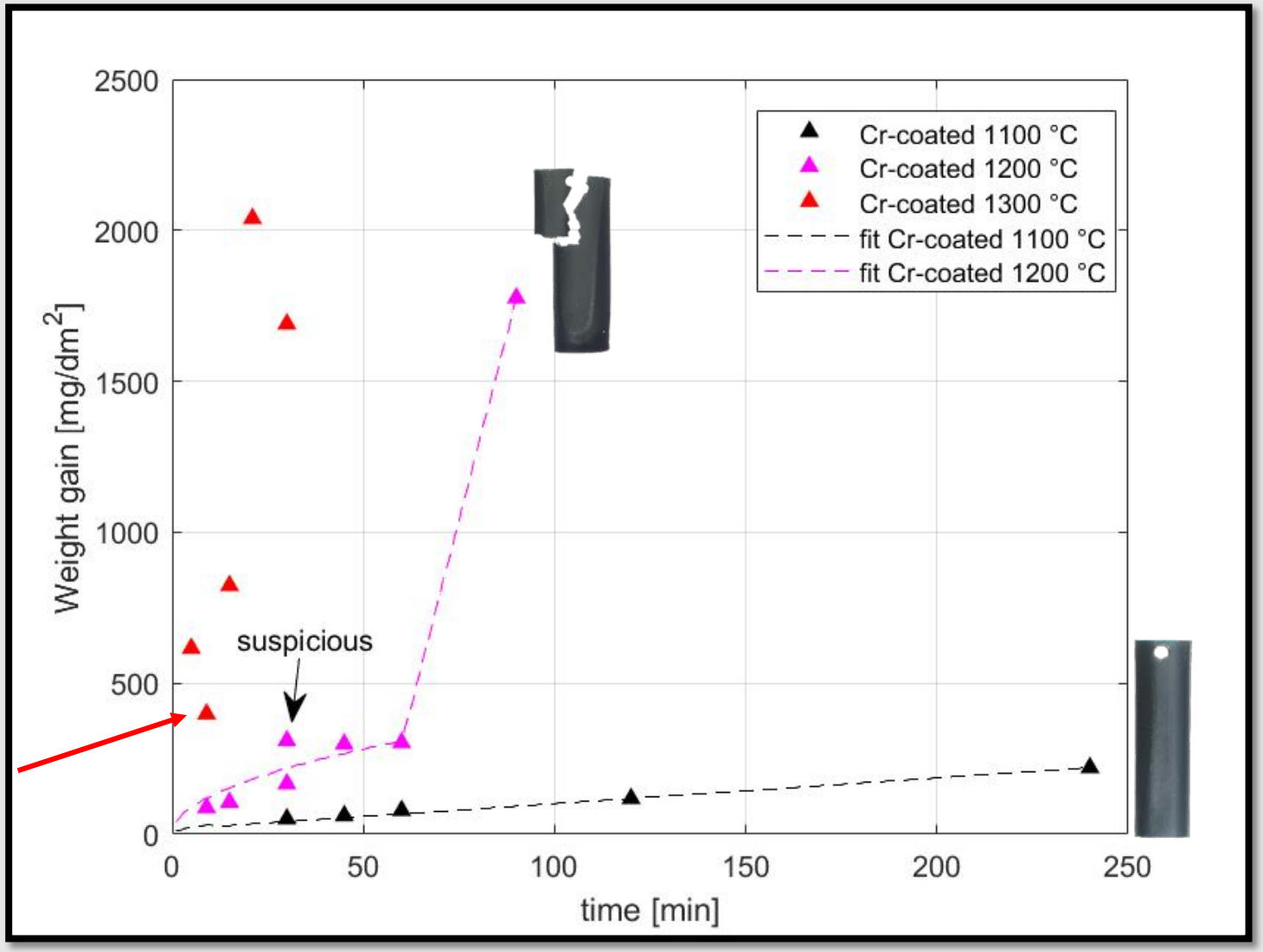




Limited Cr-Zr interdiffusion in air. Cr consumed mainly by oxidation.

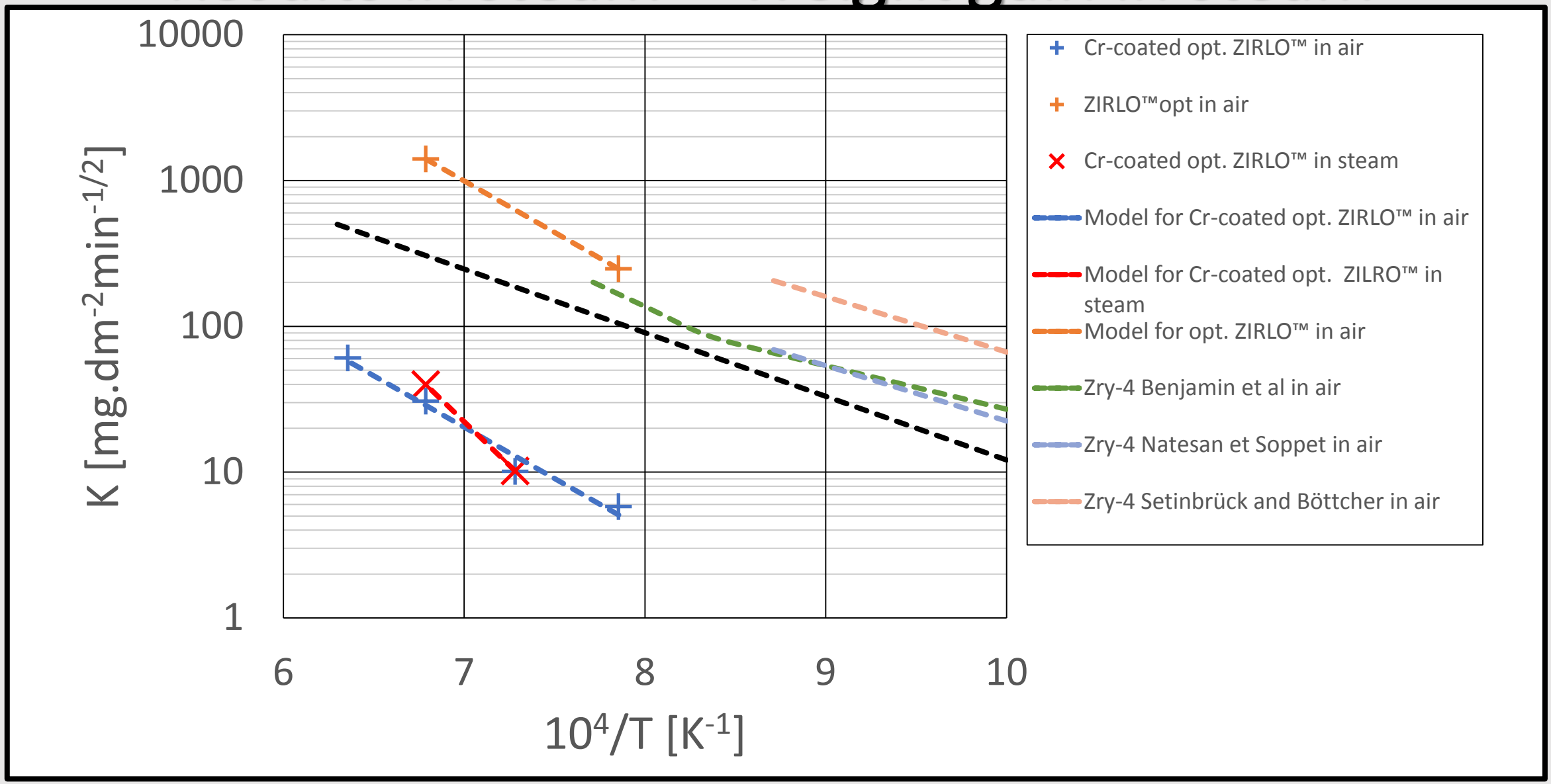


Results in steam – Weight gain in steam



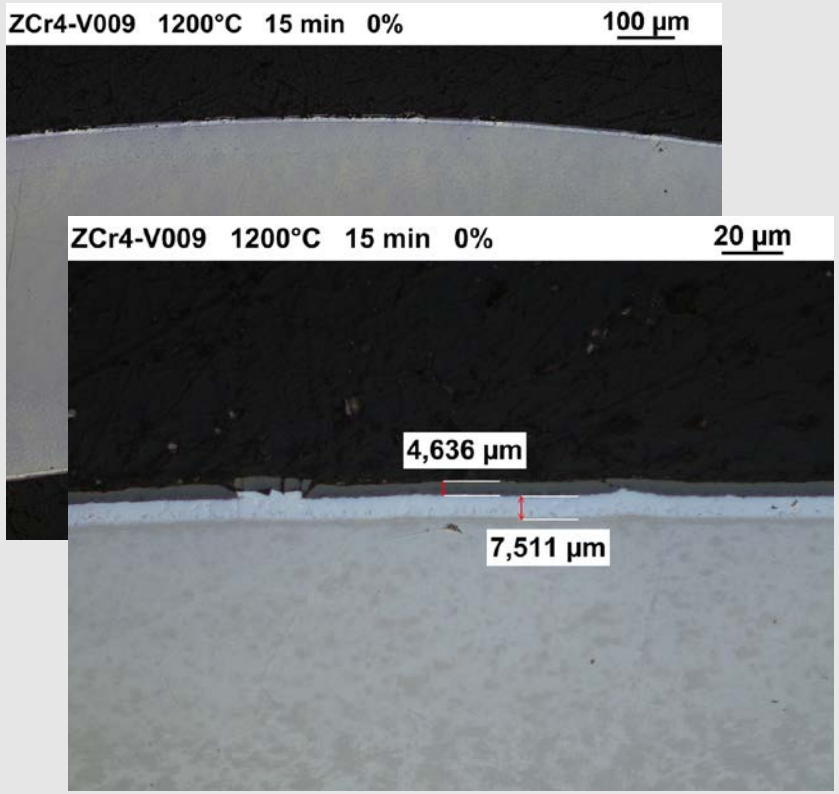
- **1100°C:** No kinetic transition up to 240 minutes
- **1200 °C:** More damaged around the hole after the kinetic transition
- **1300 °C:** Coating must have melted which suggest higher temperature

Results in steam – Weight gain in steam

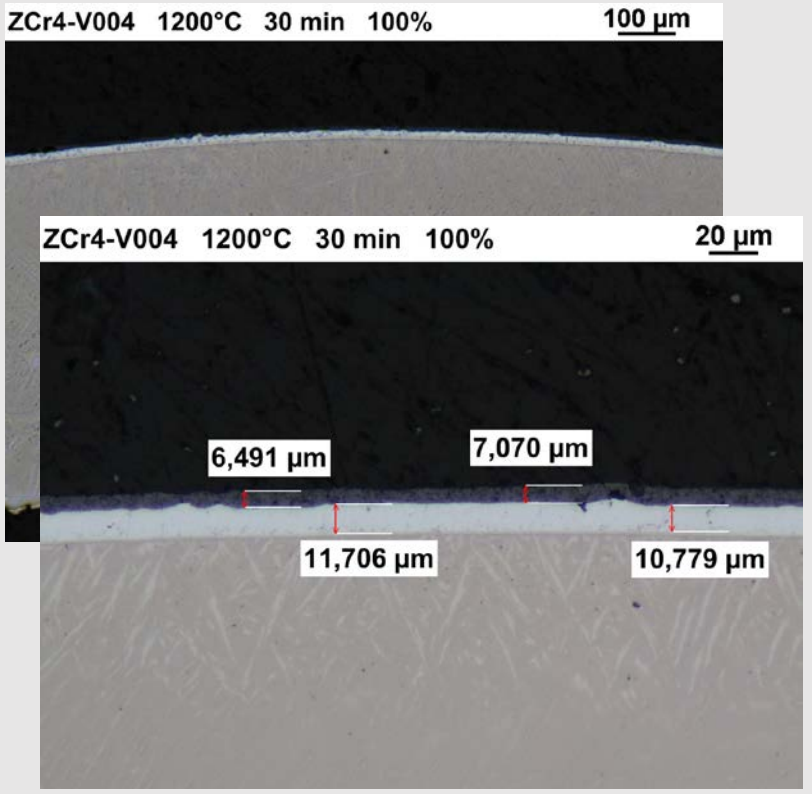


Results in steam – Microstructures

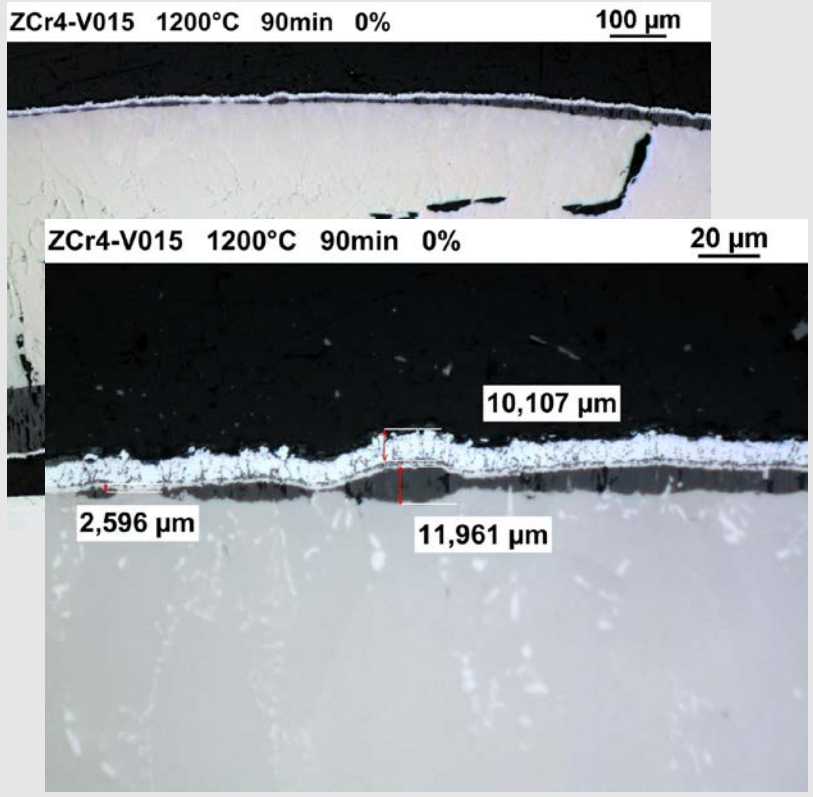
Cr-coated Optimized Zirlo™
15 min -1200 °C



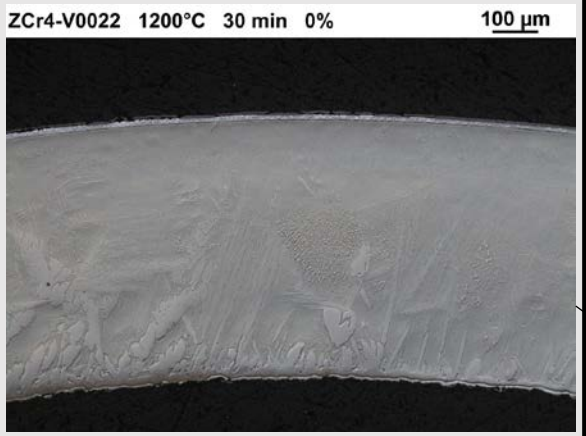
Cr-coated Optimized Zirlo™
45 min -1200 °C

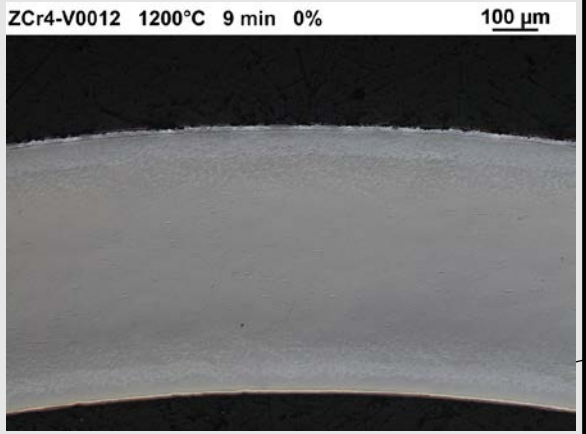


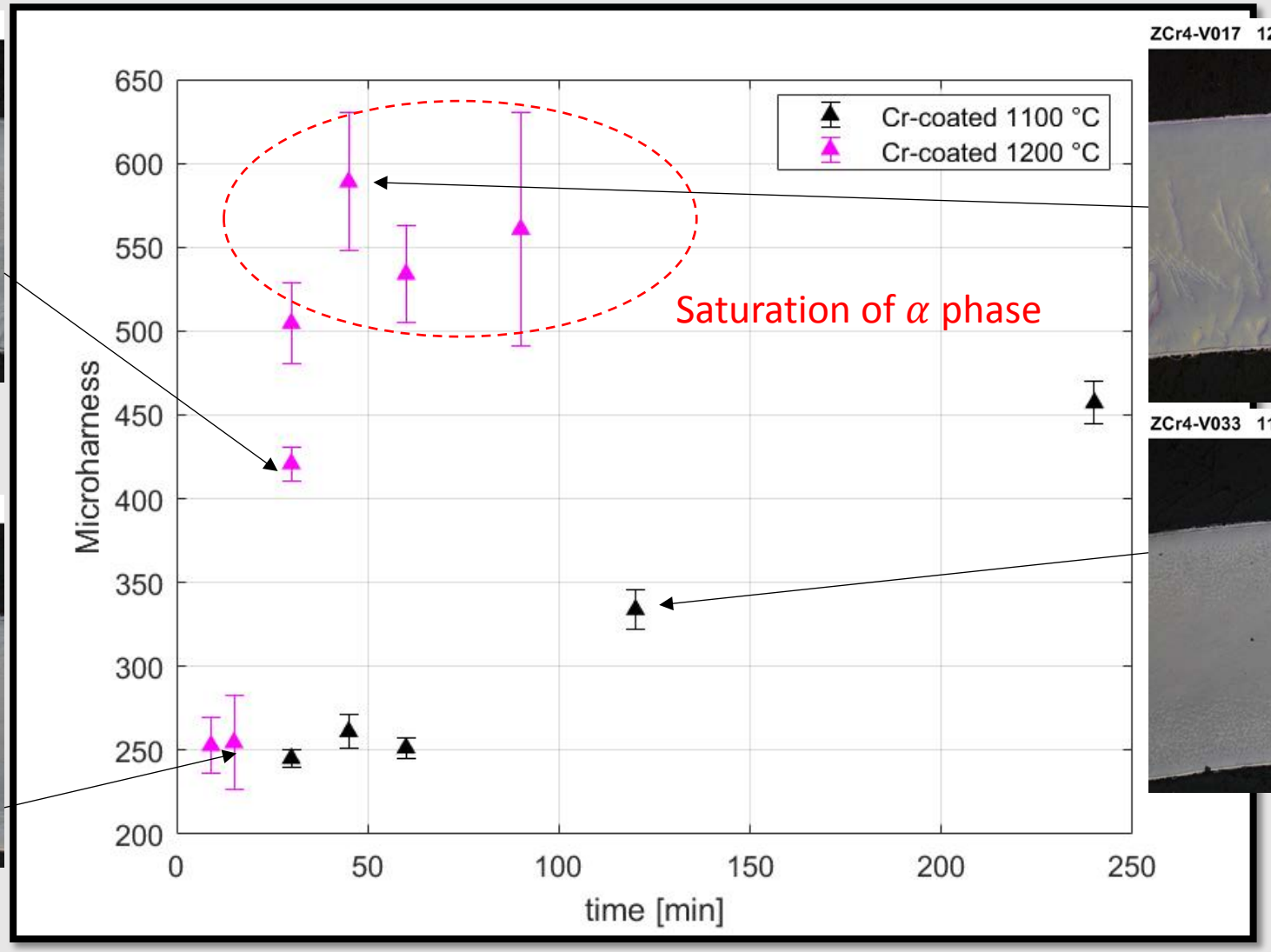
Cr-coated Optimized Zirlo™
90 min -1300 °C

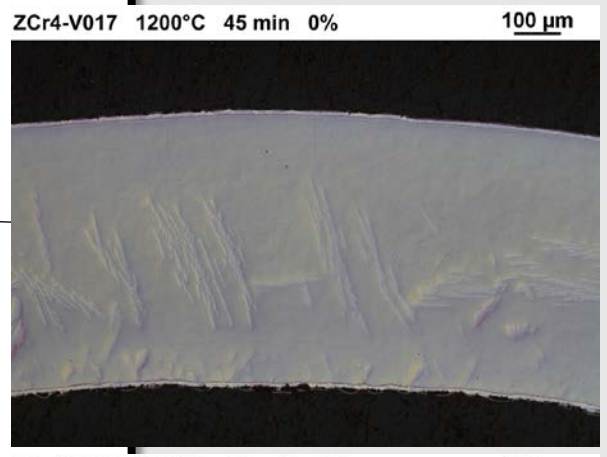


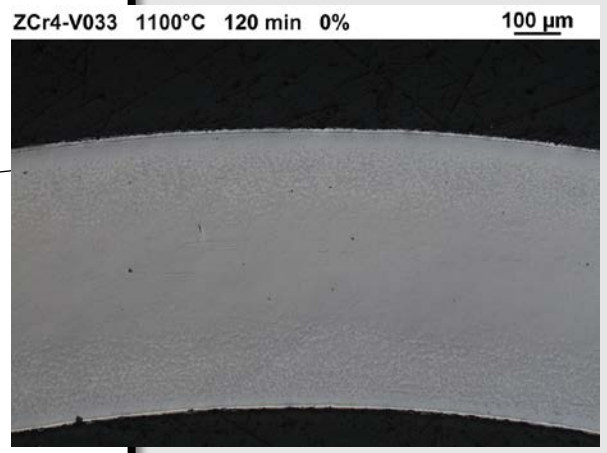
Results in steam – Microhardness



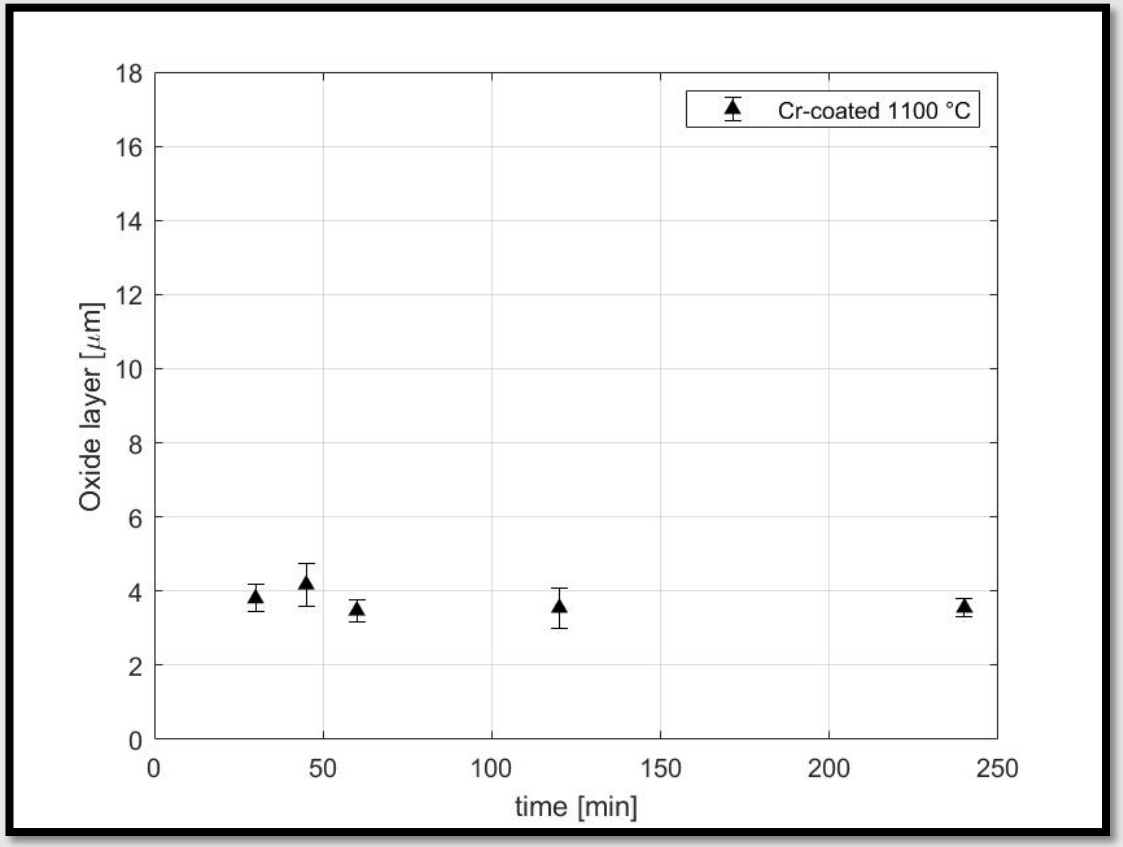


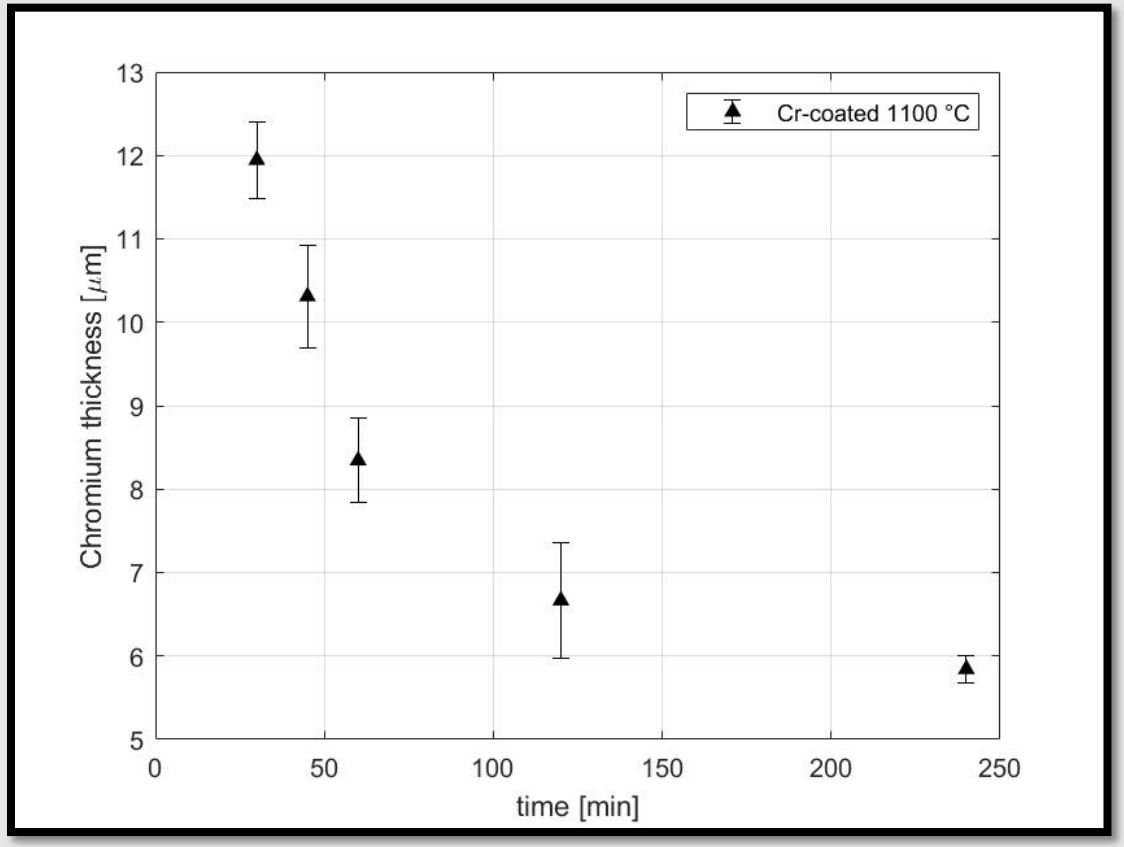






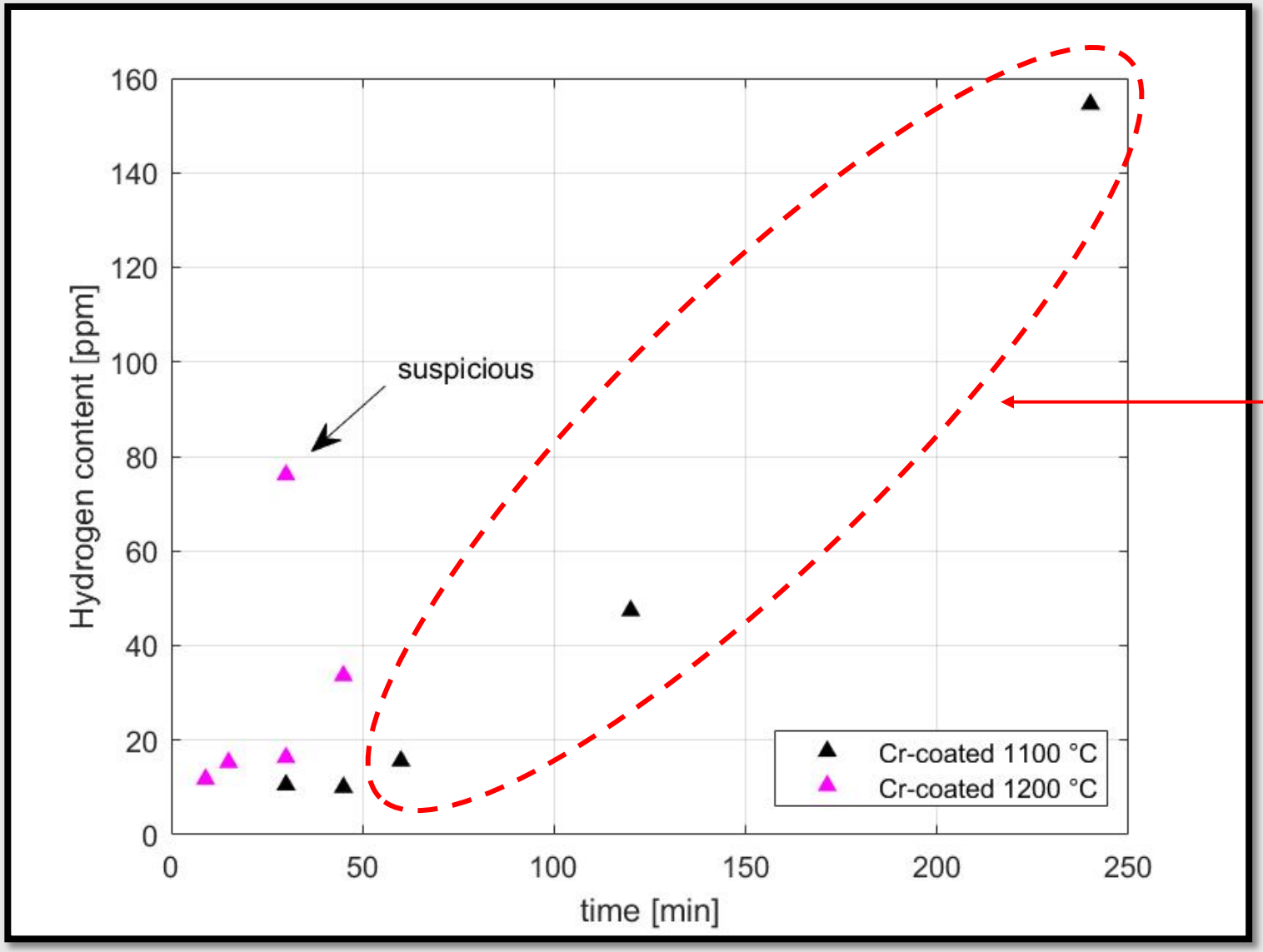
Results in steam – Microstructures





Oxide layer stable but chromium layer still decrease → higher Cr diffusion in steam

Results in steam – Hydrogen content



Rapid increase of hydrogen content **without** oxidation kinetic change

Conclusion

- Chromium coating reduces oxidation in air and steam
- There is a breakaway for both oxidation atmosphere. However it happens later than for uncoated samples
- Results might be affected by the drilled hole, the thinner inner coating and double size oxidation. However full rod may have even better corrosion resistance.
- Less oxygen concentration in the cladding with air oxidation (confirmed by mircohardness)
- Cr diffusion lower in air due to nitride at Zr/Cr interface
- Unexpected high hydrogen concentration before breakaway in steam at 1100 °C

Acknowledgements

- The author would like to thank Westinghouse Electric Corporation for providing Optimized Zirlo™

- The author would like to thank IAEA for the grant they provided to the author

References

- M.M. Stempniewicz. “Air oxidation of Zircaloy,Part 1- Review of correlations”. In: Nuclear Engineering and Design (2016).
- C. Duriez, T. Dupont, B. Schmet, F. Enoch b. *Zircaloy-4 and M5 high temperature oxidation and nitriding in air,* Journal of nuclear material 2018.
- W.M Rumball. “The Effect of Chromium, Oxygen and Microstructure on the Hardness of Zirconium-Chromium Alloys”. In: Journal of the Less-Common Metals 39 (1975), pp. 35–42.
- Y. Yan, T.A. Burtseva, and M.C. Billone. “High-temperature steam-oxidation behavior of Zr-1Nb cladding alloy E110”. In: Journal of Nuclear Materials 393.3 (2009)

CEA-Framatome-EDF presentation based on a paper submitted to Corrosion Science

Title: "High Temperature Steam Oxidation of Chromium-Coated Zirconium-Based Alloys: Kinetics and Process"

Authors: *Jean-Christophe BRACHET, Elodie ROUESNE, Joël RIBIS, Thomas GUILBERT, Stéphane URVOY, Guillaume NONY, Matthieu LE SAUX, Nihed CHAABANE, Hervé PALANCHER, Amandine DAVID, Jérémy BISCHOFF, Julien AUGEREAU, Edouard POUILLIER*

ABSTRACT:

The oxidation of chromium-coated zirconium-based alloys is studied under steam at temperatures ranging from 800°C up to 1300°C and for oxidation times ranging from a few minutes up to a few hours. Overall oxidation kinetics is nearly parabolic at the beginning of oxidation, when the Cr outer layer is protective. Finally, it significantly accelerates (Fig. 1), and hydrogen is absorbed during a short period. These steps correspond to different oxidation and diffusion mechanisms, involving: growth of outer chromia scale, Zr-Cr interdiffusion, inducing $Zr(Cr,Fe)_2$ intermetallic layer thickening - then disappearance due to re-transformation to metallic chromium and to zirconia, transport of oxygen through the residual chromium (in particular along grain boundaries) and into the zirconium substrate, and finally growth of sub-coating zirconia.

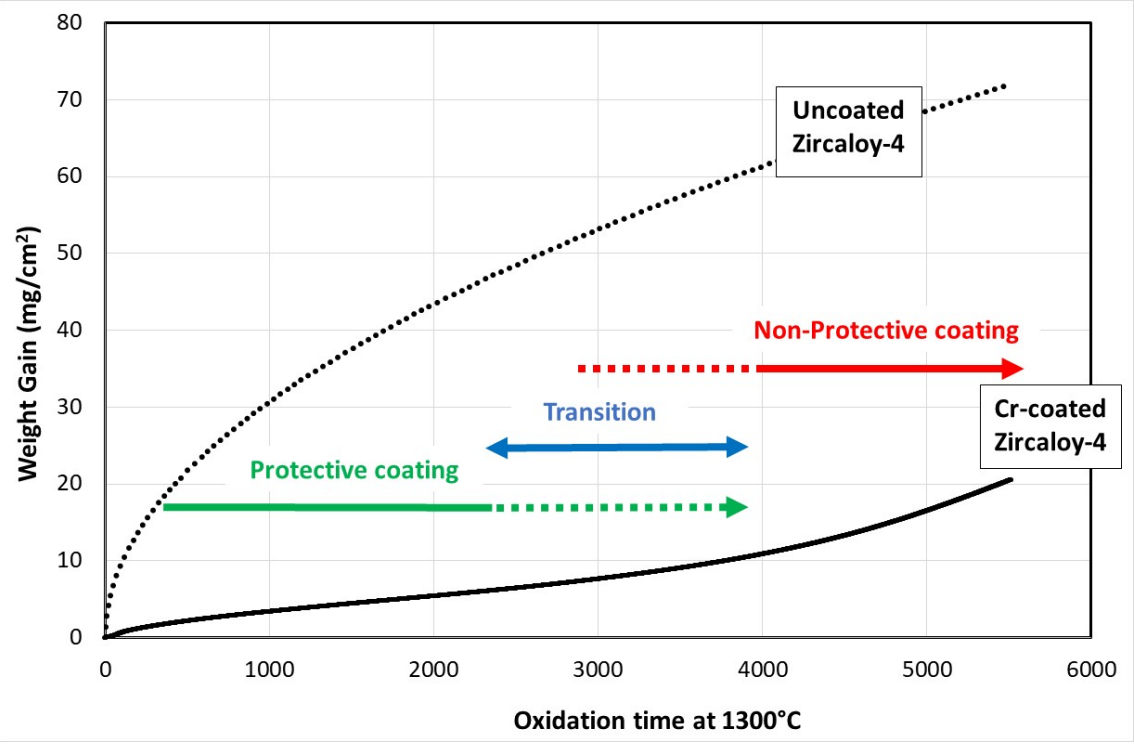


Figure 1 - Weight gain evolution measured by TGA experiments carried out in helium-oxygen mixture at 1300°C on the first generation of Cr-coated Zircaloy-4 (sheet sample geometry) compared to the weight gain evolution of uncoated Zircaloy-4


für Technologie

FROM RESEARCH TO INDUSTRY

cea den

framatome

EDF

French alternative energies and atomic energy commission
Saclay center | F91191 Gif-sur-Yvette Cedex
T. +33 (0)1 69 08 51 66 | F. +33 (0)1 69 08 82 52

Nuclear Energy Division
Nuclear Materials Department
Section for Applied Metallurgy Research

jean-christophe.brachet@cea.fr

Some Insights into High Temperature Steam Oxidation Kinetics and Process of Cr-Coated Zirconium-Based Alloys

(DBA-LOCA and beyond conditions)

Presentation based on a paper published in Corrosion Science Journal, entitled:
"High Temperature Steam Oxidation of Cr-Coated Zirconium-Based Alloys: Kinetics and Process"
https://doi.org/10.1016/j.corsci.2020.108537

J.C. BRACHET, E. ROUESNE, J. RIBIS, T. GUILBERT, S. URVOY, G. NONY, M. LE SAUX(*), N. CHAABANE, H. PALANCHER (CEA);
A. DAVID (Tescan-Analytics);
J. BISCHOFF, J. AUGEREAU (Framatome);
E. POUILLIER (EDF)
(*) present address: ENSTA-Brest, France

25th. International QUENCH Workshop
Karlsruhe Institute of Technology, Germany
(22-24 October 2019)

INTRODUCTION – (Cr-)COATED ZIRCONIUM BASED ALLOYS STUDIED AS SHORT-TERM (EVOLUTIONARY) ENHANCED-ATF CLAD CONCEPT

2005-2013: Early prospective studies carried out at CEA on several 5-10µm thick coatings (*Zirc-4 sheets substrate*), including ceramic and metallic ones
=> special PVD metallic Cr-coatings have been choosen (*Brachet et al., JNM, 2019*)

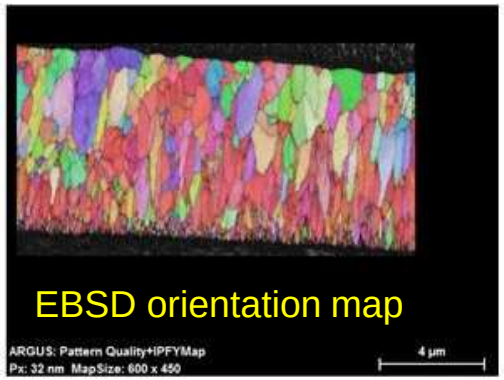
2013-2019: More recent studies carried out within CEA-Framatome-EDF framework on Cr-Coated $M5_{Framatome}$ nuclear fuel claddings (*Bischoff et al., Nucl. Eng. & Tech., 2018*)

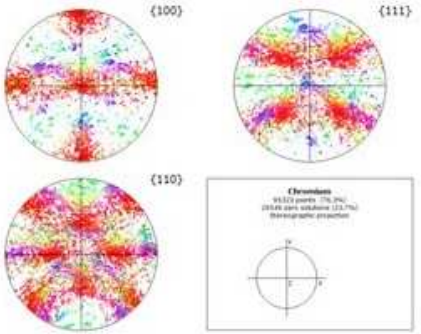
⇒ Some benefits for in-service conditions: negligible corrosion, higher wear resistance, *Zr-Cr stability under irradiation – no spallation (has to be confirmed for high BU)*…

⇒ Some benefits in LOCA and beyond conditions: HT strengthening & lower balloon and burst openings sizes + significant additional copying time before loss of clad integrity upon HT steam oxidation (*higher PQ strength/ductility…*)

Typical as-received cristallographic and morphological chromium coating textures of 1st. generation 5-10µm Cr-coated Zirc-4:

(remark: adequate coating deposition process-parameters are necessary to achieve good density-uniformity, low surface roughness and strong/stable Zr-Cr bonding)

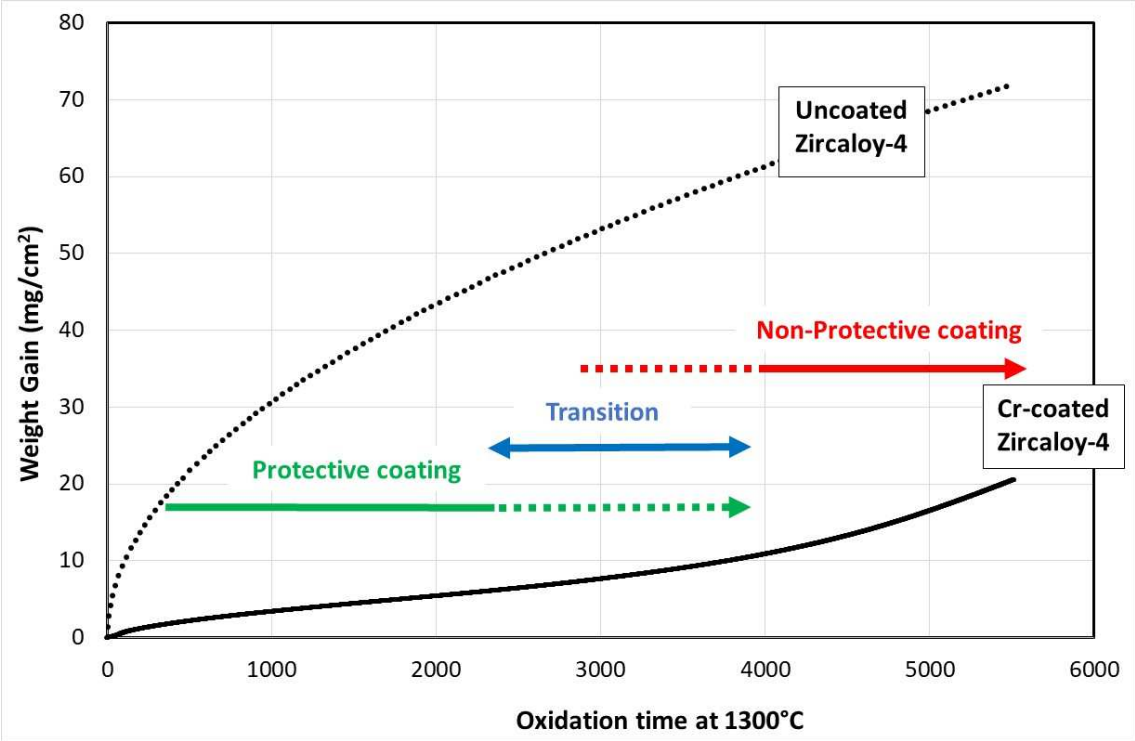




25th. Quench workshop, KIT, Oct. 2019, "HT Steam Oxidation of Cr-Coated Zr" (presentation based on paper published in Corrosion Science Journal: https://doi.org/10.1016/j.corsci.2020.108537)

OVERALL OXIDATION KINETICS OF Cr-COATED Zr BASED ALLOYS:

Weight gain evolution measured by TGA experiments carried out in helium-oxygen mixture at 1300°C on 1st generation Cr-coated Zircaloy-4 (sheet sample geometry):



Some pending questions:

- What are the underlying oxidation and diffusion mechanisms?
- Any hydrogen up-take?
- Any Cr volatilisation (*formation of CrO_3, $CrO_2(OH)_2$, CrO_2OH…*) – (*Yeom et al. JNM, 2019*)?

BEGINNING OF OXIDATION (PROTECTIVE COATING) (1/4)

For short enough HT steam oxidation time (i.e., for DBA-LOCA and slighlty beyond oxidation times):

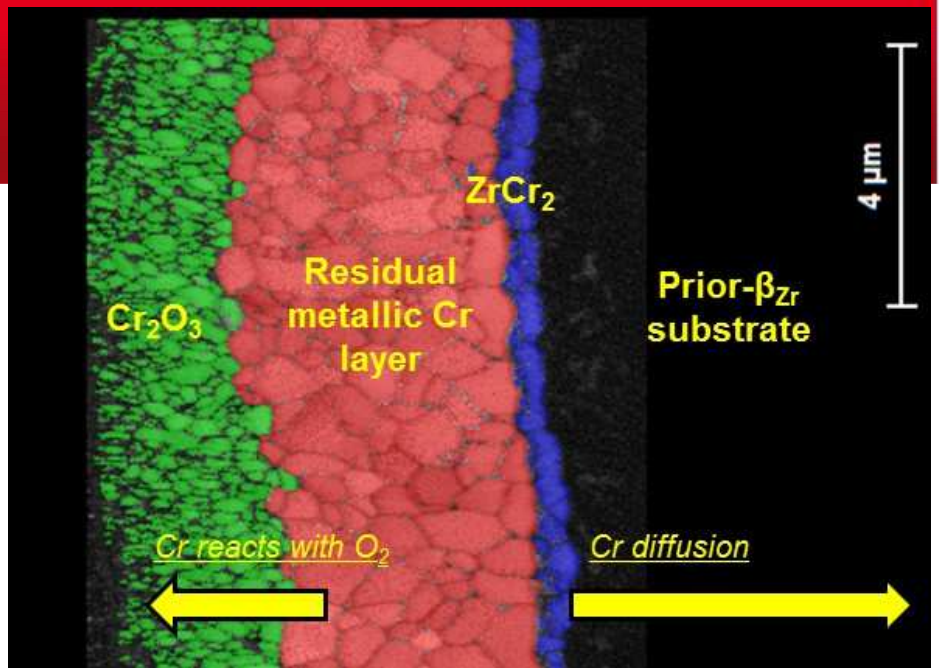
Overall parabolic, oxidation kinetics;

⇒ Cr-coating consumption by:

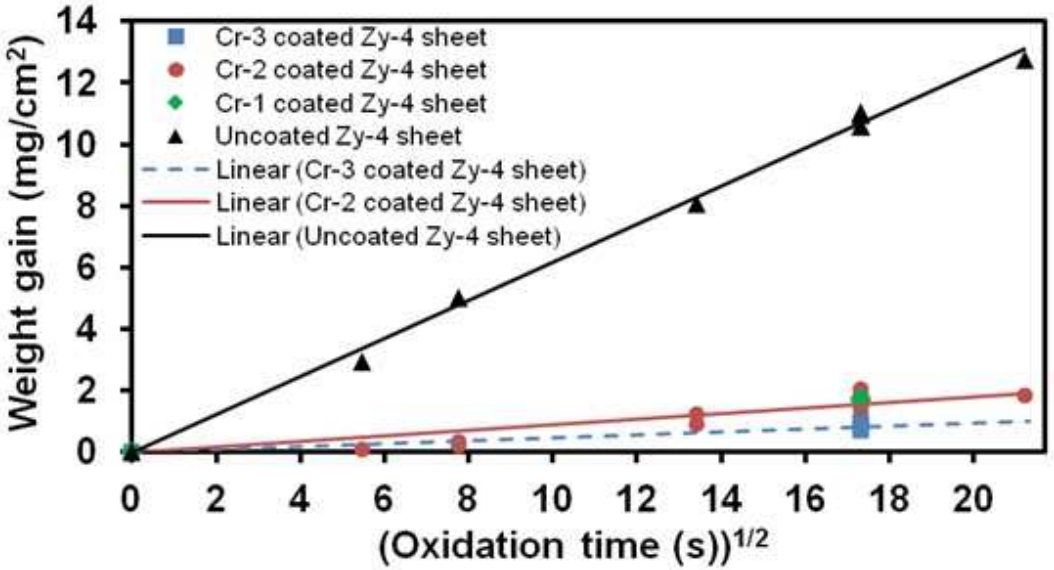
(1) outer Cr_2O_3 scale formation;

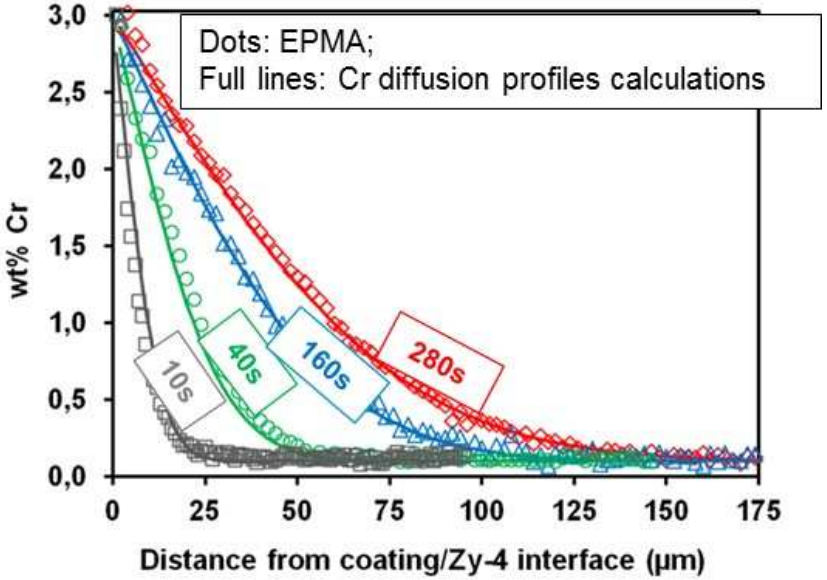
(2) inward Cr diffusion into the β_{Zr} substrate;

(3) + *Cr volatilisation? (discussed further)*



(Brachet et al., JNM, 2019)





25th. Quench workshop, KIT, Oct. 2019, "HT Steam Oxidation of Cr-Coated Zr" (presentation based on paper published in Corrosion Science Journal: https://doi.org/10.1016/j.corsci.2020.108537)

BEGINNING OF OXIDATION (PROTECTIVE COATING) (2/4)

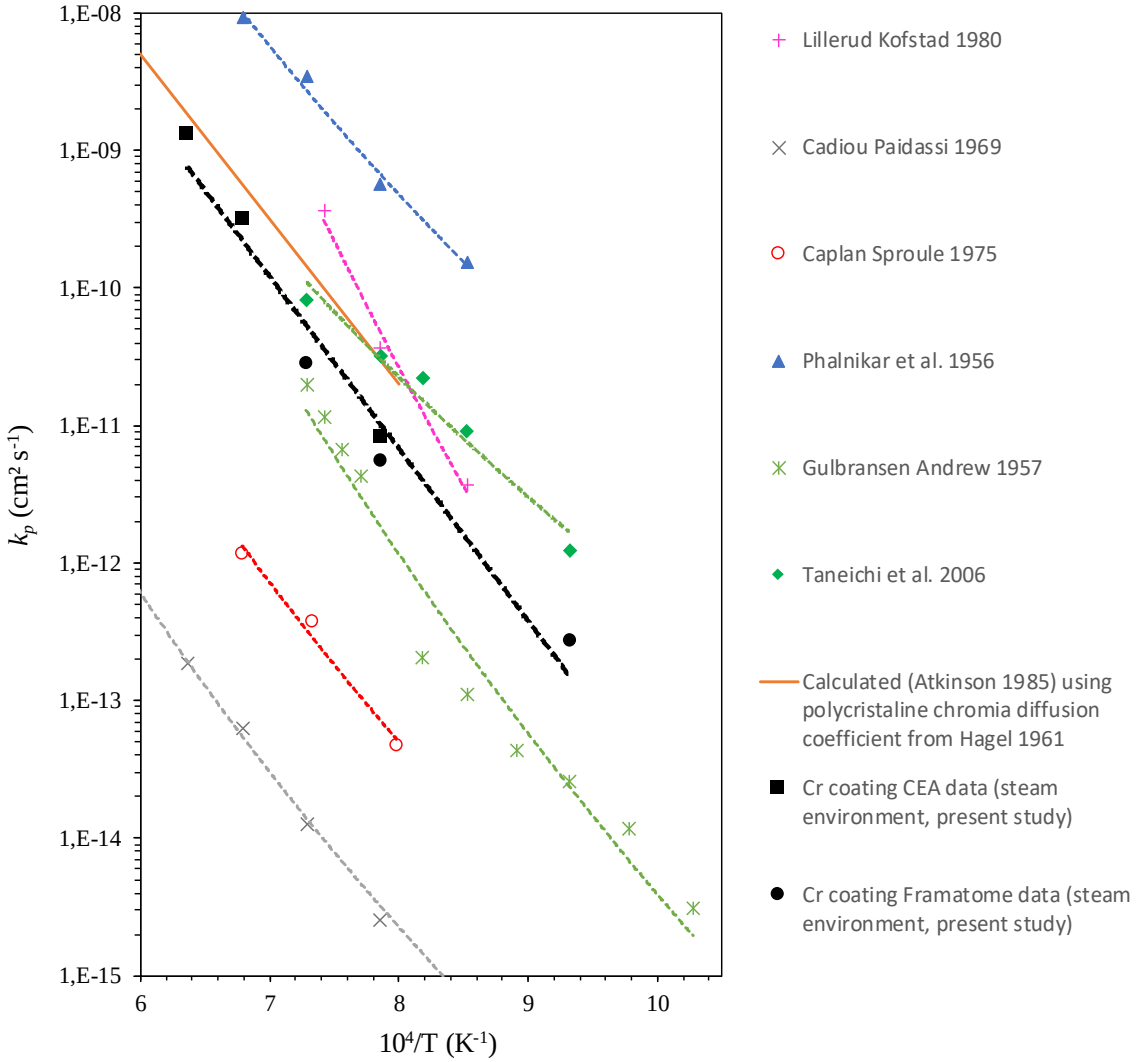
=> **Outer chromia scale thickening kinetics** under isothermal conditions:

$$X_{Cr2O3} = (Kp.t)^{1/2}$$

Kp = parabolic rate constant derived from both CEA and Framatome data / **800-1300°C**

Consistent with some literature data for HT oxidation of bulk Cr (*under oxygen or air environment*)

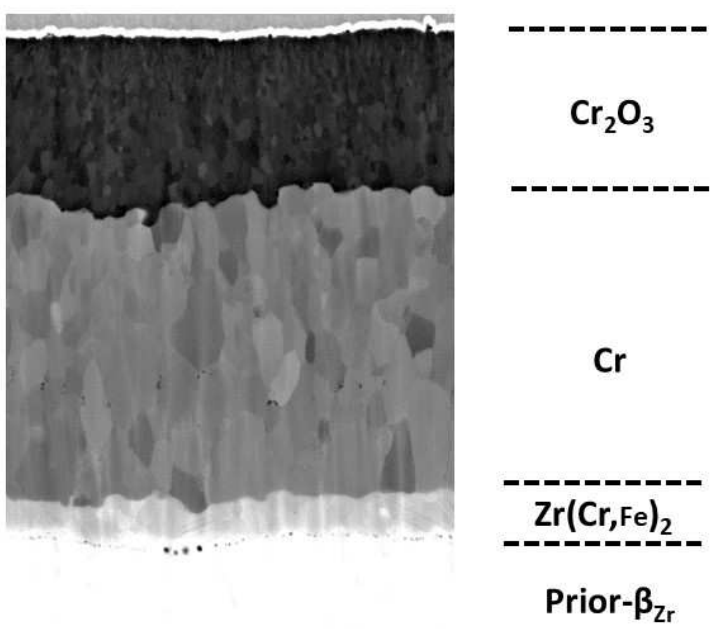
⇒ *Remark: parabolic growth kinetics of outer chromia scale only observed at short enough oxidation time*



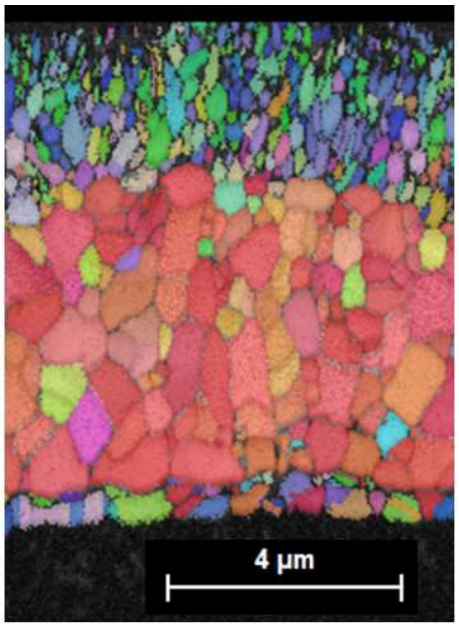
25th. Quench workshop, KIT, Oct. 2019, "HT Steam Oxidation of Cr-Coated Zr" (presentation based on paper published in Corrosion Science Journal: https://doi.org/10.1016/j.corsci.2020.108537)

BEGINNING OF OXIDATION (PROTECTIVE COATING) (3/4)
µSTRUCTURAL EXAMINATION (EBSD)

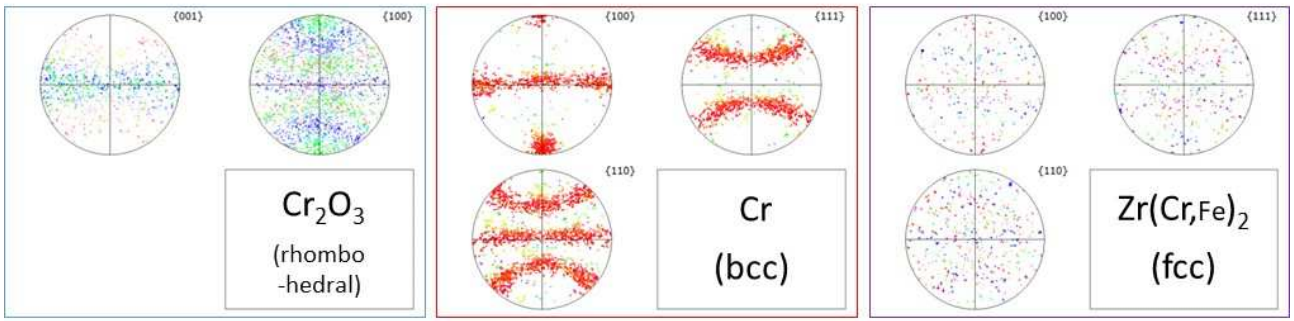
- Outer chromia scale formation with a fiber cristallographic texture;
- Sub-oxide residual metallic Cr layer with stronger cristallographic texture, likely inherited from the initial (as-received) one;
- Thickening of an intermediate intermetallic $Zr(Cr,Fe)_2$ layer (*due to the HT Zr-Cr inter-diffusion*)



(a)



(b)

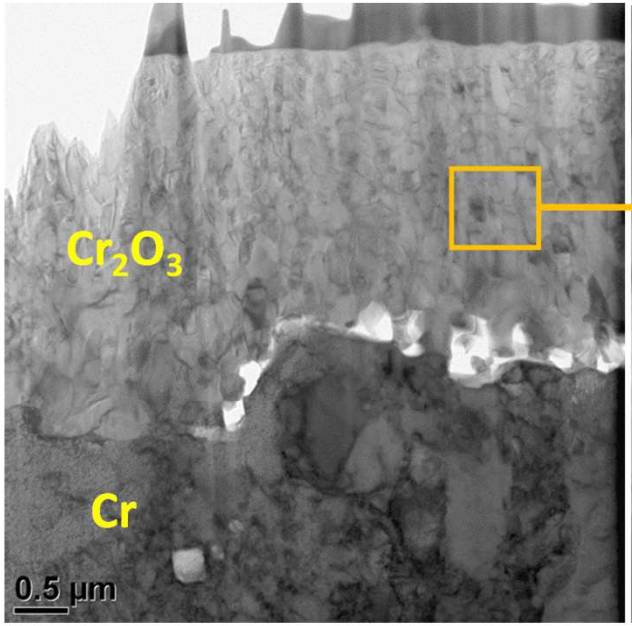


(c)

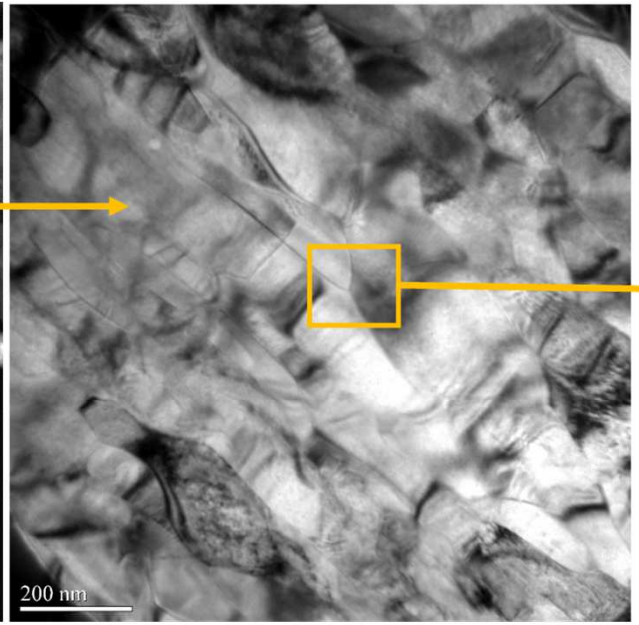
25th. Quench workshop, KIT, Oct. 2019, "HT Steam Oxidation of Cr-Coated Zr" (presentation based on paper published in Corrosion Science Journal: https://doi.org/10.1016/j.corsci.2020.108537)

BEGINNING OF OXIDATION (PROTECTIVE COATING) (4/4)
µSTRUCTURAL EXAMINATION (TEM)

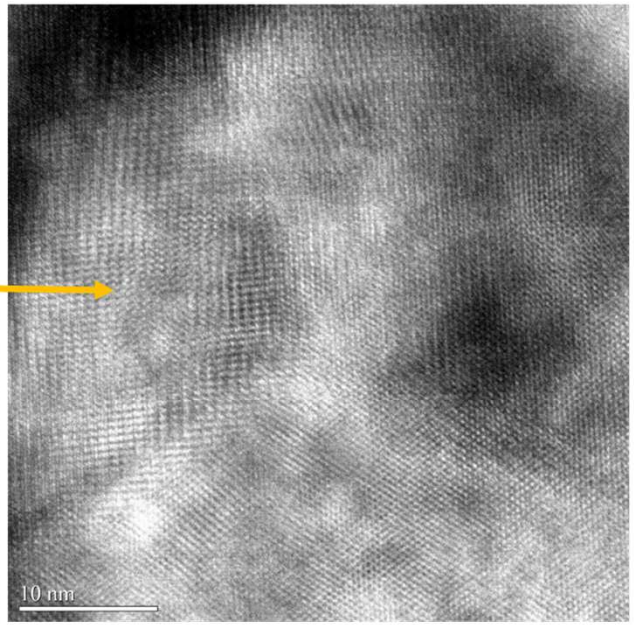
- Confirmation of dense (and thus protective) outer chromia scale formation;
- Evidence of interfacial porosities *(« Kirkendall » effects? and/or due to delamination upon final water quenching? …)*;



(a) Overall view of Cr_2O_3/Cr outer scales (low magnification)



(b) Intermediate magnification - Cr_2O_3 scale



(c) HRTEM examination of a triple grain boundary - Cr_2O_3 scale

25th. Quench workshop, KIT, Oct. 2019, "HT Steam Oxidation of Cr-Coated Zr" (presentation based on paper published in Corrosion Science Journal: https://doi.org/10.1016/j.corsci.2020.108537)

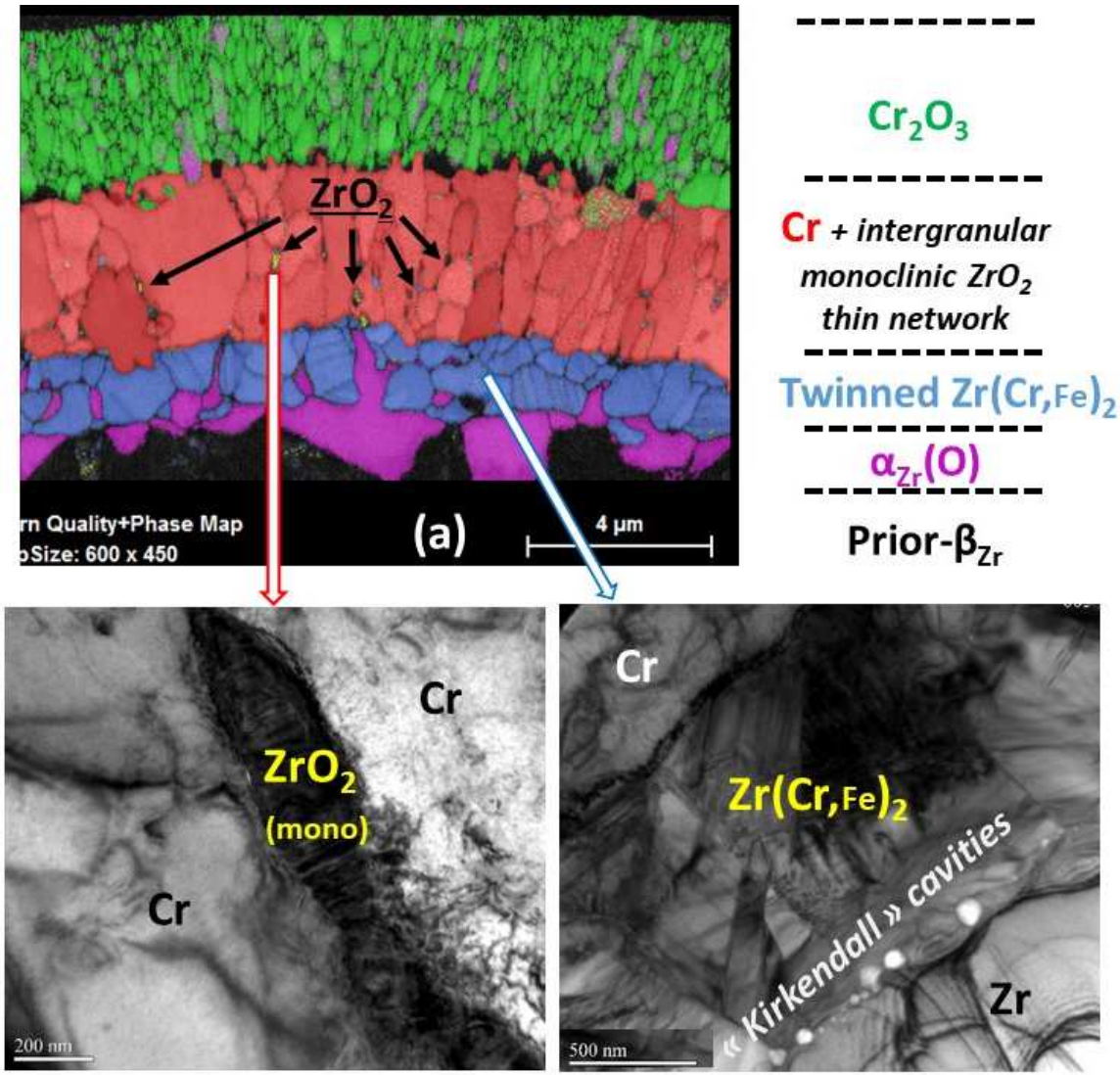
TRANSITION BETWEEN PROTECTIVE AND NON-PROTECTIVE COATING

Drastic decrease of the outer Cr_2O_3 scale thickening kinetics
=> new oxygen transport mechanism activated beneath the outer Cr_2O_3 scale:

- Inward oxygen together with outward Zr intergranular diffusion within the residual metallic Cr layer;
- Nucleation and growth of zirconia stringers at the Cr grain boundaries, *likely due to higher thermodynamic stability of zirconia vs. chromia*;

⇒ Continuous network of zirconia at Cr grain boundaries promoting further and accelerated (inward) diffusion of oxygen anions

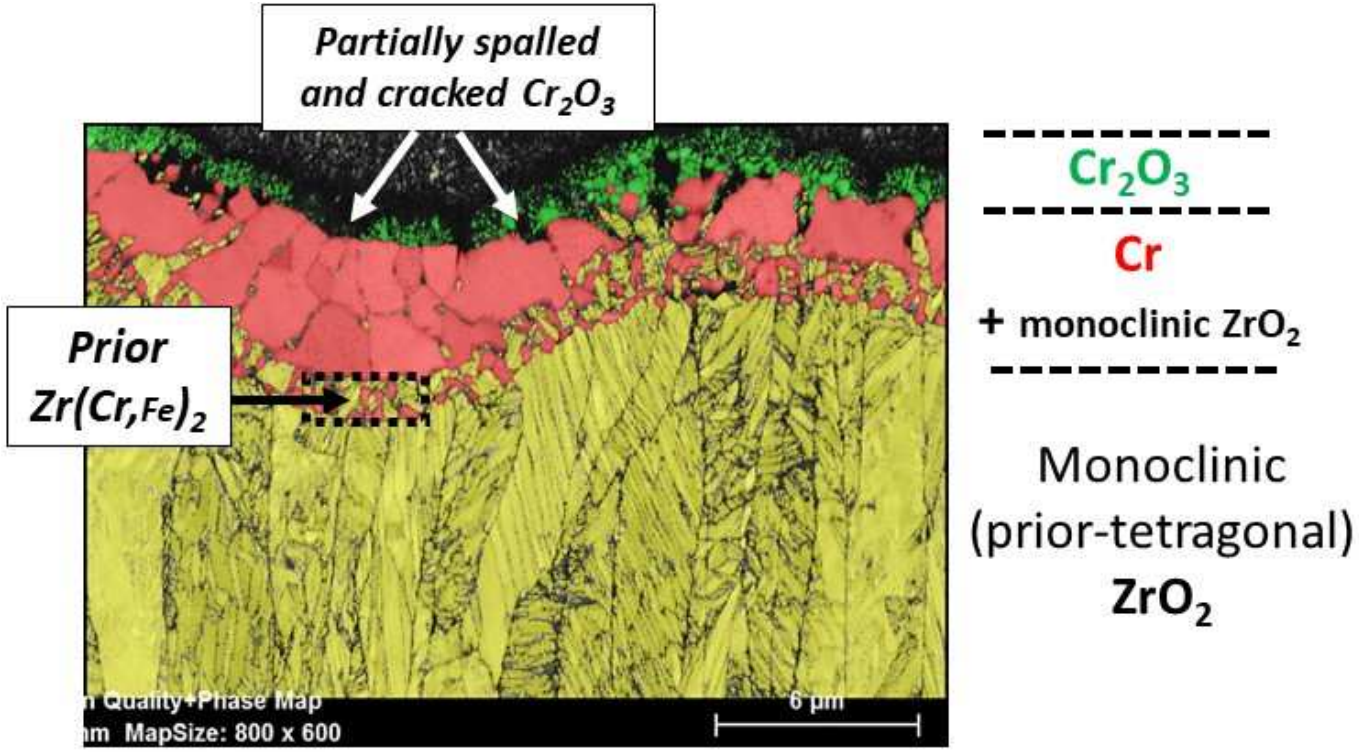
⇒ αZr(O) incursions…



25th. Quench workshop, KIT, Oct. 2019, "HT Steam Oxidation of Cr-Coated Zr" (presentation based on paper published in Corrosion Science Journal: https://doi.org/10.1016/j.corsci.2020.108537)

LONGER OXIDATION TIMES (NO LONGER PROTECTIVE COATING)

- Outer heavily damaged residual chromia scale (no more protective);
- Underlying residual metallic (not oxidized) chromium layer, showing a quasi-continuous intergranular zirconia network (accelerated diffusion path for oxygen);
- Prior-$Zr(Cr)_2$ intermediate layer has disappeared according to: $Zr(Cr)_2 + 2O \Rightarrow ZrO_2 + 2Cr$;
- Thick zirconia layer observed beneath the residual chromium-rich outer layers, consistently with the observed overall oxidation acceleration.



25th. Quench workshop, KIT, Oct. 2019, "HT Steam Oxidation of Cr-Coated Zr" (presentation based on paper published in Corrosion Science Journal: https://doi.org/10.1016/j.corsci.2020.108537)

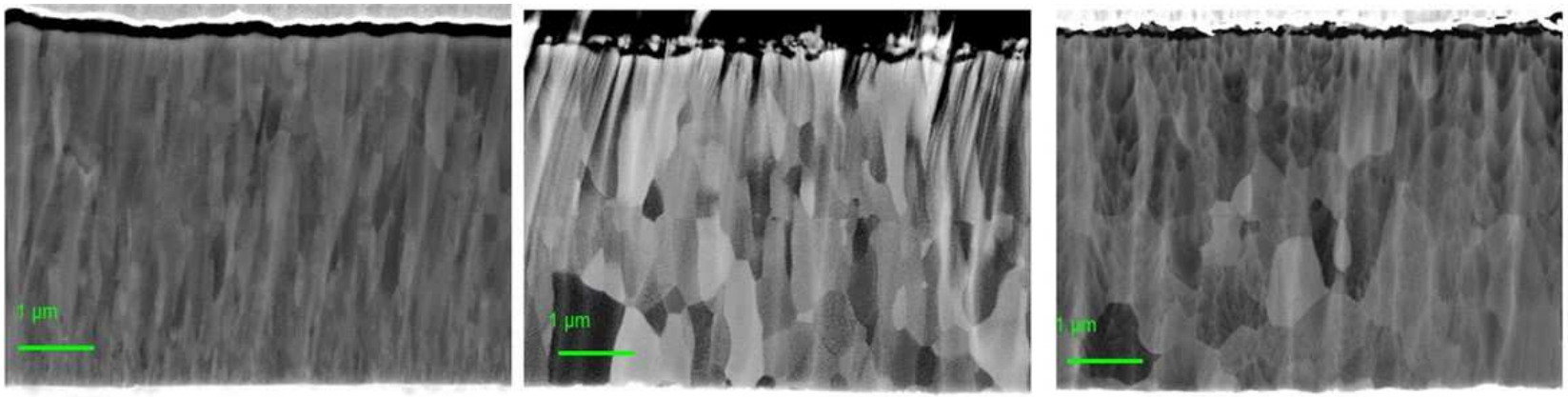
EFFECT OF PRE-ANNEALING AT 700 AND 800°C *INDUCING Cr RECRYSTALLISATION (1/3)*

- Complementary experiments carried out to assess the proposed HT oxidation mechanism, *i.e., preferential/accelerated oxygen transport along the zirconia stringers formed at Grain Boundaries (GB) of residual sub-oxide metallic Cr layer*:

⇒ 5-10µm thick Cr-coated Zr samples have been **pre-annealed at 700/800°C**

⇒ Then, submitted to one sided HT steam oxidation: **1500s at 1200°C**

⇒ **Increase of the Cr-coating grain size and more equiaxed grain structures:**



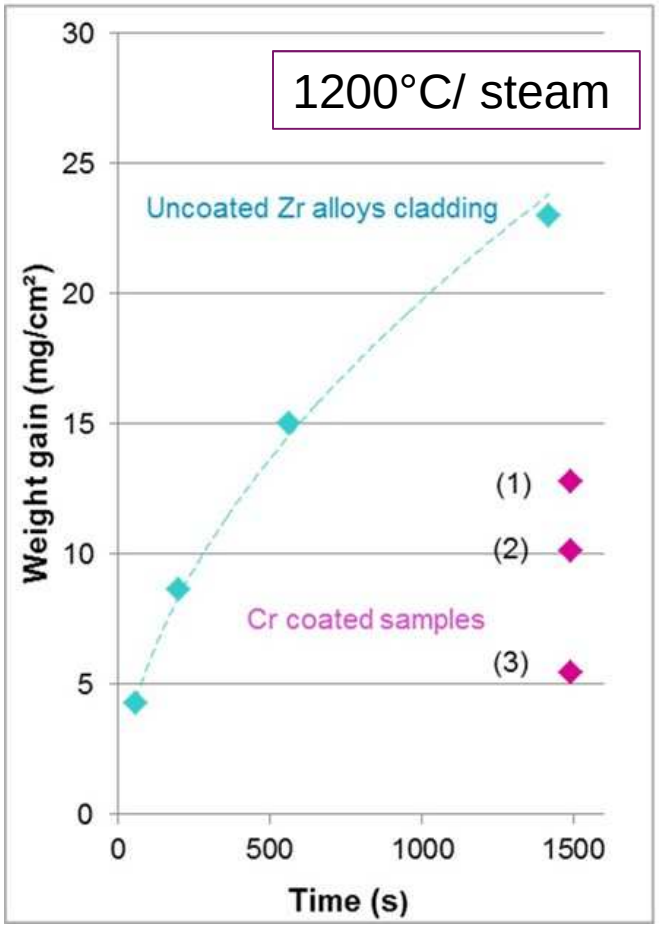
As-deposited | Sample annealed at 700°C (2h) | Sample annealed at 800°C (2h)

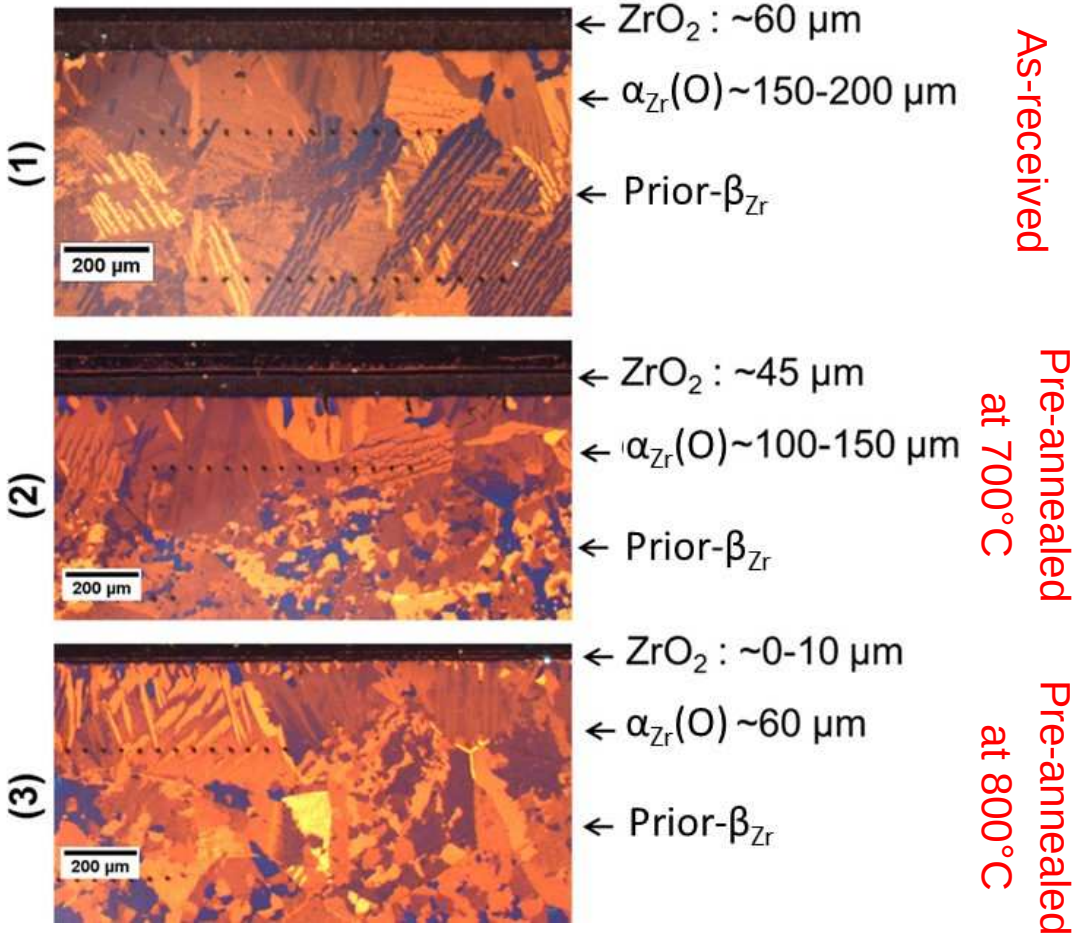
⇒ Lower GB density may induce lower preferential/accelerated diffusion footpaths for oxygen ?

⇒ Additional delay for inward oxygen diffusion/ingress ?

25th. Quench workshop, KIT, Oct. 2019, "HT Steam Oxidation of Cr-Coated Zr" (presentation based on paper published in Corrosion Science Journal: https://doi.org/10.1016/j.corsci.2020.108537)

EFFECT OF PRE-ANNEALING AT 700 AND 800°C (2/3)





25th. Quench workshop, KIT, Oct. 2019, "HT Steam Oxidation of Cr-Coated Zr" (presentation based on paper published in Corrosion Science Journal: https://doi.org/10.1016/j.corsci.2020.108537)

EFFECT OF PRE-ANNEALING AT 700 AND 800°C (3/3)

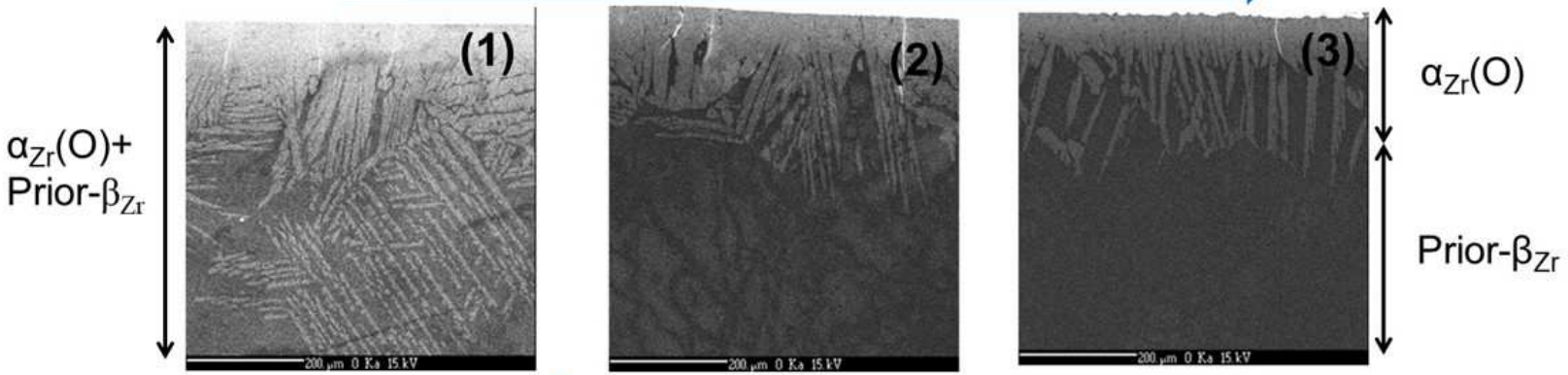
After oxidation for 1500s @ 1200°C

As-received

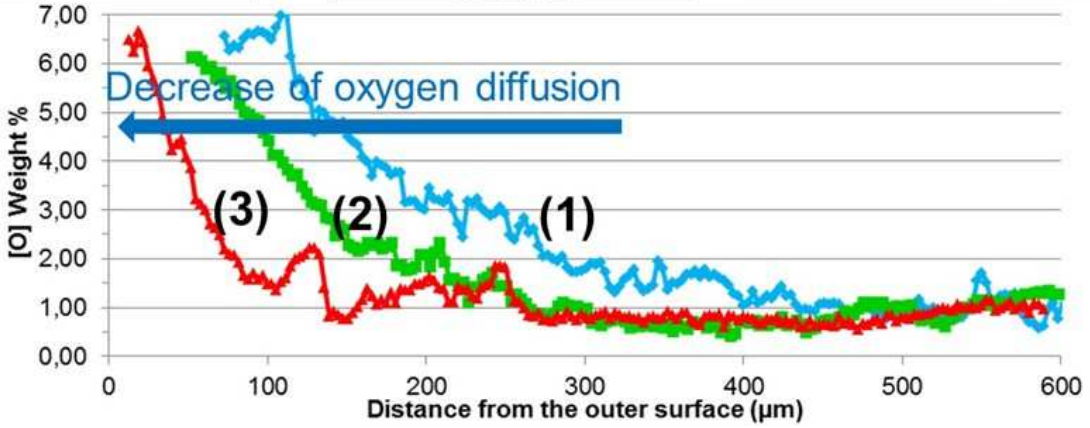
Pre-annealed @ 700°C

Pre-annealed @ 800°C

Decrease of $\alpha_{Zr}(O)$ thickness



EPMA Oxygen diffusion profiles measured from the $ZrO_2/\alpha_{Zr}(O)$ interface

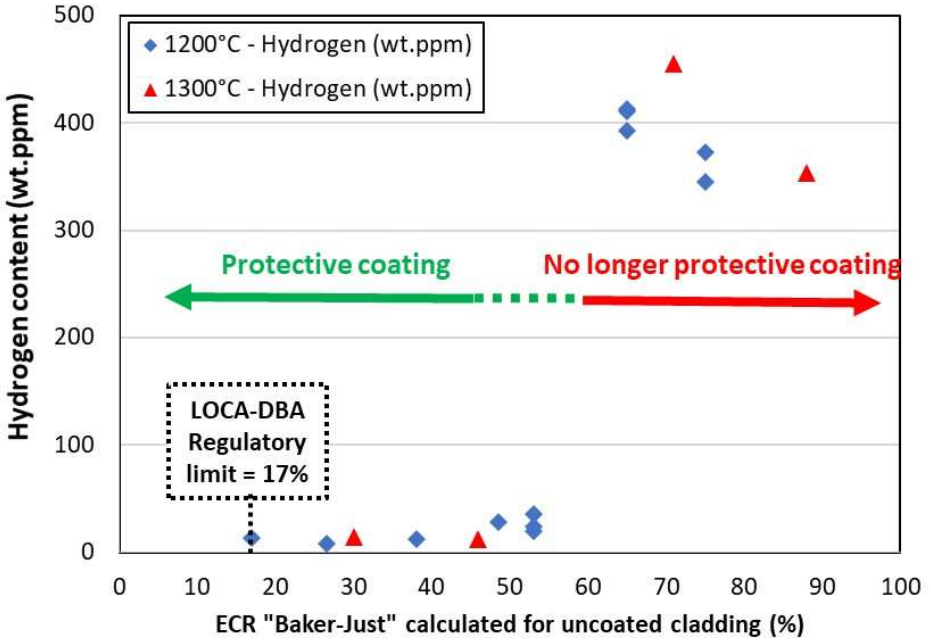


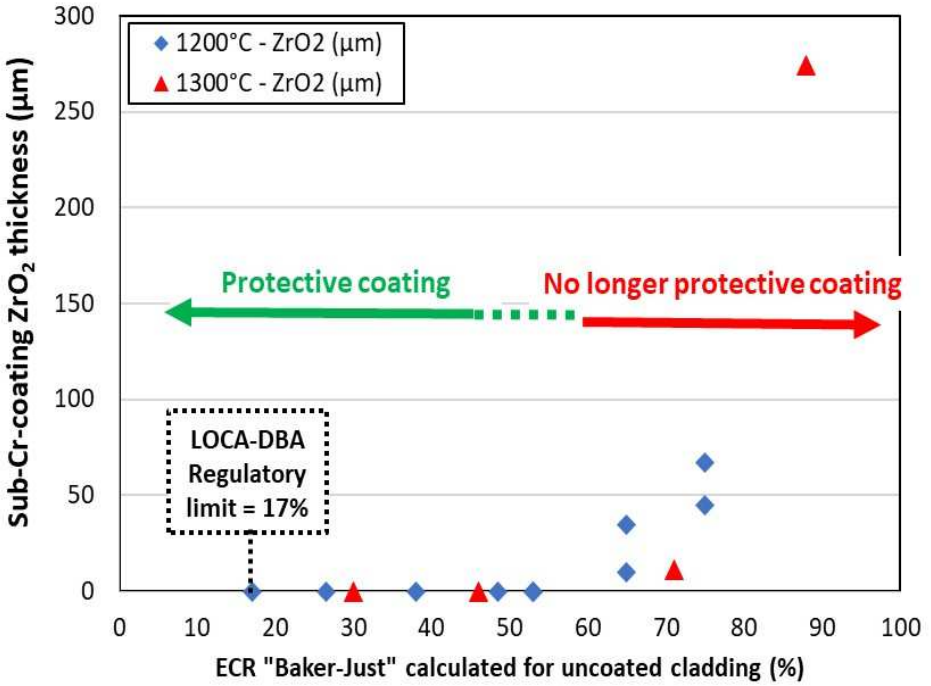
Pre-annealing + HT oxidation experiments seem to confirm the proposed HT oxidation mechanism

25th. Quench workshop, KIT, Oct. 2019, "HT Steam Oxidation of Cr-Coated Zr" (presentation based on paper published in Corrosion Science Journal: https://doi.org/10.1016/j.corsci.2020.108537)

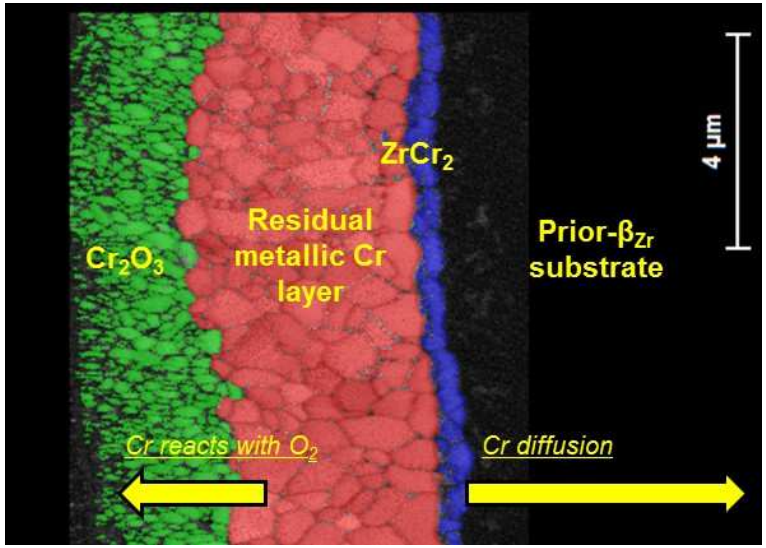
TRANSIENT HYDROGEN UP-TAKE

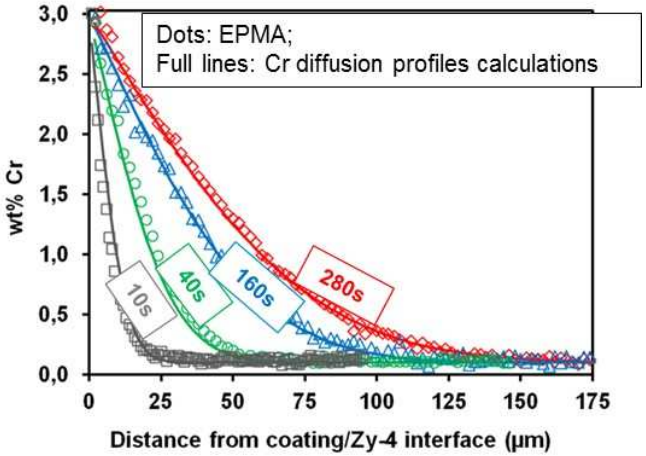
- Short time-period during which steam may have direct access to the metallic Zr-based substrate (*when the Cr-coating loses definitely its protective properties*), thus inducing transient H up-take;
- May coincide with the early formation of thin & discontinuous zirconia spots beneath the residual Cr-coating;
- Occurs at high ECR values, and limited to a few hundreds of wt.ppm;
- Hydrogen content seems to saturate after this short transient period (*thanks to formation of a fresh continuous and thus again protective Zirconia layer*) ≠ from post-breakaway situations…





Cr VOLATILISATION OR NOT?





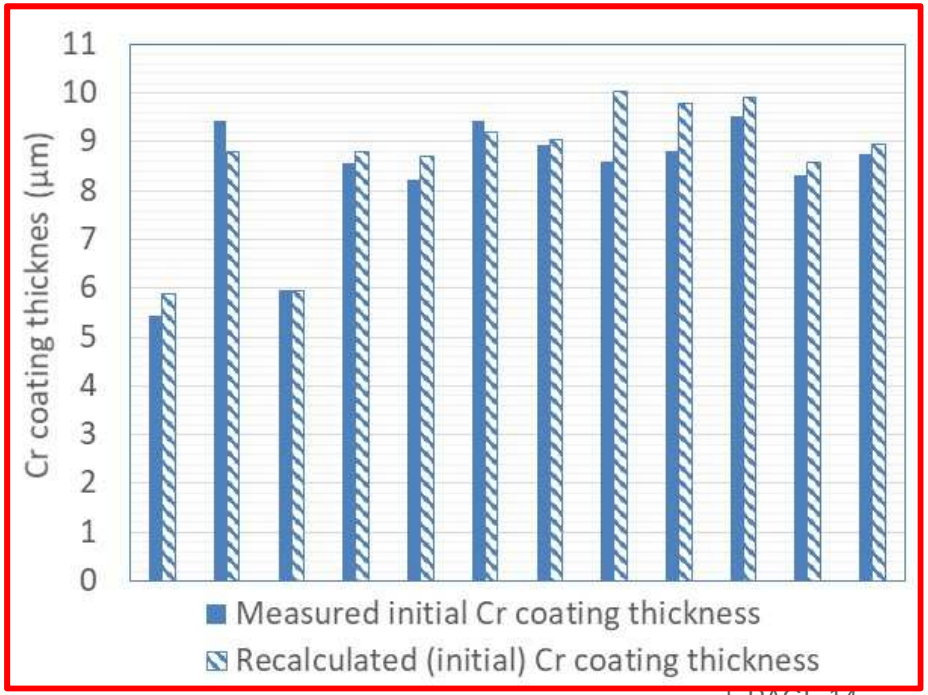
To assess if Cr volatilization is significant or not => **post-HT oxidation re-calculation of the initial Cr coating thickness**:

$X_0(Cr) = X_{Cr2O3}/PB + X(Cr)_{metal} + X(Cr)_{prior\text{-}\beta Zr}$

Where: PB ~ 2 (Pilling-Bedworth coeff. for chromia)

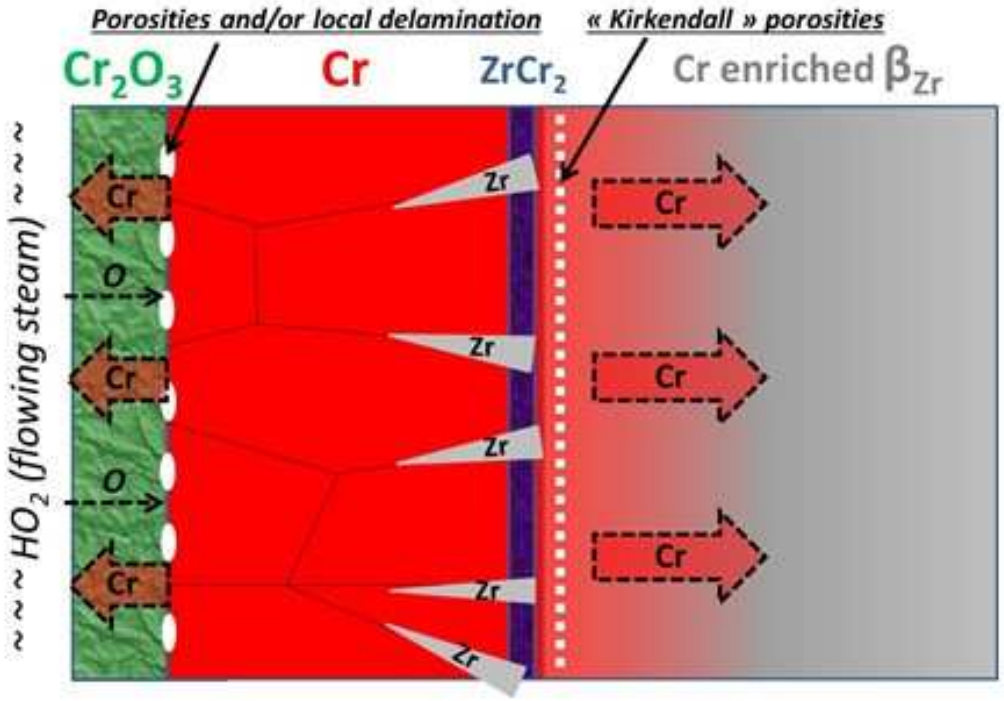
$X(Cr)_{prior\text{-}\beta Zr}$ = *integration of the Cr-diffusion profiles*

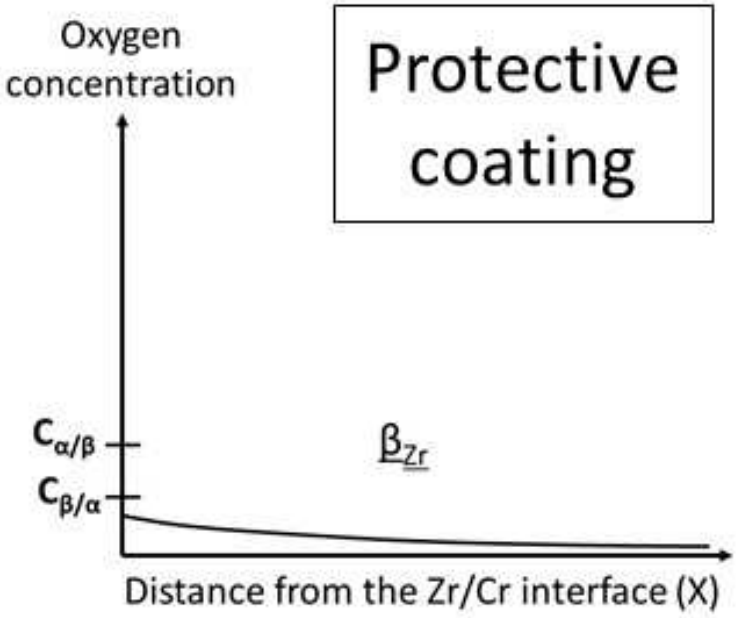
CONCLUSION: *for the oxidation times and temperature experienced here,* Cr volatilization can be neglected (consistently with some literature data)



25th. Quench workshop, KIT, Oct. 2019, "HT Steam Oxidation of Cr-Coated Zr" (presentation based on paper published in Corrosion Science Journal: https://doi.org/10.1016/j.corsci.2020.108537)

Tentative schematic summary (1/3): Beginning of oxidation

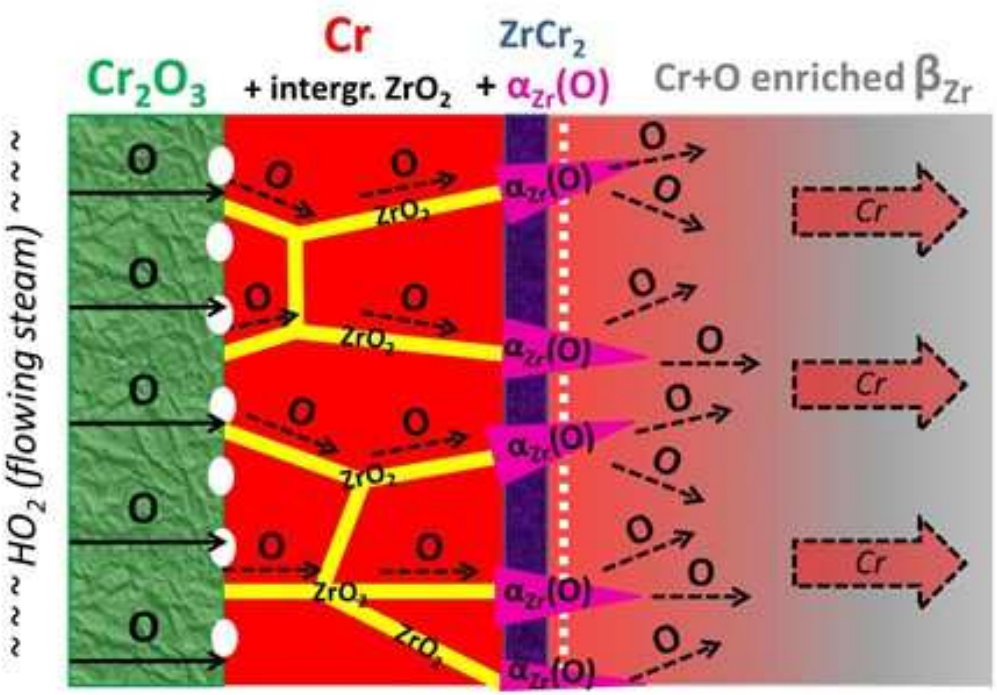


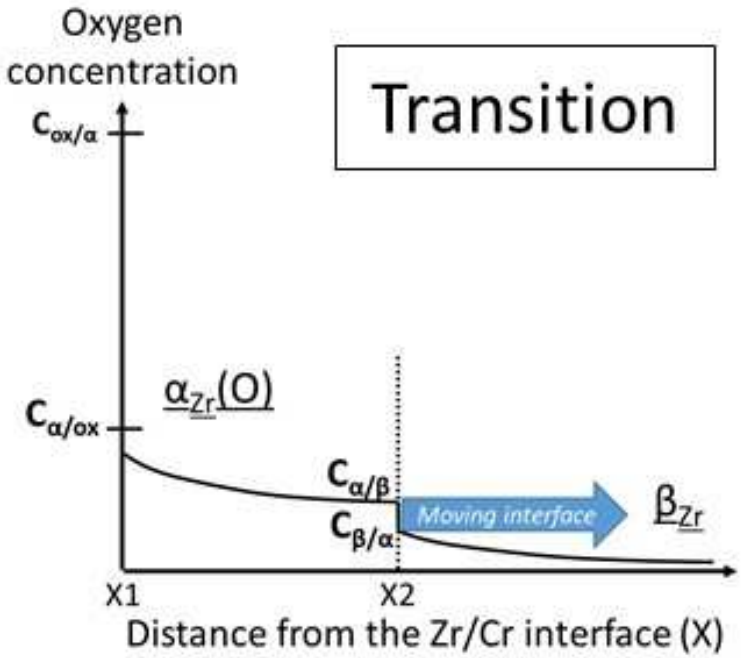


no hydrogen up-take…

25th. Quench workshop, KIT, Oct. 2019, "HT Steam Oxidation of Cr-Coated Zr" (presentation based on paper published in Corrosion Science Journal: https://doi.org/10.1016/j.corsci.2020.108537)

Summary (2/3): Transition period

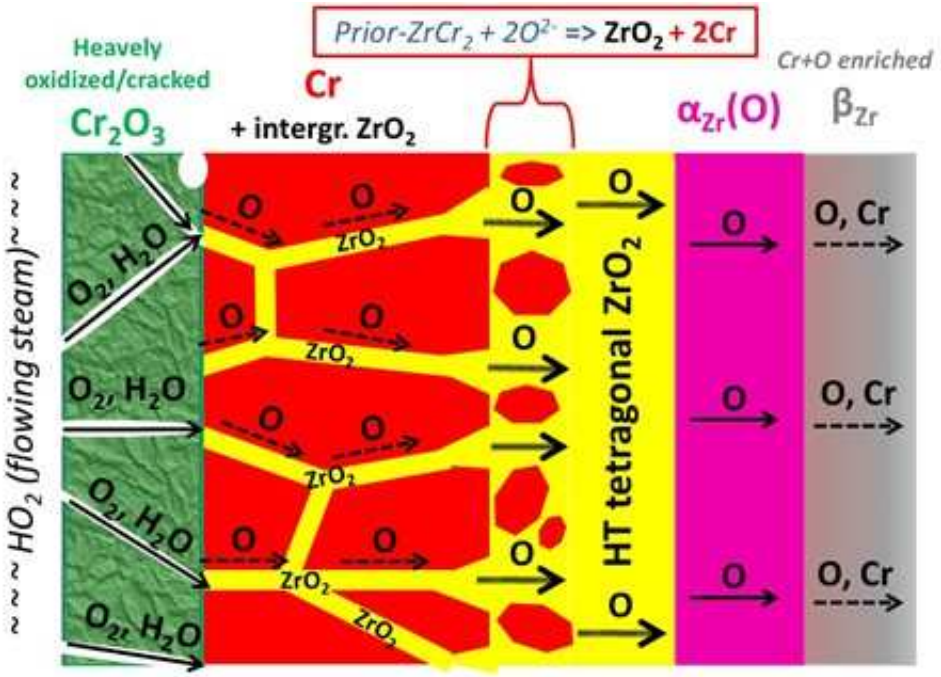


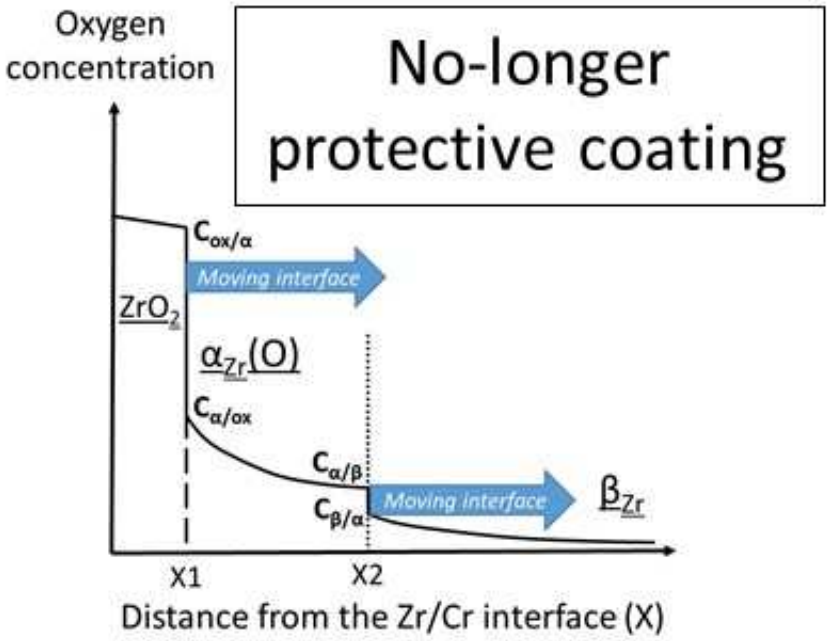


+ transient hydrogen up-take…

25th. Quench workshop, KIT, Oct. 2019, "HT Steam Oxidation of Cr-Coated Zr" (presentation based on paper published in Corrosion Science Journal: https://doi.org/10.1016/j.corsci.2020.108537)

Summary (3/3): Longer oxidation times





no more hydrogen up-take…

25th. Quench workshop, KIT, Oct. 2019, "HT Steam Oxidation of Cr-Coated Zr" (presentation based on paper published in Corrosion Science Journal: https://doi.org/10.1016/j.corsci.2020.108537)

FROM RESEARCH TO INDUSTRY

cea den

THANK YOU FOR YOUR ATTENTION

View publication stats

Some additional CEA references on Cr-coated Zr based nuclear fuel claddings:

[1] I. Idarraga et al., "Assessment at CEA of coated nuclear fuel cladding for LWRs with increased margins in LOCA and beyond conditions", in proceedings of TopFuel 2013, Charlotte, USA, (Sept. 15-19, 2013)

[2] J.C. Brachet et al., "On-going studies at CEA on Cr-coated zirconium based nuclear fuel claddings for enhanced tolerant LWRs fuel", proceedings of TopFuel 2015, Zurich, Switzerland (Sept. 13-19, 2015)

[3] J.C. Brachet et al., "Behavior under LOCA conditions of Enhanced Accident Tolerant Chromium Coated Zircaloy-4 Cladding", proceedings of TopFuel 2016, Boise, IDAHO, USA, (Sept. 11-16, 2016)

[4] J.C. Brachet et al., "Behavior of Cr-coated M5™ claddings under LOCA conditions", Proceedings of 2017 Water Reactor Fuel Performance Meeting, (Sept. 10-14, 2017), Jeju Island, Korea

[5] A. Michau, et al., "High-temperature oxidation resistance of chromium-based coatings deposited by DLI-MOCVD process for enhanced protection of the inner surface of long tubes", Surf. & Coat. Tech. (2018)

[6] J.C. Brachet, et al., « Behavior of Cr-coated M5 claddings during and after high temperature steam oxidation from 800°C up to 1500°C (LOss-of-Coolant Accident & Design Extension Conditions)", Proceedings of WRFPM/TOPFUEL 2018, (30 Sept. – 04 Oct. 2018), Prague, Czech Republic

[7] M. Dumerval, et al., « Behavior of Chromium Coated M5 Claddings upon thermal ramp tests under internal pressure (LOss-of-Coolant Accident Conditions)", Proceedings of WRFPM/TOPFUEL 2018, (30 Sept. – 04 Oct. 2018), Prague, Czech Republic

[8] J. Ribis, et al., "Atomic-scale interface structure of a Cr-coated Zirc-4 », Journ. of Mat. Sci., (2018)

[9] A. Wu, et al., "HRTEM and chemical study of an ion-irradiated chromium/zircaloy-4 Interface", Journal of Nuclear Materials 504 (2018) 289-299

[10] J.C. Brachet, et al., "Early studies on Cr-Coated Zircaloy-4 as Enhanced Accident Tolerant Nuclear Fuel Claddings for Light Water Reactors", Journal of Nuclear Materials 517 (2019) pp. 268-285

Oxidation and quenching behavior of cold spray Cr-coated Zr alloy fuel cladding

Chongchong Tang, Mirco Grosse, Martin Steinbrueck, Ulrike Stegmaier, Niek Neuraij
Institute for Applied Materials (IAM), Karlsruhe Institute of Technology (KIT), D-76021 Karlsruhe, Germany

Koroush Shirvan
Department of Nuclear Science and Engineering, Massachusetts Institute of Technology, 77, Massachusetts Avenue, Cambridge, MA 02139, USA

The Fukushima-Daiichi accidents in 2011 highlighted the demand to explore and develop advanced accident tolerant fuel (ATF) claddings that provide enhanced safety margins under accident scenarios of water-cooled nuclear reactors. One near-term evolutionary strategy can be surface modification of state-of-the-art zirconium-based alloy cladding with innovative metallic or ceramic coatings. This solution characterizes an incremental change to the currently standardized UO_2 fuel/Zr alloy cladding structures and allows more easily licensing.

Among the variety of coating materials being investigated, the pure metallic Cr coating represents one of the most attractive and promising options for near-term implementation. The Cr coatings, deposited by either cold spraying or physical vapor deposition (PVD), are featured by good adhesion strength and irradiation resistance. Formation of a superficial Cr_2O_3 layer in oxidizing environments renders the coated cladding an extremely low corrosion rate under simulated normal operational conditions and significantly improved high-temperature steam oxidation resistance with reduced cladding creep and ballooning during LOCA conditions. The eventual objective of enhanced ATF materials is to offer additional coping time in case of severe accident scenarios, however, only few works are devoted to evaluation and qualification of oxidation and quench performances of Cr coated cladding under simulated severe accident scenarios.

In this presentation, the oxidation performance and quench behavior of cold spraying Cr coated Zircaloy-2 tubes were investigated from 1100°C up to 1500°C in steam using the single-rod quench facility QUENCH-SR. The coated samples displayed improved oxidation resistance, good thermal shock resistance and higher post-quench ductility during oxidation at 1100°C and 1200°C for 1 hour accompanied by subsequent quench in water. However, substantial bending of the coated tubes was observed during oxidation at 1100°C, which led to the detachment of the coating and loss of protective effect on one side. A transient test with a heating rate of 10 K/min was performed additionally to the isothermal tests. When the temperature exceeds the Cr-Zr eutectic temperature (~1330°C), formation of liquid phase contributed to failure of the coatings at about 1500°C. A much faster oxidation rate compared to uncoated reference sample was detected at temperatures above ~1450°C.



Oxidation and quenching behavior of cold spray Cr-coated Zr alloy fuel cladding

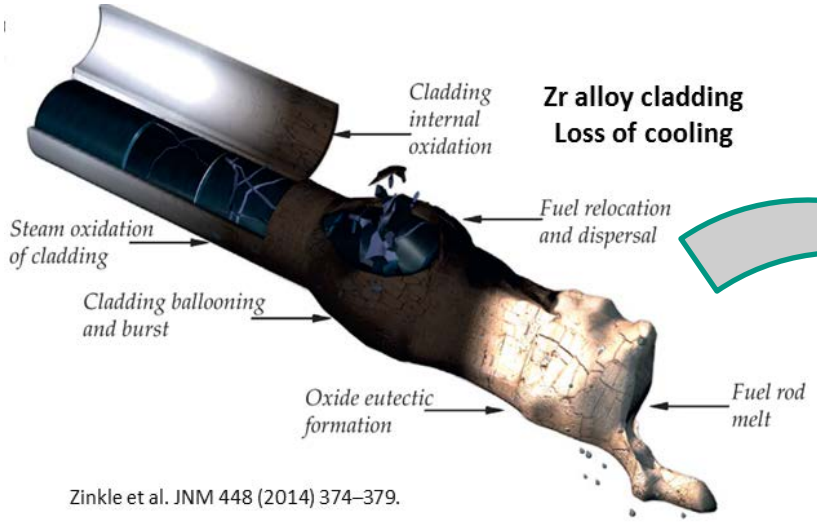
C. Tang, M. Grosse, M. Steinbrueck, U. Stegmaier, N. Neuraij
Institute for Applied Materials (IAM), Karlsruhe Institute of Technology (KIT), D-76021 Karlsruhe, Germany

K. Shirvan
Department of Nuclear Science and Engineering, Massachusetts Institute of Technology, Cambridge, MA 02139, USA

Institute for Applied Materials IAM-AWP & Program NUSAFE



Accident tolerant fuels (ATF) cladding



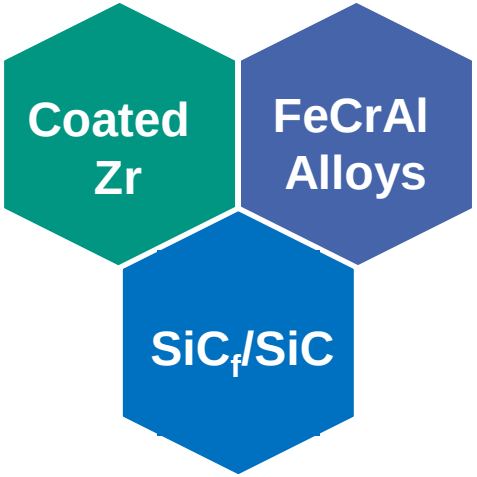
Zinkle et al. JNM 448 (2014) 374–379.

Enhanced Tolerance to Loss of Active Core Cooling

ATF

Increased Coping Time for Severe Accident Management!

ATF Concepts

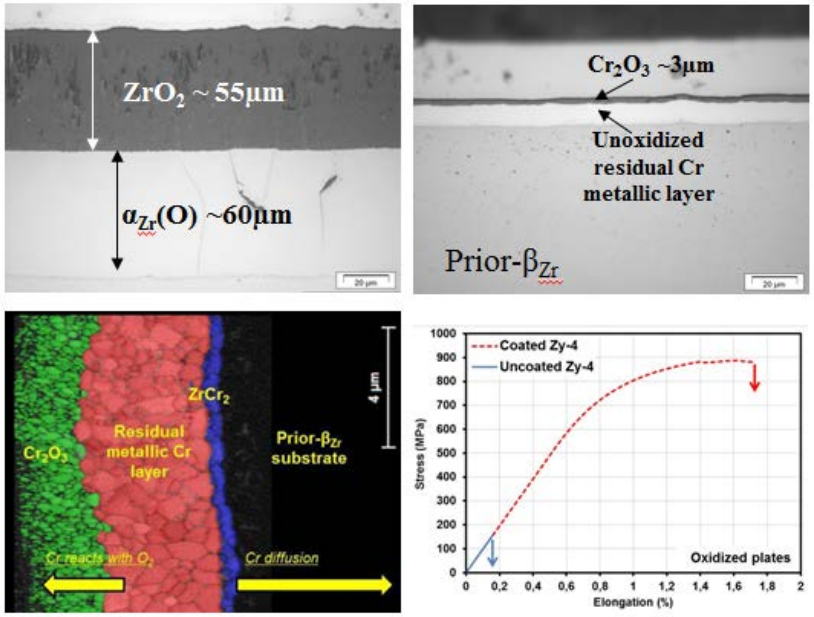


- Excellent high-temperature properties
- Compatibility with current fuel and reactor designs
- Meet regulatory and operational requirements

Cr coated Zr alloys

- Excellent adherence, high thermal conductivity, good irradiation resistance, easy fabrication
- Improvement of oxidation, hydrogen uptake, mechanical properties up to 1300°C
- Cr-Zr diffusion and eutectic at 1330°C

Properties	Cr	Zircaloy-4
Density (g/cm^3)	7.15	6.56
Crystal structure	BCC	HCP (<810°C) BCC (>810°C)
Melting point (°C)	1860	1850
Eutectic tem. (°C)	1330	1330
Thermal conductivity [W/(m·K)]	93.7	21.5
CTE (*10^{-6} K^{-1})	6.2	6.0
Specific heat capacity (J/g·°C)	0.46	0.28
Thermal neutron absorption (barn)	3.1	0.2

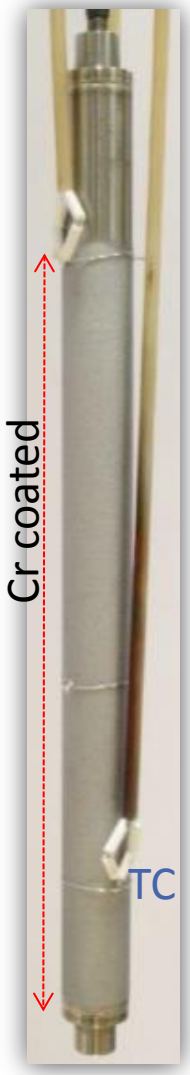


Brachet et al. TopFuel2016, JNM2019.

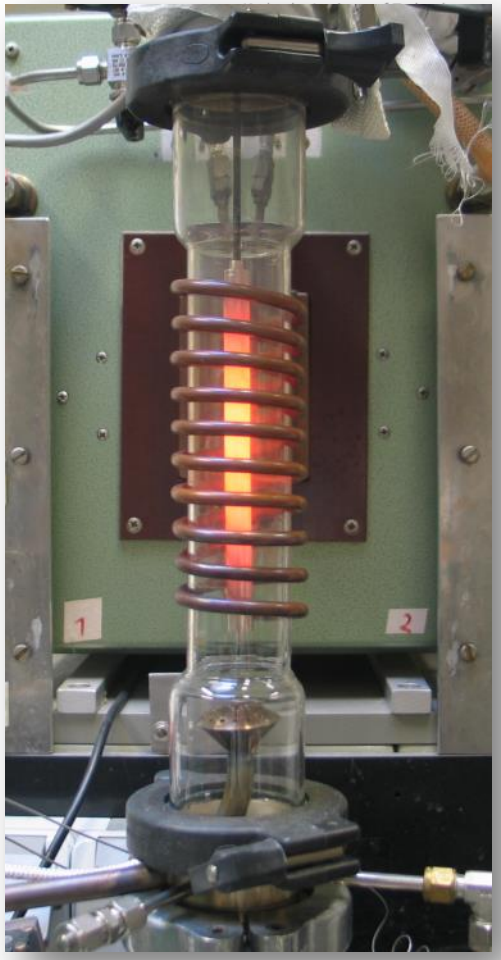
Oxidation and quench performances under simulated **severe accident scenarios beyond eutectic temperature** are still lacking.

Materials and experiment

- 13-cm long samples provided by MIT
- 20~70 μm cold sprayed Cr coating
- One end not coated
- Filled with zirconia pellets
- Oxidation in steam:
  - Isothermal tests 1 hour at nominally 1100°C, 1200°C (quench), and 1300°C
  - Transient test from 800 to 1500°C
  - Reference tests with uncoated Zry-4

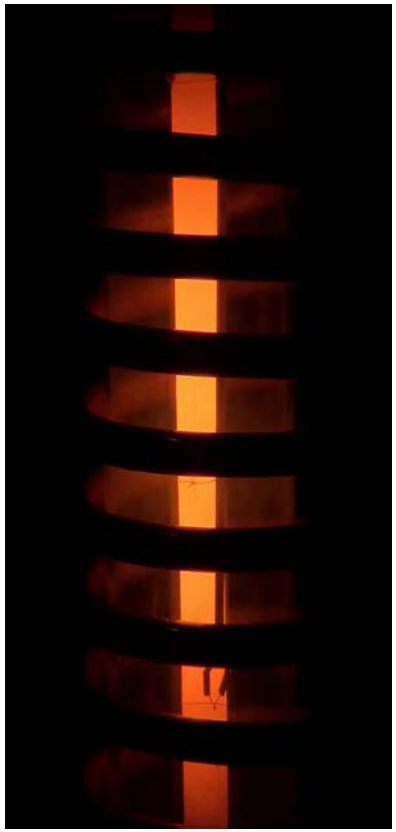


(130*9.7*0.57 mm)

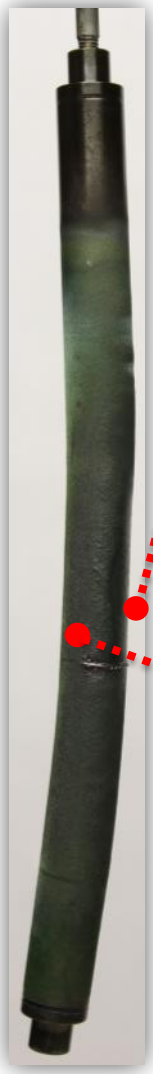


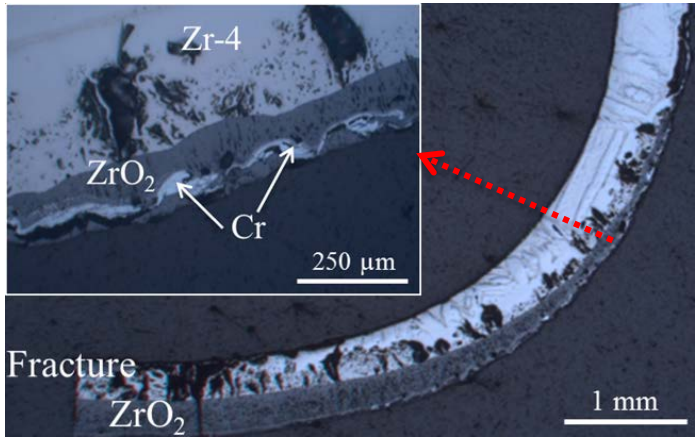
QUENCH-SR with inductive heating Ar + Steam

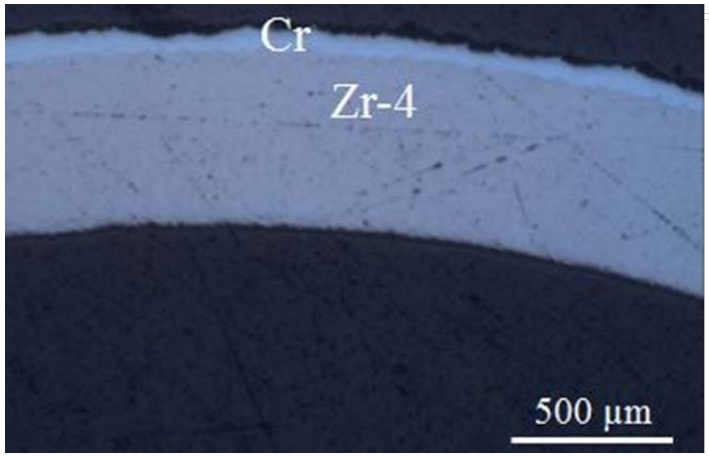
Isothermal test at 1100°C



Without quenching due bending



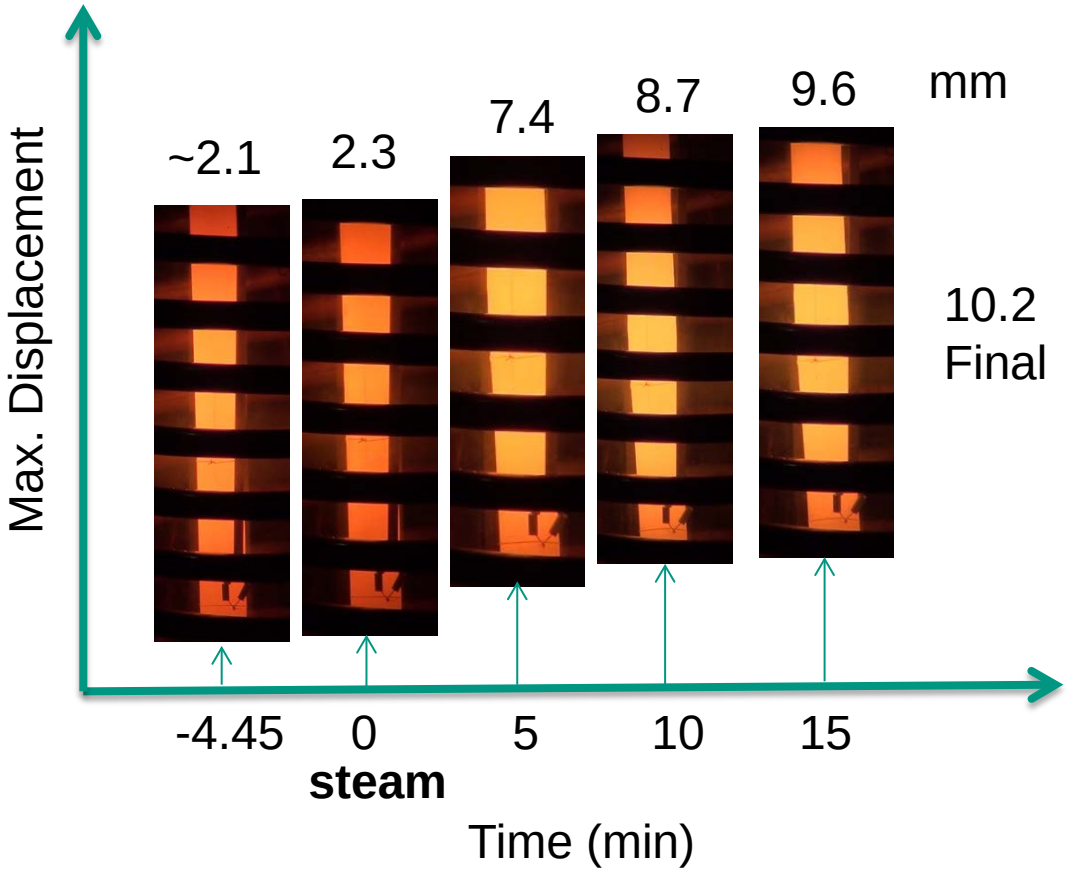


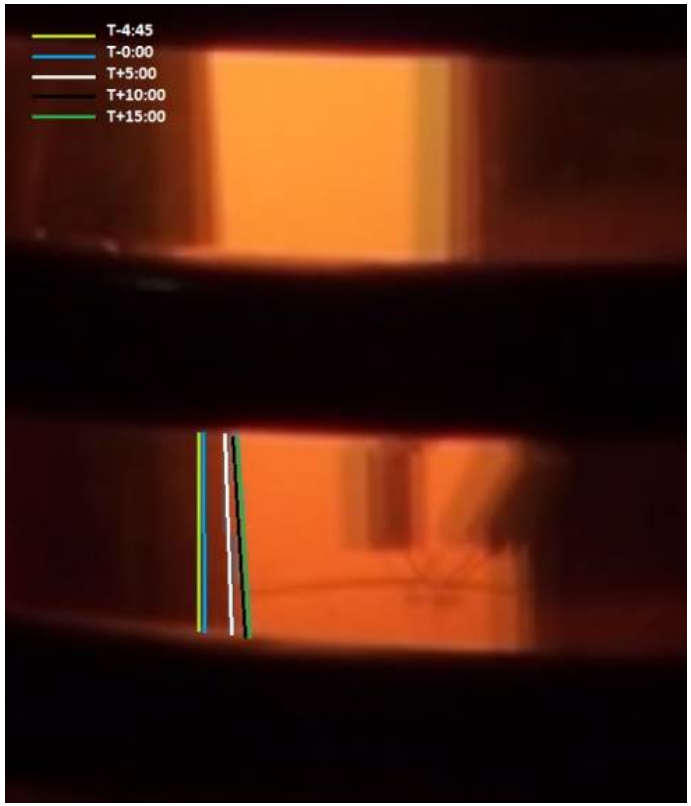


- Substantial bending during oxidation
- Loss of protective effect of the coatings on the tensile (convex) side via cracking /delamination

Isothermal test at 1100°C

- Small bending before oxidation
- Majority of the bending on first 5 minutes of steam oxidation





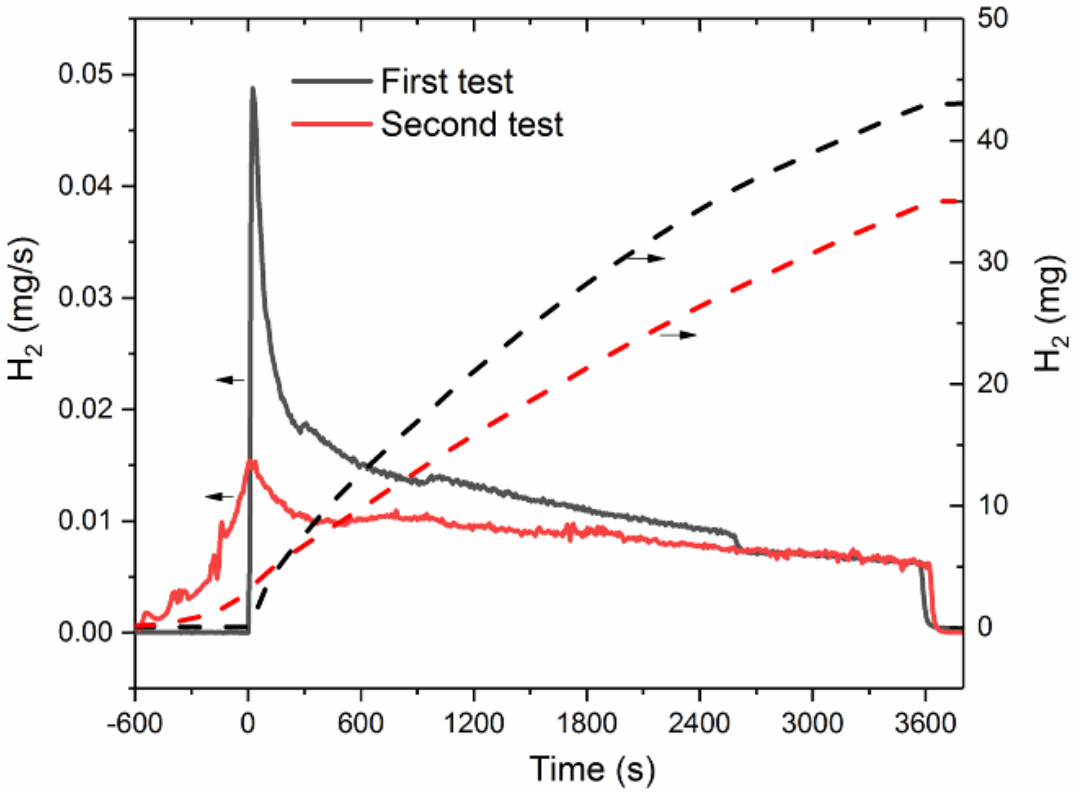
Isothermal test at 1100°C



Repeated test
Pre-oxidation from 800°C

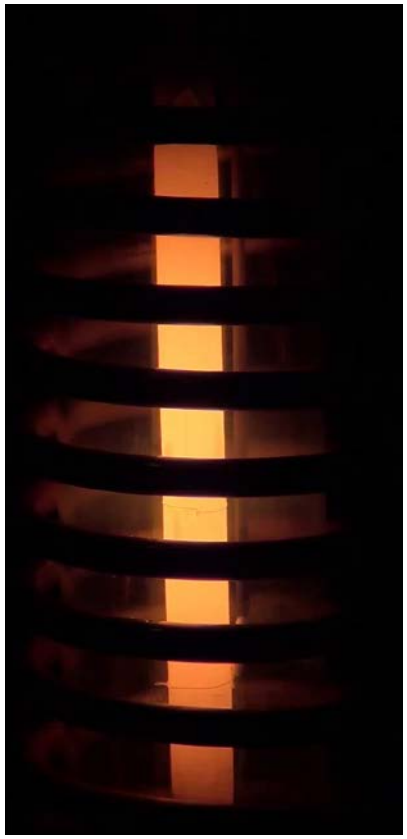
First test

Same level bending



- Bending: High-level of residual stress and stress concentration (inhomogeneity) via cold spraying

Isothermal test at 1200°C



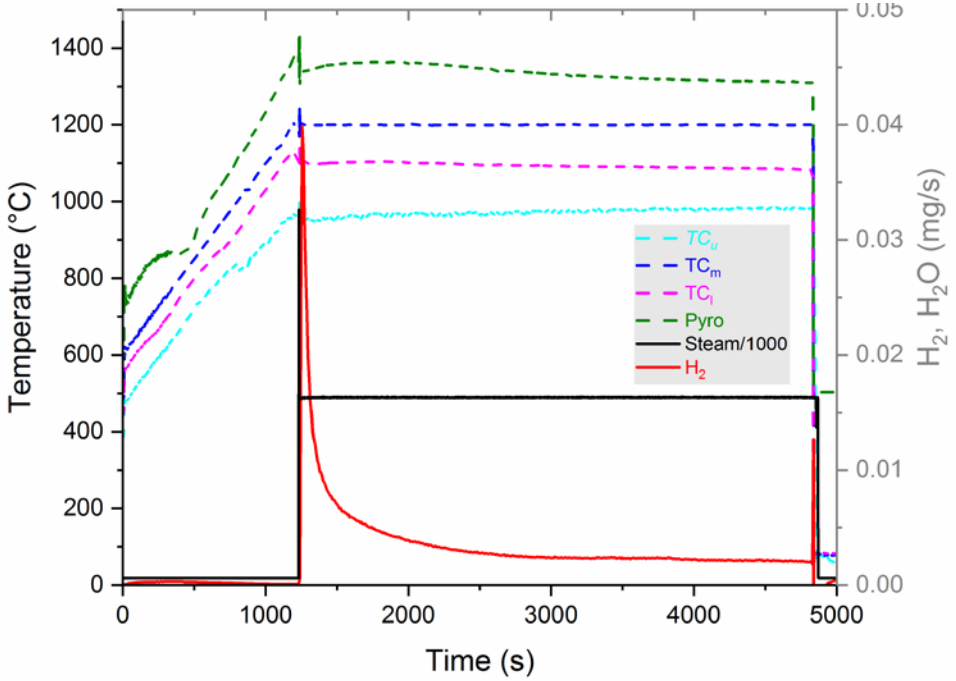
Quenching in water



Coated

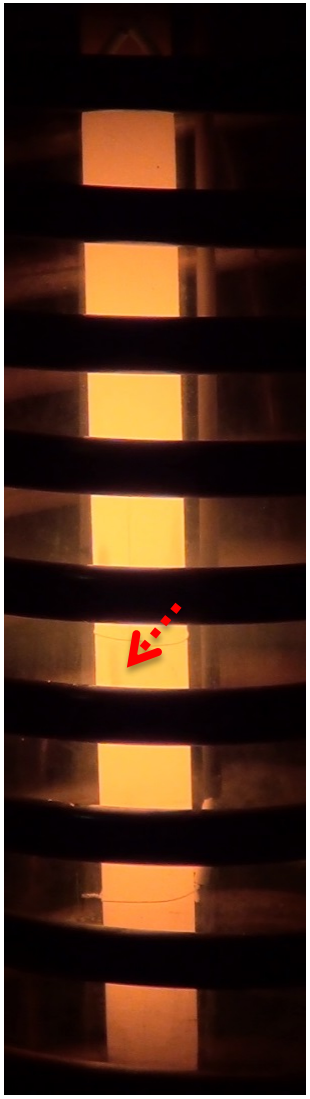


Uncoated



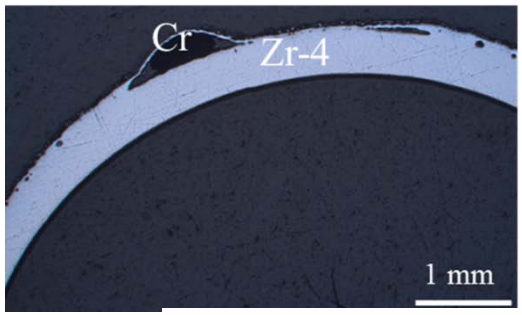
- Significantly improved oxidation resistance, good thermal shock resistance and high post-quench ductility
- H_2 production: 13.4 mg (coated),
  186.2 mg (uncoated)

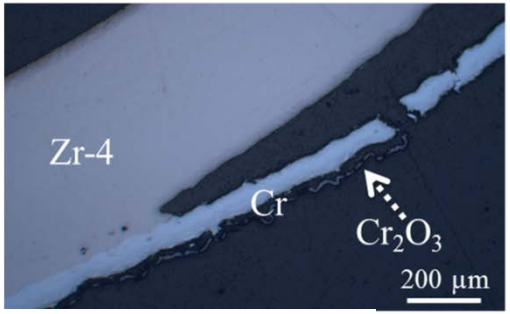
Isothermal test at 1200°C

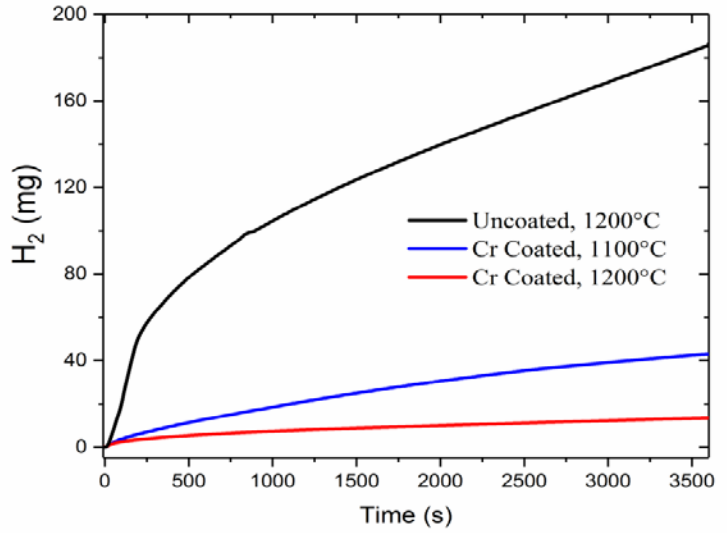






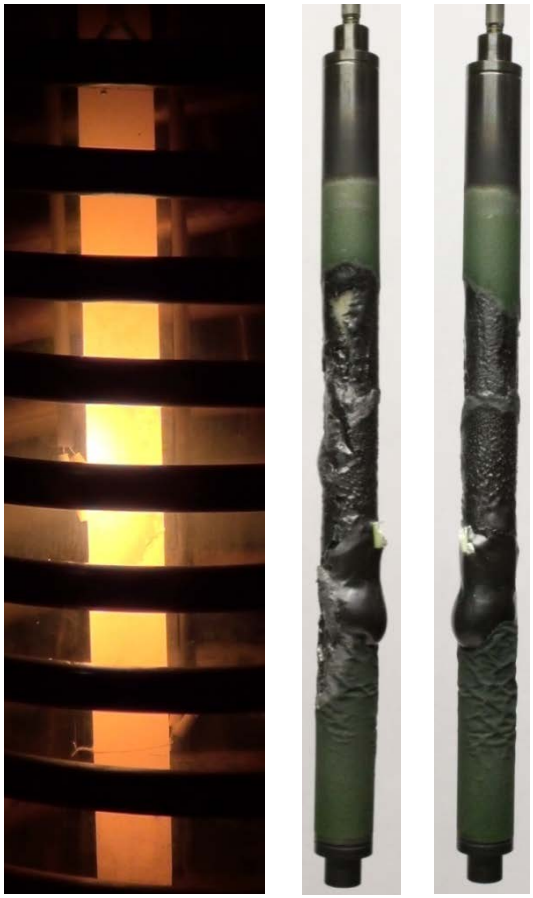




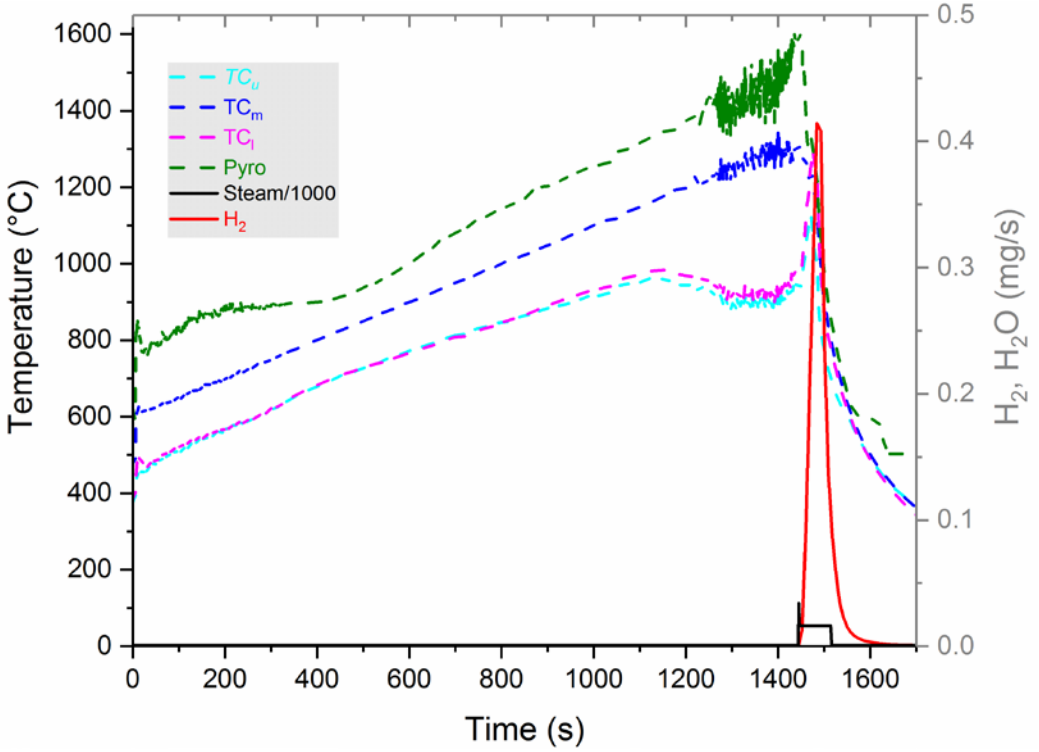


- No obvious bending
- Local delamination at two interfaces
- Less hydrogen production than at 1100°C

Isothermal test at 1300°C



Failure of temperature control (detachment of thermocouple)

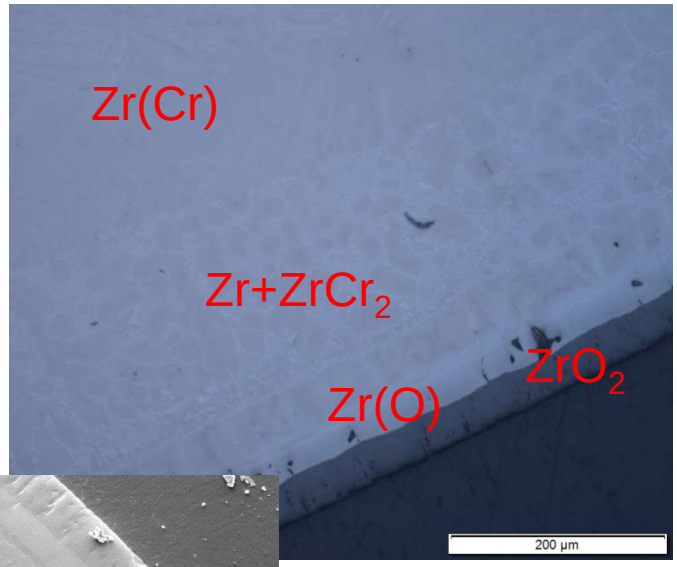


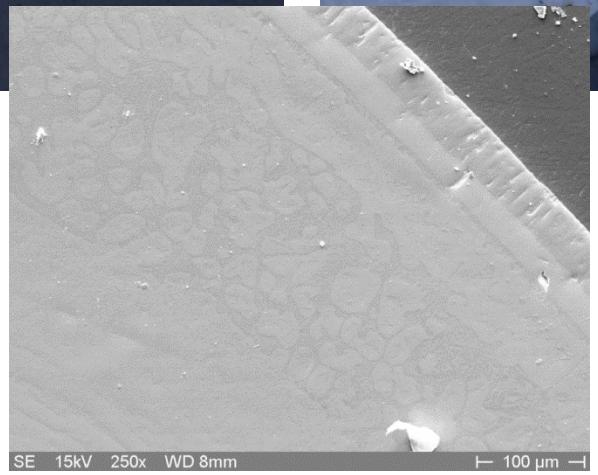
- The steam flow lasted about 70 s with a very high peak of hydrogen
- Higher temperature was anticipated, large liquid drops formation

Isothermal test at 1300°C



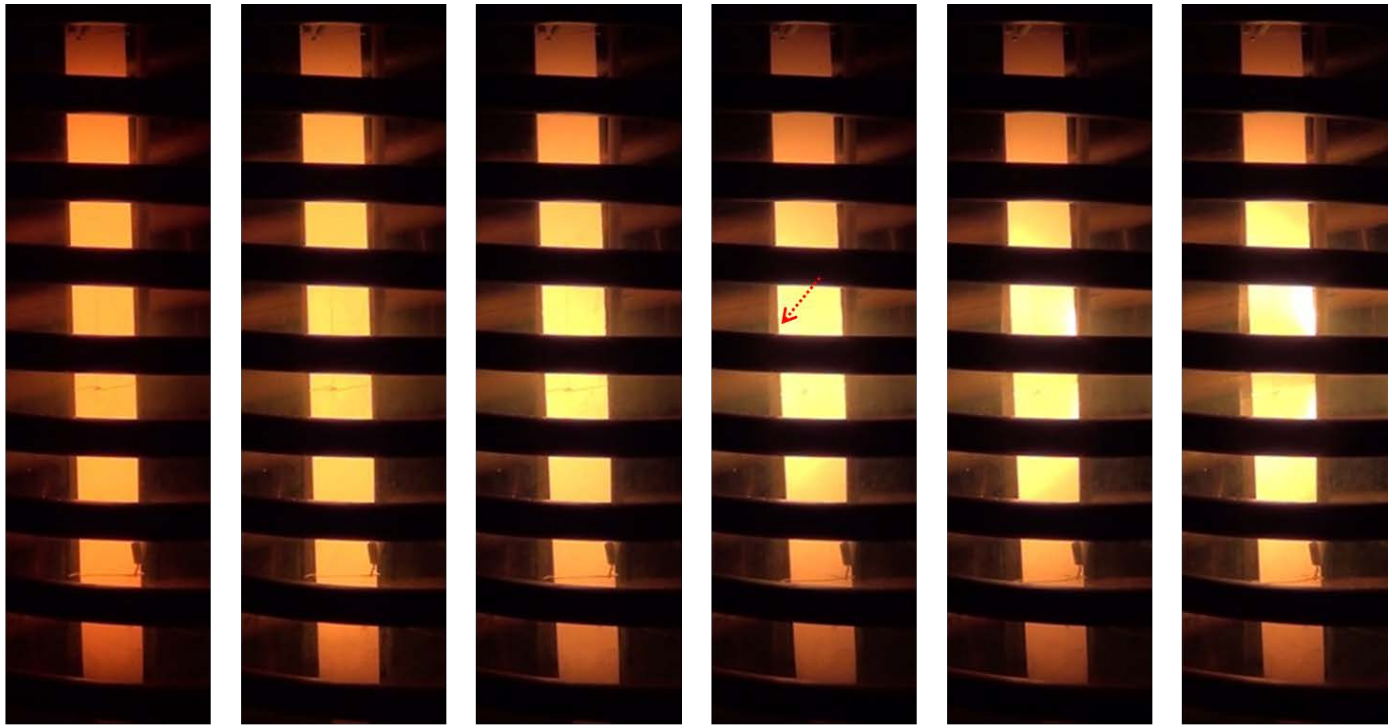






- Formation of liquid phase and its continuous displacement resulted in rapid degradation of the whole cladding tube.

Transient test 800-1500°C



1150°C 1200°C 1300°C 1400°C 1450°C 1480°C

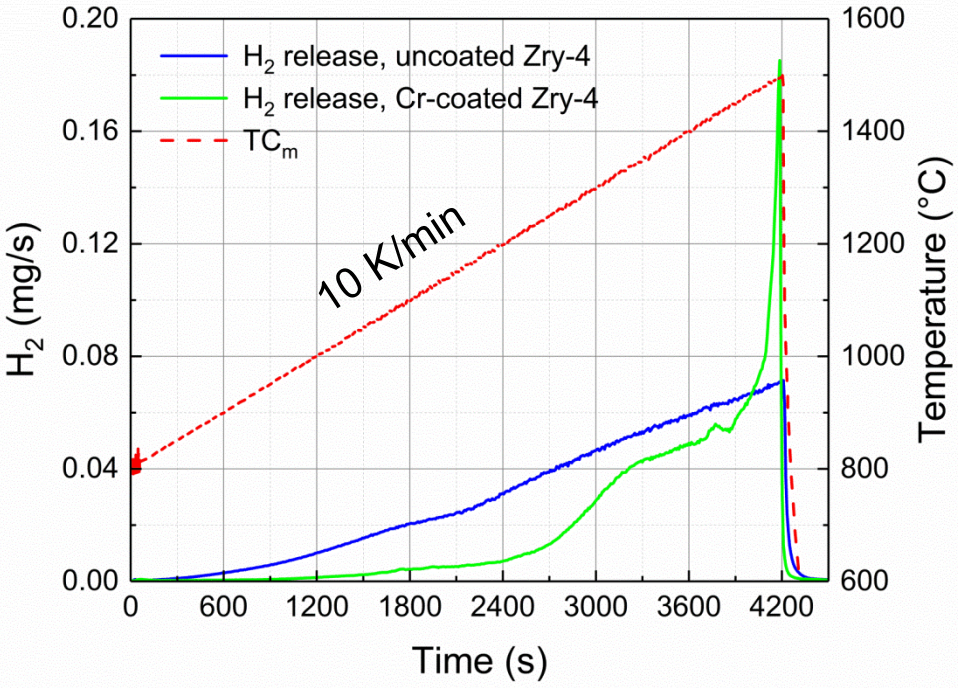


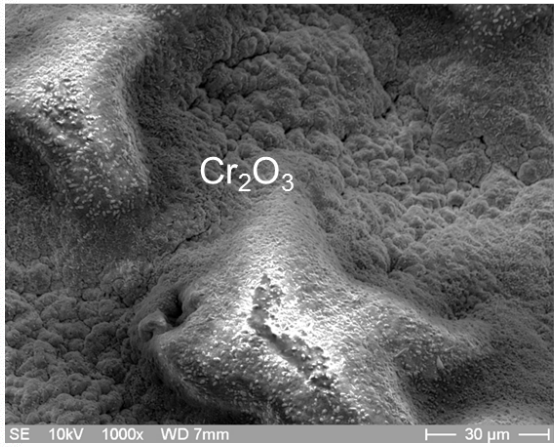
Coated

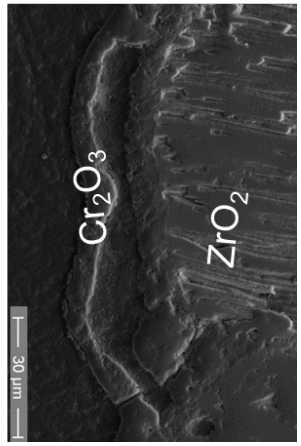


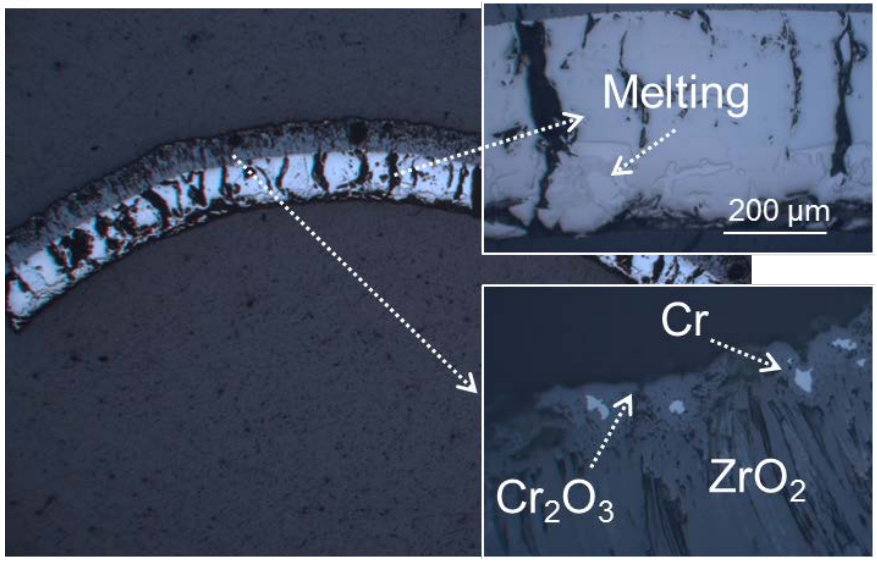
Uncoated

Transient test 800-1500°C



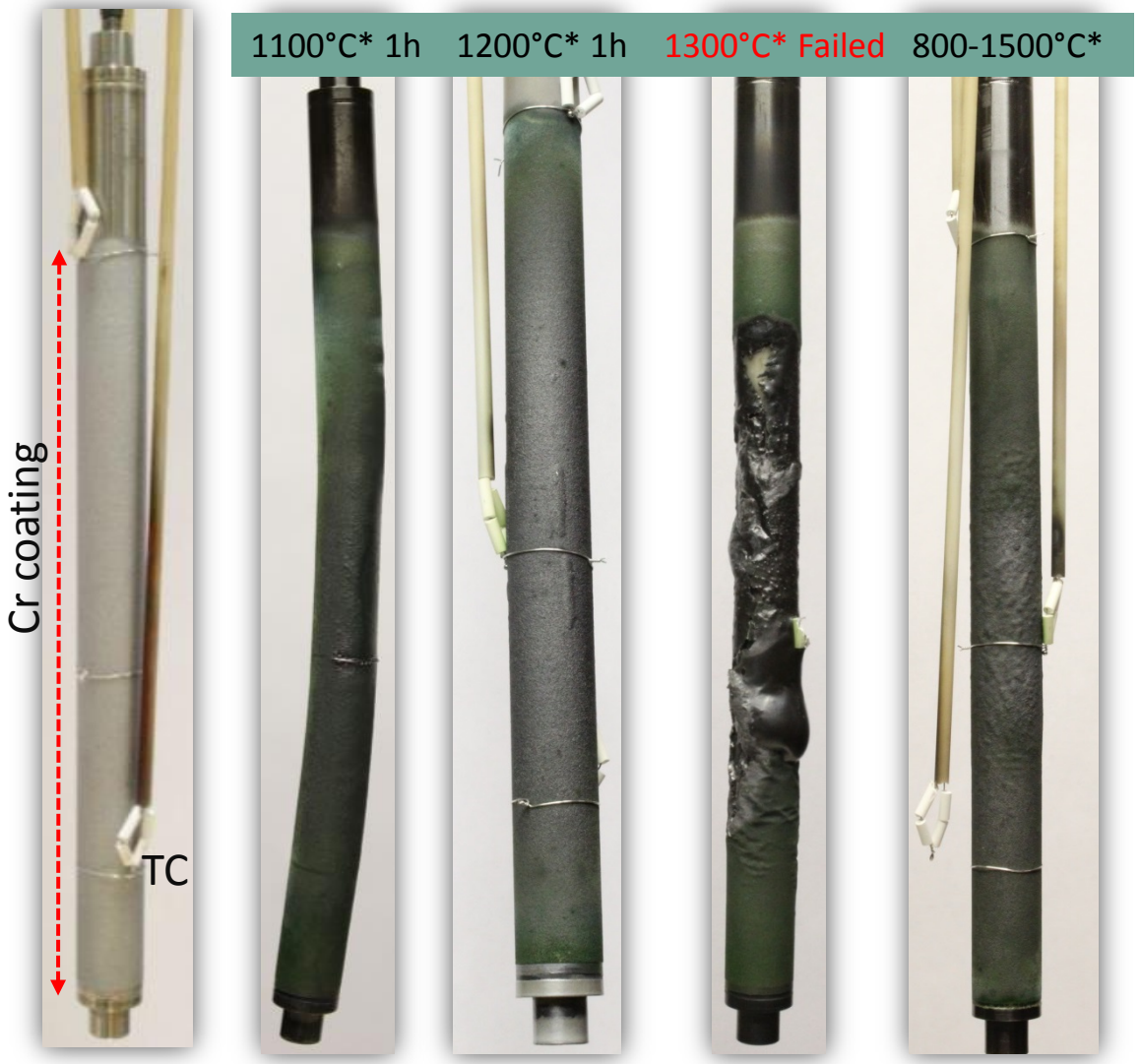






- A steeply increased hydrogen release rate above approx. 1410°C
- Oxidation (oxygen) drives inward diffusion of Cr into the inner region forming liquid phase.

Post-test appearance comparison



* *Nominal temperature; real/local temperature may differ*

Degradation modes:

- Bending with cracking/spallation and strong oxidation (ZrO_2) at convex side at 1100°C
- Local delamination at 1200°C and transient test
- Liquid phase formation at nominally 1300°C (real temperatures >1300°C)

Conclusions

- Significantly improved oxidation resistance and excellent adherence of cold spraying Cr coating.
- Undesirable substantial bending at 1100°C. Loss of protective effect at the tensile (convex) side.
- Above the Cr-Zr eutectic temperature, interdiffusion and formation of liquid phase led to quick degradation. An optimized coating thickness thus should be pursued.
- More tests are needed, including for instance large-bundle tests, to fully elucidate the material interactions, degradation phenomena and coping time during severe accidents.

Thanks the Quench group and program NUSAFE at KIT!

Thank you for your attention!

Results of corrosion and thermomechanical tests of ATF-cladding samples

Mokrushin Andrey, Urusov Alexander, Polunin Kirill (LUCH FSUE), Novokov Vladimi., Kuznetsov Vladimir, Fedotov Petr, Maslov Alexander (JSC VNIINM), Kalin Boris (NRNU MEPHI)

ABSTRACT

The claddings of ATF fuel elements were essentially fragments of commercially fabricated E110-alloy tubes with chromium-based coatings deposited on their surfaces. To form the diffusion barrier, an intermediate layer based on chrome, titanium and niobium was used in the work. Magnetron deposition was used as the technique for the coatings formation. High-temperature corrosion testing in the temperature diapason of 800 to 1200 degrees Celsius was carried out using the "GASPAR" test facility. For all the test temperatures, approximately twofold reduction of the specific weight gain is typical for the coated samples. That is, it can be said that the coatings retained their protective properties at these temperatures. Cr-coating – the metallic part of the coating is a uniform layer over its thickness present at the outer surface of the cladding, preventing oxygen from penetrating into the central part ("ex-β" – layer). The coating is firmly attached to the cladding. No signs of either spallation or oxidation were found under the coating. The results of analysis of microhardness distribution over the cross-section of the samples demonstrate that microhardness of the central region of "ex"-β layer for the coated samples is considerably lower as compared with E110. That is, the oxygen content in the layer responsible for plasticity is also reduced. Thicknesses and microhardness distribution of all structural elements from the side of the inner surface are almost identical for all the samples.



ROSATOM STATE ATOMIC ENERGY CORPORATION

Results of corrosion and thermomechanical tests of ATF-cladding samples

Mokrushin A., Urusov A., Polunin K. – LUCH FSUE
Novokov V., Kuznetsov V, Fedotov P., Maslov A. – JSC “VNIINM”
Kalin B. – MEPHI

25th QUENCH Workshop
Karlsruhe, 22 – 24/10/2019

ACCIDENT TOLERANT FUEL (ATF)

Goals of ATF fuel

- Impediment of free hydrogen release
- Improvement of the economical characteristics of the fuel, including the factors of the post-irradiation cycle
- Improvement of the thermomechanical properties of the cladding and the fuel
- Improvement of the kinetics of cladding-steam reaction
- Reduction of the fission products release

Ways to achieve the goal set

Development of protective coatings for zirconium cladding

Nb_2-Al-C
Zr-Si_2
Ti_2-Al-C
MAX-phases
Cr
Cr-(NbCrTi)-Cr

Replacement of the zirconium elements of the core

Fe-Cr-Al
SiC/SiC
Mo
Thin-walled steel claddings

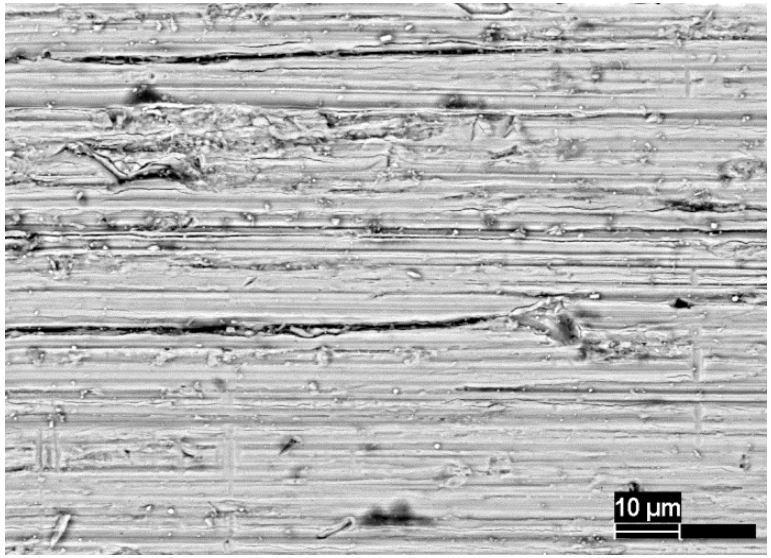
Development of a new type of fuel

U_3-Si_2
U-Zr
U-Mo
UO_2-Cr_2O_3-SiC
Dispersion fuel

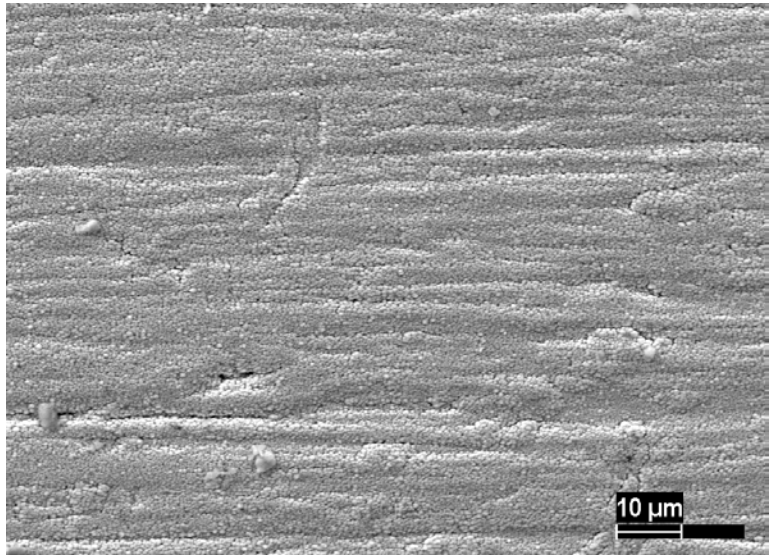
OBJECTIVE OF THE WORK

The objective of the work is to carry out the experimental studies of the corrosive characteristics of the ATF fuel element claddings studies within a temperature range of 800 to 1200 °C.

The ATF fuel element claddings were standard claddings made of E110 zirconium alloy with a chromium-based coating. Two variants of the chromium-based coating have been studied: one with an intermediate layer and the other one – without it.



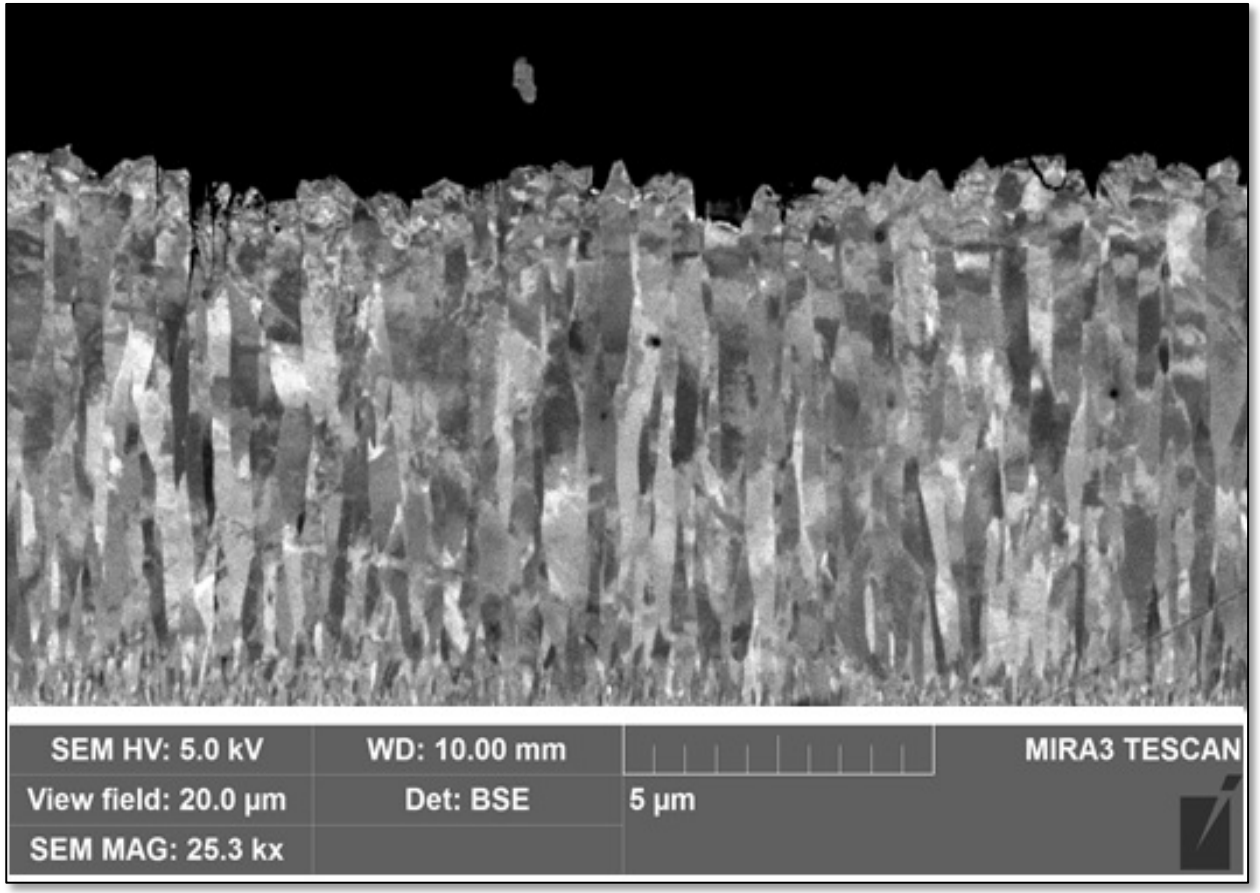
Initial



Coated

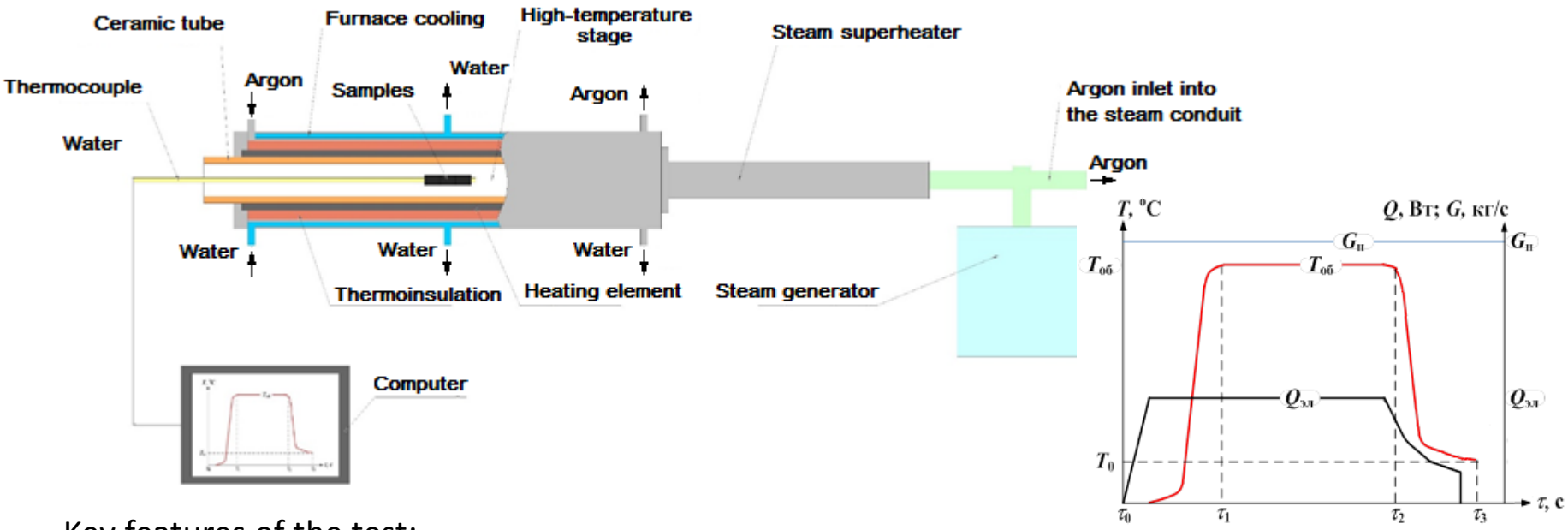
Surface of the E110 cladding

CHROMIUM-BASED COATING



Coating microstructure

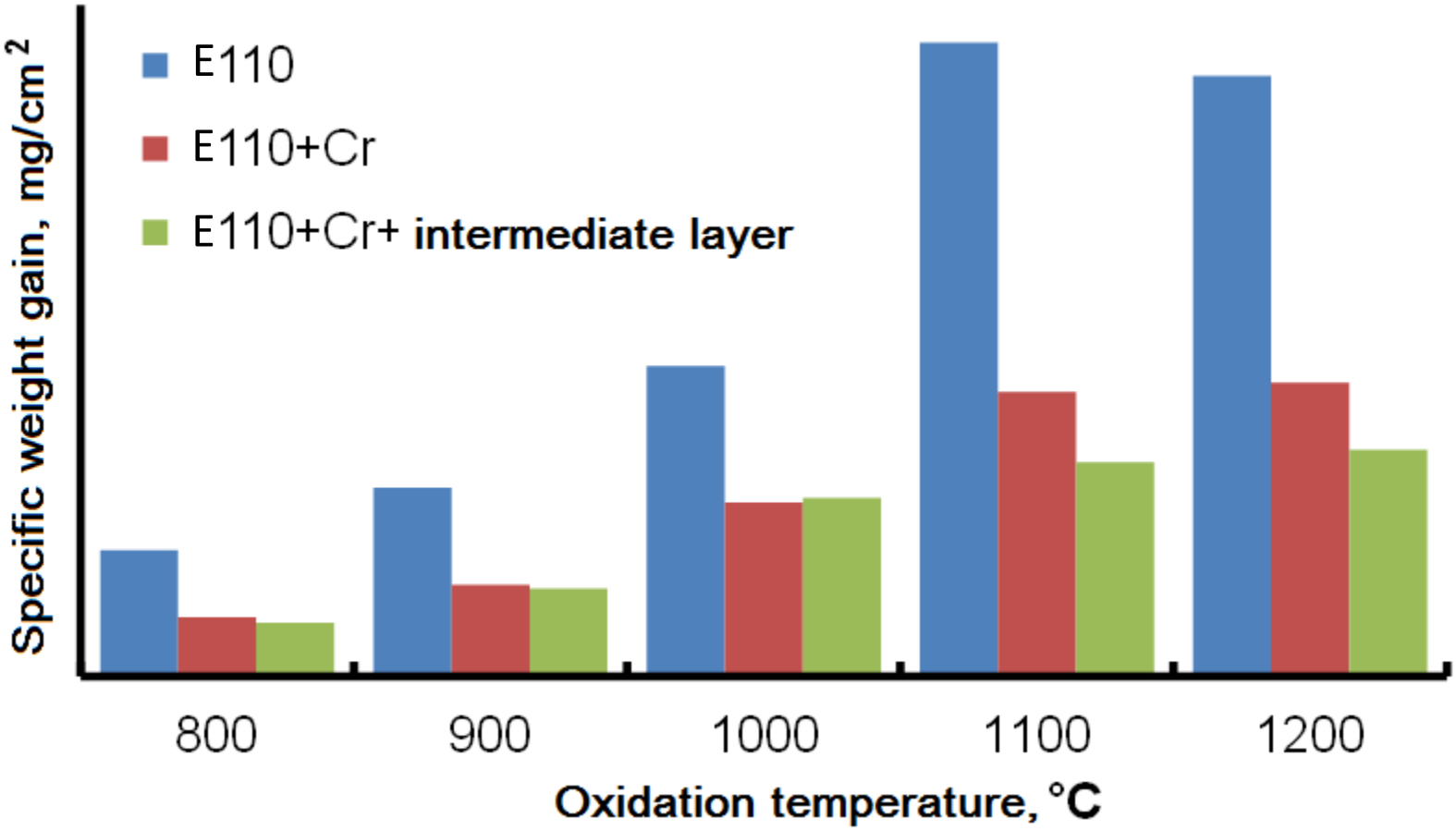
CORROSION TESTING PROCEDURE



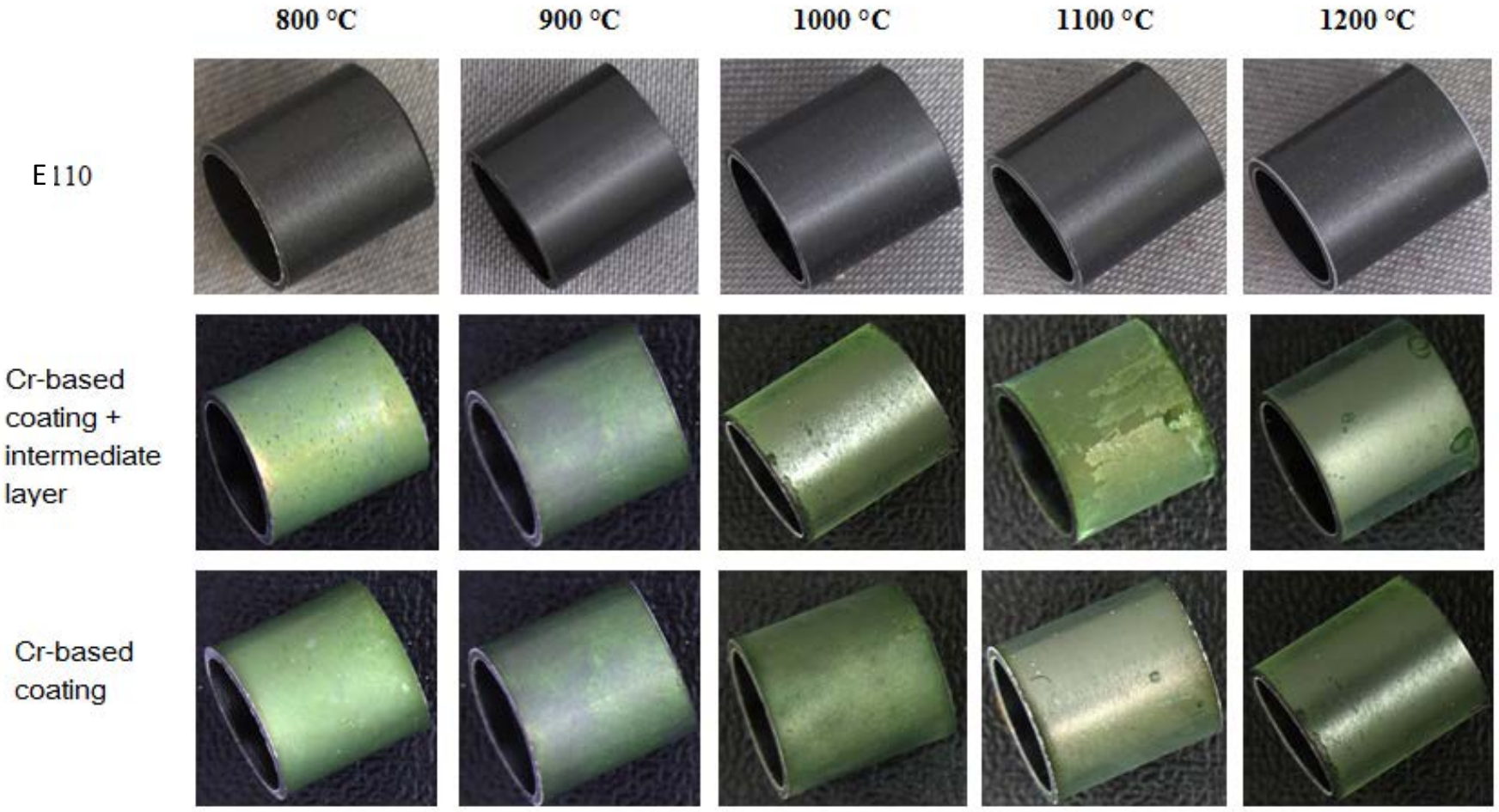
Key features of the test:

- prior to commencing the testing, the internal steam conduit of the furnace is vented with low-intensity argon flow, then saturated steam is introduced into the furnace's high-temperature region through the steam superheater
- oxidation occurs under isothermal conditions at the preset time-temperature parameters
- time of the sample heating-up to the oxidation temperature time is not to exceed 150 s
- precision of the preset temperature implementation is to be ± 1 % at worst
- cooling of the sample occurs in the cool region of the furnace at a rate of 20 °C/s

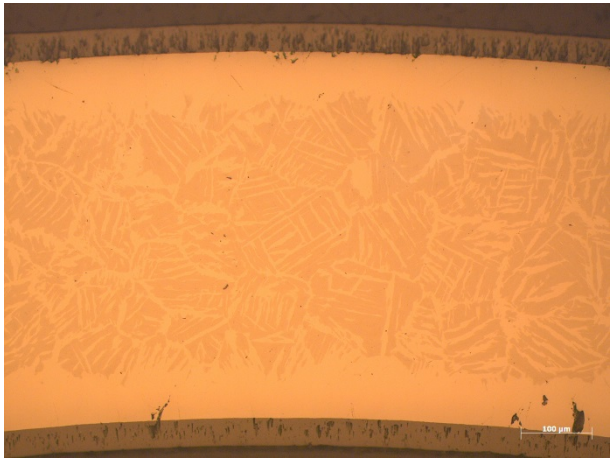
TESTING RESULTS



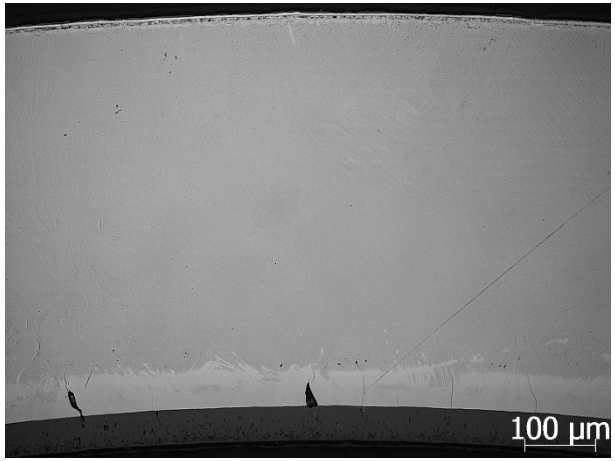
TESTING RESULTS



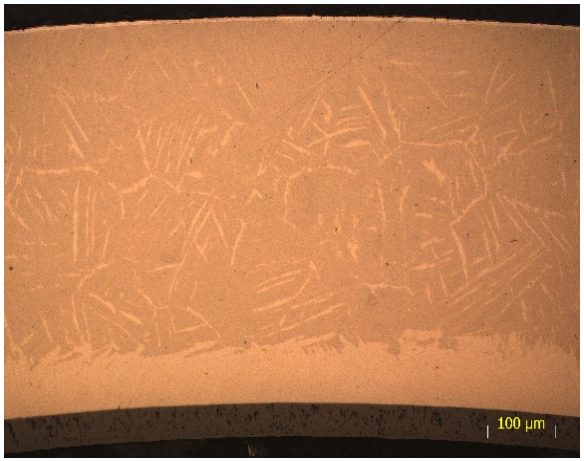
METALLOGRAPHIC ANALYSIS (1200 °C)



E110



Cr + intermediate layer



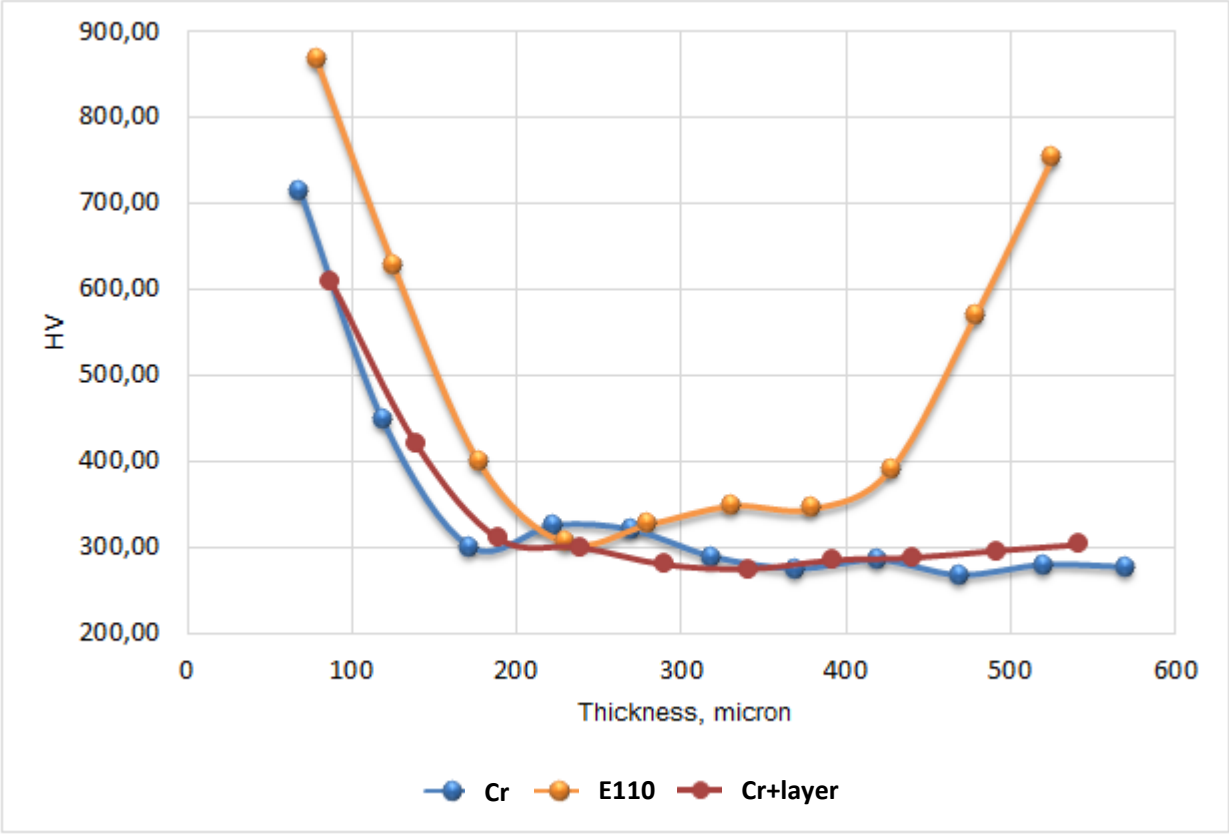
Cr-coating

E110 – typical cross-section structure.

Cr + intermediate layer the metallic part of the coating is a non-uniform layer over its thickness present at the outer surface of the cladding, preventing oxygen from penetrating into the central part (“ex-β” – layer). The coating is loosely attached to the cladding, though no signs of oxidation were found under the coating, making it possible to assume that the coating spalled because of the thermal shock.

Cr-coating – the metallic part of the coating is a uniform layer over its thickness present at the outer surface of the cladding, preventing oxygen from penetrating into the central part (“ex-β” – layer). The coating is firmly attached to the cladding. No signs of either spallation or oxidation were found under the coating.

RESULTS OF MATERIALS SCIENCE STUDIES

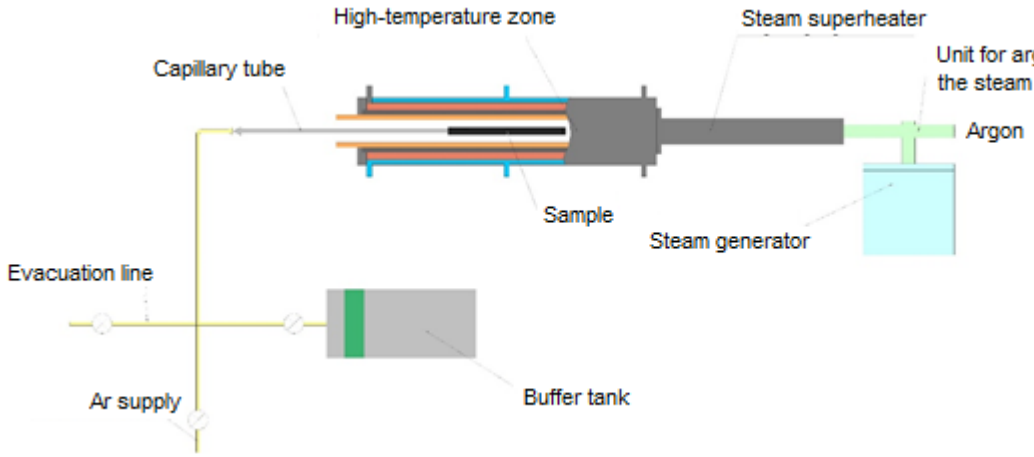


A significant reduction (down to 50 - 200 HV) of microhardness of the central region of the “ex”-β layer for the coated samples by comparison with E110.

ZrO_2 oxide layer is virtually absent for the coated samples, while being ~ (50 – 60) micron thick for E110 alloy claddings.

Thicknesses of the structural elements at the inner surface side are virtually identical for all the samples.

“BURST” TESTING PROCEDURE

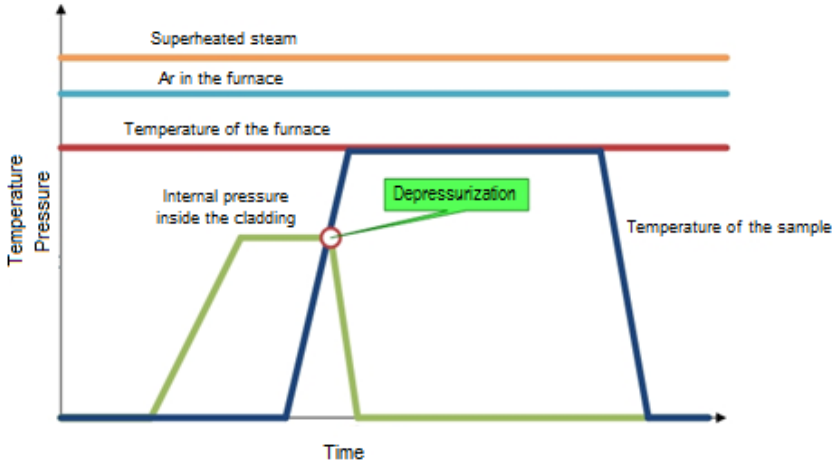


$$\text{Deformation} = \frac{L_2 - L_1}{L_1} \times 100\%$$

L_1 – circumference of the initial cladding, mm;
L_2 – maximum circumference in the spot of depressurization, mm.

Key parameters of the test:

- time of sample heating-up to the test temperature is not to exceed 150 s
- oxidation is conducted under isothermal conditions as per the timing diagram
- at the moment of depressurization the gas supply is terminated by shutting off the buffer tank
- the sample is cooled at a rate of 20 °C/s at least in the cool region of the furnace with argon flow blowing



“BURST” TESTING

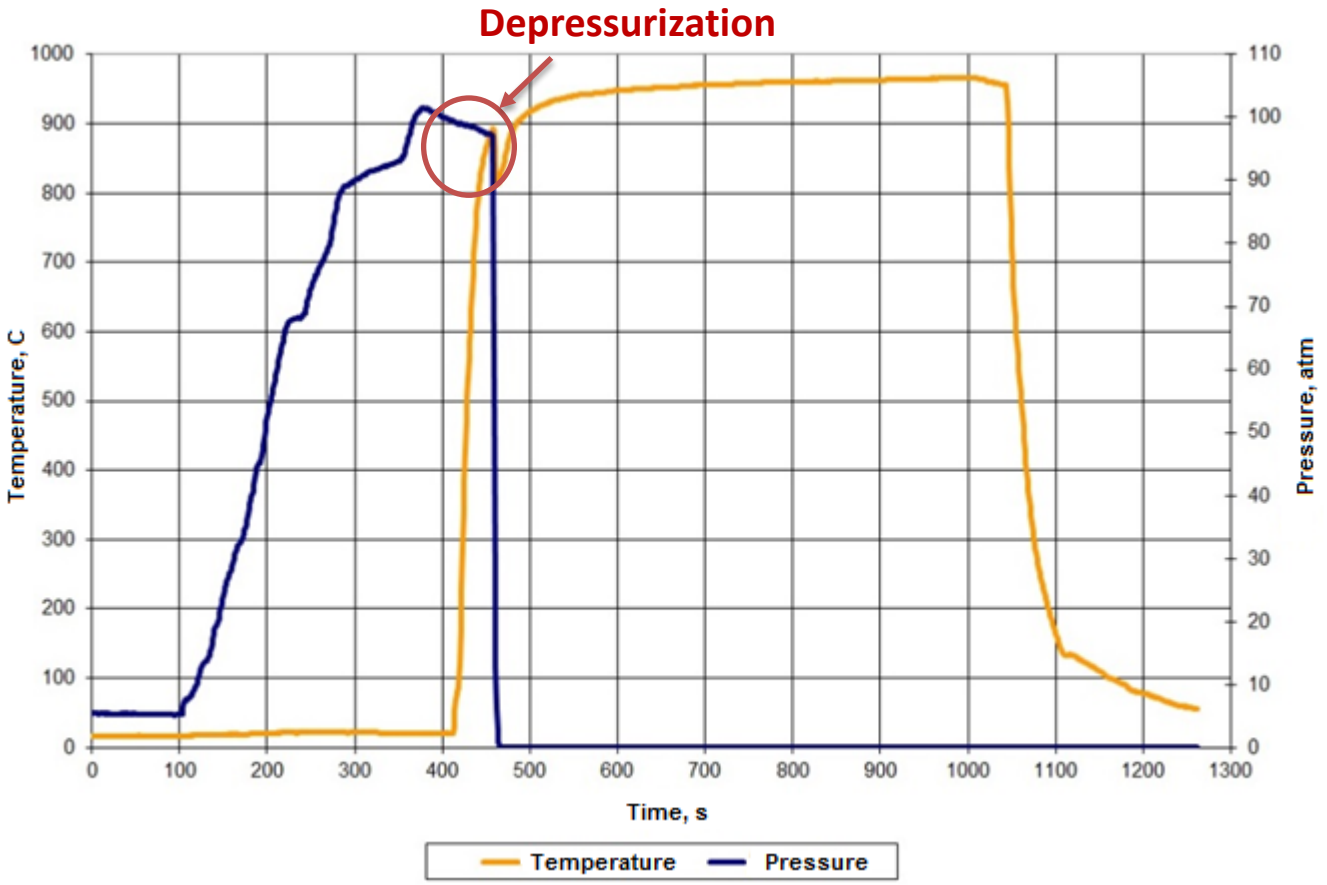
Cladding	Coating	Diameter	Pressure, MPa	Depressurization time, s	Depressurization temperature, °C	Deformation, %
1000 °C						
E110	Cr+layer	9.1	10,4	22	840	43
E110	Cr+layer	9.5	10	33	870	58
E110	Cr	9.1	9,8	39	870	26
E110	Cr	9.5	10,1	39	890	41
1200 °C						
E110	Cr+layer	9.1	11	13	870	29
E110	Cr	9.5	10	13	890	41

Depressurization of the E100 cladding samples occurs upon reaching ~ 850 °C regardless of the coating type and test temperature.

Changes of the cross-section of E110 claddings make (30 – 50) % of the initial diameter.

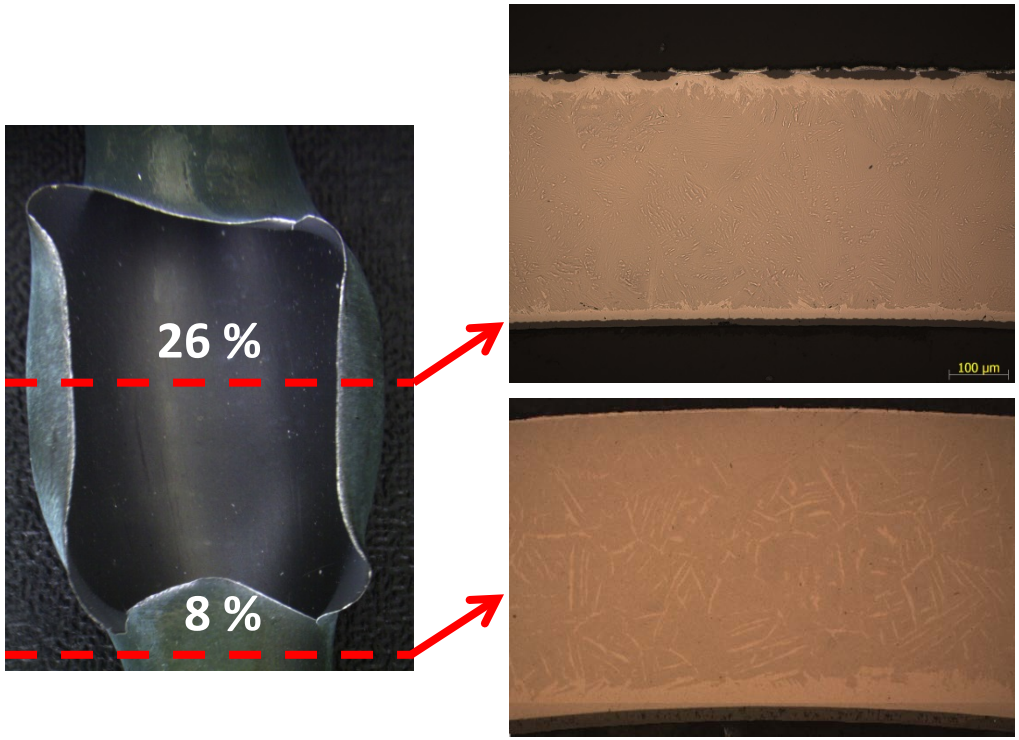
“BURST” TESTING OF COATED E110





Typical testing diagram of the cladding samples

“BURST” TESTING OF COATED E110



Microstructure of all the samples after “burst” testing exhibits layer-by-layer morphology. Presence of oxide layer at the outer surface results from the failure of the coating due to the cladding bulge at a deformation of 26 %.

With the relative deformation of roughly 8 %, no coating failure and zirconium oxide formation occur.

CONCLUSIONS

- A series of corrosion tests of the samples has been performed. Test temperature (800 – 1200) °C. Time of exposure – (70 – 500) s. Cooling rate – 20 °C/s down to 800 °C, with subsequent thermal shock.
- A complex of studies of FA-ATF fuel element claddings made of E110 coated with (Cr, Cr + intermediate layer) has been performed.
- Neither oxide or sub-oxide layers were found at the outer surface of the samples.
- In the process of burst-testing, depressurization of E110-alloy cladding samples occurs upon reaching ~ 850 °C regardless of the coating type and test temperature. It has been found, that during burst-testing with the circumferential deformation being roughly 8%, the chrome-coated cladding retains its protective properties.

Continuation of the Work

- Testing for bulging and depressurization of the samples of fuel element coated claddings in the extended ranges of pressure – up to 30 MPa and temperature 600 – 1200 °C;

- Currently, the samples of fuel elements with Cr-coated claddings undergo in-pile testing at RIAR (MIR reactor). A program of post-irradiation examination is scheduled for carrying out after completion of the testing.

High temperature oxidation of cladding material in SFP-LOCA conditions examined with Raman imaging and ^{18}O tracer techniques.

M. Mermoux[2], I. Idarraga[1,2], M. Guérain[1,2], A. Kasperski[1,2], M. Gestin[3], C. Duriez[1]

1 Institut de Radioprotection et de Sûreté Nucléaire, PSN-RES, Cadarache BP 3, 13 115 St Paul-Lez-Durance cedex, France

2 Université Grenoble Alpes, LEPMI, UMR 5279 CNRS, 38402 Saint-Martin d'Hères cedex, France

3 Ecole Nationale Supérieure des Mines, 158 Cours Fauriel, 42023 Saint-Etienne, France

Zircaloy-4 high temperature oxidation has been studied in O_2 - N_2 - steam mixed atmospheres and for temperatures in the 700-950°C range, conditions that are relevant to Spent Fuel Pool Loss-of-Coolant or Loss-of-Cooling (SFP-LOCA) scenarios.

Two different kinds of experiments using ^{18}O as a tracer will be presented: (i) Diffusion experiments, to investigate the role of the pre-oxide barrier formed during in-reactor normal operation; (ii) Oxidation experiments performed in mixed $^{18}O_2$ - $H_2{}^{16}O$ - N_2 atmospheres, as an attempt to understand the respective contributions of oxygen and steam to the oxidation mechanism.

The zirconia scales were examined using micro-Raman imaging, allowing the ^{18}O content, monoclinic and tetragonal ZrO_2 and ZrN phase distribution to be investigated. First conclusions of this work will be given.

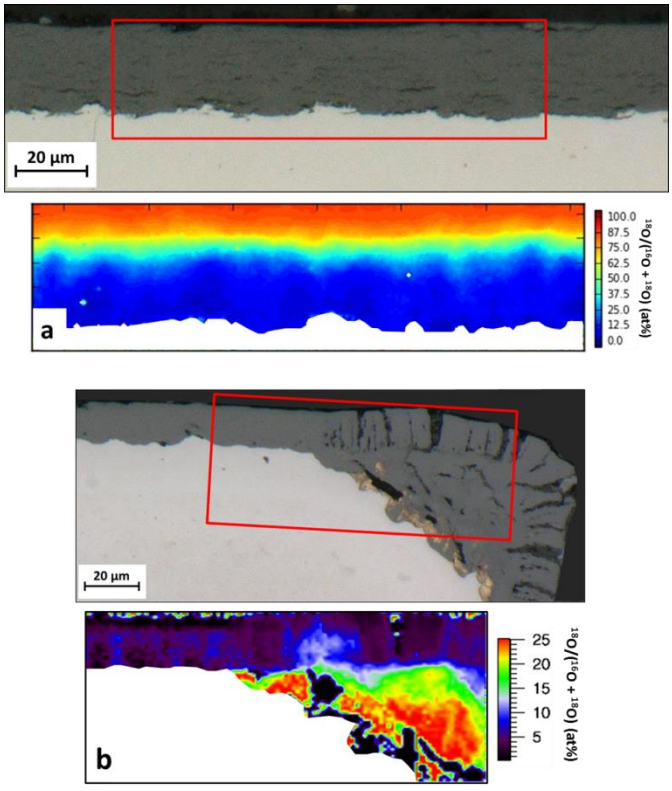


Figure: Examples of ^{18}O Raman distributions in zirconia scales
a- Pre-oxidized Zircaloy-4 exposed to pure $^{18}O_2$ at 850°C during 360 min
b- Bare Zircaloy-4 oxidized at 850°C in a $^{18}O_2$ + $H_2{}^{16}O$ + N_2 (4/16.5/79.5 vol%) atmosphere during 30 min.
The scanned areas are marked with a red rectangle on the optical images.



IRSN
INSTITUT
DE RADIOPROTECTION
ET DE SÛRETÉ NUCLÉAIRE

Enhancing nuclear safety

HT cladding oxidation in SFP-LOCA conditions examined with micro Raman imaging and ^{18}O tracer techniques

M. Mermoux[2], I. Idarraga[1,2], M. Guerain[1,2], A. Kasperski[1,2], M. Gestin[3], C. Duriez[1]

1- IRSN/PSN-RES/SEREX/LE2M, Cadarache, 13115 Saint-Paul-lez-Durance, France
2- Univ. Grenoble Alpes, CNRS/LEPMI, 38402 Saint-Martin d'Hères cedex, France
3 Ecole Nationale Supérieure des Mines, 158 Cours Fauriel, 42023 Saint-Etienne, France

25th QUENCH Workshop, Karlsruhe, 22-24 Oct. 2019

IRSN/FRM-414.ind 3

MEMBER OF
ETSON | EUROPEAN TECHNICAL SAFETY ORGANISATIONS NETWORK

Context: SFP-LOCA

For Spent Fuel Pool Loss of Cooling or Loss of coolant Accidents:

⇒ The temperature range of interest is ~ **700-1000°C**

⇒ The atmospheres considered are **air + steam** mixtures



IRSN MEMBER OF ETSON

Content

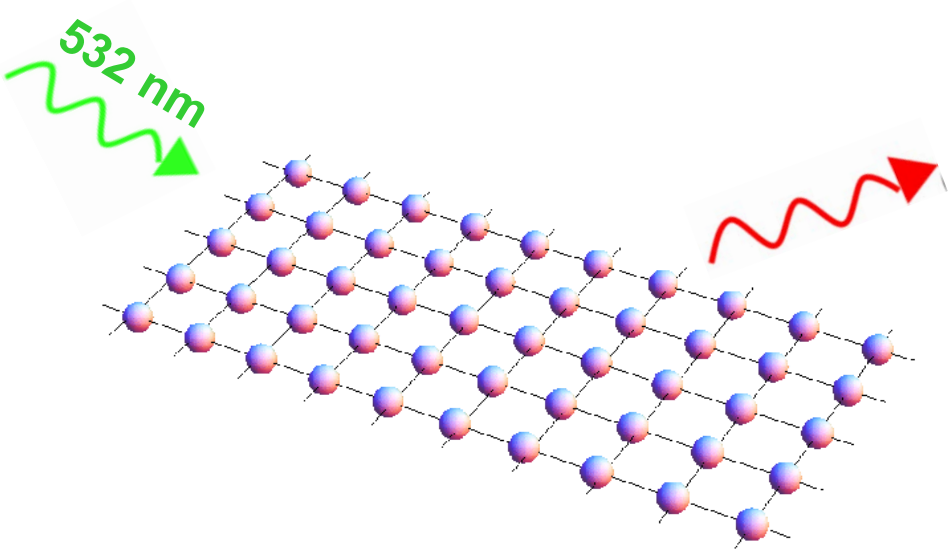
- Principle of Raman imaging → 2 slides
- Phases mapping → 2 slides
- Stress mapping → 2 slides
- ^{18}O isotopic distribution mapping
  - Principle → 1 slides
  - Two-stage diffusion experiments → 4 slides
  - HT oxidations in $^{18}O_2$ + $H_2{}^{16}O$ → 5 slides
- Summary

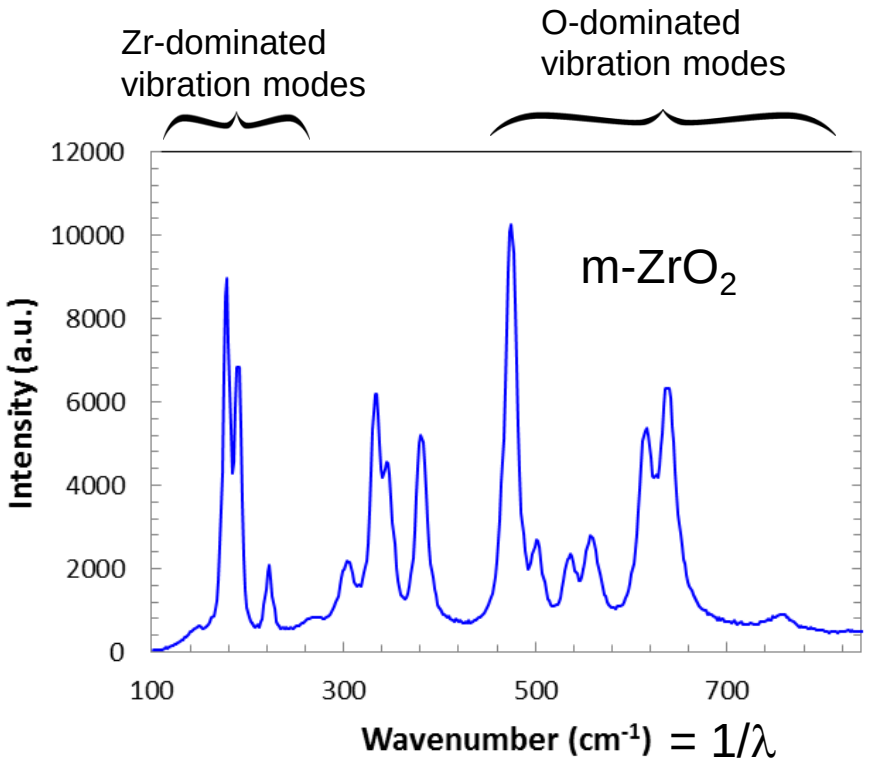
IRSN MEMBER OF ETSON

Micro-Raman spectroscopy



Raman imaging system
=
laser source
+ optical microscope
+ Raman spectrometer



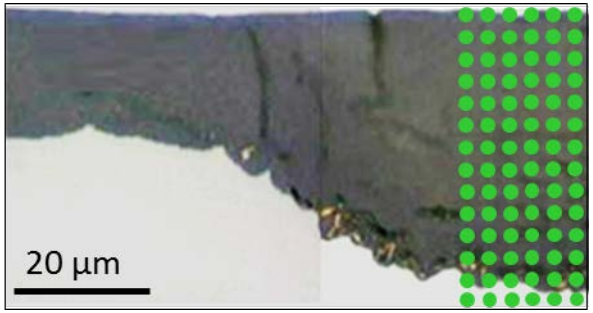


Phase identification and mapping (1/2)

1- Sample scanning: λ = 532 nm, ~1µm resolution → Dataset of experimental spectra

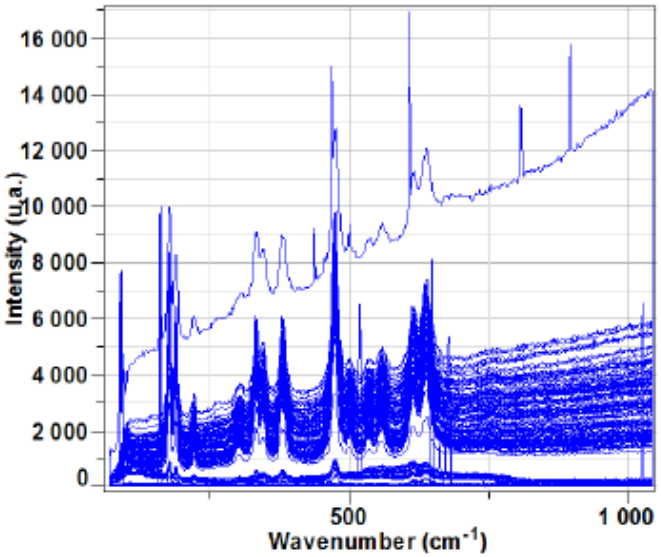
2- Visual examination of the dataset and **subtraction** between spectra → 5 pure phase spectra were identified (m-ZrO_2, t-ZrO_2, distorted t-ZrO_2, c-ZrO_2, ZrN) + 1 broad band signal likely due to substoichiometry.

Metallographic cross section of Zy-4 oxidized in air at 800°C

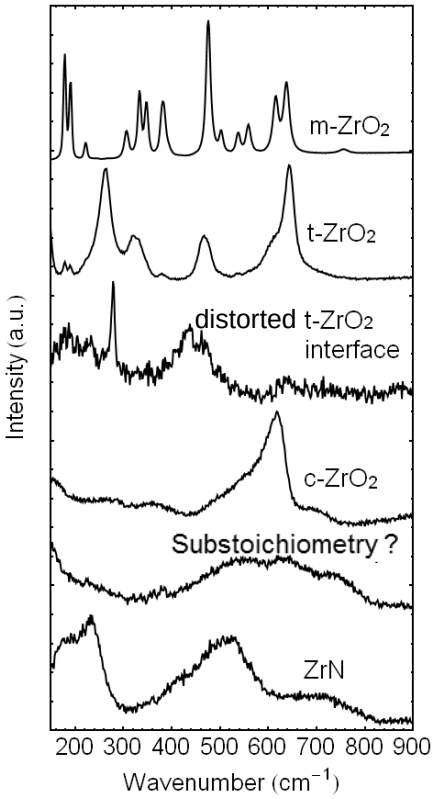


Scanned area 85 x 45 µm, step 0.7 µm

~9000 experimental spectra
~7 h acquisition



Model spectra



3- Phase maps construction: Method 1: Integrated intensity of a given line

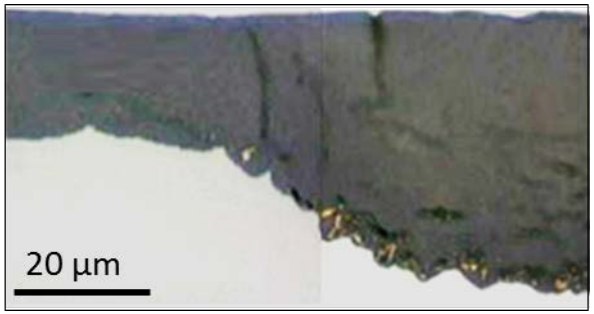
Method 2: Linear combinations of the model spectra

→ not quantitative !

IRSN MEMBER OF ETSON

Phase identification and mapping (2/2)

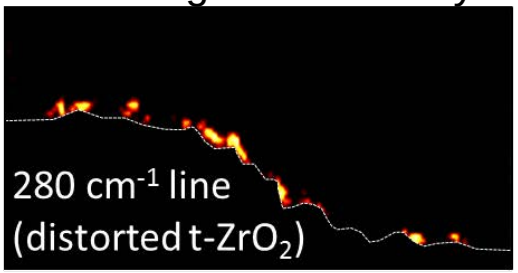
Zy-4 oxidized in air at 800°C

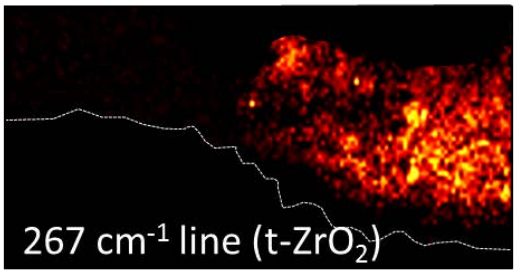


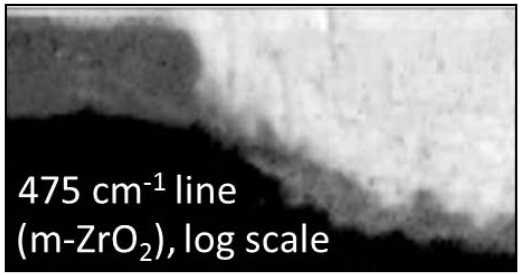
Pre-BA, dense scale

Post-BA, nitrided scale

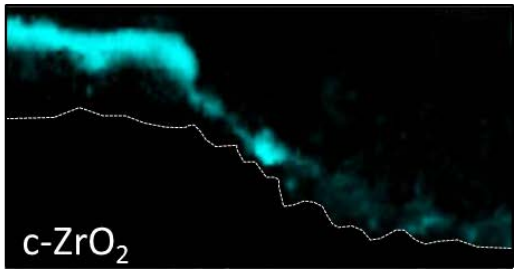
Line integrated intensity

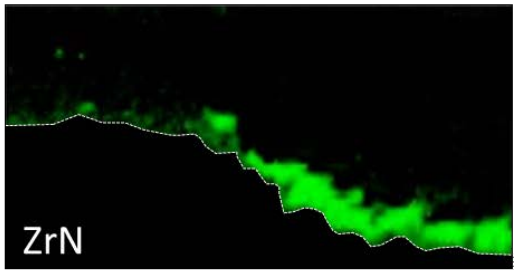






Linear combination





I. Idarraga et al, Oxid. Met. 79 (2013) pp. 289-302.

- Significant amount of t-ZrO_2 in the post-BA region (effect of nitriding ?).
- Distorted t-ZrO_2 found at the M/O interface, for both pre and post-BA regions.
- Cubic ZrO_2 detected (low amount).
- Good sensitivity for ZrN detection.
- m-ZrO_2 intensity linked to stoichiometry.

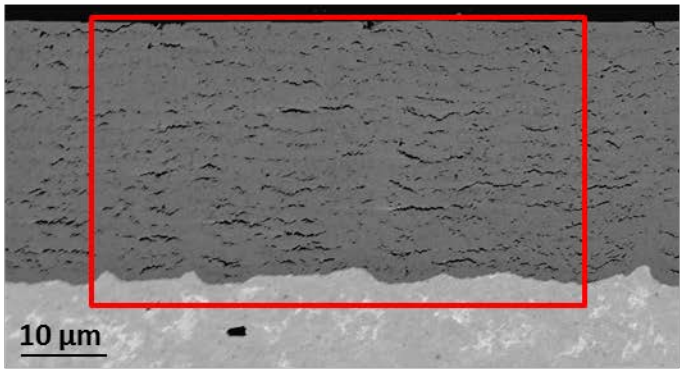
IRSN MEMBER OF ETSON

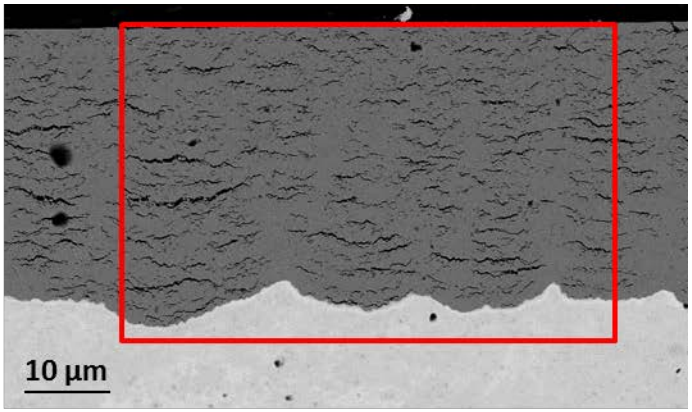
Stoichiometry of pre-oxidation scales

360°C, autoclave,1265 days

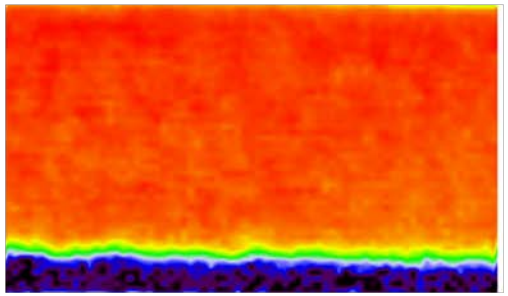
425°C, O_2 + H_2O, 250 days

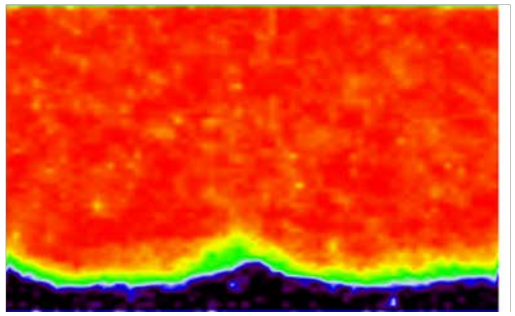
SEM/BSE





Integrated intensity of the 475 cm^{-1} line (m-ZrO_2), log scale





For both pre-oxidation conditions :

- The scales are mostly stoichiometric
- The last formed layer at the M/O interface is sub-stoichiometric.

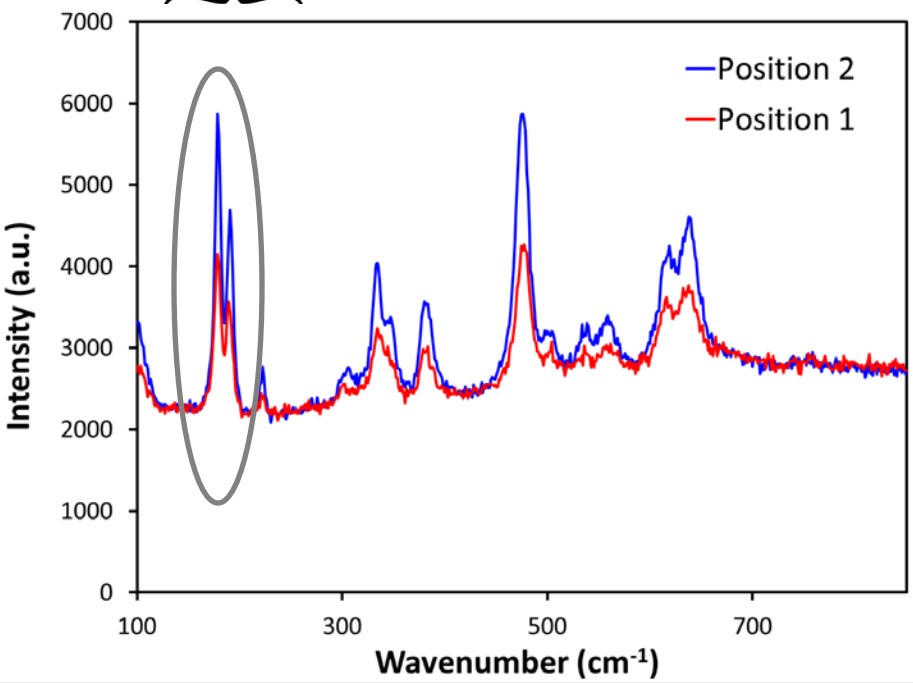
IRSN MEMBER OF ETSON

Stress mapping (1/2)

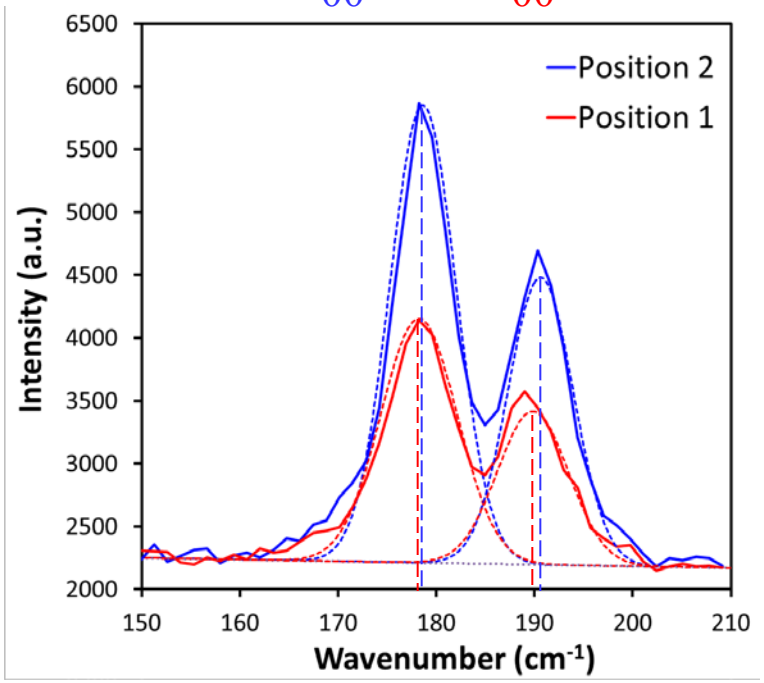
- Stress → Lattice strain → Slight shifts of Raman lines (few cm^{-1}/GPa).
- Shifts due to bi-axial stresses **cannot be calibrated** through isostatic compression tests (diamond anvil-cell).

  ⇒ **Stresses can be qualitatively mapped** by measuring the shifts of the low-frequency lines (not influenced by stoichiometry) from a reference signal (relaxed sample).

Zr-dominated vibration modes



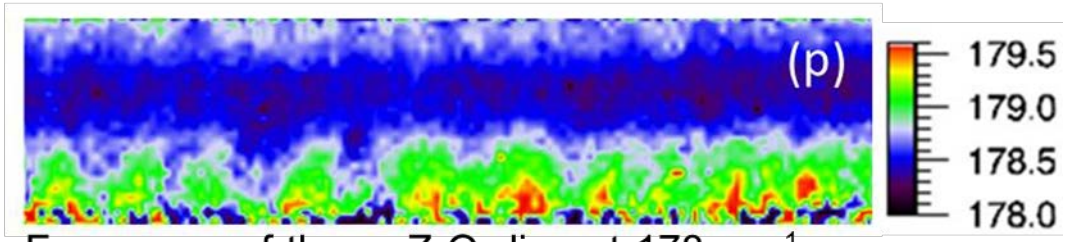
$|\sigma_{\theta\theta}| > |\sigma_{\theta\theta}|$



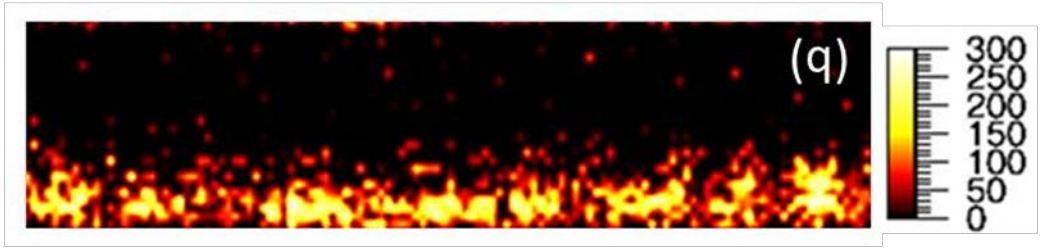
Stress mapping (2/2)

Pre-breakaway scale formed on M5 at 800°C in air





Frequency of the m-ZrO_2 line at 178 cm^{-1}



Integrated intensity of the t-ZrO_2 line at 280 cm^{-1}

I. Idarraga et al, Oxid. Met. 79 (2013) pp. 289-302.

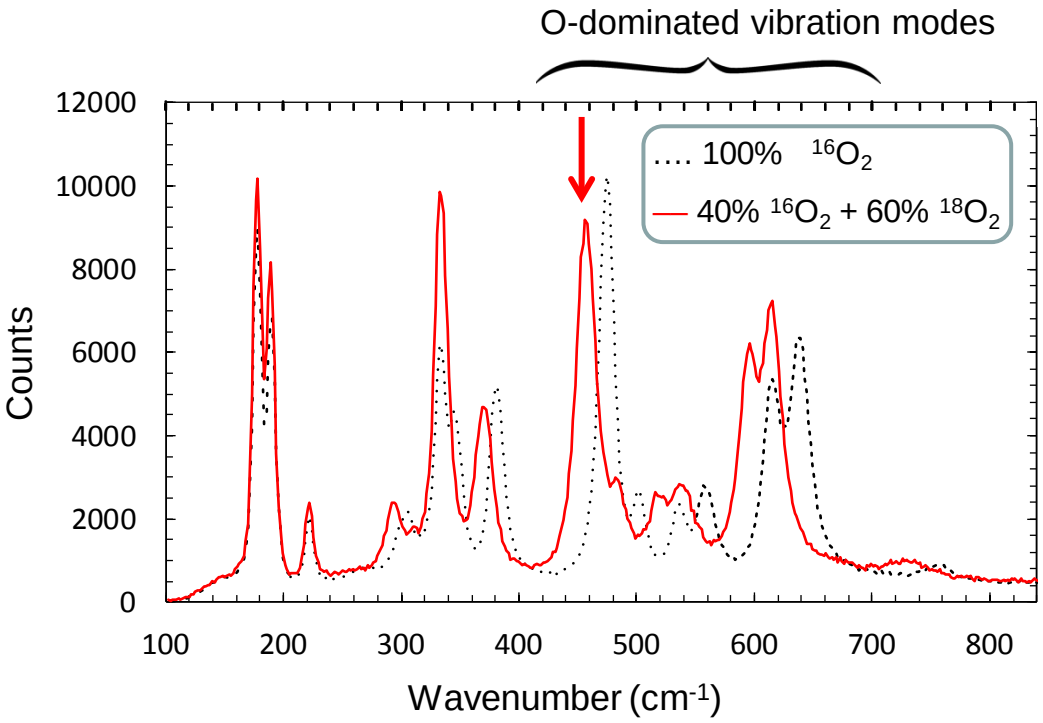
- Compressive stresses at the M/O interface.
- Distorted t-ZrO_2 distribution linked to the stress distribution.

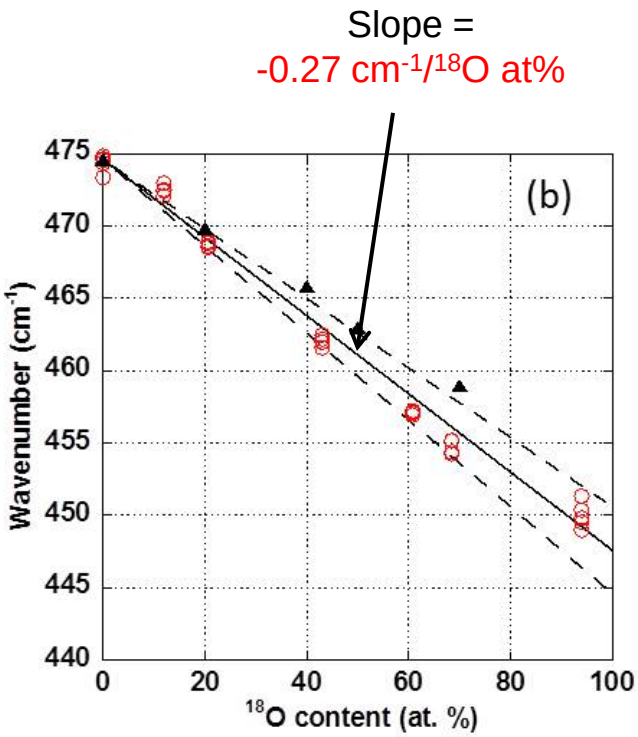
IRSN MEMBER OF ETSON

^{18}O distributions mapping

- $^{16}O \rightarrow {}^{18}O$ substitution induces strong downward shifts of **O-dominated lines** of the m-ZrO_2 Raman spectrum.
- Shifts are proportional to the ^{18}O fraction and **can be calibrated** with $Zr(^{18}O,^{16}O)_2$ standards (Powders prepared by Zy-4 total oxidation in $^{16}O_2$ + $^{18}O_2$ atmospheres).

⇒ Raman imaging can be use to quantitatively map the ^{18}O distribution in a zirconia scale by measuring the position of the **475 cm^{-1}** line.





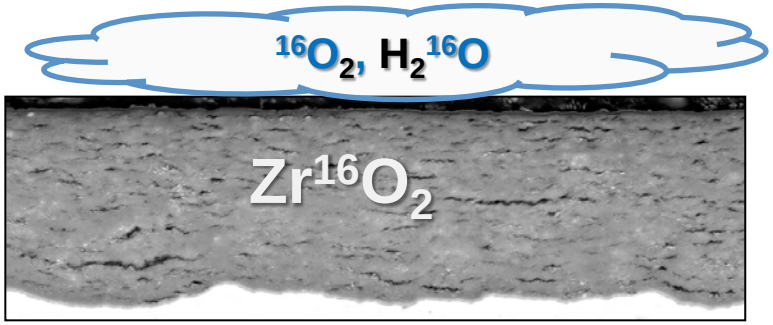
M. Guerain et al, Corrosion Science 98 (2015) 140-149

Two-stage oxidation experiments

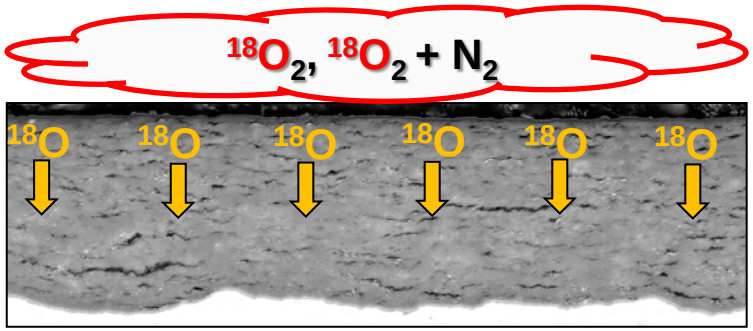
- **Objective:**
  Investigate oxygen ingress at high T through a low T pre-oxidation scale

- **Principle:**

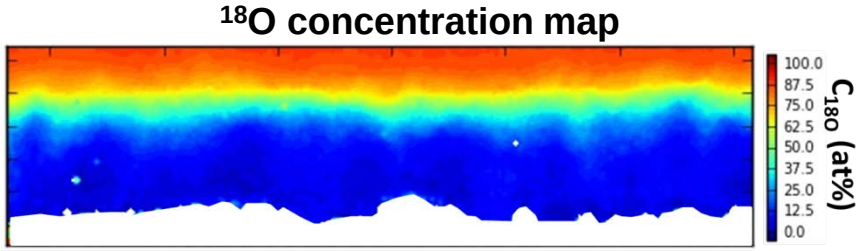
1) Low T pre-oxydation in $^{16}O_2$ + $H_2{}^{16}O$ ⇨



2) HT exposure in $^{18}O_2$ or $^{18}O_2$ + N_2 ⇨

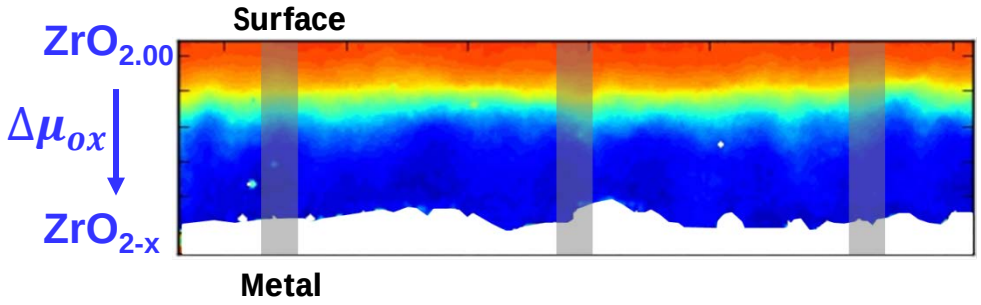


^{18}O distribution Raman mapping ⇨



IRSN MEMBER OF ETSON

^{18}O two-stage oxidation experiments: oxygen diffusion modelling

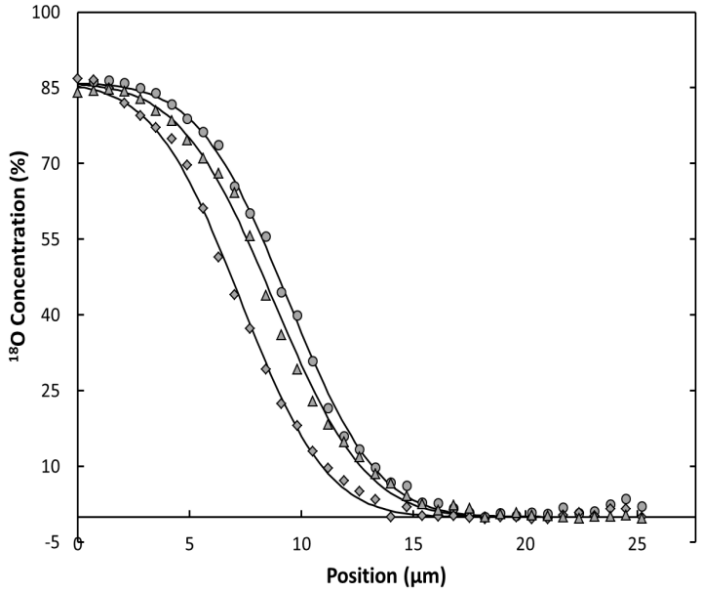


$$\frac{\partial C_{180}}{\partial t} = \frac{D_O}{RT}\frac{\Delta\mu_{ox}}{e}\frac{\partial C_{180}}{\partial x} + D_{16\leftrightarrow 18}\frac{\partial^2 C_{180}}{\partial x^2}$$

Gradient of oxygen chemical potential

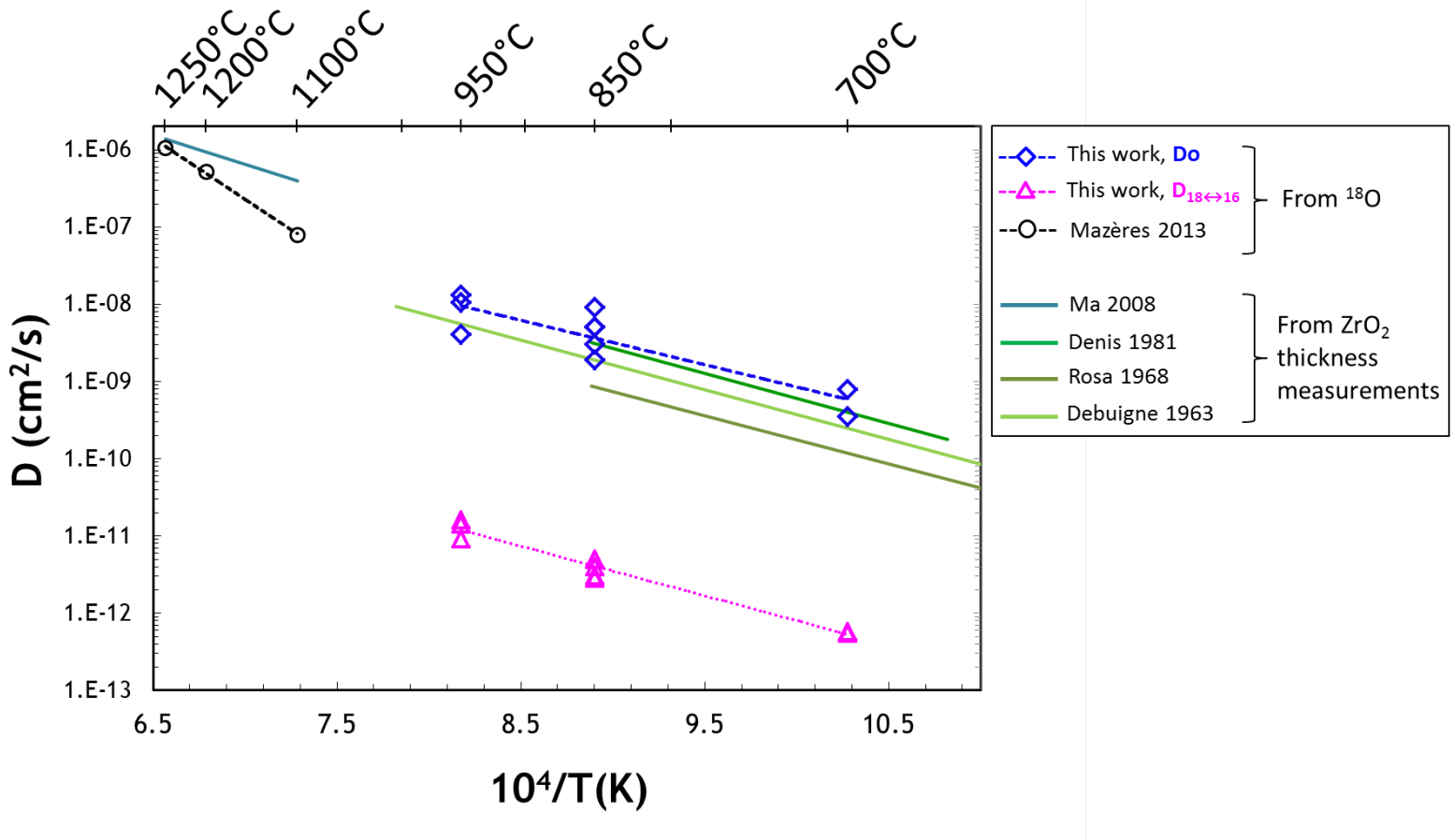
isotopic exchange

$$C_{180}(x,t) = C_s \mathrm{erfc}\left(\frac{x + \frac{D_O \Delta\mu_{ox}}{RTe}t}{2\sqrt{D_{16\leftrightarrow 18}t}}\right)$$



IRSN MEMBER OF ETSON

Oxygen diffusion coefficients



Our D_O data are comparable with apparent diffusivity derived from high T Kp

Our pre-oxide scales behave <u>at high T</u> as dense, protective scales …

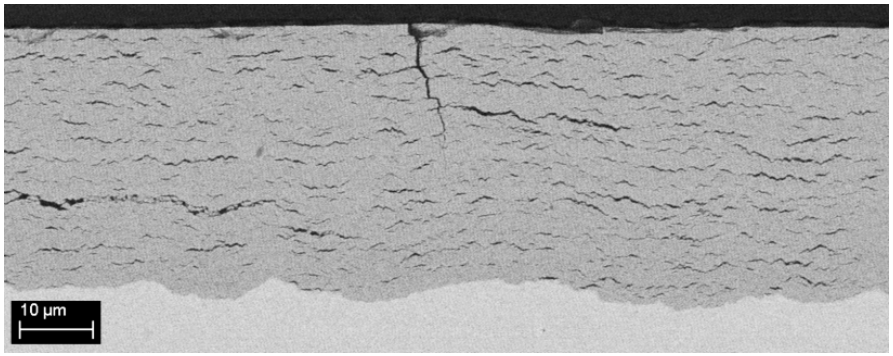
… away from radial cracks !

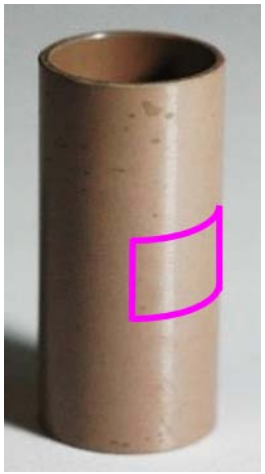
C. Duriez et al., JNM 513 (2019) 152-174.

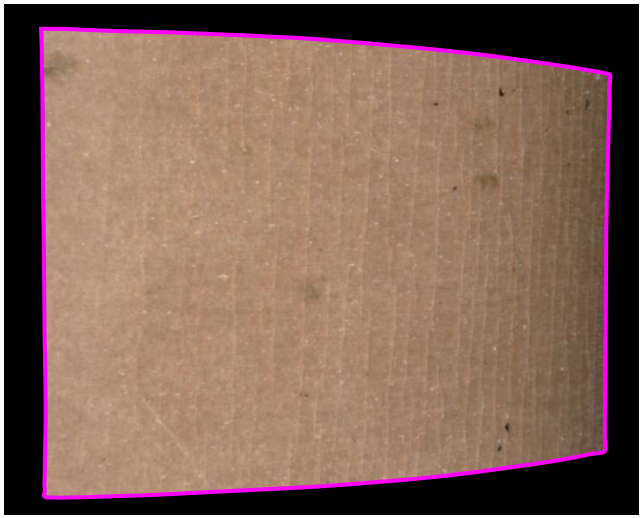
IRSN MEMBER OF ETSON

Two-stage oxidation experiments : effect of cracks

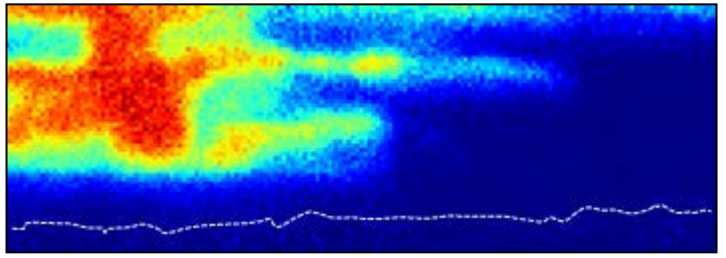
Pre-oxidation at 425°C in $^{16}O_2$ + $H_2{}^{16}O$ ⇨ 120 min at 850°C in $^{18}O_2$ + N_2



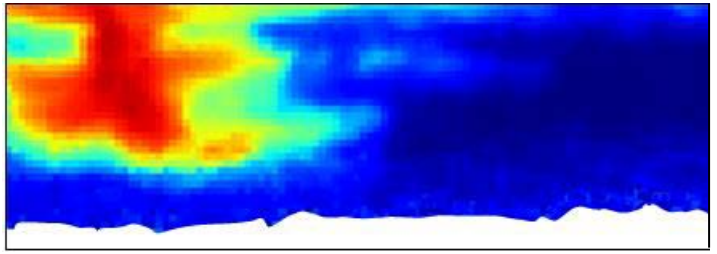


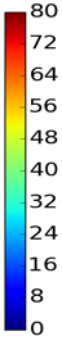


SIMS mapping



Raman mapping





A. Kasperski,, ASTM STP1597, 2018, pp. 1059-1092.

⇨ Radial cracks are preferential path for oxygen incorporation and circumferential cracks favor its lateral spreading.

→ The protective influence of the scale is lowered.

IRSN MEMBER OF ETSON

HT oxidations in $^{18}O_2 + H_2{}^{16}O + N_2$ (1/5)

- **Objective:**

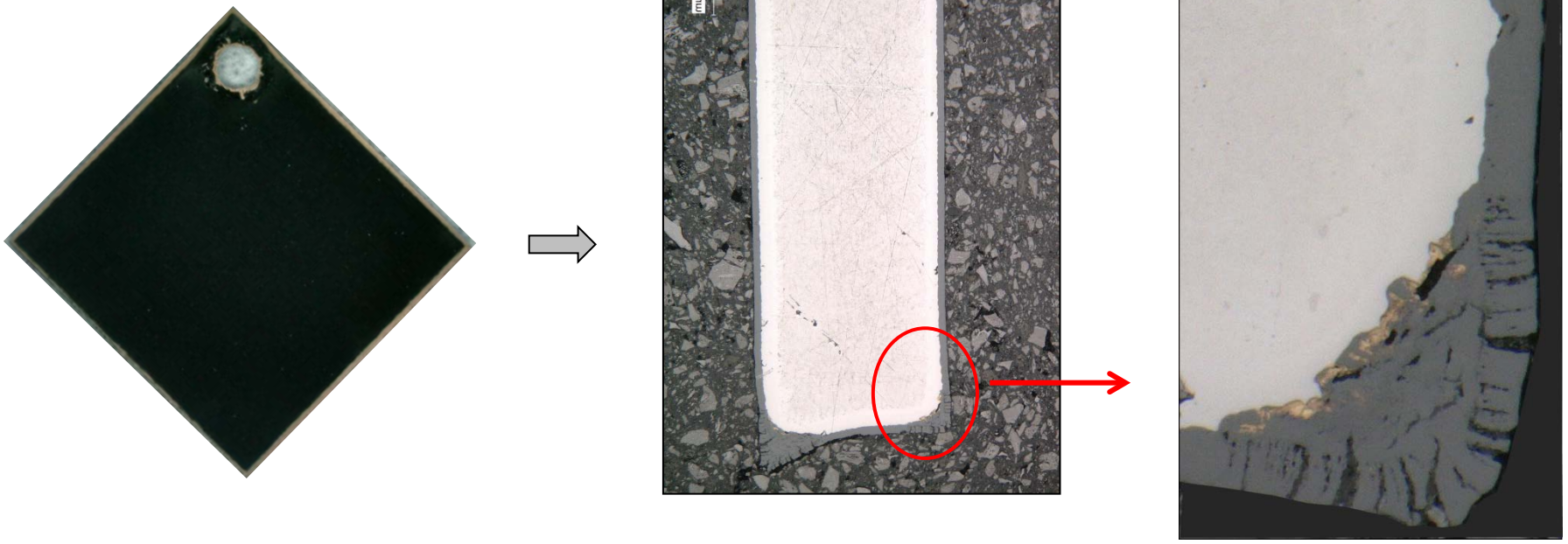
  Quantify, in mixed air + steam atmospheres, the **respective contributions** of the **O_2 and H_2O** species to the oxidation process.

- **Principle:**

  1) Bare Zy-4 plates HT oxidation in <u>flowing</u> $^{18}O_2 + H_2{}^{16}O + N_2$

  Short duration test to limit $^{18}O_2$ consumption and isotopic exchanges after oxide formation.

  2) Raman mapping at the edges ⇒ isotopic composition of <u>pre-BA</u> and <u>post-BA</u> oxides.



- **Two different composition of the gas mixture tested:**

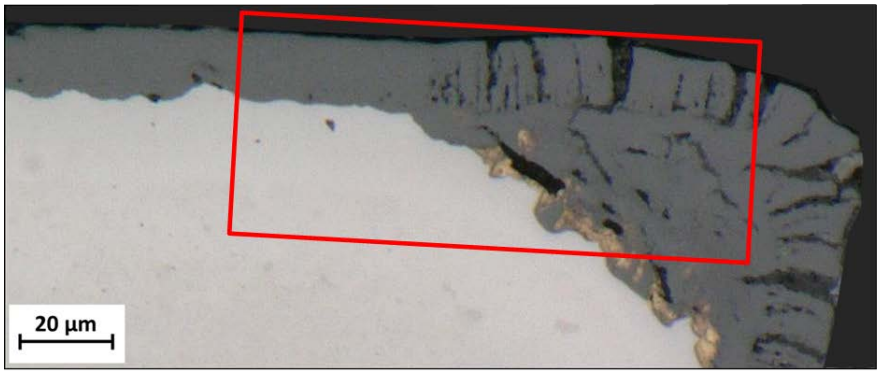
	Vol. fraction (%)			$^{18}O/(^{18}O+^{16}O)$
	$^{18}O_2$	$H_2{}^{16}O$	N_2	
« ^{18}O-poor »	4	16.5	79.5	**0.315**
« ^{18}O-rich »	14	15	71	**0.64**

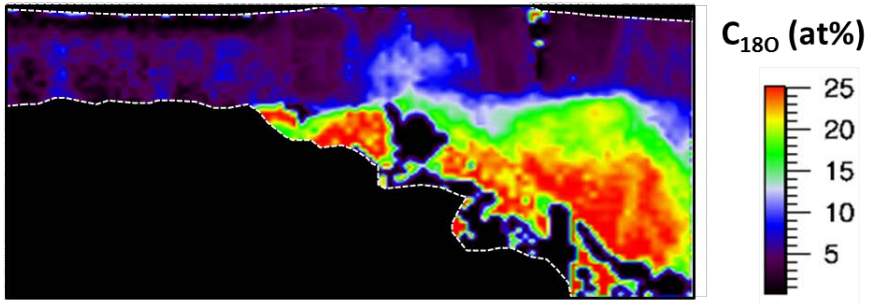
- **3 temperatures investigated:**
  - 700°C, Δt = 4 h
  - 850°C, Δt = 1 h
  - 950°C, Δt = 15 min

IRSN MEMBER OF ETSON

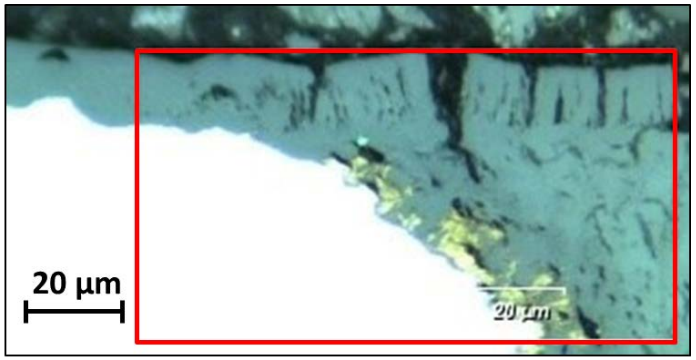
850°C, 60 min

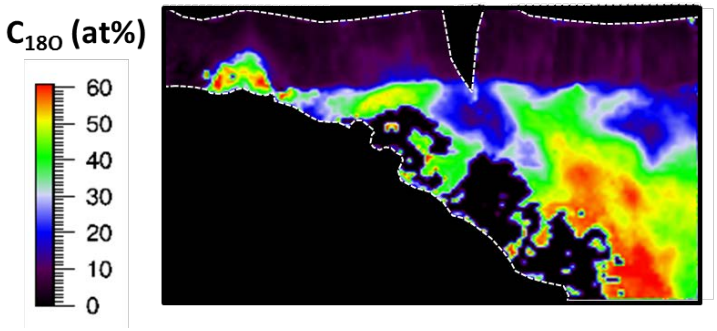
« ^{18}O-poor »





« ^{18}O-rich »



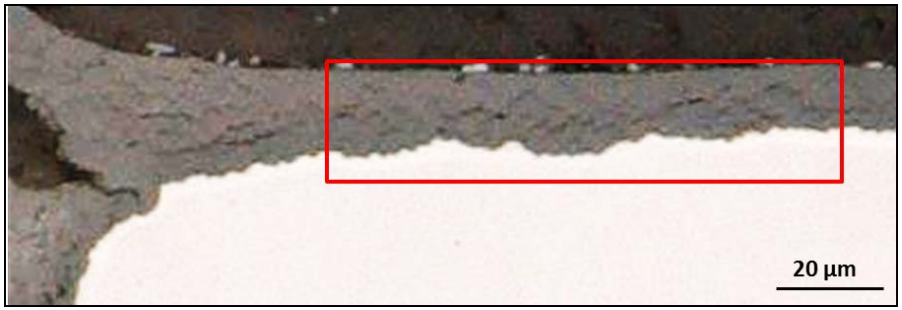


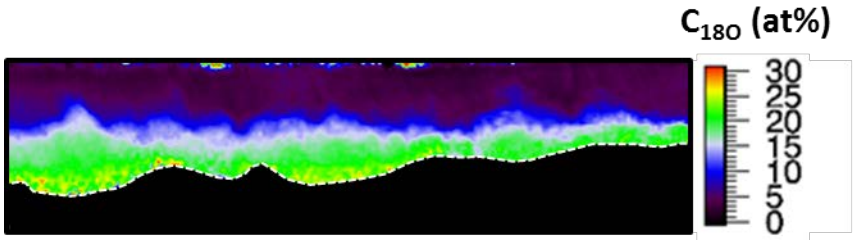
⇨

- The dense oxide has low ^{18}O content ⇒ it forms mainly from H_2O.
- The porous oxide has ~same isotopic composition than the gas mixture
  ⇒ H_2O and O_2 contribute ~ proportionally to their partial pressure.

700°C, 4h

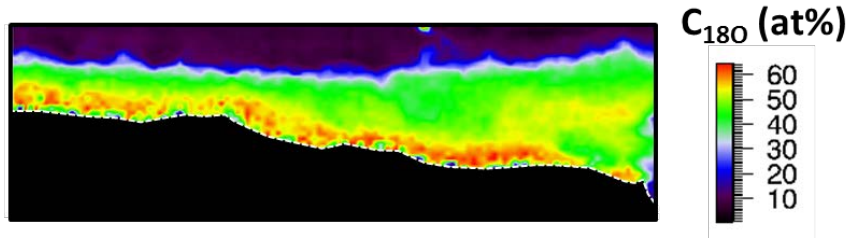
« ^{18}O-poor »





« ^{18}O-rich »



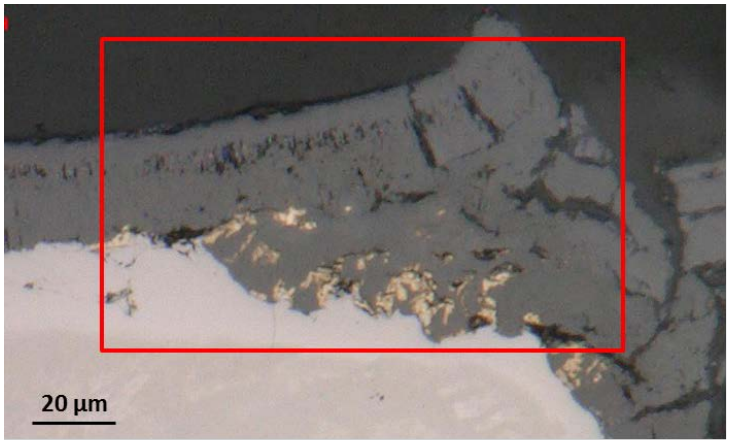


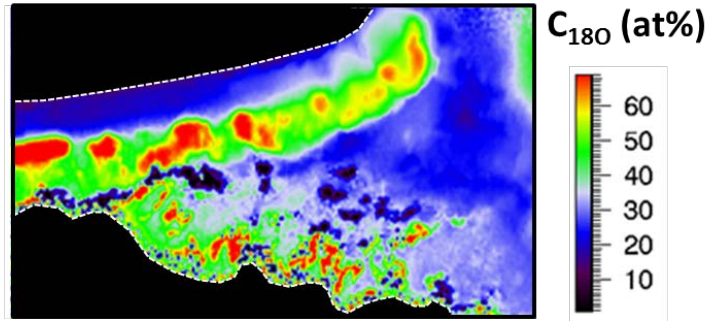
⇨ Same conclusions than at 850°C

IRSN MEMBER OF ETSON

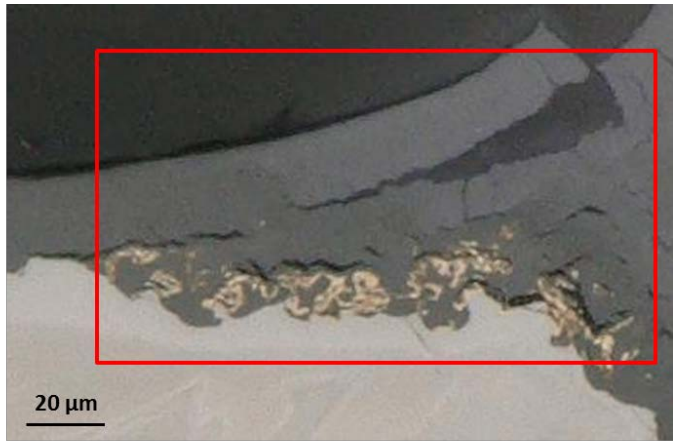
950°C, 15 min

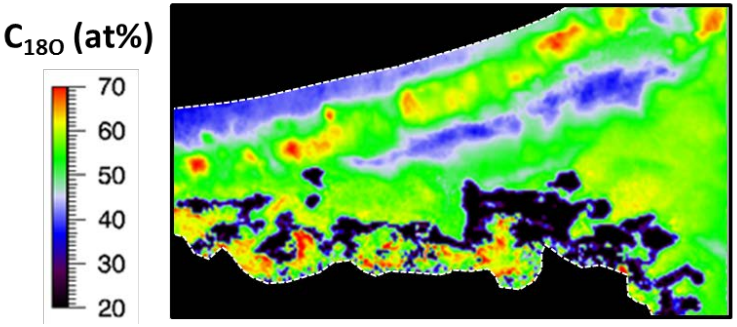
« ^{18}O-poor »





« ^{18}O-rich »





⇨

- Not as clear as at 700 and 850°C.
- Effect of isotopic exchanges after oxide formation ? → Shorter tests needed.

IRSN MEMBER OF ETSON

CONCLUSIONS

Raman imaging is a powerful tool for mapping thermally grow zirconia layers at a µm scale

⇒ Phase distribution maps (not quantitative)

⇒ Stress distribution maps (not quantitative)

⇒ ^{18}O isotopic distribution maps (quantitative)

t-ZrO_2 distributions

- **Significant t-ZrO_2 amounts** after high temperature oxidation **in air**.
- Much lower amounts after low temperature pre-oxidation.

Stress distribution

- In dense high temperature layers, **compressive stresses close to the M/O interface**.
- Low temperature, thick pre-oxidation scales **are mostly relaxed and stoichiometric**.

^{18}O distributions

- Our **pre-oxidation scales are protective** in SFP-LOCA conditions (but detrimental effect of cracks).
- In mixed air + steam atmospheres, the respective contributions of O_2 and H_2O depend on the oxidation regime. At 700-850°C, the **pre-breakaway** dense oxide forms mostly **from H_2O**.

IRSN MEMBER OF ETSON

Aknowledgments

Part of this work has been performed in the frame of the DENOPI project, funded by the French government as part of the “Investment for the Future” Program reference ANR-11-RSNR-0006

Thank you for your attention !

IRSN MEMBER OF ETSON

Additional slides

Oxidation furnaces

Pre-oxidation at 425°C in O_2 + steam





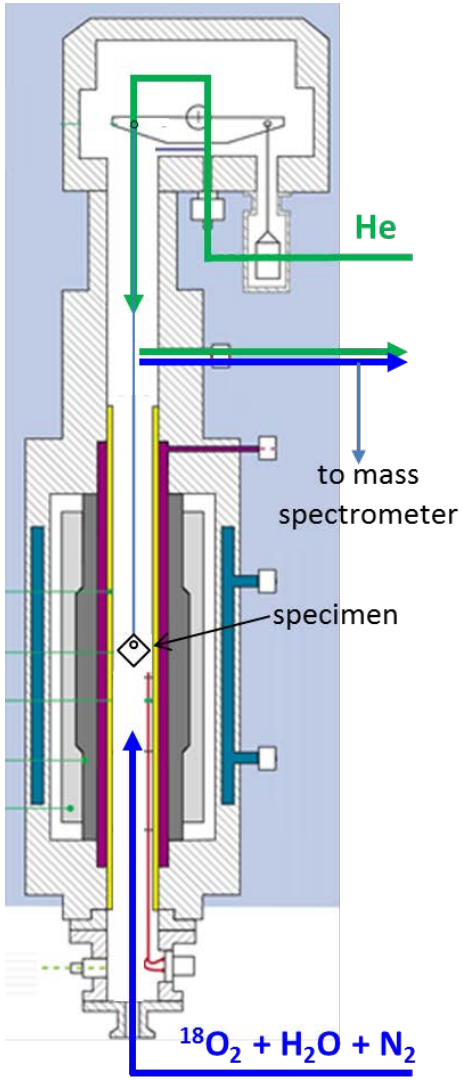


10 mm

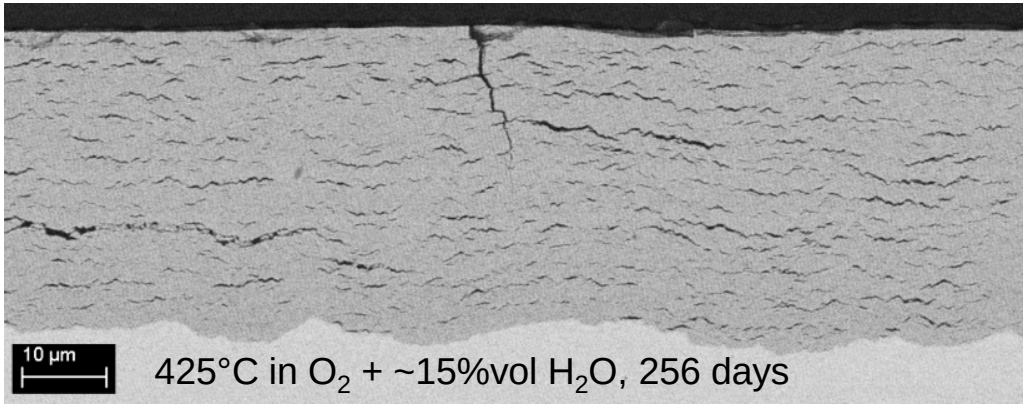


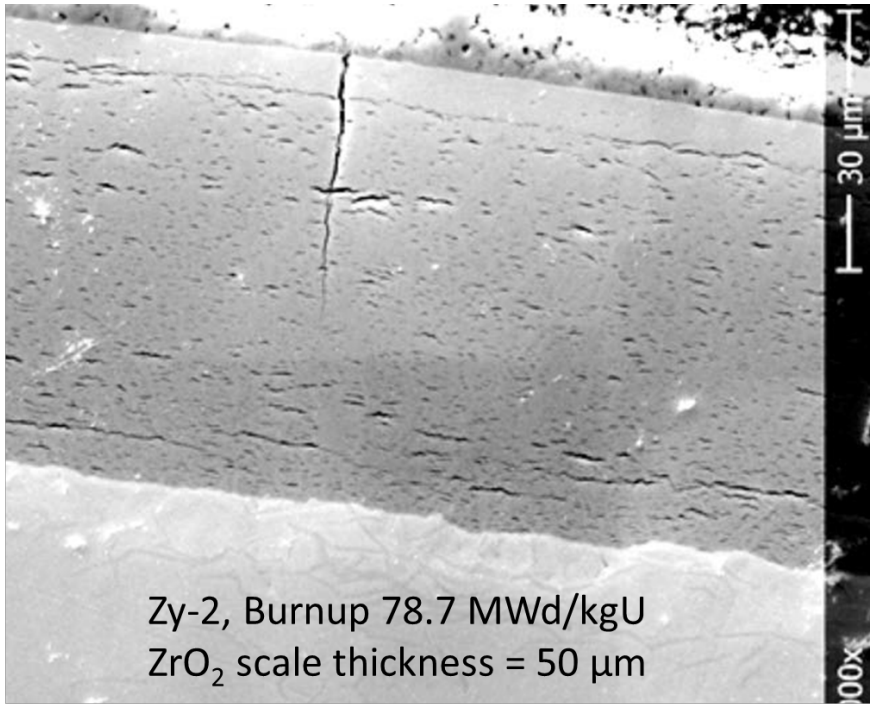
Ø 9.5 mm

HT oxidation tests in a SETARAM thermobalance



IRSN MEMBER OF ETSON





S. Abolhassani et al., *Zirconium in the Nuclear Industry, 19th International Symposium, Manchester, May 20-23, 2015.*

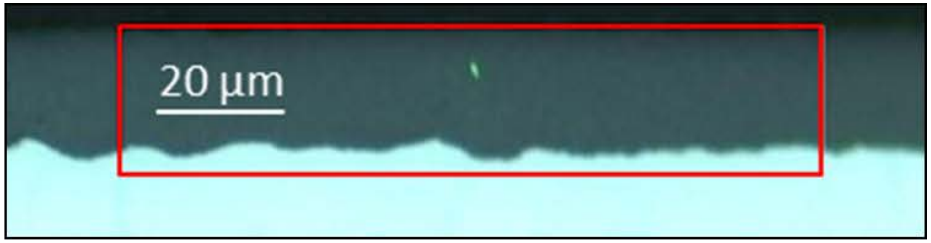
IRSN MEMBER OF ETSON

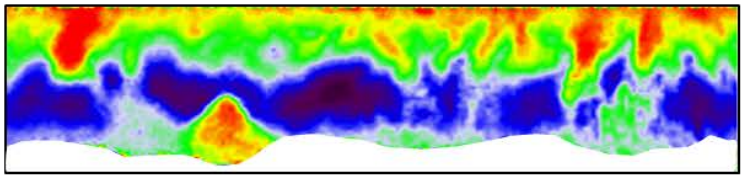
Sequential oxidations, 850 °C

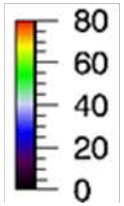
30 min $^{18}O_2$, then 60 min $H_2{}^{16}O + N_2$

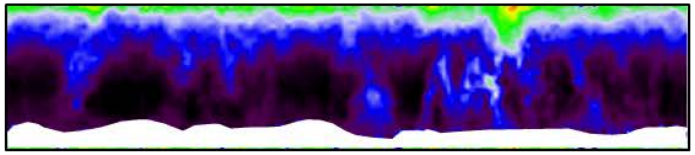
30 min $H_2{}^{16}O + N_2$, then 60 min $^{18}O_2$











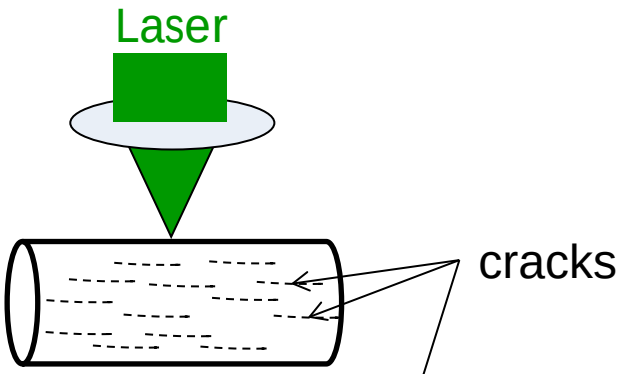
^{16}O Concentration map

^{18}O Concentration map

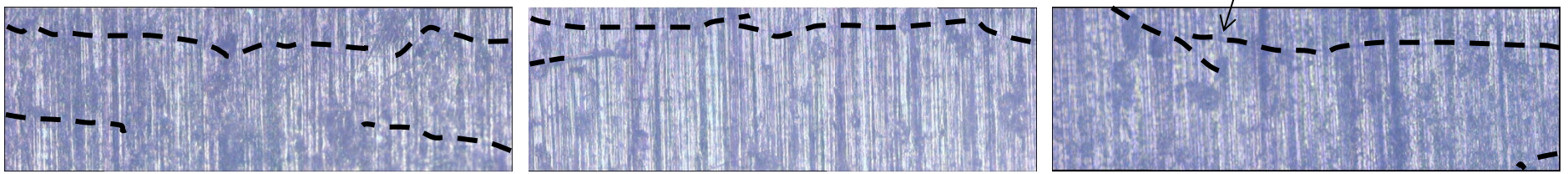
IRSN MEMBER OF ETSON

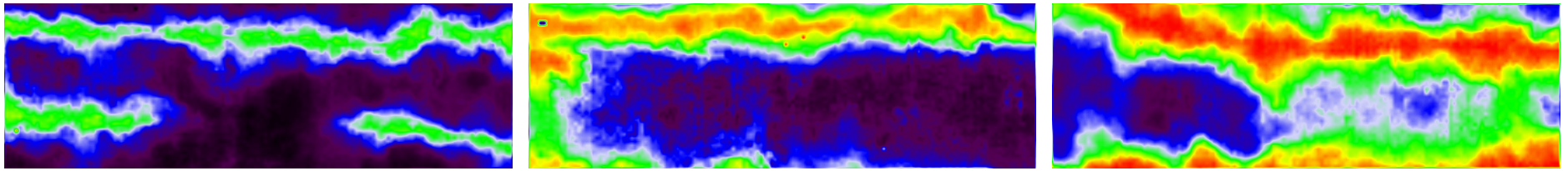
Outer oxide after exposure in $^{18}O_2$ at 850°C





30 min **60 min** **120 min**





100 µm

C_{18O} (at. %) 0 20 40 60 80

IRSN MEMBER OF ETSON

The oxidation behavior of Zr1%Nb cladding alloy in air-steam mixtures

P. Vrbka[1,2], **J. Krejčí[1]**, J. Kabátová[1], J. Kočí[1], F. Manoch[1], V. Vrtílková[1]

[1]*UJP PRAHA a.s., Nad Kamínkou 1345, 156 10 Praha - Zbraslav, Czech Republic*

[2] *Faculty of Nuclear Sciences and Physical Engineering, Czech Technical University in Prague, V Holešovičkách 2, Praha 8, 18000, Czech Republic*

The oxidation behavior of a Zr1%Nb cladding alloy in air-steam mixtures at temperatures ranging from 700 to 1200 °C was studied. Air attack under prototypical conditions with an air ingress during a severe reactor accident or a spent fuel pool accident was investigated. Oxidation in nitrogen containing atmosphere leads to major degradation of the cladding material. Steam contained in mixture can leads to hydrogen absorption, and also to hydrogen release. Exposure times covered both pre- and post-breakaway regimes.

Both, autoclave and high-temperature steam pre-oxidized specimens were exposed as well. Pre-oxidation prevents cladding surface against nitrogen attack and leads to significant decrease of the oxidation rate or to delaying the breakaway phenomena.

Measured weight gains were used for developing a new correlation to determine the oxidation kinetics of given Zr1%Nb alloy in air and air-steam mixtures at temperature range in between 700 and 1200°C.

Metallographic observations along with microhardness testing were carried out to study the material microstructure. The hydrogen content was measured and residual mechanical properties were studied using Ring Compression Tests.

Key words: high temperature oxidation, fuel cladding, severe accident, steam-air mixtures



UJP PRAHA

The oxidation behavior of Zr-1%Nb cladding alloy in air-steam mixtures

P. Vrbka[2], J. Krejčí[1,2], J. Kabátová[1], F. Manoch[1], J. Kočí[1], V. Vrtílková[1]

[1] UJP PRAHA a.s., [2] Czech Technical University in Prague



25th International QUENCH Workshop

Karlsruhe Institute of Technology, Germany

October 22-24, 2019

Presentation outlines

UJP PRAHA

Czech Technical University in Prague

- Tested material
- Experimental facility and methodology
- High temperature oxidation in air
- Influence of pre-oxidation
- Air-steam mixtures
- Influence of flow rate



Material

- Zr1%Nb cladding alloy
  - 9.1 x 7.93 x 30 mm



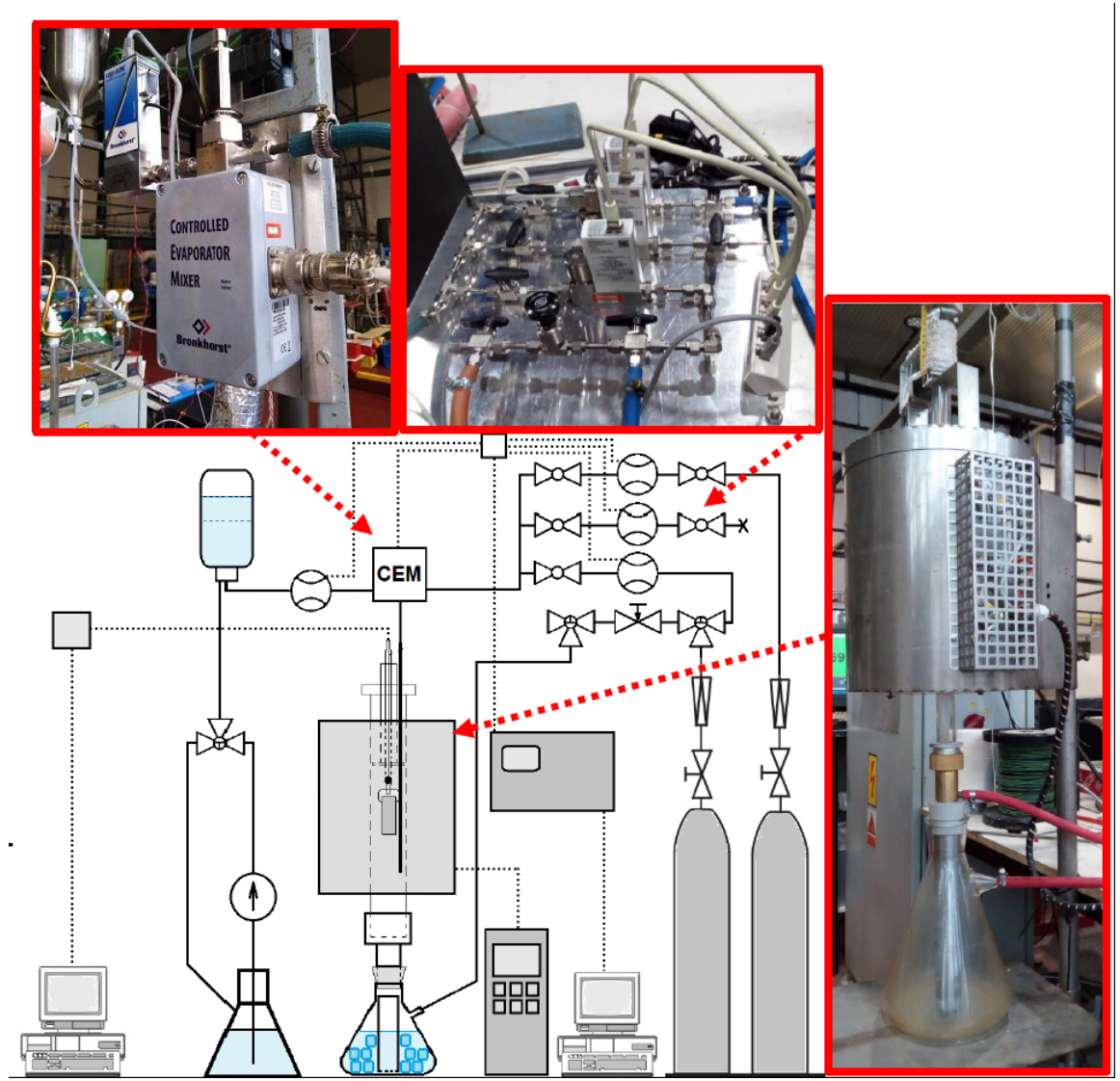
- As-received state
- Pre-oxidation
  - Autoclave: WWER environment
  - Autoclave: steam
  - High temperature steam

Alloy	Nb [%]	Fe [ppm]	O [ppm]	Zr
Zr1%Nb	1.0	500	700	sponge

Environment	Temperature [°C]	Duration	Oxide [µm]	H [ppm]
Steam 10.7 MPa	425	42 days	5	~ 22
		105 days	9,2	~ 202
Steam 0.1 MPa	814	13; 113 min	10; 20	< 20
	1016	0,5; 3; 40 min	10; 20; 40	
	1200	0,33; 18 min	40; 130	
WWER water 18.6 MPa	360	378 days	5	~ 50

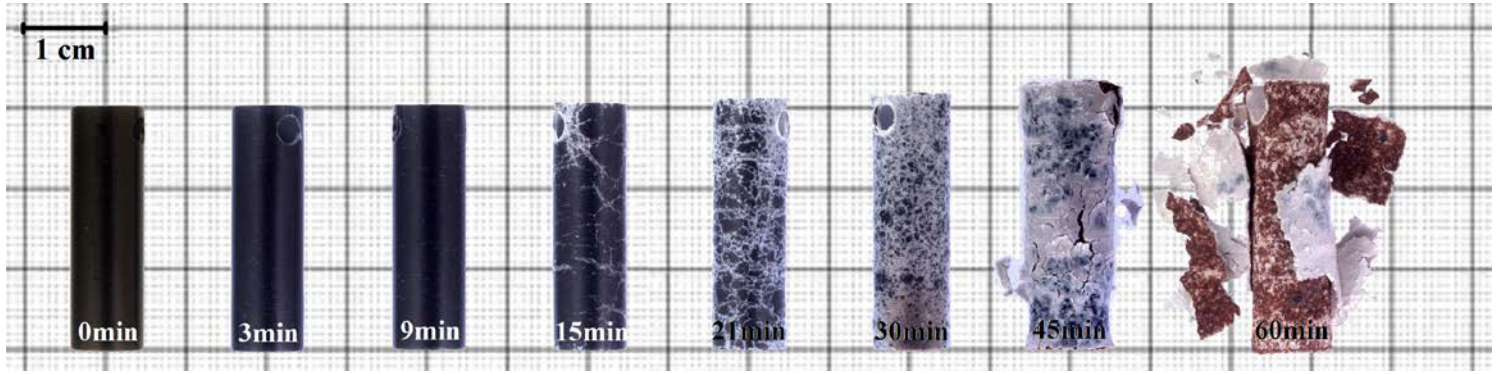
Experimental facility

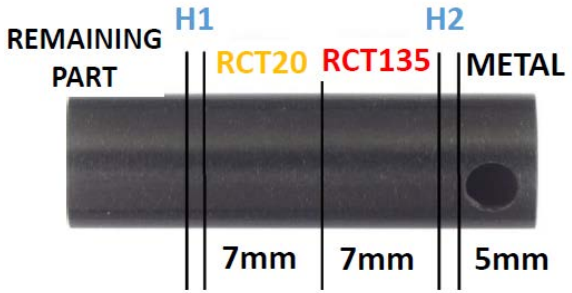
- Resistance furnace
  - Temperatures: 700-1200 °C
- CEM unit (Bronkhorst)
  - Air/steam ratio: { 0; 10; 30; 50; 70; 90; 100} %
- Gas flow rates
  - Air oxidation
    - Synthetic air 18 l/h
    - Argon 6 l/h
  - Air-steam mixtures oxidation
    - Synthetic air 0-100 l/h
    - Steam 70-0 g/h
    - Argon 50 l/h
- Specimens inserted into pre-heated furnace with stabilized flow

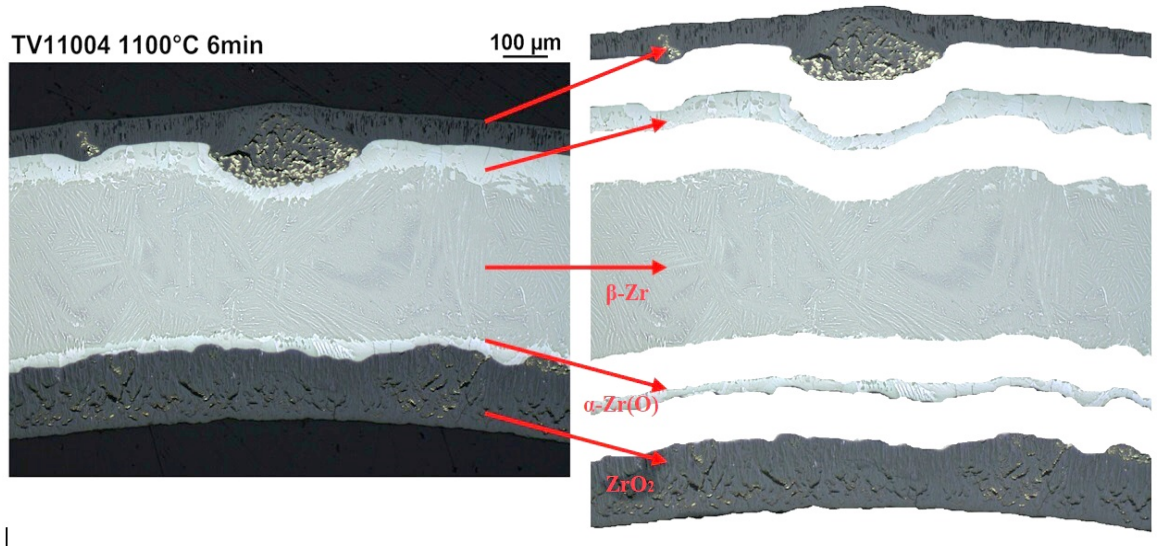


Post experimental evaluation

- Non destructive
  - Visual inspection
  - **Weight gain => oxidation kinetics**
  - Length of specimen
- Destructive evaluation
  - H-content
  - Ring compression test (20, 135 °C)
  - Metalography in 4 directions
    - ZrO_2, ZrO_2+ZrN,α-Zr(O), β-Zr
  - Microhardness (2x 10 points HV: 100 g)







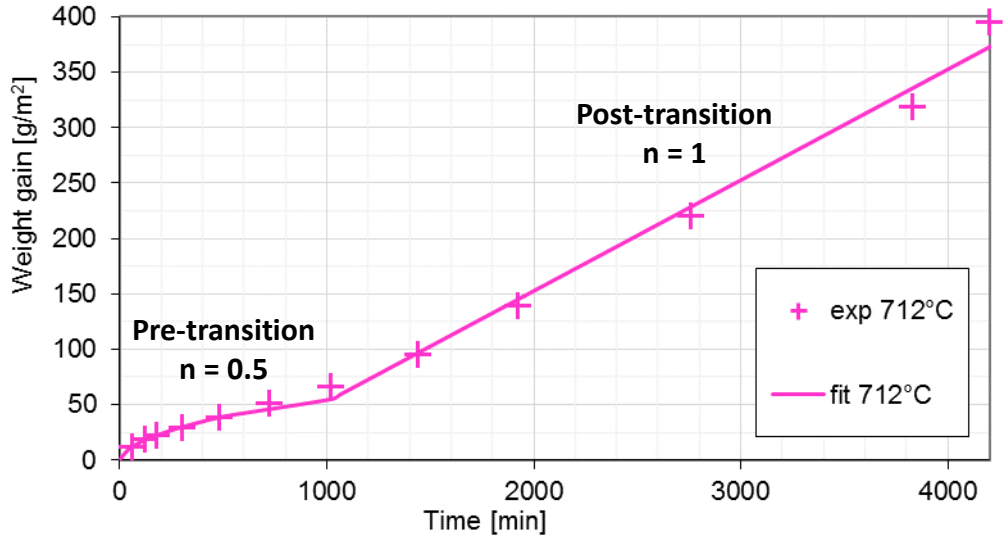
Oxidation kinetics formula

- Arrhenius formula based on air-oxidation data

$$\frac{dWG^n}{d\tau} = k = Aexp\left(-\frac{B}{T}\right)$$

- Pre-transition and after transition kinetics
- Correction factors used to include other phenomena
  - Critical region
  - Pre-oxidation
  - Air-steam mixtures
  - Flow rate

$$\frac{dWG^n}{d\tau} = k = Aexp\left(-\frac{B}{T}\right)\varepsilon_{cr}\varepsilon_{po}\varepsilon_{mix}\varepsilon_{flow}$$

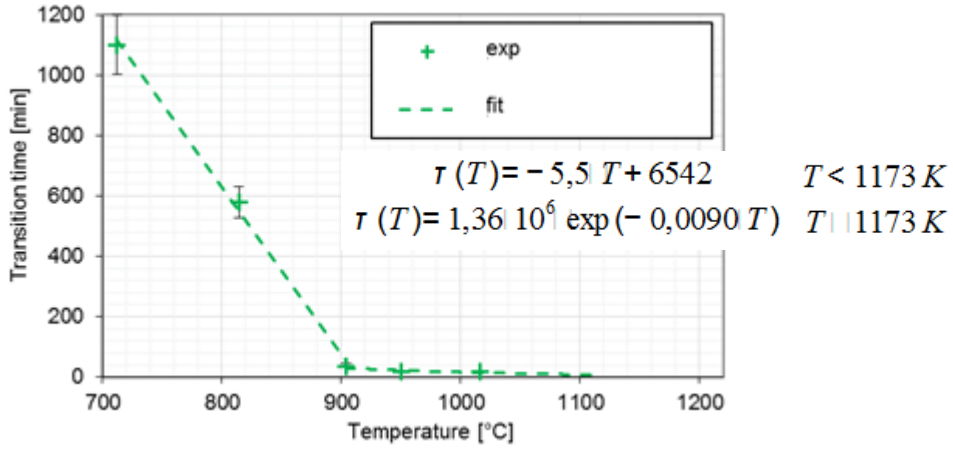


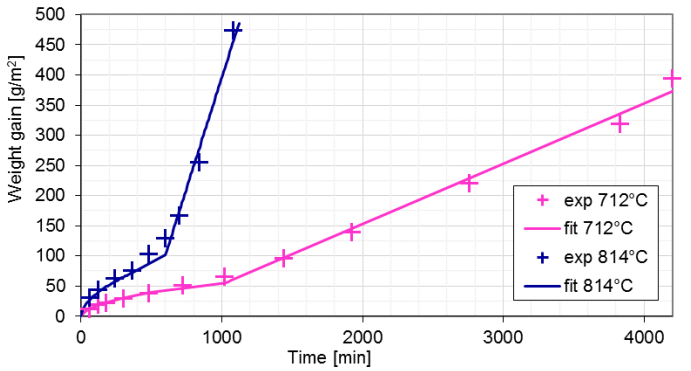
Air oxidation kinetics: fit of parameters

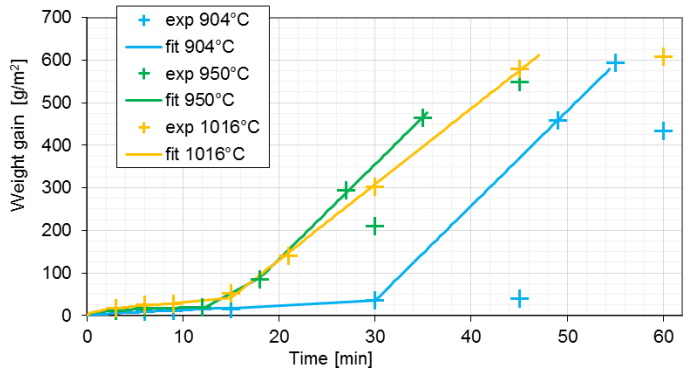
- Temperatures 712 – 1200 °C: 170 specimens
- 712-1016
  - Pre-transition kinetics: n = 0.5
  - Post-ransition kinetics: n = 1
    - Critical temperatures: 904 °C, 950 °C => enhancement
- 1100-1200
  - No transition: n = 0.66

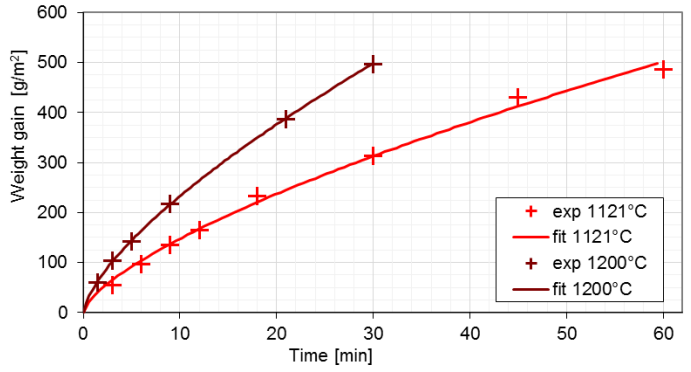
$$\epsilon_{cr} = \exp\left(1{,}268\,\frac{T_0 - T}{T_0 - 1223}\right)$$

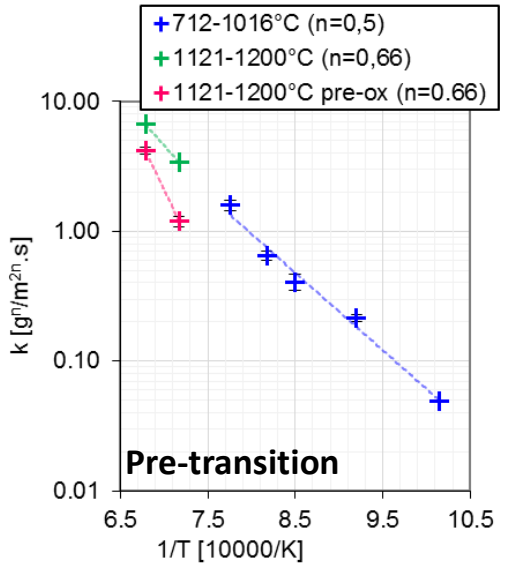
- Transition time dependend on temperature

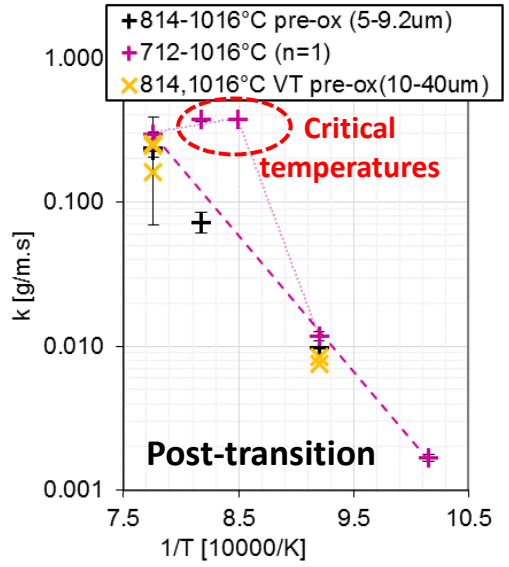






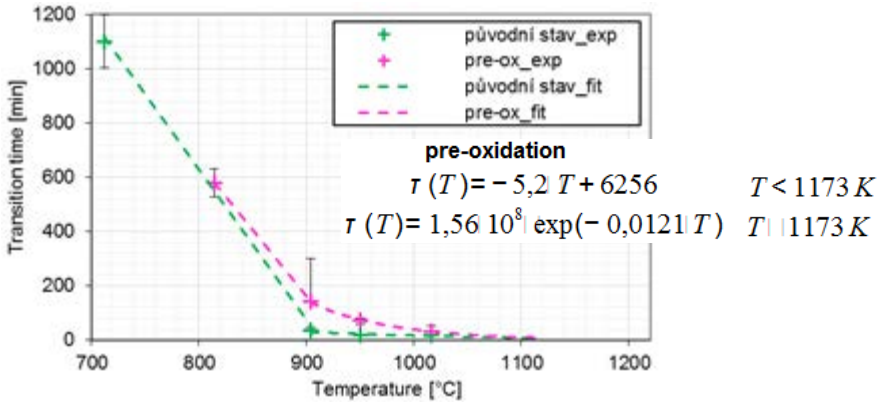




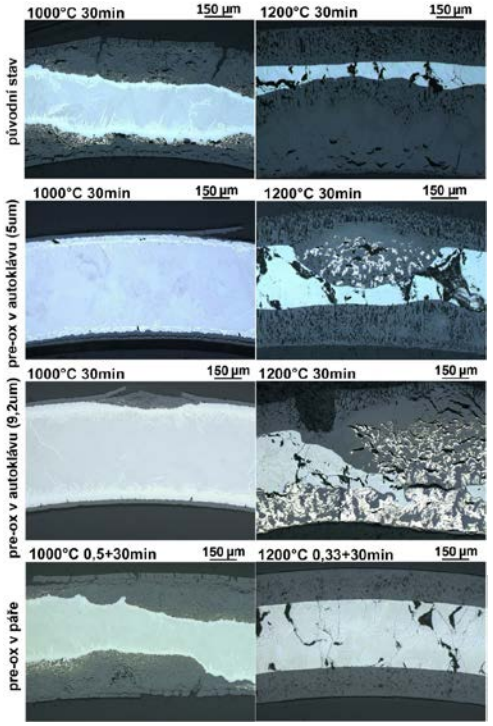


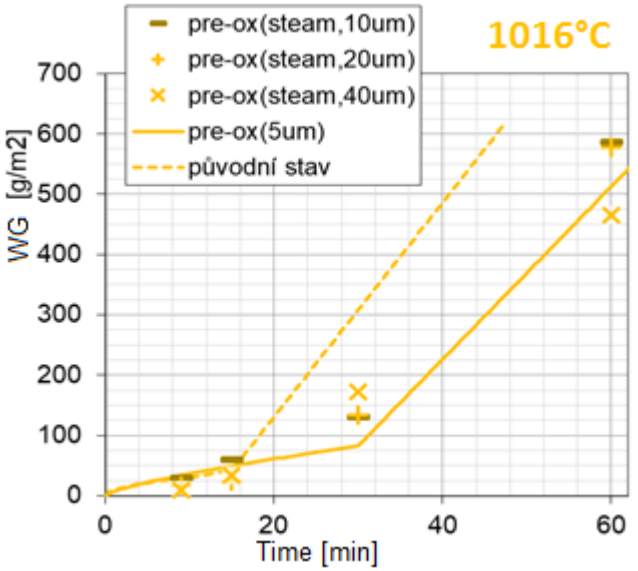
Influence of pre-oxidation

- Temperatures 800 – 1200 °C: 110 specimens
- 800 °C similar to as-received
- 900-1016 °C: transition time later, similar ox. rate



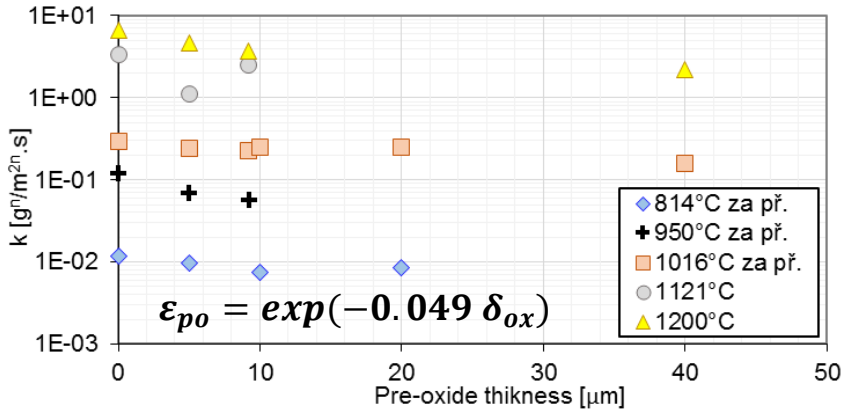


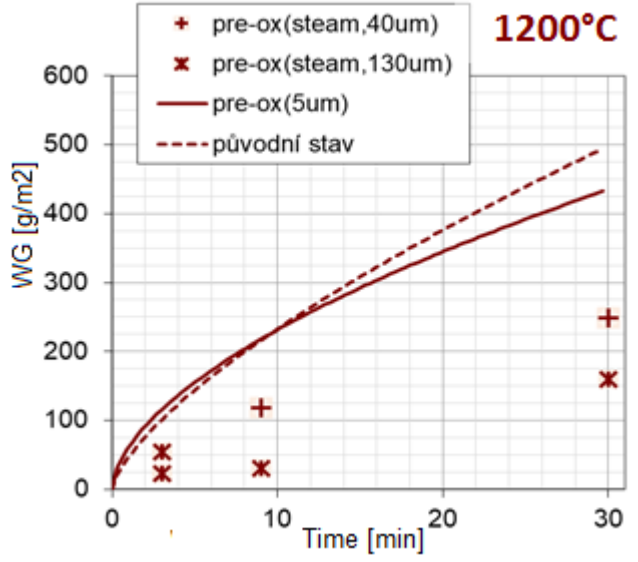




- 1100-1200 °C
  - HT pre-ox (LOCA: thick layer)

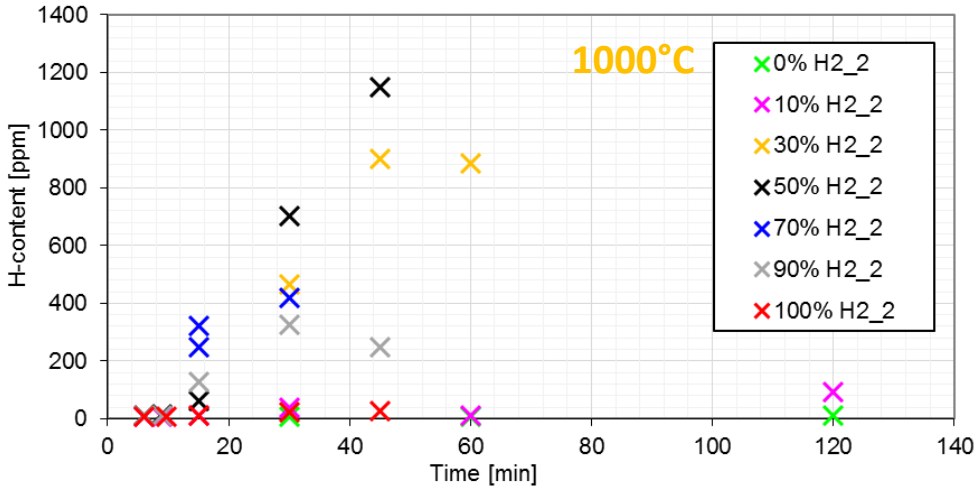
  ⇒ significant decrease of ox. rate
- Pre-oxide layer ↓ ox. rate
- **<u>No correction → conservative</u>**

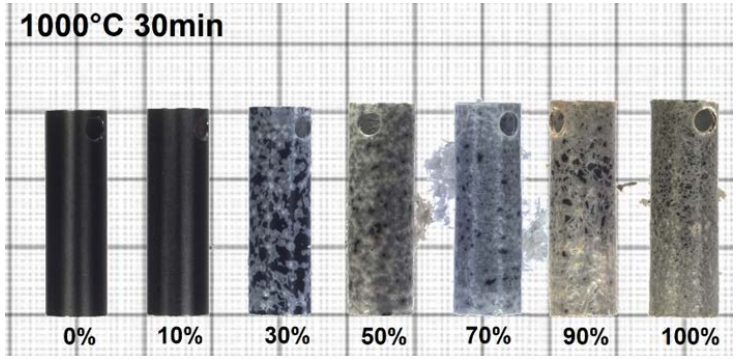


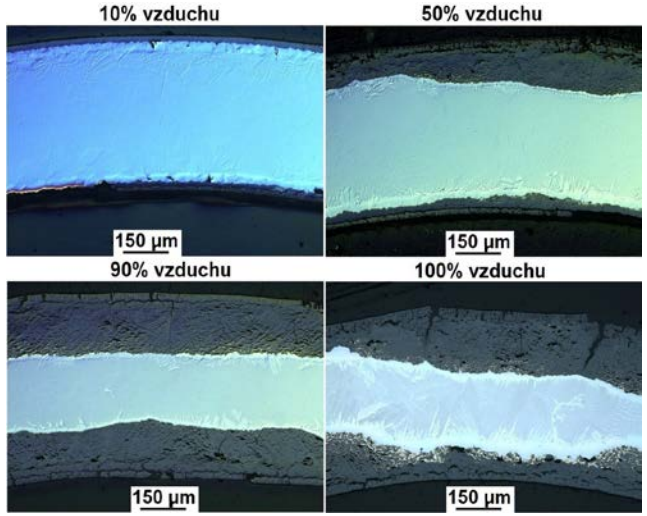


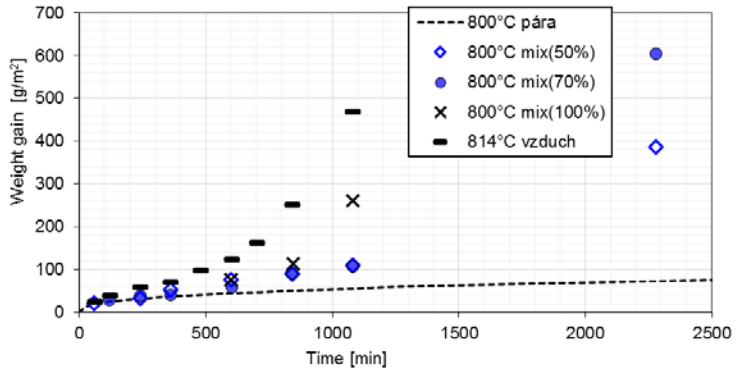
Air steam mixtures

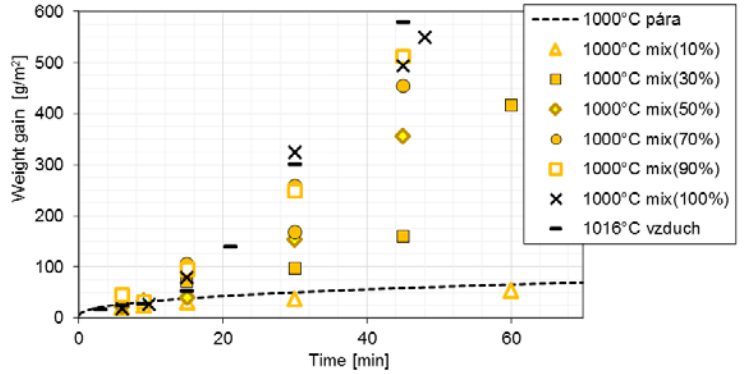
- Temperatures 800, 1000, 1200 °C
  - 100 specimens
- Air ratio influence on
  - Transition time
  - Pre and post-transient kinetics
  - Microstructure
  - Hydrogen content (highest for 30-70%)
  - Mechanical properties

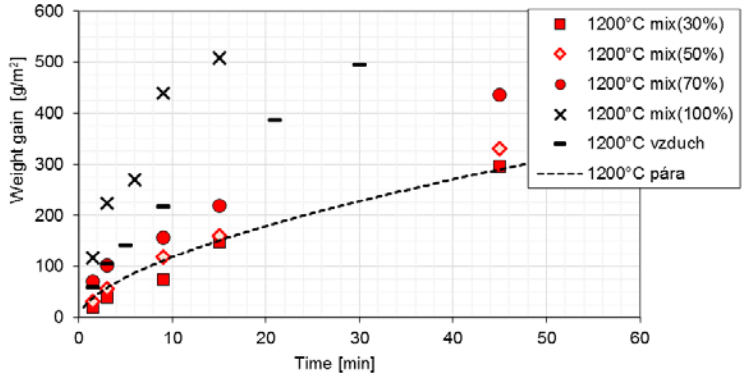












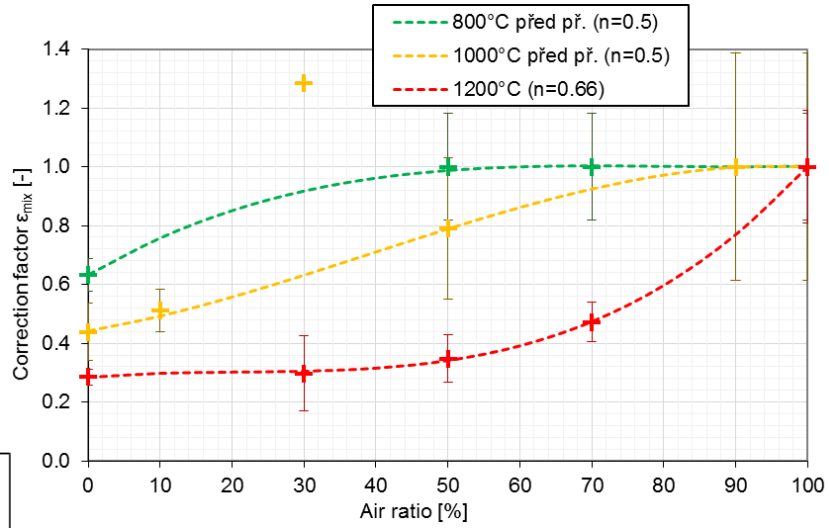
Air-steam mixtures kinetics correction factor

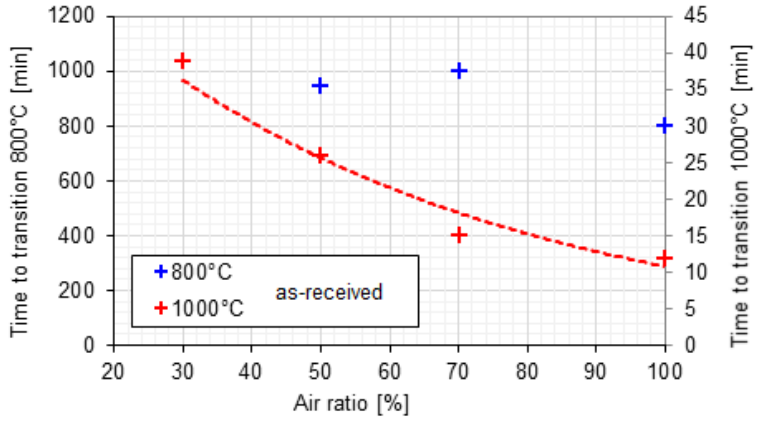
UJP PRAHA

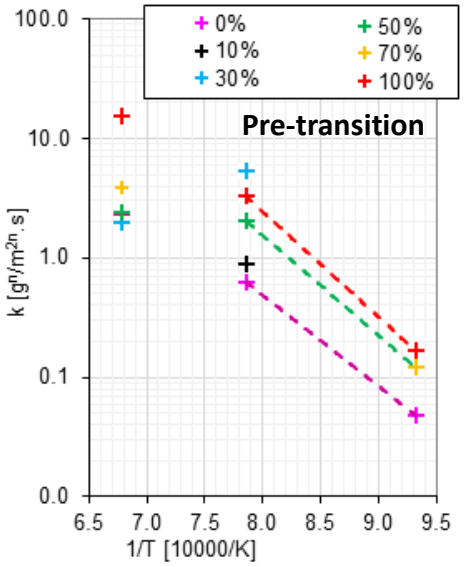
Czech Technical University in Prague

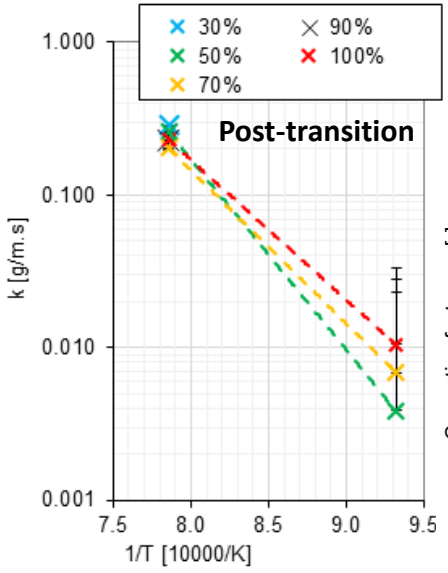
- Influence of Air volume ratio
- Pre-transition oxidation rate
  - 800 & 1000 °C: significant influence from low air ratio (local phenomena)
  - 1200 °C: significant influence from air ratio above 50 %
- Post-transition oxidation rate
  - Influence at 800 °C
- Transition time
  - Especially at 1000 °C

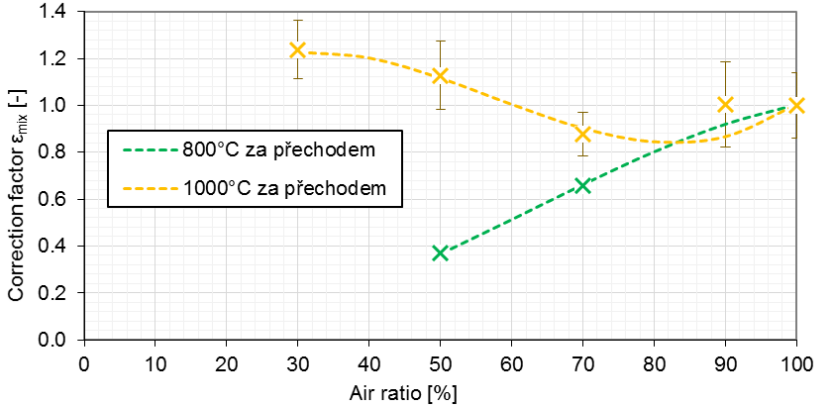
$$\varepsilon_{mix} = D\varphi_{air}^3 + E\varphi_{air}^2 + F\varphi_{air} + G$$





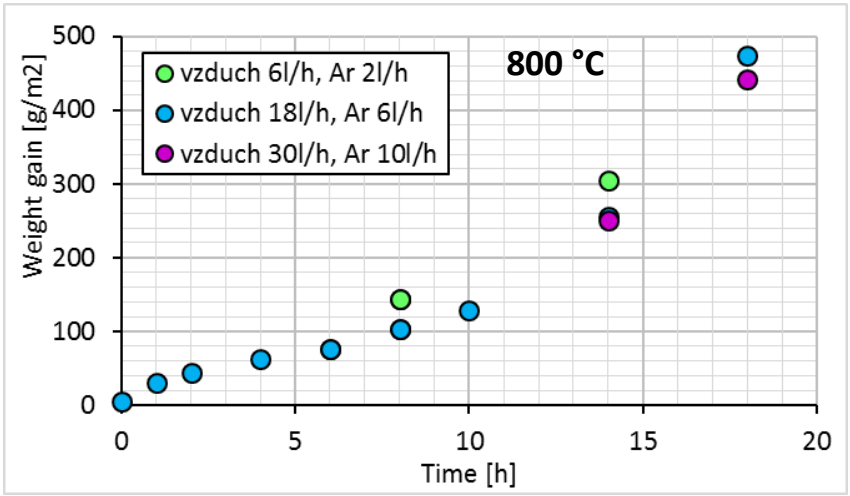


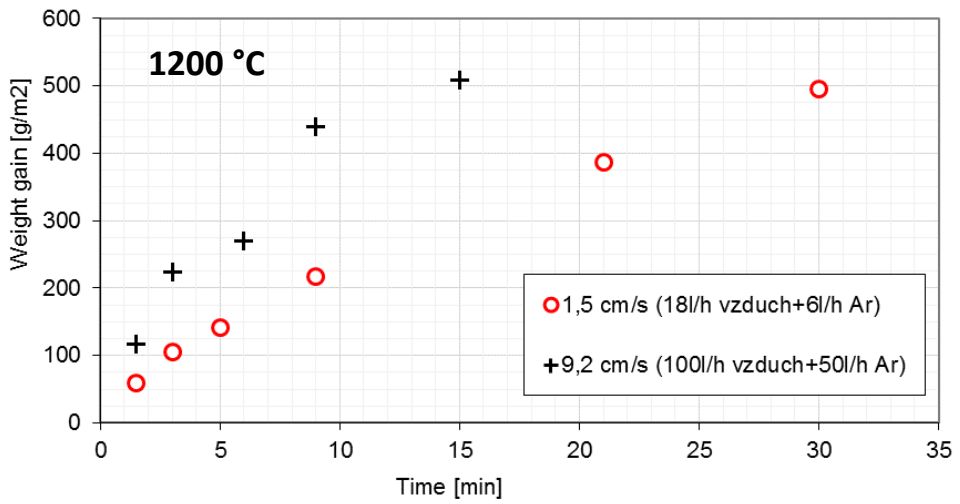


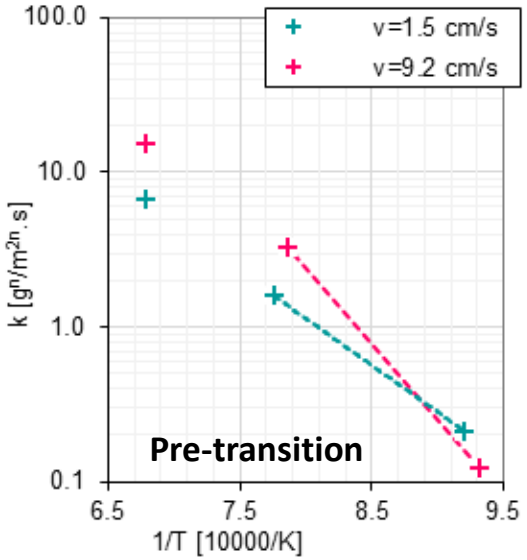


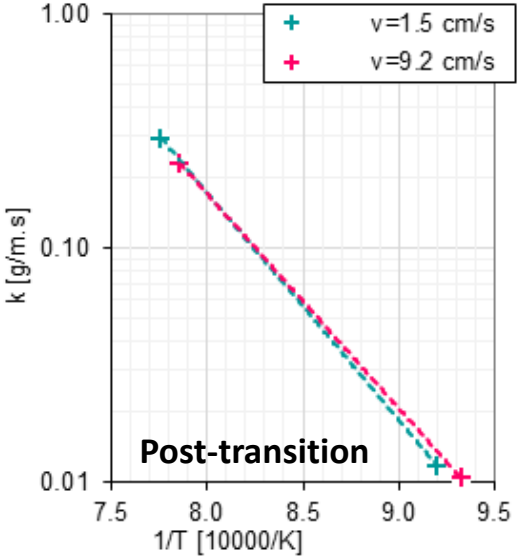
Influence of flow rate

- 30 mm specimens tested at different flow rates and quartz tube diameter
  - Not enough of experimental data for correction factor
  - More expereimtns need to be performed
- Lower temperatures: „local“ steam starvation, influence on transition time
- Higher temperatures: „global“ steam starvation
- Experiments very sensitive on flow rate (especially higher temperatures)



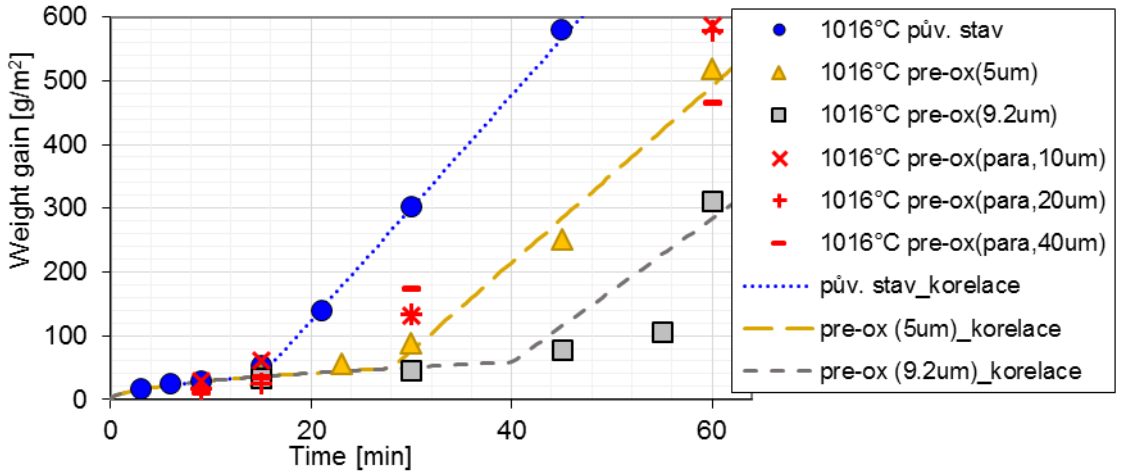


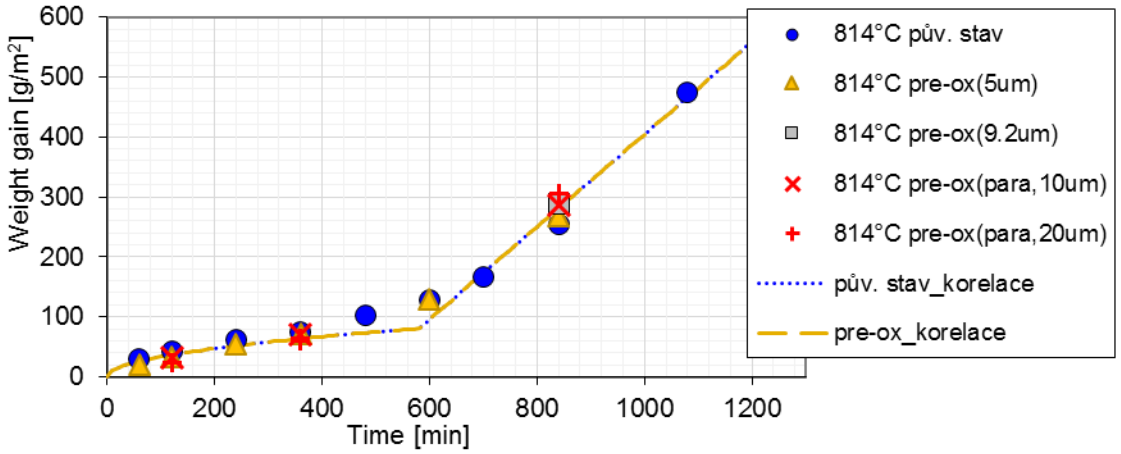


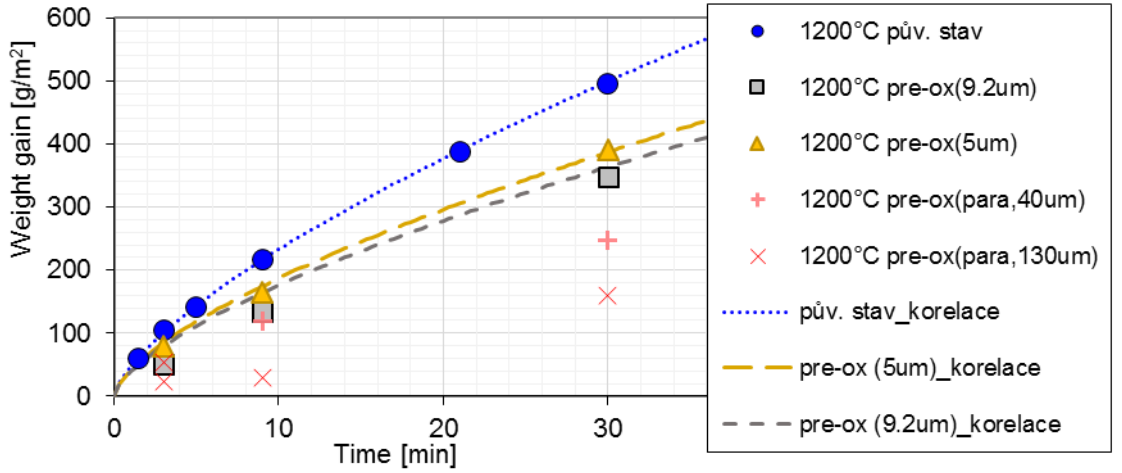


Comparison correlation and UJP data

- Air oxidation
  - as-received, pre-oxided
  - 814, 1016, 1200 °C
- Proposed correlation
  - In sufficient agreement with experimental data
  - Correction factor for low temperature pre-oxidation

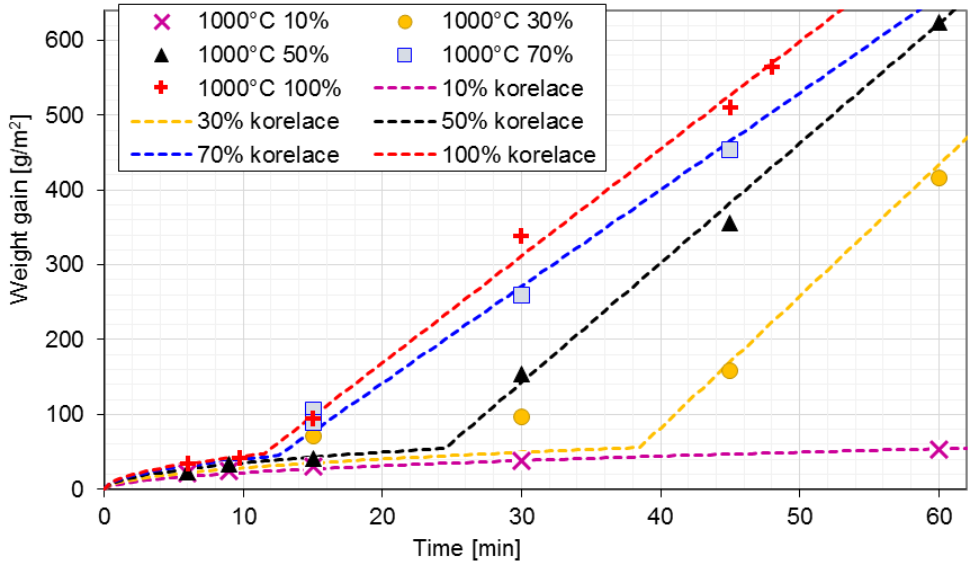


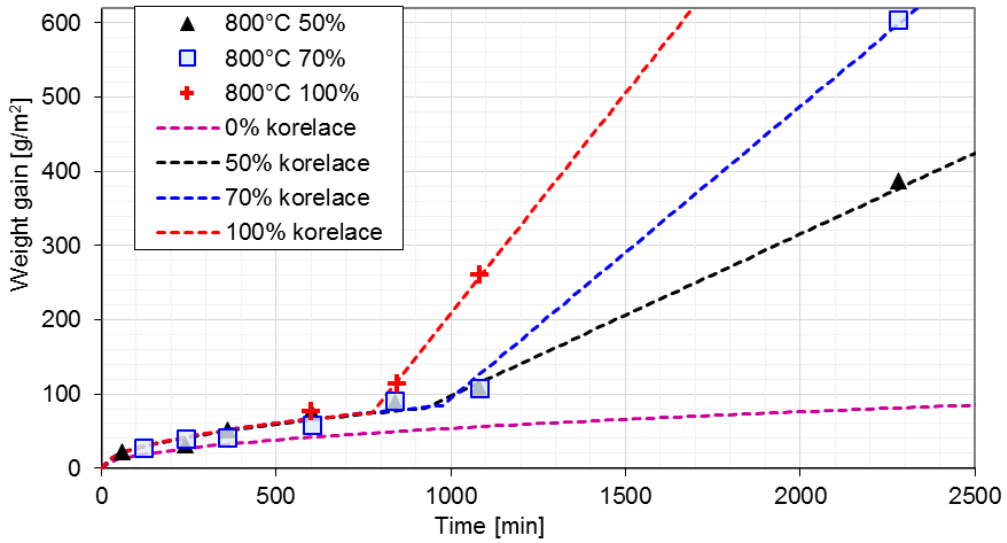


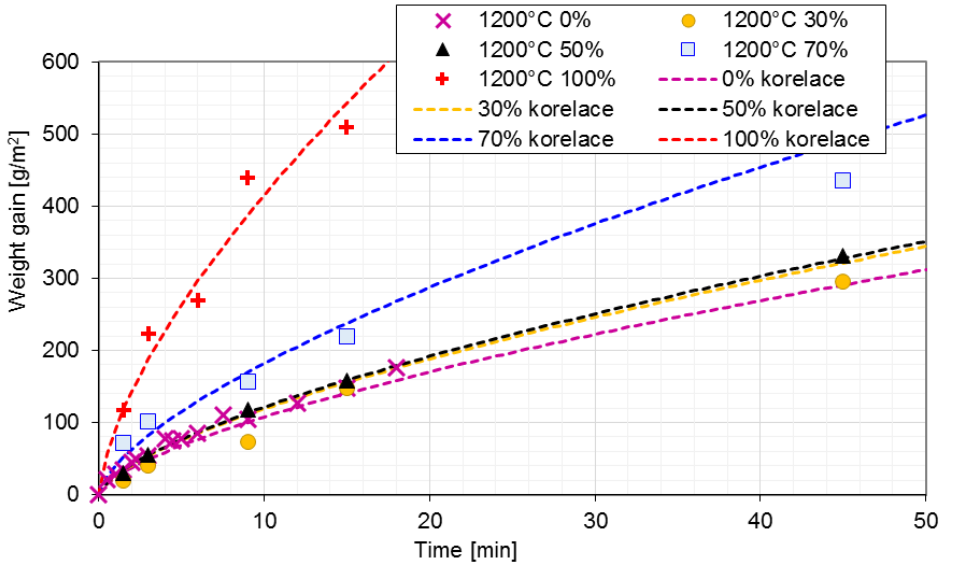


Comparison correlation and UJP data

- Air-steam mixtures
  - as-received
  - Air ratio 10 - 100%
  - 800, 1000, 1200 °C
- Correction factor for air-steam ratio
  - In sufficient agreement with experimental data
  - But data only for 3 temperatures and low amount of points

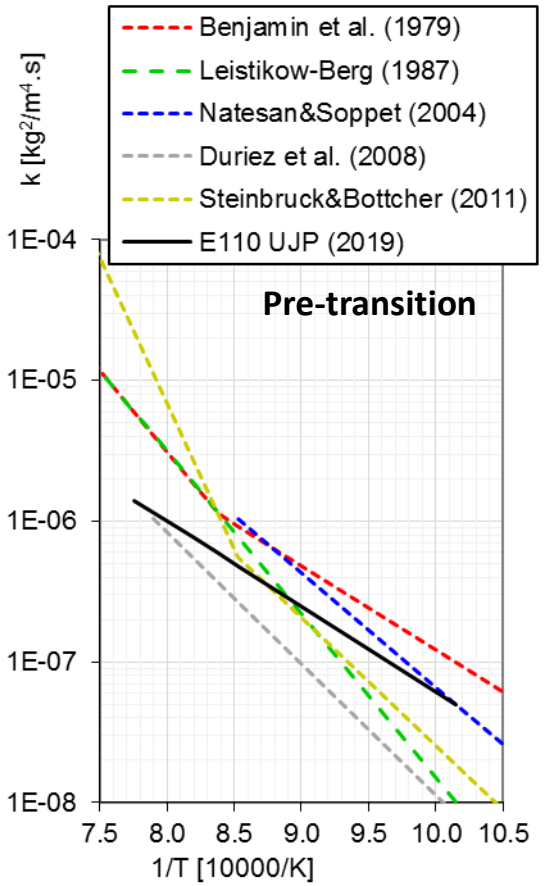


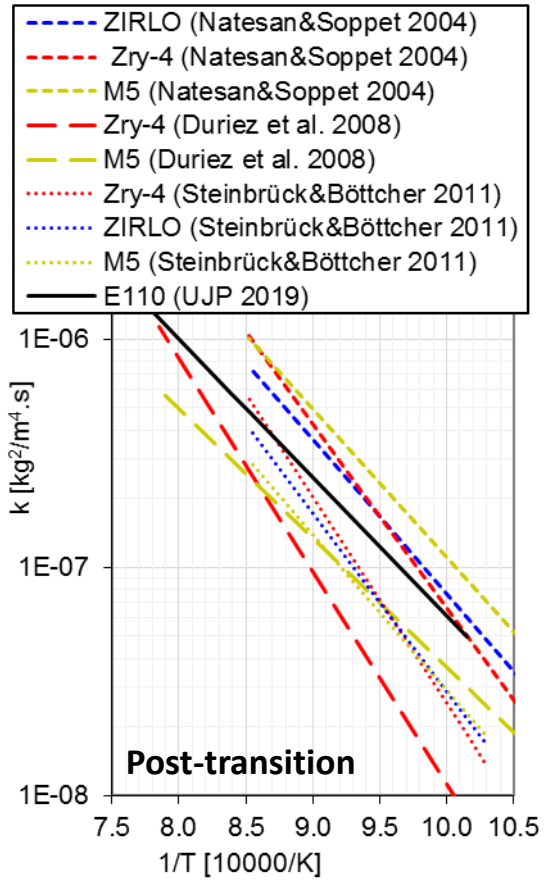




Comparison UJP correlation and others

- Air oxidation
  - Different alloys (Zircaloy-4, ZIRLO, M5)
  - In range of available correlations
  - n = 0.66 for higher temperatures





Conclusions

- Air oxidation correlation for Zr1%Nb alloy proposed
  - Based on Arrhenius equation for Air + argon mixture
  - In temperature range 700 – 1200 °C

$$\frac{dWG^n}{d\tau} = Aexp\left(-\frac{B}{T}\right)$$

Temperature (°C)	Transtion	n (-)	A ($kg^{1/n}/m^{2/n}s$)	B (10^3K)
700-1016	Pre	0.5	0.07	14.0
	Post	1.0	6.0	21.7
1100-1200	-	0.66	0.9	17.5

- Correction factors
  - Critical reagion (significant increase of oxidation rate for temperatures 900 and 950 °C)
  - Pre-oxidation (especially positive influence on transition time)
  - Air-steam ratio (pure air is conservative, more experiments especially in area 900-1000 °C)
  - Flow rate (local and global steam starvation: more experiments need to be done)

$$\frac{dWG^n}{d\tau} = Aexp\left(-\frac{B}{T}\right)\varepsilon_{cr}\varepsilon_{po}\varepsilon_{mix}\varepsilon_{flow}$$

Acknowledgements

The authors thanks to whole UJP-zirconium alloys department (D. Rada, A. Přibyl, J. Šustr, V. Rozkošný, J. Sýkora) and students (G. Bourdon, A. Chalupová, T. Tomaško) for sample preparation, running experiments, and post-experimental evaluation.

Financial support of this research through ČEZ a.s. company is gratefully acknowledged.

Also, this work was supported by the Technology Agency of the Czech Republic grants No. TH02020477, TH02020691, CZ.2.16/3.1.00/21563.

UJP PRAHA

CZECH TECHNICAL UNIVERSITY IN PRAGUE

Thank you for your attention



25. International QUENCH Workshop, 22-24 Oct 2019, KIT, Karlsruhe, Germany

Towards an improved understanding of the mechanisms involved in the increased hydrogen uptake and corrosion at high burnups in zirconium based claddings

Sousan Abolhassani, Adrienn Baris, Robin Grabherr, Jonathan Hawes, Aaron Colldeweih, Radovan Vanta, Renato Restani, Armin Hermann, Johannes Bertsch, Melanie Chollet, Goutam Kuri, Matthias Martin, Stephane Portier, Holger Wiese, Herbert Schweikert, Gerhard Bart, Katja Ammon, Guido Ledergerber, Magnus Limbäck

In contrast to the oxidation at high temperatures, the oxidation of Zr alloys at service temperature is a very slow process and the oxide growth is in the nanometric scale, in the time frame of interest for this Workshop. However, long term residence times in reactor modifies the material's microstructure and microchemistry and the oxidation and hydrogen uptake of the cladding are influenced by these changes.

In this study, the changes occurring in some Zr alloys are examined by means of different characterisation techniques, and not only the chemical composition of the cladding, but also the microporosity of the oxide is analyzed and related to the hydrides in the vicinity of the metal-oxide interface. Furthermore, the micro-mechanical and semi-conducting properties of the metal and oxide near the interface are examined for two different residence times, for the same cladding grade.

The results show that changes occurring in the material in reactor, gradually modify the nature of the cladding and they will influence its oxidation and hydrogen uptake rate. It can be demonstrated that claddings with an oxide layer showing less micro-porosity, higher conductivity and better mechanical properties in the vicinity of the metal-oxide interface, show lower hydrogen uptake and hydrogen pickup fraction.


ologie
TOSHIBA

PAUL SCHERRER INSTITUT

PSI



Sousan Abolhassani:: Senior Scientist :: Paul Scherrer Institut

Towards an improved understanding of the mechanisms involved in the increased hydrogen uptake and corrosion at high burnups in zirconium based claddings

25th Quench Workshop, Karlsruhe, 24th October 2019

PAUL SCHERRER INSTITUT

PSI



Sousan Abolhassani1, Adrienn Baris1, Robin Grabherr1, Jonathan Hawes1, Aaron Colldeweih1, Radovan Vanta1, Renato Restani1, Armin Hermann1, Johannes Bertsch1, Melanie Chollet1, Goutam Kuri1, Matthias Martin1, Stephane Portier1, Holger Wiese1, Herbert Schweikert1, Gerhard Bart1, Katja Ammon2, Guido Ledergerber2, Magnus Limbäck3

1Laboratory for Nuclear Materials, Nuclear Fuels Group, NES, and AHL, NES, Paul Scherrer Institut, 5232 Villigen PSI, Switzerland.
2Kernkraftwerk Leibstadt AG, CH-5325 Leibstadt, Switzerland,
3 Westinghouse Electric Sweden AB, SE-72163 Västerås, Sweden.

The aim of the project

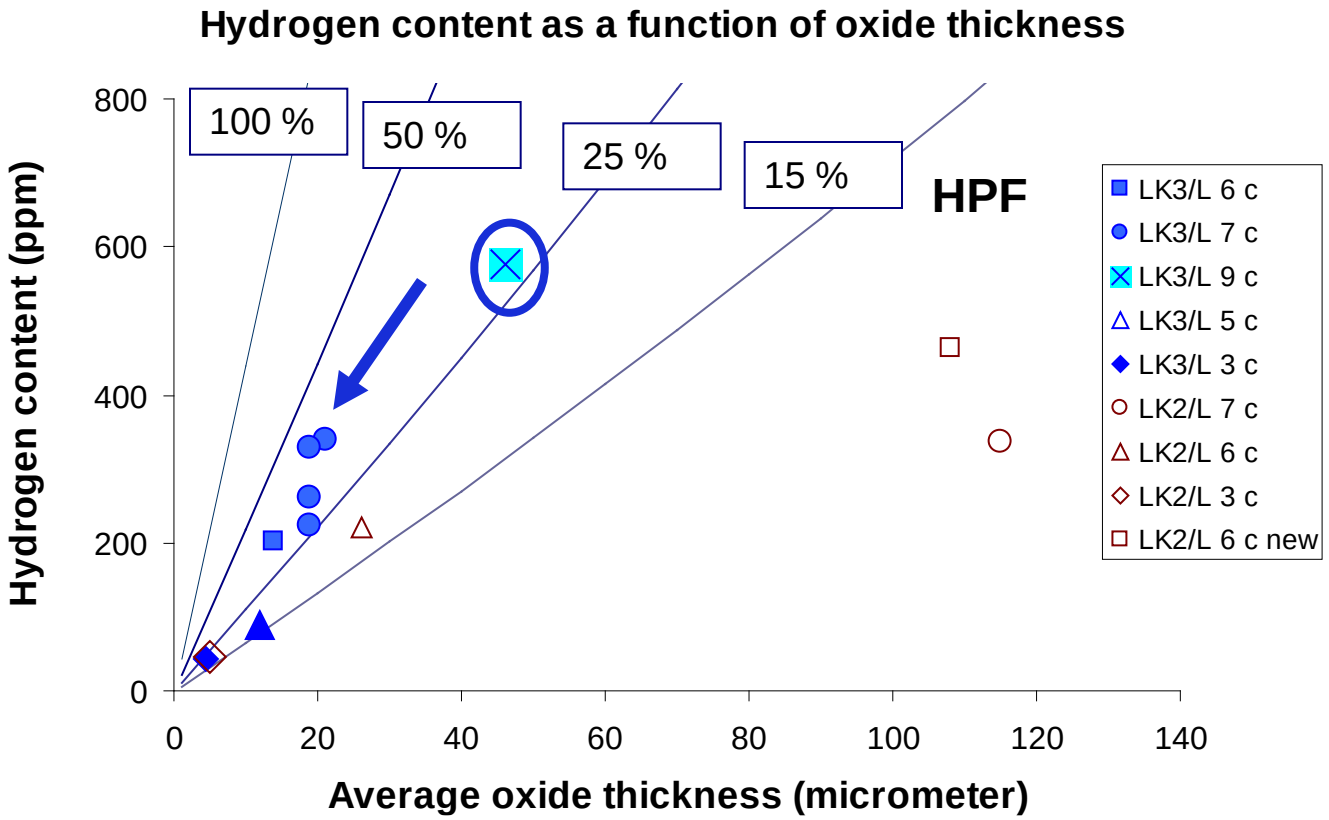
- To search for the causes of increased H Uptake at high burnups
- A Strategy selected:
  - Step 1: To study a very high burnup cladding (here a 9-cycle BWR) and look at the hints pointing to changes in characteristics.
  - Step-2: Then extrapolate the changes to lower burnup examples of the same cladding grade under very similar conditions
  - Step-3: Determine the indicators
  - Step-4: Check if they are valid in other alloys or other reactors
- Evaluate which regime is acting at which stage?

Hydrogen Uptake Project

- The objective of the project is to examine the role of alloy composition, residence time and burnup on the extent of hydrogen uptake and the mechanisms involved.
- To compare the hydrogen uptake phenomena in BWR and in PWR type of reactors.
- The aim is to understand why certain alloys have a much better performance even to high burnups.

Parameters influencing hydrogen distribution

Correlation between oxidation and hydrogen content (example of a BWR)



Different alloys (LK3/L and LK2/L cladding) behave differently. For identical elevation hydrogen uptake increases with the burnup, the hydrogen pickup fraction (HPF) is not constant and it increases with the high burnup in one alloy and decreases in a second alloy. Data in graph is for mid-span peak burn-up elevation, approx. 2000 mm.

[Abolhassani et al. ASTM 17th, 2013].

PAUL SCHERRER INSTITUT

Outline

- i. Study of the 9-cycle Zircaloy-2, LK3/L from KKL (BWR) cladding to look for great changes
- ii. Comparison with a low burnup (here 3-cycle) and an intermediate burnup (here 6-cycle) cladding from the same grade material and the same reactor; to verify the validity of indicators
- iii. Examination of mechanical and semi-conducting properties of the oxide layers in the case of the two extreme cases
- iv. Verification of PWR material to search for general phenomena
- v. The use of the data to define the determinant indicators
- vi. Correlation with the known parameters
- vii. Conclusion

Materials selected for the current study

Comp. Specimen	Sn	Fe	Cr	Ni	Nb	Fe+Cr(+Ni)	C ppm	O ppm	Si ppm	H.T.
LK3/L (Zircaloy-2)* wt%	1.34	0.18	0.11	0.05		0.34	-	1320	70	logA* -14.2
LK3/L (Zircaloy-2) at%	1.02	0.29	0.19	0.077		0.557				
Low-tin Zircaloy-4 wt%	1.20	0.22	0.107	-	-	0.337	140	1730	-	504°C SRA
Low-tin Zircaloy-4 at%	0.914	0.356	0.186	-	-	0.542				
Zr-2.5%Nb wt%	-	0.07	-	-	2.5	-	180	1170	60	500°C PRX
Zr-2.5%Nb at%										

The chemical composition of alloys used for the current study, (H.T.: heat treatment, SRA: stress relieve annealed, and PRX: partially recrystallized condition) [13], [17] and [19]

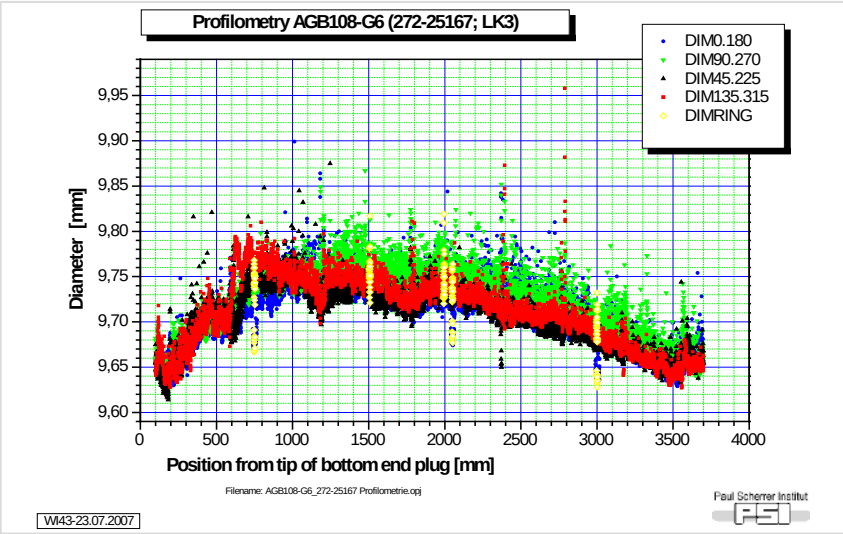
Outline

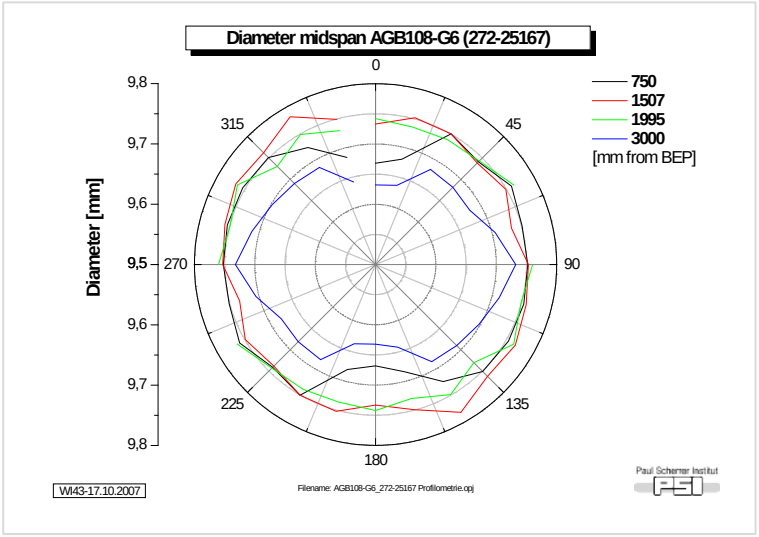
- i. Study of the 9-cycle Zircaloy-2, LK3/L from KKL (BWR) cladding to look for great changes
- ii. Comparison with a low burnup (here 3-cycle) and an intermediate burnup (here 6-cycle) cladding from the same grade material and the same reactor; to verify the validity of indicators
- iii. Examination of mechanical and semi-conducting properties of the oxide layers in the case of the two extreme cases
- iv. Verification of PWR material to search for general phenomena
- v. The use of the data to define the determinant indicators
- vi. Correlation with the known parameters
- vii. Conclusion

Step 1

- i. Study a very high burnup cladding to look for great changes (in this case a Zirc-2 with LK3/L grade from KKL after 9 cycles)
  - a- Observation of macroscopic changes in the cladding from PIE: NDT and DT
  - b- Observation of microscopic changes in the cladding: from EPMA, TEM, 3D FIB, micropillar compression test, etc.

a- Observation of macroscopic changes in the cladding from PIE: NDT and DT

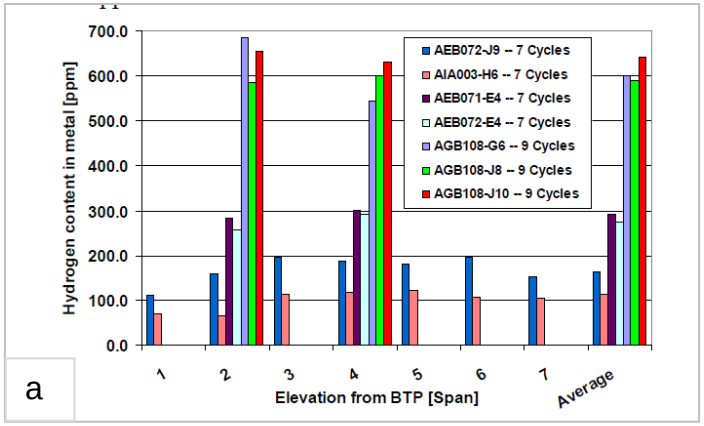




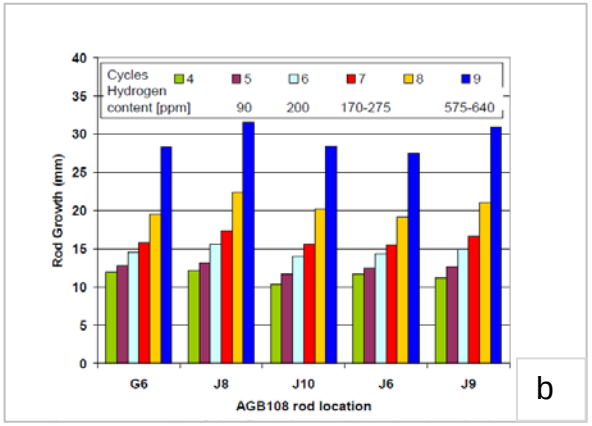
Results of profilometry of rod AGB108-G6 diameter plot at different orientations: 0°, 45°, 90°, 135° (corrected for comparison with other data)

Azimuthal plot of rod diameter at different elevations.

a- Observation of macroscopic changes in the cladding from PIE: NDT and DT



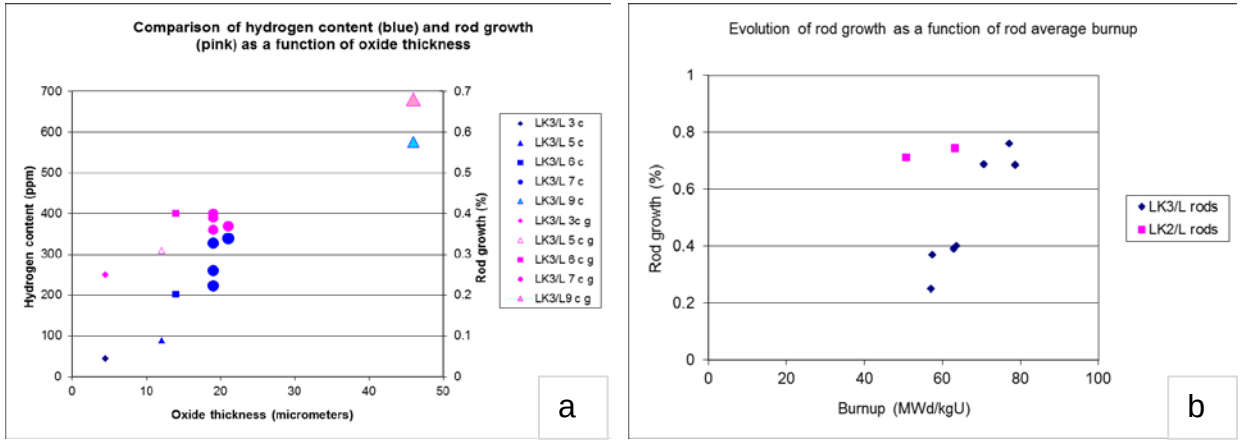
a



b

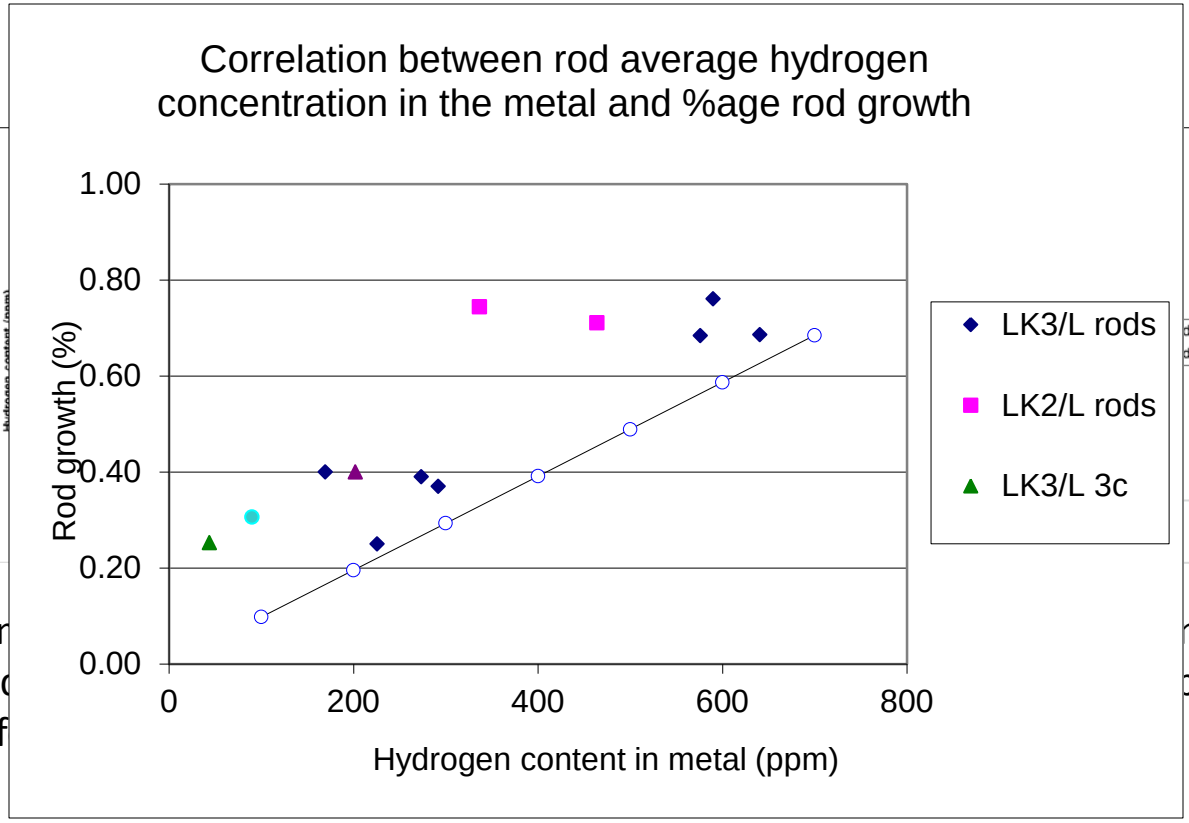
Comparison of hydrogen content (DT) at different elevations (a) and rod growth (b) from pool side NDT investigations; for LK3/L cladding grade and as a function of number of cycles. As can be observed, the 9 cycle rod shows a rapid rod growth.

a- Observation of macroscopic changes in the cladding from PIE: NDT and DT



Comparison of hydrogen content (DT) and rod growth (NDT), (a) as a function of oxide thickness, for LK3/L cladding grade and (b) as a function of burnup for two different cladding grades

a- Observation of macroscopic changes in the cladding from PIE: NDT and DT

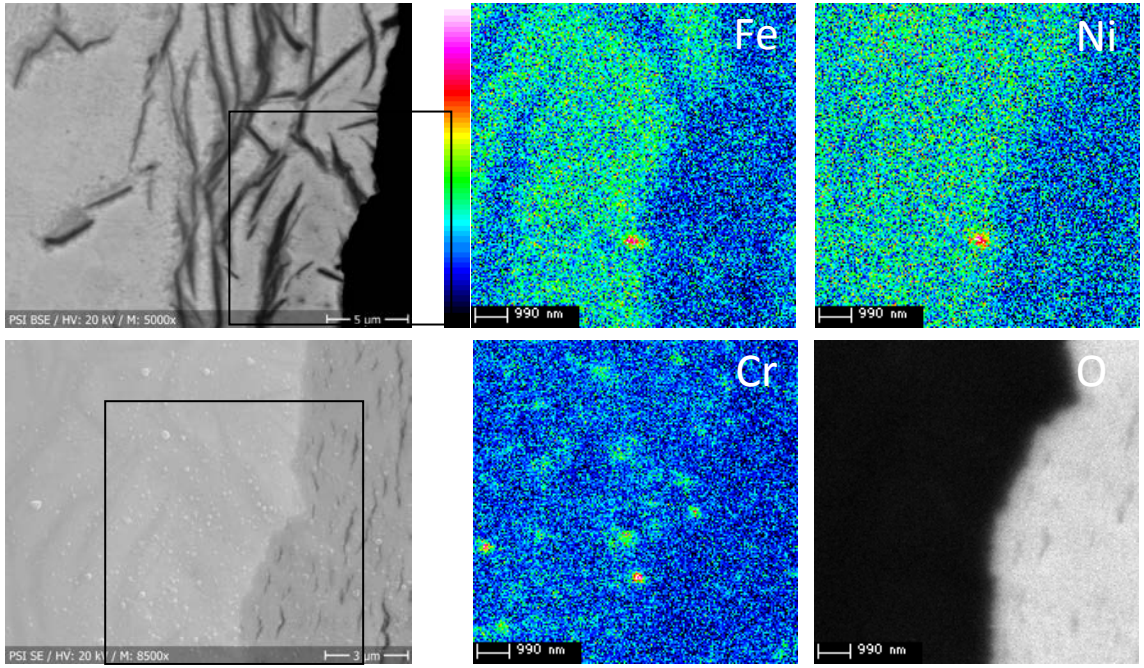


Cor nction of
oxi for two
diff

Step 1

- i. Study a very high burnup cladding to look for great changes (in this case a Zirc-2 with LK3/L grade from KKL after 9 cycles)
  - a- Observation of macroscopic changes in the cladding from PIE: NDT and DT
  - b- Observation of microscopic changes in the cladding: from EPMA, TEM, 3D FIB, micropillar compression test, etc.

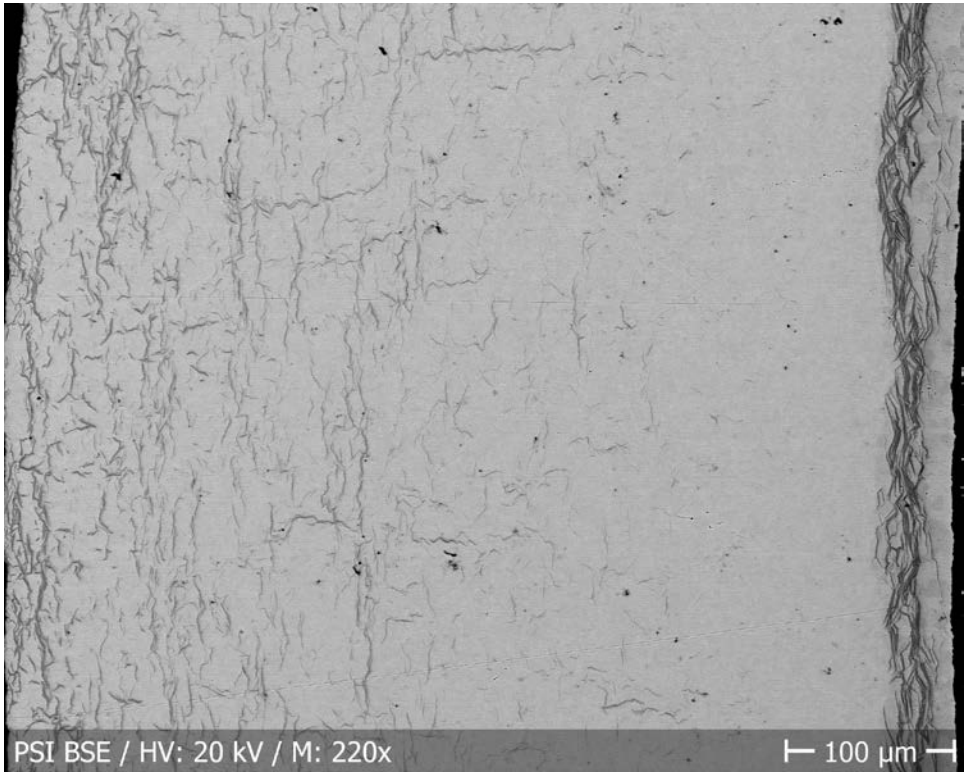
b- Observation of microscopic changes in the cladding: from EPMA, TEM, 3D FIB...



AGB108-G6-GF: SEM, BSE and EPMA distribution mappings of Cladding at the Metal/Oxide interface; at orientation of (200^0). HV 15kV, 200nA, 120 ms/pix (192 x 192 pix.) Large hydrides in the metal side, depleted from Fe and to some extent Ni.

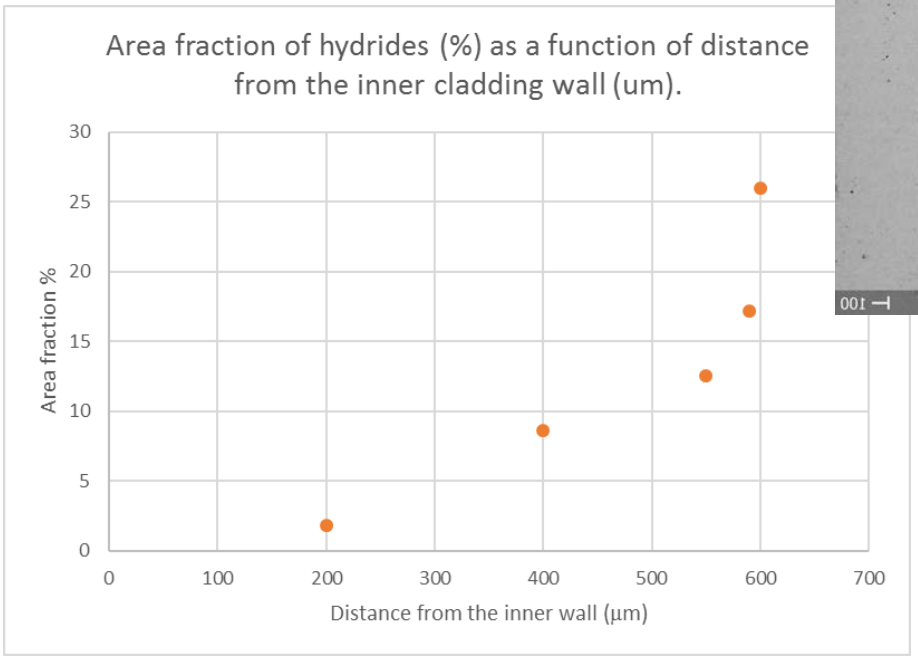
A. Baris et al. "Chemical and microstructural characterization of a 9 cycle Zircaloy-2 cladding using EPMA and FIB tomography"; Journal of Nuclear Materials, 2018, 504, pp. 144-160.

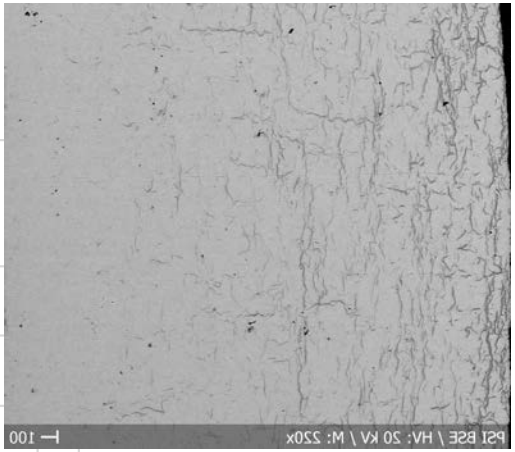
b- Observation of microscopic changes in the cladding: from EPMA, TEM, 3D FIB, micropillar compression test, …



Distribution of hydride precipitates, in the 9-cycle LK3/L observed in the EPMA, with no etching. Hydrides are distributed unevenly and the waterside rim has a higher density of hydrides.

b- Observation of microscopic changes in the cladding: from EPMA, TEM, 3D FIB, micropillar compression test, …





Area fraction of hydrides along the 9-cycle LK3/L cladding wall from inner to the outer surface of the tube. The hydride present in the liner is not taken into consideration in this graph.

b- Observation of microscopic changes in the cladding: from EPMA, TEM, 3D FIB ...

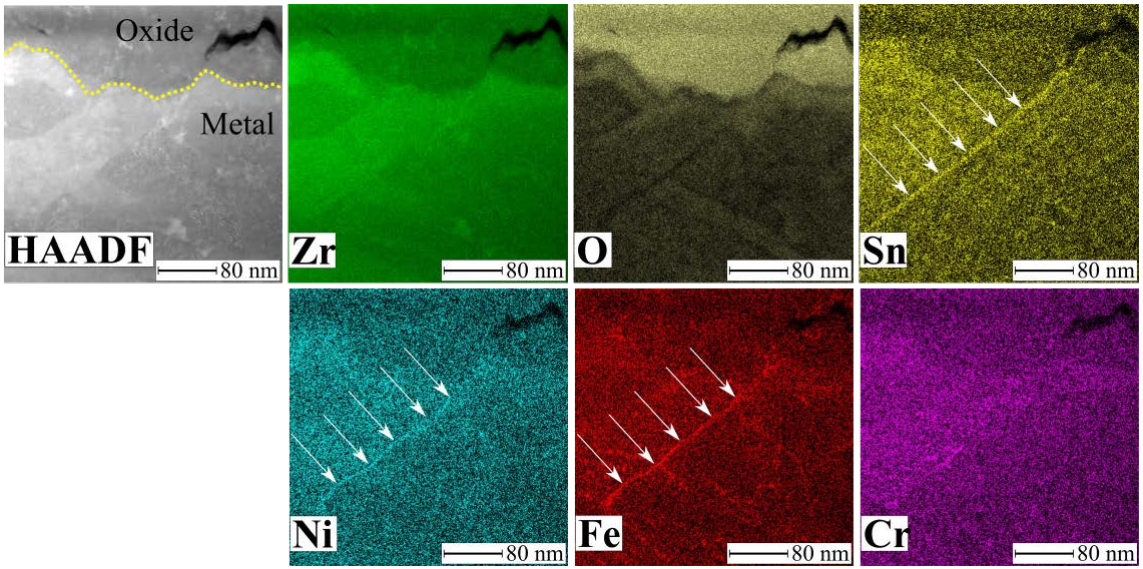
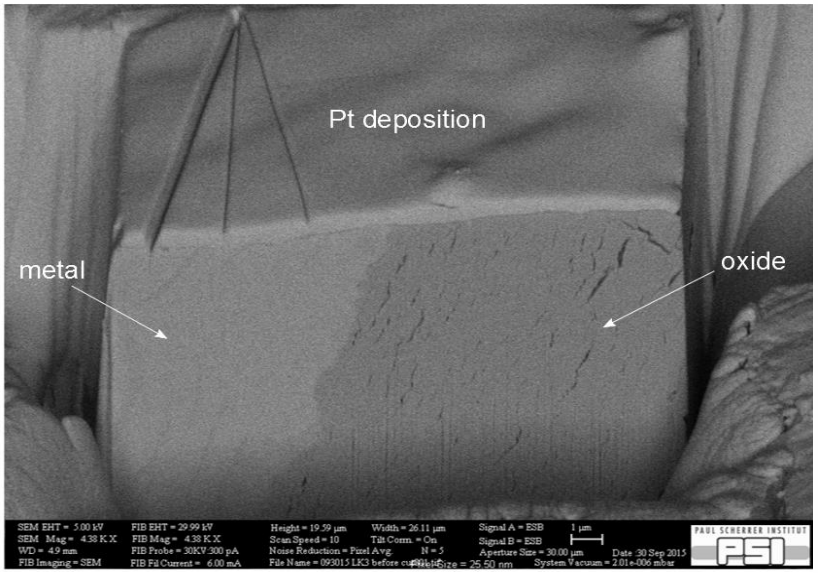
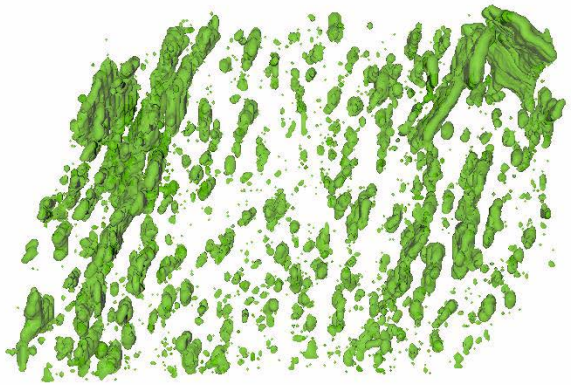


Fig. 5: HAADF and Chemi-STEM maps of 9-cycle LK3/L showing the grain boundary segregation in the metal side of the interface [19].

A. Baris et al. «Causes of increased corrosion and hydrogen uptake of Zircaloy-2 cladding at high burnups – A comparative study of the chemical composition of a 3 cycle and a 9 cycle cladding»; Proceedings of the TopFuel Conference, 2018.

3D imaging of the FIB cut layers (example of the metal-oxide region in the cladding)

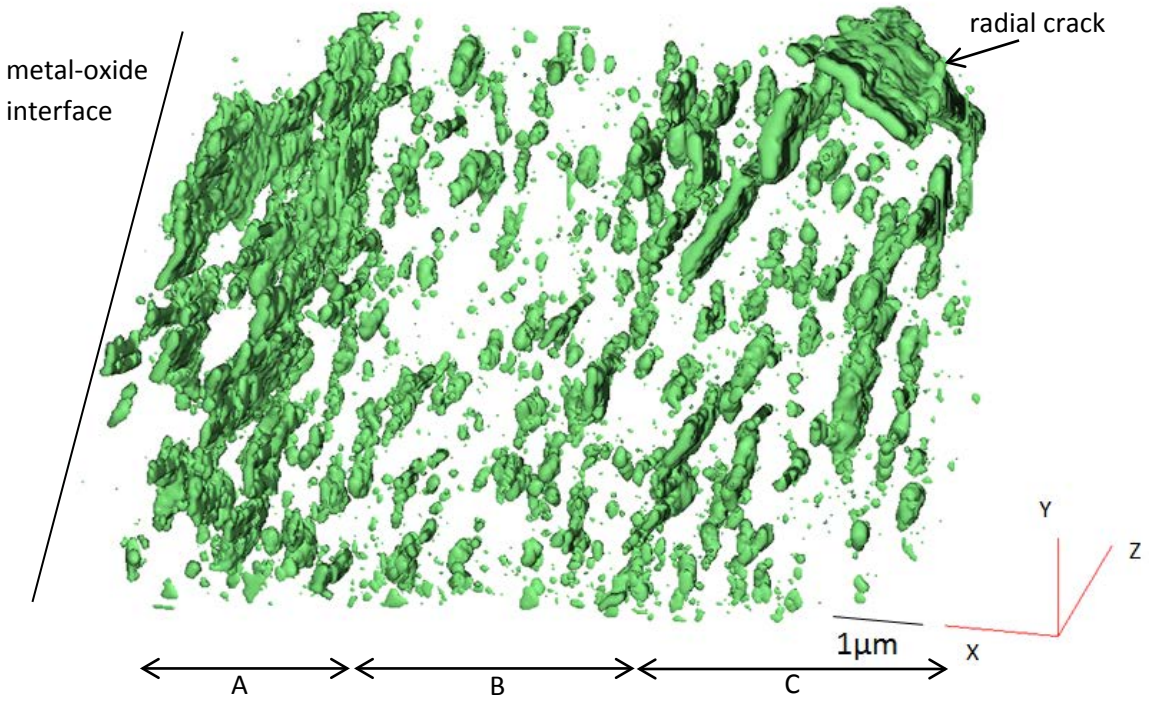




Example of a FIB segment cut into the Metal-oxide interface of the fuel from a 9 cycle cladding and prepared for 3D reconstruction. The pores and cracks in the oxide are reconstructed (right).

A. Baris et al. "Chemical and microstructural characterization of a 9 cycle Zircaloy-2 cladding using EPMA and FIB tomography"; Journal of Nuclear Materials, 2018, 504, pp. 144-160.

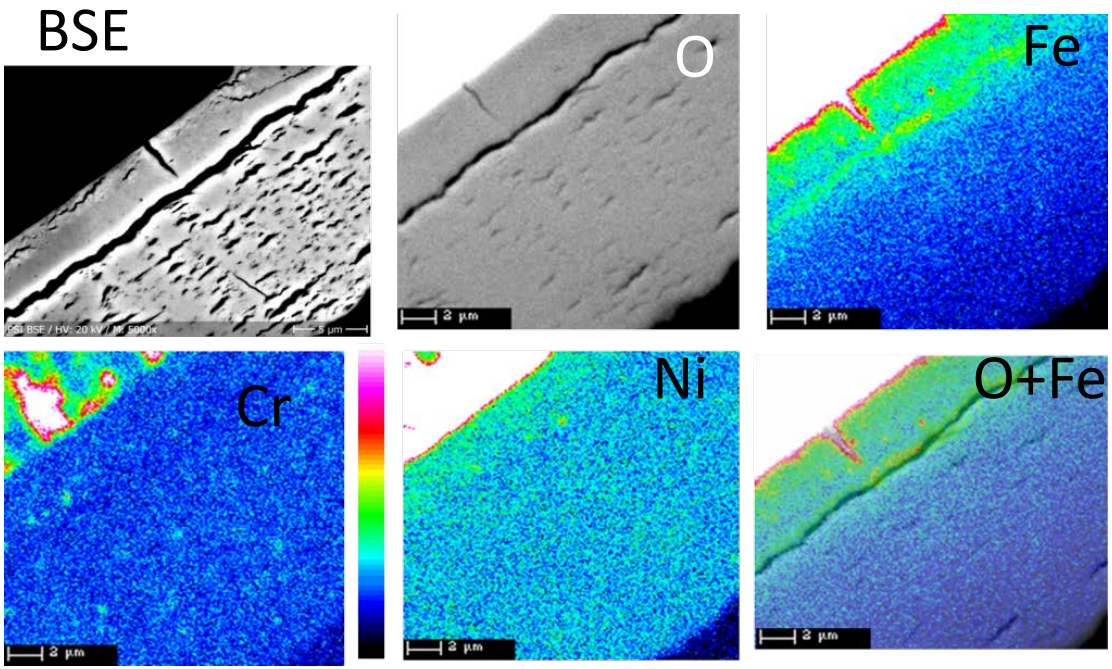
3D imaging of the FIB cut layers (example of the metal-oxide region in the cladding)



Cracks of the oxide formed in the last cycle, i.e. close to the metal-oxide interface. A, B and C indicates the possible subdivision of the cracks.

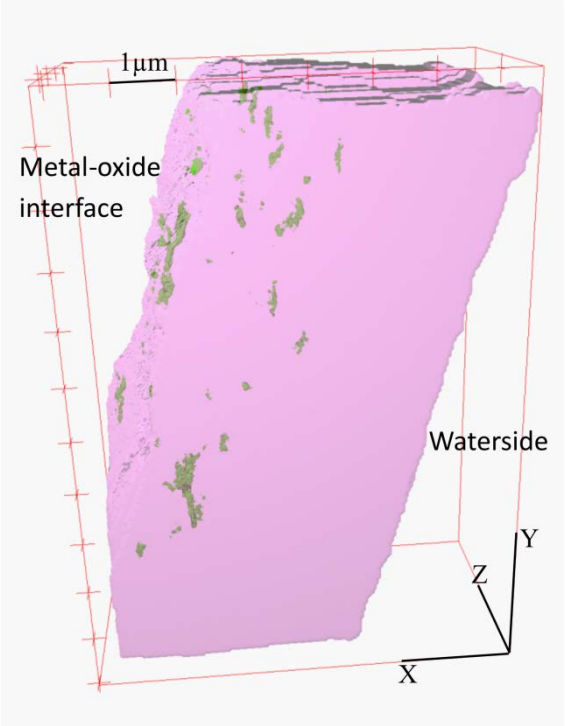
A. Baris et al. "Chemical and microstructural characterization of a 9 cycle Zircaloy-2 cladding using EPMA and FIB tomography"; Journal of Nuclear Materials, 2018, 504, pp. 144-160.

EPMA map of the outer oxide of the 9 cycle LK3/L cladding



AGB108-G6-GF: SEM, BSE and EPMA distribution mappings of Cladding at the water side oxide. HV 15kV, 200nA, 120 ms/pix (192 x 192 pix.)

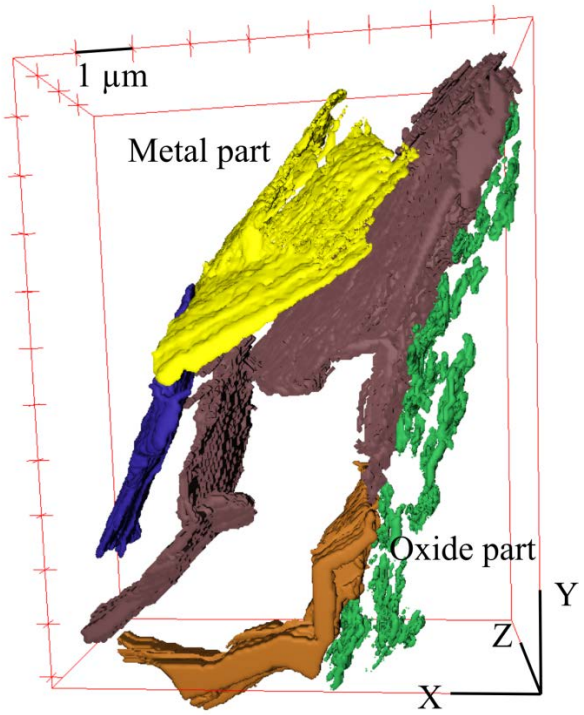
3D imaging of the FIB cut layers (example of the metal-oxide region in the cladding)



3D reconstruction of the waterside oxide of the 9 cycle sample from the waterside oxide.
Green objects: cracks, transparent pink object: oxide matrix.

A. Baris et al. "Chemical and microstructural characterization of a 9 cycle Zircaloy-2 cladding using EPMA and FIB tomography"; Journal of Nuclear Materials, 2018, 504, pp. 144-160.

3D imaging of the FIB cut layers (example of the metal-oxide region in the cladding)



The 3D reconstruction of the metal-oxide interface of the 9 cycle material. Green objects: cracks in the oxide. Hydrides in the metal are shown in different colours.

A. Baris et al. "Chemical and microstructural characterization of a 9 cycle Zircaloy-2 cladding using EPMA and FIB tomography"; Journal of Nuclear Materials, 2018, 504, pp. 144-160.

PAUL SCHERRER INSTITUT

Outline

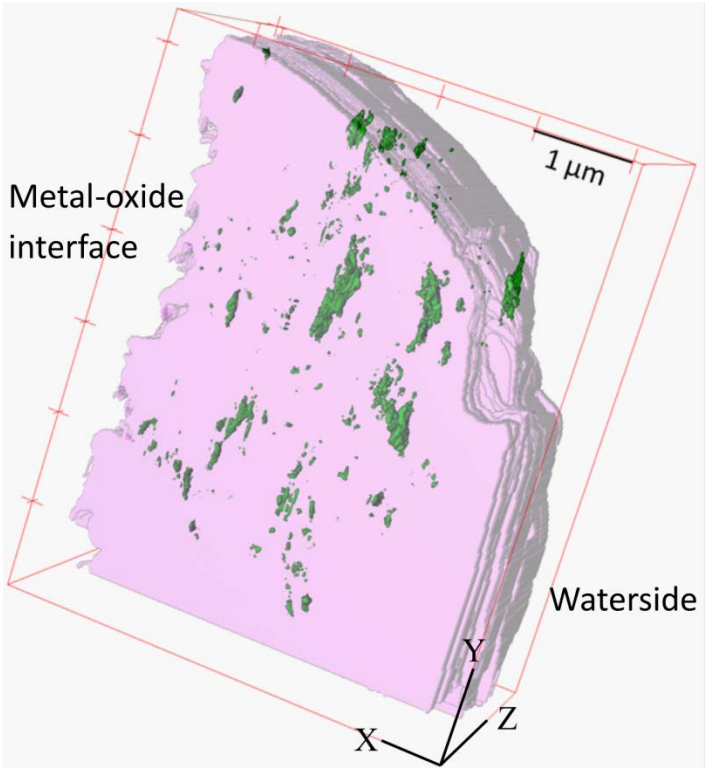
- i. Study of the 9-cycle Zircaloy-2, LK3/L from KKL (BWR) cladding to look for great changes
- ii. Comparison with a low burnup (here 3-cycle) and an intermediate burnup (here 6-cycle) cladding from the same grade material and the same reactor; to verify the validity of indicators
- iii. Examination of mechanical and semi-conducting properties of the oxide layers in the case of the two extreme cases
- iv. Verification of PWR material to search for general phenomena
- v. The use of the data to define the determinant indicators
- vi. Correlation with the known parameters
- vii. Conclusion

PAUL SCHERRER INSTITUT

Step 2

- Step-2: Then extrapolate the changes to lower burnup examples of the same cladding grade under very similar conditions
  - Will only report the recent destructive results:
  - Observation of microscopic changes in the cladding: from EPMA, TEM, 3D FIB, micropillar compression test, etc.

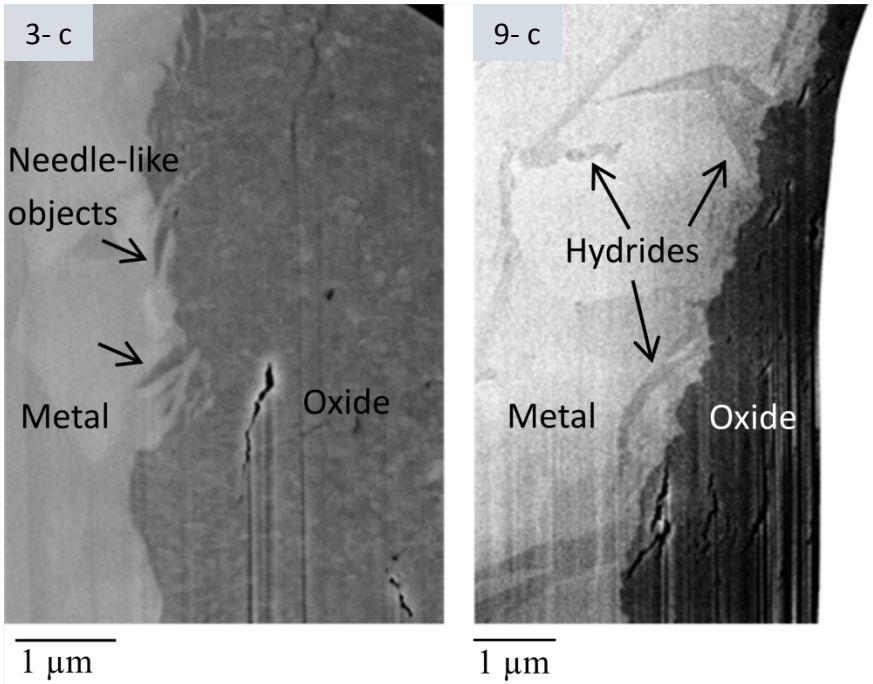
3D imaging of the FIB cut layers (example of the metal-oxide region in the cladding)... Comparison with lower burnup materials



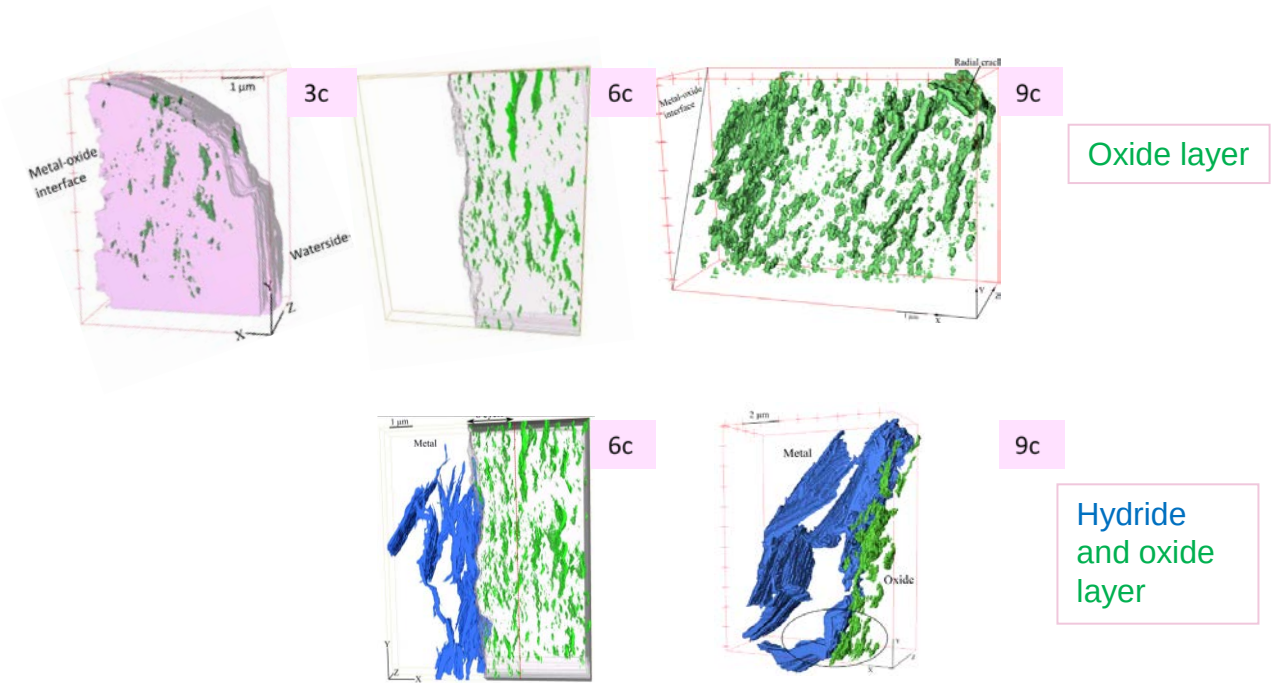
3D reconstruction of the oxide of the 3-cycle sample. Green objects: cracks, transparent pink object: oxide matrix.

A. Baris et al. "Chemical and microstructural characterization of a 9 cycle Zircaloy-2 cladding using EPMA and FIB tomography"; Journal of Nuclear Materials, 2018, 504, pp. 144-160.

3D imaging of the FIB cut layers (example of the metal-oxide region in the cladding)... Comparison with lower burnup materials

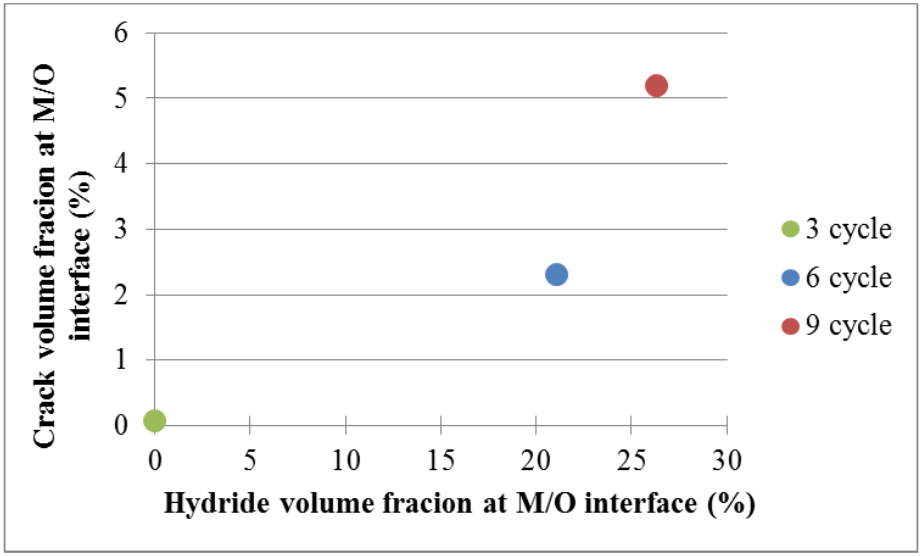


b- 3D- Distribution of hydrides in the metal and the microcracks in the oxide … Comparison with lower burnup materials



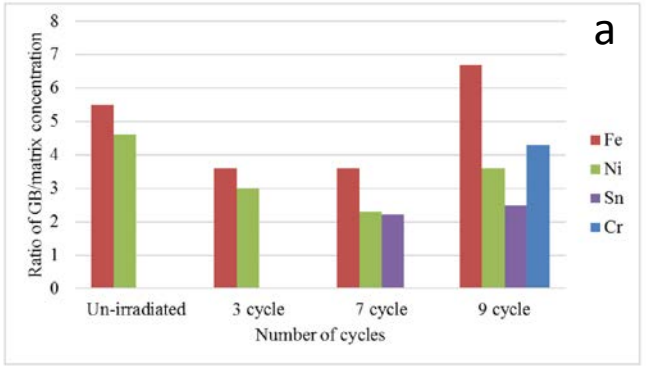
Microcrack distribution in the oxide (upper tomograms) as a function of number of cycles in the reactor, and the distribution of hydrides in the metal side of the interface (lower tomogram) indicating the large hydride objects.

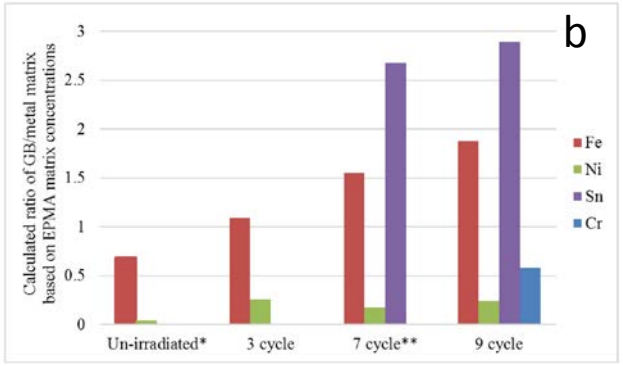
b- 3D- Distribution of hydrides in the metal and the microcracks in the oxide ... Comparison with lower burnup materials; Quantification of volume fractions



The correlation of volume fraction of hydrides, as a function of volume fraction of micropores in the oxide, at 1 micrometer on the two sides of the metal-oxide interface [30].

b- Observation of microscopic changes in the cladding: from EPMA, TEM, 3D FIB, micropillar compression test, … Comparison with lower burnup materials





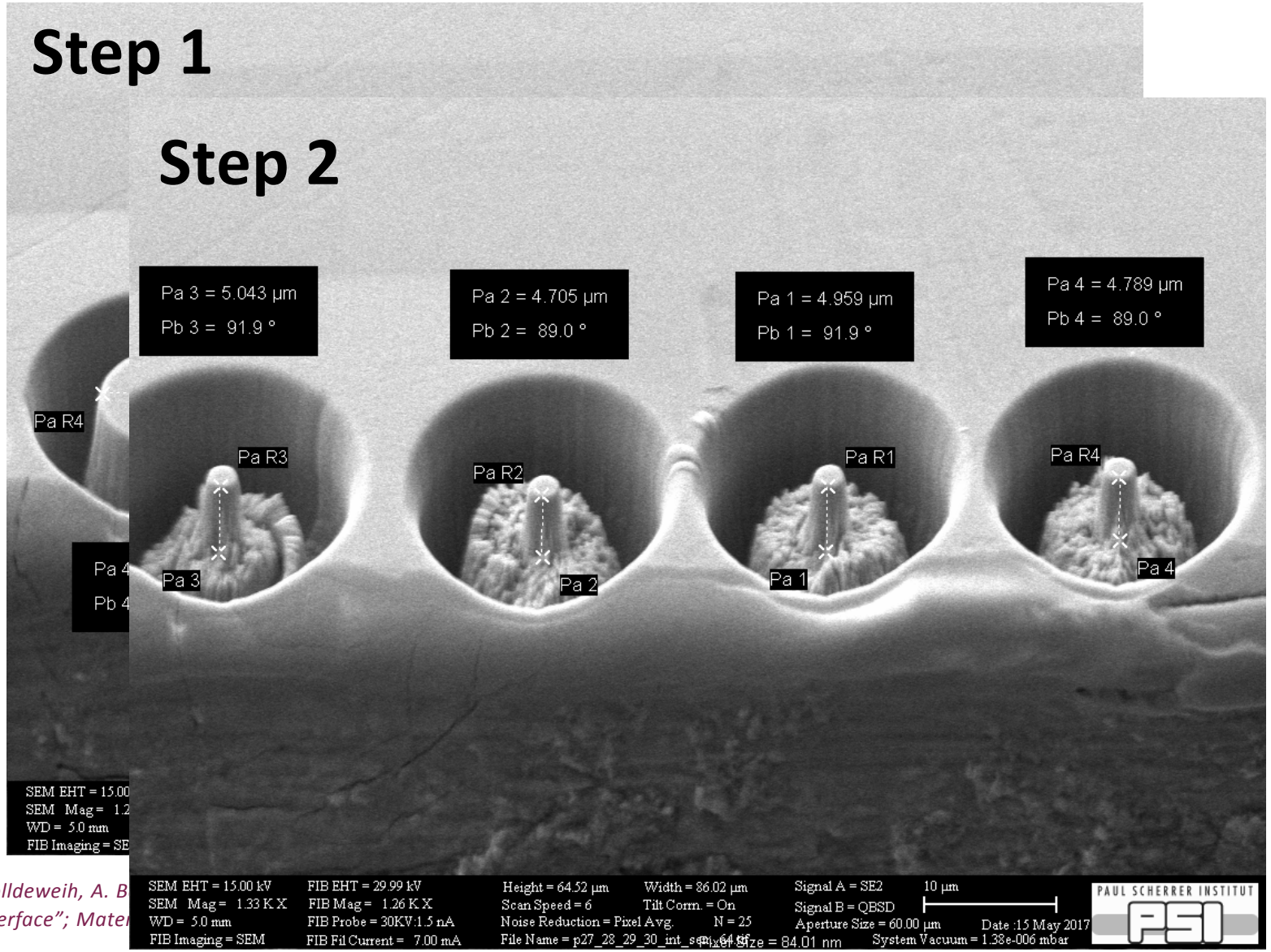
(a) grain boundary segregation as a function of number of cycles represented as the ratio of alloying element in the GB with respect to the matrix. Cr segregation was observed only at limited sites of the GB after 9 cycles.(b) Data from Fig. (a) normalized using the matrix concentrations in EPMA. [30].

PAUL SCHERRER INSTITUT

Outline

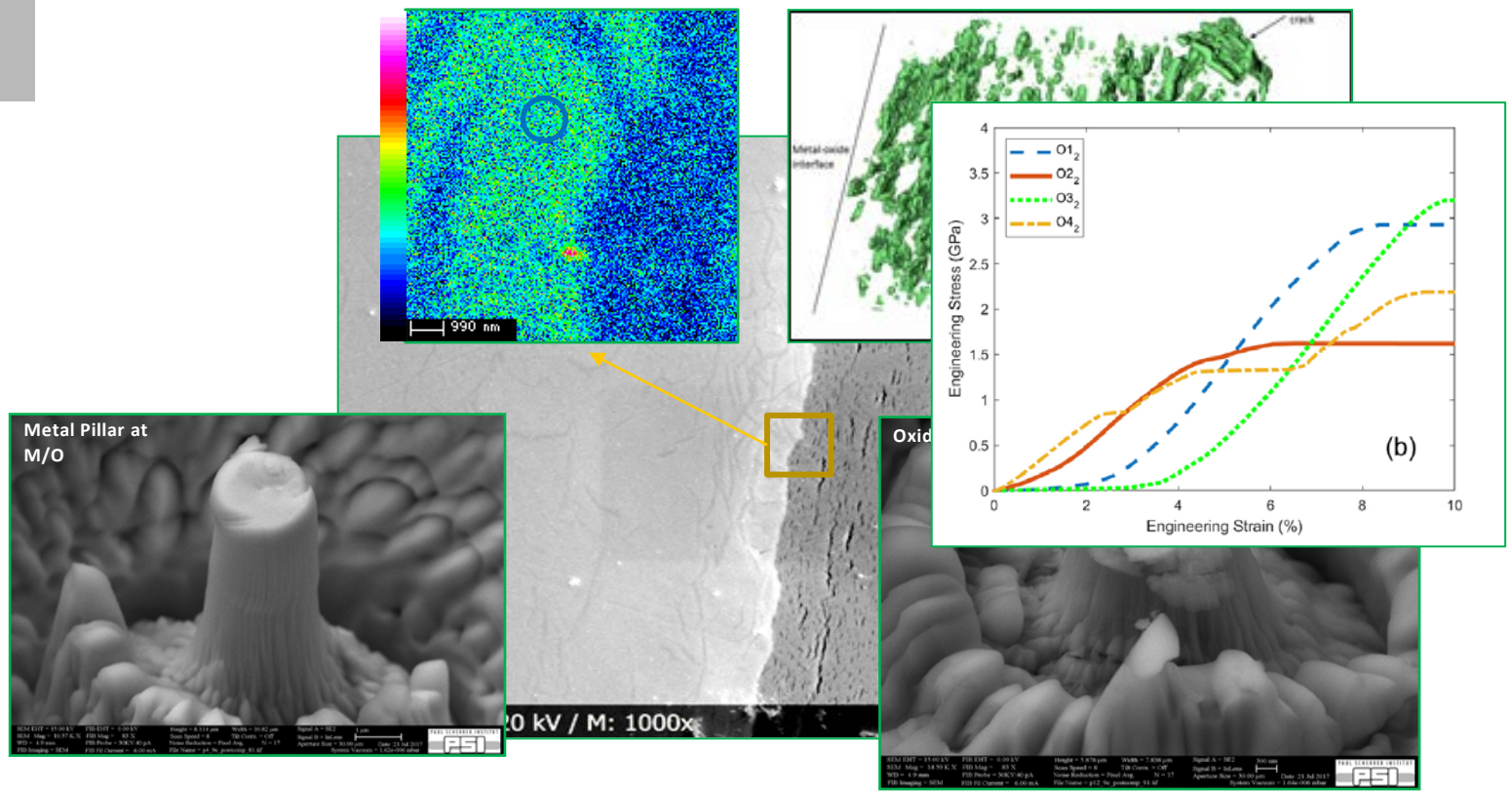
- i. Study of the 9-cycle Zircaloy-2, LK3/L from KKL (BWR) cladding to look for great changes
- ii. Comparison with a low burnup (here 3-cycle) and an intermediate burnup (here 6-cycle) cladding from the same grade material and the same reactor; to verify the validity of indicators
- iii. Examination of mechanical and semi-conducting properties of the oxide layers in the case of the two extreme cases
- iv. Verification of PWR material to search for general phenomena
- v. The use of the data to define the determinant indicators
- vi. Correlation with the known parameters
- vii. Conclusion

I. Examination of Mechanical properties: Micropillar Fabrication by FIB



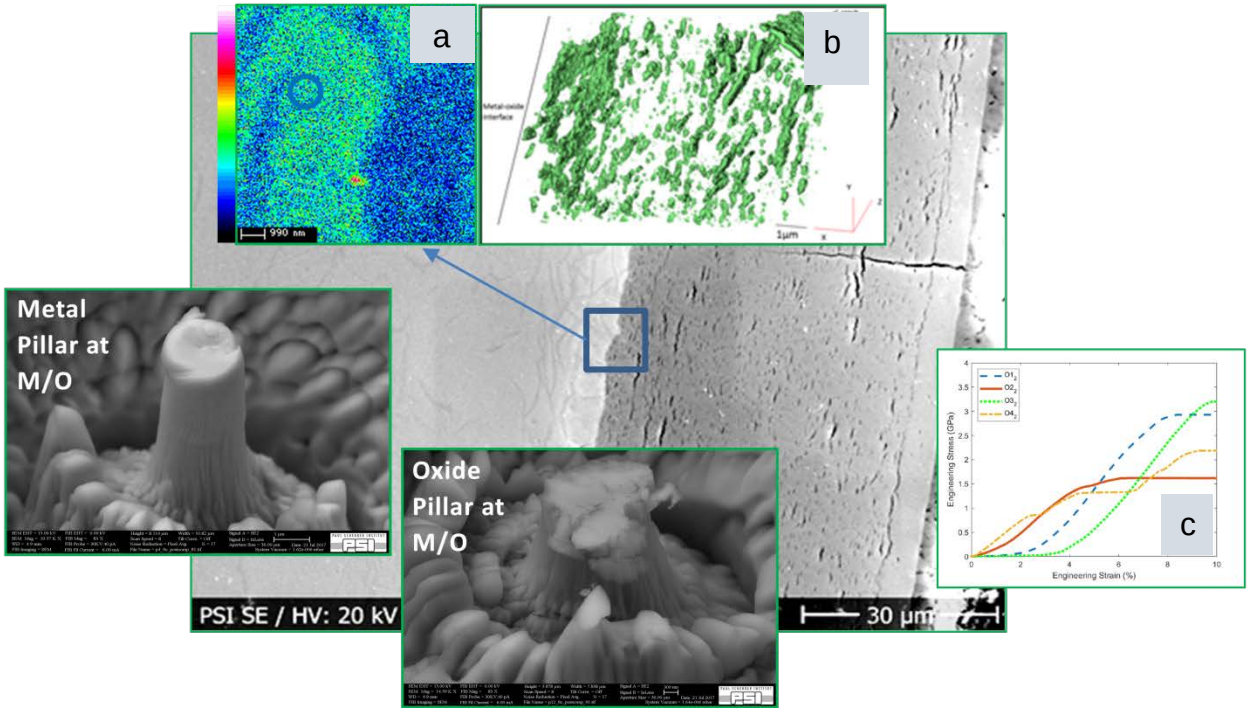
[A. W. Colldeweih, A. B
oxide Interface"; Mater

I. Examination of Mechanical properties: Micro-compression results



Example of 9-cycle cladding

I. Examination of Mechanical properties: Micro-compression results 9-cycle LK3/L



Presentation of the micropillar experiment: approximate sizes of regions examined; examples of a metal and an oxide micropillars, for the 9-cycle LK3/L cladding. The EPMA map of Fe of the square indicated in the bulk sample is shown in the inset (a), together with the microcrack structure (b) to describe the nature of the metal and the oxide being examined in this material. The ring depicted in the map of Fe shows schematically the relative size of the regions analyzed by the micro-pillars. The stress-strain curve in the inset indicates the behavior of oxide in the same material (c).

I. Examination of Mechanical properties: Micro-compression results

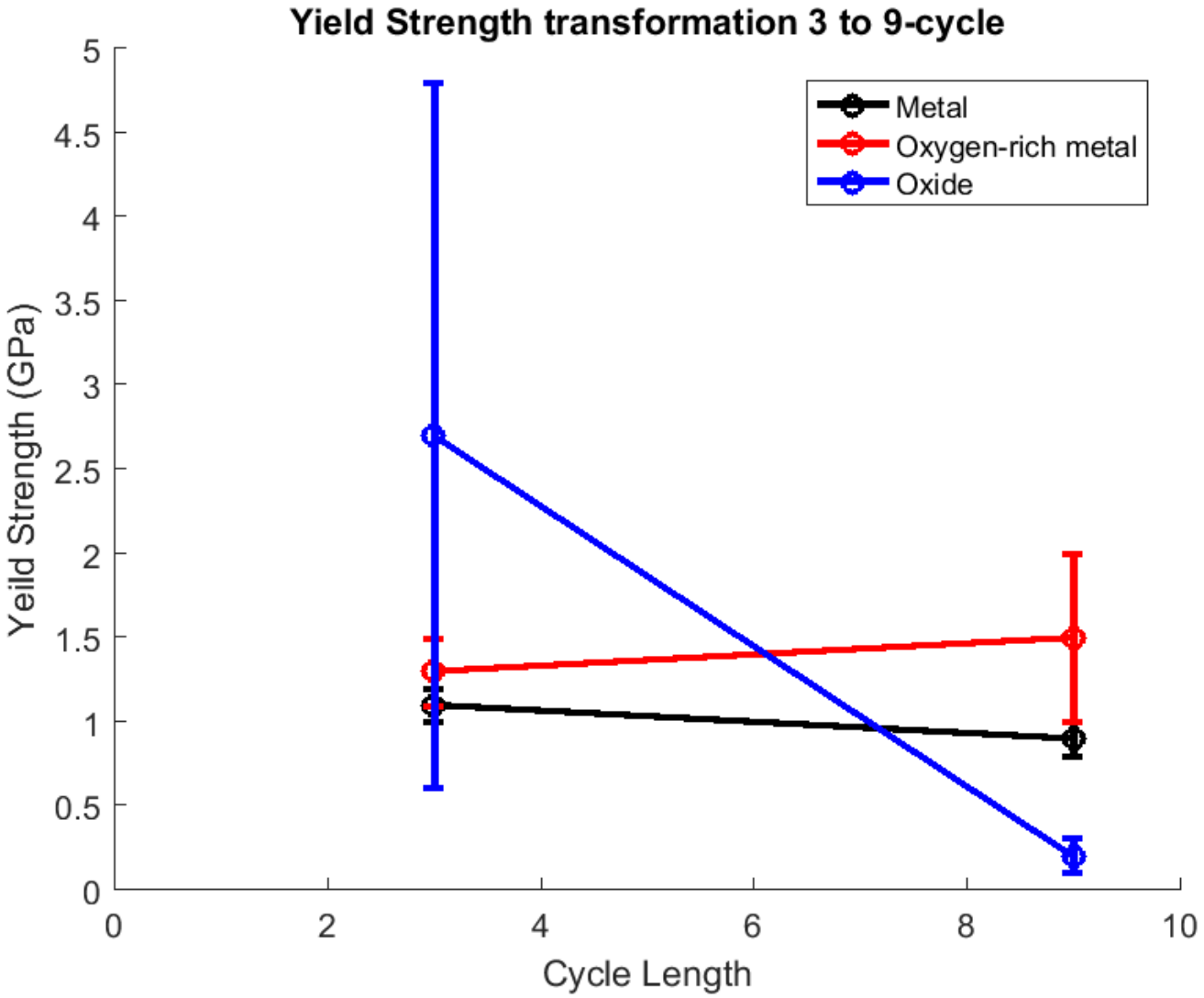
Material	Metal- E (GPa)	Metal- YS (GPa)	Metal strain (Y) YS/E	Oxygen rich region- E (GPa)	Oxygen rich region- YS (GPa)	Oxygen rich region- strain (Y) YS/E	Oxide- E (GPa)	Oxide- YS (GPa)	Oxide Strain (Y) YS/E
3-cycle	62.3	1.1	0.018	39	1.3	0.033	26-106	1 - 5.1	0.076
9-cycle	39.5	0.9	0.023	36.5	1.5	0.041	23 - 60	0.1 - 3.2	0.026
Fuel Cladding unirr [Yagnik]	95-103	0.6		-	-				
Fuel cladding irr [Yagnik]	-	0.8		-	-				
Oxide bulk [refxx]							190-200		
Oxide bulk [refyy]							100-250	0.12-0.78 /(1.2-5)*	

*The values between parentheses show the compressive strength for comparison

Mechanical properties of micro-pillars at Metal-Oxide interface. LK3/L 3-cycle and 9-cycle claddings. Previous measurements from the literature or the general information about zirconia provided for comparison.

I. Examination of Mechanical properties: Micro-compression results

Comparison of yield strength 3 and 9-cycle LK3/L

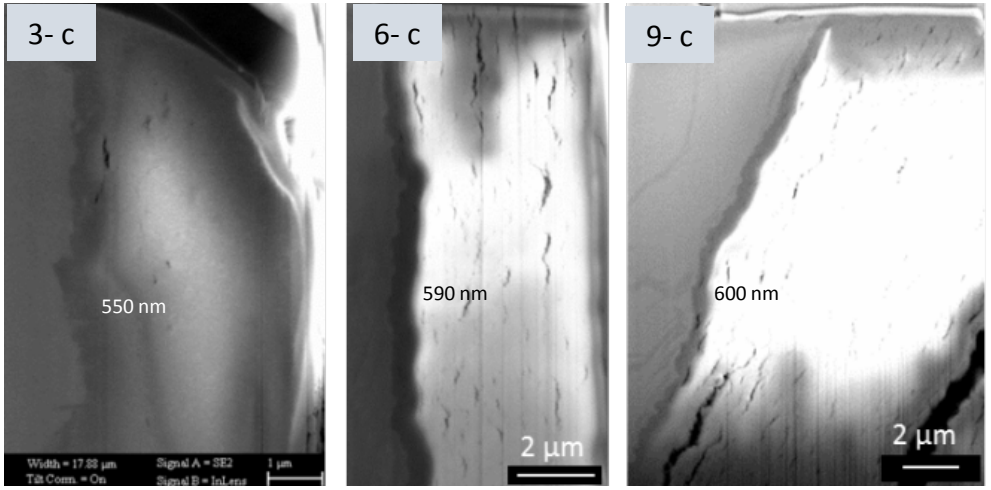


PAUL SCHERRER INSTITUT

Outline

- i. Study of the 9-cycle Zircaloy-2, LK3/L from KKL (BWR) cladding to look for great changes
- ii. Comparison with a low burnup (here 3-cycle) and an intermediate burnup (here 6-cycle) cladding from the same grade material and the same reactor; to verify the validity of indicators
- iii. Examination of mechanical and semi-conducting properties of the oxide layers in the case of the two extreme cases
- iv. Verification of PWR material to search for general phenomena
- v. The use of the data to define the determinant indicators
- vi. Correlation with the known parameters
- vii. Conclusion

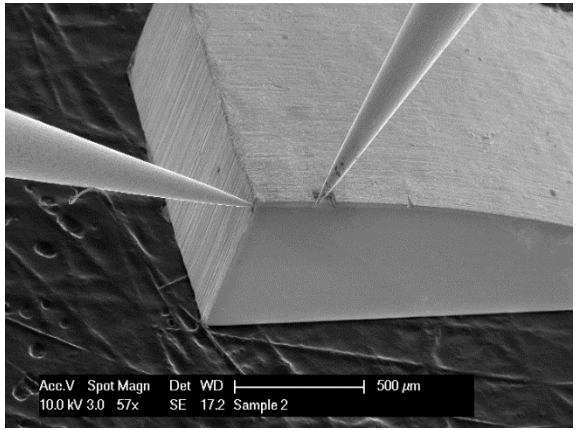
II. Examination of Semi-conducting properties: SEM observations

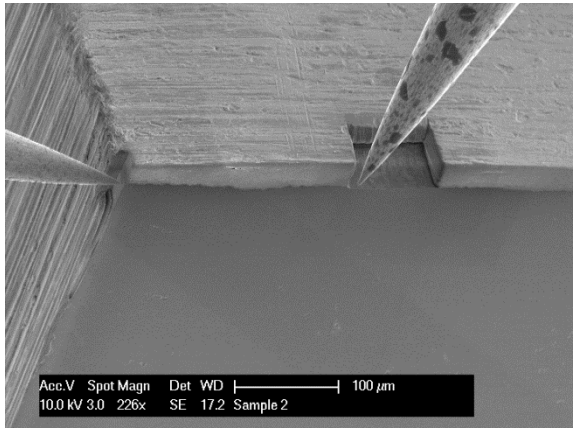


SEM micrographs from 3, 6 and 9-cycle LK3/L materials at the metal-oxide interface, during the FIB cuts showing the charging effects and the small non-charging layer close to the metal-oxide interface. The thickness of this very small layer seems to be rather similar for the material after the different residence times.

C- Micromanipulators for conductivity measurement

New method to determine electrical properties of the material at the micro and nanometric level

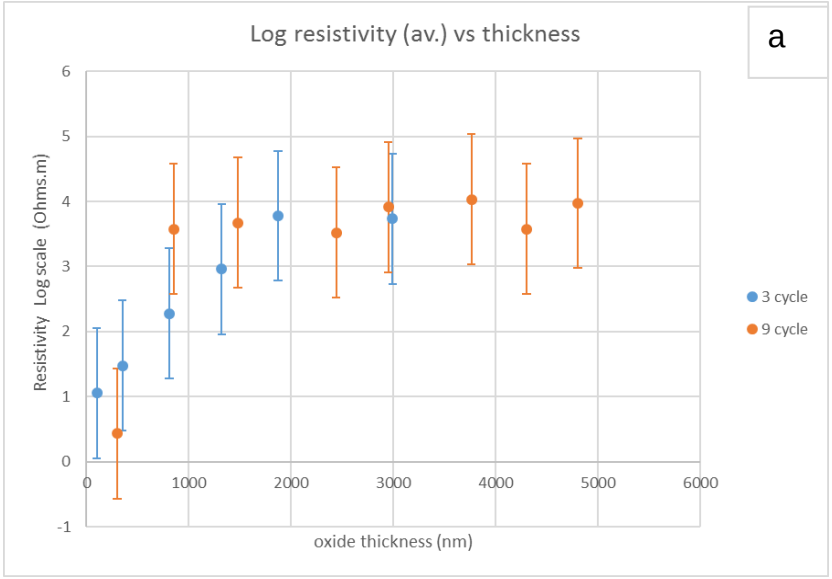




In this example, the metal electrode has been created at an angle of 90° w.r.t. the wedge, for the ease of access.

Radovan Vanta et al.: "Examination of semiconducting properties of oxides in the vicinity of metal-oxide interfaces for selected alloys"; The 16th European Microscopy Congress 2016; DOI: 10.1002/9783527808465.EMC2016.6954

II. Examination of Semi-conducting properties: Micromachining and micromanipulator observations



Examples of resistivity calculations from the measurement of semi-conducting properties of the oxide in the vicinity of interface by means of micromanipulators in the SEM. (a) Results for LK3/L; 3 and 9-cycle claddings (BWR). (b) the same measurements for low-tin Zircaloy-4 and Zr2.5%Nb materials from PWR.

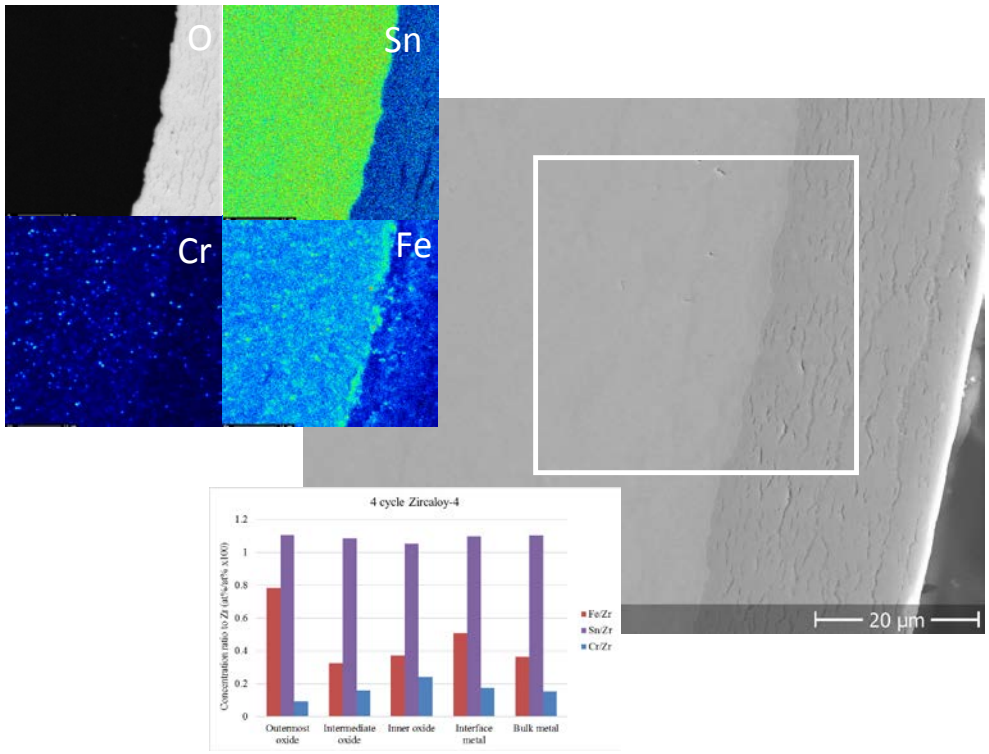
Hawes et al. To be submitted.

PAUL SCHERRER INSTITUT

Outline

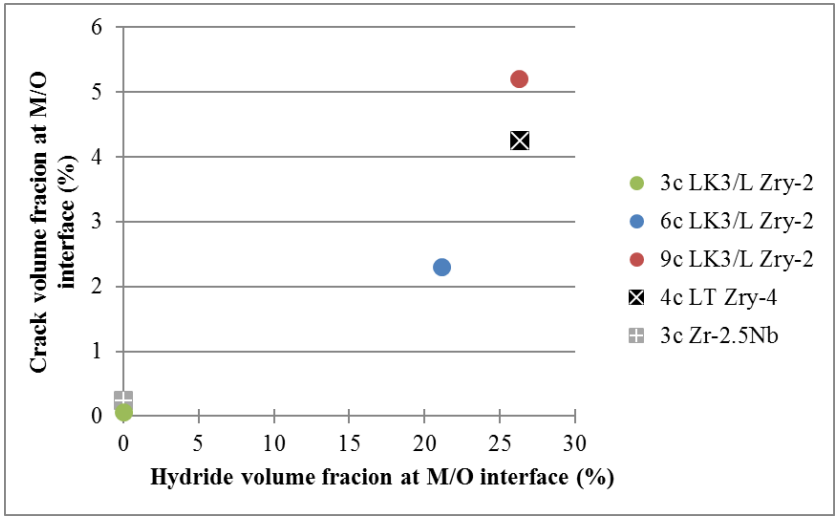
- i. Study of the 9-cycle Zircaloy-2, LK3/L from KKL (BWR) cladding to look for great changes
- ii. Comparison with a low burnup (here 3-cycle) and an intermediate burnup (here 6-cycle) cladding from the same grade material and the same reactor; to verify the validity of indicators
- iii. Examination of mechanical and semi-conducting properties of the oxide layers in the case of the two extreme cases
- iv. Verification of PWR material to search for general phenomena
- v. The use of the data to define the determinant indicators
- vi. Correlation with the known parameters
- vii. Conclusion

Observation of microscopic changes in the cladding: from EPMA … Comparison with PWR materials



An example of EPMA map for low-tin Zircaloy-4 and the distribution of alloying elements in the metal, oxide and along the metal-oxide interface. Higher concentration of Fe in the metal side of the interface is observed. The histograms in the inset indicate the distribution of alloying elements in the different regions of the metal and oxide.

b- 3D- Distribution of hydrides in the metal and the microcracks in the oxide … All materials studied represented; Quantification of volume fractions

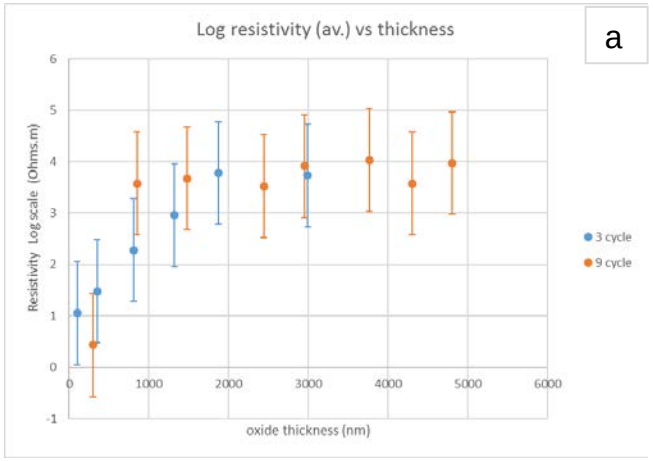


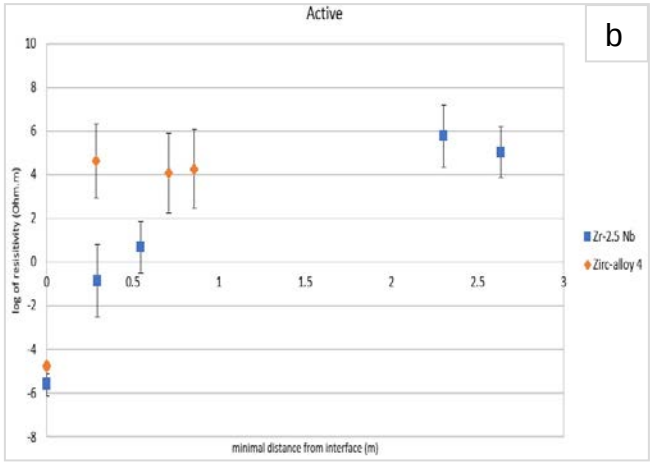
The correlation of volume fraction of hydrides, as a function of volume fraction of micropores in the oxide, at 1 micrometer on the two sides of the metal-oxide interface for all claddings from BWR and PWR [30].

Baris A., PhD thesis.

II. Examination of Semi-conducting properties: Micromachining and micromanipulator observations

All materials studied represented; Quantification of resistivity of different oxide regions





Examples of resistivity calculations from the measurement of semi-conducting properties of the oxide in the vicinity of interface by means of micromanipulators in the SEM. (a) Results for LK3/L; 3 and 9-cycle claddings (BWR). (b) the same measurements for low-tin Zircaloy-4 and Zr2.5%Nb materials from PWR.

Radovan Vanta et al.: "Examination of semiconducting properties of oxides in the vicinity of metal-oxide interfaces for selected alloys"; The 16th European Microscopy Congress 2016; DOI: 10.1002/9783527808465.EMC2016.6954

PAUL SCHERRER INSTITUT

Outline

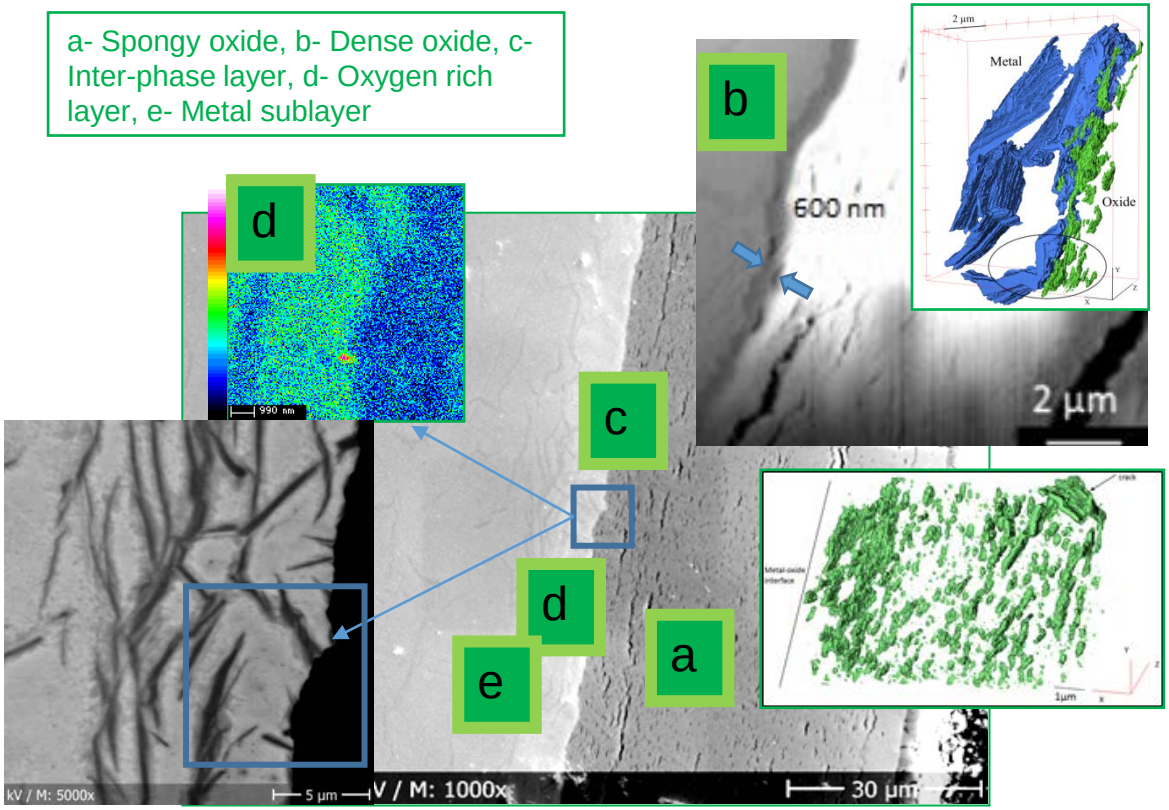
- i. Study of the 9-cycle Zircaloy-2, LK3/L from KKL (BWR) cladding to look for great changes
- ii. Comparison with a low burnup (here 3-cycle) and an intermediate burnup (here 6-cycle) cladding from the same grade material and the same reactor; to verify the validity of indicators
- iii. Examination of mechanical and semi-conducting properties of the oxide layers in the case of the two extreme cases
- iv. Verification of PWR material to search for general phenomena
- v. The use of the data to define the determinant indicators
- vi. Correlation with the known parameters
- vii. Conclusion

Determination of Indicators

- A. microscopic factors
  - i- the chemical composition of the metal and the oxide
  - ii- the distribution of hydrides near the metal oxide interface
  - iii- the volume fraction of microcracks in the oxide side of the interface
  - iv- the extent of grain boundary segregation close to the metal-oxide interface
  - v- the coupled mechanical properties of the interface
  - vi- the semi-conducting properties of the oxide sublayer and its extent

- B. macroscopic factors
  - vii- pellet clad interactions
  - viii- dimensional changes and increase of rod radius
  - ix- rod growth
  - x- inner clad-wall compression through constant pellet swelling
  - xi- pellet swelling and fission gas release

a- Spongy oxide, b- Dense oxide, c- Inter-phase layer, d- Oxygen rich layer, e- Metal sublayer



PAUL SCHERRER INSTITUT

Outline

- i. Study of the 9-cycle Zircaloy-2, LK3/L from KKL (BWR) cladding to look for great changes
- ii. Comparison with a low burnup (here 3-cycle) and an intermediate burnup (here 6-cycle) cladding from the same grade material and the same reactor; to verify the validity of indicators
- iii. Examination of mechanical and semi-conducting properties of the oxide layers in the case of the two extreme cases
- iv. Verification of PWR material to search for general phenomena
- v. The use of the data to define the determinant indicators
- vi. Correlation with the known parameters
- vii. Conclusion

Stages of oxidation and hydrogen uptake in-reactor

- Suggest at least three stages:

- Stage 1: A very tenacious oxide, the oxidation governed by diffusion , the mechanical properties of oxide allow for stresses induced from oxidation and from the cladding dimensional changes, hydrides are small precipitates, extended semi-conducting oxide at the metal-oxide interface (e.g. 3-cycle LK3/L)
- Stage 2: Oxide composition has changed, the oxide has developed microcracks, the oxidizing species percolate into the inner layer, the gradual dimensional changes of the cladding increase due to growth from different origins (e.g. irradiation and hydride precipitation), the mechanical properties of oxide change and the oxide is less resistant to crack formation, hydride rims induce more microcracks, the semi-conducting properties will evolve.
- Stage 3: The indicators reach the threshold, and the above mentioned behaviors become macroscopically measureable.

Our thanks go to

- PSI
- KKL
- KKG
- Swissnuclear
- Westinghouse
- Areva
- MUZIC-3



Steam Oxidation of Hafnium at high Temperature.

Guilbert-Banti S.[1], Viretto A.[1], Barrachin M.[1], Steinbrück M.[2], Tanguy C.[2], Stuckert J.[2]

1- IRSN/PSN-RES, Cadarache, 13115 Saint-Paul-lez-Durance, France
2- KIT, IAM-AWP, Hermann-von-Helmholtz-Platz 1, 76344 Eggenstein-Leopoldshafen, Germany

Due to its high thermal neutron absorption cross section and good corrosion resistance at low temperature, hafnium has been used in the nuclear reactors as control rods or shut-off rods since the late 1950's. Its use in commercial reactors declined in the 1990's, due, in part, to its ability to pick-up hydrogen and swell. However, hafnium received a renewed interest, theses last years. For instance, in France, it is planned to generalize the introduction of absorber rods of hafnium not sheathed in fuel assemblies positioned in the core periphery in order to reduce the neutronic flux received by the vessel in the 900 MWe power plants.

This paper presents IRSN and KIT[1] results on the oxidation behaviour of hafnium up to 1400°C, i.e. in temperature conditions relevant to severe accidents. Samples, with different surface conditions (rods/tubes) were oxidized in steam/argon mixtures, either in a furnace or in a thermogravimetric analyser (TGA). Metallographic examinations, hydrogen measurements and Electron Probe Micro Analysis (EPMA) oxygen profiles were then performed.

All the tests confirm that hafnium exhibits better resistance to oxidation at high temperature than zirconium alloys. For hafnium rods, metallographic examinations show the presence of a dense and protective oxide film, whereas, on hafnium tubes, a white and porous layer is observed. No or little hydrogen is measured in the metallic part of the rod specimens while significant hydrogen amount is picked up by hafnium tubes.

Regarding hafnium rods, the reaction rate may be described by a parabolic law in the investigated temperature range, and the value determined from the experimental data in steam is in good agreement with the ones published in the literature for oxygen. The oxygen diffusion coefficient was estimated at each temperature by fitting the experimental profile obtained on hafnium rods. A linear regression of the data allows an estimate of the temperature dependence of the diffusion coefficient of oxygen in hafnium in the temperature range 700-1400°C.

Hafnium tubes led to weight gain twice as high as the ones measured on hafnium rods. However, it remains well below the oxidation rate of zirconium alloys in the same temperature range. Above 800°C, the reaction rate for hafnium tubes cannot be modelled by a parabolic law, which confirms that the oxide layer formed on this material, is not protective.

These tests highlighted the influence of the surface conditions on the oxidation rate of hafnium in steam.

[1] In a different context, KIT performed oxidation experiments of Hf tubes during the preparation of the QUENCH-17 test.



Hafnium Oxidation in Steam at High Temperature

S.Guilbert-Banti[1], A. Viretto[1],M. Barrachin[1], C. Tanguy[2], M. Steinbrück[2], J. Stuckert[2]

1- IRSN/PSN-RES, Cadarache, 13115 Saint-Paul-lez-Durance, France
2 – KIT/IAM-AWP, Hermann-von-Helmholtz-Platz 1
76344 Eggenstein-Leopoldshafen, Germany

25th QUENCH Workshop, Karlsruhe, 22-24 Oct. 2019

IRSN/FRM-414 ind 3

Contents

- Context
- Experimental devices
- Materials & Methods
- Experimental results
- Summary

Context

- EDF plans to generalize the introduction of absorber rods of hafnium not sheathed in the 12 assemblies positioned in the core periphery in order to reduce the flux received by the vessel (900 MWe)

- $Hf + 2H_2O \rightarrow HfO_2 + 2H_2$: $\Delta_r H°$ (1500°C)=-611 kJ/mol

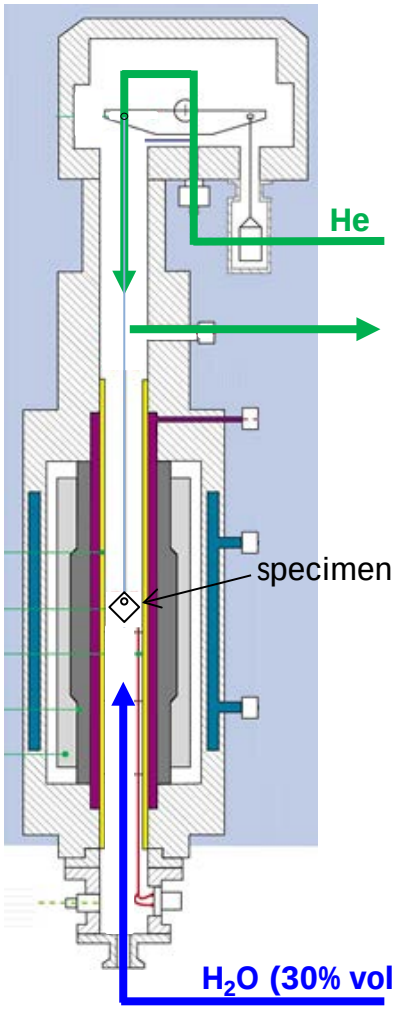
- In SA, possible existence of a runaway temperature of the reaction between Hf and H_2O ?
  - This runaway could lead to an early acceleration of the oxidation phenomena of the surrounding materials (and in particular the Zry-4) with increased hydrogen production and heat release.

- Hf/H_2O interaction investigated in the past
  - Most studies at LT (< 700°C)
  - Only one study in steam at 700-1200°C by D'yachkov (2006)
  - Indicative of better resistance of Hf than Zr

- Hf/H_2O interaction tests at KIT and at IRSN
  - KIT objective : to prepare the QUENCH-debris test
  - 600°C to 1400°C
  - Different materials (disc, rods and cladding)

Experimental devices at IRSN and KIT

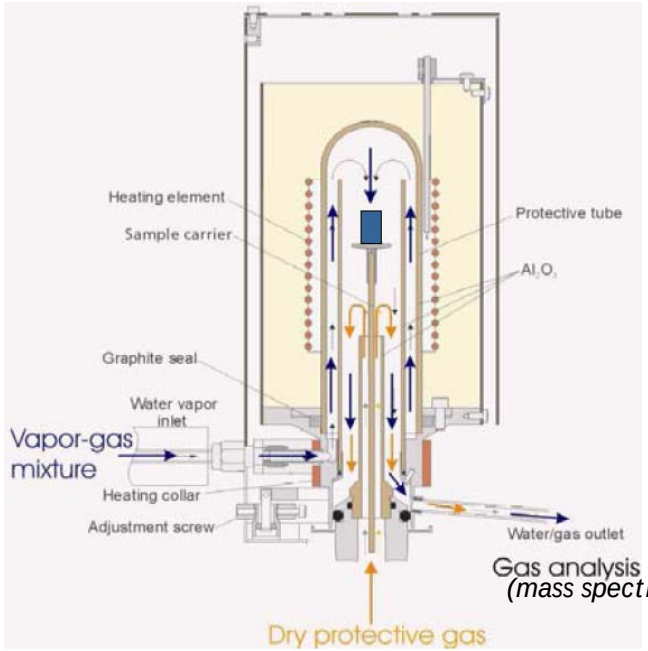
SETARAM thermobalance

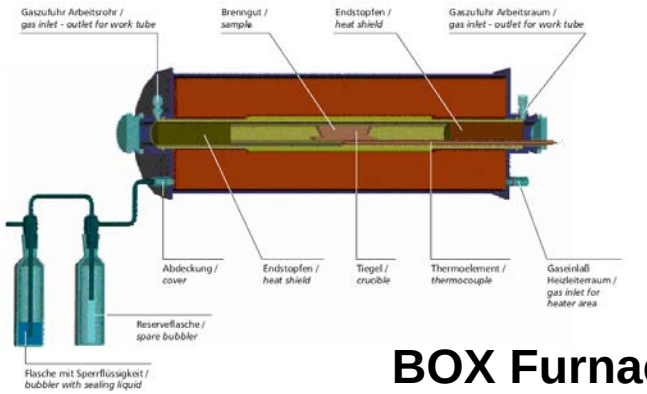


HT Furnace



NETZSCH STA 409 thermobalance





BOX Furnace

Oxidation temperature range: 600-1400°C - Isothermal tests up to 60h

Materials & Methods

- Hafnium rods, discs and cladding

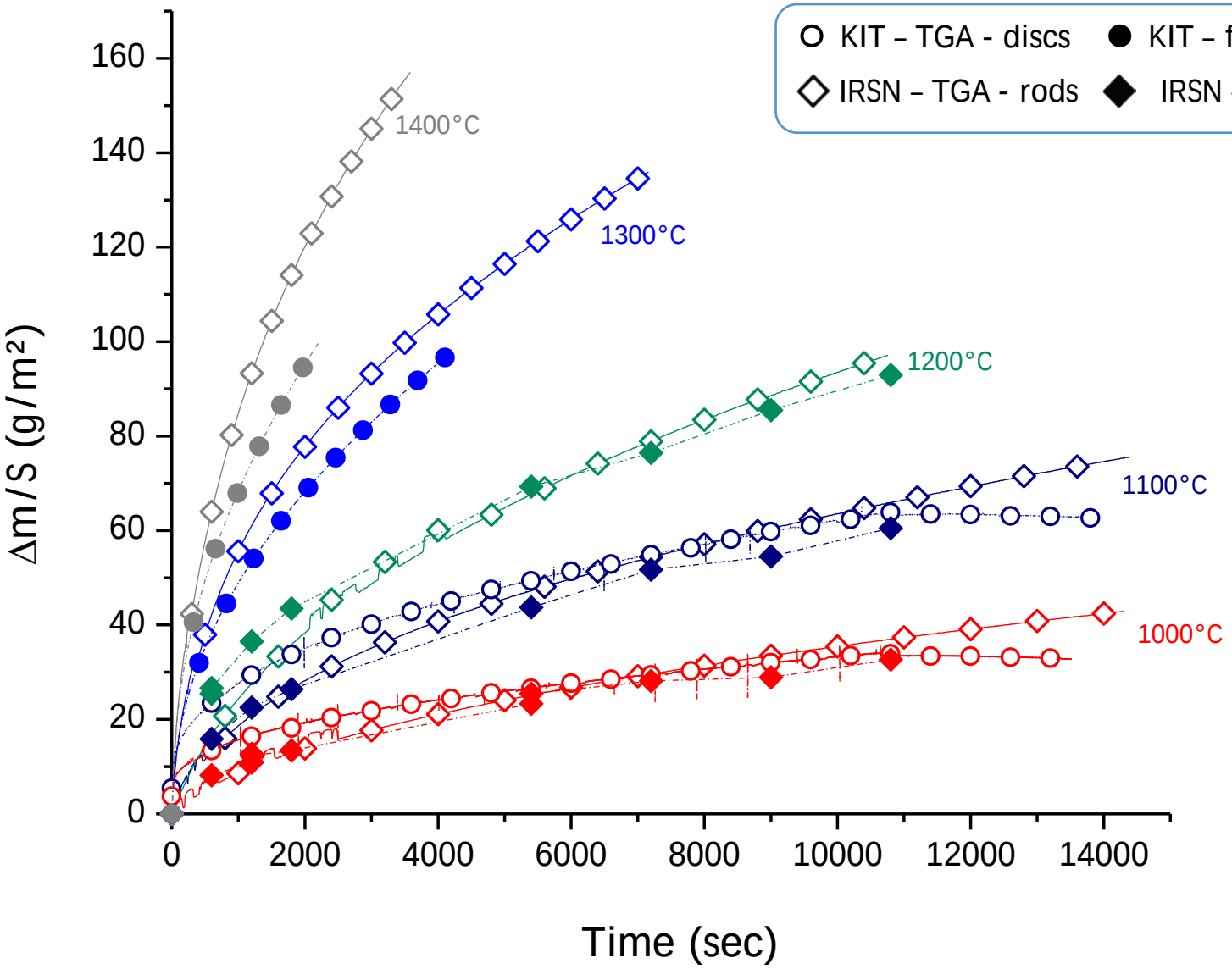


- Weight gain, metallography, EPMA, hydrogen measurements



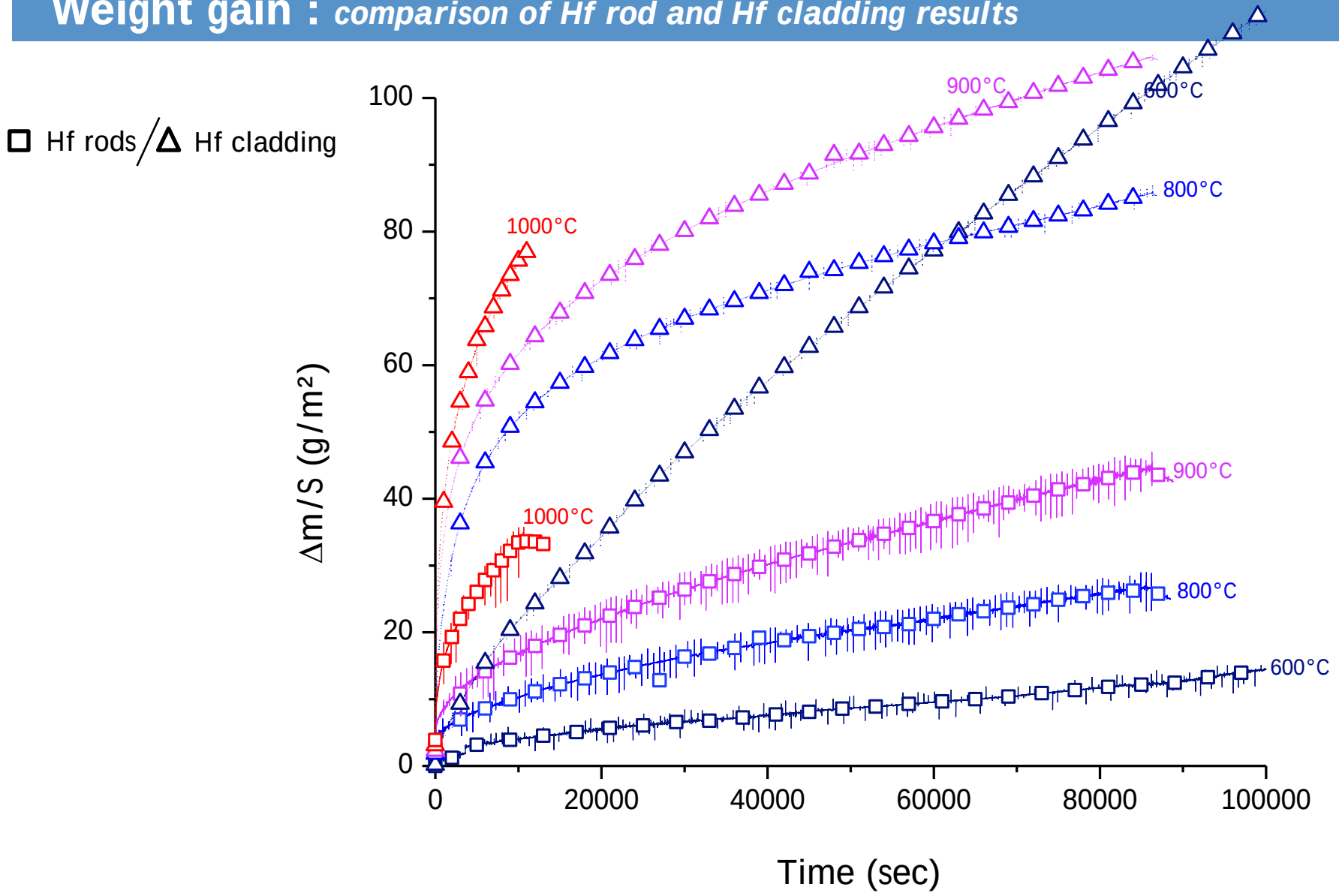


Weight gain: *comparison of furnace and TGA experiments*



- Good agreement between furnace and TGA experiments

Weight gain : *comparison of Hf rod and Hf cladding results*

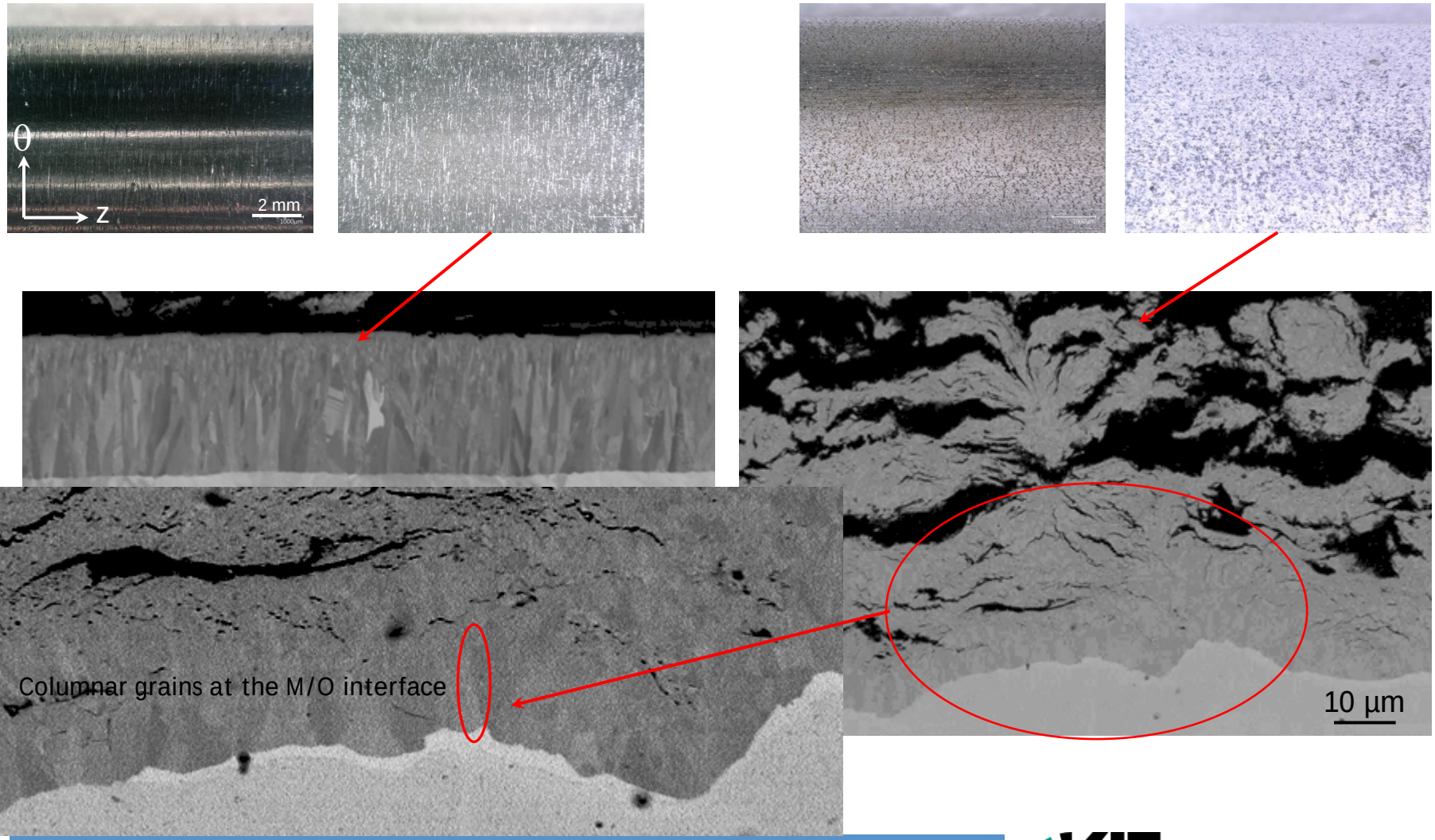


- Large difference in oxidation kinetics between Hf rods and cladding….

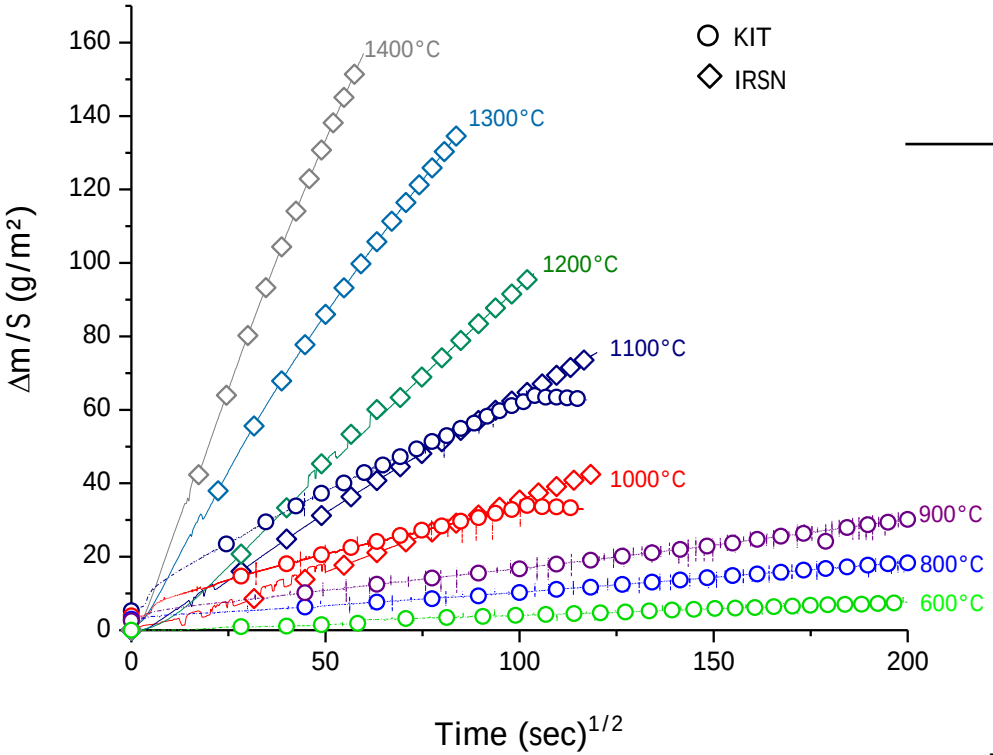
Oxide microstructure: *comparison of Hf rod and Hf tube results*

- …..linked to a difference in oxide microstructure

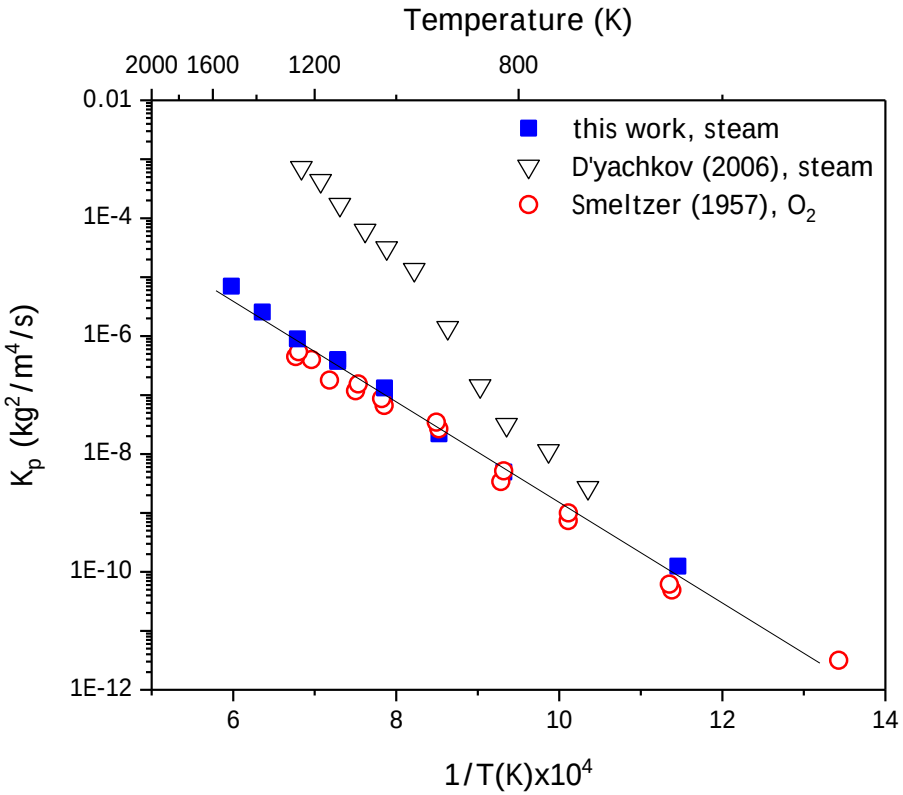
as-received Hf rod *after ox900°C, 22h* *as-received Hf cladding* *after ox900°C, 22h*



Parabolic rate constant K_p for hafnium rods/discs



$$\left(\frac{\Delta m}{S}\right)^2 = K_p \times t$$

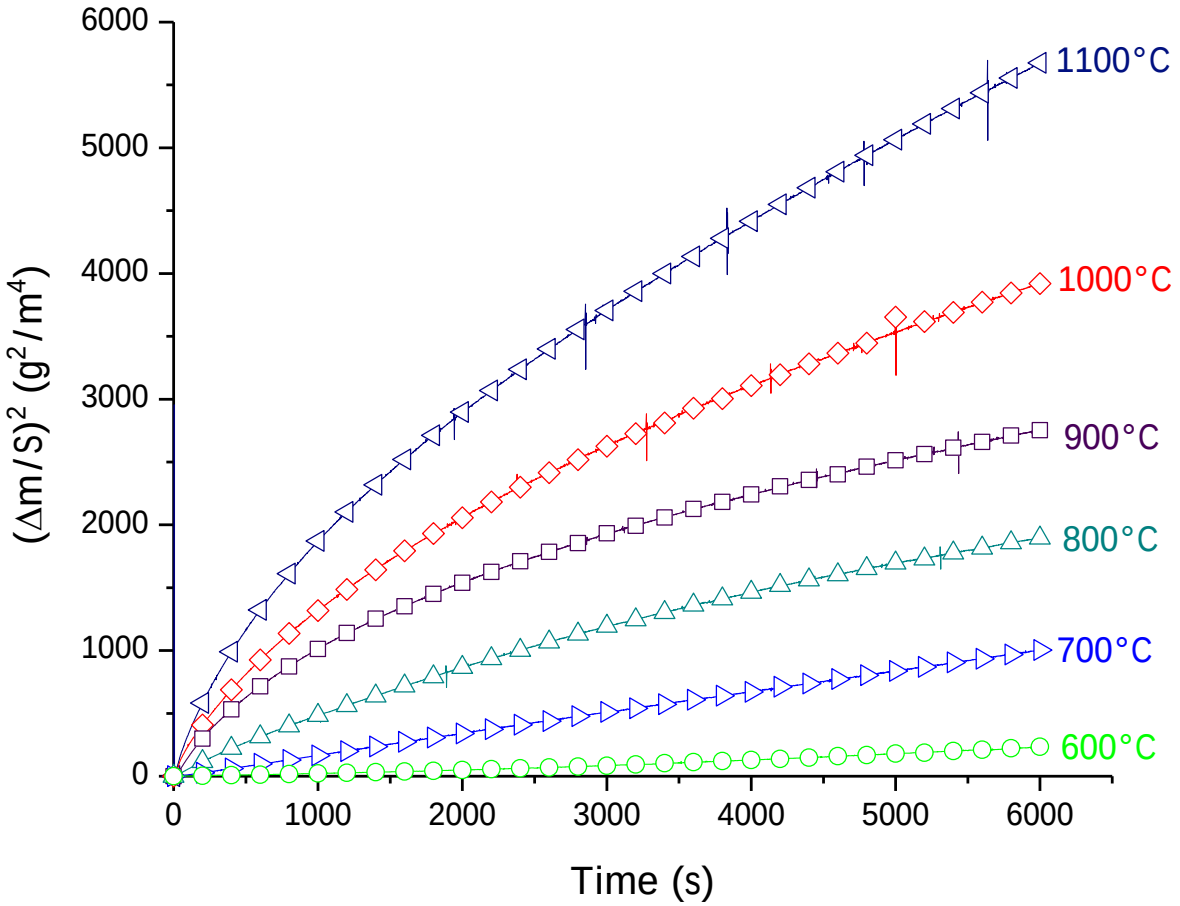


$$K_p = A exp \frac{-E_a}{RT}$$

with E_a = 189,2 kJ.mol^{-1}

- in good agreement with the activation energy obtained by Smelter and Pemsler

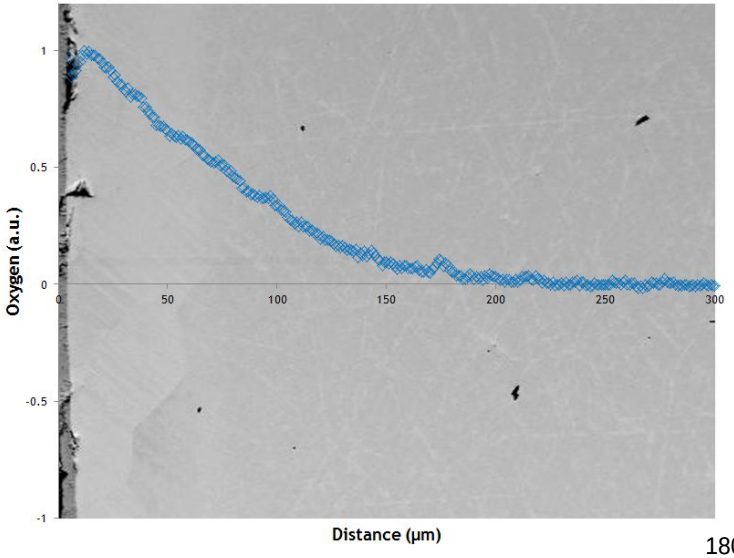
Oxidation of Hafnium cladding



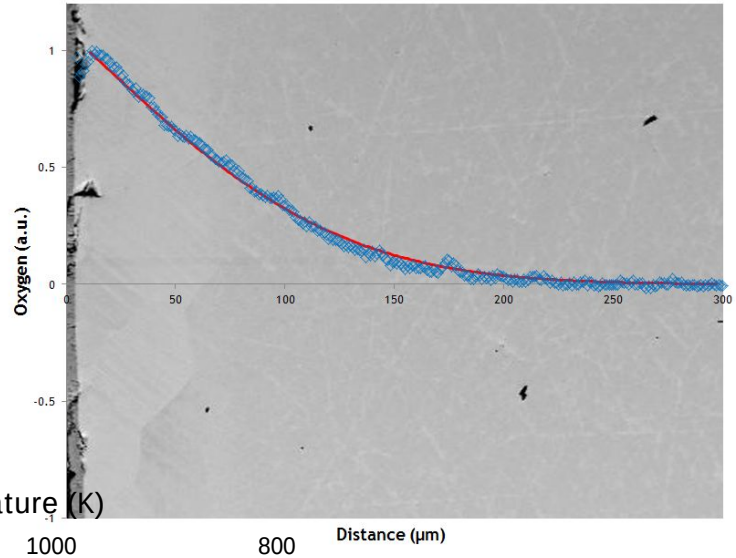
- The oxidation rate is not parabolic above 700°C
- The higher oxidation rate seems to be associated to hydrogen pickup

  (>600 ppm after oxidation at 900°C for 22h)

Oxidation of Hafnium rods: oxygen diffusion in metal

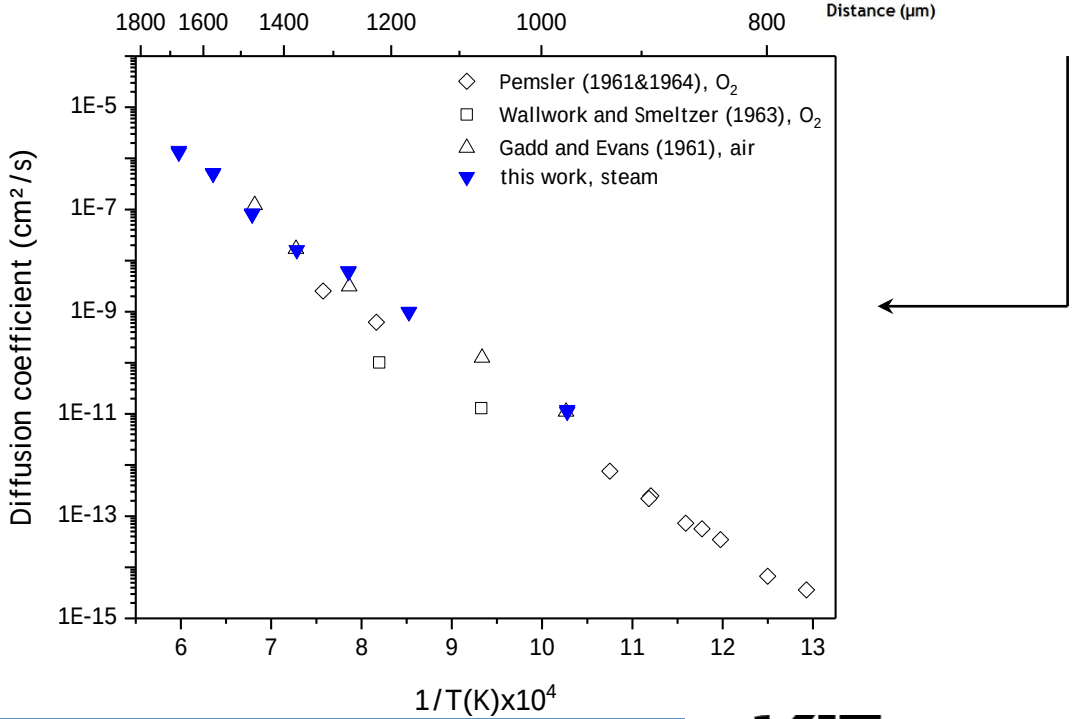


$$\frac{C}{C_0} = erfc\left(\frac{x}{\sqrt{Dt}}\right)$$

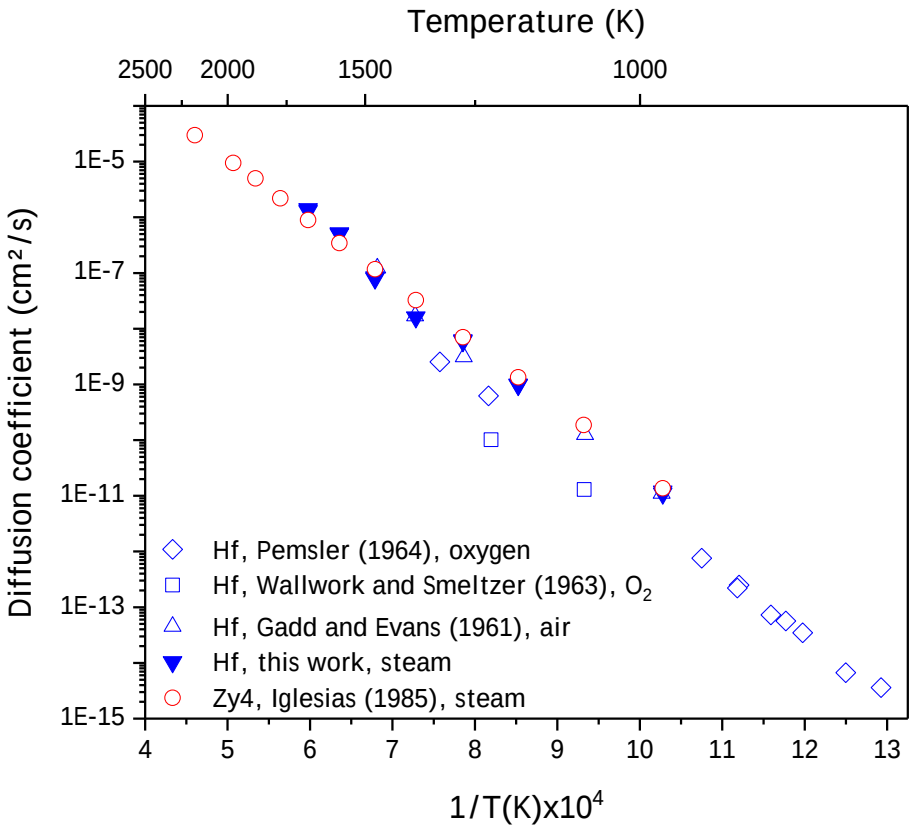


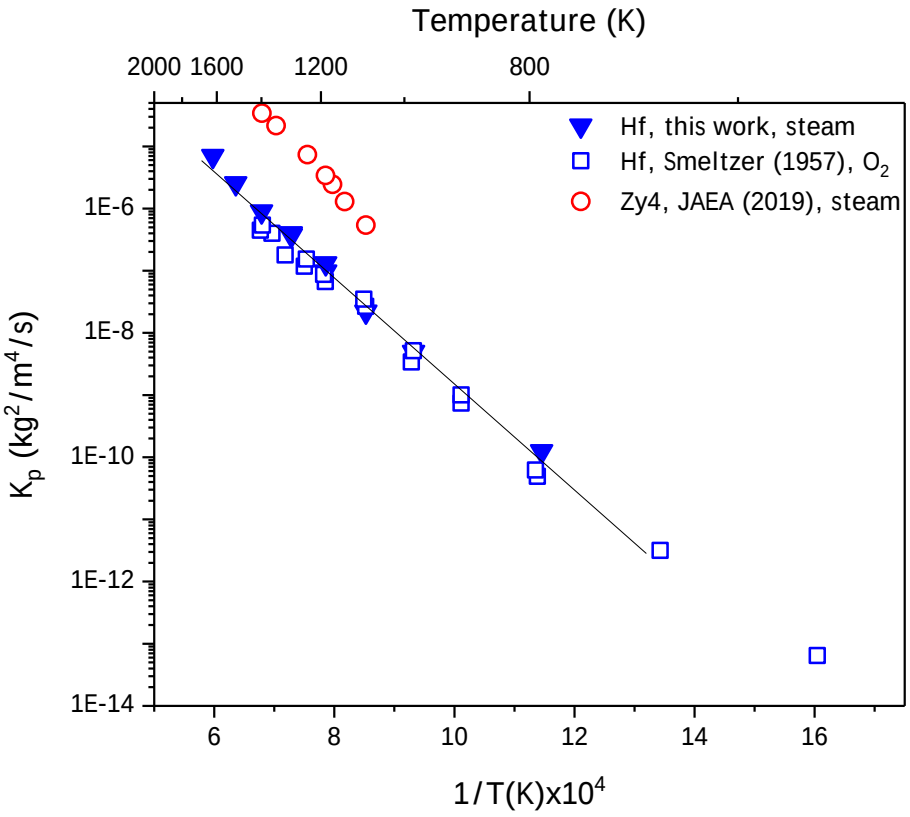
$$D = Aexp\frac{-E_a}{RT}$$

with E_a = 224,3 kJ.mol^{-1}



K_p rate constant and oxygen diffusivity : Hf versus Zy4





- The oxygen diffusivity in hafnium and in Zircaloy-4 is of the same order
- However, the parabolic rate constant is much lower than in Zircaloy-4

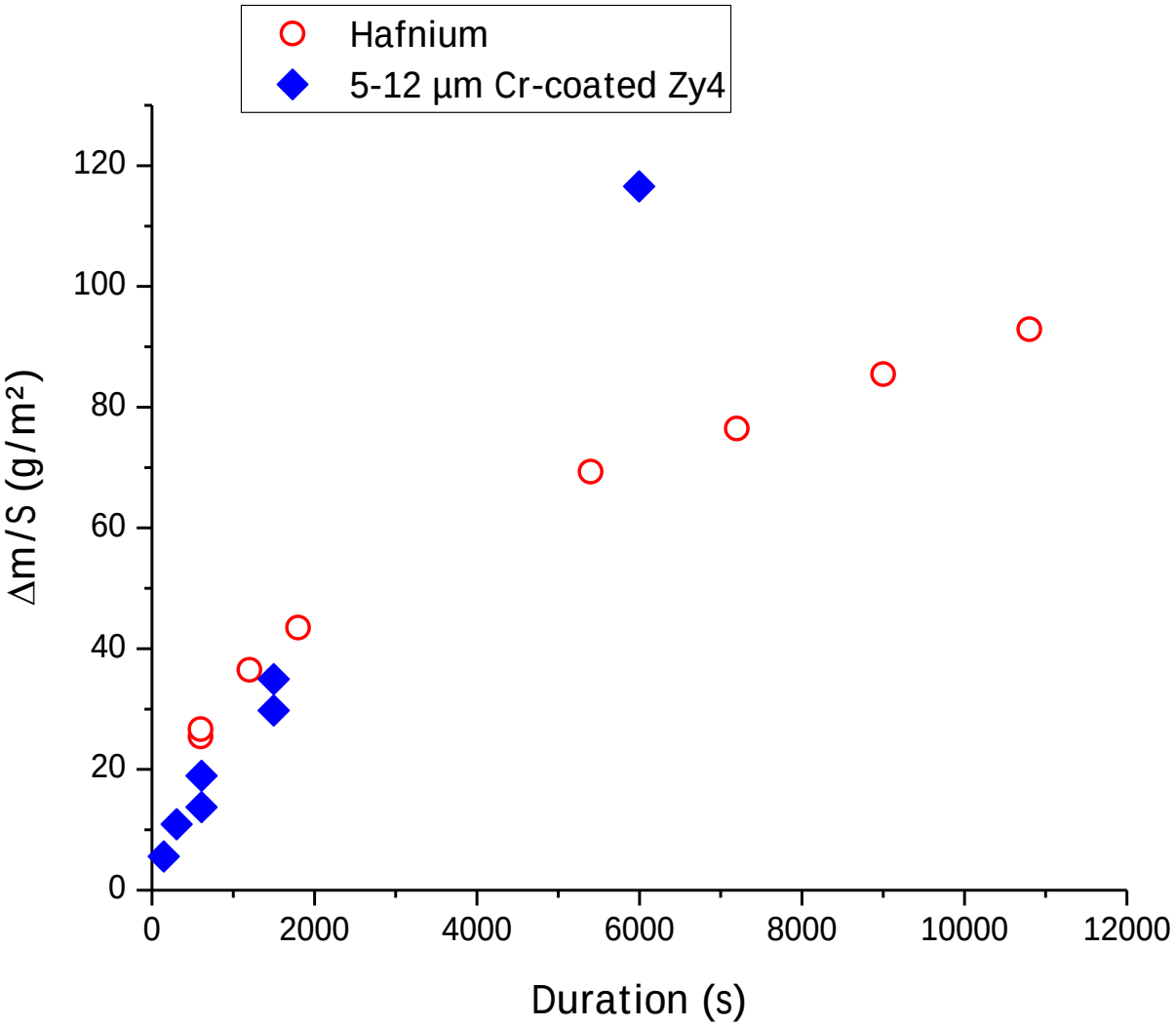
Summary and conclusions

- The oxidation rate of hafnium in steam was determined in the temperature range 600-1400°C,
- The parabolic rate constant and the diffusion coefficient in the metal were estimated for hafnium rods/discs,
- Clearly, the oxidation rate depends on the surface conditions of the samples
- However, it remains well below the oxidation rate of Zircaloy-4
- First calculations show little impact on accident progression but, interactions between hafnium and core materials should be investigated to confirm this result.

Karlsruhe Institute of Technology IRSN MEMBER OF ETSON

Thank you for your attention !

Comparison with Cr-coated Zy-4 at 1200°C



Brachet, JNM 517, 2019

The CODEX-NITRO experiment

Róbert Farkas, Imre Nagy, Nóra Vér, Zoltán Hózer, Péter Szabó, Gergely Szabó
Hungarian Academy of Sciences Centre for Energy Research (MTA EK), Budapest

A CODEX-NITRO experiment was carried out at the Centre for Energy Research (MTA EK) in order to simulate loss of coolant accident with injection of nitrogen from the hydroaccumulators during the last phase of the event. The reference scenario was taken from safety analyses for the VVER-440 units of the Paks NPP.

Seven-rod electrically heated VVER type bundle was used with 600 mm heated length. The bundle was covered by Zr shroud. The composition of outlet gases was monitored with mass spectrometer.

During the experiment the maximum cladding temperature reached 1700 °C. The presence of nitrogen in the atmosphere accelerated the oxidation of Zr components. Applying low steam flowrates, steam starvation conditions were established and intense nitriding took place in the upper section of the bundle. The post-test examination confirmed that thick oxide and nitride layers were formed and part of the bundle suffered brittle failure.


KIT

CENTRE FOR ENERGY RESEARCH HUNGARIAN ACADEMY OF SCIENCES

THE CODEX-NITRO EXPERIMENT

R. Farkas, I. Nagy, N. Vér, Z. Hózer, M. Horváth, P. Szabó

25th International QUENCH Workshop

OBJECTIVE

- The CODEX-NITRO experiment was carried out at the Centre for Energy Research.

- Reference scenario: simulate loss of coolant accident with injection of nitrogen from the hydroaccumulators during the last phase of the event.

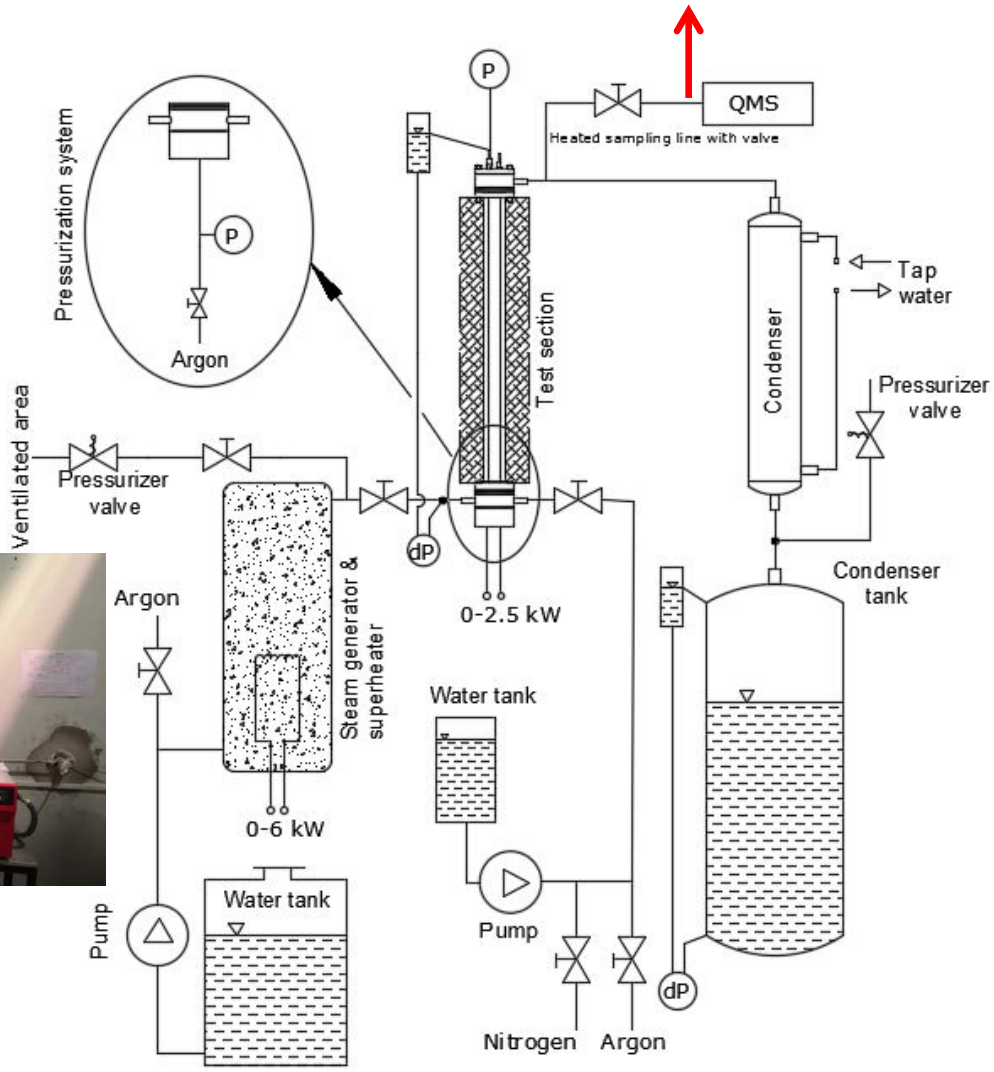
- Reference scenario was taken from safety analyses for the VVER-440 units of the Paks NPP.
- Pre-test calculations performed by NUBIKI.

- The presence of nitrogen in the atmosphere accelerated the oxidation of Zr components.
- Applying low steam flowrates, steam starvation conditions were established and intense nitriding took place in the upper section of the bundle.
- Slow cool-down was applied to provide information on bundle state before quench.

CODEX FACILITY

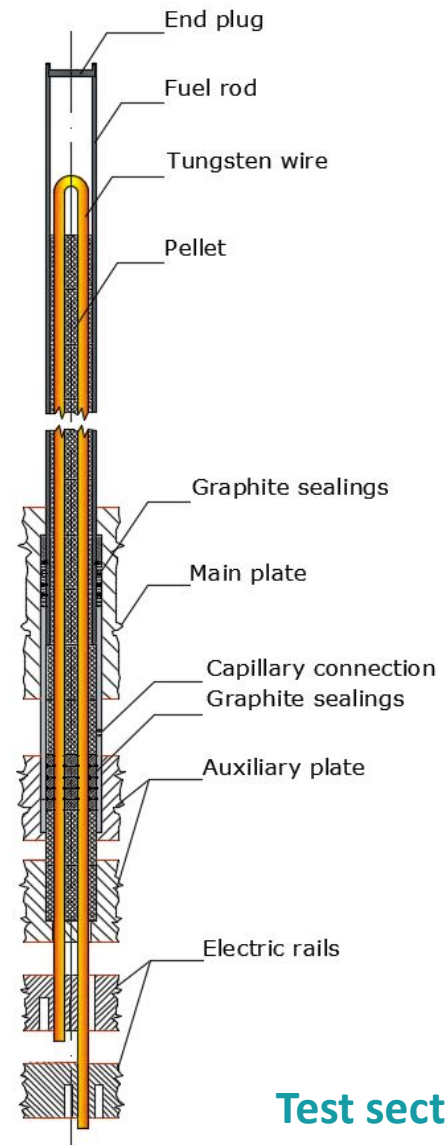
- Water tank & gas inlet
- Steam generator & superheater
- Test section
- Condenser
- Condenser tank
- Pressurisation system

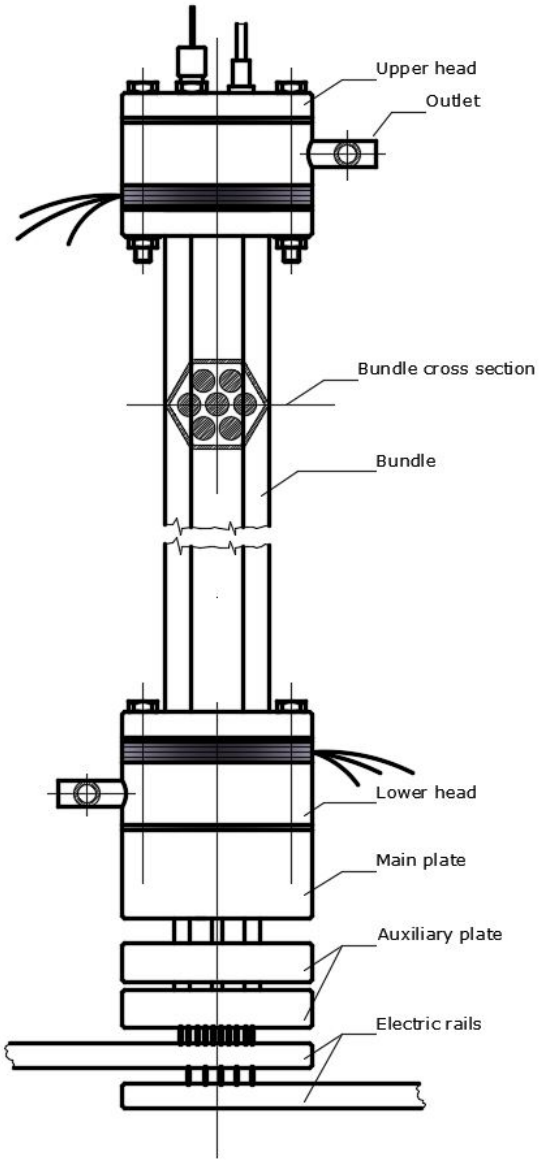




BUNDLE DESING

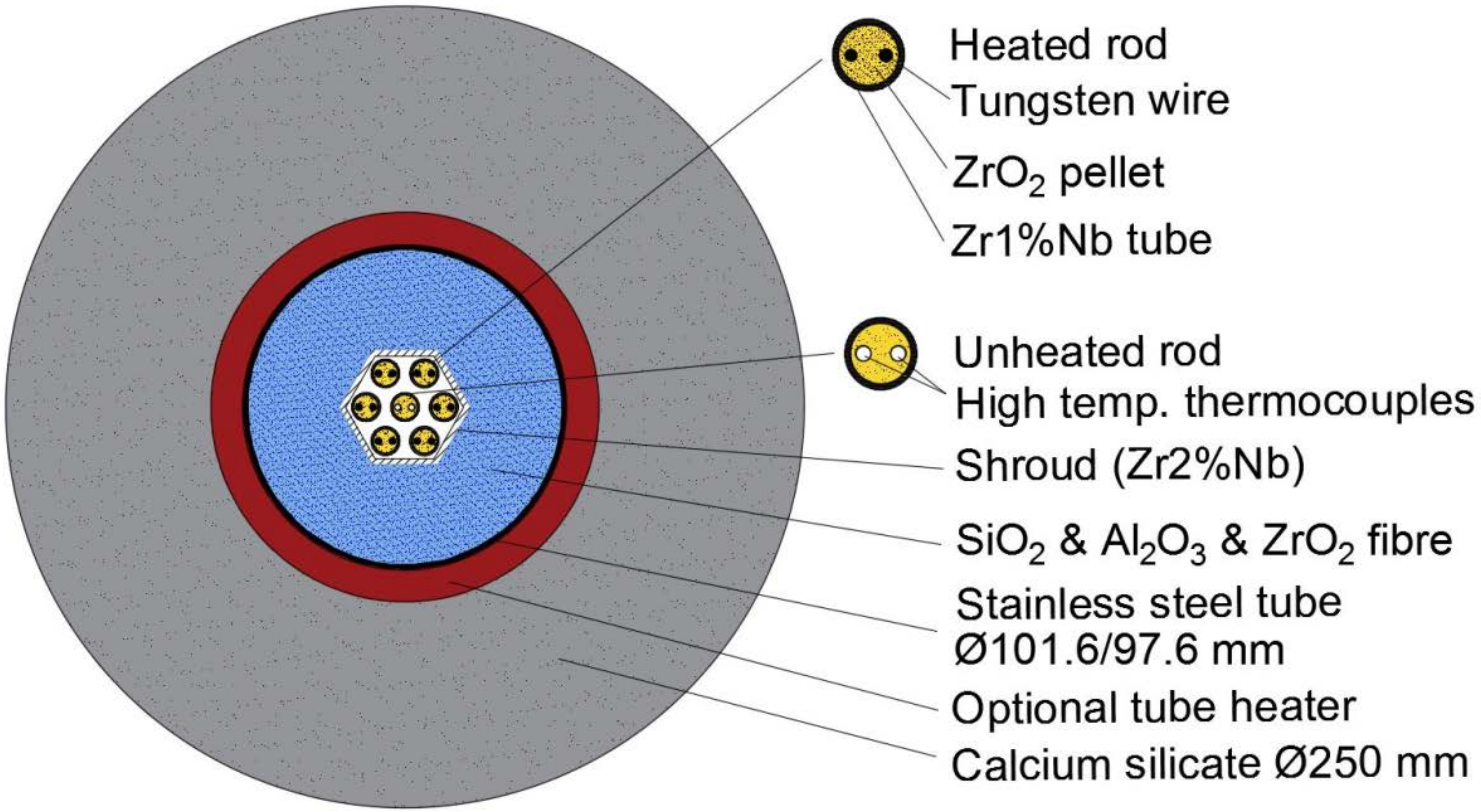
- VVER bundle type:
  hexagonal arrangement of 7 rods
- Height of rods: 600 mm
  - 6 rods (periphery)
    electrically heated - no pressurized
  - 1 rod (in the center)
    unheated - pressurized
- Cladding material: E110, E110G, E110h.p. alloy
- ZrO_2 ceramic pellets
- Tungsten heaters (580 mm)
- 2 spacer grids (Zr1%Nb alloy)
- Hexagonal shroud (Zr2.5%Nb alloy, 1000 mm)





Test section with seven-rod bundle

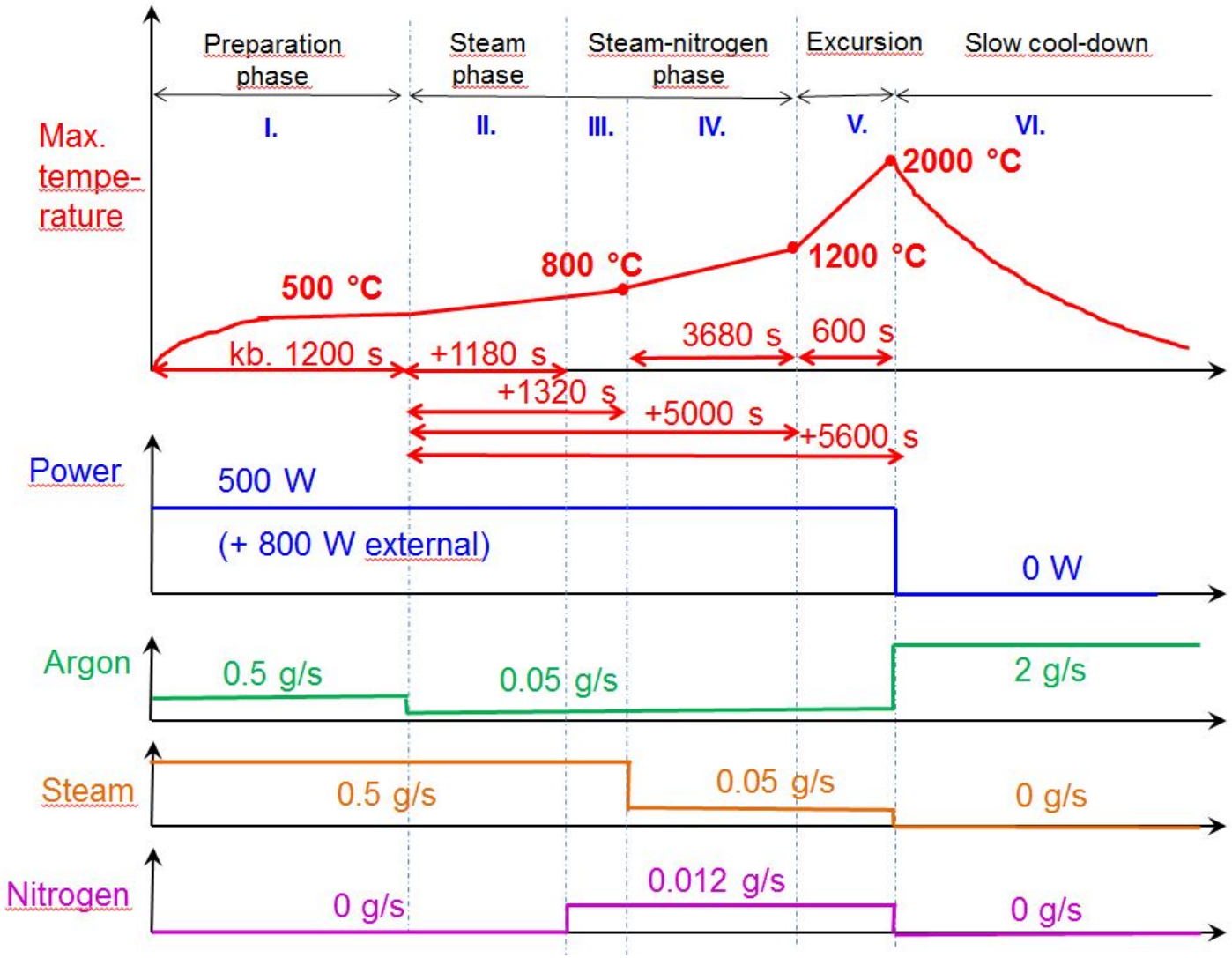
CROSS SECTION OF THE TEST SECTION WITH THERMAL INSULATIONS



MEASUREMENT OF PARAMETERS

Parameter	Device	Placement
Temperature	K-type, W5% Re/W26% Re in Zr shield tube	Rod surfaces and inner side
	K-type	Others (coolant , off-gas, stainless steel tube, …)
Argon/nitrogen flowrate	Calibrated flowmeter	Gas supply system
Steam flowrate	Calibrated pump	Pump
Gas composition	Mass spectrometer	Gas outlet
Power	DC power units	Rail of electric connections
System pressure	P transducer, 6 bar/4-20 mA	Test section upper head
Fuel rod pressure	P transducer, 100 bar/4-20 mA	Pressurization system
Water level	DP transducer device	Condenser tank

SPECIFIED SCENARIO



Targets in the pre-test calculations:

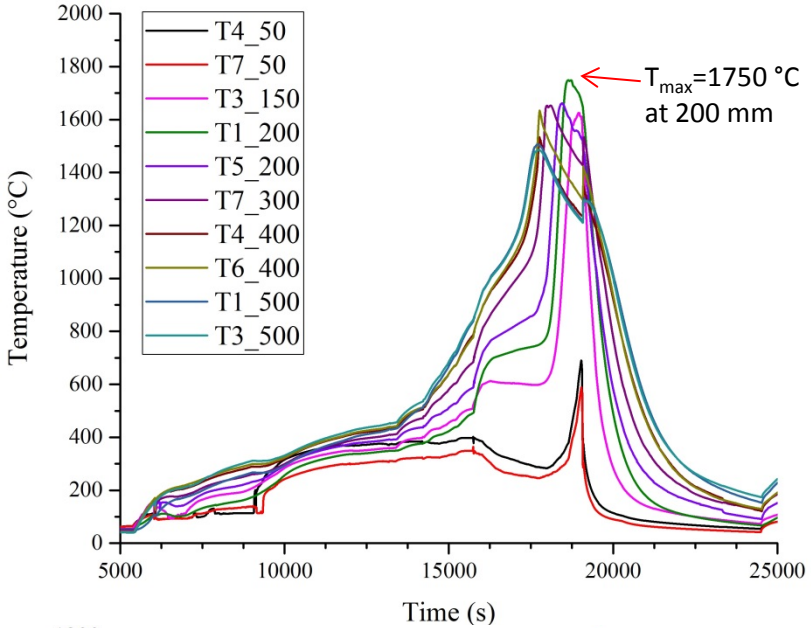
Pre-oxidation phase:

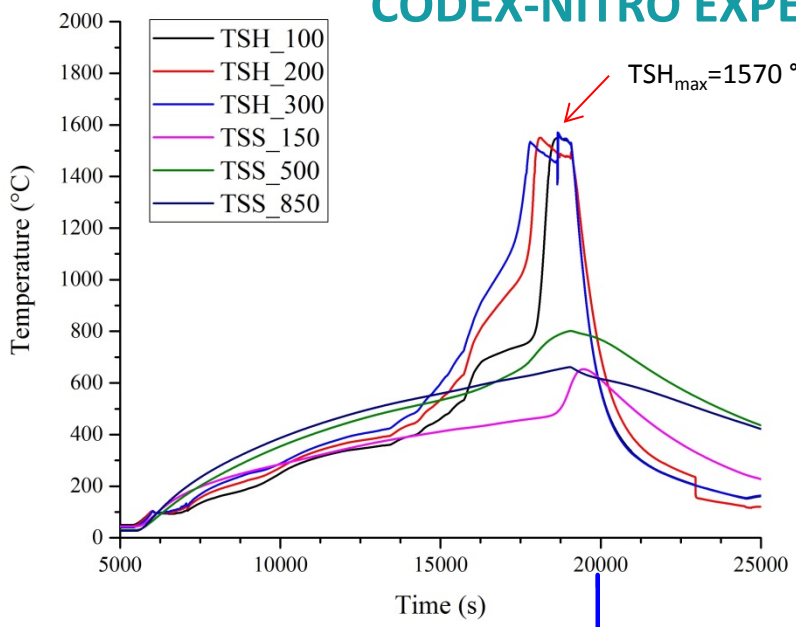
- T_{max} = 1200 °C

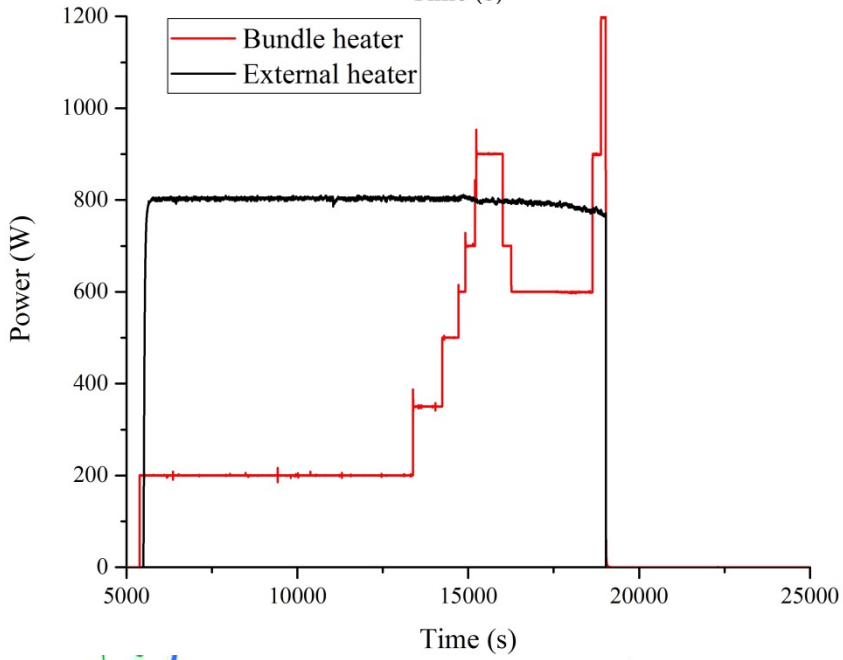
Excursion phase:

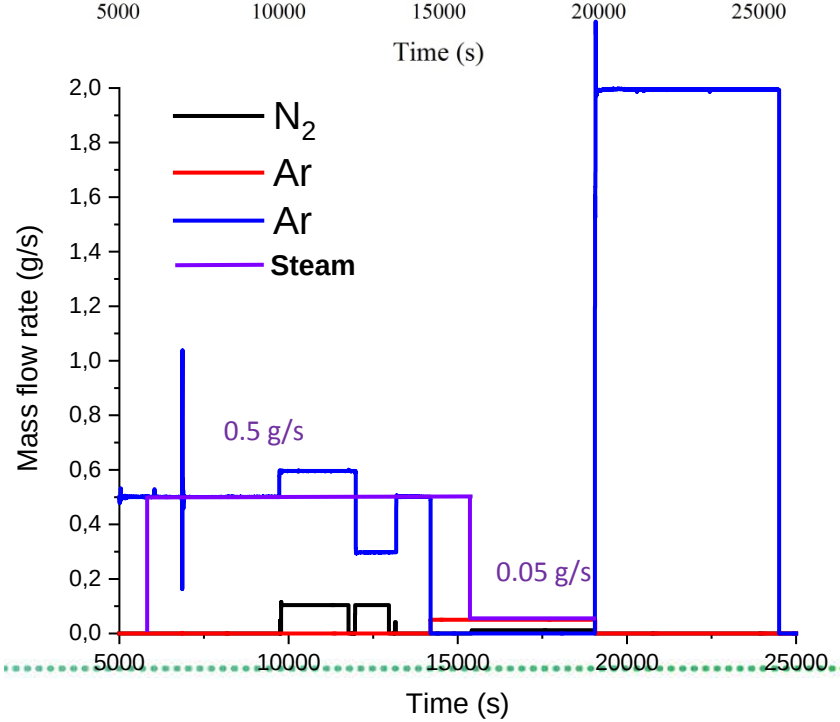
- Rapid temperature increase
- t ≈ 10 min.
- T_{max} = 2000 °C

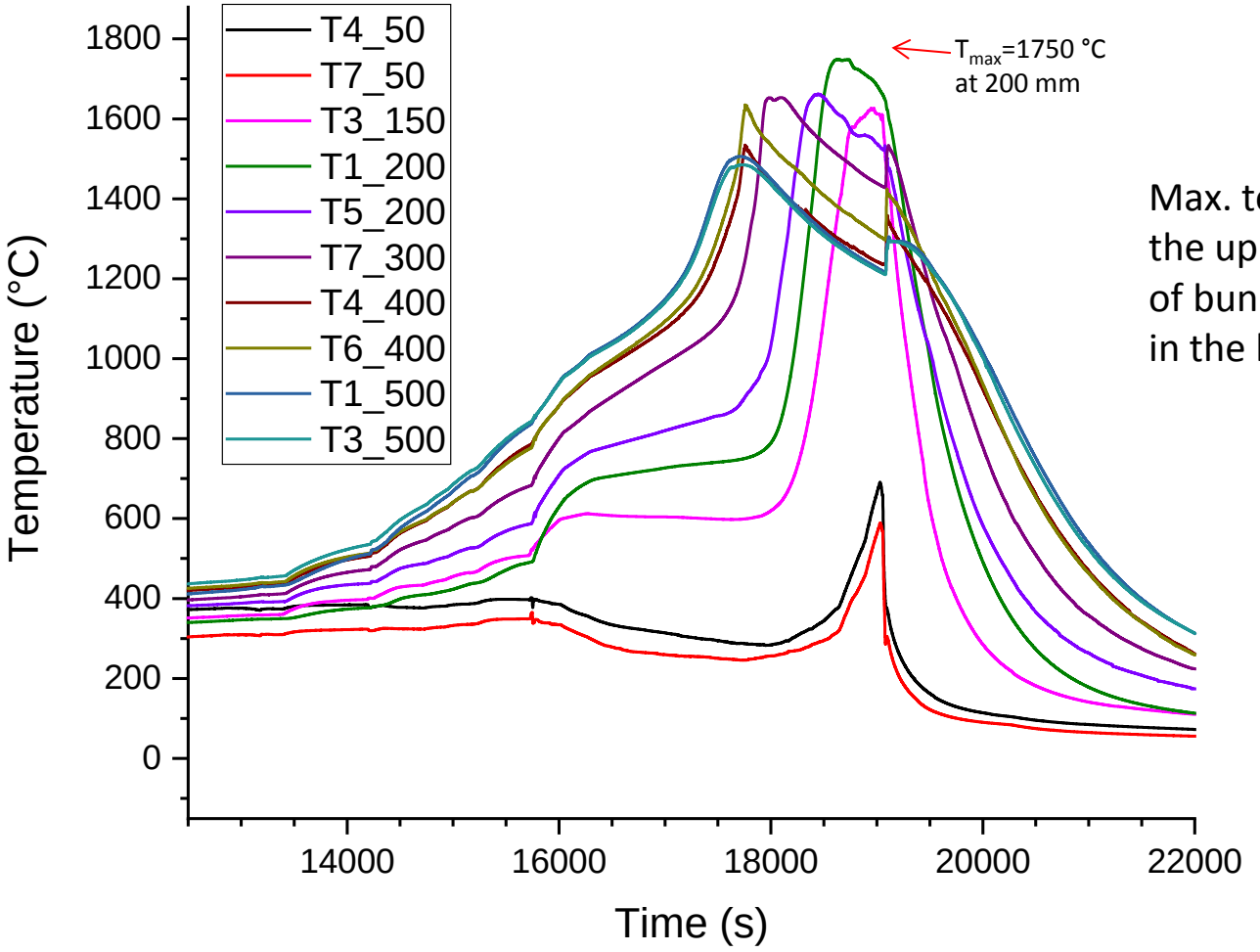
CODEX-NITRO EXPERIMENT







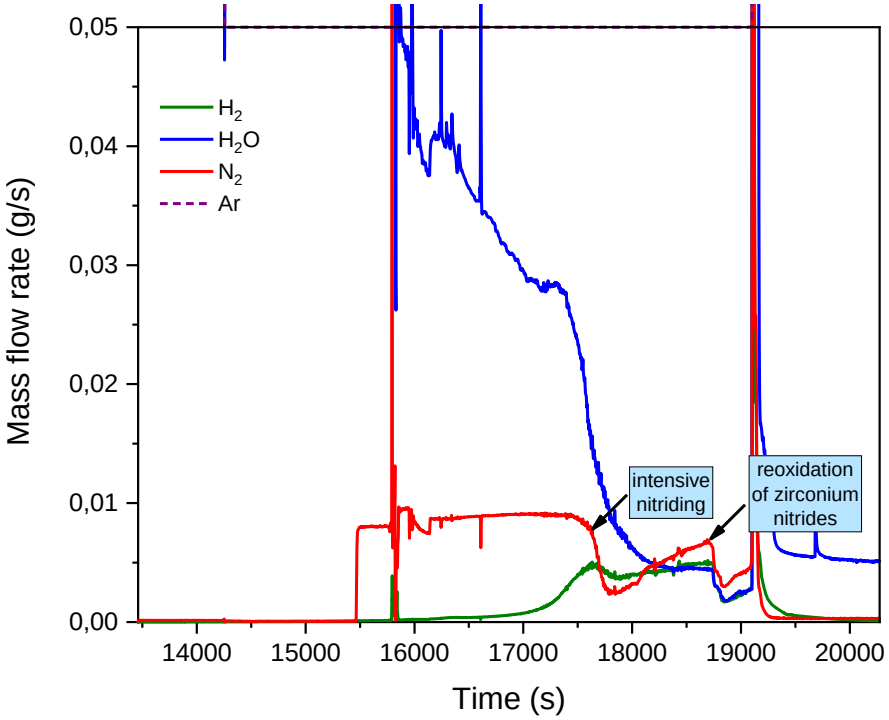


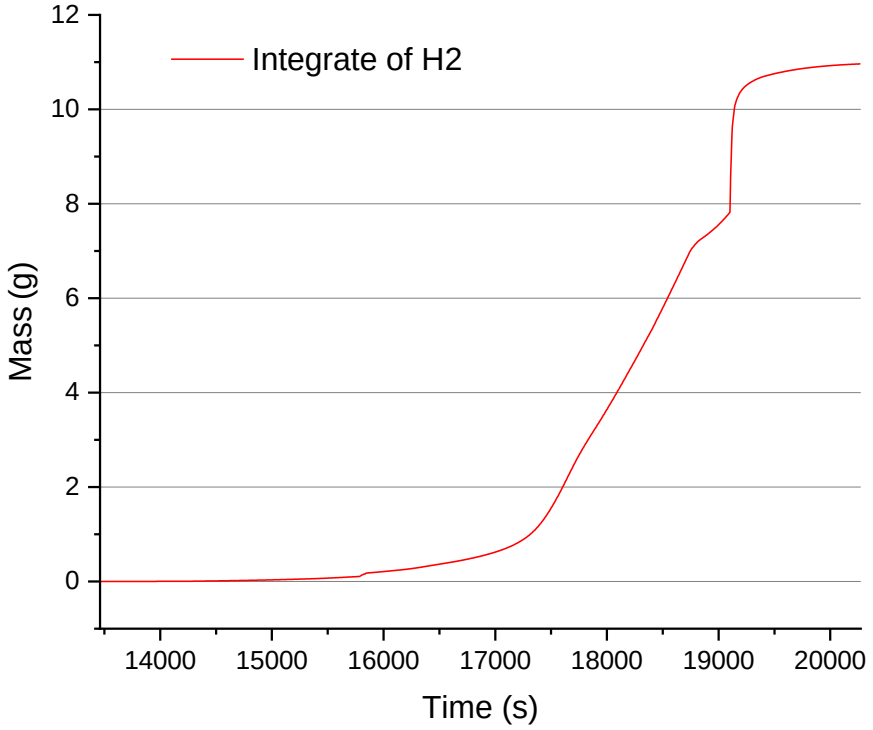


Max. temperature moved from the upper section to the middle of bundle (chemical interactions in the less oxidised central part)

CODEX-NITRO EXPERIMENT

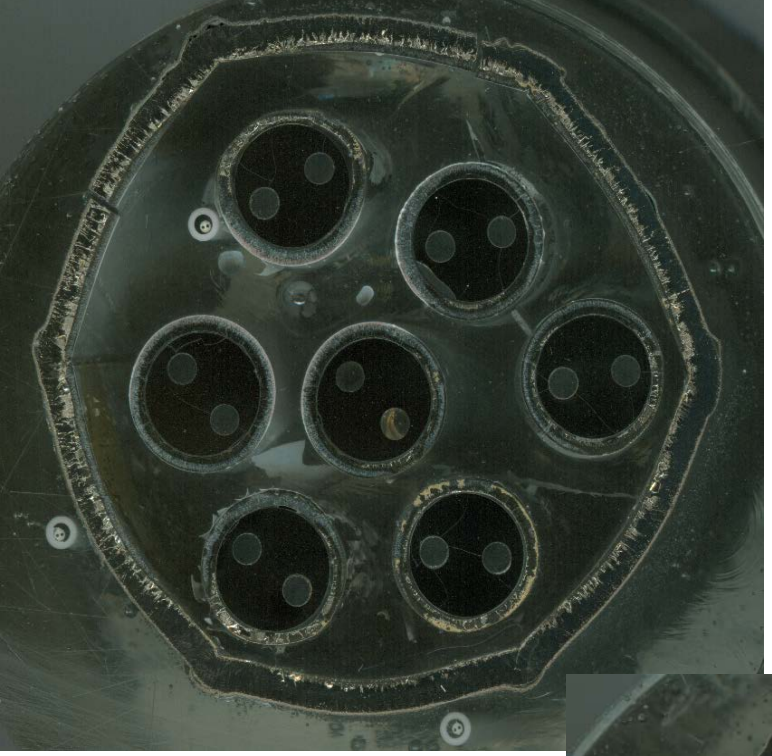
QMS measured data in steam-nitrogen phase

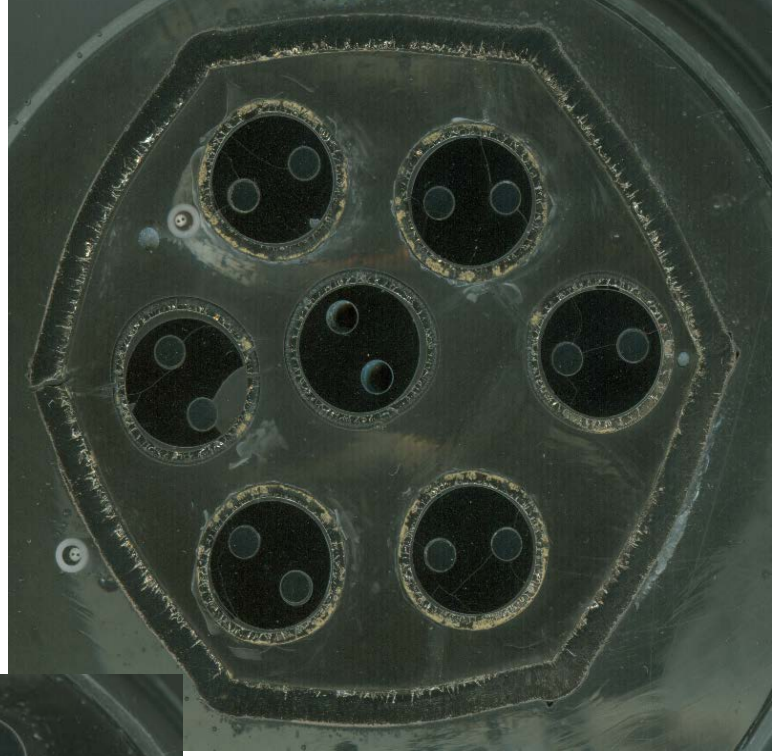


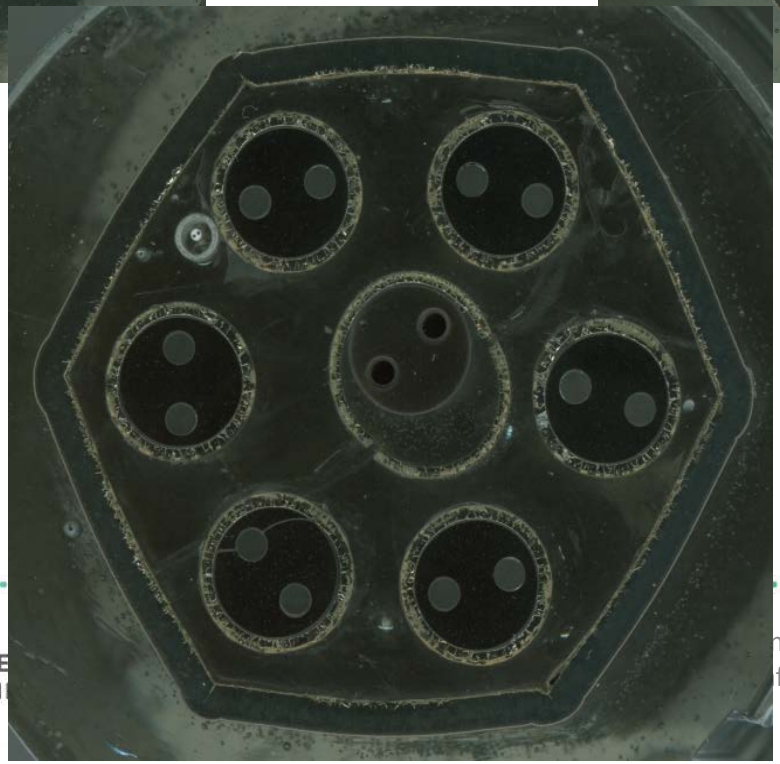


Total H_2 generation ≈ 11 g

Cross sections of bundle







250 mm

In lower section:
-strong oxidation
-rods moved from the original position

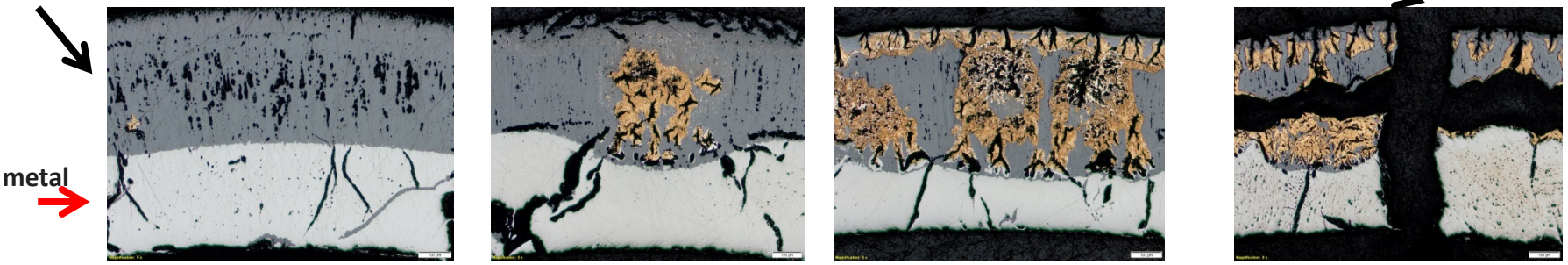
350 mm

Upper section:
-strong nitriding

Inhomogeneous nitriding+ oxidation (stagnant zones with low gas velocity)

550 mm

Cross sections of rods



SUMMARY

- The CODEX-NITRO test was successfully performed on the 7th December 2018.
- The experiment was carried out with temperature conditions which were close to the specified ones by pre-test calculations.
- Pre-oxidation was carried out in high flowrate steam with maximum temperature above 800 °C.
- The duration of steam-nitrogen phase was 1.5 hour and the maximum cladding temperature was slightly above 1750 °C.
- The outlet gas composition showed that during the steam-nitrogen phase steam starvation and nitriding conditions were established. The consumption of nitrogen indicated the formation of nitrides, too.

SUMMARY

- The temperature profile significantly changed during the excursion phase: the maximum temperature moved from the upper section to the middle of bundle due to the intense chemical interactions in the less oxidised central part.

- Cool-down of the bundle was performed in argon in order to provide information on bundle state before quench.

FURTHER ACTIONS

- The CODEX-SBO (Station Black Out) test was successfully performed on the 11th October 2019 – data evaluation (T_{max}=1900 °C)

ACKNOWLEDGEMENTS

The CODEX-NITRO experiment was supported by the National Research, Development and Innovation Fund of Hungary (contract number: NVKP_16-1-2016-0014).



NATIONAL RESEARCH, DEVELOPMENT AND INNOVATION OFFICE
HUNGARY

PROJECT FINANCED FROM THE NRDI FUND

MOMENTUM OF INNOVATION


Thank you for your attention!
E110 3/500 mm
Magnification: 5 x
100 µm

Experimental investigation and modelling of the Ag-Cd-In system

Barrachin M.[1], Gajavalli K.[1], Decreton A.[1], Mikaelian G.[2], Rogez J.[2], Benigni P.[2], Fischer E.[3]

1- IRSN/PSN-RES, Cadarache, 13115 Saint-Paul-lez-Durance, France
2- IM2NP Aix Marseille Univ, Univ Toulon, CNRS, 13397 Marseille, France
3- Université Grenoble Alpes, CMTC, SIMAP, 38000 Grenoble, France

In the case of a severe accident occurring on a Pressurized Water Reactor, the silver indium-cadmium absorbing alloy (80 wt% Ag, 15 wt% In, 5 wt% Cd) is ejected from the control rods ruptured by overpressurization. The ejected alloy can affect the Zircaloy cladding of the surrounding fuel rods and then impact the core degradation progression as well as the aerosol concentration and the fission product speciation (in particular iodine) in the containment atmosphere. To quantitatively evaluate these effects it is required to have a reliable description of the liquid fraction as well as the vapour pressure as a function of temperature and composition. In this context, the thermodynamic study of the Ag-Cd-In ternary system and in particular of the liquid phase and its associated equilibria is a necessary step. Liquidus temperatures were measured by the interrupted differential thermal analysis method (IHDTA) for a series of ternary alloys in the cadmium- and indium-rich regions. It will be shown that the IHDTA technique permits better equilibrium conditions than for classical DTA, and then more reliable measurements for the ternary compositions. These liquidus determinations have been combined with the existing literature data and the measurements of mixing enthalpy of liquid phase previously obtained to propose for the first time a Calphad modelling of the Ag-Cd-In ternary system. An overall consistency between the experiments and the modeling has been obtained.


TOSHIBA

IRSN
INSTITUT
DE RADIOPROTECTION
ET DE SÛRETÉ NUCLÉAIRE

Experimental Investigation of the Ag-Cd-In System

M. Barrachin, K. Gajavalli, A. Decreton (IRSN)

P. Bénigni, G. Mikaelian, J. Rogez (IM2NP, Marseille)

E. Fischer (SIMAP, Grenoble)

QUENCH Workshop | 24th October 2019 | Karlsruhe, Germany

Overview of the presentation

Context

Experiments on the Ag-Cd-In system

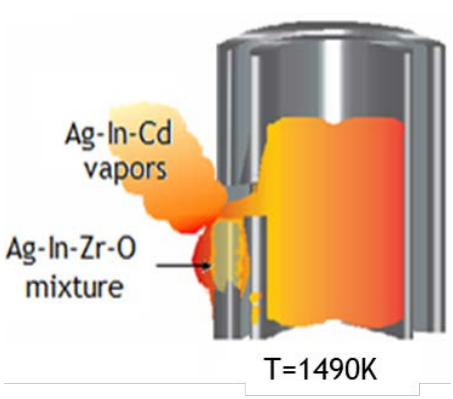
Modelling

Comparison with previous works

Conclusion

Control Rod Degradation During a Severe Accident in PWR

Ag – 80.8 at.%, In -14.3 at.%, Cd – 4.9 at.%, (SIC alloy)



Phenomenology

- In a severe accident, the control rod alloy partially liquefies,
- $(SIC)_{liq,T}$ interaction with Zry-4 due to failure of SS cladding,
- SIC constituents unconfined,
- Large amount of Ag-Cd-In aerosols generated,
- Impact on the fission products and iodine chemistry.

→ Issue: quantification of the Ag, Cd, In releases from Ag-Cd-In-Zr-O melts.

Strategy to model the complex system

- To obtain thermodynamic data in the sub-systems
- Calphad modeling of the binary and ternary sub-systems

Sub-systems poorly known

- Ag-Cd-In
- Ag-Zr
- In-Zr
- In_2O_3-ZrO_2

Ag-Cd-In Ternary System

State of the art

- Extension of the ternary solid solution based on Ag at two temperatures
- Melting point for the nominal control rod composition
- ΔH_{mix} in the ternary liquid for 5 isopleth sections by drop dissolution calorimetry at 723K
- Few uncertain liquidus measurements by DTA

This work

- Determine the liquidus surface to achieve a better description of the phase diagram
- Experimental technique : DTA

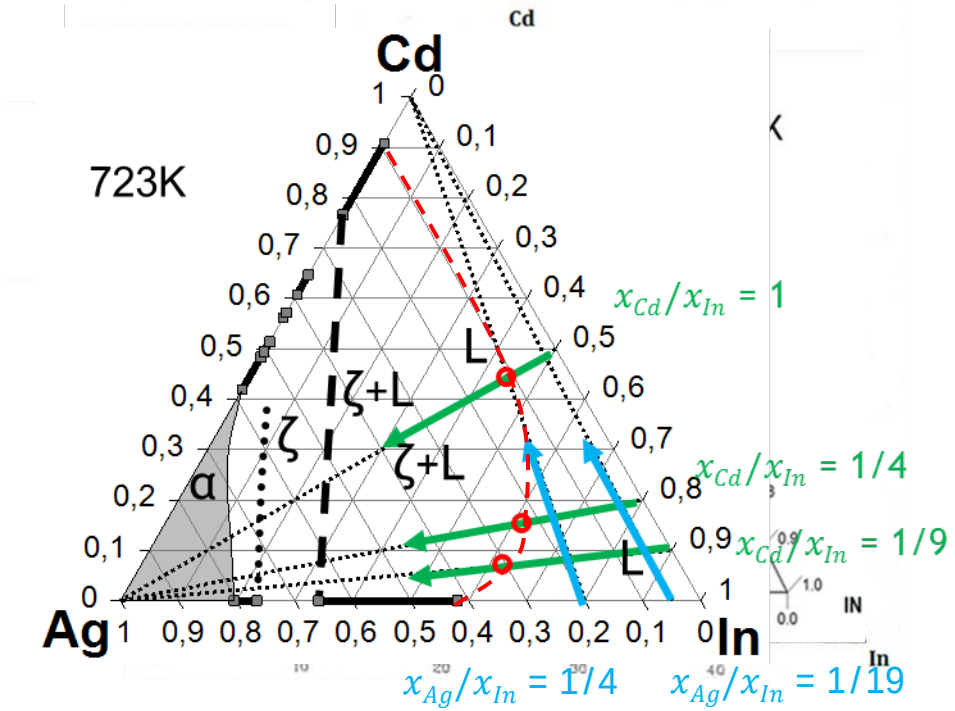


Figure adopted from ASME handbook of Phase Diagrams based on the work of: Snyder, H. J., AIME Metall. Soc. Trans. 239, 1385–1391 (1967).

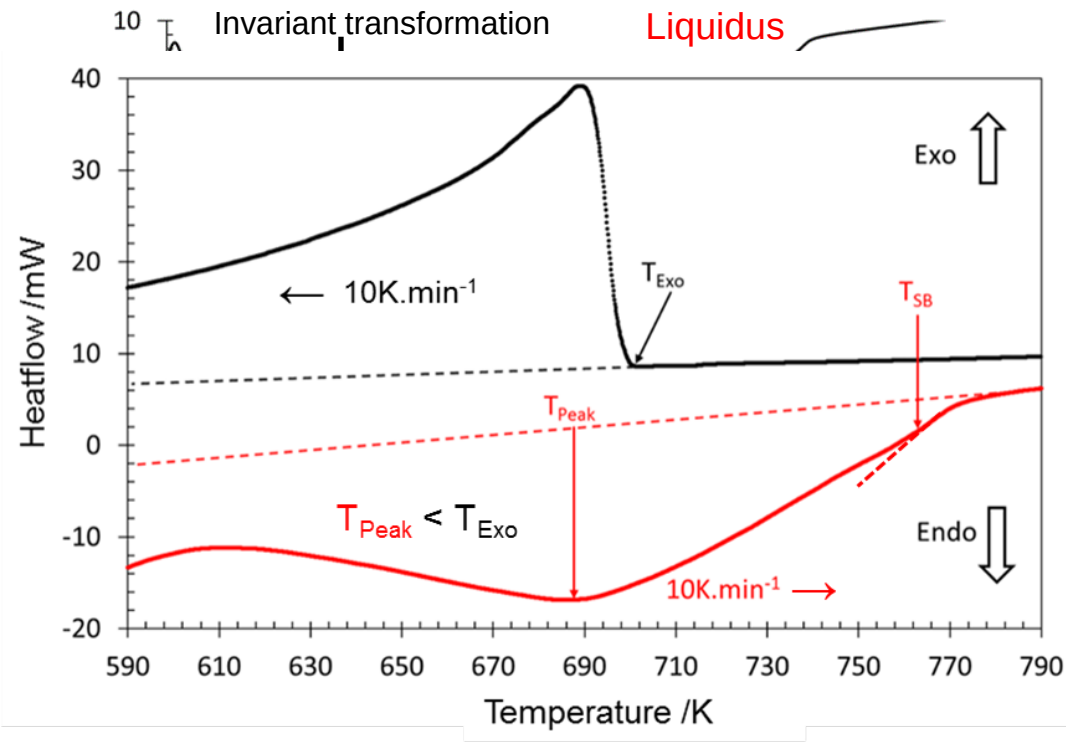
[1] Harrocks P.J., Thesis University of Manchester, 1991.
[2] Bowsher B.R., Jenkins R.A., Nichols A.L., Rowe N.A., Simpson J.A.H., UKAEA, 1986.
[3] Peña, D. A., Nucl. Technol. 84, 128–151 (1988).
[4] Steinbrück M., Stegmaier U., AMNT, Berliner Congress Center: Jahrestagung Kerntechnik, 2010.
P. Benigni, S. Hassam, A. Degreton, C. Mikaelian, K. Gajavalli, M. Barrachin, E. Fischer, J. Rogez, J. Chem. Thermodyn. **107**, 207–215 (2017).
2016.

Classical DTA

Protocol

- $T_{room} \rightarrow T_{max} \rightarrow T_{room}$
- Rates: 10, 5, 2, 1, 0.5 K/min
- True liquidus = extrapolating measured liquidus values to zero rate

Ag-35 at.%, Cd-5 at.%, In-60 at.%



Problems

- Liquidus temperature is underestimated on continuous cooling due to the undercooling required to nucleate the primary solid phase
- Liquidus temperature is hard to detect on continuous heating

Improvements for the Liquidus Detection

- Ag-Cd-In alloys likely prone to microsegregation
- Composition gradients in the solid phase during thermal analysis at constant rate
- Better estimation could be obtained by temperature cycling close to the estimated liquidus temperature [1,2]

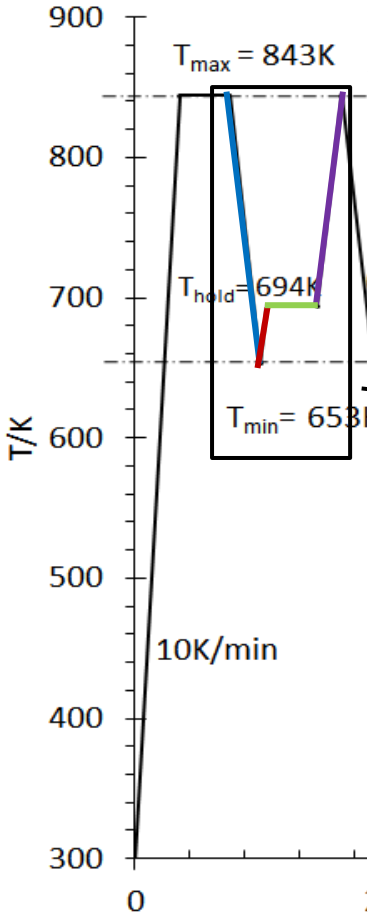
  → Interrupted Heating DTA (IHDTA)

Principle of the « new » method

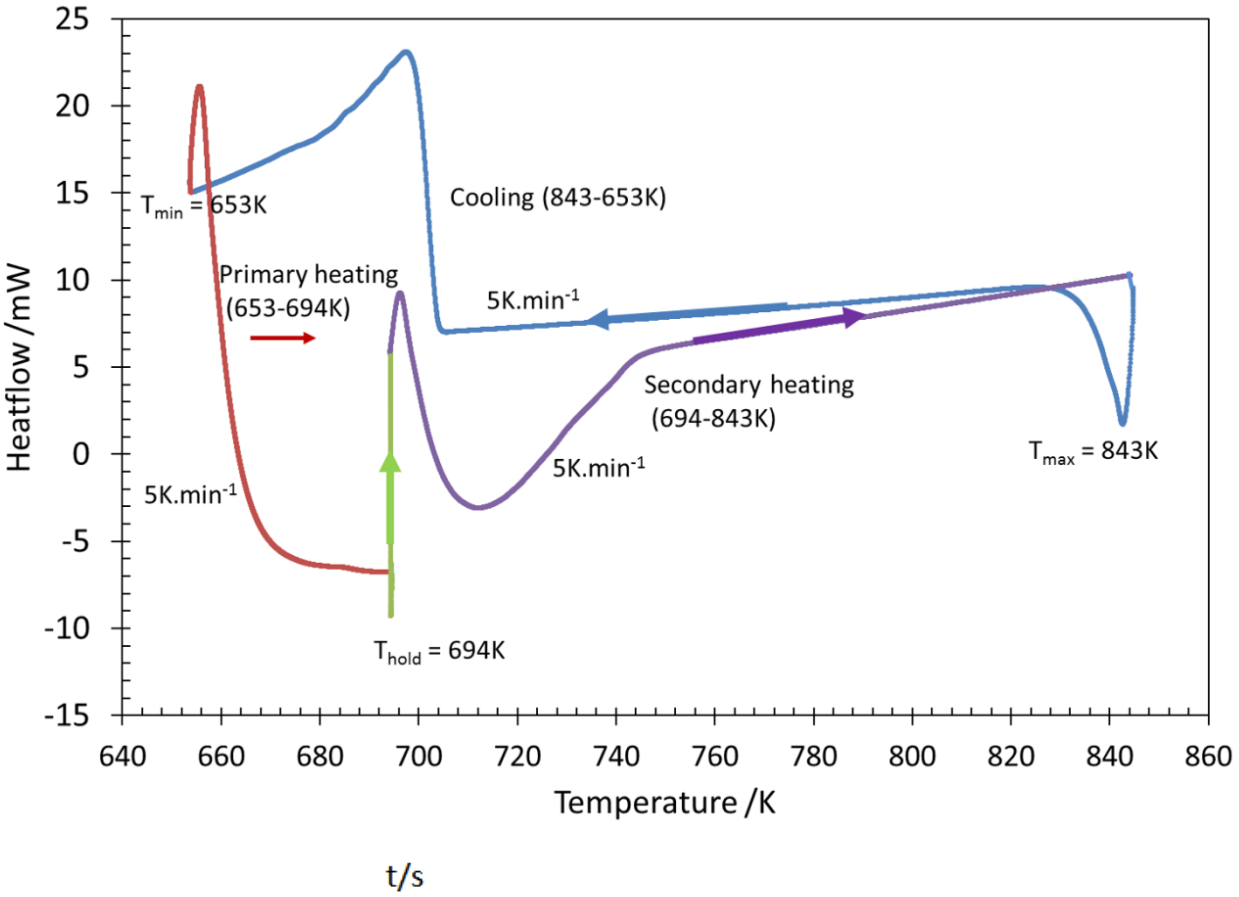
- Sample is equilibrated by isothermal holding at temperatures close to the liquidus before final heating at constant rate
- Diffusion is promoted and facilitates homogenization of the alloy

[1] R.I. Wu and J.H. Perepezko, MMT, 31(2000), 497
[2] K.W.Moon, W.J.Boettinger, U.R.Kattnet, JEM, Vol. 29(2000), 10

Interrupted Heating DTA (IHDTA) - Protocol



Ag-35 at.%, Cd-5 at.%, In-60 at.%

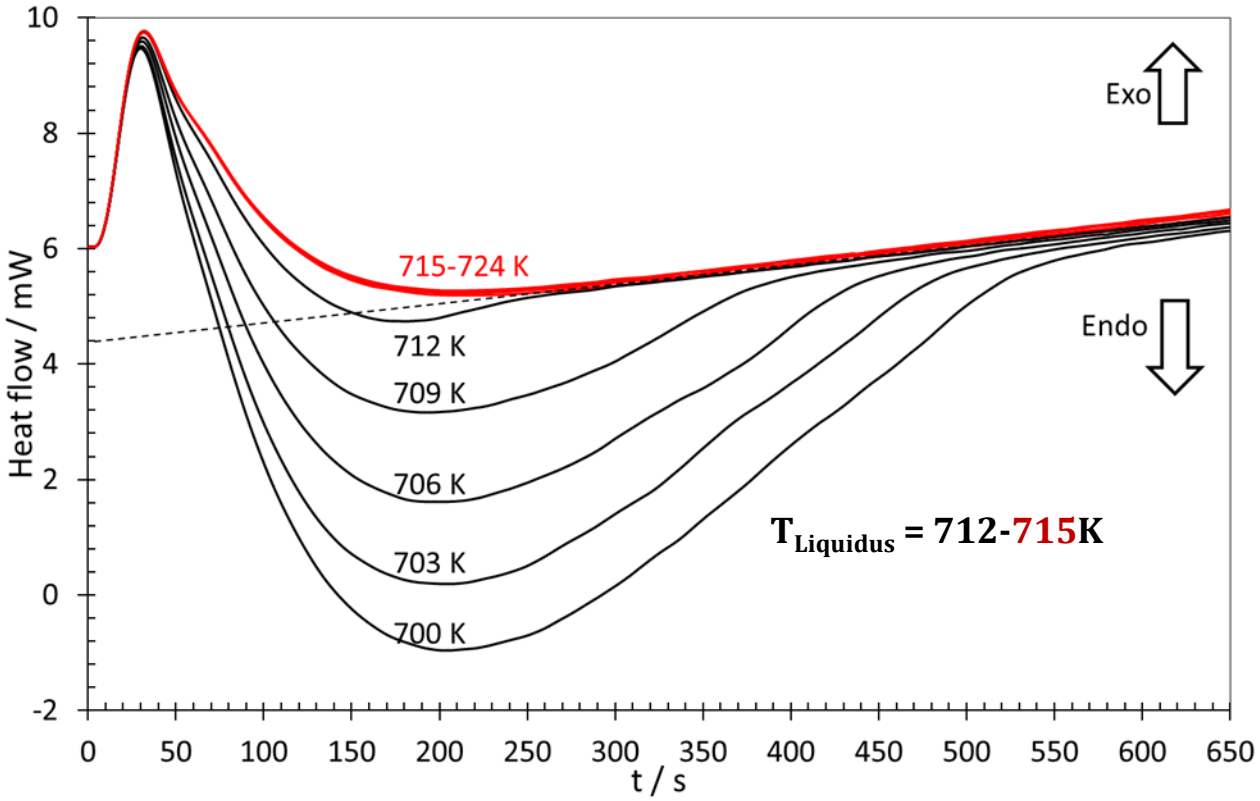


IHDTA: Method of Liquidus Detection

Analysis of secondary heating curves

- The endothermic deviation is used to determine the liquidus,
- If the deviation is absent, a fully liquid state is implied.

Ag-35 at.%, Cd-5 at.%, In-60 at.%



IHDTA: Results and Comparison

- $T_{liquidus}$ measured for 9 ternary and 1 binary compositions by IHDTA/DTA,
- Of these, 5 compositions measured by both techniques
- Significant improvement by adopting the new IHDTA protocol
  - Our data invalidate the measurements of Robinson and Jones [1]
    - → For the $Ag_{7.5}Cd_{23.1}In_{69.4}$ composition, liquidus temperature of Jones is 80K below our measured value

[1] P.J. Horrocks, Phase Diagram and Thermodynamics of the Ag–Cd–In Ternary Alloy Systems, Ph D. Thesis, Manchester University, 1991.

CALPHAD Modelling of the Ag-Cd-In System

- Description of solution phases ($\phi = \alpha, \zeta$ or L)

Gibbs energy G^{ϕ} for each solution phase

$$G^{\phi} = G^{\phi,ref} + G^{\phi,id} + G^{\phi,exbin} + G^{\phi,exter}$$

$$G^{\phi,ref} = x_{Ag}\,{}^{0}G^{\phi}_{Ag} + x_{Cd}\,{}^{0}G^{\phi}_{Cd} + x_{In}\,{}^{0}G^{\phi}_{In}$$

Gibbs energy of mechanical mixture of Ag, Cd, In

$$G^{\phi,id} = RT\left(x_{Ag}\ln x_{Ag} + x_{Cd}\ln x_{Cd} + x_{In}\ln x_{In}\right)$$

Ideal entropy of mixing

$$G^{\phi,exbin} = x_{Ag}x_{Cd}\sum_{v} {}^{v}\boldsymbol{L}^{\boldsymbol{\phi}}_{\boldsymbol{Ag,Cd}}\left(x_{Ag} - x_{Cd}\right)^{v} +$$

$$x_{Ag}x_{In}\sum_{v} {}^{v}\boldsymbol{L}^{\boldsymbol{\phi}}_{\boldsymbol{Ag,In}}\left(x_{Ag} - x_{In}\right)^{v} + x_{Cd}x_{In}\sum_{v} {}^{v}\boldsymbol{L}^{\boldsymbol{\phi}}_{\boldsymbol{Cd,In}}\left(x_{Cd} - x_{In}\right)^{v}$$

Excess binary terms, adjusted to reproduce the established information for Ag-Cd, Ag-In and Cd-In binary systems

- Adjustment of ternary excess parameters

$$G^{\phi,exter} = x_{Ag}x_{Cd}x_{In}\left(x_{Ag}\,{}^{\boldsymbol{Ag}}\boldsymbol{L}^{\boldsymbol{\phi}}_{\boldsymbol{Ag,Cd,In}} + x_{Cd}\,{}^{\boldsymbol{Cd}}\boldsymbol{L}^{\boldsymbol{\phi}}_{\boldsymbol{Ag,Cd,In}} + x_{In}\,{}^{\boldsymbol{In}}\boldsymbol{L}^{\boldsymbol{\phi}}_{\boldsymbol{Ag,Cd,In}}\right)$$

α Phase

$${}^{Ag}L^{\alpha}_{Ag,Cd,In} = {}^{Ag}a^{\alpha} + {}^{Ag}b^{\alpha}T$$
$${}^{Cd}L^{\alpha}_{Ag,Cd,In} = {}^{Cd}a^{\alpha} + {}^{Cd}b^{\alpha}T$$
$${}^{In}L^{\alpha}_{Ag,Cd,In} = {}^{In}a^{\alpha} + {}^{In}b^{\alpha}T$$

ζ Phase

$${}^{Ag}L^{\zeta}_{Ag,Cd,In} = {}^{Ag}a^{\zeta} + {}^{Ag}b^{\zeta}T$$
$${}^{Cd}L^{\zeta}_{Ag,Cd,In} = {}^{Cd}a^{\zeta} + {}^{Cd}b^{\zeta}T$$
$${}^{In}L^{\zeta}_{Ag,Cd,In} = {}^{In}a^{\zeta} + {}^{In}b^{\zeta}T$$

Liquid Phase

$${}^{Ag}L^{L}_{Ag,Cd,In} = {}^{Ag}a^{L} + {}^{Ag}b^{L}T$$
$${}^{Cd}L^{L}_{Ag,Cd,In} = {}^{Cd}a^{L} + {}^{Cd}b^{L}T$$
$${}^{In}L^{L}_{Ag,Cd,In} = {}^{In}a^{L} + {}^{In}b^{L}T$$

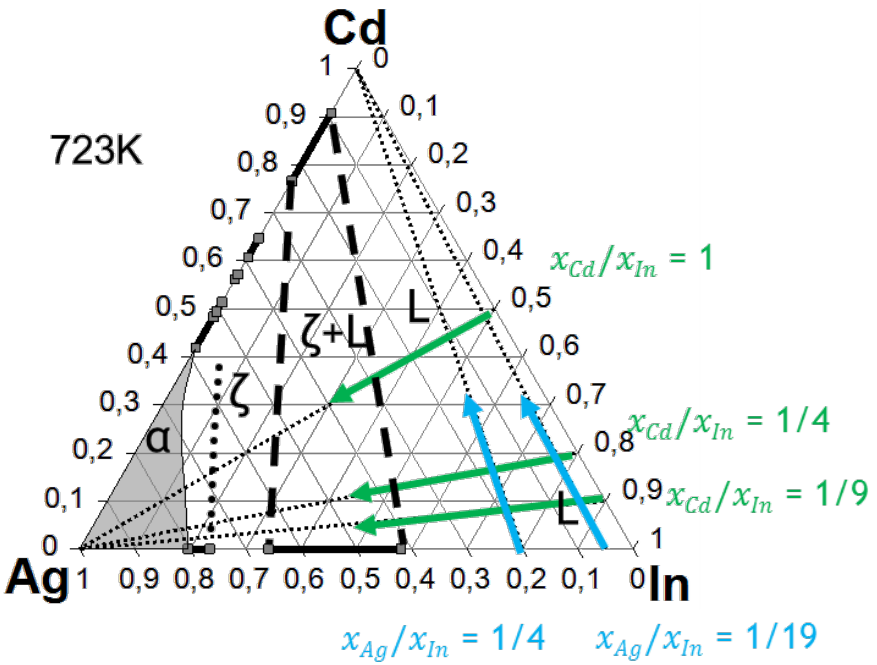
18 adjustable parameters

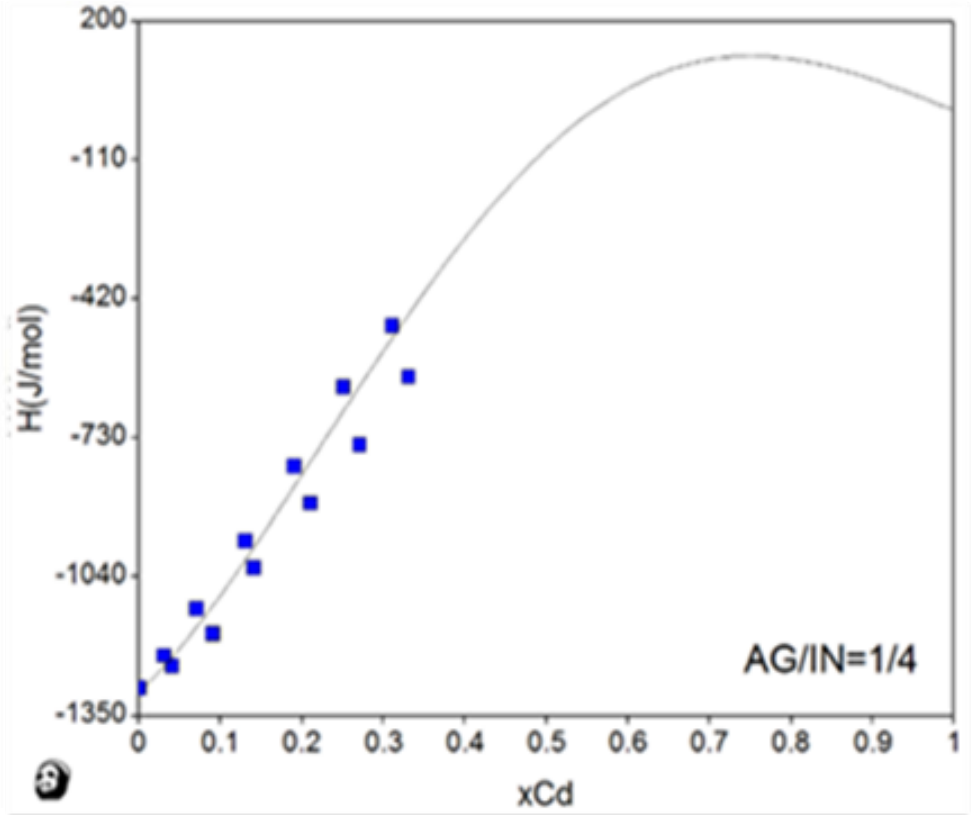
11 optimized parameters

$${}^{Ag}a^{\alpha} = {}^{Cd}a^{\alpha} = {}^{In}a^{\alpha}, \quad {}^{Ag}b^{\alpha} = {}^{Cd}b^{\alpha} = {}^{In}b^{\alpha}, \quad {}^{Ag}b^{\zeta} = {}^{Cd}b^{\zeta} = {}^{In}b^{\zeta} = 0$$

CALPHAD Modelling Results (1)

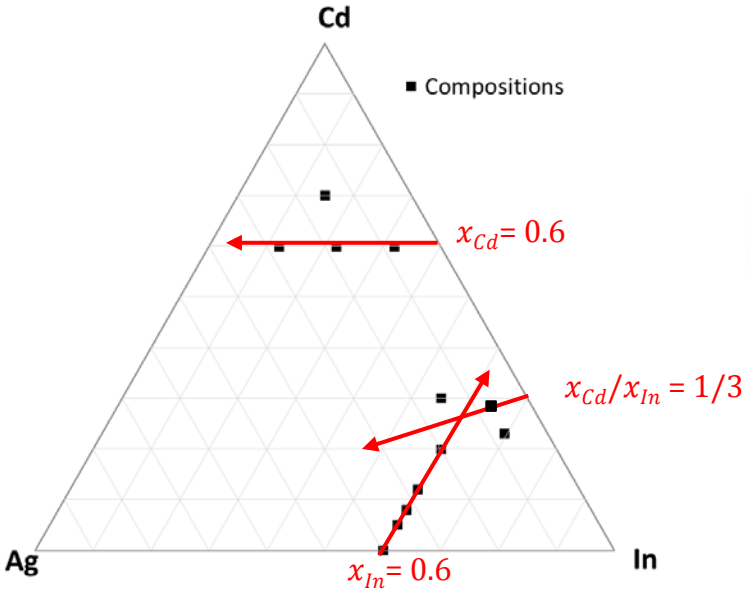
Optimization of the enthalpy terms of the Gibbs energy of the liquid phase on the basis of previous calorimetric experimental data

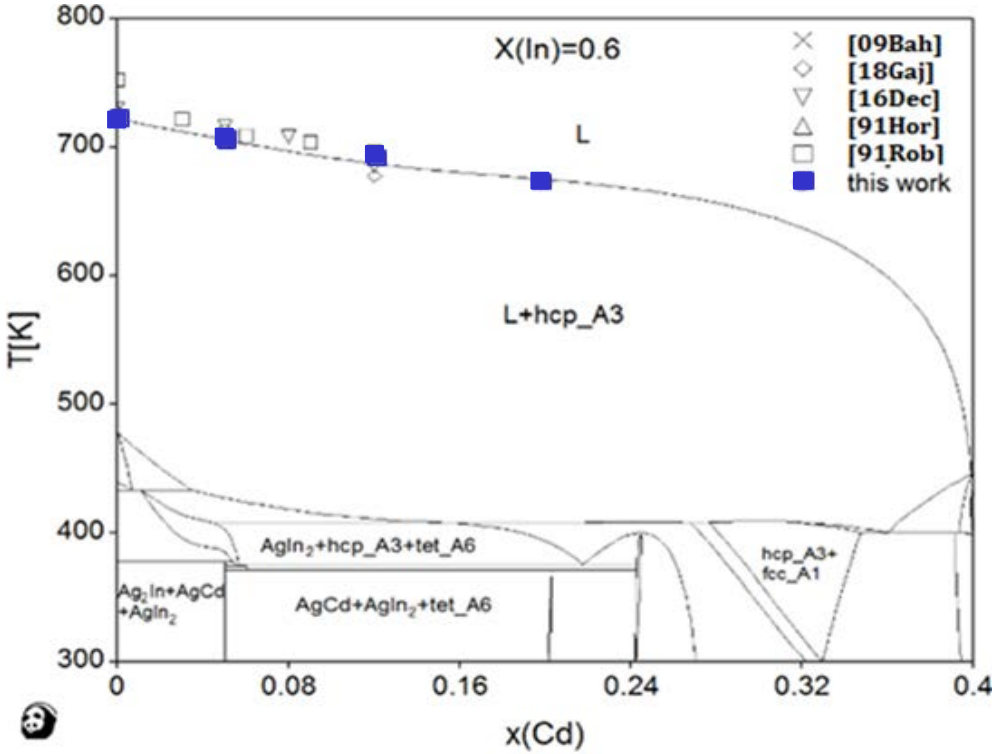




CALPHAD Modelling Results (2)

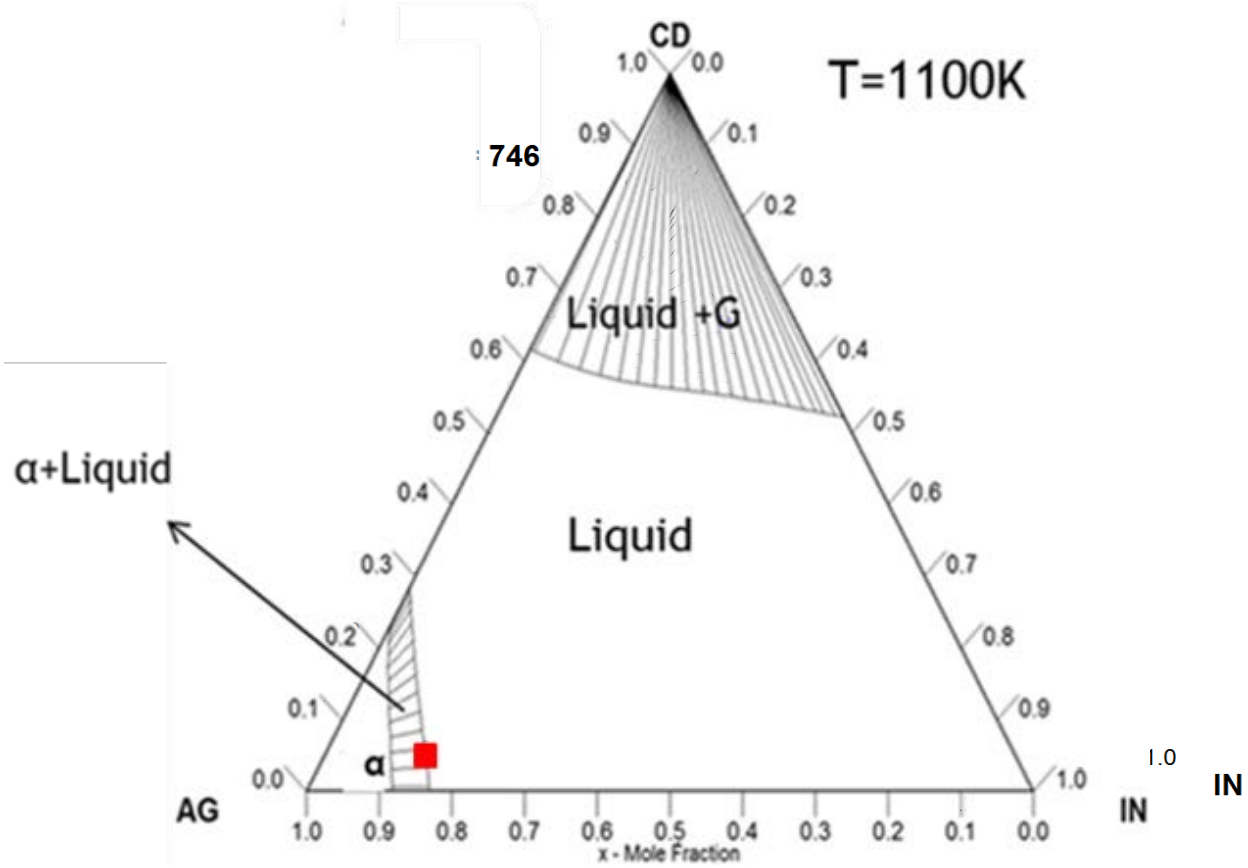
Entropic terms of the liquid phase optimized using liquidus experimental data



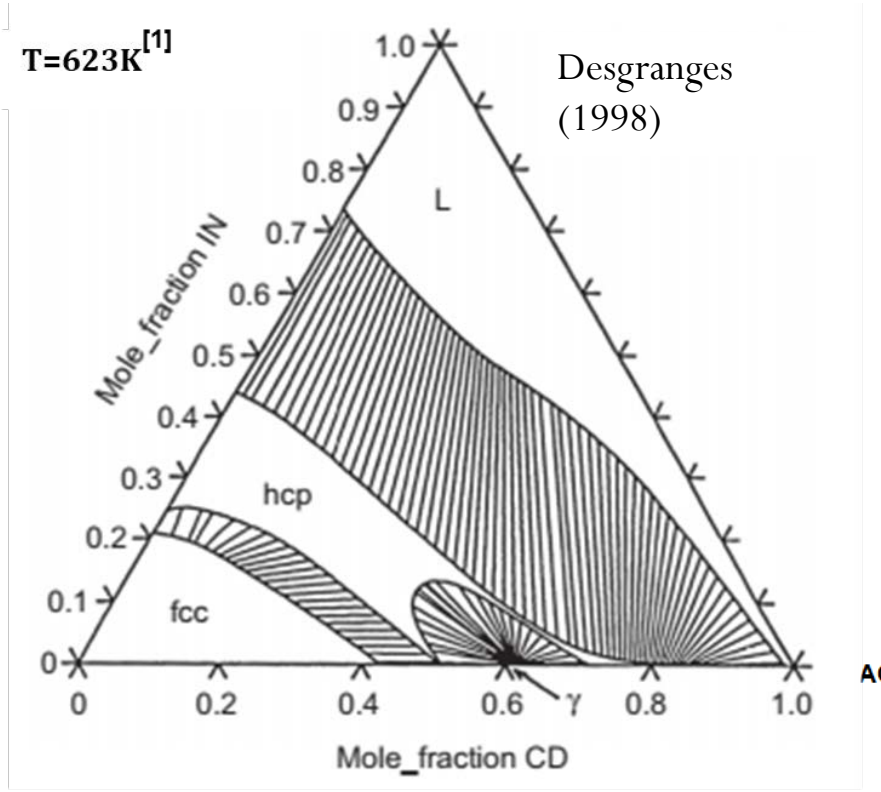


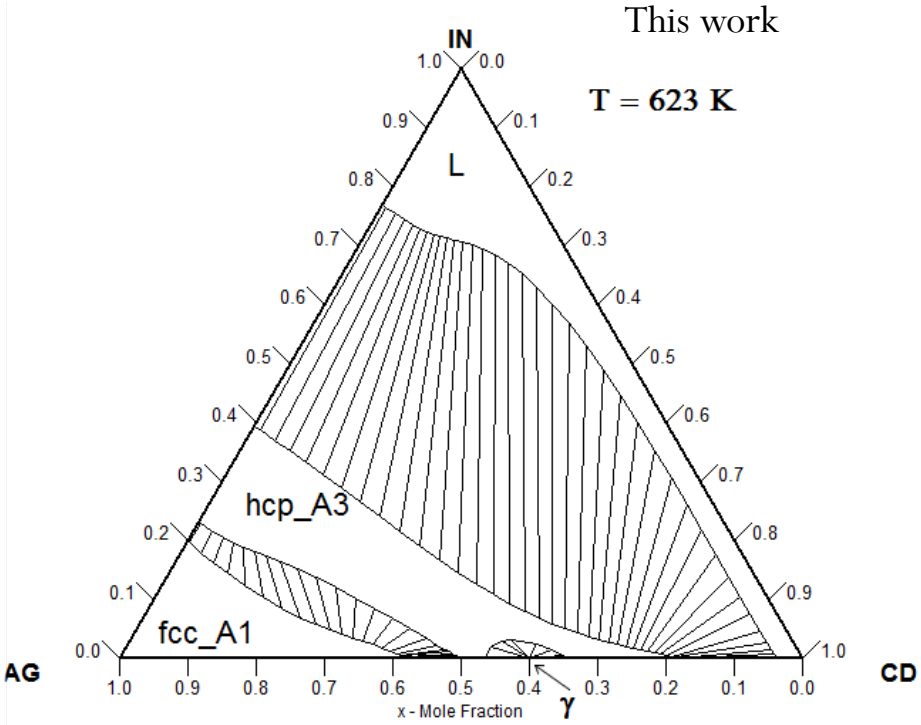
CALPHAD Modelling Results (3)

Isothermal sections



Comparison with previous works (Desgranges 1998)





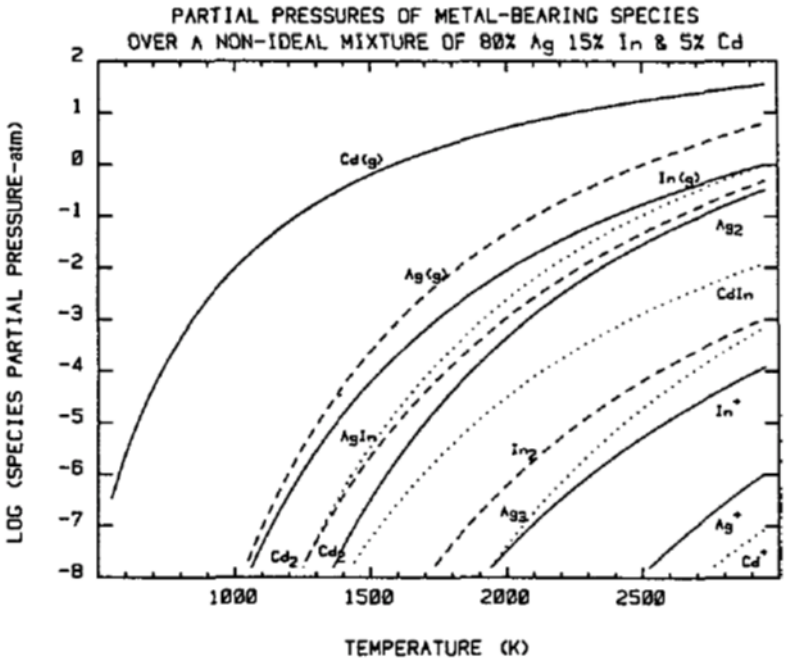
Better description of the (L+fcc) and (L+hcp) equilibria relevant to severe accident phenomenology

[1] Desgranges C. Comprehension et Prediction du Comportement sous Irradiation Neutronique D'alliages Absorbants à Base d'Argent. PhD Thesis, Paris XI University- Orsay; 1998.

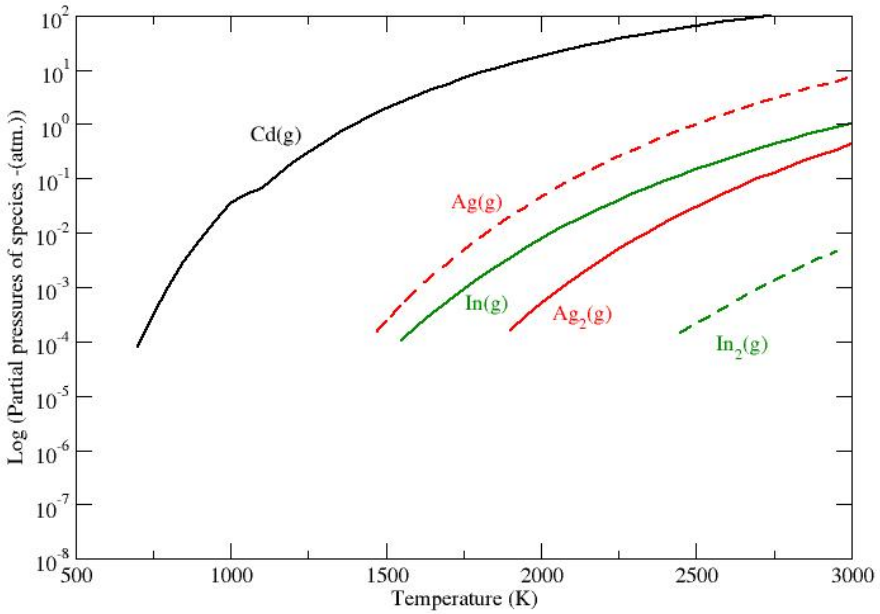
Comparison with previous works (Powers,1985) limited to the SIC composition

Vaporization of the SIC composition versus T

Powers 1985



This work



Consistency between both works but only checked for the SIC composition

Conclusions

Progress in investigation of the system in this work

- New experimental data in the Ag-Cd-In system
- First reliable ternary optimization of the system
- For the first time, possibility to consider thermodynamics both degradation and vaporization process of the SIC absorber rod

Next steps

- Impact of zirconium on the vaporization process
- To be implemented in the ASTEC code

IRSN
INSTITUT
DE RADIOPROTECTION
ET DE SÛRETÉ NUCLÉAIRE

Experimental Investigation of the Ag-Cd-In System

M. Barrachin, K. Gajavalli, A. Decreton (IRSN)

P. Bénigni, G. Mikaelian, J. Rogez (IM2NP, Marseille)

E. Fischer (SIMAP, Grenoble)

Physicochemical interaction between U-Zr-O melt and Fe-based structure during core degradation

Materials science and engineering department, Tokyo Institute of Technology
Ayumi ITOH

In the severe accident of a light water reactor, the fuel cladding materials significantly liquefies at high temperatures above approximately 2273 K then relocates downwardly forming the U-Zr-O melt and the $(U,Zr)O_{2-x}$ oxide, alpha-Zr(O) and metallic U-Zr phase are precipitated due to cooling down in the following transient. The melt has a contact with a steel structure such as the core support plate, fuel support pieces, penetrations of lower head and the lower head wall. Due to the decay heat from uranium, the melt itself produces a heat and possibly activates a chemical interaction with structures in the late phase of in-vessel core degradation. In this study, the physicochemical properties of the Fe-U-Zr-O system and related its subsystems have been investigated in order to understand the possible chemical reactions between the melt and Fe-base structures, i.e. SS. The thermodynamic calculation of the interaction between alpha-Zr(O) and Fe suggested the interaction could be exothermic at 1673 K in the case of O-poor and U-rich melt composition, which is even about 150 K lower than the melting point of iron. Moreover, the calculated heat was 10 - 30 kJ/mol that cannot be negligible compared to the latent heat of iron (13.8 kJ/mol). This result indicates that metallic rich U-Zr-O melt formation could accelerate the destruction of Fe-including structure. The calculation results of thermodynamic estimation with a small-scaled simulation of reaction will be presented in the workshop.



Physicochemical interaction between U-Zr-O melt and Fe-based structure during core degradation

A.Itoh and Y.Kobayashi (TITech)
N.Shirasu, Y.Nagae and M.Kurata (JAEA)

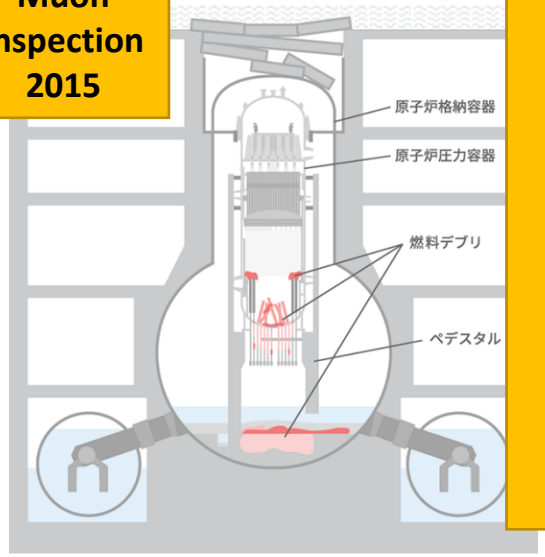
Presented at 25th international QUENCH workshop,
22th – 24th October 2019, Karlsruhe Institute of Technology, Germany.

Debris distribution estimation of FDNPP

- Distribution and status of degraded core materials has been investigated by TEPCO using muon/camera inspection.

Unit 1

Muon inspection 2015



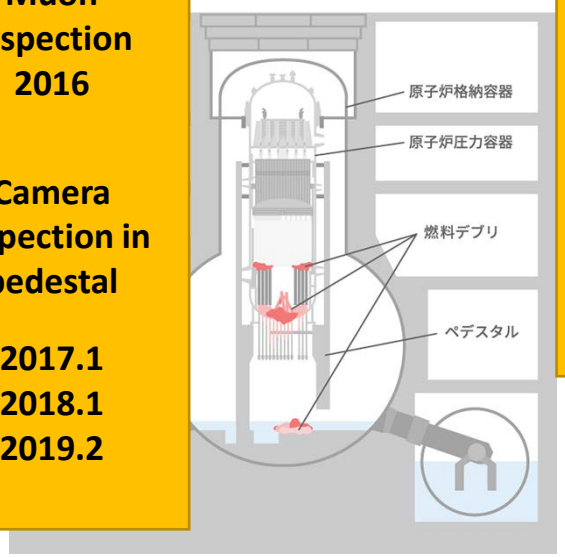
Mostly relocated to PCV

Unit 2

Muon inspection 2016

Camera inspection in pedestal

2017.1
2018.1
2019.2



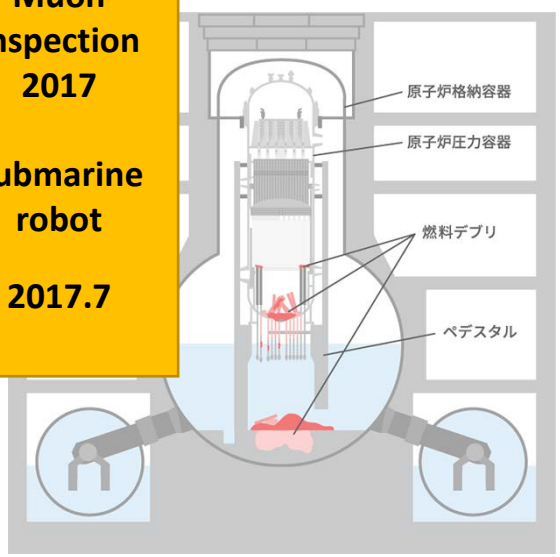
Mostly remains inside RPV and partially relocated to PCV

Unit 3

Muon inspection 2017

Submarine robot

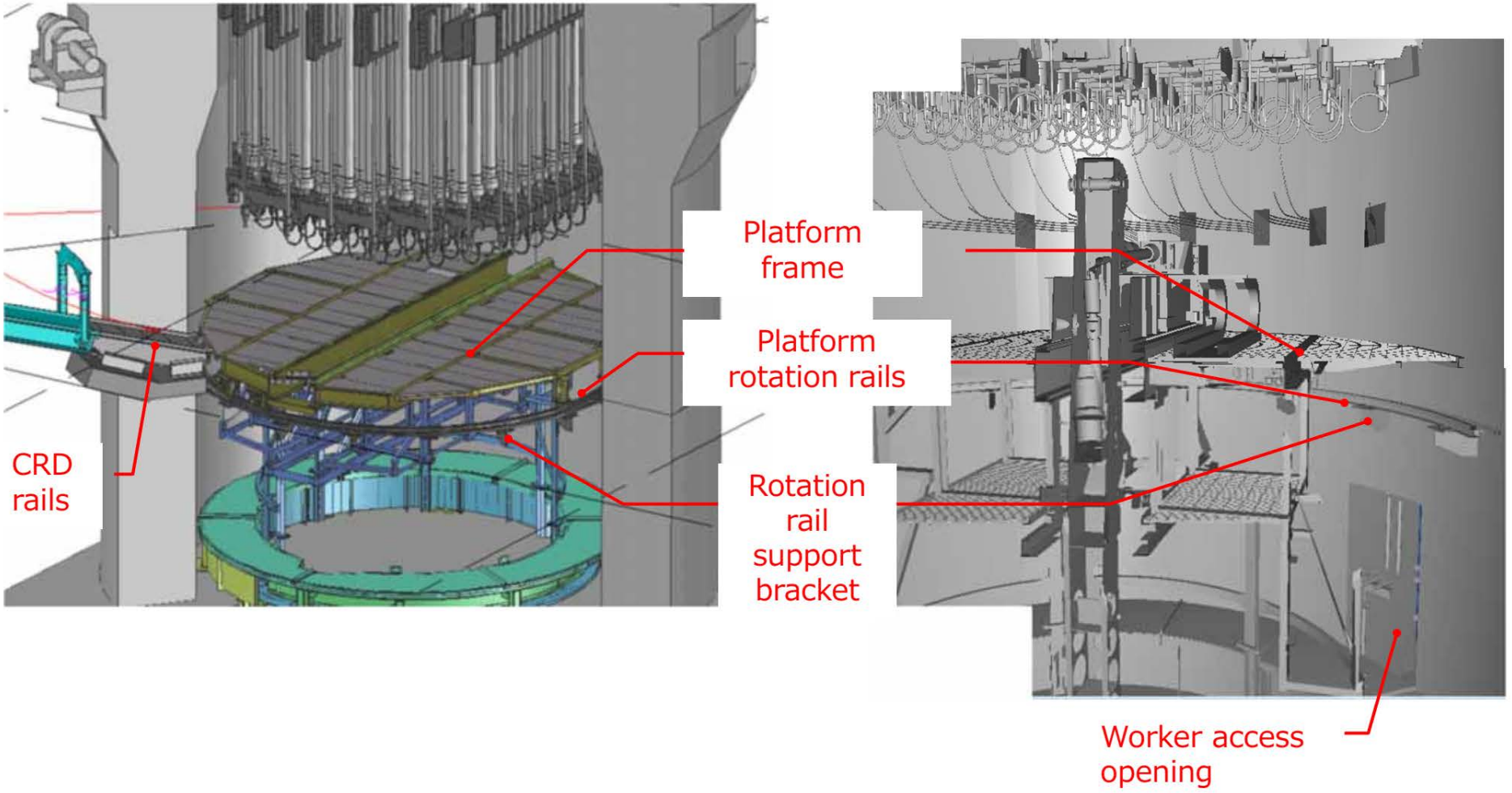
2017.7



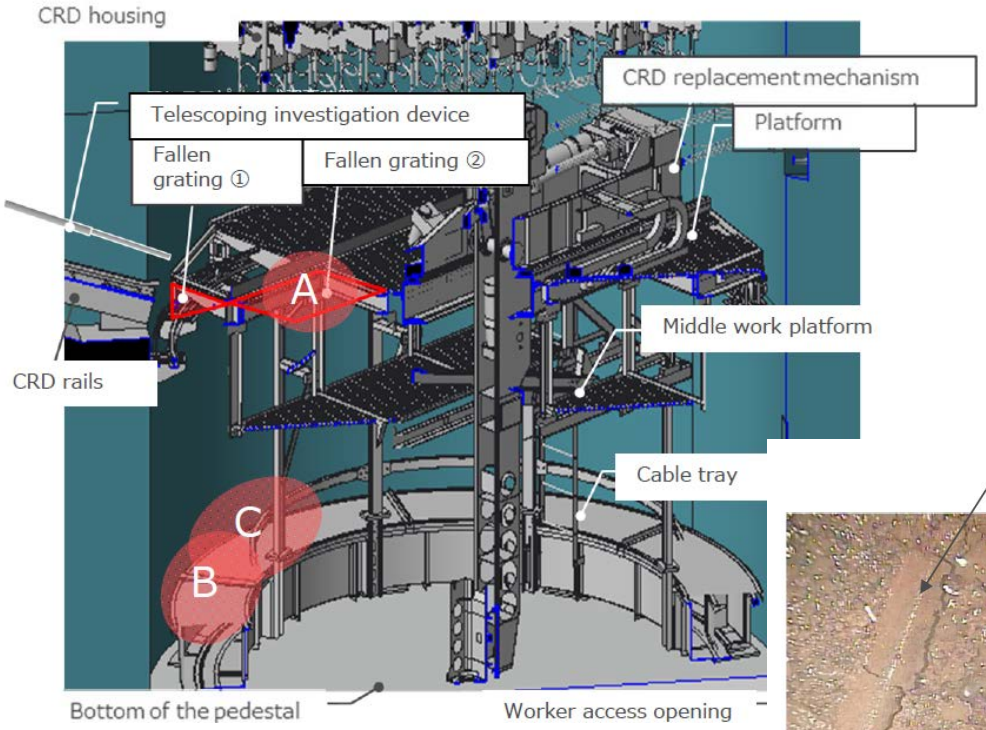
Remains partially in side RPV and “not small amount” relocated to PCV

Tokyo Electric Power Company Holdings, Inc., “Current status of fuel debris in Fukushima Daiichi nuclear power plants,” 2019, [Online] Available: http://www.tepco.co.jp/decommission/progress/retrieval/index-j.html (in Japanese).

Structure inside the pedestal



PCV inspection at unit 2 (Jan. 2018)



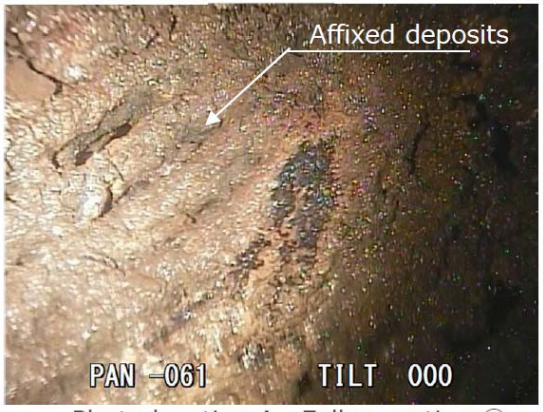


Photo location A Fallen grating ②

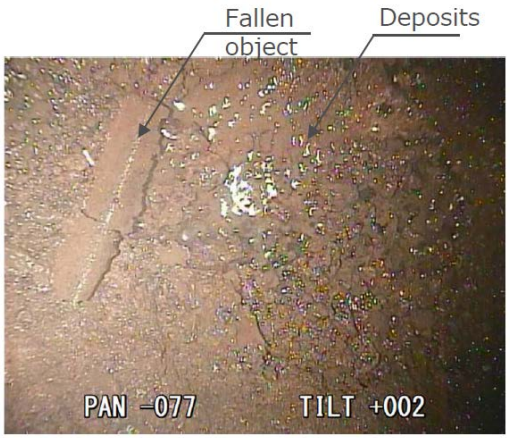


Photo location B Bottom of pedestal

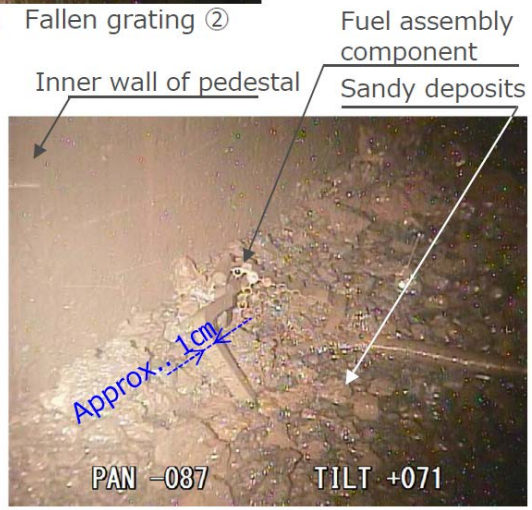


Photo location C Bottom of pedestal

- The entire bottom of the pedestal was covered with **sandy and clay-like deposits**. (app. 40-50 cm in thickness)
- Underneath the platform-fallen area, the accumulation is thicker than other areas.
- Some **fuel assembly components** (top tie-plate) have fallen to the bottom of the pedestal, which were found in the vicinity of these sandy and clay-like deposits.

These suggest that the deposits could relocate from RPV via the fallen part of platform, and a hole ~ ϕ=15 cm exists at the peripheral region to let the part of assembly pass through.

Tokyo Electric Power Company Holdings, Inc., "Fukushima Daiichi Nuclear Power Station Unit 2 Primary Containment Vessel Internal Investigation Results," 2018, [Online] Available: http://www.tepco.co.jp/en/nu/fukushima-np/handouts/2018/images/handouts_180201_01-e.pdf.

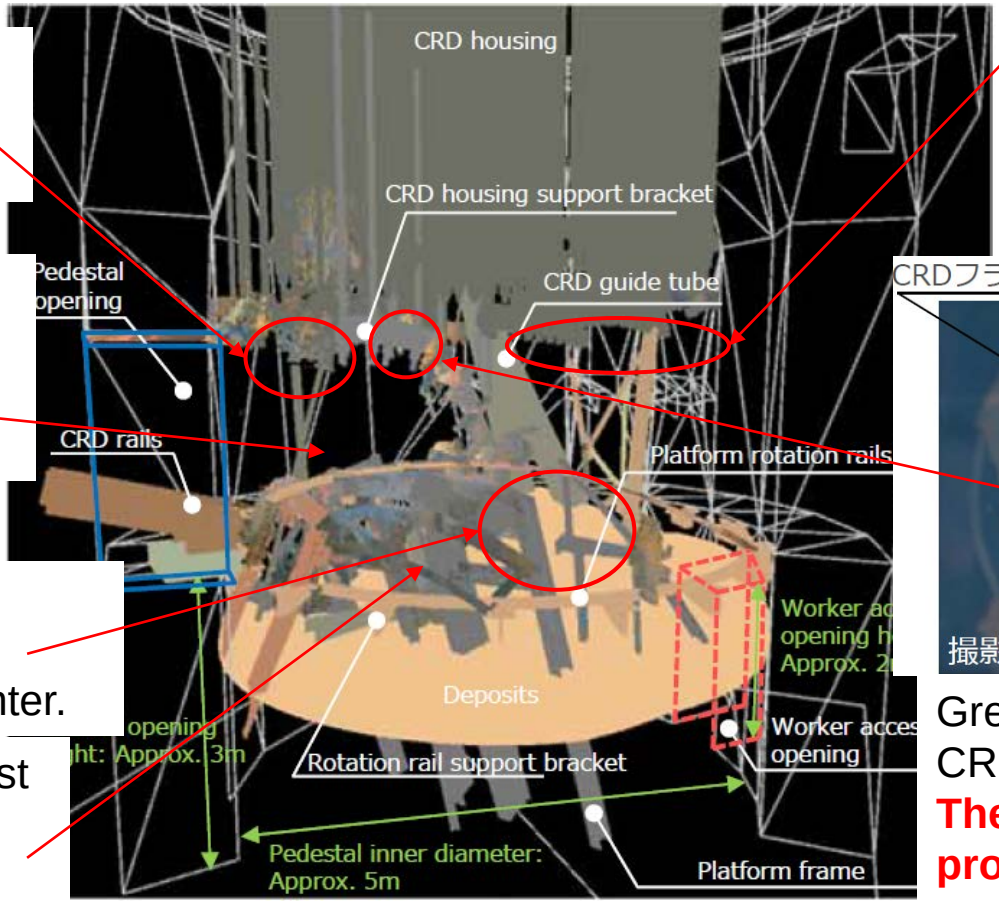
PCV inspection at unit 3 (Jul. 2017)

The bottom end of these CRDs looks lower than others.

The platform dislodged from the rail and a portion buried in deposits.

Mountain-like accumulation was observed in the center.

The deposits highest in the center with structural materials



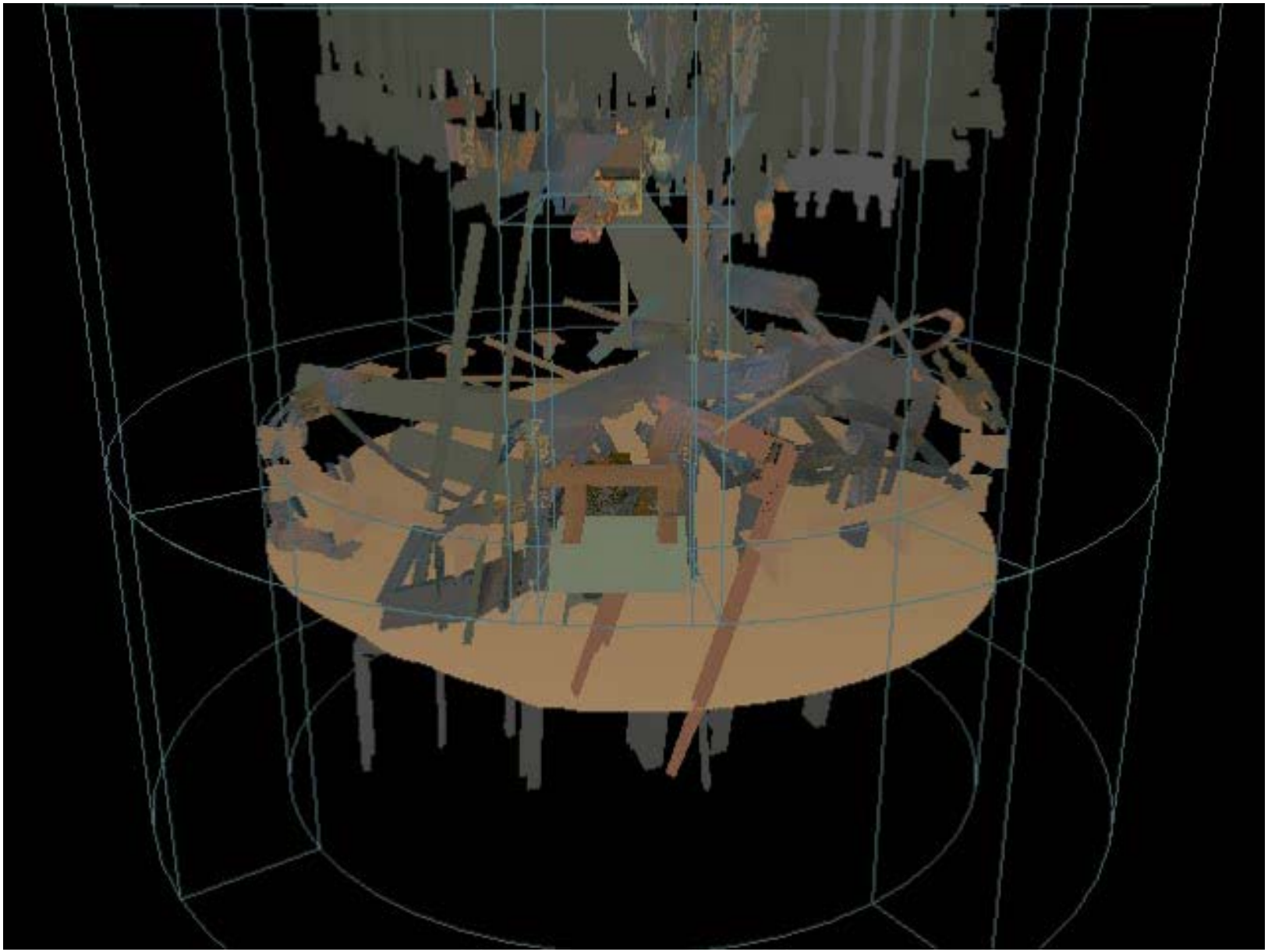
CRD support structure is mostly gone.



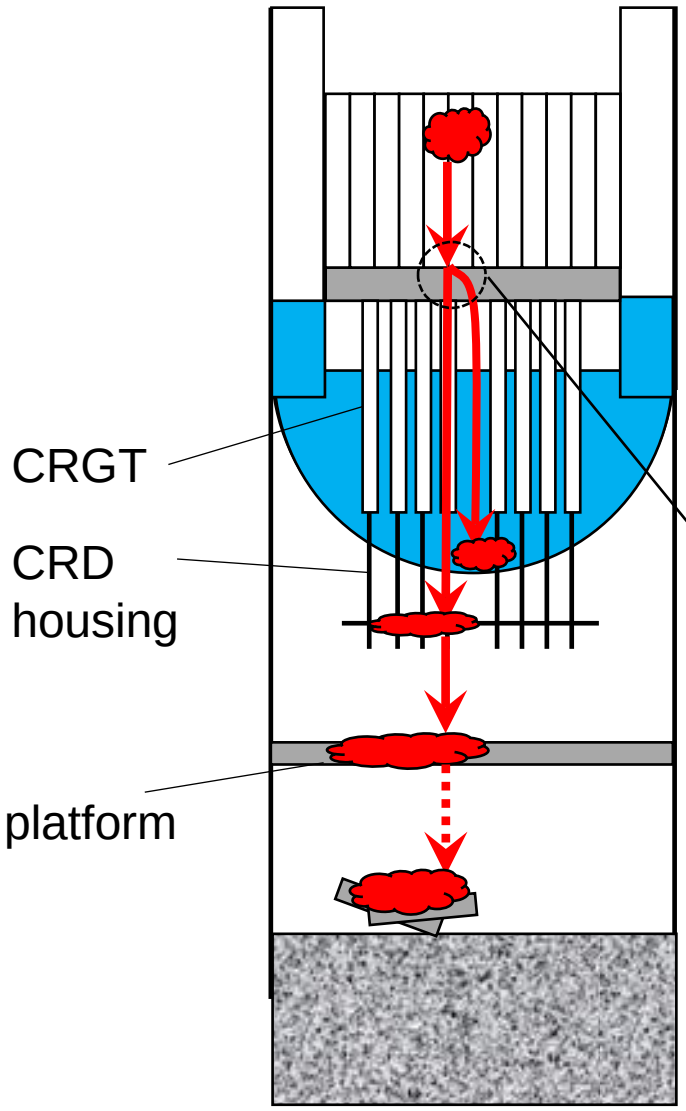
Grey material deposited on CRD flange.

The appearance might propose the high viscosity.

- ➔ **Considering the fact that the platform dislodged, the CRD support structure is mostly gone, the thick deposits is observed, it is suggested that molten material, containing fuel debris, could fall on top of the structures deposits.**
- ➔ **The appearance of thick accumulation might propose relatively lower temperature relocation of debris from RPV with several hours.**



Possible relocation scenario

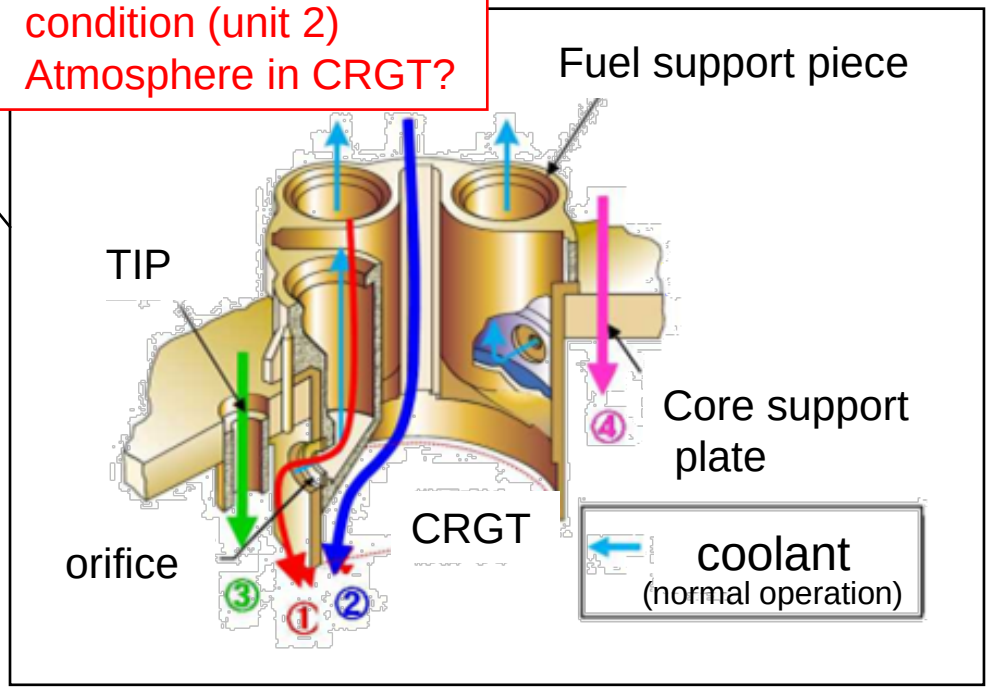


How is it possible for fuel-origin metallic melt to relocate outside RPV?

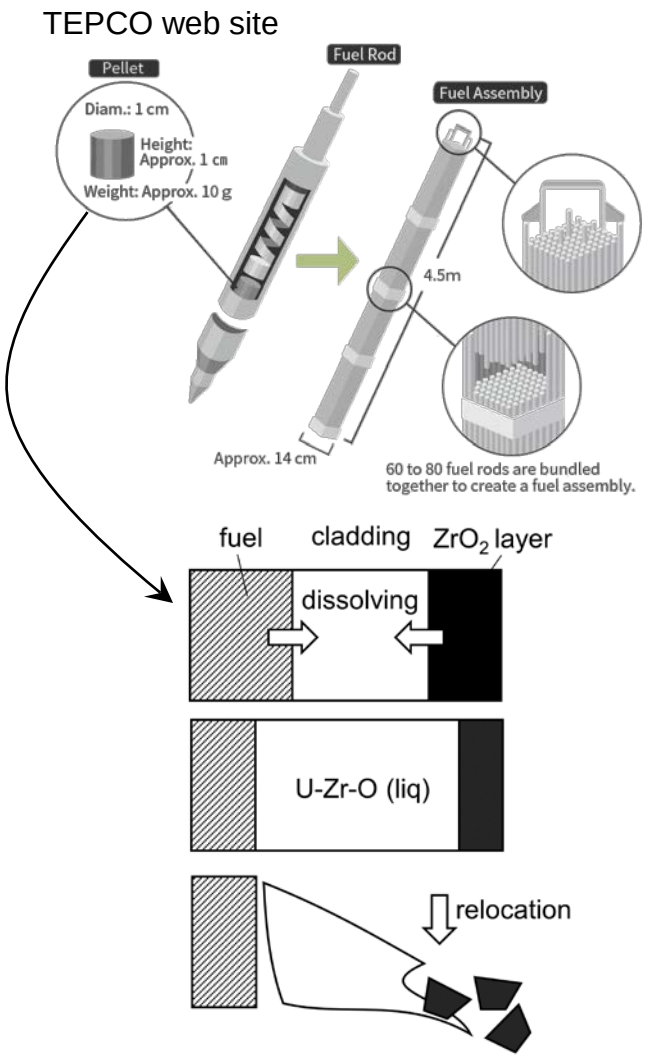
Molten fuel (U-Zr-O) →

- Core support plate →(failure)→ lower head
- Fuel support piece → lower head
- CRGT →(CRD housing) → CRD support

- ✓ Likely steam starved condition (unit 2)
- ✓ Atmosphere in CRGT?

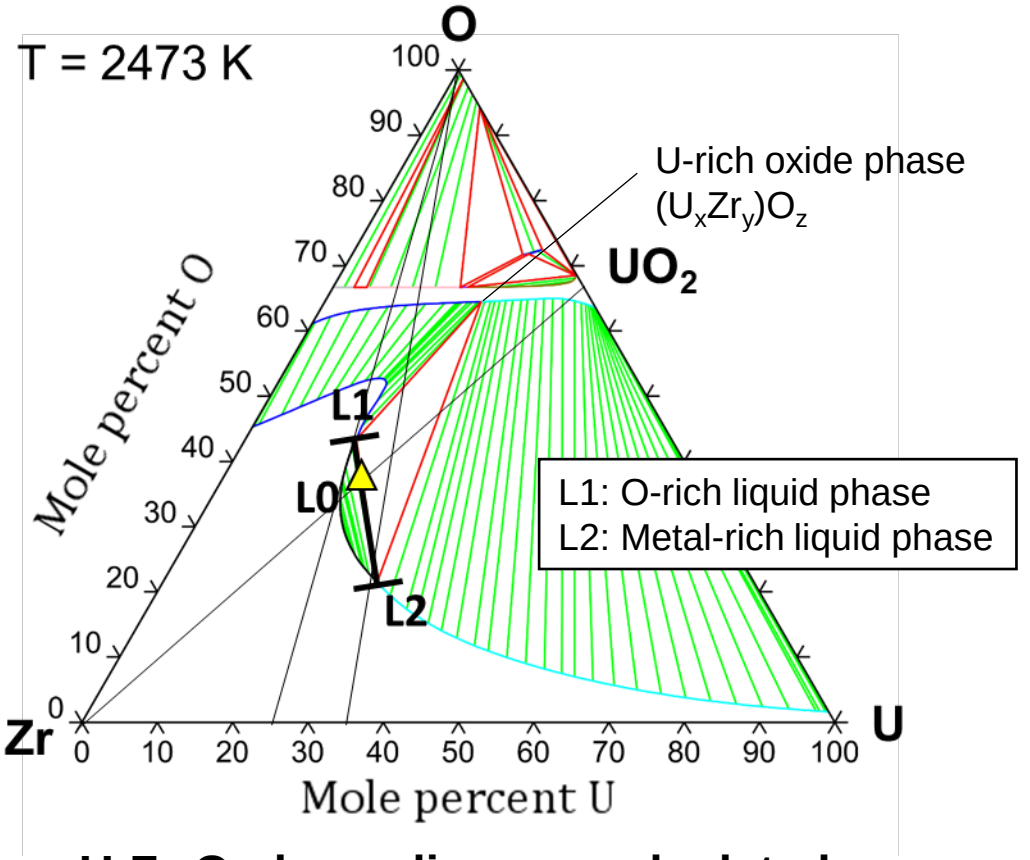


U-Zr-O composition at fuel liquefaction



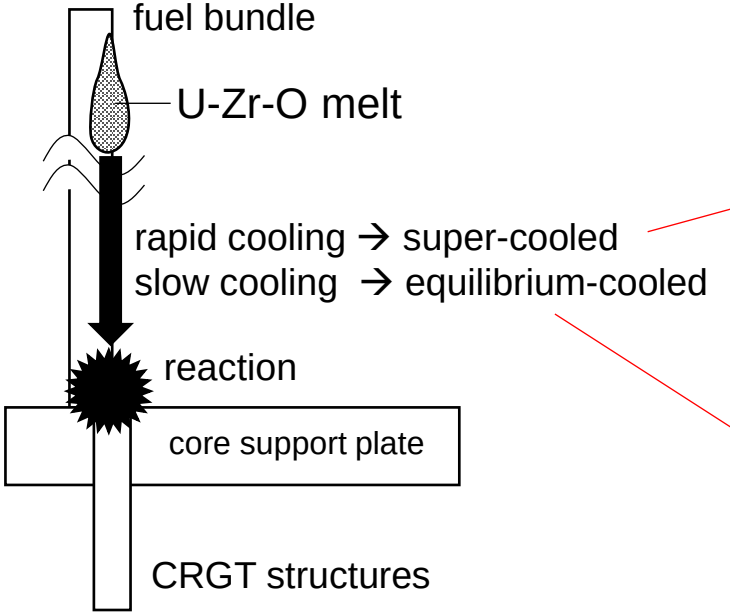
Schematic image of fuel dissolution & relocation

- Thickness ZrO2 cladding oxide layer affects UO2 dissolution behavior (thicker one results in more oxygen diffusion → $(U,Zr)O_{2-x}$ ceramic precipitates in the melt).
- Massive fuel degradation and relocation at about 2473 K was observed in the integral experiment (Phebus FPT3).

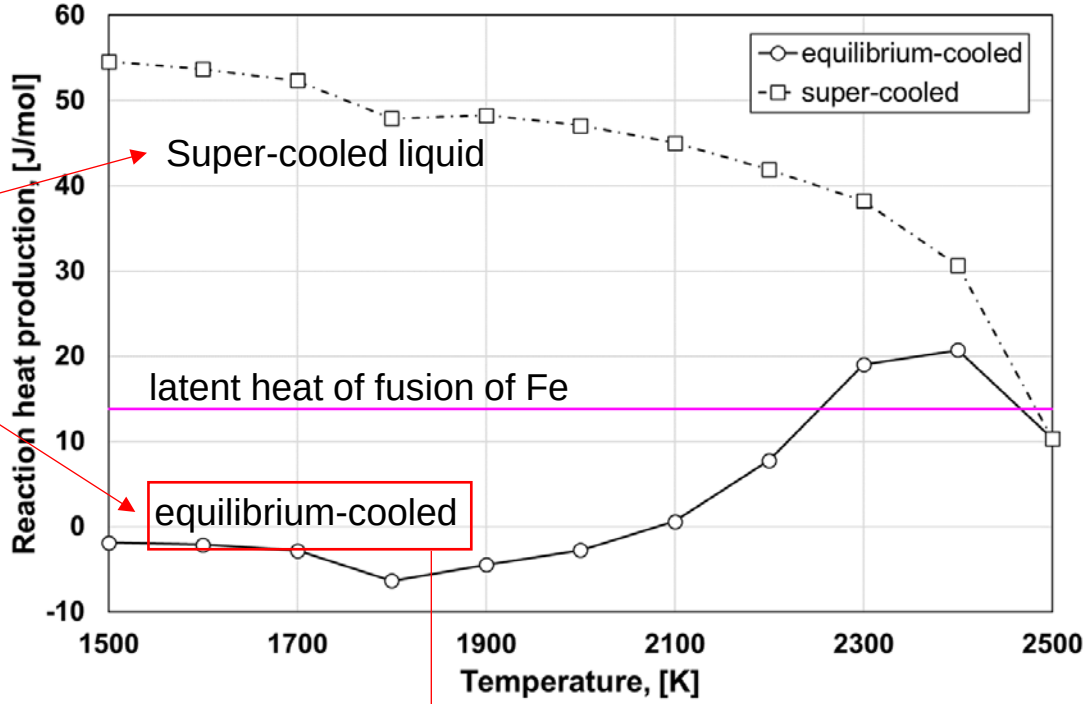


U-Zr-O phase diagram calculated by TAF-ID database

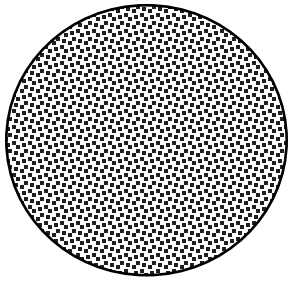
Potential heat production of U-Zr-O vs Fe



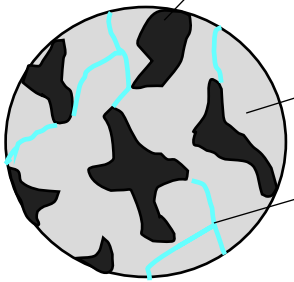
U-Zr-O (O-rich) vs Fe (U-Zr-O:Fe=9:1 mol%)



Super-cooled liquid
short-order disordering







Zr(O) **reactive with Fe forming $Fe_2Zr + ZrO_2$**

$(U,Zr)O_{2-x}$

L (U-Zr)

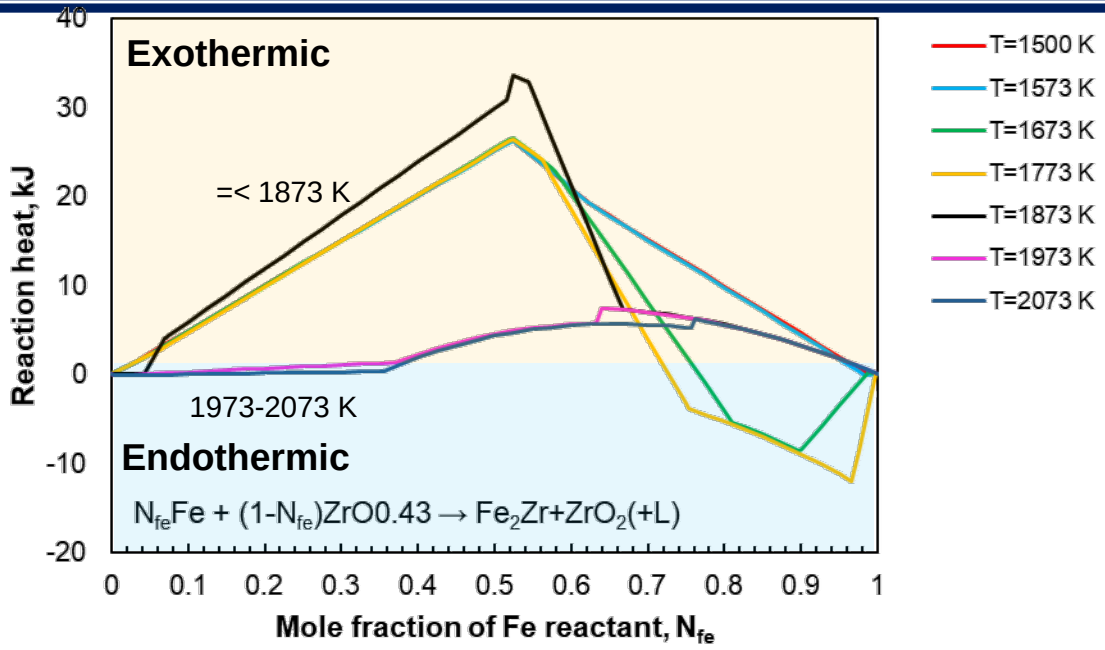
Negative mixing enthalpy of Fe-U-Zr

Heat generation of Zr(O) – Fe reaction

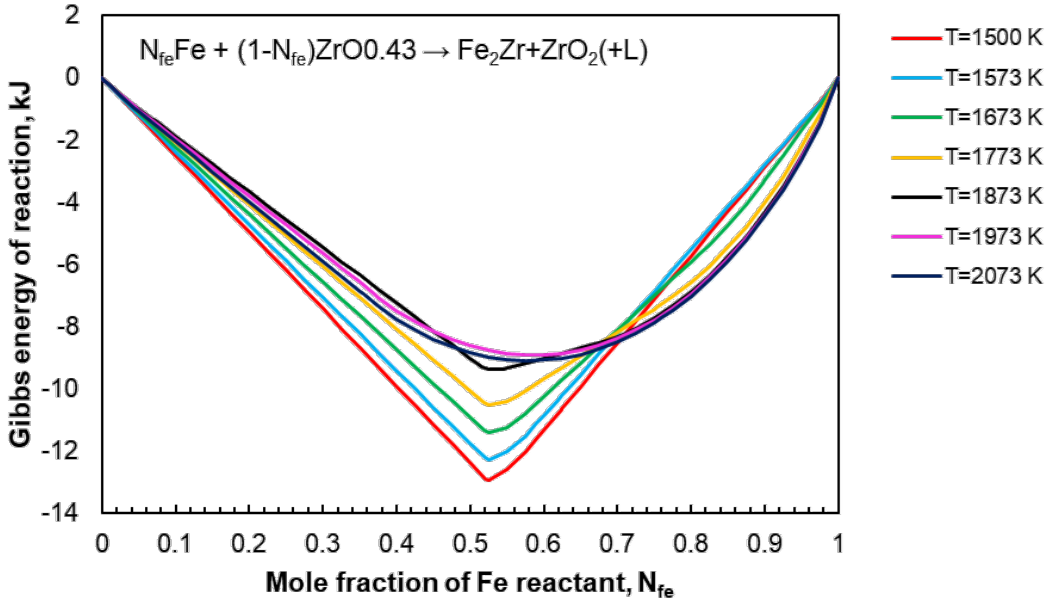
Reaction heat

- Heat generation was calculated by enthalpy difference between reactants and products using the TAF-ID database.
- Formation of ZrO_2/Fe_2Zr precipitates produces large heat (20 – 30 kJ per 1 mole of system at 0.5 mole-fraction of Fe).

Not negligible against the latent heat of fusion of Fe (13.8 kJ/mol)



Gibbs energy of reaction

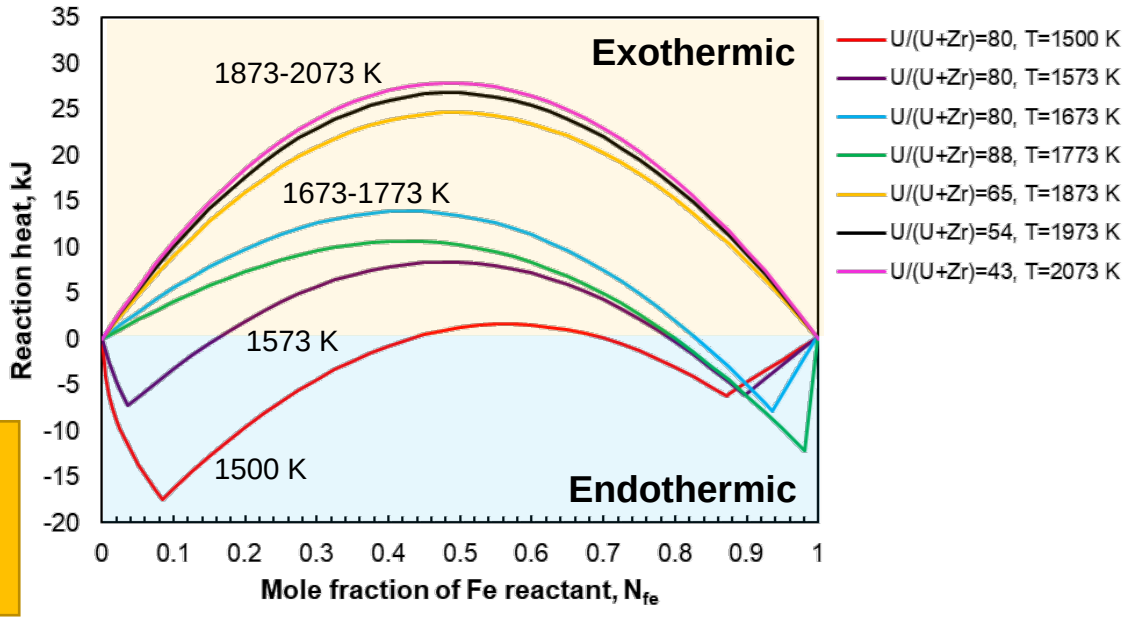


Heat generation of (U,Zr) – Fe reaction

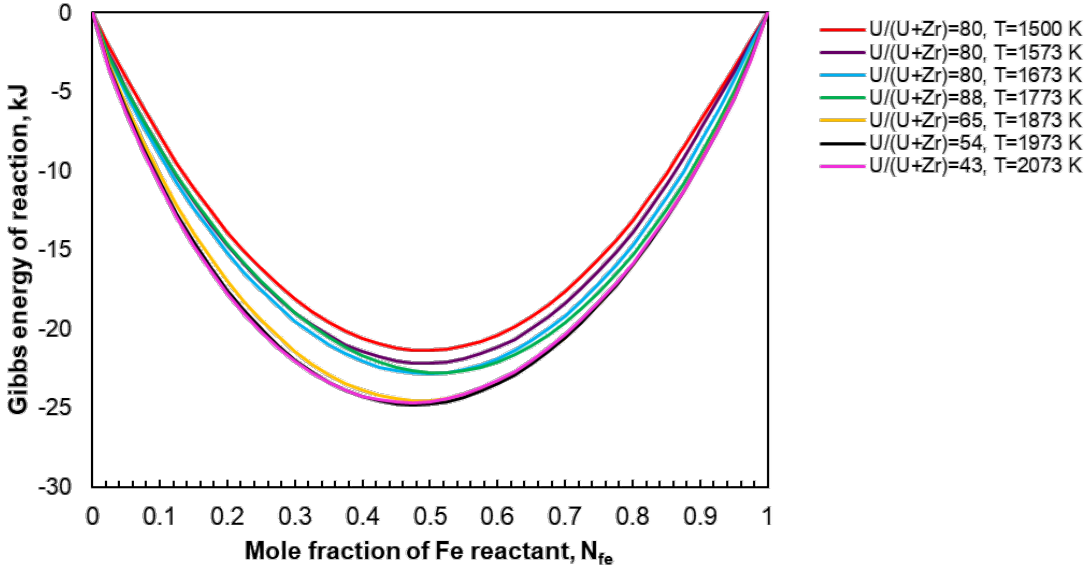
Reaction heat

- Heat generation was calculated by enthalpy difference between reactants and products using the TAF-ID database.
- Mixing heat gets high above 1673 K (5 – 30 kJ per 1 mole of system at 0.4 mole-fraction of Fe).

Not negligible against the latent heat of fusion of Fe (13.8 kJ/mol)

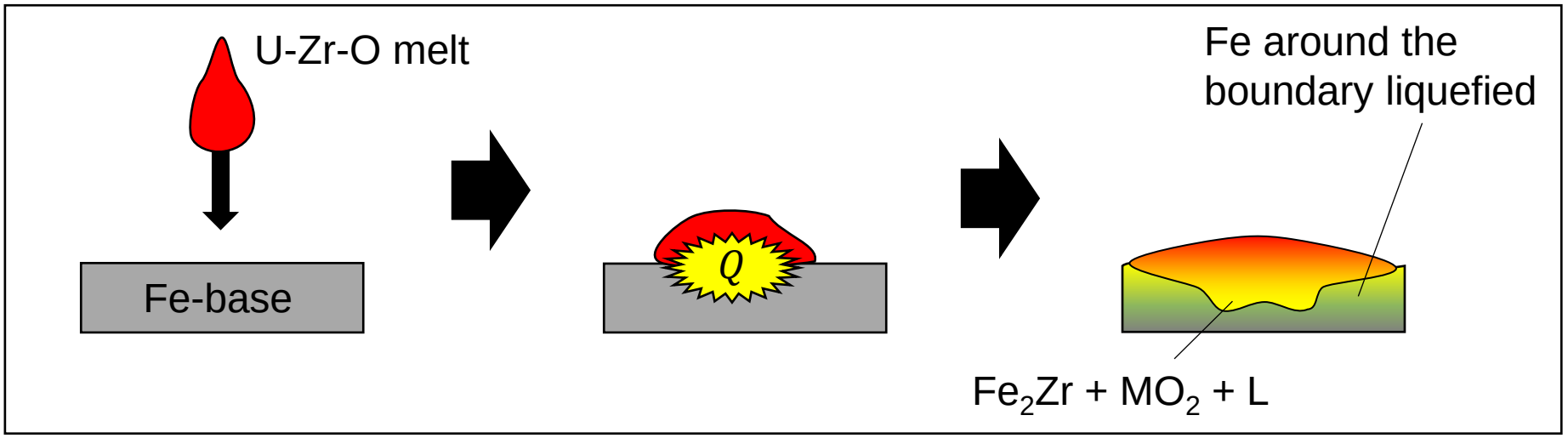


Gibbs energy of reaction



Possible reaction mechanism

- Possible interaction between U-Zr-O melt and Fe are
  1) **heat transfer** from U-Zr-O melt to Fe,
  2) **latent heat of precipitation** of stable solid phases (Fe_2Zr, MO_2) and
  3) **heat of mixing** of U-Zr-Fe.
- Subsequent heat production can lead to **dissolution of Fe**.
- **Interaction will be accelerated** because the reaction scheme is changed to solid-liquid from solid-solid.

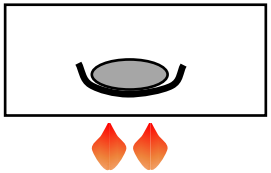


Experimental issues → next step

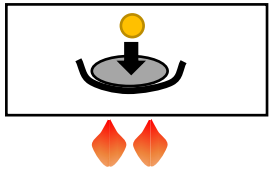
- How quickly does these reactions take place?
- What is an activity of Zr(O) in the U-Zr-O melt?
- Influence of oxygen potential? What if we use SUS304 instead of pure Fe?
- Can a super-cooled liquid form under the accident progression?

Experiment and simulation plan

Separate-effect test



- thermodynamic properties of reactants and products
- phase relation



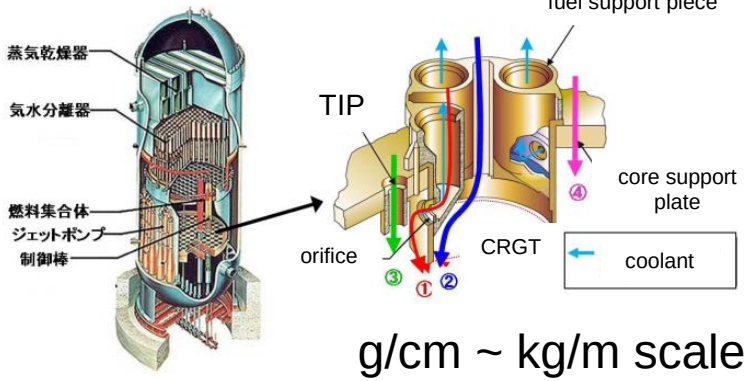
- reaction kinetics of system
- heat generation

mg/mm ~ g/cm scale

atomic diffusion scale model

simulation of materials + structures

CFD for middle scale

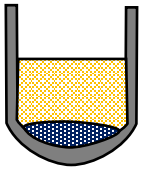


g/cm ~ kg/m scale

design

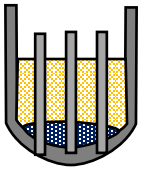
Middle scale integral test

Ar or H_2+H_2O



- the most basic case SS crucible + materials + atmosphere

Ar or H_2+H_2O



- practical shapes ex) crucible + obstacles
- See destructive flow movement

g/cm ~ kg/m scale

continuous convective scale model (→ SA code)

Thank you for your attention.







Difference in oxidation behavior of heterogeneous BWR fuel assembly under steam-starved condition

Yuji Nagae, Susumu Yamashita and Masaki Kurata
Japan Atomic Energy Agency

BWR has heterogeneous configuration of fuel assembly, especially control blade. Growth and reduction behavior of oxidation depend on steam fraction. The oxidation behavior affects the reaction between SUS and Zry in an early stage of accident progression. According to ANSYS-fluent using oxidation growth and reduction models depending on steam fraction, oxidation behavior drastically change above 1200 C. Steam fraction on the surface of channel box covered by control blade decreases up to steam-starved condition around 1200 degree C, which means oxidation growth rate decreases depending on steam fraction. Oxidized layer grows continuously even steam-starved condition using a model of oxidation behavior independent of steam fraction.

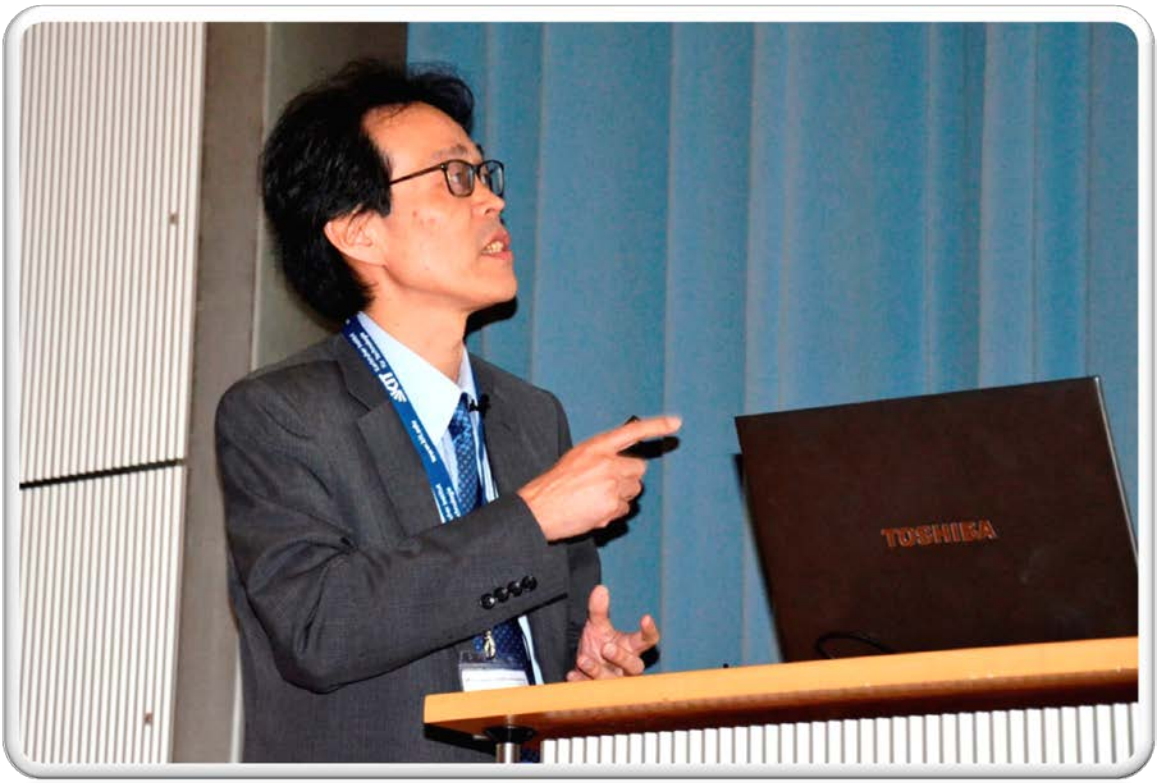
According to experimental integral tests (1.2m height, 0.1m square) without pre-oxidation[*1], a reaction between SUS-B4C and Zry occurs under low steam flow rate because the reaction rate is higher in the case of thin oxidized layer. Almost full oxidization occurs on the surface of Zry under a sufficient steam flow condition, except for thin oxidation at a top part of the test body. The reaction between control rod and Zry occurs at the top part. In addition, an observation of oxidation behavior in an integral test with pre-oxidation show us that a thickness of oxidized layer in a part of Zry covered by control blade is thinner and the interaction between SUS-B4C and Zry begins even pre-oxidation[*2].

The model will be implemented into JUPITER (JAEA Utility Program with Immersed boundary Technic and Equations of multi-phase flow analysis to simulate Relocation behavior of molten materials)[*3] developed by Nuclear Science and Engineering Center.

*1 H. Shibata et al., “Control blade degradation test under temperature gradient in steam atmosphere”, Top Fuel 2016, (2016) 11-15.

*2 A. Pshenichnikov et al., “The Behavior of materials in case of solidified absorber melt oxidized BWR channel box interaction revealed after CLADS-MADE-01 test”, Proc. FDR2019 (2019).

*3 S. Yamashita et al., “A numerical simulation method for molten material behavior in nuclear reactors”, Nuclear Engineering and Design, 322 (2017) 301-312.


TOSHIBA

Difference in oxidation behavior of heterogeneous BWR fuel assembly under steam-starved condition

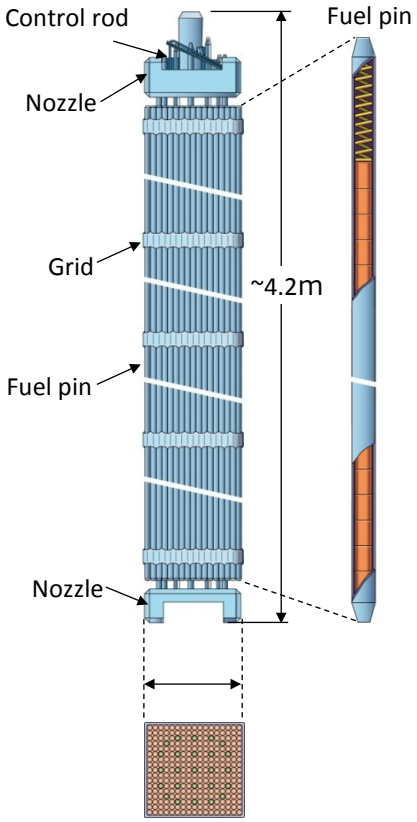
October 24, 2019

Yuji NAGAE, Susumu YAMASHITA and Masaki KURATA

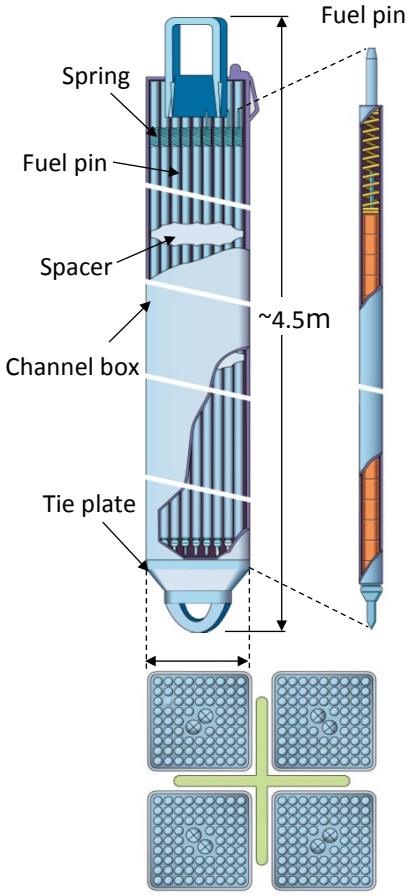
Japan Atomic Energy Agency

Collaborative Laboratories for Advanced Decommissioning Science (CLADS)

Difference in BWR and PWR fuel assembly



PWR fuel assembly



BWR fuel assembly

Characteristics of BWR fuel assembly

- **Relatively complicated and heterogeneous configuration (ex. control blade)**
- Larger amount of Zry (mainly by “channel box” and “thicker” fuel cladding)
- Larger amount of S.S. (mainly by control rod guide tube, steam separation equipment, etc.)
- Different absorber material (B_4C instead of Ag-In-Cd)

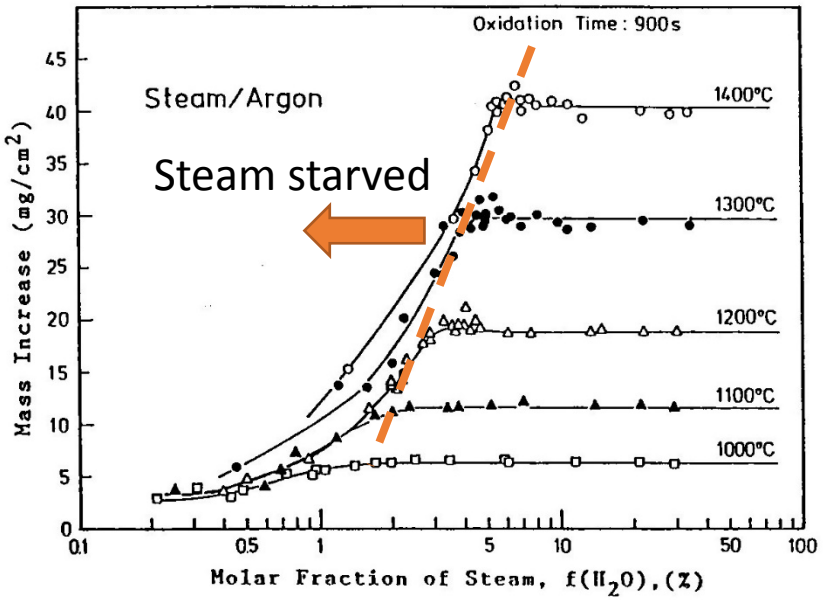
Early stage in accident

- Abrupt temperature increase by steam/Zry-interaction (**>1200℃**).
- Local eutectic interaction among core component (S.S., absorber materials) and fuel cladding (Zry).
  - ✓ Variations along with fuel length (~4m) to be taken into consideration.
    ex. sudden decrease in coolant level and significant oxidation in lower part of fuel assembly can generate "steam-starved condition" and can accelerate local eutectic.
    ➔ ***a possible scenario of unit-2***

Oxidation behavior should be considered in order to understand core degradation in steam-starved conditions more preciously.

Previous study on oxidation behavior under steam starved condition

Mass increase depending steam fraction*1



The mass increase settles on the constant level in the range of $f(H_2O)$ above the certain critical value, while **the mass increase due to oxidation decreases sharply with decreasing $f(H_2O)$ below the critical value**.

Reduction in ZrO_2 layer

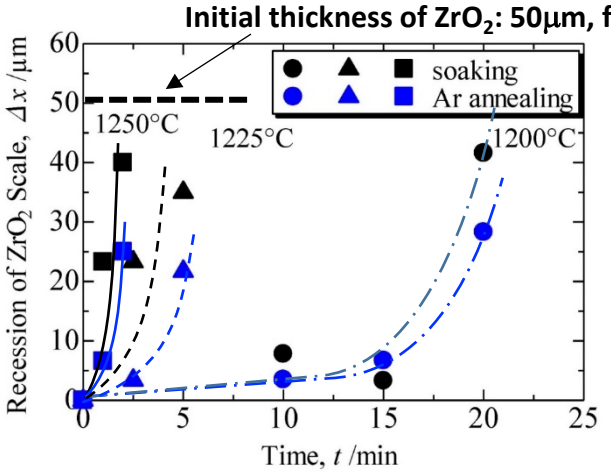
- FZK

  Oxide layer reduction processes was investigated.

  J. Stuckert, U. Stegmaier. "Degradation of the cladding oxide layer under steam starvation conditions". 8th Quench Workshop, Karlsruhe, Oct. 29-31, 2002.
  J. Stuckert, M. S. Veshchunov, "Behaviour of Oxide Layer of Zirconium-Based Fuel Rod Cladding under Steam Starvation Conditions", FZKA7373, 2008

- Nagaoka Univ. and JAEA

  Oxide layer reduction rate was investigated.

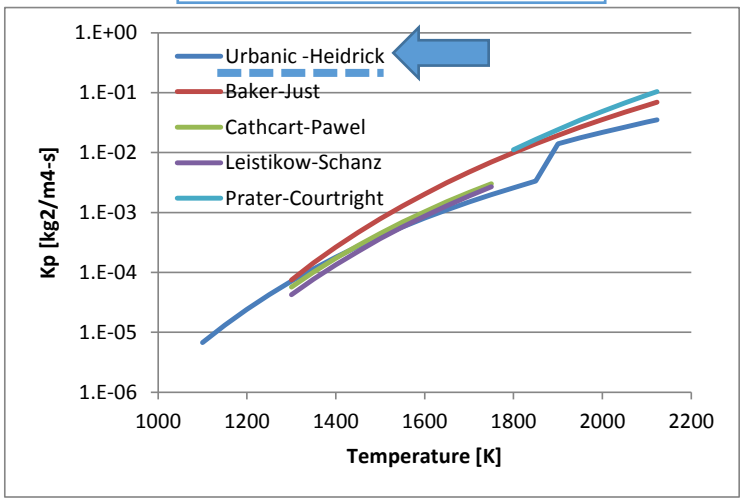


*1 H. Uetsuka et al., High Temperature Oxidation of Zircaloy-4 in Diluted Steam, J. Nuclear Science and Technology, 26, 1989, pp.240-248.

Outline of analysis by ANSYS-fluent

Computational fluid dynamics (CFD) software: ANSYS FLUENT Ver. 16.2

Oxidation models



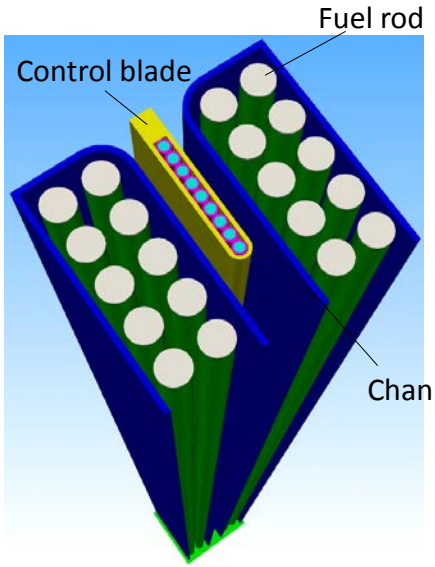
Reduction of oxidized layer

Sensitivity analysis;

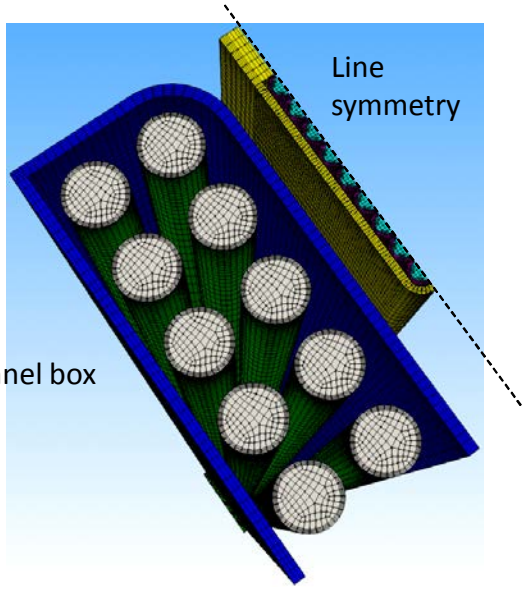
Assumption:

Reduction of ZrO_2 occurs below a cut-off of molar fraction of steam.

Cut-off of molar fraction of steam = 0.2, 0.1, 0.05



Analysis system



Mesh

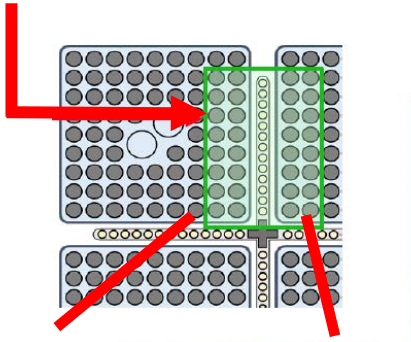
Conditions

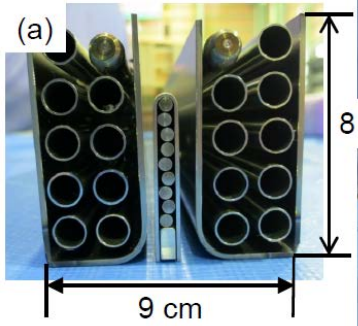
Test ID	Steam flow rate [g/min]	Ar flow rate [g/min]
CRFCBF03	50	17
CRFCBF04	15	15

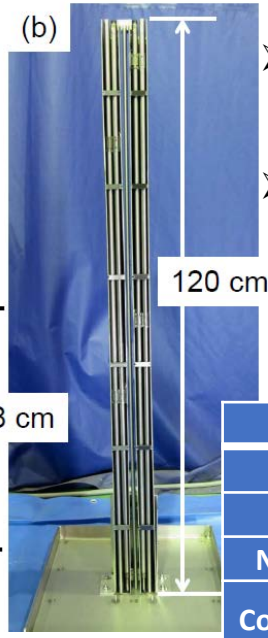
Outline of experimental tests

- **Oxidation behavior depends on steel flow rate and tendency of control blade degradation possibly has threshold condition. Critical condition for reaction between molten control rod and channel box can be recognized.**

Cross section of BWR fuel assembly







- These materials are equivalent to those applied for typical BWRs in Japan.
- Thickness of pre-oxidized layer on Zry:
  ～ 0 (fuel rod)
  a few μm (channel box)

Parts	Materials
Fuel cladding	Zry-2
Channel box	Zry-4
Neutron absorber	B_4C
Control rod cladding	S.S304L
Control blade	S.S316L

Appearance of test piece (before)

Control blade and channel box was co-degraded.



15 g/min

Only the control blade was degraded at the upper part.

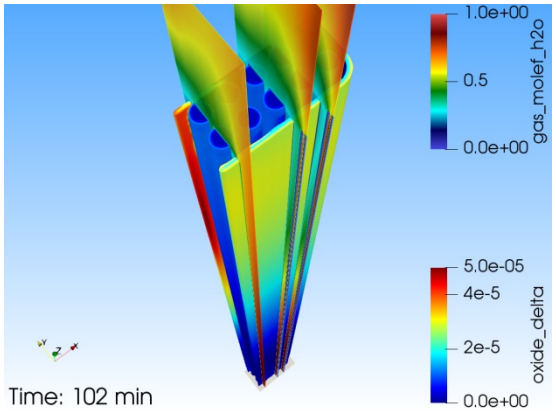
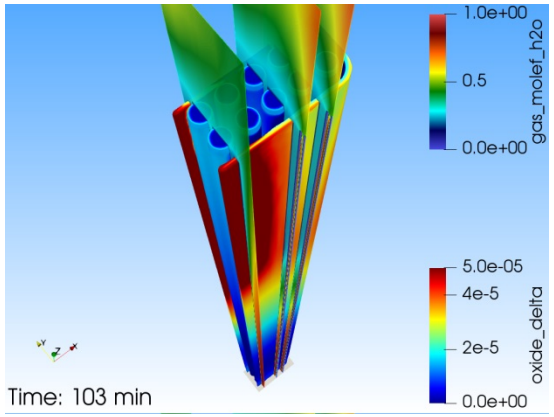
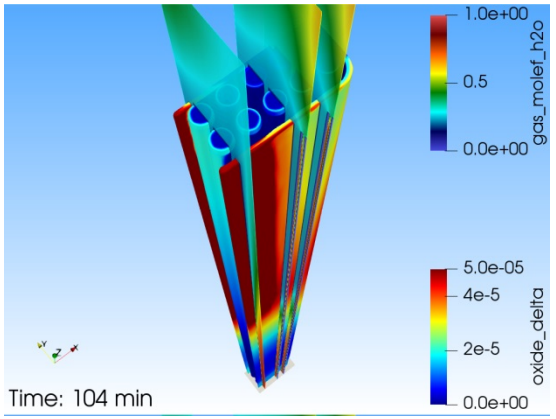
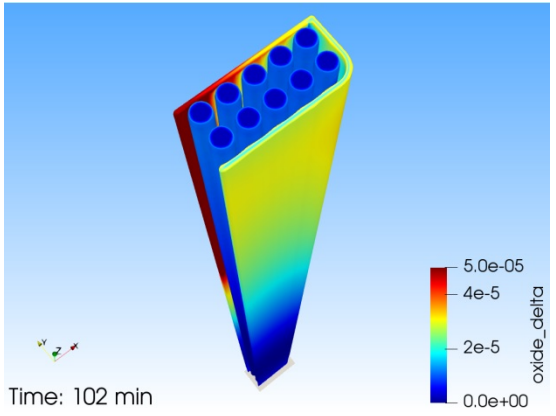
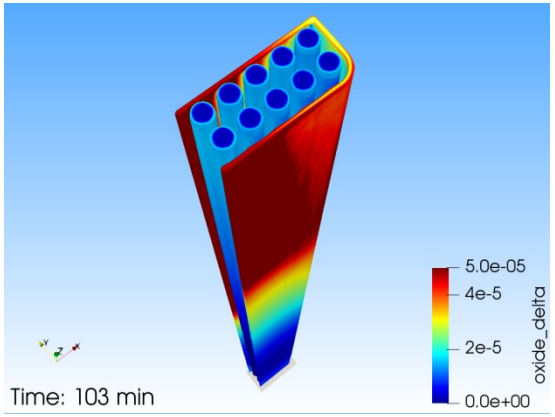
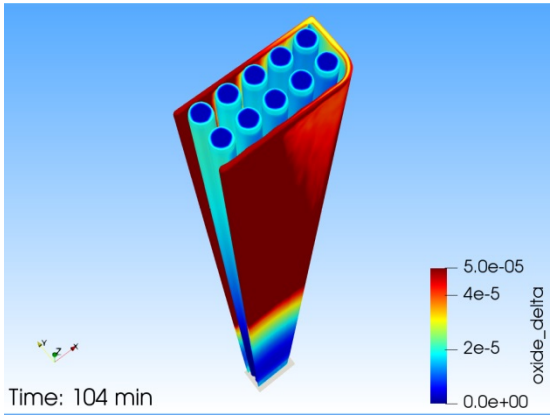


50 g/min

Steam flow rate

Appearance of test piece (after)

Analysis of oxidation behavior
- Sufficient steam flow (50 g/min) -

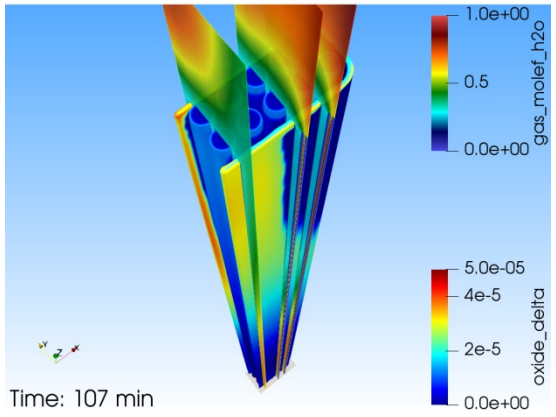
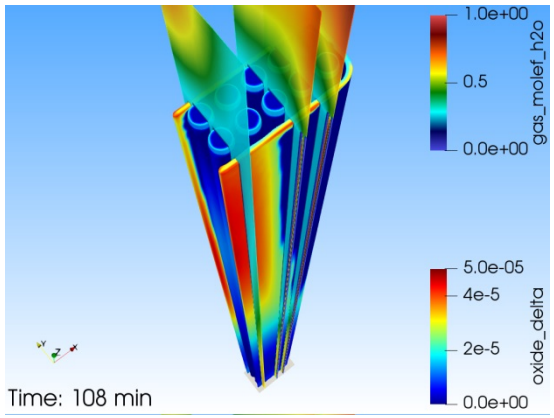
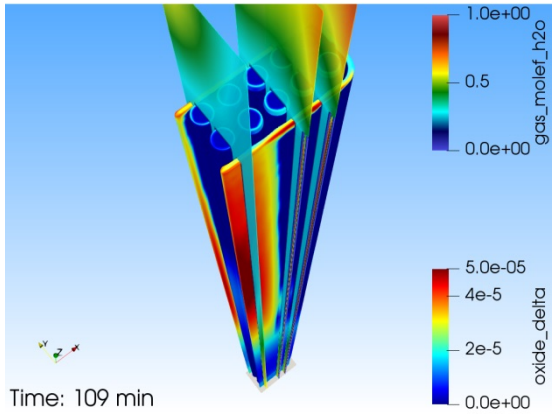
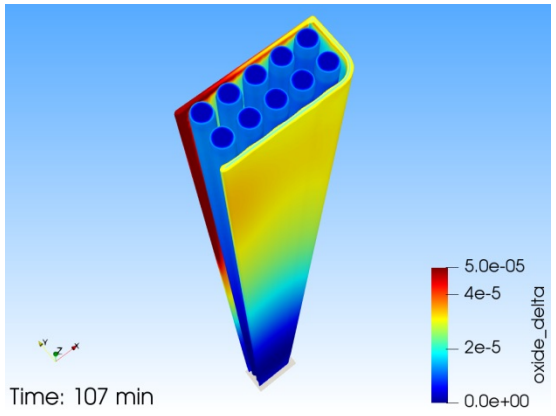
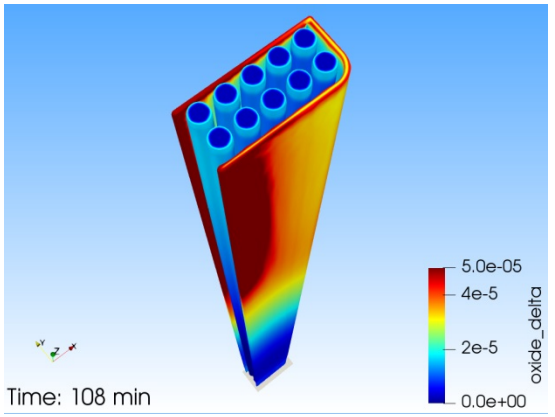
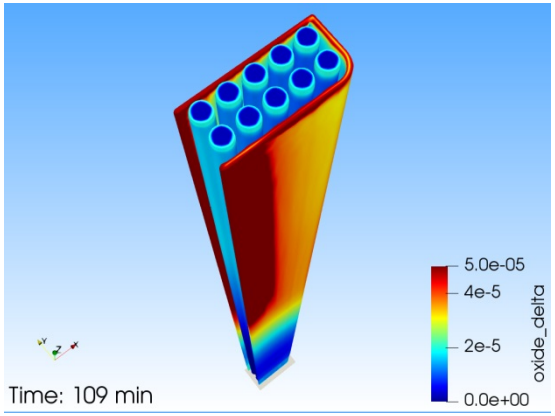
Temp.	1200 ℃ → (heating rate: 1K /s) 1260℃ → 1320℃		
Reduction of oxidized layer below cut-off value (0.2)			
Oxidation growth rate independent of steam flow			

Note

Still oxidation behavior depending temperature gradient

Different oxidation behavior due to lower steam fraction on the surface of channel box covered by control blade

Analysis of oxidation behavior
- Insufficient steam flow (15 g/min) -

Temp.	1200 ℃ → (heating rate: 1K /s) 1260℃ → 1320℃		
Reduction of oxidized layer below cut-off value (0.2)			
Oxidation growth rate independent of steam flow			

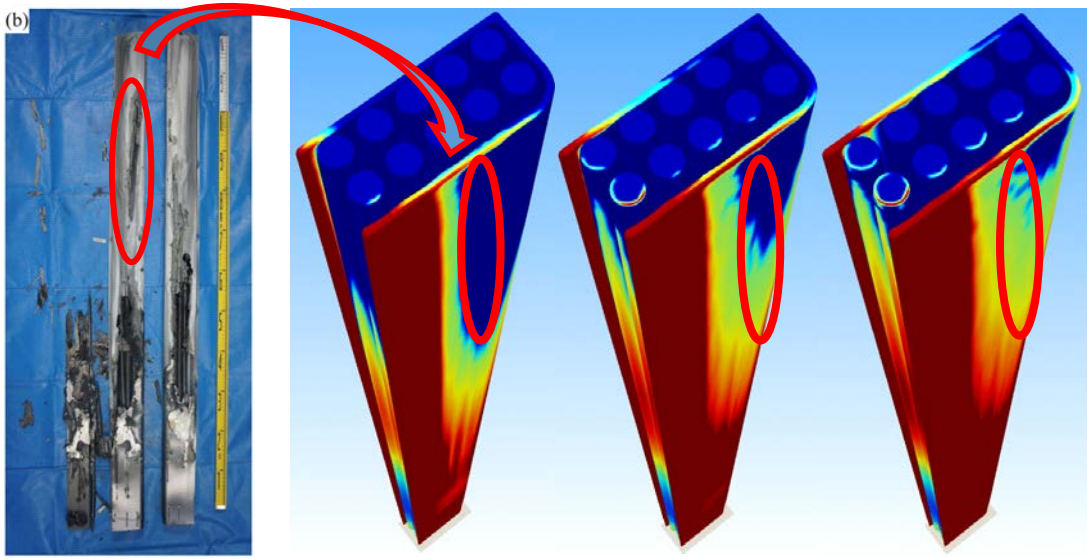
Note

Already different oxidation behavior due to steam starvation

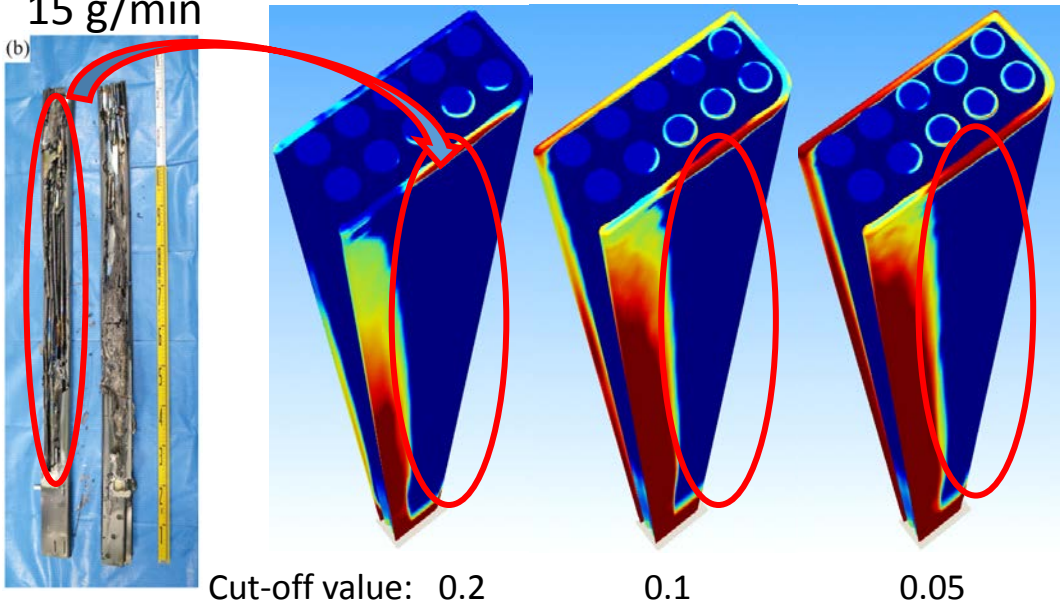
Different oxidation behavior due to lower steam fraction on the surface of channel box covered by control blade

Possibility of reaction of Zry/molten S.S./B_4C

50 g/min

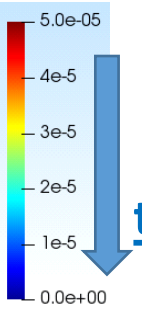


15 g/min



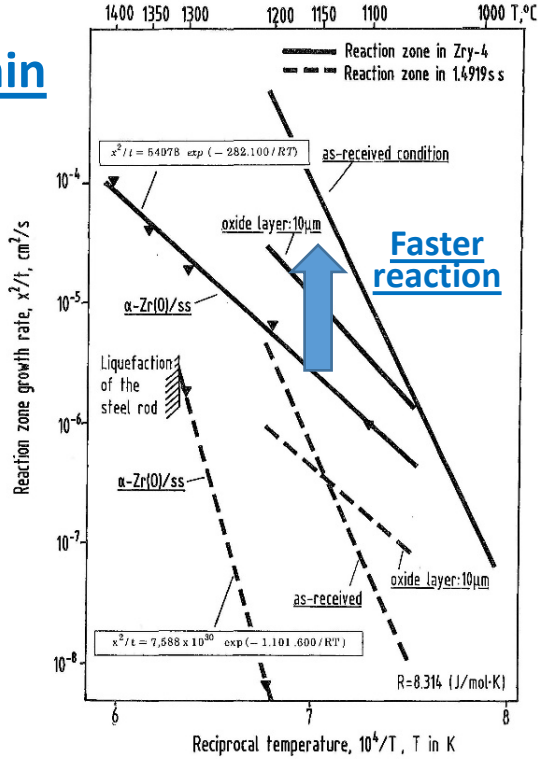
Cut-off value: 0.2 0.1 0.05

Thickness of ZrO_2 / m



thin

Reaction rate increases in case of lower thickness.



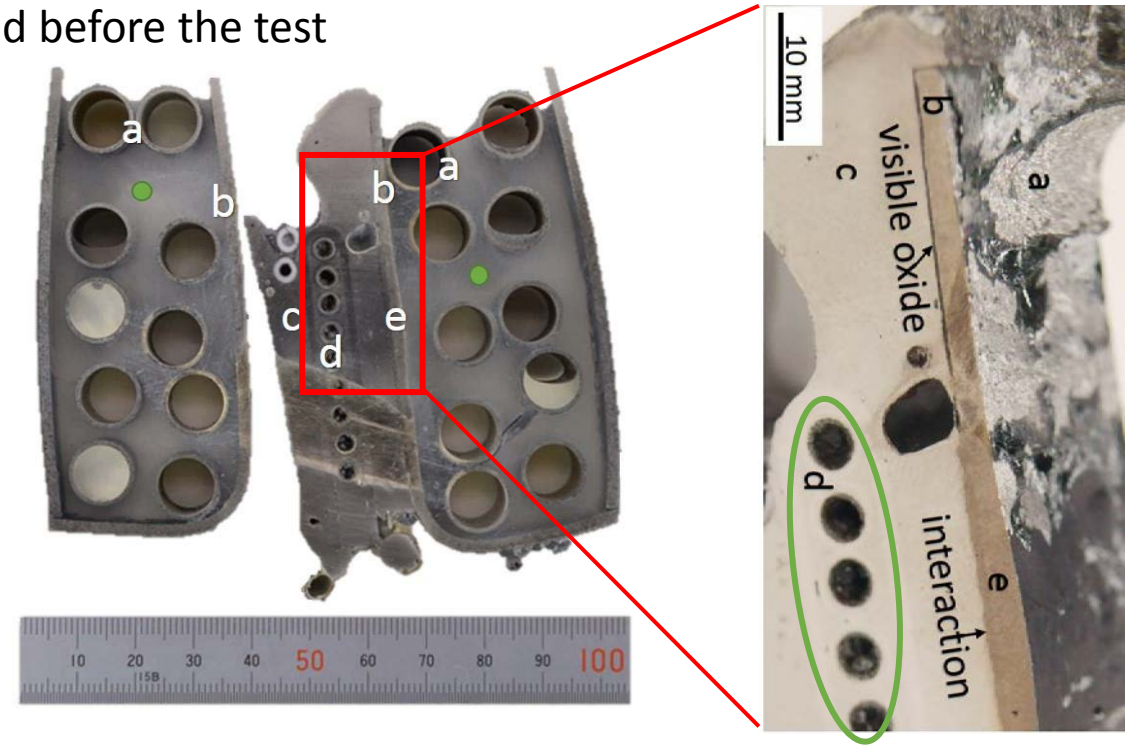
Faster reaction

P. Hofmann et al., KfK 5106, 1994.

Reaction between molten S.S.-B_4C and Zry could be analyzed by considered oxidation growth and reduction of oxidized layer.

Difference in oxidation behavior due to presence of control blade

Pre-oxidized before the test



Cross-sectional view in the middle part of large scaled test piece[*1].

Zone “b”: Some part of the channel box was protected by surface oxide.

Zone “e”: An interaction between the hot melt and the channel box occurred in the part of control blade, which means there is possibility of thinner oxidized layer.

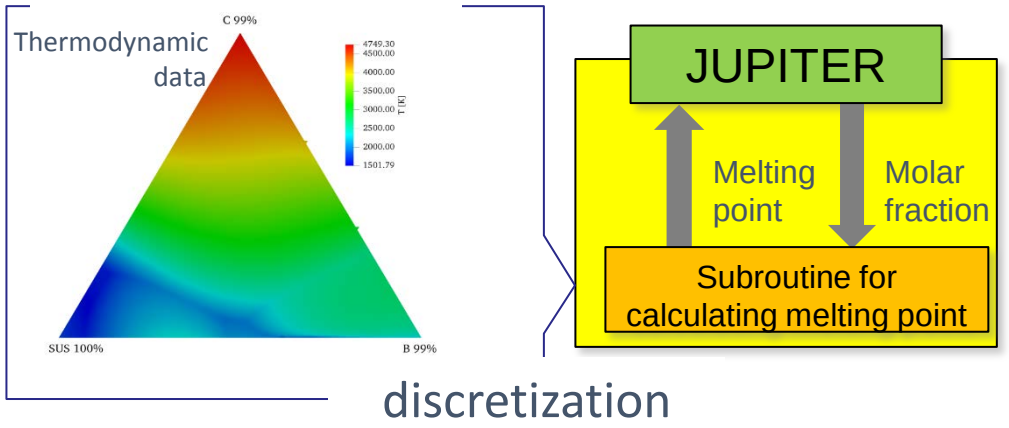
*1 A. Pshenichnikov et al., Proc. of FDR2019, International Topical Workshop on Fukushima Decommissioning Research, May 24-26, Japan

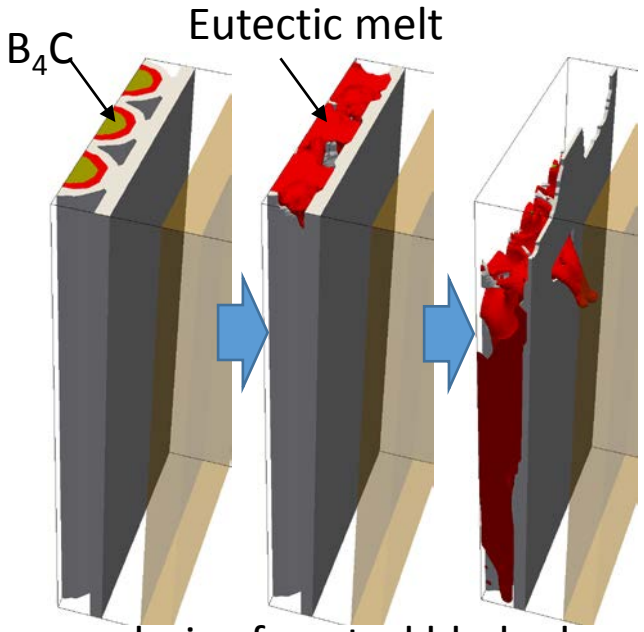
JUPITER code developed by JAEA

JUPITER code developed by Nuclear Science and Engineering Center

(JAEA Utility Program with Immersed boundary Technic and Equations of multi-phase flow analysis to simulate Relocation behavior of molten materials)

- **Computational fluid dynamics (CFD)** including the three dimensional multiphase thermal-hydraulic simulation models.
- **Reaction models based on thermodynamic data** for boron carbide (absorber), stainless steel (control rod, fuel support structure, etc.), Zircaloy (channel box and fuel cladding) in order to deal with complicated melt relocation behaviors.





Preliminary analysis of control blade degradation

Summary

- Growth and reduction of oxidized layer should be considered in order to understand control degradation in steam-starved conditions preciously.
- The growth and reduction model will be implemented into JUPITER code developed by JAEA.

Thank you for your attention.

Acknowledgement

This study is performed in the framework of “Advanced Multi-scale Modeling and Experimental Tests on Fuel Degradation in Severe Accident Conditions” supported by Ministry of Economy, Trade and Industry, Japan (METI).

25th international QUENCH Workshop
October 22–24, 2019
Karlsruhe, Germany

Post-test analysis of the CMMR-4 test bundle

Hiroshi Madokoro, Takuya Yamashita, Ikken Sato
Japan Atomic Energy Agency (JAEA)
Collaborative Laboratories for Advanced Decommissioning Science (CLADS)
4002 Naritacho, Oarai, Ibaraki Pref. 311-1396

Abstract

Decommissioning of the Fukushima Daiichi Nuclear Power Plant (1F) is a challenging issue due to its complex final distribution and the characteristics of the core materials. Severe accident analysis codes have a large uncertainty in predicting BWR core relocation behavior according to their assumed accident progression scenarios: TMI-2 like path (molten fuel pool formation and relocation) or Continuous Drainage Path" (fuel relocation basically without melting). The MAAP-MELCOR Crosswalk has revealed that this uncertainty cannot be resolved by existing experimental data and knowledge. In order to fill in the gap of the knowledge, a series of the CMMR (Core-Material Melting and Relocation) experiment has been conducted. The test bundle of the latest test CMMR-4 consists of 48 fuel rods filled with ZrO2 simulant pellets with Zircaloy claddings, a control blade with B4C particles in SS tube and sheath, two Zircaloy channel box walls, and lower support structures. The height of the test bundle was 80 cm and the heating system of the test was the plasma heating, which enabled melting of the oxide simulant fuel pellets. The test confirmed that macroscopic gas permeability existed until the ceramic-fuel melted and that the hot fuel rods tended to remain as columns in the core region, which suggests the heating of the support structure in earlier phase is unlikely. This information is useful not only for 1F decommissioning but also for further understanding of a BWR severe accident progression.

The test bundle was cut by using the abrasive waterjet (AWJ) technique that uses abrasive garnet of 150–300 μm with feed rate of approximately 1.5 kg/min. In order to cut off about 30 mm of ZrB_2 spot contained in the relocated melts, 750 liters of water, 84 kg of garnet and one nozzle replacement were necessary. The EPMA and XRD analyses of the cross-section showed that the place where repelled the garnet-contained waterjet contained ZrB_2. Since the cutting by AWJ technique has the property of selectively abrading the soft spots of the material, it must be noted that, in case of utilizing the technique in 1F decommissioning, garnet might be repelled by a hard boride and abrades places which were not expected.

Hiroshi Madokoro <madokoro.hiroshi@jaea.go.jp>



Post-test analysis of the CMMR-4 test bundle

Hiroshi Madokoro
Takuya Yamashita
Ikken Sato

Japan Atomic Energy Agency (JAEA)

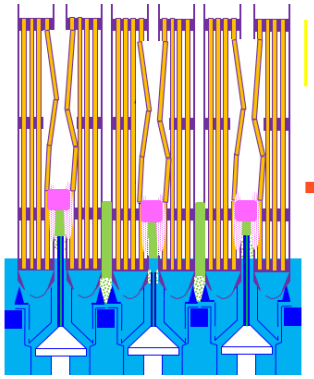
Uncertainty in BWR accident progression

- Fukushima-Daiichi (1F)(BWR) and TMI-2 (PWR) have different reactor designs.
- Accident progression of 1F may be quite different from that of TMI-2.

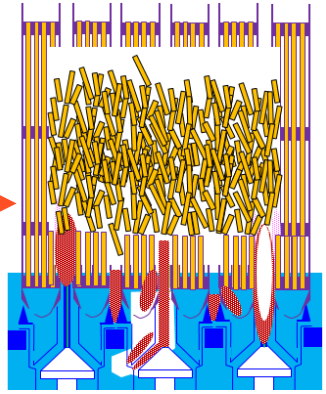
Typical accident progression of BWR:

Core Material Relocation

Early phase (dry condition) | **Uncertainties in CMR of BWR**



Melt through of control blade and channel box



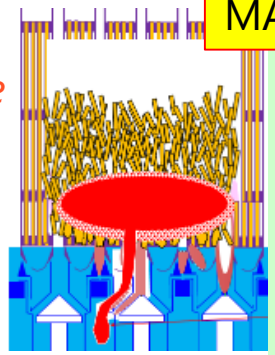
Cladding oxidation and melting through of metals

Gas permeability of degraded fuel assemblies

Downward penetration of unmolten core materials through bypass and its effect on structure heating

TMI-like path

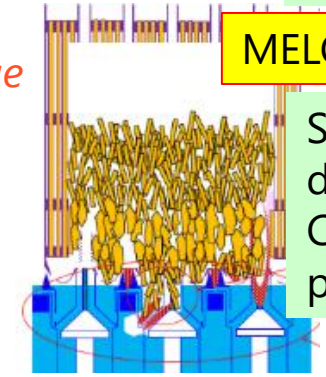
Drainage path



MAAP5

Molten pool formation

Mixed liquid/solid-phase CMR to lower plenum

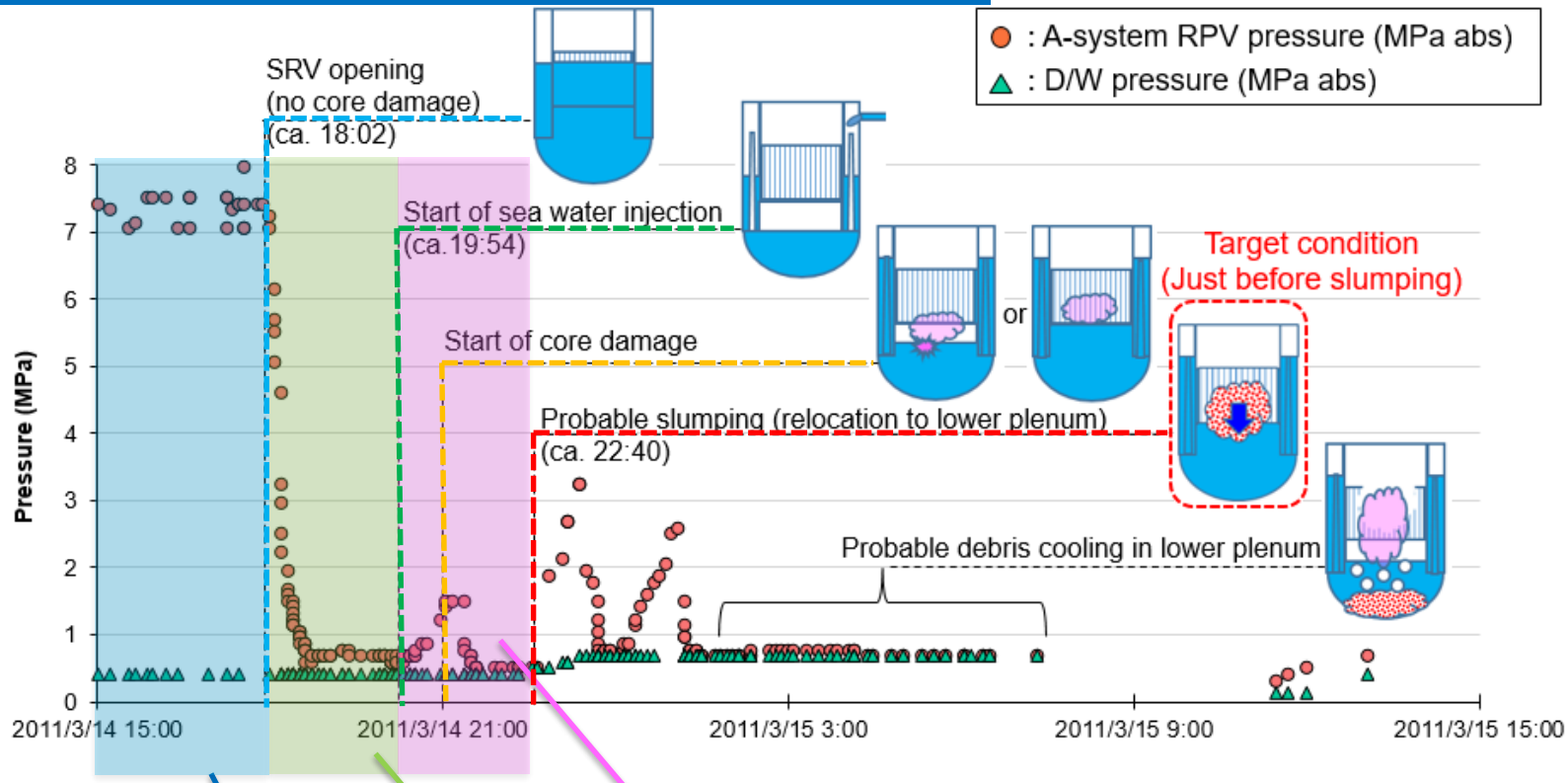


MELCOR

Solid material dominant CMR to lower plenum

Selection of target test condition

Fukushima Daiichi Unit2 (1F2) accident progression



No core damage is expected

Core region filled with steam and hydrogen

Core heat up
Water level dropped below the core region

CMMR : Core Material Melting and Relocation

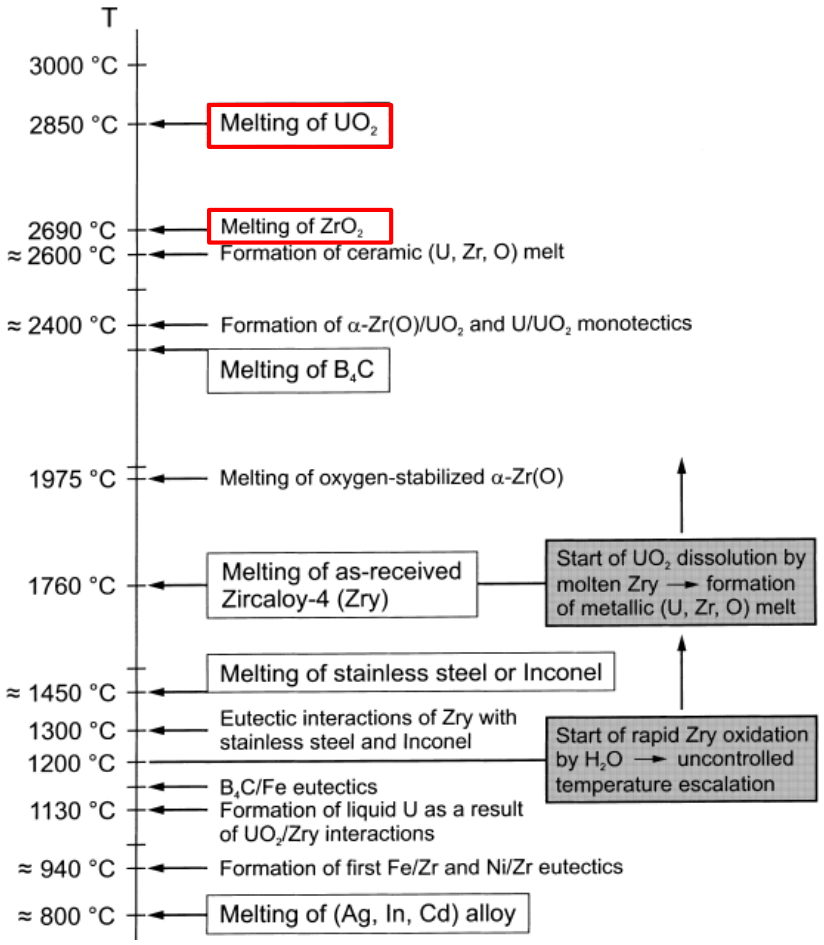
Test bundle

- Simulant fuel assembly ($UO_2 \rightarrow ZrO_2$ pellets)

Non-radiation test

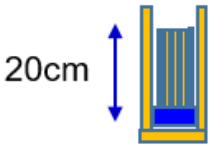
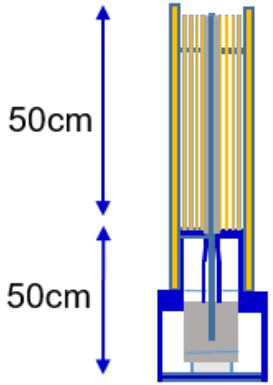
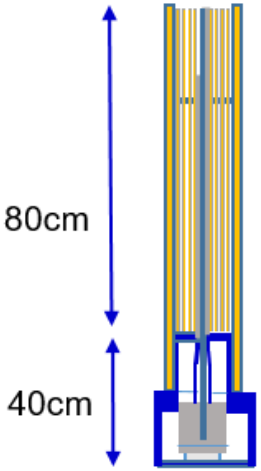
Heating system

- Plasma heating

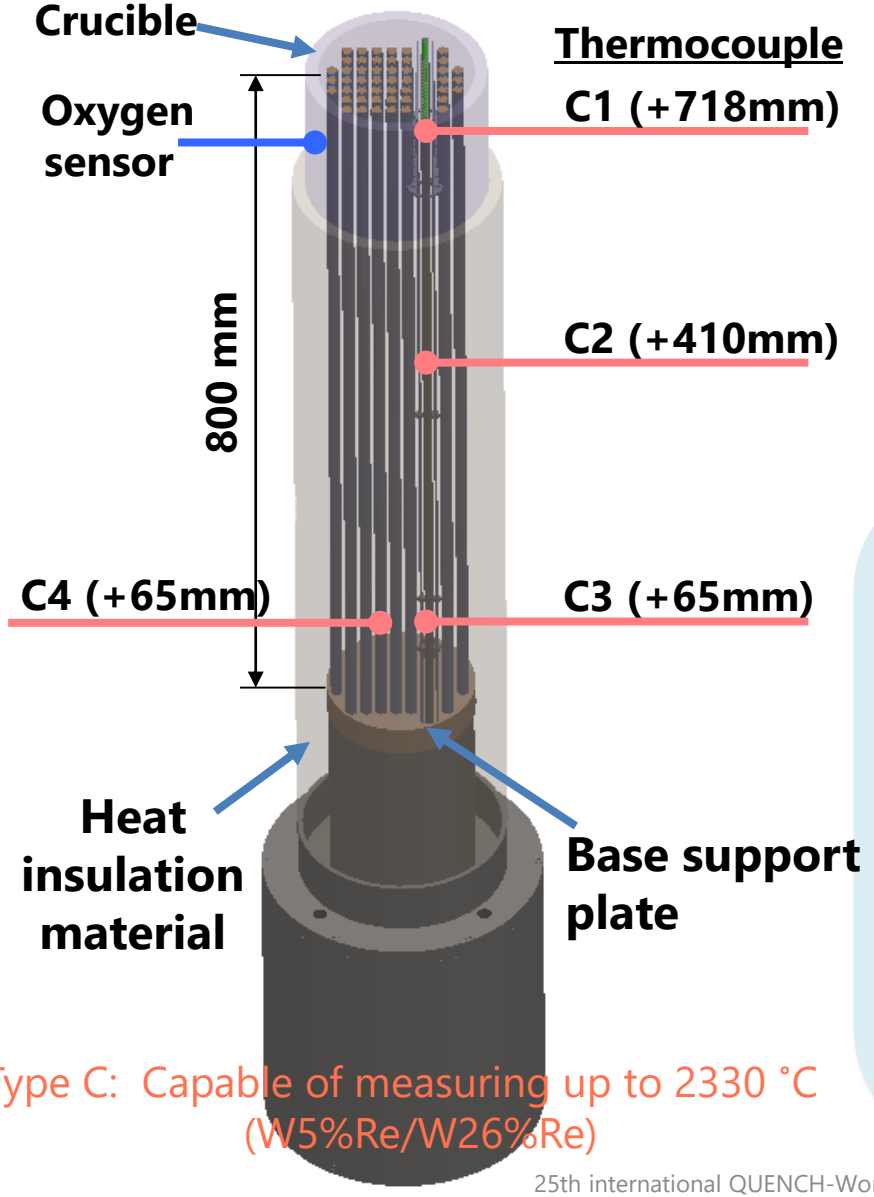


P. Hofmann, "Current knowledge on core degradation phenomena, a review", Journal of Nuclear Materials, Vol.270, 1999, pp.194-211.

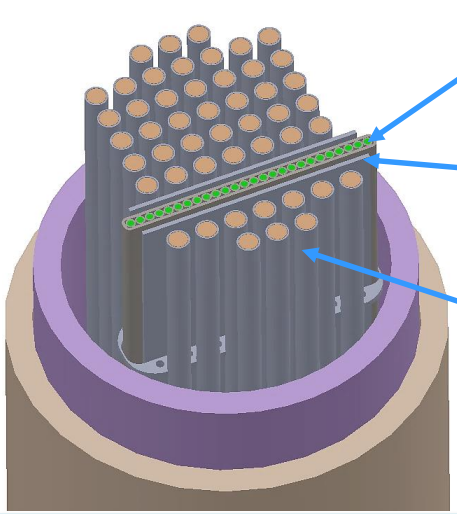
The CMMR program

JFY2014, Phase-I (Preliminary test)	JFY2015, Phase-II (Preliminary test)	JFY2016, Phase-III (Main test)	JFY2017, Phase-IV (Main test)
Small-scale tests #1, #2 and #3	Plasma torch failure	CMMR-1	CMMR-3
	CMMR-0	CMMR-2 Increased heating rate	CMMR-4 Melting of pellet was achieved
With high O_2 concentration (ca.5%)		*With low O_2 concentration (<0.2%)*	
			

CMMR-4 test bundle

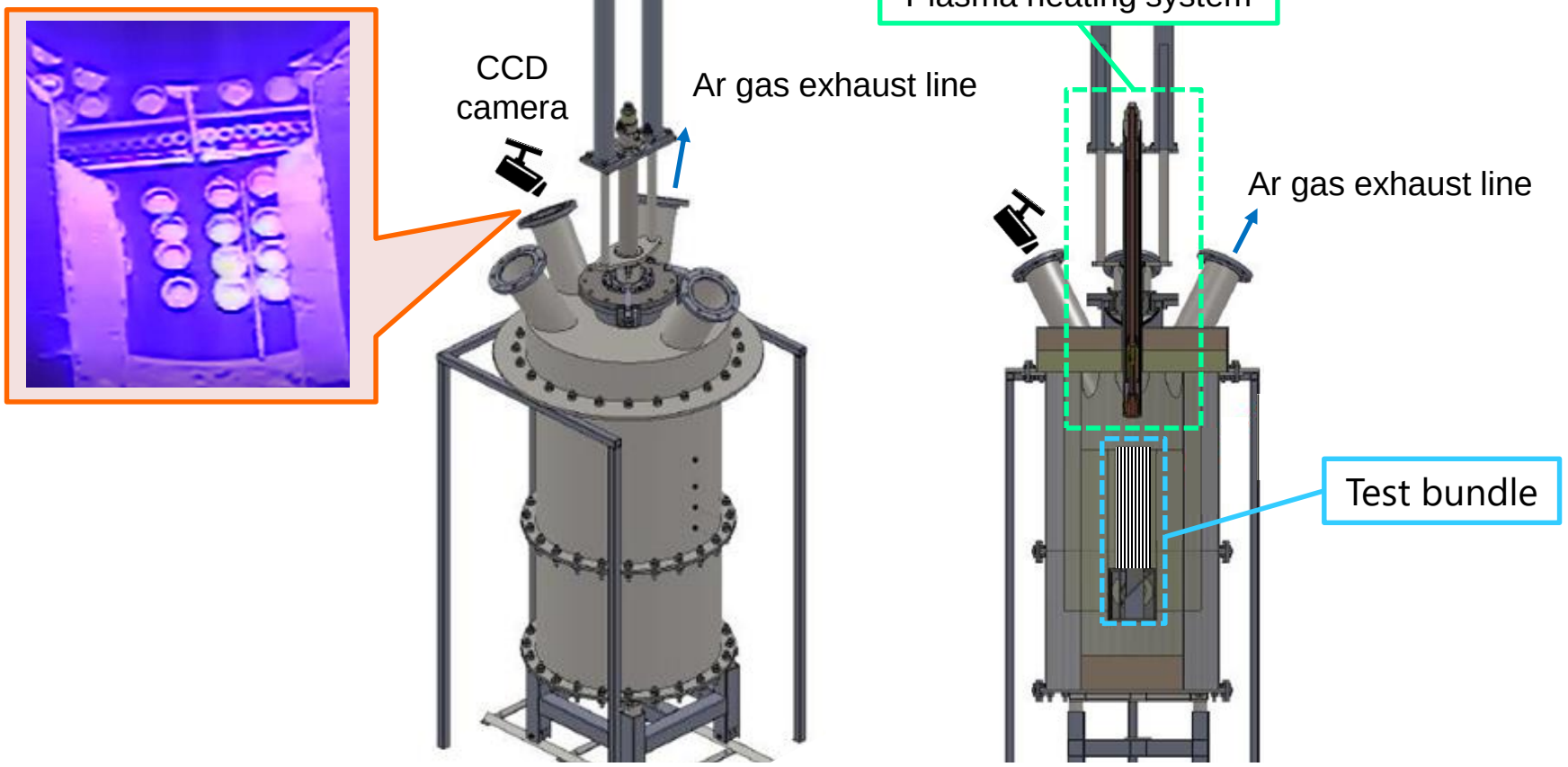


Type C: Capable of measuring up to 2330 ˚C (W5%Re/W26%Re)



- The control blade contains B_4C powder placed in stainless steel tubes within a stainless steel outer containment shell.
- The channel box and the cladding tubes are made of zirconium alloys such as Zircadyne 702.
- To observe temperature and material melting behavior, 4 thermocouples and an oxygen sensor were installed in the simulated fuel assembly.

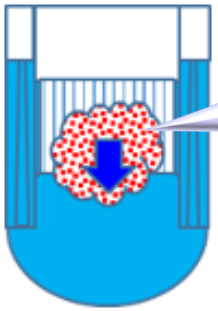
Test reactor



The basic boundary of the test reactor vessel was an outer steel shell. The shell contained layers of insulating materials comprising combinations of refractory materials such as alumina castable, ceramic zirconia, fibrous zirconia, and zirconia felt.

Test conditions

Target condition : 1F2 just before slumping



Core region : Dry core
(Oxide concentration <0.1%)

Fuel temperature : Close to the melting point

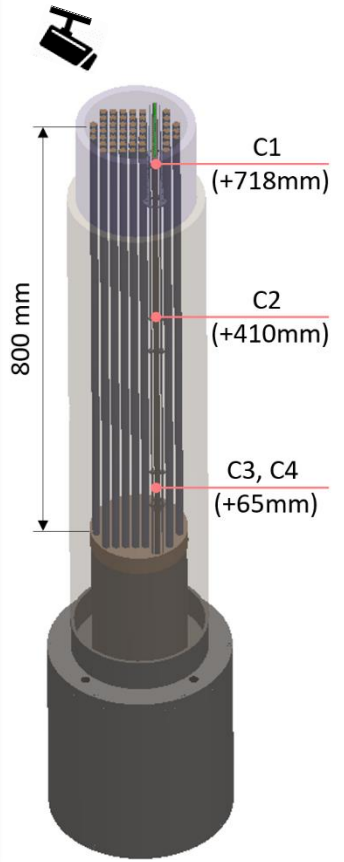
Heating rate : unknown

Test conditions

Core condition	Dry
Oxygen concentration	Less than 0.1% (in Ar gas atmosphere)
Maximum temperature	Close to the melting point of ZrO_2 pellets (~2500 ˚C)
Heating rate at the top (<500 ˚C)	As quickly as possible
(>500 ˚C)	40 ˚C/min

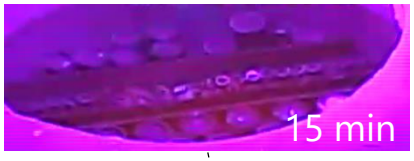
Camera view of CMMR-4 (x30 speed)





Heating history

B_4C/Fe eutectics



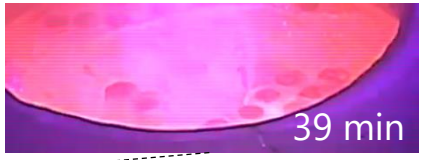
Control blade completely melted, except B_4C

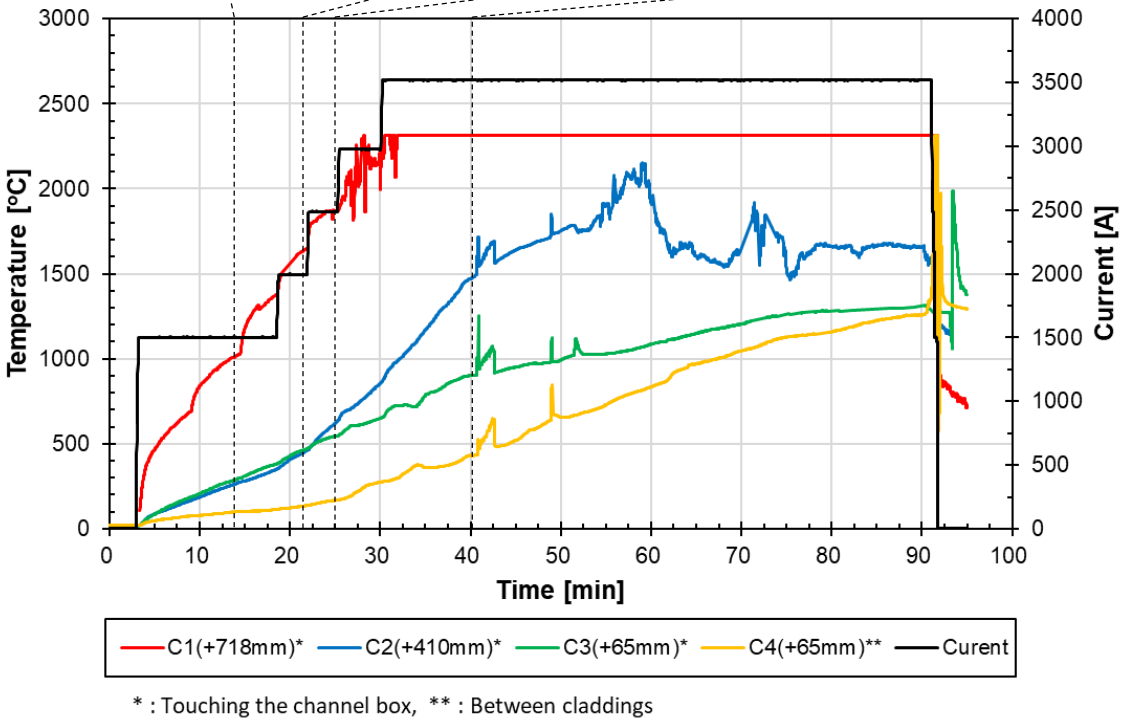


Channel box melt



ZrO_2 pellets melt

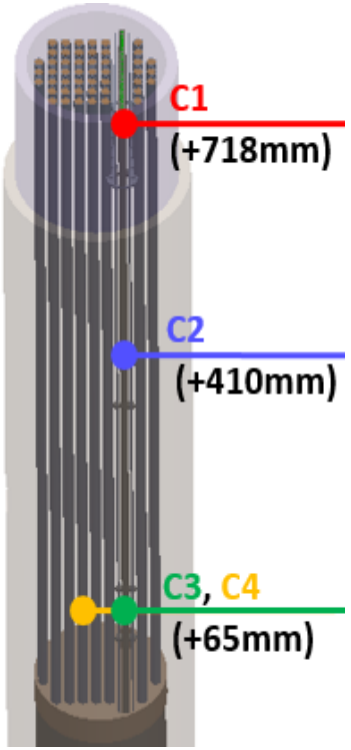




* : Touching the channel box, ** : Between claddings



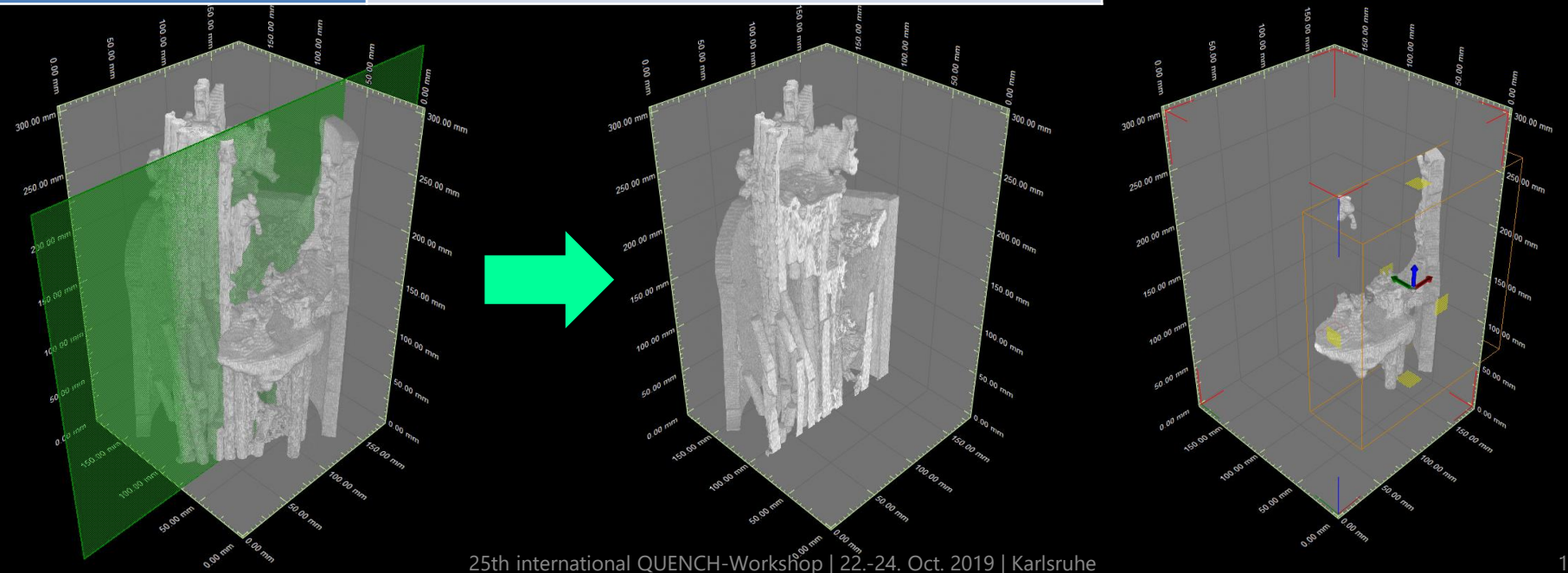
800 mm



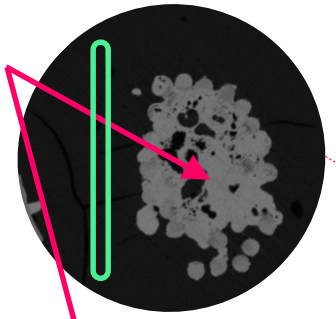
- The test atmosphere was controlled: oxygen less than 0.1%.
- TC C1 broke at the maximum temperature of a type C TC (2330 C).

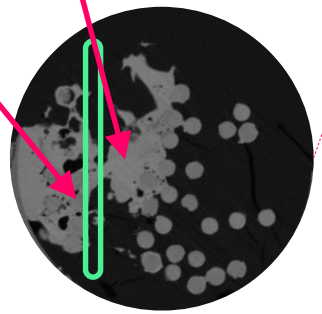
X-ray CT images of the test bundle (1/2)

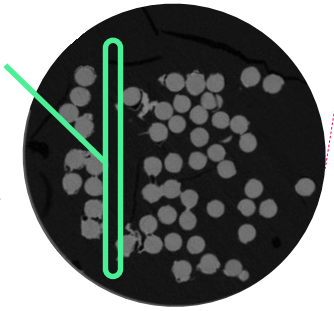
CT measurement method	Translate/Rotate
X-ray source	Maximum electron energy: 9 MeV Maximum power: 520 mC/kg/min
X-ray device	Silicon semiconductor detector • Number of channels: 0.06° × 100 Tungsten collimator • Slit size: 0.1 mm W × 2 mm H × 230 mm L • Number of slits: 100
Measuring time	Normal imaging: 20 min/cross section Fine imaging: 80 min/cross section

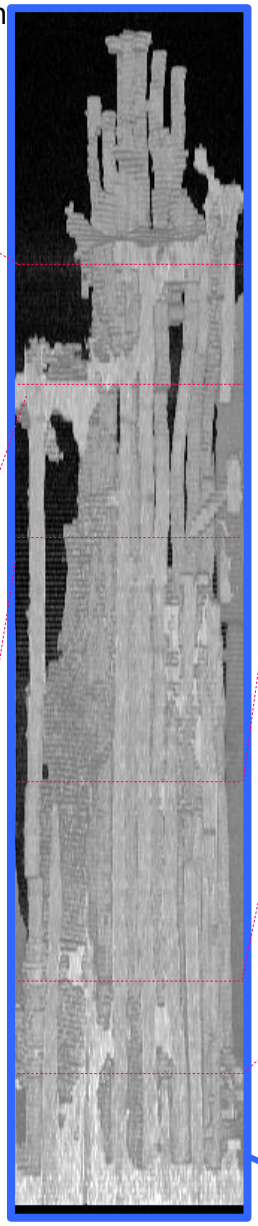


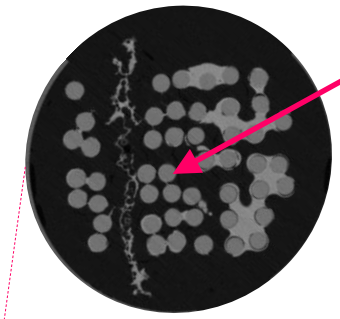
X-ray CT images of the test bundle (2/2)

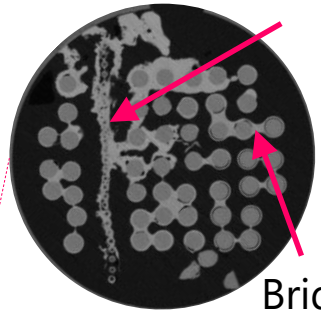


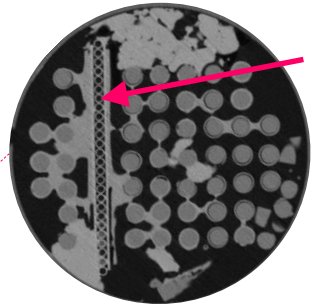












+800 mm

+625 mm

Molten pool of melted ZrO_2 pellets

+550 mm

Metallic melts including Fe and Zr

Control blade and channel box were completely gone

+430 mm

Hot-gas flow channel was created

-2 mm

+250 mm

Cladding tube were melted at this level or higher

+110 mm

Channel box partially molten

Bridge of molten cladding

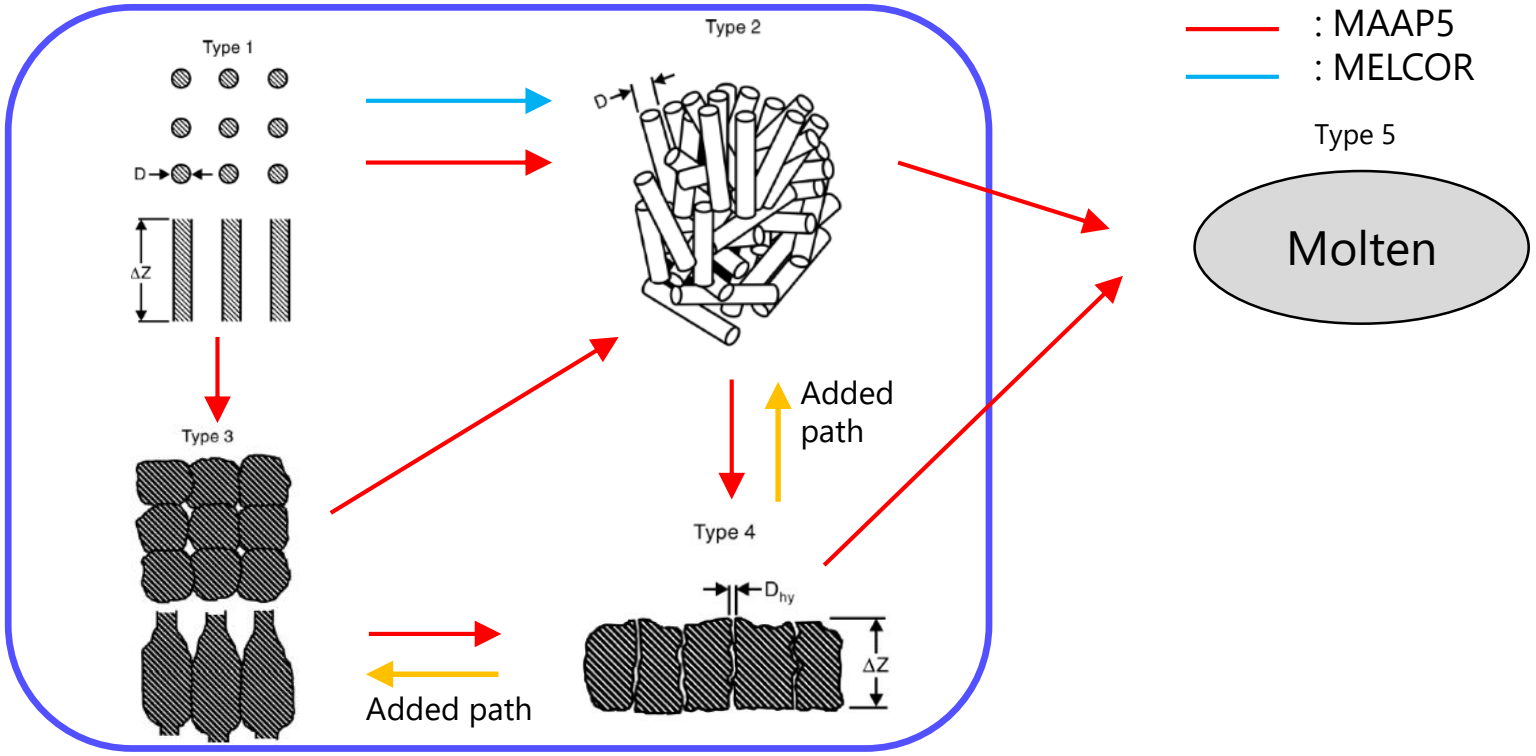
+50 mm

Control blade looks intact

There were selective draining paths near the control blade, and a complete blockage was not formed.

The simulant fuel columns survived

Influence on modeling of SA codes



a. The macroscopic gas permeability of the heated up core until ceramic fuel melting will be kept.
b. The hot fuel tends to remain as columns thus “effective fuel relocation” removing hottest fuel from the middle of the core and effectively heating the support structure is unlikely.

Cutting of a sampling target –AWJ technique

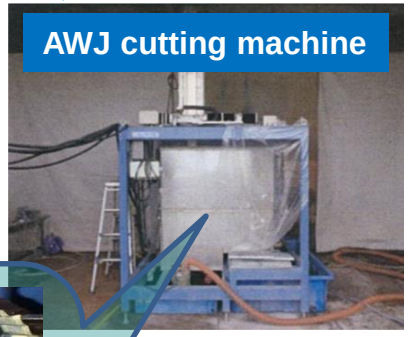
- Device
  - High pressure pump, Ecomaster Magnum MARK III.
    - Maximum discharge pressure: 245 MPa
  - Suspension unit, ANT
    - Abrasive: Garnet (150-300 μm)
    - Feed rate: 0.5-2.0 kg/min
  - AWJ cutting machine
    - 3-axis movable
    - Water tank capacity: 2 m^3



High pressure water
&
Abrasive (Garnet)

High pressure water

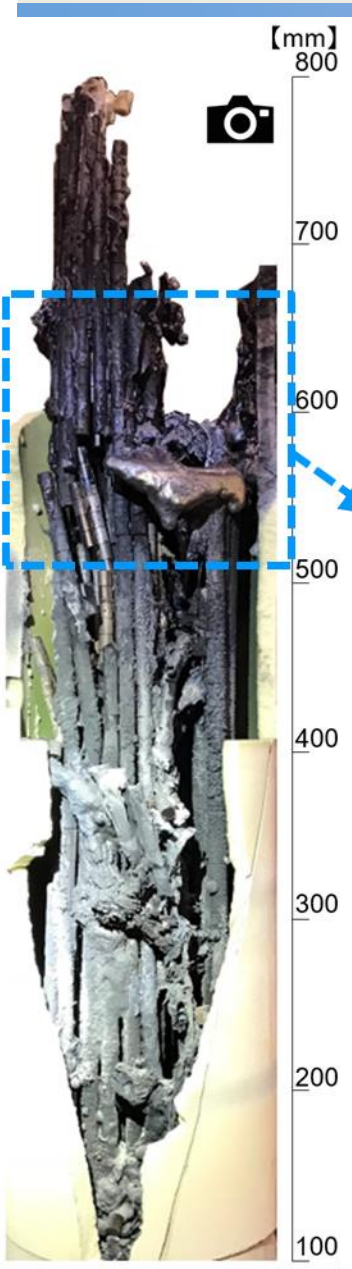


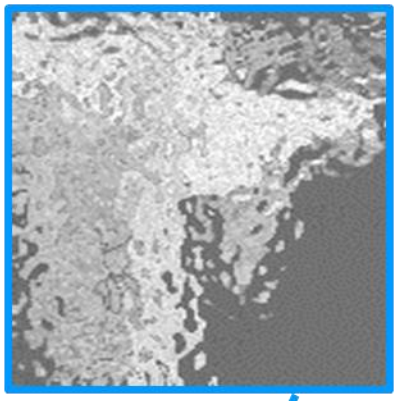


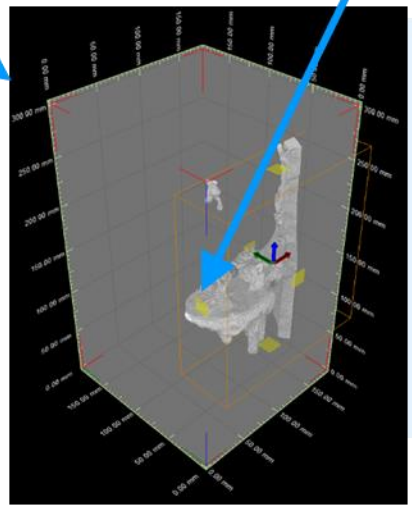


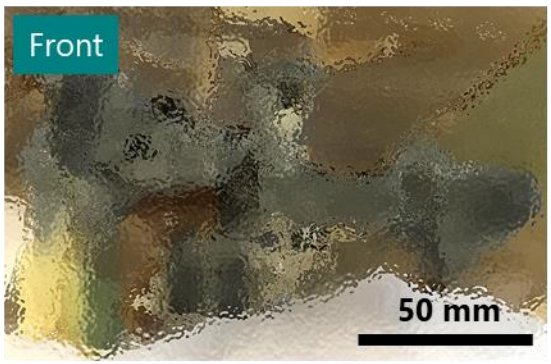
- Cutting conditions
  - Atmosphere: under water
  - Abrasive feed rate: approx. 1.5 kg/min
  - Cutting rate: 5 mm/min

Cutting of a sampling target

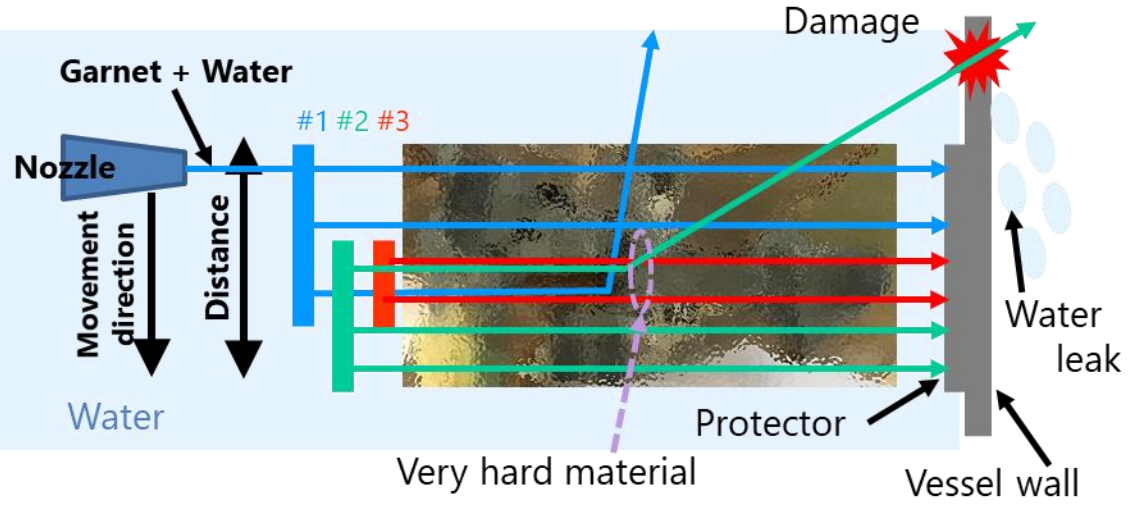












This page has been modified from the original version due to copyright.

EPMA and XRD analyses

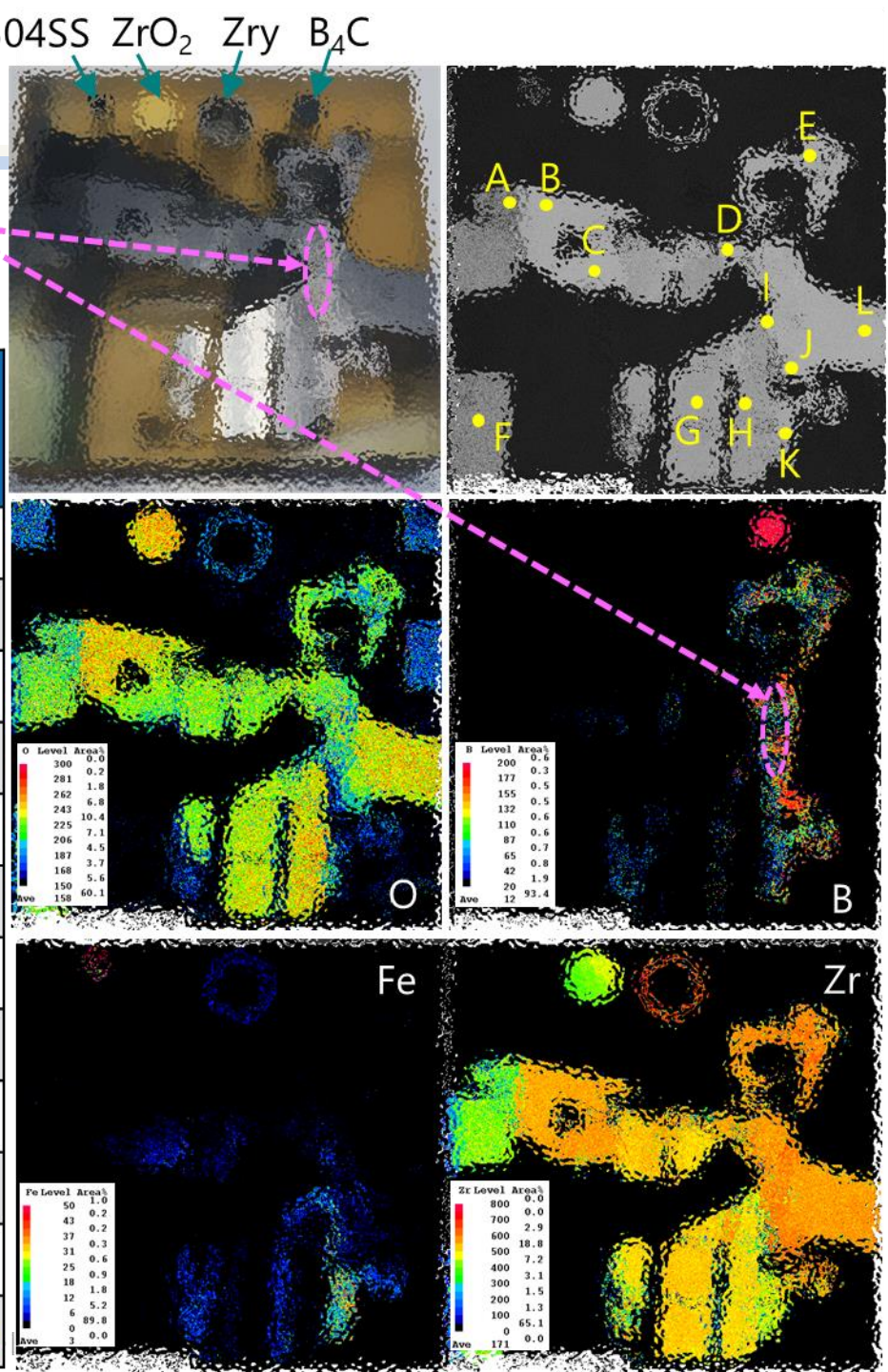
Hard material

Material distribution

Numbering in order of peak intensity

	Zr	ZrB_2	ZrC	ZrO	ZrO_2		Mg-Zr Oxide	Fe-Zr Oxide
					tetrag -onal	mono -clinic		

This page has been modified from the original version due to copyright.



Summary

- Melting and relocation of metals (the control blade, the channel box, and the cladding tube) were widely observed.
- Selective draining paths near the control blade were found; no complete blockage.
- The simulant fuel columns survived, although they have been exposed to high-temperature near the melting of ZrO_2 pellets.

This page has been modified from the original version due to copyright.

- The cutting by AWJ technique has the property of selectively abrading the soft spot of melts. Therefore, garnet may be repelled by a hard boride, and it may abrade places which were not expected.

a. **Macroscopic gas permeability** of the core was confirmed in reaching ceramic-fuel melting under the 1F2-like condition.
   - Selective formation of molten-metal draining paths preventing macroscopic blockage.
   - Absence of solid fuel swelling or sticking together reducing flow channels.

b. The **hot simulant core remained as columns**, suggesting a possible actual BWR scenario.
   - Remaining of the upper core part would result in coherent collapse of fuel columns rather than pellet-wise relocation.
   - The hottest part of the fuel might not relocate "effectively" down to the core support structure.

c. **Challenges in cutting by AWJ technique**:
   - The generation of a large amount of secondary waste
   - The damage of the non-target parts.

Thank you for your attention!
Collaborative works are always welcome!!

H. Madokoro <madokoro.hiroshi@jaea.go.jp>
T. Yamashita <yamashita.takuya38@jaea.go.jp>

References

- T. Yamashita, "Cutting of the CMMR-4 test bundle after test by the AWJ technique," Poster presented in Fukushima Research Conference, July 10-12, (2019).
- T. Yamashita, I. Sato, "The CMMR Program: BWR Core Degradation in the CMMR-4 test," Proc. 9th European Review Meeting on Severe Accident Research (ERMSAR2019), Czech Republic, March 18-20, (2019).

Status and first results of the CLADS-MADE-02 BWR control blade degradation test under steam-rich conditions related to 1F Unit 3 accident

Anton Pshenichnikov, Saishun Yamazaki, Yuji Nagae, Masaki Kurata

Japan Atomic Energy Agency (JAEA), Collaborative Laboratories for Advanced Decommissioning Science (CLADS)

790-1 Motooka Ohtsuka, Tomioka, Futaba district, Fukushima prefecture, 979-1151, Japan.

Abstract

The programme for investigation of a BWR control blade degradation under severe accident conditions of Fukushima Dai-Ichi reactors is ongoing. Previous researchers' results and recent JAEA activities are helpful in understanding of all details of Fukushima Dai-Ichi (1F) accident for each 1F reactor. However, there are still many uncertainties around 1F Unit 3, where accident was likely to develop under intermediate heating rate in sufficient steam environment. New experimental information and especially video of an accident progression is necessary for describing of materials behaviour at the beginning phase of the accident. Control blade debris, obtained in oxidative environment could have different chemical composition, which is very important to know during decommissioning of 1F reactors. Another important concern is possibility of B_4C interaction with steam, and consequences of it reaction with surrounding stainless steel and Zr changing materials compositions and properties. Thus, it was proposed to perform a test maximally close to 1F Unit 3 accident scenario.

A Large-scale Equipment for Investigation of Severe Accidents in Nuclear reactors (LEISAN) was utilized to conduct a Mock-up Assembly Degradation test (CLADS-MADE-02). In situ video of the experiment and mass-spectrometric analysis of the output gases (H_2, CO, CO_2) were carried out during tests. Preliminarily oxidized test bundle of 1.2 m long consisted of one control blade surrounded by two channel boxes each contained ten simulated fuel rods. It was subjected to an initial heating rate at 0.6 K/s in its hottest position. In the other points of the bundle due to temperature gradient the heating rate was lower. Steam flow rate was increased stepwise 5, 20, 30, 50 g/min during transient heating to simulate oxidation during boil-away. During heating no signs of temperature runaway was detected. After reaching ≈ 1600 °C the heating was maintained isothermal for 15 minutes to stabilize the temperature in the sample. At the moment an axial temperature gradient reached 525 °C/m. The final hottest and coldest temperature was 1605 °C and 975 °C respectively. Finally, the assembly was cooled down by natural heat losses in Ar.

Preliminarily it can be concluded, that the results of the present study were found to be in accord with the data from all previous BWR tests and complement them providing new data for scenario of 1F Unit 3 in the oxidative environment. Concerning melt progression, it is in accord with findings of LOFT LP-FP-2 test. In particular, problem of heterogeneous core degradation, causing the origination of two melt waves – first wave is metallic melt and second wave – oxidic melt, is extremely important in case of 1F accident. Because first wave of melt creates a blockage of metallic solidified melt, which later can be remelted and further relocate many times. However, oxidative environment was found to influence this behaviour, making secondary melting of the blockage material happened in a little bit different manner compared to steam-starved conditions. It can be seen that in oxidative environment some interesting effect of blockage surface bubbling of liquid melt can be observed. A possible mechanism of control blade melt relocation and liquid melt bubbling are under discussion.

The post-test investigation is ongoing.

This study is performed in "Advanced Multi-scale Modeling and Experimental Tests on Fuel Degradation in Severe Accident Conditions" supported by Ministry of Economy, Trade and Industry, Japan (METI).

The characterization of the CLADS-MADE-01 and -02 BWR control blade degradation test debris by Raman spectroscopy

Anton Pshenichnikov, Yuji Nagae, Masaki Kurata

Japan Atomic Energy Agency (JAEA), Collaborative Laboratories for Advanced Decommissioning Science (CLADS)

790-1 Motooka Ohtsuka, Tomioka, Futaba district, Fukushima prefecture, 979-1151, Japan.

Abstract

Characterization of potential debris from Fukushima Dai-Ichi (1F) damaged reactors will be a challenging task. To avoid future difficulties, it is worth studying a formation mechanism and properties of simulated debris resulted from the JAEA's control blade degradation tests CLADS-MADE-01 and -02, because the mechanism of their formation can be quite similar to the 1F debris.

The conventional SEM/EDS mapping of cross-sections forced difficulties because of overlapping of B and C peak areas, which made the exact determination problematic and not precise. Thus it was decided to check the debris by a promising Raman spectroscopy technique.

Polished cross-sections of control blade debris after the CLADS-MADE-01 and -02 tests [1] were investigated using a Raman imaging microscope (532 nm) (Thermo Fisher Scientific Inc., WI, USA). Raman spectra were collected from the area of 500 × 500 μm has with a 1 μm step size. A mapping of chemical compounds was possible after each spectrum was compared by the software for a correlation with reference ones.

It was established, that there were lots of unreacted B_4C material encapsulated in the metallic melt under the temperature ≈ 1500 °C much higher than Fe-B eutectic point and stainless steel melting range. The reacted traces of previous B_4C contained only pure graphite. The surrounding material represented by solidified metallic melt. Thus the mechanism of B4C granules degradation was defined as isolated decomposition of B_4C resulted in graphitization in the places of direct contact with metallic melt both under steam-starved and full steam conditions.

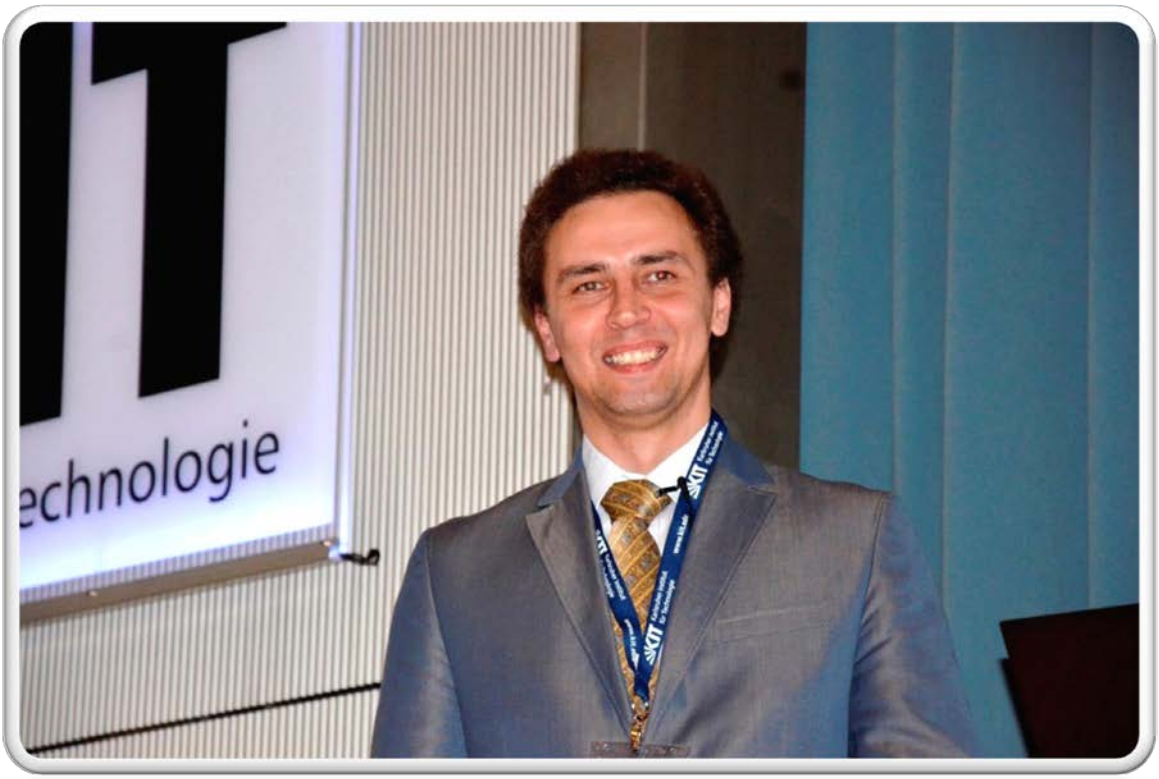
Established encapsulation of B_4C makes an idea of direct interaction with hot steam in case of granules not realistic. Two scenarios were detected when temperature increased: in a case of steam-starved conditions graphite remained in the structure, which promoted complicated $(Fe,Cr)_x(B,C)_y$ carboboride mixed phases formation; In case of oxidative environment, oxygen can be transferred through the liquid melt and oxidize the C to CO_x gases, which causes bubbling effect. Removal of C from the debris by oxygen will promote more borides formation in the structure of debris.

This knowledge would provide new insights for understanding of the absorber blade degradation mechanism under specific accident conditions close to 1F Unit 2 and Unit 3 reactors.

This study is performed in "Advanced Multi-scale Modeling and Experimental Tests on Fuel Degradation in Severe Accident Conditions" supported by Ministry of Economy, Trade and Industry, Japan (METI).

References

[1] Pshenichnikov, A., Yamazaki, S., Bottomley, D., Nagae, Y. and Kurata, M. "Features of a control blade degradation observed in situ during severe accidents in boiling water reactors", Journal of Nuclear Science and Technology, Vol. 56, No. 5 (2019), pp. 440 453.


echnologie

Status and first results of the CLADS-MADE-02 BWR control blade degradation test under steam-rich conditions related to 1F Unit 3 accident

Anton Pshenichnikov, Saishun Yamazaki, Yuji Nagae, Masaki Kurata

Presentation at 25th QUENCH workshop

Collaborative Laboratories for Advanced Decommissioning Science



Part 1
Introduction

CLADS-MADE-02 test

Purpose of this study:
Investigation of the mock-up assembly degradation under steam and temperature conditions which are most likely happened during the beginning phase of the accident at Fukushima-1 Nuclear Power Station (1F) at the unit 3

According to the TEPCO 5th progress report, 2017: there is a difference: Unit 2 was steam-starved for a prolonged time and Unit 3 had sufficient steam during the onset of control blade melting and relocation

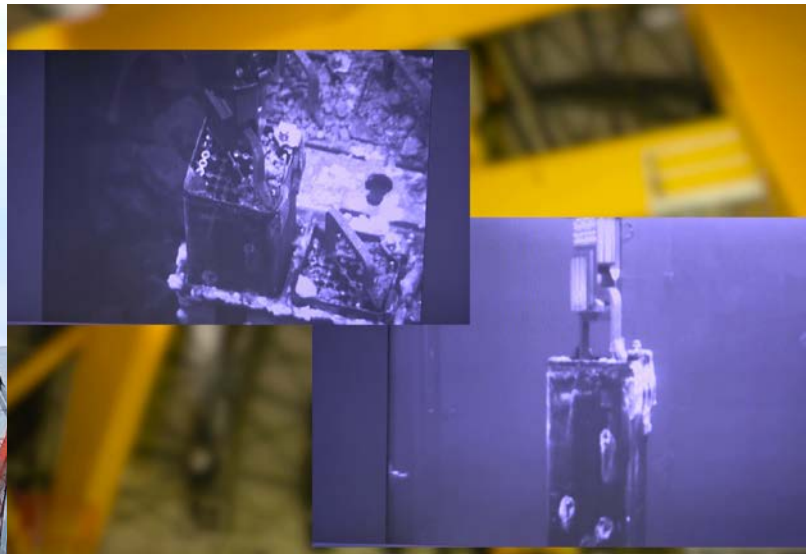


Fukushima-1, Unit 3 Mar. 2011

source, TEPCO's web-site



Jul. 2018



Jul. 2019 spent fuel removal



Part 2
Mock-up Assembly DEgradation test (CLADS-MADE-02)

JAEA/CLADS Test technology development group

Large-scale Equipment for Investigation of Severe Accidents in Nuclear reactors (LEISAN)

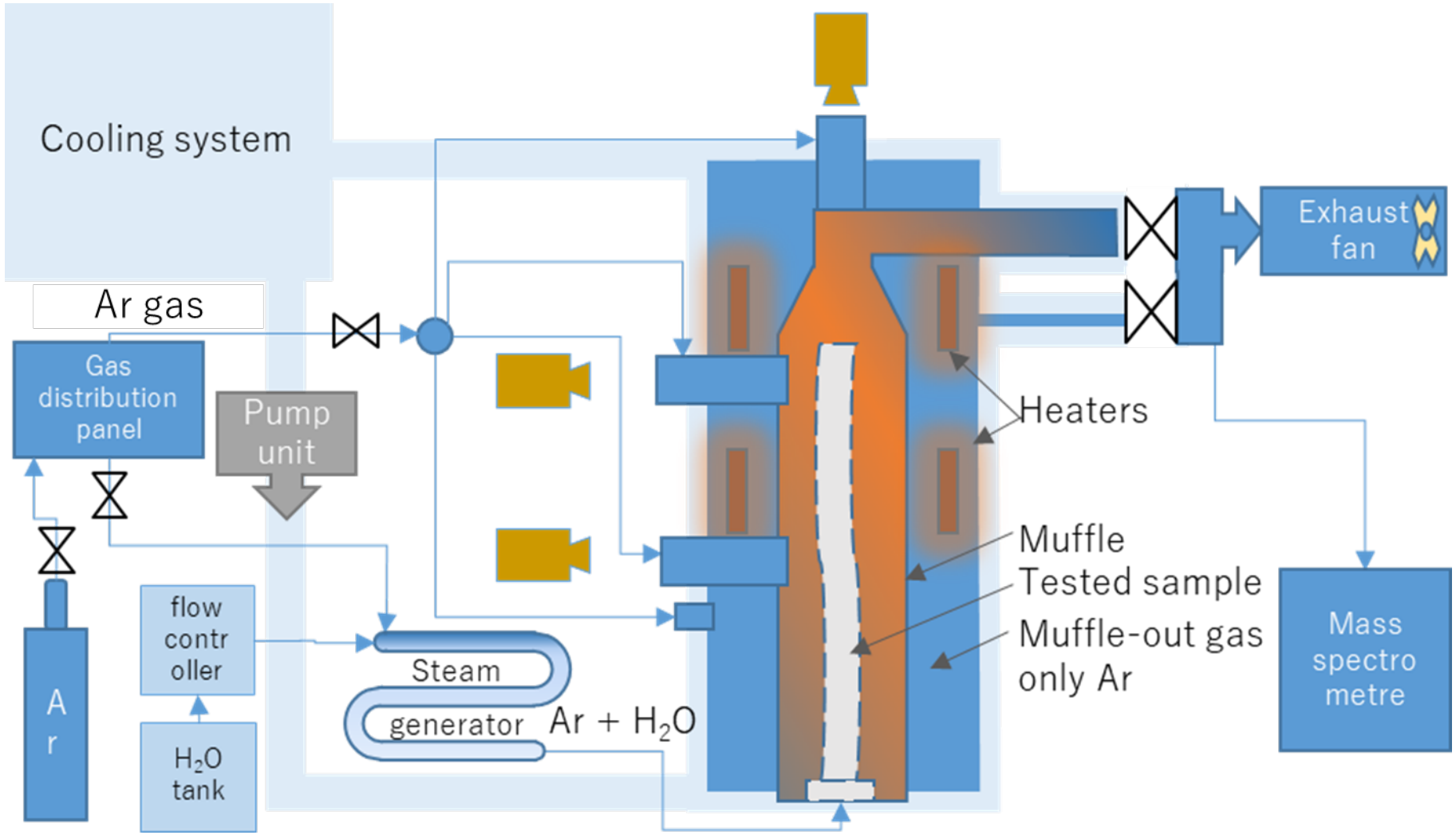






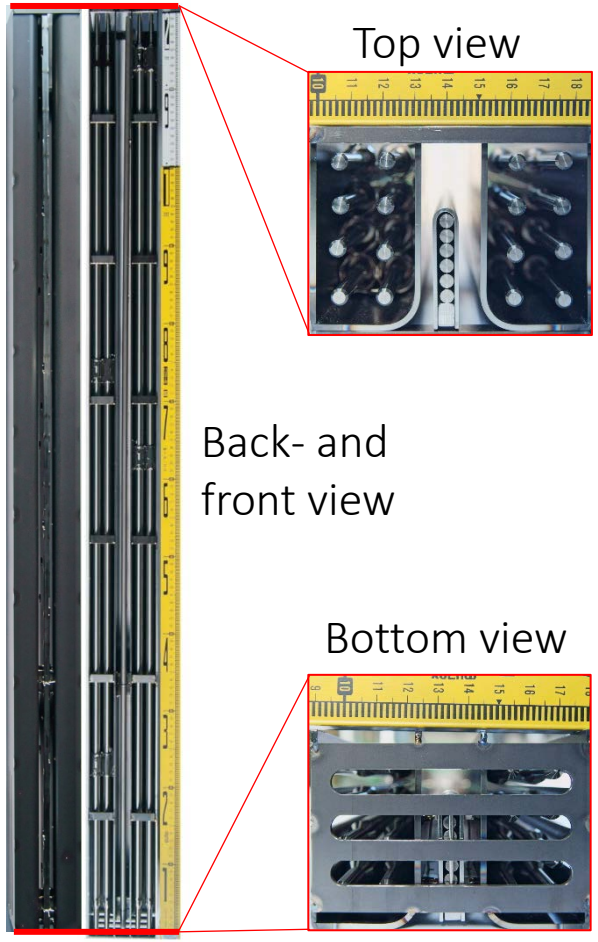
Specification	
Max assembly size for steam oxidation (limited by current muffle design)	20 ×20×120 cm
Max sample size for Ar environment (limited by furnace inner dimensions)	45×40 ×159 cm
Max temperature	2073 K / 1800 ℃
Atmosphere	Steam + Ar, pure Ar
Steam flow rate	0 – 50 g/min
Ar pre-heating temperature	Max. 300 ℃
Heating control	PID-controller
Heating rate (in steam / in Ar)	(< 1 K/s, < 4 K/s)
Form of samples	Customized assemblies
Test materials	Nonradioactive

LEISAN facility flow diagram



CLADS-MADE-02 sample overview

Produced by Japanese nuclear fuel manufacturer
Using real BWR materials (except pellets)

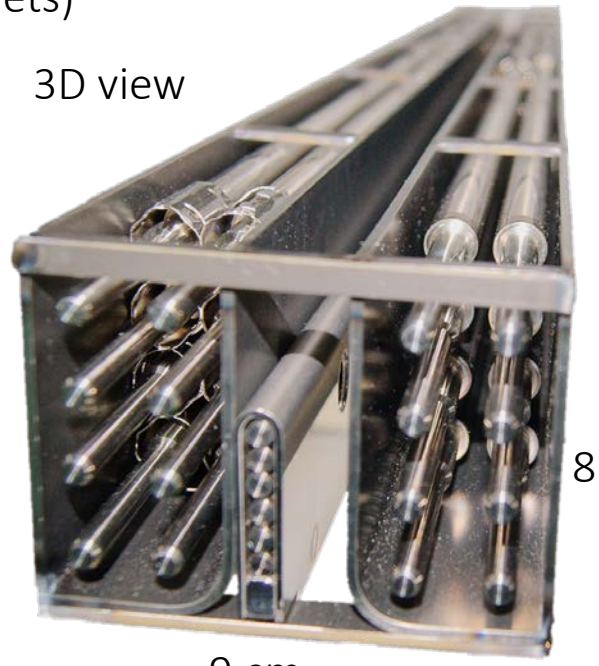


Top view

Back- and
front view

Bottom view

3D view



9 cm

8 cm

Covered by muffle



Inside of the
LEISAN facility



1.2 m long



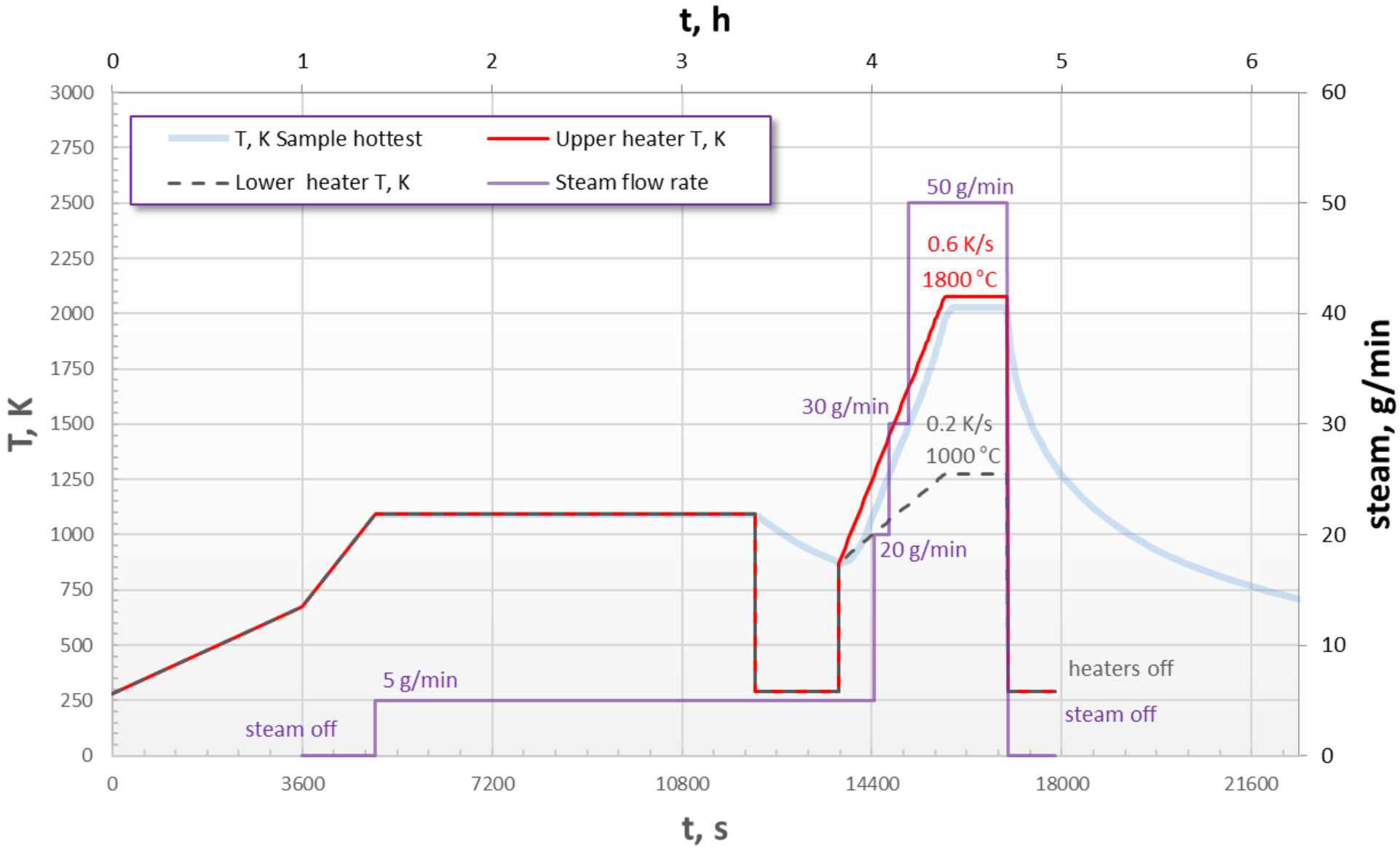
Full weight
with pellets and
a control blade

CLADS-MADE-02 planned test scenario

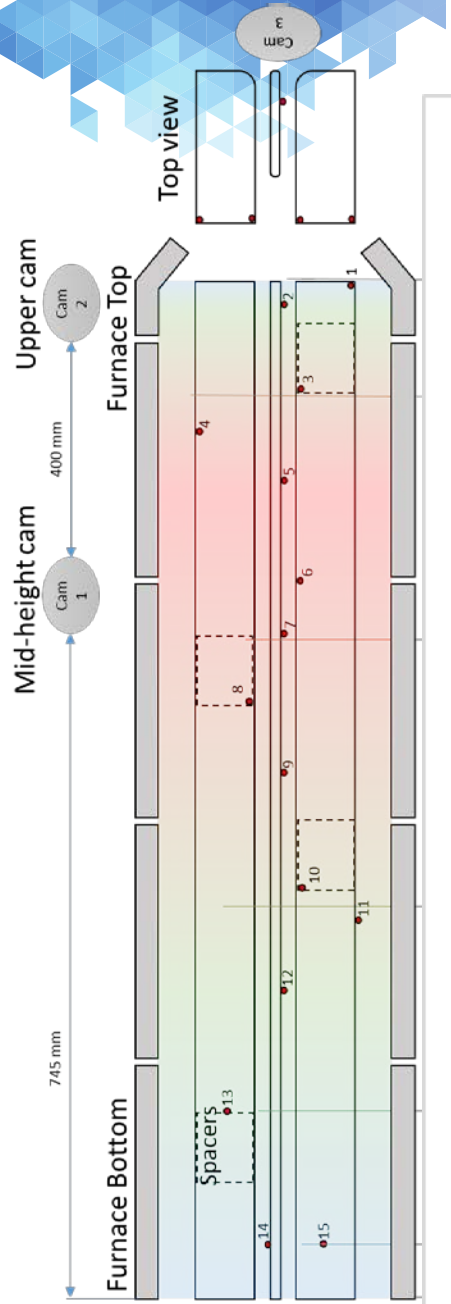
1F Unit 3 had steam production greatly decreased due to the decreased reactor water level
(TEPCO 5th progress report, 2017)

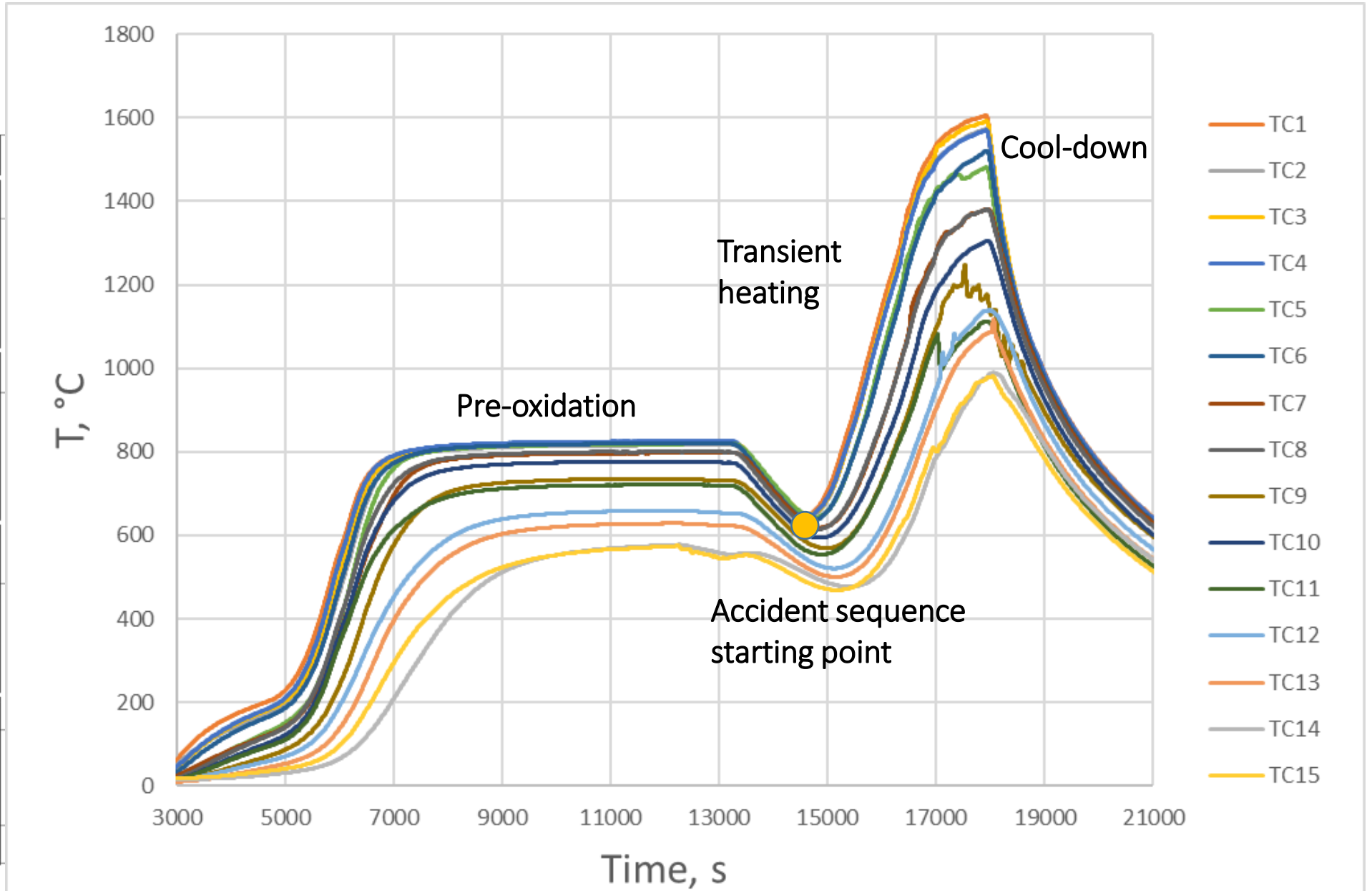
Probably the accident conditions were far from steam-rich. However, keeping in mind the amount of generated H_2 we assume the steam was sufficient.

The main steaming difference between units: Unit 2 (starved) and Unit 3 (sufficient)

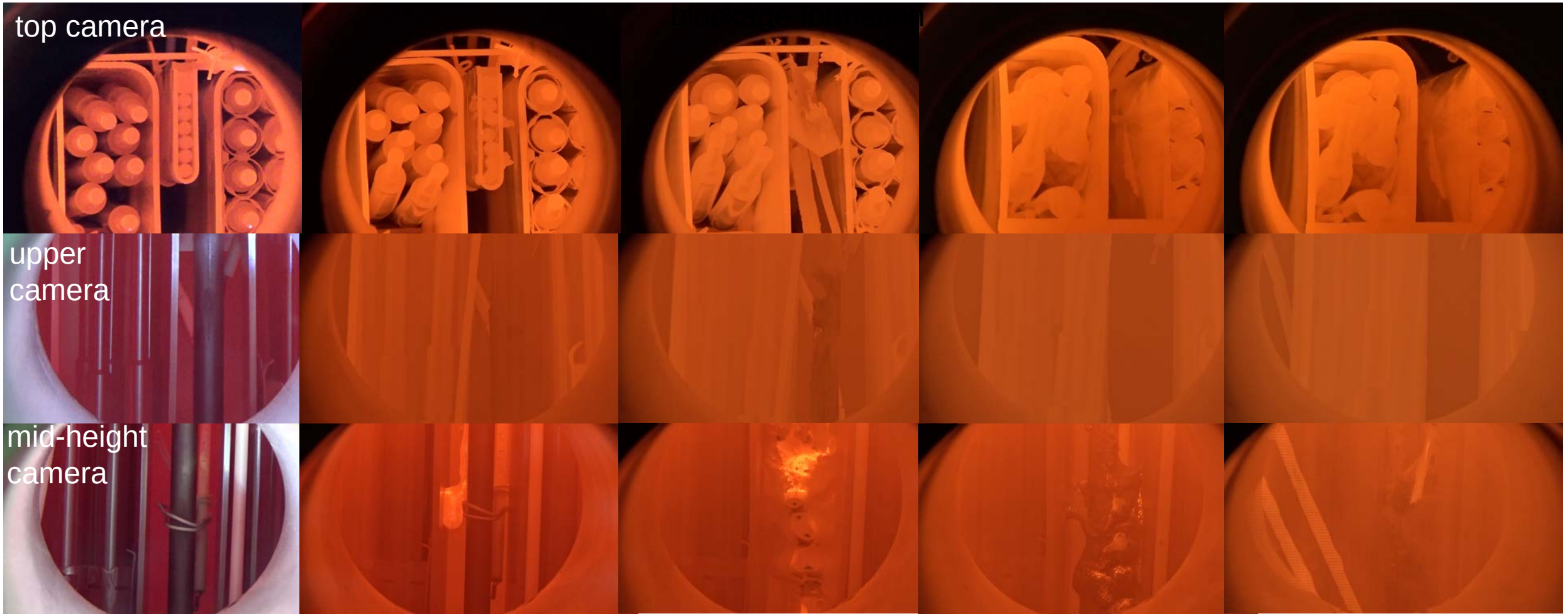


CLADS-MADE-02 measured temperatures





Mock-up of BWR fuel assembly during test



In situ video data during test

x16.68 times speed-up video



Top view cam
1200 mm



Upper cam
1150-1200 mm



Mid-height cam
740-790 mm

CLADS-MADE-02 has been performed on 18th of March 2019, Tomioka, Fukushima, Japan, International Collaborative Decommissioning Research Centre, JAEA/CLADS,

Dr. Anton P. Pshenichnikov, Dr. Saishun Yamazaki, Dr. Yuji Nagae, Dr. Masaki Kurata

Mock-up of BWR fuel assembly after test



before



after





Oxidized upper part



Solidified melt
In the middle part



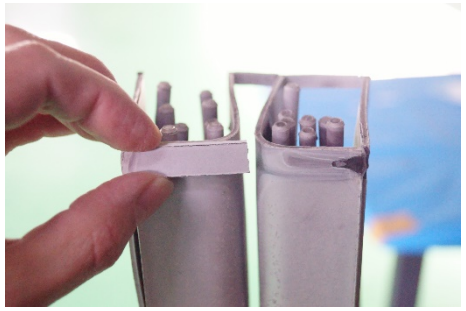


Lower part
Slight oxidation

First samples for post-test analysis

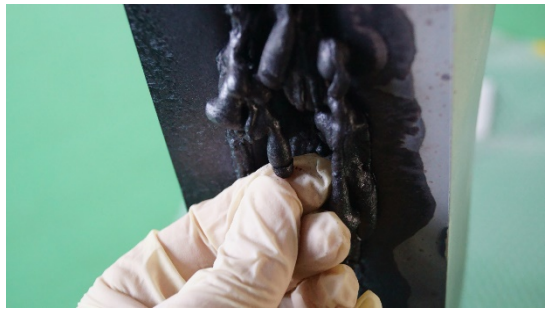



Sample supporting plate after test



Zr channel box in the oxidized upper part





Solidified melt samples in the middle part





Partially molten, then fallen control blade remnants

Cutting cross-sections (ongoing)

1200 mm Tmax ≈ 1605 °C

Control blade

intact **degraded**

Blade sheath 316L
Initial Tm=1371-1399 °C
partially molten

Control blade melt rivulet

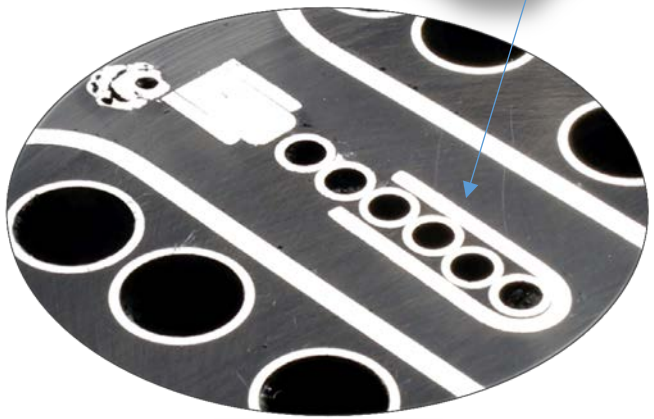
No. 1



No. 8



Channel box
no melt-through,
But traces of melt attack





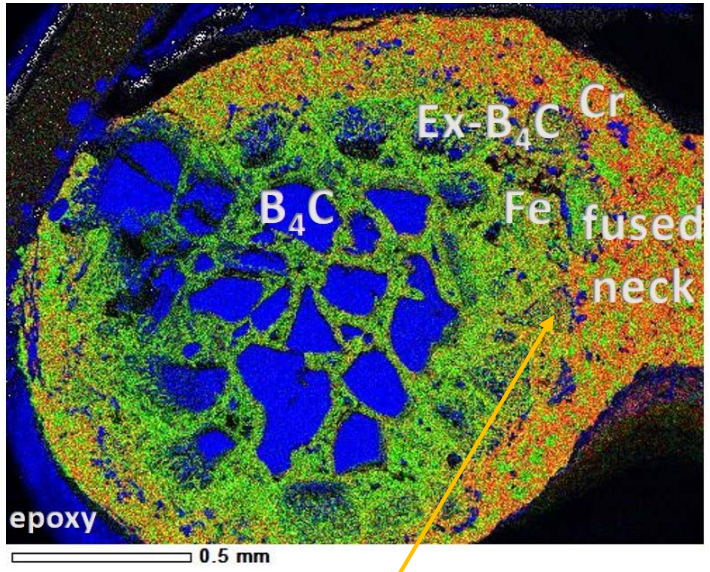


No. 8
620-640 mm
Tmax ≈ 1305 °C
(>1300 °C 150 s)

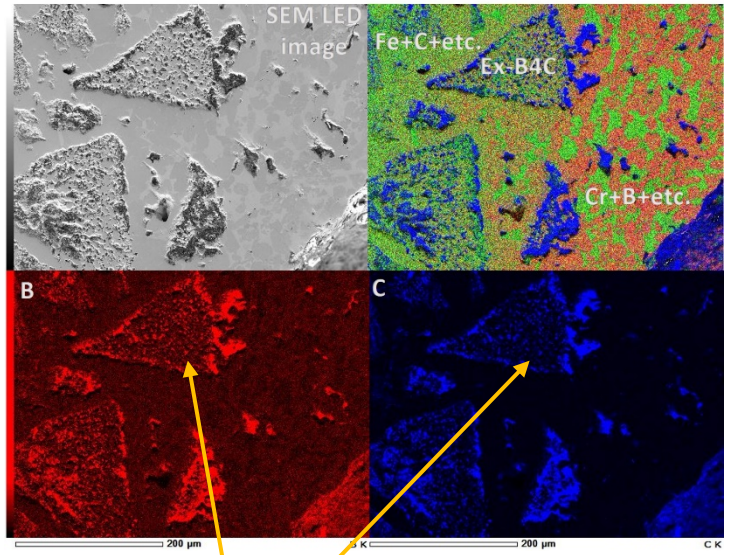
No. 1
60-80 mm
Tmax ≈ 990 °C

Scanning electron microscopy

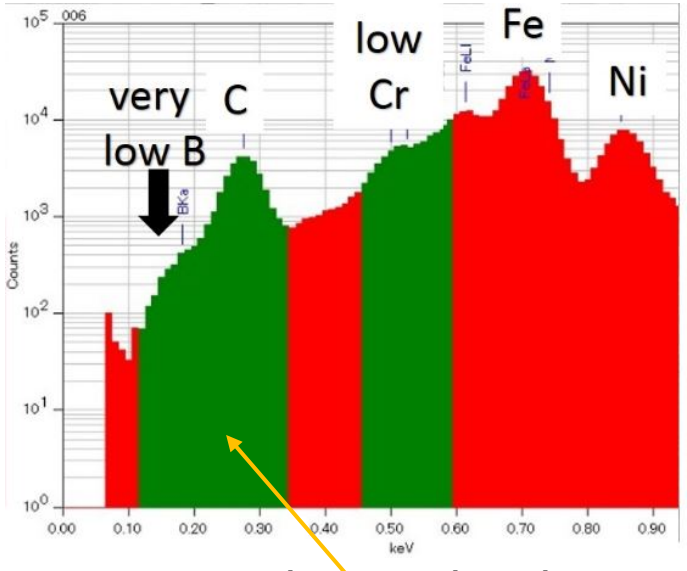
- Two tests with simulated fuel bundle in steam-starved and sufficient steam environment for understanding of the BWR control blade behavior in a case of a nuclear accident in 1F have been performed;
- Sim-debris analysis findings could help uncovering the physical mechanisms, which improves our knowledge;
- SEM EDS has some limitations in determining B and C together;



How did this happen?



Is it B or C or both as B_4C?



B and C overlapping - not ok for mapping!

- Let us try Raman spectroscopy measurement and mapping

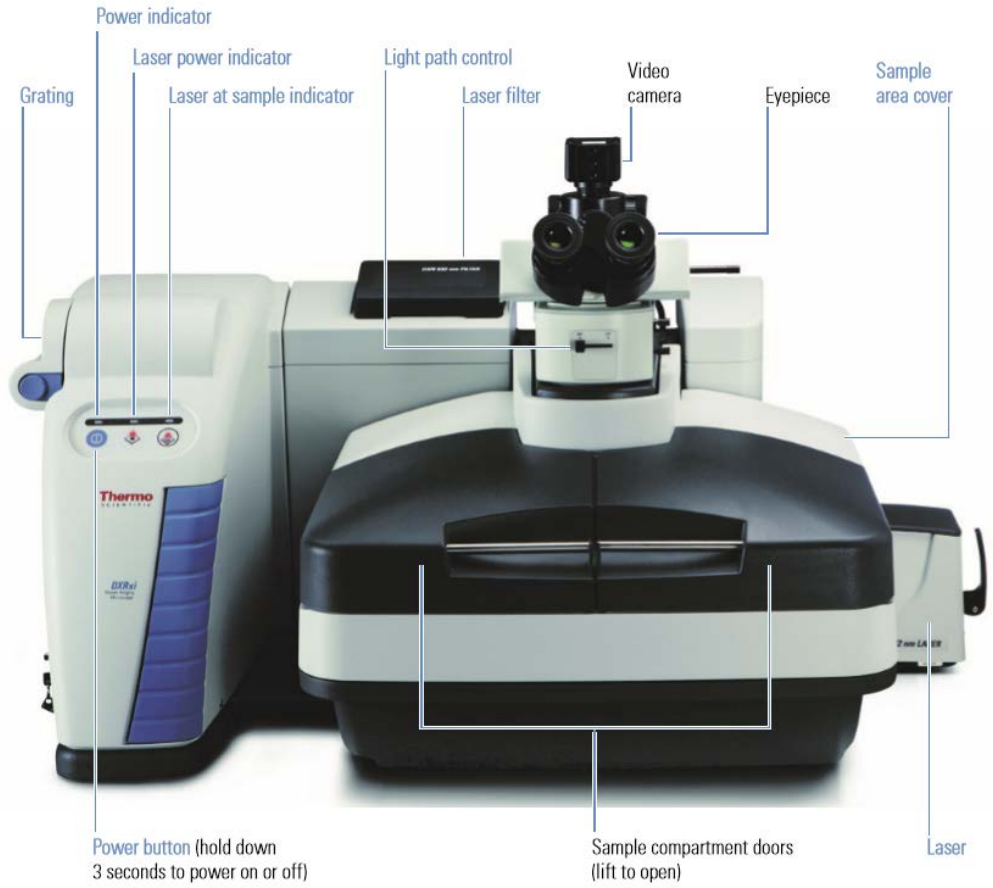
Raman imaging microscope

Advantages:

- Allows to study chemical material composition by dispersive Raman spectroscopy
- 532 nm laser
- Mapping scale is from μm^2 to mm^2
- High spatial resolution of ≈ 1-2 µm
- Solid (cristalline, amorphous), liquid, gas – any type of materials if there is a chemical bonding can be analysed
- Simple preparation of samples
- Simple operation

Disadvantage:

- Opened database is under development, that makes it difficult to analyse the spectra of unknown or nonstoichiometric compounds



*Picture quoted from User guide

Sample and choice of cross-sections for Raman

Not everything melts by Fe-B eutectic at 1200 °C,
there were control blade debris survived at 1500 °C

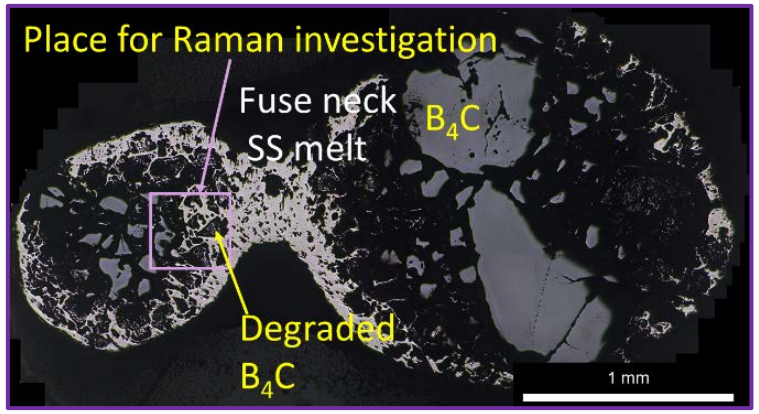


No melt bubbles observed

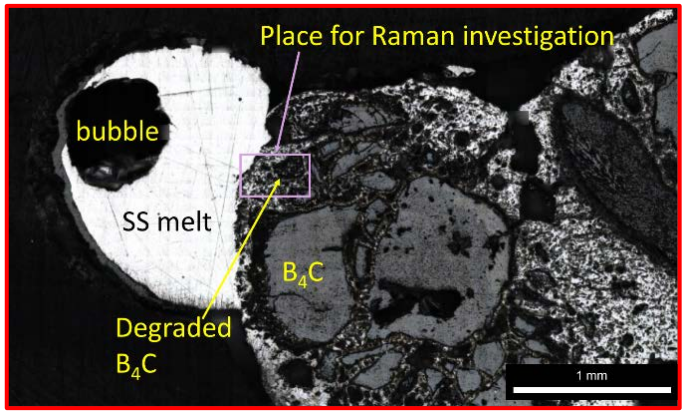


melt bubbles solidified!

10 mm



CLADS-MADE-01 test



CLADS-MADE-02 test

Representative Raman spectra

Pure B_4C

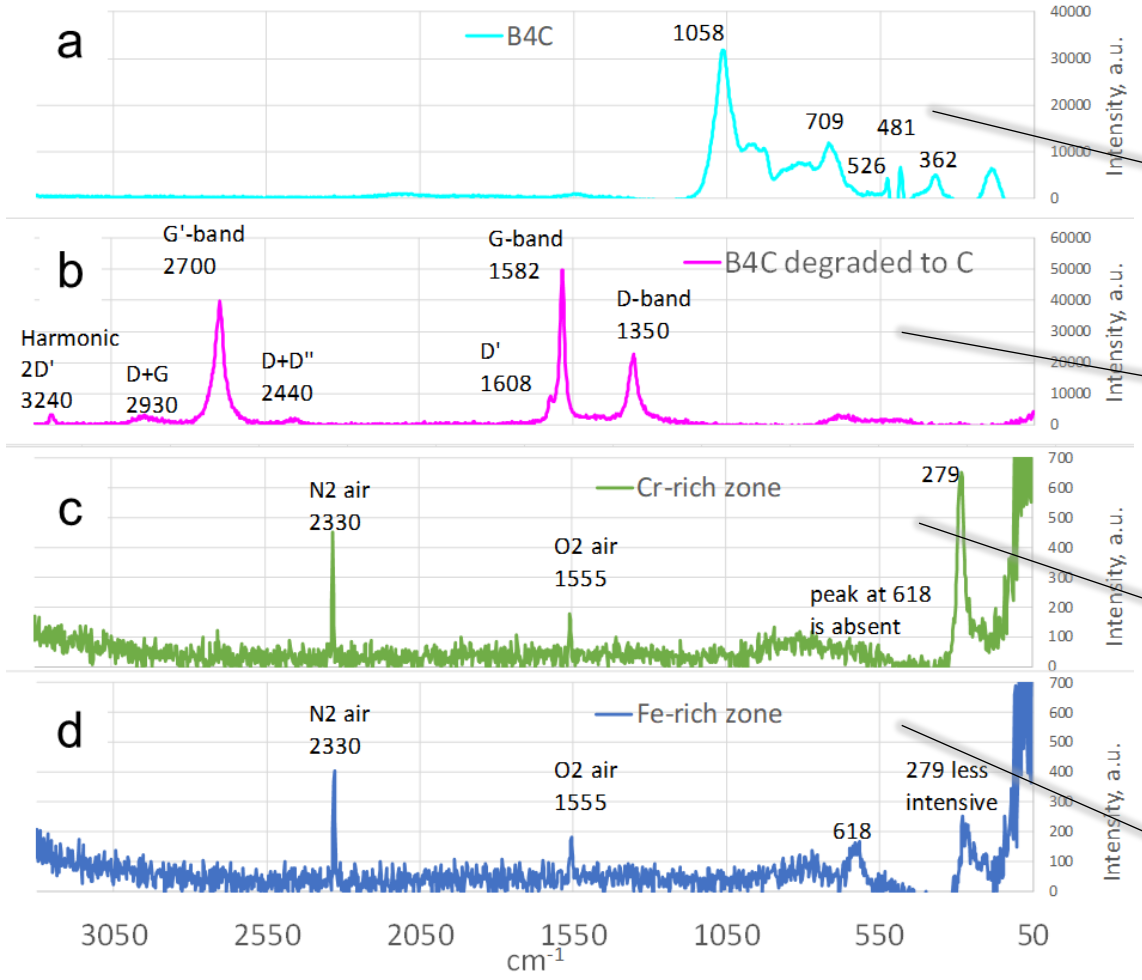
From Tallant, et al. Physical review B, Vol. 40, No. 8 (1989)

Pure graphite

From Bokobza et al. C, Vol. 1, (2015)

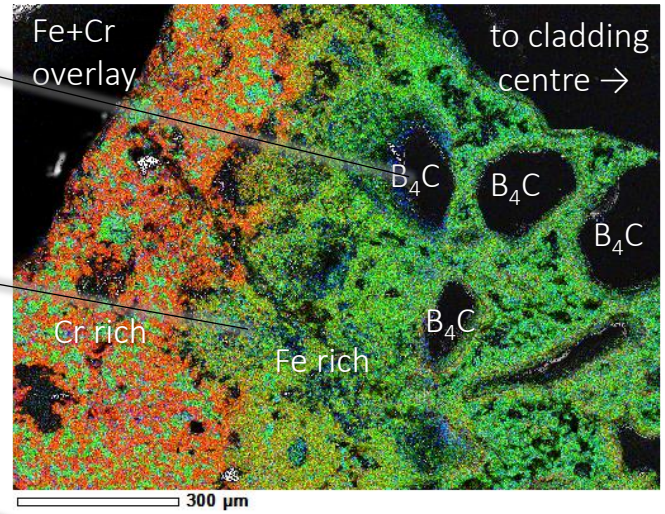
Metallic melt

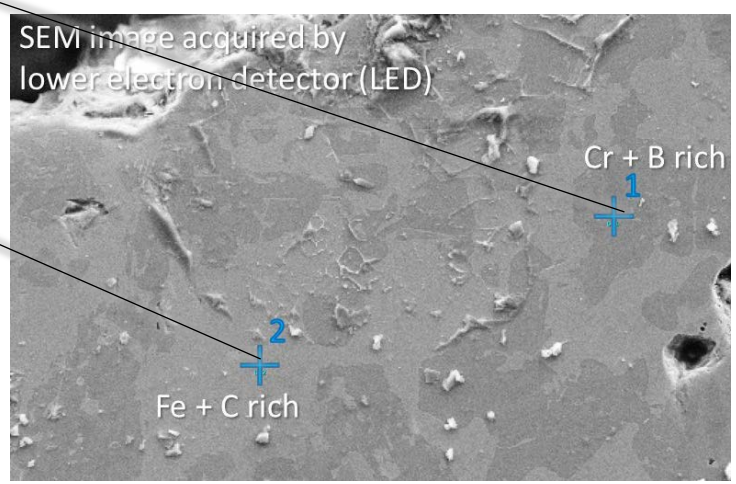
N_2 and O_2 peaks from Hippler, Analytical Chemistry, Vol. 83, (2015)



Only 4 spectra in all sample had been detected

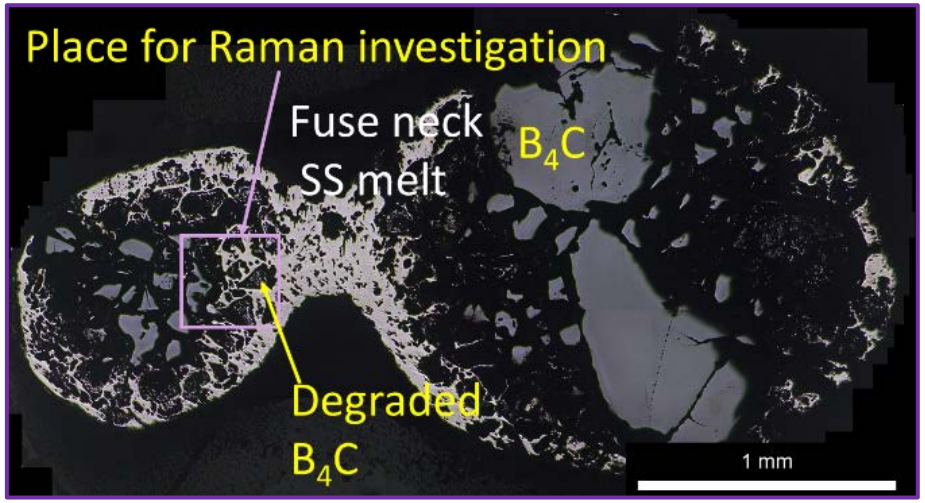
CLADS-MADE-01 test

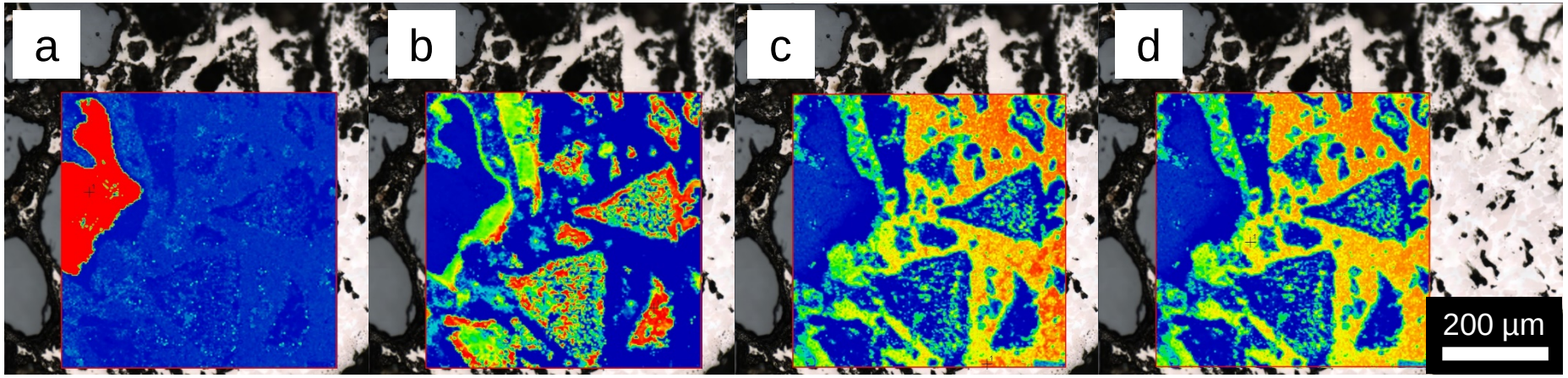




Raman mapping with obtained spectra

CLADS-MADE-01 test

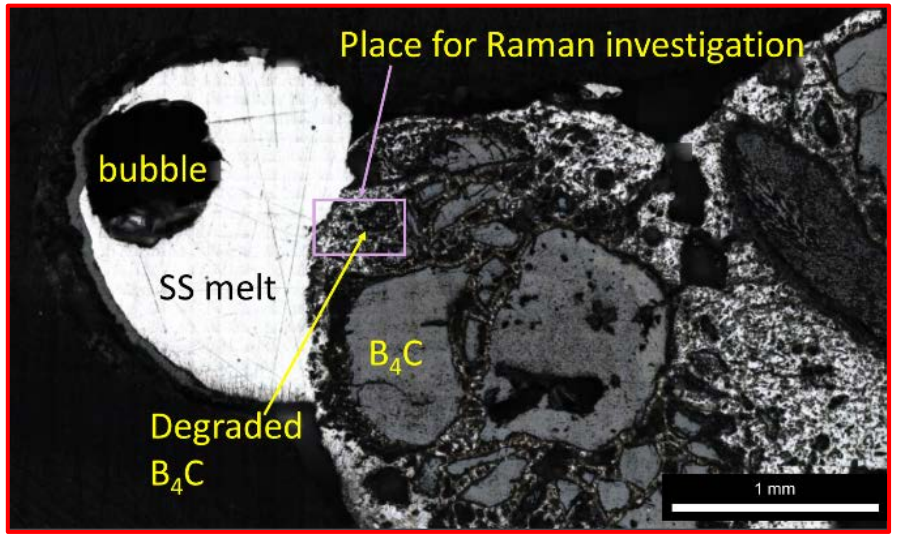


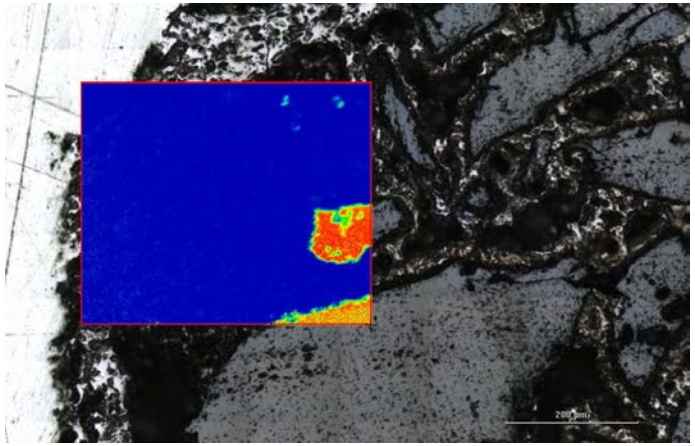


Pure B_4C | Pure C | Cr-rich metallic | Fe-rich metallic

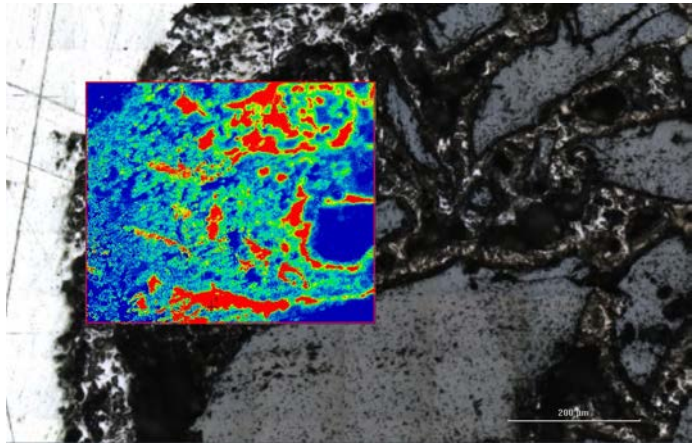
Raman mapping with obtained spectra

CLADS-MADE-02 test

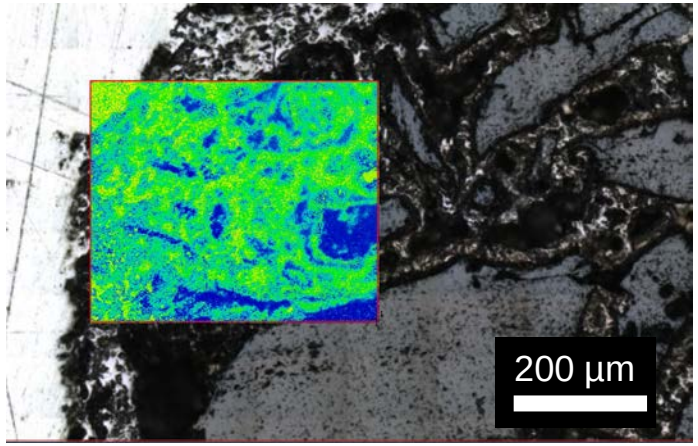




Pure B_4C



Pure C



Fe-rich metallic

Cr-rich metallic regions were too small as detected earlier by SEM hence, not resolved at this magnification

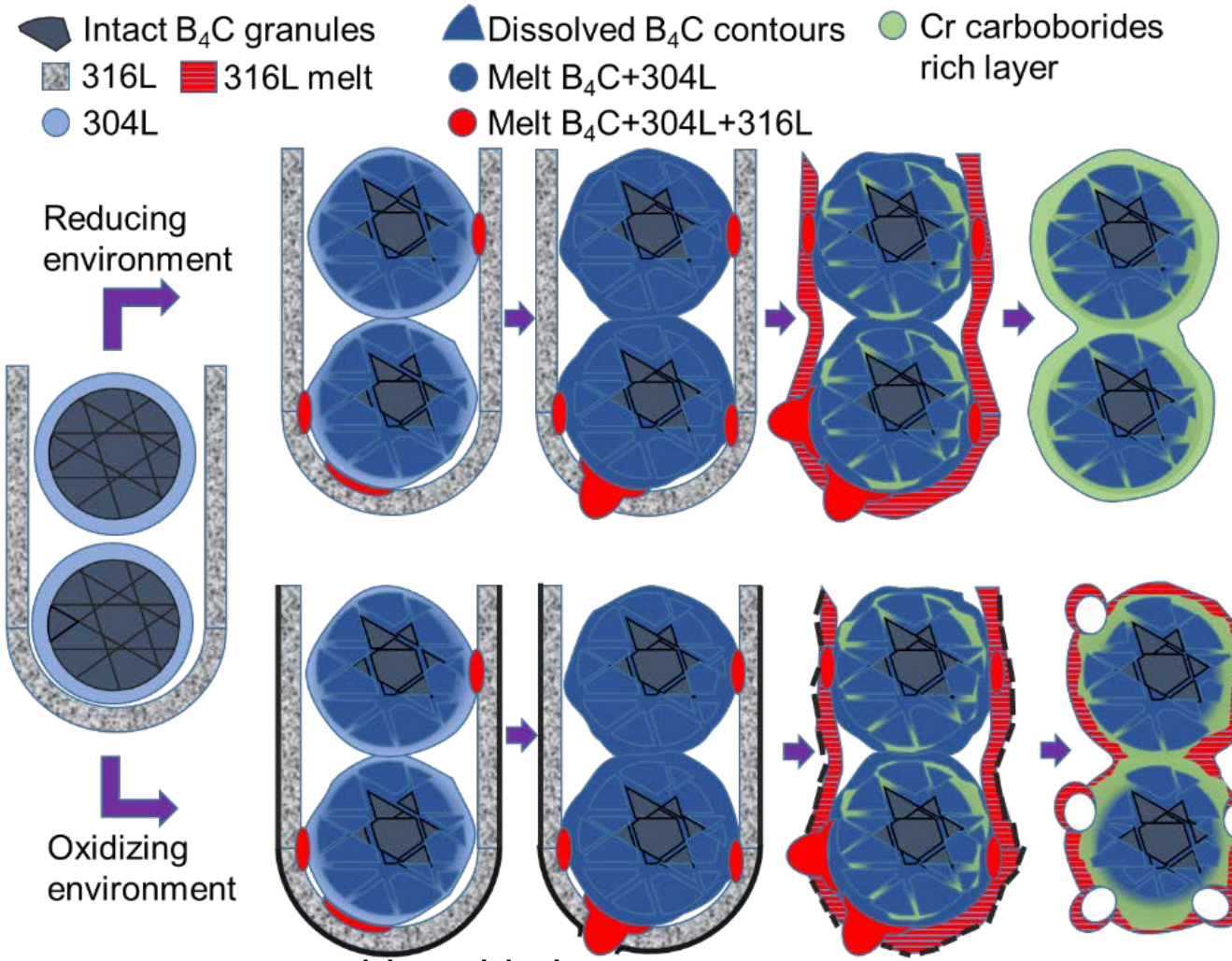


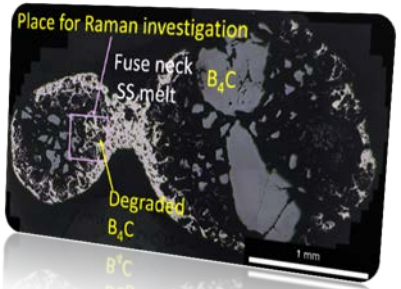
Part 3
Discussion

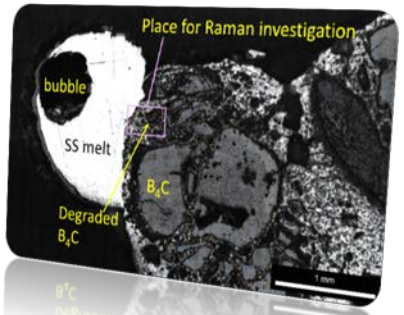
JAEA-CLADS Test technology development group

Raman mapping with obtained spectra

Pure C graphite found at the place where B_4C granules were







Understanding of B_4C degradation mechanism updated

Conclusions 1/2

- CLADS-MADE-01 test for Fukushima-1 Unit 3 accident scenario (sufficient steam) has been successfully performed;
- In situ video allowed thorough analysis of melt relocation features: onset, progress, candling, blockage formation and its subsequent melting with surface bubbling were directly observed using video cameras;
- Boron carbide (B_4C) blade remnants were degraded by melting but stayed in the hot region until they were mechanically broken by a falling massive upper sheath part;
- Melt blockage between channel boxes existed where the temperature conditions were ≈ 1174 °C - 1250 °C;
- Blockage can be remelted again many times, as soon as temperature increases above the eutectic point 1174 °C (1447 K);
- Channel boxes (≈ 20 μm preox.) were intact after direct contact with hot liquid melt proving high resistance of zirconium oxide; Threshold thickness that resist melt-through is still to confirm;
- During melt relocation no significant oxidation of melt happened probably because relocation from hot to cold region was fast and because Zr was not involved into melting;
- No temperature escalation was observed, though small temperature increase due to melt relocation was detected;
- Under oxidizing conditions like in Unit 3 during second and later remelting, it is confirmed, that less and less metallic melt will be relocating in comparison to the Unit 2 steam-starved conditions and more oxidized debris will be generated;
- Control blade debris and melt post-test detailed investigations are underway;

Conclusions 2/2

- Raman spectroscopy of debris from the control blade degradation tests has been successfully performed;
- In situ video catched bubbling of melt, which advanced us towards understanding of B_4C degradation mechanism;
- The new mechanism of B_4C granules degradation by graphitization has been identified both under steam-starved and full steam conditions;
- Direct B_4C oxidation by steam at the beginning phase of the accident seems not realistic as it is isolated in the centre of debris; Instead of this, B_4C degradation to graphite and then graphite oxidation in melt is quite possible;
- In the case of steam-starved conditions C cannot be effectively oxidized, thus remains in the structure, which promotes carboboride mixed phases formation $(Fe, Cr)_x(B, C)_y$, whereas in oxidative environment C removal would promote more borides formation;
- Data on control blade melt relocation is important for updating of existing severe accident models specially for BWR case.

Acknowledgement

This study is performed in the framework of "Advanced Multi-scale Modelling and Experimental Tests on Fuel Degradation in Severe Accident Conditions" supported by Ministry of Economy, Trade and Industry, Japan.

The authors would like to thank JAEA colleagues Dr. H.V. Pham helping us during different stages of the test and Dr. V. Cantarel for discussion on Raman spectroscopy questions.

Thank you for your attention

The talk was given by:

Dr. Anton Pshenichnikov

Special topic researcher,

Japan Atomic Energy Agency (JAEA)

Collaborative laboratories for Advanced Decommissioning Science (CLADS)

Fuel Debris Characterization & Core Status Evaluation Division

Simulation Test Technology Development Group

E-mail: pshenichnikov.anton@jaea.go.jp

Collaborative Laboratories for Advanced Decommissioning Science

25th International QUENCH Workshop, Karlsruhe Institute for Technology, 22-24 October 2019
Participants

Nr.	Family Name	First Name	Institution	Country	e-mail
1	Abolhassani Dadras	Sousan	Paul Scherrer Institut	Switzerland	sousan.abolhassani@psi.ch
2	Algama	Don	USNRC	USA	Don.Algama@nrc.gov
3	Allison	Chris	Innovative Systems Software	USA	ISS@SRV.NET
4	Barrachin	Marc	IRSN	France	marc.barrachin@irsn.fr
5	Boldt	Felix Maximilian	GRS	Germany	felix.boldt@grs.de
6	Bottomley	Paul David William	JAEA	Japan	dboksb3@gmail.com
7	Bourdon	Gauthier	CVUT	France	gauthier.bourdon@grenoble-inp.org
8	Brachet	Jean-Christophe	CEA	France	jean-christophe.brachet@cea.fr
9	Chalupová	Adéla	Faculty of Nuclear Sciences and Physical Engineering	Czech Republic	chaluade@fjfi.cvut.cz
10	Choi	Boyeon	KIT	Germany	boyeon.choi@partner.kit.edu
11	Chun	Tae-Hyun	KAERI	Korea, South	thchun@kaeri.re.kr
12	D'Alessandro	Christophe	GRS Garching	Germany	christophe.dalessandro@grs.de
13	De Malmazet	Erik	EDF	France	erik.de-malmazet@edf.fr
14	DURIEZ	Christian	IRSN	France	christian.duriez@irsn.fr
15	Farkas	Róbert	MTA Centre for Energy Research	Hungary	farkas.robert@energia.mta.hu
16	Fluhrer	Beatrix	KIT	Germany	beatrix.fluhrer@kit.edu
17	Freis	Daniel	European Commission - JRC	Germany	daniel.freis@ec.europa.eu
18	Gabrielli	Fabrizio	KIT	Germany	fabrizio.gabrielli@kit.edu

25th International QUENCH Workshop, Karlsruhe Institute for Technology, 22-24 October 2019
Participants

Nr.	Family Name	First Name	Institution	Country	e-mail
19	Gaus-Liu	Xiaoyang	KIT	Germany	xiaoyang.gaus-liu@kit.edu
20	Große	Mirco	KIT	Germany	Mirco.Grosse@KIT.edu
21	Guilbert-Banti	Séverine	IRSN	France	severine.guilbert@irsn.fr
22	Hagen	Siegfried	former FZK	Germany	siegfried.hagen@bitpri.de
23	Haste	Timothy	Imperial College	United Kingdom	t.haste@imperial.ac.uk
24	He	Xiaojun	China Institute of Atomic Energy	P.R.China	ciae.hexiaojun@gmail.com
25	Hering	Wolfgang	KIT	Germany	hering@kit.edu
26	Hollands	Thorsten	Gesellschaft für Anlagen- und Reaktorsicherheit (GRS) gGmbH	Germany	thorsten.hollands@grs.de
27	Howell	Jutta	KIT	Germany	jutta.howell@kit.edu
28	Hózer	Zoltán	MTA EK	Hungary	zoltan.hozer@energia.mta.hu
29	Ito	Ayumi	Tokyo Institute of Technology	Japan	itoh.a.ae@m.titech.ac.jp
30	Jäckel	Bernd	Paul-Scherrer-Institut	Switzerland	bernd.jaeckel@psi.ch
31	Joshi	Aniket	Imperial College London	United Kingdom	acj18@ic.ac.uk
32	Kaliatka	Tadas	Lithuanian Energy Institute	Lithuania	Tadas.Kaliatka@lei.lt
33	König	Tobias	KIT	Germany	koenig.tobias@kit.edu
34	Krejci	Jakub	UJP PRAHA a.s.	Czech Republic	krejci@ujp.cz
35	Krist	Florian	Ruhr-Universität Bochum	Bochum	krist@pss.rub.de
36	Laier	Jutta	KIT	Germany	jutta.laier@kit.edu

25th International QUENCH Workshop, Karlsruhe Institute for Technology, 22-24 October 2019
Participants

Nr.	Family Name	First Name	Institution	Country	e-mail
37	Le Belguet	Alix	EDF Lab	France	alix.le-belguet@edf.fr
38	Lovasz	Liviusz	GRS	Germany	liviusz.lovasz@grs.de
39	Madokoro	Hiroshi	JAEA	Japan	madokoro.hiroshi@jaea.go.jp
40	Matocha	Vitezslav	UJV Rez, a. s.	Czech Republic	vitezslav.matocha@ujv.cz
41	Moch	Jürgen Alexander	KIT	Germany	juergen.moch@kit.edu
42	Mokrushin	Andrey	FSUE SRI SIA LUCH	Russia	mokrushinaa@sialuch.ru
43	Muscher	Heinrich	KIT	Germany	heinrich.muscher@kit.edu
44	Nagae	Yuji	Japan Atomic Energy Agency	Japan	nagae.yuji@jaea.go.jp
45	Nigbur	Corbinian	University of Stuttgart	Germany	corbinian.nigbur@ike.uni-stuttgart.de
46	Ott	Larry	Oak Ridge National Laboratory (retired)	USA	LJOtt13@gmail.com
47	Peschel	Jan Mathis	Ruhr-Universität Bochum	Germany	Jan.Peschel@pss.rub.de
48	Peters	Ursula	KIT	Germany	Ursula.Peters@kit.edu
49	Petroff	Markus	Universität Stuttgart	Germany	markus.petroff@ike.uni-stuttgart.de
50	Pshenichnikov	Anton	JAEA/CLADS	Japan	pshenichnikov.anton@jaea.go.jp
51	Sartowska	Bożena	Institute of Nuclear Chemistry and Technology	Poland	b.sartowska@ichtj.waw.pl
52	Schubert	Arndt	Joint Research Centre	Germany	Arndt.Schubert@ec.europa.eu
53	Sevecek	Martin	Czech Technical University in Prague	Czech Republic	martin.sevecek@fjfi.cvut.cz
54	Sidelev	Dmitrii	Tomsk Polytechnic University	Russia	sidelevdv@tpu.ru

25th International QUENCH Workshop, Karlsruhe Institute for Technology, 22-24 October 2019
Participants

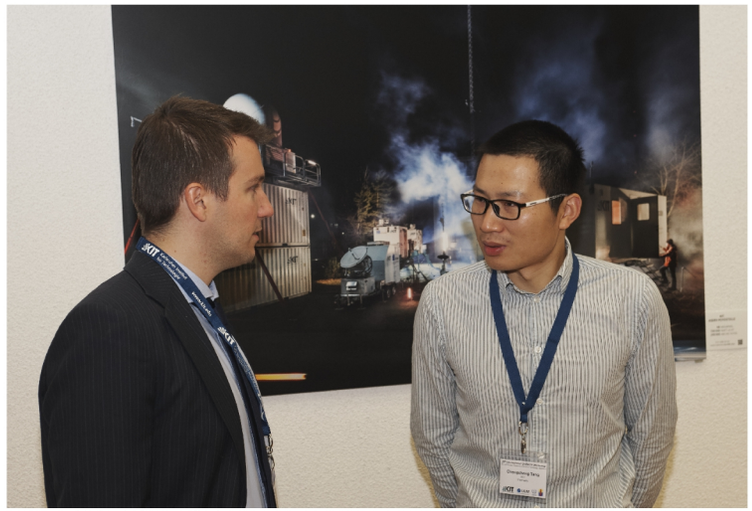
Nr.	Family Name	First Name	Institution	Country	e-mail
55	Stakhanova	Anastasia	KIT	Germany	anastasia.stakhanova@kit.edu
56	Stegmaier	Ulrike	KIT	Germany	ulrike.stegmaier@kit.edu
57	Steinbrück	Martin	KIT	Germany	martin.steinbrueck@kit.edu
58	Stevanka	Kamil	Faculty of Electrical Engineering, Brno University of Technology	Czech republic	kamil.stevanka@vutbr.cz
59	Stuckert	Juri	KIT	Germany	juri.stuckert@kit.edu
60	Tang	Chongchong	KIT	Germany	chongchong.tang@kit.edu
61	Tiborcz	Livia	Gesellschaft für Anlagen- und Reaktorsicherheit (GRS) gGmbH	Germany	livia.tiborcz@grs.de
62	Tromm	Th. Walter	KIT	Germany	walter.tromm@kit.edu
63	Van Uffelen	Paul	European Commission, Joint Research Centre	Germany	Paul.Van-Uffelen@ec.europa.eu
64	Vasiliev	Alexander	IBRAE	Russia	vasil@ibrae.ac.ru
65	Veshchunov	Mikhail	IAEA	Austria	m.veshchunov@iaea.org
66	Wang	Shisheng	KIT	Germany	Shisheng.Wang@kit.edu





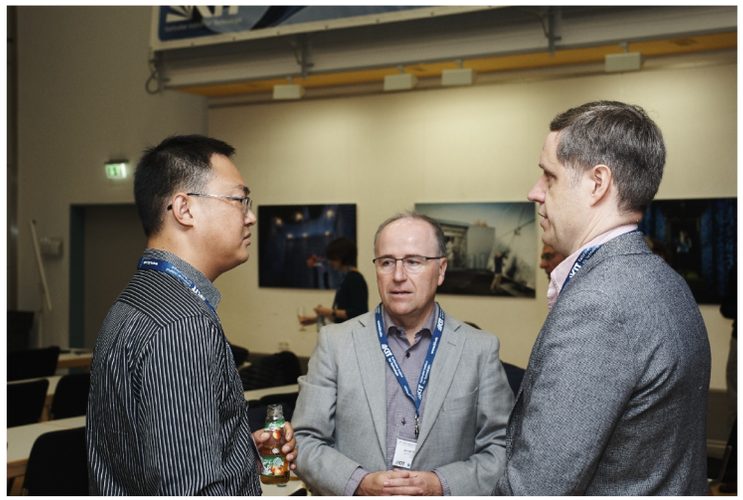






















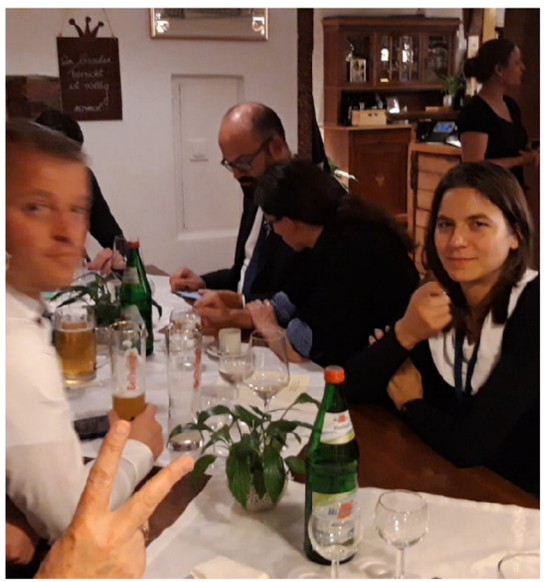


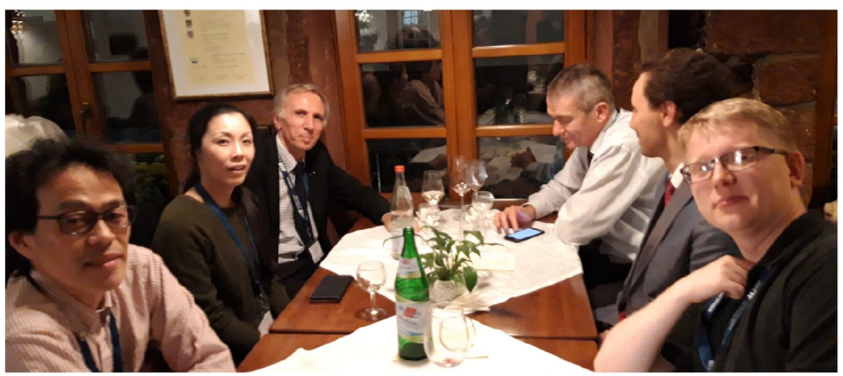















KASPER



















